

NUMERICAL ANALYSIS OF CONDITIONS NECESSARY FOR  
NEAR-SURFACE SNOW METAMORPHISM

by

Andrew Edward Slaughter

A dissertation submitted in partial fulfillment  
of the requirements for the degree

of

Doctor of Philosophy

in

Engineering

MONTANA STATE UNIVERSITY  
Bozeman, Montana

April 2010

UMI Number: 3403060

All rights reserved

INFORMATION TO ALL USERS

The quality of this reproduction is dependent upon the quality of the copy submitted.

In the unlikely event that the author did not send a complete manuscript and there are missing pages, these will be noted. Also, if material had to be removed, a note will indicate the deletion.



UMI 3403060

Copyright 2010 by ProQuest LLC.

All rights reserved. This edition of the work is protected against unauthorized copying under Title 17, United States Code.



ProQuest LLC  
789 East Eisenhower Parkway  
P.O. Box 1346  
Ann Arbor, MI 48106-1346



© Copyright

by

Andrew Edward Slaughter

2010

All Rights Reserved

APPROVAL

of a dissertation submitted by

Andrew Edward Slaughter

This dissertation has been read by each member of the dissertation committee and has been found to be satisfactory regarding content, English usage, format, citations, bibliographic style, and consistency, and is ready for submission to the Division of Graduate Education.

Dr. Edward E. Adams

Approved for the Department of Civil Engineering

Dr. Brett W. Gunnink

Approved for the Division of Graduate Education

Dr. Carl Fox

## STATEMENT OF PERMISSION TO USE

In presenting this dissertation in partial fulfillment of the requirements for a doctoral degree at Montana State University, I agree that the Library shall make it available to borrowers under rules of the Library. I further agree that copying of this dissertation is allowable only for scholarly purposes, consistent with "fair use" as prescribed in the U.S. Copyright Law. Requests for extensive copying or reproduction of this dissertation should be referred to ProQuest Information and Learning, 300 North Zeeb Road, Ann Arbor, Michigan 48106, to whom I have granted "the exclusive right to reproduce and distribute my dissertation in and from microform along with the non-exclusive right to reproduce and distribute my abstract in any format in whole or in part."

Andrew Edward Slaughter

April 2010

## ACKNOWLEDGMENTS

First, I would like to thank my advisor, Dr. Adams, for all of his assistance through the years, for securing various sources of funding to keep me going, and mostly for allowing me to discover my own path. Thanks to Dr. McKittrick for his guidance with numerical analysis and setting up servers for all my projects. And, thank you to my entire committee for their time and patience.

This dissertation would not be possible without the dedicated Yellowstone Club Ski Patrol that helped produce a world-class data set, specifically Tom Leonard, Doug McCabe, Irene Henninger, Doug Catherine, and Henry Munter. I would also like to thank my fellow graduate students for their assistance in gathering data, the conversations, and the encouragement. A special thanks to those I shared an office with: Peter Gammelgard, Patrick Staron, and Rich Schertzer. Thank you to Dave Neal for my experience in his 5th grade class. Thank you to my parents as well as all of my family and friends for their support. Thank you to my beautiful wife, Deanne, for her patience, emotional and financial support, editing skills, and mostly for her love. Lastly, I am thankful for the fortitude granted by our heavenly Father to continue the pursuit of this achievement.

## TABLE OF CONTENTS

1. INTRODUCTION .....	1
2. SIGNIFICANCE AND BACKGROUND OF SURFACE WEAK LAYERS .....	5
2.1 Introduction .....	5
2.2 Significance of the Near-Surface Layers .....	5
2.2.1 Avalanches .....	5
2.2.2 Climate .....	6
2.2.3 Synopsis .....	8
2.3 A Review of Surface Hoar .....	9
2.4 A Review of Near-Surface Facets .....	17
2.5 Conclusions .....	21
3. FIELD INVESTIGATION OF SURFACE HOAR .....	24
3.1 Introduction .....	24
3.2 Methods.....	25
3.2.1 Weather stations .....	25
3.2.2 Instrumentation .....	25
3.2.3 Snow observations .....	26
3.3 Results.....	27
3.4 2007/2008 Surface Hoar Events .....	29
3.4.1 Event A-1: January 24, 2008.....	29
3.4.2 Event A-2: February 15, 2008 .....	31
3.4.3 Event A-3: February 19–21, 2008 .....	32
3.4.4 Event A-4: February 22, 2008 .....	36
3.4.5 Event A-5: February 26, 2008 .....	38
3.4.6 Event A-6: March 10, 2008 .....	40
3.4.7 Event A-7: March 30, 2008 .....	42
3.5 2008/2009 surface hoar events .....	44
3.5.1 Event B-1: January 23, 2009 .....	44
3.5.2 Event B-2: January 30–31, 2009 .....	45
3.5.3 Event B-3: February 4, 2009 .....	47
3.5.4 Event B-4: February 7–8, 2009 .....	49
3.5.5 Event B-5: February 13–14, 2009.....	51
3.5.6 Event B-6: February 28, 2009.....	52
3.5.7 Event B-7: March 13, 2009 .....	53
3.6 Analysis .....	55
3.7 Future Considerations .....	59
3.8 Conclusion .....	60

## TABLE OF CONTENTS – CONTINUED

4. FIELD INVESTIGATION OF NEAR-SURFACE FACETS .....	61
4.1 Introduction .....	61
4.2 Methods.....	61
4.3 Results.....	63
4.4 2007/2008 Near-surface Facet Events .....	66
4.4.1 Event C-1: January 21, 2008 .....	66
4.4.2 Event C-2: February 14–16, 2008.....	66
4.4.3 Event C-3: February 18–20, 2008.....	69
4.4.4 Event C-4: February 26–27, 2008.....	71
4.4.5 Event C-5: March 6, 2008 .....	75
4.4.6 Event C-6: March 10, 2008 .....	75
4.4.7 Event C-7: March 13, 2008 .....	77
4.4.8 Event C-8: March 15, 2008 .....	78
4.4.9 Event C-9: March 19, 2008 .....	79
4.4.10 Event C-10: March 22, 2008 .....	81
4.4.11 Event C-11: March 28, 2008 .....	82
4.4.12 Event C-12: March 30, 2008 .....	82
4.4.13 Event C-13: April 2–4, 2008 .....	84
4.4.14 Event C-14: April 6, 2008 .....	85
4.4.15 Event C-15: April 8, 2008 .....	87
4.5 2008/2009 Near-surface Facet Events .....	89
4.5.1 Event D-1: February 4, 2009 .....	89
4.5.2 Event D-2: February 8, 2009 .....	90
4.5.3 Event D-3: February 12–14, 2008 .....	92
4.5.4 Event D-4: February 19, 2009 .....	93
4.5.5 Event D-5: February 21, 2009 .....	95
4.5.6 Event D-6: February 27–28, 2009 .....	97
4.5.7 Event D-7: March 7, 2009.....	99
4.5.8 Event D-8: March 12–14, 2009 .....	101
4.5.9 Event D-9: March 20, 2009 .....	104
4.5.10 Event D-10: March 30, 2009.....	105
4.5.11 Event D-11: April 6, 2009 .....	107
4.6 Analysis .....	108
4.7 Conclusions .....	111
5. SNOW THERMAL MODEL .....	114
5.1 Introduction.....	114

## TABLE OF CONTENTS – CONTINUED

5.2 Background.....	115
5.3 Model Development .....	117
5.3.1 Conservation of Energy.....	117
5.3.2 Application .....	120
5.3.3 Numerical Solution.....	121
General Numeric Equation .....	121
Boundary Conditions .....	123
Matrix Solution .....	124
5.3.4 Short-wave Radiation .....	125
5.3.5 Surface Flux Terms .....	127
5.3.6 Boundary Layer Application .....	130
5.3.7 Material Properties.....	132
5.4 Analysis with VIS/NIR Components.....	133
5.5 Reliability of Model .....	136
5.6 Closing Remarks.....	137
6. SOBOL SENSITIVITY ANALYSIS: THEORY AND EXAMPLES .....	139
6.1 Introduction.....	139
6.2 Sensitivity Defined.....	142
6.3 Decomposition of Variance .....	144
6.3.1 Closed Variance.....	145
6.3.2 Total-effect Variance.....	145
6.4 SOBOL Method .....	146
6.4.1 Basic Premise.....	147
6.4.2 Improved SOBOL Method .....	149
6.4.3 A “Less Expensive” SOBOL .....	153
6.5 Confidence Levels and Bias Correction.....	153
6.5.1 $BC_\alpha$ Confidence Level Intervals .....	155
6.5.2 Bias Correction .....	157
6.6 Example 1: SOBOL .....	157
6.7 Example 2: Temporal Analysis .....	160
6.8 Closing Remarks.....	161
7. IMPLEMENTATION OF NUMERICAL ANALYSIS TECHNIQUES.....	162
7.1 Introduction.....	162
7.2 Thermal Model Input Distributions .....	162
7.3 Model Evaluations .....	168

## TABLE OF CONTENTS – CONTINUED

7.4 Sensitivity Analysis.....	168
7.5 Monte Carlo Analysis .....	170
7.6 Highest Density Regions.....	170
7.7 Empirical Probability Density Functions .....	173
7.8 Goodness-of-fit Hypothesis Test.....	174
7.9 Closing Remarks.....	175
8. NUMERICAL ANALYSIS OF SURFACE HOAR .....	176
8.1 Introduction.....	176
8.2 Methods.....	177
8.3 Results: Sensitivity Analysis .....	178
8.3.1 Mean Mass-Flux, $\bar{\Phi}$ .....	178
8.3.2 Minimum and Maximum Mass-flux ( $\Phi^{min}$ and $\Phi^{max}$ ).....	180
8.3.3 Positive and Negative Mean Mass-flux ( $\bar{\Phi}_{pos}$ and $\bar{\Phi}_{neg}$ ) .....	182
8.4 Discussion: Sensitivity Analysis .....	186
8.5 Results and Discussion: Monte Carlo Simulations .....	188
8.6 Analysis: Comparison with Field Observations .....	191
8.7 Closing Remarks.....	199
9. SENSITIVITY ANALYSIS OF NEAR-SURFACE FACETS .....	202
9.1 Introduction.....	202
9.2 Methods.....	202
9.3 Results and Discussion.....	205
9.3.1 Snow Temperatures .....	205
Snow Surface Temperature.....	205
Snow Temperatures at Depth .....	211
9.3.2 Temperature Gradient .....	216
Gradient Computed at 2 cm.....	216
“Knee” Temperature Gradient.....	219
9.4 Closing Remarks.....	223
10. MONTE CARLO SIMULATIONS OF NEAR-SURFACE FACETS .....	225
10.1 Introduction .....	225
10.2 Methods.....	225
10.3 Results .....	228
10.4 Discussion .....	232
10.5 Analysis .....	234



## TABLE OF CONTENTS – CONTINUED

Control Location .....	237
North Location.....	238
South Location.....	239
10.6 Closing Remarks.....	241
11. CONCLUSIONS .....	243
REFERENCES CITED.....	247
APPENDICES .....	258
APPENDIX A: Yellowstone Club Weather Stations .....	259
APPENDIX B: YCweather User Manual .....	305
APPENDIX C: Thermal Model Software User Manual .....	343
APPENDIX D: Sensitivity Analysis Software User Manual .....	366
APPENDIX E: Sensitivity Analysis Results for Surface Hoar .....	391
APPENDIX F: Sensitivity Analysis Results for Near-Surface Facets .....	413
APPENDIX G: Yellowstone Club Daily Logs .....	468

## LIST OF TABLES

Table	Page
2.1 A summary of the conditions necessary for surface hoar growth as reported in the literature reviewed.....	16
2.2 A summary of the conditions necessary for near-surface facet growth as reported in the literature reviewed.....	22
2.3 Summary of quantifiable parameters shown to lead to the formation of (a) surface hoar and (b) near-surface facets as presented in the available literature.....	23
3.1 Detailed information on each of the three weather stations situated on Pioneer Mountain.....	26
3.2 Summary of mean nightly weather conditions for all days recorded as surface hoar events.....	28
3.3 Summary of the snow conditions for the layer underlying the surface hoar, as recorded in the field notes.....	28
3.4 Kolmogorov-Smirnov test results comparing the distributions set shown in Figures 3.31 and 3.30; the null hypothesis ( $H_0$ ) was that the data are from the same distribution.....	57
3.5 Percentiles of environmental variables coupled to the formation of surface hoar.....	58
4.1 Summary of snow conditions prior to the near-surface facet events as recorded in the field notes. Events tagged with an asterisk (*) indicate events, as noted in the field notes, that were likely dominated by non-radiation processes.....	64
4.2 Summary of mean daily weather conditions for all days recorded as near-surface facets events.....	65
4.3 Kolmogorov-Smirnov test results comparing the distribution sets shown in Figures 4.52 and 4.53; the null hypothesis ( $H_0$ ) was that the data were from the same distribution.....	109
4.4 Percentiles of environmental variables coupled to the observed formation of near-surface facets.....	110
5.1 List of constant variables utilized for computing the heat source term of Equation (5.30). .....	128

## LIST OF TABLES – CONTINUED

Table	Page
6.1 Matrix detailing the output vectors ( $\vec{a}$ ) used to compute the necessary sensitivity parameters. This table was adapted from Saltelli (2002) and should be used in conjunction with Equations (6.33) through (6.40). Note, the $j$ superscript is omitted for simplicity. ....	152
6.2 Improved SOBOL sensitivity indices, expresses as percentages, of Equation (6.51). ....	158
7.1 List of input parameters, their associated symbol, and index ( $i$ ) referenced in the analysis throughout Chapters 8–10. ....	163
7.2 Snow property uniform distribution parameters used for sensitivity analysis and Monte Carlo simulations. ....	165
7.3 Environmental input parameter distribution sets used for sensitivity analysis and Monte Carlo simulations; the coefficients (a, b, and c) correspond to the parameters provided in Equations (7.1)–(7.4). ....	166
8.1 List of input parameters, associated symbol, and reference index used in the analysis throughout this chapter. ....	178
8.2 Table summarizing the sensitivity analysis parameters for the Control location calculated from $\bar{\Phi}$ . ....	180
8.3 Summary of crystal size, long-wave radiation ( $LW$ ), and II observed surface hoar events at the North and South Stations. ....	192
8.4 Regions of mass-flux and expected surface hoar crystal size. ....	198
9.1 First-, second-, total-, and higher-order sensitivity indices for the South/ $KTG^{mid}$ results (see Table 7.1 for reference). ....	222
10.1 Summary of results from laboratory experiments conducted by Morstad <i>et al.</i> (2007) and Slaughter <i>et al.</i> (2009). ....	227
A.1 Detailed location information on each of the three weather stations situated on Pioneer Mountain. ....	260
A.2 List of output data from North and South weather stations. ....	263
A.3 Summary of the instrumentation utilized at each weather station during each winter season. ....	265

## LIST OF TABLES – CONTINUED

Table	Page
A.4 Summary of calibration constants of weather station sensors. The values inside the brackets give the serial number of the sensor and all calibration numbers are given as W/m <sup>2</sup> /mV. ....	268
A.5 Tabular wiring layout for North and South weather stations. ....	269
E.1 Control / Mass Flux with Time (Total-effect).....	393
E.2 Control / Mass Flux / Mid-day .....	393
E.3 South / Mass Flux with Time (Total-effect) .....	394
E.4 South / Mass Flux / Mid-day.....	394
E.5 North / Mass Flux with Time (Total-effect) .....	395
E.6 North / Mass Flux / Mid-day.....	395
E.7 Control / Mass Flux / Mean .....	396
E.8 South / Mass Flux / Mean.....	396
E.9 North / Mass Flux / Mean.....	396
E.10 Control / Positive Mass Flux with Time (Total-effect) .....	397
E.11 Control / Mass Flux / Positive Mid-day.....	397
E.12 South / Positive Mass Flux with Time (Total-effect).....	398
E.13 South / Mass Flux / Positive Mid-day .....	398
E.14 North / Positive Mass Flux with Time (Total-effect).....	399
E.15 North / Mass Flux / Positive Mid-day .....	399
E.16 Control / Mass Flux / Positive Mean.....	400
E.17 South / Mass Flux / Positive Mean .....	400
E.18 North / Mass Flux / Positive Mean .....	400
E.19 Control / Negative Mass Flux with Time (Total-effect) .....	401
E.20 Control / Mass Flux / Negative Mid-Day.....	401
E.21 South / Negative Mass Flux with Time (Total-effect) .....	402
E.22 South / Mass Flux / Negative Mid-Day .....	402

## LIST OF TABLES – CONTINUED

Table	Page
E.23 North / Negative Mass Flux with Time (Total-effect) .....	403
E.24 North / Mass Flux / Negative Mid-Day .....	403
E.25 Control / Mass Flux / Negative Mean .....	404
E.26 South / Mass Flux / Negative Mean .....	404
E.27 North / Mass Flux / Negative Mean .....	404
E.28 Control / Mass Flux / Maximum .....	405
E.29 South / Mass Flux / Maximum .....	405
E.30 North / Mass Flux / Maximum .....	405
E.31 Control / Mass Flux / Minimum .....	406
E.32 South / Mass Flux / Minimum .....	406
E.33 North / Mass Flux / Minimum .....	406
E.34 Control / Temp. at 0cm with Time (Total-effect) .....	407
E.35 Control / Temp. at 0cm / Mid-day .....	407
E.36 South / Temp. at 0cm with Time (Total-effect) .....	408
E.37 South / Temp. at 0cm / Mid-day .....	408
E.38 North / Temp. at 0cm with Time (Total-effect) .....	409
E.39 North / Temp. at 0cm / Mid-day .....	409
E.40 Control / Temp. at 0cm / Mean .....	410
E.41 South / Temp. at 0cm / Mean .....	410
E.42 North / Temp. at 0cm / Mean .....	410
E.43 Control / Temp. at 0cm / Maximum .....	411
E.44 South / Temp. at 0cm / Maximum .....	411
E.45 North / Temp. at 0cm / Maximum .....	411
E.46 Control / Temp. at 0cm / Minimum .....	412
E.47 South / Temp. at 0cm / Minimum .....	412

## LIST OF TABLES – CONTINUED

Table	Page
E.48 North / Temp. at 0cm / Minimum .....	412
F.1 Control / Temp. at 0cm with Time (Total-effect) .....	415
F.2 Control / Temp. at 0cm / Mid-day .....	415
F.3 South / Temp. at 0cm with Time (Total-effect).....	416
F.4 South / Temp. at 0cm / Mid-day .....	416
F.5 North / Temp. at 0cm with Time (Total-effect).....	417
F.6 North / Temp. at 0cm / Mid-day .....	417
F.7 Control / Temp. at 0cm / Mean.....	418
F.8 South / Temp. at 0cm / Mean .....	418
F.9 North / Temp. at 0cm / Mean .....	418
F.10 Control / Temp. at 0cm / Maximum .....	419
F.11 South / Temp. at 0cm / Maximum.....	419
F.12 North / Temp. at 0cm / Maximum.....	419
F.13 Control / Temp. at 0cm / Minimum.....	420
F.14 South / Temp. at 0cm / Minimum .....	420
F.15 North / Temp. at 0cm / Minimum .....	420
F.16 Control / Temp. at 2cm with Time (Total-effect) .....	421
F.17 Control / Temp. at 2cm / Mid-day .....	421
F.18 South / Temp. at 2cm with Time (Total-effect).....	422
F.19 South / Temp. at 2cm / Mid-day .....	422
F.20 North / Temp. at 2cm with Time (Total-effect).....	423
F.21 North / Temp. at 2cm / Mid-day .....	423
F.22 Control / Temp. at 2cm / Mean.....	424
F.23 South / Temp. at 2cm / Mean .....	424
F.24 North / Temp. at 2cm / Mean .....	424

## LIST OF TABLES – CONTINUED

Table	Page
F.25 Control / Temp. at 2cm / Maximum .....	425
F.26 South / Temp. at 2cm / Maximum.....	425
F.27 North / Temp. at 2cm / Maximum.....	425
F.28 Control / Temp. at 2cm / Minimum.....	426
F.29 South / Temp. at 2cm / Minimum .....	426
F.30 North / Temp. at 2cm / Minimum .....	426
F.31 Control / Temp. at 5cm with Time (Total-effect) .....	427
F.32 Control / Temp. at 5cm / Mid-day.....	427
F.33 South / Temp. at 5cm with Time (Total-effect).....	428
F.34 South / Temp. at 5cm / Mid-day .....	428
F.35 North / Temp. at 5cm with Time (Total-effect).....	429
F.36 North / Temp. at 5cm / Mid-day .....	429
F.37 Control / Temp. at 5cm / Mean.....	430
F.38 South / Temp. at 5cm / Mean .....	430
F.39 North / Temp. at 5cm / Mean .....	430
F.40 Control / Temp. at 5cm / Maximum .....	431
F.41 South / Temp. at 5cm / Maximum.....	431
F.42 North / Temp. at 5cm / Maximum.....	431
F.43 Control / Temp. at 5cm / Minimum.....	432
F.44 South / Temp. at 5cm / Minimum .....	432
F.45 North / Temp. at 5cm / Minimum .....	432
F.46 Control / Temp. at 8cm with Time (Total-effect) .....	433
F.47 Control / Temp. at 8cm / Mid-day.....	433
F.48 South / Temp. at 8cm with Time (Total-effect).....	434
F.49 South / Temp. at 8cm / Mid-day .....	434

## LIST OF TABLES – CONTINUED

Table	Page
F.50 North / Temp. at 8cm with Time (Total-effect).....	435
F.51 North / Temp. at 8cm / Mid-day .....	435
F.52 Control / Temp. at 8cm / Mean.....	436
F.53 South / Temp. at 8cm / Mean .....	436
F.54 North / Temp. at 8cm / Mean .....	436
F.55 Control / Temp. at 8cm / Maximum .....	437
F.56 South / Temp. at 8cm / Maximum.....	437
F.57 North / Temp. at 8cm / Maximum.....	437
F.58 Control / Temp. at 8cm / Minimum.....	438
F.59 South / Temp. at 8cm / Minimum .....	438
F.60 North / Temp. at 8cm / Minimum .....	438
F.61 Control / “Knee” Temp. with Time (Total-effect).....	439
F.62 Control / “Knee” Temp. / Mid-day .....	439
F.63 South / “Knee” Temp. with Time (Total-effect).....	440
F.64 South / “Knee” Temp. / Mid-day .....	440
F.65 North / “Knee” Temp. with Time (Total-effect).....	441
F.66 North / “Knee” Temp. / Mid-day .....	441
F.67 Control / “Knee” Temp. / Mean .....	442
F.68 South / “Knee” Temp. / Mean.....	442
F.69 North / “Knee” Temp. / Mean .....	442
F.70 Control / “Knee” Temp. / Maximum .....	443
F.71 South / “Knee” Temp. / Maximum.....	443
F.72 North / “Knee” Temp. / Maximum.....	443
F.73 Control / “Knee” Temp. / Minimum .....	444
F.74 South / “Knee” Temp. / Minimum.....	444



## LIST OF TABLES – CONTINUED

Table	Page
F.75 North / “Knee” Temp. / Minimum .....	444
F.76 Control / Temp. Gradient at 2cm with Time (Total-effect) .....	445
F.77 Control / Temp. Gradient at 2cm / Mid-day .....	445
F.78 South / Temp. Gradient at 2cm with Time (Total-effect) .....	446
F.79 South / Temp. Gradient at 2cm / Mid-day .....	446
F.80 North / Temp. Gradient at 2cm with Time (Total-effect) .....	447
F.81 North / Temp. Gradient at 2cm / Mid-day .....	447
F.82 Control / Temp. Gradient at 2cm / Mean .....	448
F.83 South / Temp. Gradient at 2cm / Mean .....	448
F.84 North / Temp. Gradient at 2cm / Mean .....	448
F.85 Control / Temp. Gradient at 2cm / Maximum .....	449
F.86 South / Temp. Gradient at 2cm / Maximum .....	449
F.87 North / Temp. Gradient at 2cm / Maximum .....	449
F.88 Control / Temp. Gradient at 2cm / Minimum .....	450
F.89 South / Temp. Gradient at 2cm / Minimum .....	450
F.90 North / Temp. Gradient at 2cm / Minimum .....	450
F.91 Control / Temp. Gradient at 5cm with Time (Total-effect) .....	451
F.92 Control / Temp. Gradient at 5cm / Mid-day .....	451
F.93 South / Temp. Gradient at 5cm with Time (Total-effect) .....	452
F.94 South / Temp. Gradient at 5cm / Mid-day .....	452
F.95 North / Temp. Gradient at 5cm with Time (Total-effect) .....	453
F.96 North / Temp. Gradient at 5cm / Mid-day .....	453
F.97 Control / Temp. Gradient at 5cm / Mean .....	454
F.98 South / Temp. Gradient at 5cm / Mean .....	454
F.99 North / Temp. Gradient at 5cm / Mean .....	454

## LIST OF TABLES – CONTINUED

Table	Page
F.100 Control / Temp. Gradient at 5cm / Maximum .....	455
F.101 South / Temp. Gradient at 5cm / Maximum.....	455
F.102 North / Temp. Gradient at 5cm / Maximum.....	455
F.103 Control / Temp. Gradient at 5cm / Minimum.....	456
F.104 South / Temp. Gradient at 5cm / Minimum .....	456
F.105 North / Temp. Gradient at 5cm / Minimum .....	456
F.106 Control / Temp. Gradient at 8cm with Time (Total-effect) .....	457
F.107 Control / Temp. Gradient at 8cm / Mid-day.....	457
F.108 South / Temp. Gradient at 8cm with Time (Total-effect).....	458
F.109 South / Temp. Gradient at 8cm / Mid-day .....	458
F.110 North / Temp. Gradient at 8cm with Time (Total-effect).....	459
F.111 North / Temp. Gradient at 8cm / Mid-day .....	459
F.112 Control / Temp. Gradient at 8cm / Mean.....	460
F.113 South / Temp. Gradient at 8cm / Mean .....	460
F.114 North / Temp. Gradient at 8cm / Mean .....	460
F.115 Control / Temp. Gradient at 8cm / Maximum .....	461
F.116 South / Temp. Gradient at 8cm / Maximum.....	461
F.117 North / Temp. Gradient at 8cm / Maximum.....	461
F.118 Control / Temp. Gradient at 8cm / Minimum.....	462
F.119 South / Temp. Gradient at 8cm / Minimum .....	462
F.120 North / Temp. Gradient at 8cm / Minimum .....	462
F.121 Control / “Knee” Temp. Gradient with Time (Total-effect).....	463
F.122 Control / “Knee” Temp. Gradient / Mid-day .....	463
F.123 South / “Knee” Temp. Gradient with Time (Total-effect).....	464
F.124 South / “Knee” Temp. Gradient / Mid-day .....	464

## LIST OF TABLES – CONTINUED

Table	Page
F.125 North / “Knee” Temp. Gradient with Time (Total-effect) .....	465
F.126 North / “Knee” Temp. Gradient / Mid-day .....	465
F.127 Control / “Knee” Temp. Gradient / Mean .....	466
F.128 South / “Knee” Temp. Gradient / Mean.....	466
F.129 North / “Knee” Temp. Gradient / Mean .....	466
F.130 Control / “Knee” Temp. Gradient / Maximum .....	467
F.131 South / “Knee” Temp. Gradient / Maximum .....	467
F.132 North / “Knee” Temp. Gradient / Maximum.....	467

## LIST OF FIGURES

Figure	Page
2.1 Example images of (a) surface hoar (Cooperstein <i>et al.</i> , 2004) and (b) near-surface faceted snow crystals (Morstad, 2004). .....	9
3.1 Image from event A-1 of surface hoar (1 mm grid) captured from the North Station on January 24, 2008. ....	29
3.2 Weather data for event A-1 (January 24, 2008) recorded for both the (a,b) North and (c,d) South weather stations.....	30
3.3 Image from event A-2 of surface hoar (1 mm grid) captured from the North Station on February 15, 2008. ....	31
3.4 Weather data for event A-2 (February 15, 2008) recorded for a the North weather Station. ....	32
3.5 Images from event A-3 of surface hoar captured from the (a) North and (b) South Stations on February 19, 2008 and surface hoar from the (c) South Station that was recorded on February 20.....	33
3.6 North Station weather data for event A-3 (February 19–21, 2008).....	34
3.7 South Station weather data for event A-3 (February 19–21, 2008).....	35
3.8 Images from event A-4 of surface hoar captured from the (a) North and (b) South Stations on February 22, 2008 and at the (c) North station the following day after the surface hoar was buried by new snow. ....	36
3.9 Weather data for event A-4 (February 22, 2008) for both the (a,b) North and (c,d) South weather stations. ....	37
3.10 Images from event A-5 of surface hoar captured from the (a) North and (b) South Stations on February 26, 2008. ....	38
3.11 Weather data for event A-4 (February 26, 2008) for both the (a,b) North and (c,d) South weather stations. ....	39
3.12 Images from event A-6 of surface hoar captured from the (a) North and (b) South Stations on March 10, 2008. ....	40
3.13 Weather data for event A-6 (March 10, 2008) for both the (a,b) North and (c,d) South weather stations. ....	41
3.14 Images from event A-7 of surface hoar captured from the (a) North and (b) South Stations on March 30, 2008. ....	42

## LIST OF FIGURES – CONTINUED

Figure	Page
3.15 Weather data for event A-7 (March 30, 2008) for both the (a,b) North and (c,d) South weather stations. ....	43
3.16 Images from event B-1 of surface hoar (2 mm grid) captured from the North Station on January 23, 2009. ....	44
3.17 North Station weather data for event B-1 (January 23, 2009). ....	45
3.18 Images from event B-2 of surface hoar captured from the (a) North and (b) South Stations on January 30, 2009 and the (c) North Station on January 31, 2009. ....	46
3.19 North Station weather data for event B-2 (January 30–31, 2009). ....	47
3.20 Images from event B-3 of surface hoar captured from the (a) North and (b) South Stations on February 4 and (c) the North Station on February 5, 2009. ....	48
3.21 North Station weather data for event B-3 (February 4, 2008). ....	49
3.22 Images from event B-4 of surface hoar captured from the North and South Stations on (a) February 7 and (b,c) 8, 2009. ....	50
3.23 South Station weather data for event B-4 (February 7, 2009). ....	50
3.24 Images from event B-5 of surface hoar captured from the North Station on (a) February 13 and (b) 14, 2009. ....	51
3.25 North Station weather data for event B-5 (February 13–14, 2009). ....	52
3.26 Images from event B-6 of surface hoar captured from the North Station on February 28, 2009. ....	53
3.27 North Station weather data for event B-6 (February 28, 2009). ....	53
3.28 Images from event B-7 of surface hoar captured from the North Station on March 13, 2009. ....	54
3.29 Weather data for event B-7 (March 13, 2009) for the North Station. ....	54
3.30 Histogram comparing the daily average air/snow temperature difference for the entire season (all data), along with the days associated with surface hoar events at either the North or South Stations. ....	55

## LIST OF FIGURES – CONTINUED

Figure	Page
3.31 Histograms comparing the frequency of recorded daily average weather conditions at both the North and South Stations (all data), along with the days associated with surface hoar events observed at the North or South Stations.....	56
4.1 Recorded short- and long-wave radiation at the Aspirit Station as well as the air and snow surface temperatures at the South Station for January 21–22, 2008 (C-1). .....	67
4.2 Four images of a near-surface facet event at the South Station on February 14, 2008 (C-2): (a) initial observation (1100) at the South Station, (b) second observation (1400) at the South Station, (c) observations at a near-by south facing slope, and (d) following day (Feb. 15) South Station observation (1100). .....	68
4.3 Recorded short- and long-wave radiation at the Aspirit Station as well as the air and snow surface temperatures at the South Station for February 14–16, 2008 (C-3). .....	69
4.4 Facets formed on February 14, 2008 at the South Station that persisted through warmer temperatures and new snow until February 16 <sup>th</sup> . .....	69
4.5 Images of near-surface facets at the South station described as diurnal recrystallization., that formed on February 18–20, 2008 (C-3). .....	70
4.6 Graph of air temperature and snow surface temperature at the South Station on February 17–20, 2008 (C-3). .....	71
4.7 Images taken at the South Station of (a) surface hoar formed the day prior to the (b) near-surface facets that formed on February 27, 2008 (C-4) and persisted through (c) the following day. ....	73
4.8 Recorded short- and long-wave radiation at the Aspirit Station as well as the air and snow surface temperatures at the South Station on February 26–28, 2008 (C-4). .....	74
4.9 Snow temperature profiles from February 26, 2008 (C-4) at the South Station.....	74
4.10 Images from March 6, 2008 (C-5) near-surface facet event at the South Station: (a) initial observation at 1100 and (b) second observation at 1330. 75	

## LIST OF FIGURES – CONTINUED

Figure	Page
4.11 Image of near-surface facets observed on March 10, 2008 (C-6) at the South Station. ....	76
4.12 Recorded short- and long-wave radiation at the Aspirit station (C-6) as well as the air and snow surface temperatures at the South station for March 10, 2008. ....	77
4.13 Recorded short- and long-wave radiation at the Aspirit Station as well as the air and snow surface temperatures at the South Station on March 12–13, 2008 (C-7). ....	78
4.14 Images taken at the South Station during the (a) March 15, 2008 (C-8) near-surface facet event; this layer persisted the following two days (b and c). ....	79
4.15 Recorded short- and long-wave radiation at the Aspirit Station as well as the air and snow surface temperatures at the South Station on March 15–17, 2008 (C-8). ....	80
4.16 Recorded short- and long-wave radiation at the Aspirit Station as well as the air and snow surface temperatures at the South Station on March 19, 2008 (C-9). ....	80
4.17 Images from the (a) March 22, 2008 (C-10) near-surface facet event at the South Station and (b) facets that persisted through the following day. .	81
4.18 Recorded short- and long-wave radiation at the Aspirit Station as well as the air and snow surface temperatures at the South Station for March 22–24, 2008 (C-10). ....	82
4.19 Recorded short- and long-wave radiation at the Aspirit Station as well as the air and snow surface temperatures at the South Station, on March 28, 2008 (C-11). ....	83
4.20 Recorded short- and long-wave radiation at the Aspirit Station as well as the air and snow surface temperatures at the South Station on March 30, 2008 (C-12). ....	84
4.21 Image of near-surface facets formed on March 30, 2008 (C-12) at the South Station. ....	84
4.22 Images of surface snow at (a) 1130 and (b) 1430 at the South Station on April 3, 2008 (C-13) showing formation of near-surface facets . ....	85

## LIST OF FIGURES – CONTINUED

Figure	Page
4.23 Recorded short- and long-wave radiation at the Aspirit Station, as well as the air and snow surface temperatures at the South Station, on April 2–4, 2008 (C-13). . . . .	86
4.24 Images of surface snow at (a) 1030 and (b) 1430 on April 6, 2008 (C-14) showing formation of near-surface facets at the South Station. . . . .	87
4.25 Recorded short- and long-wave radiation at the Aspirit station, as well as the air and snow surface temperatures at the South Station, on April 6, 2008 (C-14). . . . .	87
4.26 Recorded short- and long-wave radiation at the Aspirit station as well as the air and snow surface temperatures at the South station for April 8–9, 2008. . . . .	88
4.27 Image near-surface facets formed on April 8, 2008. . . . .	89
4.28 Image of near-surface facets formed (a) at the South Station on February 4, 2009 (D-1) ; the facets persisted through the night and were also observed (b) on Feb. 5. . . . .	90
4.29 Recorded weather data from the South Station on February 4, 2009 (D-1); due to instrumentation malfunctions the data prior to 1200 on Feb. 4 was not recorded. . . . .	90
4.30 Images of a near-surface facet event that occurred on February 8, 2009 (D-2) at the South Station. Images include facets observed (a) at the initial observation, (b and c) at the second observation, and (d) the following day despite being buried underneath new snow. . . . .	91
4.31 Recorded weather data from the South Station on February 8, 2009 (D-2).. 92	92
4.32 Images of near-surface facet event that occurred at the South Station on (a,b) February 12, 2009 (D-3) and that continued on (c) Feb. 13 and (d) 14.93	93
4.33 Recorded weather data from the South Station on February 12–14, 2009 (D-3). . . . .	94
4.34 Images of a near-surface facet event (D-3) that occurred at the South Station and persisted beneath 9 cm of new snow falling on the night of Feb. 14. . . . .	94
4.35 Image of near-surface facets observed at the South Station on February 19, 2009 (D-4). . . . .	95



## LIST OF FIGURES – CONTINUED

Figure	Page
4.36 Recorded weather data from the South Station on February 19, 2009 (D-4).	95
4.37 Recorded weather data from the South and North stations on February 21, 2009 (D-5). .....	96
4.38 Images of near-surface facets on February 21, 2009 (D-5) that formed small-faceted crystals at both the South and North Stations.....	97
4.39 Recorded weather data from the South Station on February 27–28, 2009 (D-6). .....	98
4.40 Images of radiation-recrystallized near-surface facets from Event D-6 that formed at the South Station on (a,b) February 27 and (c,d) 28, 2009. ....	99
4.41 Images of a near-surface facet event that occurred at the South Station on March, 7 2009 (D-7).....	100
4.42 Recorded weather data from the South Station on March 7, 2009 (D-7). ..	100
4.43 Recorded weather data from the South Station on March 12–14, 2009 (D-8). .....	101
4.44 Images of event a near-surface facet event (D-8) that occurred on three consecutive days (March 12–14, 2009) at the South Station. ....	103
4.45 Images of large near-surface facets captured at the South Station during the second observation (1440) on March 14, 2009 (D-8).....	104
4.46 Recorded weather data from the South Station on March 20, 2009 (D-9)..	105
4.47 Image of slight faceting that occurred at the South Station on March, 20 2009 (D-9).....	105
4.48 Images from two observations—(a) 1130 and (b) 1315—of a near-surface facet event that occurred at the South Station on March, 30 2009 (D-9)...	106
4.49 Recorded weather data from the South Station on March 30, 2009 (D-10).	106
4.50 Image from near-surface facet event that occurred at the South Station on April 6, 2009 (D-11). .....	107
4.51 Recorded weather data from the South Station on April 6, 2009 (D-11). ..	108
4.52 Histograms comparing daily average radiation conditions for the entire data set (2007/2008 and 2008/2009 seasons) against the days associated with near-surface facet events. ....	112

## LIST OF FIGURES – CONTINUED

Figure	Page
4.53 Histograms comparing the daily average weather conditions—(a) air temperature, (b) snow surface temperature, (c) wind speed, (d) wind direction, and (e) relative humidity—for the entire data set (2007/2008 and 2008/2009 seasons ) against the days associated with near-surface facet events at the South Station. ....	113
5.1 Schematic of the arbitrary control volume ( $CV$ ) enclosed by the control surface ( $CS$ ).....	119
5.2 Schematic of snowpack layering utilized for numerical solution of snow temperatures with time. The superscript $j$ represents the $j$ -th time step and the subscript $i$ represents the layer number. ....	122
5.3 Schematic that demonstrates the application of short-wave attenuation in a layered snowpack. ....	127
5.4 Example of temperature differences observed by differing application of the Neumann boundary condition. ....	131
5.5 Resulting output distributions—(a) snow surface temperature and (b) temperature gradient—from the Monte Carlo simulations.....	132
5.6 Comparison between six model evaluations with varying irradiation inputs.	136
5.7 Graphs demonstrating the model behavior with respect to measurement error including (a) a contour plot of the largest deviation from the input evaluation and (b) 90% confidence intervals with input evaluation and measured values.....	138
6.1 Results from the SOBOL sensitivity analysis of Equation (6.51), including the first-order ( $S_i$ ) and total-effect sensitivity ( $S_{T_i}$ ) terms. (The error bars reflect the 90% confidence intervals.) ....	158
6.2 First- and second-order indices for the first input parameter ( $x_1$ ) from analysis of Equation (6.51). ....	160
6.3 Stacked area plot of the time-dependent total-effect indices resulting from the analysis of Equation (6.52). ....	161
7.1 Probability distribution functions for input data based on measured data.	167
7.2 Comparison of 3-D representations of (a) the raw data as a scatter plot and (b) the data encapsulated by 5% (inner), 50% (middle), and 95% (outer) HDRs. ....	172

## LIST OF FIGURES – CONTINUED

Figure	Page
7.3 The (a) bi-variate probability density function was constructed from the raw data points shown in sub-figure b; the probability distribution was then sliced such that 95% of raw data had a probability density greater than this value resulting in a highest density region trace also shown in sub-figure b. ....	172
7.4 Example of tri-variate data analysis including (a) a 3-D scatter plot of raw data, (b) a 3-D 95% HDR, (c) 2-D HDRs encapsulating specific bands of $\Psi$ , and (d) the 10%, 50%, 90%, and 95% HDRs of complete data set (the number of data points used to construct each region is included in the parenthesis). ....	174
8.1 Total-effect indices for $\bar{\Phi}$ for each of the three locations considered, see Table 8.1 for reference. ....	179
8.2 Total-effect indices for (a) $\Phi^{min}$ and (b) $\Phi^{max}$ for each of the three locations considered (see Table 8.1 for reference). ....	181
8.3 Total-effect indices for (a) $\bar{\Phi}_{neg}$ and (b) $\bar{\Phi}_{pos}$ for each of the three locations considered (see Table 8.1 for reference). ....	182
8.4 First-, second- and higher-order indices for $\bar{\Phi}_{pos}$ for control location and each of the four important inputs: $LW(6)$ , $V_w(9)$ , $T_a(10)$ , and $RH(11)$ (see Table 8.1 for reference). The higher-order interactions for these terms are provided in the $S_h$ grouping. ....	184
8.5 First-, second- and higher-order indices for $\bar{\Phi}_{pos}$ for North location and each of the four important inputs: $\rho(1)$ , $T_s^{int}(4)$ , $LW(6)$ , $V_w(9)$ , $T_a(10)$ , and $RH(11)$ (see Table 8.1 for reference). The higher-order interactions for these terms are provided in the $S_h$ grouping. ....	185
8.6 First-, second- and higher-order indices for $\bar{\Phi}_{pos}$ for South location and each of the six important inputs: $\rho(1)$ , $T_s^{int}(4)$ , $LW(6)$ , $V_w(9)$ , $T_a(10)$ , and $RH(11)$ (see Table 8.1 for reference). The higher-order interactions for these terms are provided in the $S_h$ grouping. ....	186
8.7 Highest density regions (95%) comparing Monte Carlo simulation results for $LW(6)$ and $\Pi$ for (a) all values with $T_a < 0$ and (b) $\bar{\Phi}_{SH}$ . ....	190
8.8 Highest density regions (95%) comparing the complete set (All) of Monte Carlo simulation results to the data limited to surface hoar formation (SH) for the (a) Control, (b) North, and (c) South locations. ....	191

## LIST OF FIGURES – CONTINUED

Figure	Page
8.9 Comparison of Control/ $\bar{\Phi}_{SH}$ highest density regions with field observations from the North- and South-facing stations.....	193
8.10 Comparison of 99% (outer) and 50% (inner) HDRs for the Control/ $\bar{\Phi}_{SH}$ results and all recorded field data with the field observations from the North- and South-facing stations. ....	194
8.11 Comparison of 99% (outer) and 50% (inner) HDRs for the $\bar{\Phi}_{SH}$ results and all recorded field data with the field observations from the (a) South- and (b) North-facing stations.....	196
8.12 Comparison of North/ $\bar{\Phi}_{SH}$ highest density regions with field observations from the North-facing station. ....	197
8.13 Highest density regions based on the North location and various mass-flux rates. ....	199
9.1 Schematic of “knee” temperature profile and related sensitivity analysis output parameters. ....	204
9.2 Stacked area charts of normalized total-effect sensitivity ( $S_T^*$ ) for $T_0(t)$ for the (a) Control, (b) North, and (c) South locations. The regions are stacked from bottom to top in order as listed in Table 7.1. ....	206
9.3 Total-effect sensitivity indices for the Control, South, and North locations for (a) $\bar{T}_0$ , (b) $T_0^{max}$ , and (c) $T_0^{mid}$ (see Table 7.1 for reference).....	208
9.4 First-, second-, and higher-order indices for (a) the South/ $T_0^{mid}$ sensitivity analysis and (b) a zoomed view focusing on $\alpha(8)$ (see Table 7.1 for reference). ....	209
9.5 First-, second-, and higher-order indices for the (a) Control/ $T_0^{mid}$ and (b) North/ $T_0^{mid}$ sensitivity analysis (see Table 7.1 for reference). ....	211
9.6 Stacked area charts of normalized total-effect sensitivity as a function of model evaluation time at the (a) “knee”, (b) 2 cm, (c) 5 cm, and (d) 8 cm depth for the South locations. The regions are stacked from bottom to top in order as listed in Table 7.1. ....	212
9.7 Stacked area charts of normalized total-effect sensitivity as a function of model evaluation time at the 2 cm depth for the (a) Control and (b) North locations. The regions are stacked from top to bottom in order as listed in Table 7.1 (see Table 7.1 for reference).....	213

## LIST OF FIGURES – CONTINUED

Figure	Page
9.8 Total-effect sensitivity indices for the Control, South, and North locations for $TK^{mid}$ (see Table 7.1 for reference).....	214
9.9 First-, second-, and higher-order indices for $TK^{mid}$ sensitivity analysis for the (a) Control, (b) North, and (c) South locations (see Table 7.1 for reference).....	215
9.10 Stacked area charts of normalized total-effect sensitivity of $TG2(t)$ for the (a) Control, (b) North, and (c) South locations and (d) the total-effect indices computed from $TG2^{mid}$ output. The regions are stacked from bottom to top in order as listed in Table 7.1.....	217
9.11 Contour plots of snow temperature with incoming short-wave radiation of (a) 300 W/m <sup>2</sup> and (b) 400 W/m <sup>2</sup> . (see Table 7.1 for reference) .....	218
9.12 First-, second-, and higher-order indices for $TG2^{mid}$ sensitivity analysis for the South location, which highlights the overwhelming importance of higher-order interactions. (see Table 7.1 for reference).....	219
9.13 Stacked area charts of normalized total-effect sensitivity of $KTG(t)$ for the (a) Control, (b) North, and (c) South locations. The regions are stacked from bottom to top in order as listed in Table 7.1.....	220
9.14 Grouped bar charts of total-effect sensitivity for $KTG^{mid}$ for all three locations. (see Table 7.1 for reference) .....	221
9.15 First-, second-, and higher-order indices for $KTG^{mid}$ sensitivity analysis for the (a) Control and (b) North locations. (see Table 7.1 for reference) .	221
10.1 Comparison between the two seasons (2007/2008 and 2008/2009) of recorded long-wave radiation values for near-surface facet events.....	229
10.2 Probability distribution functions for snow properties including the complete (all) input distribution and data limited by $KTG^{mid}$ from 200–600 °C/m (limited) . Table 7.1 (p. 163) defines the variables and the units for each graph. ....	231
10.3 Probability distribution functions for radiation inputs including the complete (all) input distribution and data limited by $KTG^{mid}$ from 200–600 °C/m (limited) . Table 7.1 (p. 163) defines the variables and the units for each graph. ....	232

## LIST OF FIGURES – CONTINUED

Figure	Page
10.4 Comparison of the complete input (A) with the input limited by $KTG^{mid}$ from 200–600°C/m (B) for the (a) Control, (b) North, and (c) South locations. ....	235
10.5 Comparison of tri-variate PDF of all input (A) with the input limited by $KTG^{mid}$ from 200–600°C/m (B) for the South location. ....	236
10.6 Contour plot of HDRs for the Control results including the field observations from Chapter 4 and laboratory data of Morstad <i>et al.</i> (2007) and Slaughter <i>et al.</i> (2009). ....	238
10.7 Contour plot of HDRs for the North location including the field observations from Chapter 4 and laboratory data of Morstad <i>et al.</i> (2007) and Slaughter <i>et al.</i> (2009). ....	239
10.8 Contour plot of HDRs for the South location including the field observations from Chapter 4 and laboratory data of Morstad <i>et al.</i> (2007) and Slaughter <i>et al.</i> (2009). ....	240
10.9 Chart showing the relationship of $\rho$ , $k$ , and $\gamma$ as well as two commonly utilized $\rho$ and $k$ relationships as presented by Sturm <i>et al.</i> (1997). ....	241
A.1 Google Earth images of Pioneer Mountain showing the locations of (a) the South and (b) the North and American Spirit weather stations. ....	261
A.2 Wiring schematic for North and South weather stations. ....	267
A.3 Comparison of incoming short-wave radiation at the Yellow Mule RAWS and Aspirit weather stations. ....	279
B.1 YCweather Program Control window. ....	308
B.2 Example of the Data List window. ....	310
B.3 Example graph showing dual-axis capabilities. ....	311
B.4 Example of a YCweather workspace. ....	317
B.5 Prompt that appears by default when opening a workspace. ....	318
B.6 YCweather preferences window. ....	320
B.7 Example of the image viewer for YCweather. ....	323
B.8 Examples of the daily log options available in YCweather. ....	325

## LIST OF FIGURES – CONTINUED

Figure	Page
B.9 Program Control with all side panels showing.....	326
B.10 Example workspace showing a graph of thermocouple data.....	327
B.11 (a) RadTherm/RT file exporter and (b) an example output file. ....	330
B.12 Example of file structure of the database directory used by YCweather. ...	334
B.13 Example format file utilized by YCweather. ....	335
B.14 Example format file utilized by YCweather that includes the thermo- couple ID for plotting temperature profile data (this is not a complete file).....	337
B.15 Example entries for prescribing units within the <code>units.txt</code> file, which is utilized by the <code>getunit.m</code> function. ....	340
C.1 Flow chart demonstrating how the various functions discussed in Section C.2 and C.3 interact. ....	345
C.2 Example of the (a) “SnowProperties” and (b) “AtmosphericSettings” worksheets for Excel file read by <code>xls_input.m</code> . ....	348
C.3 Example of the “Constants” worksheets for Excel file read by <code>xls_input.m</code> .	349
C.4 MATLAB implementation of <code>runmodel.m</code> and the resulting data structure.	350
C.5 Required data structure of <code>albedo.mat</code> .....	352
C.6 Graphical user interface for implementing the snow thermal model. ....	354
C.7 Example graphs of snowpack temperatures demonstrated the two graph- ing options available: (a) profiles and (b) contours.....	356
C.8 Example graphs of snowpack temperature demonstrated the two graphing options available for displaying confidence level intervals: (a) C.I. profiles and (b) C.I. contours. ....	357
D.1 Flow chart of the main sensitivity analysis function <code>sobol.m</code> and associ- ated sub functions.....	370
D.2 MATLAB code for <code>saFANG.m</code> function.....	371
D.3 MATLAB code for <code>saG.m</code> function. ....	371
D.4 Syntax for implementation of <code>saMODEL2.m</code> .....	374

## LIST OF FIGURES – CONTINUED

Figure	Page
D.5 MATLAB code demonstrating the definition of the input *.mat files for the saMODEL2.m function. ....	375



## NOMENCLATURE

Variables

<i>Variable(s)</i>	<i>Description</i>
$\vec{a}^j$	Sensitivity analysis vectors of for the $j$ th model output vectors, Eq. (6.32)
$\widehat{acc}$	Acceleration of bootstrap confidence level intervals, Eq. (6.48)
$a, b, c, d$	Coefficients for numeral solution of heat equation (Eq. (5.18)); coefficients of probability density functions (Sec. 7.2)
$\underline{b}$	Arbitrary vector used in Gauss' theorem, Eq. (5.6)
$B$	Number of bootstrap re-samplings (Sec. 6.5)
$bias_B$	Bootstrap-computed estimate of bias, Eq. (6.50a)
$C$	Number of computations required for SOBOL method (Chap. 6)
$c_p, c_{pa}$	Specific heat capacity of snow and air, respectively
$CS$	Control surface, Fig. 5.1
$CV$	Control volume, Fig. 5.1
$e_a, e_s$	Water-vapor pressure above and at the snow surface, respectively (Sec. 5.3.5)
$e_0$	Reference vapor pressure, Tab. 5.1
$E$	Internal energy, Eq. (5.1)
$E(y^j)$	Expected value of the $j$ th output parameter (Chap. 6)
$Ec$	Eckert number (Sec. 8.4)
$h$	Specific heat supply (Sec. 5.3.1)

<i>Variable(s)</i>	<i>Description</i>
$\mathbf{k}$	Thermal conductivity tensor (Chap. 6)
$k$	Thermal conductivity scalar (Chapter 5); shape parameter for generalized extreme value and generalized Pareto distributions (Sec. 7.2)
$K_e, K_h$	Transfer coefficients for latent and sensible heat equations, Tab. 5.1
$KE$	Kinetic energy, Eq. (5.1)
$K$	Number of Monte Carlo simulations for SOBOL method (Chap. 6)
$L_s$	Latent heat of sublimation phase change, Tab. 5.1
$LW, LW^a$	Incoming long-wave radiation, the superscript $a$ (Tab. 4.2) denotes the American Spirit Station
$M_a, M_v$	Dry-air and water-vapor molecular weights, respectively, Tab. 5.1
$m$	Number of output parameters for SOBOL analysis (Chap. 6)
$n$	Number of input parameters for SOBOL analysis (Chap. 6)
$\hat{n}$	Outward normal vector of the control surface, Fig. 5.1
$N$	Matrix of inputs for computing SOBOL output vectors (Chap. 6)
$N_b$	Number of bootstrap estimates greater than the test statistic (Sec. 6.5)
$p$	The $p$ -value test statistic for goodness-of-fit (Sec. 7.8)
$p_i$	Probability density function of $i$ th SOBOL input parameter, Eq. (6.3)
$P$	Composite probability density function of all inputs, Eq. (6.3)

<i>Variable(s)</i>	<i>Description</i>
$P_{atm}$	Atmospheric pressure, Eq. (5.34)
$\vec{q}$	Weighting function vector for use in the $g$ -function for sensitivity analysis example (Sec. 6.6)
$\underline{q}$	Heat flux vector across the control surface, Fig. 5.1
$q_i$	Short-wave heat flux (Chap. 5)
$q_{VIS_i}$	Short-wave heat flux in visible wavebands (Chap. 5)
$q_{NIR_i}$	Short-wave heat flux in near-infrared wavebands (Chap. 5)
$q_s$	Heat flux at the snow surface (Chap. 5)
$q_{LW}$	Long-wave heat flux, Eq. (5.31)
$q_e, q_h$	Latent and sensible heat flux, respectively (Sec. 5.3.5)
$R$	Rate of heat input, Eq. (5.1)
$R_a$	Specific gas constant for air, Tab. 5.1
$R_v$	Specific gas constant for water vapor, Tab. 5.1
$RH$	Relative humidity
$S_h$	Higher-order sensitivity analysis index
$S_i, S_{i,l}$	First- and second-order sensitivity indices (Chaps. 8 and 9), an alternate representation of the following term
$S_i^j, S_{il}^j$	First- and second-order sensitivity indices with respect to the $j$ th output parameter (Chap. 6)
$S_i^T$	Total-effect sensitivity index (Chaps. 7–10), an alternate representation of the following term

<i>Variable(s)</i>	<i>Description</i>
$S_{T_i}^j$	Total-effect sensitivity with respect to the $j$ th output parameter (Chap. 6)
$S_T^*$	Normalized total-effect sensitivity index (Sec. 6.7 and Chap. 9)
$S_{T_i}^{j*}$	Normalized total-effect sensitivity index with respect to $j$ th output parameter (Sec. 6.7)
$SW$	Incoming short-wave radiation
$t$	Time
$T$	Temperature
$T_a, T_s$	Air and snow surface temperature, respectively
$T_s^{int}$	Initial snow temperature at the start of thermal model evaluations (Chaps. 7–10)
$T_0$	Reference temperature, Tab. 5.1
$T_0, T_2, T_5, T_8$	Modeled snow temperatures at 0, 2, 5, and 8 cm depths, respectively (Chap. 10)
$TK$	Modeled snow temperature at the “knee” location (Chap. 10)
$TG_2, TG_5, TG_8$	Modeled snow temperature gradients between the snow surface and 2, 5, and 8 cm depths, respectively (Chap. 10)
$KTG$	Modeled snow temperature gradient between the surface and the “knee” temperature (Chap. 10)
$\vec{u}$	A subsample vector of the input vector $\vec{x}$ (Sec. 6.4)
$U_i^j$	A parameters used to defined the sensitivity $S_i^j$ (Chap. 6)
$\hat{U}_i^{jc}, \hat{U}_{-i}^{jc}, \hat{U}_{il}^{jc}$	Estimates of the “closed” $U$ -terms for computation of sensitivity indices (Chap. 6)

<i>Variable(s)</i>	<i>Description</i>
$\vec{v}$	A subsample vector of the input vector $\vec{x}$ (Sec. 6.4)
$V^j$	Total variance of $j$ th output parameter (Chap. 6)
$V_i^j, V_{il}^j$	First- and second-order partial variance of $i$ th input parameter with respect to the $j$ th output parameter (Chap. 6)
$V_i^{jc}, V_{il}^{jc}$	“Closed” first- and second-order partial variance with respect to the $j$ th output parameter (Chap. 6)
$V_{T_i}^j$	Total-effect variance with respect to the $j$ th output parameter (Chap. 6)
$V_w$	Wind velocity
$W$	Rate of work acting on the system, Eq. (5.1)
$W, W'$	Replicates of the Monte Carlo input matrices used for computing $N$ (Eq. (6.29))
$\vec{x}$	Vector of input parameters, where $\vec{x} = x_i \mid i = 1, 2, \dots, n$ (Chap. 6)
$\vec{x}^{*b}$	The $b$ th bootstrap re-sampling of input parameters of $\vec{x}$ (Sec. 6.5)
$\vec{y}$	Vector of output parameters, where $\vec{y} = y^j \mid j = 1, 2, \dots, m$ (Chap. 6)
$z$	Distance (Chap. 5)
$\hat{z}_0$	An estimate of bias for computing bootstrap confidence levels (Sec. 6.5)
$z^\alpha, z^{1-\alpha}$	Standard normal percentiles for computing bootstrap confidence levels (Sec. 6.5)
$\alpha$	Snow albedo; shape parameter (Eq. (7.3)) for Weibull distribution

<i>Variable(s)</i>	<i>Description</i>
$\alpha^{hi}, \alpha^{lo}$	Upper and lower percentiles for computation of bootstrap confidence intervals (Sec. 6.5)
$\beta$	Scale parameter for Weibull distribution, Eq. (7.3)
$\gamma$	location parameter for Weibull and lognormal distribution (Eq. (7.3) and (7.4)); thermal diffusivity (Chap. 10)
$\Delta T$	Difference between the air and snow temperature (Chap. 3)
$\varepsilon$	Emissivity of snow
$\hat{\theta}$	Test statistic (Sec. 6.5)
$\hat{\theta}^{*b}$	Test statistic computed from bootstrap re-samplings (Sec. 6.5)
$\hat{\theta}_{(r)}$	The $r$ th jackknife statistic (Sec. 6.5)
$\hat{\theta}_{(\cdot)}$	The sum of the jackknife statistics (Sec. 6.5)
$\hat{\theta}_{(\cdot)}^{*b}$	Mean of the bootstrap estimates of the test statistic (Sec. 6.5)
$\vartheta$	Specific internal energy (Sec. 5.3.1)
$\kappa$	Extinction coefficient for snow
$\mu$	Location parameter for generalized extreme value and generalized Pareto distributions; continuous shape parameter of lognormal distribution (Sec. 7.2)
$\Pi$	Dimensionless parameter, Eq. (8.2)
$\Pi_1, \Pi_2$	Arbitrary terms utilized in highest density region examples (Sec. 7.6)
$\rho, \rho_a$	Density of snow and air, respectively

<i>Variable(s)</i>	<i>Description</i>
$\sigma$	Scale parameter for generalized extreme value and generalize Pareto distributions (Sec. 7.2); continuous shape parameter for lognormal distribution (Sec. 7.2); standard deviation (Chap. 10)
$\Phi$	Standard normal distribution (Sec. 6.5); mass-flux at the snow surface (Chap. 8)
$\Psi$	Arbitrary term utilized in highest density region examples (Sec. 7.6)
$\Omega$	Dimensionless parameter, Eq. (10.3)
$\vec{\nabla}$	Del vector operator (Sec. 5.3.1)

### Indices

<i>Variable(s)</i>	<i>Description</i>
$b$	Index for bootstrap re-samplings, $b = 1, 2, \dots, B$ (Sec. 6.5)
$i$	Index for depth in numerical solution of heat equation (Chap. 5); index for SOBOL input parameters, $i = 1, 2, \dots, n$ (Chap. 6)
$-i$	Short-hand notation used to represent “all except $i$ ” (Chap. 6)
$i(-i)$	Short-hand notation used to represent the coupling of the $i$ th value with all values except $i$ (Chap. 6)
$j$	Index for time in numerical solution (Chap. 5); index for SOBOL output parameters, $j = 1, 2, \dots, m$ (Chap. 6)
$l$	Index of input parameters, $l = 1, 2, \dots, n$ and $l \neq i$ (Chap. 6)
$r$	Index for sensitivity analysis Monte Carlo replicates, $r = 1, 2, \dots, K$ (Chap. 6)

## ABSTRACT

Faceted snow crystals develop at or near the snow surface due to temperature gradients. After burial, snow avalanches regularly fail on these layers. Generally, surface hoar deposits when the snow surface is cooler than the surrounding environment; near-surface facets form when the subsurface is warmed by solar radiation and the surface is cooled by radiative, convective, and latent heat exchange.

Field research stations were established that included daily observations and meteorological data. In two seasons, 14 surface hoar and 26 near-surface facet events were recorded. Statistical analysis of the surface hoar events indicated three factors that were related to surface hoar growth: incoming long-wave radiation, snow surface temperature, and relative humidity. The ideal conditions for each of these parameters were 190–270 W/m<sup>2</sup>, -22 to -11 °C, and 45–80%, respectively. For near-surface facet formation, long- and short-wave radiation and relative humidity were statistically linked to the events. The ideal conditions for these parameters ranged from 380–710 W/m<sup>2</sup>, 210–240 W/m<sup>2</sup>, and 23–67%, respectively.

Using a thermal model, sensitivity analysis, and Monte Carlo simulations the conditions that lead to facet formation were explored. Based on computed mass-flux, the formation of surface hoar was mainly driven by changes in long-wave radiation, air temperature, wind velocity, and relative humidity. From these terms graphical tools were developed to predict surface hoar; the numerical results matched reasonably well with the field observations. Based on the presence of a specific temperature gradient understood to lead to near-surface facets, three terms were determined to be the most influential: density, thermal conductivity, and incoming long-wave radiation. Using these terms, albedo, and incoming short-wave radiation—a requirement for radiation-recrystallization—a means for predicting the presence of near-surface facets was presented.

The physical and analytical data presented indicates that incoming long-wave radiation is the most influential parameter governing the conditions that lead to surface hoar and near-surface facet growth. The analysis suggests that snow with low density and high thermal conductivity may be conducive to the formation of near-surface facets.



## CHAPTER 1

### INTRODUCTION

Within the avalanche community, surface hoar and near-surface facets are established areas of importance and have been reported to account for up to 73% of human-triggered avalanches (Schweizer and Jamieson, 2001; Tremper, 2001). Moreover, the influence of these surface layers on the environment extends well beyond the scope of avalanche prediction into the domain of global climatology. Seasonally, snow covers 46,000,000 km<sup>2</sup> of the earth, which is about 31% of the Earth's land surface (Weast, 1981; Frei *et al.*, 1999). Consequently, the extent of snow cover affects the global temperature, principally due to the reflectivity of snow—in contrast to the reflectivity of soil or vegetation. However, the crystal structure of snow itself can alter its reflectivity, since the optical properties of particles are controlled by the size and shape of the particle. The presence of a layer such as surface hoar (crystals that form via vapor deposition on the snow surface) could have global effects, especially when considering the vast extent of snow cover that exists. Leathers *et al.* (1995) stated that “a thorough knowledge of the dynamics of snow cover to atmosphere interactions is needed if an understanding of present climate variations and long-term climate change is desired.”

Qualitative data regarding the formation of both surface hoar and near-surface facets is readily available, and the processes for both are driven by radiation processes. Surface hoar is known to form when the snow surface cools due to a radiation loss and water vapor condenses on the surface. Near-surface facets form when radiation heats the snow just below the surface and the surface is cooled because of radiation losses. In both cases, large temperature and vapor pressure gradients develop resulting in the formation of facets.

While conceptual knowledge of conditions leading to the morphology of such a faceted layer is important, a quantitative definition of these conditions is the ultimate goal of this dissertation. There has only been a modicum of prior success in this effort. The work that coined the term “near-surface facets” focused heavily on the temperature gradient near the surface, which was generally 100–300 °C/m (Birke-land *et al.*, 1998). A study in the Bolivian Andes reinforced these findings with the meteorological and snow profile data collected after two avalanches claimed several lives. Prior to the fatal avalanche the average nighttime near-surface temperature gradient was determined to be 160 °C/m (Hardy *et al.*, 2001). Perhaps the most conclusive quantitative study to date regarding facet formation was a laboratory study of radiation-recrystallization (Morstad, 2004; Morstad *et al.*, 2004, 2007). Thirteen experiments were performed where environmental conditions including short-wave and long-wave radiation, snow density, and humidity were controlled . Ten of these experiments produced 1/4–1 mm faceted crystals near the surface.

The study of the near-surface snow environment is well-founded. However, a solid qualitative comprehension of the environmental parameters necessary to yield facet formation has not been established. Considering that the micro-structure of snow is a critical component of avalanche research and climatology, an antecedent need is an understanding of the environmental and micro-structural factors that drive snow morphology—the overriding objective for this dissertation. To meet this general objective two specific tasks were completed, the details of which are the basis for this dissertation:

1. Two extensive weather stations, at north- and south-facing locations, were coupled with rigorous daily observations and grain scale images of the snow surface.

The data collected from this investigation contains two complete winter seasons

of observations and comprises the most extensive and detailed field study of near-surface facets and surface hoar.

2. Both field and laboratory research of snow metamorphism are limited by time and nature, thus a numerical exploration was conducted that provided quantitative results in two capacities. A sensitivity analysis defines the relative importance of the various driving factors known to influence the snowpack and using Monte Carlo simulations the specific quantities for the factors deemed important were defined.

The work presented in this dissertation is divided into nine chapters, plus this introduction and a short conclusion. These chapters generally were written to be self supporting. The dissertation is also divided into four parts. Part I includes a single chapter (2) that begins with providing additional details regarding the relevance of the research and then provides a literature review of the two near-surface morphologies of snow considered: near-surface facets and radiation-recrystallization. This review focuses mainly on research that investigated the environmental conditions leading to the formation of these two types of crystals.

Part II, which includes two chapters (3 and 4), details the first accomplishment listed above, the field investigation of surface hoar and near-surface facets respectively. Within each chapter the recorded events were summarized with images of the snow crystals (before and after metamorphism) and graphs of the weather conditions surrounding the event. Also, based on the recorded events, the environmental conditions were analyzed providing physically based evidence of the most influential environmental parameters.

The next portion of the dissertation, Part III, includes the methods. In Chapter 5 the thermal model used for the numerical investigation is derived. Additional analysis

in this chapter examines the importance of various wave lengths for incoming short-wave radiation and the influence of measurement error on the model output. Chapter 6 presents the theory and application of a sensitivity analysis methodology used for the numerical investigation portion of this dissertation.

Part IV of the dissertation includes four chapters (7–10). Chapter 7 summarizes all the methods defined in Part III, which includes the development of input distributions for the thermal model, a discussion of sensitivity analysis, methods used to develop the Monte Carlo simulations, and various data analysis techniques employed for analyzing the results. Chapter 8 includes both the sensitivity analysis and Monte Carlo simulation results for surface hoar formation.

Part IV continues with an analysis of near-surface facet formation separated into two chapters. Chapter 9 focuses on the sensitivity analysis and quantifies the most influential inputs on a variety of model outputs. Chapter 10 continues by applying the results of the sensitivity analysis in conjunction with Monte Carlo simulation data to define specific regions of inputs that are likely to result in near-surface facet development.

## CHAPTER 2

### SIGNIFICANCE AND BACKGROUND OF SURFACE WEAK LAYERS

#### 2.1 Introduction

The introduction (Chapter 1) of this dissertation provided a brief overview of the importance of examining the near-surface layer of a snowpack and sets the stage for the main objective of the entire body of work presented. The objective of which is to improve the current understanding of near-surface facet and surface hoar formation. Along these lines, the first step to obtaining such an understanding is to compile the preexisting data, which is the purpose of this chapter. That is, to define the state of the art concerning the driving factors associated with the development of surface hoar and near-surface facets.

#### 2.2 Significance of the Near-Surface Layers

##### 2.2.1 Avalanches

On the regional scale the importance of studying the near-surface layer of snow lies with predicting avalanche hazards. Tremper (2001) provided myriad statistics regarding avalanche fatalities within the United States and Western Europe from 1953 through 2000. It is reported that the average fatalities in the U.S. increased from approximately 5 annually in the 1960s to near 25 in the late 1990s. The Colorado Avalanche Information Center (CAIC, 2010) provided more recent statistics up to 2008, and reported that the current U.S. average is now approaching 30 fatalities per year. The avalanche concern is not limited to the U.S. For example, according to McClung and Schaerer (2006) Switzerland alone averaged nearly 30 fatalities per year between 1983 and 2003.

In addition to fatalities, property damage due to avalanches is a serious concern. In alpine countries (Switzerland, Austria, and France) property damage is often 20 times as great as in the U.S. (McClung and Schaerer, 2006). McClung and Schaerer (1993, 2006) pointed out that the true cost of avalanches to society is difficult to define, but the collateral costs such as the cost of avalanche protection—typically four times that of annual property damage—as well as indirect costs that result from highway and rail closures drive up the financial liability of avalanche activity. Inarguably avalanches are a deadly threat and have a significant associated cost.

The most common weak layer associated with avalanches develops in the surface layer as near-surface facets or surface hoar. Schweizer and Jamieson (2001) reported that in approximately 73% of 103 investigated avalanches in Canada and Switzerland, the weak layer was composed of facets (excluding depth hoar) and surface hoar. Furthermore, of the 45 avalanches investigated by Schweizer and Lutschg (2001) the weak layer or interface layer (layers adjacent to the failure plane) of 29 were composed of facets or surface hoar. In studying the processes associated with near-surface facets in southwest Montana, Birkeland (1998) reported that of 51 avalanches investigated 90% had a weak layer composed of near-surface facets (59%) or surface hoar (31%). Additionally, research had indicated that such layers are persistent over time and can be hazardous well after the layer initially formed (Lang *et al.*, 1984; Davis *et al.*, 1996; Hachikubo and Akitaya, 1996).

### 2.2.2 Climate

On a global scale the surface layer of snow has perhaps more significant implications than avalanche formation, that is, the link between this uppermost layer of snow and the global climate. Globally, snow covers approximately 46,000,000 km<sup>2</sup> annually during January and February (Frei *et al.*, 1999), which is nearly one third

of the Earth's total land surface (Weast, 1981). Consequentially, snow can have a vast effect on the climate, specifically on air temperature (Karl *et al.*, 1993; Leathers and Robinson, 1993; Groisman *et al.*, 1994a). For example, Groisman *et al.* (1994b) explained that snow cover increases planetary albedo and reduces outgoing long-wave radiation. It was shown that the changing radiation balance from decreasing snow cover in the northern hemisphere between 1979 and 1990 may account for 0.5 °C of the recorded 0.98 °C temperature increase (Groisman *et al.*, 1994b).

Leathers *et al.* (1995) examined temperature depressions associated with snow cover in the Northeastern United States and concluded that a snow cover of greater than 2.5 cm caused temperature depressions near 5 °C during early and late portions of the season. Utilizing a snow pack model and data from four cold air masses moving across the United States Great Plains, Ellis and Leathers (1999) reported that decreasing the albedo affects the air temperature significantly. Changing the uniform albedo for the region from 0.9 to 0.5 increased mean daytime air temperature 3–6 °C and maximum day temperatures by 7–12 °C (Ellis and Leathers, 1999). Additionally, snow depth variations between 30 cm, 15 cm, and 2.5 cm yielded little difference in the change of air temperature (Ellis and Leathers, 1999). Ellis and Leathers (1999) explained that the temperature differences developed from the model agree with those of the measured data and stated that the difference in temperature may be due to sensible and possibly latent heat fluxes.

The snow albedo is an important factor when considering climatic changes in areas that are covered in snow. Typically, snow albedo is reported as a singular value or all-wave albedo that includes the solar (short-wave) electromagnetic spectrum, but the albedo for each wavelength varies. The solar reflectance of radiation is highest in the ultraviolet and visible range (0.2–0.8  $\mu\text{m}$ ) and decreases to nearly zero in the

near-infrared range (0.7–5.0  $\mu\text{m}$ ); hence, a majority of the radiation absorbed is in the near-infrared spectra (Oke, 1978; Warren and Wiscombe, 1980; Warren, 1984).

The albedo of snow also varies on snow age and grain size; Oke (1978) indicated that snow albedo ranges from 0.4 to 0.95 for old and new snow, respectively. Albedo has been shown to change dramatically due to aging and contamination of the snow, but albedo also varies due to physical changes in the surface morphology (Oke, 1978; Armstrong and Brun, 2008). Additionally, it is reported that the albedo of snow reduces upon aging due to its increasing grain size as well as the introduction of impurities such as carbon soot, particularly in the near-infrared (Warren, 1982, 1984).

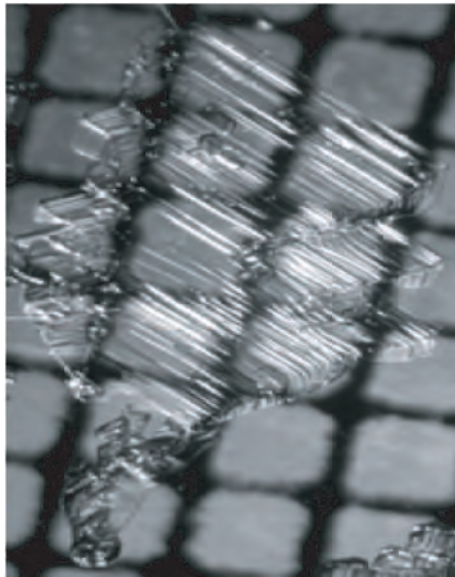
As mentioned previously, grain size is a critical component when discussing the optical or solar adsorption properties of snow (Mellor, 1965; Bohren and Barkstrom, 1974; Warren, 1982). Moreover, Kokhanovsky and Zege (2004) indicated that current reflectivity studies of snow are limited to spherical grains, but pointed out that the shape of the grains has a profound effect on the reflectivity of snow. These researchers provided a “new approach to snow optics with a more realistic model of snow as a medium with non-spherical and close-packed snow grains.”

### 2.2.3 Synopsis

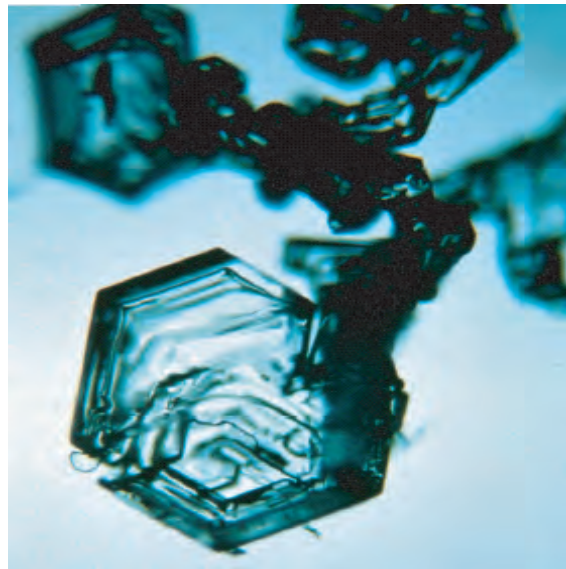
On the surface of a snow pack, the grain size and shape impact the albedo and consequently the surrounding climate. In this respect, near-surface facets and surface hoar are critical, since both develop either at the surface, as in the case of surface hoar, or in the upper few centimeters of a snowpack (Birkeland *et al.*, 1996; Birkeland, 1998; Morstad *et al.*, 2007). Additionally, these layers are known to be associated with avalanche release. Surface hoar and near-surface faceted crystals associated with skier-triggered avalanches were typically around 2 mm in size (Schweizer and Lutschg, 2001). However, surface hoar crystals have been observed to grow up to 10 mm in



the mountains of southwest Montana (Tremper, 2001; Cooperstein *et al.*, 2004), but typically range from 1–5 mm (McClung and Schaerer, 2006). Near-surface facets are smaller in size. Tremper (2001) reported that near-surface facets range from 0.5–2.0 mm. While Cooperstein *et al.* (2004) indicated that a majority of crystals observed were less than 0.5 mm. In a laboratory study, artificially grown near-surface facets ranged from 0.1–1.0 mm (Morstad *et al.*, 2007). Figure 2.1 provides examples of near-surface faceted and surface hoar crystals.



(a) Surface Hoar



(b) Near-surface Facet

Figure 2.1: Example images of (a) surface hoar (Cooperstein *et al.*, 2004) and (b) near-surface faceted snow crystals (Morstad, 2004).

### 2.3 A Review of Surface Hoar

Surface hoar has been studied for nearly 75 years (Seligman, 1936) and in a discussion of observations collected regarding the accumulation and stratification of snow, Gow (1965) observed “spike-like crystals” now referred to as surface hoar. These

crystals were reported to form during periods of still weather and clear skies, and were more prominent on snow dunes and sastrugi (sharp irregular ridges on the snow surface formed by wind erosion). Gow (1965) theorized that this hoar frost may originate from the condensing of water originating in the dune itself. Furthermore, Gow (1965) emphasized that hoar frost only forms during “exceptionally” calm weather.

As with the aforementioned research, work regarding the accumulation of moisture on Antarctic ice has also been examined by Linkletter and Warburton (1976). Their work took into consideration the accumulation due to surface hoar and rime (crystals formed from liquid water condensation as opposed to vapor deposition that forms surface hoar) and determined that these processes may contribute 5–10% of the annual accumulation on the Ross Ice Shelf. Their observations indicated that both rime and surface hoar develop during super-cooled fog events. The fog events typically occurred with a light wind from 0–5 m/s and frequently demonstrated temperature oscillations as rapid as 0.5 °C/min with fluctuations as large as 5 °C (Linkletter and Warburton, 1976). However, surface hoar was also shown to develop on three occasions when no visible fog was present (Linkletter and Warburton, 1976).

Lang *et al.* (1984) proclaimed that their research was the first “thorough quantitative study of surface hoar.” The study utilized a thermocouple stack that recorded temperatures of the air above and within first the few centimeters of the snowpack. In an overnight experiment, Lang *et al.* (1984) observed that surface hoar formation was associated with significant differences between the snow surface temperature and the air temperature, with the major growth occurring when the gradient in the air was largest at 380 °C/m. Additionally, a temperature gradient reversal was observed between the -2 cm temperature in the snow and the snow surface; the gradient reversed from -80 °C/m to 70 °C/m during the growth of the surface hoar (Lang *et al.*, 1984). Snow surface temperatures were observed to range between -21°C and -12.5

°C when surface hoar crystals developed. These results agree with work conducted by Mason *et al.* (1963), who reported the growth of snow crystals from the vapor phase. This study indicated the dendritic, feather-like crystals grew with the air temperature between -12 °C and -16 °C. Lang *et al.* (1984) concluded that “a large near-surface air temperature gradient, due to nocturnal clear sky conditions, is insufficient in itself for significant condensation onto the snow surface to occur.” It also explained that any horizontal air movement close to the surface was observed to prohibit surface hoar growth—a result that has been disputed (Colbeck, 1988).

In maritime climates, Breyfogle (1986) determined that two dominant scenarios exist for the development of surface hoar. The first of the two formation scenarios outlined by Breyfogle (1986) occurred when a cold air front moved into the region causing a “highly saturated environment at the snow/air interface;” this was associated with radiation cooling of the snow surface to the dew point, hence deposition occurred. Generally, surface hoar tended to develop when the air temperature was between -6 °C and -12 °C at the snow surface, relative humidity was at least 70%, and the formation occurred in low-wind conditions. The second observed formation conditions occurred in an under-saturated environment, but a secondary source of water vapor must be present (Breyfogle, 1986). This secondary source was similar to that of the aforementioned research by Linkletter and Warburton (1976); Breyfogle (1986) indicated that the source of vapor was supercooled cloud decks that established a large vapor flux when clear sky and low humidity conditions prevailed above the cloud deck; in these conditions the cloud deck acted as a radiator and this layer was termed the “peripheral zone.”

Breyfogle (1986) provided two examples of the latter scenario that occurred during a four day period where air temperature and relative humidity were monitored continuously. During two nights the relative humidity dropped from near 100% during

the day to near 60% at night. Additionally, the air temperatures increased during the night by approximately 2–3 °C. These environmental observations we observed at a station located 300 m above the study plot, directly in the peripheral zone. During both of these events surface hoar was shown to form precisely when the observation station was within the peripheral zone.

Colbeck (1988) calculated the importance of temperature profiles and humidity to form surface hoar by employing a theory for temperature decay of a surface being cooled by outgoing radiation explained by Sutton (1953). The theory is an exponential function based on environmental conditions such as long-wave radiation, thermal conductivity, temperature gradient within the snow, latent heat, and heat capacity, among others. Using a number of assumptions from the literature, Colbeck (1988) considered a no-wind condition which was described as necessary by Lang *et al.* (1984). The study concluded that “some wind” is a necessity to supply vapor to the snow surface causing surface hoar growth and such wind could be due to “near-surface, low-speed gravity drainage.” These winds are common in mountainous areas undergoing radiation cooling, which causes pools of cool air to accumulate in constricted areas that suddenly release (Colbeck, 1988). Thus, no detectable wind may be present for a majority of the time, but surges could supply vapor necessary for the growth of surface hoar.

Surface hoar crystals were found to persist on the surface of a snow pack for many days despite evaporation during the day. During two multi-day case studies, surface hoar formed during the clear, humid nights with air temperatures between -6 and -10 °C and snow surface temperatures around -15 °C (Hachikubo and Akitaya, 1996, 1998). Hachikubo and Akitaya (1996) indicated that the surface hoar did not degrade as expected during the daytime hours. Data indicated that hoar crystals developed during a positive latent heat flux with condensation of 74 gm/m<sup>2</sup>. Evaporation of 62

gm/m<sup>2</sup> occurred during the day, indicating that the crystals should have been reduced; however, they persisted. One possible explanation provided by the researchers was that the vapor lost due to evaporation may have been from the underlying layer of snow, a few centimeters below the surface. Hachikubo and Akitaya (1996) suggested that “the surface hoar crystals were cooled by outgoing radiation even in the daytime and kept their size, while the snow grains underneath the surface were warmed by solar radiation and evaporated.” These are precisely the near-surface faceted crystals that shall be discussed in Section 2.4.

As previously discussed, wind has been presented as both necessary (Colbeck, 1988) and destructive (Lang *et al.*, 1984) for surface hoar formation. Hachikubo and Akitaya (1997) provided sufficient evidence that the presence of wind is significant in the formation of surface hoar crystals and made the general statement that surface hoar grew “when the snow surface temperature was 5 °C (or more) lower than the air temperature, the humidity was higher than 90%, and the wind speed was 1 to 2 m/s at 0.1 m high.” Additionally, Hachikubo and Akitaya (1997) stated that the net radiation (sum of sensible, latent, and conductive heat fluxes) slowly decreased during formation, as did the bulk transfer coefficient. The bulk transfer coefficient is utilized as an estimate for condensation rate, which was shown to increase as the surface hoar forms. Hence, the formation of surface hoar itself increases the surface roughness of snow thus increasing the bulk transfer rate. In other words, a feedback process exists for the means of condensation and surface hoar formation (Hachikubo and Akitaya, 1997). An investigation by Höller (1998) and values inferred from the work of Hachikubo and Akitaya (1997) suggest that surface hoar is far more likely to form in open areas than in forested or partially forested areas. This conclusion was based upon a preliminary study that examined three study plots in open and

forested areas by comparing the air temperature, relative humidity, wind speed, and total radiation balance at each site (Höller, 1998).

Hachikubo (2001) conducted a comparison between field data and two numerical models—the “Simple” and the “Crocus.” Crocus is a snow model originally developed by Brun *et al.* (1992). Hachikubo (2001) concluded that when relative humidity was less than 80% there existed a wind speed at which the sublimation rate was maximized. For example, at 60% the sublimation rate reached its maximum around 2 m/s, while at 70% it was greatest near 3.5 m/s (Hachikubo, 2001). For conditions with a relative humidity greater than 90% sublimation increased with wind speed in the range examined from 0–6 m/s. The two models explored both disagreed with field experiments in some capacity. The Crocus Model underestimated snow surface temperature and the Simple Model disagreed with results when clouds were present (Hachikubo, 2001).

A more recent study of surface hoar and near-surface facets compared the differences between aspect (north versus south) with respect to crystal formation. In two examples given by Cooperstein *et al.* (2004), surface hoar formed larger crystals on the north-facing site when compared to the south-facing site. The conditions were similar in both examples: the temperature gradient at the snow/air interface was larger on the north site, the snowpack absorbed less short-wave radiation, and the snow surface temperatures were lower. Interestingly, the second example discussed also exhibited growth of near-surface faceted crystals, which formed better on the south-facing slope.

In a study examining the spatial variability of surface hoar formation, Feick *et al.* (2007) reported three surface hoar events that occurred at three weather stations. Feick *et al.* (2007) provided exhaustive details of these events. To summarize, the events occurred with air temperatures of approximately  $-10$  to  $-5$  °C, with snow

surface temperatures approximately 10 °C colder, and with wind speeds less than 2.5 m/s. The study concluded that wind and short-wave radiation contributed to the destruction of the surface hoar and that wind speed was key to predicting formation and destruction. This conclusion suggests that forecasting is nearly impossible due to the difficulties of modeling wind speeds across complex terrain.

Finally, Colbeck *et al.* (2008) detailed an investigation into a specific mechanism for surface hoar formation due to valley clouds. This work explained that in order to achieve growth rates observed, the surface hoar likely formed as the cloud expanded up-slope where the wind speeds were between 1 and 2 m/s and the snow was still exposed to the cold sky allowing for radiative losses at the snow surface.

Overall, the study of surface hoar has progressed during the years from simple observations to complex numerical modeling. Throughout all the literature presented, three major variables are consistently explored: wind speed, air/snow temperature gradients, and relative humidity. Wind speed has been shown to be critical for forming surface hoar by providing a source of moisture for condensation on the surface. The research presented indicated that winds in the range of a few meters per second are optimum. A temperature difference between the snow surface and the air must be present; this difference was shown to be near 5 °C, with air temperature being the higher value. Finally, humidity varies greatly depending on the conditions. Although not mentioned in a majority of the literature, another critical factor is the radiation balance and heat exchange, which was shown to be slightly negative but changed little during surface hoar formation. Table 2.1 summarizes the work presented within this section, highlighting the chief focus of each article reviewed.



Table 2.1: A summary of the conditions necessary for surface hoar growth as reported in the literature reviewed.

Author	Surface Hoar Observations
Mason <i>et al.</i> (1963)	Dendritic feather-like crystals grew from vapor phase between -12 °C and -16 °C with supersaturation with respect to ice greater than 20%.
Gow (1965)	Surface hoar formed during clear and still weather; on dunes and sastrugi; theorized that condensed moisture may have originated from dune feature.
Linkletter and Warburton (1976)	Crystals formed in association with fog events (in addition to three periods without fog) and with light winds of 0–5 m/s; fog had rapid (0.5 °C/min) and large (5 °C) temperature variations.
Lang <i>et al.</i> (1984)	Surface hoar formed with snow surface to air temperature gradients in excess of 300 °C/m, a gradient reversal of snow to snow-surface (-80 to 70 °C/m), snow surface temperatures between -12 and -16 °C, and no horizontal wind movement.
Breyfogle (1986)	Formation tended to occur with air temperatures between -6 and -12 °C with humidity of 70%; two dominant processes occurred: 1) a highly saturated condition with low wind and 2) an undersaturated condition with the presence of a secondary vapor source.
Colbeck (1988)	Formation required low wind conditions such as provided by gravity drainage winds; pure diffusion of water vapor was unable to account for growth rates observed.
Hachikubo and Akitaya (1996, 1998)	Surface hoar growth occurred during clear humid nights; air temperature was between -6 and -10 °C; snow surface temperature was near -15 °C.
Hachikubo and Akitaya (1997)	Growth occurred with a surface temperature 5 °C lower than the air temperature, humidity greater than 90%, wind speed between 1–2 m/s at 0.1 m above snow, and as net radiation decreased from -85 to -50 W/m <sup>2</sup> .
Höller (1998)	Environment for surface hoar growth suggested to be open terrain compared to forested areas with 20% and 80% canopy coverage.
Hachikubo (2001)	Sublimation was maximized between wind speeds from 0–6 m/s when relative humidity was less than 90%; when humidity was over 90%, sublimation increased throughout the range tested.
Cooperstein <i>et al.</i> (2004)	Surface hoar crystals up to 10 mm formed with temperature gradients up to 92 °C/m at the snow/air interface, net short-wave of 181 W/m <sup>2</sup> , average surface temperature of -10 °C, and average wind speed of 2.1 m/s.
Feick <i>et al.</i> (2007)	Various extents of surface hoar was observed at three weather stations in a single basin. The surface hoar developed with air temperatures of -5 to -10 °C, wind speeds of less than 2.5 m/s, and a snow surface temperature approximately 10 °C less than the air temperature.



#### 2.4 A Review of Near-Surface Facets

Colbeck (1989) conducted one of the first studies specifically examining near-surface faceted crystal formation, although previous research exists (LaChapelle, 1970; LaChapelle and Armstrong, 1977; Armstrong, 1985; Akitaya and Shimizu, 1987). Colbeck (1989) developed a “theory of spatial and temporal variations in temperature with sinusoidally varying surface temperature and periodic solar radiation at the surface.” Colbeck (1989) examined three scenarios using the theory developed: seasonal, high-altitude, and polar ice-sheet snow covers. The seasonal snow cover was assumed to be 1 m thick, have a 30 °C air temperature swing, and have a peak solar radiation absorption of 70 W/m<sup>2</sup>. Under these conditions Colbeck (1989) explained that the conditions necessary for increased crystal growth just beneath the surface existed, especially when the diurnal effects were coupled with penetration solar radiation.

Field observations and laboratory experiments were conducted by Fukuzawa and Akitaya (1993) with regard to the formation of faceted crystals near the snow surface. A January case study consisted of 3 cm of new snow (70 kg/m<sup>3</sup>) on top of a lightly compacted layer (170 kg/m<sup>3</sup>). The snow surface metamorphosed into faceted grains over two nights of clear skies (Fukuzawa and Akitaya, 1993). These grains formed due to temperature gradients that averaged 159 °C/m, occurred at about 1 cm depth, were subjected to high solar radiation during the day and radiative cooling at night, and experienced low wind speeds averaging 1.0 m/s (Fukuzawa and Akitaya, 1993). Similar results were found during March, except that the growth rates were double that of January, which was likely due to the increased solar radiation during this month. Fukuzawa and Akitaya (1993) constructed an experimental setup that established a temperature gradient across a snow sample and were able to explore the effects of high temperature gradients on low density snow as observed in the field. During these

experiments faceted crystals grew from fine ice particles into 0.2 mm facets within 16 hr and into 0.4 mm facets in 48 hr. Fukuzawa and Akitaya (1993) concluded that three conditions were necessary to form faceted crystals near the surface: (1) a low density layer (less than 3 cm) must overlay older, denser snow, (2) the subsurface snow temperature must increase due to diurnal solar radiation, and (3) the surface temperature must decrease rapidly due to upward long-wave radiation.

The process of diurnal heating of the snow beneath the surface applies to more than just the formation of faceted crystals. Oke (1978) explains such a process and its importance to understanding the boundary layer climate, and Ozeki and Akitaya (1996) explained a similar process that lead to the formation of ice crusts.

Fierz (1998) explained the formation of a near-surface faceted layer similarly to Fukuzawa and Akitaya (1993), including the three key factors pointed out. Fierz (1998) reported that 11 cm of new low-density snow ( $70\text{--}110\text{ kg/m}^3$ ) accumulated on a denser pack ( $260\text{ kg/m}^3$ ) that was followed by clear weather. The result was a crust 5 mm thick on the surface with 1.5–2 mm facets underneath.

The establishment of near-surface faceted crystals as an specific area of expanded study is partially due to work conducted by Birkeland *et al.* (1996), Birkeland (1998), and Birkeland *et al.* (1998), in which the term “near-surface facets” was coined to describe “snow formed by near-surface vapor pressure gradients resulting from temperature gradients near the snow surface.” Birkeland (1998) defined three specific processes that lead to the formation of near-surface facets:

In a case study in the mountains of Montana, diurnal recrystallization was shown to develop 1 mm facets within 36 hours during a period characterized by fresh snowfall (5–10 cm) followed by clear weather (Birkeland *et al.*, 1996; Birkeland, 1998). Temperatures during the day were near  $-3\text{ }^\circ\text{C}$ , which was proceeded by nighttime temperatures near  $-15\text{ }^\circ\text{C}$ . This shift in temperature caused a large temperature gra-

dient in the upper 5 cm of the snow pack. A gradient of  $-250\text{ }^{\circ}\text{C}/\text{m}$  (in this paper a negative gradient is associated with warmer temperatures at depth) was recorded during the night followed by a  $100\text{ }^{\circ}\text{C}/\text{m}$  gradient during the day, resulting in faceted crystals up to 1 mm in size.

In an investigation of two avalanches, one of which claimed the lives of two climbers, Hardy *et al.* (2001) suggested that the conditions existed in high-altitude tropical mountains that led to the formation of a thick (10 cm), well-developed layer of large-faceted grains (3–5 mm). Although specific measurements regarding the formation of the faceted layer were not available, using data from a nearby weather station Hardy *et al.* (2001) concluded that a layer of buried facets (27–37 cm deep) was once at the surface and exposed to clear and cold conditions. Additionally, high amounts of incoming short-wave solar radiation are typical of these high-altitude areas ( $950\text{ W}/\text{m}^2$ ) and temperature gradients of  $161\text{ }^{\circ}\text{C}/\text{m}$  were recorded, both of which have been shown to be sufficient for the formation of near-surface faceted crystals (Hardy *et al.*, 2001).

Aspect was also shown to affect the formation of near-surface faceted crystals. Cooperstein *et al.* (2004) reported that faceted crystals were better developed on south-facing slopes compared to a north-facing aspect with similar elevations. During a 24 hour period in which near-surface faceted crystals were observed to form, the southern exposure had a larger temperature gradient and exhibited a reversal while the opposing site did not show a reversal (Cooperstein *et al.*, 2004). As mentioned in the previous section, this near-surface facet event was coupled with the formation of surface hoar, which grew larger on the north site.

To re-examine the effects of canopy coverage on facet formation Höller (2004) conducted a study similar to that summarized in the preceding section on surface hoar. The effects of tree cover were examined between an open area, a clearing (30%

canopy coverage), and a forest (75% canopy coverage). Temperature gradients were shown to be as high as 130 °C/m for the open area, 42 °C/m in the clearing, and less than 25 °C/m for the forest region. Using snow profiles during three different winter seasons, Höller (2004) did not observe any near-surface faceted crystals forming in the forest areas, but observed faceting in the open area and the clearing.

The most complete quantitative study of near-surface faceting was conducted under laboratory conditions, utilizing an environmental chamber that allows for the control of incoming long-wave and short-wave radiation, among other variables. Morstad *et al.* (2007) successfully grew radiation recrystallized near-surface facets in a lab setting, whence facets ranged from 1/8 to 1 mm in size. The complete results from this endeavor are provided in Morstad (2004). Of the thirteen experiments performed, 10 produced 1/4–1 mm faceted crystals near the surface. The environmental conditions were controlled as follows: short-wave radiation ranged from 595–1180 W/m<sup>2</sup>, long-wave was relatively constant near 280 W/m<sup>2</sup>, density varied between 175–10 kg/m<sup>3</sup>, and humidity was between 15% and 40%. The temperature gradients found during the facet formation were between 100–550 °C/m.

Slaughter *et al.* (2009) detailed the work originally presented in McCabe *et al.* (2008) and Slaughter *et al.* (2008) that included field observations of near-surface facets and laboratory simulations of three events. McCabe *et al.* (2008) summarized six radiation-recrystallization events that formed facets under similar conditions: a warm, melting subsurface overlain by a frozen surface. The temperature gradient between the melt-layer and surface was estimated to range from 240–400 °C/m and short-wave input ranged from 575–840 W/m<sup>2</sup> at a weather station with a clear view of the sky. The facets formed in new snow in each event. Slaughter *et al.* (2009, 2008) mimicked these three observed events in a laboratory environment. Despite that the

experiments utilized old, rounded snow, facets developed, albeit not to the extent observed in the field.

In summary, according to the literature reviewed the formation of near-surface faceted crystals was driven by a temperature gradient that forms in the upper few centimeters of the snowpack. This gradient may be established in any number of ways, including radiation penetration into the snow surface, long-wave radiative losses, or because of the presence of a buried layer of warmer snow from a melt cycle. This gradient was also shown to be both positive and negative. Generally speaking, a temperature gradient of equal to or greater than 100 °C/m was required for facets to form. Table 2.2 summarizes each article reviewed regarding the formation of near-surface faceted crystals.

## 2.5 Conclusions

The near-surface layer is important with respect to global climatology and avalanche safety. A significant portion of the Earth's surface is coated by a layer of snow seasonally. Thus, the changing and aging of a snowpack can have a large effect on the environment due to the drastic changes in albedo that may occur in snow. Additionally, avalanches are a significant societal hazard accounting for numerous deaths and high cost to highway departments in mountainous regions.

Avalanche research with respect to snow crystal metamorphism has been ongoing for a number of years, a portion of which has focused on two specific formations at the snow surface: near-surface facets and surface hoar. However, minimal quantitative work has been completed regarding the driving environmental conditions that lead to the formation of each of these crystals. Tables 2.3a and 2.3b summarize the quantifiable parameters found in the research reviewed. Researchers indicate that

Table 2.2: A summary of the conditions necessary for near-surface facet growth as reported in the literature reviewed.

Author	Near-Surface Facet Observations
Colbeck (1989)	Radiation recrystallization formed crystals at 0.1 m below the surface with a peak solar radiation of $126 \text{ W/m}^2$ and a temperature swing of $20 \text{ }^\circ\text{C}$ .
Fukuzawa and Akitaya (1993)	Formation required temperature gradients between $100\text{--}300 \text{ }^\circ\text{C/m}$ and a low density layer (3 cm) overlaying an old denser layer.
Fierz (1998)	Facets (1.5–2 mm) formed under a 5 mm crust when 11 cm of new low-density snow ( $70\text{--}110 \text{ kg/m}^3$ ) accumulated on a denser pack ( $260 \text{ kg/m}^3$ ) followed by days of clear weather.
Birkeland <i>et al.</i> (1996); Birkeland (1998); Birkeland <i>et al.</i> (1998)	Diurnal recrystallization occurred on a layer of new snow 5 to 10 cm thick with temperature gradients shifting from $-250$ to $100 \text{ }^\circ\text{C/m}$ between the $-20 \text{ }^\circ\text{C}_{\text{night}}$ and $-3 \text{ }^\circ\text{C}_{\text{day}}$ .
Hardy <i>et al.</i> (2001)	Temperature gradients of $161 \text{ }^\circ\text{C/m}$ and incoming short-wave radiation of $950 \text{ W/m}^2$ , were shown to account for a 10 cm layer of large-faceted crystals using dust and chloride concentration evidence.
Cooperstein <i>et al.</i> (2004)	Well-developed facets formed with temperature gradients between $126$ and $-60 \text{ }^\circ\text{C/m}$ just below the surface, with net short-wave of $587 \text{ W/m}^2$ and an average surface temperature of $-7 \text{ }^\circ\text{C}$ .
Höller (1998)	Near-surface facet growth was observed in an open region and forest clearing (30% canopy coverage) with maximum temperature gradients of $130 \text{ }^\circ\text{C/m}$ and $42 \text{ }^\circ\text{C/m}$ , respectively.
Morstad (2004); Morstad <i>et al.</i> (2004, 2007)	Ten experiments produced near surface faceted crystals with $1/4\text{--}1 \text{ mm}$ grains and temperature gradients between $100\text{--}550 \text{ }^\circ\text{C/m}$ . The environmental conditions were controlled: short-wave ranged from $595\text{--}1180 \text{ W/m}^2$ , long-wave was near $280 \text{ W/m}^2$ , snow density varied between $175\text{--}410 \text{ kg/m}^3$ , and humidity was between 15% and 40%.
McCabe <i>et al.</i> (2008); Slaughter <i>et al.</i> (2008, 2009)	Six radiation-recrystallization events were observed in the field with temperature gradients in the surface layer ranging from $240\text{--}400 \text{ }^\circ\text{C/m}$ with incoming short-wave radiation ranging from $575\text{--}840 \text{ W/m}^2$ at a station with a clear view of the ski. Three of these events were reproduced in laboratory simulations, producing facets despite drastically different snowpacks from those observed in the field.

surface hoar forms due to large temperature gradients between the snow and the overlying subfreezing air. Near-surface facets tend to form in the top few centimeters of the snowpack, with high solar radiation, and with various snow densities. As with surface hoar, a temperature gradient is necessary to induce growth of near-surface faceted crystals, however in the case of the latter phenomenon this gradient exists within the snowpack.

Table 2.3: Summary of quantifiable parameters shown to lead to the formation of (a) surface hoar and (b) near-surface facets as presented in the available literature.

(a) Surface Hoar	
Quantitative Parameter	Range Adapted From Literature
Air temperature	-6 to -16 °C
Difference in surface and air temperature	5 °C
Humidity	60 to 100%
Net radiation	-85 to -50 W/m <sup>2</sup>
Net shortwave radiation	181 to 587 W/m <sup>2</sup>
Temperature gradient (snow/air)	0 to 300 °C/m

(b) Near-surface Facets	
Quantitative Parameter	Range Adapted From Literature
Changes in air temperature	17 to 20 °C
Humidity	15 to 40%
Snow density	0 to 410 kg/m <sup>3</sup>
Short-wave radiation	587 to 1180 W/m <sup>2</sup>
Long-wave radiation	280 W/m <sup>2</sup>
Temperature gradient	-250 to 550 °C/m

Overall, the research that has been performed to date marks a significant step in developing an understanding of the surface environment of a snowpack. A solid conceptual understanding of the formation process exists, but further work is required to quantify these parameters. Quantification is a requirement for greater comprehension of the processes that alter the snow surface, which affects the environment and presents a risk to the life of people who work and recreate in mountainous regions.

## CHAPTER 3

### FIELD INVESTIGATION OF SURFACE HOAR

#### 3.1 Introduction

Surface hoar is a snow crystal that forms on a surface, typically on seasonal snow, via vapor deposition from the surrounding environment. When buried by additional snowfall, this layer is a particularly dangerous weak-layer that leads to a significant number of avalanches. Approximately 30% of skier-triggered avalanches have been associated with surface hoar (Birkeland, 1998; Schweizer and Lutschg, 2001). This layer is known to be persistent (McClung and Schaerer, 2006), thus understanding the conditions surrounding the formation of surface hoar has been the topic of numerous research projects. A complete review of surface hoar is provided in Chapter 2.

Despite the body of research that exists for surface hoar formation, minimal research exists that defines specific environmental conditions that surround surface hoar formation. To this end, two weather stations were established and daily observations and crystal-scale photographs of the snow surface were taken. The goal of these stations and extensive observations was to quantify the conditions necessary to yield surface hoar formation for use in subsequent research. The following chapter summarizes the results obtained from a field investigation of surface hoar, which is only one portion of an ongoing investigation resulting from the collaborative efforts of researchers at the Subzero Science and Engineering Research Facility at Montana State University and the Yellowstone Club (YC) Ski Patrol.



## 3.2 Methods

### 3.2.1 Weather stations

Two study plots were chosen, one on a north-facing and another on a south-facing slope. Data collection began during the 2005/2006 season; however, snow observations did not begin until the following season (2006/2007) and images were added to the observations during the 2007/2008 season. All three forms of data (weather, observations, and images) continued through 2008/2009, and will continue as the project is ongoing. Both sites were used in previous research: Cooperstein *et al.* (2004) used these locations in a study of surface hoar and near-surface facet development; Staples *et al.* (2006) utilized the weather data when modeling snow surface temperatures; Slaughter *et al.* (2009) performed laboratory experiments mimicking conditions observed at the south location; Adams *et al.* (2009) used recorded data as a basis for spatial modeling of weak-layers; and Slaughter and Adams (2009) used the weather data for the basis of a sensitivity analysis of the conditions leading to the formation of near-surface facets and surface hoar.

The North and South study plots are located on Pioneer Mountain at the Yellowstone Club near Big Sky, Montana. A third station (Aspirit), which is maintained by the YC Ski Patrol, is positioned near the top of a ridge at the American Spirit chair lift. This location has a nearly clear view of the sky for gathering unobstructed radiation data. The locations and elevations for each station are detailed in Table 3.1. Both the North and South study plots have a slope angle of approximately 30°.

### 3.2.2 Instrumentation

The North and South sites were similarly instrumented to measure air temperature and humidity (Campbell Scientific, Inc. CS215 with 41303-5 naturally aspirated

Table 3.1: Detailed information on each of the three weather stations situated on Pioneer Mountain.

Station	Latitude	Longitude	Elevation	Aspect
Aspirit	45°14'23.0"N	111°26'34.5"W	2690 m	n/a
North	45°14'52.3"N	111°27'21.8"W	2530 m	0°
South	45°13'47.7"N	111°26'33.0"W	2740 m	187°

radiation shield), snow depth (NovaLynx Corp.), snow surface temperature (Everest Interscience, Inc. 4000.4ZL), incoming long-wave radiation (Eppley Lab., Inc. PIR and Kipp & Zonen CGR3), slope-parallel incoming and reflected shortwave radiation (LI-COR, Inc. Li200 and Kipp & Zonen CGR3), wind speed and direction (Met One Instruments, Inc. 034B-L), and subsurface snow temperature taken at 2 cm intervals (Omega Eng., Inc. type T thermocouples). Data was recorded with Campbell Scientific, Inc. (CSI) CR10(x) dataloggers. The third location, Aspirit, measured unobstructed incoming short- and long-wave radiation (Eppley Lab., Inc. PSP and PIR). Appendix A includes a completed discussion of the instrumentation.

### 3.2.3 Snow observations

Each season, from mid-January to early April each season the YC Ski Patrol daily maintained visual observations and images describing the upper 5 cm of the snowpack. Snow crystal images were captured using a Panasonic PV-500, Olympus SP-510 UZ, or a Nikon Coolpix fitted with a 10× loupe from a Brunel 8×30 ocular. The same Brunel scope was utilized for the crystal classification. The daily records and images were cataloged in a custom weather software package, YCweather, designed for use in this project. The software also includes regional weather data and extensive graph creation capabilities (see Appendix B). Complete copies of all the daily logs are included in Appendix G.

### 3.3 Results

During the 2007/2008 (A) and 2008/2009 (B) winter seasons, 14 significant events of surface hoar were recorded. These events occurred at both the South and North weather stations, but not always both. Table 3.2 includes the mean values of the measured weather data for each event at the station(s) that crystals were observed. The means were computed using the data from the night prior to event date shown, from dusk to dawn. The difference between the air ( $T_a$ ) and snow surface ( $T_s$ ) temperature ( $\Delta T = T_a - T_s$ ) was also computed.

Throughout the field notes more references to surface hoar exist than those discussed here; however, some of this data was omitted as the event was minimal (i.e., the field notes and images did not demonstrate that the surface hoar was widespread or the surface hoar crystals only accounted for a small portion of the surface layer). The surface hoar often developed in newer snow at the North site while it developed on melt-freeze crusts at the South location. Table 3.3 summarizes the snow underlying the surface hoar on the day of observation.

In all but a few events, complete weather data as well as grain-scale images of the crystals exist. The following sections summarize each of the events recorded. These summaries provide a brief overview of the event and include the weather data surrounding the events and images of the surface hoar observed. Images included in this chapter are un-cropped and are representative of all the images captured for that event.

Table 3.2: Summary of mean daily weather conditions for all days recorded as surface hoar events, including long-wave ( $LW$ ) radiation, air ( $T_a$ ) and snow surface ( $T_s$ ) temperature, wind speed ( $V_w$ ) and direction ( $Dir$ ), relative humidity ( $RH$ ), and the difference between the air and snow temperatures ( $\Delta T$ ). Blank regions indicate that surface hoar was not observed at that location.

Event	Date	$LW$ W/m <sup>2</sup>	$T_a$ W/m <sup>2</sup>	$T_s$ °C	$V_w$ °C	$Dir$ m/s	$RH$ deg.	$\Delta T$ °C	$LW$ W/m <sup>2</sup>	$T_a$ W/m <sup>2</sup>	$T_s$ °C	$V_w$ °C	$Dir$ m/s	$RH$ deg.	$\Delta T$ °C	
A-1	01/24/2008	252	-13.1	-22.1	1.0	155	71	9.0	354	-10.5	-19.7	1.3	82	40	9.2	
A-2	02/15/2008	225	-11.1	-16.3	1.1	117	78	5.2								
A-3a	02/19/2008	217	-4.8	-15.3	1.2	142	54	10.5	376	-4.7	-11.5	1.4	76	51	6.8	
A-3b	02/20/2008								417	-0.9	-9.7	1.6	45	18	8.8	
A-4	02/22/2008	206	-8.2	-18.0	1.4	151	64	9.9	371	-6.6	-10.5	1.1	53	57	3.9	
A-5	02/26/2008	274	-8.8	-15.0	1.1	132	81	6.2	277	-9.8	-15.8	0.9	93	84	5.9	
A-6	03/10/2008	206	-7.6	-17.6	1.2	165	57	10.0	369	-7.5	-15.0	1.4	122	57	7.4	
A-7	03/30/2008	199	-15.9	-22.4	1.3	152	79	6.5	267	-15.9	-22.4	1.1	89	74	6.5	
B-1	01/23/2009	263	-5.7	-9.0	0.5	165	83	3.4								
B-2a	01/30/2009	226	-5.8	-12.4	1.5	105	72	6.6								
B-2b	01/31/2009	210	-6.4	-15.1	1.4	119	61	8.7								
B-3	02/04/2009	202	-6.2	-15.4	1.3	159	63	9.2								
B-4a	02/07/2009	<i>Surface hoar observed, data missing</i>														
B-4b	02/08/2009	<i>Surface hoar observed, data missing</i>								190	-7.1	-14.9	1.2	246	55	7.8
B-5a	02/13/2009	188	-14.0	-21.3	1.4	159	72	7.3								
B-5b	02/14/2009	193	-14.1	-20.8	1.2	155	69	6.7								
B-6	02/28/2009	175	-14.7	-22.4	1.3	159	75	7.7								
B-7	03/13/2009	317	-8.3	-17.5	1.3	134	50	9.2								

Table 3.3: Summary of the snow conditions for the layer underlying the surface hoar, as recorded in the field notes. Blank regions indicate that surface hoar was not observed at that location.

Event	Event Date	North: Description of Snow	South: Description of Snow
A-1	1/24/2008	1–3 mm stellars, plates	1 mm decomposing new snow
A-2	2/15/2008	stellars 2 mm, facets 0.5 mm	
A-3a	2/19/2008	0.5–1 mm decomposing stellar crystals	0.25x1 mm spaghetti chains
A-3b	2/20/2008		melt freeze/sun crust
A-4	2/22/2008	0.5–1 mm decomposing snow	moist melt freeze crust
A-5	2/26/2008	broken stellars 2–3 mm	rimed new snow, 2mm
A-6	3/10/2008	partly decomposed 1 mm	melt freeze crust (frozen/dry) 1.5 mm
A-7	3/30/2008	highly broken 0.25 mm	melt freeze crust
B-1	1/23/2009	0.5 mm decomposing	
B-2	1/30/2009	0.5–1 mm decomposing	
B-3	2/4/2009	1 mm rounds	melt freeze crust
B-4a	2/7/2009	2 mm new snow, 0.25 mm decomposing	
B-4b	2/8/2009	0.25 mm highly decomposed	melt-freeze (moist)
B-5a	2/13/2009	Decomposing stellars 0.5–1 mm	
B-5b	2/14/2009	0.5 mm decomposing and rounds	
B-6	2/28/2009	0.25 mm highly decomposed	
B-7	3/13/2009	1 mm highly decomposed particles	

### 3.4 2007/2008 Surface Hoar Events

#### 3.4.1 Event A-1: January 24, 2008

Surface hoar measuring 2–3 mm in height formed the between January 23 and 24, 2008 at the North Station; “decomposing surface hoar” 1–2 mm in size was recorded at the South location. Figure 3.1 is an image of the surface hoar from the North location; no images showing the surface hoar at the South station were captured. Figure 3.2 contains graphs of the weather data surrounding the event. At both locations the surface hoar formed on new snow. At the South the short-wave radiation was beginning to break down the crystals at the time of observation.

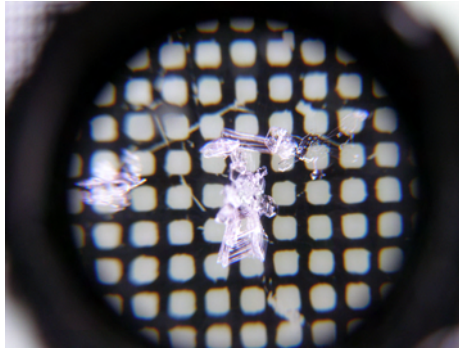


Figure 3.1: Image from event A-1 of surface hoar (1 mm grid) captured from the North Station on January 24, 2008.

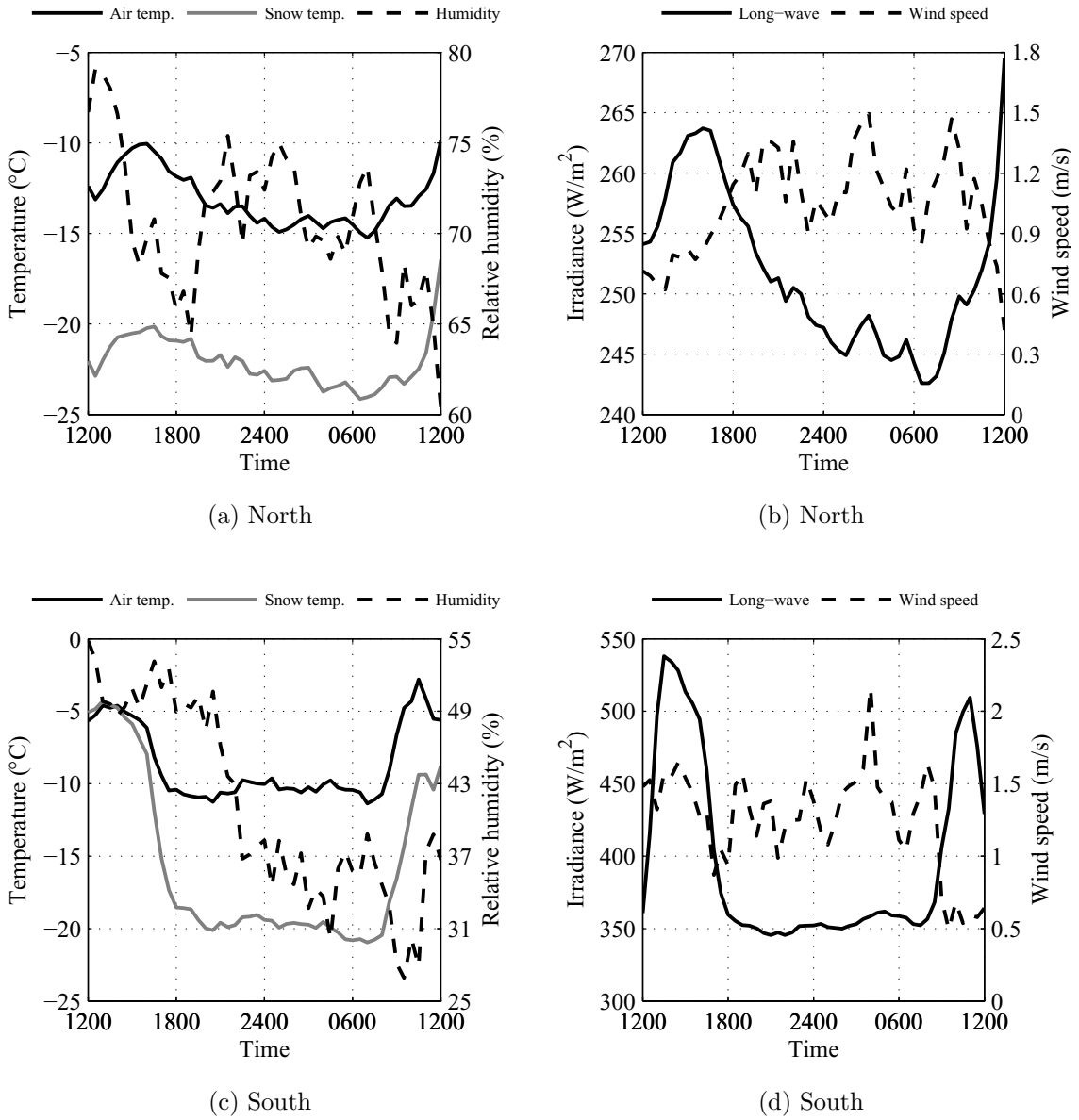


Figure 3.2: Weather data for event A-1 (January 24, 2008) recorded for both the (a,b) North and (c,d) South weather stations.

### 3.4.2 Event A-2: February 15, 2008

The second significant surface hoar event occurred on February 15, 2008 primarily at the North Station. The field notes from the South Station indicated that surface hoar was present, but only constituted “a very small percent of the surface snow,” thus it was assumed that the significant growth only occurred at the North Station. Figure 3.3 is an image showing the faceted surface hoar that developed on the stellar arms of new snow. The weather data from the North Station (Figure 3.4) indicates that the surface hoar likely began forming just after midnight, which is marked by a rapid decrease in incoming long-wave radiation and subsequent snow surface cooling.

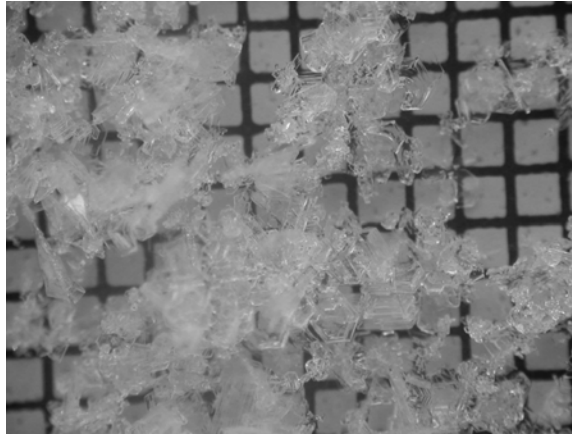


Figure 3.3: Image from event A-2 of surface hoar (1 mm grid) captured from the North Station on February 15, 2008.

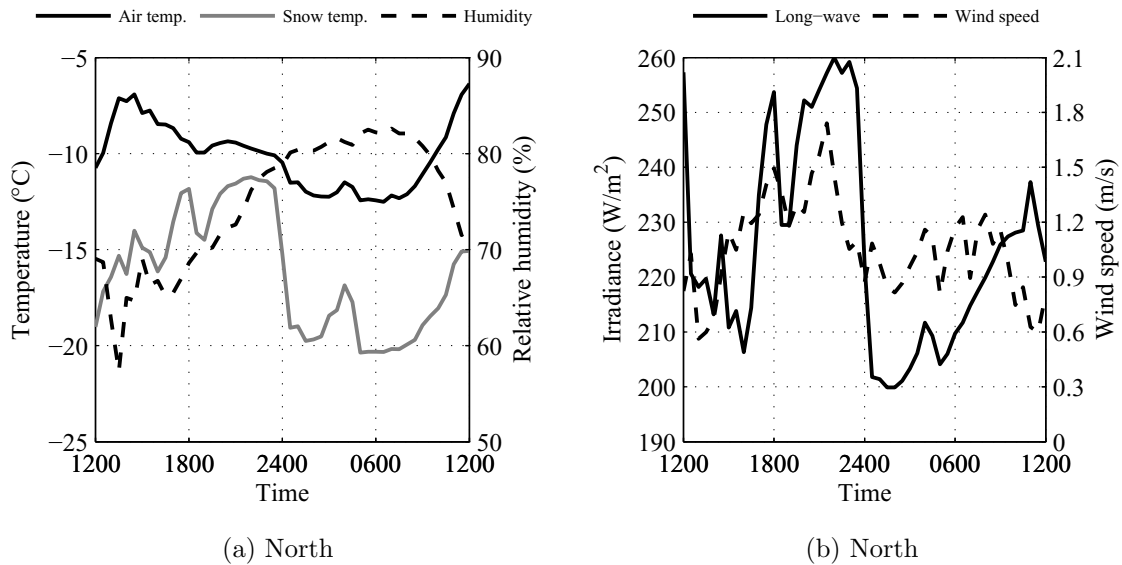


Figure 3.4: Weather data for event A-2 (February 15, 2008) recorded for the North weather Station.

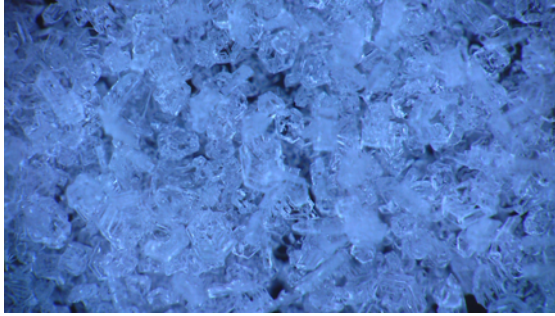
### 3.4.3 Event A-3: February 19–21, 2008

The field notes from the North Station indicated that small (0.5 mm) surface hoar formed in the night prior to the February 19, 2008 and persisted nearly unaltered until the following day, at which point it degraded. However, the surface hoar was still visible on the February 21. The field notes stated that the “snow appeared very similar to [the] previous two days, but had signs of having dried out.” The notes also indicated that surface hoar was observed at the South Station, but these crystals were intermingled with “spaghetti chains” of near-surface facets. Images from both stations on February 19 are provided in Figure 3.5 and the weather data from both stations is provided in Figures 3.6 and 3.7.

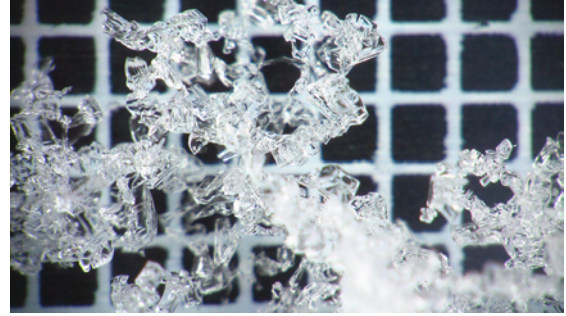
Interestingly, the field notes from the South Station on the February 20 stated that “surface hoar was barely attached to the crust below, suggesting [that] it [formed]



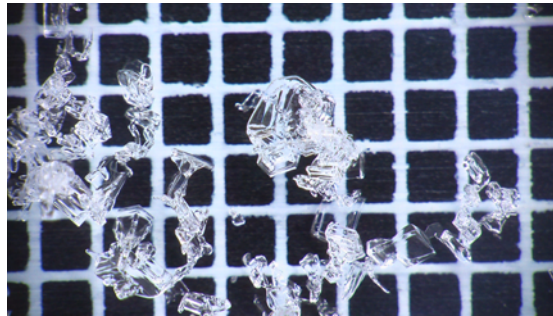
last night” since the surface hoar observed on the previous day was “well-linked to the crystal below it.”



(a) North: Feb. 19

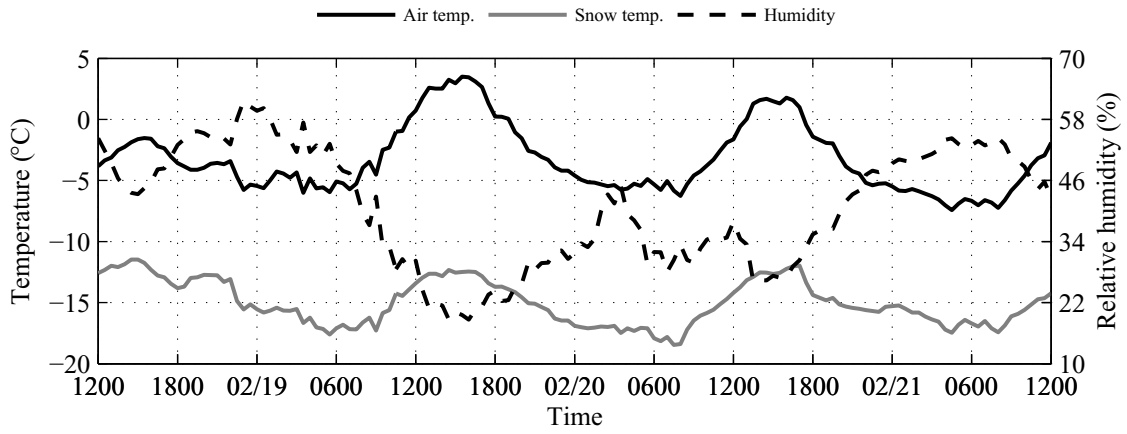


(b) South: Feb. 19 (1 mm grid)

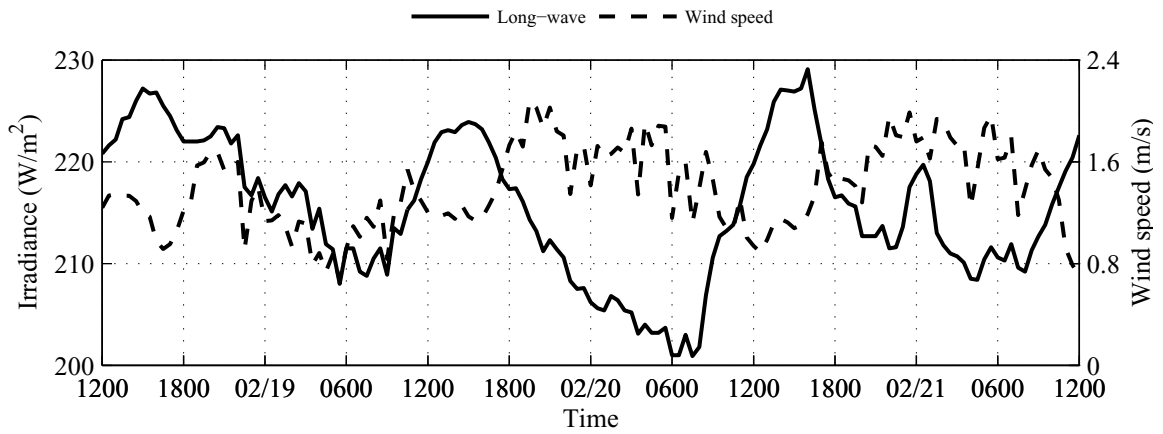


(c) South: Feb. 20 (1 mm grid)

Figure 3.5: Images from event A-3 of surface hoar captured from the (a) North and (b) South Stations on February 19, 2008 and surface hoar from the (c) South Station that was recorded on February 20.

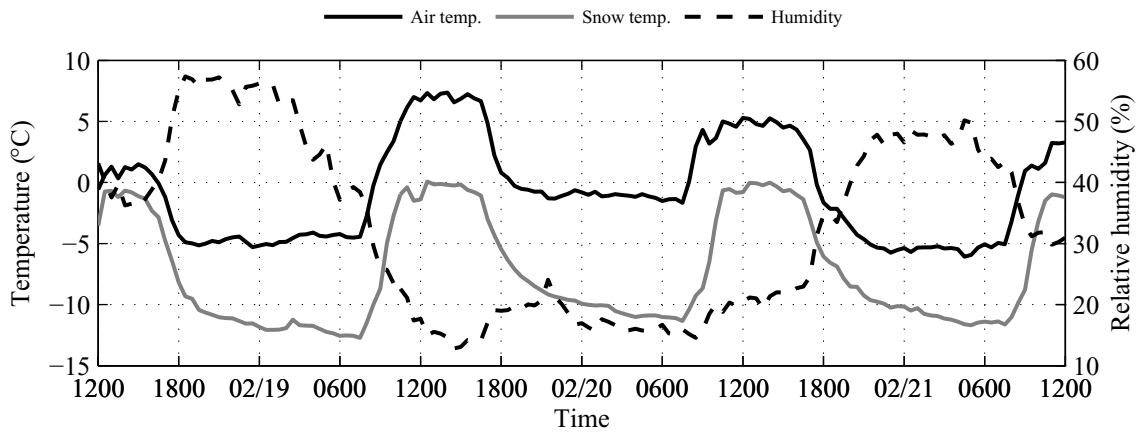


(a) North

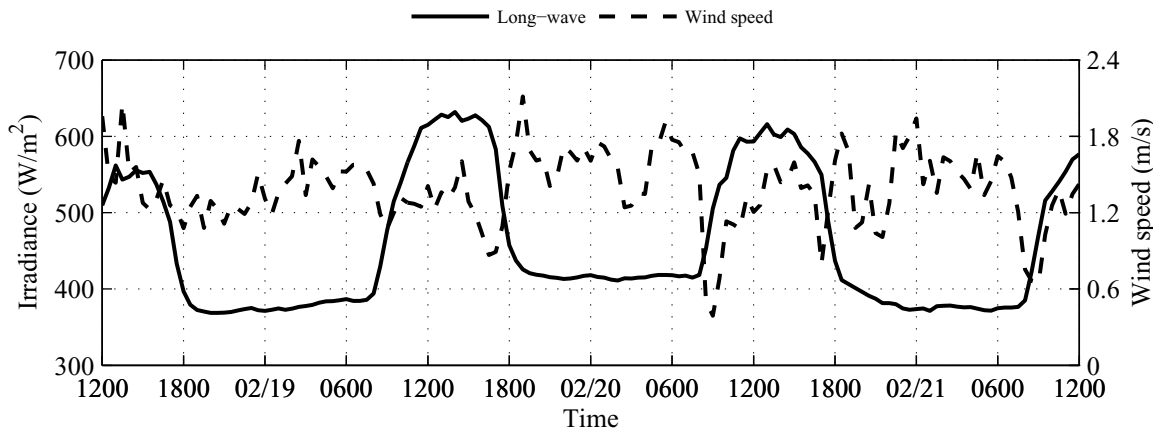


(b) North

Figure 3.6: North Station weather data for event A-3 (February 19–21, 2008).



(a) South

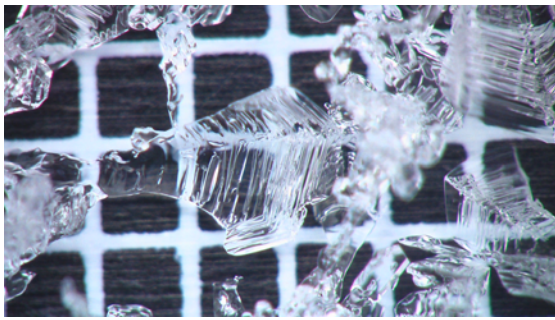


(b) South

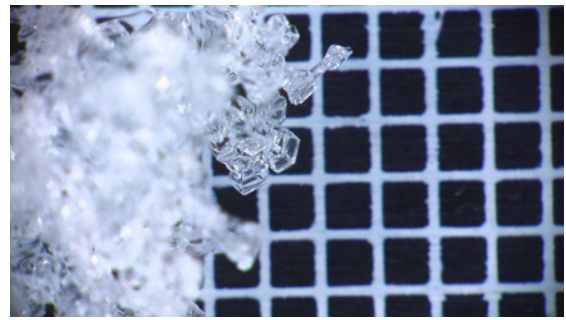
Figure 3.7: South Station weather data for event A-3 (February 19–21, 2008).

#### 3.4.4 Event A-4: February 22, 2008

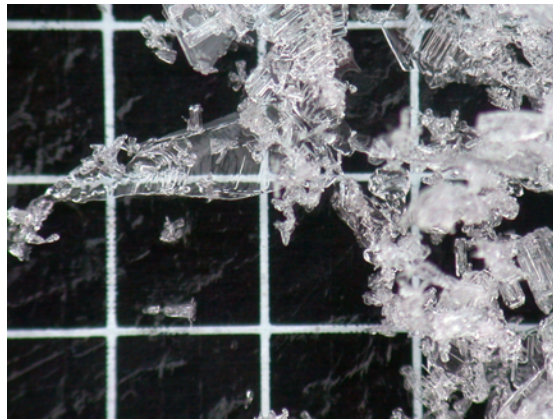
A widespread surface hoar event occurred on the night prior to February 22, 2008. Well-defined 1–2 mm surface hoar was observed at the North site. Smaller crystals were found at the South Station, which were growing on a “moist melt-freeze crust.” Images from February 22 for both sites are included in Figure 3.8 as well as an image of the surface hoar at the North Station the following day, after being buried under a few centimeters of new snow. The weather data for the night surrounding the formation is included in Figure 3.9.



(a) North: Feb. 22 (1 mm grid)



(b) South: Feb. 22 (1 mm grid)



(c) North: Feb. 23 (3 mm grid)

Figure 3.8: Images from event A-4 of surface hoar captured from the (a) North and (b) South Stations on February 22, 2008 and at the (c) North station the following day after the surface hoar was buried by new snow.

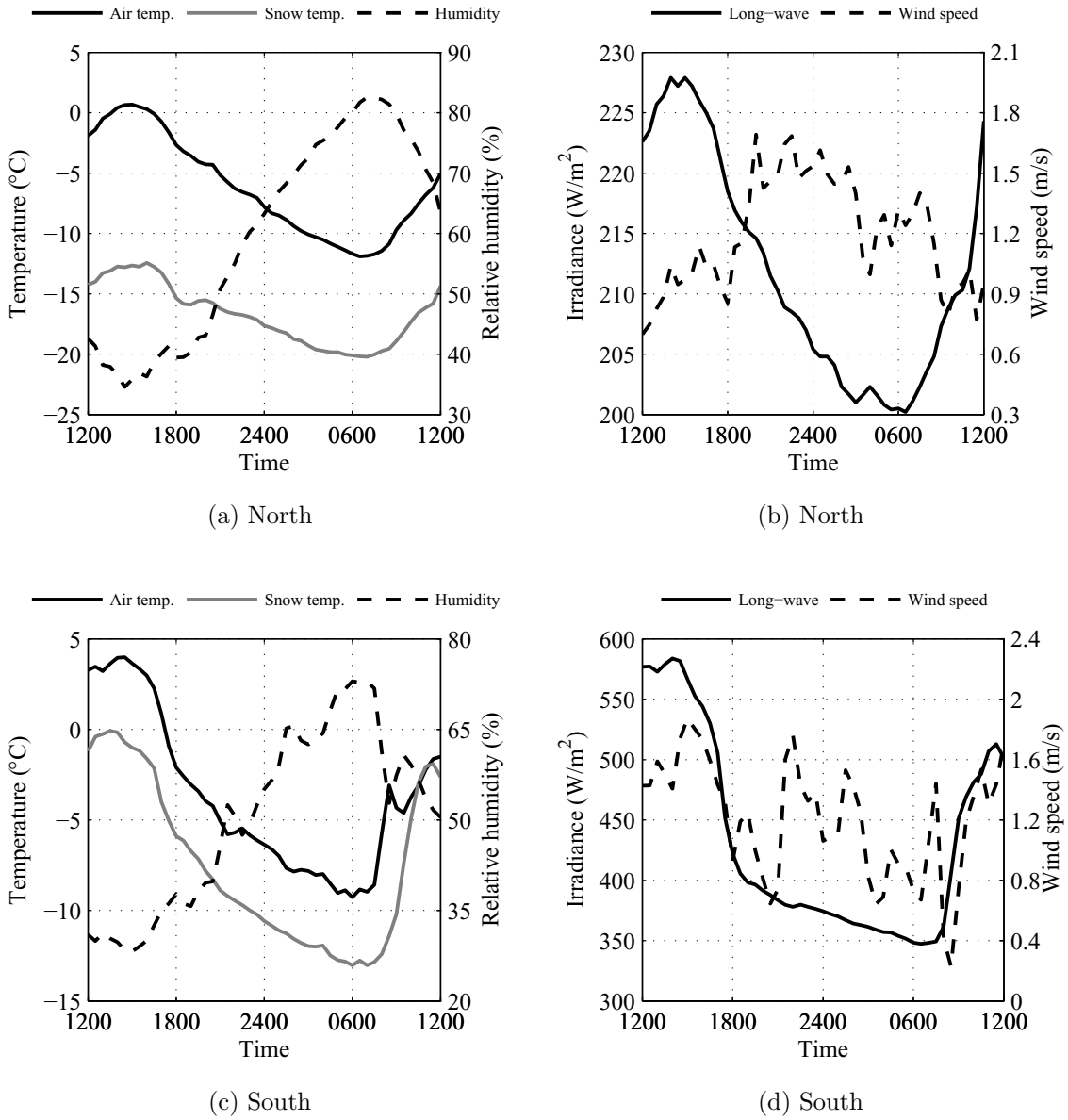


Figure 3.9: Weather data for event A-4 (February 22, 2008) for both the (a,b) North and (c,d) South weather stations.

### 3.4.5 Event A-5: February 26, 2008

Large surface hoar formed at both the North (4–8 mm) and South (2–4 mm) Stations the night prior to February 26, 2008. According to the field notes the surface hoar persisted at the North Station through the following few days, despite being buried by a few centimeters of new snow. Examples of these crystals are shown in Figure 3.10 and the weather data is provided in Figure 3.11.

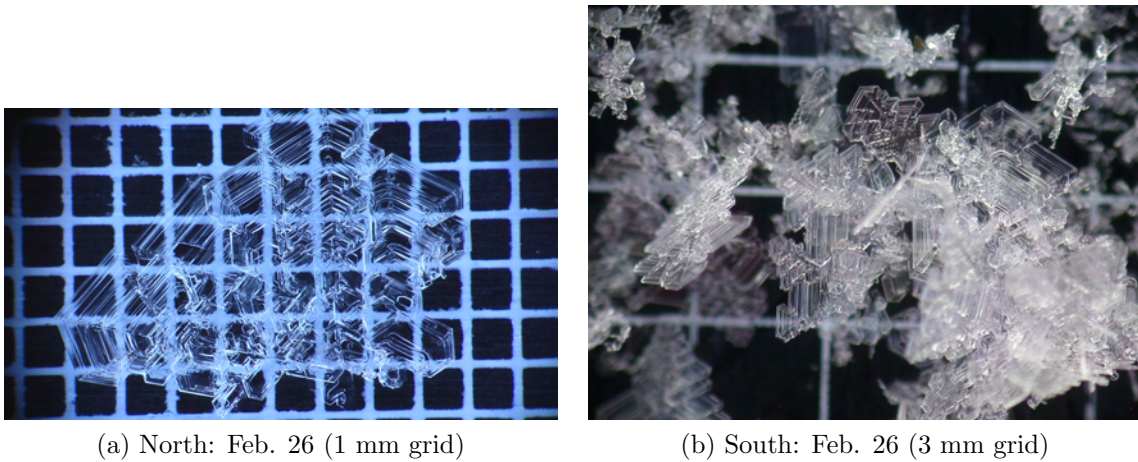


Figure 3.10: Images from event A-5 of surface hoar captured from the (a) North and (b) South Stations on February 26, 2008.



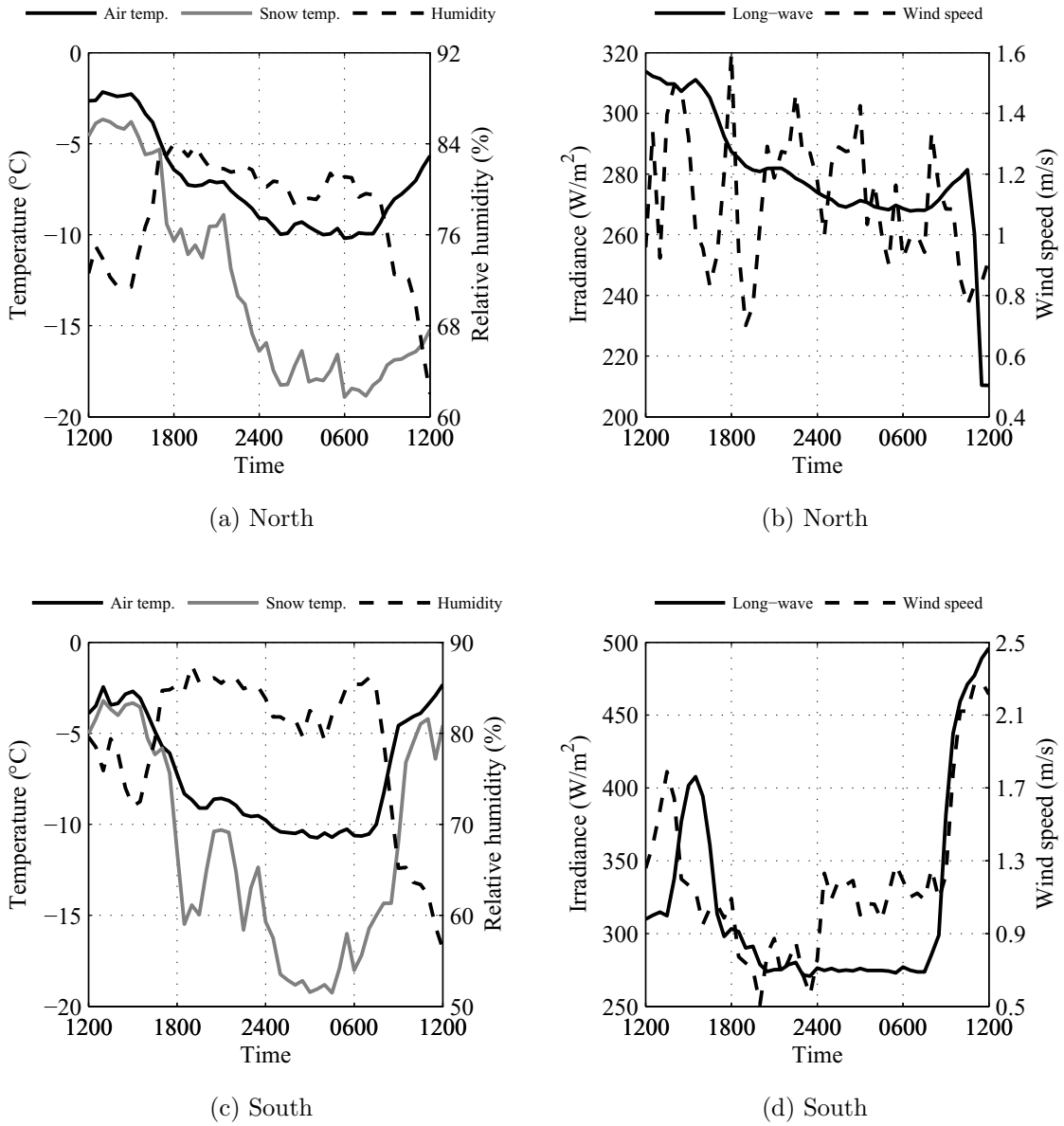
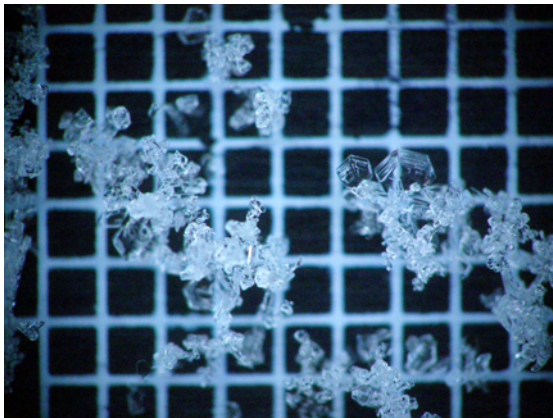


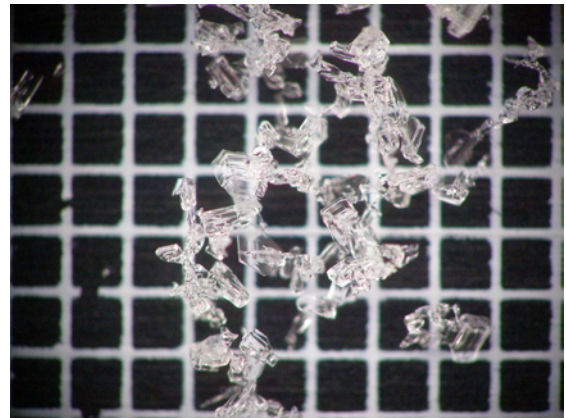
Figure 3.11: Weather data for event A-4 (February 26, 2008) for both the (a,b) North and (c,d) South weather stations.

### 3.4.6 Event A-6: March 10, 2008

On March 10, 2008 small (1 mm) surface hoar, as shown in Figure 3.12, was observed at both the North and South Stations. The weather conditions around this event were similar to many of the prior events and characterized by the snow temperature dropping upwards of 10 °C below the air temperature, see Figure 3.13. The surface hoar on the North site persisted to the following day, as the field log noted “0.5 mm decomposing surface hoar” on March 11.



(a) North (1 mm grid)



(b) South (1 mm grid)

Figure 3.12: Images from event A-6 of surface hoar captured from the (a) North and (b) South Stations on March 10, 2008.



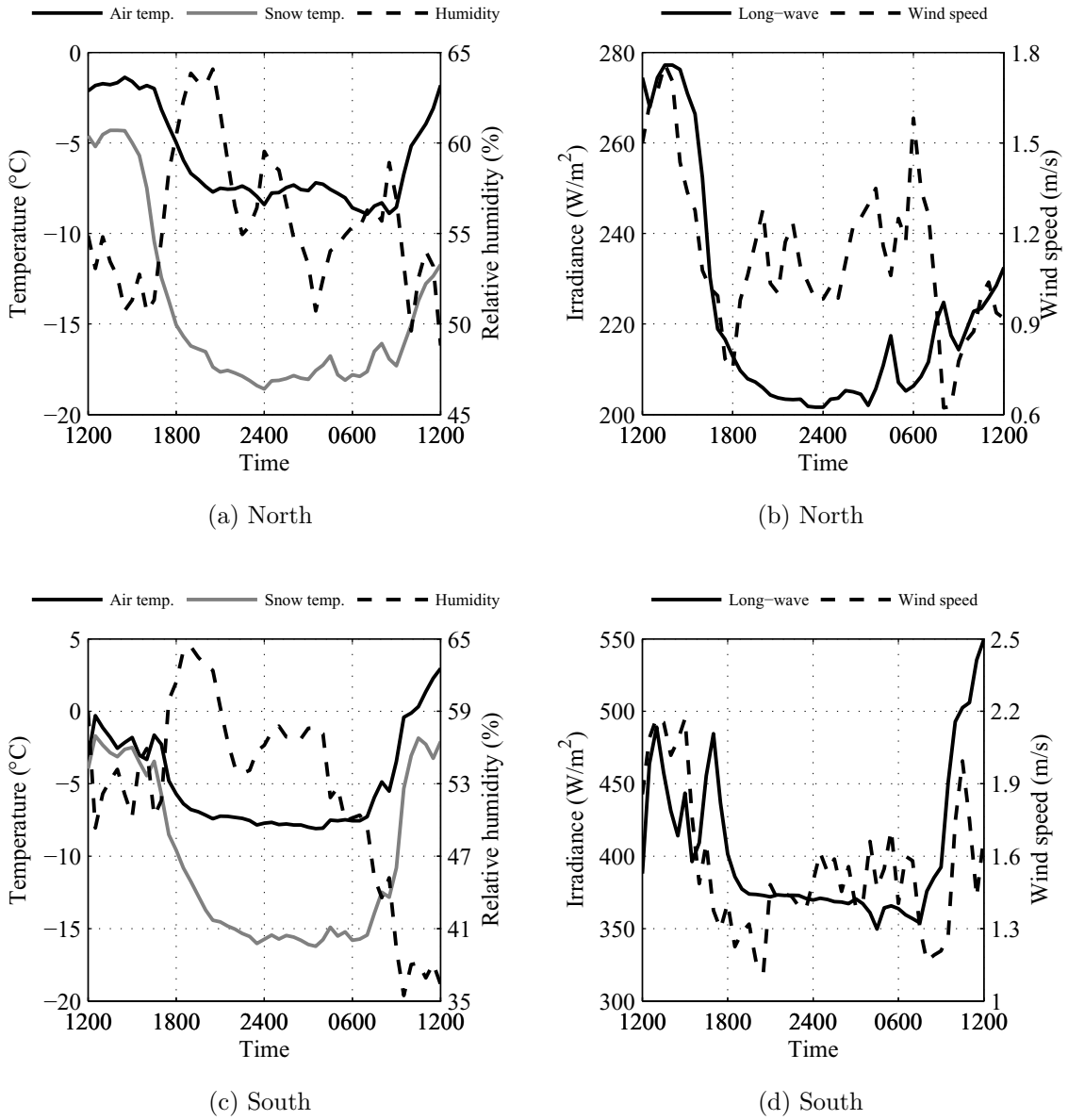


Figure 3.13: Weather data for event A-6 (March 10, 2008) for both the (a,b) North and (c,d) South weather stations.

### 3.4.7 Event A-7: March 30, 2008

The final significant surface hoar event of the 2007/2008 season occurred on the night prior to March 30, 2008, resulting in 1 mm and 0.3–0.5 mm crystals at the North and South stations, respectively. Images from both locations are included in Figure 3.14. The weather data surrounding the event is included in Figure 3.15. The field notes indicated that the crystals did not persist beyond the initial day of observation.

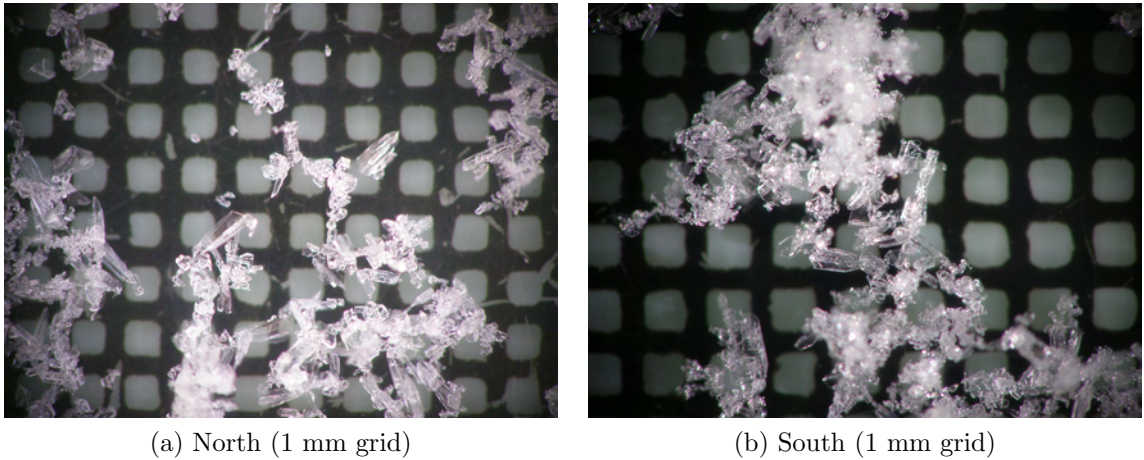


Figure 3.14: Images from event A-7 of surface hoar captured from the (a) North and (b) South Stations on March 30, 2008.

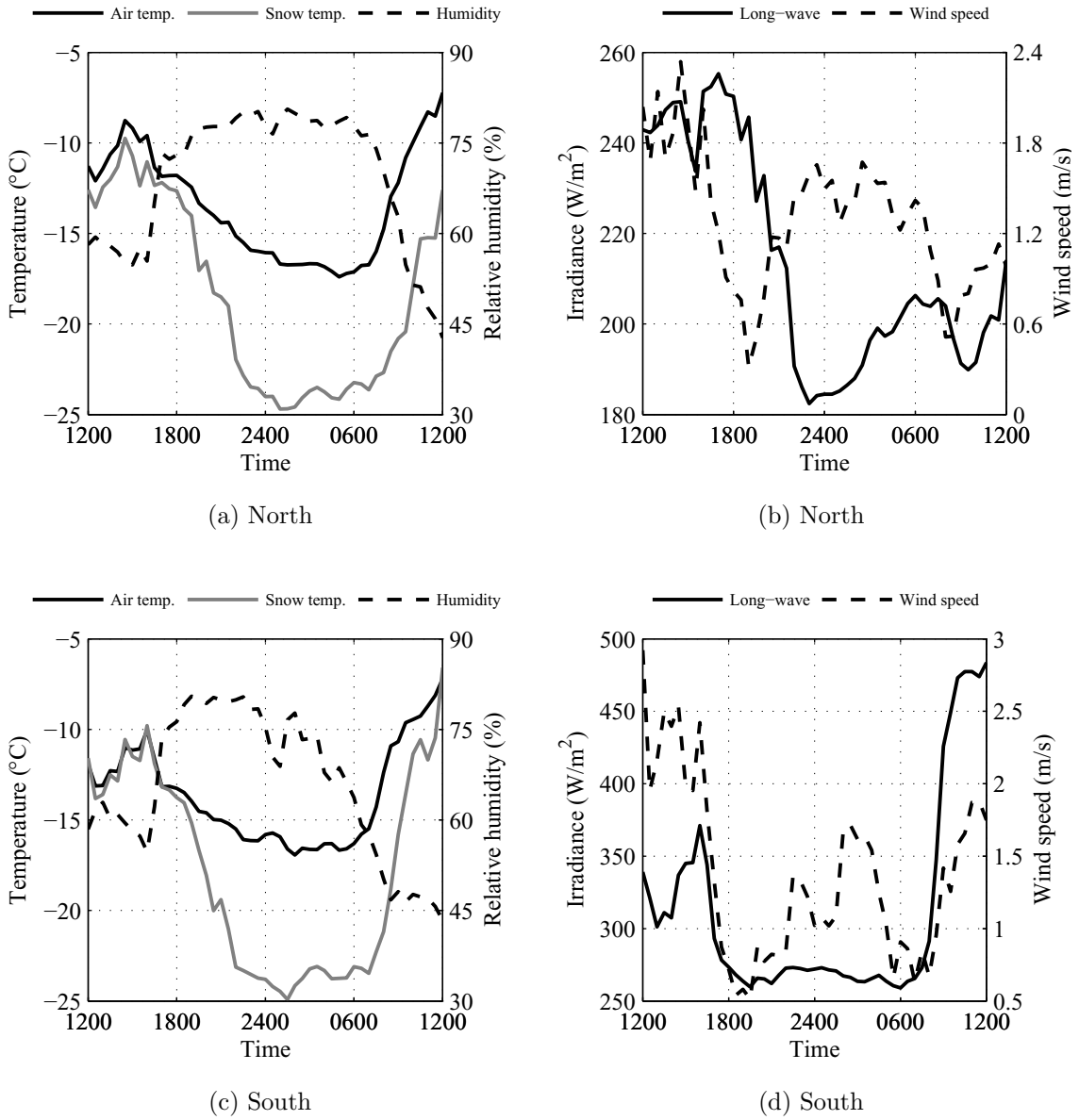


Figure 3.15: Weather data for event A-7 (March 30, 2008) for both the (a,b) North and (c,d) South weather stations.

### 3.5 2008/2009 surface hoar events

#### 3.5.1 Event B-1: January 23, 2009

The first surface hoar event of the 2008/2009 season resulted in 0.5–4 mm crystals developing the night between January 22 and 23, 2009, as shown in Figure 3.16. The field notes indicated that the surface hoar was 0.5 mm in size. However, the images indicated crystals as large as 4 mm. It is likely that these larger crystals were not as widespread, but photographed preferentially due to their size. The weather conditions from the North Station surrounding this event are provided in Figure 3.17. Note, this event occurred on the first full day of fully operational weather stations, thus the weather data that begins the previous day was not recorded.

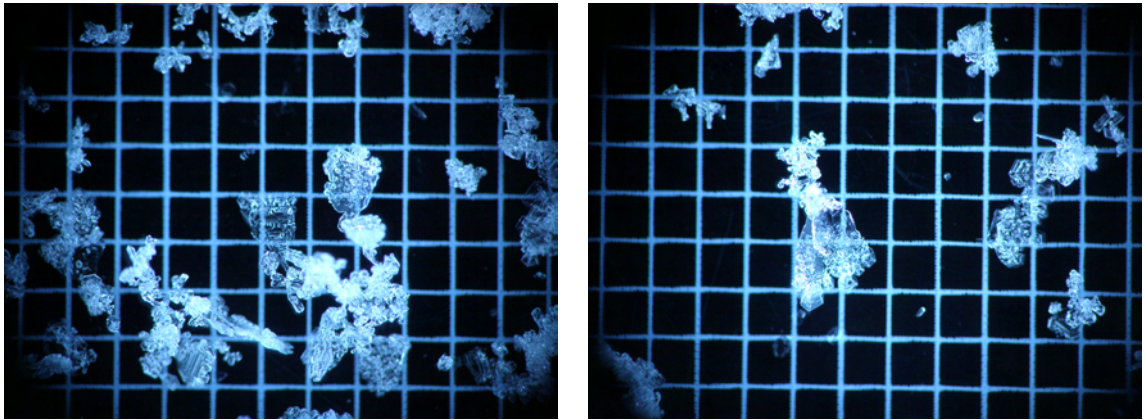


Figure 3.16: Images from event B-1 of surface hoar (2 mm grid) captured from the North Station on January 23, 2009.

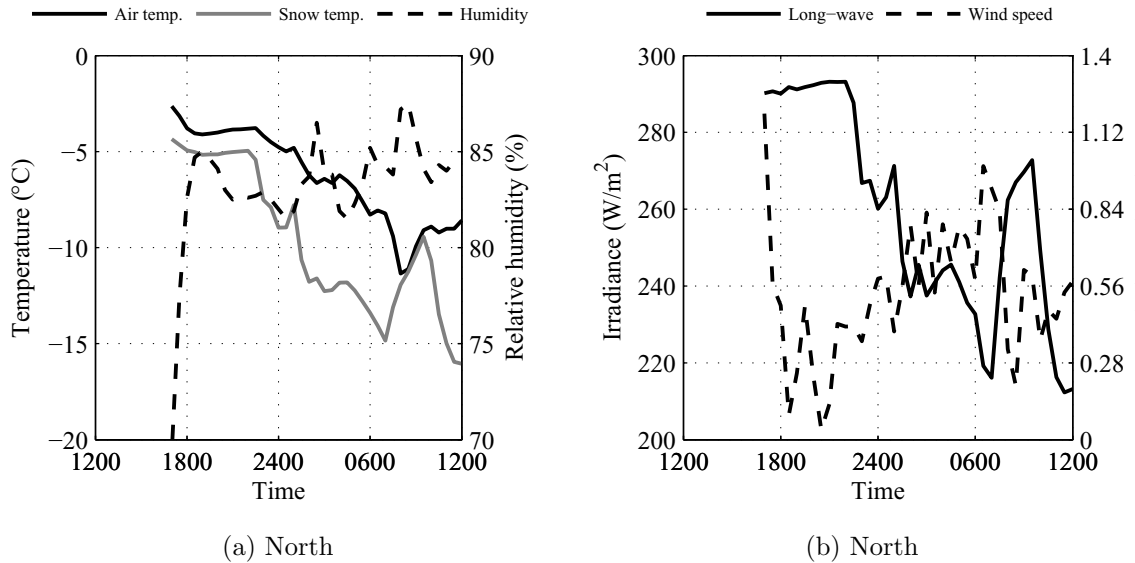


Figure 3.17: North Station weather data for event B-1 (January 23, 2009).

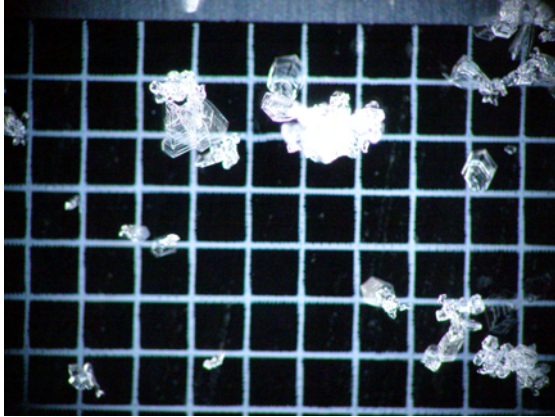
### 3.5.2 Event B-2: January 30–31, 2009

Event B-2 was a wide-spread surface hoar event that resulted in crystals forming at both the North and South Stations the night between January 29 and 30, 2009. The weather data from the North Station surrounding the event is included in Figure 3.19. The field notes from the North Station indicated 0.5 mm facets; however, the image in Figure 3.18 indicates that larger crystals existed. Interestingly, the images from the South Station show much larger and more pronounced surface hoar crystals than from the North, but only images from the South station were taken on this day. Also, the weather data from the South Station surrounding the event was absent due to a technical difficulty, thus the observation at this station cannot not be confirmed. An example of the well-defined surface hoar crystals is provided in Figure 3.18.

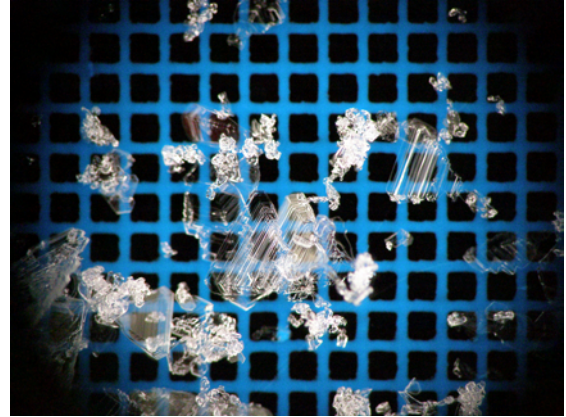
The surface hoar on the North site persisted and likely became larger the following night. The field notes for January 31 indicated 1 mm surface hoar. As shown in Figure 3.18, the crystals were more pronounced than previous day. The images from



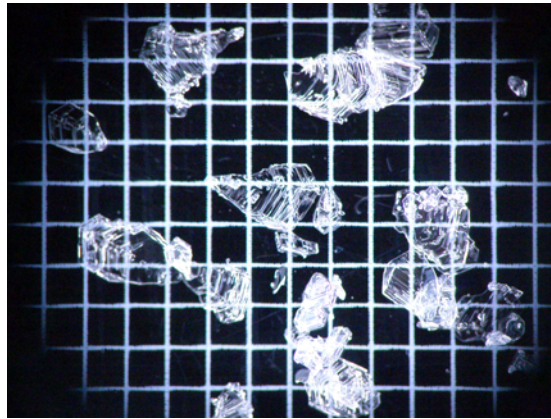
the South Station indicated that the surface hoar degraded, as it was not evident from in the images on the January 31.



(a) North: Jan. 30 (2 mm grid)



(b) South: Jan. 30 (1 mm grid)



(c) North: Jan. 31 (2 mm grid)

Figure 3.18: Images from event B-2 of surface hoar captured from the (a) North and (b) South Stations on January 30, 2009 and the (c) North Station on January 31, 2009.

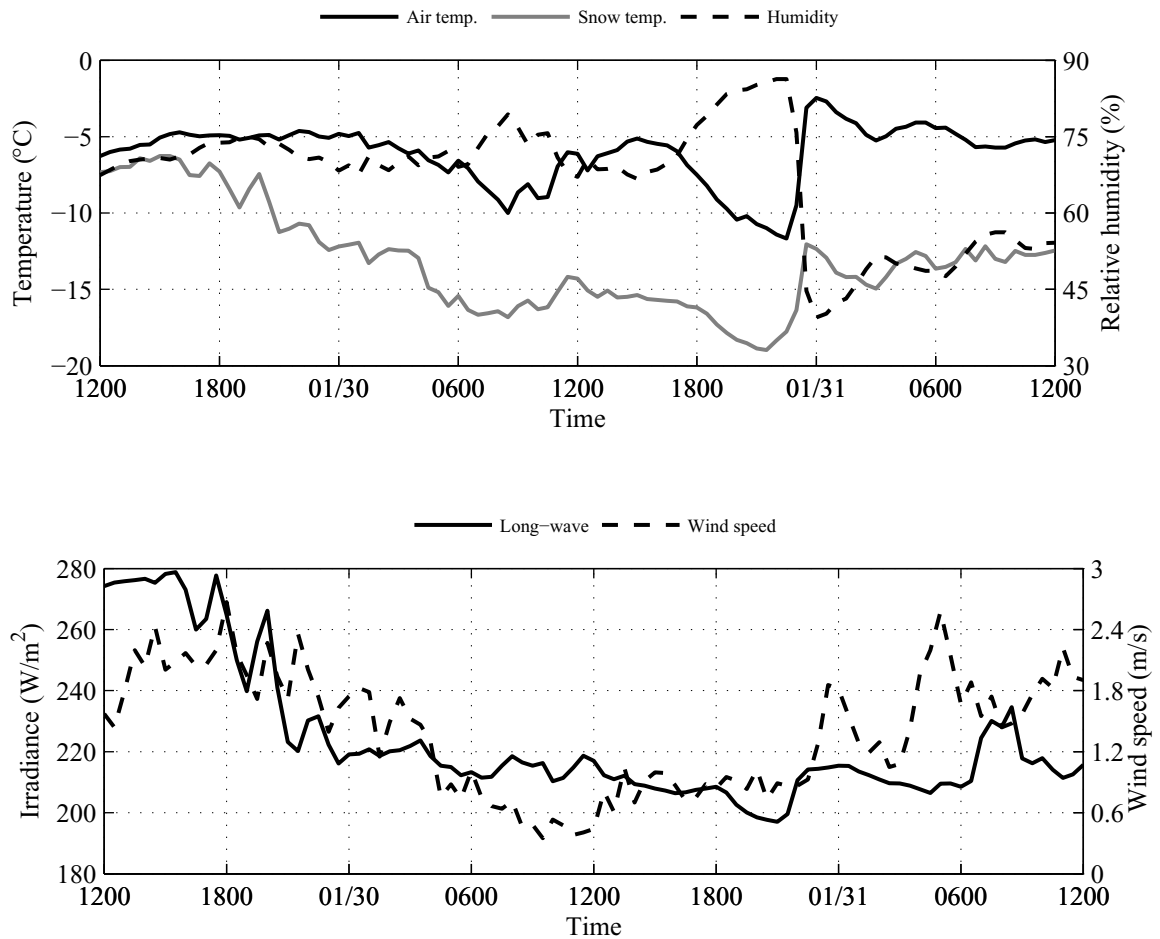


Figure 3.19: North Station weather data for event B-2 (January 30–31, 2009).

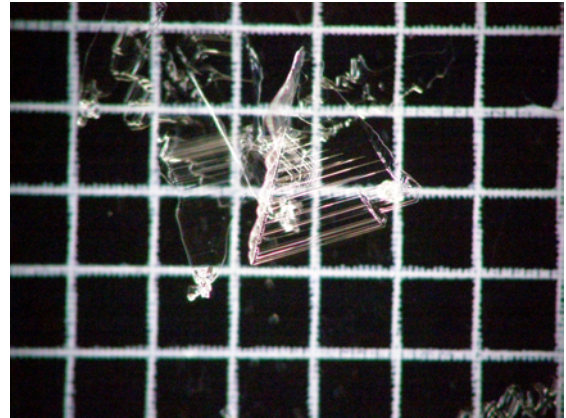
### 3.5.3 Event B-3: February 4, 2009

Large (5 mm) surface hoar developed at both the North and South Stations on February 4, 2009 as shown in Figure 3.20. At the North Station the surface hoar persisted to the following day (February 5), but was noticeably decomposing. No evidence of the crystals were reported in the notes after the February 5. At the South Station, the field notes indicated that facets were present, but it was unclear if these crystals were near-surface facets or decomposed surface hoar. Figure 3.21 includes the weather data for both the North and South Stations surrounding this

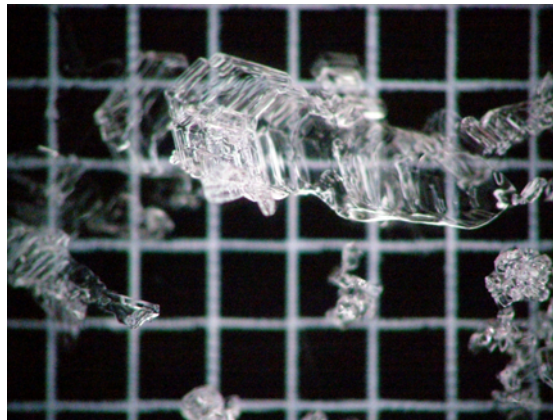
event. Unfortunately, as with the previous event, the weather data for the South Station was unavailable due to technical difficulties.



(a) North: Feb. 4 (2 mm grid)



(b) South: Feb. 4 (2 mm grid)



(c) North: Feb. 5 (2 mm grid)

Figure 3.20: Images from event B-3 of surface hoar captured from the (a) North and (b) South Stations on February 4 and (c) the North Station on February 5, 2009.



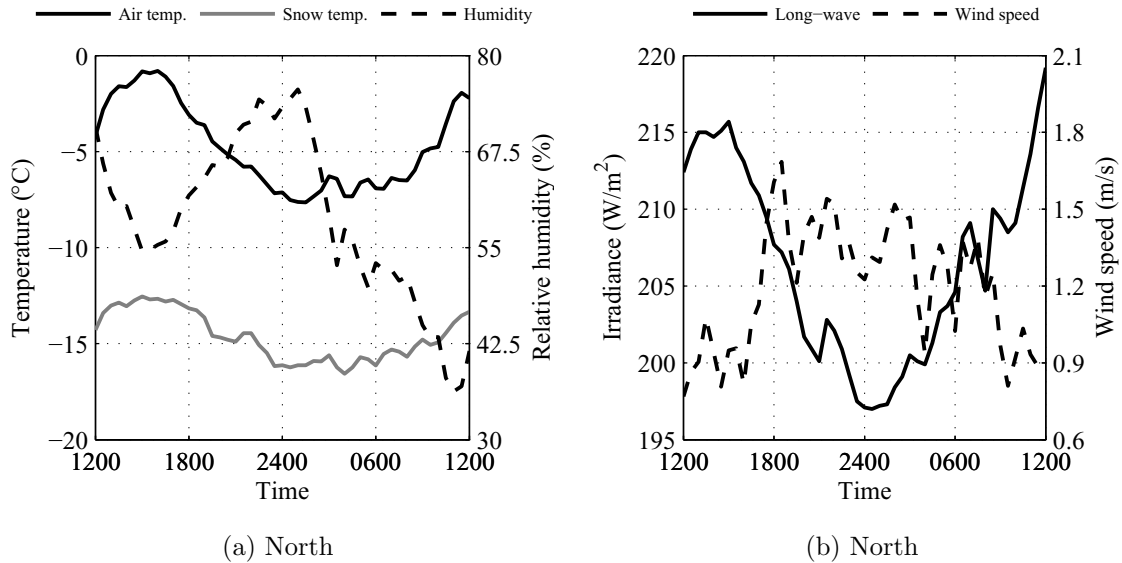


Figure 3.21: North Station weather data for event B-3 (February 4, 2008).

### 3.5.4 Event B-4: February 7–8, 2009

On February 7, 2009 1 mm surface hoar developed on new snow at the North station (Figure 3.22). No evidence of surface hoar was reported at the South station. On the following day, surface hoar was reported at both stations, 1 mm at the South and 5 mm at the North (Figure 3.22). The surface hoar from the North Station persisted through the February 8 and was visible underneath a few centimeters of new snow on February 9. On February 10, after 14 cm of new snow, no evidence of the layer was found in the snowpack. The weather data surrounding this event at the South Station is included in Figure 3.23. The weather data from the North Station is unavailable due to a battery failure during the event.

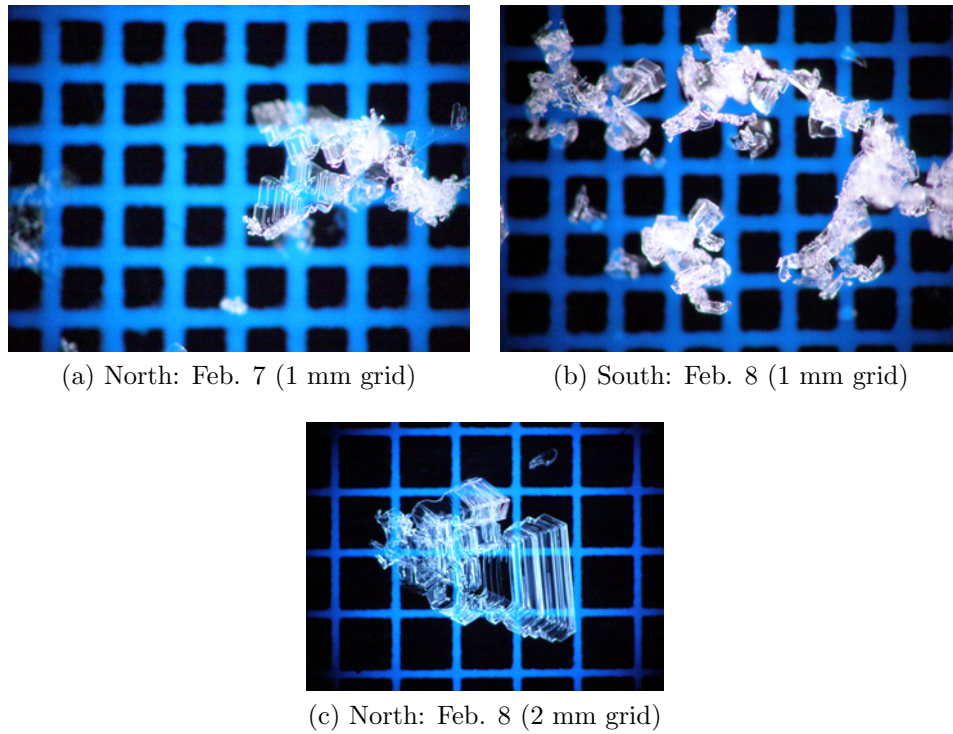


Figure 3.22: Images from event B-4 of surface hoar captured from the North and South Stations on (a) February 7 and (b,c) 8, 2009.

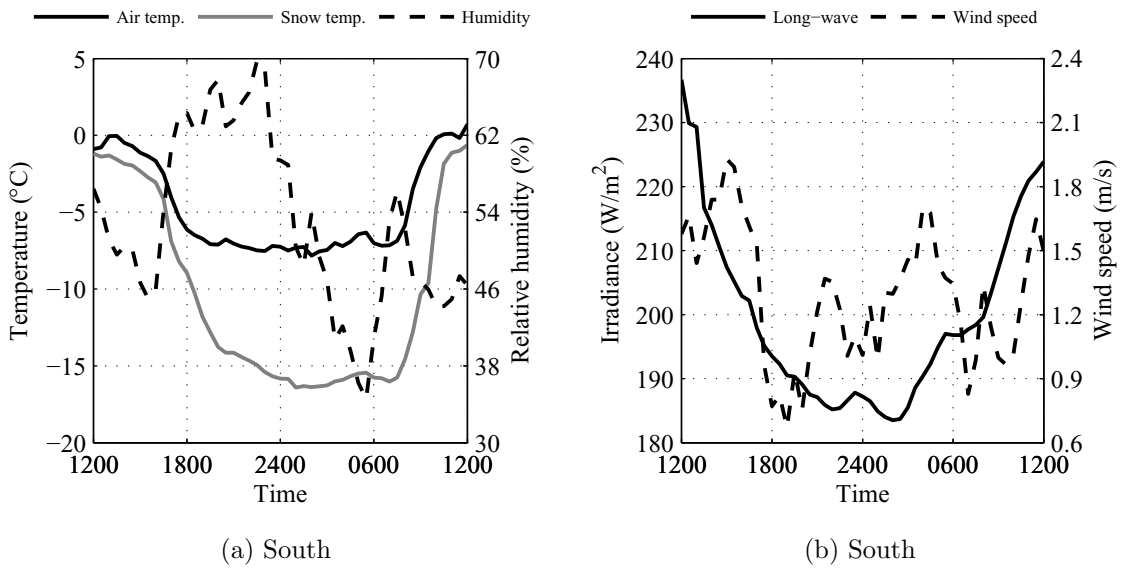


Figure 3.23: South Station weather data for event B-4 (February 7, 2009).

### 3.5.5 Event B-5: February 13–14, 2009

Surface hoar was reported at the North site on two consecutive days: February 13 and 14, 2009. On February 13, the surface hoar was reported as “[half] surface hoar and [half] decomposing stellars” 1 mm in size. The following day, February 14, the surface hoar was more pronounced and reported as 1.5 mm in size. Images from both days are included in Figure 3.24 and the weather data from the North site is included in Figure 3.25.

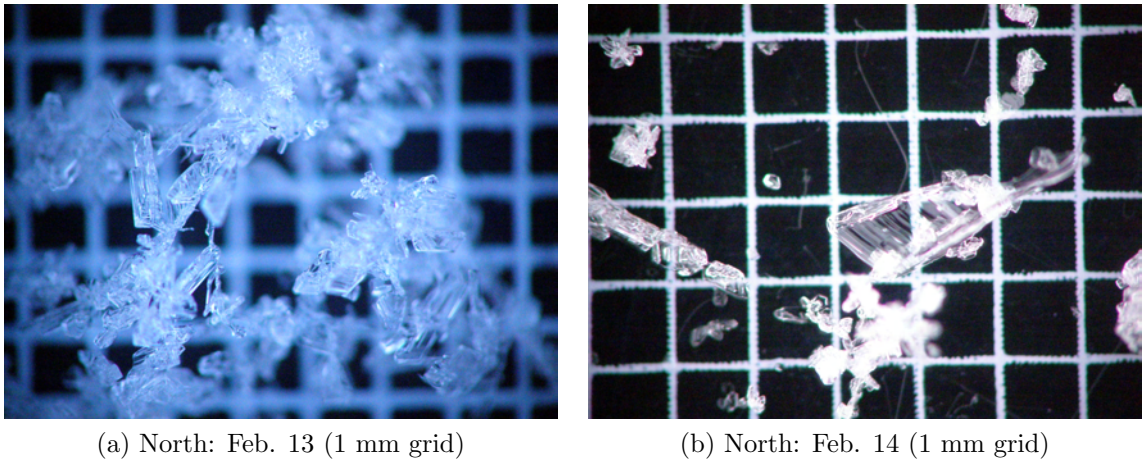


Figure 3.24: Images from event B-5 of surface hoar captured from the North Station on (a) February 13 and (b) 14, 2009.

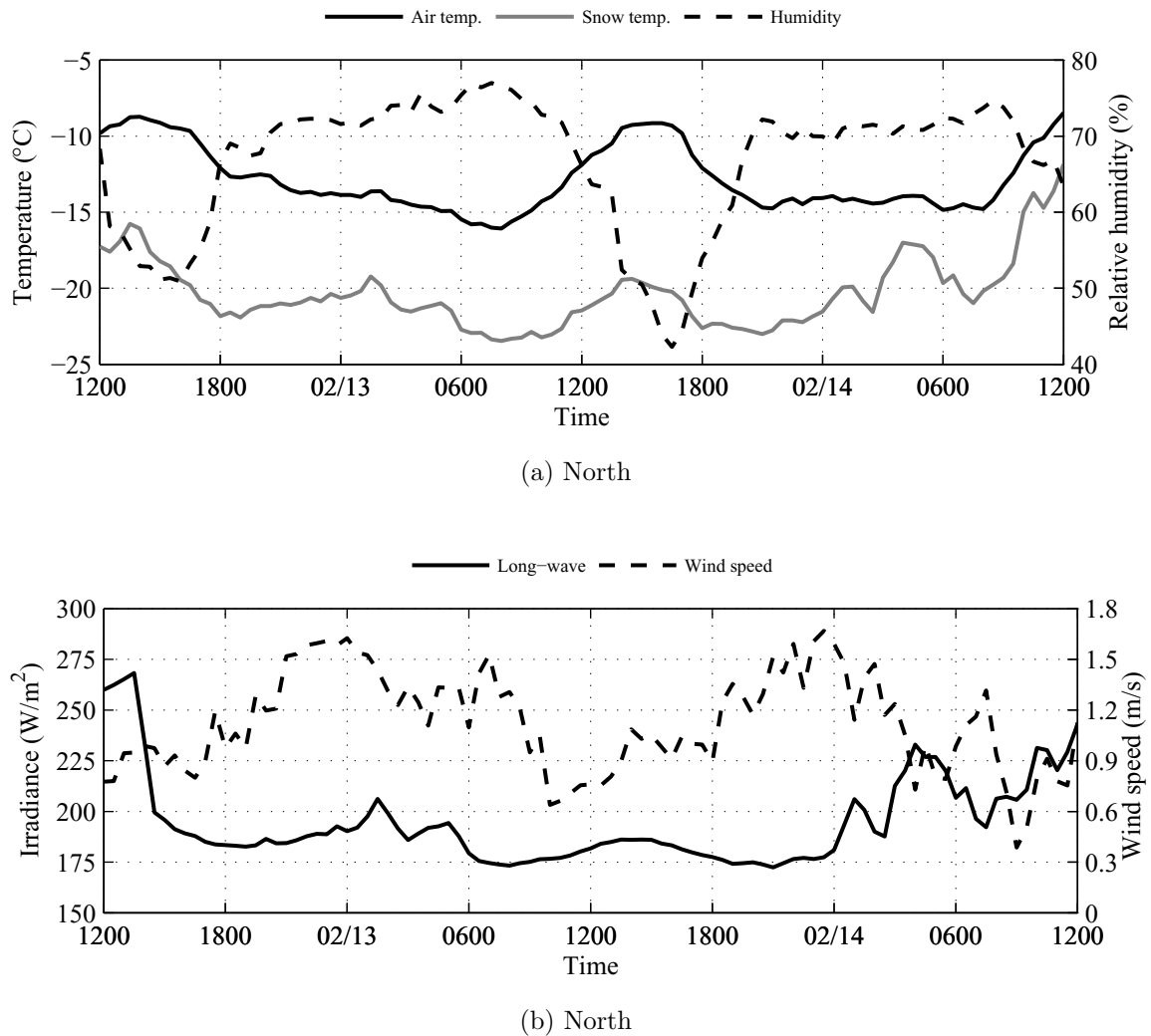


Figure 3.25: North Station weather data for event B-5 (February 13–14, 2009).

### 3.5.6 Event B-6: February 28, 2009

Surface hoar crystals 1.5 mm in size were reported at the North Station on February 28, 2009. These crystals persisted to the following day, but were reported to be “decomposing” on March 1. Images of crystals from these events are included in Figure 3.26 and the weather data surrounding the event is included in Figure 3.27.

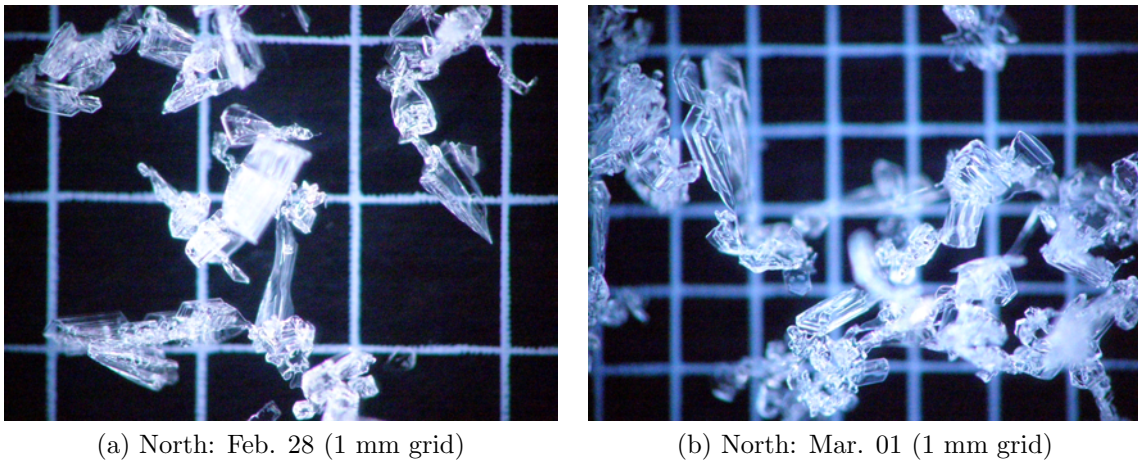


Figure 3.26: Images from event B-6 of surface hoar captured from the North Station on February 28, 2009.

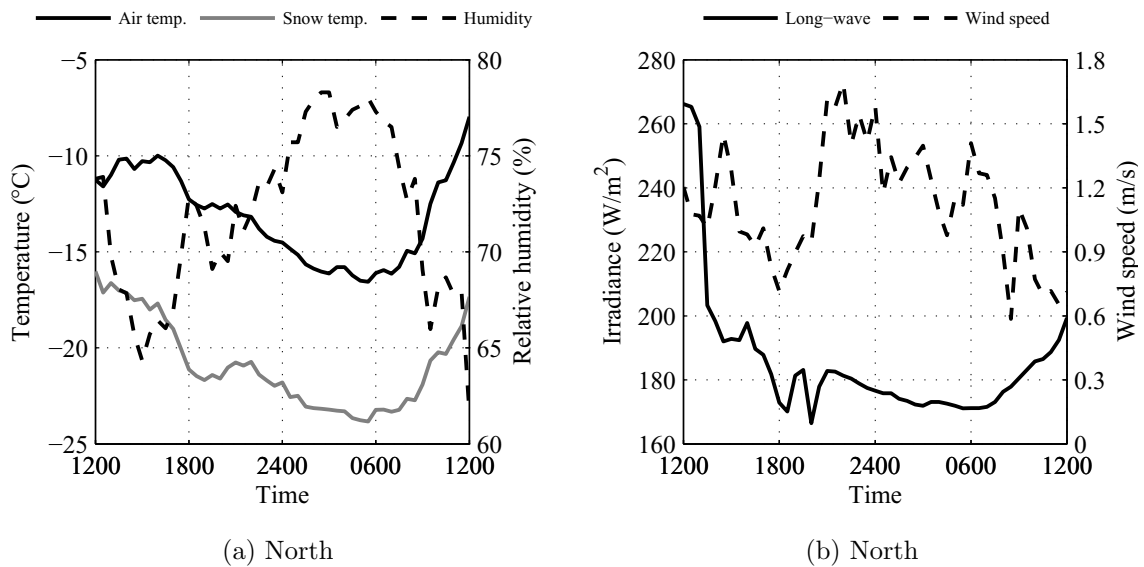


Figure 3.27: North Station weather data for event B-6 (February 28, 2009).

### 3.5.7 Event B-7: March 13, 2009

Small (0.5–1 mm) surface hoar, as shown in Figure 3.28, was reported at the North weather station on March 13, 2009. This was the final surface hoar event for the 2008/2009 season. The event only occurred at the North station and the surface



hoar did not persist beyond the observation date. The weather data surrounding this event is provided in Figure 3.15.

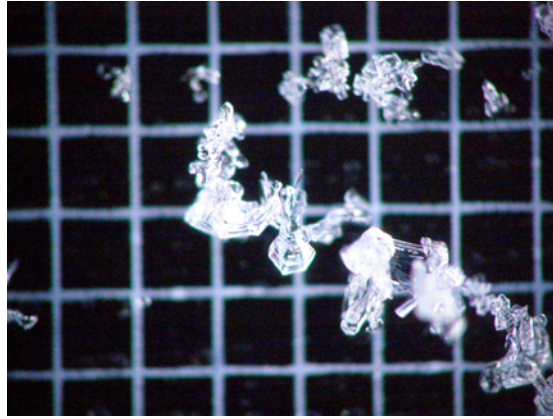


Figure 3.28: Images from event B-7 of surface hoar captured from the North Station on March 13, 2009.

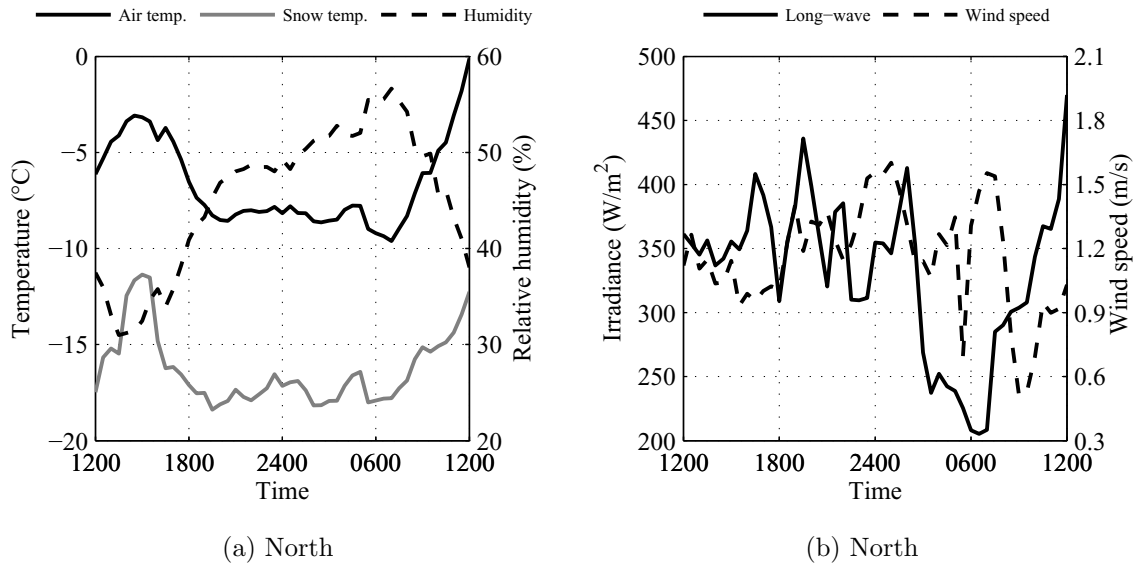


Figure 3.29: Weather data for event B-7 (March 13, 2009) for the North Station.

### 3.6 Analysis

The data presented in this chapter was used to assess the weather conditions that lead to the formation of surface hoar. First, the data from both stations was combined into a single set. This was performed primarily due to the small number of surface hoar events that occurred, which would make statistical analysis difficult if the values were not combined. Next, the mean nightly averages from each event (Table 3.2) were compared to the nightly averages from each day recorded during the two seasons at both stations.

Histograms showing all the measured data, with the surface hoar events superimposed, are included Figure 3.30 and 3.31. The thickness of the histogram bar for the North and South sites provides the frequency. For example, the bar above the 200 W/m<sup>2</sup> tick mark in Figure 3.31 indicates that the North site includes 8 events and the South 1 event. The height of the all data provides the actual frequency.

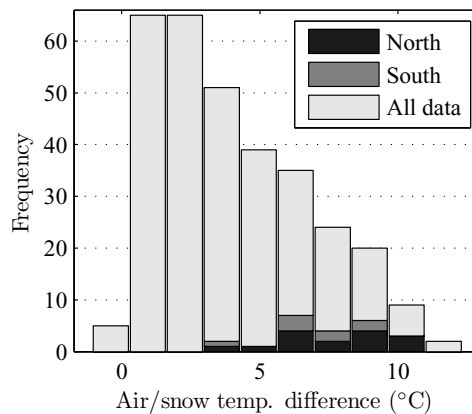


Figure 3.30: Histogram comparing the daily average air/snow temperature difference for the entire season (all data), along with the days associated with surface hoar events at either the North or South Stations.

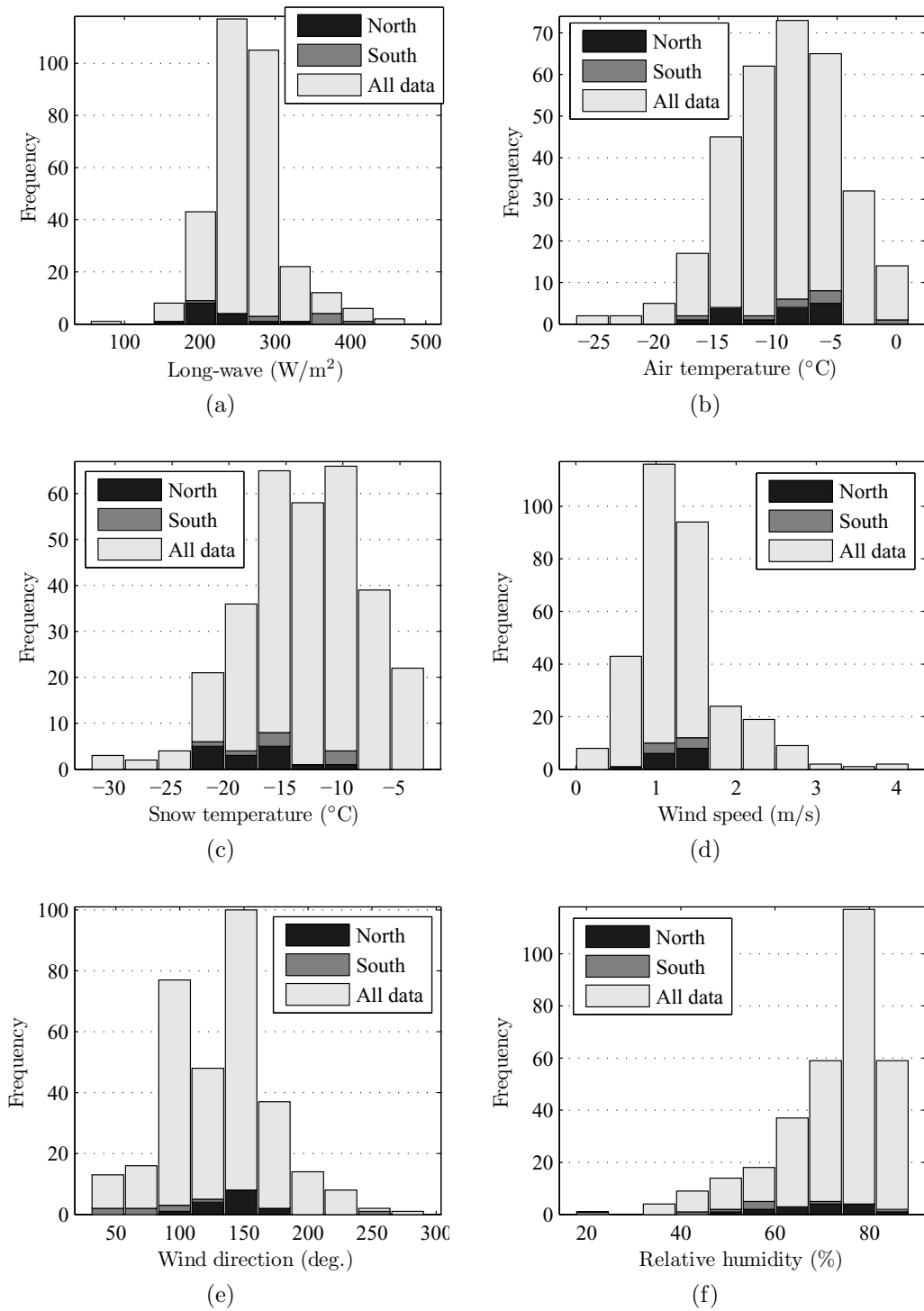


Figure 3.31: Histograms comparing the frequency of recorded daily average weather conditions at both the North and South Stations (all data), along with the days associated with surface hoar events observed at the North or South Stations.



Using a Kolmogorov-Smirnov test (KS-test), the two distributions—all days and event-only days (i.e., days when surface hoar was observed)—were compared (Massey, 1951). The test provided a means for determining if the two data sets were from the same distribution. The results of these comparisons are provided in Table 3.4, where the null hypothesis ( $H_0$ ) was that the two data sets were from the same distribution at the 5% significance level. The hypothesis test stated that  $p$ -values less than 0.05 (i.e., 5% significance level) would result in a failure to reject the null hypothesis, meaning that the distributions were likely different.

Table 3.4: Kolmogorov-Smirnov test results comparing the distributions set shown in Figures 3.31 and 3.30; the null hypothesis ( $H_0$ ) was that the data are from the same distribution.

Figure	Variable	$H_0$ result	$P$ -value
3.31a	Long-wave	reject	0.01
3.31b	Air temperature	fail to reject	0.84
3.31c	Snow temperature	reject	$2.17 \times 10^{-3}$
3.31d	Wind speed	fail to reject	0.19
3.31e	Wind direction	fail to reject	0.94
3.31f	Relative humidity	reject	0.02
3.30	Air/snow temp. difference	reject	$1.28 \times 10^{-7}$

The results from the K-S test indicated that incoming long-wave radiation, snow surface temperature, relative humidity, and air/snow temperature difference likely originate from different distributions. Thus, it is assumed that these factors are related to the formation of surface hoar. Surprisingly, considering the body of research discussing its importance, wind speed was not one of the these factors. This is likely an artifact of the weather station locations, which typically had wind speeds from 1–2 m/s (see Figure 3.31d). These values are within the range typically reported as necessary for surface hoar formation (Linkletter and Warburton, 1976; Hachikubo and Akitaya, 1997; Feick *et al.*, 2007).

The event-only distributions deemed significant via the KS-test were used to assign a range of “optimum” conditions for surface hoar development. Using the Bootstrap Method (Efron and Tibshirani, 1993), the percentiles of the empirical distribution function for each event-only result were developed and presented in Table 3.5. The percentiles are a simple quantification of the distribution. For example, referring to Table 3.5, the 10% percentile of long-wave radiation is 190 W/m<sup>2</sup>, which means that 90% of the observed events had a higher value of incoming long-wave radiation. If a normal distribution is assumed, the percentiles are proportional to the probability, i.e., the 50% percentile would be the most probable for the formation of surface hoar. Also, assuming a normal distribution, 68.2% of the data fits between the 15.9 and 84.1 percentiles, which is one standard deviation.

Table 3.5: Percentiles of environmental variables coupled to the formation of surface hoar.

Variable	Units	10%	20%	30%	40%	50%	60%	70%	80%	90%
Long-wave	W/m <sup>2</sup>	190	199	208	220	238	261	291	332	369
Snow temperature	°C	-22.0	-20.8	-19.1	-17.4	-16.2	-15.3	-14.5	-13.0	-10.9
Relative humidity	%	45	53	57	61	65	70	73	77	81
Air/snow temp. difference	°C	5.0	6.1	6.6	7.0	7.5	8.1	8.7	9.2	9.7

Cooperstein *et al.* (2004) detailed two surface hoar events that occurred at the same locations used for the data presented in this chapter, where minimum snow surface temperatures were reported as -15.1 and -14.2 °C for the North site and -11.1 and -12.5 °C at the South Station. Mean values for the night were not reported by Cooperstein *et al.* (2004), but the minimum value in many of the events reported in this chapter was representative of the mean (i.e., the snow surface temperature remained relatively constant through the night). The values from the North fell near the 70<sup>th</sup> and 80<sup>th</sup> percentile, which is within one standard deviation. Thus these values match well with the events presented in this chapter. The South temperatures

lie between the 80<sup>th</sup> and 90<sup>th</sup> percentiles, which indicate that surface hoar formation is less probable at the South site than at the North. These results are expected for two reasons. First, if Figure 3.31c is examined, the snow temperatures from the South events tended to occur at slightly warmer temperatures. Secondly, Cooperstein *et al.* (2004) concluded that the surface hoar at the South Station was less developed than at the North station, which indicated that the conditions are less favorable for development.

A similar analysis to the above may be performed using two surface hoar events recorded in Japan (Hachikubo and Akitaya, 1996), which identified two multi-day surface hoar events. The average snow surface temperatures for the five nights reported were one of three temperatures: -12, -14, and -16 °C. These values are within the range defined in Table 3.5 and the -16 °C value reported corresponds with the most probable temperature for surface hoar formation defined by the data set presented in this chapter.

### 3.7 Future Considerations

The results presented in both this chapter as well as in Chapter 4, which covers near-surface facets, show that surface hoar and near-surface facets often occur in conjunction with each other. Nearly 60% of the dates summarized in Table 3.2 occurred the night before or after a near-surface event reported in Table 4.2. For example, on February 14, 2008 near-surface facets were observed (C-2) the day following 1 mm surface hoar (A-2). Similarly, on March 10, 2009 surface hoar was observed (C-6) followed by the observation of near-surface facets on the snow surface (A-6) that same day. This relationship is also evident in one of the surface hoar events described by Cooperstein *et al.* (2004) at the same locations. To the author's knowledge, no

other investigation has shown this relationship. As such, it should be the topic of future investigations.

### 3.8 Conclusion

Throughout two seasons, 2007/2008 and 2008/2009, 14 surface hoar events were observed at north- and south-facing weather stations. Four parameters—incoming long-wave radiation, snow surface temperature, relative humidity, and the air/snow surface temperature difference—were shown to be the weather factors important to the formation of surface hoar. The analysis of the data defined the following optimum conditions for surface hoar formation for each of the aforementioned factors, respectively: 190–270 W/m<sup>2</sup>, -22 to -11°C, 45–80%, and 5-10 °C.

The ranges developed in this chapter may be used as one tool among many for determining if surface hoar growth is likely based on weather data. However, the data presented was developed from only two locations on the same mountain and only for two seasons of data, thus increasing the data set would likely provide a more reliable tool. This project is ongoing therefore the data set will be expanding. The methodology presented herein may be easily applied, thus forecasting agencies with reliable weather data and daily observations of the snow surface could perform a similar analysis and build probability charts for their own region.

## CHAPTER 4

### FIELD INVESTIGATION OF NEAR-SURFACE FACETS

#### 4.1 Introduction

Dry slab avalanches cause extensive property damage and fatalities each year throughout the world. A majority of these avalanches slide on a weak layer that was formed at or near the snow surface and were subsequently buried (Schweizer and Lutschg, 2001; Birkeland, 1998). Specifically, near-surface facets—a layer that forms at or near the snow surface due to temperature gradients—accounted for 59% of avalanches in a case study in Southwest Montana (Birkeland, 1998), which is also the location of the field investigation presented herein. Chapter 2 includes a review of the of the body of literature discussing the conditions leading to near-surface facet development.

#### 4.2 Methods

A discussion of the methods used for this investigation are provided in the methods section of Chapter 3 and a complete discussion of the instrumentation is included in Appendix A. for the sake of brevity, the details are not repeated. However, it should be noted that Chapter 3 is a discussion of surface hoar that almost exclusively develops at night. Thus, the short-wave radiation was not considered. As short-wave radiation is crucial to the formation of near-surface facets, the focus of this chapter, two items related to the short-wave radiation need to be mentioned: solar contamination of long-wave radiation and short-wave radiation sensor orientation.

Long-wave radiation data from the 2007/2008 season at the South Station is considered unreliable due to solar contamination—a problem discussed by Albrecht and

Cox (1977)—associated with the instruments used, the Eppley Lab Inc., PIR. The PIR sensor measures the incoming long-wave radiation, but the protective dome and the case of the instrument also contribute to this value when their temperatures differ from that of the sensor itself. Generally, correcting for the case temperature, as was done, is adequate (PIR, 2007). However, in certain applications of intense solar (short-wave) radiation the dome temperature must also be adjusted, this is the situation at the South station (Albrecht and Cox, 1977). The sensors were mounted slope parallel, hence nearly in-line with the solar zenith angle. This problem was corrected during the 2008/2009 season by upgrading to Kipp and Zonen CGR3 instruments that account for this problem.

Slope parallel orientation is also used for the upward- and downward-facing short-wave sensors. Therefore, the sensors are measuring both incoming as well as reflected radiation from the surrounding environment (i.e., albedo), which includes snow from the slope below the research site. Slope parallel orientation is desired at the stations as the sensor is intended to measure the radiation actually impacting the snow, but causes the recorded values to be higher than expected. For comparison, peak irradiation values at the South Station often exceed over  $1200 \text{ W/m}^2$ . Values of this magnitude are within the range of values expected based on ASTM G-173, which reports an average value of  $1000 \text{ W/m}^2$  for terrestrial direct radiation (ASTM G-173, 2003) at a  $37^\circ$  latitude (i.e., average for the continental United States) as well as the solar standard of  $1367 \text{ W/m}^2$ .

### 4.3 Results

The 2007/2008 (C) and 2008/2009 (D)<sup>1</sup> seasons include detailed weather data, observations, and images of 26 near-surface facet events. Though weather data was collected prior to 2007, the results are excluded here due to the lack of snow crystal images. All except three of these events (C-3, C-7, and D-5), as noted in the field notes, were likely dominated by radiation processes. The results presented here does not differentiate these events since it was not possible to determine if these events were not due to radiation. In many cases, the events have before and after images and observations showing facet development in a manner of hours. Table 4.1 summarizes the type of snow that existed prior to the formation of facets, as reported in the field notes.

Each event of near-surface facets that occurred is summarized in Sections 4.4 and 4.5. The summaries presented attempt to provide a brief but thorough overview of each event, with minimal interpretation. Images included in this document are uncropped and selected as a representative of all the images taken on each day.

The event summaries for the 2007/2008 season (C) utilize long- and short-wave data from the Aspirit Station. As mentioned in Section 4.2, the long-wave sensors at the station were unreliable during this season. Thus, for consistency among the reported long- and short-wave radiation values, unless otherwise noted data from the Aspirit Station was used throughout the summaries for the 2007/2008 season.

The summaries for the 2008/2009 season (D) utilize the radiation data at the station itself, thus the values mentioned in the summaries are not comparable between the seasons. However, Table 4.2 provides the complete data set for both stations and

---

<sup>1</sup>The C and D notations are used to differentiate event references from Chapter 4.

seasons, allowing for a comparison to be made. This table includes daily mean values at both the South and Aspirit Stations for each event including short- and long-wave radiation, snow surface and air temperature, wind speed and direction, and relative humidity. The mean values for all parameters were calculated for the duration in which short-wave radiation was greater than zero.

Table 4.1: Summary of snow conditions prior to the near-surface facet events as recorded in the field notes. Events tagged with an asterisk (\*) indicate events, as noted in the field notes, that were likely dominated by non-radiation processes.

Event	Event Date	Description of Snow
C-1	1/21/2008	rimed stellars and plates 0.2–0.5 mm
C-2	2/14/2008	new snow, stellars rimed 2 mm, plates 1 mm
C-3*	2/18/2008	rimed stellars
C-4	2/26/2008	2–3 mm stellar dendrites, some heavily rimed, some not at all
C-5	3/6/2008	1 mm rimed stellars, 2 mm stellars
C-6	3/10/2008	highly broken 0.25 mm (dry)
C-7*	3/13/2008	2 mm stellars, 1 mm decomposing stellars, 1 mm facets
C-8	3/15/2008	stellars rimed 1–2 mm
C-9	3/19/2008	rimed new snow, 1–2 mm
C-10	3/22/2008	1 mm plates, columns, capped columns, stellars
C-11	3/28/2008	decomposing rimed new snow
C-12	3/30/2008	highly broken new snow, 0.5 mm
C-13	4/2/2008	rimed stellars, 1 mm
C-14	4/6/2008	new snow, rimed irregular grains, 1 mm
C-15	4/8/2008	new snow, 1mm
D-1	2/4/2009	1–2 mm graupel
D-2	2/8/2009	1.5 mm new snow
D-3	2/12/2009	1 mm new snow
D-4	2/19/2009	1–2 mm new snow
D-5*	2/21/2009	1 mm stellars
D-6	2/27/2009	0.5–3 mm new snow
D-7	3/7/2009	1–2 mm new snow
D-8	3/12/2009	0.5–1 mm decomposing snow and 0.1–0.3 mm surface hoar
D-9	3/20/2009	1 mm graupel
D-10	3/30/2009	1–2 mm new snow
D-11	4/6/2009	0.5–3 mm new snow and some surface hoar



Table 4.2: Summary of mean daily weather conditions for all days recorded as near-surface facets events, including short-wave ( $SW$ ) and long-wave ( $LW$ ) radiation, air ( $T_a$ ) and snow surface ( $T_s$ ) temperature, relative humidity ( $RH$ ), and wind speed ( $V_w$ ) and direction ( $Dir$ ). The superscript  $a$  denotes Aspirit station. Events tagged with an asterisk (\*) indicate events that were likely dominated by non-radiation processes.

Event	Date	$SW$ W/m <sup>2</sup>	$LW$ W/m <sup>2</sup>	$T_a$ °C	$T_s$ °C	$V_w$ m/s	$Dir$ deg.	$RH$ %	$\frac{LW}{SW}$	$SW^a$ W/m <sup>2</sup>	$LW^a$ W/m <sup>2</sup>	$\frac{LW^a}{SW^a}$
C-1	01/21/2008	607	340	-16.1	-16.6	0.7	157	68	1.79	170	166	1.03
C-2	02/14/2008	547	414	-7.2	-9.2	1.0	187	58	1.32	292	190	1.54
C-3a*	02/18/2008	593	479	-2.0	-5.4	1.4	232	45	1.24	291	202	1.44
C-3b*	02/19/2008	680	558	4.3	-3.2	1.3	151	20	1.22	318	192	1.65
C-3c*	02/20/2008	664	549	3.4	-3.2	1.2	209	21	1.21	310	197	1.57
C-4	02/26/2008	675	440	-4.0	-6.5	1.9	150	60	1.53	383	196	1.95
C-5	03/06/2008	626	432	-6.6	-7.9	1.6	216	63	1.45	413	194	2.13
C-6	03/10/2008	619	484	1.0	-4.2	1.6	154	43	1.28	404	218	1.85
C-7*	03/13/2008	262	348	-4.9	-5.8	1.1	207	68	0.75	221	265	0.84
C-8	03/15/2008	506	403	-6.3	-7.8	1.5	165	60	1.25	375	221	1.70
C-9	03/19/2008	416	388	-3.9	-7.8	2.1	146	52	1.07	306	230	1.33
C-10	03/22/2008	669	458	-6.7	-10.2	1.4	177	47	1.46	423	171	2.47
C-11	03/28/2008	499	380	-9.5	-12.8	1.9	171	50	1.31	365	207	1.77
C-12	03/30/2008	614	434	-8.6	-11.7	1.5	198	43	1.41	441	185	2.39
C-13a	04/02/2008	508	400	-6.8	-10.2	1.9	163	48	1.27	383	213	1.80
C-13b	04/03/2008	647	455	-4.0	-7.8	1.9	154	44	1.42	487	185	2.64
C-13c	04/04/2008	356	393	-2.1	-6.1	2.3	150	38	0.90	286	243	1.17
C-14	04/06/2008	506	386	-5.2	-7.3	1.9	156	58	1.31	399	229	1.75
C-15	04/08/2008	564	396	-5.4	-7.4	1.6	136	60	1.43	448	220	2.03
D-1	02/04/2009	706	230	5.7	-0.9	2.0	122	24	3.07	306	–	–
D-2	02/08/2009	504	240	-1.0	-3.9	1.2	156	51	2.10	211	224	0.94
D-3	02/12/2009	691	224	-7.6	-8.9	1.2	121	56	3.08	208	172	1.21
D-4	02/19/2009	608	220	-5.8	-7.5	2.0	101	64	2.76	313	202	1.55
D-5*	02/21/2009	687	215	-0.2	-5.2	1.9	107	37	3.20	334	201	1.67
D-6a	02/27/2009	516	229	-9.8	-9.7	1.5	111	65	2.26	363	190	1.92
D-6b	02/28/2009	711	197	-2.1	-7.0	1.2	131	31	3.61	372	180	2.07
D-7	03/07/2009	685	221	-7.2	-9.3	2.0	106	57	3.09	399	197	2.02
D-8a	03/12/2009	704	194	-4.6	-8.6	1.3	163	33	3.62	438	180	2.43
D-8b	03/13/2009	640	222	0.0	-5.7	1.8	126	35	2.89	416	211	1.97
D-8c	03/14/2009	661	222	-1.0	-5.5	2.3	124	34	2.98	422	211	2.00
D-9	03/20/2009	690	238	3.7	-2.1	1.9	107	48	2.90	337	213	1.58
D-10	03/30/2009	488	247	-8.5	-9.2	1.2	150	66	1.98	436	221	1.97
D-11	04/06/2009	739	218	4.4	-3.8	1.7	97	24	3.39	578	204	2.83

#### 4.4 2007/2008 Near-surface Facet Events

##### 4.4.1 Event C-1: January 21, 2008

The first event (C-1) of the 2007/2008 season was reported as both a surface hoar and near-surface facet event on January 22, 2008. The surface was described as “surface hoar 4–6 mm” and the subsurface at 1, 2, and 3 cm depth was described as facets with broken stellars still slightly visible with a grain size of less than 0.5 mm. The observations occurred at 0900, thus it is likely that the facets formed the day prior (Jan. 21). No images were taken of this event.

The air and snow surface temperatures as well as the incoming short- and long-wave radiation from Aspirit for this event are included in Figure 4.1. New snow was reported on Jan. 20 and then the weather cleared. On the 21<sup>st</sup>, short-wave peaked at 340 W/m<sup>2</sup> and long-wave was approximately 170 W/m<sup>2</sup> throughout the daylight hours. During daylight on Jan. 21 the snow was also warmer than the air, confirming the absorption of significant short-wave radiation. It is assumed that facets formed during the sunny conditions and persisted, and perhaps grew, until the observation the following day.

##### 4.4.2 Event C-2: February 14–16, 2008

Event C-2 was a considerable and wide-spread near-surface facet event and has been the subject of additional analysis (McCabe *et al.*, 2008; Slaughter *et al.*, 2008, 2009). Initial observations occurred at 1100 on the South Station. It was reported that evidence of minimal amounts of surface hoar existed. The YC ski patrol made additional observations at 1400 showing additional needle-like growth. Figures 4.2a–4.2c include before and after images taken at the South Station as well as images

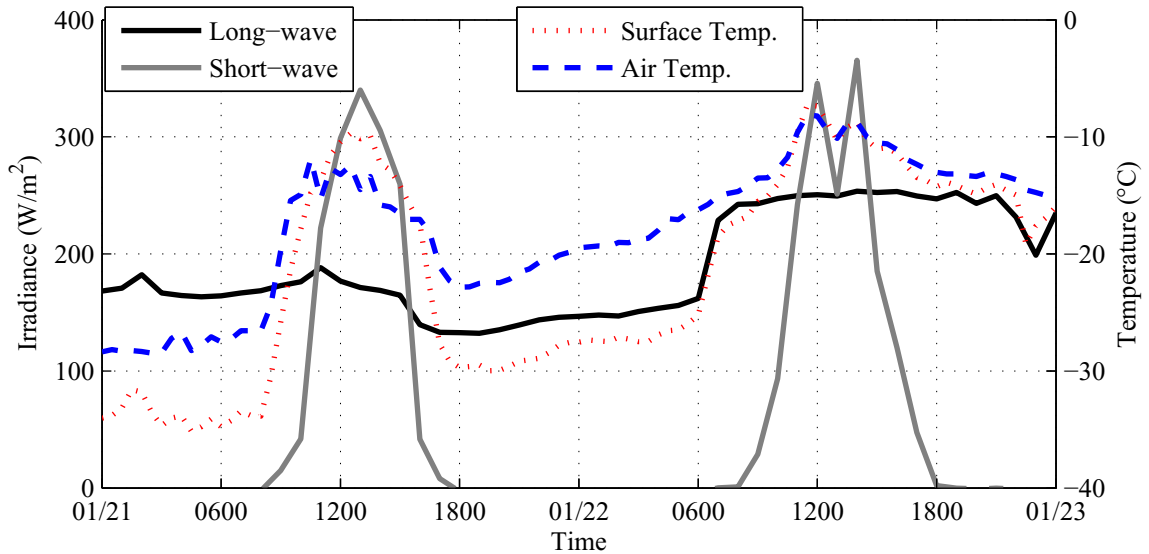


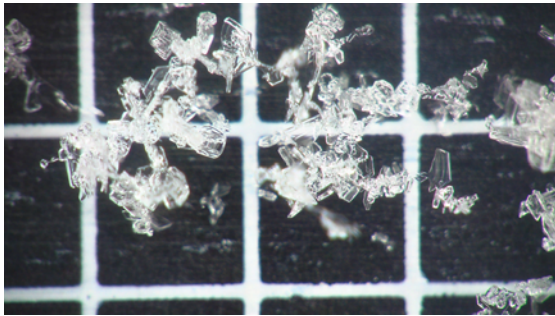
Figure 4.1: Recorded short- and long-wave radiation at the Aspirit Station as well as the air and snow surface temperatures at the South Station for January 21–22, 2008 (C-1).

taken from the Pinnacles area, which is a near-by slope with an elevation of 2800 m, aspect of  $182^\circ$ , and slope angle of  $28\text{--}38^\circ$ .

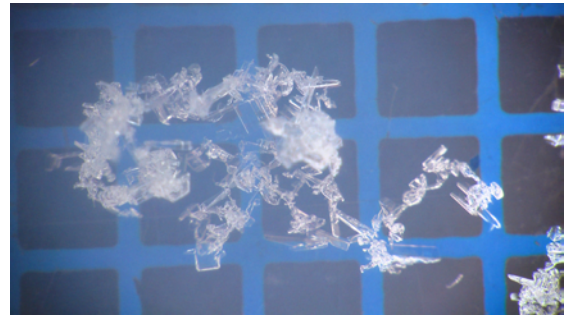
The formation of these crystals occurred with air temperatures that rose between 600 and 1400 from  $-17^\circ\text{C}$  to  $-4^\circ\text{C}$  and snow surface temperatures that increased from  $-25^\circ\text{C}$  to  $-4^\circ\text{C}$ , as shown in Figure 4.3. The facets formed in new snow that fell the previous day; the density was reported as  $20\text{ kg/m}^3$ . This warming was more pronounced in the subsurface, and it was reported the snow between 1 cm and 5 cm was moist. Thus, the temperature gradient in the upper centimeter of snow was approximately  $400^\circ\text{C/m}$ . Figure 4.3 confirms that the sky was clear: long-wave radiation was only  $160\text{ W/m}^2$  and short-wave peaked at  $575\text{ W/m}^2$ .

On Feb. 15 facets were observed again in the surface layer at 1100, as shown in Figure 4.4. The radiative conditions were nearly identical on Feb. 14 and 15; however, the air temperature on Feb. 15 increased to  $2^\circ\text{C}$  (see Figure 4.3). No

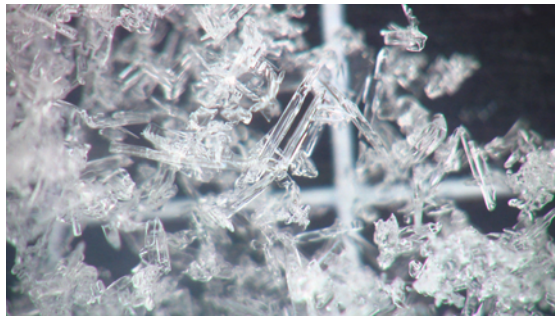
secondary observations were made on Feb. 15. The facets persisted despite being buried on Feb. 16 by 4–5 cm of new snow, as recorded in the field notes: “facets are still visible on the upper crust interface” (see Figure 4.4). No mention of the layer of facets was recorded after this day.



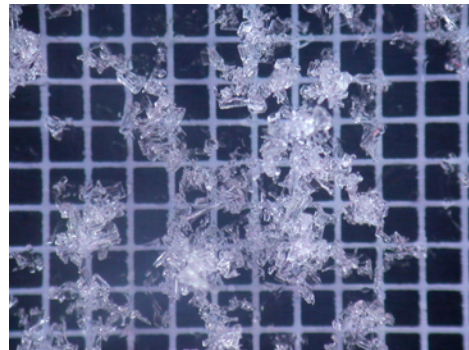
(a) South at 1100 (2 mm grid)



(b) South at 1400 (2 mm grid)



(c) Pinnacles (2 mm grid)



(d) South at 1100 on Feb. 15 (2 mm grid)

Figure 4.2: Four images of a near-surface facet event at the South Station on February 14, 2008 (C-2): (a) initial observation (1100) at the South Station, (b) second observation (1400) at the South Station, (c) observations at a near-by south facing slope, and (d) following day (Feb. 15) South Station observation (1100).

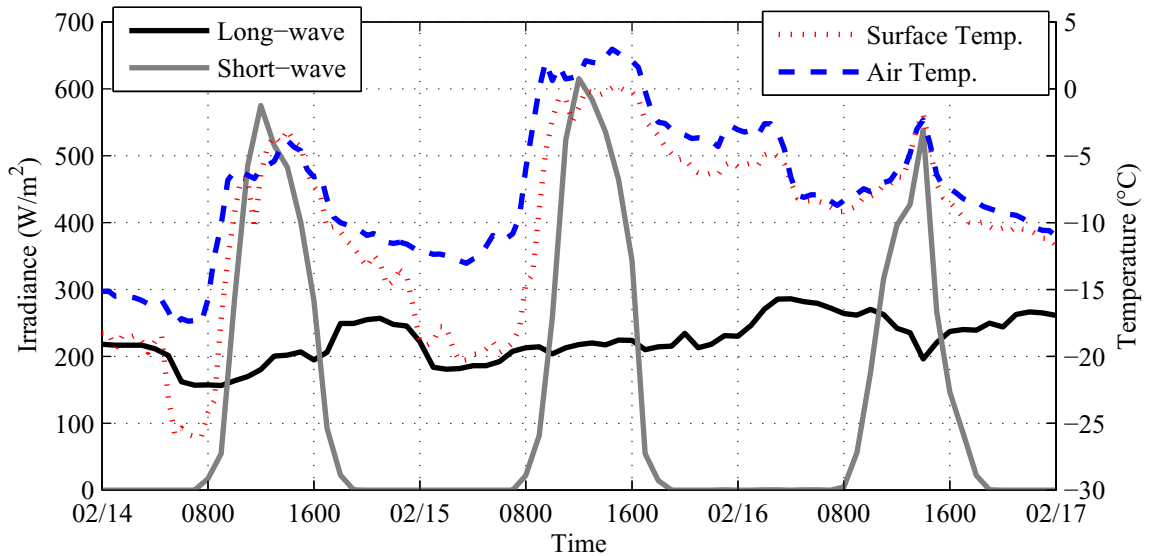


Figure 4.3: Recorded short- and long-wave radiation at the Aspirit Station as well as the air and snow surface temperatures at the South Station for February 14–16, 2008 (C-3).

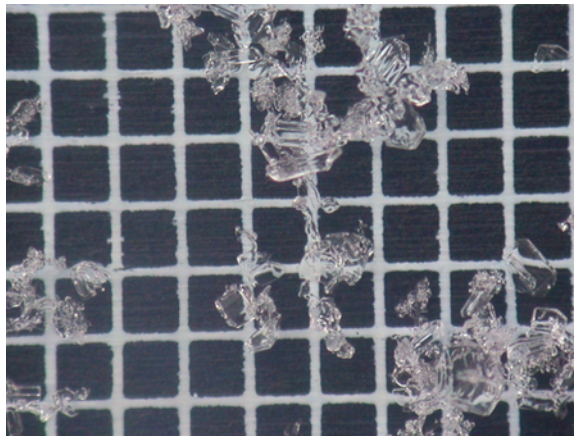


Figure 4.4: Facets formed on February 14, 2008 at the South Station that persisted through warmer temperatures and new snow until February 16<sup>th</sup>.

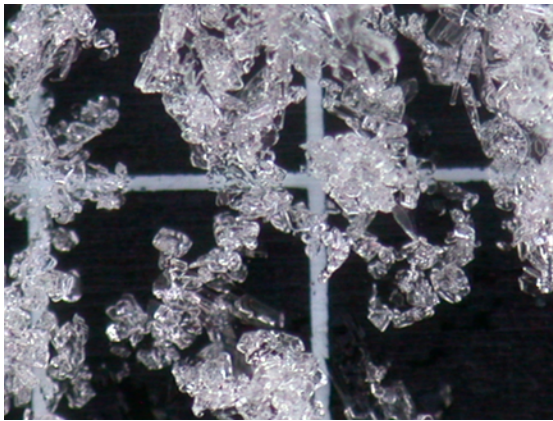
#### 4.4.3 Event C-3: February 18–20, 2008

Event C-3 consisted of an observation of small (0.5 mm) facets in the surface layer at 0924 on February 18, 2008 followed by two days (Feb. 19 and 20) in which the field notes indicated the presence of facets underlying surface hoar crystals. The

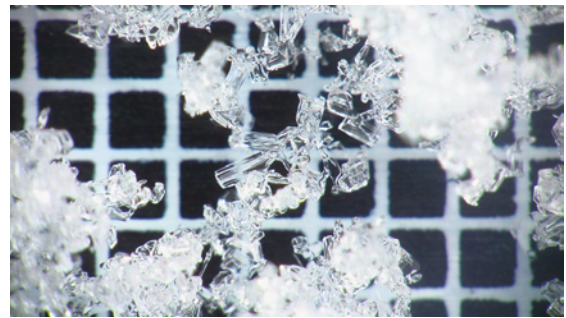


facets were described as “spaghetti of diurnal-recrystallization chains.” Figure 4.5 includes an image from each of these three days.

The recorded weather conditions indicated drastic changes in the snow surface temperature (see Figure 4.6). During these three days the snow surface temperature changed an average of 13 °C between daylight and night, with the biggest change being a 17 °C increase from night to daylight on Feb. 18. The changes occurred in a matter of hours.



(a) Feb. 18 (2 mm grid)



(b) Feb. 19 (1 mm grid)



(c) Feb. 20 (1 mm grid)

Figure 4.5: Images of near-surface facets at the South station described as diurnal recrystallization., that formed on February 18–20, 2008 (C-3).

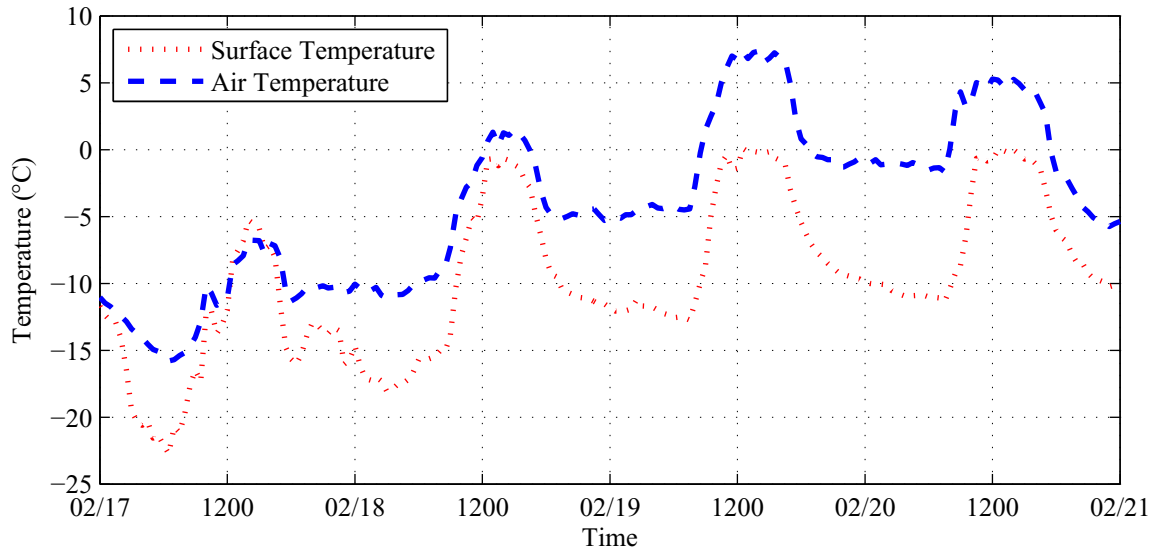


Figure 4.6: Graph of air temperature and snow surface temperature at the South Station on February 17–20, 2008 (C-3).

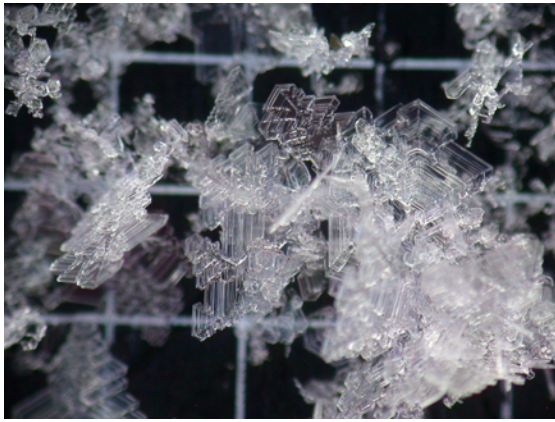
#### 4.4.4 Event C-4: February 26–27, 2008

The field notes explained that “1 mm columns [and] needles” formed on February 27, 2008 (C-4). New snow (10 inches) fell two days prior (Feb. 25), surface hoar formed the following day, and distinct facets were then found on Feb. 27. These facets persisted for the following two days. Figure 4.7 includes images of the preceding surface hoar and subsequent near-surface facets.

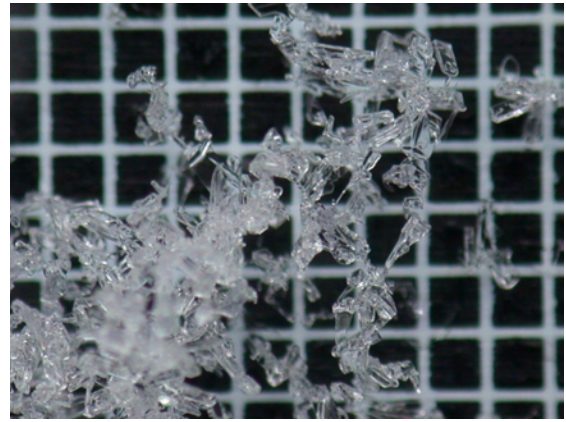
Figure 4.8 is a graph of the radiation and temperature data for the days surrounding the C-4 event. The near-surface facets likely formed during the day on Feb. 26, were reported on Feb. 27, and persisted for several overcast days after formation. The observation on Feb. 26 was made at 0830 and showed significant surface hoar; however, the short-wave was high ( $640 \text{ W/m}^2$  at Aspirit at mid-day) and the incoming long-wave was less than  $200 \text{ W/m}^2$  throughout the day. The following day (Feb. 27) short-wave was much lower ( $490 \text{ W/m}^2$ ) and long-wave was higher ( $250\text{--}290 \text{ W/m}^2$ ). Thus, it is possible that the near-surface facets formed on Feb. 26.

An examination of the snow temperature data from the thermocouple array placed in the snow provided further evidence that the facets may have formed on Feb. 26. Figure 4.9 includes measured temperature profiles during the daylight hours on Feb. 26, which indicate subsurface heating and surface cooling. Note, the data was suspect due to solar contamination of the thermocouples (above freezing snow temperature), however the general trend of the temperature measurements indicated a temperature gradient near the snow surface with the subsurface warmer than the surface. On Feb. 27 temperature profiles indicate that the snow surface was the warmest portion of the snowpack; however these measurements were invalid due to melting around the thermocouple array. On Feb. 26 three thermocouples were exposed to the air and the following day 10 were exposed. Thus, melting of the snow caused 14 cm of the array to become exposed over 24 hours.

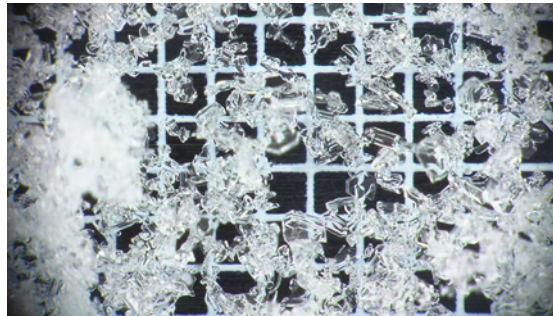




(a) Feb. 26 (3 mm grid)



(b) Feb. 27 (1 mm grid)



(c) Feb. 28 (1 mm grid)

Figure 4.7: Images taken at the South Station of (a) surface hoar formed the day prior to the (b) near-surface facets that formed on February 27, 2008 (C-4) and persisted through (c) the following day.

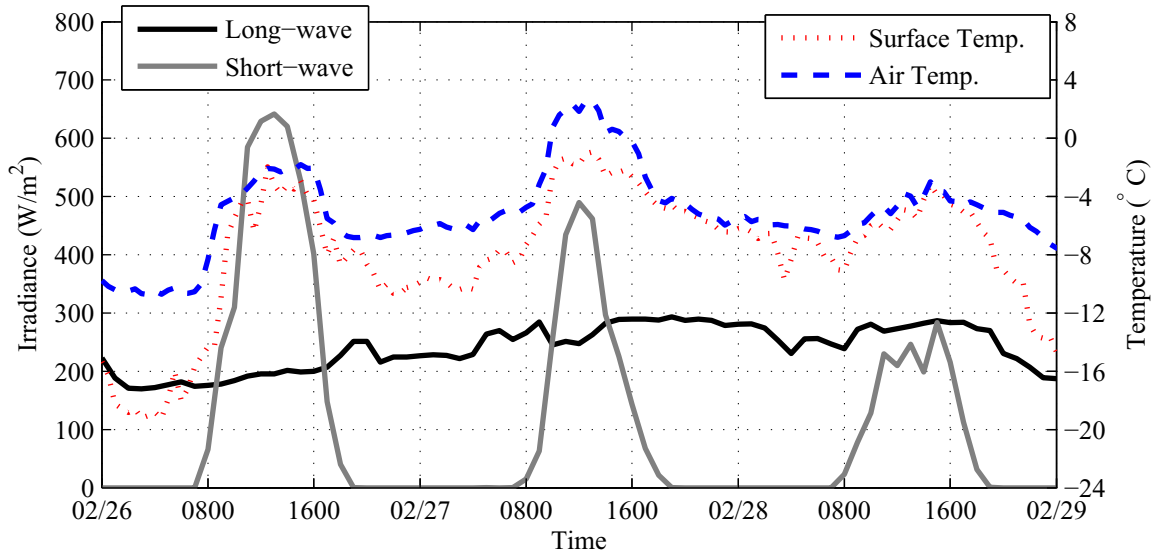


Figure 4.8: Recorded short- and long-wave radiation at the Aspirit Station as well as the air and snow surface temperatures at the South Station on February 26–28, 2008 (C-4).

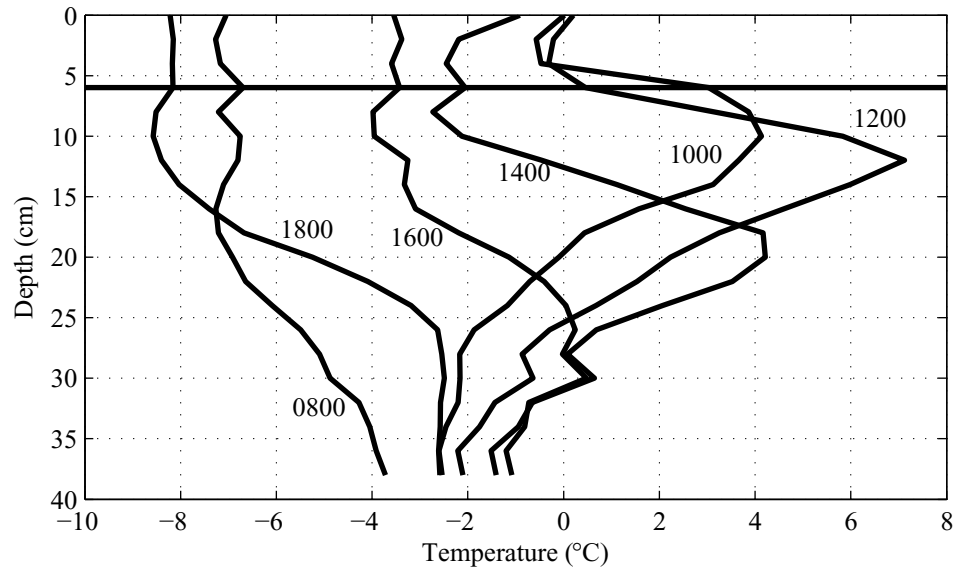


Figure 4.9: Snow temperature profiles from February 26, 2008 (C-4) at the South Station. The horizontal line represents the snow surface.

#### 4.4.5 Event C-5: March 6, 2008

Observations at the South Station were made at 1100 and 1330 on March 6, 2008. The initial observation reported the “surface snow [was] composed of 2–3 mm stellars and stellar fragments throughout the top ten centimeters. . . no surface hoar or other faceting was present.” In the second observation the field report stated that “small cups and needles were observed in the cold snow on the surface.” Figure 4.10 includes images from both observations. This event has been discussed and analyzed in prior research (McCabe *et al.*, 2008; Slaughter *et al.*, 2008, 2009).

On Mar. 6 the short-wave radiation at Aspirit peaked at  $690 \text{ W/m}^2$  and long-wave radiation remained constant at approximately  $200 \text{ W/m}^2$  throughout the day. Air temperature increased from  $-15 \text{ }^\circ\text{C}$  at sunrise to  $-4 \text{ }^\circ\text{C}$  during the daylight. This event occurred after five consecutive days of snow totaling 25 mm of snow water equivalent and a depth of 30 cm.

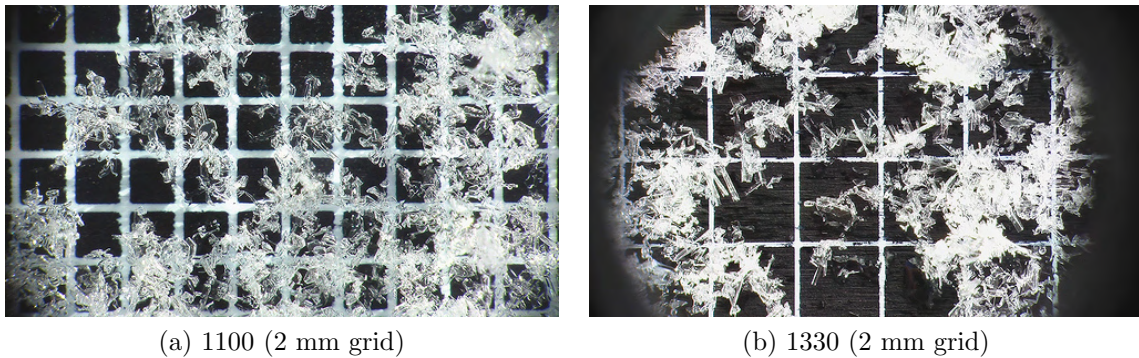


Figure 4.10: Images from March 6, 2008 (C-5) near-surface facet event at the South Station: (a) initial observation at 1100 and (b) second observation at 1330.

#### 4.4.6 Event C-6: March 10, 2008

Near-surface facets and surface hoar were observed on March 10, 2008 (C-6). The faceted crystals were “0.5 mm to 1 mm in size and mostly rectangular in shape; some

chaining [was] observed.” Chaining refers to the facets being arranged in long, narrow chains. The field notes also reported that distinct surface hoar grains were visible. Figure 4.11 is an image of near-surface facets located at the snow surface. The facets were reported to persist until Mar. 12 on the surface; the field notes indicated facets on the surface “from [Mar. 10] surface hoar event.”

The air temperature was mild on Mar. 10, rising to 5 °C. The snow surface temperature reached 0 °C for a few hours at mid-day. The short- and long-wave radiation at Aspirit were similar to the previous event: short-wave peaked at 660 W/m<sup>2</sup> and long-wave was approximately 220 W/m<sup>2</sup> throughout the day.

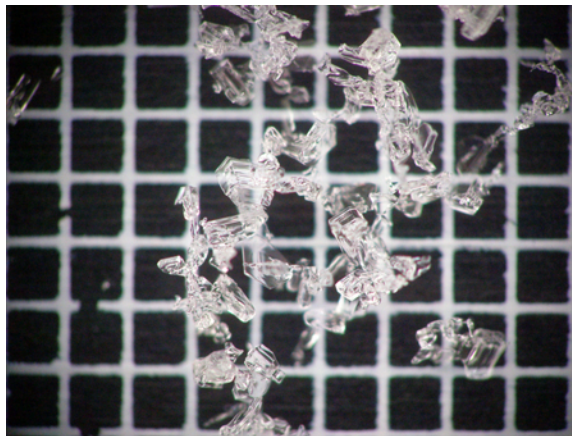


Figure 4.11: Image of near-surface facets observed on March 10, 2008 (C-6) at the South Station.

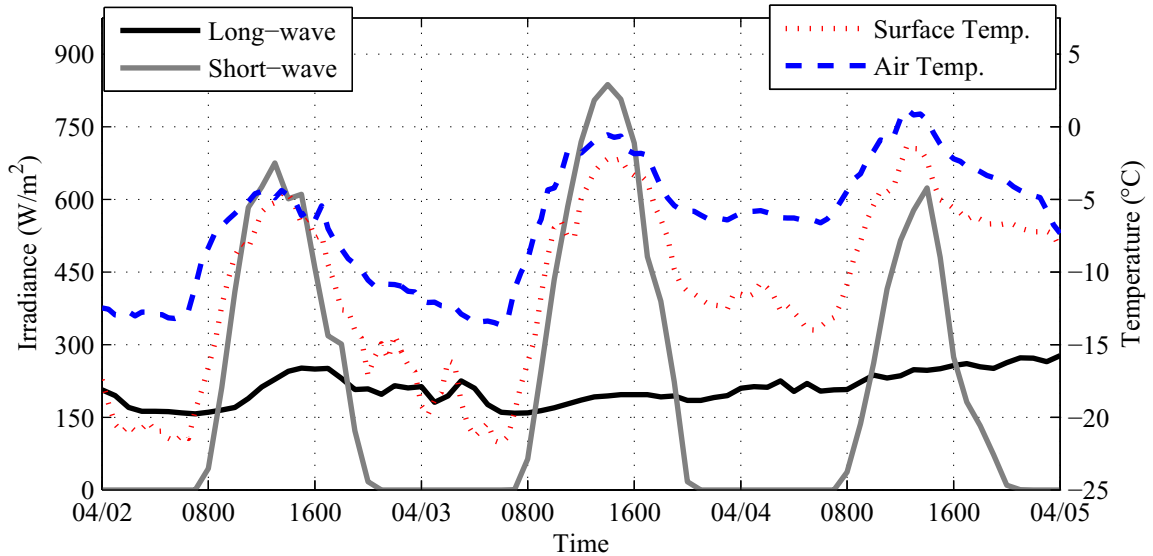


Figure 4.12: Recorded short- and long-wave radiation at the Aspirit station (C-6) as well as the air and snow surface temperatures at the South station for March 10, 2008.

#### 4.4.7 Event C-7: March 13, 2008

A layer of 0.5 mm facets was observed 4–5 cm below the surface on March 13, 2008 (C-7). This layer was between two crusts and the facets were described as “small and relatively round, but very [non-cohesive].” The weather data, Figure 4.13, was not as conducive to radiation-recrystallization when compared to the previous event described. Long-wave radiation was  $280 \text{ W/m}^2$  during the day and short-wave peaked at only  $350 \text{ W/m}^2$ . The prior days conditions were similar to other events, but no indication of facets was recorded at the 1245 observation. Thus, the resulting facets may have formed due to the diurnal temperature change (the snow surface temperature changed over  $10 \text{ }^\circ\text{C}$  between day and night) or melt-layer recrystallization as indicated by the presence of crusts surrounding the layer.

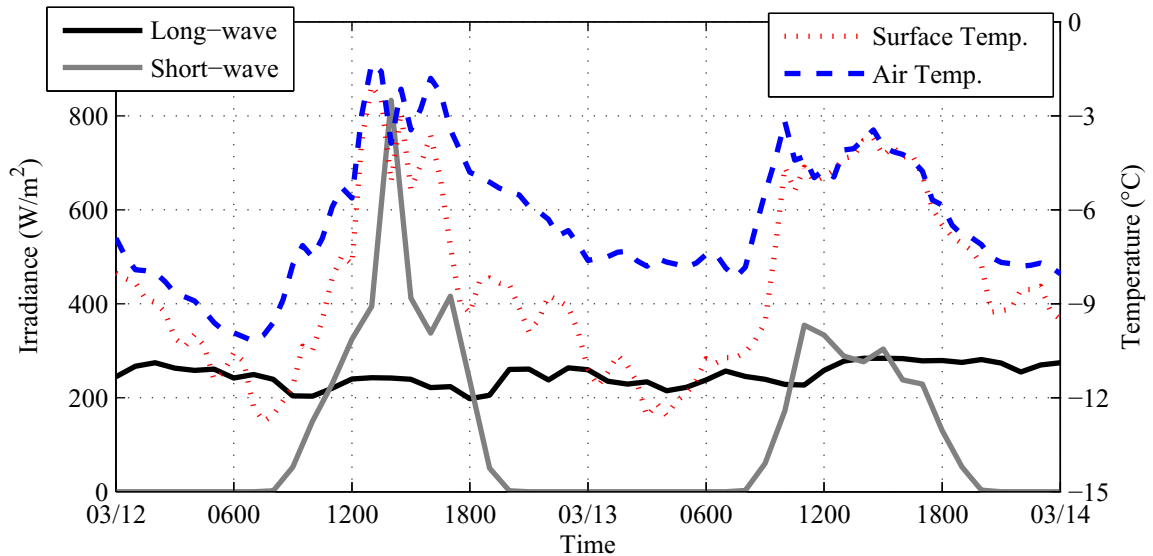


Figure 4.13: Recorded short- and long-wave radiation at the Aspirit Station as well as the air and snow surface temperatures at the South Station on March 12–13, 2008 (C-7).

#### 4.4.8 Event C-8: March 15, 2008

Event C-8 was marked by an observation of small (0.5 mm) facets (Figure 4.14a) above a crust that was 2 cm below the surface at 1045 and 1400 on March 15, 2008. Approximately 8 cm of new snow fell the day prior (Mar. 14). The short-wave radiation at Aspirit peaked at  $770 \text{ W/m}^2$  and long-wave was approximately  $210 \text{ W/m}^2$  throughout the day. The facets persisted (Figures 4.14b and 4.14c) through the following two days despite being covered by approximately 3 cm of new snow. The radiation and temperature data for March 15–17 is included in Figure 4.15.



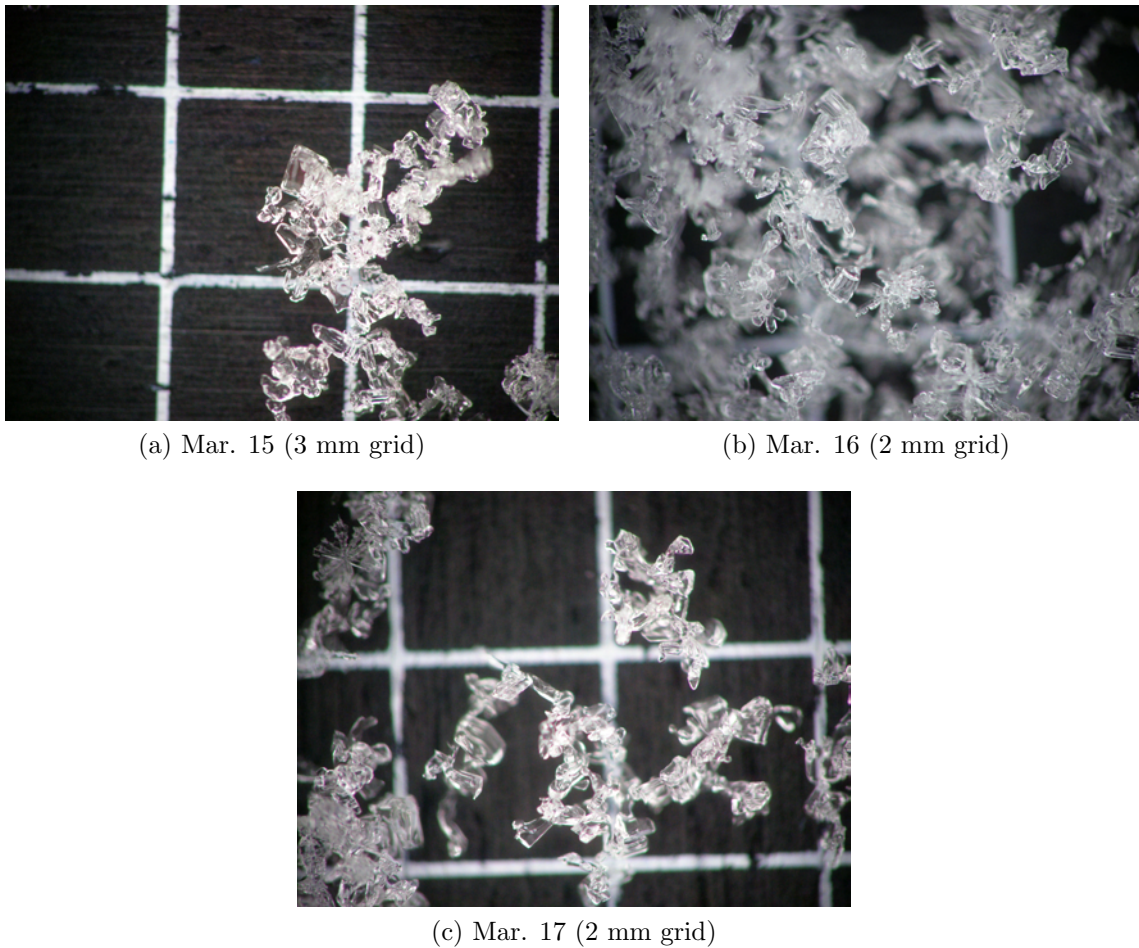


Figure 4.14: Images taken at the South Station during the (a) March 15, 2008 (C-8) near-surface facet event; this layer persisted the following two days (b and c).

#### 4.4.9 Event C-9: March 19, 2008

Small (0.25–0.5 mm) facets were observed at 1330 on March 19, 2008 (C-9). These facets formed in new snow under cool, clear conditions. Short-wave radiation at Aspirit peaked at  $550 \text{ W/m}^2$  and long-wave radiation increased from  $166 \text{ W/m}^2$  at sunrise to  $275 \text{ W/m}^2$  at sunset. Air temperatures reached  $-2 \text{ }^\circ\text{C}$  at mid-day; the snow surface peaked at  $-4 \text{ }^\circ\text{C}$ . No images were taken of this event. The radiation and temperature data for the event are included in Figure 4.16.

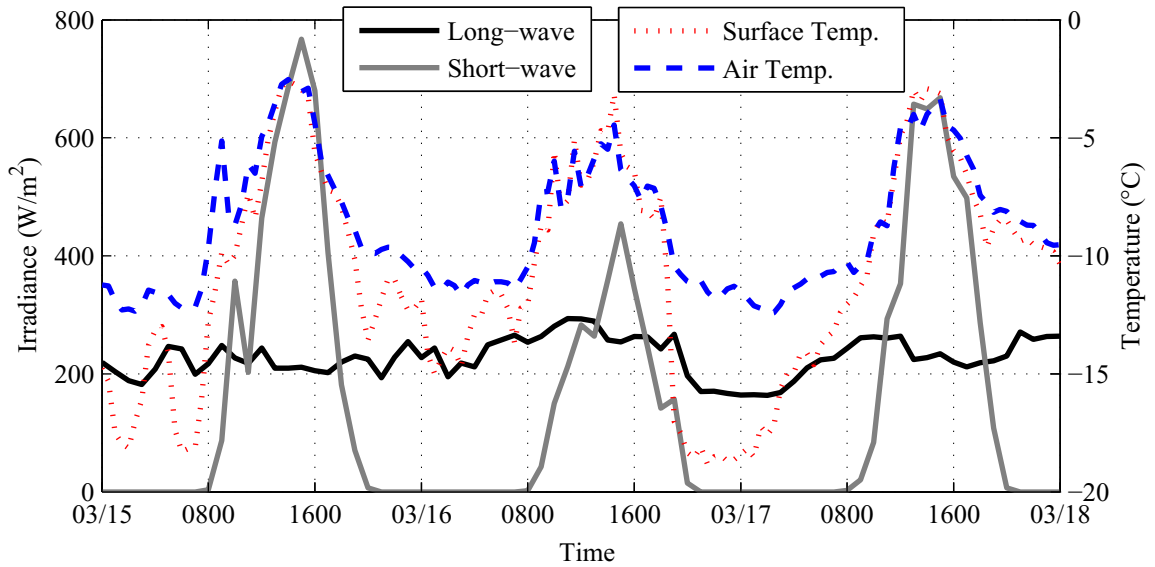


Figure 4.15: Recorded short- and long-wave radiation at the Aspirit Station as well as the air and snow surface temperatures at the South Station on March 15–17, 2008 (C-8).

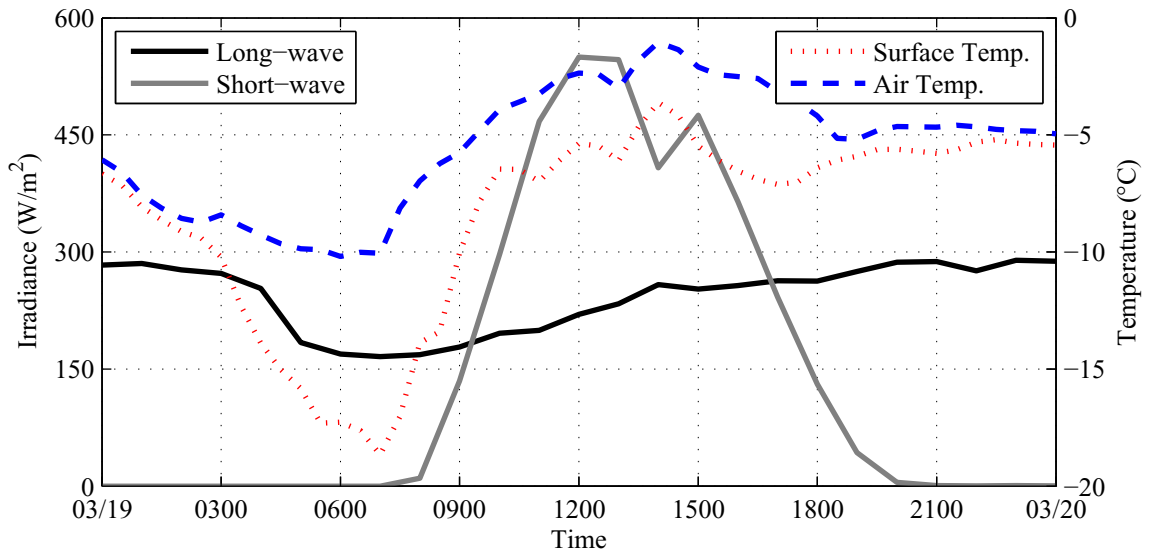


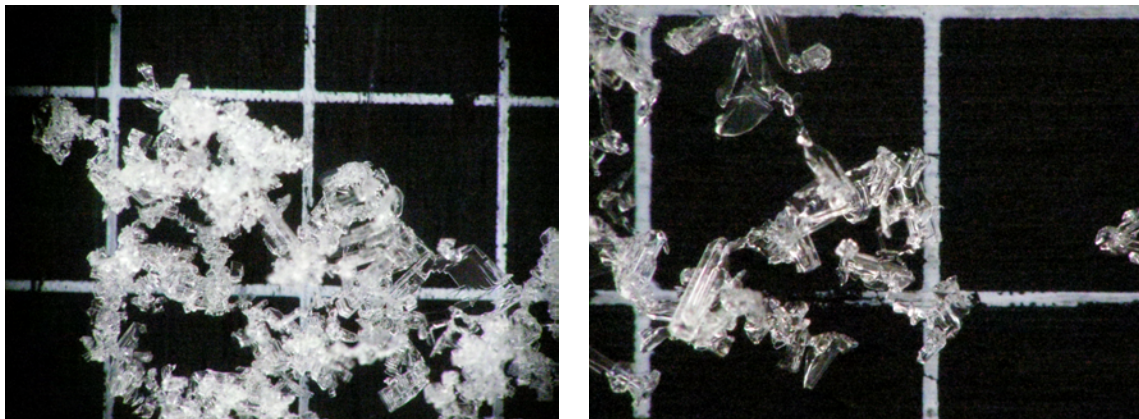
Figure 4.16: Recorded short- and long-wave radiation at the Aspirit Station as well as the air and snow surface temperatures at the South Station on March 19, 2008 (C-9).



#### 4.4.10 Event C-10: March 22, 2008

The conditions of Event C-10 on March 22, 2008 were very similar to Event C-2 on February 14–16, 2008 (Section 4.4.2). Widespread 0.3–1.5 mm facets were found at the South Station on March 22, 2008 and persisted until Mar. 25. The facets formed in new snow that fell two days prior. Images of the facets observed are included in Figure 4.17.

On Mar. 22 both the snow surface and air temperature reached  $-4\text{ }^{\circ}\text{C}$ , short-wave at Aspirit peaked at  $800\text{ W/m}^2$ , and long-wave was between  $160\text{ W/m}^2$  and  $190\text{ W/m}^2$ . On subsequent days following the event, air temperatures and long-wave radiation increased, while short-wave decreased compared to the event day. The field notes on Mar. 25 indicated that new snow had fallen but the facets were still observable beneath the new snow. The temperature and radiation data for Mar. 22–24 is included in Figure 4.18.



(a) Mar. 22 (2 mm grid)

(b) Mar. 23 (2 mm grid)

Figure 4.17: Images from the (a) March 22, 2008 (C-10) near-surface facet event at the South Station and (b) facets that persisted through the following day.

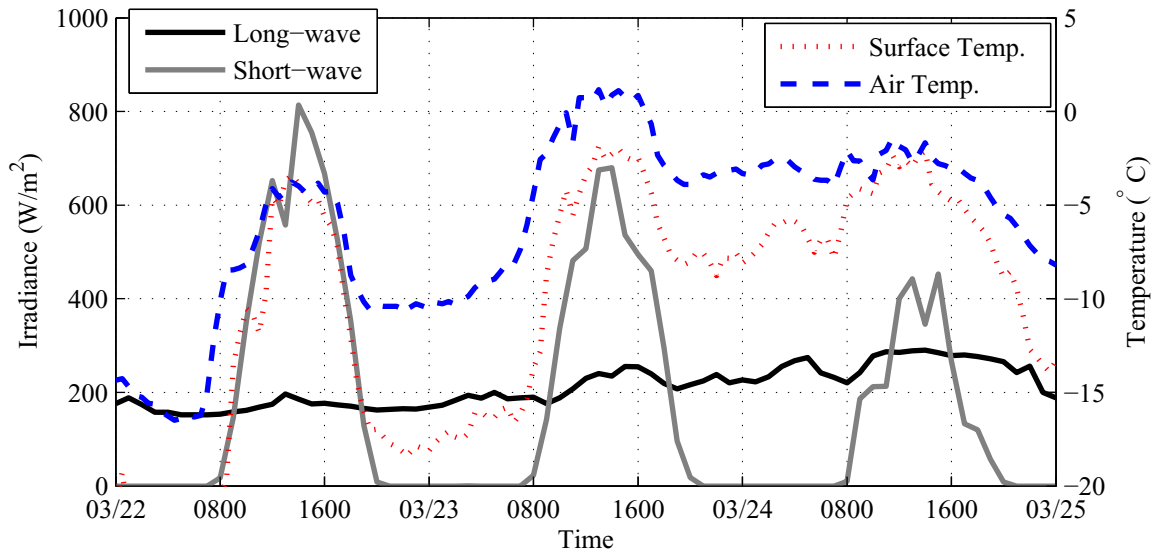


Figure 4.18: Recorded short- and long-wave radiation at the Aspirit Station as well as the air and snow surface temperatures at the South Station for March 22–24, 2008 (C-10).

#### 4.4.11 Event C-11: March 28, 2008

Event C-11 occurred on March 28, 2008, facets measuring 0.5 mm were observed. The field notes indicated difficulty deciphering if the observed crystals were surface hoar or near-surface facets; however, the field notes also stated “it did appear that the [facets were] slightly subsurface.” No images were taken on this day. The weather data, Figure 4.19, showed that the conditions were similar to the previously mentioned events: short-wave at Aspirit peaked at 630 W/m<sup>2</sup> and long-wave ranged from 150 W/m<sup>2</sup> to 250 W/m<sup>2</sup> throughout the day. The increase in long-wave radiation throughout the day may be why only a “small amount” of faceting was observed.

#### 4.4.12 Event C-12: March 30, 2008

Event C-12 on March 30, 2008 was similar to many of the previously mentioned events: short-wave at Aspirit peaked at 760 W/m<sup>2</sup> and long-wave remained below

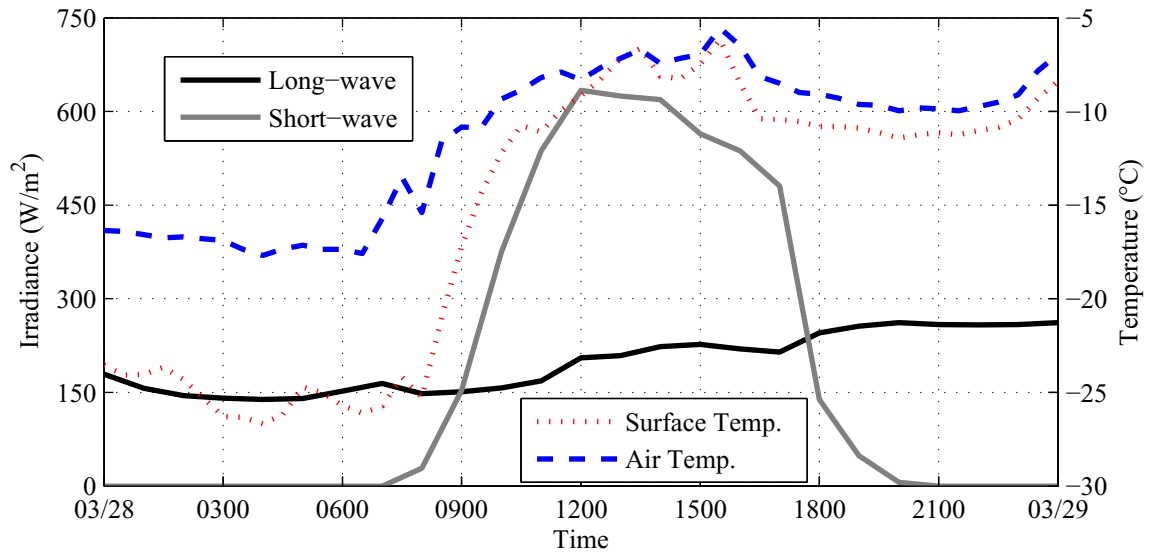


Figure 4.19: Recorded short- and long-wave radiation at the Aspirit Station as well as the air and snow surface temperatures at the South Station, on March 28, 2008 (C-11).

200 W/m<sup>2</sup> during the entire day. Air temperature increased from -15 °C at night to -5 °C at midday. The radiation and temperature data for Mar. 30 are included in Figure 4.20 and an image of the crystals observed is shown in Figure 4.21. The facets formed in 3 cm of new snow that fell on the night between Mar. 29 and 30. The field notes stated that the surface snow “was mostly 1 mm facets with some forms that appeared to be surface hoar.”

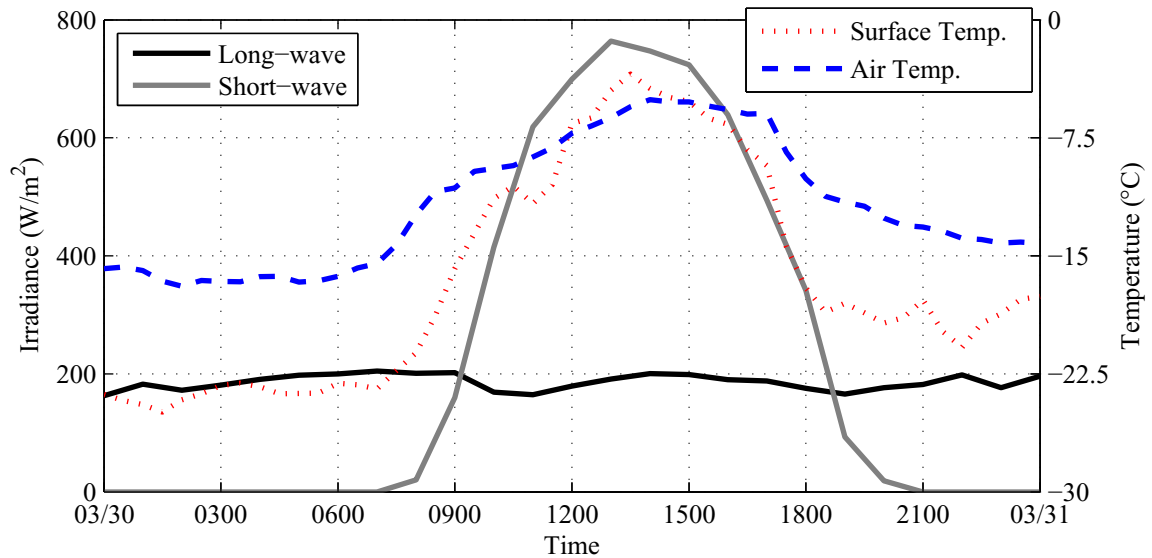


Figure 4.20: Recorded short- and long-wave radiation at the Aspirit Station as well as the air and snow surface temperatures at the South Station on March 30, 2008 (C-12).

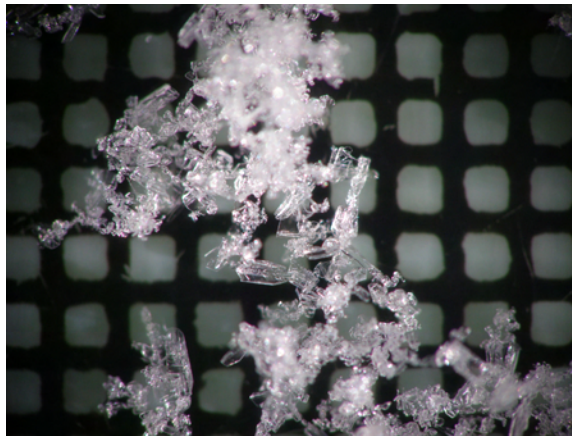


Figure 4.21: Image of near-surface facets formed on March 30, 2008 (C-12) at the South Station.

#### 4.4.13 Event C-13: April 2–4, 2008

Facets were observed at the South Station on three consecutive days in early April, 2008 (C-13). At 1200 on Apr. 2 facets measuring 0.5–1 mm were observed in the upper 1 cm of the snowpack. The following day (Apr. 3) small facets were observed

at 1130 and at 1430; the field notes indicated that “additional facet growth” had occurred. Also, only the top 1 cm of the snow remained frozen. Figure 4.22 includes images from the two observations made on Apr. 3. On Apr. 4, well-developed facets were observed at the surface; they were described as “needles and sheath, striated cups.” Additional faceting was observed 3 cm below the surface between melt-freeze crusts.

The radiation and temperature weather data for April 2–4, 2008 is displayed in Figure 4.23. The conditions for both Apr. 2 and 3 are similar to many of the events discussed in this chapter: high short-wave peaks and long-wave radiation near 200 W/m<sup>2</sup>. On Apr. 4 conditions change: short-wave radiation decreased to a peak of 600 W/m<sup>2</sup> and long-wave radiation increased to 280 W/m<sup>2</sup> by sunset.

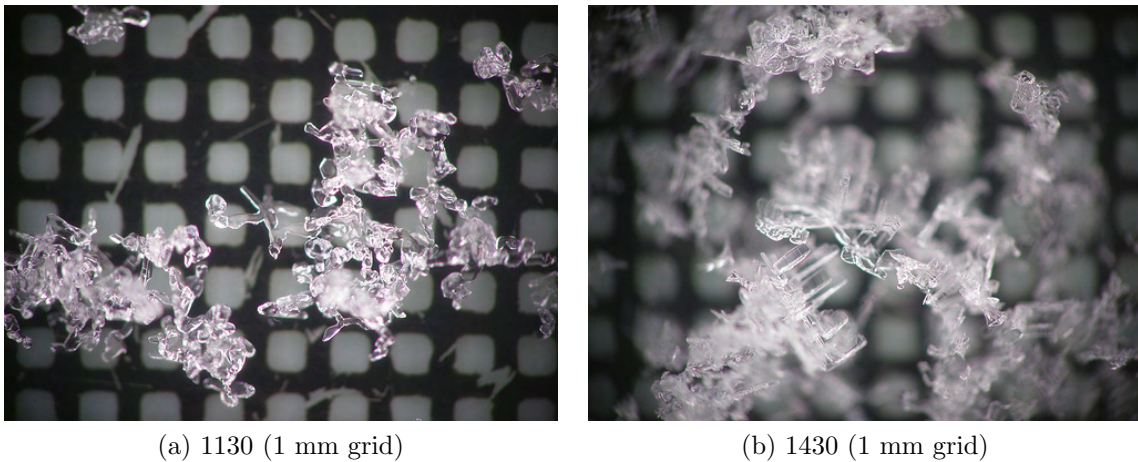


Figure 4.22: Images of surface snow at (a) 1130 and (b) 1430 at the South Station on April 3, 2008 (C-13) showing formation of near-surface facets .

#### 4.4.14 Event C-14: April 6, 2008

Event C-14 occurred April 6, 2008. The initial (1030) observation at the South Station reported 1 mm surface hoar and 2–3 mm stellars; at 1430 facets measuring 1 mm were reported. The field notes state that “it was clear that the observed snow

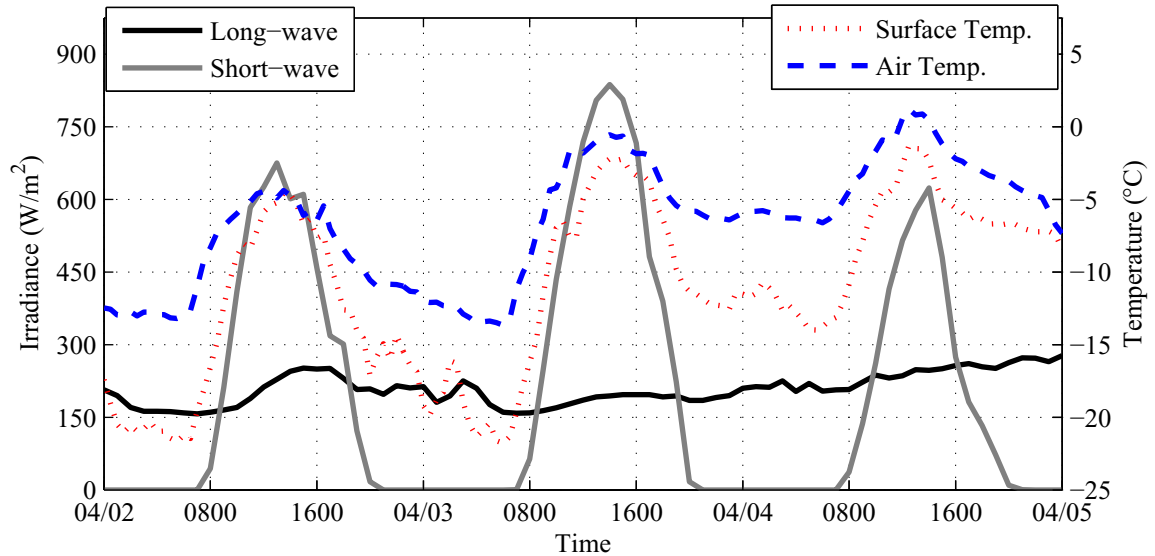


Figure 4.23: Recorded short- and long-wave radiation at the Aspirit Station, as well as the air and snow surface temperatures at the South Station, on April 2–4, 2008 (C-13).

was more faceted in the [afternoon] than in the [morning].” The facets that formed during the day were described as “champagne glass facets.” Figure 4.24 includes images from both observations.

The temperature and radiation data are provided in Figure 4.25. The day prior was overcast as indicated by the low incoming short-wave radiation and light snow was reported in the field notes. The night prior to the event, the skies cleared and some surface hoar formed, this is indicative of the large gradient between air and snow temperatures. The near-surface facets formed during the day under similar conditions as many of the other events described: incoming short-wave radiation peaked at 837  $\text{W}/\text{m}^2$  and long-wave radiation remained near 230  $\text{W}/\text{m}^2$  throughout the day.



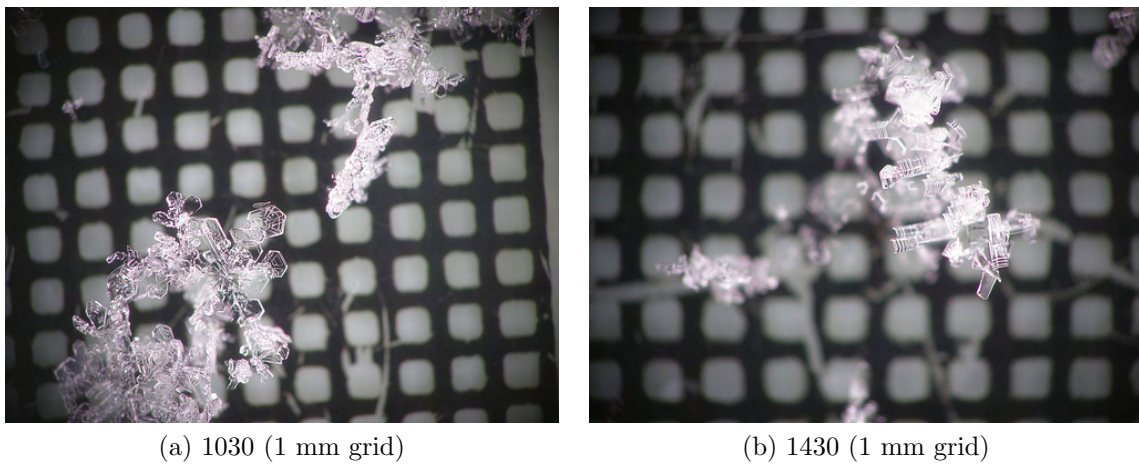


Figure 4.24: Images of surface snow at (a) 1030 and (b) 1430 on April 6, 2008 (C-14) showing formation of near-surface facets at the South Station.

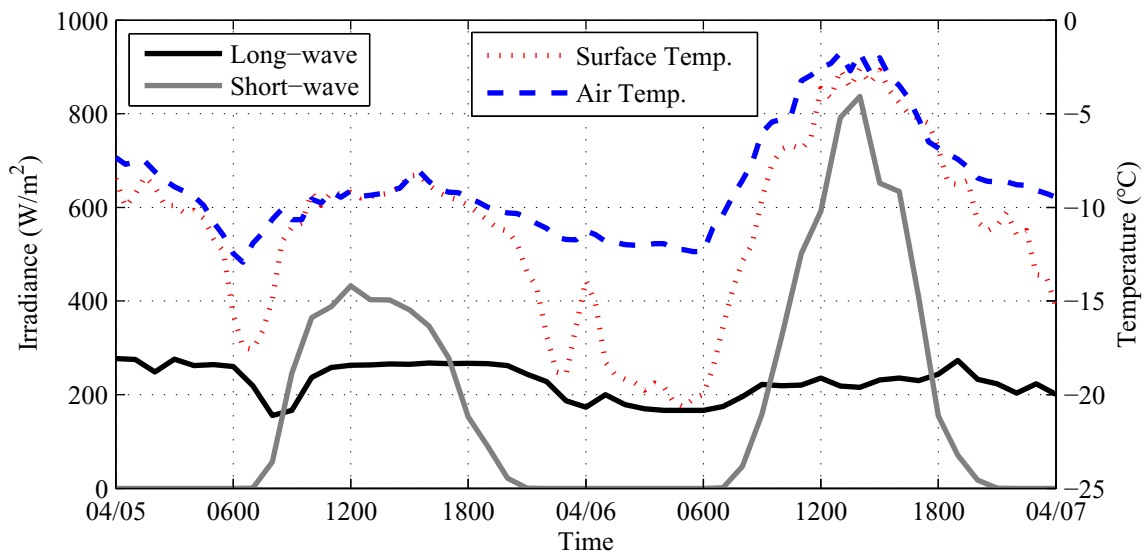


Figure 4.25: Recorded short- and long-wave radiation at the Aspirit station, as well as the air and snow surface temperatures at the South Station, on April 6, 2008 (C-14).

#### 4.4.15 Event C-15: April 8, 2008

The final event (C-15) recorded during the 2007/2008 occurred on April 8, 2008 at the South Station. Again the conditions were similar to other events described: days were characterized by high incoming short-wave radiation (peaked at  $800 \text{ W/m}^2$ ) and

long-wave radiation (average around  $220 \text{ W/m}^2$  throughout the day). The field notes indicated that 10 cm of new snow fell the night prior to the event; this is noticeable in the weather data presented in Figure 4.26, which shows a jump in incoming long-wave radiation on Apr. 9.

The actual event was not recorded in the notes until Apr. 9, the entry stated that “at [0930] pictures were taken of facets in [the] 3 mm layer on top of [a] melt freeze crust; presumably, these facets formed during yesterday’s clear skies in a radiation process.” These facets persisted through the following day and were buried by new snow that began falling at 1200, as stated in the notes: “at [1400] 5 mm of new snow had fallen on this [faceted] layer, which appears to have survived today’s radiation, which lasted until noon or so. In the photos, the facets are still observable underneath the newly fallen stellar crystals.” Photographs of the facets taken on Apr. 9 are included in Figure 4.27.

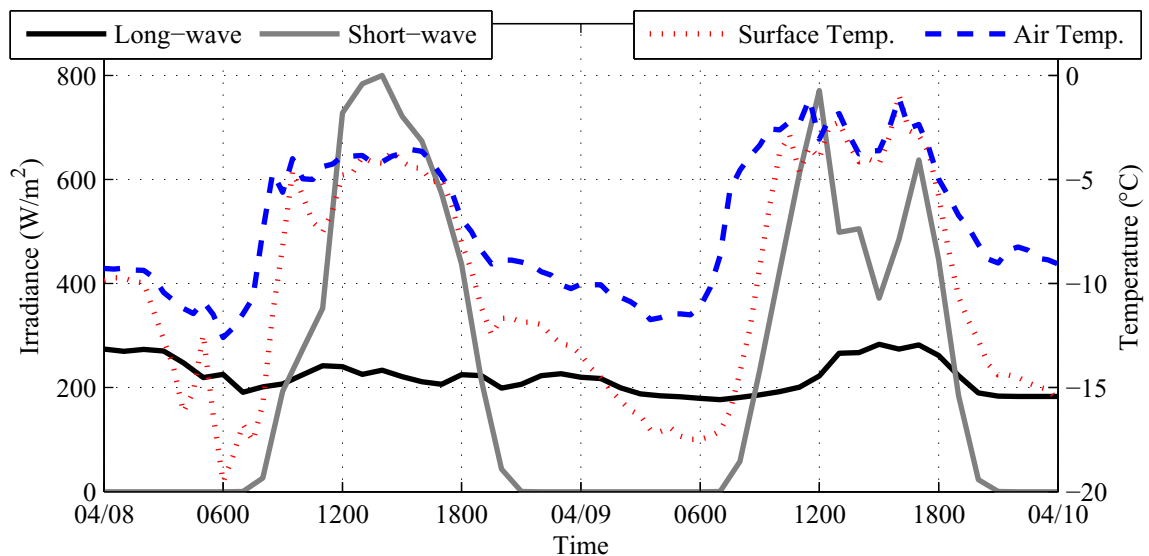


Figure 4.26: Recorded short- and long-wave radiation at the Aspirit station as well as the air and snow surface temperatures at the South station for April 8–9, 2008.



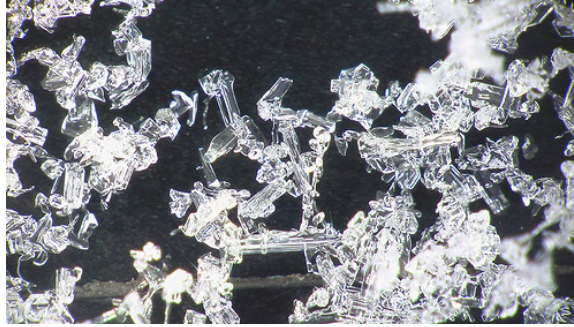


Figure 4.27: Image near-surface facets formed on April 8, 2008 (C-15). Photo was taken on April 9 after buried by new snow, the scale is unknown.

#### 4.5 2008/2009 Near-surface Facet Events

##### 4.5.1 Event D-1: February 4, 2009

The first recorded event (D-1) of the 2008/2009 season occurred on February 4, 2009 at the South station. The field notes reported 0.5 mm facets at the surface, as shown in Figure 4.28a. Due to a malfunction with the weather station instrumentation, the weather data for this event does not begin until 1200 on Feb. 4, see Figure 4.29. Nonetheless, the data showed that short-wave radiation peaked near  $1090 \text{ W/m}^2$  at the South Station and  $520 \text{ W/m}^2$  at Aspirit. The long-wave radiation averaged  $230 \text{ W/m}^2$  throughout the day at the South Station. Air temperatures were well above freezing ( $6.7 \text{ }^\circ\text{C}$ ) and the snow surface was  $0^\circ\text{C}$  at midday.

The facets persisted through the night and were observed the following day (Feb. 5). However, as shown in Figure 4.28b, they appeared to be decomposing. The field notes indicated that subsurface melting occurred beneath the thin layer of facets on the snow surface.

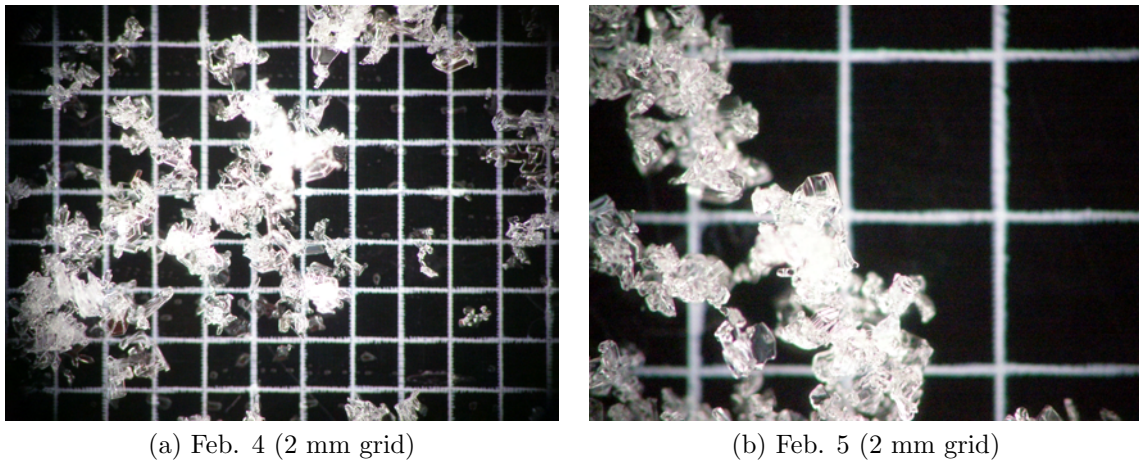


Figure 4.28: Image of near-surface facets formed (a) at the South Station on February 4, 2009 (D-1) ; the facets persisted through the night and were also observed (b) on Feb. 5.

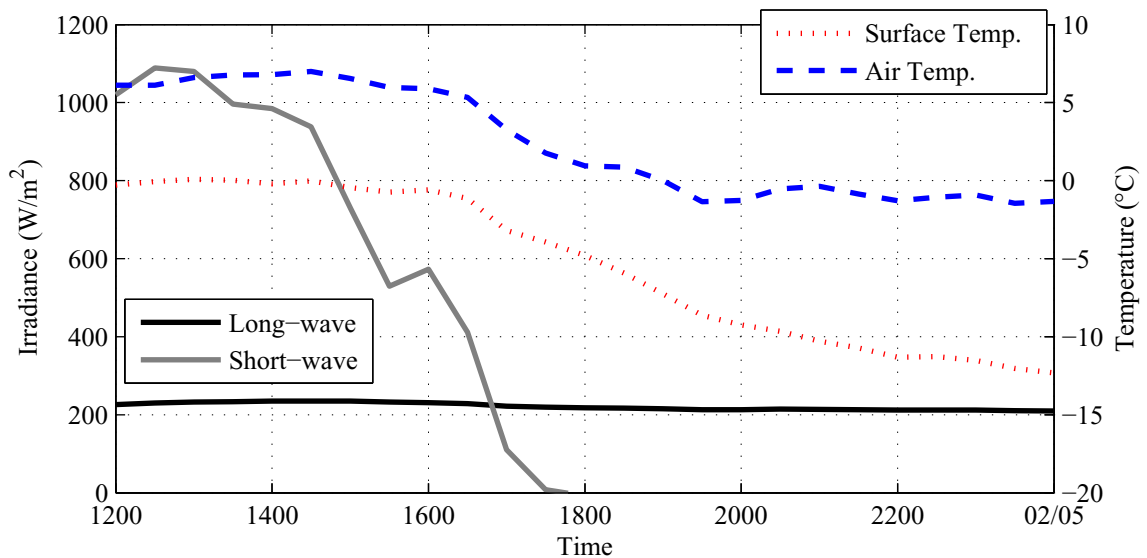
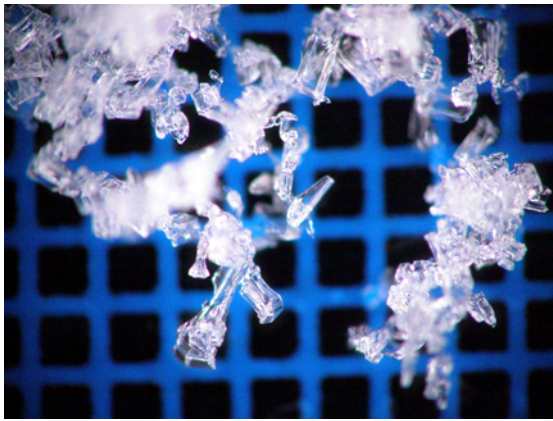


Figure 4.29: Recorded weather data from the South Station on February 4, 2009 (D-1); due to instrumentation malfunctions the data prior to 1200 on Feb. 4 was not recorded.

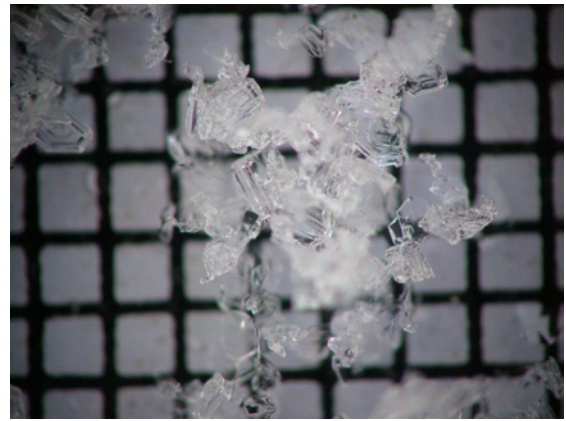
#### 4.5.2 Event D-2: February 8, 2009

An initial observation of the surface snow was conducted at 1045 on February 8, 2009 (D-2) at the South Station, which indicated widespread faceting. A second

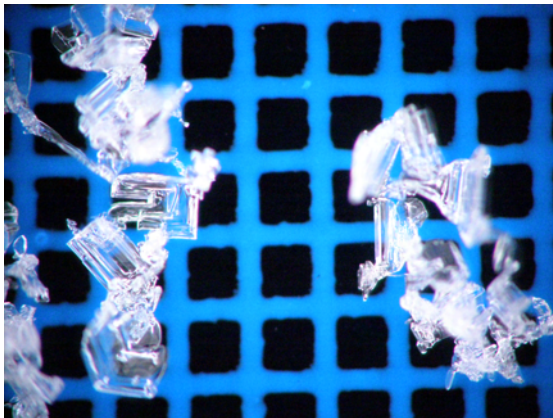
observation was made at 1300 that “found additional faceting.” The facets persisted until the following day (Feb. 9), despite being buried by 2–3 cm of new snow. Images from both observations on Feb. 8 as well as those taken on the following day, are included in Figure 4.30. The weather conditions for Event D-2 were similar to the previous event, only slightly cooler as shown in Figure 4.31. This event was perhaps one of the most obvious of all events, the images show facets that were easily distinguishable and were present in a variety of forms.



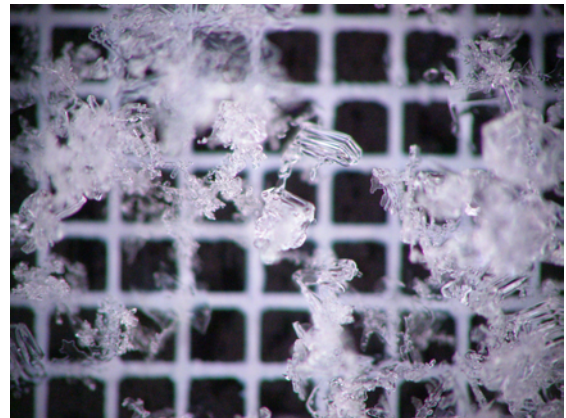
(a) 1045 Feb. 8



(b) 1300 Feb. 8 (#1)



(c) 1300 Feb. 8 (#2)



(d) 1130 Feb. 9

Figure 4.30: Images of a near-surface facet event that occurred on February 8, 2009 (D-2) at the South Station. Images include facets observed (a) at the initial observation, (b and c) at the second observation, and (d) the following day despite being buried underneath new snow.

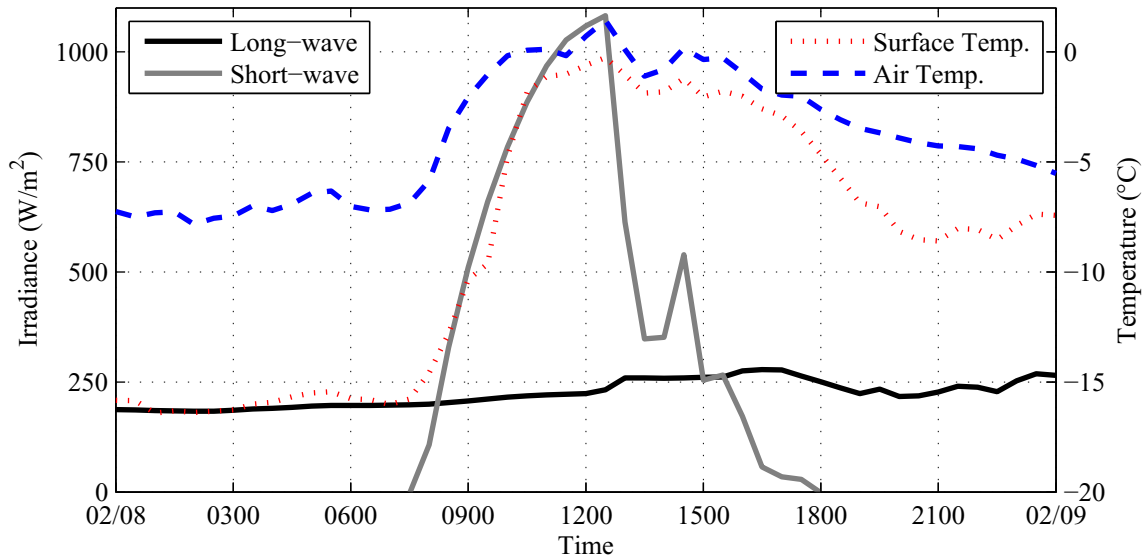


Figure 4.31: Recorded weather data from the South Station on February 8, 2009 (D-2).

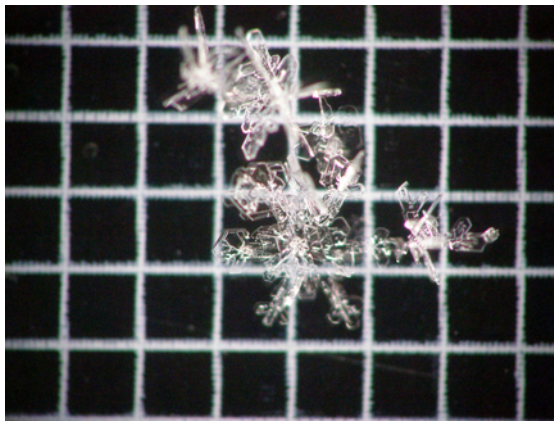
#### 4.5.3 Event D-3: February 12–14, 2008

Event D-3 occurred on February 12, 2009, observations showed that new snow became faceted in a manner of hours. The initial observation at 1015 reported 1–2 mm of new snow (Figure 4.32a). At 1245 facets measuring 1 mm were observed (Figure 4.32b) at the snow surface with a moist layer between 2 and 5 cm. Facets at the surface were observed for the following two days (Figures 4.32c and 4.32d). The field notes on Feb. 14 stated, “[the facets] look larger than yesterday, but not as many striations are noted [and they] don’t seem to be standard [radiation recrystallized near-surface facets].” Hence, it is unknown if the facets observed on the days following the initial event formed during the day, night, or both.

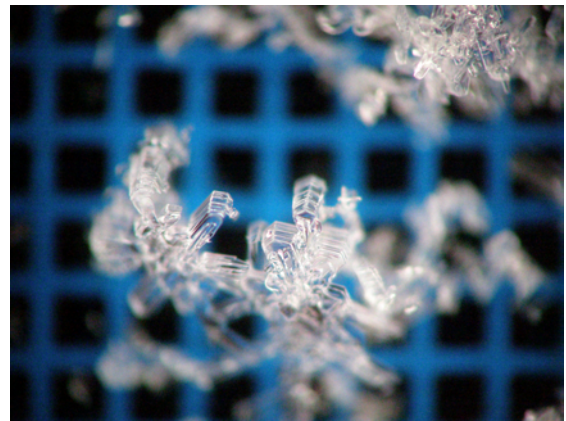
Weather data, including snow and air temperatures as well as long- and short-wave radiation, is provided in Figure 4.33. The conditions for each day were similar to many other events described herein: high incoming short-wave radiation and long-wave radiation near 200 W/m<sup>2</sup>.



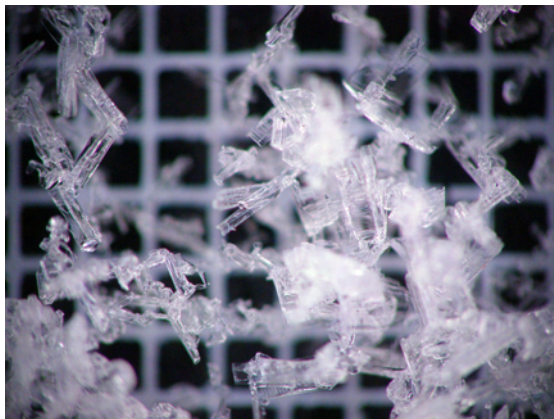
On the night of Feb. 14 new snow (9 cm) was recorded. The following day (Feb. 15) at 0845 the facets detailed in Event D-3 were intact underneath this layer, as shown in Figure 4.34a. At 1300 the buried facets were also observed, although significant decomposition (Figure 4.34b).



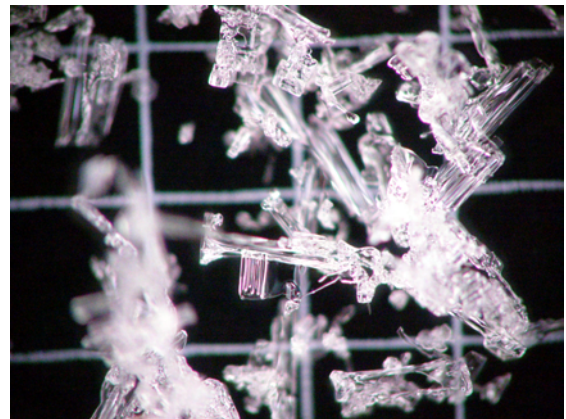
(a) 1015 Feb. 12 (1 mm grid)



(b) 1245 Feb.12(1 mm grid)



(c) Feb. 13 (1 mm grid)



(d) 1245 Feb.14(2 mm grid)

Figure 4.32: Images of near-surface facet event that occurred at the South Station on (a,b) February 12, 2009 (D-3) and that continued on (c) Feb. 13 and (d) 14.

#### 4.5.4 Event D-4: February 19, 2009

Small 0.3 mm facets were observed on February 19, 2008 (D-4) at 1245 at the South Station, as shown in Figure 4.35. The facets appeared intermixed with the 8

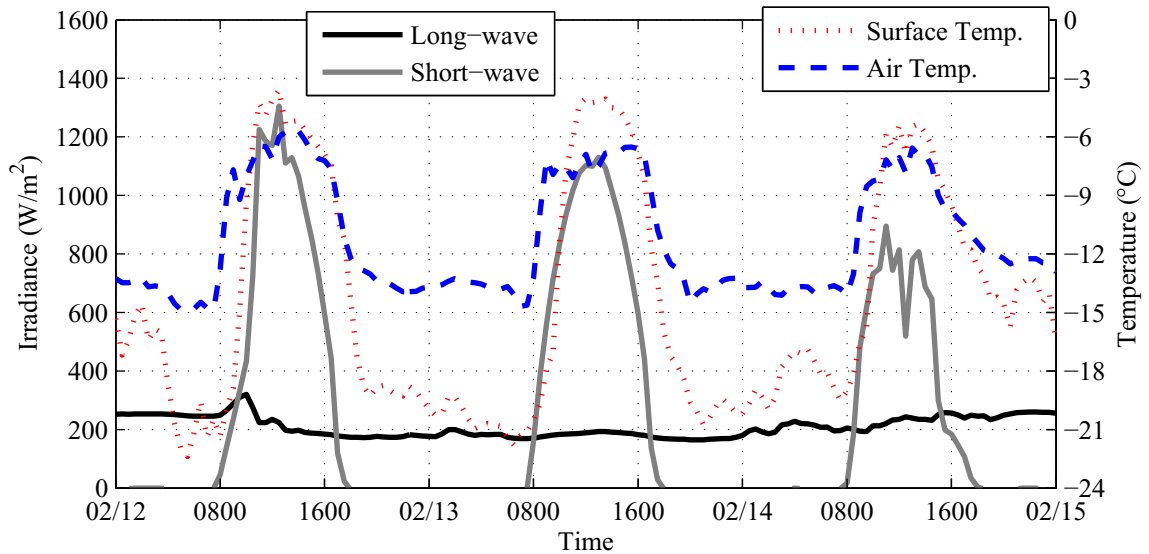
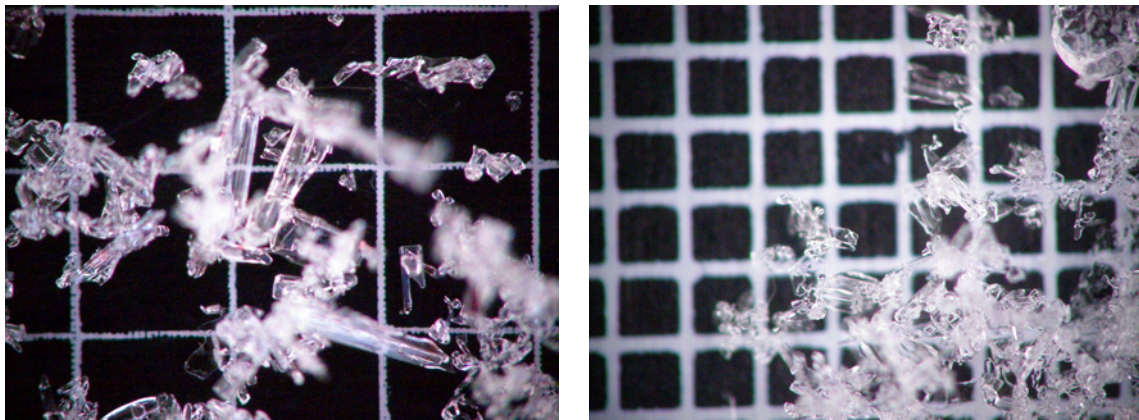


Figure 4.33: Recorded weather data from the South Station on February 12–14, 2009 (D-3).



(a) 0845 (2 mm grid)

(b) 1300 (1 mm grid)

Figure 4.34: Images of a near-surface facet event (D-3) that occurred at the South Station and persisted beneath 9 cm of new snow falling on the night of Feb. 14.

cm of new snow that was recorded at 0700. The weather conditions (Figure 4.36) were typical of many of the other events described throughout this chapter.

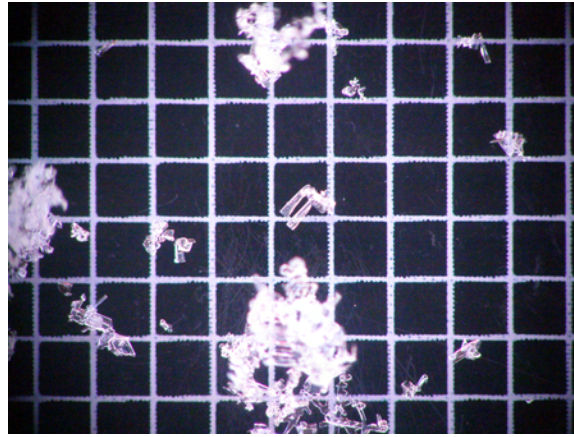


Figure 4.35: Image of near-surface facets observed at the South Station on February 19, 2009 (D-4).

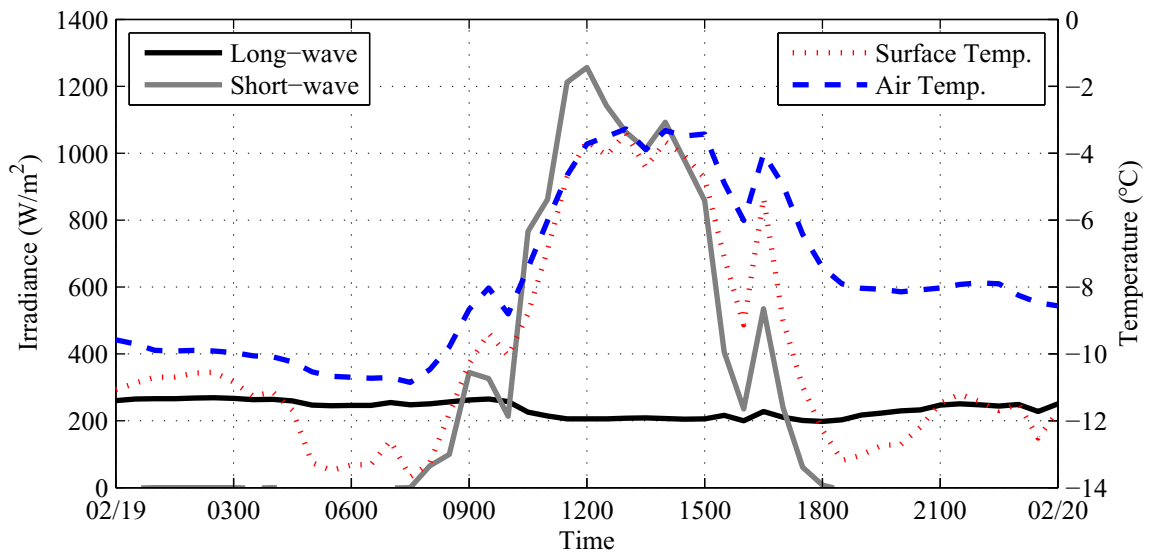


Figure 4.36: Recorded weather data from the South Station on February 19, 2009 (D-4).

#### 4.5.5 Event D-5: February 21, 2009

Small 0.5 mm facets were observed at the South Station in the snow surface at 1045 on February 21, 2009 (D-5), the weather data surrounding the event is provided in Figure 4.37. Similar facets were observed at the North Station at 0900. The field notes from the South Station stated that “as with the north plot, there seems to be

some small facets at the surface. Not that many advanced forms and it doesn't look like surface hoar." The field notes from the North Station also stated that "a few [of the facets] look like the classic [radiation-recrystallized near-surface facets] we saw last year at the South plot." Figures 4.38a and 4.38b are images from the South and North Stations, respectively.

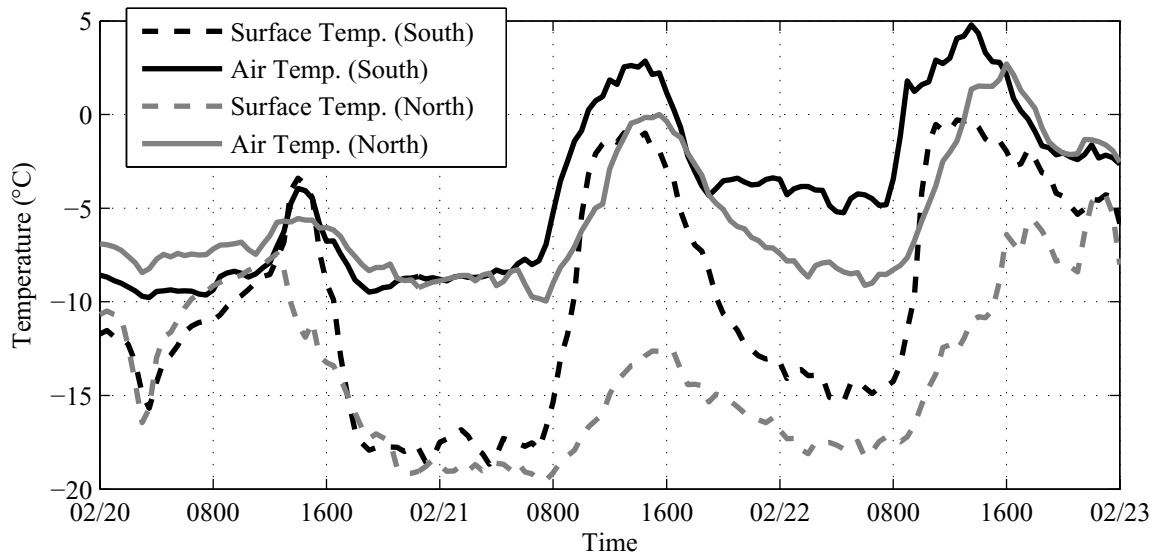


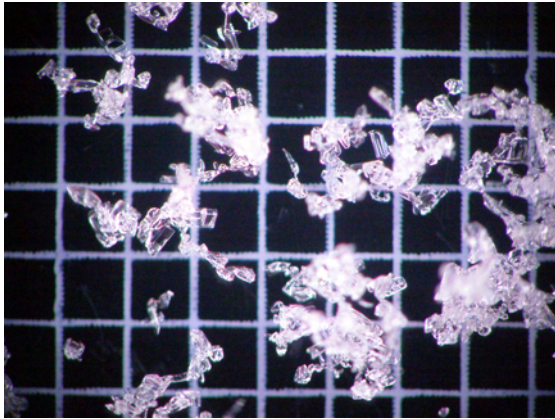
Figure 4.37: Recorded weather data from the South and North stations on February 21, 2009 (D-5).

The following day, facets were reported at both the South and North sites once again. At the North Station "0.5 mm mixed facets" were reported between 1 cm and 3 cm. At the South Station 0.5 mm facets were reported at the snow surface. Images of the facets from the South are included in Figure 4.38c; no images were taken from the North Station.

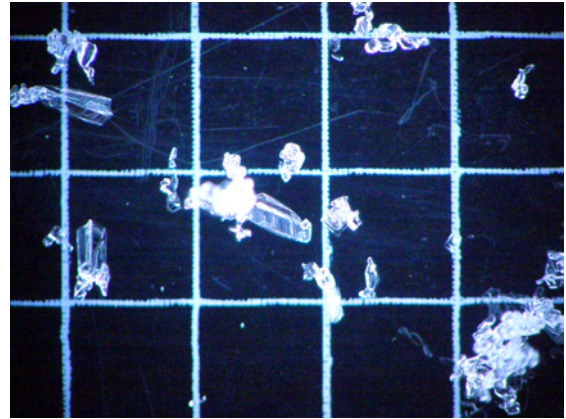
Since these crystals were observed at both locations, it is assumed that they formed due to diurnal temperature fluctuations, or possibly they were the beginnings of surface hoar crystals. Figure 4.37 shows the snow surface and air temperatures surrounding the event for both the North and South locations. The night prior to



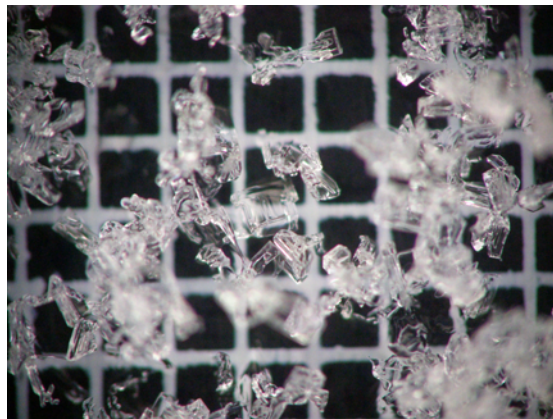
the event, the conditions at both sites were nearly identical: air temperatures near  $-9\text{ }^{\circ}\text{C}$  and snow surface temperature near  $-18\text{ }^{\circ}\text{C}$ .



(a) 1045 Feb. 21 at South Station (2 mm grid)



(b) 0900 Feb. 21 at North Station (2 mm grid)



(c) 1300 Feb. 22 at South Station (1 mm grid)

Figure 4.38: Images of near-surface facets on February 21, 2009 (D-5) that formed small-faceted crystals at both the South and North Stations.

#### 4.5.6 Event D-6: February 27–28, 2009

Event D-6 consisted of an occurrence of radiation-recrystallization at the South Station on consecutive days: February 27 and 28, 2009. The daily weather conditions were typical of the events discussed throughout this chapter, as shown in Figure 4.39.

The two-day conditions where day two was warmer than day one were similar to Events C-2 and C-4.

At 1200 on Feb. 27 the field notes stated that the snow surface was composed of “some small facets (0.25 mm) mixed with new snow.” A second observation was made at 1400; the notes explained that the “surface had changed to 0.5–1 mm facets.” Images of these two observations are included in Figure 4.40.

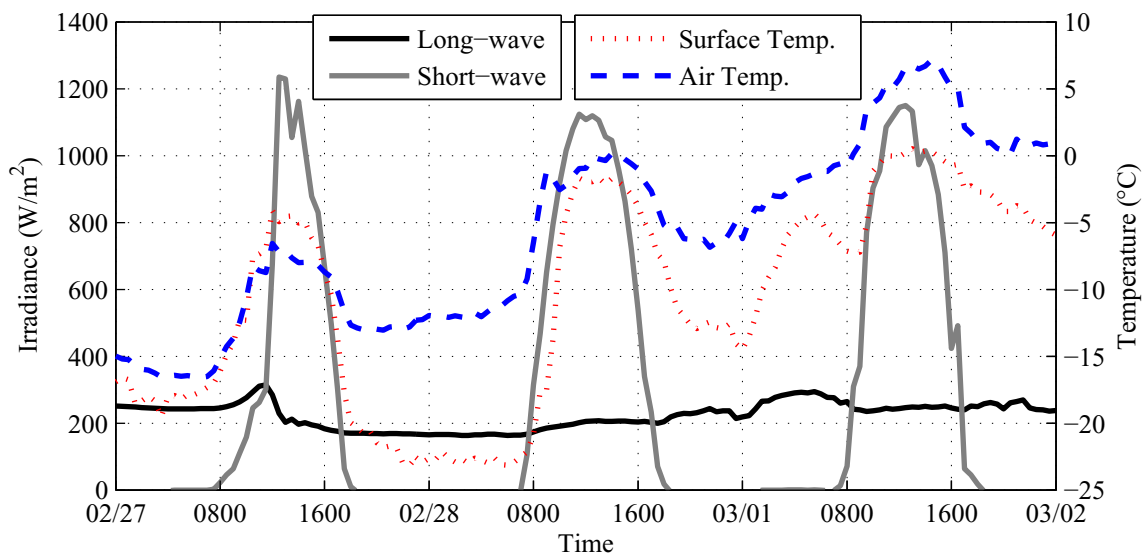


Figure 4.39: Recorded weather data from the South Station on February 27–28, 2009 (D-6).

The following day (Feb. 28) an observation was made at 1000; the notes explained that the facets “from yesterday [were] still visible, but a bit more rounded.” A second observation at 1430 detailed that the “facets in the surface snow appear to have grown some amount since [the] morning [observation].” Images of the two observations from this day are also included in Figure 4.40. The field notes also explained that the “pictures don’t really do it justice” and that “some facet forms look like surface hoar; this was not observed in the [morning].” The facets were also observed on March 1, 2009 but melted during the day due to warm temperatures.

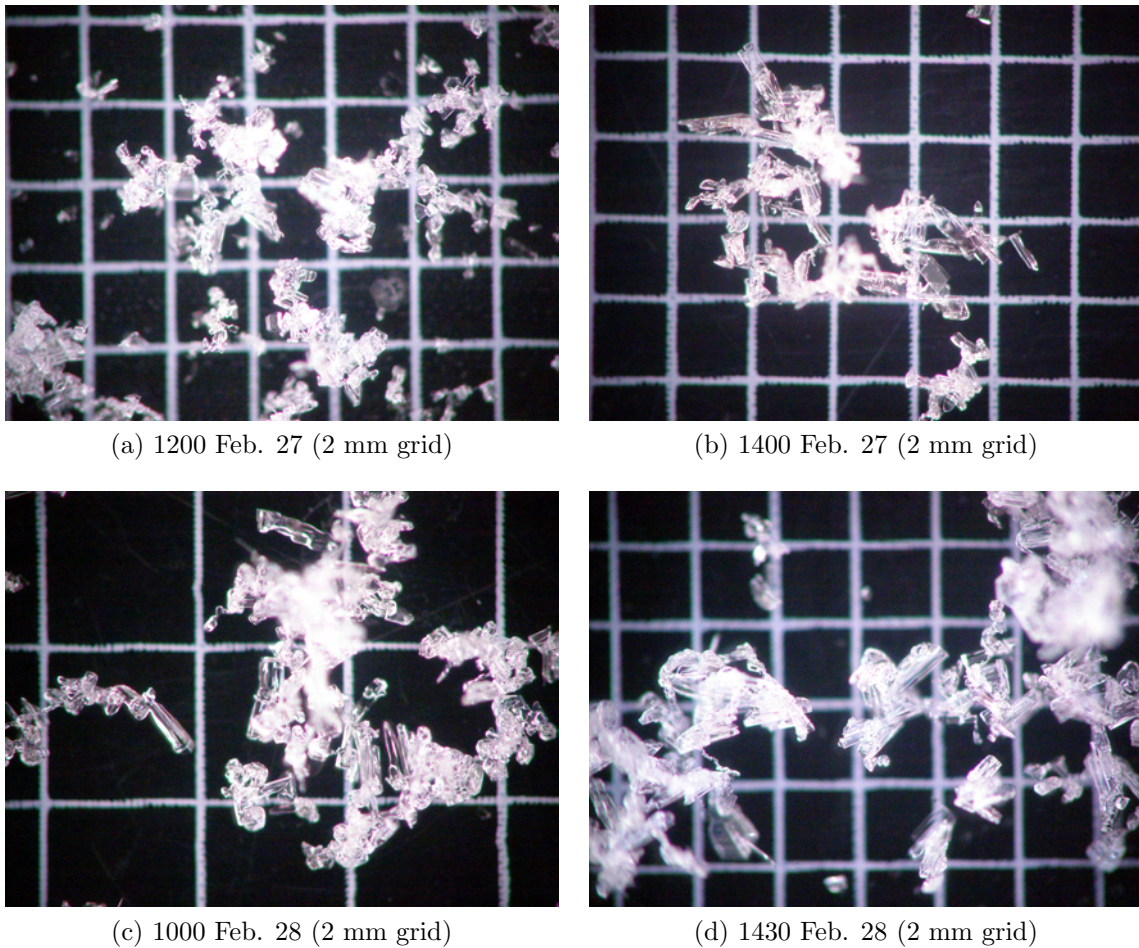


Figure 4.40: Images of radiation-recrystallized near-surface facets from Event D-6 that formed at the South Station on (a,b) February 27 and (c,d) 28, 2009.

#### 4.5.7 Event D-7: March 7, 2009

Event D-7 occurred on March 7, 2009. In the initial observation at 0945 new snow was reported at the South Station, as shown in Figure 4.41a. A second observation was made at 1315 in which “small 0.5 mm facets” were found on the surface layer at the South Station, as pictured in Figure 4.41b. The subsurface at the second observation was moist between 1 cm and 3 cm deep.

Air and snow surface temperatures as well as long- and short-wave radiation for Event D-7 are shown in Figure 4.42. Short-wave radiation peaked near  $1200 \text{ W/m}^2$



and long-wave averaged  $200 \text{ W/m}^2$ . The drop in temperatures and short-wave radiation at 1200 is due to a “brief period of mostly cloudy sky” that occurred around 1145.

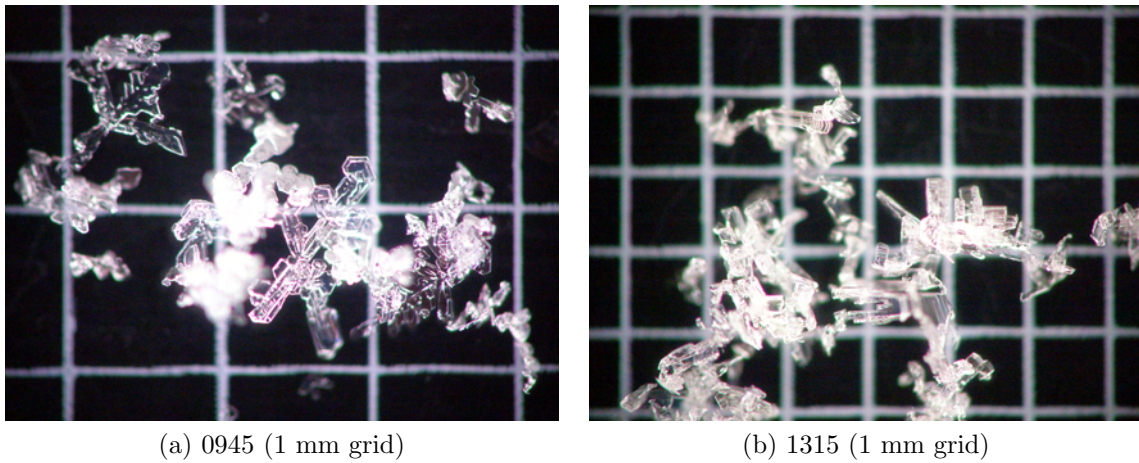


Figure 4.41: Images of a near-surface facet event that occurred at the South Station on March, 7 2009 (D-7).

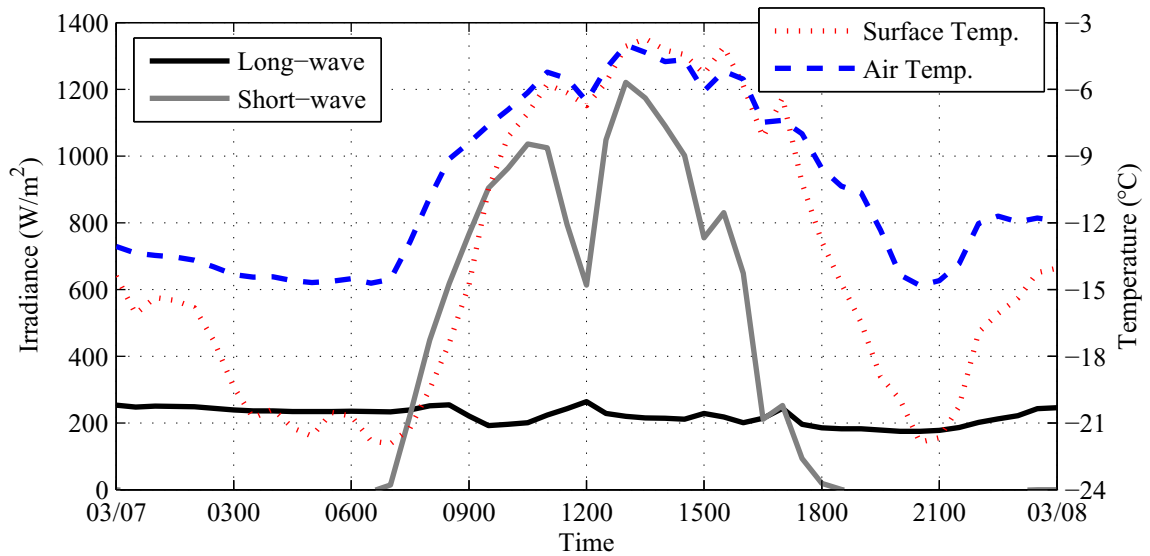


Figure 4.42: Recorded weather data from the South Station on March 7, 2009 (D-7).

#### 4.5.8 Event D-8: March 12–14, 2009

Event D-8 was composed of three consecutive days (March 12–14, 2009) of near-surface facet formation at the South Station. The temperature and radiation data for all three days is presented in Figure 4.43. The prior day (Mar. 11) small 0.1–0.3 mm facets were observed. These small facets persisted throughout the day without change, and at the North Station 1–3 mm surface hoar was reported. The night prior to Mar. 11 the air temperatures ( $-18\text{ }^{\circ}\text{C}$ ) and snow surface temperatures ( $-26\text{ }^{\circ}\text{C}$ ) were the same at both weather stations. Thus, these facets were assumed to be small surface hoar.

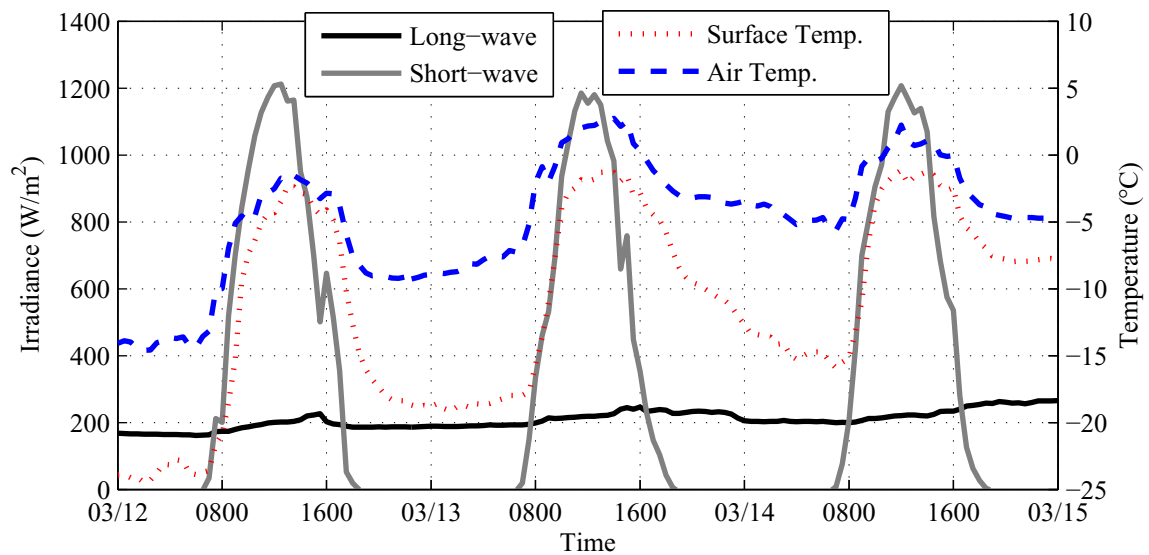


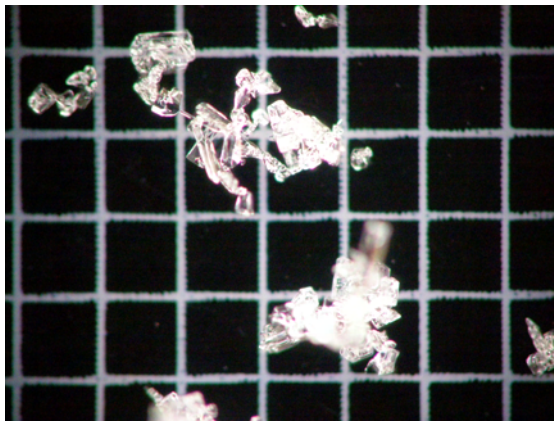
Figure 4.43: Recorded weather data from the South Station on March 12–14, 2009 (D-8).

Facets 0.5 mm in size were reported at the South Station during the initial observation (0945) on Mar. 12. Later that day (at 1345) near-surface facets 1 mm in size were reported on the surface. Images of both observations are shown in Figures 4.44a and 4.44b.

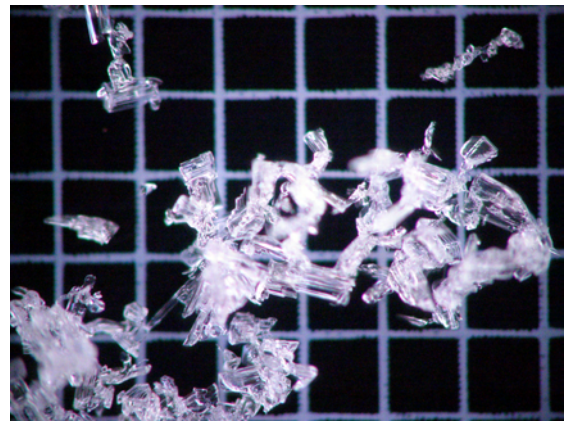
On Mar. 13, the field notes explained that facets observed on the surface at the South Station were composed of “easily visible needles [seen with] the naked eye.” Two sets of images were taken: an AM and PM. However, the field notes did not distinguish the times—only a single time was given of 1220. Figures 4.44c and 4.44d include images from each of the observations made on the second day.

The third day of Event D-8 included two observations at the South Station made at 1120 and 1440. Images of from the snow surface for these observations are included in Figures 4.44e and 4.44f. The field notes described that facets on the snow surface ranged in size from 0.5–2 mm and that the snow was melting to a depth of 15 cm. Examining the images taken, the facets observed clearly changed between the two observations on Mar. 14. The initial images show crisp rectangular facets, while the images show facets that seem to be mixing with melting snow and are more hexagonal. These hexagonal crystals also tended to be the some of the largest observed (measuring over 4 mm) for any of the events over the two seasons reported herein. Figure 4.45 includes two examples of these large hexagonal crystals.

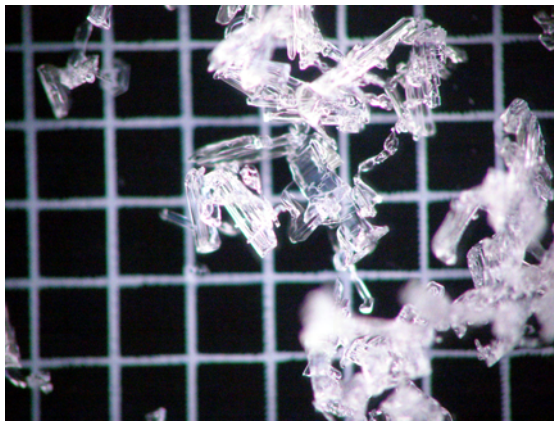
The facets formed during Event D-8 were still visible on Mar. 15 and 16. The field notes stated that the crystals were melted into the top of the melt-freeze crust that developed due to a slight decrease in incoming short-wave radiation and increased wind speed on Mar. 15.



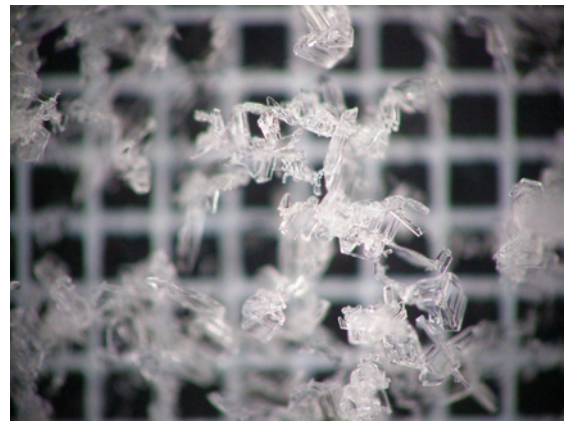
(a) 0945 Mar. 12 (1 mm grid)



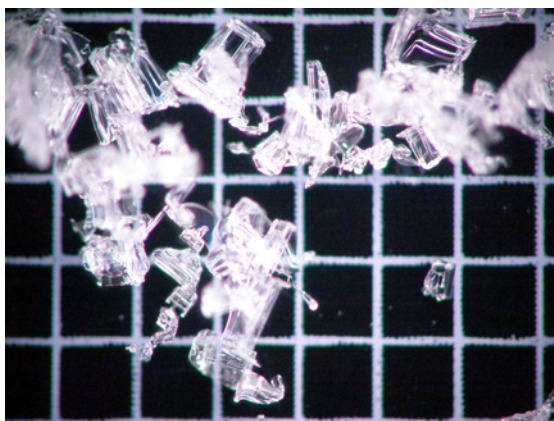
(b) 1345 Mar. 12 (1 mm grid)



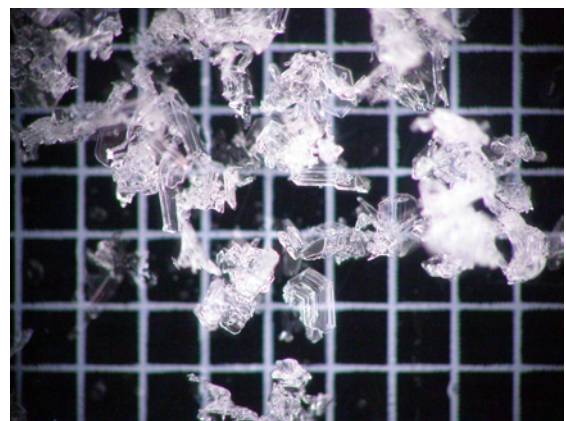
(c) Mar. 13 AM (1 mm grid)



(d) Mar. 13 PM (1 mm grid)



(e) 1120 Mar. 14 (2 mm grid)



(f) 1440 Mar. 14 (1 mm grid)

Figure 4.44: Images of event a near-surface facet event (D-8) that occurred on three consecutive days (March 12–14, 2009) at the South Station.



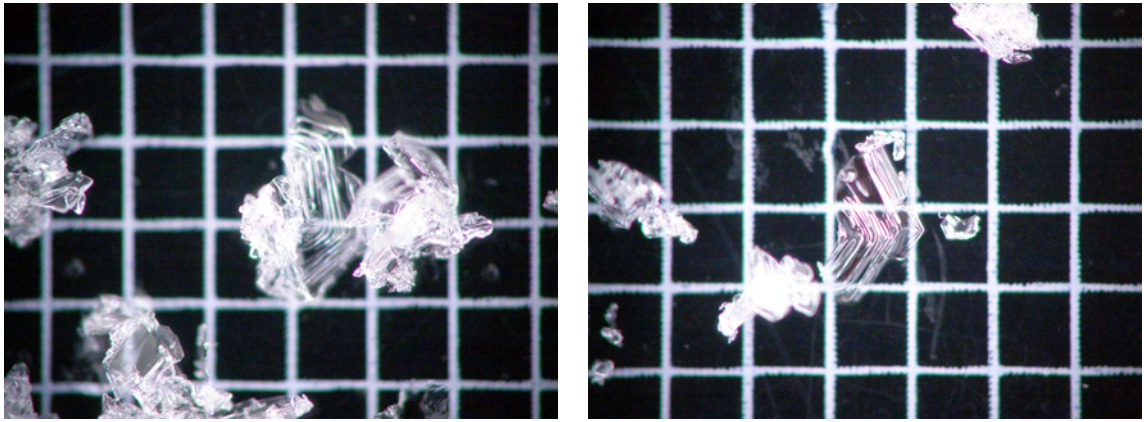


Figure 4.45: Images of large near-surface facets captured at the South Station during the second observation (1440) on March 14, 2009 (D-8).

#### 4.5.9 Event D-9: March 20, 2009

An occurrence of radiation-recrystallized “forms” was recorded on March 20, 2009 (D-9) at the South Station. The weather data shown in Figure 4.46 corresponded well with many of the other events discussed: short-wave radiation peaked at  $1200 \text{ W/m}^2$  and long-wave averaged  $240 \text{ W/m}^2$ . However, the images from this event showed only a few hints of faceted crystals, see Figure 4.47. Observations were made at 1120 when air temperatures were reaching nearly  $7 \text{ }^\circ\text{C}$ ; thus, this event was likely on the cusp between melting and near-surface faceting.

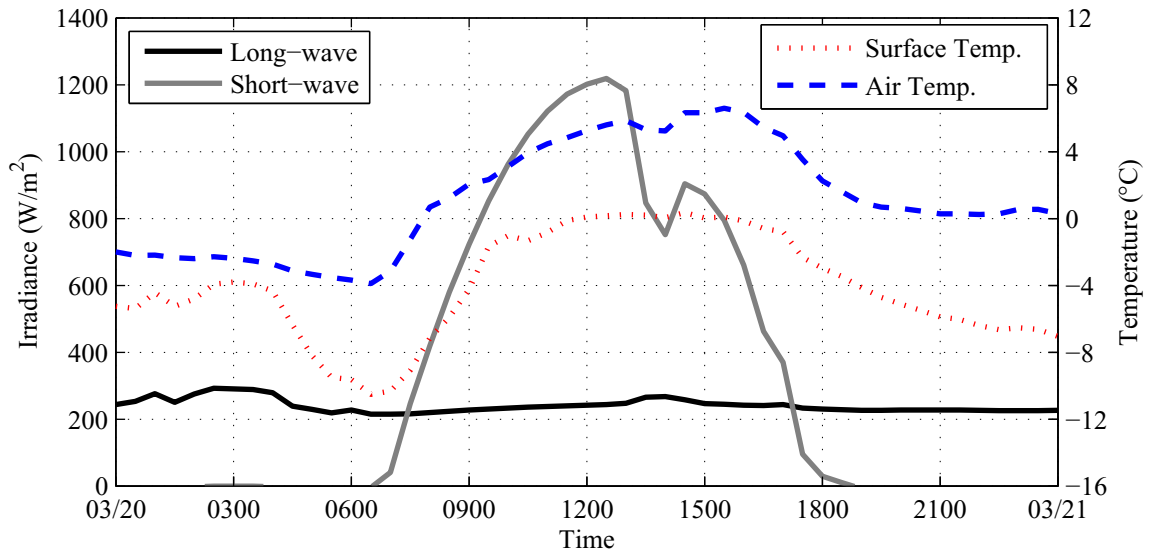


Figure 4.46: Recorded weather data from the South Station on March 20, 2009 (D-9).

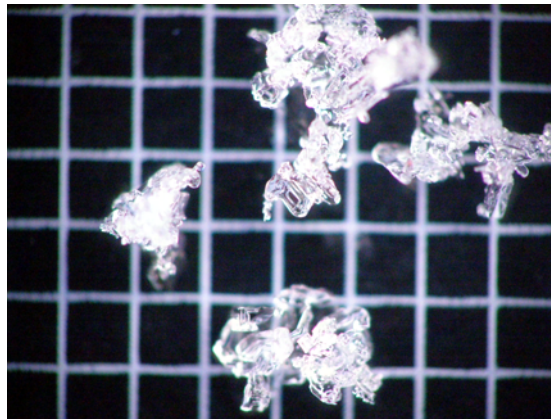


Figure 4.47: Image of slight faceting that occurred at the South Station on March, 20 2009 (D-9).

#### 4.5.10 Event D-10: March 30, 2009

Event D-10 occurred on March 30, 2009 at the South Station. Initial observations at 1130 indicated that the snow surface was composed of 1–2 mm new snow, see Figure 4.48a. A second observation at 1415 reported that stellars had 0.3 mm facets attached, as shown in Figure 4.48b. The weather data, see Figure 4.49, shows that

the skies likely cleared between 1000 and 1100, just prior to the initial observations. At this time the long-wave radiation decreased from 300 W/m<sup>2</sup> to 200 W/m<sup>2</sup>.

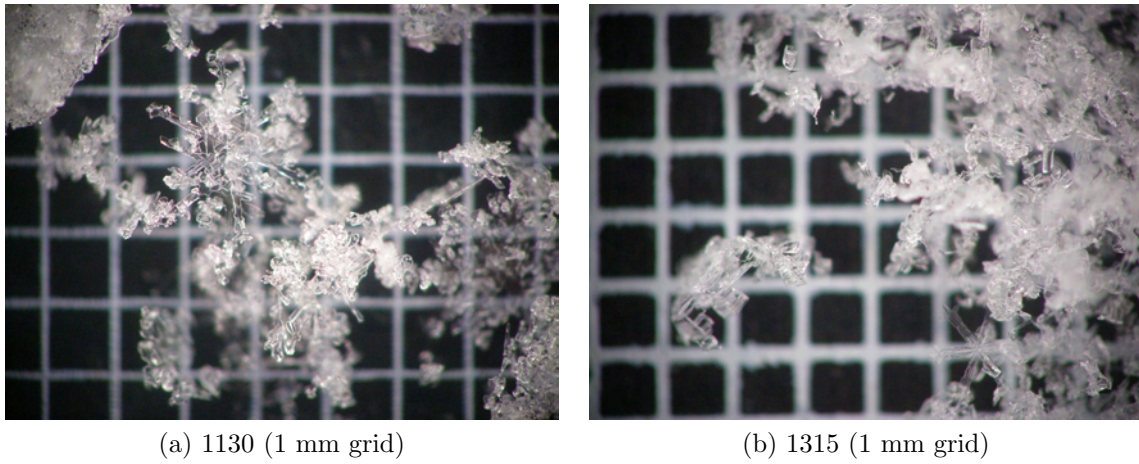


Figure 4.48: Images from two observations—(a) 1130 and (b) 1315—of a near-surface facet event that occurred at the South Station on March, 30 2009 (D-9).

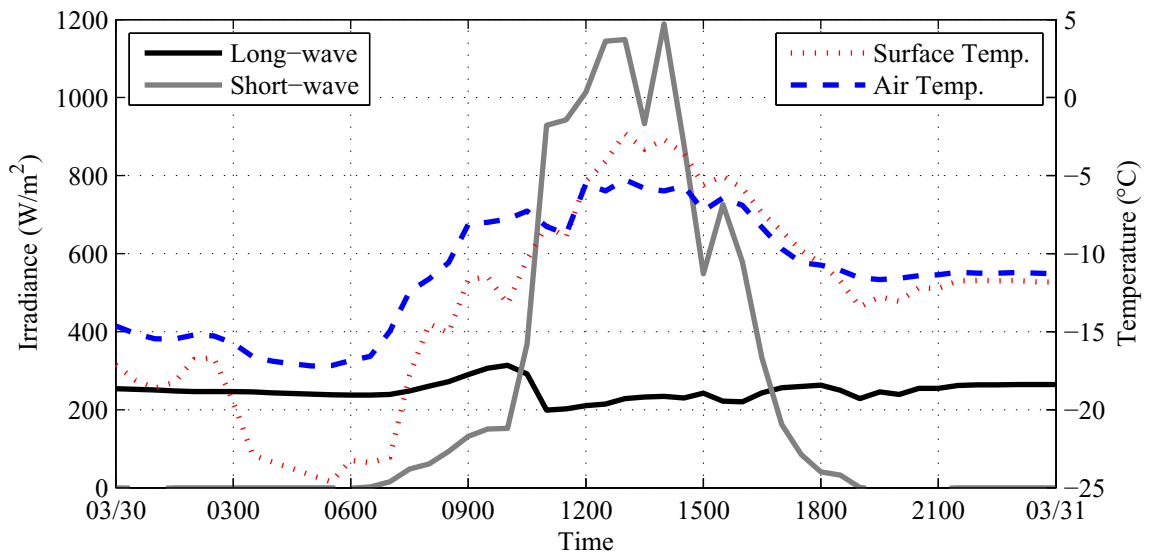


Figure 4.49: Recorded weather data from the South Station on March 30, 2009 (D-10).

#### 4.5.11 Event D-11: April 6, 2009

The final near-surface event (D-11) of the 2008/2009 winter season occurred on April 6, 2009 at the South Station. This event was very similar to Event D-9, though the snow surface temperature remained a few degrees cooler resulting in more identifiable facets, as shown in Figure 4.50. The temperature and radiation data for this event is included in Figure 4.51.

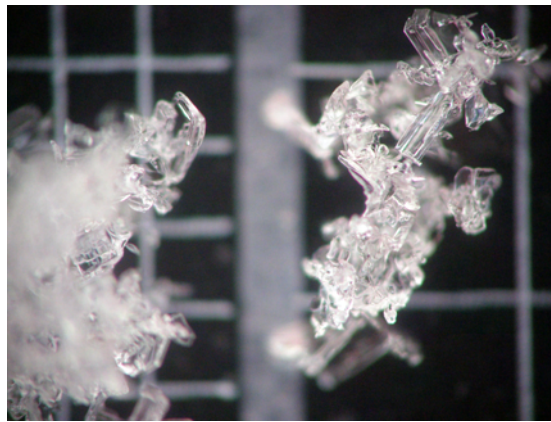


Figure 4.50: Image from near-surface facet event that occurred at the South Station on April 6, 2009 (D-11).

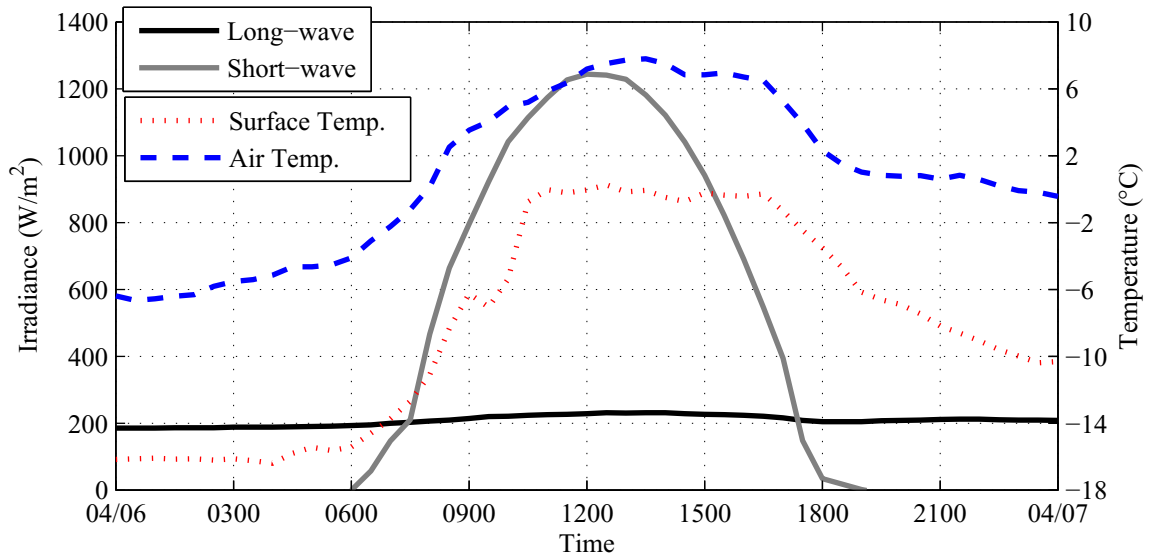


Figure 4.51: Recorded weather data from the South Station on April 6, 2009 (D-11).

#### 4.6 Analysis

The data collected throughout both seasons presented herein may be utilized to help pinpoint the conditions favorable for near-surface facet development, particularly due to radiation recrystallization. This was accomplished by comparing daily averages of all recorded weather data over the two seasons with the specific days associated with the near-surface facet events.

Figures 4.52 and 4.53 include histograms showing the frequency of all data observed superimposed with the data on each day with a near-surface facet event. Figure 4.52 contains the radiation data, including short- and long-wave, as well as the ratio of the two for both the South and Aspirit Stations. The long-wave radiation, and consequently the ratio with short-wave radiation from the South Station only contains data from the 2008/2009 (B) season due to unreliable short-wave radiation data (see Section 3.2.2). Figure 4.53 contains the histograms of air and snow surface

temperature, wind speed and direction, and relative humidity from the South Station for both seasons.

For each of these histograms, the complete daily averages were compared to the event-only data. This was accomplished via the two-sample Kolmogorov-Smirnov test (KS-test), which determines if the two data sets are from the same distribution. The results of these comparisons are included in Table 4.3, where the null hypothesis ( $H_0$ ) was that two data sets were from the same distribution with a 5% significance level. The hypothesis test stated that  $p$ -values less than 0.05 (i.e., 5% significance level) would result in a failure to reject the null hypothesis, that is the distributions are likely different.

Table 4.3: Kolmogorov-Smirnov test results comparing the distribution sets shown in Figures 4.52 and 4.53; the null hypothesis ( $H_0$ ) was that the data were from the same distribution.

Figure	Variable	$H_0$ Result	$p$ -value
4.52a	Short-wave (South)	Reject	$5.32 \times 10^{-9}$
4.52b	Short-wave (Aspirit)	Reject	$3.19 \times 10^{-3}$
4.52c	Long-wave (South 08/09)	Reject	$8.23 \times 10^{-7}$
4.52d	Long-wave (Aspirit)	Reject	$3.27 \times 10^{-8}$
4.52e	SW:LW (South 08/09)	Reject	$7.14 \times 10^{-4}$
4.52f	SW:LW (Aspirit)	reject	$1.73 \times 10^{-7}$
4.53a	Air Temp.	Fail to reject	0.12
4.53b	Snow Temp	Fail to reject	0.35
4.53c	Wind Speed	Fail to reject	0.18
4.53d	Wind Dir.	Fail to reject	1.00
4.53e	Relative Humidity	Reject	$2.97 \times 10^{-5}$

The KS-test results showed that the entire weather data set from both seasons (2007/2008 and 2008/2009) and the event-only weather data are different for both long- and short-wave radiation as well as relative humidity. Thus, the ranges observed could be linked to the formation of the near-surface facet crystals. Using the Bootstrap method, percentiles for the daily mean values of each environmental variable



were determined (Efron and Tibshirani, 1993). Table 4.4 includes the percentiles for the environmental variables of interest that were coupled to the near-surface facet events observed in the field (these variables resulted in a rejection of the null hypothesis). The percentiles presented in the table provide a tool for predicting environmental conditions conducive to near-surface facet formation.

Table 4.4: Percentiles of environmental variables coupled to the observed formation of near-surface facets.

Variable	Units	5%	10%	20%	30%	40%	50%	60%	70%	80%	90%	95%
Short-wave (South)	W/m <sup>2</sup>	376	450	508	542	587	621	648	670	685	701	714
Short-wave (Aspirit)	W/m <sup>2</sup>	199	203	212	218	221	223	225	229	234	240	243
Long-wave (South 08/09)	W/m <sup>2</sup>	209	242	292	316	341	368	389	407	425	450	489
Long-wave (Aspirit)	W/m <sup>2</sup>	172	178	186	192	198	203	208	214	220	230	242
SW:LW (South 08/09)		2.09	2.20	2.48	2.74	2.90	3.00	3.08	3.18	3.33	3.50	3.56
SW:LW (Aspirit)		0.99	1.14	1.41	1.57	1.68	1.80	1.91	2.00	2.14	2.41	2.59
Relative humidity	%	22.9	26.7	34.1	39.9	44.8	48.9	53.3	57.6	61.1	64.7	66.5

Morstad *et al.* (2007) successfully formed radiation-recrystallized near-surface facets in ten laboratory experiments. The mean short-wave radiation for these experiments was one of three values: 595, 755, or 1180 W/m<sup>2</sup>. Long-wave radiation ranged from 270–320 W/m<sup>2</sup> and relative humidity ranged between 15 and 40%. A comparison of these values with the tabulated data in Table 4.4 indicated that only the experiment conducted with short-wave at 595 W/m<sup>2</sup> fell within the range of average values observed in the field at the South Station. Interestingly, this experiment resulted in the largest facets (1 mm) of any experiment conducted by Morstad *et al.* (2007, Table 1). The long-wave radiation and relative humidity from the Morstad *et al.* (2007) experiments fell in the lower portion of the values observed in the field observation discussed in this Chapter. Finally, a computation of the ratio of short-to long-wave radiation from the laboratory experiments yielded four values: 2.2, 2.4, 2.7, and 3.9. These values, with exception of the 3.9, fit between the 10<sup>th</sup> and 30<sup>th</sup>



percentiles. Observations made at the South Station by Cooperstein *et al.* (2004) reported near-surface facet growth during  $587 \text{ W/m}^2$  of short-wave radiation, which falls at the 40<sup>th</sup> percentile of the data presented in this work.

#### 4.7 Conclusions

Throughout two seasons of observations, 26 near-surface events were observed on a south-facing slope with no conclusive events recorded at the north-facing slope. The events reported at the South station in this work typically formed under clear skies. A comparison of the daily mean environmental conditions from the near-surface facet events with that of the daily means entire data set support that only short- and long-wave radiation as well as relative humidity demonstrate statistically significant differences. Slope parallel incident short-wave radiation ranged from  $380\text{--}710 \text{ W/m}^2$ , long-wave ranged from  $210\text{--}240 \text{ W/m}^2$ , and relative humidity between 23% and 67% for all near-surface facet events. However, these results are only based on a small set of data from two locations. Further research documenting near-surface facet formation is needed from various locations for multiple seasons.

The formation of near-surface facets seemed to be dominated by the interaction of short-wave radiation gain just below the surface and cooling at the snow surface due to long-wave radiation loss. This was evident through field notes that indicated that a majority of the events showed crystals which appeared to develop during the daylight hours and that the facets were often diminished the day following the event. However, this was not the case for all events. This finding emphasizes that the traditional separation of diurnal- and radiation-recrystallized facet formation as separate processes may not be appropriate. These processes likely occur simultaneously and radiation-recrystallization may be more prevalent than previous research suggests.

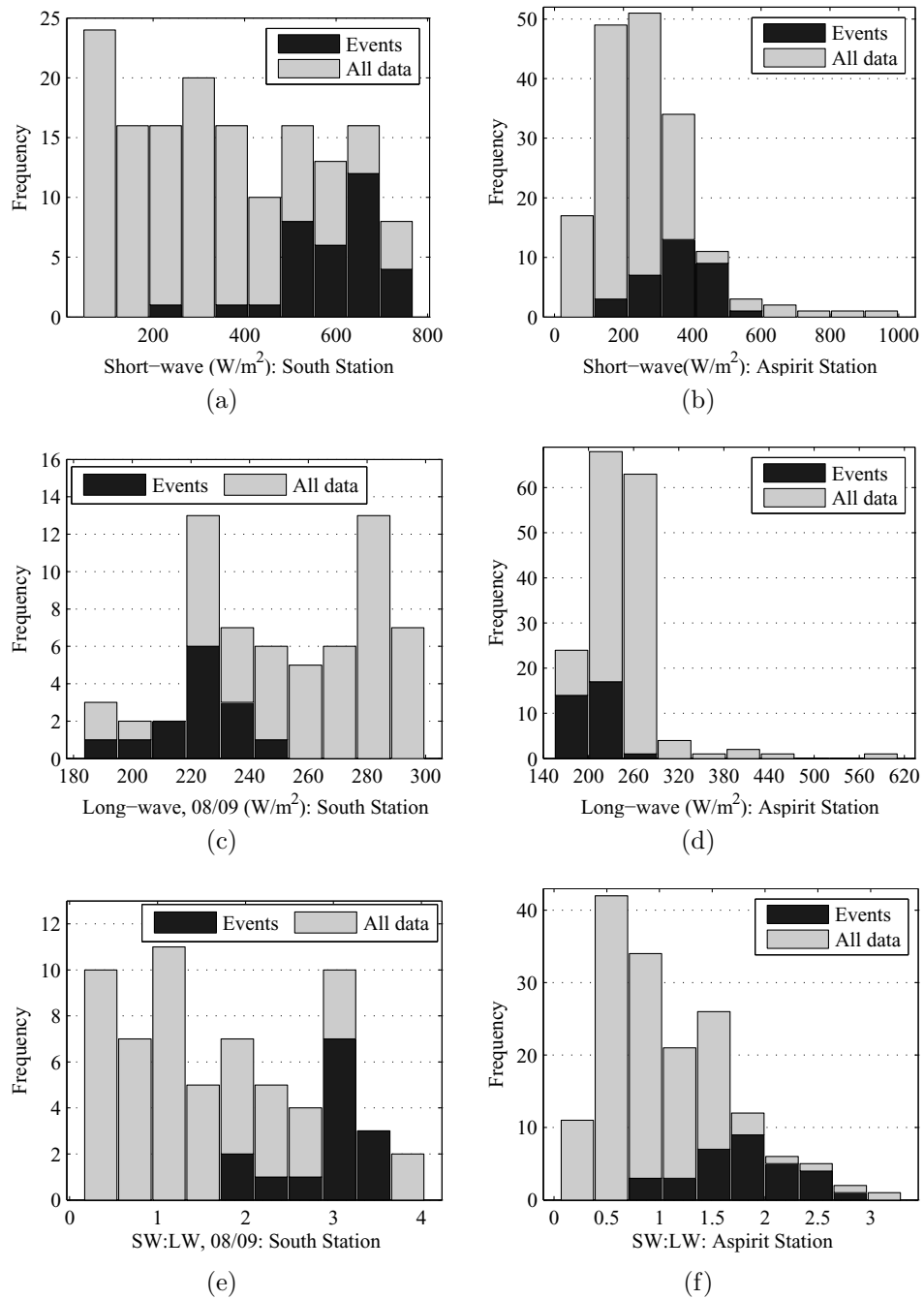


Figure 4.52: Histograms comparing daily average radiation conditions for the entire data set (2007/2008 and 2008/2009 seasons) against the days associated with near-surface facet events: (a) short-wave radiation at the South Station, (b) short-wave radiation at the Apsirit station, (c) long-wave radiation at South Station for 2008/2009 season, (d) long-wave radiation at the Apsirit Station, (e) the ratio of short- to long-wave radiation (SW:LW) at South Station for 2008/2009 season, and (f) the ratio between short- and long-wave radiation at the Apsirit station.

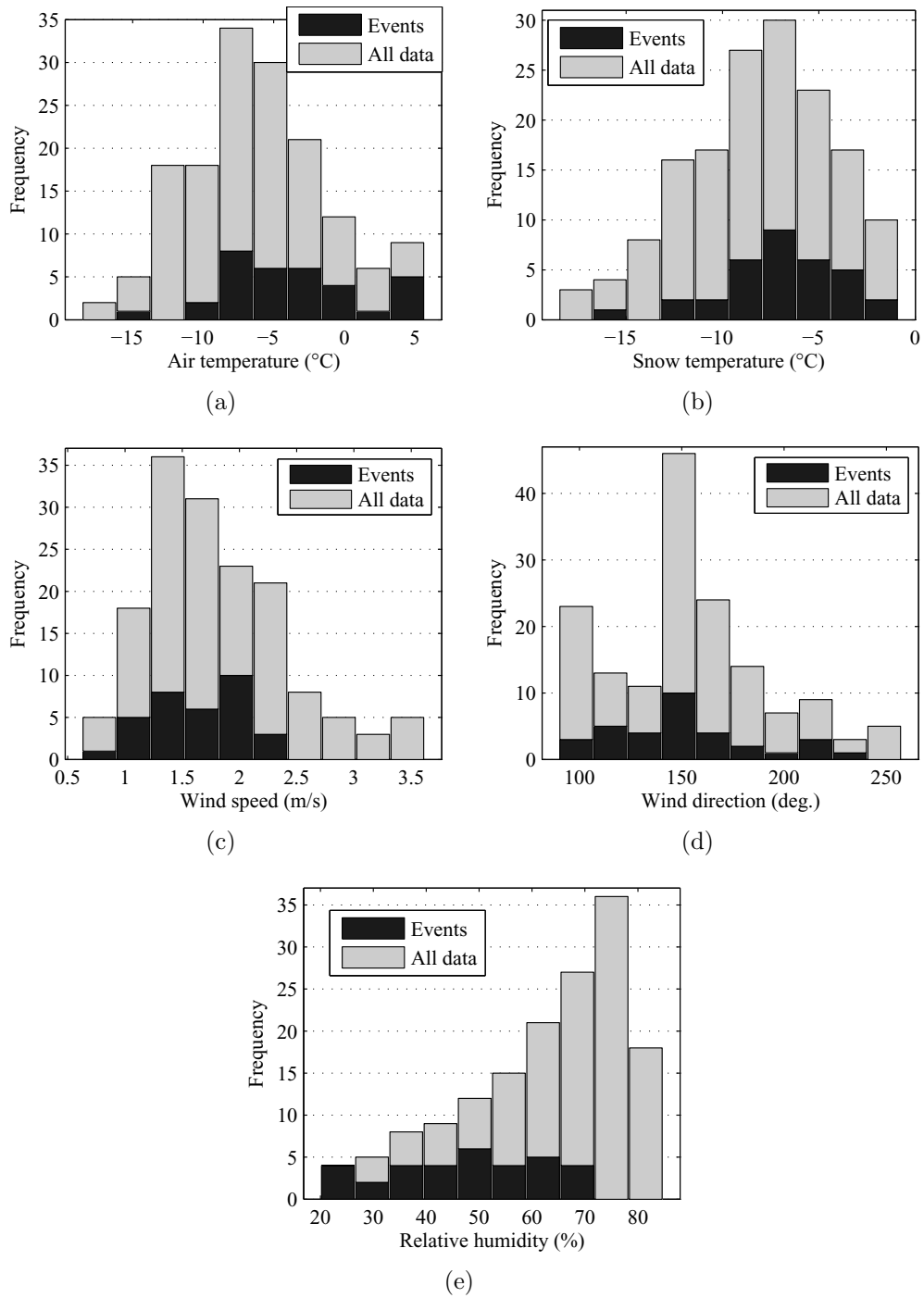


Figure 4.53: Histograms comparing the daily average weather conditions—(a) air temperature, (b) snow surface temperature, (c) wind speed, (d) wind direction, and (e) relative humidity—for the entire data set (2007/2008 and 2008/2009 seasons ) against the days associated with near-surface facet events at the South Station.

## CHAPTER 5

### SNOW THERMAL MODEL

#### 5.1 Introduction

Various models exist for snow that range from simple 1-D conduction to complete 3-D finite element constructs. Section 5.2 provides a broad overview of various modeling endeavors, including the model discussed in this chapter. The model presented is a simple 1-D heat equation-based energy balance model, written in MATLAB (The Mathworks, Inc.), which includes attenuation of short-wave radiation for computing snowpack temperatures.

This chapter serves to highlight the details surrounding the model development, including the theoretical derivation, numerical representation, example usage, and the reliability of the output. Details regarding the usage of the model, including the source code, are included in the user manual in Appendix C. The model presented herein was originally implemented by Morstad *et al.* (2007) and was subsequently re-developed, as presented here, to improve the application of the boundary conditions, improve computational efficiency, and enhance usability for future researchers. Increasing the computational efficiency was necessary to perform the analysis presented in Chapters 7–10, which required millions of model evaluations. Additionally, visible (VIS) and near-infrared (NIR) components were added to the short-wave radiation attenuation to allow snow material properties related to radiation to vary between these two wavebands.

## 5.2 Background

Modeling the thermal behavior of snow is not a new endeavor. LaChapelle (1960) cited papers from as early as 1892 that examined temperature profiles of snow. In his critique, experimental and theoretical means were explored regarding thermal conductivity and vapor transport, all of which show a high degree of associated uncertainty. This uncertainty is expected considering that snow is a complex system that consists of a porous, phase-changing material that is subject to atmospheric radiation. Adams and Sato (1993) explored modeling thermal conductivity using an idealized snowpack; the findings indicated that, under certain geometric conditions, the theoretical results were in close agreement with empirical data and, as expected, the geometry of the snow grains was critical to determining the thermal conductivity. A significant amount of work has examined snow using a continuum mechanics theory of mixtures (Adams and Brown, 1989, 1990; Morland *et al.*, 1990; Bader and Weilenmann, 1992; Brown *et al.*, 1994, 1999). However, Boone and Etchevers (2001) indicated that the application of such models can be unattractive due to computation time; therefore a detailed comparison with simpler models was explored that yielded comparable results.

A non-dimensional approach was utilized by Gray and Morland (1994) that reduced a mixture theory analysis (Morland *et al.*, 1990) to a set of four differential equations using a variety of simplifications. Then, contour plots were developed for varying non-dimensional time and depth using non-dimensional parameters for snow temperature, snow density, and surface air velocity. However, the results obtained were developed for long time scales (winter season) but neglected to account for the effects of solar penetration. Additional non-dimensional work was later conducted to assess the snow for shorter time scales (15 min) and small layers (mm scale) (Bartelt

*et al.*, 2004). Using a thermal non-equilibrium approach, this study also indicated that temperature differences between the pore air and ice particles in the uppermost layer of snow (within 0.2 m of the surface) were on the order of  $\pm 5$  °C and that interfacial heat exchange between snow crystals played a significant role in determining the temperature profile.

Perhaps the most comprehensive model developed to date is the SNOWPACK model, which was designed to improve avalanche warnings (Lehning *et al.*, 1999). The model was intended to provide snowpack information using data from a number of automated weather stations. Initial results examining the accuracy of the model were considered a “reasonable representation” (Lehning *et al.*, 1999). SNOWPACK has been explained in detail in a series of papers (Bartelt and Lehning, 2002; Lehning *et al.*, 2002a,b). The model was explained as a one-dimensional three-phase (ice, water, and air) model that accounts for heat transfer, water transport, vapor diffusion, and mechanical deformation with special conditions for wind drifting and snow ablation (Bartelt and Lehning, 2002). Research conducted in an attempt to validate the SNOWPACK model yielded reasonable results: The predicted temperature profiles were stated to be “fairly accurate” by Lundy *et al.* (2001), but Fierz and Lehning (2001) encouraged additional work regarding the initial stage of snow metamorphism, specifically the processes involving particles changing to small faceted or rounded crystals.

Attempts to model the metamorphism of snow due to temperature gradients using a heat-transfer approach has been attempted by many authors; some of the earliest work was presented by Adams and Brown (1982a,b, 1983). Adams and Brown (1982a) initially examined vapor transport through a pore space of two snow crystals as established by the presence of a temperature gradient. The results agreed with experimental work conducted by other researchers. Adams and Brown (1983) expanded

upon this effort by including a heat-conduction equation that considered internal heat generation. This was the basis of the model utilized by Morstad *et al.* (2007) as well as the model presented in this chapter. The aforementioned models were based on general heat transfer principles, the basic equation of which may be found in introductory heat transfer textbooks (e.g., Incropera *et al.*, 2007). However, the model has been refined significantly with respect to the input terms, specifically the supply term. Morstad *et al.* (2007) included the surface effects of long-wave radiation exchange, latent heat, and sensible heat as well as the internal heat generation of absorbed shortwave radiation. This augmentation is similar to many other models including SNOWPACK (Lehning *et al.*, 2002b) and is common when assessing the energy balance of a snowpack (Armstrong and Brun, 2008). The governing equations for each of these terms were adopted from a variety of sources and a detailed description of each is contained in Morstad (2004) as well as the following sections. It is important to note that other similar models have been developed, but with varying supply terms. Singh and Gan (2005) compared three models that vary the input terms and determined that a model that approximates heat flow into the snow using a periodic boundary (diurnal) temperature forcing at the surface was shown to be the most statistically accurate for determining snow surface temperature.

### 5.3 Model Development

#### 5.3.1 Conservation of Energy

The First Law of Thermodynamics, also known as conservation of energy, states (e.g., Narashimhan, 1993):

The time rate of change of the sum total of the kinetic energy and the internal energy in the body is equal to the sum of the rates of work done by



the surface and body loads in producing the deformation (or flow) together with the heat energy that may leave or enter the body at a certain rate.

As a mathematical expression, this principle may be written as

$$\frac{d}{dt}(KE + E) = W + R, \quad (5.1)$$

which, as stated above, is a function of macroscopic kinetic energy ( $KE$ ), internal energy ( $E$ ), rate of work acting on the system ( $W$ ), and rate of heat input ( $R$ ).

The system is assumed to remain at rest, thus macroscopic kinetic energy is neglected. Additionally, it shall be assumed that no mechanical work is being performed on the system, so the work rate term is also neglected. Finally, the rate of heat input may be broken into two parts: the heat added to the system across its surface boundary and the heat generated internally or supplied to the volume, that is

$$R = \oint_{CS} -\underline{\xi} \cdot \underline{\hat{n}} dA + \int_{CV} \rho h dV. \quad (5.2)$$

This relationship is best described using a control volume as shown in Figure 5.1, which is an illustration detailing that the rate of heat input ( $R$ ) is equivalent to the sum flux of heat ( $\underline{\xi}$ ), across the control surface ( $CS$ ) and the internally generated heat ( $\rho h$ ). The outward normal vector ( $\underline{\hat{n}}$ ) defines the surface and the internal heat is defined as the product of the material density ( $\rho$ ) and the specific heat supply ( $h$ ). The negative sign preceding the flux vector defines flux of heat into the control volume as positive (i.e., the dot product of the flux and outward normal vector is negative when the flux is entering the control volume).

The internal energy may be described using specific internal energy ( $\vartheta$ ) as

$$\frac{d}{dt}E = \frac{d}{dt} \int_{CV} \rho \vartheta dV. \quad (5.3)$$

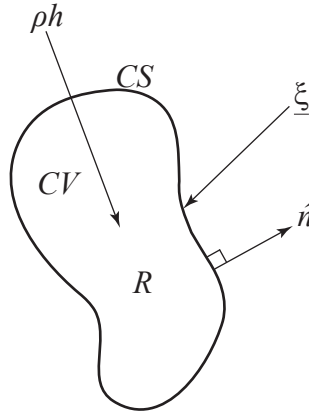


Figure 5.1: Schematic of the arbitrary control volume ( $CV$ ) enclosed by the control surface ( $CS$ ). The rate of heat generation ( $R$ ) is a result of the heat flux across the surface ( $\underline{\xi}$ ) and the heat supply ( $\rho h$ );  $\underline{\hat{n}}$  is the outward normal vector.

Therefore, Equation (5.1), with the aforementioned assumptions, may be rewritten as

$$\frac{d}{dt} \int_{CV} \rho \vartheta dV = \oint_{CS} -\underline{\xi} \cdot \underline{\hat{n}} dA + \int_{CV} \rho h dV. \quad (5.4)$$

Using the Reynolds Transport Theorem and the continuity equation, assuming the specific internal energy is a continuous and differentiable function, the left-side of this relationship may be rewritten as (Reddy, 2008, Eq. 5.2.28)

$$\frac{d}{dt} \int_{CV} \rho \vartheta dV = \int_{CV} \frac{d}{dt} \rho \vartheta dV. \quad (5.5)$$

Gauss' Theorem (Liu, 2002) is defined as

$$\oint_{CS} \underline{b} \cdot \underline{\hat{n}} dA = \int_{CV} \underline{\nabla} \cdot \underline{b} dV, \quad (5.6)$$

where  $\underline{b}$  is an arbitrary vector. This expression allows the area integral of Equation (5.4) to be represented as a volume integral. By applying both Equations (5.5) and (5.6), Equation (5.4) may again be rewritten as

$$\int_{CV} \left[ \frac{d}{dt} \rho \vartheta + \underline{\nabla} \cdot \underline{\xi} - \rho h \right] dV = 0. \quad (5.7)$$

For Equation (5.7) to be valid for an arbitrary control volume, the integrand must be zero. The resulting relationship is the differential form of the First Law of Thermodynamics, commonly referred to as the local form of conservation of energy with the absence of mechanical processes:

$$\frac{d}{dt}\rho\vartheta + \vec{\nabla} \cdot \underline{\xi} - \rho h = 0. \quad (5.8)$$

This relationship was the basis of the thermal model for snow presented in this chapter.

### 5.3.2 Application

The following section details the application of Equation (5.8) to the form used for developing the thermal model. The internal energy component of Equation (5.8) is expressed in terms of the specific heat capacity ( $c_p$ ) at a constant pressure, density ( $\rho$ ), and the time rate of change of the material temperature ( $T$ ) as follows,

$$\frac{d}{dt}\rho\vartheta = \rho c_p \frac{\partial T}{\partial t}. \quad (5.9)$$

The heat flux across the control surface ( $\underline{\xi}$ ) is separated into two components such that

$$\underline{\xi} = \underline{q}_k + \underline{q}, \quad (5.10)$$

where  $\underline{q}_k$  is the heat flux due to conduction and  $\underline{q}$  is an additional heat flux component. The latter is detailed in Section 5.3.4, which includes heat flux due to short-wave radiation. This radiation term may be considered a volumetric heat source that would be accounted for in the  $\rho h$  term of Equation (5.8). However, due to the method used to compute and measure this term as a heat flux ( $\text{W}/\text{m}^2$ ); radiation was implemented here as an additional flux term ( $\underline{q}$ ) As such, the  $\rho h$  term of Equation (5.8) is zero.

Fourier's Law of Conduction is defined as

$$\underline{q}_k = -\mathbf{k}\vec{\nabla}T, \quad (5.11)$$

where  $\mathbf{k}$  is the thermal conductivity tensor (Narashimhan, 1993). Using this relationship, Equation (5.10), and the aforementioned assumption that  $\rho h = 0$ , Equation (5.8) may be written as

$$\rho c_p \frac{\partial T}{\partial t} = \vec{\nabla} \cdot (\mathbf{k}\vec{\nabla}T) - \vec{\nabla} \cdot \underline{q}. \quad (5.12)$$

Finally, the material in question is assumed to be thermally isotropic (i.e., thermal conductivity is a scalar,  $k$ ) and reduced to one-dimensional heat flow in the vertical direction,  $z$ . Thus, Equation (5.12) becomes

$$\rho c_p \frac{\partial T}{\partial t} = k \frac{\partial^2 T}{\partial z^2} - \frac{\partial q}{\partial z}. \quad (5.13)$$

Each additive term in this equation has units of W/m<sup>3</sup>, which may be described as the rate of change of energy per unit volume within the system. This equation is an adaptation of the 1-D heat diffusion equation (Incropera *et al.*, 2007) and used for the basis of the thermal model presented in this chapter.

### 5.3.3 Numerical Solution

General Numeric Equation: Equation (5.13) may be solved numerically for the temperature ( $T$ ) of a layered system throughout time ( $t$ ). Referring to Equation (5.13), the Crank-Nicolson Method may be applied as (Chapra and Canale, 2002, p. 849)

$$\rho c_p \frac{\partial T}{\partial t} \cong \rho_i c_{p_i} \left[ \frac{T_i^{j+1} - T_i^j}{\Delta t} \right] \quad (5.14)$$

and

$$k \frac{\partial^2 T}{\partial z^2} \cong \frac{k_i}{2} \left[ \frac{T_{i+1}^j - 2T_i^j + T_{i-1}^j}{(\Delta z)^2} + \frac{T_{i+1}^{j+1} - 2T_i^{j+1} + T_{i-1}^{j+1}}{(\Delta z)^2} \right], \quad (5.15)$$

where the  $j$  index represents the  $j$ -th time step and the layer index is  $i = 1, 2, \dots, n$ , where  $n$  is the number of layers.

Additionally, the heat flux ( $q$ ) from Equation (5.13) may be rewritten as a numerical representation using the forward difference approximation (Chapra, 2005):

$$-\frac{\partial q}{\partial z} \cong \frac{q_i^j - q_{i+1}^j}{\Delta z}. \quad (5.16)$$

Throughout this chapter the layer thickness is assumed constant, thus the  $i$  index is dropped from  $\Delta z$  term; this is done for simplicity and is not a requirement of the method. Figure 5.2 is a schematic showing the layered snowpack for the numerical solution presented here, which includes the temperatures at each node ( $T_i^j$ ) and heat flux across the layer ( $q_i^j$ ), for the  $j$ -th time step. The node above the surface is considered a “phantom” node, which is necessary for the application of the upper boundary condition.

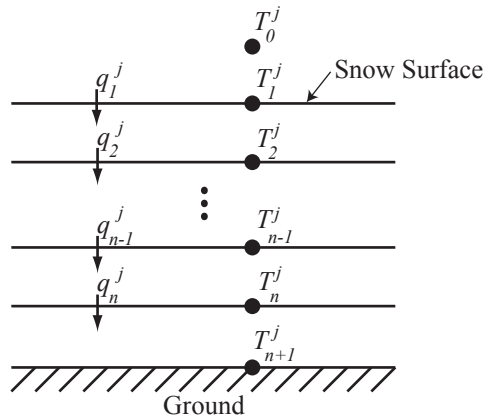


Figure 5.2: Schematic of snowpack layering utilized for numerical solution of snow temperatures with time. The superscript  $j$  represents the  $j$ -th time step and the subscript  $i$  represents the layer number.

The numerical representation of Equations (5.14)–(5.16), may be substituted into Equation (5.13). The result of this substitution yields

$$\frac{\rho_i c_{p_i} T_i^{j+1}}{\Delta t} - \frac{k_i}{2(\Delta z)^2} (T_{i+1}^{j+1} - 2T_i^{j+1} + T_{i-1}^{j+1}) = \dots$$

$$\frac{\rho_i c_{p_i} T_i^j}{\Delta t} - \frac{k_i}{2(\Delta z)^2} (T_{i+1}^j - 2T_i^j + T_{i-1}^j) + \frac{q_i^j - q_{i+1}^j}{\Delta z}, \quad (5.17)$$

where all of the  $j + 1$  and  $j$  temperature terms are relocated to the left and right sides, respectively.

The constant terms of Equation (5.17) may be grouped together as

$$a_i = \frac{k_i}{(\Delta z)^2}, \quad (5.18a)$$

$$b_i = \frac{\rho_i c_{p_i}}{\Delta t}, \quad (5.18b)$$

$$c_i = b_i + a_i, \text{ and} \quad (5.18c)$$

$$d_i = b_i - a_i. \quad (5.18d)$$

In conjunction with the coefficients defined in Equation (5.18), the general numerical representation of the heat equation is written as

$$\frac{-a_i T_{i-1}^{j+1}}{2} + c_i T_i^{j+1} + \frac{-a_i T_{i+1}^{j+1}}{2} = \frac{a_i T_{i-1}^j}{2} + d_i T_i^j + \frac{a_i T_{i+1}^j}{2} + \frac{q_i^j - q_{i+1}^j}{\Delta z}. \quad (5.19)$$

Boundary Conditions: The bottom temperature of the snowpack is assumed to be constant, thus the bottom boundary condition may be defined as

$$T_{n+1}^j = T_{bottom}, \quad (5.20)$$

where  $T_{bottom}$  is a constant temperature.

The top boundary condition is defined as

$$k \frac{\partial T}{\partial z} \Big|_{z=0} = q_s, \quad (5.21)$$

where  $q_s$  is the heat flux across the surface layer at node  $i = 1$ . This flux boundary condition is known as the Neumann condition (Incropera *et al.*, 2007), which states that the flux entering the system at the surface is conducted into the uppermost layer of the system. Section 5.3.5 details the components of  $q_s$ . It may be written numerically—using the central difference approximation (Chapra, 2005)—for the current ( $j$ ) and future ( $j + 1$ ) time steps as

$$q_s^j = k_1 \frac{T_0^j - T_2^j}{2\Delta z} \quad \text{and} \quad (5.22a)$$

$$q_s^{j+1} = k_1 \frac{T_0^{j+1} - T_2^{j+1}}{2\Delta z}. \quad (5.22b)$$

Next, it is assumed the heat flux at the surface in the present time step may be applied to the future time step. This allows Equation (5.22) to be solved for  $T_0^j$  and  $T_0^{j+1}$ , which results in

$$T_0^j = \frac{2q_s^j \Delta z}{k_1} + T_2^j \quad \text{and} \quad (5.23a)$$

$$T_0^{j+1} = \frac{2q_s^j \Delta z}{k_1} + T_2^{j+1}. \quad (5.23b)$$

Equations (5.23a) and (5.23b) are then substituted into Equation (5.19) to produce the upper boundary condition as

$$c_1 T_1^{j+1} - a_1 T_2^{j+1} = d_1 T_1^j + a_1 T_2^j + 2 \frac{q_s^j}{\Delta z} + \frac{q_1^j - q_2^j}{\Delta z}. \quad (5.24)$$

Matrix Solution: Equations (5.19), (5.20), and (5.24) may be represented in matrix form as shown in Equation (5.25),



$$\underbrace{\begin{bmatrix} c_1 & -a_1 & 0 & 0 & \cdots & 0 & 0 & 0 \\ \frac{-a_2}{2} & c_2 & \frac{-a_2}{2} & 0 & \cdots & 0 & 0 & 0 \\ 0 & \frac{-a_3}{2} & c_3 & \frac{-a_3}{2} & \cdots & 0 & 0 & 0 \\ 0 & 0 & \frac{-a_4}{2} & c_4 & \cdots & 0 & 0 & 0 \\ \vdots & \vdots & \vdots & \vdots & \ddots & \vdots & \vdots & \vdots \\ 0 & 0 & 0 & 0 & \cdots & \frac{-a_n}{2} & c_n & \frac{-a_n}{2} \\ 0 & 0 & 0 & 0 & \cdots & 0 & 0 & 1 \end{bmatrix}}_{[A]} \underbrace{\begin{bmatrix} T_1^{j+1} \\ T_2^{j+1} \\ T_3^{j+1} \\ T_4^{j+1} \\ \vdots \\ T_n^{j+1} \\ T_{n+1}^{j+1} \end{bmatrix}}_{\underline{x}} = \underbrace{\begin{bmatrix} d_1 T_1^j + a_1 T_2^j + 2 \frac{q_s^j}{\Delta z} + \frac{q_1^j - q_2^j}{\Delta z} \\ \frac{a_2}{2} T_1^j + d_2 T_2^j + \frac{a_2}{2} T_3^j + \frac{q_2^j - q_1^j}{\Delta z} \\ \frac{a_3}{2} T_2^j + d_3 T_3^j + \frac{a_3}{2} T_4^j + \frac{q_3^j - q_2^j}{\Delta z} \\ \frac{a_4}{2} T_3^j + d_4 T_4^j + \frac{a_4}{2} T_5^j + \frac{q_4^j - q_3^j}{\Delta z} \\ \vdots \\ \frac{a_n}{2} T_{n-1}^j + d_n T_n^j + \frac{a_n}{2} T_{n+1}^j + \frac{q_n^j - q_{n-1}^j}{\Delta z} \\ T_{bottom}^j \end{bmatrix}}_{\underline{b}}, \quad (5.25)$$

which is in the form  $[A]\underline{x} = \underline{b}$ . Thus, the temperatures given in  $\underline{x}$  may be solved using the temperatures from the previous time step, such that  $\underline{x} = [A]^{-1}\underline{b}$ . Hence, the model must be initialized with a temperature profile and it is assumed that material properties ( $k$ ,  $\rho$ , and  $c_p$ ; see Section 5.3.7) as well as the heat flux terms ( $q$  and  $q_s$ ) are known model inputs.

#### 5.3.4 Short-wave Radiation

The heat flux term ( $q$ ) of Equation (5.13) comprises the short-wave radiative (0.28–2.8  $\mu\text{m}$ ) heat flux that penetrates the snow surface and is absorbed throughout

the snow; the amount absorbed is a strong function of wavelength (Armstrong and Brun, 2008). The total radiative flux absorbed by the snow ( $SW^{in}$ ) is computed using snow all-wave albedo ( $\alpha$ ) in this range. Albedo is the ratio of reflected to incident irradiance. It is assumed that both  $SW^{in}$  and  $\alpha$  are known model inputs. Numerically, for the  $j$ -th time step, the incoming short-wave radiation flux in the first layer ( $i = 1$ ), that is  $q_1^j$ , may be described as

$$q_1^j = SW^{in}(1 - \alpha). \quad (5.26)$$

The remaining short-wave radiation penetrates the snowpack and is assumed to be absorbed following an exponential decay function, as presented by Gray and Male (1981). This decay function is applied to the layered snowpack, for  $i > 1$ , with the following relationship:

$$q_{i+1}^j = q_i^j \cdot \exp(-\kappa_i \Delta z). \quad (5.27)$$

The extinction coefficient,  $\kappa$ , has units of  $1/m$  and is multiplied by the layer thickness,  $\Delta z$ . Figure 5.3 graphically shows the application of these relationships to a layered snowpack. Notice that the extinction coefficient may differ for each layer, this allows for the inclusion of different types of snow such as contaminated snow or an ice layer. In application, i.e., Equation (5.25), the following relationship is useful:

$$q_i^{absj} = q_i^j - q_{i+1}^j = q_i^j \cdot (1 - \exp(-\kappa_i \Delta z)). \quad (5.28)$$

As mentioned previously, short-wave absorption is a strong function of wavelength. Thus, the model presented in this chapter divides the short-wave flux term into two components: a visible (VIS) and near-infrared (NIR). This allows the short-wave flux term to be written as

$$q_i^j = q_{VISi}^j + q_{NIRi}^j. \quad (5.29)$$

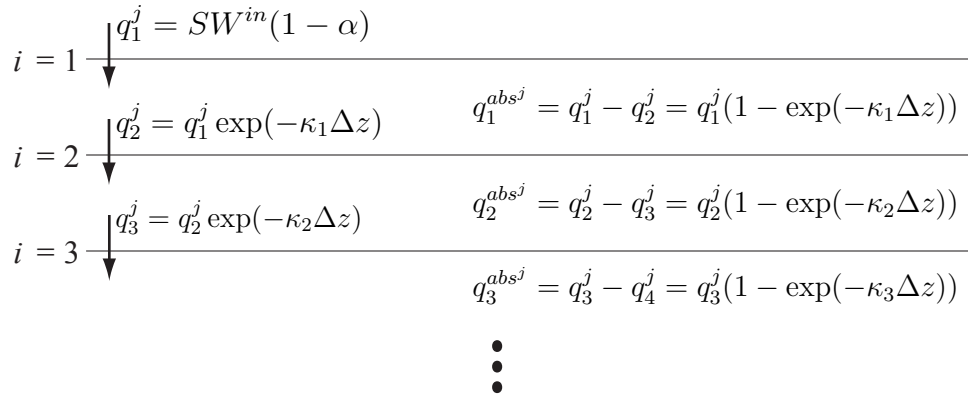


Figure 5.3: Schematic that demonstrates the application of short-wave attenuation in a layered snowpack.

Both of these components behave as shown in Figure 5.3, but allow for different albedo and extinction coefficients to be defined for the two wavebands: 380–700 nm (VIS) and 700–1400 nm (NIR); see Appendix C for additional details.

### 5.3.5 Surface Flux Terms

For application to snow, the heat flux at the surface ( $q_s$ ) includes three energy balance inputs: the heat flux input due to long-wave radiation ( $q_{LW}$ ), sensible heat ( $q_e$ ), and latent heat ( $q_h$ ), which may be written as

$$q_s = q_{LW} + q_e + q_h. \quad (5.30)$$

This may be directly substituted into Equation (5.25).

As mentioned in Section 5.2, the energy balance factors have been used in various forms in many models. Morstad (2004) detailed the factors summarized in the following sections, and Armstrong and Brun (2008) provided a detailed overview of each energy balance component. Table 5.1 summarizes the various constant values used throughout this section, specifically Equations (5.31) through (5.35).

Table 5.1: List of constant variables utilized for computing the heat source term of Equation (5.30).

Variable	Description	Value
$L_s$	Latent heat of sublimation phase change [kJ/kg]	2833
$K_e$	Transfer coefficient for water vapor	0.0023
$K_h$	Transfer coefficient	0.0023
$M_v/M_a$	Ratio of dry-air to water-vapor molecular weights	0.622
$R_a$	Gas constant for air [kJ/(kg· K)]	0.287
$R_v$	Gas constant for water vapor [kJ/(kg· K)]	0.462
$T_0$	Reference temperature for vapor pressure [°C]	-5
$e_0$	Reference vapor pressure [kPa]	0.402
$\varepsilon$	Emissivity of snow	0.988

Long-wave radiation (3.5–50  $\mu\text{m}$ ) is simply another name for thermal radiation. The heat flux due to long-wave radiation is a balance between the incoming and outgoing radiation. The incoming radiation ( $q_{LW}^{in}$ ) is assumed to be a known or measured value. The outgoing radiation is governed by the Stefan-Boltzman Law (Wetly *et al.*, 2008, p. 365), which is a function of the snow emissivity ( $\varepsilon$ ) the snow temperature ( $T_s$ ) and the Stefan-Boltzman constant ( $\sigma = 5.670 \times 10^{-8} \text{W}/(\text{m}^2 \cdot \text{K}^4)$ ). The emissivity is assumed constant at 0.988, the same as for pure ice in the spectrum defined for long-wave radiation. The net long-wave radiation may be written as

$$q_{LW} = q_{LW}^{in} - \varepsilon \sigma T_s^4. \quad (5.31)$$

If  $q_{LW}$  is computed as a negative value, then the surface is cooling or losing heat. The same convention applies to the  $q_e$  and  $q_h$  parameters.

Latent heat is the result of energy associated with phase-change and is driven by the water-vapor pressure gradients at the snow surface, i.e., changes in the energy state of the snow cause phase changes rather than temperature changes. Latent heat may be estimated as (Martin and Lejeune, 1998; Ishikawa *et al.*, 1999)

$$q_e = \frac{(M_v/M_a)\rho_a L_s K_e V_w (e_a \frac{RH}{100\%} - e_s)}{P_{atm}}. \quad (5.32)$$

Based on this equation, latent heat ( $q_e$ ) is a function of the latent heat of sublimation ( $L_s$ ), the transfer coefficient for water-vapor ( $K_e$ ), the water-vapor pressures above the snow surface ( $e_a$ ) and at the snow surface ( $e_s$ ), the ratio of dry-air to water-vapor molecular weights ( $M_v/M_a$ ), the density of air ( $\rho_a$ ), wind velocity ( $V_w$ ), and the atmospheric pressure (assumed to be a known model input,  $P_{atm}$ ).

The saturation water-vapor pressures above and at the snow surface may be calculated with the the Clausius-Clapeyron Equation for water-vapor (Gray and Male, 1981; Bejan, 1997):

$$e_i = e_0 \cdot \exp \left[ \frac{L_s}{R_v} \left( \frac{1}{T_0} - \frac{1}{T_i} \right) \right]. \quad (5.33)$$

The variables  $e_0$  and  $T_0$  are reference values,  $R_v$  is the gas constant for water vapor, and the temperature,  $T_i$ , represents either the air ( $i = a$ ) or snow temperature ( $i = s$ ). The air density is calculated via the ideal gas law, which uses the gas constant for air ( $R_a$ ), atmospheric pressure, and air temperature:

$$\rho_a = \frac{P_{atm}}{R_a T_a}. \quad (5.34)$$

At the snow surface, saturation is assumed, but above the snow surface (i.e., in the air) the calculated partial pressure of water-vapor ( $e_a$ ) must be adjusted for undersaturated conditions. Therefore, the relative humidity ( $RH$ ) is multiplied by  $e_a$  in Equation (5.32).

Sensible heat,  $q_h$ , is calculated using Equation (5.35),

$$q_h = \rho_a c_{pa} K_h V_w (T_a - T_s), \quad (5.35)$$

and is a function of the convection between the air and snow surface. Sensible heat is associated with a change in energy state of the material that results in a temperature change. Sensible heat is dependent on the density of air ( $\rho_a$ ), specific heat capacity

of air ( $c_{pa}$ ), the transfer coefficient ( $K_h$ ), wind speed ( $V_w$ ), and the snow and air temperatures ( $T_s$  and  $T_a$ , respectively).

Both the latent and sensible heat relationships are based on simple bulk transfer formulations (Armstrong and Brun, 2008);  $q_h$  is a direct application of the convective heat flux equation:  $q_h = h(T_1 - T_2)$  (Wetly *et al.*, 2008, p. 302). The transfer coefficients  $K_e$  and  $K_h$  are based on melting snow (Martin and Lejeune, 1998; Ishikawa *et al.*, 1999). Armstrong and Brun (2008) detailed another common method for determining transfer coefficients based on surface roughness parameterization. These methods were used in the SNOWPACK model (Lehning *et al.*, 2002b), which was also based on experiments examining wet snow (Calanca, 2001). Hence, for application to dry snow these coefficients do not directly apply, but are utilized nonetheless since a suitable alternative does not exist.

### 5.3.6 Boundary Layer Application

The implementation of surface heat flux ( $q_s$ ) from Equation (5.30) and the application of short-wave radiation (Section 5.3.4) differ from that presented by Morstad *et al.* (2007). This research assumed that the surface heat flux applied to the Neumann boundary condition was composed of the three components defined in Equation (5.30) as well as a fourth component that includes the amount of short-wave radiation absorbed between the surface and mid-point of the first layer (Morstad *et al.*, 2007).

In general, the difference in the computed temperatures between the two methods were on the order of tenths of a degree, as shown in Figure 5.4, which is a comparison of Experiment #1 from Morstad *et al.* (2007) evaluated using the two methods. Additionally, Monte Carlo simulations with 500 replicates of the model were conducted with the two different model setups. For both models, the inputs were varied as detailed in Chapter 7 (“Control” location). Two of the resulting output distributions, as

shown in Figure 5.5, were compared: the snow surface temperature with the “night” (Figure 5.5a) and the temperature gradient computed between the surface and 2 cm (Figure 5.5b) with the “day-light” configuration (see Chapter 7). Statistically, at the 5% confidence level interval using the Kolmogorov-Smirnov (Massey, 1951) and Ansari and Bradley (1960) tests, the distributions between the two models do not differ.

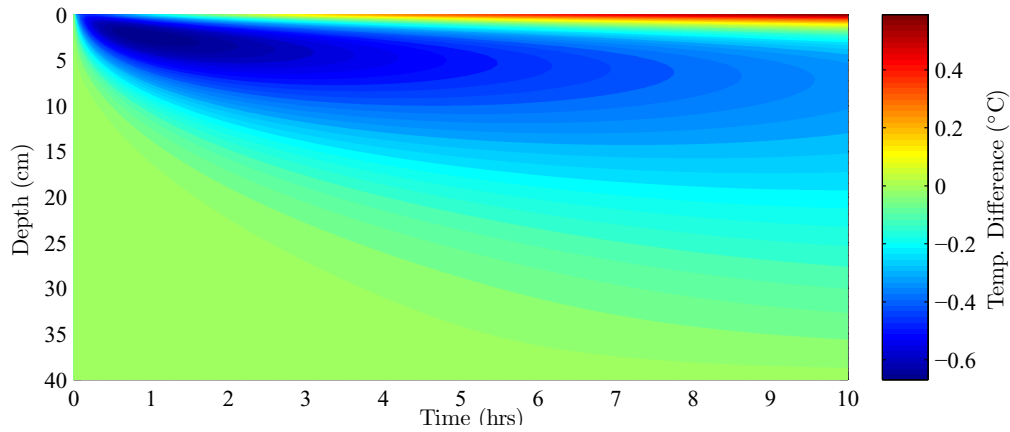


Figure 5.4: Example of temperature differences observed by differing application of the Neumann boundary condition.

The discrepancy in the boundary condition application of Morstad *et al.* (2007) was not identified until after the analysis in this dissertation was complete, as such the application of the Neumann boundary condition as conducted by Morstad *et al.* (2007) was utilized throughout this dissertation. Since statistically the resulting distributions do not differ between the two versions of the model, the results presented in the subsequent chapters should agree with the analysis if it were performed with the derivation presented here. However, the derivation presented in this chapter is more rigorous and is recommended for future applications of the thermal model.



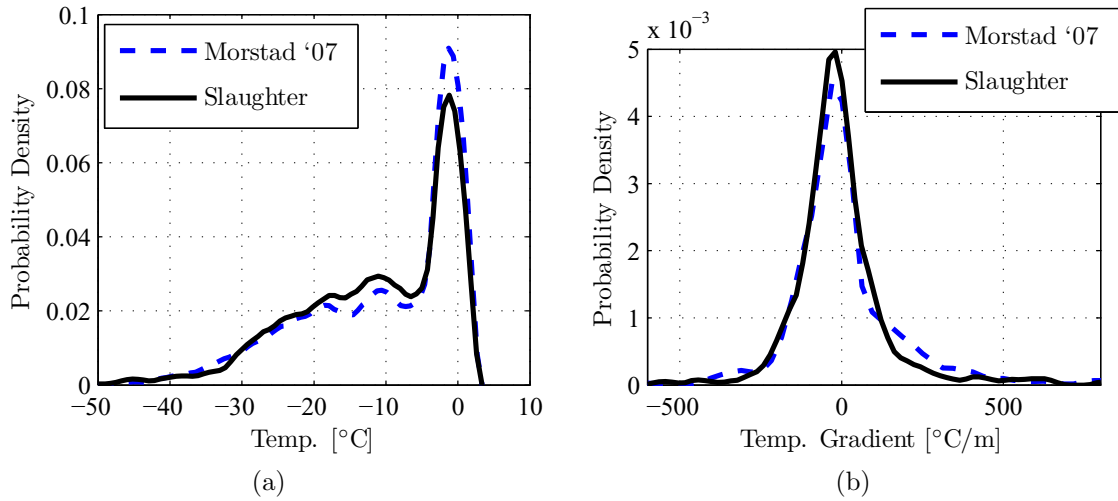


Figure 5.5: Resulting output distributions—(a) snow surface temperature and (b) temperature gradient—from the Monte Carlo simulations.

### 5.3.7 Material Properties

Equation (5.8) requires three material properties of snow: density ( $\rho$ ), specific heat capacity ( $c_p$ ), and thermal conductivity ( $k$ ). The density is assumed to be a measured or known value, thus is not discussed. The specific heat of snow is assumed to be only a function of its temperature ( $T$  in °C), according to the relationship in Equation (5.36) as was utilized by Morstad *et al.* (2007),

$$c_p = 1000 \cdot (2.115 + 0.00779 \cdot T), \quad (5.36)$$

which is a relationship for ice (Gray and Male, 1981).

The thermal conductivity,  $k$ , relationship used by Gray and Male (1981) is given in Equation (5.37),

$$k = 0.021 + 2.5 \cdot \left( \frac{\rho}{1000} \right)^2, \quad (5.37)$$

which is a strict function of density,  $\rho$  ( $kg/m^3$ ). The conductivity is expressed as effective thermal conductivity because it is assumed to account for various aspects of heat-transfer including conduction through the air and ice matrix as well as heat

transfer across the pore-space from vapor diffusion. This is only one of many relationships that exist for modeling thermal conductivity; Sturm *et al.* (1997) compiled an extensive list of experimentally attained relationships.

In Chapters 9–10 the thermal conductivity and specific heat were assumed to be known, thus the relationships of Equations (5.36) and (5.37) were not utilized.

#### 5.4 Analysis with VIS/NIR Components

The equations defined in the previous sections were used to build a thermal model which is solved using MATLAB (The Mathworks, Inc.). The complete program is detailed in Appendix C, including instructions for operating the model via the MATLAB command-line or via a graphical interface. This section highlights the inclusion of the NIR and VIS short-wave radiation components. Besides the code being written more efficiently, the inclusion of these radiation components is the only substantial difference between the model presented herein and that used by Morstad *et al.* (2007). This detail was added to improve the model behavior with respect to attenuating radiation.

The sun emits radiation primarily in the visible (VIS, 0.3–0.8  $\mu\text{m}$ ) and near-infrared (NIR, 0.8–1.5  $\mu\text{m}$ ) wavelengths. ASTM G-173 (2003) provided a standard reference for direct incident short-wave radiation. According to this standard over the entire electromagnetic spectrum that reaches the Earth's surface (0.28–4  $\mu\text{m}$ ) the average total irradiation is 1000  $\text{W}/\text{m}^2$ , at a latitude of 37°. Of this value, 54.5% is in the visible range, 27.4% is in the near-infrared, and 8.7% is in the short-wave infrared range (SWIR, 1.5–2.8  $\mu\text{m}$ ). The remaining 9.4% of the incident irradiation is for wavelengths greater than 2.8  $\mu\text{m}$ . A negligible amount of incident irradiation is due to the bands omitted from this analysis: 0.28–0.3  $\mu\text{m}$ . The wavebands presented

here differ slightly from the formal definitions, but were defined to align with bands presented by Armstrong and Brun (2008) for analysis purposes.

Experiment two in Morstad *et al.* (2007) resulted in 1 mm near-surface facets due to radiation recrystallization; this experiment was utilized here to demonstrate the VIS/NIR component added to the model. Morstad (2004) provided complete details on this experiment, which used a constant value of  $650 \text{ W/m}^2$  for short-wave irradiance. This value was measured using an Eppley PSP radiation sensor, which measures between  $0.3$  and  $1.5 \mu\text{m}$ . Thus, this value may be divided into VIS, NIR, and SWIR components based on the aforementioned divisions. The resulting components are  $391$ ,  $196$ , and  $62 \text{ W/m}^2$ , respectively. This division is reasonable, even for the laboratory experiments, because the solar simulation system is within  $2.6\%$  of the CIE (1989) standard (Scott, 2001).

Morstad *et al.* (2007) measured the albedo for this experiment to be  $0.81$ . This value is similar to the albedo of  $0.78$  reported by Armstrong and Brun (2008, p. 57) for a Class 1 snow type. This class of snow has albedo values for the VIS, NIR, and SWIR of  $0.94$ ,  $0.80$ , and  $0.59$ , respectively, and extinction coefficient,  $\kappa$ , values of  $40 \text{ m}^{-1}$  and  $110 \text{ m}^{-1}$  for the VIS and NIR spectral ranges, respectively, which average to a value of  $75 \text{ m}^{-1}$ . Morstad *et al.* (2007) used  $82 \text{ m}^{-1}$  for the extinction coefficient. In the SWIR range,  $\kappa$  is reported as infinite, therefore it acts only at the snow surface.

In addition to the SWIR irradiance, a small band between  $2.8 \mu\text{m}$  and  $3.5 \mu\text{m}$  was unmeasured. Wavelengths between  $3.5 \mu\text{m}$  and  $50 \mu\text{m}$  were measured by a long-wave sensor (Eppley Lab., Inc. PIR) and applied to the snow surface, since in these wavebands snow acts nearly as a blackbody (Warren, 1982; Armstrong and Brun, 2008). Using the ASTM G-173 (2003),  $3.2\%$  of the total incoming radiation is in this “missing” range. This value may be estimated using the measured value of  $650 \text{ W/m}^2$ , which is measured over the wavelengths that comprise  $91.3\%$  of radiation

emitted by the sun. Therefore, the missing portion of the spectrum may be estimated as  $(0.032)\left(\frac{650 \text{ W/m}^2}{0.913}\right) = 0.035 \cdot 650 \text{ W/m}^2 = 23 \text{ W/m}^2$ . A missing portion on the order of 3.5% may seem insignificant, but once the albedo values are applied to the incident radiation the value yielded— $23 \text{ W/m}^2$ —becomes a significant contributor to the energy balance.

Using the irradiance, albedo, and extinction coefficient values defined here, the thermal model presented in this chapter was executed for six scenarios defined below:

1. “AS-IS” was executed as in Morstad *et al.* (2007) but with  $\alpha = 0.78$  and  $\kappa = 75 \text{ m}^{-1}$ .
2. “VIS” was executed with only visible irradiation.
3. “NIR” was run with only near-infrared irradiation.
4. “VIS-NIR” used both the visible and near-infrared values.
5. “SWIR(1)” was the same as the previous simulation, except the  $25 \text{ W/m}^2$  from the SWIR range was added to the long-wave radiation component that acts at the snow surface ( $62 \text{ W/m}^2(1 - 0.59) = 25 \text{ W/m}^2$ ).
6. “SWIR(2)” was the same as the “SWIR(1)” simulation, except the “missing”  $23 \text{ W/m}^2$  was also added to the long-wave radiation component.

Figure 5.6 compares the model evaluations with the measured values after eight hours, which was when the largest facets were observed in the experiment. This figure also shows the importance of including each of the radiation components. As expected, the “AS-IS” model evaluation behaves almost identically to the evaluations presented in Morstad (2004). Notice, this evaluation tended towards a melt-layer beneath the snow surface, which was not as prominent in the measured data. The

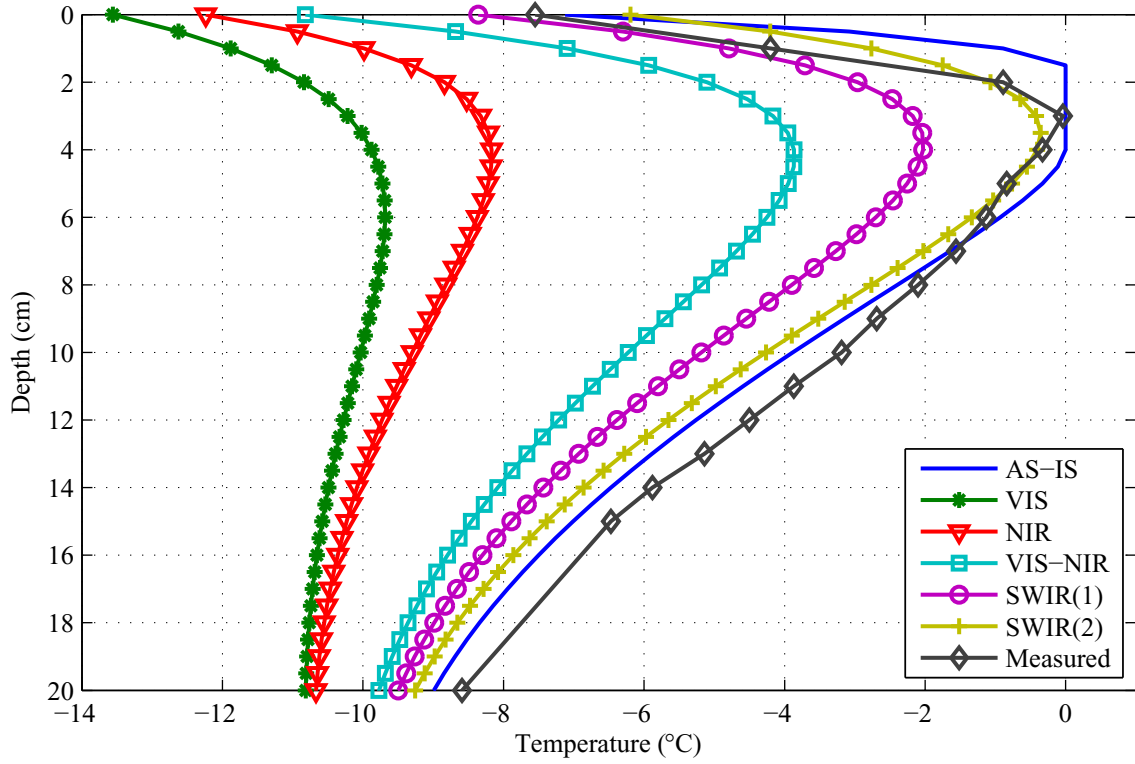


Figure 5.6: Comparison between six model evaluations with varying irradiation inputs.

melt-layer in the model was common (9 of 13 experiments) in the model/experiment comparisons in Morstad (2004). Additionally, the “SWIR(2)” evaluation matches the measured data the closest, particularly in the inflection point region. This single example highlights the importance of considering, with as much detail as available, the various components of radiation that impact the energy balance.

### 5.5 Reliability of Model

Often, the thermal model presented here is used in comparison with measured temperature data using various environmental sensors for input. Thus, each input factor has an associated measurement error. Using 1,000 re-samplings, the 95% confidence level intervals were computed using the bootstrap percentile method (Press

*et al.*, 1986; Efron, 1987). Based on the “SWIR(2)” evaluation from the previous section, confidence intervals were calculated assuming that all input parameters have an associated measurement error that is  $\pm 5\%$  of the desired value and which may be described by a normal distribution such that the 1% tails of the distribution occur at the 5% values.

Figure 5.7a contains a contour plot showing the maximum deviation from the mean value of the 1,000 samplings over a 10-hour period, which indicates that the largest error is approximately 2 °C and occurs just below the snow surface. Figure 5.7b depicts a single profile at the 8-hour mark that includes the confidence level intervals, the “SWIR(2)” model evaluation, and the measured values from Morstad *et al.* (2007) Experiment Two. Note, the analysis presented here was simply an example. Confidence level intervals, a feature available in the thermal model software presented in Appendix C, need to be computed for any model evaluation. Nonetheless, both Figures 5.7a and 5.7b show that accurate measurements are crucial when using the model to compare modeled and measured data.

## 5.6 Closing Remarks

This chapter summarized the theoretical and numerical development of a 1-D model for computing snowpack temperatures, which was utilized for additional numerical computation in Chapters 7–10. In addition to the model development, an example was presented that highlights the importance of the short-wave radiation attenuation. This example indicated that using both visible and near-infrared components may provide more accurate results than using the all-wave component alone. Finally, in another example, the computed temperature profiles were shown to be

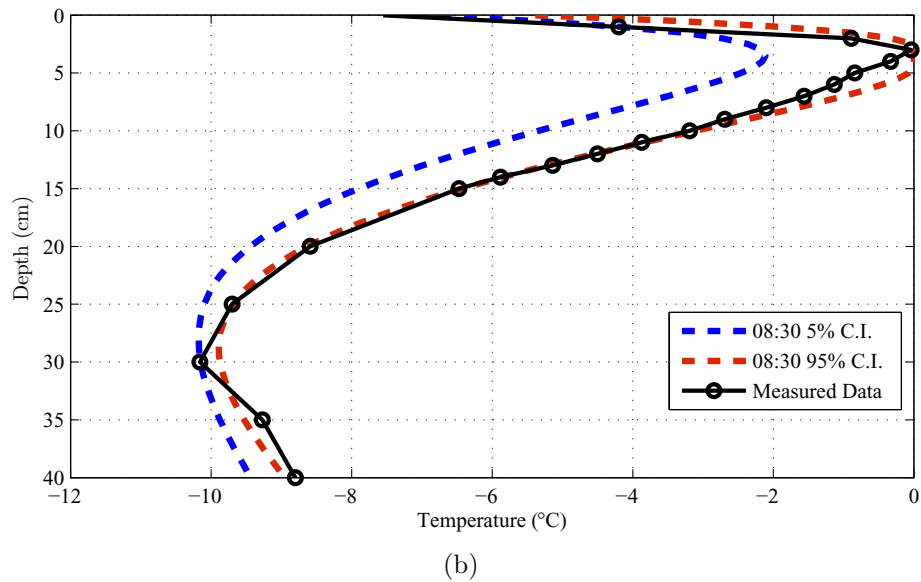
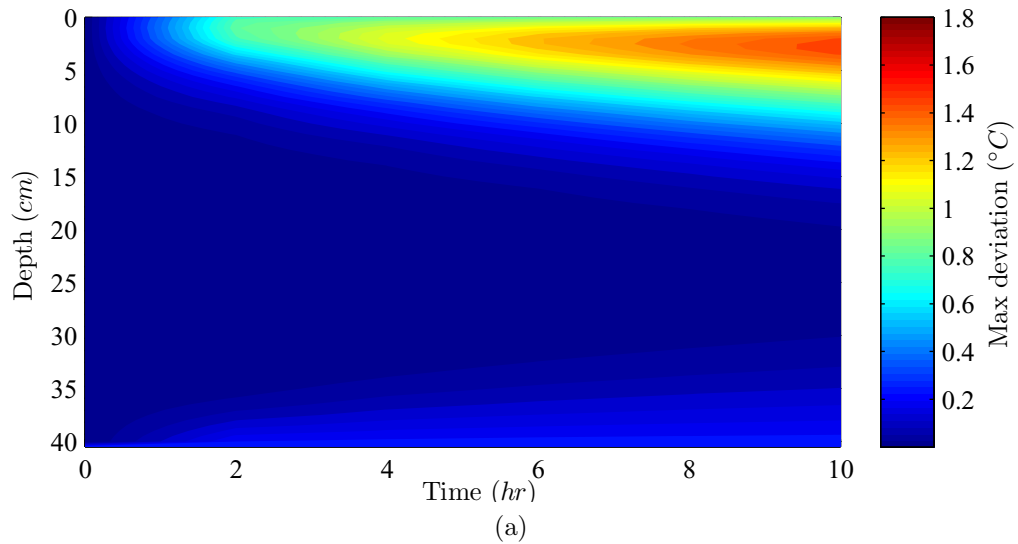


Figure 5.7: Graphs demonstrating the model behavior with respect to measurement error including (a) a contour plot of the largest deviation from the input evaluation and (b) 90% confidence intervals with input evaluation and measured values.

affected by measurement error when measured data was used for the input terms.

Thus, it is critical that care is taken when using measured data.



## CHAPTER 6

## SOBOL SENSITIVITY ANALYSIS: THEORY AND EXAMPLES

6.1 Introduction

Sensitivity analysis is used to examine the output of a model and how the variation of this output can be apportioned to the various input factors. The typical purpose for performing such an analysis is to determine how important the input parameters are to the overall outcome. Chan *et al.* (2000) elaborated on the importance of sensitivity analysis stating that it “is a prerequisite for model building in any setting. . . .”

Two methods of global, variance-based sensitivity analysis (see Saltelli *et al.*, 2008) shall be briefly discussed: the Fourier Amplitude Sensitivity Test (FAST) and an extension of the SOBOL method, which was named after I.M. Sobol (1993). FAST relies on transforming the input parameters into the frequency domain and then analyzing the variance via the Fourier coefficients. The improved SOBOL method assesses the variance via Monte Carlo samplings. Cukier *et al.* (1977) explained the advantages of using the FAST method, as detailed in the excerpt below.

The sensitivity analysis presented here is *nonlinear* so that it permits us to examine large deviations from the nominal parameter values. In addition, since all parameters are varied simultaneously, one explores regions of parameter space where more than one parameter is far from its nominal value. Because of this thorough exploration of the parameter space, it often turns out that sensitivities of an unexpected nature are revealed. A careful study of the model will then reveal some complex coupling between variables, unexpected prior to the analysis, which leads to observed sensitivity. . . . Another frequent and important finding is that a number of

sensitivity coefficients corresponding to a large set of parameters turn out to be negligible. This permits one to focus one's attention on a greatly reduced set of Equations.

Since that publication, the SOBOL method has become an equally, if not more, effective method of sensitivity analysis. FAST was developed throughout a series of papers to analyze chemical rate equations (Cukier *et al.*, 1973; Schaibly and Shuler, 1973; Cukier *et al.*, 1975) and is centered around theories presented by Weyl (1938). However, as stated by the creator, the method is not limited to chemical rate equations. In fact, in a later comprehensive review Cukier *et al.* (1978) stated that FAST was developed for sensitivity analysis of large systems of coupled nonlinear equations. Since the creation of FAST it has been implemented in a variety of applications (McRae *et al.*, 1982; Uliasz, 1988; Collins and Avissar, 1994; Colonna *et al.*, 1994). Additionally, variations and improvements have been applied to the method (Smith and Ginsburg, 1977; Saltelli and Bolado, 1998; Saltelli *et al.*, 1999; Fang *et al.*, 2003). These papers are not an exhaustive list of the applications and modifications of FAST; additional references exist for each of the references given here, and Frey and Patil (2002) provided even more references as well as a review of many other sensitivity analysis procedures.

Both FAST and the SOBOL method provide sensitivity indices that communicate the relative importance of each input parameter. The power of the methods is that both are capable of determining the importance of each factor independent from the others as well as the importance of the interactions between the inputs. The results are typically reported as first-order, second-order, and/or total-effect sensitivity indices; first-order yields sensitivity without any interactions, second-order yields the interactions between pairs of inputs, and total-effect results in the combined effect of

first-order and all interactions. The originally FAST was only capable of computing first-order, but Saltelli *et al.* (1999) developed an extended FAST method capable of computing the total-effect indices.

Saltelli (2002) developed an improvement of the SOBOL method that advanced the computational efficiency beyond that of the extended FAST, which was previously the most efficient method for computing “total-effect” indices. The SOBOL method was originally introduced by Sobol (1990, 1993) and been reported and improved by various authors (Saltelli *et al.*, 1993; Chan *et al.*, 1997; Sobol, 2001; Saltelli, 2002; Saisana *et al.*, 2005). The improvements made by Saltelli (2002) allow for the calculation of first- and second-order sensitivity indices as well as the total-effect indices that reduces computational cost by nearly 50% compared to other methods.

Due to the superior computational efficiency offered by the SOBOL method, it was selected for the analysis performed in Chapters 8 and 9. This chapter focuses solely on the theory and application of the SOBOL method. Appendix D includes the complete program code capable of implementing both methods, which was used for the examples in this chapter as well as the analysis detailed in later chapters.

This chapter was designed to be a generic, model-independent explanation of the improved SOBOL method of sensitivity analysis. The chapter begins with a general discussion of variance and variance-based sensitivity parameters. Then, theoretical development and stepwise instructions for implementing the SOBOL method are given. A method for computing confidence levels and adjusting for bias that does not require any additional model evaluations is then presented. Finally, examples are included that illustrate the usage and interpretation of the results.

## 6.2 Sensitivity Defined

The following derivation of sensitivity was gathered primarily from Saltelli (2002), and is one of many derivations presented in the literature (see also Ishigami and Homma, 1990; Chan *et al.*, 1997, 2000; Homma and Saltelli, 1996). The SOBOL method is applicable to any function that has a discrete input and output. The only stipulation is that the input parameters must be independent. Consider the generic mathematical function

$$\vec{y} = f(\vec{x}), \quad (6.1)$$

where  $\vec{y} = y^j \mid j = 1, 2, \dots, m$  are the model outputs if the function  $f$  is evaluated for the model input parameters,  $\vec{x} = x_i \mid i = 1, 2, \dots, n$ .

The mean of the output parameters,  $E(y^j)$ , may be represented as an ensemble, as:

$$E(y^j) = \int \int \dots \int y^j(x_1, x_2, \dots, x_n) P(x_1, x_2, \dots, x_n) dx_1 dx_2 \dots dx_n, \quad (6.2)$$

where  $P(x_1, x_2, \dots, x_n)$  is the combined probability density function of all the input parameters in  $\vec{x}$ .

Equation (6.2) is also known as the expected output for all possible inputs (Cacuci, 2003). For further discussion of the mean ensemble, including a simplified two-parameter example, review McRae *et al.* (1982). The expected value computation for sensitivity analysis relies on the knowledge of each input parameters' probability density function,  $p_i(x_i)$ , and that each is independent of the others. Thus the total probability becomes

$$P(x_1, x_2, \dots, x_n) = \prod_{i=1}^n p_i(x_i). \quad (6.3)$$

Using the total probability as defined in Equation (6.3), the expected output may be re-written as (Saltelli, 2002)

$$E(y^j) = \int \int \cdots \int y^j(x_1, x_2, \dots, x_n) \prod_{i=1}^n p_i(x_i) dx_i, \quad (6.4)$$

where the  $dx_i$  is inserted into the product results in the  $dx_1 dx_2 \dots dx_n$  in Equation (6.2). In similar fashion the total variance of the output may be expressed as (Saltelli, 2002)

$$V(y^j) = \int \int \cdots \int (y^j(x_1, x_2, \dots, x_n))^2 \prod_{i=1}^n p_i(x_i) dx_i - E(y^j)^2. \quad (6.5)$$

Next, one of the input values,  $x_k$ , is fixed to an arbitrary value,  $\tilde{x}_k$ , where  $k$  is an arbitrary value of the index  $i$  representing  $x_k$ . The resulting variance of the desired function is then re-written as

$$V(y^j | x_k = \tilde{x}_k) = \int \int \cdots \int (y^j(x_1, x_2, \dots, x_k, \dots, x_n))^2 \prod_{\substack{i=1 \\ i \neq k}}^n p_i(x_i) dx_i - E(y^j | x_k = \tilde{x}_k)^2. \quad (6.6)$$

The main purpose of a sensitivity analysis is to remove the necessity for fixing values. Thus Equation (6.6) is integrated over the probability distribution of the fixed term  $\tilde{x}_k$ , resulting in the expected value of the variance for the  $k$ th input,

$$E(V(y^j | x_k)) = \int \int \cdots \int (y^j(x_1, x_2, \dots, x_n))^2 \prod_{i=1}^n p_i(x_i) dx_i - \int E(y^j | x_k = \tilde{x}_k)^2 p_k(\tilde{x}_k) dx_k. \quad (6.7)$$

Subtracting Equation (6.7) from Equation (6.5) results in

$$V(y^j) - E(V(y^j | x_k)) = \int (E(y^j | x_k = \tilde{x}_k))^2 p_k(\tilde{x}_k) dx_k - (E(y^j))^2. \quad (6.8)$$

The left side of Equation (6.8) is equivalent to the variance of the expected value of the  $j$ th output of the function  $y$  for the factor  $x_k$ , which is written as  $V(E(y^j | x_k))$

(Saltelli, 2002). This is the fundamental quantity of variance-based sensitivity analysis. When normalized with respect to the total variance,  $V(y^j)$ , it is exactly the first-order sensitivity index  $S_k^j$ , where

$$S_k^j = \frac{V^j(E(y^j|x_k))}{V(y^j)}. \quad (6.9)$$

Recalling that  $k$  is an arbitrary value of the  $i$  index, this relationship is redefined as

$$S_i^j = \frac{V^j(E(y^j|x_i))}{V(y^j)}. \quad (6.10)$$

This basic relationship, Equation (6.10), is also commonly referred to as the correlation ratio (Chan *et al.*, 1997). An estimation of this parameter is the foundation of the SOBOL method.

### 6.3 Decomposition of Variance

Before presenting the details specific to the SOBOL method of sensitivity analysis, an understanding of how the variance may be separated into parts is necessary. This section defines various ways in which variance may be separated into components as well as some notational conventions that will be used in Section 6.4 when the specific method of SOBOL is detailed.

As discussed previously, Equation (6.10) is equivalent to the first-order sensitivity index  $S_i^j$  (Chan *et al.*, 2000). This measure of sensitivity yields the portion of the total variance that may be contributed to the  $i$ th input parameter.  $S_i^j$  refers to the  $i$ th parameter only, uncoupled with any other factors. However, each input factor may be coupled with each of the other input parameters, thus higher order terms exist. For example,  $S_{il}^j$  refers to the  $i$ th second-order indices, where  $l = 1, 2, \dots, n$  and  $l \neq i$ . The second-order indices give the portion of the total variance due to the  $i$ th and  $l$ th inputs interacting.

The denominator of Equation (6.10) is the total-variance, which is renamed here for simplicity as  $V_i^j$ . The total variance may also be expressed as a summation of the various components and interactions as follows (Chan *et al.*, 2000):

$$V^j = \sum_{i=1}^n V_i^j + \sum_{i=1}^n \sum_{\substack{g=1 \\ g \neq i}}^n V_{il}^j + \sum_{i=1}^n \sum_{\substack{l=1 \\ l \neq i}}^n \sum_{\substack{h=1 \\ h \neq l \neq i}}^n V_{ilh}^j + \dots \quad (6.11)$$

For example, in a three-input parameter model the total-variance would break down into three components: first-, second-, and third-order components, namely

$$V^j = \underbrace{V_1^j + V_2^j + V_3^j}_{\text{1st Order}} + \underbrace{V_{12}^j + V_{13}^j + V_{23}^j}_{\text{2nd Order}} + \underbrace{V_{123}^j}_{\text{3rd Order}}. \quad (6.12)$$

### 6.3.1 Closed Variance

As done for a single parameter in Section 6.2, the variance of the expected value for multiple input factors may also be determined, i.e.,  $V(E(y^j|x_i, x_l))$ . In sensitivity analysis, this is called a “closed” variance (Saltelli *et al.*, 2004). A closed variance is the variance associated with respect to specific input parameters, namely

$$V(E(y^j|x_i)) = V_i^{j^c} = V_i^j, \quad (6.13a)$$

$$V(E(y^j|x_i, x_l)) = V_{il}^{j^c} = V_i^j + V_l^j + V_{il}^j, \text{ and} \quad (6.13b)$$

$$V(E(y^j|x_i, x_l, x_g)) = V_{ilg}^{j^c} = V_i^j + V_l^j + V_g^j + V_{il}^j + V_{ig}^j + V_{lg}^j + V_{ilg}^j. \quad (6.13c)$$

Notice, for the three parameter case ( $n = 3$ ) the variance  $V_{ilg}^{j^c}$  equals  $V^j$  because it contains all the possible variance in the function.

### 6.3.2 Total-effect Variance

The total-effect variance,  $V_{T_i}^j$ , is introduced as

$$V_{T_i}^j = V_i^j + V_{i(-i)}^j \quad (6.14)$$



where the  $-i$  indicates “all except  $i$ ” (Homma and Saltelli, 1996; Chan *et al.*, 1997; Saltelli and Bolado, 1998; Saltelli *et al.*, 2000; Chan *et al.*, 2000). The subscript  $i(-i)$  represents the coupled interactions of the  $i$ th input parameter with all other parameters. For example, referring to the three parameter model, the total-effect index for the first ( $i = 1$ ) parameter may be written as

$$V_{T_1}^j = V_1^j + \underbrace{V_{12}^j + V_{13}^j + V_{123}^j}_{V_{1(-1)}^j}. \quad (6.15)$$

As such, the total variance of Equation (6.11) may be reduced to a summation of three terms:

$$V_i^j = \sum_{i=1}^n [V_i^j + V_{i(-i)}^j + V_{-i}^j]. \quad (6.16)$$

This introduces a third term,  $V_{-i}^j$ , which is the variance not coupled to the  $i$ th parameter. For the first parameter of a three parameter model this term would be

$$V_{-1}^j = V_2^j + V_3^j + V_{23}^j. \quad (6.17)$$

#### 6.4 SOBOL Method

In the preceding sections (6.2 and 6.3), no applications specific to the SOBOL method were defined. This section details the application of the SOBOL method developed by Saltelli (2002) and further summarized in Saltelli *et al.* (2004) and Saltelli *et al.* (2008). This method is an adaptation of the original SOBOL method introduced by Sobol (1993).

### 6.4.1 Basic Premise

Equation (6.10) was defined as the basic relationship for computing sensitivity parameters, which is redefined by breaking the numerator into two components:

$$S_i^j = \frac{U_i^j - E(y^j)^2}{V^j}. \quad (6.18)$$

Referring to Equation (6.8),

$$U_i^j = \int E(y^j|x_i)^2 p_i(x_i) dx_i. \quad (6.19)$$

The SOBOL method relies on the estimation of  $U_i^j$  in Equation (6.19);

$$\begin{aligned} \widehat{U}_i^j = & \int \int \cdots \int y^j(x_1, x_2, \dots, x_i, \dots, x_n) y^j(x'_1, x'_2, \dots, x_i, \dots, x'_n) \\ & \prod_{i=1}^n p_i(x_i) dx_i \prod_{\substack{l=1 \\ l \neq i}}^n p_l(x_l) dx_l. \end{aligned} \quad (6.20)$$

The theory of this transformation is beyond the scope of this summary, but a detailed derivation is presented in Ishigami and Homma (1990) as well as a summary in Saltelli *et al.* (1993) and Saltelli (2002). This transformation may be considered a representation of the square of the expected value,  $E(y^j|x_i)^2$ , of a new function that is defined as the product of  $y^j$  evaluated with two different input sets,  $\vec{x}$  and  $\vec{x}'$ . The sets are produced via uniform Monte Carlo samplings, both with  $K$  replicates of each input parameter, i.e.,  $x_{r,i} \mid r = 1, 2, \dots, K$ .

The use of these Monte Carlo input parameters allows Equation (6.20) to be estimated as a summation:

$$\widehat{U}_i^j = \frac{1}{K} \sum_{r=1}^K y^j(x_{r,1}, x_{r,2}, \dots, x_{r,i}, \dots, x_{r,n}) y^j(x'_{r,1}, x'_{r,2}, \dots, x'_{r,i}, \dots, x'_{r,n}). \quad (6.21)$$

This simplification is only representative provided that the Monte Carlo sample size is adequately large; Saltelli (2002) utilized  $K = 1024$ . The multiplier prior to the

summation differs slightly from that of Saltelli (2002), who used  $\frac{1}{K-1}$  instead of  $\frac{1}{K}$ . The value of  $\frac{1}{K}$  was used here for simplicity. With respect to variance, both methods can be utilized, however for large  $K$ ,  $\frac{1}{K} \approx \frac{1}{K-1}$  (Freund and Simon, 1995).

Next, the integral function that defines the expected value,  $E(y^j)$ , and total variance,  $V^j$ , that is Equations (6.4) and (6.5), may be estimated in a similar fashion:

$$\widehat{E}(y^j) = \frac{1}{K} \sum_{r=1}^K y^j(x_{r,1}, x_{r,2}, \dots, x_{r,n}) \quad (6.22)$$

and

$$\widehat{V}^j = \frac{1}{K} \sum_{r=1}^K [y^j(x_{r,1}, x_{r,2}, \dots, x_{r,n})]^2 - E(y^j)^2. \quad (6.23)$$

As alluded to in Section 6.3, a further extension of SOBOL involves the computation of variance subsets. For example, consider a function with four input parameters ( $n = 4$ ), where  $\vec{u} = \{x_{r,2}, x_{r,3}\}$  and  $\vec{v} = \{x_{r,1}, x_{r,4}\}$ . Recalling the definition of closed variance in Equation (6.13), the effect of  $\vec{v}$  on the total variance may be estimated as

$$\widehat{V}(E(y^j|\vec{v})) = \widehat{V}_{\vec{v}}^{j^c} = \widehat{U}_{\vec{v}}^{j^c} - \widehat{E}(y^j)^2, \quad (6.24)$$

where,

$$\widehat{U}_{\vec{v}}^{j^c} = \frac{1}{K} \sum_{r=1}^K f(x_{r,1}, x_{r,2}, x_{r,3}, x_{r,4}) f(x_{r,1}, x'_{r,2}, x'_{r,3}, x_{r,4}). \quad (6.25)$$

Hence,  $\widehat{U}_i^j$ ,  $\widehat{U}_{-i}^j$ , and  $\widehat{U}_{il}^{j^c}$  may be written as

$$\widehat{U}_i^j = \frac{1}{K} \sum_{r=1}^K f(x_{r,1}, x_{r,2}, \dots, x_{r,i}, \dots, x_{r,n}) f(x'_{r,1}, x'_{r,2}, \dots, x_{r,i}, \dots, x'_{r,n}), \quad (6.26)$$

$$\widehat{U}_{-i}^j = \frac{1}{K} \sum_{r=1}^K f(x_{r,1}, x_{r,2}, \dots, x_{r,i}, \dots, x_{r,n}) f(x_{r,1}, x_{r,2}, \dots, x'_{r,i}, \dots, x_{r,n}), \quad (6.27)$$

and

$$\widehat{U}_{il}^{j^c} = \frac{1}{K} \sum_{r=1}^K f(x_{r,1}, x_{r,2}, \dots, x_{r,i}, \dots, x_{r,n}) f(x'_{r,1}, x'_{r,2}, \dots, x_{r,i}, \dots, x_{r,l}, \dots, x'_{r,n}). \quad (6.28)$$

The ability to estimate the variance of subsets, as done here, provides the basis for the improved SOBOL method which is detailed in the following section (Saltelli, 2002). This method is capable of computing first-order, second-order, and total-effect sensitivity parameters.

#### 6.4.2 Improved SOBOL Method

The improved method of SOBOL derived by Saltelli (2002) relies on two Monte Carlo sampling matrices, each with  $K$  replicates of the input variables. These two matrices are considered the “sample” ( $W$ ) and “re-sample” ( $W'$ ) matrices:

$$W = \begin{bmatrix} x_{1,1} & x_{1,2} & \cdots & x_{1,n} \\ x_{2,1} & x_{2,2} & \cdots & x_{2,n} \\ \vdots & \vdots & \ddots & \vdots \\ x_{K,1} & x_{K,2} & \cdots & x_{K,n} \end{bmatrix} \quad \text{and} \quad W' = \begin{bmatrix} x'_{1,1} & x'_{1,2} & \cdots & x'_{1,n} \\ x'_{2,1} & x'_{2,2} & \cdots & x'_{2,n} \\ \vdots & \vdots & \ddots & \vdots \\ x'_{K,1} & x'_{K,2} & \cdots & x'_{K,n} \end{bmatrix}. \quad (6.29)$$

These two matrices are used to develop the  $N_i$  and  $N_{-i}$  matrices:

$$N_i = \begin{bmatrix} x'_{1,1} & x'_{1,2} & \cdots & x'_{1,i-1} & x_{1,i} & x'_{1,i+1} & \cdots & x'_{1,n} \\ x'_{2,1} & x'_{2,2} & \cdots & x'_{2,i-1} & x_{2,i} & x'_{2,i+1} & \cdots & x'_{2,n} \\ \vdots & \vdots & \vdots & \vdots & \vdots & \vdots & \ddots & \vdots \\ x'_{K,1} & x'_{K,2} & \cdots & x'_{K,i-1} & x_{K,i} & x'_{K,i+1} & \cdots & x'_{K,n} \end{bmatrix} \quad (6.30)$$

and

$$N_{-i} = \begin{bmatrix} x_{1,1} & x_{1,2} & \cdots & x_{1,i-1} & x'_{1,i} & x_{1,i+1} & \cdots & x_{1,n} \\ x_{2,1} & x_{2,2} & \cdots & x_{2,i-1} & x'_{2,i} & x_{2,i+1} & \cdots & x_{2,n} \\ \vdots & \vdots & \vdots & \vdots & \vdots & \vdots & \ddots & \vdots \\ x_{K,1} & x_{K,2} & \cdots & x_{K,i-1} & x'_{K,i} & x_{K,i+1} & \cdots & x_{K,n} \end{bmatrix}. \quad (6.31)$$

In Equations (6.32)a–(6.32)d a set of vectors of length  $K$  is introduced. Recalling that  $i = 1, 2, \dots, n$  and  $l = 1, 2, \dots, n | l \neq i$ , these vectors are defined as follows:

$$\vec{a}_0^j = y^j(W), \quad (6.32a)$$

$$\vec{a}_i^j = y^j(N_i), \quad (6.32b)$$

$$\vec{a}_{-i}^j = y^j(N_{-i}), \quad \text{and} \quad (6.32c)$$

$$\vec{a}_K^j = y^j(W'). \quad (6.32d)$$

These vectors refer to the output of the function evaluated with the various input matrices defined in Equations (6.29) through (6.31). The output vectors  $a_0^j$  and  $a_K^j$  are  $j \times K$  dimensional and  $a_i^j$  and  $a_{-i}^j$  are  $j \times K \times n$  dimensional. Therefore, the necessary evaluations of the function in question results in  $C = K(2n + 2)$  model evaluations.

Saltelli (2002) presented a table to aid with calculating the sensitivity analysis parameters, which assumed a five-parameter model with a single output variable. Table 6.1 was developed from this table, but was simplified to contain only values pertinent to the discussion at hand. Saltelli (2002) demonstrated that results when  $n < 5$  are a special case of this table. However, the methodology presented here may be applied to all cases; the differences arise in the off-diagonal terms that were excluded in Table 6.1.

Using the results from Equations in (6.32)a–d and Table 6.1 as a guide, the first-order, second-order, and total-effect sensitivity indices may be computed. Recognizing that the scalar products of two  $\vec{a}_i^j$  output vectors  $\vec{a}$  are proportional to  $\hat{E}(y^j)$ ,

$\widehat{V}(y^j)$ ,  $\widehat{U}^j$ ,  $\widehat{U}_{-i}^{jc}$ , and  $\widehat{U}_{il}^{jc}$  these estimates may be redefined as

$$\widehat{E}(y^j)^2 = \frac{1}{K} \vec{a}_0^j \cdot \vec{a}_K^j = \frac{1}{K} \vec{a}_i^j \cdot \vec{a}_{-i}^j, \quad (6.33)$$

$$\widehat{V}^j = \frac{1}{K} \vec{a}_i^j \cdot \vec{a}_i^j - \widehat{E}(y^j)^2 = \frac{1}{K} \vec{a}_0^j \cdot \vec{a}_0^j - \widehat{E}(y^j)^2 = \frac{1}{K} \vec{a}_K^j \cdot \vec{a}_K^j - \widehat{E}(y^j)^2, \quad (6.34)$$

$$\widehat{U}_i^j = \frac{1}{K} \vec{a}_0^j \cdot \vec{a}_{-i}^j = \frac{1}{K} \vec{a}_i^j \cdot \vec{a}_K^j, \quad (6.35)$$

$$\widehat{U}_{-i}^{jc} = \frac{1}{K} \vec{a}_0^j \cdot \vec{a}_i^j = \frac{1}{K} \vec{a}_{-i}^j \cdot \vec{a}_K^j, \quad (6.36)$$

and

$$\widehat{U}_{il}^{jc} = \frac{1}{K} \vec{a}_i^j \cdot \vec{a}_{-l}^j = \frac{1}{K} \vec{a}_{-i}^j \cdot \vec{a}_l^j. \quad (6.37)$$

Notice each of the above equations has multiple relationships that may be used for estimation; this results in double estimates of the first, second, and total-effect indices (Saltelli, 2002). Recalling the break-down of the closed variance in Equation (6.13), the desired sensitivity parameters are calculated as follows:

$$S_i^j = \frac{\widehat{U}_i^j - \widehat{E}(y^j)^2}{\widehat{V}^j}, \quad (6.38)$$

$$S_{il}^{jc} = \frac{\widehat{U}_{il}^{jc} - \widehat{E}(y^j)^2 - \widehat{V}_i^j - \widehat{V}_l^j}{V^j} = \frac{\widehat{V}_{il}^{jc} - \widehat{V}_i^j - \widehat{V}_l^j}{V^j}, \quad (6.39)$$

and

$$S_{T_i}^j = 1 - \frac{\widehat{U}_{-i}^j - \widehat{E}(y^j)^2}{\widehat{V}^j}. \quad (6.40)$$

Saltelli (2002) provided the following restrictions on the usage of the total variance,  $V^j$ , and expected value,  $E(y^j)$ , estimates, which ensured that all the estimates available were applied:

1. In computing the first-order indices,  $S_i^j$ ,  $\vec{a}_0^j$ , and  $\vec{a}_K^j$  should be used for  $\widehat{E}(y^j)^2$  and  $\vec{a}_K^j$  should be used for the computation of  $\widehat{V}^j$ .

2. The total-effect indices should be computed using  $\vec{a}_0^j$  only for  $\widehat{E}(y^j)^2$ , while  $\vec{a}_0^j$  and  $\vec{a}_K^j$  should be used for  $\widehat{V}^j$ .
3. Computation of the second-order indices is completed using one of the output vectors in the same row or column, i.e.,  $\widehat{V}_{il}^{jc}$  should be calculated using  $\vec{a}_{-i}^j$  and  $\vec{a}_i^j$  for  $\widehat{E}(y^j)^2$  and using  $\vec{a}_{-l}^j$  and  $\vec{a}_{-l}^j$  for  $\widehat{V}^j$ .

Finally, the higher-order interaction sensitivity indices may be computed via Equation (6.41),

$$S_{i(-il)}^j = S_{T_i}^j - S_i^j - \sum_{\substack{l=1 \\ l \neq i}}^n S_{il}^j \quad (6.41)$$

which accounts for any higher-order variance not accounted for by the first- or second-order indices.

Table 6.1: Matrix detailing the output vectors ( $\vec{a}$ ) used to compute the necessary sensitivity parameters. This table was adapted from Saltelli (2002) and should be used in conjunction with Equations (6.33) through (6.40). Note, the  $j$  superscript is omitted for simplicity.

	$\vec{a}_0$	$\vec{a}_1$	$\vec{a}_2$	$\vec{a}_3$	$\vec{a}_4$	$\vec{a}_5$	$\vec{a}_{-1}$	$\vec{a}_{-2}$	$\vec{a}_{-3}$	$\vec{a}_{-4}$	$\vec{a}_{-5}$	$\vec{a}_K$
$\vec{a}_0$	$\widehat{V}(y)$											
$\vec{a}_1$	$S_{T_1}$	$\widehat{V}(y)$										
$\vec{a}_2$	$S_{T_2}$		$\widehat{V}(y)$									
$\vec{a}_3$	$S_{T_3}$			$\widehat{V}(y)$								
$\vec{a}_4$	$S_{T_4}$				$\widehat{V}(y)$							
$\vec{a}_5$	$S_{T_5}$					$\widehat{V}(y)$						
$\vec{a}_{-1}$	$S_1$	$\widehat{E}(y)^2$	$\widehat{V}_{12}^c$	$\widehat{V}_{13}^c$	$\widehat{V}_{14}^c$	$\widehat{V}_{15}^c$	$\widehat{V}(y)$					
$\vec{a}_{-2}$	$S_2$	$\widehat{V}_{12}^c$	$\widehat{E}(y)^2$	$\widehat{V}_{23}^c$	$\widehat{V}_{24}^c$	$\widehat{V}_{24}^c$		$\widehat{V}(y)$				
$\vec{a}_{-3}$	$S_3$	$\widehat{V}_{13}^c$	$\widehat{V}_{23}^c$	$\widehat{E}(y)^2$	$\widehat{V}_{34}^c$	$\widehat{V}_{35}^c$			$\widehat{V}(y)$			
$\vec{a}_{-4}$	$S_4$	$\widehat{V}_{14}^c$	$\widehat{V}_{24}^c$	$\widehat{V}_{34}^c$	$\widehat{E}(y)^2$	$\widehat{V}_{45}^c$				$\widehat{V}(y)$		
$\vec{a}_{-5}$	$S_5$	$\widehat{V}_{15}^c$	$\widehat{V}_{24}^c$	$\widehat{V}_{35}^c$	$\widehat{V}_{45}^c$	$\widehat{E}(y)^2$					$\widehat{V}(y)$	
$\vec{a}_K$	$\widehat{E}(y)^2$	$S_1$	$S_2$	$S_3$	$S_4$	$S_5$	$S_{T_1}$	$S_{T_2}$	$S_{T_3}$	$S_{T_4}$	$S_{T_5}$	$\widehat{V}(y)$



### 6.4.3 A “Less Expensive” SOBOL

Saltelli (2002) presented a second approach that is computationally less expensive ( $C = K(n + 2)$ ) than the aforementioned method. Two disadvantages to this method are that only single estimates are produced and the second-order indices may not be computed. To perform this analysis, solve the desired relationship to obtain the output vectors listed in Equations (6.32)a–d, except omit (6.32)c. The first-order and total-effect indices can be computed as previously described using the Equations (6.33)–(6.40), but without including any  $-i$  vectors. Table 6.1 and the steps listed on page 151 may still be utilized to perform the calculations; simply overlook the  $\vec{a}_{-i}$  terms and the third step.

## 6.5 Confidence Levels and Bias Correction

The SOBOL method for computing sensitivity indices, as shown in the previous sections, is based on estimates of variance. Therefore, confidence should be applied to the results. When computing the confidence intervals, traditional statistical techniques may not be appropriate, especially for models that require significant computation time. For example, using traditional statistics, the sensitivity analysis would be repeated to develop a set of sensitivity indices from which confidence intervals may be computed. This may be unreasonable for models that require significant computation time. To circumvent this issue the bootstrap method is presented for calculating the confidence levels of the SOBOL analysis. The bootstrap method allows for these calculations without any additional model evaluations. Additionally, a bootstrap method for estimating the bias is presented.

The theory behind the computations presented in this section is beyond the scope of this chapter. The information presented is meant to be an overview as required for

implementation. For further details discussion of bootstrap analysis, refer to Efron and Tibshirani (1993). Additional information may also be found in Efron (1987), DiCiccio and Efron (1996), Hesterberg *et al.* (2005), and Manly (2007).

Bootstrap calculations are based on re-samplings of the input parameters to create replicate, or bootstrap, samples. Consider, for example, the data set  $\vec{x} = \{1, 5, 6, 8\}$ . Bootstrap data sets are created by randomly selecting replacement parameters from the original data set to create another of the same size, which might be  $\vec{x}^{*1} = \{8, 5, 1, 8\}$ . This process is repeated  $B$  times, resulting in  $B$  bootstrap samples:  $\vec{x}^{*1}, \vec{x}^{*2}, \dots, \vec{x}^{*B}$ . Each set of bootstrap samples is then used to calculate a new bootstrap estimate of the statistic of interest, for example

$$\hat{\theta} = f(\vec{x}) \quad (6.42a)$$

and

$$\hat{\theta}^{*b} = f(\vec{x}^{*b}) \mid b = 1, 2, \dots, B \quad (6.42b)$$

where  $\hat{\theta}$  is the value computed using the original data set ( $\vec{x}$ ) and  $\hat{\theta}^{*b}$  is computed with the bootstrap data sets ( $\vec{x}^{*b}$ ).

With the SOBOL method, the samplings are generated from output vectors defined in Equation (6.32). The re-sampling procedure is performed for each of the output vectors in a fashion that is consistent across the vectors, such that model evaluations are not disordered. As expected, the statistics of interest are the sensitivity indices:  $S_i^j$ ,  $S_{il}^j$ , and  $S_{T_i}^j$ . For example, referring to Equation (6.38) and (6.33)–(6.35), the first-order index would be computed as follows, the superscript  $j$  and the double estimates were omitted for simplicity:

$$S_i^{*b} = \frac{\hat{U}_i^{*b} - (\hat{E}(y)^{*b})^2}{\hat{V}^{*b}} \quad (6.43)$$

where,

$$(\widehat{E}(y)^{*b})^2 = \frac{1}{K} \bar{a}^{*b} \cdot \bar{a}_K^{*b}, \quad (6.44)$$

$$\widehat{V}^{*b} = \frac{1}{K} \bar{a}_i^{*b} \cdot \bar{a}_i^{*b} - (\widehat{E}(y)^{*b})^2, \quad (6.45)$$

and

$$\widehat{U}_i^{*b} = \frac{1}{K} \bar{a}_0^{*b} \cdot \bar{a}_{-i}^{*b}. \quad (6.46)$$

Performing re-sampling and computing  $B$  bootstrap sensitivity analysis parameters results in data sets from which confidence intervals are computed following the general procedure detailed in the following section.

### 6.5.1 BC<sub>a</sub> Confidence Level Intervals

Efron and Tibshirani (1993) explained that the BC<sub>a</sub> method—an abbreviation for *bias-corrected and accelerated*—is a “good” method for automatic computation of confidence level intervals. The bias correction accounts for the difference in expectation of the original statistic,  $\hat{\theta}$ , and bootstrap estimates,  $\hat{\theta}^{*b}$ . The acceleration accounts for the rate of change between the standard error of  $\hat{\theta}$  and the true value. For details regarding calculation of the BC<sub>a</sub> confidence levels refer to Efron and Tibshirani (1993).

The BC<sub>a</sub> method begins by computing an estimate of bias,  $\hat{z}_0$  that is

$$\hat{z}_0 = \Phi^{-1} \left( \frac{N_b}{B} \right), \quad (6.47)$$

which is a function of the number of bootstrap estimates,  $\hat{\theta}^{*b}$ , that are less than the measured statistic  $\hat{\theta}$ , which is defined here as  $N_b$ . This value is normalized against the total number of bootstrap samples,  $B$ , and then applied to the inverse of the standard normal cumulative distribution function,  $\Phi^{-1}$ .

The acceleration,  $\widehat{acc}$ , is computed based on the jackknife values of the statistic  $\hat{\theta}_{(r)}$ . The subscript  $r$  is used here because the computation of the jackknife statistic in the SOBOL method is based on the  $k$  Monte Carlo re-sampling. These values are determined by computing the value of the statistics with the  $i$ th input parameter removed, for example  $\hat{\theta}_{(r)} = f(a_{-r})$ . The function  $f(a_{-r})$  in the SOBOL method refers to the computation of the sensitivity analysis parameters using all except the  $r^{\text{th}}$  Monte Carlo re-samplings. Equation (6.48) utilizes these jackknife values to compute acceleration,

$$\widehat{acc} = \frac{\sum_{r=1}^K (\hat{\theta}_{(\cdot)} - \hat{\theta}_{(r)})^3}{6 [\sum_{i=r}^K (\hat{\theta}_{(\cdot)} - \hat{\theta}_{(r)})^2]^{3/2}} \quad (6.48)$$

where  $\hat{\theta}_{(\cdot)} = \sum_{r=1}^K \frac{\hat{\theta}_{(r)}}{K}$ .

The  $BC_a$  adjusted percentiles are computed using the relationships in Equation (6.49),

$$\alpha_{lo} = \Phi \left( \hat{z}_0 + \frac{\hat{z}_0 + z^{(\alpha/2)}}{1 - \widehat{acc}(\hat{z}_0 + z^{(\alpha/2)})} \right) \quad (6.49a)$$

$$\alpha_{hi} = \Phi \left( \hat{z}_0 + \frac{\hat{z}_0 + z^{(1-\alpha/2)}}{1 - \widehat{acc}(\hat{z}_0 + z^{(1-\alpha/2)})} \right) \quad (6.49b)$$

where  $z^{(\alpha)}$  and  $z^{(1-\alpha)}$  are computed using the standard normal cumulative distribution. The  $\alpha$ -value corresponds to the percentile interval desired, e.g.,  $\alpha = 0.1$  results in confidence intervals between the 5% and 95% values of the bootstrap estimates of  $\hat{\theta}^{*b}$ . For example, if  $\alpha = 0.1$  then  $z^{(0.95)} = \Phi^{-1}(0.95) = 1.645$ .

The confidence level intervals are then determined using the  $\alpha_{lo}$  and  $\alpha_{hi}$  values. Take for example, a  $BC_a$  bootstrap sample size of  $B = 2000$  and calculated intervals  $\alpha_{lo} = 0.110$  and  $\alpha_{hi} = 0.985$ . The confidence levels would be the 220<sup>th</sup> and 1970<sup>th</sup> ordered values of  $\hat{\theta}^{*b}$ .

### 6.5.2 Bias Correction

An unbiased result is defined as  $E(\hat{\theta}) = \theta$ , i.e., the expected value is equal to the true value. Using the bootstrap replicates, an estimate of the bias may be computed. Note, this estimate is different from the bias calculation in the previous section. The bias estimate method presented here should be applied to the computed value of the SOBOL sensitivity indices, whereas the previous estimate should be used with the confidence intervals. The bootstrap bias,  $bias_B$ , is easily estimated from the mean of the bootstrap estimates:

$$\hat{\theta}_{(\cdot)}^{*b} = \sum_{b=1}^B \hat{\theta}^{*b} / B \quad \text{and} \quad (6.50a)$$

$$bias_B = \hat{\theta}_{(\cdot)}^{*b} - \hat{\theta}. \quad (6.50b)$$

### 6.6 Example 1: SOBOL

The test case presented here is based on the “g function,” which is commonly used throughout the literature. This function, as defined below, is used here as an example of the SOBOL technique.

$$g(x_1, x_2, \dots, x_n) = \prod_{i=1}^n \frac{|4x_i - 2| + q_i}{1 + q_i}. \quad (6.51)$$

The vector,  $\vec{q}$  is defined as  $\vec{q} = \{0, 0.5, 3, 9, 99, 99\}$  and acts as a weighting parameter for the  $x_i$  inputs. Small values cause the associated input to become more important. Each input parameter,  $x_i$ , is uniformly distributed between 0 and 1, where  $i = 1, 2, \dots, 6$  (i.e.,  $n = 6$ ). A SOBOL sensitivity analysis was performed on this function where  $K = 10,000$  replicates of the input parameters. Bootstrap confidence level intervals were computed using  $B = 10,000$  bootstrap re-samplings. The results indicate the importance of each  $x_i$ .

Figure 6.1 provides the results of this analysis for the first-order and total-effect indices. This figure can be directly compared to Saltelli (2002, Fig. 3), which shows similar results. Additionally, bias-corrected first-order, second-order, and total-effect indices are provided in Table 6.2.

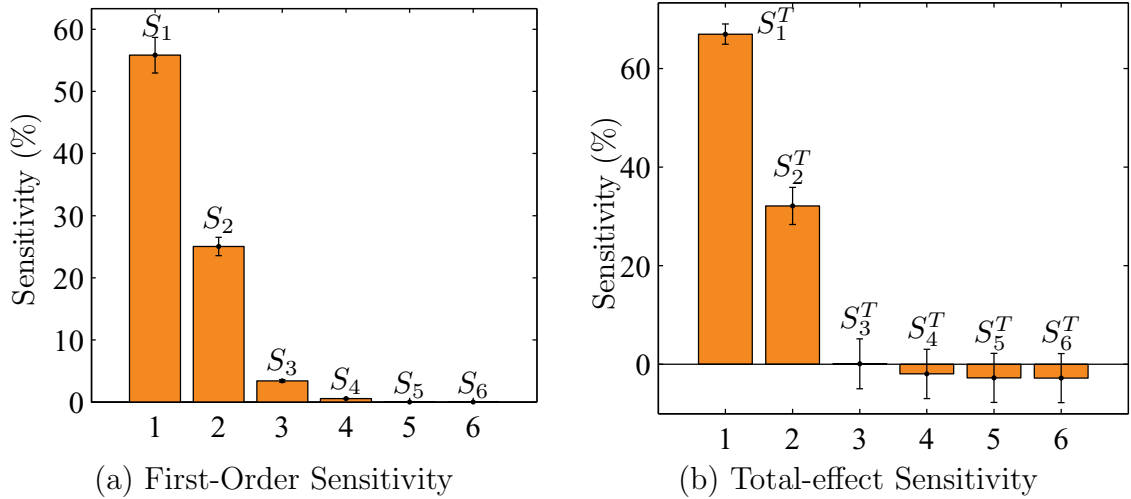


Figure 6.1: Results from the SOBOL sensitivity analysis of Equation (6.51), including the first-order ( $S_i$ ) and total-effect sensitivity ( $S_{T_i}$ ) terms. (The error bars reflect the 90% confidence intervals.)

Table 6.2: Improved SOBOL sensitivity indices, in percent, of Equation (6.51); the values on the diagonal are the first-order indices, the off-diagonal terms are the second-order indices (e.g.,  $S_{12} = 14.19\%$ ), and the bottom row reflects the total-effect indices. The table is a symmetric matrix, but the upper triangular values were omitted for readability.

i,l	1	2	3	4	5	6
1	57.26					
2	14.19	25.73				
3	3.61	1.61	3.51			
4	-0.67	-0.29	0.04	0.58		
5	0.03	0.02	0.00	0.00	0.00	
6	0.02	-0.02	0.00	0.00	0.00	0.00
$S_T$	68.30	34.73	3.51	0.00	0.00	0.00

This example allows for an analysis that is indicative of what is desired from a sensitivity of a given function. The first two parameters are the most significant, as both the first- and second-order indices reveal. It may also be possible to state that the  $x_3, \dots, x_6$  terms are negligible and may be omitted in future analyses. The importance of computing the total-effect and/or the second-order indices is also illustrated.  $S_{12}$  accounts for 14% of the total variance. Without computing the total-effect or second-order indices this would remain undetected.

This example also highlights the importance of computing confidence intervals. Recall the total-effect index includes individual sensitivity and the sensitivity of all interactions. Thus, the sum of the columns in Table 6.2 should comprise a value less than the total-effect. Performing this computation for the first column yields a value of approximately 75%, which differs from the reported total-effect index in the table (68.3%). This difference is likely due to the uncertainty present in the calculation of the first- and second-order indices, which when added compounds; Figure 6.2 shows the uncertainty in these terms. This uncertainty is not compounded in the calculation of the indices themselves, since each is determined from different estimates according to the criteria listed in Section 6.4.2.

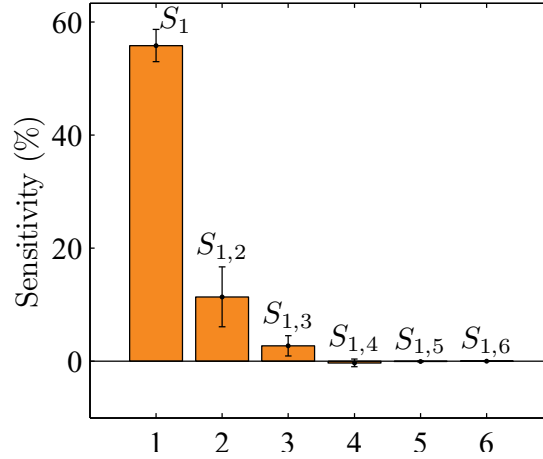


Figure 6.2: First- and second-order indices for the first input parameter ( $x_1$ ) from analysis of Equation (6.51).

### 6.7 Example 2: Temporal Analysis

In situations that are time dependent SOBOL is particularly useful. The following example considers an arbitrary function that is dependent on time  $t$ :

$$y(t) = \frac{1}{t^2} \sin(x_1) + 7t \sin^2(x_2) + 0.1t^2 x_3^4 \sin(x_1). \quad (6.52)$$

For any given set of input parameters this function may be evaluated at any time  $t$ . For example, SOBOL is implemented as usual, but instead of incorporating a single output as in the previous example, the function will output  $m$  values, i.e.,  $y^j = y(t_j) \mid j = 1, 2, \dots, m$ . Thus, when SOBOL is performed  $m$  sets of sensitivity indices are computed. This allows the sensitivity indices to be plotted with time, as in Figure 6.3, which depicts the aforementioned time dependent relationship for  $t$  between 1 and 5. Using this figure, it is possible to examine the contribution of each parameter to the total of all values. For example, at  $t = 4$  the normalized total-effect  $S_{T_i}^*$  indices are 0.58, 0.05, and 0.37, respectively. The asterisk indicates that the total-effect indices are normalized to the sum of all the total-effect indices,



thus guaranteeing that the individual indices are between 0 and 1. For additional examples and illustrations refer to Saltelli *et al.* (2000).

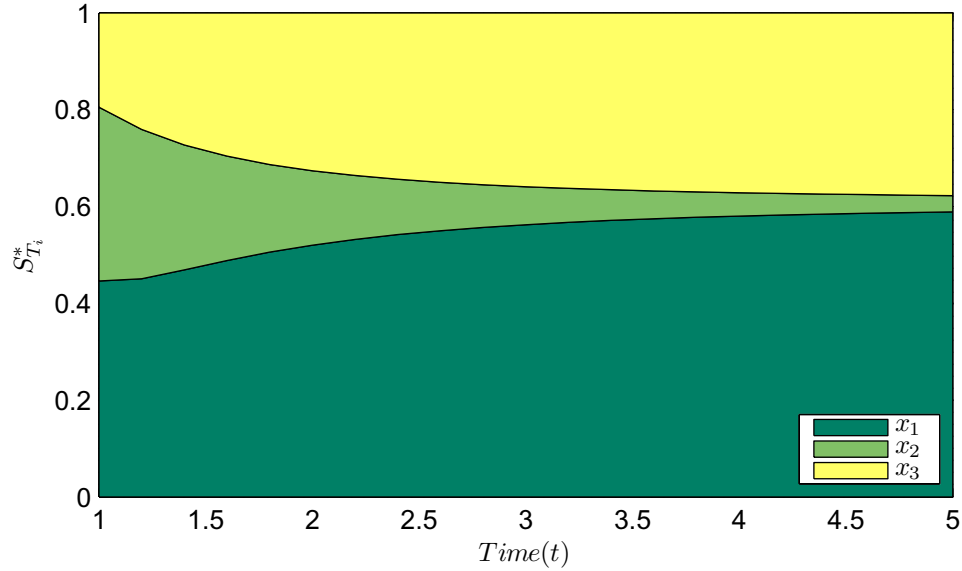


Figure 6.3: Stacked area plot of the time-dependent total-effect indices resulting from the analysis of Equation (6.52).

### 6.8 Closing Remarks

This chapter summarizes the theory behind the SOBOL method of sensitivity analysis, which is a variance-based method capable of computing first-order, second-order, and total-effect sensitivity indices. The methods defined here have been utilized by a variety of researchers to analyze chemical rate equations and climate energy balance models, among others. The tools defined here, including a set of MATLAB (The Mathworks, Inc.) functions (see Appendix D), were used for analyzing the critical parameters of the formation weak-layers on the snow surface that often lead to subsequent avalanches, Chapters 8–10.

## CHAPTER 7

### IMPLEMENTATION OF NUMERICAL ANALYSIS TECHNIQUES

#### 7.1 Introduction

The main objective of the research presented throughout this dissertation was to define the conditions favorable for surface hoar and near-surface facet development. To achieve this goal, two numerical analysis techniques—sensitivity analysis (see Chapter 6 for details) and Monte Carlo simulation—were employed, these provide complementary products. The sensitivity analysis quantified the amount of variance in the model output that was due to the variance of the input parameters, simply stated, it quantifies the importance of each input on the output. The Monte Carlo simulations supplemented this analysis by providing a means for determining the set of inputs that led to a certain output. That is, this technique allowed for a range of inputs to be associated with a range of outputs. This chapter provides the information necessary to understand how these methods, as well as two additional data analysis techniques, were implemented for the problem at hand. This chapter sets the stage for the work detailed in Chapters 8–10.

#### 7.2 Thermal Model Input Distributions

The analysis presented in Chapters 8–10 is based on a snowpack model derived from the heat equation (Equation (5.13)). For details regarding the model used, refer to Chapter 5. This model was chosen for two reasons. First, a nearly identical model is implemented in RadTherm/RT (ThermoAnalytics, Inc.<sup>1</sup>) that has been shown to

---

<sup>1</sup><http://www.thermoanalytics.com/>

be successful in predicting snow surface temperatures and mass-flux over spatially complex terrain (Staples *et al.*, 2006; Adams *et al.*, 2009). Secondly, the analysis presented in this chapter is computationally expensive. The method used required hundreds of thousands of model evaluations. Therefore, a computationally efficient thermal model was advantageous. The evaluation time of the model presented in Chapter 5 is on the order of a few tenths of a second (Hewlett Packer dv9000; Windows Vista x64; Intel T9300 at 2.50 GHz; 4 GB RAM).

The model used in the analysis required either 8 or 11 input parameters which are listed in Table 7.1 along with its respective index reference ( $i$ ) and assigned symbol (Sym.) that are referenced throughout the remainder of this chapter and Chapters 8–10. The parameters listed are divided into two groups: snow properties— $\rho(1)$ ,  $k(2)$ ,  $c_p(3)$ ,  $\kappa(5)$ , and  $\alpha(8)$ —and environmental conditions.

Table 7.1: List of input parameters, their associated symbol, and index ( $i$ ) referenced in the analysis throughout Chapters 8–10.

$i$	Sym.	Units	Name
1	$\rho$	kg/m <sup>3</sup>	Snow density
2	$k$	W/(m K)	Thermal conductivity
3	$c_p$	kJ/(kg K)	Specific heat capacity
4	$T_s^{int}$	°C	Initial snow temperature
5	$\kappa$	m <sup>-1</sup>	Extinction coefficient
6	$LW$	W/m <sup>2</sup>	Incoming long-wave radiation
7	$SW$	W/m <sup>2</sup>	Incoming short-wave radiation
8	$\alpha$		Albedo
9	$V_w$	m/s	Wind speed
10	$T_a$	°C	Air temperature
11	$RH$	%	Relative humidity

Both the sensitivity analysis and Monte Carlo simulations required that each input be assigned a continuous distribution function. The distributions were then sampled randomly so that all possible values and combinations for each input were evaluated. Two scenarios were considered in the analysis: “day-light” and “night.”

The day-light sets considered all the input parameters including solar input ( $SW(7)$ ) and the related snow properties, albedo ( $\alpha(8)$ ) and extinction coefficient ( $\kappa(5)$ ). The night sets were executed in absence of these three “solar” parameters, which explains the difference between the number of input parameters considered. Within each of these two scenarios, three locations were developed: a Control set that used uniform distributions, a South set based on weather data from the South-facing weather station, and a North set based on the North-facing weather station. The term “control” is used loosely to refer to the synthetic location created based only on reasonable values of each of the input parameters; i.e., if no location specific weather conditions existed, the distributions defined by Control location may be reasonable estimates of the input parameters. From this point forward these data sets will be referred to as scenario/location, e.g., night/North or day-light/South.

Due to limited information regarding the snow properties, uniform distributions consistent with data published by Armstrong and Brun (2008) were used in all cases for the five terms listed in Table 7.2. The remaining terms—the environmental conditions—were fit to distributions based on two seasons of recorded weather data from two weather stations at the Yellowstone Club ski area located near Big Sky, Montana. Using a distribution-fitting software package, EasyFit 5.0 (Mathwave Technologies), these distributions were determined based on mean values of the input parameters measured at the weather stations for the day-light or night scenarios, with one exception. Namely, the initial snow temperature  $T_s^{int}(4)$  for the entire snowpack was assumed to be the temperature of the snow prior to the onset of day-light or night.

All the Control input sets were composed of uniform distributions that spanned reasonable values, these values also served as limits for the South and North data set distribution functions. For each of the North and South input data sets, the best-

Table 7.2: Snow property uniform distribution parameters used for sensitivity analysis and Monte Carlo simulations.

	min.	max.
$\rho$	50	500
$k$	0.01	0.7
$c_p$	1795	2115
$\alpha$	0.4	0.95
$\kappa$	40	200

fitting distributions functions, based on a Kolomogorov-Smirnov test, were selected that were also available in MATLAB (The Mathworks, Inc.). Four different distribution functions were utilized: generalized extreme value (gev), generalized Pareto (gp), Weibull (wbl), and lognormal (logn), as defined in the probability density functions (EasyFit 5.0, 2009) which follow. The functions chosen were the

The resulting distributions for each parameter are tabulated in Table 7.3, with the relevant distribution functions provided in Equations (7.1)–(7.4). Each input distribution utilized is graphed in Figure 7.1. The distributions presented indicate the probability that the inputs equal the mean for any given day or night during the two seasons. Figure 7.1 includes the probability density functions for the input parameters based on measured data.

$$f_{gev}(x) = \begin{cases} \frac{1}{\sigma} \exp(-(1 + kz)^{-1/k})(1 + kz)^{-1-1/k} & k \neq 0, \\ \frac{1}{\sigma} \exp(-z - \exp(-z)) & k = 0, \end{cases} \quad (7.1)$$

where  $z = \frac{x-\mu}{\sigma}$  and  $k$ ,  $\sigma$ , and  $\mu$  are the shape, scale, and location parameters, respectively, which correspond to  $a$ ,  $b$ , and  $c$ , respectively, in Table 7.3.

$$f_{gp}(x) = \begin{cases} \frac{1}{\sigma} \left(1 + k \frac{x-\mu}{\sigma}\right)^{-1-1/k} & k \neq 0, \\ \frac{1}{\sigma} \exp\left(-\frac{x-\mu}{\sigma}\right) & k = 0, \end{cases} \quad (7.2)$$

where  $k$ ,  $\sigma$ , and  $\mu$  are the shape, scale, and location parameters, respectively, which correspond to  $a$ ,  $b$ , and  $c$ , respectively, in Table 7.3.

$$f_{wbl}(x) = \frac{\alpha}{\beta} \left( \frac{x - \gamma}{\beta} \right)^{\alpha-1} \exp \left( - \left( \frac{x - \gamma}{\beta} \right)^\alpha \right), \quad (7.3)$$

where  $\alpha$ ,  $\beta$ , and  $\gamma$  are the shape, scale, and location parameters, respectively, which correspond to  $a$ ,  $b$ , and  $c$ , respectively, in Table 7.3.

$$f_{logn}(x) = \frac{\exp \left( - \frac{1}{2} \left( \frac{\ln(x-\gamma)-\mu}{\sigma} \right)^2 \right)}{(x - \gamma)\sigma\sqrt{2\pi}}, \quad (7.4)$$

where  $\sigma$  and  $\mu$  are the continuous shape parameters and  $\gamma$  is the location parameter, which correspond to  $a$ ,  $b$ , and  $c$ , respectively, in Table 7.3.

Table 7.3: Environmental input parameter distribution sets used for sensitivity analysis and Monte Carlo simulations; the coefficients ( $a$ ,  $b$ , and  $c$ ) correspond to the parameters provided in Equations (7.1)–(7.4).

		South			North				Control		
		Type*	$a$	$b$	$c$	Type*	$a$	$b$	$c$	Min.	Max.
Day-light	$T_s^{int}$	gev	-0.39	5.80	-16.34	gev	-0.36	6.15	-16.13	-40	0
	LW	gev	-0.09	63.62	287.97	gev	-0.04	33.85	245.29	100	600
	SW	gp	-0.89	575.79	39.09	wbl	128.08	2.20	0.00	50	800
	$V_w$	logn	0.52	0.33	0.00	gev	-0.09	0.28	1.05	0	4
	$T_a$	gev	-0.24	4.47	-8.19	gev	-0.39	4.68	-7.59	-30	10
	RH	gev	-0.66	15.92	60.43	gev	-0.73	13.33	62.99	0	100
Night	$T_s^{int}$	gev	-0.45	5.32	-12.65	gev	-0.40	5.19	-13.15	-40	0
	LW	gev	-0.25	42.46	262.03	gev	0.07	35.84	236.83	100	600
	$V_w$	gev	0.00	0.54	1.17	gev	-0.17	0.35	1.02	0	10
	$T_a$	gev	-0.28	4.51	-11.33	gev	-0.41	4.68	-10.11	-30	10
	RH	gev	-0.99	13.72	72.14	gev	-0.80	11.26	70.90	0	100

\* gev = generalized extreme value; gp = generalized Pareto; wbl = Weibull; logn = lognormal

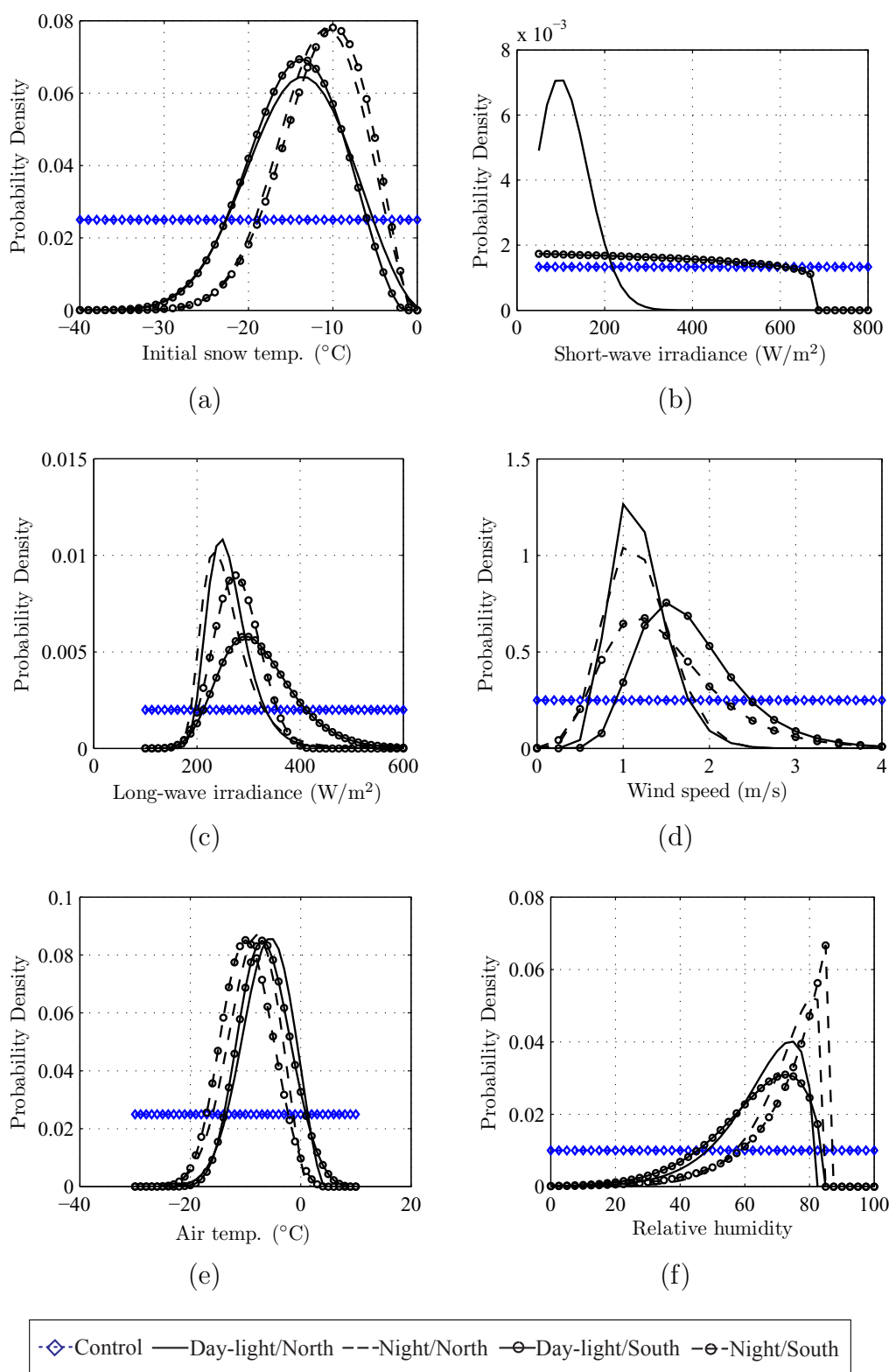


Figure 7.1: Probability distribution functions for input data based on measured data.

### 7.3 Model Evaluations

The sensitivity analysis and Monte Carlo simulations rely on a multitude of model evaluations. In each model evaluation, with the exception of short-wave radiation, all of the input parameters remained constant through time. For each evaluation the inputs were selected from the input distributions randomly, i.e., random numbers that follow the assigned distributions defined in Table 7.3. Initially, the entire snowpack was assumed to begin at the same temperature defined by  $T_s^{int}(4)$ , and the model was evaluated for a 10-hour period. Data for use in computation was exported in 20 minute intervals. Short-wave radiation was defined as a sine function that had a mean value equivalent to the mean value recorded in the field measurements.

### 7.4 Sensitivity Analysis

The extended SOBOL variance-based sensitivity method (Saltelli, 2002) quantifies the contribution of the variance of each input parameter (see Table 7.1) and the interactions between input parameters to the total variance of the model output. The theory behind the method used here, as well as a detailed discussion of variance with respect to sensitivity, is provided in Chapter 6.

The SOBOL method was performed using the thermal model and a sampling size of 10,000 replicates ( $K$ , see Section 6.4.2) to compute output based on the input parameters and associated statistical distributions. . The 90% confidence intervals were calculated using the bootstrap BCa method (Efron and Tibshirani, 1993) with 10,000 re-samplings ( $B$ , see Section 6.5). The basic methodology is summarized by the following steps:



1. The input distributions previously defined in Section 7.2 were re-sampled twice each, 10,000 times in this case, to form two input matrices.
2. These two matrices are used systematically, as defined by the improved SOBOL method in Section 6.4.2, to construct sets of input parameters for evaluation.
3. These sets of input data are analyzed with the thermal model thus producing sets of output vectors associated with each of the input parameters, see Chapter 5 and Section 7.3.
4. These vectors are combined using the improved SOBOL methodology to estimate the various sensitivity parameters detailed below, see Section 6.4.2.
5. Confidence level intervals for each parameter are obtained by re-sampling the output vectors, in this case 10,000 times, creating 10,000 values for each sensitivity parameter from which the 90% confidence intervals were computed, see Section 6.5.

The results discussed include four terms: the first-order index ( $S_i$ ) gives the contribution of the  $i^{th}$  input parameter; the second-order index  $S_{i,l}$  gives the contribution due to interaction between  $i^{th}$  and  $l^{th}$  terms; the higher-order index ( $S_h$ ) that includes all interactions greater than second-order; and the total-effect index ( $S_i^T$ ) provides the contribution of the  $i^{th}$  parameter and all associated interactions to the  $k^{th}$  order (e.g.,  $S_1^T = S_1 + S_{1,2} + S_{1,3} + \dots + S_{1,k} + S_h$ ), where  $k$  is the number of input factors (i.e., 8 or 11 here), see Section 6.3.2. The  $i$  and  $l$  subscripts refer to the variable numbers in Table 7.1. The term “residual” is also used throughout this chapter and refers to all variance not associated with the parameter under consideration.

### 7.5 Monte Carlo Analysis

While the SOBOL method quantifies the significance of the input parameters, its limitation is that it does not directly link inputs to a particular output. The specific outputs utilized are defined in Chapters 8 and 9 and include mass flux, snow temperatures, and temperature gradients. Thus, Monte Carlo simulations (Press *et al.*, 1986) were utilized to further quantify the environmental conditions and snow properties by separating the portion of critical input parameters that led to a specific output, e.g., the levels of long-wave radiation that are associated with mass-flux rates typical of surface hoar formation (see Section 8.2). To perform this analysis, no additional model evaluations were necessary; it was sufficient to rearrange—as described below—the input and output from the SOBOL method to create a large set of Monte Carlo simulated data.

The use of this reordered data is a natural extension, as the SOBOL method is based on Monte Carlo simulations organized in a certain manner. Referring to Chapter 6 (Section 6.4.2), this is accomplished by gathering the input matrices ( $W$ ,  $W'$ ,  $N_i$  and  $N_{-i}$ ; see Equations (6.29)–(6.31)) with the corresponding output vectors ( $\vec{a}_0^j$ ,  $\vec{a}_K^j$ ,  $\vec{a}_{-i}^j$ , and  $\vec{a}_K^j$ ; see Equation (6.32)). Using the results from the SOBOL a Monte Carlo data set was produced with 240,000 and 180,000 replicates for the day-light and night data sets, respectively.

### 7.6 Highest Density Regions

A methodology for analyzing the Monte Carlo simulation data is presented; the data in this section is hypothetical and used simply as an example of how this analytical tool was applied in the following chapters. Using the Monte Carlo simulations it

was possible to separate the inputs responsible for a specified output. Thus, subsets of the complete Monte Carlo data were defined. These subsets may contain any number of data points, so it was necessary to define a region that surrounded the data. The information in this section demonstrates the usage of highest density regions (HDRs), as defined by Hyndman (1996).

An HDR is defined by cropping the probability density function (PDF) such that the desired amount of data remains, 95% for example. Imagine slicing a plane through a normal distribution such that 95% of the data has a probability density greater than that of the plane. Hence, it may be stated that an observation from within the population (i.e., a model evaluation) has a 95% chance of falling within this range (Hyndman, 1996). The HDR region is defined by the slice of the PDF function that encapsulates the data. By definition this region is the smallest possible region that satisfies this condition (Hyndman, 1996). Additional discussions of the usage of HDRs may be found in Scott (1992) and Martinez (2008).

Consider the data presented in Figure 7.2a, which includes an arbitrary output value ( $\Phi$ ) that is a function of two additional variables ( $\Pi_1$  and  $\Pi_2$ ). A 3-D HDR was used to enclose the data in a region that contained a certain amount of the data. To compute the HDR, first a tri-variate PDF was defined. This is done using the normal Product Kernel (Martinez, 2008) that resulted in an empirical multi-variate distribution function. Based on the distribution, HDRs were defined. Figure 7.2b shows the 5%, 50%, and 90% HDRs of the Monte Carlo simulations based on the data points in Figure 7.2a.

The 3-D HDRs were not a practical graphic for gathering useful information regarding the data presented. Therefore, the 3-D HDR shown in Figure 7.2 is simplified into a 2-D plot, ignoring the vertical dimension. As was done with the 3-D data, a Kernel Product estimation of the probability density function (PDF) was defined,

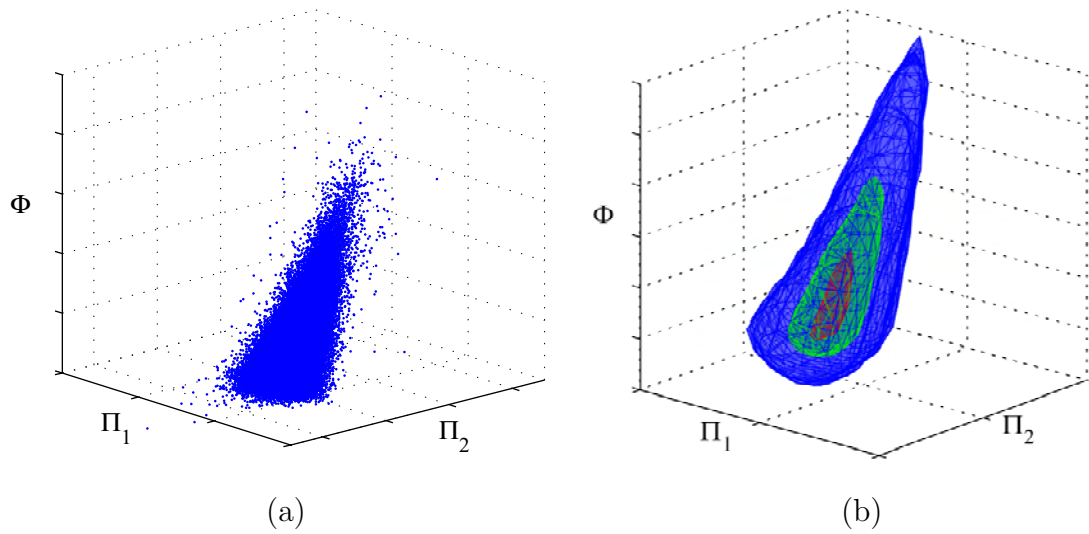


Figure 7.2: Comparison of 3-D representations of (a) the raw data as a scatter plot and (b) the data encapsulated by 5% (inner), 50% (middle), and 95% (outer) HDRs.

resulting in the bi-variate distribution shown in Figure 7.3a. This PDF was then used to define the region that encapsulates 95% of the data, as shown in Figure 7.3b.

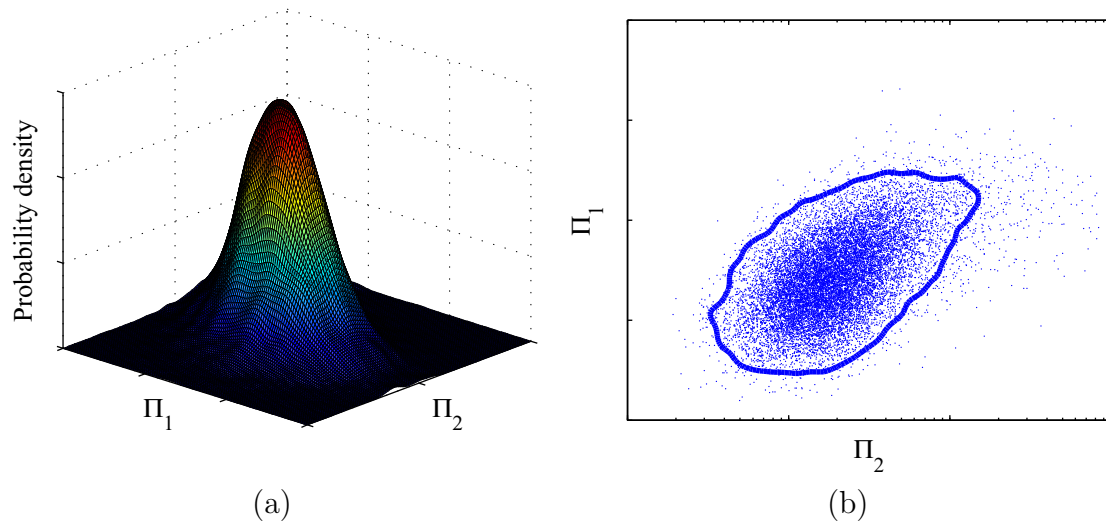


Figure 7.3: The (a) bi-variate probability density function was constructed from the raw data points shown in sub-figure b; the probability distribution was then sliced such that 95% of raw data had a probability density greater than this value resulting in a highest density region trace also shown in sub-figure b.

A second example of data set was then considered, where  $\Psi = f(\Pi_1, \Pi_2)$ . First, for comparison, the raw data as shown in Figure 7.4a was encapsulated by a 95% HDR, as was performed in the previous example. Again, utilizing the 3-D representation is problematic so the data was reduced to a 2-D representation. In Figure 7.4c the vertical dimension, represented by  $\Psi$ , was not ignored but separated into three bands. The bands only included inputs resulting in the output for the prescribed bands (i.e., inputs resulting in values of  $\Psi$  of 100-200, 200-300, and 300-400 in Figure 7.4c). For each band the 95% HDR are shown in Figure 7.4c. For the data in this example, as demonstrated in Figure 7.4c,  $\Pi_2$  exhibited a much larger range for values of  $\Psi$  above 200. Figure 7.4d considers all the data without banding, but includes four different HDRs: 95%, 90%, 50%, and 10%. This example demonstrates that 50% of the data is expected to have  $\Pi_1 \approx 0.25-0.7$  and  $\Pi_2 \approx -0.2-0.2$ . Both of these analysis techniques were utilized throughout Chapters 8–10.

### 7.7 Empirical Probability Density Functions

The highest density regions discussed in the previous section required the computation of the multi-variate probability distribution functions. This was accomplished, as mentioned, using a product kernel estimate (Scott, 1992; Martinez, 2008) with a Gaussian kernel. In addition to the multivariate PDFs used in the HDR computations, one-dimensional PDFs were also used for displaying data. In this case, the kernel estimate was also used, but with an Epanechnikov kernel (Scott, 1992; Martinez, 2008).

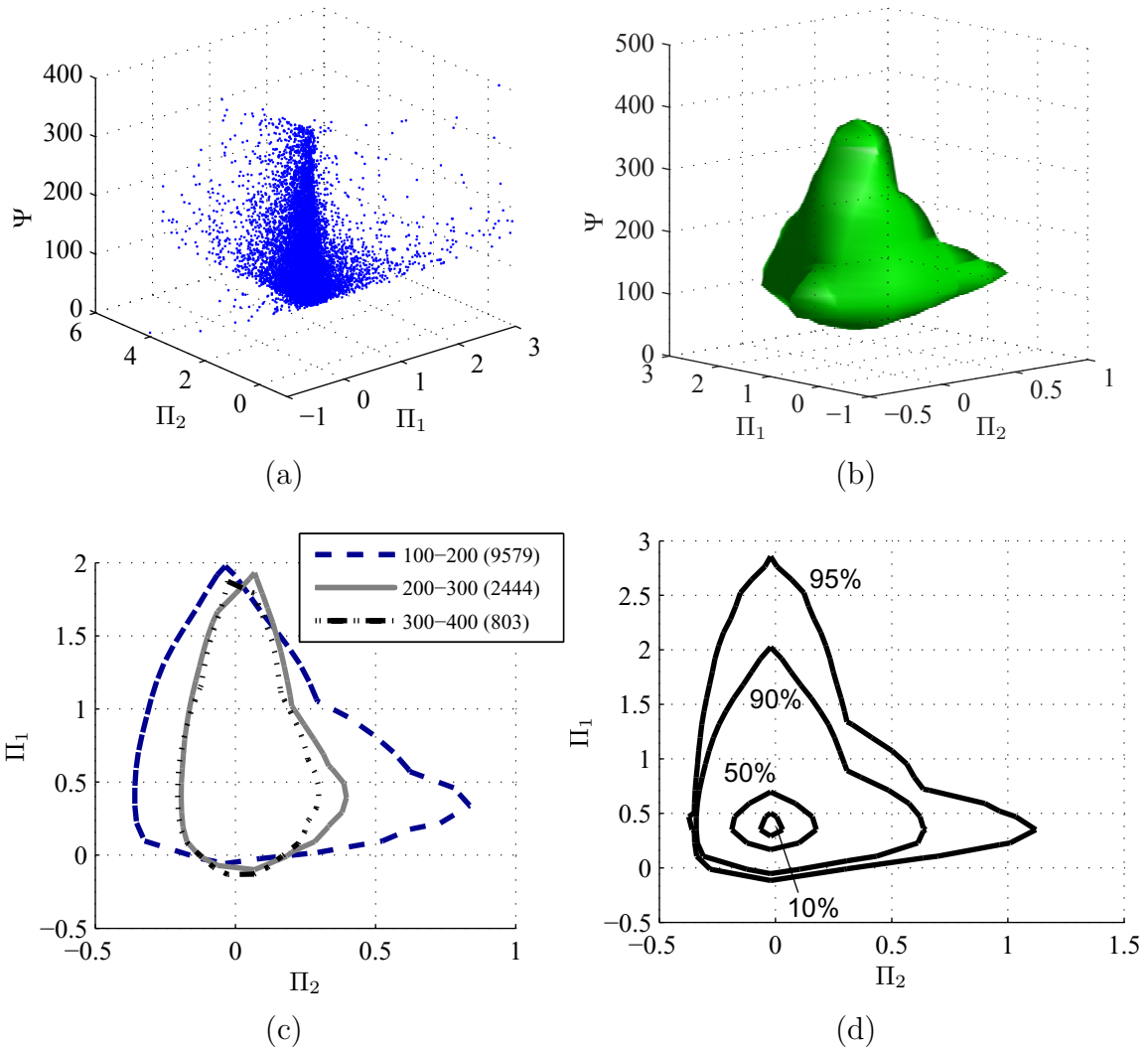


Figure 7.4: Example of tri-variate data analysis including (a) a 3-D scatter plot of raw data, (b) a 3-D 95% HDR, (c) 2-D HDRs encapsulating specific bands of  $\Psi$ , and (d) the 10%, 50%, 90%, and 95% HDRs of complete data set (the number of data points used to construct each region is included in the parenthesis).

### 7.8 Goodness-of-fit Hypothesis Test

Throughout Chapters 8–10 distributions of data were compared using the Kolmogorov-Smirnov Test (Massey, 1951). In all cases the null hypothesis was that the two distributions being compared were from the same distribution. The test

returns a  $p$ -value; if the  $p$ -value is greater than the level of significance desired then the null hypothesis is rejected. For example, if two distributions returned  $p = 0.074$ , then at the 5% significance level the null hypothesis would be rejected and it may be concluded that the two distributions are likely from different populations. However, at a 10% significance level the test would fail to reject the null hypothesis, meaning the distributions may be from the same population.

### 7.9 Closing Remarks

The methods presented in this chapter summarize the tools utilized throughout the following analytical chapters. The sensitivity analysis quantifies the important factors influencing the thermal model output. The Monte Carlo simulations allow for the identification of the input parameters responsible for the desired conditions. To aid in the visualization of the data, highest density regions were defined. Finally, throughout the analysis, the Kolmogorov-Smirnov test for goodness-of-fit was employed to quantify the similarity or difference between various distributions.

## CHAPTER 8

### NUMERICAL ANALYSIS OF SURFACE HOAR

#### 8.1 Introduction

Surface hoar is a particular morphology of faceted snow crystals that forms on the snow surface. When buried, it is often a contributor to snow avalanches. The environmental and snow material properties that are conducive to surface hoar formation have been investigated by a number of authors (Mason *et al.*, 1963; Lang *et al.*, 1984; Hachikubo and Akitaya, 1997; Cooperstein *et al.*, 2004; Feick *et al.*, 2007). A review of the literature provided in Chapter 2 reports that surface hoar forms when air temperature is between  $-5\text{ }^{\circ}\text{C}$  and  $-15\text{ }^{\circ}\text{C}$ , relative humidity is between 60% and 100%, and when the snow surface is about  $5\text{ }^{\circ}\text{C}$  cooler than the air temperature. Despite the research that exists, a minimal amount of quantifiable data is available to firmly determine the necessary conditions for surface hoar formation.

The information presented in this chapter expands on the current understanding of the conditions surrounding surface hoar formation. Using numerical methods, namely the SOBOL method of sensitivity analysis (Saltelli, 2002) as well as Monte Carlo simulations (Press *et al.*, 1986), augmented with observed surface hoar events, the conditions were explored with a simple 1-D snow thermal model similar to that used by Morstad *et al.* (2007). The main objectives of the analysis presented were two-fold:

1. To identify the most important environmental conditions and snow properties causing surface hoar formation.
2. To provide a tool for determining when surface hoar forms based on environmental and snow conditions.



## 8.2 Methods

Chapter 7 describes the methods used throughout this chapter, including the input data set development. The variables considered for this analysis are repeated here, Table 8.1, for convenience. Since surface hoar typically forms at night, only the night input scenario was considered. However, all three locations—Control, North, and South—were considered. The Control location was designed to be generic in nature and was developed assuming uniform distributions for each of the 11 input parameters. As the names suggest, the North and South locations were developed based on site specific weather conditions. Refer to Section 7.2 for a description of the locations and details of the input distributions.

In the case of surface hoar, one output “class”<sup>1</sup> was analyzed: mass-flux ( $\Phi$ ) at the snow surface. The mass-flux was computed as

$$\Phi = \frac{q_e}{L_s}, \quad (8.1)$$

where  $q_e$  is the latent heat flux computed from Equation (5.35) on page 129 and  $L_s$  is the latent heat of sublimation of ice (see Table 5.1).

Various calculations, referred to as “types,” were considered including the mean, minimum, and maximum for the 10-hour model evaluations. For reference the mean, minimum, and maximum of  $\Phi$  are respectively named as  $\bar{\Phi}$ ,  $\Phi^{min}$ , and  $\Phi^{max}$ . In addition to considering mass-flux in general, output considering only positive ( $\Phi_{pos}$ ) and negative ( $\Phi_{neg}$ ) values was also considered. This was accomplished in each case by setting mass-flux values equal to zero for  $\Phi < 0$  and  $\Phi > 0$  for the positive and negative cases, respectively. Only the mean values were considered for the positive and negative  $\Phi$  outputs, referred respectively to as  $\bar{\Phi}_{pos}$  and  $\bar{\Phi}_{neg}$ .

<sup>1</sup>The term class is used here to remain consistent with Chapter 9, which uses multiple classes.

The consideration of three locations, one class, and five types generated 15 different outputs data sets. The results shall be referred to by the convention of location/class-type, e.g., North/ $\Phi^{min}$ . The complete tabulated results are provided in Appendix E. Also, in all cases the sensitivity indices are listed as percentages, that indicate the percent of the total variance that may be attributed to the parameter under consideration (e.g.,  $S_1 = 15\%$  indicates that 15% of the total variance is due to the  $\rho$  acting independently).

Table 8.1: List of input parameters, associated symbol, and reference index used in the analysis throughout this chapter.

$i$	$Sym.$	$Units$	$Name$
1	$\rho$	kg/m <sup>3</sup>	Snow density
2	$k$	W/(m K)	Thermal conductivity
3	$c_p$	kJ/(kg K)	Specific heat capacity
4	$T_s^{int}$	°C	Initial snow temperature
6	$LW$	W/m <sup>2</sup>	Incoming long-wave radiation
9	$V_w$	m/s	Wind speed
10	$T_a$	°C	Air temperature
11	$RH$	%	Relative humidity

### 8.3 Results: Sensitivity Analysis

#### 8.3.1 Mean Mass-Flux, $\bar{\Phi}$

The total-effect indices ( $S_i^T$ ) result from analyzing  $\bar{\Phi}$  for each of the three locations are presented in Figure 8.1. The figure is a grouped bar chart, with a group of bars for each of the model inputs. Within each group a bar exists that represents  $S_i^T$  for the specified location, ordered from left to right for the Control, North, and South input locations. For example, the total-effect index for  $LW(6)$  was approximately 40% for the Control and 75% for the North input. The error bars provide the 90% confidence levels for each index. In all cases,  $k(2)$  and  $c_p(3)$  were irrelevant to the

mass-flux at the snow surface. The North results demonstrated the most dramatic results, where  $LW(6)$  dominated the other factors and all of the contributing factors interacted with each other.

Table 8.2 includes the first-, second-, and higher-order as well as the total-effect sensitivity indices computed for  $\bar{\Phi}$  from the Control/ $\bar{\Phi}$  results. The second-order interactions included  $\rho(1)$  interacting with  $T_s^{int}(4)$  and  $V_w(9)$ ; both of these interactions were of similar magnitude to the first-order index, indicating that the interaction of these parameters interacting was as important as  $\rho(1)$  itself. A similar relationship existed between  $T_a(10)$  and  $RH(11)$ . The first-order indices for these parameters were approximately 9.0% and 10.7%, respectively, and the second-order index  $S_{10,11} \approx 7.9\%$ . The similarity of these values also indicated that the interaction of these two parameters was as important as either parameter individually.

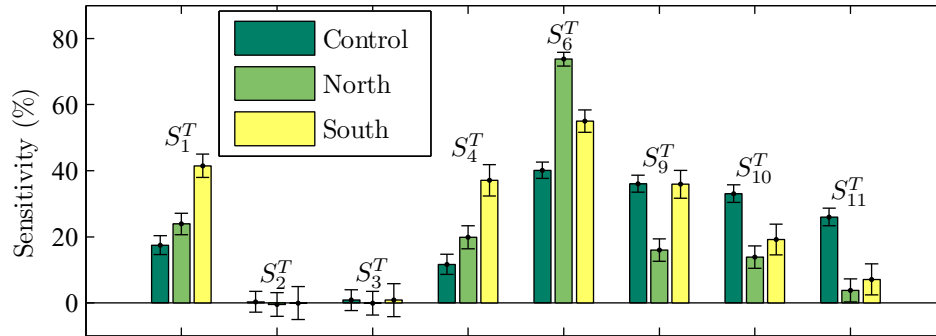


Figure 8.1: Total-effect indices for  $\bar{\Phi}$  for each of the three locations considered, see Table 8.1 for reference.

The second-order interactions of the parameters observed in the Control/ $\bar{\Phi}$  results were nearly non-existent when the North and South inputs were considered. In fact, only the interaction of  $\rho(1)$  with the  $T_s^{int}(4)$  ( $S_{1,4}$ ) was non-zero:  $4.5\% \leq S_{1,4} \leq 8.6\%$  and  $4.1\% \leq S_{1,4} \leq 9.4\%$  for the North and South, respectively. However, the results from all locations included significant higher-order interactions, see the tables provided in Appendix E for the specific values.

Table 8.2: Table summarizing the sensitivity analysis parameters (in percent) for the Control location calculated from  $\bar{\Phi}$ . The *italic* ranges indicate the confidence levels of each parameter; the first-order indices ( $S_i$ ) are along the diagonal, the second-order indices ( $S_{i,j}$ ) are on the off-diagonal (e.g.,  $S_{1,2} = 0.6$ ), the total-effects ( $S_i^T$ ) are listed in the bottom row, and the higher-order interactions ( $S_h$ ) in the row labeled “Higher.”

i \ j	1	2	3	4	6	9	10	11
1	1.7 <i>0.8-2.5</i>	0.6 <i>-0.8-2.1</i>	0.6 <i>-0.8-2.1</i>	2.3 <i>0.8-3.7</i>	0.2 <i>-1.7-2.2</i>	1.6 <i>0.1-3.0</i>	0.3 <i>-1.3-1.9</i>	0.9 <i>-0.6-2.5</i>
2	0.6 <i>-0.8-2.1</i>	0.1 <i>0.0-0.2</i>	-0.2 <i>-0.4-0.0</i>	-0.1 <i>-0.3-0.1</i>	-0.2 <i>-1.2-0.8</i>	-0.5 <i>-1.1-0.1</i>	-0.3 <i>-0.7-0.1</i>	0.0 <i>-0.4-0.4</i>
3	0.6 <i>-0.8-2.1</i>	-0.2 <i>-0.4-0.0</i>	0.0 <i>-0.1-0.2</i>	-0.1 <i>-0.4-0.3</i>	-0.2 <i>-1.2-0.8</i>	-0.4 <i>-1.0-0.2</i>	-0.3 <i>-0.7-0.2</i>	-0.0 <i>-0.5-0.4</i>
4	2.3 <i>0.8-3.7</i>	-0.1 <i>-0.3-0.1</i>	-0.1 <i>-0.4-0.3</i>	-0.3 <i>-1.0-0.5</i>	0.2 <i>-1.6-1.9</i>	0.2 <i>-1.1-1.5</i>	0.4 <i>-1.1-1.9</i>	0.4 <i>-1.0-1.9</i>
6	0.2 <i>-1.7-2.2</i>	-0.2 <i>-1.2-0.8</i>	-0.2 <i>-1.2-0.8</i>	0.2 <i>-1.6-1.9</i>	24.6 <i>23.2-26.0</i>	3.0 <i>0.7-5.3</i>	2.2 <i>0.1-4.3</i>	-0.1 <i>-2.0-1.8</i>
9	1.6 <i>0.1-3.0</i>	-0.5 <i>-1.1-0.1</i>	-0.4 <i>-1.0-0.2</i>	0.2 <i>-1.1-1.5</i>	3.0 <i>0.7-5.3</i>	11.5 <i>10.3-12.6</i>	1.6 <i>0.2-2.9</i>	4.2 <i>2.9-5.5</i>
10	0.3 <i>-1.3-1.9</i>	-0.3 <i>-0.7-0.1</i>	-0.3 <i>-0.7-0.2</i>	0.4 <i>-1.1-1.9</i>	2.2 <i>0.1-4.3</i>	1.6 <i>0.2-2.9</i>	9.0 <i>7.7-10.3</i>	7.9 <i>5.6-10.3</i>
11	0.9 <i>-0.6-2.5</i>	0.0 <i>-0.4-0.4</i>	-0.0 <i>-0.5-0.4</i>	0.4 <i>-1.0-1.9</i>	-0.1 <i>-2.0-1.8</i>	4.2 <i>2.9-5.5</i>	7.9 <i>5.6-10.3</i>	10.7 <i>9.7-11.8</i>
Higher	9.2	1.0	1.4	8.7	10.5	14.9	12.3	1.9
Total	17.5 <i>14.6-20.3</i>	0.3 <i>-2.8-3.5</i>	0.9 <i>-2.3-4.0</i>	11.6 <i>8.6-14.7</i>	40.1 <i>37.7-42.6</i>	36.1 <i>33.5-38.6</i>	33.1 <i>30.4-35.8</i>	26.0 <i>23.4-28.7</i>

An interesting result was evident in the behavior of the  $RH(11)$ . As shown in Figure 8.1,  $RH(11)$  was only significant for the Control/ $\bar{\Phi}$  data. Therefore, relative humidity at the North- and South-facing location had little effect on mass-flux, at least with respect to the model used here and  $\bar{\Phi}$ . This result may find reason in the range of relative humidity recorded in the field, which was typically between 40% and 80%; refer to Figure 7.1f (p.167). Field observations (see Chapter 3) at the same locations demonstrated that surface hoar formed with relative humidities across this entire range.

### 8.3.2 Minimum and Maximum Mass-flux ( $\Phi^{min}$ and $\Phi^{max}$ )

The sensitivity analysis results based on the minimum and maximum mass-flux over the 10-hours simulation provided information regarding the dominant direction

of mass-flux. The results of the  $\Phi^{min}$  analysis are presented in Figure 8.2a. When compared, the  $\bar{\Phi}$  and  $\Phi^{min}$  results were similar. For example, statistically speaking the value of  $S_6^T$  ( $LW$ ) did not differ between the mean and minimum results for all three locations (see Appendix E). This behavior was not observed when comparing  $\bar{\Phi}$  and  $\Phi^{min}$ .

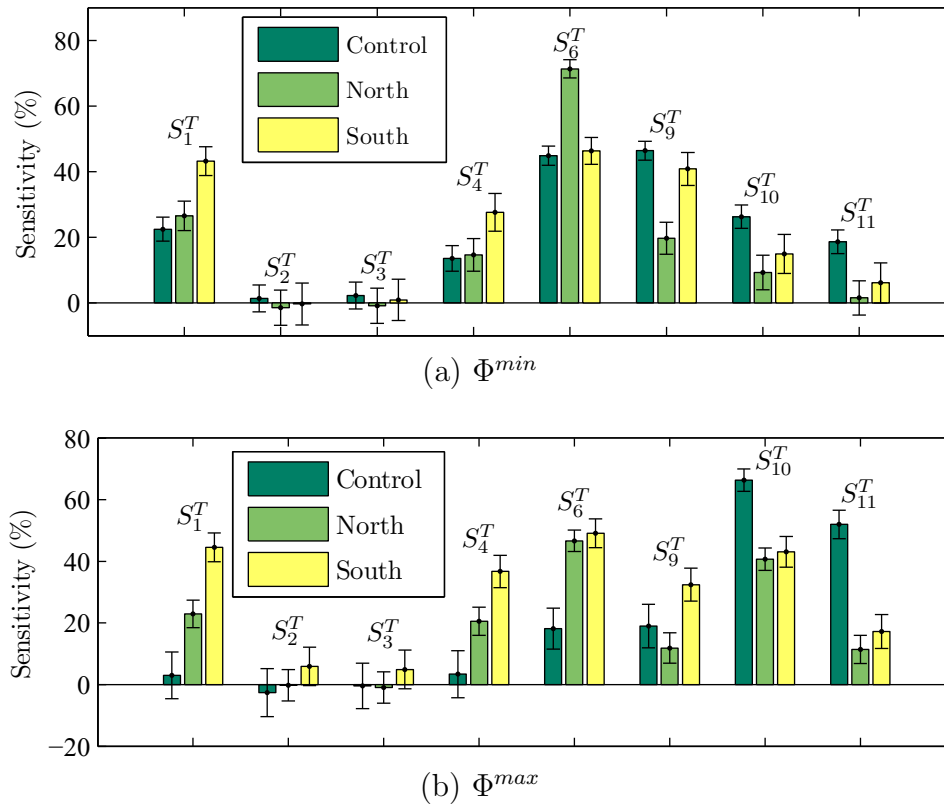


Figure 8.2: Total-effect indices for (a)  $\Phi^{min}$  and (b)  $\Phi^{max}$  for each of the three locations considered (see Table 8.1 for reference).

The  $\Phi^{min}$  results (Figure 8.2b) show a diminished importance of  $LW$  (6) and  $V_w$  (9) and increased importance of  $T_a$  (10) and  $RH$  (11) of the Control location. For the Control/ $\Phi^{min}$  results,  $T_a$  (10) and  $RH$  (11) overshadowed all other inputs. The difference between the  $\Phi^{min}$  and  $\bar{\Phi}$  results likely indicates that negative mass-flux (i.e., smaller values) are dominant. However, making this conclusion definitively is difficult

since the  $\Phi^{min}$  and  $\bar{\Phi}$  output used to compute the result does not distinguish the sign, just the largest or smallest value observed for the model evaluations.

### 8.3.3 Positive and Negative Mean Mass-flux ( $\bar{\Phi}_{pos}$ and $\bar{\Phi}_{neg}$ )

The dominance of negative mass-flux values was confirmed by considering the positive and negative mass-flux results separately; the total-effect results are shown in Figure 8.3. These results did not statistically differ from the minimum and maximum data shown in Figure 8.2, as the confidence levels for all terms overlapped. Making this distinction is critical for applying these results to surface hoar formation, which forms with a mass-flux onto the surface.

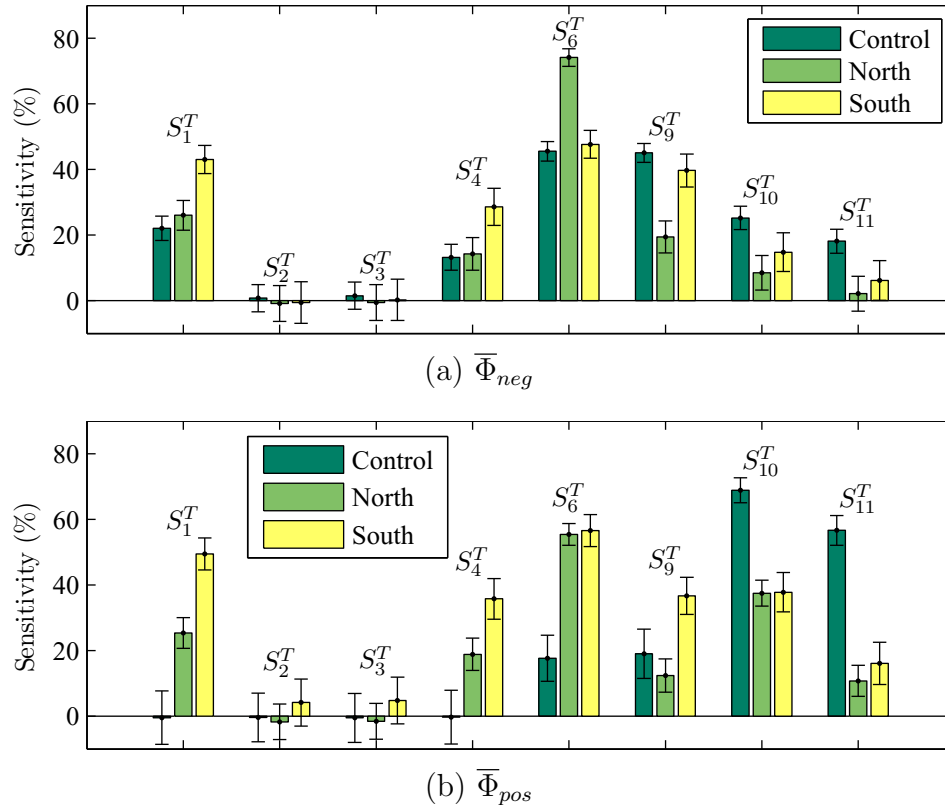


Figure 8.3: Total-effect indices for (a)  $\bar{\Phi}_{neg}$  and (b)  $\bar{\Phi}_{pos}$  for each of the three locations considered (see Table 8.1 for reference).

For the model used here a positive mass-flux was defined as mass being added to the snow surface. Therefore, the use of the  $\bar{\Phi}$  results shown in Figure 8.1 is not appropriate, since the results presented in Figures 8.2 and 8.3 indicate that the negative terms dominate the sensitivity of  $\bar{\Phi}$ . For the remainder of the analysis, the  $\bar{\Phi}_{pos}$  results will be utilized.

The main objective of the sensitivity analysis was to identify as well as quantify the most important model inputs for surface hoar formation. The results of  $\bar{\Phi}_{pos}$  (Figure 8.3b) indicated that the important factors differ depending on the input location being considered. Also, the total-effect index ( $S_i^T$ ) included interaction terms, so it is important to examine the role these play to truly determine the critical terms. First the Control location was considered for  $\bar{\Phi}_{pos}$ ; An examination of Figure 8.3b indicates that only  $LW(6)$ ,  $V_w(9)$ ,  $T_a(10)$ , and  $RH(11)$  contributed to the variance of the output  $\bar{\Phi}_{pos}$ . As such were the only parameters that must be considered for this location.

Figure 8.4 is a grouped bar chart that differs from the charts already displayed therefore requires some explanation. The groups include four bars, one for each of the parameters listed as important for Control/ $\bar{\Phi}_{pos}$ :  $LW(6)$ ,  $V_w(9)$ ,  $T_a(10)$ , and  $RH(11)$ . If the corresponding bars in each group were summed it would equal the total-effect value provided in 8.3b. The height of the bars provides either the first-, second-, or higher-order index for the parameter associated with the bar. Consider the following example, the left-most bar in each group of four refers to  $LW(6)$ . The first-order index ( $S_6$ ) for this term is located in the sixth group, which is labeled  $S_{6,i}$ . The  $i$  is replaced by the index of the parameter being considered, in this case  $i = 6$ , thus represents  $S_{6,6} = S_6$ —the first-order index of  $LW(6)$ . All other locations in the same group yield the second-order index for this term, e.g., the first column in the  $S_{10,i}$  group represents the interaction of  $LW(6)$  with  $T_a(10)$ , since the  $i$  is replaced with

the corresponding index for the column reference it becomes  $S_{10,6}$ . This is the second-order index representing the second-order interaction of  $LW(6)$  with  $T_a(10)$ . Finally, the higher-order index is provided in the last group labeled  $S_h$ . For  $LW(6)$  this value was near zero. Error bars were excluded from this value because it was computed post-analysis directly from  $S_i^T$ ; as such the error is similar in magnitude from the error associated with the total-effect index.

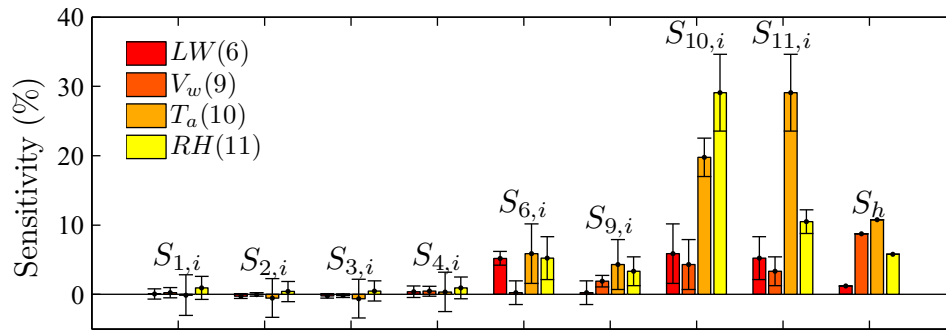


Figure 8.4: First-, second- and higher-order indices for  $\bar{\Phi}_{pos}$  for control location and each of the four important inputs:  $LW(6)$ ,  $V_w(9)$ ,  $T_a(10)$ , and  $RH(11)$  (see Table 8.1 for reference). The higher-order interactions for these terms are provided in the  $S_h$  grouping.

The sensitivity results presented in Figure 8.4 indicate that the most important parameter for causing changes in  $\bar{\Phi}_{pos}$  was the interaction of  $T_a(10)$  and  $RH(11)$ :  $23.6\% \leq S_{10,11} \leq 34.6\%$ . Note, the  $S_{10,11}$  and  $S_{11,10}$  terms are exactly equal. The first-order index,  $T_a(10)$  acting independently, was second in importance:  $17.0\% \leq S_{10} \leq 22.5\%$ . The total of the first- and second-order indices for  $T_a(10)$  and  $RH(11)$  ( $S_{10} + S_{11} + S_{10,11}$ ) is approximately 59.4%. This means that nearly 60% of the variance observed in the output parameter  $\bar{\Phi}_{pos}$  for the Control location was due to changes in these two parameters.

Next, the sensitivity terms for  $\bar{\Phi}_{pos}$  based on the North location were considered in a similar fashion. The total-effect results (shown in Figure 8.3b) indicated that six terms are non-zero:  $\rho(1)$ ,  $T_s^{int}(4)$ ,  $LW(6)$ ,  $V_w(9)$ ,  $T_a(10)$ , and  $RH(11)$ . Each of these



terms was grouped and displayed in Figure 8.5. The North location showed results that differed greatly from those of the Control location. The most dominant term in this case was  $S_6$ , i.e., the effect of  $LW(6)$  acting alone, where  $27.1\% \leq S_6 \leq 31.5\%$ . The next most important term was the effect of  $T_a(1)$  acting alone,  $16.1\% \leq S_{10} \leq 19.3\%$ , followed by the higher-order terms except for  $S_h$  associated with  $RH(11)$ . Also significant was the interaction between  $LW(6)$  and  $T_a(10)$ :  $4.7\% \leq S_{6,10} \leq 11.9\%$ . The significance of the higher-order terms indicated that the North location was more interactive than the Control.

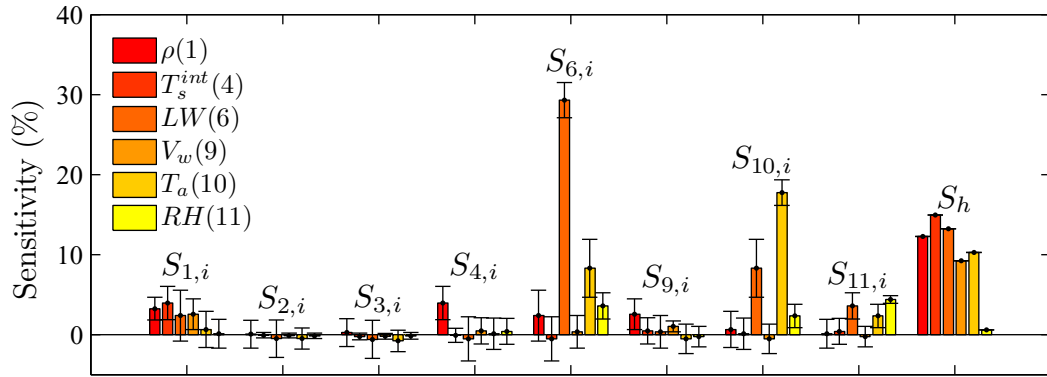


Figure 8.5: First-, second- and higher-order indices for  $\bar{\Phi}_{pos}$  for North location and each of the four important inputs:  $\rho(1)$ ,  $T_s^{int}(4)$ ,  $LW(6)$ ,  $V_w(9)$ ,  $T_a(10)$ , and  $RH(11)$  (see Table 8.1 for reference). The higher-order interactions for these terms are provided in the  $S_h$  grouping.

Despite the larger role of interactions, a majority of the variance observed in the North/ $\bar{\Phi}$  results may be attributed to only two parameters:  $LW(6)$  and  $T_a(10)$ . If the mean values of the first- and second-order terms are considered ( $S_6 + S_{10} + S_{6,10}$ ), 55.3% of the variance is accounted for by these two parameters alone. And, if the higher-order terms are included then it may be stated that approximately 79% of the variance of  $\bar{\Phi}$  is in some way attributed to changes in  $LW(6)$  and  $T_a(10)$  for the North location.

The total-effect results from the south/ $\bar{\Phi}_{pos}$  shown in Figure 8.3b indicate that the same six terms as the south/ $\bar{\Phi}_{pos}$  data were non-zero:  $\rho(1)$ ,  $T_s^{int}(4)$ ,  $LW(6)$ ,  $V_w(9)$ ,  $T_a(10)$ , and  $RH(11)$ . However, as shown in Figure 8.6, the sensitivity results differ. For the South location, mass-flux is highly interactive, since the higher-order terms dominate. Only the first-order index for  $LW(6)$  ( $18.8\% \leq S_6 \leq 24.0\%$ ) was on the same scale as the higher-order terms, with the exception of  $RH(11)$ . The highly interactive results shown here indicated that only in certain situations, when many terms work together, were the conditions able to influence the positive mass-flux output.

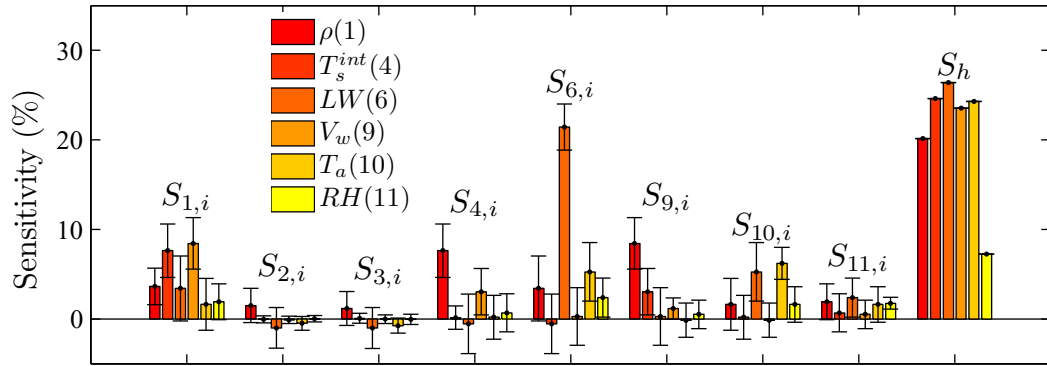


Figure 8.6: First-, second- and higher-order indices for  $\bar{\Phi}_{pos}$  for South location and each of the six important inputs:  $\rho(1)$ ,  $T_s^{int}(4)$ ,  $LW(6)$ ,  $V_w(9)$ ,  $T_a(10)$ , and  $RH(11)$  (see Table 8.1 for reference). The higher-order interactions for these terms are provided in the  $S_h$  grouping.

#### 8.4 Discussion: Sensitivity Analysis

The sensitivity analysis presented in the previous section demonstrated that at all locations four parameters— $LW(6)$ ,  $V_w(9)$ ,  $T_a(10)$ , and  $RH(11)$ —were important to positive values of mass-flux at the snow surface. The results from South/ $\bar{\Phi}_{pos}$  were shown to be highly interactive. As such specific critical parameters were difficult to

identify and therefore these results were not considered here. The North/ $\bar{\Phi}_{pos}$  data also indicated that both  $\rho(1)$  and  $T_s^{int}(4)$  influenced  $\bar{\Phi}_{pos}$  to some respect. Examining the mean values of the sensitivity indices indicated that only 7.7% of the variance of  $\bar{\Phi}_{pos}$  may be attributed to these terms alone ( $S_1$ ,  $S_4$ , and  $S_{1,4}$ ). Due to this relatively small influence, these terms were assumed to be secondary influences. Therefore, the sensitivity analysis indicated that  $\bar{\Phi}_{pos}$  may be approximated as a function of four terms:  $\bar{\Phi}_{pos} \approx f(LW, V_w, T_a, RH)$ . Through the use of a dimensionless parameter  $\Pi$ , defined as

$$\Pi = \frac{-V_w^2}{C_{p,air} T_a} \cdot RH, \quad (8.2)$$

the five-dimensional function is re-written as  $\bar{\Phi}_{pos} \approx f(LW, \Pi)$ .

The relationship in Equation 8.2 is analogous the Eckert number ( $Ec$ ), which is defined as  $Ec = \frac{U^2}{c_p T_0}$  and is important for dissipation problems, where  $U$  is the free-stream velocity,  $T_0$  the fluid reference temperature (White, 1999, 2006),  $c_p$  the specific heat of the fluid. The fluid for the problem at hand is air, thus the specific heat of air is assumed to be a constant of 1001 kJ/(kg°K)(Armstrong and Brun, 2008). The negative sign is applied such that the result becomes positive (this is discussed further in Section 8.5). The appearance of the Eckert number is reasonable, since dissipation is defined as a system losing energy resulting in heat generation due to friction or turbulence—a process that is likely occurring at the snow surface to some extent. Hence, the dimensionless term in Equation 8.2 is analogous to  $Ec \cdot RH$ , but not equal to this parameter, since the thermal model is simplistic and assumes nothing regarding a boundary layer. The velocity ( $V_w$ ) and temperature ( $T_a$ ) discussed throughout this chapter were assumed to act precisely at the snow surface. Finally,  $RH$ —being a dimensionless term itself—is simply applied to make the mass-flux relationship as a function of two variables.

### 8.5 Results and Discussion: Monte Carlo Simulations

Before delving into the Monte Carlo simulation results, two problems with relating surface hoar formation to  $\bar{\Phi}_{pos}$  must be addressed. The issues are rooted in how  $\bar{\Phi}_{pos}$  is computed from Equation (8.1) on page 177. The basic premise of the problem is that  $\bar{\Phi}_{pos}$  alone does not lead to surface hoar formation, other conditions must be satisfied, namely the wind speed and air temperature.

In the latent heat equation,  $V_w(9)$  is a simple linear relationship, thus the higher the wind speed, when the air temperature is warmer than the snow, the higher the mass-flux to the snow. With respect to surface hoar formation this behavior is not accurate; surface hoar formation becomes inhibited by the high wind (Colbeck, 1988). However, the wind speeds used here were limited to 4 m/s, which is within the realm observed by other researchers (see Chapter 2). So, this problem was assumed to be irrelevant for the results presented here.

The second problem that must be addressed is that of air temperature, which may be as high as 10 °C. The thermal model simply returns a mass-flux and says nothing of the phase. Based on the literature reviewed in Chapter 2, when air temperature is above freezing surface hoar would likely not form, even though the mass-flux is well within the range defined previously. To account for this problem, an assumption was made that surface hoar only forms with below-freezing air temperatures. Therefore, a negative value assigned to the  $\Pi$ -term of Equation 8.2 will always result in a positive quantity.

Knowing that  $\bar{\Phi}_{pos}$  is a function of two parameters— $LW(6)$  and  $\Pi$ —it was possible to separate the inputs that lead to a specific output through the use of Monte Carlo simulations. For the results presented in this section, only the inputs from the Monte Carlo simulations resulting in a positive mass-flux onto the snow surface over a range

from  $1.5 \times 10^{-4}$ – $3.0 \times 10^{-3}$  gm/(m<sup>2</sup>s) were considered. This range was defined by a mass-flux known to be reasonable for surface hoar formation based on recorded data published by Feick *et al.* (2007) that reported average mass-flux rates of  $1.3 \times 10^{-3}$  gm/(m<sup>2</sup>s) over a 24-hour period resulting in approximately 1 cm surface hoar. For comparison, Hachikubo and Akitaya (1997) reported mass-flux values of similar magnitude. Using this value, the time frame was shifted to 10 hours and surface hoar from 0.5–10 mm was assumed possible. This yielded the range of mass-flux defined. The size of the surface hoar considered here was consistent with the sizes observed in the field events discussed in Chapter 4, which are used in the following section. The mass-flux limited as such is defined referred to as  $\bar{\Phi}_{SH}$  herein.

As mentioned previously, for the analysis presented here  $T_a(10)$  was limited to sub-freezing values. Making this assumption reduced the number of simulations being assessed from 180,000 to 135,333, 179,028, and 177,172 for the Control, North, and South locations respectively. From these data sets, the 95% highest density region (HDR) was computed for each location. These regions surround the data such that 95% is contained within the area traced. Chapter 7 Section 7.6 provides details regarding HDRs.

An HDR comparison between the locations of all possible values of  $LW(6)$  and  $\Pi$  with  $T_a > 0$  is included in Figure 8.7a. Limiting mass-flux to the range previously defined resulted in Figure 8.7b. These regions are composed of 10.0%, 35.0%, and 17.6% of the simulations considered for the Control, North, and South locations, respectively.

The simulations shown in Figure 8.7b indicate that in the most general case, based on the Control location  $LW(6)$  ranges from approximately 100–400 W/m<sup>2</sup> and  $\Pi$  ranges from approximately  $10^{-4}$ – $10^0$ . However at both the North and South locations, the ranges of  $LW(6)$  is reduced to 200–300 W/m<sup>2</sup> and  $10^{-3}$ – $10^0$ , respectively.

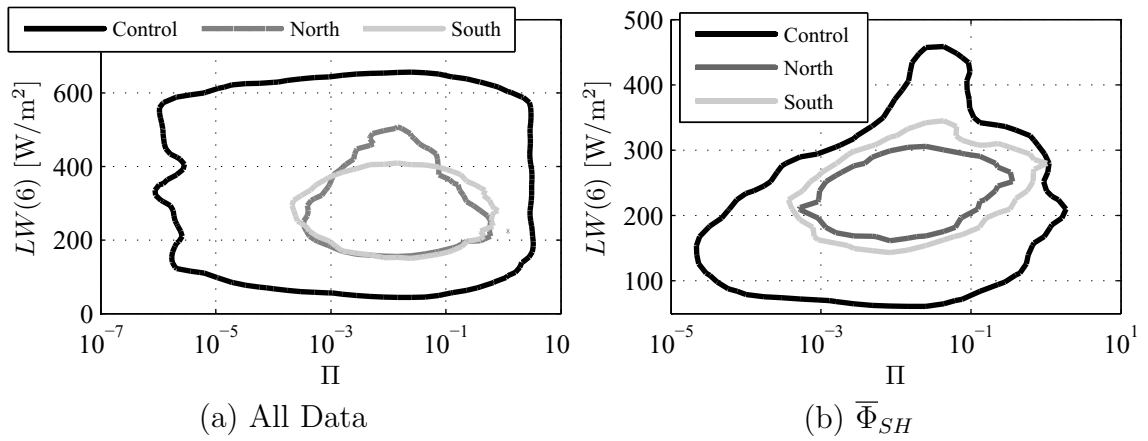


Figure 8.7: Highest density regions (95%) comparing Monte Carlo simulation results for  $LW(6)$  and  $\Pi$  for (a) all values with  $T_a < 0$  and (b)  $\bar{\Phi}_{SH}$ .

This difference may be attributed to the differences in the input distributions; values of less than  $200 \text{ W/m}^2$  are improbable (see Chapter 7 Section 7.2). Comparing these results with the entire data set presented in Figure 8.7a showed that the values of  $LW(6)$  and  $\Pi$  for  $\bar{\Phi}_{SH}$  were concentrated to a region in the lower-right corner.

All the Monte Carlo simulations were compared with the  $\bar{\Phi}_{SH}$  simulations for each location in Figure 8.8. Aspect seemed to have a minimal affect on the regions, which should be expected since the conditions at night should be similar irrespective of aspect: short-wave radiation is not contributing. The similarity of the North and South input data sets was evident in Figure 7.1 (p. 167) of Chapter 7. Despite the similarities in the input distributions, the number of data points resulting in each region differs by about 50%; the South location is composed of about one-half the number of points as the North location. This difference, along with the vastly different and interactive results obtained from the sensitivity analysis, make drawing specific conclusions on the regions difficult.

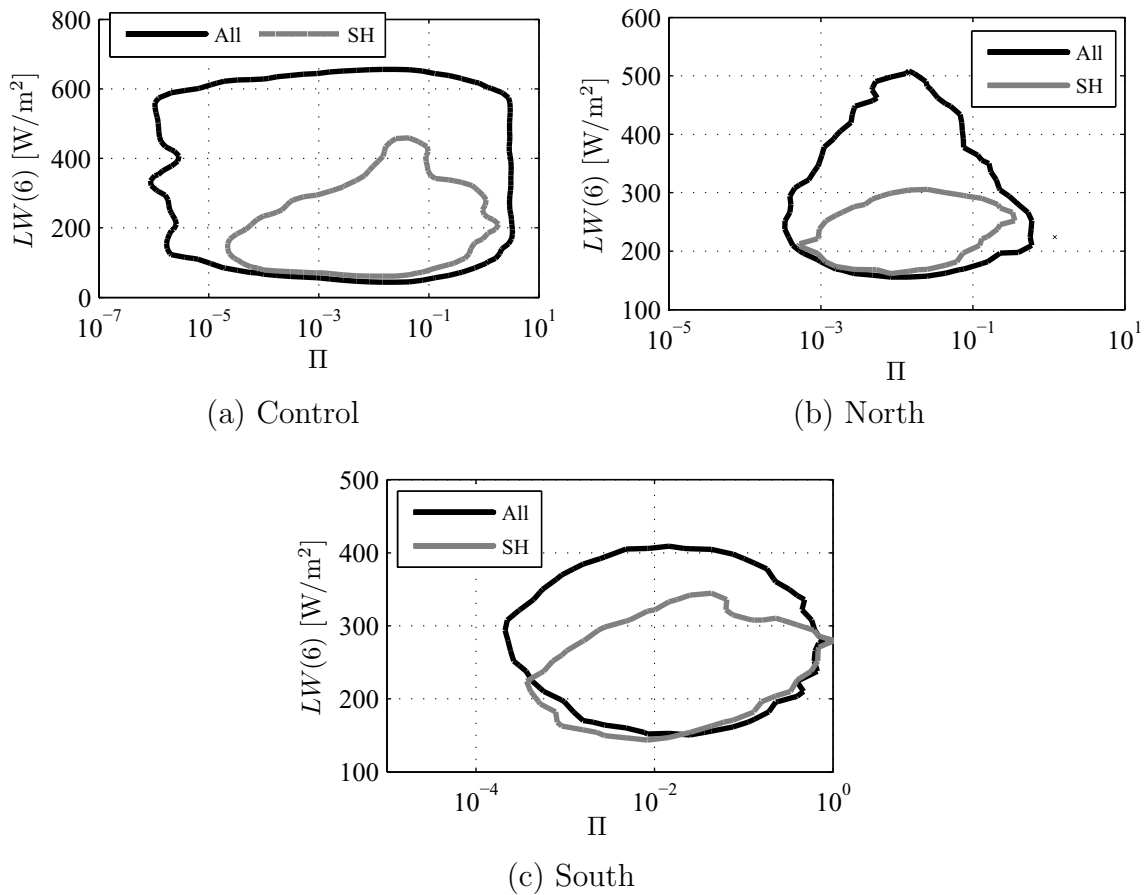


Figure 8.8: Highest density regions (95%) comparing the complete set (All) of Monte Carlo simulation results to the data limited to surface hoar formation (SH) for the (a) Control, (b) North, and (c) South locations.

### 8.6 Analysis: Comparison with Field Observations

The sensitivity analysis (Section 8.3) defined the critical parameters governing mass-flux onto the snow surface, while the Monte Carlo simulations (Section 8.5) provided a means for identifying values of these parameters that may be conducive to surface hoar formation. In this section, the Monte Carlo simulation results are compared with observed events.

Chapter 3 details 14 surface hoar events that occurred on the North- and South-facing slopes—the same locations that the weather station data utilized for the numerical examination presented in this chapter was collected. Based on the weather data recorded, as well as the field notes describing the surface hoar crystals, values for crystal size were determined. Table 8.3 includes the average crystal size as well as  $LW(6)$  and  $\Pi$  for each event. In total, 23 observations were made: 15 at the North Station and 8 at the South Station. The average crystal size observed ranged from 0.5–8 mm. The mass-flux rate of  $0.0015 \text{ gm}/(\text{m}^2\text{s})$  defined in the previous section results in a 0.5 cm crystal in 10 hours.

Event	North			South		
	Size (mm)	$LW$ $\text{W}/\text{m}^2$	$\Pi$	Size (mm)	$LW$ $\text{W}/\text{m}^2$	$\Pi$
A-1	2–3	252	5.87E-03	1–2	354	6.87E-03
A-2	0.5	225	9.13E-03			
A-3a	0.5	217	1.58E-02	1	376	2.07E-02
A-3b				0.5	417	5.02E-02
A-4	1–2	206	1.51E-02	0.5–1	371	9.93E-03
A-5	4–8	274	1.18E-02	2–4	277	7.55E-03
A-6	1	206	1.01E-02	1	369	1.57E-02
A-7	1	199	8.96E-03	<0.5	267	5.57E-03
B-1	0.5–4	263	4.08E-03			
B-2a	0.5	226	2.80E-02			
B-2b	2–4	210	1.79E-02			
B-3	5	202	1.85E-02			
B-4b				1	190	1.06E-02
B-5a	1	188	9.43E-03			
B-5b	1.5	193	7.56E-03			
B-6	1.5	175	8.18E-03			
B-7	0.5–1	317	1.03E-02			

Table 8.3: Summary of crystal size, long-wave radiation ( $LW$ ), and  $\Pi$  observed surface hoar events at the North and South Stations.

The field observations were first compared with the numerical results from the Control location. Figure 8.9 includes HDRs for  $\text{Control}/\bar{\Phi}_{SH}$  results as well as the field observations for both the South- and North-facing weather stations listed in Table 8.3. To some respect the observations fit the regions: 43% (10/23) of the



observations fell within the 50% HDR and all the data points were within the 99% HDR. The later results was particularly interesting considering the 99% HDR contains an abnormality that the encompassed five points that may otherwise have not fit in the region. On the other hand, 26% (6/23) of the data points fell outside the 90% HDR, where only two or three should have been in this region. The discrepancy between the observations and numerical results was likely caused by two factors:

1. Very small values of  $\Pi$  (on the order of  $10^{-3}$  or less) resulted due to decimal values of  $V_w(9)$  that were raised to the second power and to a lesser extent large values of  $\Pi$  resulted from similarly small decimal values of  $T_a(10)$ .
2. The observations of surface hoar were limited by the conditions observed in the field.

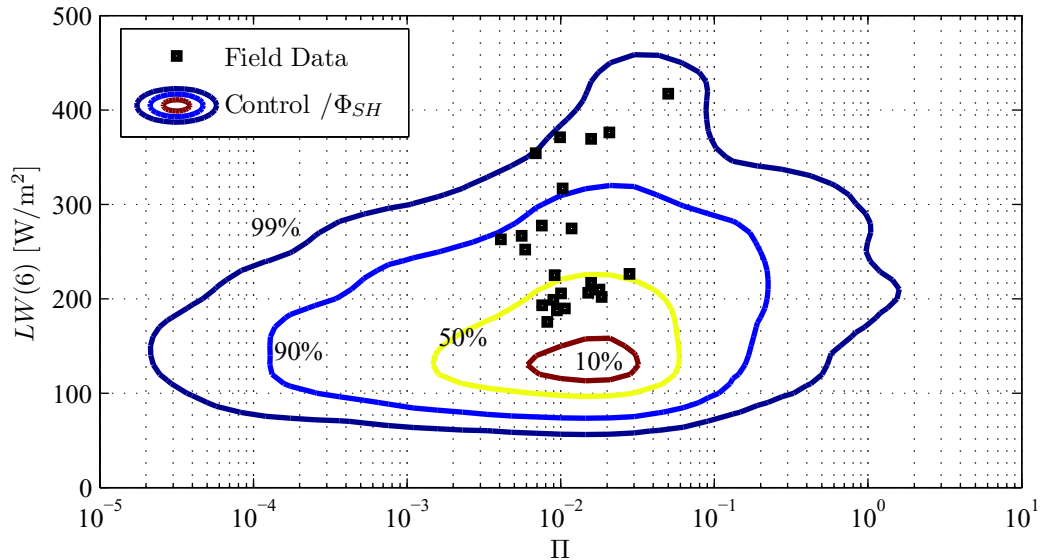


Figure 8.9: Comparison of  $\text{Control}/\bar{\Phi}_{SH}$  highest density regions with field observations from the North- and South-facing stations.

To account for the first of the two problems defined, two adjustments to the numerical data were made. First, Figure 8.10 must be introduced. This figure includes

two sets of HDRs. The first set was generated from the Monte Carlo simulations as discussed above. The second set was generated from daily means from the entire weather data set—the same data used to generate the location-specific input distributions, as detailed in Section 7.2. Two restrictions to the Monte Carlo simulation data were implemented to minimize the small-number issues introduced:  $V_w(9)$  was limited to values greater than 0.25 m/s and  $T_a(10)$  to values less than  $-0.1$  °C. These values were selected such that the extent of the  $\Pi$  values in Figure 8.10 were approximately the same magnitude for the two region sets displayed. These adjustments are included in the following analysis.

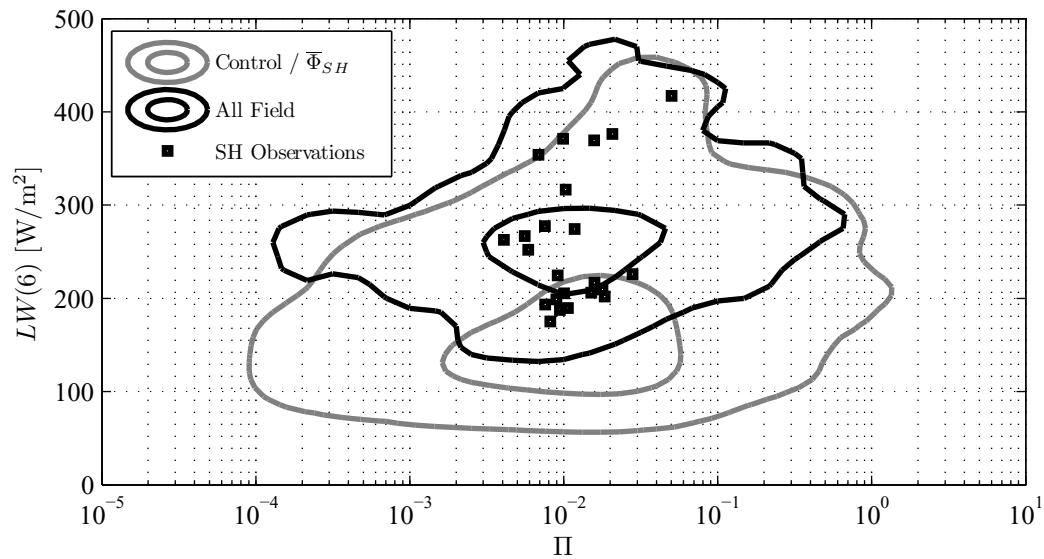


Figure 8.10: Comparison of 99% (outer) and 50% (inner) HDRs for the Control/ $\bar{\Phi}_{SH}$  results and all recorded field data with the field observations from the North- and South-facing stations.

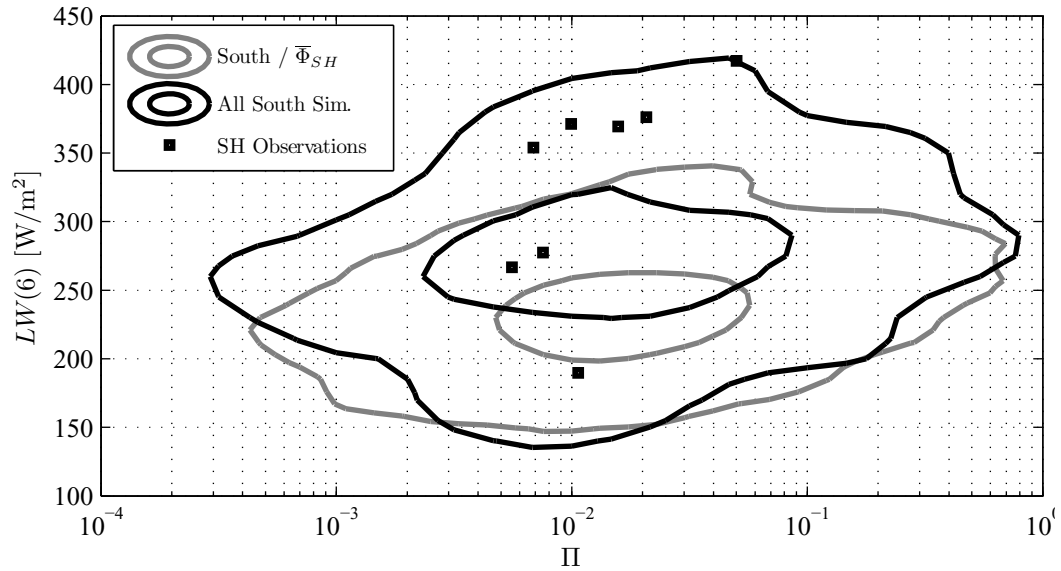
The Control results yielded promising results. Referring to Figure 8.10, all of the observed surface hoar events fell within the 99% HDR from the field data. Although, if the observed events were a purely randomly selected subset, half of the points would lie inside the 50% HDR, but only 30% (7/23) were within this region. So, it is

reasonable to state that the observed surface hoar events were not a random sample of the complete data set. Next, if the observed surface hoar events were a sample from the numerically generated data, then half of the points would lie within the 50% HDR of the Control/ $\bar{\Phi}_{SH}$  results. As stated earlier, 10 of the 23 events (43%) were within this region; this is promising considering a major portion of this 50% HDR is outside the conditions attainable in the field on any given day.

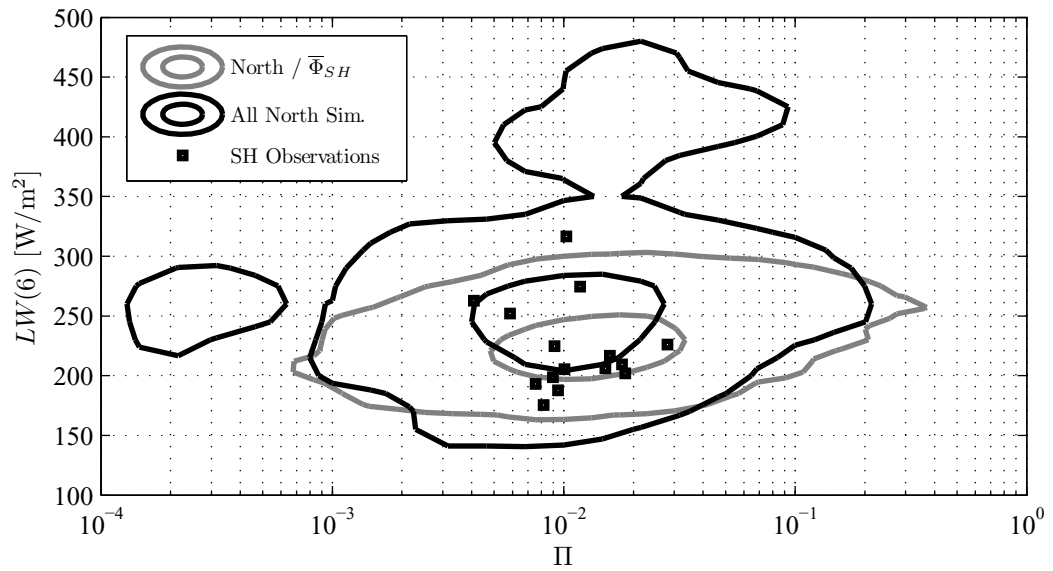
A similar analysis was performed for the North and South locations exclusively, as shown in Figure 8.11, but the HDRs were limited to the numerical Monte Carlo simulations results only. Hence, the North/ $\bar{\Phi}_{SH}$  and South/ $\bar{\Phi}_{SH}$  regions were computed from the data limited to mass-flux rates defined as conducive for surface hoar development. And the regions labeled at “All South Sim.” and “All North Sim.” were developed from all values of the inputs (i.e., not limited). The “Sim.” identifier is added to decipher this data from that of Figure 8.10 that displays regions computed from the measured field data, whereas the regions in 8.11 were computed entirely from simulated data (i.e., “Sim.”).

In Figure 8.11a, the results from the South indicated that the numerical results did not correlate with the observed field data. Due to this lack of correlation, as well as the sensitivity analysis results that yielded little in the way of definitive results, the data from the South was excluded from further analysis.

The most promising results were obtained from the data based on the North-facing station, as shown in Figure 8.11b. First, as expected, all of the observed events were within the field data 99% HDR. Also, only 27% (4/15) of the data was within the 50% HDR of the field data, which indicated that the observed events at the North Station were not a random sample of the complete data set itself. With respect to the numerically generated 50% HDR from the North/ $\bar{\Phi}_{SH}$  results, 53% (8/15) of the observed events were within this region. To illustrate this result further, Figure 8.12



(a) South



(b) North

Figure 8.11: Comparison of 99% (outer) and 50% (inner) HDRs for the  $\bar{\Phi}_{SH}$  results and all recorded field data with the field observations from the (a) South- and (b) North-facing stations.

was generated to compare various HDRs from the numerical results with the observed events.

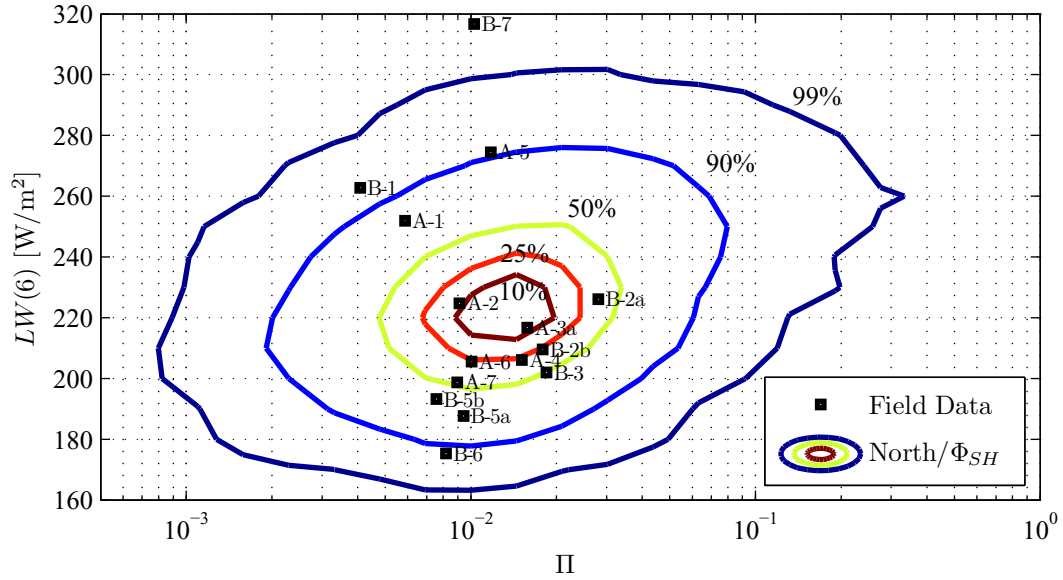


Figure 8.12: Comparison of  $\text{North}/\bar{\Phi}_{SH}$  highest density regions with field observations from the North-facing station.

Comparing the HDRs and observations in Figure 8.12 demonstrated that the observations fit reasonably well within the numerically generated data. For example, 1 of 15 (7%) points were within the 10% HDR, 3 of 15 (20%) were within the 25% HDR, 8 of 15 (53%) were within the 50% HDR, and 14 of 15 (93%) were within the 99% HDR.

This apparent fit was confirmed using the Kolmogorov-Smirnov goodness-of-fit test (KS-test) for both  $LW$  and  $\Pi$ . These KS-tests were performed independently on the two parameters comparing the Monte Carlo simulation data,  $\text{North}/\bar{\Phi}_{SH}$ , with the observed events. The results were  $p$ -values of 0.198 and 0.094, for  $LW(6)$  and  $\Pi$  respectively. The null hypothesis was that the observed events and the Monte Carlo simulation data were from the same distribution. Hence, for both terms, the hypothesis fails to be rejected at the 5% confidence level indicating that the two data sets were likely from the same distribution. Interestingly, the  $\Pi$  data fit better than the  $LW(6)$  data (larger  $p$ -value for  $\Pi$ ), which does not seem to be the case visually.

However, the B-7 event likely caused this result for the  $LW(6)$  data since it was well outside the  $North/\overline{\Phi}_{SH}$  data.

Finally, the surface hoar size was examined. Table 8.4 defines four ranges of mass-flux and the expected size of the surface hoar crystal based on the previously defined rate. Figure 8.13 includes 95% HDRs for each of these. Upon examining the size of the observed events reported in Table 8.3 as well as the over lap of the regions, it was obvious that the regions did not correspond to surface hoar size. This figure does however demonstrate the bias in the model towards large values of  $\Pi$  for large mass-flux values. This bias was likely, as previously discussed, due to the nature of the latent heat equation utilized that unequivocally increased as wind velocity and air temperature increased. This result confirmed that mass-flux alone is insufficient for predicting the size of surface hoar formation.

Since surface hoar size and mass-flux were uncorrelated in Figure 8.13, a KS-test was performed in similar fashion as done previously for the  $North/\Phi_{SH}$ , but here the field data was compared to all positive values of mass-flux for the North location:  $North/\Phi > 0$ . The goodness-of-fit results obtained in this differed significantly from the  $North/\Phi_{SH}$  results. In the case of  $LW(6)$  the fit actually improved significantly ( $p = 0.84$ ), but the  $\Pi$  goodness-of-fit decreased markedly ( $p \approx 0$ ). Therefore, with respect to  $\Pi$  simply considering a positive mass-flux is not appropriate. So, Figures 8.9 and 8.12 may be the best tools for determining if a positive mass-flux exists conducive to surface hoar formation.

Table 8.4: Regions of mass-flux and expected surface hoar crystal size.

Mass-flux rate $10^{-3}\text{gm}/(\text{m}^2\text{s})$	Crystal size
0–0.15	<0.5 mm
0.15–3	0.5–10 mm
3–6	1–2 cm
6–30	2–10 cm

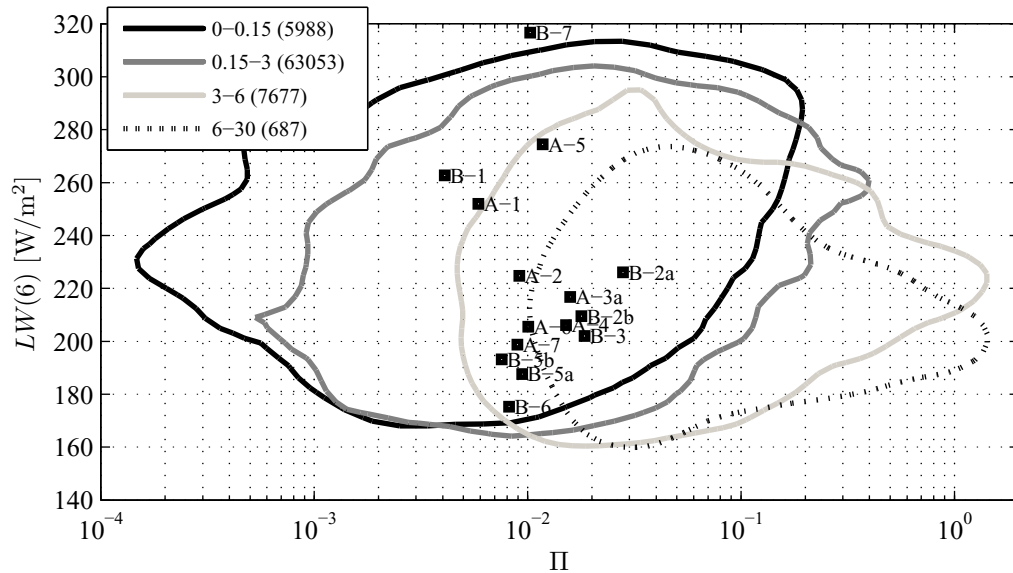


Figure 8.13: Highest density regions based on the North location and various mass-flux rates.

### 8.7 Closing Remarks

Using SOBOL sensitivity analysis, four parameters—incoming long-wave radiation, air temperature, wind velocity, and relative humidity—were defined to be the most important based on their effect on mass-flux rate at the snow surface. An input data set composed of conditions that varied uniformly demonstrated that air temperature and relative humidity were the most important, with long-wave radiation and wind velocity playing a secondary role. However, data sets derived from measured data indicated the long-wave radiation was the most important parameter, accounting for 20–30% of the total variance observed in mass-flux by itself. When interactions were considered, approximately 60% of the mass-flux observed was in some way related to incoming long-wave radiation. This finding may be the most significant finding to result from the work presented in this chapter. To the author’s knowledge previous field studies—excluding the data presented in Chapter 4—typically neglect

to consider incoming long-wave radiation, but this study indicates that such data may be vital for identifying the conditions leading to surface hoar development.

The shortfall of this study lies in trying to relate surface hoar formation to mass-flux rates. Thus, the results obtained which indicated that incoming long-wave radiation is a critical parameter was limited by the use of mass-flux as the indicator variable. The Monte Carlo simulation data demonstrated that mass-flux alone was insufficient for predicting surface hoar.

In Section 8.6 the results from the Monte Carlo simulations were explored and compared with observed surface hoar events. The results indicated, based on the model evaluation presented here, that mass-flux was insufficient for predicting surface hoar particularly in characterizing the size of the surface hoar. Out of the three data sets explored—Control, South, and North—the North input set resulted in the best correlation. However, this correlation was limited strictly to the presence of a positive mass-flux. As such, Figures 8.9 and 8.12 were presented as possible tools for assessing if a positive mass-flux exists that would be conducive to surface hoar formation. Based on this data, long-wave radiation of 100–200 W/m<sup>2</sup> and a value of  $\Pi$  from  $10^{-2.9}$ – $10^{-1.5}$  may be considered the optimum conditions for positive mass-flux to occur, which is necessary of surface hoar formation. This range was defined from a 50% HDR of the most general case (the Control location). If the North location is used this range narrows to long-wave of 200–250 W/m<sup>2</sup> and  $\Pi$  from  $10^{2.5}$ – $10^{-1.7}$  (see Figure 8.12). These charts demonstrate the ultimate goal for the work presented throughout this chapter: to develop a methodology for assessing surface hoar formation based on modeled data that may then be applied spatially via the RadTherm/RT software package. The results presented here require additional validation for such application, but are a stepping stone to this end.



The work presented shows the potential for sensitivity analysis, Monte Carlo simulations, and similar numerical methods to aid in exploring the behavior of the snowpack to an extent not possible with laboratory or field experimentation alone. But, in the case of surface hoar formation, the application of these methods is restricted by the limited knowledge that exists of surface hoar formation on the micro-structural and micro-meteorological scale. This knowledge is critical for taking the next step in spatial modeling.

## CHAPTER 9

## SENSITIVITY ANALYSIS OF NEAR-SURFACE FACETS

9.1 Introduction

Faceted snow crystals form at or near the snow surface due to temperature gradients that are induced by a variety of sources including diurnal temperature changes, melt-layers, and solar radiation (Fukuzawa and Akitaya, 1993; Hardy *et al.*, 2001; Morstad *et al.*, 2007; Slaughter *et al.*, 2009). However, the specific environmental conditions required to form near-surface facets are not well understood. A review of the literature investigating these conditions is presented in Chapter 2.

The research presented in this chapter used a numerical methodology to expand the knowledge surrounding the formation of near-surface facets, particularly focused on the process of radiation-recrystallization. The main objective was to quantify the most critical environmental and snow micro-structure parameters that lead to near-surface metamorphism, which was accomplished using variance-based sensitivity analysis. The data presented sets the stage for Chapter 10 that further quantified—through the use of Monte Carlo simulations—the specific conditions necessary for facet formations.

9.2 Methods

This chapter employed the variance-based sensitivity analysis method of SOBOL (Saltelli, 2002), which was summarized in Section 7.4 and described in detail in Chapter 6. The input parameters used in this chapter are defined in Table 7.1, which includes the index (*i*), symbol (Sym.), and description that are used for referencing

the inputs. The short-wave radiation input ( $SW(7)$ ) was assumed to vary temporally according to a sine-wave (see Section 7.3).

For this analysis three input data sets were considered based on the “location” from which the distributions were developed: Control, South, and North. The development of these data sets was explained in Section 7.2. For each location, nine different output “classes” were considered:

- the snow temperature at the surface, 2, 5, and 8 cm deep ( $T_0$ ,  $T_2$ ,  $T_5$ , and  $T_8$  respectively);
- the snow temperature at the depth of the “knee” temperature gradient ( $TK$ );
- the temperature gradient between the snow surface and 2, 5, and 8 cm deep ( $TG_2$ ,  $TG_5$ , and  $TG_8$  respectively); and
- a “knee” temperature gradient ( $KTG$ ).

The “knee” related outputs were defined according to the temperature profile that is characteristic of solar penetration and surface radiative cooling (Figure 9.1), which is typically associated with radiation-recrystallization. In this case, the gradient was calculated between the surface and the inflection point. If the “knee” shape was not present a value of zero was assigned to the output, otherwise the magnitude of the gradient was utilized.

For each class mentioned above various model output calculations were performed. These various outputs of the thermal model were used in the SOBOL sensitivity analyses. First, a sensitivity analysis was performed temporally at 20 minute intervals for each of the classes mentioned, resulting in 30 sets of indices for each class. Next, the temporal data from the thermal model was reduced to a single output in the

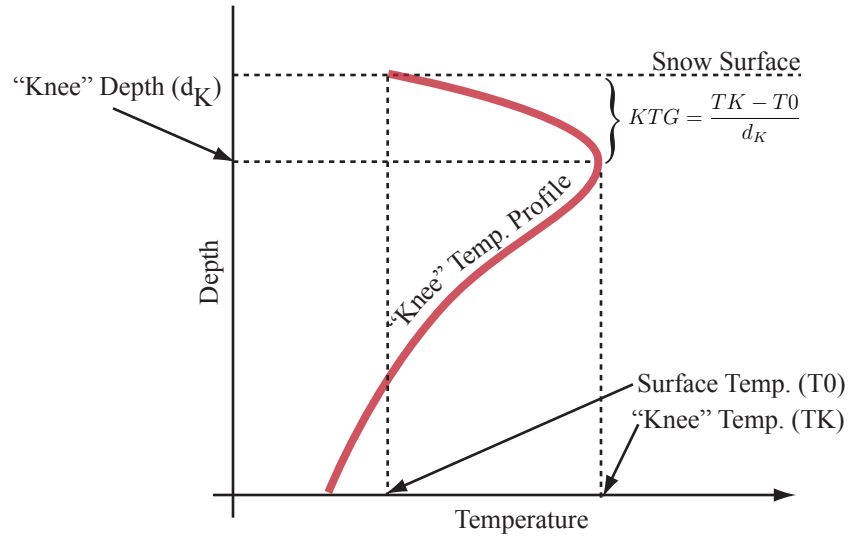


Figure 9.1: Schematic of “knee” temperature profile and related sensitivity analysis output parameters.

form of the mean, maximum, minimum, and mid-day values from the entire 10-hour simulations. The results from all of these sensitivity analyses are denoted by modifying the class previously defined as:

- The temporal results list the symbols as a function of time, e.g.,  $T0(t)$ .
- The mean results utilizes the bar, e.g.,  $\overline{T0}$ .
- The minimum (min) and maximum (max) for each evaluation and mid-day utilize a superscript, e.g.,  $T0^{min}$ ,  $T0^{max}$ ,  $T0^{mid}$ .

The input and output combinations will henceforth be referred to as location/symbol, where symbol is the modified class symbols listed above. For example, South/ $\overline{KTG}$  was used when considering the mean “knee” temperature gradient for the South input location and Control/ $T5^{max}$  when the maximum temperature at a depth of 5 cm was considered based on the Control input location.

### 9.3 Results and Discussion

The sensitivity analyses results presented use the various combinations of input locations (i.e., Control, South, and North) and outputs (e.g.,  $T5^{max}$  or  $TG2^{min}$ ) to provide a better understanding of what inputs are the most important to the formation of near-surface facets. Due to the enormity of the data produced, considering all the results is impossible and it is easy to become enveloped in the subtle nuances of the analyses conducted. To make the data presented in this chapter accessible, a majority of the results are presented graphically and specific quantities are kept to a minimum, only being listed when deemed to be a significant finding with respect to radiation-recrystallization. Also, when quantities are reported only the mean values are given, however each parameter has defined confidence levels associated. Appendix F includes the complete results from the sensitivity analyses presented here, with the exception of the temporal data, which only includes the total-effect results with time and the complete results at mid-day.

#### 9.3.1 Snow Temperatures

All of the gradient computations are based on the gradient between the snow surface and a temperature at depth. Hence, analyzing the results of the snow surface temperature ( $T0$ ) is an obvious starting point. The critical input parameters affecting the snow surface temperature, the temperatures at 2 cm, 5 cm, and 8 cm depth ( $T2$ ,  $T5$ , and  $T8$ , respectively), and the temperature at the “knee” ( $TK$ ) were considered.

Snow Surface Temperature: The total-effect indices as a function of model evaluation time for the three locations are included in Figure 9.2. The indices in these figures are expressed as the normalized total-effect indices ( $S_T^*$ ; see Chapter 6

Section 6.7). Two obvious results arise: (1)  $LW(6)$  is the most influential input at all locations and (2) the importance of  $SW(7)$  and  $\alpha(8)$  differ with location.

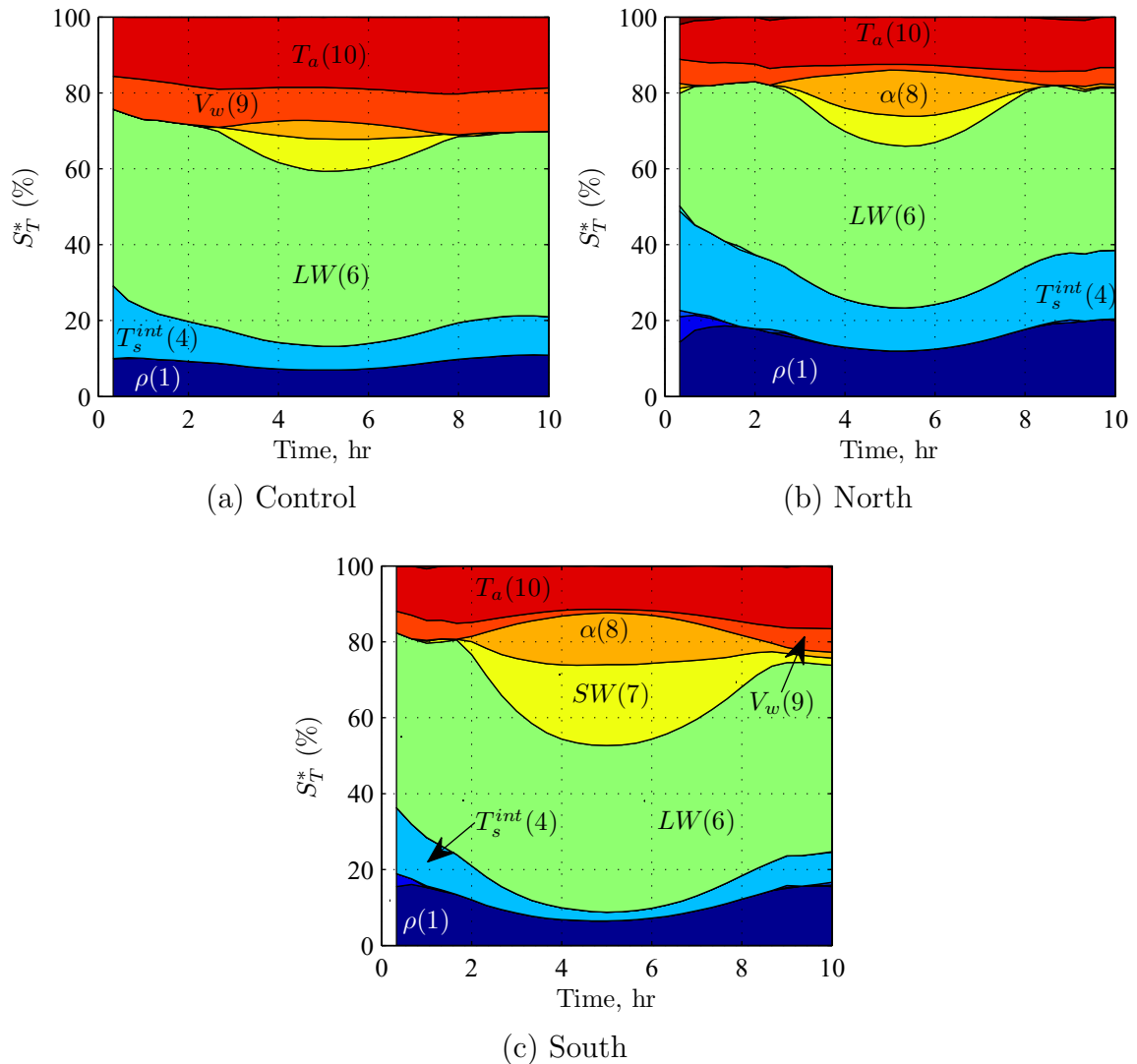


Figure 9.2: Stacked area charts of normalized total-effect sensitivity ( $S_T^*$ ) for  $T0(t)$  for the (a) Control, (b) North, and (c) South locations. The regions are stacked from bottom to top in order as listed in Table 7.1.

The area charts shown are useful for monitoring the progression of the sensitivity parameters over time, but two difficulties arise when trying to gather specific quantities. Figure 9.2 only includes the total-effect results, which incorporate interactions,

but do not decipher distinctly the components of the interactions. To determine what interactions are important, the first- and second-order indices must be considered, but doing so would require 11 area charts (one for each input parameter) for every output under consideration, which is not practical. Secondly, the area charts do not display the confidence bounds. Therefore, it is necessary to establish a suitable single parameter capable of capturing the important information contained in the temporal data.

First, the mean surface temperature is considered, as presented in Figure 9.3a. For the  $\overline{T_0}$  analysis  $LW(6)$  is the most influential parameter—two-thirds of the output variance is due to some respect with changes in  $LW(6)$ . The only other parameters that influence the snow surface temperature (i.e., a non-zero total-effect index) are  $\rho(1)$ ,  $T_s^{int}$ , and  $T_a(10)$ . Additionally, the results did not differ with location. However, the lack of significance of the  $SW(7)$  and  $\alpha(8)$  indicated that the mean does not reflect the conditions during the day.

The results obtained by considering the maximum value of the surface temperature (i.e.,  $T_0^{max}$ ) were considered first, see Figure 9.3b. These results yielded total-effect indices consistent with the temporal data, that is the  $SW(7)$  and  $\alpha(8)$  inputs contributed to the output variance. Upon further scrutiny the  $T_0^{max}$  results were problematic in practice, since the sensitivity analysis does not decipher when the maximum occurs, the maximum used for computation could then be from any point during the simulations. With respect to radiation-recrystallization the fluctuation due to solar radiation may be missed. Therefore, the mid-day results were computed (see Figure 9.3c) and assumed to be the most relevant to the problem at hand, which is explored in further detail in the following sections.

The  $T_0^{mid}$  results, by definition, align exactly with the five hour point on each of the graphs in Figure 9.2. Overwhelmingly,  $LW(6)$  was the most influential input.

Also,  $\rho(1)$ ,  $T_s^{int}(4)$ ,  $SW(7)$ ,  $\alpha(8)$ ,  $V_w(9)$ , and  $T_a(10)$  each influence the snow surface to some extent, depending on the location. Before specific conclusions may be stated regarding the most influential terms on snow surface temperature the interactions should be considered, as shown in Figure 9.4 for the South location.

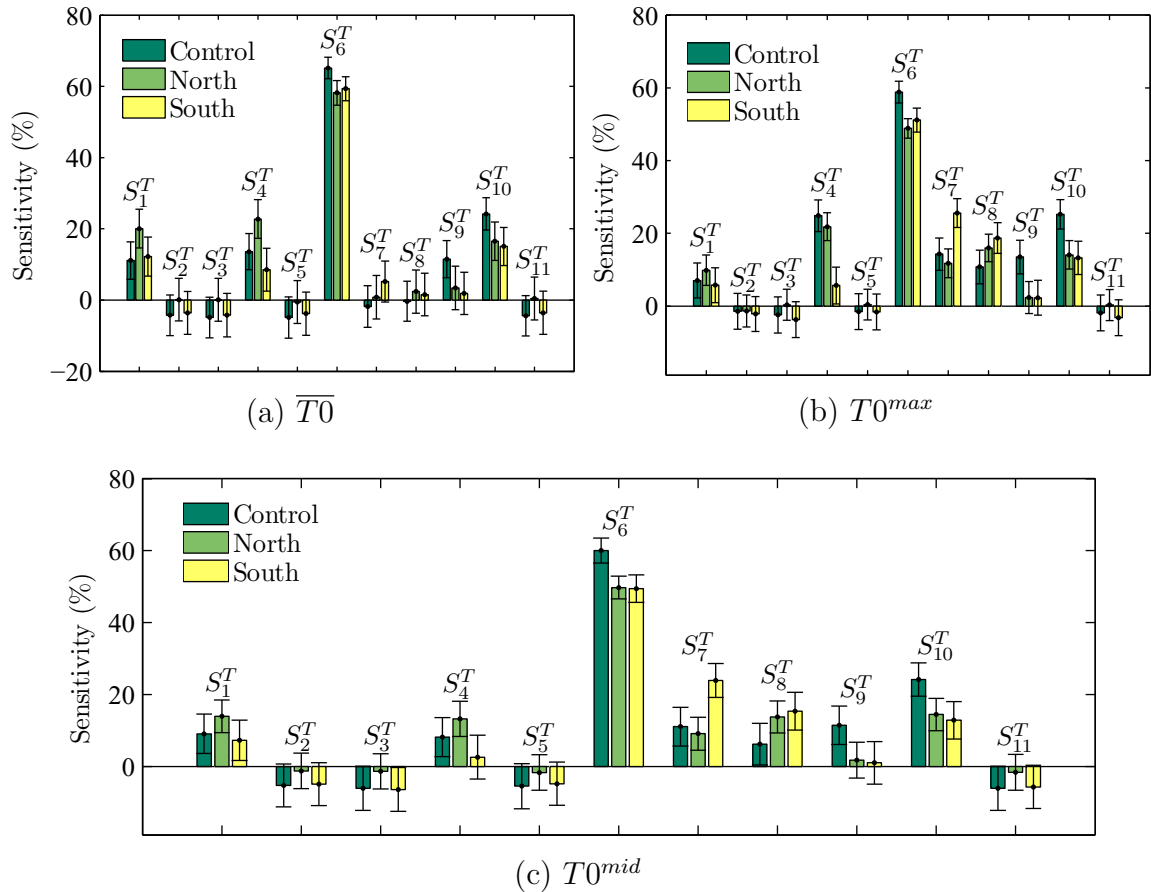
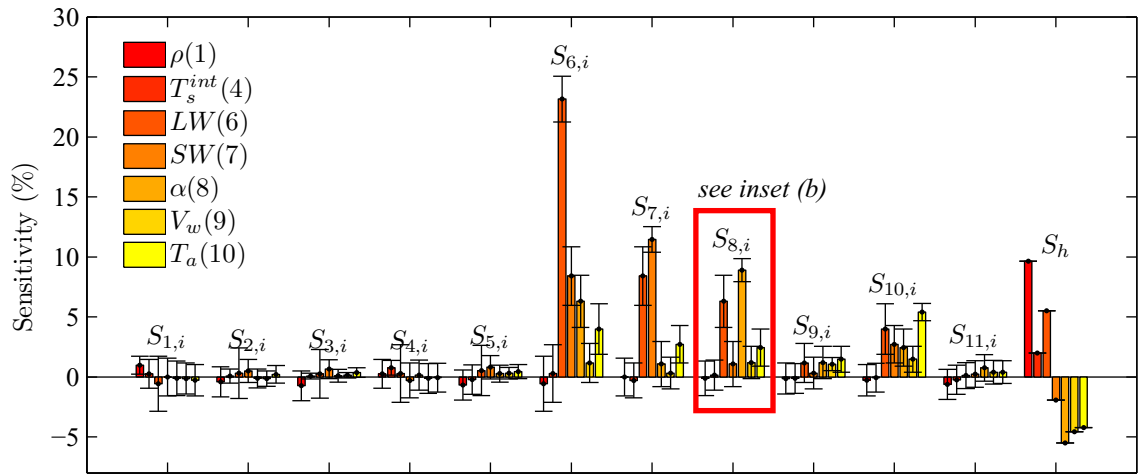


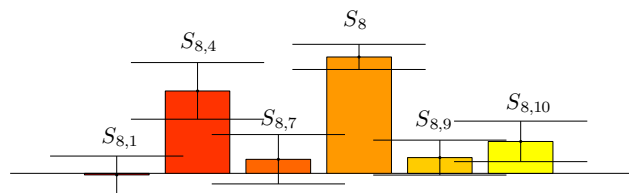
Figure 9.3: Total-effect sensitivity indices for the Control, South, and North locations for (a)  $\overline{T_0}$ , (b)  $T_0^{max}$ , and (c)  $T_0^{mid}$  (see Table 7.1 for reference).

The first-, second-, and higher-order interactions for the South location are presented in Figure 9.4 and for the Control and North locations in Figure 9.5. These figures only include data for the values listed previously— $\rho(1)$ ,  $T_s^{int}(4)$ ,  $LW(6)$ ,  $SW(7)$ ,  $\alpha(8)$ ,  $V_w(9)$ , and  $T_a(10)$ —as important from the total-effect results. These grouped bar charts require explanation, they differ from the charts already presented, but





(a) South/ $T_0^{mid}$



(b) Zoom inset of  $\alpha(8)$

Figure 9.4: First-, second-, and higher-order indices for (a) the South/ $T_0^{mid}$  sensitivity analysis and (b) a zoomed view focusing on  $\alpha(8)$  (see Table 7.1 for reference).

are similar to the charts used in Chapter 8 (see p. 183). For each chart, the bars are grouped. Each group includes seven bars, one for each of the parameters listed above as important. The height of the bars provides either the first- or second-order index for the parameter associated with the bar. Consider the inset in Figure 9.4b, it provides a zoomed view of the group associated with  $\alpha(8)$  from Figure 9.4a. For each bar in the group the  $i$  is replaced with the corresponding input term in the legend. For example, the first bar corresponds with  $\rho(1)$ , thus becomes  $S_{8,1}$ , which is the interaction of  $\alpha(8)$  and  $\rho(1)$ . In this example, the first-order index occurs with  $i = 8$  ( $S_{8,8} = S_8$ ). The higher-order interactions—labeled as  $S_h$ —for each term are

provided in similar fashion. Based upon the data presented in Figures 9.4 and 9.5 the following may be stated:

1. Control/ $T0^{mid}$  (Figure 9.5a): The output variance is mainly related to  $LW(6)$ , which accounts for approximately 60% of the variance, if the total-effect is considered ( $S_6^T \approx 60\%$ ). The next most important term is  $S_{10}^T$ , approximately 25% of the output variance may be attributed to this term.
2. North/ $T0^{mid}$  (Figure 9.5b): A vast majority of the output variance (80%) was due to the first-order indices. Over one-third (35%) of the output is attributed to  $LW(6)$  alone, 21% to  $T_a(10)$ , 12% to  $\alpha(8)$ , 9% to  $SW(7)$ , and 2% to  $T_s^{int}(4)$ .
3. South/ $T0^{mid}$  (9.4): A majority (59%) of the total variance may be attributed to the first- and second-order results for  $LW(6)$ ,  $SW(7)$ , and  $\alpha(8)$  (i.e.,  $S_6 + S_7 + S_8 + S_{6,7} + S_{6,8} + S_{7,8} \approx 59\%$ ). The remainder of the variance is associated with  $T_a(10)$  or the higher-order interactions.

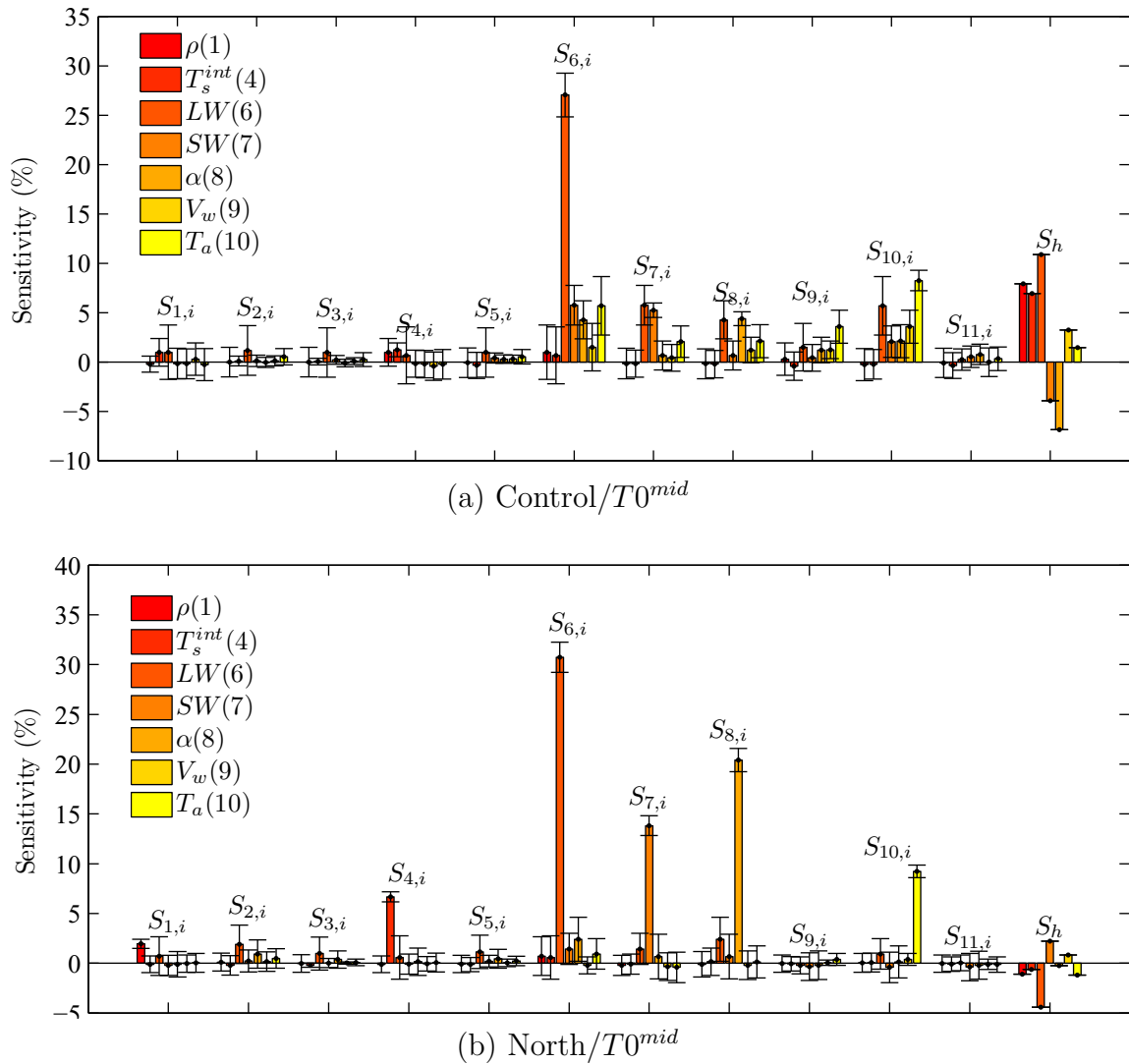


Figure 9.5: First-, second-, and higher-order indices for the (a) Control/ $T_0^{mid}$  and (b) North/ $T_0^{mid}$  sensitivity analysis (see Table 7.1 for reference).

Snow Temperatures at Depth: The time-dependent sensitivity analysis results for snow temperature at various depths— $TK(t)$ ,  $T2(t)$ ,  $T5(t)$ ,  $T8(t)$ —for the South location are provided in Figure 9.6. The most obvious result gained was the similarity between  $TK(T)$  and  $T2(t)$ . In fact, at mid-day the  $TK(t)$  values do not statistically differ from the  $T2(t)$  results; for all the inputs parameters the confidence intervals overlapped. This result was also true for the Control and North locations. Therefore,

it is reasonable to conclude that the “knee” is located at approximately 2 cm deep in the snowpack. For comparison, Figure 9.7 includes the  $TK(t)$  results for the Control and North locations.

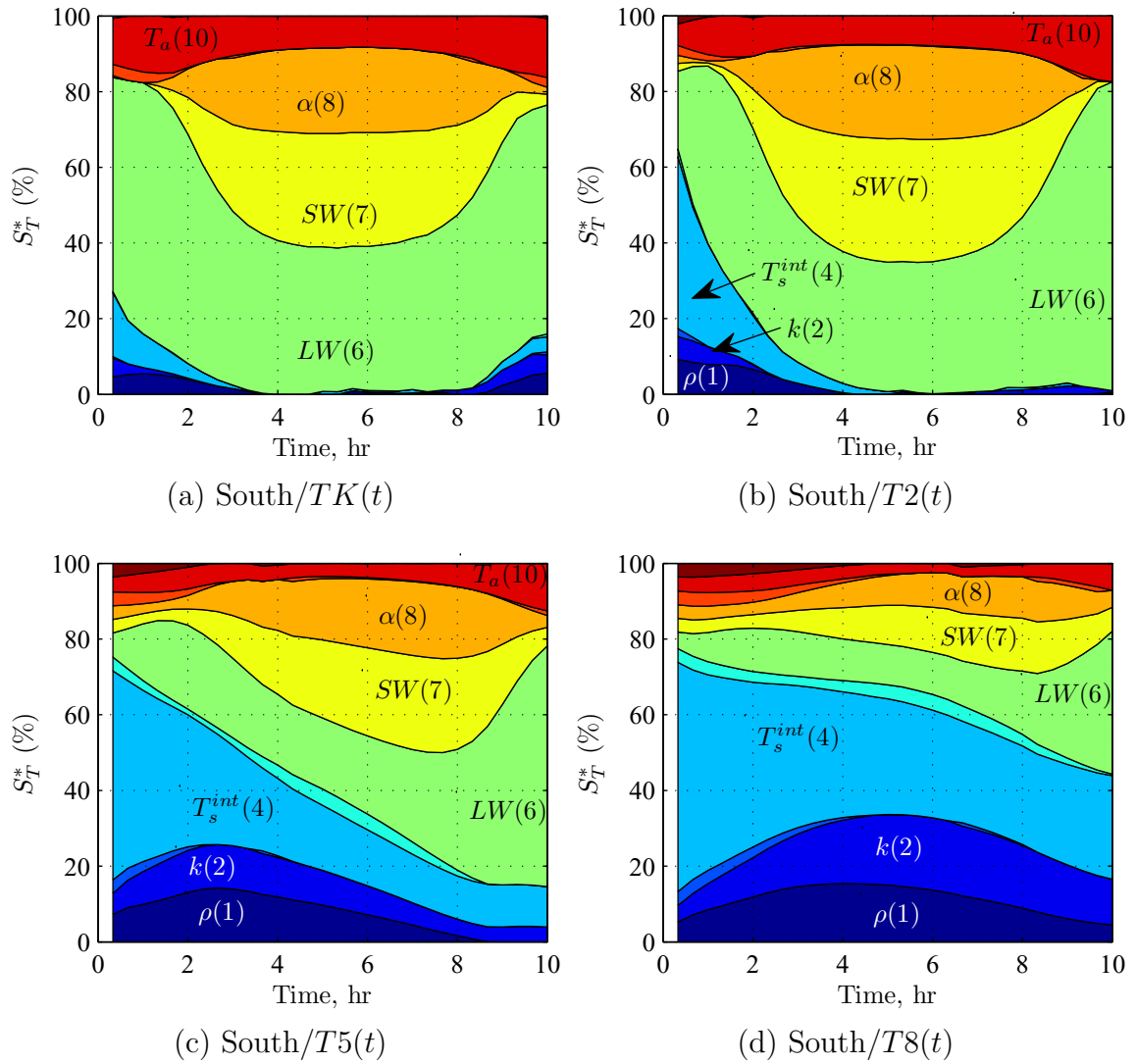


Figure 9.6: Stacked area charts of normalized total-effect sensitivity as a function of model evaluation time at the (a) “knee”, (b) 2 cm, (c) 5 cm, and (d) 8 cm depth for the South locations. The regions are stacked from bottom to top in order as listed in Table 7.1.

Conceptually, the  $T2(t)$ ,  $T5(t)$ , and  $T8(t)$  results in Figures 9.6b–d demonstrate the attenuation of short-wave radiation expected. At 8 cm the role of  $SW(7)$  and  $\alpha(8)$  are greatly diminished. Interestingly, the extinction coefficient ( $\kappa(5)$ ) appears to be negligible with respect to effecting the snow temperature at depth. As discussed, the time-dependent results are not practical for providing quantitative results. Thus, considering the focus of this chapter on the radiation-recrystallization process, only the  $TK$  results are analyzed further. Additionally, given the findings for the snow surface temperature ( $T0$ ) only the mid-day values are considered. The total-effect results for  $TK^{mid}$  are presented in Figure 9.8.

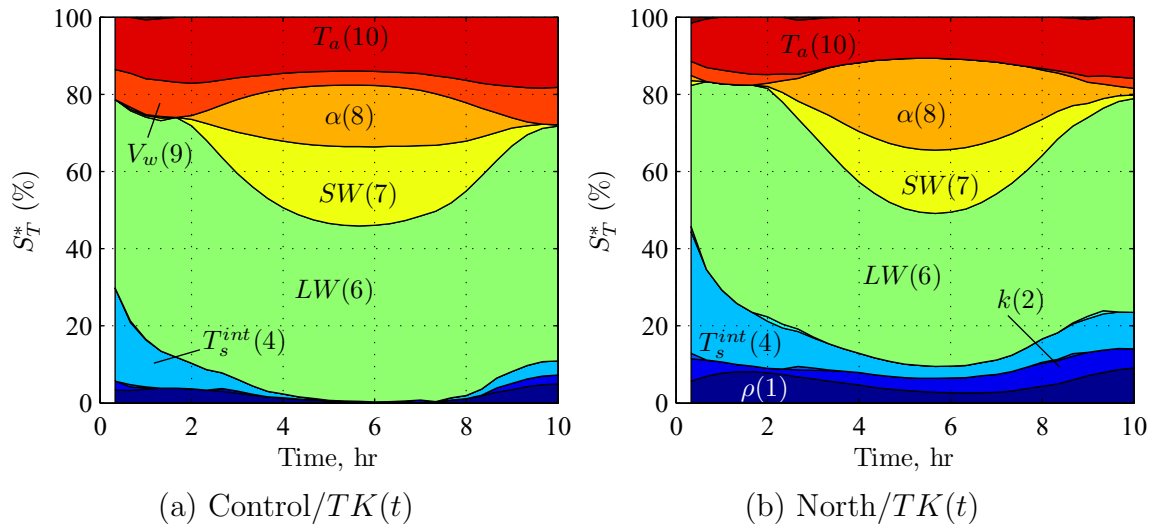


Figure 9.7: Stacked area charts of normalized total-effect sensitivity as a function of model evaluation time at the 2 cm depth for the (a) Control and (b) North locations. The regions are stacked from top to bottom in order as listed in Table 7.1 (see Table 7.1 for reference).

Based on the total-effect results in Figure 9.8 only four parameters influenced the “knee” temperature:  $LW(6)$ ,  $SW(7)$ ,  $\alpha(8)$ , and  $T_a(10)$ . For all three locations  $LW(6)$  was the most influential term. However, both  $SW(7)$  and  $\alpha(8)$  approach the total-effect of  $LW(6)$  for the South location. Again, to truly quantify the important

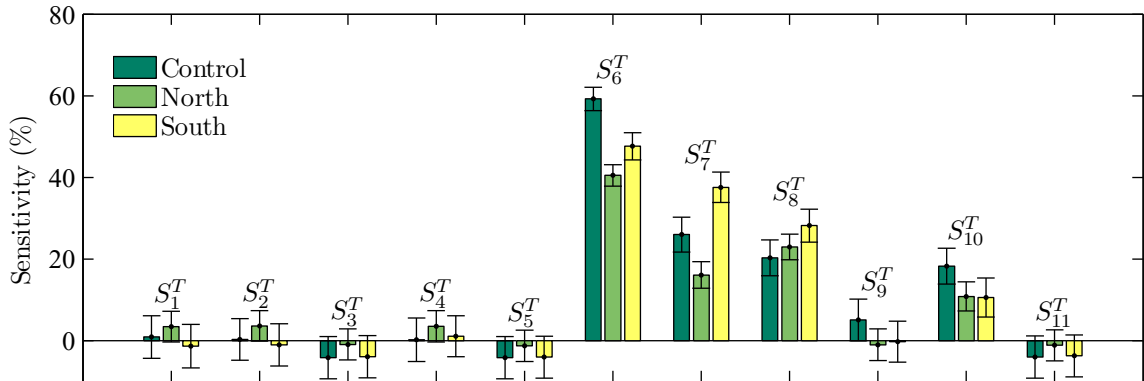


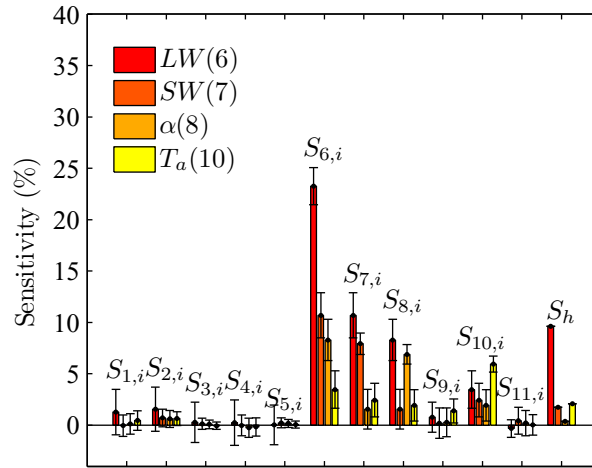
Figure 9.8: Total-effect sensitivity indices for the Control, South, and North locations for  $TK^{mid}$  (see Table 7.1 for reference).

parameters the interactions must also be considered. The first-, second-, and higher-order sensitivity indices are provided in Figure 9.9. This figure only includes the four terms listed above as influential on the  $TK^{mid}$  output.

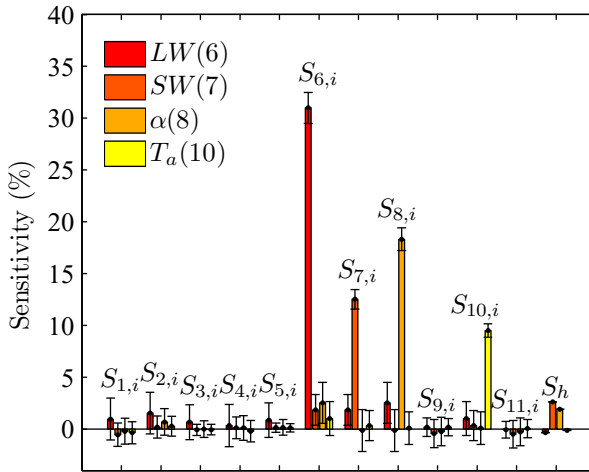
In similar fashion as the snow surface temperature, the following statements are provided based on the sensitivity analysis results of the “knee” temperature at mid-day ( $TK^{mid}$ ):

1. Control/ $TK^{mid}$  (9.9a): Approximately 44% of the output variance is due solely to three terms— $LW(6)$ ,  $SW(7)$ ,  $\alpha(8)$ , and  $T_a(10)$ —without any interactions, with 23% from  $LW(6)$  alone. The second-order interactions of these four terms account for an additional 29% of the total variance, the remainder is associated with higher-order interactions.
2. North/ $TK^{mid}$  (9.9b): A vast majority of the output variance (72%) was due to the first-order indices: 31% from  $LW(6)$ , 13% from  $SW(7)$ , 18% from  $\alpha(8)$ , and 10% from  $T_a(10)$ . The remainder of the output variance is due to a variety of second- and higher-order interactions.

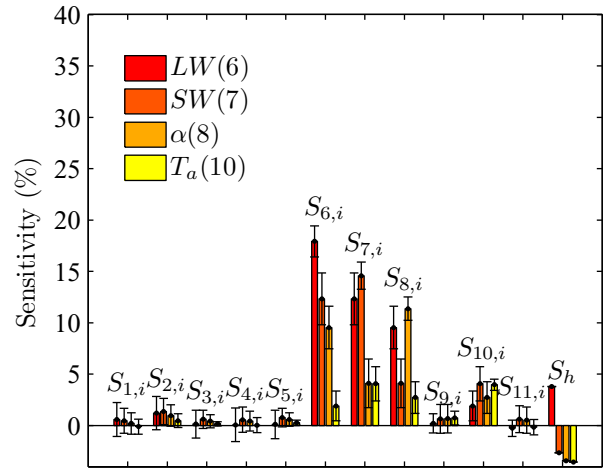
3. South/ $T0^{mid}$  (9.9c): A majority (69%) of the total variance may be attributed to the first- and second-order results for  $LW(6)$ ,  $SW(7)$ , and  $\alpha(8)$  (i.e.,  $S_6 + S_7 + S_8 + S_{6,7} + S_{7,8} + S_{7,8} \approx 69\%$ ). An additional 11% of the output variance is due to the total-effect of  $T_a(10)$  and the remainder from higher-order interactions.



(a) Control/ $TK^{mid}$



(b) North/ $TK^{mid}$



(c) South/ $TK^{mid}$

Figure 9.9: First-, second-, and higher-order indices for  $TK^{mid}$  sensitivity analysis for the (a) Control, (b) North, and (c) South locations (see Table 7.1 for reference).

### 9.3.2 Temperature Gradient

As shown in the previous section, the sensitivity results for snow temperature at a depth of 2 cm were statistically identical to the results for the “knee” temperature. Therefore, only the *TG2* and *KTG* results are considered in this section.

Gradient Computed at 2 cm: The *TG2(t)* results for each location are included in Figure 9.10a–c. The results shown in this figure indicated that sensitivity indices for the input parameters did not change significantly with time. The exception was *SW(7)* and  $\alpha(8)$  that became evident after about 2 hours of model evaluation time. Generally speaking, three terms— $\rho(1)$ ,  $T_s^{int}$ , and *LW(6)*—dominate the charts. Additionally, as was done for temperature, the mid-day value (*TG2<sup>mid</sup>*) was used to simplify the temporal results. Figure 9.10d shows the total-effect results for *TG2<sup>max</sup>*, which indicates six terms as influencing the gradient:  $\rho(1)$ ,  $k(2)$ ,  $T_s^{int}(4)$ , *LW(6)*,  $V_w(9)$ , and  $T_a(10)$ . Interestingly, in both the *TG2(t)* and *TG2<sup>mid</sup>* neither *SW(7)* or  $\alpha(8)$  appear to influence the gradient to a significant extent.

The reason behind this behavior is due to subsurface melting.<sup>1</sup> Consider the scenario where the only parameter altered is short-wave radiation. For example, two different temperature contour plots are shown in Figure 9.11. In these figures, all inputs—except for *SW(7)*—were held constant:  $\rho(1) = 150$ ,  $k(2) = 0.08$ ,  $c_p(3) = 2030$ ,  $T_s^{int}(4) = -10$ ,  $\kappa(5) = 60$ ,  $LW(6) = 250$ ,  $\alpha(8) = 0.8$ ,  $V_w(9) = 1$ ,  $T_a(10) = -10$ , and  $RH(11) = 50$  (units are consistent with values in Table 7.1). The value of *SW(7)* was changed from 300 W/m<sup>2</sup> to 400 W/m<sup>2</sup>, but despite this change the temperature gradient computed at 2 cm for both scenarios is approximately 600 °C/m, since the subsurface is at 0°C and the surface at -12°C. Hence, despite changes in *SW(7)*, the

<sup>1</sup>The thermal model presented in Chapter 5 is constrained such that the temperature of the snow remains at or below 0°C and it does not model melting snow.



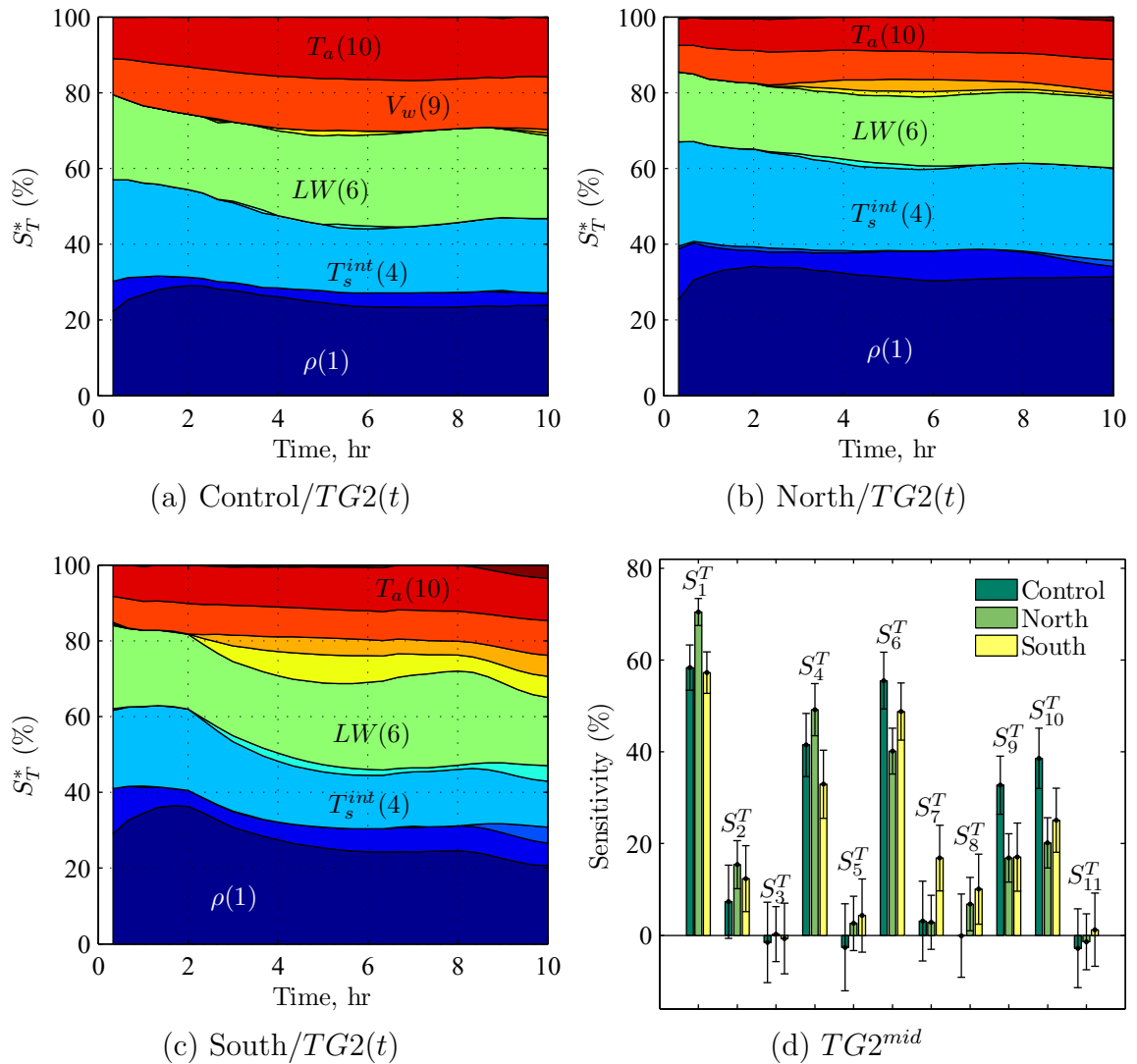


Figure 9.10: Stacked area charts of normalized total-effect sensitivity of  $TG2(t)$  for the (a) Control, (b) North, and (c) South locations and (d) the total-effect indices computed from  $TG2^{mid}$  output. The regions are stacked from bottom to top in order as listed in Table 7.1.

gradient remains the same. This behavior is the culprit behind the low values for the sensitivity indices reported previously.

This result coincides with observed near-surface facet events described in Chapter 4, which often were reported to occur with subsurface melting. Typically radiation-

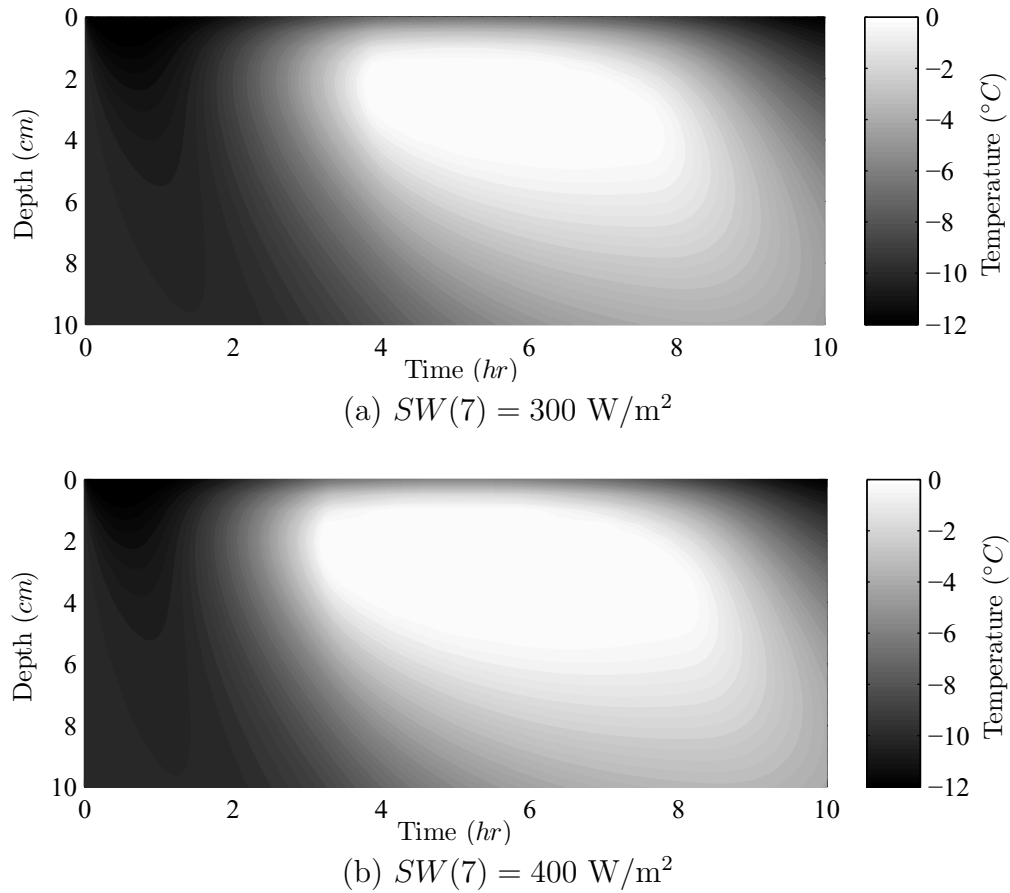


Figure 9.11: Contour plots of snow temperature with incoming short-wave radiation of (a)  $300 \text{ W/m}^2$  and (b)  $400 \text{ W/m}^2$ . (see Table 7.1 for reference)

recrystallization is explained as requiring incoming short-wave radiation, which is true, but the intensity is less important than the intensity of the incoming long-wave radiation.

Next, the interactions should be considered before providing specific results. The total-effect results for  $TG2^{mid}$  indicate that only three parameters— $c_p(3)$ ,  $\kappa(4)$ , and  $RH(11)$ —may be neglected at all locations. Hence, Figure 9.12 is presented that includes the first-, second-, and higher-order indices for each of the other parameters. This figures contains far too many factors to be easily used, but is presented to illustrate one point—the overwhelming importance of the higher-order interactions. This

result indicates that temperature gradient is only affected when certain combinations exist of the various input parameters.

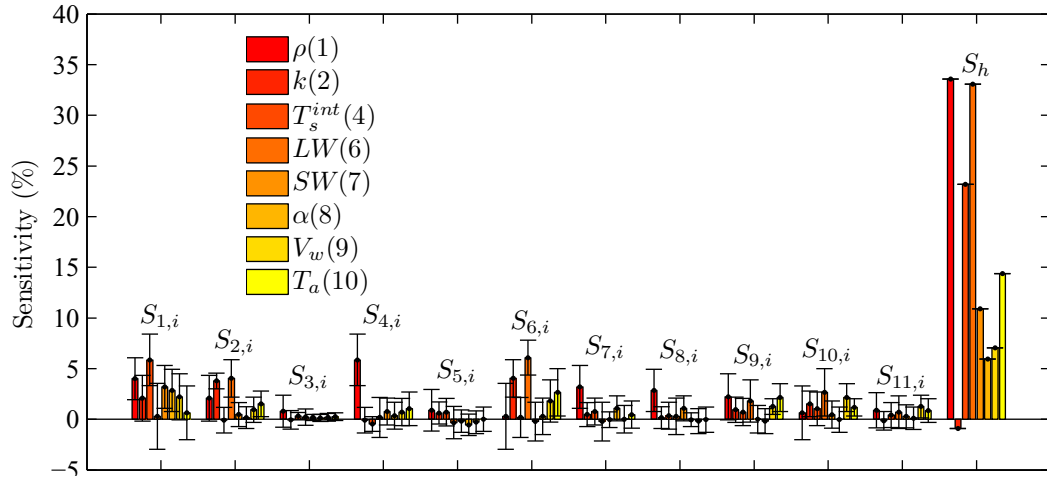


Figure 9.12: First-, second-, and higher-order indices for  $TG2^{mid}$  sensitivity analysis for the South location, which highlights the overwhelming importance of higher-order interactions. (see Table 7.1 for reference)

“Knee” Temperature Gradient: Unlike the temperature results, the  $KTG$  data differed slightly from  $TG2$  results. The temporal results for each location for the “knee” temperature gradient ( $KTG(t)$ ) are included in Figure 9.13. The  $KTG(t)$  results were less uniform than observed for  $TG2(t)$  (see Figure 9.10),  $k(2)$  became the dominant input around mid-day, and  $T_s^{int}(4)$  and  $LW(6)$  had a diminished importance.

The total-effect indices for  $KTG^{mid}$  are provided in Figure 9.14. Two characteristics of the  $KTG(t)$  (Figure 9.13) data were captured by the mid-day results: (1) the importance of  $k(2)$  is evident and (2) the  $SW(7)$  and  $\alpha(8)$  inputs also show some level of importance depending on the location being considered. The large error associated with the total-effect may be attributed to the nature of the  $KTG$  calculation, which sets all input scenarios that did not yield a “knee” temperature profile to a value

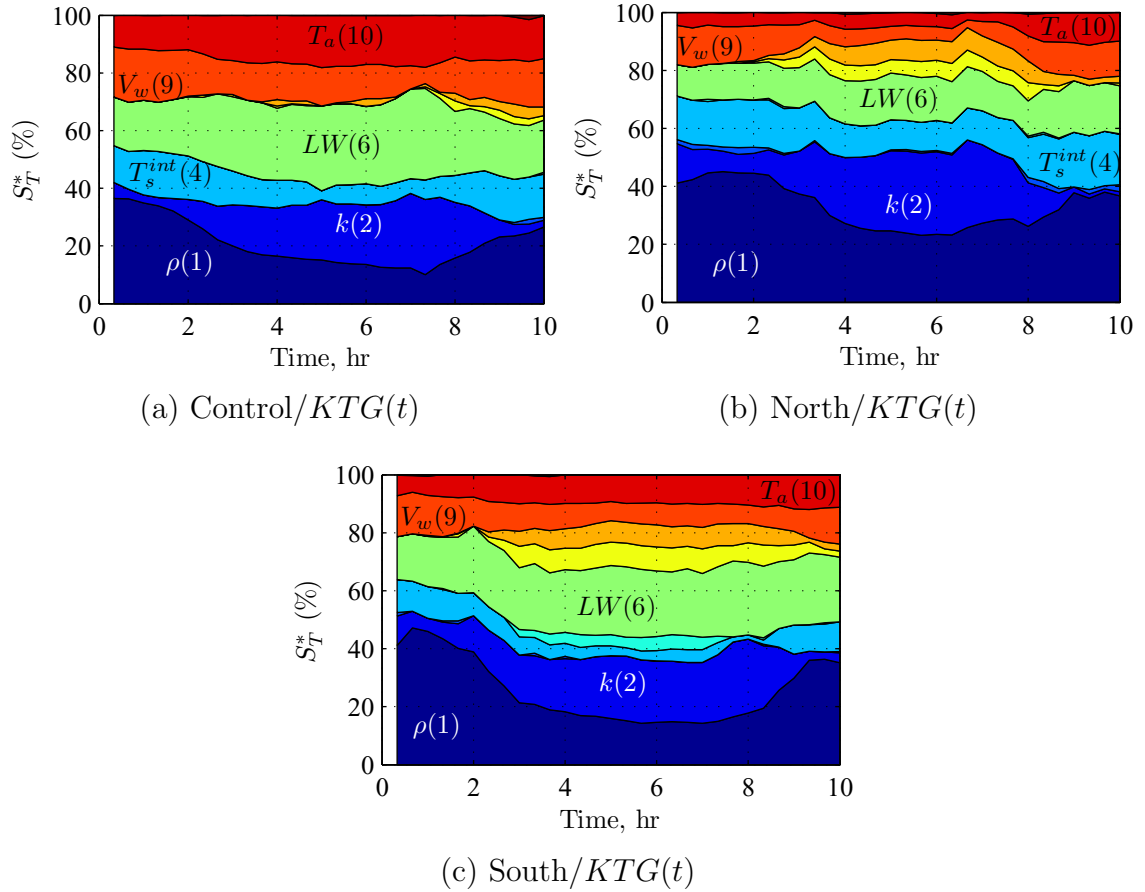


Figure 9.13: Stacked area charts of normalized total-effect sensitivity of  $KTG(t)$  for the (a) Control, (b) North, and (c) South locations. The regions are stacked from bottom to top in order as listed in Table 7.1.

of zero, this effectively reduces the number of simulations from which the sensitivity parameters were computed, inducing greater error.

The total-effect results also differed significantly with locations. Figure 9.15a presents the indices from the Control location, which include  $\rho(1)$ ,  $k(2)$ ,  $LW(6)$ ,  $V_w(9)$ , and  $T_a(10)$ . The total-effect results for the North/ $KTG^{mid}$  indicated that five terms— $\rho(1)$ ,  $k(2)$ ,  $T_s^{int}$ ,  $LW(6)$ , and  $\alpha(8)$ —influenced the temperature gradient, thus Figure 9.15b is presented. Finally, considering that the South/ $KTG^{mid}$  were influenced by seven terms, a complete table of these results is provided in Table 9.1.

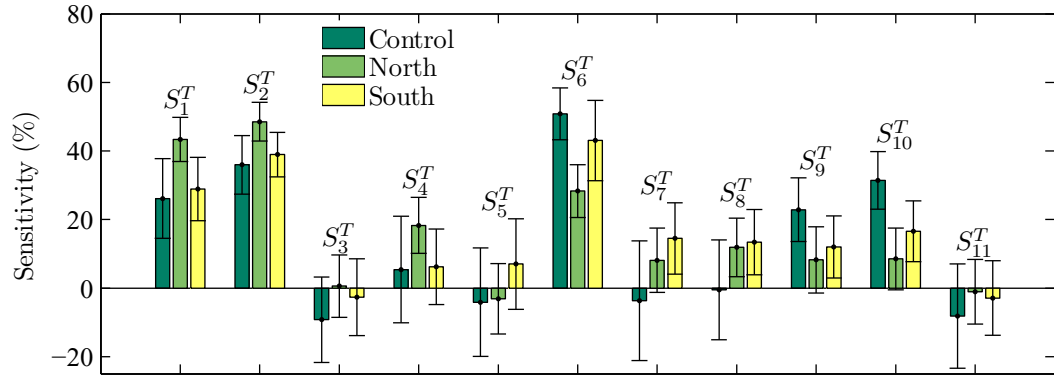
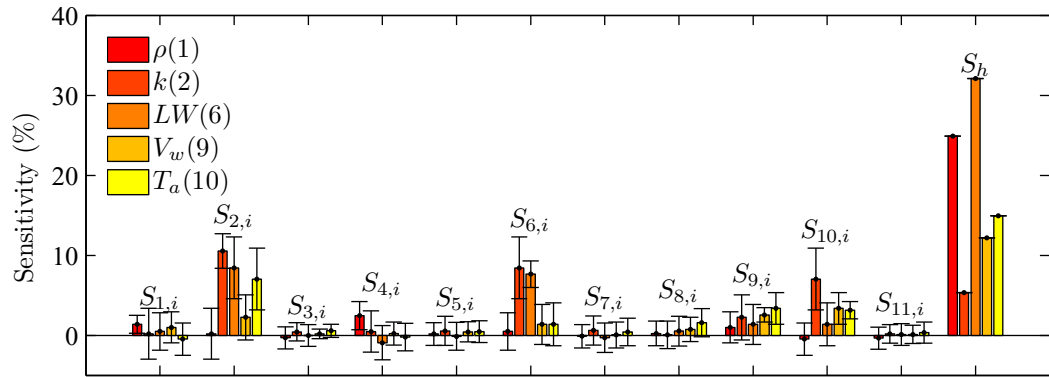
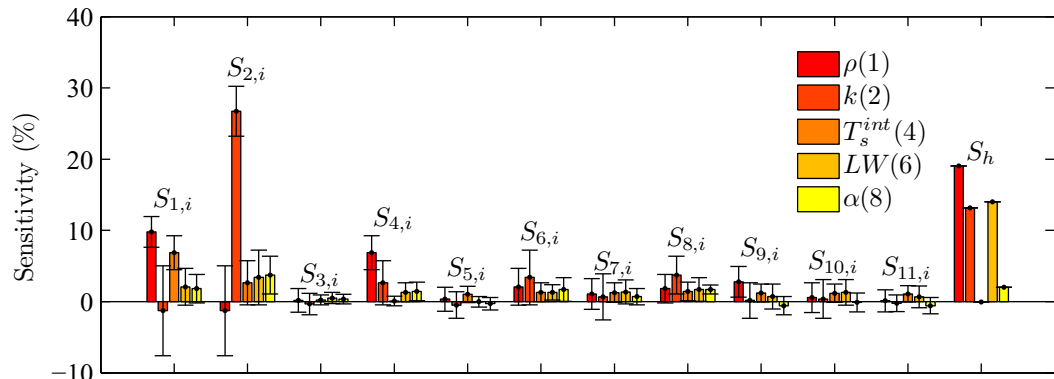


Figure 9.14: Grouped bar charts of total-effect sensitivity for  $KTG^{mid}$  for all three locations. (see Table 7.1 for reference)



(a) Control/ $KTG^{mid}$



(b) North/ $KTG^{mid}$

Figure 9.15: First-, second-, and higher-order indices for  $KTG^{mid}$  sensitivity analysis for the (a) Control and (b) North locations. (see Table 7.1 for reference)

Table 9.1: First-, second-, total-, and higher-order sensitivity indices for the South/ $KTG^{mid}$  results (see Table 7.1 for reference).

i \ j	1	2	3	4	5	6	7	8	9	10	11
1	<b>1.8</b> <i>0.1-3.5</i>	3.3 <i>-0.7-7.4</i>	1.2 <i>-0.5-2.8</i>	<b>3.1</b> <i>1.2-5.0</i>	1.8 <i>-0.3-3.8</i>	0.1 <i>-2.6-2.9</i>	<b>2.5</b> <i>0.2-4.8</i>	<b>2.6</b> <i>0.5-4.7</i>	<b>3.4</b> <i>1.3-5.6</i>	1.9 <i>-0.6-4.4</i>	1.4 <i>-0.3-3.1</i>
2	3.3 <i>-0.7-7.4</i>	<b>13.2</b> <i>10.9-15.4</i>	<b>1.2</b> <i>0.0-2.4</i>	<b>2.3</b> <i>0.1-4.4</i>	<b>1.8</b> <i>0.1-3.5</i>	<b>5.4</b> <i>1.4-9.4</i>	-0.7 <i>-3.6-2.1</i>	0.4 <i>-1.9-2.8</i>	<b>3.7</b> <i>1.2-6.1</i>	<b>4.4</b> <i>1.4-7.4</i>	1.1 <i>-0.1-2.2</i>
3	1.2 <i>-0.5-2.8</i>	<b>1.2</b> <i>0.0-2.4</i>	-0.2 <i>-0.4-0.1</i>	0.5 <i>-0.1-1.0</i>	0.3 <i>-0.3-0.8</i>	-0.2 <i>-1.6-1.2</i>	0.3 <i>-0.3-0.9</i>	0.5 <i>-0.1-1.1</i>	0.5 <i>-0.0-1.0</i>	0.4 <i>-0.2-1.1</i>	0.3 <i>-0.1-0.8</i>
4	<b>3.1</b> <i>1.2-5.0</i>	<b>2.3</b> <i>0.1-4.4</i>	0.5 <i>-0.1-1.0</i>	-0.2 <i>-0.7-0.2</i>	0.3 <i>-0.7-1.4</i>	-0.7 <i>-2.4-0.9</i>	0.5 <i>-0.5-1.4</i>	0.5 <i>-0.4-1.5</i>	0.8 <i>-0.2-1.7</i>	0.4 <i>-0.6-1.4</i>	0.3 <i>-0.6-1.2</i>
5	1.8 <i>-0.3-3.8</i>	<b>1.8</b> <i>0.1-3.5</i>	0.3 <i>-0.3-0.8</i>	0.3 <i>-0.7-1.4</i>	0.1 <i>-0.7-0.9</i>	-0.4 <i>-2.4-1.6</i>	0.1 <i>-1.5-1.6</i>	0.3 <i>-1.2-1.9</i>	0.5 <i>-1.0-2.1</i>	-0.1 <i>-1.8-1.7</i>	0.3 <i>-1.1-1.7</i>
6	0.1 <i>-2.6-2.9</i>	<b>5.4</b> <i>1.4-9.4</i>	-0.2 <i>-1.6-1.2</i>	-0.7 <i>-2.4-0.9</i>	-0.4 <i>-2.4-1.6</i>	<b>9.3</b> <i>7.4-11.1</i>	-0.1 <i>-2.7-2.5</i>	0.3 <i>-2.0-2.7</i>	1.4 <i>-1.0-3.9</i>	0.6 <i>-2.1-3.3</i>	-0.3 <i>-2.2-1.6</i>
7	<b>2.5</b> <i>0.2-4.8</i>	-0.7 <i>-3.6-2.1</i>	0.3 <i>-0.3-0.9</i>	0.5 <i>-0.5-1.4</i>	0.1 <i>-1.5-1.6</i>	-0.1 <i>-2.7-2.5</i>	-0.5 <i>-1.8-0.9</i>	0.7 <i>-1.4-2.9</i>	0.4 <i>-1.9-2.6</i>	0.3 <i>-2.1-2.6</i>	-0.0 <i>-2.0-2.0</i>
8	<b>2.6</b> <i>0.5-4.7</i>	0.4 <i>-1.9-2.8</i>	0.5 <i>-0.1-1.1</i>	0.5 <i>-0.4-1.5</i>	0.3 <i>-1.2-1.9</i>	0.3 <i>-2.0-2.7</i>	0.7 <i>-1.4-2.9</i>	-0.1 <i>-1.1-1.0</i>	1.0 <i>-0.8-2.8</i>	0.8 <i>-1.2-2.7</i>	0.9 <i>-0.7-2.5</i>
9	<b>3.4</b> <i>1.3-5.6</i>	<b>3.7</b> <i>1.2-6.1</i>	0.5 <i>-0.0-1.0</i>	0.8 <i>-0.2-1.7</i>	0.5 <i>-1.0-2.1</i>	1.4 <i>-1.0-3.9</i>	0.4 <i>-1.9-2.6</i>	1.0 <i>-0.8-2.8</i>	<b>1.6</b> <i>0.8-2.3</i>	<b>1.4</b> <i>0.0-2.8</i>	0.5 <i>-0.5-1.6</i>
10	1.9 <i>-0.6-4.4</i>	<b>4.4</b> <i>1.4-7.4</i>	0.4 <i>-0.2-1.1</i>	0.4 <i>-0.6-1.4</i>	-0.1 <i>-1.8-1.7</i>	0.6 <i>-2.1-3.3</i>	0.3 <i>-2.1-2.6</i>	0.8 <i>-1.2-2.7</i>	<b>1.4</b> <i>0.0-2.8</i>	<b>2.0</b> <i>0.7-3.3</i>	-0.2 <i>-2.1-1.7</i>
11	1.4 <i>-0.3-3.1</i>	1.1 <i>-0.1-2.2</i>	0.3 <i>-0.1-0.8</i>	0.3 <i>-0.6-1.2</i>	0.3 <i>-1.1-1.7</i>	-0.3 <i>-2.2-1.6</i>	-0.0 <i>-2.0-2.0</i>	0.9 <i>-0.7-2.5</i>	0.5 <i>-0.5-1.6</i>	-0.2 <i>-2.1-1.7</i>	0.0 <i>-0.2-0.2</i>
Higher	5.7	2.9	-7.5	-1.5	2.0	27.5	11.1	5.3	-3.1	4.6	-7.3
Total	<b>28.9</b> <i>19.7-38.2</i>	<b>38.9</b> <i>32.4-45.5</i>	-2.6 <i>-13.9-8.6</i>	6.3 <i>-4.8-17.3</i>	7.0 <i>-6.2-20.2</i>	<b>43.1</b> <i>31.3-54.8</i>	<b>14.5</b> <i>4.1-24.9</i>	<b>13.4</b> <i>3.9-22.9</i>	<b>12.0</b> <i>3.0-21.0</i>	<b>16.6</b> <i>7.7-25.4</i>	-2.9 <i>-13.8-8.0</i>

Given the data presented in this section, the following statements are provided based on the sensitivity analysis results of the “knee” temperature gradient at mid-day ( $KTG^{mid}$ ):

1. Control/ $KTG^{mid}$  (9.15a): A majority of the variance observed in the output was due to three terms and their associated interactions. The variance due to  $\rho(1)$  and  $LW(6)$  was primarily from higher-order interactions, while the variance due to  $k(2)$  was primarily from the first-order index and second-order interactions with  $\rho(1)$  and  $T_a(10)$ .
2. North/ $KTG^{mid}$  (9.15b): Two terms— $\rho(1)$  and  $k(2)$ —were the most influential on the output variance, with  $LW(6)$  having a secondary effect. The first-order index for  $k(2)$  was the most significant accounting for approximately 27% of the total variance observed.

3. South/ $KTG^{mid}$  (9.1): A majority of the observed variance was due to  $\rho(1)$ ,  $k(2)$ , and  $LW(6)$ , which had total-effect indices of approximately 29%, 39%, and 43%, respectively. Both  $\rho(1)$  and  $k(2)$  were composed of a significant number of second-order interactions.  $SW(7)$  and  $\alpha(8)$  were also shown to affect the output, but this effect was composed of interactions with  $\rho(1)$  directly or high-order terms, the first-order indices were approximately zero.

#### 9.4 Closing Remarks

As stated the goal of this chapter is to identify the inputs that influence the temperature gradient, specifically gradients induced by short-wave radiation gains that are known to lead to radiation-recrystallization. The snow temperatures were affected by a number of inputs and the relative importance shifted with evaluation time. However, considering the mid-day temperatures the snow temperatures were mainly affected by five parameters:  $T_s^{int}(4)$ ,  $LW(6)$ ,  $SW(7)$ ,  $\alpha(8)$ , and  $T_a(10)$ .

The broadest conclusion that may be drawn from the results presented in this chapter is that incoming long-wave radiation is the most influential parameter that effects snow temperature, temperature gradient, and “knee” related outputs. Also, that  $c_p(3)$ ,  $\kappa(5)$ , and  $RH(11)$  are negligible in this regard.

Another conclusion that may be drawn from the data presented in this chapter is that incoming short-wave radiation is a necessary, but secondary influence on the “knee” temperature gradient assumed to be associated with radiation-recrystallization. In general, three terms governed changes in the temperature gradient:  $\rho(1)$ ,  $k(2)$ , and  $LW(6)$ . And, only when interacting with one or more other parameters did  $SW(7)$  influence the gradient. This indicated that only in specific

situations did the “knee” gradient develop, defining these situations is the topic of Chapter 10.

The minimal influence of  $SW(7)$  was due to subsurface melting. Changes in  $SW(7)$  caused alterations in the extent of subsurface melting that occurred. This was evident in the sensitivity analyses focused on snow temperature that showed both  $SW(7)$  and  $\alpha(8)$  as dominant. However, the snow surface temperature, at least with respect to the model used here, was not affected by short-wave radiation to the extent of other parameters, namely  $LW(6)$ . Thus, when the gradient is considered both the subsurface temperature (near melting) and the surface temperature are not influenced significantly by changes in short-wave radiation. This finding indicates that the “knee” temperature gradient is often associated with subsurface melting. Based on the snow temperature results this melting occurs near a depth of 2 cm. The observed near-surface facets events provided in Chapter 4 present physical evidence of this behavior, as many of the events occurred under these conditions.



## CHAPTER 10

## MONTE CARLO SIMULATIONS OF NEAR-SURFACE FACETS

10.1 Introduction

Conceptually the process of near-surface faceting of snow is well understood, however the quantitative data detailing the conditions under which these crystals form is based on limited field and laboratory data. Using a simple thermal model, in Chapter 9 sensitivity analysis was employed to quantify the most influential model inputs on the snow temperatures and temperature gradients. The inputs included both snow properties and environmental conditions. Based on these results, through the use of Monte Carlo simulations, it is possible to examine specific quantities of each input that resulted in a specific output. This type of numerical analysis allows for an infinite number of input parameter combinations to be explored, which is impossible with physical experiments.

The results and analysis presented throughout this chapter aim to meet a single objective: to provide a graphical tool for assessing the likelihood of radiation-recrystallization based on snow and environmental conditions.

10.2 Methods

Details of the methods used in this section are provided in Chapter 7. The Monte Carlo simulations (Section 7.5) performed were constructed from the evaluations from the sensitivity analysis discussed in Chapter 9. The reference scheme defined in Section 9.2 is also used throughout this chapter. The input parameters discussed remain the same as in Chapters 7–9, these values are listed in Table 7.1. In total, 240,000 model evaluations were performed for each of the three locations: Control,

North, and South. Examining the data from such a large number of simulations required the use of highest density regions (see Section 7.6), which simply offer a means to encompass a percentage of the simulations by a region or contour.

In addition to the data generated from the simulations, three physically based data sets were used for comparison: (1) the near-surface facet events detailed in Chapter 3, (2) the laboratory experiments conducted by Morstad *et al.* (2007), and (3) laboratory experiments conducted by Slaughter *et al.* (2009). The laboratory data from Morstad *et al.* (2007) and Slaughter *et al.* (2009) is provided in Table 10.1. The bottom four entries in the table were conducted by Slaughter *et al.* (2009), which included six total experiments, but two were missing long-wave radiation data and thus excluded. The thermal conductivity ( $k$ ) values reported for this work were estimated from the measured density using the relationship proposed by Sturm *et al.* (1997). The work by Morstad *et al.* (2007) was the result of 13 laboratory experiments, 10 of which resulted in near-surface facet formation. The data in this table includes only the parameters used in this chapter, for complete results refer to Morstad (2004). The thermal diffusivity ( $\gamma$ ) was used here for convenience, where

$$\gamma = \frac{k}{\rho c_p}. \quad (10.1)$$

A constant value of  $c_p = 2030 \text{ J}/(\text{kg} \cdot \text{K})$  of ice was used for the calculations presented in Table 10.1. Diffusivity is presented with units of  $\text{m}^2/\text{s}$  were used throughout this chapter. The  $\Omega$  term is introduced in Section 10.4 as the ratio of  $SW(1 - \alpha)$  and  $LW$ .

Chapter 4 detailed 26 near-surface facet events observed at the South-facing weather station. The observations did not include micro-structural parameters, as such estimates for  $\rho$ ,  $k$ , and  $\alpha$  were required. Rather than use a single estimate

Table 10.1: Summary of results from laboratory experiments conducted by Morstad *et al.* (2007) and Slaughter *et al.* (2009).

Exp. #	Size mm	TG °C/m	SW W/m <sup>2</sup>	LW W/m <sup>2</sup>	$\alpha$	$\rho$ kg/m <sup>3</sup>	$k$ W/(m·K)	$\log(\gamma)$	$\Omega$
1		200	330	254	0.75	195	0.20	-6.30	0.32
2	1.0	350	595	273	0.81	174	0.10	-6.55	0.41
3	3/4	550	755	280	0.81	175	0.10	-6.55	0.51
4	1/2	400	1180	300	0.78	200	0.12	-6.53	0.87
5	1/4	400	755	280	0.76	250	0.18	-6.45	0.65
6	1/2	300	755	280	0.84	187	0.11	-6.54	0.43
7	1/2	150	755	280	0.85	270	0.20	-6.44	0.40
8		100	208	242	0.73	170	0.15	-6.36	0.23
9	1/4	170	755	280	0.79	257	0.40	-6.12	0.57
10	1/4	200	755	320	0.78	540	0.17	-6.81	0.52
11	1/8	200	755	280	0.78	410	0.75	-6.05	0.59
12		20	0	207		303	0.25	-6.39	
13	1/2	200	755	280	0.75	300	0.25	-6.39	0.67
Feb14#3			443	315	0.92	284	0.11	-6.71	0.11
Mar6			701	272	0.87	350	0.18	-6.59	0.34
Apr#1			679	286	0.91	284	0.11	-6.71	0.21
Apr3#2			638	330	0.89	320	0.15	-6.65	0.21

of these properties a range of values was assigned based on published data, thus a confidence region was defined to encapsulate the observed events.

Nearly all the measured near-surface facet events reported in Chapter 4 occurred after recent snowfall events, thus a density range was assigned as such. Armstrong and Brun (2008, p. 59) state that newly fallen snow typically ranges between 60 kg/m<sup>3</sup> and 120 kg/m<sup>3</sup>. Using the raw data from the entire body of thermal conductivity measurements presented by Sturm *et al.* (1997, Fig. 4),  $k$  was assumed to vary from 0.04–0.25 W/(m·K). The specific heat capacity is assumed to be a constant value of  $c_p = 2030$  J/(kg·K). For the estimated range of  $\gamma$ , both  $\rho$  and  $k$  were assumed to vary according to a normal distribution such that the aforementioned limits were at the 95% tails (i.e., two standard deviations from the mean). This resulted in  $\log(\gamma)$  having an estimated range of -6.57 to -5.81.

To determine the range of  $\alpha$ , first it was assumed the new snow metamorphosed into facets of class 1, 2, or 3 (Armstrong and Brun, 2008, p. 28). This assumption allowed for tabulated values (see Armstrong and Brun (2008, p. 57)) of  $\alpha$  to be utilized for determining the possible extent of  $\alpha$ . However, the tabulated data alone is insufficient due to the wavelength dependence of albedo. Using a weighted average determined from the various wavebands defined by ASTM G-173 (see Section 5.4) and the tabulated values of Armstrong and Brun (2008, p. 57),  $\alpha$  is assumed to range from 0.8–0.87.

As discussed in Chapter 4, the long-wave radiation sensors used during the 2007/2008 winter season were influenced by preferential heating from incoming short-wave radiation, particularly at the south-facing slope. This problem was corrected in the 2008/2009 data. The histogram of Figure 10.1 is an illustration of the long-wave radiation data that highlights the difference in the recorded values between the two seasons. To account for this problem a correction is applied to the 2007/2008 data based on a comparison with the American Spirit (Aspirit) radiation data (see Chapter 4). The mean daily incoming long-wave radiation values of the events at the South Station were 2.07 times that of Aspirit during the 2007/2008 season and 1.11 for the 2008/2009 season (see Table 4.2). Assuming the 2008/2009 ratio applies to the previous season, the long-wave values reported in Table 4.2 were reduced by a factor of 0.54 (1.11/2.07) for usage in the analysis presented here.

### 10.3 Results

Near-surface facets are known to form with significant temperature gradients, the values reported in the literature range from approximately 100–600 °C/m (Fukuzawa and Akitaya, 1993; Hardy *et al.*, 2001; Morstad *et al.*, 2007; Slaughter *et al.*, 2009).

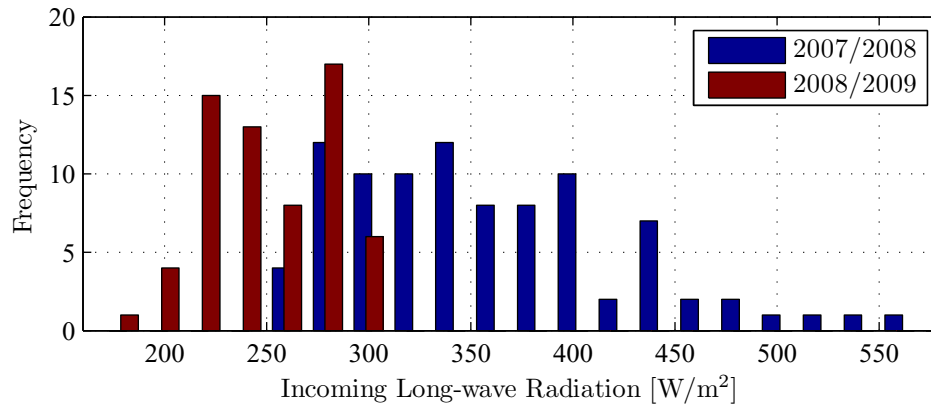


Figure 10.1: Comparison between the two seasons (2007/2008 and 2008/2009) of recorded long-wave radiation values for near-surface facet events.

The data presented from Morstad *et al.* (2007) in Table 10.1 indicates that gradients on the order of 100 °C/m may be inadequate (Exp. #8). One experiment is of little value for making such a claim, but this statement gains traction considering the work of Pinzer and Schneebeli (2009). Their work provides additional evidence that on time scales of less than a day that “temperature gradients on the order of 100 °C/m do not lead necessarily to faceting...” Considering that the simulations presented here only spanned 10 hours, a lower limit of 200 °C/m was assumed to be necessary for facet formation to occur. This is in agreement with observations in Chapter 4 as well as in Slaughter *et al.* (2009). The upper limit was assumed to remain at 600 °C/m. Values larger than this were observed in the simulations but assumed to be unrealistic.

In Chapter 10, the temperature gradient (both  $TG2$  and  $KTG$ ) was demonstrated to be primarily affected by  $\rho$ ,  $k$ , and  $LW$ . Additionally, relying on the results from sensitivity analysis of  $KTG^{mid}$ , four other terms influence the gradient for the Control and South locations:  $SW$ ,  $\alpha$ ,  $V_w$ , and  $T_a$ . However, as discussed in the analysis in Section 10.4, the  $V_w$  and  $T_a$  were not utilized. Therefore, the remainder of the results

focused on five parameters listed— $\rho$ ,  $k$ ,  $LW$ ,  $SW$ , and  $\alpha$ —as well as the above temperature gradient range.

The input parameters under investigation were divided into two groups: snow properties ( $\rho$ ,  $k$ , and  $\alpha$ ) and radiation input ( $SW$  and  $LW$ ). Based on the  $KTG^{mid}$  values these five inputs were limited to values with a  $KTG^{mid}$  from 200–600 °C/m resulting from the simulations. Limiting the data as such reduced the simulations considered to 27,893 (11.6%), 24,251 (10.1%), and 22,257 (9.3%) for the Control, North, and South locations, respectively. Estimated probability distribution functions (PDFs) for the snow properties are provided in Figure 10.2 and for the radiation inputs in Figure 10.3. Each graph includes the PDFs for the complete (all) input data set and the limited data (limited). For the snow properties the “all” input distributions do not differ between the locations. The PDFs were computed via the kernel estimate method, see Section 7.7.

Negative values appeared in the PDFs of  $\rho$ ,  $k$ , and  $SW$ , which is impossible considering the parameters. However, this was strictly a graphical issue due to the computation method used, which was only employed to visualize the results, no numerical computations used these distributions.

As shown in Figures 10.2 and 10.3, the PDFs had various differences, which were compared in two ways: (1) for each location and input parameter the complete input was compared with the  $KTG^{mid}$  limited data and (2) the limited data for each parameter was compared across the locations (e.g., the limited data from the Control locations was compared with the limited data from the South location). In all cases, despite apparent similarities—such as for  $\rho$  in Figure 10.2a—statistically the distributions are different. Using the Kolmogorov-Smirnov test (KS-test; see Section 7.8), a  $p$ -value of approximately zero for each comparison was computed.

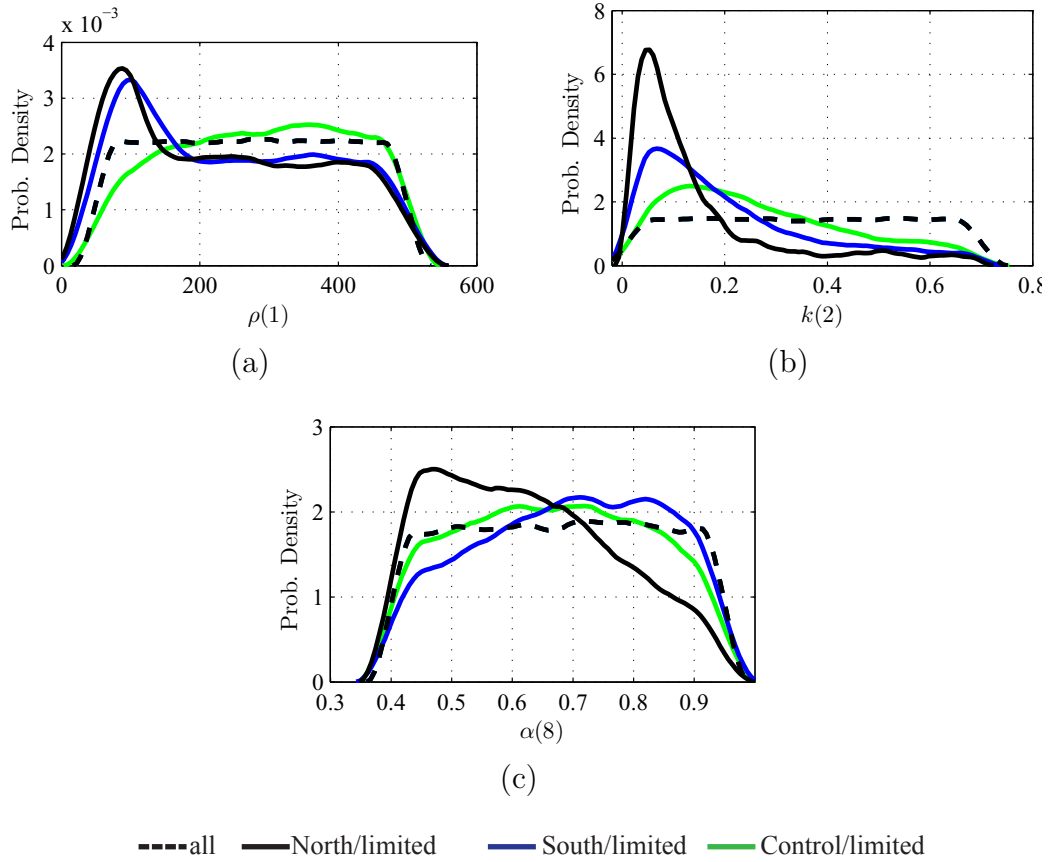
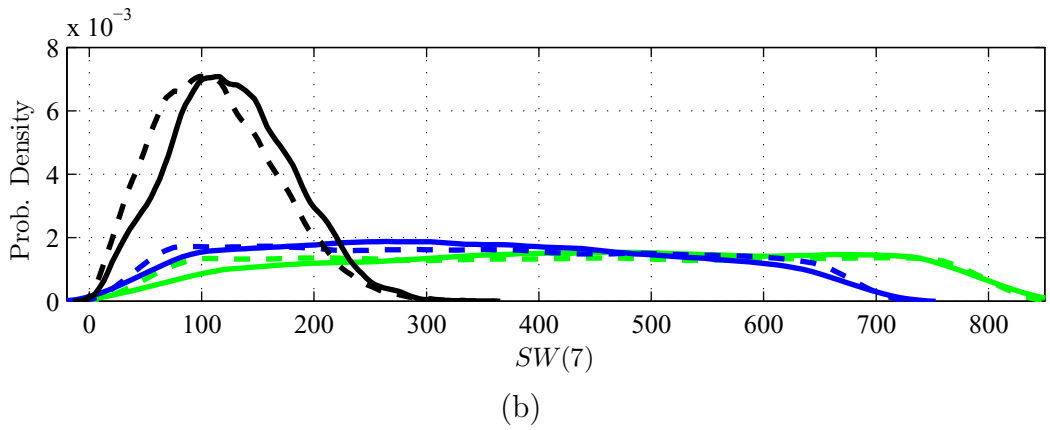
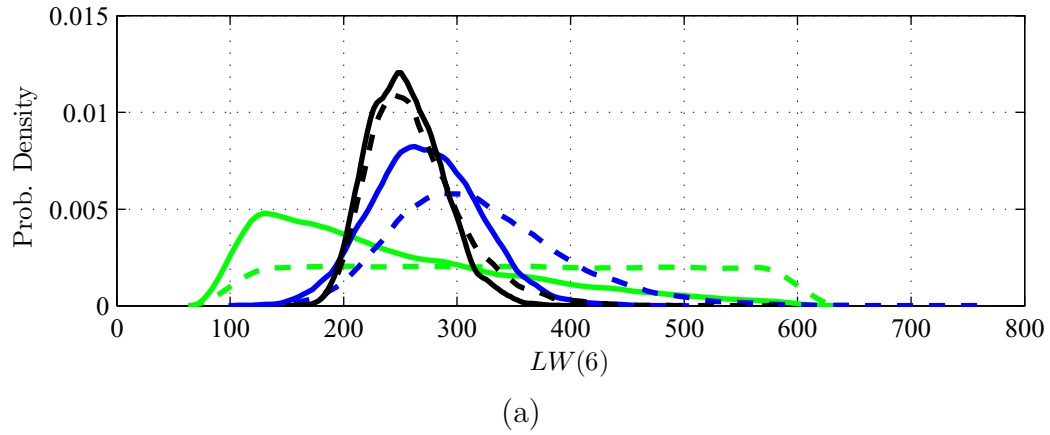


Figure 10.2: Probability distribution functions for snow properties including the complete (all) input distribution and data limited by  $KTG^{mid}$  from 200–600 °C/m (limited) . Table 7.1 (p. 163) defines the variables and the units for each graph.

Visually, substantial changes in the distributions occurred. The most notable change was the spike in probability density for values of  $\rho$  near 100 kg/m<sup>3</sup> for the North and South locations. This spike was not observed in the Control location data and the probability density actually became lower in that same region. Thermal conductivity ( $k$ ) yielded drastically different distributions for all locations and incoming short-wave radiation showed little change.



-----North/all    —North/limited    - - - - -South/all    —South/limited    - - - - -Control/all    —Control/limited

Figure 10.3: Probability distribution functions for radiation inputs including the complete (all) input distribution and data limited by  $KTG^{mid}$  from 200–600 °C/m (limited) . Table 7.1 (p. 163) defines the variables and the units for each graph.

#### 10.4 Discussion

Based on the sensitivity analysis of Chapter 9,  $\rho$ ,  $k$ , and  $LW$  were determined to be the influential parameters on temperature gradient, particularly the “knee” gradient typical of radiation-recrystallization. Hence, a simple function was defined using the thermal diffusivity ( $\gamma$ ) as

$$TG \approx f(\gamma, LW), \quad (10.2)$$



where  $TG$  is used as a generic temperature gradient not associated with any specific computation method such as  $KTG$  or  $TG2$ . Including the specific heat,  $c_p$ , was simply a natural selection when grouping  $\rho$  and  $k$ .

Conceptually, Equation 10.2 seems lacking, considering the focus of this research is radiation-recrystallization, so naturally the incoming short-wave should be included. Excluding short-wave radiation, as well as the albedo negates, the North and South data sets for practical application, since there is nothing to distinguish the locations. An unexpected result was the number of resulting simulations with  $KTG^{mid}$  limited from 200–600 °C/m: 10.1% and 9.3% for the North and South locations, respectively. Intuitively, the South location should yield a larger portion of “knee” gradients. The likely culprit behind this result was the range of  $\alpha$  assumed, which was 0.4–0.9. Examining Figure 10.2c demonstrates that the North location favors low values and the South high values of  $\alpha$ . Therefore, it is assumed here that the important parameter to consider is the absorbed short-wave radiation. When combined with  $LW$  a convenient dimensionless term arises:

$$\Omega = \frac{SW}{LW}(1 - \alpha). \quad (10.3)$$

Therefore, Equation 10.2 is redefined as

$$TG \approx f(\gamma, \Omega). \quad (10.4)$$

Including the  $SW$  and  $\alpha$  terms is not only natural but offers some statistical advantage—although only a small advantage considering the sensitivity analysis—since the variability associated with these terms is included.

Similarly, if  $V_w$  and  $T_a$  were included all of the variance in the system would be accounted for since no other input terms would remain that influenced the variance of  $KTG^{mid}$ , refer to Figure 9.1. In this case,  $TG = f(\rho, k, LW, SW, \alpha, V_w, T_a)$ , notice the approximation sign used in Equation (10.4) would be inappropriate for this complete

equation. The sensitivity analysis demonstrated, at least with respect to the model and  $KTG^{mid}$  output considered, that only these seven terms alone caused changes in the temperature gradient. An attempt was made to analyze all the parameters, but it was deemed impractical and made an already complex analysis even more so. Therefore, the relationship defined in Equation 10.4 was used for the remainder of the analysis presented.

### 10.5 Analysis

Using Equation 10.4, the Monte Carlo simulation inputs and temperature gradient output were simplified to a three-dimensional data set. First, the inputs of  $\gamma$  and  $LW$  are compared in similar fashion as done in the previous section. However, here the variables are considered together using two-dimensional PDFs, as shown in Figure 10.4.

Visually these 2-D PDFs illustrate the most profound difference in the complete data set and the data limited by  $KTG^{mid}$  from 200–600 °C/m, the bi-modal behavior. The low point or saddle of the bi-modal distributions coincided with the peak of the complete data set. This indicates that the most common value of  $\gamma$  in the simulations is unfavorable for the developing a strong temperature gradient. The 2-D PDFs in Figure 10.4 were the basis of the end result of the work presented in this chapter that includes comparison with field and laboratory measurements of near-surface facets. However, before continuing it is important to explain that the full analysis of Equation 10.4 requires a tri-variate PDF. An example of which is presented in Figure 10.5.

The tri-variate, 38% HDR for the South location is provided in Figure 10.5. The 38% HDR was selected because it is akin to a confidence level of  $\pm\frac{1}{2}\sigma$  for a normal distribution (i.e., a probable outcome), where  $\sigma$  is the standard deviation. In this

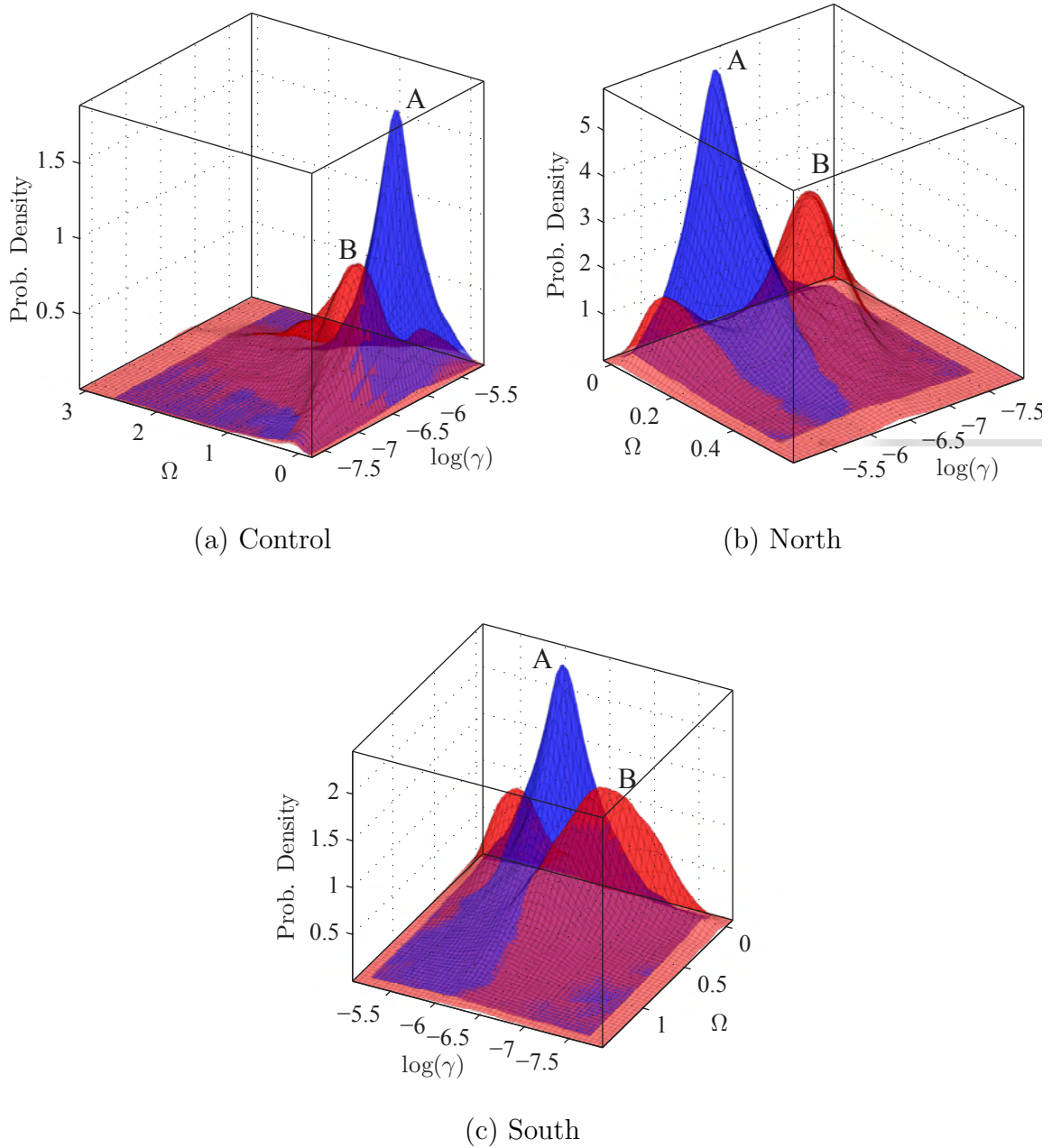


Figure 10.4: Comparison of the complete input (A) with the input limited by  $KTG^{mid}$  from 200–600°C/m (B) for the (a) Control, (b) North, and (c) South locations.

figure the  $TG2^{mid}$  output comprises the vertical axis because it produced output for the complete data set. The limited data was still based on the  $KTG^{mid}$  criteria, but the associated  $TG2^{mid}$  quantities were displayed for consistency. The two regions of

the limited data, clearly shows the bi-modal behavior of the data, which indicated that there are two regions of  $\Omega$  and  $\gamma$  likely to induce significant “knee” temperature gradients.

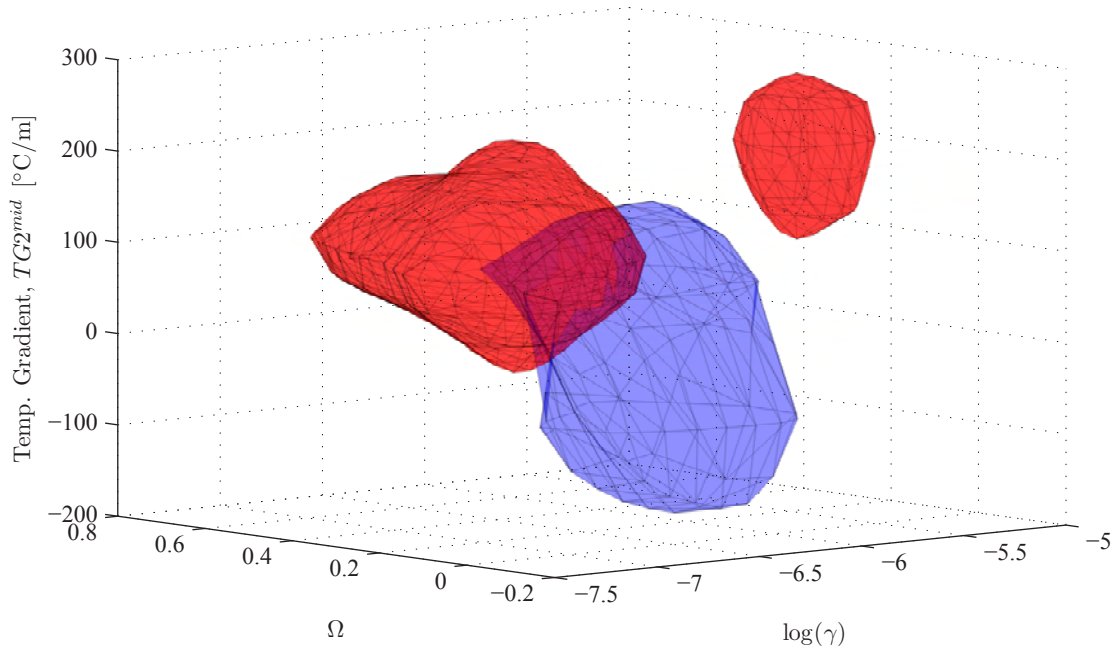


Figure 10.5: Comparison of tri-variate PDF of all input (A) with the input limited by  $KTG^{mid}$  from 200–600°C/m (B) for the South location.

In any dimension, one, two, or three, the PDFs presented throughout this chapter may be thought of in the same fashion. Consider the  $KTG^{mid}$  limited distribution for the South location presented in Figure 10.4 and the following hypothetical situation. If  $\gamma$  was determined to be approximately  $10^{-6}$ , then the most likely scenario to lead to gradients of 200–600 °C/m would be an  $\Omega$  of approximately 0.17, which is located in the depression between the two peaks. Based on a comparison with the other probability densities it is then possible to assess how likely it is that a gradient will develop. Even at the peak of the distributions it is never possible to state, with certainty, that the gradient will develop because the data includes additional variance. Sources of additional variance included: known variance in terms not considered such

as  $T_a$  and  $V_w$ , unknown variance due to uncertainty associated with the sensitivity analyses (i.e., the error bars shown throughout Chapter 9), and errors associated with the non-infinite sample size in the Monte Carlo simulations.

Control Location: Contour plots computed from the 2-D probability distributions in Figure 10.4 were computed. First, the Control results are considered, as presented in Figure 10.6. The contours are composed of the 95%, 68%, 38%, 20%, and 10% HDRs. These ranges were selected because they were approximately proportional to confidence levels typically associated with a normal distribution. And, if the data was normally distributed these HDRs would be equivalent to  $2\sigma$ ,  $1\sigma$ ,  $\frac{1}{2}\sigma$ ,  $\frac{1}{4}\sigma$ , and  $\frac{1}{8}\sigma$  confidence regions.

The region labeled “field” estimates the location of all 26 observations from the field data presented in Chapter 4. The regions were defined using the ranges for  $\gamma$  and  $\alpha$  defined in Section 10.2. Assuming a uniform distribution for these terms, these distributions were sampled 10,000 times for each observed event, thus constructing a synthetic set of data of likely values from which the 95% HDR was computed. Simply stated, the field observations likely fall somewhere within this region.

Statistically comparing the Monte Carlo simulation computed HDRs with the observed laboratory and field near-surface facets is not appropriate. The laboratory data of Morstad *et al.* (2007) was exploratory in nature so the conditions were explicitly selected based on success of facet formation. However, nearly all of the laboratory experiments shown are within the 38% HDR. On the other hand, two of these points (Exp. #1 and #8) did not result in near-surface facet formation, but considering how tight the contours are in this region, a small error in  $\Omega$  could shift these parameters outside of the most probable regions.

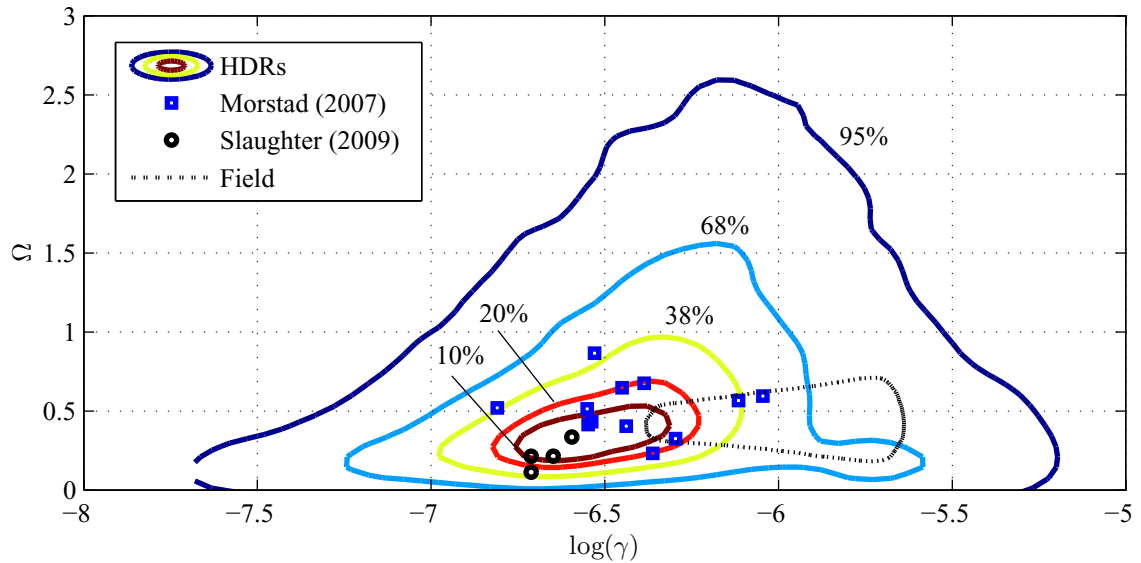


Figure 10.6: Contour plot of HDRs for the Control results including the field observations from Chapter 4 and laboratory data of Morstad *et al.* (2007) and Slaughter *et al.* (2009).

Although only composed of four experiments, the data presented by Slaughter *et al.* (2009) were all near the center of the regions. Since these laboratory experiments were based on observed events from the South-facing weather station (see Chapter 4) it is reasonable to expect these values to be well predicted by the Monte Carlo simulations. However, such is not the case for the field estimate region presented, which did not seem to align well with the regions.

North Location: Figure 10.7 includes the Monte Carlo simulations results computed from the North location. Generally, the observed field and laboratory data match poorly with the results from the North location, which is expected considering that much of the physical data was developed by examining data from the South-facing weather station. The North HDR regions are skewed to lower values of  $\Omega$  when compared to the Control results of Figure 10.6, this is expected considering the lower values of  $\alpha$  observed in Figure 10.2c.

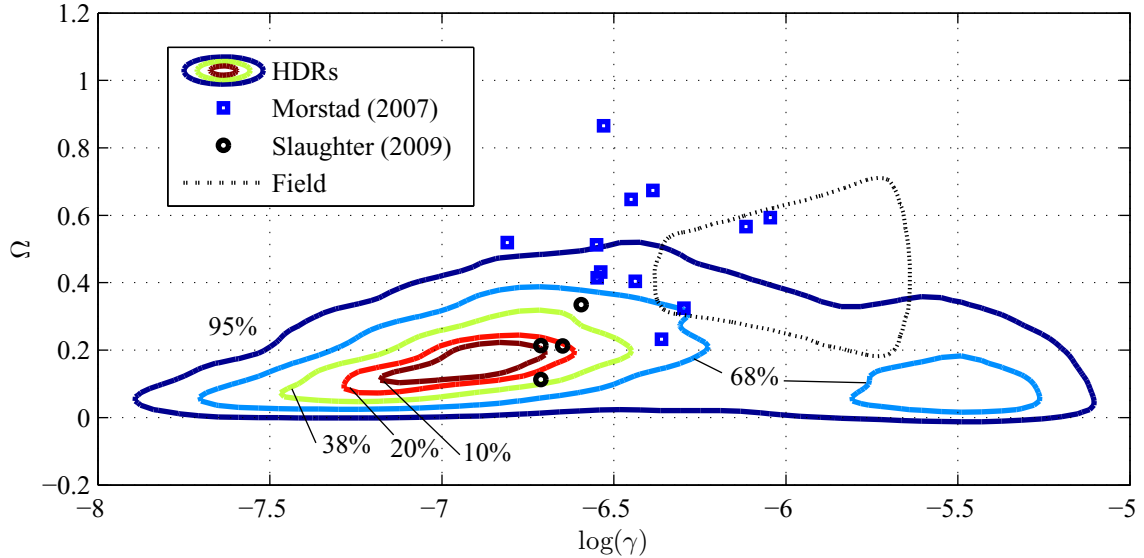


Figure 10.7: Contour plot of HDRs for the North location including the field observations from Chapter 4 and laboratory data of Morstad *et al.* (2007) and Slaughter *et al.* (2009).

South Location: The results from the South location were the most intriguing. As shown in Figure 10.8, the bi-modal behavior observed is the most prominent in this data set. This is evident by the 38% and 20% HDRs located with  $\gamma \approx 10^{-5.6}$ . Unfortunately, the correlation with the laboratory data and field data in this region is weak, so it is not possible to make any definitive statements. Visually, the laboratory experiments particularly those conducted by Morstad *et al.* (2007) do not seem to correlate.

It is important to point out that the most probable regions for both the North and South locations (Figures 10.7 and 10.8) were similar to the Control set. In fact, in direct comparison the North and South data appear to be subsets of the Control location. This is expected considering the Control input was designed to a generic unbiased approach with the North and South being oriented, as their name suggests, with different aspects.

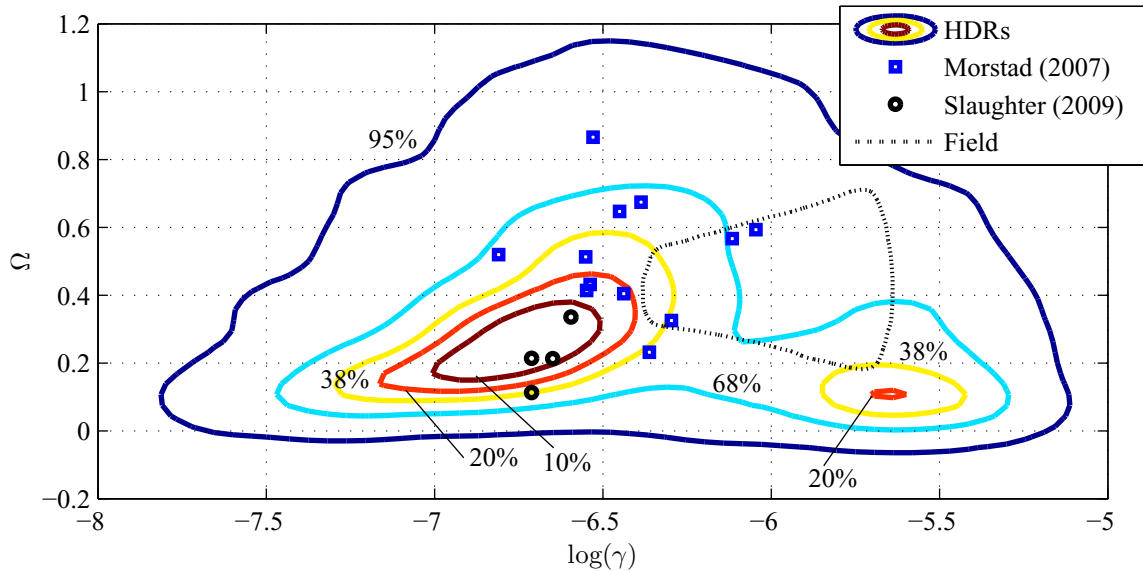


Figure 10.8: Contour plot of HDRs for the South location including the field observations from Chapter 4 and laboratory data of Morstad *et al.* (2007) and Slaughter *et al.* (2009).

Returning to the bi-modality of the data observed. Conceptually the reality of this behavior may be explored. Figure 10.9 is a reconstruction of a figure presented by Sturm *et al.* (1997) relating  $\rho$  and  $k$ , but here it also includes the value of  $\gamma$  associated as well as two relationships commonly used for relating  $\rho$  and  $k$ . Consider the larger of the two spikes in the probability distribution function, which occurred with values of  $\gamma$  approximately from  $10^{-7.25}$ – $10^{-6.25}$ . The other peak occurred with  $\gamma \approx 10^{-5.6}$ . Using Figure 10.9, the first range is in the realm of reasonable values of  $\gamma$ , especially when compared to the raw data presented by Sturm *et al.* (1997, Fig. 4).

The second peak was associated with low density snow with high  $k$  values, which is counter intuitive, i.e., based on the typical relationships used for relating conductivity and density. The data presented in Chapter 4 indicated facets commonly form in low-density snow. The only observed data to approach this region in the numerical results was the field observations. And, since this field data region was constructed assuming



typical  $\rho$ - $k$  relationship this misalignment is expected. Hence, this second region may be physical evidence that supports the existence of the low-density, high-conductivity region. This conclusion is not unfounded, theoretically  $k$  used here can be assumed to be due to any mode of heat transfer such as conduction or vapor diffusion. In fact, this deviation from the typical  $\rho$ - $k$  relationship is discussed to some extent by Sturm *et al.* (1997).

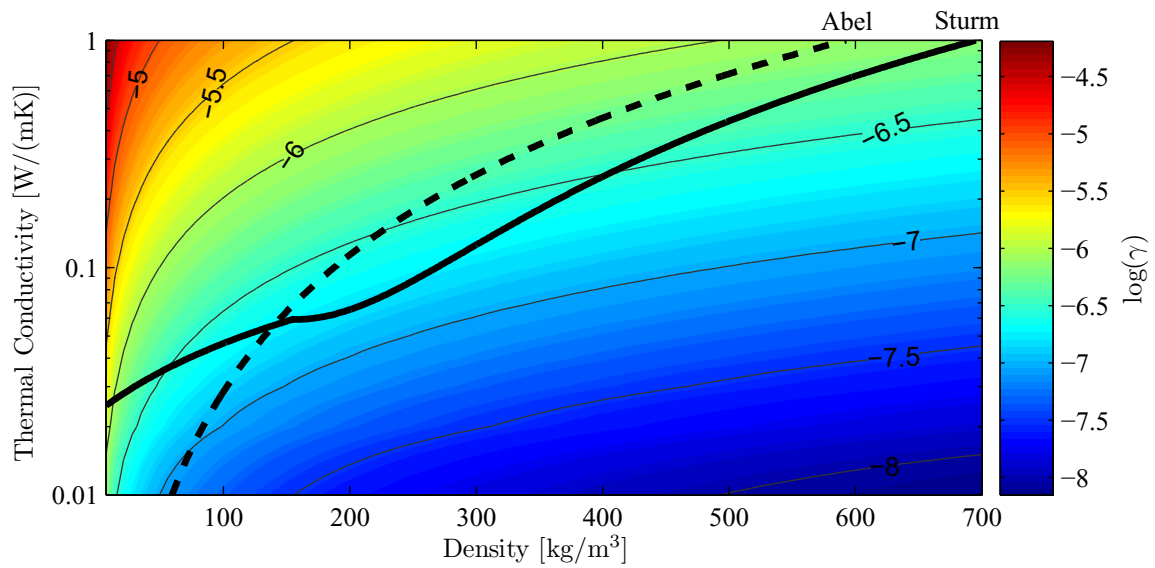


Figure 10.9: Chart showing the relationship of  $\rho$ ,  $k$ , and  $\gamma$  as well as two commonly utilized  $\rho$  and  $k$  relationships as presented by Sturm *et al.* (1997).

### 10.6 Closing Remarks

The main objective of this chapter was to present a tool for assessing near-surface faceting due to radiation-recrystallization, which was accomplished with Figures 10.6–10.8. These figures related the non-dimensional term  $\Omega$  to thermal diffusivity ( $\gamma$ ). Based on the numerical simulations performed it was possible to define the ideal conditions that lead to strong temperature gradients (200–600 °C/m) that have a temperature profile conducive to radiation-recrystallization. In the most general case,

irrespective of aspect, the optimum region for facet formation is  $\Omega$  from 0.2–0.5 and  $\gamma$  from  $10^{-6.3}$ – $10^{-6.7}$ . If aspect is considered these levels shift, for the North location the ideal conditions are  $\Omega$  from 0.1–0.2 and  $\gamma$  from  $10^{-6.3}$ – $10^{-7.2}$  and for the South location  $\Omega$  ranges from 0.2–0.4 and  $\gamma$  from  $10^{-6.5}$ – $10^{-7}$ .

Qualitatively, these results matched reasonably well with observed values for both laboratory and field observations of near-surface facet formation. A strict, statistical comparison was not possible due to the nature of the observed data. Hence, the regions defined are not a definitive answer to the question of when near-surface facets form. The regions are defined to offer a postulate that these regions are of importance and require further research. Of particular interest are the two discrete regions mainly observed in the South location results that indicated that near-surface facets form generally under two scenarios: (1) with  $\rho$  and  $k$  following the basic trend of traditional regression based relationships and (2) with low-density, high-thermal conductivity snow, a postulate that is supported by the results presented in Chapter 4 of this dissertation. That is, low-density snow subjected to a strong temperature gradient includes significant heat-transfer due to vapor diffusion, thus the effective thermal conductivity may be higher than expected.

## CHAPTER 11

### CONCLUSIONS

The review provided in Chapter 2 demonstrates the importance of studying the metamorphic processes in snow, particularly surface hoar and near-surface facets. This review set the stage for the main objective of the work presented in this dissertation: to further quantify the necessary conditions for the formation of both surface hoar and near-surface facets.

To this end, weather stations and observations were established on a north- and south-facing slope in southwest Montana. Throughout two winter seasons, 14 surface hoar and 26 near-surface facet events were observed at one or both of the stations. Beginning with the surface hoar events, see Chapter 3, it was determined that three environmental parameters were statistically significant in leading to their formation: long-wave radiation, snow temperature, and relative humidity. Based on percentiles of recorded events, the ideal conditions to cause surface hoar formation were nightly mean values of long-wave radiation of  $220 \text{ W/m}^2$ , snow temperature of  $-16 \text{ }^\circ\text{C}$ , and relative humidity of 65%.

In the case of near-surface facets, 26 events were observed during the two winter seasons that data was collected, see Chapter 4. However, in this case the crystals almost exclusively formed at the South weather station and were due to radiation-recrystallization. The prevalence of near-surface facets formed due to radiation indicated that the conditions in southwest Montana are sufficient for the development of these crystals. A comparison of the mean daily values of all days with the values from days with near-surface facet events suggested three parameters were statistically significant: short- and long-wave radiation and relative humidity. Again, based on percentiles of the observed events, the optimum conditions for facet formation, using

mean daily values at the South-facing weather station, were short-wave radiation of  $620 \text{ W/m}^2$ , long-wave radiation of  $220 \text{ W/m}^2$ , and relative humidity of 49%.

Using a thermal model (Chapter 5) and various numerical analysis techniques (Chapters 6 and 7), an analytical investigation was conducted to meet the main objective for both surface hoar formation (Chapter 8) and near-surface formation due to radiation recrystallization (Chapters 9 and 10). In general, the surface hoar analysis (Chapter 8) indicated that long-wave radiation and air temperature were the most influential inputs affecting positive mass-fluxes at the snow surface; these terms alone attributed to over 50% of the variance observed in positive values of mass-flux. Also, Figures 8.9 and 8.12 were presented as possible tools for assessing if the conditions are conducive to surface hoar formation. For example, at north-facing aspects the following optimum conditions were presented: long-wave radiation from  $200\text{--}250 \text{ W/m}^2$  and  $\Pi$  from  $10^{2.5}\text{--}10^{-1.7}$  (see Figure 8.12), where  $\Pi$  is defined in Equation (8.2). However, with respect to surface hoar size, mass-flux alone is inadequate for determining the size of the crystals.

The results obtained for near-surface facets indicated that three parameters—snow density, thermal conductivity, and incoming long-wave radiation—were the most influential on the presence of a temperature gradient conducive to radiation-recrystallization. In similar fashion as for surface hoar, Figures 10.6–10.8 were presented as tools for assessing the likelihood of facet formation. In the most general case, irrespective of aspect, the optimum region for facet formation is  $\Omega = \frac{SW}{LW}(1 - \alpha)$  from  $0.2\text{--}0.5$  and  $\gamma$  from  $10^{-6.3}\text{--}10^{-6.7}$ , where  $\Omega$  is defined by Equation (10.4) and  $\gamma$  is the thermal diffusivity of the snow. If aspect is considered these levels shift; for north-facing aspects the ideal conditions are  $\Omega$  from  $0.1\text{--}0.2$  and  $\gamma$  from  $10^{-6.3}\text{--}10^{-7.2}$  and for south-facing aspects  $\Omega$  from  $0.2\text{--}0.4$  and  $\gamma$  from  $10^{-6.5}\text{--}10^{-7}$ .

Perhaps the most interesting result obtained throughout this dissertation was the region of low-density, high-thermal conductivity snow conducive to the development of near-surface facets (see Figure 10.8). Traditional relationships of density and thermal conductivity, i.e., those defined by Sturm *et al.* (1997) indicate that this scenario is unlikely. However, the analysis presented throughout this dissertation made no assumptions regarding the mode of thermal conductivity. Thus, if heat transport due to water vapor diffusion is significant, this density and thermal conductivity may be reasonable. Considering that the majority of the observed near-surface facet events described in Chapter 4 occurred with recently fallen snow, this scenario is likely a real phenomenon.

If only one conclusion should be drawn from the work presented, it is the importance of incoming long-wave radiation. Throughout the entire dissertation long-wave radiation appeared as a dominant factor for both surface hoar and near-surface facets. As presented here, long-wave is a crucial parameter and should be the focus of additional research.

Finally, both sensitivity analysis and Monte Carlo simulations were presented here as a tool for examining the conditions important to snow morphologies. And, the work presented only scratches the surface of the potential use of these methods to improve the current understanding of the most influential terms. Additional research should be conducted exploring a variety of scenarios including layered snowpack, melt-layers, and diurnal fluctuations to name a few. Furthermore, the analysis should be applied to more detailed models such as SNOWPACK that include micro-structure parameters. The potential applications are only limited by computation time and imagination.

REFERENCES CITED

- Adams, E. and Brown, R. (1982a). Further results on studies of temperature-gradient metamorphism. *Journal of Glaciology*, **28**(98).
- Adams, E. and Brown, R. (1982b). A model for crystal development in dry snow. *Geophysical Research Letters*, **9**(11), 1287–1289.
- Adams, E. and Brown, R. (1983). Metamorphism of dry snow as a result of temperature gradient and vapor density differences. *Annals of Glaciology*, **4**.
- Adams, E. and Brown, R. (1989). A constitutive theory for snow as a continuous multiphase mixture. *International Journal of Multiphase Flow*, **15**(4), 553–572.
- Adams, E. and Brown, R. (1990). A mixture theory for evaluating heat and mass transport processes in nonhomogeneous snow. *Continuum Mechanics and Thermodynamics*, **2**, 31–63.
- Adams, E. and Sato, A. (1993). Model for effective thermal conductivity of a dry snow cover composed of uniform ice spheres. *Annals of Glaciology*, **18**.
- Adams, E., McKittrick, L., Slaughter, A., Staron, P., Shertzer, R., Miller, D., Leonard, T., McCabe, D., Henninger, I., Catherine, D., Cooperstein, M., and Laveck, K. (2009). Modeling variation of surface hoar and radiation recrystallization across a slope. In *International Snow Science Workshop*, Davos, CH.
- Akitaya, E. and Shimizu, H. (1987). Observations of weak layers in a snow cover. *Low temperature science. Series A, Physical sciences*, **46**, 67–75.
- Albrecht, B. and Cox, S. (1977). Procedures for improving pyrgeometer performance. *Journal of Applied Meteorology*, **16**, 188–197.
- Ansari, A. and Bradley, R. (1960). Rank-sum tests for dispersions. *The Annals of Mathematical Statistics*, **31**(4), 1174–1189.
- Armstrong, R. (1985). *Metamorphism in a subfreezing, seasonal snow cover: The role of thermal and vapor pressure conditions*. Ph.D. thesis, University of Colorado.
- Armstrong, R. L. and Brun, E. (2008). *Snow and Climate: Physical Processes, Surface Energy Exchange, and Modeling*. Cambridge University Press.
- ASTM G-173 (2003). Standard tables for reference solar spectral irradiances: Direct normal and hemispherical on 37° tilted surface. ASTM International.
- Bader, H. and Weilenmann, P. (1992). Modeling temperature distribution, energy and mass flow in a (phase-changing) snowpack. I. Model and case studies. *Cold Regions Science and Technology*, **20**, 157–181.

- Baldrige, A., Hook, S., Grove, C., and Rivera, G. (2009). The ASTER spectral library version 2.0. *Remote Sensing of Environment*, **113**(4), 711–715.
- Bartelt, P. and Lehning, M. (2002). A physical snowpack model for the swiss avalanche warning. Part 1: numerical model. *Cold Regions Science and Technology*, **35**, 123–145.
- Bartelt, P., Buser, O., and Sokratov, S. A. (2004). A nonequilibrium treatment of heat and mass transfers in alpine snowcovers. *Cold Regions Science and Technology*, **39**, 219–242.
- Bejan, A. (1997). *Advanced engineering thermodynamics*. Wiley New York.
- Birkeland, K. W. (1998). Terminology and predominant processes associated with the formation of weak layers of near-surface faceted crystals in the mountain snowpack. *Arctic and Alpine Research*, **30**(2), 193–199.
- Birkeland, K. W., Johnson, R. F., and Schmidt, D. S. (1996). Near-surface faceted crystals: Conditions necessary for growth and contribution to avalanche formation, Southwest Montana, U.S.A. In *In Proceedings: International Snow Science Workshop*, Banff, AB.
- Birkeland, K. W., Johnson, R. F., and Schmidt, D. S. (1998). Near-surface facet crystals formed by diurnal recrystallization: A case study of weak layer formation in the mountain snowpack and its contribution to snow avalanches. *Arctic and Alpine Research*, **30**(2), 200–204.
- Bohren, C. and Barkstrom, B. (1974). Theory of the optical properties of snow. *Journal of Geophysical Research*, **79**(30).
- Boone, A. and Etchevers, P. (2001). An intercomparison of three schemes of varying complexity coupled to the same land surface model: local-scale evaluation at an alpine site. *Journal of Hydrometeorology*, **2**, 374–394.
- Breyfogle, S. (1986). Growth characteristics of hoarfrost with respect to avalanche occurrence. In *International Snow Science Workshop*, Tahoe.
- Brown, R., Adams, E., and Barber, M. (1994). Non-equilibrium thermodynamics applied to metamorphism of snow. In *Proceedings of Snowsymp - 94*, Manali, H.P., India.
- Brown, R., Edens, M., and Barber, M. (1999). Mixture theory of mass transfer based upon microstructure. *Defense Science Journal*, **49**(5), 393–409.
- Brun, E., David, P., Sudul, M., and Brunot, G. (1992). A numerical model to simulate snow-cover stratigraphy for operational avalanche forecasting. *Journal of Glaciology*, **38**(128), 13–22.



- Cacuci, D. G. (2003). *Volume I: Sensitivity and Uncertainty Analysis Theory*. Chapman and Hall/CRC.
- CAIC (2010). Colorado Avalanche Information Center - Avalanche Statistics.
- Calanca, P. (2001). A note on the roughness length for temperature over melting snow and ice. *Quarterly Journal of the Royal Meteorological Society*, **127**(571).
- Chan, K., Saltelli, A., and Tarantola, S. (1997). Sensitivity analysis of model output: Variance-based methods make the difference. In *In Proceedings: Winter Simulation Conference*.
- Chan, K.-S., Tarantola, S., Saltelli, A., and Sobol, I. M. (2000). *Sensitivity Analysis*, chapter 8: Variance-Based Methods, pages 167–197. John Wiley & Sons, Inc.
- Chapra, S. (2005). *Applied Numerical Methods with MATLAB for Engineers and Scientists*. McGraw-Hill.
- Chapra, S. and Canale, R. (2002). *Numerical methods for engineers*. McGraw-Hill, 4th edition.
- CIE (1989). Solar spectral irradiance. Technical Report 85, International Commission of Illumination.
- Colbeck, S. (1988). On the micrometeorology of surface hoar growth on snow in mountainous area. *Boundary-Layer Meteorology*, **44**, 1–12.
- Colbeck, S. (1989). Snow-crystal growth with varying surface temperatures and radiation penetration. *Journal of Glaciology*, **35**(119), 23–29.
- Colbeck, S., Jamieson, B., and Crowe, S. (2008). An attempt to describe the mechanism of surface hoar growth from valley clouds. *Cold Regions Science and Technology*, **54**(2), 83–88.
- Collins, D. C. and Avissar, R. (1994). An evaluation with the Fourier Amplitude Sensitivity Test (FAST) of which land-surface parameters are of greatest importance in atmospheric modeling. *American Meteorological Society*, **7**, 681–703.
- Colonna, G., Longo, S., Esposito, F., and Capitelly, M. (1994). Fourier-transform sensitivity analysis: Application to XeCl self-sustained discharge-laser kinetics. *Applied Physics B, Laser and Optics*, **59**, 61–72.
- Cooperstein, M. S., Birkeland, K. W., and Hansen, K. J. (2004). The effects of slope aspect on the formation of surface hoar and diurnally recrystallized near-surface faceted crystals: Implications for avalanche forecasting. In *International Snow Science Workshop*, pages 83–93, Jackson Hole, Wyoming.

- Cukier, R., Fortuin, C., Shuler, K., Petschek, A., and Schaibly, J. (1973). Study of the sensitivity of coupled reaction systems to uncertainties in rate coefficients. I Theory. *The Journal of Chemical Physics*, **59**, 3873–3878.
- Cukier, R., Schaibly, J., and Shuler, K. (1975). Study of the sensitivity of coupled reaction systems to uncertainties in rate coefficients. III. Analysis of approximations. *The Journal of Chemical Physics*, **63**, 1140–1149.
- Cukier, R., Levine, H., and Shuler, K. (1977). Nonlinear sensitivity analysis of multiparameter model systems. *The Journal of Physical Chemistry*, **81**, 2365–2366.
- Cukier, R., Levine, H., and Schuler, K. (1978). Review: Non-linear sensitivity analysis of multiparameter model systems. *Journal of Computational Physics*, **26**, 1–42.
- Davis, R., Jamieson, B., Hughes, J., and Johnston, C. (1996). Observations on buried surface hoar - persistent failure planes for slab avalanches in British Columbia, Canada. In *International Snow Science Workshop*, Banff, AB.
- DiCiccio, T. J. and Efron, B. (1996). Bootstrap confidence intervals. *Statistical Science*, **11**(3), 189–228.
- Efron, B. (1987). Better bootstrap confidence intervals. *Journal of the American Statistical Association*, **82**(397), 171–185.
- Efron, B. and Tibshirani, R. J. (1993). *An introduction to the Bootstrap*. Chapman and Hall.
- Ellis, A. W. and Leathers, D. J. (1999). Analysis of cold airmass temperature modification across the U.S. Great Plains as a consequence of snow depth and albedo. *Journal of Applied Meteorology*, **38**, 696–711.
- Fang, S., Gertner, G. Z., Shinkareva, S., Wang, G., and Anderson, A. (2003). Improved generalized Fourier amplitude sensitivity test (fast) for model assessment. *Statistics and Computing*, **13**, 221–226.
- Feick, S., Kronholm, K., and Schweizer, J. (2007). Field observations on spatial variability of surface hoar at the basin scale. *Journal of Geophysical Research-Earth Surface*, **112**(F2), F02002.
- Fierz, C. (1998). Field observations and modelling of weak-layer evolution. *Annals of Glaciology*, **26**, 7–13.
- Fierz, C. and Lehning, M. (2001). Assessment of the microstructure-based snow-cover model snowpack: Thermal and mechanical properties. *Cold Regions Science and Technology*, **33**, 123–131.

- Frei, A., Robinson, D. A., and Hughes, M. G. (1999). North American snow extent: 1900-1994. *International Journal of Climatology*, **19**, 1517–1534.
- Freund, J. and Simon, G. (1995). *Statistics: A First Course*. Prentice Hall, Inc., 6 edition.
- Frey, H. C. and Patil, S. R. (2002). Identification and review of sensitivity analysis methods. *Risk Analysis*, **3**, 553–578.
- Fukuzawa, T. and Akitaya, E. (1993). Depth-hoar crystal growth in the surface layer under high temperature gradient. *Annals of Glaciology*, **18**, 39–45.
- Gow, A. J. (1965). On the accumulation and seasonal stratification of snow at the south pole. *Journal of Glaciology*, **5**(40), 467–477.
- Gray, D. and Male, D. (1981). Handbook of snow: Principles, processes, management & use.
- Gray, J. and Morland, L. (1994). A dry snow pack model. *Cold Regions Science and Technology*, **22**, 135–148.
- Groisman, P. Y., Karl, T. R., Knight, R. W., and Stenchikov, G. L. (1994a). Changes of snow cover, temperature, and radiative heat balance over the Northern Hemisphere. *Journal of Climate*, **7**, 1633–1656.
- Groisman, P. Y., Karl, T. R., and Knight, R. W. (1994b). Observed impact of snow cover on the heat balance and the rise of continental spring temperatures. *Science*, **263**(5144), 198–200.
- Hachikubo, A. (2001). Numerical modelling of sublimation on snow and comparison with field measurements. *Annals of Glaciology*, **32**, 27–32.
- Hachikubo, A. and Akitaya, E. (1996). Surface hoar growing for several days. In *International Snow Science Workshop*, Banff, AB.
- Hachikubo, A. and Akitaya, E. (1997). Effect of wind on surface hoar growth on snow. *Journal of Geophysical Research*, **102**(D4), 4367–4373.
- Hachikubo, A. and Akitaya, E. (1998). Daytime preservation of surface-hoar layer. *Annals of Glaciology*, **26**, 22–26S.
- Hardy, D., Williams, M. W., and Escobar, C. (2001). Near-surface faceted crystals, avalanches and climate in high-elevation, tropical mountains of Bolivia. *Cold Regions Science and Technology*, **33**, 291–302.
- Hesterberg, T., Moore, D. S., Monaghan, S., Clipson, A., and Epstein, R. (2005). *Introduction to the Practice of Statistics*, chapter 14: Bootstrap Methods and Permutation Tests. W. H. Freeman.

- Höller, P. (1998). Tentative investigations on surface hoar in mountain forests. *Annals of Glaciology*, **26**, 31–34.
- Höller, P. (2004). Near-surface faceted crystals on a slope covered with stone pine trees. In *International Snow Science Workshop*, Jackson Hole, WY.
- Homma, T. and Saltelli, A. (1996). Importance measures in global sensitivity analysis of nonlinear models. *Reliability Engineering and System Safety*, **52**, 1–17.
- Hyndman, R. (1996). Computing and Graphing Highest Density Regions. *The American Statistician*, **50**(2).
- Incropera, F., Dewitt, D., Bergman, T., and Lavine, A. (2007). *Introduction to Heat Transfer*. John Wiley & Sons, Inc., Hoboken, NJ, 5th edition.
- Ishigami, T. and Homma, T. (1990). An importance quantification technique in uncertainty analysis for computer models. In *International Symposium on Uncertainty Modelling and Analysis (ISUMA'90)*, Dec. 3–6, University of Maryland.
- Ishikawa, N., Narita, H., and Kajiya, Y. (1999). Contributions of heat from traffic vehicles to snow melting on roads. *Transportation Research Record: Journal of the Transportation Research Board*, **1672**(-1), 28–33.
- Karl, T. R., Groisman, P. Y., Knight, R. W., and Heim, R. R. J. (1993). Recent variations of snow cover and snowfall in North America and their relation to precipitation and temperature variations. *Journal of Climate*, **6**, 1327–1344.
- Kokhanovsky, A. and Zege, E. (2004). Scattering optics of snow. *Applied Optics*, **43**(7), 1589–1602.
- LaChapelle, E. (1960). Critique on heat and vapor transfer in snow. *U.S. Department of Agriculture, Alta Avalanche Study Center, Progress Report No. 1*.
- LaChapelle, E. (1970). Principles of avalanche forecasting. In L. Gold and G. Williams, editors, *Ice engineering and avalanche forecasting and control*, pages 106–112. National Research Council of Canada. Associate Committee on Geotechnical Research, Ottawa.
- LaChapelle, E. and Armstrong, R. (1977). Temperature patterns in an alpine snow cover and their influence on snow metamorphism. Technical report, University of Colorado Institute of Arctic and Alpine Research.
- LaLonde, A., Norton, M., McIlroy, D., Zhang, D., Padmanabhan, R., Alkhateeb, A., Han, H., Lane, N., and Holman, Z. (2005). Metal coatings on SiC nanowires by plasma-enhanced chemical vapor deposition. *Journal of Materials Research*, **20**(3), 549–553.

- Lang, R., Leo, B., and Brown, R. (1984). Observations on the growth process and strength characteristics of surface hoar. In *International Snow Science Workshop*, Aspen, CO.
- Leathers, D. J. and Robinson, D. A. (1993). The association between extremes in North American snow cover extent and United States temperature. *Journal of Climate*, **6**, 1345–1355.
- Leathers, D. J., Ellis, A. W., and Robinson, D. A. (1995). Characteristics of temperature depressions associated with snow cover across the Northeast United States. *American Meteorological Society*, **34**, 381–390.
- Lehning, M., Bartelt, P., Brown, R., Russi, T., Stekli, U., and Zimmerli, M. (1999). Snowpack model calculations for avalanche warning based upon a network of weather and snow stations. *Cold Regions Science and Technology*, **30**, 145–157.
- Lehning, M., Bartelt, P., Brown, R., Fierz, C., and Satyawali, P. (2002a). A physical snowpack model for the swiss avalanche warning. Part II: Snow microstructure. *Cold Regions Science and Technology*, **35**, 147–176.
- Lehning, M., Bartelt, P., Brown, R., and Fierz, C. (2002b). A physical snowpack model for the swiss avalanche warning. Part III: Meteorological forcing, thin layer formation and evaluation. *Cold Regions Science and Technology*, **35**, 169–184.
- Linkletter, G. and Warburton, J. (1976). A note on the contribution of rime and surface hoar to the accumulation on the ross ice shelf, antarctica. *Journal of Glaciology*, **17**(76), 351–353.
- Liu, I. (2002). *Continuum Mechanics*. Springer-Verlag, Berlin.
- Lundy, C., Brown, R., Adams, E., Birkeland, K., and Lehning, M. (2001). A statistical validation of the snowpack model in a Montana climate. *Cold Regions Science and Technology*, **33**(237-246).
- Manly, B. F. (2007). *Randomization, Bootstrap and Monte Carlo Methods in Biology*. Chapman and Hall, 3 edition.
- Martin, E. and Lejeune, Y. (1998). Turbulent fluxes above the snow surface. *Annals of Glaciology*, **26**, 179–183.
- Martinez, A. (2008). *Computational statistics handbook with MATLAB*. CRC Press, 2 edition.
- Mason, B., Bryant, G., and Van den Heuvel, A. (1963). The growth habits and surface structure of ice crystals. *Philosophical Magazine*, **8**, 505–526.

- Massey, Frank J., J. (1951). The Kolmogorov-Smirnov test for goodness of fit. *Journal of the American Statistical Association*, **46**(253), 68–78.
- McCabe, D., Munter, H., Catherine, D., Henninger, I., Cooperstein, M., Leonard, T., Slaughter, A. E., Staron, P. J., and Adams, E. E. (2008). Near-surface faceting on south aspects in southwest Montana. In *International Snow Science Workshop*, pages 147–154, Whistler, B.C.
- McClung, D. and Schaerer, P. (1993). *The Avalanche Handbook*. The Mountaineers, Seattle, WA.
- McClung, D. and Schaerer, P. (2006). *The Avalanche Handbook*. The Mountaineers, Seattle, WA, 3rd edition.
- McRae, G. J., Tilden, J. W., and Seinfeld, J. H. (1982). Global sensitivity analysis—a computational implementation of the Fourier Amplitude Sensitivity Test (FAST). *Computers and Chemical Engineering*, **6**, 15–25.
- Mellor, M. (1965). Some optical properties of snow. In *Symp. Int. sur les Aspects Sci. de Avalanches de Neige, 5-10, Avril 1965*, pages 128–140, Davos, Suisse. Ass. Int. d'Hydrol. Sci., Gentbrugge, Belgium 1966.
- Morland, L., Kelly, R., and Morris, E. (1990). A mixture theory for a phase-changing snowpack. *Cold Regions Science and Technology*, **17**, 271–285.
- Morstad, B. (2004). *Analytical and Experimental Study of Radiation-Recrystallized Near-Surface Facets in Snow*. Master's thesis, M.S. Thesis, Montana State University.
- Morstad, B., Adams, E., and McKittrick, L. (2004). Experimental study of radiation-recrystallized near-surface facets in snow. In *International Snow Science Workshop*, Jackson Hole, WY.
- Morstad, B., Adams, E., and McKittrick, L. (2007). Experimental and analytical study of radiation-recrystallized near-surface facets in snow. *Cold Regions Science and Technology*, **47**(1-2), 90–101.
- Narashimhan, M. (1993). *Principles of Continuum Mechanics*. John Wiley & Sons, Inc., New York.
- Oke, T. (1978). *Boundary Layer Climates*. Methuen & Co. Ltd., London.
- Ozeki, T. and Akitaya, E. (1996). Field observations of sun crust formation in Hokkaido, Japan. *Arctic and Alpine Research*, **28**(2), 244–248.

- Pinzer, B. and Schneebeli, M. (2009). Snow metamorphism under alternating temperature gradients: Morphology and recrystallization in surface snow. *Geophysical Research Letters*, **36**(23), L23503.
- PIR (2007). *Eppley PIR Precision Infrared Radiometer (Application Note 2RA-H)*. Campbell Scientific, Inc., 815 W. 1800 N., Logan, UT 84321-1784.
- Press, W. H., Flannery, B. P., Teukolsky, S. A., and Vetterling, W. T. (1986). *Numerical Recipes*. Cambridge University Press.
- Reda, I., Gotseff, P., Stoffel, T., and Webb, C. (2003). Evaluation of improved pyrgeometer calibration method. In *Thirteenth ARM Science Team Meeting Proceedings*, Broomfield, Colorado.
- Reddy, J. (2008). *An introduction to continuum mechanics: with applications*. Cambridge University Press.
- Saisana, M., Saltelli, A., and Tarantola, S. (2005). Uncertainty and sensitivity analysis techniques as tools for the quality assessment of composite indicators. *Journal of the Royal Statistical Society. Series A*, **168**, 307323.
- Saltelli, A. (2002). Making best use of model evaluations to compute sensitivity indices. *Computer Physics Communications*, **145**, 280–297.
- Saltelli, A. and Bolado, R. (1998). An alternative way to compute Fourier Amplitude Sensitivity Test (FAST). *Computational Statistics and Data Analysis*, **26**, 445–460.
- Saltelli, A., Andres, T., and Homma, T. (1993). Sensitivity analysis of model output: An investigation of new techniques. *Computational Statistics and Data Analysis*, **15**, 211–238.
- Saltelli, A., Tarantola, S., and Chan, K.-S. (1999). A quantitative model-independent method for global sensitivity analysis of model output. *American Statistical Association*, **41**, 39–55.
- Saltelli, A., Tarantola, S., and Campolongo, F. (2000). Sensitivity analysis as an ingredient of modeling. *Statistical Science*, **15**(4), 377–395.
- Saltelli, A., Tarantola, S., Campolongo, F., and Ratto, M. (2004). *Sensitivity Analysis in Practice: A Guide to Assessing Scientific Models*. John Wiley & Sons, Inc.
- Saltelli, A., Ratto, M., Andres, T., Campolongo, F., Cariboni, J., Gatelli, D., Saisana, M., and Tarantola, S. (2008). *Global Sensitivity Analysis: The Primer*. John Wiley & Sons, Inc.



- Schaibly, J. and Shuler, K. (1973). Study of the sensitivity of coupled reaction systems to uncertainties in rate coefficients. II: Applications. *The Journal of Chemical Physics*, **59**, 3879–3888.
- Schweizer, J. and Jamieson, J. B. (2001). Snow cover properties for skier triggering of avalanches. *Cold Regions Science and Technology*, **33**(2-3), 201–221.
- Schweizer, J. and Lutschg, M. (2001). Characteristics of human-triggered avalanches. *Cold Regions Science and Technology*, **33**, 147–162.
- Scott, D. (1992). *Multivariate density estimation: theory, practice, and visualization*. Wiley-Interscience.
- Scott, K. P. (2001). Shedding some numbers on light. *Sun Spots*, **30**(64).
- Seligman, G. (1936). *Snow structure and ski fields*. Macmillan London.
- Singh, P. R. and Gan, Y. T. (2005). Modelling snowpack surface temperature in the canadian prairies using simplified heat flow models. *Hydrological Processes*, **19**, 3481–3500.
- Slaughter, A. and Adams, E. (2009). Numerical investigation of factors causing near-surface metamorphism. In *International Snow Science Workshop*, Davos, CH.
- Slaughter, A., McCabe, D., Munter, H., Staron, P., Adams, E., Catherine, D., Henninger, I., Cooperstein, M., and Leonard, T. (2009). An investigation of radiation-recrystallization coupling laboratory and field studies. *Cold Regions Science and Technology*, **59**(2-3), 126–132.
- Slaughter, A. E., Staron, P. J., Adams, E. E., McCabe, D., Munter, H., Catherine, D., Henninger, I., Cooperstein, M., and Leonard, T. (2008). Laboratory simulations of radiation-recrystallization events in Southwest Montana. In *International Snow Science Workshop*.
- Smith, P. K. and Ginsburg, J. L. (1977). Improved frequency sets for fourier sensitivity analysis. *Journal of Chemical Physics*, **67**, 5978.
- Sobol, I. M. (1990). Sensitivity estimates for nonlinear mathematical models (in Russian). *Mathematical Models*, **2**, 112–118.
- Sobol, I. M. (1993). Sensitivity estimates for nonlinear mathematical model. *Mathematical Modeling and Computational Experiments*, **1**(4), 407–414.
- Sobol, I. M. (2001). Global sensitivity indices for nonlinear mathematical models and thier Monte Carlo estimates. *Mathematics and Computers in Simulation*, **55**, 271–280.



- Staples, J., Adams, E., Slaughter, A., and McKittrick, L. (2006). Slope scale modeling of snow surface temperature in topographically complex terrain. In *International Snow Science Workshop*, pages 806–814, Telluride, CO.
- Stoffel, T., Reda, I., Jickey, J., Dutton, E., and Michalsky, J. (2006). Pyrgeometer calibrations for the atmospheric radiation measurement program: Updated approach. In *Sixteenth ARM Science Team Meeting Proceedings*, Albuquerque, NM.
- Sturm, M., Holmgren, J., and Knig, M. (1997). The thermal conductivity of seasonal snow. *Journal of Glaciology*, **43**(143), 26–41.
- Sutton, O. (1953). *Micrometeorology*. McGraw-Hill, New York.
- Tremper, B. (2001). *Staying Alive in Avalanche Terrain*. The Mountaineers, Seattle, WA.
- Uliasz, M. (1988). Application of the FAST method to analyze the sensitivity-uncertainty of a largangian model of Sulphur transport in Europe. *Water, Air, and Soil Pollution*, **40**, 33–49.
- Warren, S. (1982). Optical properties of snow. *Reviews of Geophysics and Space Physics*, **20**(1), 67–89.
- Warren, S. (1984). Impurities in snow: Effects on albedo and snowmelt (review). *Annals of Glaciology*, **5**.
- Warren, S. and Wiscombe, W. (1980). A model for the spectral albedo of snow. II: Snow containing atmospheric aerosols. *Journal of the Atmospheric Sciences*, **37**(12), 2734–3745.
- Weast, R. C. (1981). *CRC Handbook of Chemistry and Physics 61st edition*. Chemical Rubber Co.
- Wetly, J., Wicks, C., Wilson, R., and Rorrer, G. (2008). *Fundamentals of Momentum, Heat, and Mass Transfer*. John Wiley & Sons, Inc., 4th edition.
- Weyl, H. (1938). Mean motion. *American Journal of Mathematics*, **60**(4), 889–896.
- White, F. (1999). *Fluid Mechanics*. McGraw-Hill Companies, Inc., 4th edition.
- White, F. M. (2006). *Viscous Fluid Flow*. McGraw-Hill, 3rd edition.

APPENDICES

APPENDIX A

YELLOWSTONE CLUB WEATHER STATIONS

### A.1 Introduction

Two weather stations were installed on Pioneer Mountain near Big Sky, Montana at the Yellowstone Club. These stations were set up to gather data regarding the environmental conditions that lead to the formation of near-surface faceted snow crystals on two different aspects, north and south. The stations were originally established during the winter season of 2005/2006. The instrumentation was changed since this time and the information presented here focuses on the current configuration. The purpose of this document is to provide details regarding the configuration and set up of the Yellowstone Club weather stations.

### A.2 Location

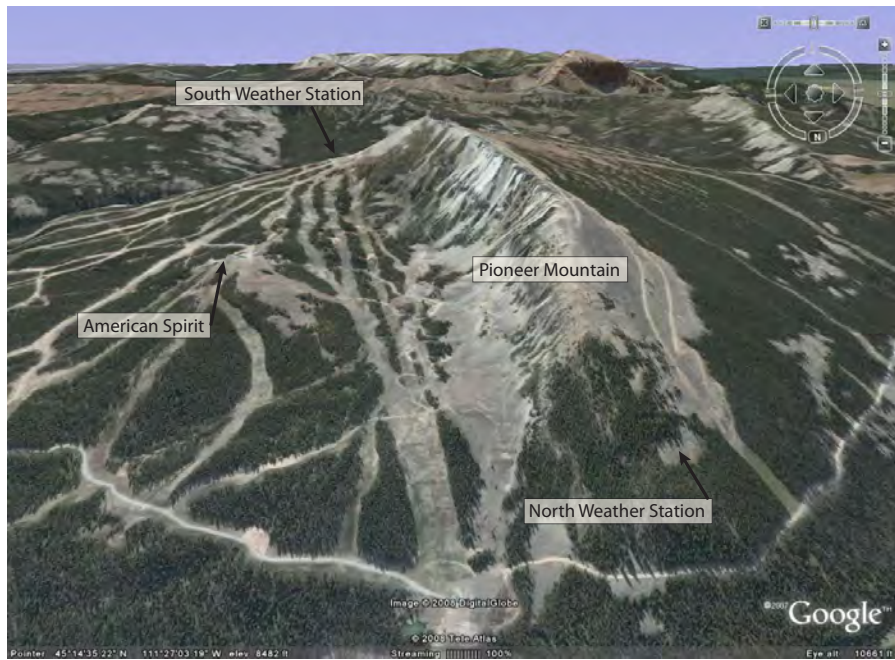
Two complete weather stations were established on Pioneer Mountain near Big Sky, Montana. These sites are referred to as North and South in this document. Both the North and South stations are on a slope of approximately  $30^\circ$ . Additionally, a third station shall be referred to: American Spirit (Aspirit). This station is maintained by the Yellowstone Club Ski Patrol and is located near the top of the American Spirit chair lift. Figure A.1 shows the location of each weather station on Pioneer Mountain and Table A.1 details the location of each site.

Table A.1: Detailed location information on each of the three weather stations situated on Pioneer Mountain.

Station	Latitude	Longitude	Elevation	Aspect
Aspirit	$45^\circ 14' 23.0'' \text{N}$	$111^\circ 26' 34.5'' \text{W}$	2690 m	n/a
South	$45^\circ 13' 47.7'' \text{N}$	$111^\circ 26' 33.0'' \text{W}$	2740 m	$187^\circ$
North	$45^\circ 14' 52.3'' \text{N}$	$111^\circ 27' 21.8'' \text{W}$	2530 m	$0^\circ$



(a)



(b)

Figure A.1: Google Earth images of Pioneer Mountain showing the locations of (a) the South and (b) the North and American Spirit weather stations.

### A.3 Data Acquisition

The North and South stations use CR10(x) dataloggers that were programmed with Campbell Scientific (CSI) PC208w software<sup>1</sup>. The connection between the computer is made via a serial connection with a SC32B (CSI) between the CR10(x) and computer. Data was acquired in the field using a PDA equipped with Campbell Scientific PConnect software. The PDA connection requires a PDA to SC I/O connection, which was included with the PConnect software. The dataloggers were powered with CSI PS12 power supplies and utilized CSI AM416 multiplexers for additional measurements. For instructions on using the PC208w or PConnect software, please refer to the respective user manuals.

Weather data was recorded every 2 minutes during the 2005/2006 season and 3 minutes thereafter; these readings were averaged every 30 minutes. The weather data was written to output array 100 on the dataloggers every thirty minutes. The data is downloaded and saved as a \*.dat file and acquired via a PDA. This file is a ASCII comma delimited file. Table A.2 summarizes the data that is output for both the North and South stations.

---

<sup>1</sup>[www.campbellsci.com/pc208w](http://www.campbellsci.com/pc208w).

Table A.2: List of output data from North and South weather stations, where LW = longwave, SW = shortwave, and TC = thermocouple.

	05/06 Season		05/06 & 07/08 Seasons		08/09 Season	
	Description	Units	Description	Units	Description	Units
1	Array ID		Array ID		Array ID	
2	Year	yyyy	Year	yyyy	Year	yyyy
3	Day	dd	Day	dd	Day	dd
4	Hour/minute	hhmm	Hour/minute	hhmm	Hour/minute	hhmm
5	Battery	V	Battery	V	Battery	V
6	Wind speed	m/s	Wind speed	m/s	Wind speed	m/s
7	Wind direction	deg	Wind direction	deg	Wind direction	deg
8	Surface #1	°C	Surface Temp.	°C	Surface Temp.	°C
9	Surface #2	°C	Incoming SW	W/m <sup>2</sup>	Incoming SW	W/m <sup>2</sup>
10	Incoming SW	W/m <sup>2</sup>	Reflected SW	W/m <sup>2</sup>	Reflected SW	W/m <sup>2</sup>
11	Reflected SW	W/m <sup>2</sup>	LW	W/m <sup>2</sup>	LW	W/m <sup>2</sup>
12	LW	W/m <sup>2</sup>	Depth	cm	Depth	cm
13	Depth	cm	Air (NovaLynx)	°C	Air (CS215)	°C
14	Air (NovaLynx)	°C	Air (CS215)	°C	Humidity	%
15	Air (CS215)	°C	Humidity	%	LW voltage	mV
16	Humidity	%	LW voltage	mV	LW resistance	Ω
17	LW voltage	mV	LW resistance	Ω	TC (0 cm)	°C
18	LW resistance	Ω	TC (0 cm)	°C	TC (2 cm)	°C
19	TC (0 cm)	°C	TC (2 cm)	°C	TC (4 cm)	°C
20	TC (1 cm)	°C	TC (4 cm)	°C	TC (6 cm)	°C
21	TC (2 cm)	°C	TC (6 cm)	°C	TC (8 cm)	°C
22	TC (3 cm)	°C	TC (8 cm)	°C	TC (10 cm)	°C
23	TC (4 cm)	°C	TC (10 cm)	°C	TC (12 cm)	°C
24	TC (5 cm)	°C	TC (12 cm)	°C	TC (14 cm)	°C
25	TC (6 cm)	°C	TC (14 cm)	°C	TC (16 cm)	°C
26	TC (7 cm)	°C	TC (16 cm)	°C	TC (18 cm)	°C
27	TC (8 cm)	°C	TC (18 cm)	°C	TC (20 cm)	°C
28	TC (9 cm)	°C	TC (20 cm)	°C	TC (22 cm)	°C
29	TC (10 cm)	°C	TC (22 cm)	°C	TC (24 cm)	°C
30	TC (11 cm)	°C	TC (24 cm)	°C	TC (26 cm)	°C
31	TC (12 cm)	°C	TC (26 cm)	°C	TC (28 cm)	°C
32	TC (13 cm)	°C	TC (28 cm)	°C	TC (30 cm)	°C
33	TC (14 cm)	°C	TC (30 cm)	°C	TC (32 cm)	°C
34	TC (15 cm)	°C	TC (32 cm)	°C	TC (34 cm)	°C
35	TC (16 cm)	°C	TC (34 cm)	°C	TC (36 cm)	°C
36	TC (17 cm)	°C	TC (36 cm)	°C	TC (38 cm)	°C
37	TC (18 cm)	°C	TC (38 cm)	°C	TC (40 cm)	°C
38	TC (19 cm)	°C	TC (40 cm)	°C	TC (ground)	°C
39	TC (20 cm)	°C	TC (ground)	°C		

Continued on next page...

... continued from previous page

	05/06 Season		05/06 & 07/08 Seasons		08/09 Season	
	Description	Units	Description	Units	Description	Units
40	TC (21 cm)	°C				
41	TC (22 cm)	°C				
42	TC (23 cm)	°C				
43	TC (24 cm)	°C				
44	TC (25 cm)	°C				
45	TC (26 cm)	°C				
46	TC (27 cm)	°C				
47	TC (28 cm)	°C				
48	TC (29 cm)	°C				
49	TC (30 cm)	°C				
50	TC (ground)	°C				

#### A.4 Instrumentation

The weather station equipment was mounted on a cross arm and tower placed on the slope before snow was present. Table A.3 provides the make and model of each instrument implemented at each site for the different setups utilized during all winter seasons. The North and South stations include incoming short-wave radiation, reflected short-wave radiation, incoming long-wave radiation, air temperature, relative humidity, snow surface temperature, wind speed, wind direction, ground temperature, and a stack of type T thermocouples for measuring snow temperatures at depth.



Table A.3: Summary of the instrumentation utilized at each weather station during each winter season.

Measurement	2005/2006 Season		2006/2007 & 2007/2008 Seasons		2008/2009 Season	
	North	South	North & South	Aspirt	North & South	Aspirt
Incoming Longwave Radiation (Radiometer)	Eppley Laboratory, Inc. PIR	Eppley Laboratory, Inc. PIR	Eppley Laboratory, Inc. PIR		Kipp & Zonen CGR3	Eppley Laboratory, Inc. PIR
Incoming Shortwave Radiation (Pyranometer)	Eppley Laboratory, Inc. PSP	LI-COR LI-200 Pyranometer	LI-COR LI-200 Pyranometer	Eppley Laboratory, Inc. PSP	Kipp & Zonen CMP3	Eppley Laboratory, Inc. PSP
Reflected Shortwave Radiation	Eppley Laboratory, Inc. PSP	LI-COR LI-200 Pyranometer	LI-COR LI-200 Pyranometer		Kipp & Zonen CMP3	
Air Temperature and Relative Humidity	Campbell Scientific CS215	Campbell Scientific CS215	Campbell Scientific CS215		Campbell Scientific CS215	
Snow Depth Sensor	NovaLynx 260-700	NovaLynx 260-700	NovaLynx 260-700		NovaLynx 260-700	
Snow Surface Temperature	Everest Interscience Inc. 4000.4ZL	Everest Interscience Inc. 4000.4ZL	Everest Interscience Inc. 4000.4ZL		Everest Interscience Inc. 4000.4ZL	
Anemometer	Met One 034A-LC	Met One 034A-LC	Met One 034A-LC		Met One 034A-LC	
Snow Temperature (Type T thermocouples)	30 spaced at 1 cm	30 spaced at 1 cm	20 spaced at 2 cm		20 spaced at 2 cm	

## A.5 Programing and Wiring

A complete wiring diagram for the current (2008/2009) setup is included in Figure A.2 and Table A.5 summarizes the wiring in tabular format. Generally, each sensor is wired as defined in the sensor documentation and/or the Campbell Scientific literature. The following sections (A.5.1 and A.5.2) detail programs utilized at the weather stations. The sections step through the entire program including the program initialization, sensor measurements, and data output. The only difference between the North and South station program are the calibration constants for a few sensors. For quick reference, Table A.4 includes the calibration multipliers that differ between the stations. Finally, the complete programs for each station are included in Section A.6.

Programming with the CR10(x) was completed using PC208w, the following are a few important points to understand when reading the programs described herein.

- The “;” character indicates a comment. The comments are omitted in the following sections but included in the complete programs in Section A.6.
- Each action in the CR10(x) programs is sequentially numbered and also includes an instruction code. For example, 03: Temp (107) (P11) is the 3rd instruction and has a code of P11. The options corresponding to this command are indented underneath this first line. The instruction code is the important identifier, and when referred to in this document are enclosed in brackets (e.g., [P11]).

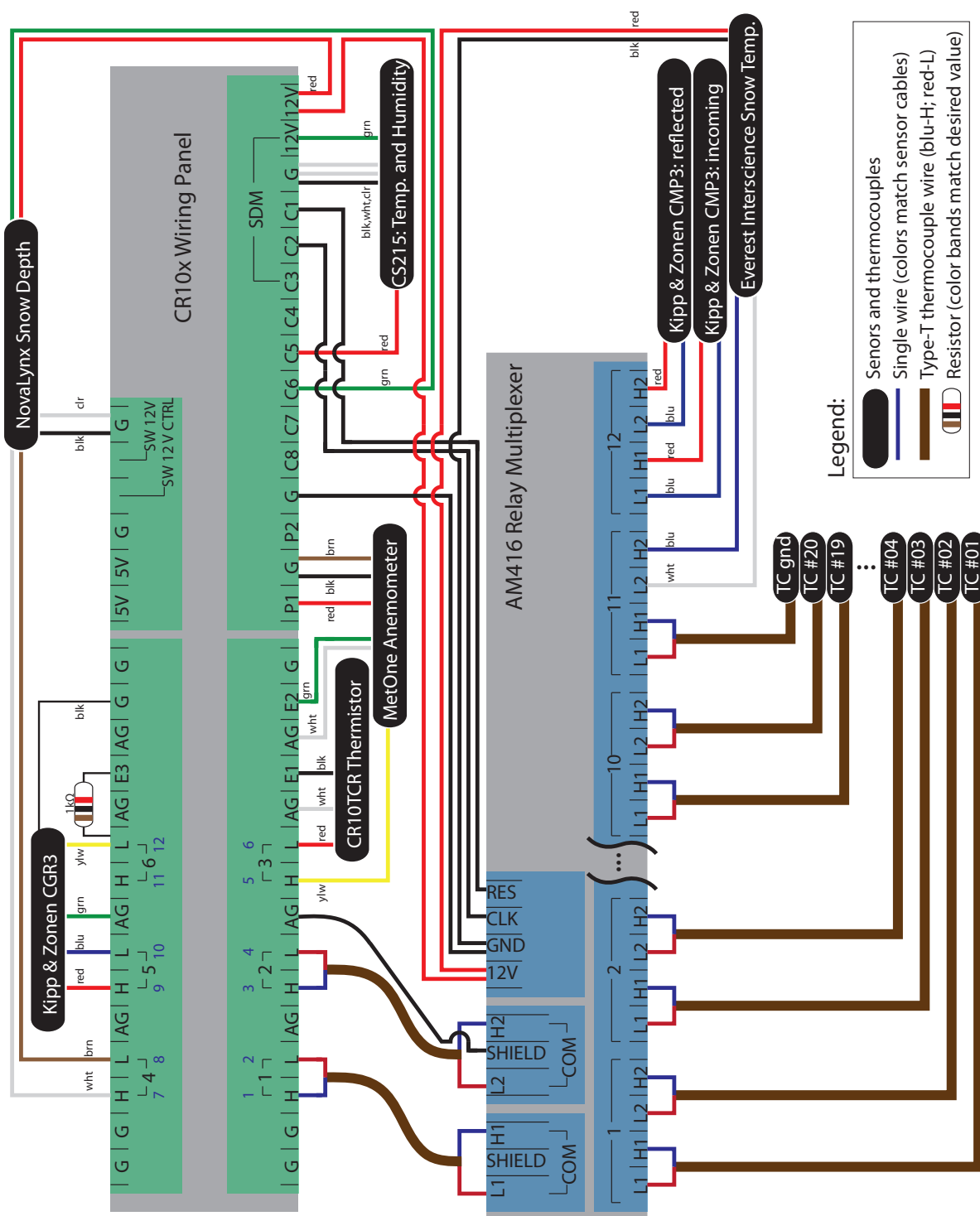


Figure A.2: Wiring schematic for North and South weather stations.

Table A.4: Summary of calibration constants of weather station sensors. The values inside the brackets give the serial number of the sensor and all calibration numbers are given as  $W/m^2/mV$ .

	North	South	Aspirt
CGR3	156.495 (070108)	84.531 (070112)	n/a
CMP3, incoming	70.47 (080194)	70.87 (080193)	n/a
CMP3, reflected	65.87 (080191)	69.74 (080192)	n/a
Aspirt, PSP	n/a	n/a	122.55 (32530F3)
Aspirt, PIR	n/a	n/a	256.89 (33586F3)

Table A.5: Tabular wiring layout for North and South weather stations.

Sensor	Wire	CR10(x)	Sensor	Wire	AM416	Description	AM416	CR10(x)
CR10TCR	blk	E1	Thermocouple #1	blu	1:H1	AM416 to CR10(x)	COM L1	L1
	wht	AG		red	1:L1		COM H1	H1
	red	SE6		blu	1:H2		COM L2	L2
Kipp & Zonen CGR3 (1 kΩ Res. SE12 to E3)	red	H5	Thermocouple #2	red	1:L2	AM416 to CR10(x)	SHIELD	AG
	blu	L5		...	...		COM H2	H2
	grn	AG		blue	10:H1		12V	12V
	ylw	SE12		red	10:L1		GND	G
	blk	G		blue	10:H2		CLK	C2
Nova Lynx Snow Depth	wht	H4	Thermocouple #20	red	10:L2		RES	C1
	brn	L4		blu	11:H1			
	blk,clr	G		red	11:L1			
MetOne Anemometer	red	12V	Everest Interscience Temp.	blu	11:H2			
	grn	C6		wht	11:L2			
	ylw	SE5		red	12V			
	grn	E2		blk	GND			
	red	P1		red	12:H1			
CS215 Temp. and Humidity	blk,brn	G	Kipp & Zonen CMP3 (incoming)	blu	12:L1			
	wht	AG		red	12:H2			
	red	12V		blu	12:L2			
CS215 Temp. and Humidity	blk,wht,clr	G	Kipp & Zonen CMP3 (reflected)	red	12:H2			
	grn	C5		blu	12:L2			

### A.5.1 North and South Station Program

Program Initialization: The first three commands in the program establish the program storage location on the CR10(x), measure the battery voltage with [P10], and turn off the data logger when the battery voltage drops belows 11 volts with [P89].

---

```
*Table 1 Program
01: 180      Execution Interval (seconds)

1: Batt Voltage (P10)
1: 14      Loc [ Battery ]

2: If (X<=>F) (P89)
1: 14      X Loc [ Battery ]
2: 4       <
3: 11      F
4: 0       Go to end of Program Table
```

---

Reference Temperature (CR10TCR): The reference temperature captured with [P11], as measured by the CR10TCR, is used to adjust for the temperature of the AM416 multiplexer terminals, where the thermocouples are attached. Thus, the thermistor should be placed on the multiplexer.

---

```
3: Temp (107) (P11)
1: 1       Reps
2: 6       SE Channel
3: 1       Excite all reps w/E1
4: 1       Loc [ RefTemp__ ]
5: 1.0     Mult
6: 0.0     Offset
```

---

Activate AM416 Multiplexer: The AM416 multiplexer is activated by turning the attached port (C1) to high with [P86], i.e., “on”. As will be detailed in the next section, the multiplexers operate by first being activated. When the port (C2) connected to CLK on the multiplexer is pulsed the signal form the first pair of channels is transfered through the COM connections. The next time C2 is pulsed the second pair is transfered and so forth.

---

```
4: Do (P86)
1: 41      Set Port 1 High
```

---

Thermocouple Array: The thermocouple array in the snow contains 20 sensors, thus the 10 pairs of thermocouples must be measured. First, a loop is established with [P87]. On each execution of this loop the C2 is pulsed with [P86] causing the multiplexer to cycle through the first 10 terminal pairs. [P90] indicates that the subsequent command, [P14], should be executed twice. Finally, the loop is ended with [P95].

The -- in front of step 6 of [P14] indicates that each time this command is executed that the storage location should be incremented. In this case, this results in TC\_1, TC\_2, etc.

---

```
5: Beginning of Loop (P87)
1: 0      Delay
2: 10     Loop Count

6: Do (P86)
1: 72     Pulse Port 2

7: Step Loop Index (P90)
1: 2      Step

8: Thermocouple Temp (DIFF) (P14)
1: 2      Reps
2: 1      2.5 mV Slow Range
3: 01     DIFF Channel
4: 1      Type T (Copper-Constantan)
5: 1      Ref Temp (Deg. C) Loc [ RefTemp__ ]
6: 20     -- Loc [ TC_1      ]
7: 1.0    Mult
8: 0.0    Offset

9: End (P95)
```

---

Ground and Snow Surface Temperature: After reading the 20 thermocouples the multiplexer is triggered again by pulsing C2 with [P86], this causes the 11th terminal pair to be measured, which is the thermocouple at the ground ([P14]) and

the snow surface temperature ([P2]). The surface temperature requires a multiplier of 0.1 °C/m, which is consistent between stations.

---

```

10: Do (P86)
1: 72      Pulse Port 2

11: Thermocouple Temp (DIFF) (P14)
1: 1      Reps
2: 1      2.5 mV Slow Range
3: 1      DIFF Channel
4: 1      Type T (Copper-Constantan)
5: 1      Ref Temp (Deg. C) Loc [ RefTemp__ ]
6: 40     Loc [ TCgnd      ]
7: 1.0    Mult
8: 0.0    Offset

12: Volt (Diff) (P2)
1: 1      Reps
2: 5      2500 mV Slow Range
3: 2      DIFF Channel
4: 9      Loc [ SurTemp_1 ]
5: 0.1    Mult
6: 0.0    Offset

```

---

Incoming and Reflected Short-wave: As done for the previous readings, the multiplexer is triggered by pulsing C2 with [P86], this causes the 12th terminal pair to be measured, which is the two short-wave radiation sensors both of which are voltages read using [P2].

---

```

13: Do (P86)
1: 72      Pulse Port 2

14: Volt (Diff) (P2)
1: 1      Reps
2: 3      25 mV Slow Range
3: 1      DIFF Channel
4: 4      Loc [ ShortUP   ]
5: 72.43  Mult
6: 0.0    Offset

15: Volt (Diff) (P2)
1: 1      Reps
2: 22     7.5 mV 60 Hz Rejection Range
3: 2      DIFF Channel
4: 5      Loc [ ShortDOWN ]
5: 200    Mult
6: 0.0    Offset

```

---

Deactivate AM416 Multiplexer: The AM416 multiplexer is turned off by setting Port 1 (C1) to low with [P86].



---

```
16: Do (P86)
1: 51      Set Port 1 Low
```

---

Wind Speed and Direction: The MetOne anemometer first measures the wind speed by reading the value from pulse input 1 using [P3]. Then instructions [P89], [P30], and [P95] (not shown) set negative values to zero, which occur in still conditions due to instrument noise. These instructions are included in the complete program in Section A.6.

---

```
17: Pulse (P3)
1: 1      Reps
2: 1      Pulse Input Channel
3: 22     Switch Closure, Output Hz
4: 2      Loc [ WindSpd  ]
5: 0.7990 Mult
6: 0.2811 Offset
```

---

The wind direction is measured with [P5] via the voltage across a resistor in the anemometer, which requires a current. The current is supplied as an excitation voltage from E2 and the voltage measured on SE5. The offsets and multipliers are consistent between the two stations.

---

```
21: AC Half Bridge (P5)
1: 1      Reps
2: 25     2500 mV 60 Hz Rejection Range
3: 5      SE Channel
4: 2      Excite all reps w/Exchan 2
5: 2500   mV Excitation
6: 3      Loc [ WindDir  ]
7: 360    Mult
8: 0.0    Offset
4: Do (P86)
1: 41     Set Port 1 High
```

---

Long-wave Radiation: The Kipp & Zonen long-wave sensor requires two measurements, a voltage and a resistance. The voltage is measured with [P2] and is used to adjust for variations between the case and sensor temperatures. The resistance measurement requires an excitation to acquire the voltage across the resistor using

[P5]. This value is then converted to a resistance with instruction [P59]. The multiplier for this instruction should be the value of the reference resistor wired from SE12 to E3.

These two values are converted to long-wave radiation ( $\text{W}/\text{m}^2$ ) using subroutines #1 and #2 that are called with instruction [P86]. These subroutines use Equations (A.1)–(A.3), where the incoming long-wave radiation  $L_{d\downarrow}$  is computed from the voltage reading  $U_{emf}$ , the case resistance  $R_c$ , and the constants  $\alpha$ ,  $\beta$ ,  $\gamma$ , and  $S$ . The constant  $S$  is the sensor sensitivity included in Table A.4. The constants, for both the Eppley and Kipp & Zonen sensors, are defined as  $\alpha = 1.0295 \times 10^{-3}$ ,  $\beta = 2.391 \times 10^{-4}$ , and  $\gamma = 1.568 \times 10^{-7}$ . The complete subroutines are provided in Section A.6.

$$L_{net} = \frac{U_{emf}}{S} \quad (\text{A.1})$$

$$T_c = \frac{1}{\alpha + [\beta \cdot (\ln(R_c) + \gamma(\ln(R_c))^3)]} \quad (\text{A.2})$$

$$L_{d\downarrow} = L_{net} + 5.67 \times 10^{-8} \cdot T_b^4 \quad (\text{A.3})$$

---

```

25: Volt (Diff) (P2)
  1: 1      Reps
  2: 1      2.5 mV Slow Range
  3: 5      DIFF Channel
  4: 100    Loc [ Uemf   ]
  5: 1.0    Mult
  6: 0.0    Offset

26: AC Half Bridge (P5)
  1: 1      Reps
  2: 15     2500 mV Fast Range
  3: 12     SE Channel
  4: 3      Excite all reps w/Exchan 3
  5: 2500   mV Excitation
  6: 101    Loc [ Case_Res ]
  7: 1.0    Mult
  8: 0.0    Offset

27: BR Transform Rf[X/(1-X)] (P59)
  1: 1      Reps
  2: 101    Loc [ Case_Res ]
  3: 1000   Multiplier (Rf)

28: Do (P86)
  1: 1      Call Subroutine 1

```

29: Do (P86)  
1: 2            Call Subroutine 2

---

Snow Depth: The Nova Lynx ultrasonic snow depth sensor operates in various modes. The method presented in the Nova Lynx user manual proved to be unreliable in the field. Thus, the method presented here is recommended. First, the sensor is turned on using communication port 6 via [P22]. Then the program waits two seconds, [P22], for the sensor to perform the measurement, which is accomplished with the excitation with delay command, but notice that the excitation voltage is set to zero. Next, the voltage returned from the sensor is collected via [P2] and the sensor is powered off with [P86].

In order for the Nova Lynx sensor to operate correctly both dip switch #1 and #3 must be in the “on” position, refer to the sensor user manual for setting these switches. The voltage range should be from 0–5 V, which results in the use of the multiplier of -0.25 cm/mV. The resulting depth is not temperature adjusted and should be compensated for temperature using the multiplier ( $CF$ ) computed using Equation (A.4) and the measured temperature ( $T$ ) from the CS215 sensor. This sensor provides a more accurate reading of temperature than the Nova Lynx sensor itself. This portion of the code is included in the complete program in Section A.6.

$$CF = \left[ \frac{T + 273.15}{273.15} \right]^{\frac{1}{2}} \quad (\text{A.4})$$

The offset value should be set to the distance from the sensor to bare ground. A value of 200 cm was used for both stations; this value was an assumed value because only the occurrence of new snow was desired.

---

30: Do (P86)  
1: 46            Set Port 6 High  
31: Excitation with Delay (P22)

```

1: 2      Ex Channel
2: 200    Delay W/Ex (units = 0.01 sec)
3: 0000   Delay After Ex (units = 0.01 sec)
4: 0000   mV Excitation

32: Volt (Diff) (P2)
1: 1      Repts
2: 5      2500 mV Slow Range
3: 4      DIFF Channel
4: 116    Loc [ rawdepth ]
5: -0.25  Mult
6: 200    Offset

33: Do (P86)
1: 56     Set Port 6 Low

```

---

Temperature and Humidity: The CS215 sensor has a specific instruction, [P105], designed for reading the sensor. The temperature is returned to the location specified (6) and the humidity in the following location (7).

```

40: SDI-12 Recorder (P105)
1: 00     SDI-12 Address
2: 00     SDI-12 Command
3: 5      Port
4: 6      Loc [ TempCS215 ]
5: 1.0    Mult
6: 0.0    Offset

```

---

Data Storage: To store the data the output flags must be set to high, which is accomplished with instruction [P92], in this case the data is written every 30 minutes. Before writing the data, the storage location is set to 100 with [P80], which is an arbitrary value. The storage location allows you to write various sets of data to a single file. For example, it is common to write 30 minute data as well as the 24 hour averages in different storage arrays.

First, the time stamp is output using [P77] as three values: year, day, and hour/minute. Next, the 30 minute averages of all recorded data are output using [P71], with the exception of the battery voltage in which the minimum is reported with [P74]. Only two commands are shown in the code here, for the complete output see Section A.6.

---

```

41: If time is (P92)
1: 0000    Minutes (Seconds --) into a
2: 30      Interval (same units as above)
3: 10      Set Output Flag High

42: Set Active Storage Area (P80)
1: 1       Final Storage Area 1
2: 100     Array ID

43: Real Time (P77)
1: 1220    Year,Day,Hour/Minute (midnight = 2400)

44: Minimum (P74)
1: 1       Reps
2: 00      Time Option
3: 14      Loc [ Battery ]

46: Average (P71)
1: 1       Reps
2: 9       Loc [ Surface ]

```

---

Complete Main Program: The main program does not require any ending statement. However, the two commands shown here must be present. The first may be used for a second program and the second indicates the beginning of the subroutines, which must be present regardless of the presence of subroutines.

---

```

*Table 2 Program
02: 0.0000    Execution Interval (seconds)

```

---

```

*Table 3 Subroutines

```

---

Subroutines: The subroutines require a beginning statement, [P85], and an ending statement of [P95]. The operations desired from the subroutine should be in between these two statements. The subroutines have complete access to read and write input values. For a complete example of a subroutine see the programs in Section A.6.

---

```

1: Beginning of Subroutine (P85)
1: 1       Subroutine 1

13: End (P95)

```

---

### A.5.2 American Spirit Weather Station

The Aspirit station and program are maintained by the Yellowstone Club Ski Patrol. The Eppley PIR long-wave sensor at this station requires the same instructions as the the North and South stations, as detailed in Section A.5.1.9. For the North and South stations Kipp & Zonen sensors were purchased because of their ability to adjust for solar contamination of the sensor, which is a problem with the Eppley PIR sensors (Albrecht and Cox, 1977). To avoid this contamination with the Eppley PIR long-wave sensor, an additional resistance measurement and computation is required. Currently this additional adjustment is not included at the Aspirit station. A comparison with the nearby Yellow Mule (YLWM8) RAWS<sup>2</sup> weather station indicates that solar contamination has a minimal effect. As shown in Figure A.3, the short-wave solar irradiance is similar between the RAWS and Aspirit weather stations.

Nonetheless, the details regarding the implementation of this adjustment are presented here for future application by other researchers. Contrary to the CSI application note recommended setup, in certain situations the dome thermistor correction should be included in the computation of incoming long-wave radiation. Details regarding this adjustment are given by Albrecht and Cox (1977), which explains that under intense solar radiation the case and dome temperatures can differ by 10°C resulting in errors between 300 and 400 W/m<sup>2</sup>, such was the case at the South location that motivated the usage of the Kipp & Zonen sensors.

Equation (A.5) is used to adjust for the dome temperature,

$$L_{d\downarrow} = L_{net} + \sigma T_b^4 - k\sigma(T_d^4 - T_b^4), \quad (\text{A.5})$$

where  $\sigma = 5.67 \times 10^{-8}$ . This is an extension of Equation (A.3). Thus, the Eppley PIR requires three measurements:  $U_{emf}$ ,  $R_d$ , and  $R_c$ . The net radiation  $L_{net}$  is calculated

<sup>2</sup>Remote Automated Weather Station ([www.fs.fec.us/raWS](http://www.fs.fec.us/raWS))

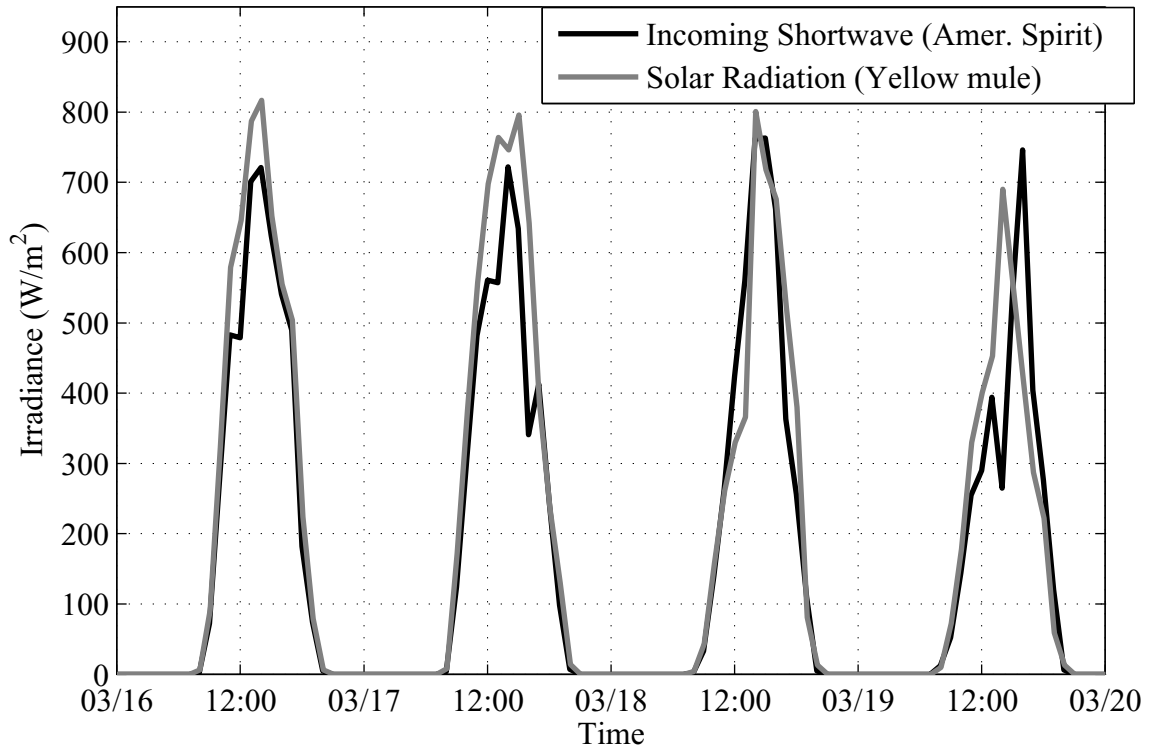


Figure A.3: Comparison of incoming short-wave radiation at the Yellow Mule RAWS and Aspirit weather stations.

using Equation (A.1) and the temperatures  $T_d$  and  $T_c$  are computed using Equation (A.2) using the appropriate resistance value. As with the Kipp & Zonen the sensitivity  $S$  is provided by the manufacturer. Finally, the  $k$  is yet another constant that is not provided; upon contacting a CSI representative it was recommended that a value of  $k = 3.5$  be used. This estimation can be eliminated by performing one of many calibration procedures. Additional information on calibration may be found in Reda *et al.* (2003) and Stoffel *et al.* (2006).

## A.6 Complete Weather Station Programs

### A.6.1 North Weather Station Program

```

1  ;{CR10X}
2  ;-----
3  ; A PROGRAM BY:
4  ;
5  ;   ANDREW E. SLAUGHTER
6  ;   205 Cobleigh Hall, MSU-Bozeman
7  ;   P.O. Box 173900
8  ;   Bozeman, MT 59717-3900
9  ;   (406)994-2293
10 ;
11 ;*****
12 ;
13 ; BACKGROUND:
14 ;   The following program utilizes the Campbell Scientific, Inc. (SCI) CR10(x)
15 ;   datalogger and two CSI AM418 multiplexer to acquire basic weather data that
16 ;   includes snow surface temperature, snow depth, humidity, air temperature,
17 ;   wind speed, wind direction, longwave radiation, and shortwave radiation.
18 ;   Additionally, the station has an array of thermocouples that measures the
19 ;   snowpack temperature at various depths below the surface.
20 ;
21 ;   The objective of the site is to collect field data regarding the growth
22 ;   of near-surface faceted and surface hoar crystals for the use in verifying both
23 ;   lab and analytical models of the near-surface processes.
24 ;
25 ;   Last Updated: December 2008
26 ;
27 ;*****
28 ;
29 ; WIRING SCHEME:
30 ;
31 ; -> CR10TCR Thermistor
32 ;   Wht - AG
33 ;   Blk - E1
34 ;   Red - SE6
35 ;
36 ; -> AM418 MULTIPLEXIERS
37 ;   Wiring (CR10 - AM416):
38 ;       C1 - REM
39 ;       C2 - CLK
40 ;       H1 - ComH1
41 ;       L1 - ComL1
42 ;       H2 - ComH2
43 ;       L2 - ComL2
44 ;
45 ; -> THERMOCOUPLES (wired to AM416)
46 ;       1H1,1L1 - TC_1
47 ;       1H2,1L2 - TC_2
48 ;       ...
49 ;       11H1,11L1 - TC_21 (TC to Grnd)
50 ;
51 ; -> KIPP & ZONEN CMP3 (shortwave, wired to AM416#1)
52 ;-----
53 ;   Up Mult. = 14.19 uV/W/m^2 = 70.47 W/m^2/mV (SN:080194)
54 ;   Dn Mult. = 15.18 uV/W/m^2 = 65.87 W/m^2/mV (SN:080191)
55 ;-----
56 ;       Incoming (up)      Reflected (down)
57 ;       Red - 12:H1         Grn - 12:L2
58 ;       Blk - 12:L1         Blu - 12:H2
59 ;
60 ; -> KIPP & ZONEN CGR3 (longwave);
61 ;-----
62 ;   Mult. = 6.39 uV/W/m^2 = 156.495 W/m^2/mV (SN:070108)
63 ;-----
64 ;       Red - L5
65 ;       Blu - H5
66 ;       Ylw - SE12
67 ;       Grn - G
68 ;       1kOhm Resistor from SE12 - E3
69 ;
70 ; -> METONE ANEMOMETER
71 ;       Yel - SE5
72 ;       Wht - AG
73 ;       Grn - E2
74 ;       Blk - G
75 ;       Brn - G
76 ;       Red - P1
77 ;
78 ; -> EVEREST INTERSCIENCE SNOW SURFACE TEMPERATURE

```



```

79 ;           Blu - 11:H2
80 ;           Wht - 11:L2
81 ;           Red - 12V
82 ;           Blk - G
83 ;
84 ; -> CAMPBELL SCIENTIFIC HUMIDITY AND TEMP
85 ;           Blk ,Wht,Clr - G
86 ;           Red - 12V
87 ;           Grn - C5
88 ;
89 ; -> NOVALYNX ULTRASONIC SNOW DEPTH
90 ;           Red - 12V
91 ;           Blk - G
92 ;           Clr - G
93 ;           Grn - C6
94 ;           Wht - 4H
95 ;           Brn - 4L
96 ;
97 ;
98 ;*****
99 ;**** Begin Program *****
100 ;
101 ;EXECUTION INTERVAL IN SECONDS
102 *Table 1 Program
103   01: 180           Execution Interval (seconds)
104 ;
105 ;*****
106 ;**** Battery Voltage *****
107 ;
108 1: Batt Voltage (P10)
109 1: 14           Loc [ Battery ]
110 ;
111 ;*****
112 ;**** Stop if Battery < 11V *****
113 ;
114 2: If (X<=>F) (P89)
115 1: 14           X Loc [ Battery ]
116 2: 4           <
117 3: 11          F
118 4: 0           Go to end of Program Table
119 ;
120 ;*****
121 ;**** Reference Temperature *****
122 ;
123 3: Temp (107) (P11)
124 1: 1           Repts
125 2: 6           SE Channel
126 3: 1           Excite all repts w/EI
127 4: 1           Loc [ RefTemp-- ]
128 5: 1.0         Mult
129 6: 0.0         Offset
130 ;
131 ;*****
132 ;**** Thermocouples, SW Radiation, & Surface Temp *****
133 ;
134 ;TRIGGER MULTIPLEXER
135 4: Do (P86)
136 1: 41           Set Port 1 High
137 ;
138 ;MEASURE THERCOUPLES 1 THRU 20
139 5: Beginning of Loop (P87)
140 1: 0           Delay
141 2: 10          Loop Count
142 ;
143 6: Do (P86)
144 1: 72          Pulse Port 2
145 ;
146 ;INDICATE TWO READINGS PER SET
147 7: Step Loop Index (P90)
148 1: 2           Step
149 ;
150 ;READ 20 THERMOCOUPLES
151 8: Thermocouple Temp (DIFF) (P14)
152 1: 2           Repts
153 2: 1           2.5 mV Slow Range
154 3: 01          DIFF Channel
155 4: 1           Type T (Copper-Constantan)
156 5: 1           Ref Temp (Deg. C) Loc [ RefTemp-- ]
157 6: 20          -- Loc [ TC.1 ]
158 7: 1.0         Mult
159 8: 0.0         Offset
160 ;
161 ;END THE LOOP FOR READING THERMOCOUPLES
162 9: End (P95)

```

```

166
167 ;READ THE GROUND THERMOCOUPLE AND THE SURFACE TEMPERATURE
168 10: Do (P86)
169 1: 72 Pulse Port 2
170
171 11: Thermocouple Temp (DIFF) (P14)
172 1: 1 Reps
173 2: 1 2.5 mV Slow Range
174 3: 1 DIFF Channel
175 4: 1 Type T (Copper-Constantan)
176 5: 1 Ref Temp (Deg. C) Loc [ RefTemp-- ]
177 6: 40 Loc [ TCgnd ]
178 7: 1.0 Mult
179 8: 0.0 Offset
180
181 12: Volt (Diff) (P2)
182 1: 1 Reps
183 2: 5 2500 mV Slow Range
184 3: 2 DIFF Channel
185 4: 9 Loc [ Surface ]
186 5: 0.1 Mult
187 6: 0.0 Offset
188
189 ;READ THE SHORTWAVE SENSORS (UP & DOWN)
190 13: Do (P86)
191 1: 72 Pulse Port 2
192
193 ;Incoming (up)
194 14: Volt (Diff) (P2)
195 1: 1 Reps
196 2: 3 25 mV Slow Range
197 3: 1 DIFF Channel
198 4: 4 Loc [ ShortUP ]
199 5: 70.47 Mult
200 6: 0.0 Offset
201
202 ;Reflected (Down)
203 15: Volt (Diff) (P2)
204 1: 1 Reps
205 2: 3 25 mV Slow Range
206 3: 1 DIFF Channel
207 4: 5 Loc [ ShortDOWN ]
208 5: 65.87 Mult
209 6: 0.0 Offset
210
211 ;TURN OFF MULTIPLEXER
212 16: Do (P86)
213 1: 51 Set Port 1 Low
214
215
216 ;*****
217 ;**** Wind Speed and Direction *****
218 ;-----
219 ; WindSpd = m/s2
220 ; WindDir = 0-360 (N=0=360)
221 ;-----
222
223 ;MEASURE WIND SPEED
224 17: Pulse (P3)
225 1: 1 Reps
226 2: 1 Pulse Input Channel
227 3: 22 Switch Closure, Output Hz
228 4: 2 Loc [ WindSpd ]
229 5: 0.7990 Mult
230 6: 0.2811 Offset
231
232 ;IF WIND SPEED IS NEGATIVE SET TO ZERO
233 18: If (X<=>F) (P89)
234 1: 2 X Loc [ WindSpd ]
235 2: 1 =
236 3: 0.2811 F
237 4: 30 Then Do
238
239 19: Z=F (P30)
240 1: 0 F
241 2: 0 Exponent of 10
242 3: 2 Z Loc [ WindSpd ]
243
244 20: End (P95)
245
246 21: AC Half Bridge (P5)
247 1: 1 Reps
248 2: 25 2500 mV 60 Hz Rejection Range
249 3: 5 SE Channel
250 4: 2 Excite all reps w/Exchan 2
251 5: 2500 mV Excitation
252 6: 3 Loc [ WindDir ]

```

```

253 7: 360      Mult
254 8: 0.0      Offset
255
256
257 ;*****
258 ;**** Longwave Radiation *****
259 ;
260 ;MEASURE VOLTAGE FOR THERMOPILE
261 22: Volt (Diff) (P2)
262 1: 1        Repts
263 2: 1        2.5 mV Slow Range
264 3: 5        DIFF Channel
265 4: 100      Loc [ Uemf      ]
266 5: 1        Mult
267 6: 0.0      Offset
268
269 ;MEASURE THERMISTOR
270 23: AC Half Bridge (P5)
271 1: 1        Repts
272 2: 15       2500 mV Fast Range
273 3: 12       SE Channel
274 4: 3        Excite all repts w/Exchan 3
275 5: 2500     mV Excitation
276 6: 101      Loc [ Case_Res  ]
277 7: 1.0      Mult
278 8: 0.0      Offset
279
280 ;CONVERT THERMISTOR MEASURE TO RESISTANCE
281 24: BR Transform Rf[X/(1-X)] (P59)
282 1: 1        Repts
283 2: 101      Loc [ Case_Res  ]
284 3: 1000     Multiplier (Rf)
285
286 ;CONVERT RESISTANCE TO TEMPERATURE
287 25: Do (P86)
288 1: 1        Call Subroutine 1
289
290 ;CORRECT FOR CASE TEMPERATURE -> OUTPUT LONGWAVE RADIATION
291 26: Do (P86)
292 1: 2        Call Subroutine 2
293
294 ;*****
295 ;**** Snow Depth *****
296
297 27: Do (P86)
298 1: 46       Set Port 6 High
299
300 ; Wait 2 seconds for sensor to warm-up and measure depth
301 28: Excitation with Delay (P22)
302 1: 2        Ex Channel
303 2: 200      Delay W/Ex (units = 0.01 sec)
304 3: 0000     Delay After Ex (units = 0.01 sec)
305 4: 0000     mV Excitation
306
307 ;Depth given in mV and scaled to cm, offset = mounting height
308 29: Volt (Diff) (P2)
309 1: 1        Repts
310 2: 5        2500 mV Slow Range
311 3: 4        DIFF Channel
312 4: 116      Loc [ rawdepth  ]
313 5: -0.25    Mult
314 6: 200      Offset
315
316 30: Do (P86)
317 1: 56       Set Port 6 Low
318
319 ; Compute the temperature corrected depth
320 31: Z=X+F (P34)
321 1: 6        X Loc [ TempCS215 ]
322 2: 273.15   F
323 3: 117      Z Loc [ d1      ]
324
325 32: Z=F (P30)
326 1: 273.15   F
327 2: 00       Exponent of 10
328 3: 118      Z Loc [ kelvin  ]
329
330 33: Z=X/Y (P38)
331 1: 117      X Loc [ d1      ]
332 2: 118      Y Loc [ kelvin  ]
333 3: 119      Z Loc [ d2      ]
334
335 34: Z=F (P30)
336 1: 0.5      F
337 2: 00       Exponent of 10
338 3: 120      Z Loc [ exp    ]
339

```

```

340 35: Z=X*Y (P47)
341 1: 119 X Loc [ d2 ]
342 2: 120 Y Loc [ exp ]
343 3: 121 Z Loc [ CF ]
344
345 36: Z=X*Y (P36)
346 1: 121 X Loc [ CF ]
347 2: 116 Y Loc [ rawdepth ]
348 3: 12 Z Loc [ Depth ]
349
350
351 ;*****
352 ;*** Humidity & Air Temperature *****
353
354 37: SDI-12 Recorder (P105)
355 1: 00 SDI-12 Address
356 2: 00 SDI-12 Command
357 3: 5 Port
358 4: 6 Loc [ TempCS215 ]
359 5: 1.0 Mult
360 6: 0.0 Offset
361
362 ;*****
363 ;*** Data Storage Allocation *****
364
365 ;SET TIME AND STORAGE
366 38: If time is (P92)
367 1: 0000 Minutes (Seconds --) into a
368 2: 30 Interval (same units as above)
369 3: 10 Set Output Flag High
370
371 39: Set Active Storage Area (P80)
372 1: 1 Final Storage Area 1
373 2: 100 Array ID
374
375 40: Real Time (P77)
376 1: 1220 Year,Day,Hour/Minute (midnight = 2400)
377
378 ;OUTPUT MINIMUM BATTERY VOLTAGE
379 41: Minimum (P74)
380 1: 1 Reps
381 2: 00 Time Option
382 3: 14 Loc [ Battery ]
383
384 ;READ WIND SPEED AND DIRECTION
385 42: Average (P71)
386 1: 1 Reps
387 2: 2 Loc [ WindSpd ]
388
389 43: Average (P71)
390 1: 1 Reps
391 2: 3 Loc [ WindDir ]
392
393 ;SURFACE TEMPERATURE AVERAGES
394 44: Average (P71)
395 1: 1 Reps
396 2: 9 Loc [ Surface ]
397
398 ;AVERAGE LONG/SHORTWAVE RADATION
399 45: Average (P71)
400 1: 1 Reps
401 2: 4 Loc [ ShortUP ]
402 46: Average (P71)
403 1: 1 Reps
404 2: 5 Loc [ ShortDOWN ]
405
406 47: Average (P71)
407 1: 1 Reps
408 2: 11 Loc [ Longwave ]
409
410 ;SNOW DEPTH AVERAGE
411 48: Average (P71)
412 1: 1 Reps
413 2: 12 Loc [ Depth ]
414
415 49: Average (P71)
416 1: 1 Reps
417 2: 116 Loc [ rawdepth ]
418
419 50: Average (P71)
420 1: 1 Reps
421 2: 121 Loc [ CF ]
422
423 51: Average (P71)
424 1: 1 Reps
425 2: 8 Loc [ DpthTEMP ]
426

```

```

427 ;ATMOSPHERE TEMP/HUMID AVERAGES
428 52: Average (P71)
429 1: 1 Reps
430 2: 6 Loc [ TempCS215 ]
431
432 53: Average (P71)
433 1: 1 Reps
434 2: 7 Loc [ HumdCS215 ]
435
436 ;AVERAGE RAW DATA FOR LONGWAVE
437 54: Average (P71)
438 1: 1 Reps
439 2: 122 Loc [ ----- ]
440
441 55: Average (P71)
442 1: 1 Reps
443 2: 101 Loc [ Case_Res ]
444
445 ;THERMOCOUPLE AVERAGES
446 56: Average (P71)
447 1: 1 Reps
448 2: 20 Loc [ TC.1 ]
449 57: Average (P71)
450 1: 1 Reps
451 2: 21 Loc [ TC.2 ]
452 58: Average (P71)
453 1: 1 Reps
454 2: 22 Loc [ TC.3 ]
455 59: Average (P71)
456 1: 1 Reps
457 2: 23 Loc [ TC.4 ]
458 60: Average (P71)
459 1: 1 Reps
460 2: 24 Loc [ TC.5 ]
461 61: Average (P71)
462 1: 1 Reps
463 2: 25 Loc [ TC.6 ]
464 62: Average (P71)
465 1: 1 Reps
466 2: 26 Loc [ TC.7 ]
467 63: Average (P71)
468 1: 1 Reps
469 2: 27 Loc [ TC.8 ]
470 64: Average (P71)
471 1: 1 Reps
472 2: 28 Loc [ TC.9 ]
473 65: Average (P71)
474 1: 1 Reps
475 2: 29 Loc [ TC.10 ]
476 66: Average (P71)
477 1: 1 Reps
478 2: 30 Loc [ TC.11 ]
479 67: Average (P71)
480 1: 1 Reps
481 2: 31 Loc [ TC.12 ]
482 68: Average (P71)
483 1: 1 Reps
484 2: 32 Loc [ TC.13 ]
485 69: Average (P71)
486 1: 1 Reps
487 2: 33 Loc [ TC.14 ]
488 70: Average (P71)
489 1: 1 Reps
490 2: 34 Loc [ TC.15 ]
491 71: Average (P71)
492 1: 1 Reps
493 2: 35 Loc [ TC.16 ]
494 72: Average (P71)
495 1: 1 Reps
496 2: 36 Loc [ TC.17 ]
497 73: Average (P71)
498 1: 1 Reps
499 2: 37 Loc [ TC.18 ]
500 74: Average (P71)
501 1: 1 Reps
502 2: 38 Loc [ TC.19 ]
503 75: Average (P71)
504 1: 1 Reps
505 2: 39 Loc [ TC.20 ]
506 76: Average (P71)
507 1: 1 Reps
508 2: 40 Loc [ TCgnd ]
509
510 *Table 2 Program
511 02: 0.0000 Execution Interval (seconds)
512
513 *Table 3 Subroutines

```

```

514
515
516 ;**** SUBROUTINE #1 *****
517
518 1: Beginning of Subroutine (P85)
519 1: 1 Subroutine 1
520
521 ;CONVERT RESISTANCE TO TEMPERATURE
522 -----
523 ;T = 1/(A+B*Ln(R) + C*(Ln(R))^3)
524 ;T = Temp in Deg. Kelvin
525 ;A = 0.0010295
526 ;B = 0.0002391
527 ;C = 0.0000001568
528 ;R = Measured resistance of thermistor
529 -----
530
531 ; Constant A
532 2: Z=F (P30)
533 1: 1.0295 F
534 2: -3 Exponent of 10
535 3: 102 Z Loc [ ConstA ]
536
537 ; Constant B
538 3: Z=F (P30)
539 1: 2.391 F
540 2: -4 Exponent of 10
541 3: 103 Z Loc [ ConstB ]
542
543 ; Constant C
544 4: Z=F (P30)
545 1: 1.568 F
546 2: -7 Exponent of 10
547 3: 104 Z Loc [ ConstC ]
548
549 ; Natural Log of Resistance
550 5: Z=LN(X) (P40)
551 1: 101 X Loc [ Case_Res ]
552 2: 105 Z Loc [ Ln_Res ]
553
554 ; B*Ln(R)
555 6: Z=X*Y (P36)
556 1: 103 X Loc [ ConstB ]
557 2: 105 Y Loc [ Ln_Res ]
558 3: 107 Z Loc [ bLn.res ]
559
560 ; Squre and Cube Natural Log
561 7: Z=X*Y (P36)
562 1: 105 X Loc [ Ln_Res ]
563 2: 105 Y Loc [ Ln_Res ]
564 3: 108 Z Loc [ Ln.res2 ]
565
566 8: Z=X*Y (P36)
567 1: 105 X Loc [ Ln_Res ]
568 2: 108 Y Loc [ Ln.res2 ]
569 3: 109 Z Loc [ Ln.res3 ]
570
571 ; C*(Ln(R))^3
572 9: Z=X*Y (P36)
573 1: 104 X Loc [ ConstC ]
574 2: 109 Y Loc [ Ln.res3 ]
575 3: 110 Z Loc [ CLn.res3 ]
576
577 ; Add A and B Terms
578 10: Z=X+Y (P33)
579 1: 102 X Loc [ ConstA ]
580 2: 107 Y Loc [ bLn.res ]
581 3: 111 Z Loc [ case.temp ]
582
583 ; Add C Term to A/B Term
584 11: Z=X+Y (P33)
585 1: 111 X Loc [ case.temp ]
586 2: 110 Y Loc [ CLn.res3 ]
587 3: 111 Z Loc [ case.temp ]
588
589 ; Take Reciporcal of case.temp
590 12: Z=1/X (P42)
591 1: 111 X Loc [ case.temp ]
592 2: 111 Z Loc [ case.temp ]
593
594 13: End (P95)
595
596
597 ;**** SUBROUTINE #2 *****
598
599 14: Beginning of Subroutine (P85)
600 1: 2 Subroutine 2

```

```

601
602 ;CORRECT PIR CASE TEMPERATURE
603 -----
604 ; CorrectOutput = A + (C*T^4)
605 ; A = Thermopile Output
606 ; C = Stefan-Boltzman Cnst = 5.6697e-8 Wm-2K-4
607 ; T = Case Temperature in Kelvin
608 ; S = F = 6.39 uV/W/m^2 = 156.495 mV/W/m^2 (SN:070108)
609 -----
610
611 ;CONVERT THERMOPILE TO Wm-2
612 15: Z=X*F (P37)
613 1: 100 X Loc [ Uemf ]
614 2: 156.495 F
615 3: 112 Z Loc [ PIR.Aterm ]
616
617 ;Load 4 for raising to forth
618 16: Z=F (P30)
619 1: 4 F
620 2: 0 Exponent of 10
621 3: 113 Z Loc [ Power4 ]
622
623 ;Raise to 4th Power
624 17: Z=X^Y (P47)
625 1: 111 X Loc [ case_temp ]
626 2: 113 Y Loc [ Power4 ]
627 3: 111 Z Loc [ case_temp ]
628
629 ;Load Boltzman
630 18: Z=F (P30)
631 1: 5.669 F
632 2: -8 Exponent of 10
633 3: 114 Z Loc [ PIR.Bterm ]
634
635 ;Mutliply Boltzman by T^4
636 19: Z=X*Y (P36)
637 1: 114 X Loc [ PIR.Bterm ]
638 2: 111 Y Loc [ case_temp ]
639 3: 114 Z Loc [ PIR.Bterm ]
640
641 ;Add A to Bterm -> OUTPUTS THE LONGWAVE RADIATION
642 20: Z=X+Y (P33)
643 1: 112 X Loc [ PIR.Aterm ]
644 2: 114 Y Loc [ PIR.Bterm ]
645 3: 11 Z Loc [ Longwave ]
646
647 21: End (P95)
648
649 End Program
650
651 -Input Locations-
652 1 RefTemp-- 1 2 1
653 2 WindSpd 1 2 2
654 3 WindDir 1 1 1
655 4 ShortUP 5 1 1
656 5 ShortDOWN 1 1 2
657 6 TempCS215 9 2 2
658 7 HumdCS215 9 1 1
659 8 DpthTEMP 17 1 1
660 9 Surface 1 1 1
661 10 ----- 1 0 0
662 11 Longwave 9 1 4
663 12 Depth 9 1 4
664 13 ----- 9 0 3
665 14 Battery 9 2 4
666 15 ----- 13 0 3
667 16 ----- 9 0 3
668 17 ----- 9 0 4
669 18 ----- 25 0 4
670 19 ----- 9 0 1
671 20 TC.1 13 1 2
672 21 TC.2 25 1 2
673 22 TC.3 9 1 1
674 23 TC.4 9 1 1
675 24 TC.5 9 1 1
676 25 TC.6 9 1 1
677 26 TC.7 9 1 1
678 27 TC.8 9 1 1
679 28 TC.9 9 1 1
680 29 TC.10 9 1 1
681 30 TC.11 17 1 1
682 31 TC.12 1 1 0
683 32 TC.13 1 1 0
684 33 TC.14 1 1 0
685 34 TC.15 1 1 0
686 35 TC.16 1 1 0
687 36 TC.17 1 1 0

```

688	37	TC_18	1	1	0
689	38	TC_19	1	1	0
690	39	TC_20	1	1	0
691	40	TCgnd	1	1	1
692	41	-----	0	0	0
693	42	-----	0	0	0
694	43	-----	0	0	0
695	44	-----	0	0	0
696	45	-----	0	0	0
697	46	-----	0	0	0
698	47	-----	0	0	0
699	48	-----	1	0	0
700	49	-----	1	0	0
701	50	-----	1	0	0
702	51	-----	1	0	0
703	52	-----	1	0	0
704	53	-----	1	0	0
705	54	-----	1	0	0
706	55	-----	1	0	0
707	56	-----	1	0	0
708	57	-----	1	0	0
709	58	-----	1	0	0
710	59	-----	1	0	0
711	60	-----	1	0	0
712	61	-----	1	0	0
713	62	-----	1	0	0
714	63	-----	1	0	0
715	64	-----	1	0	0
716	65	-----	1	0	0
717	66	-----	1	0	0
718	67	-----	1	0	0
719	68	-----	1	0	0
720	69	-----	1	0	0
721	70	-----	1	0	0
722	71	-----	1	0	0
723	72	-----	1	0	0
724	73	-----	1	0	0
725	74	-----	1	0	0
726	75	-----	1	0	0
727	76	-----	1	0	0
728	77	-----	1	0	0
729	78	-----	1	0	0
730	79	-----	1	0	0
731	80	-----	1	0	0
732	81	-----	1	0	0
733	82	-----	1	0	0
734	83	-----	0	0	0
735	84	-----	0	0	0
736	85	-----	0	0	0
737	86	-----	0	0	0
738	87	-----	0	0	0
739	88	-----	0	0	0
740	89	-----	0	0	0
741	90	-----	0	0	0
742	91	-----	0	0	0
743	92	-----	0	0	0
744	93	-----	0	0	0
745	94	-----	0	0	0
746	95	-----	0	0	0
747	96	-----	0	0	0
748	97	-----	0	0	0
749	98	-----	0	0	0
750	99	-----	0	0	0
751	100	Uemf	1	1	1
752	101	Case_Res	1	3	2
753	102	ConstA	1	1	1
754	103	ConstB	1	1	1
755	104	ConstC	1	1	1
756	105	Ln_Res	1	4	1
757	106	-----	1	0	0
758	107	bLn_res	1	1	1
759	108	Ln_res2	1	1	1
760	109	Ln_res3	1	1	1
761	110	CLn_res3	1	1	1
762	111	case_temp	1	4	4
763	112	PIR_Aterm	1	1	1
764	113	Power4	1	1	1
765	114	PIR_Bterm	1	2	2
766	115	SurTemp_2	1	0	0
767	116	rawdepth	1	2	1
768	117	d1	1	1	1
769	118	kelvin	1	1	1
770	119	d2	1	1	1
771	120	exp	1	1	1
772	121	CF	1	2	1
773	122	-----	1	1	0
774	Program Security				



```

775 0000
776 0000
777 0000
778 -Mode 4-
779 -Final Storage Area 2-
780 0
781 -CR10X ID-
782 0
783 -CR10X Power Up-
784 3

```

## A.6.2 South Weather Station Program

```

1  ;{CR10}
2  ;-----
3  ; A PROGRAM BY:
4  ;
5  ;   ANDREW E. SLAUGHTER
6  ;   205 Cobleigh Hall, MSU-Bozeman
7  ;   P.O. Box 173900
8  ;   Bozeman, MT 59717-3900
9  ;   (406)994-2293
10 ;
11 ;*****
12 ;
13 ; BACKGROUND:
14 ;   The following program utilizes the Campbell Scientific, Inc. (SCI) CR10(x)
15 ;   datalogger and two CSI AM418 multiplexer to acquire basic weather data that
16 ;   includes snow surface temperature, snow depth, humidity, air temperature,
17 ;   wind speed, wind direction, longwave radiation, and shortwave radiation.
18 ;   Additionally, the station has an array of thermocouples that measures the
19 ;   snowpack temperature at various depths below the surface.
20 ;
21 ;   The objective of the site is to collect field data regarding the growth
22 ;   of near-surface faceted and surface hoar crystals for the use in verifying both
23 ;   lab and analytical models of the near-surface processes.
24 ;
25 ;   Last Updated: December 2008
26 ;
27 ;*****
28 ;
29 ; WIRING SCHEME:
30 ;
31 ; -> CR10TCR Thermistor
32 ;   Wht - AG
33 ;   Blk - E1
34 ;   Red - SE6
35 ;
36 ; -> AM418 MULTIPLEXIERS
37 ;   Wiring (CR10 - AM416):
38 ;   C1 - REM
39 ;   C2 - CLK
40 ;   H1 - ComH1
41 ;   L1 - ComL1
42 ;   H2 - ComH2
43 ;   L2 - ComL2
44 ;
45 ; -> THERMOCOUPLES (wired to AM416)
46 ;   1H1,1L1 - TC.1
47 ;   1H2,1L2 - TC.2
48 ;   ...
49 ;   11H1,11L1 - TC.21 (TC to Grnd)
50 ;
51 ; -> KIPP & ZONEN CMP3 (shortwave, wired to AM416#1)
52 ;
53 ;   Up Mult. = 14.11 uV/W/m^2 = 70.87 W/m^2/mV (SN:080193)
54 ;   Dn Mult. = 14.34 uV/W/m^2 = 69.74 W/m^2/mV (SN:080192)
55 ;
56 ;   Incoming (up)      Reflected (down)
57 ;   Red - 12:H1        Grn - 12:L2
58 ;   Blk - 12:L1        Blu - 12:H2
59 ;
60 ; -> KIPP & ZONEN CGR3 (longwave);
61 ;
62 ;   Mult. = 11.83 uV/W/m^2 = 84.531W/m^2/mV (SN:070108)
63 ;
64 ;   Red - L5
65 ;   Blu - H5
66 ;   Ylw - SE12

```

```

67 ;           Grn - G
68 ;           1kOhm Resistor from SE12 - E3
69 ;
70 ; -> METONE ANEMOMETER
71 ;           Yel - SE5
72 ;           Wht - AG
73 ;           Grn - E2
74 ;           Blk - G
75 ;           Brn - G
76 ;           Red - P1
77 ;
78 ; -> EVEREST INTERSCIENCE SNOW SURFACE TEMPERATURE
79 ;           Blu - 11:H2
80 ;           Wht - 11:L2
81 ;           Red - 12V
82 ;           Blk - G
83 ;
84 ; -> CAMPBELL SCIENTIFIC HUMIDITY AND TEMP
85 ;           Blk ,Wht,Clr - G
86 ;           Red - 12V
87 ;           Grn - C5
88 ;
89 ; -> NOVALYNX ULTRASONIC SNOW DEPTH
90 ;           Red - 12V
91 ;           Blk - G
92 ;           Clr - G
93 ;           Grn - C6
94 ;           Wht - 4H
95 ;           Brn - 4L
96 ;
97 ;
98 ;*****
99 ;**** Begin Program *****
100 ;
101 ;EXECUTION INTERVAL IN SECONDS
102 *Table 1 Program
103   01: 180           Execution Interval (seconds)
104 ;
105 ;*****
106 ;**** Battery Voltage *****
107 ;
108 1: Batt Voltage (P10)
109   1: 14           Loc [ Battery   ]
110 ;
111 ;*****
112 ;**** Stop if Battery < 11V *****
113 ;
114 2: If (X<=>F) (P89)
115   1: 14           X Loc [ Battery   ]
116   2: 4            <
117   3: 11          F
118   4: 0            Go to end of Program Table
119 ;
120 ;*****
121 ;**** Reference Temperature *****
122 ;
123 3: Temp (107) (P11)
124   1: 1            Repts
125   2: 6            SE Channel
126   3: 1            Excite all repts w/EI
127   4: 1            Loc [ RefTemp-- ]
128   5: 1.0          Mult
129   6: 0.0          Offset
130 ;
131 ;*****
132 ;**** Thermocouples, SW Radiation, & Surface Temp *****
133 ;
134 ;TRIGGER MULTIPLEXER
135 4: Do (P86)
136   1: 41           Set Port 1 High
137 ;
138 ;MEASURE THERCOUPLES 1 THRU 20
139 5: Beginning of Loop (P87)
140   1: 0            Delay
141   2: 10           Loop Count
142 ;
143 6: Do (P86)
144   1: 72           Pulse Port 2
145 ;
146 ;INDICATE TWO READINGS PER SET
147 7: Step Loop Index (P90)
148   1: 2            Step
149 ;
150 ;READ 20 THERMOCOUPLES
151 ;

```

```

154 8: Thermocouple Temp (DIFF) (P14)
155 1: 2      Repts
156 2: 1      2.5 mV Slow Range
157 3: 01     DIFF Channel
158 4: 1      Type T (Copper-Constantan)
159 5: 1      Ref Temp (Deg. C) Loc [ RefTemp-- ]
160 6: 20     -- Loc [ TC_1      ]
161 7: 1.0    Mult
162 8: 0.0    Offset
163
164 ;END THE LOOP FOR READING THERMOCOUPLES
165 9: End (P95)
166
167 ;READ THE GROUND THERMOCOUPLE AND THE SURFACE TEMPERATURE
168 10: Do (P86)
169 1: 72     Pulse Port 2
170
171 11: Thermocouple Temp (DIFF) (P14)
172 1: 1      Repts
173 2: 1      2.5 mV Slow Range
174 3: 1      DIFF Channel
175 4: 1      Type T (Copper-Constantan)
176 5: 1      Ref Temp (Deg. C) Loc [ RefTemp-- ]
177 6: 40     Loc [ TCgnd      ]
178 7: 1.0    Mult
179 8: 0.0    Offset
180
181 12: Volt (Diff) (P2)
182 1: 1      Repts
183 2: 5      2500 mV Slow Range
184 3: 2      DIFF Channel
185 4: 9      Loc [ Surface    ]
186 5: 0.1    Mult
187 6: 0.0    Offset
188
189 ;READ THE SHORTWAVE SENSORS (UP & DOWN)
190 13: Do (P86)
191 1: 72     Pulse Port 2
192
193 ;Incoming (up)
194 14: Volt (Diff) (P2)
195 1: 1      Repts
196 2: 3      25 mV Slow Range
197 3: 1      DIFF Channel
198 4: 4      Loc [ ShortUP     ]
199 5: 70.87  Mult
200 6: 0.0    Offset
201
202 ;Reflected (Down)
203 15: Volt (Diff) (P2)
204 1: 1      Repts
205 2: 3      25 mV Slow Range
206 3: 1      DIFF Channel
207 4: 5      Loc [ ShortDOWN   ]
208 5: 69.74  Mult
209 6: 0.0    Offset
210
211 ;TURN OFF MULTIPLEXER
212 16: Do (P86)
213 1: 51     Set Port 1 Low
214
215
216 ;*****
217 ;**** Wind Speed and Direction *****
218 ;-----
219 ; WindSpd = m/s2
220 ; WindDir = 0-360 (N=0=360)
221 ;-----
222
223 ;MEASURE WIND SPEED
224 17: Pulse (P3)
225 1: 1      Repts
226 2: 1      Pulse Input Channel
227 3: 22     Switch Closure, Output Hz
228 4: 2      Loc [ WindSpd    ]
229 5: 0.7990 Mult
230 6: 0.2811 Offset
231
232 ;IF WIND SPEED IS NEGATIVE SET TO ZERO
233 18: If (X<=>F) (P89)
234 1: 2      X Loc [ WindSpd  ]
235 2: 1      =
236 3: 0.2811 F
237 4: 30     Then Do
238
239 19: Z=F (P30)
240 1: 0      F

```

```

241 2: 0      Exponent of 10
242 3: 2      Z Loc [ WindSpd  ]
243
244 20: End (P95)
245
246 ; MEASURE WIND DIRECTION
247 21: AC Half Bridge (P5)
248 1: 1      Reps
249 2: 25     2500 mV 60 Hz Rejection Range
250 3: 5      SE Channel
251 4: 2      Excite all reps w/Exchan 2
252 5: 2500   mV Excitation
253 6: 3      Loc [ WindDir  ]
254 7: 360    Mult
255 8: 0.0    Offset
256
257
258 ;*****
259 ;**** Longwave Radiation *****
260 ;
261 ;MEASURE VOLTAGE FOR THERMOPILE
262 22: Volt (Diff) (P2)
263 1: 1      Reps
264 2: 1      2.5 mV Slow Range
265 3: 5      DIFF Channel
266 4: 100    Loc [ Uemf      ]
267 5: 1      Mult
268 6: 0.0    Offset
269
270 ;MEASURE THERMISTOR
271 23: AC Half Bridge (P5)
272 1: 1      Reps
273 2: 15     2500 mV Fast Range
274 3: 12     SE Channel
275 4: 3      Excite all reps w/Exchan 3
276 5: 2500   mV Excitation
277 6: 101    Loc [ Case_Res  ]
278 7: 1.0    Mult
279 8: 0.0    Offset
280
281 ;CONVERT THERMISTOR MEASURE TO RESISTANCE
282 24: BR Transform Rf[X/(1-X)] (P59)
283 1: 1      Reps
284 2: 101    Loc [ Case_Res  ]
285 3: 1000   Multiplier (Rf)
286
287 ;CONVERT RESISTANCE TO TEMPERATURE
288 25: Do (P86)
289 1: 1      Call Subroutine 1
290
291 ;CORRECT FOR CASE TEMPERATURE -> OUTPUT LONGWAVE RADIATION
292 26: Do (P86)
293 1: 2      Call Subroutine 2
294
295 ;*****
296 ;**** Snow Depth *****
297
298 27: Do (P86)
299 1: 46     Set Port 6 High
300
301 ; Wait 2 seconds for sensor to warm-up and measure depth
302 28: Excitation with Delay (P22)
303 1: 2      Ex Channel
304 2: 200    Delay W/Ex (units = 0.01 sec)
305 3: 0000   Delay After Ex (units = 0.01 sec)
306 4: 0000   mV Excitation
307
308 ;Depth given in mV and scaled to cm, offset = mounting height
309 29: Volt (Diff) (P2)
310 1: 1      Reps
311 2: 5      2500 mV Slow Range
312 3: 4      DIFF Channel
313 4: 116    Loc [ rawdepth  ]
314 5: -0.25  Mult
315 6: 200    Offset
316
317 30: Do (P86)
318 1: 56     Set Port 6 Low
319
320 ; Compute the temperature corrected depth
321 31: Z=X+F (P34)
322 1: 6      X Loc [ TempCS215 ]
323 2: 273.15 F
324 3: 117    Z Loc [ d1      ]
325
326 32: Z=F (P30)
327 1: 273.15 F

```

```

328 2: 00      Exponent of 10
329 3: 118      Z Loc [ kelvin  ]
330
331 33:  Z=X/Y (P38)
332 1: 117      X Loc [ d1      ]
333 2: 118      Y Loc [ kelvin  ]
334 3: 119      Z Loc [ d2      ]
335
336 34:  Z=F (P30)
337 1: 0.5      F
338 2: 00      Exponent of 10
339 3: 120      Z Loc [ exp    ]
340
341 35:  Z=X`Y (P47)
342 1: 119      X Loc [ d2      ]
343 2: 120      Y Loc [ exp    ]
344 3: 121      Z Loc [ CF      ]
345
346 36:  Z=X*Y (P36)
347 1: 121      X Loc [ CF      ]
348 2: 116      Y Loc [ rawdepth ]
349 3: 12       Z Loc [ Depth   ]
350
351
352 ;*****
353 ;**** Humidity & Air Temperature *****
354
355 37:  SDI-12 Recorder (P105)
356 1: 00      SDI-12 Address
357 2: 00      SDI-12 Command
358 3: 5       Port
359 4: 6       Loc [ TempCS215 ]
360 5: 1.0     Mult
361 6: 0.0     Offset
362
363 ;*****
364 ;**** Data Storage Allocation *****
365
366 ;SET TIME AND STORAGE
367 38:  If time is (P92)
368 1: 0000    Minutes (Seconds --) into a
369 2: 30      Interval (same units as above)
370 3: 10      Set Output Flag High
371
372 39:  Set Active Storage Area (P80)
373 1: 1       Final Storage Area 1
374 2: 100     Array ID
375
376 40:  Real Time (P77)
377 1: 1220    Year,Day,Hour/Minute (midnight = 2400)
378
379 ;OUTPUT MINIMUM BATTERY VOLTAGE
380 41:  Minimum (P74)
381 1: 1       Reps
382 2: 00      Time Option
383 3: 14      Loc [ Battery  ]
384
385 ;READ WIND SPEED AND DIRECTION
386 42:  Average (P71)
387 1: 1       Reps
388 2: 2       Loc [ WindSpd  ]
389
390 43:  Average (P71)
391 1: 1       Reps
392 2: 3       Loc [ WindDir  ]
393
394 ;SURFACE TEMPERATURE AVERAGES
395 44:  Average (P71)
396 1: 1       Reps
397 2: 9       Loc [ Surface  ]
398
399 ;AVERAGE LONG/SHORTWAVE RADATION
400 45:  Average (P71)
401 1: 1       Reps
402 2: 4       Loc [ ShortUP   ]
403 46:  Average (P71)
404 1: 1       Reps
405 2: 5       Loc [ ShortDOWN ]
406
407 47:  Average (P71)
408 1: 1       Reps
409 2: 11      Loc [ Longwave  ]
410
411 ;SNOW DEPTH AVERAGE
412 48:  Average (P71)
413 1: 1       Reps
414 2: 12      Loc [ Depth    ]

```

```

415
416 49: Average (P71)
417 1: 1 Reps
418 2: 116 Loc [ rawdepth ]
419
420 50: Average (P71)
421 1: 1 Reps
422 2: 121 Loc [ CF ]
423
424 51: Average (P71)
425 1: 1 Reps
426 2: 8 Loc [ DpthTEMP ]
427
428 ;ATMOSPHERE TEMP/HUMID AVERAGES
429 52: Average (P71)
430 1: 1 Reps
431 2: 6 Loc [ TempCS215 ]
432
433 53: Average (P71)
434 1: 1 Reps
435 2: 7 Loc [ HumdCS215 ]
436
437 ;AVERAGE RAW DATA FOR LONGWAVE
438 54: Average (P71)
439 1: 1 Reps
440 2: 122 Loc [ ----- ]
441
442 55: Average (P71)
443 1: 1 Reps
444 2: 101 Loc [ Case_Res ]
445
446 ;THERMOCOUPLE AVERAGES
447 56: Average (P71)
448 1: 1 Reps
449 2: 20 Loc [ TC.1 ]
450 57: Average (P71)
451 1: 1 Reps
452 2: 21 Loc [ TC.2 ]
453 58: Average (P71)
454 1: 1 Reps
455 2: 22 Loc [ TC.3 ]
456 59: Average (P71)
457 1: 1 Reps
458 2: 23 Loc [ TC.4 ]
459 60: Average (P71)
460 1: 1 Reps
461 2: 24 Loc [ TC.5 ]
462 61: Average (P71)
463 1: 1 Reps
464 2: 25 Loc [ TC.6 ]
465 62: Average (P71)
466 1: 1 Reps
467 2: 26 Loc [ TC.7 ]
468 63: Average (P71)
469 1: 1 Reps
470 2: 27 Loc [ TC.8 ]
471 64: Average (P71)
472 1: 1 Reps
473 2: 28 Loc [ TC.9 ]
474 65: Average (P71)
475 1: 1 Reps
476 2: 29 Loc [ TC.10 ]
477 66: Average (P71)
478 1: 1 Reps
479 2: 30 Loc [ TC.11 ]
480 67: Average (P71)
481 1: 1 Reps
482 2: 31 Loc [ TC.12 ]
483 68: Average (P71)
484 1: 1 Reps
485 2: 32 Loc [ TC.13 ]
486 69: Average (P71)
487 1: 1 Reps
488 2: 33 Loc [ TC.14 ]
489 70: Average (P71)
490 1: 1 Reps
491 2: 34 Loc [ TC.15 ]
492 71: Average (P71)
493 1: 1 Reps
494 2: 35 Loc [ TC.16 ]
495 72: Average (P71)
496 1: 1 Reps
497 2: 36 Loc [ TC.17 ]
498 73: Average (P71)
499 1: 1 Reps
500 2: 37 Loc [ TC.18 ]
501 74: Average (P71)

```

```

502 1: 1      Repts
503 2: 38     Loc [ TC.19      ]
504 75: Average (P71)
505 1: 1      Repts
506 2: 39     Loc [ TC.20      ]
507 76: Average (P71)
508 1: 1      Repts
509 2: 40     Loc [ TCgnd      ]
510
511 *Table 2 Program
512 02: 0.0000 Execution Interval (seconds)
513
514 *Table 3 Subroutines
515
516
517 ;**** SUBROUTINE #1 ****
518
519 1: Beginning of Subroutine (P85)
520 1: 1      Subroutine 1
521
522 ;CONVERT RESISTANCE TO TEMPERATURE
523 -----
524 ;T = 1/(A+B*Ln(R) + C*(Ln(R))^3)
525 ;T = Temp in Deg. Kelvin
526 ;A = 0.0010295
527 ;B = 0.0002391
528 ;C = 0.000001568
529 ;R = Measured resistance of thermistor
530 -----
531
532 ; Constant A
533 2: Z=F (P30)
534 1: 1.0295 F
535 2: -3     Exponent of 10
536 3: 102    Z Loc [ ConstA  ]
537
538 ; Constant B
539 3: Z=F (P30)
540 1: 2.391 F
541 2: -4     Exponent of 10
542 3: 103    Z Loc [ ConstB  ]
543
544 ; Constant C
545 4: Z=F (P30)
546 1: 1.568 F
547 2: -7     Exponent of 10
548 3: 104    Z Loc [ ConstC  ]
549
550 ; Natural Log of Resistance
551 5: Z=LN(X) (P40)
552 1: 101    X Loc [ Case_Res ]
553 2: 105    Z Loc [ Ln_Res   ]
554
555 ; B*Ln(R)
556 6: Z=X*Y (P36)
557 1: 103    X Loc [ ConstB  ]
558 2: 105    Y Loc [ Ln_Res   ]
559 3: 107    Z Loc [ bLn_res  ]
560
561 ; Squire and Cube Natural Log
562 7: Z=X*Y (P36)
563 1: 105    X Loc [ Ln_Res   ]
564 2: 105    Y Loc [ Ln_Res   ]
565 3: 108    Z Loc [ Ln_res2  ]
566
567 8: Z=X*Y (P36)
568 1: 105    X Loc [ Ln_Res   ]
569 2: 108    Y Loc [ Ln_res2  ]
570 3: 109    Z Loc [ Ln_res3  ]
571
572 ; C*(Ln(R))^3
573 9: Z=X*Y (P36)
574 1: 104    X Loc [ ConstC  ]
575 2: 109    Y Loc [ Ln_res3  ]
576 3: 110    Z Loc [ CLn_res3 ]
577
578 ; Add A and B Terms
579 10: Z=X+Y (P33)
580 1: 102    X Loc [ ConstA  ]
581 2: 107    Y Loc [ bLn_res  ]
582 3: 111    Z Loc [ case_temp ]
583
584 ; Add C Term to A/B Term
585 11: Z=X+Y (P33)
586 1: 111    X Loc [ case_temp ]
587 2: 110    Y Loc [ CLn_res3 ]
588 3: 111    Z Loc [ case_temp ]

```

```

589
590 ; Take Reciporcal of case_temp
591 12: Z=1/X (P42)
592 1: 111      X Loc [ case_temp ]
593 2: 111      Z Loc [ case_temp ]
594
595 13: End (P95)
596
597
598 ;**** SUBROUTINE #2 *****
599
600 14: Beginning of Subroutine (P85)
601 1: 2        Subroutine 2
602
603 ;CORRECT PIR CASE TEMPERATURE
604 -----
605 ; CorrectOutput = A + (C*T^4)
606 ; A = Thermopile Output
607 ; C = Stefan-Boltzman Cnst = 5.6697e-8 Wm-2K-4
608 ; T = Case Temperature in Kelvin
609 ; S = F = 11.83uV/W/m^2 = 84.531 W/m^2/mV (SN:070112)
610 -----
611
612 ;CONVERT THERMOPILE TO Wm-2
613 15: Z=X*F (P37)
614 1: 100      X Loc [ Uemf      ]
615 2: 84.531   F
616 3: 112      Z Loc [ PIR_Aterm ]
617
618 ;Load 4 for raising to forth
619 16: Z=F (P30)
620 1: 4        F
621 2: 0        Exponent of 10
622 3: 113      Z Loc [ Power4   ]
623
624 ;Raise to 4th Power
625 17: Z=X^Y (P47)
626 1: 111      X Loc [ case_temp ]
627 2: 113      Y Loc [ Power4   ]
628 3: 111      Z Loc [ case_temp ]
629
630 ;Load Boltzman
631 18: Z=F (P30)
632 1: 5.669    F
633 2: -8       Exponent of 10
634 3: 114      Z Loc [ PIR_Bterm ]
635
636 ;Mutlply Boltzman by T^4
637 19: Z=X*Y (P36)
638 1: 114      X Loc [ PIR_Bterm ]
639 2: 111      Y Loc [ case_temp ]
640 3: 114      Z Loc [ PIR_Bterm ]
641
642 ;Add A to Bterm -> OUTPUTS THE LONGWAVE RADIATION
643 20: Z=X+Y (P33)
644 1: 112      X Loc [ PIR_Aterm ]
645 2: 114      Y Loc [ PIR_Bterm ]
646 3: 11       Z Loc [ Longwave  ]
647
648 21: End (P95)
649
650 End Program
651
652 -Input Locations-
653 1 RefTemp__ 1 2 1
654 2 WindSpd   1 2 2
655 3 WindDir   1 1 1
656 4 ShortUP   5 1 1
657 5 ShortDOWN 1 1 2
658 6 TempCS215 9 2 2
659 7 HumdCS215 9 1 1
660 8 DpthTEMP  17 1 1
661 9 Surface   1 1 1
662 10 ----- 1 0 0
663 11 Longwave 9 1 4
664 12 Depth    9 1 4
665 13 ----- 9 0 3
666 14 Battery  9 2 4
667 15 ----- 13 0 3
668 16 ----- 9 0 3
669 17 ----- 9 0 4
670 18 ----- 25 0 4
671 19 ----- 9 0 1
672 20 TC.1     13 1 2
673 21 TC.2     25 1 2
674 22 TC.3     9 1 1
675 23 TC.4     9 1 1

```



676	24	TC_5	9	1	1
677	25	TC_6	9	1	1
678	26	TC_7	9	1	1
679	27	TC_8	9	1	1
680	28	TC_9	9	1	1
681	29	TC_10	9	1	1
682	30	TC_11	17	1	1
683	31	TC_12	1	1	0
684	32	TC_13	1	1	0
685	33	TC_14	1	1	0
686	34	TC_15	1	1	0
687	35	TC_16	1	1	0
688	36	TC_17	1	1	0
689	37	TC_18	1	1	0
690	38	TC_19	1	1	0
691	39	TC_20	1	1	0
692	40	TCgnd	1	1	1
693	41	-----	0	0	0
694	42	-----	0	0	0
695	43	-----	0	0	0
696	44	-----	0	0	0
697	45	-----	0	0	0
698	46	-----	0	0	0
699	47	-----	0	0	0
700	48	-----	1	0	0
701	49	-----	1	0	0
702	50	-----	1	0	0
703	51	-----	1	0	0
704	52	-----	1	0	0
705	53	-----	1	0	0
706	54	-----	1	0	0
707	55	-----	1	0	0
708	56	-----	1	0	0
709	57	-----	1	0	0
710	58	-----	1	0	0
711	59	-----	1	0	0
712	60	-----	1	0	0
713	61	-----	1	0	0
714	62	-----	1	0	0
715	63	-----	1	0	0
716	64	-----	1	0	0
717	65	-----	1	0	0
718	66	-----	1	0	0
719	67	-----	1	0	0
720	68	-----	1	0	0
721	69	-----	1	0	0
722	70	-----	1	0	0
723	71	-----	1	0	0
724	72	-----	1	0	0
725	73	-----	1	0	0
726	74	-----	1	0	0
727	75	-----	1	0	0
728	76	-----	1	0	0
729	77	-----	1	0	0
730	78	-----	1	0	0
731	79	-----	1	0	0
732	80	-----	1	0	0
733	81	-----	1	0	0
734	82	-----	1	0	0
735	83	-----	0	0	0
736	84	-----	0	0	0
737	85	-----	0	0	0
738	86	-----	0	0	0
739	87	-----	0	0	0
740	88	-----	0	0	0
741	89	-----	0	0	0
742	90	-----	0	0	0
743	91	-----	0	0	0
744	92	-----	0	0	0
745	93	-----	0	0	0
746	94	-----	0	0	0
747	95	-----	0	0	0
748	96	-----	0	0	0
749	97	-----	0	0	0
750	98	-----	0	0	0
751	99	-----	0	0	0
752	100	Uemf	1	1	1
753	101	Case_Res	1	3	2
754	102	ConstA	1	1	1
755	103	ConstB	1	1	1
756	104	ConstC	1	1	1
757	105	Ln_Res	1	4	1
758	106	-----	1	0	0
759	107	bLn_res	1	1	1
760	108	Ln_res2	1	1	1
761	109	Ln_res3	1	1	1
762	110	CLn_res3	1	1	1

```

763 111 case_temp 1 4 4
764 112 PIR_Aterm 1 1 1
765 113 Power4 1 1 1
766 114 PIR_Bterm 1 2 2
767 115 SurTemp_2 1 0 0
768 116 rawdepth 1 2 1
769 117 d1 1 1 1
770 118 kelvin 1 1 1
771 119 d2 1 1 1
772 120 exp 1 1 1
773 121 CF 1 2 1
774 122 ----- 1 1 0
775 -Program Security-
776 0000
777 0000
778 0000
779 -Mode 4-
780 -Final Storage Area 2-
781 0

```

### A.6.3 American Spirit Weather Station Program

```

1  ;{CR10X}
2  ;Program: Yellowstone Club
3  ;American Spirit Lift - Tower 18
4  ;Elevation: 8840'
5  ;1-17-08
6  ;Phone Number: 993-2679
7  ;45.2397 N 111.4429 W
8
9  ;Instrument Wiring
10
11  ;      CS 500 Temp/RH Probe
12  ;      Red 12V
13  ;      Black 1H (SE chan 1 Temp)
14  ;      Brown 1L (SE chan 2 RH)
15  ;      Green G
16  ;      Clear G
17
18  ;      R. M. Young 05103 Wind Monitor-Tower 18
19  ;      1 - Clear G
20  ;      2 - Black G
21  ;      3 - Brown AG
22  ;      4 - Red 2H
23  ;      5 - Green E1
24  ;      6 - White P1
25
26  ;      Epply PSP Shortwave Solar
27  ;      Red H3
28  ;      Black L3
29
30  ;      Epply PIR Longwave Solar
31  ;      Purple 4H
32  ;      Grey 4L
33  ;      Orange SE12
34  ;      Black G
35  ;      Yellow G
36  ;      SE12 - SE12 wire a 1kOhm resistor
37
38
39  ;FSL Tables:
40
41  ;60 Output_Table 60.00 Min
42  ;1 60 L
43  ;2 Year_RTM L
44  ;3 Day_RTM L
45  ;4 Hour_Minute_RTM L
46  ;5 Wind_Spd_S_WVT L
47  ;6 Wind_Dir_D1_WVT L
48  ;7 Wind_Spd_MAX L
49  ;8 Temp_F_AVG L
50  ;9 Rel_Humid L
51  ;10 Shortwave_AVG L
52  ;11 Longwave_AVG L
53  ;12 Battery_MIN L
54
55  ;240 Output_Table 1440.00 Min
56  ;1 240 L
57  ;2 Year_RTM L

```

```

58 ;3 Day_RTM L
59 ;4 Hour_Minute_RTM L
60 ;5 Wind_Spd_S_WVT L
61 ;6 Wind_Dir_D1_WVT L
62 ;7 Wind_Spd_MAX L
63 ;8 Wind_Spd_Hr_Min_MAX L
64 ;9 Temp_F_MIN L
65 ;10 Temp_F_Hr_Min_MIN L
66 ;11 Temp_F_MAX L
67 ;12 Temp_F_Hr_Min_MAX L
68 ;13 Temp_F_AVG L
69 ;14 Rel_Humid_AVG L
70 ;15 Shortwave_AVG L
71 ;16 Longwave_AVG L
72 ;17 Shortwave_MIN L
73 ;18 Shortwave_Hr_Min_MIN L
74 ;19 Shortwave_MAX L
75 ;20 Shortwave_Hr_Min_MAX L
76 ;21 Battery_MIN L
77
78 ;Estimated Total Final Storage Locations used per day 309
79
80 *Table 1 Program
81 01: 5 Execution Interval (seconds)
82
83 ;Measure wind speed -----
84
85 1: Pulse (P3)
86 1: 1 Reps
87 2: 1 Pulse Channel 1
88 3: 21 Low Level AC, Output Hz
89 4: 1 Loc [ Wind_Spd ]
90 5: .2192 Mult
91 6: 0 Offset
92
93 ;Measure wind direction -----
94
95 2: Excite-Delay (SE) (P4)
96 1: 1 Reps
97 2: 5 2500 mV Slow Range
98 3: 3 SE Channel
99 4: 1 Excite all reps w/Exchan 1
100 5: 2 Delay (units 0.01 sec)
101 6: 2500 mV Excitation
102 7: 2 Loc [ Wind_Dir ]
103 8: .142 Mult
104 9: 0 Offset
105
106 ;Measure Datalogger internal temp in degree F-----
107
108 3: Internal Temperature (P17)
109 1: 6 Loc [ Ref.Temp ]
110
111 4: Z=X*F (P37)
112 1: 6 X Loc [ Ref.Temp ]
113 2: 1.8 F
114 3: 6 Z Loc [ Ref.Temp ]
115
116 5: Z=X+F (P34)
117 1: 6 X Loc [ Ref.Temp ]
118 2: 32 F
119 3: 6 Z Loc [ Ref.Temp ]
120
121 ;Measure air temp in degree F and relative humidity in %-----
122
123 6: Volt (SE) (P1)
124 1: 1 Reps
125 2: 25 2500 mV 60 Hz Rejection Range
126 3: 1 SE Channel
127 4: 3 Loc [ Temp.F ]
128 5: 0.18 Mult
129 6: -40.0 Offset
130
131 7: Volt (SE) (P1)
132 1: 1 Reps
133 2: 25 2500 mV 60 Hz Rejection Range
134 3: 2 SE Channel
135 4: 4 Loc [ Rel_Humid ]
136 5: .1 Mult
137 6: 0 Offset
138
139 ;Inst. 8 - 11 limit rel humidity to a max of 100%-----
140
141 8: If (X<=>F) (P89)
142 1: 4 X Loc [ Rel_Humid ]
143 2: 3 >=
144 3: 100 F

```

```

145 4: 30      Then Do
146
147 9: Z=F (P30)
148 1: 100     F
149 2: 0       Exponent of 10
150 3: 4       Z Loc [ Rel.Humid ]
151
152 10: End (P95)
153
154 11: Batt Voltage (P10)
155 1: 5       Loc [ Battery ]
156
157 ; Measure incoming shortwave solar with Eply -----
158
159 12: Volt (Diff) (P2)
160 1: 1       Reps
161 2: 3       25 mV Slow Range
162 3: 3       DIFF Channel
163 4: 7       Loc [ Shortwave ]
164 5: 122.55 Mult
165 6: 0.0     Offset
166
167 ; Measure incoming longwave with Eply -----
168
169 ;MEASURE VOLTAGE FOR THERMOPILE
170
171 13: Volt (Diff) (P2)
172 1: 1       Reps
173 2: 1       2.5 mV Slow Range
174 3: 4       DIFF Channel
175 4: 19      Loc [ PIR.mV ]
176 5: 1.0     Mult
177 6: 0.0     Offset
178
179 ;MEASURE THERMISTOR
180
181 14: AC Half Bridge (P5)
182 1: 1       Reps
183 2: 15      2500 mV Fast Range
184 3: 12      SE Channel
185 4: 3       Excite all reps w/Exchan 3
186 5: 2500    mV Excitation
187 6: 12      Loc [ Case_Res ]
188 7: 1.0     Mult
189 8: 0.0     Offset
190
191 ;CONVERT THERMISTOR MEASURE TO RESISTANCE
192
193 15: BR Transform Rf[X/(1-X)] (P59)
194 1: 1       Reps
195 2: 12      Loc [ Case_Res ]
196 3: 1000    Multiplier (Rf)
197
198 ;CONVERT RESISTANCE TO TEMPERATURE
199
200 16: Do (P86)
201 1: 1       Call Subroutine 1
202
203 ;CORRECT FOR CASE TEMPERATURE -> OUTPUT LONGWAVE RADIATION
204
205 17: Do (P86)
206 1: 2       Call Subroutine 2
207
208 ;Output 1 hour data-----
209
210 18: If time is (P92)
211 1: 0       Minutes (Seconds --) into a
212 2: 60      Interval (same units as above)
213 3: 10      Set Output Flag High
214
215 19: Set Active Storage Area (P80)^6084
216 1: 1       Final Storage Area 1
217 2: 60      Array ID or Loc [ ----- ]
218
219 20: Real Time (P77)^17297
220 1: 1220    Year,Day,Hour/Minute (midnight = 2400)
221
222 21: Wind Vector (P69)^25081
223 1: 1       Reps
224 2: 0       Samples per Sub-Interval
225 3: 1       S, 1 Polar
226 4: 1       Wind Speed/East Loc [ Wind_Spd ]
227 5: 2       Wind Direction/North Loc [ Wind_Dir ]
228
229 22: Maximize (P73)^30846
230 1: 1       Reps
231 2: 0       Value Only

```

```

232 3: 1      Loc [ Wind_Spd ]
233
234 23: Average (P71)^2969
235 1: 1      Repts
236 2: 3      Loc [ Temp_F ]
237
238 24: Sample (P70)^2494
239 1: 1      Repts
240 2: 4      Loc [ Rel_Humid ]
241
242 ;This inst eliminates -#'s-----
243
244 25: If (X<=>F) (P89)
245 1: 7      X Loc [ Shortwave ]
246 2: 4      <
247 3: 0      F
248 4: 30     Then Do
249
250 26: Z=F*x*10^n (P30)
251 1: 0.0    F
252 2: 00     Exponent of 10
253 3: 7      Z Loc [ Shortwave ]
254
255 27: End (P95)
256
257 28: Average (P71)^2969
258 1: 1      Repts
259 2: 7      Loc [ Shortwave ]
260
261 29: Average (P71)^18739
262 1: 1      Repts
263 2: 8      Loc [ Longwave ]
264
265 30: Minimum (P74)^29813
266 1: 1      Repts
267 2: 00     Time Option
268 3: 5      Loc [ Battery ]
269
270 ;Output 24hr data -----
271
272 31: If time is (P92)
273 1: 0      Minutes (Seconds--) into a
274 2: 1440   Interval (same units as above)
275 3: 10     Set Output Flag High
276
277 32: Set Active Storage Area (P80)^32715
278 1: 1      Final Storage Area 1
279 2: 0240   Array ID
280
281 33: Real Time (P77)^24613
282 1: 1220   Year, Day, Hour/Minute (prev day at midnight, 2400 at midnight)
283
284 34: Wind Vector (P69)^7005
285 1: 1      Repts
286 2: 0      Samples per Sub-Interval
287 3: 1      S, 1 Polar
288 4: 1      Wind Speed/East Loc [ Wind_Spd ]
289 5: 2      Wind Direction/North Loc [ Wind_Dir ]
290
291 35: Maximum (P73)^15417
292 1: 1      Repts
293 2: 10     Value with Hr-Min
294 3: 1      Loc [ Wind_Spd ]
295
296 36: Minimize (P74)^2028
297 1: 1      Repts
298 2: 10     Value with Hr-Min
299 3: 3      Loc [ Temp_F ]
300
301 37: Maximum (P73)^24663
302 1: 1      Repts
303 2: 10     Value with Hr-Min
304 3: 3      Loc [ Temp_F ]
305
306 38: Average (P71)^3412
307 1: 1      Repts
308 2: 3      Loc [ Temp_F ]
309
310 39: Average (P71)^24183
311 1: 1      Repts
312 2: 4      Loc [ Rel_Humid ]
313
314 ;This inst eliminates -#'s-----
315
316 40: If (X<=>F) (P89)
317 1: 7      X Loc [ Shortwave ]
318 2: 4      <

```

```

319 3: 0      F
320 4: 30     Then Do
321
322      41: Z=F x 10^n (P30)
323      1: 0.0      F
324      2: 00      n, Exponent of 10
325      3: 7      Z Loc [ Shortwave ]
326
327 42: End (P95)
328
329 43: Average (P71)^2969
330 1: 1      Repts
331 2: 7      Loc [ Shortwave ]
332
333 44: Do (P86)
334 1: 29     Set Intermed. Proc. Disable Flag Low (Flag 9)
335
336 45: Do (P86)
337 1: 21     Set Flag 1 Low
338
339 46: Average (P71)^24559
340 1: 1      Repts
341 2: 8      Loc [ Longwave ]
342
343 47: Minimum (P74)^16675
344 1: 1      Repts
345 2: 10     Value with Hr-Min
346 3: 7      Loc [ Shortwave ]
347
348 48: Maximum (P73)^8487
349 1: 1      Repts
350 2: 10     Value with Hr-Min
351 3: 7      Loc [ Shortwave ]
352
353 49: Minimum (P74)^15889
354 1: 1      Repts
355 2: 00     Time Option
356 3: 5      Loc [ Battery ]
357
358 *Table 2 Program
359 02: 0      Execution Interval (seconds)
360
361 *Table 3 Subroutines
362
363 ;**** SUBROUTINE #1 *****
364
365 1: Beginning of Subroutine (P85)
366 1: 1      Subroutine 1
367
368 ;CONVERT RESISTANCE TO TEMPERATURE
369 -----
370 ;T = 1/(A+B*Ln(R) + C*(Ln(R))^3)
371 ;T = Temp in Deg. Kelvin
372 ;A = 0.0010295
373 ;B = 0.0002391
374 ;C = 0.0000001568
375 ;R = Measured resistance of thermistor
376 -----
377
378 ; Constant A
379 2: Z=F (P30)
380 1: 1.0295  F
381 2: -3     Exponent of 10
382 3: 9      Z Loc [ ConstA ]
383
384 ; Constant B
385 3: Z=F (P30)
386 1: 2.391  F
387 2: -4     Exponent of 10
388 3: 10     Z Loc [ ConstB ]
389
390 ; Constant C
391 4: Z=F (P30)
392 1: 1.568  F
393 2: -7     Exponent of 10
394 3: 11     Z Loc [ ConstC ]
395
396 ; Natural Log of Resistance
397 5: Z=LN(X) (P40)
398 1: 12     X Loc [ Case-Res ]
399 2: 13     Z Loc [ Ln-Res ]
400
401 ; B*Ln(R)
402 6: Z=X*Y (P36)
403 1: 10     X Loc [ ConstB ]
404 2: 13     Y Loc [ Ln-Res ]
405 3: 14     Z Loc [ bLn-res ]

```

```

406
407 ; Squire and Cube Natural Log
408 7: Z=X*Y (P36)
409 1: 13 X Loc [ Ln_Res ]
410 2: 13 Y Loc [ Ln_Res ]
411 3: 15 Z Loc [ Ln_res2 ]
412
413 8: Z=X*Y (P36)
414 1: 13 X Loc [ Ln_Res ]
415 2: 15 Y Loc [ Ln_res2 ]
416 3: 16 Z Loc [ Ln_res3 ]
417
418 ; C*(Ln(R))^3
419 9: Z=X*Y (P36)
420 1: 11 X Loc [ ConstC ]
421 2: 16 Y Loc [ Ln_res3 ]
422 3: 17 Z Loc [ CLn_res3 ]
423
424 ; Add A and B Terms
425 10: Z=X+Y (P33)
426 1: 9 X Loc [ ConstA ]
427 2: 14 Y Loc [ bLn_res ]
428 3: 18 Z Loc [ case_temp ]
429
430 ; Add C Term to A/B Term
431 11: Z=X+Y (P33)
432 1: 18 X Loc [ case_temp ]
433 2: 17 Y Loc [ CLn_res3 ]
434 3: 18 Z Loc [ case_temp ]
435
436 ; Take Reciporcal of case_temp
437 12: Z=1/X (P42)
438 1: 18 X Loc [ case_temp ]
439 2: 18 Z Loc [ case_temp ]
440
441 13: End (P95)
442
443 ;**** SUBROUTINE #2 *****
444
445 14: Beginning of Subroutine (P85)
446 1: 2 Subroutine 2
447
448 ;CORRECT PIR CASE TEMPERATURE
449 -----
450 ; CorrectOutput = A + (C*T^4)
451 ; A = Thermipile Output
452 ; C = Stefan-Boltzman Cnst = 5.6697e-8 Wm-2K-4
453 ; T = Case Temperature in Kelvin
454 -----
455
456 ;CONVERT THERMOPILE TO Wm-2
457 15: Z=X*F (P37)
458 1: 19 X Loc [ PIR_mV ]
459 2: 256.89 F
460 3: 20 Z Loc [ PIR_Aterm ]
461
462 ;Load 4 for raising to forth
463 16: Z=F (P30)
464 1: 4 F
465 2: 0 Exponent of 10
466 3: 21 Z Loc [ Power4 ]
467
468 ;Raise to 4th Power
469 17: Z=X^Y (P47)
470 1: 18 X Loc [ case_temp ]
471 2: 21 Y Loc [ Power4 ]
472 3: 18 Z Loc [ case_temp ]
473
474 ;Load Boltzman
475 18: Z=F (P30)
476 1: 5.669 F
477 2: -8 Exponent of 10
478 3: 22 Z Loc [ PIR_Bterm ]
479
480 ;Mutliply Boltzman by T^4
481 19: Z=X*Y (P36)
482 1: 22 X Loc [ PIR_Bterm ]
483 2: 18 Y Loc [ case_temp ]
484 3: 22 Z Loc [ PIR_Bterm ]
485
486 ;Add A to Bterm -> OUTPUTS THE LONGWAVE RADIATION
487 20: Z=X+Y (P33)
488 1: 20 X Loc [ PIR_Aterm ]
489 2: 22 Y Loc [ PIR_Bterm ]
490 3: 8 Z Loc [ Longwave ]
491
492 21: End (P95)

```

```

493
494 End Program
495
496 -Input Locations-
497 1 Wind_Spd 1 4 1
498 2 Wind_Dir 1 2 1
499 3 Temp_F 1 4 1
500 4 Rel_Humid 1 3 2
501 5 Battery 1 2 1
502 6 Ref_Temp 1 2 3
503 7 Shortwave 1 6 3
504 8 Longwave 1 2 1
505 9 ConstA 1 1 1
506 10 ConstB 1 1 1
507 11 ConstC 1 1 1
508 12 Case_Res 1 2 2
509 13 Ln_Res 1 4 1
510 14 bLn_res 1 1 1
511 15 Ln_res2 1 1 1
512 16 Ln_res3 1 1 1
513 17 CLn_res3 1 1 1
514 18 case_temp 1 4 4
515 19 PIR_mV 1 1 1
516 20 PIR_Aterm 1 1 1
517 21 Power4 1 1 1
518 22 PIR_Bterm 1 2 2
519 23 ----- 0 0 0
520 24 ----- 0 0 0
521 25 ----- 0 0 0
522 26 ----- 0 0 0
523 27 ----- 0 0 0
524 28 ----- 0 0 0
525 -Program Security-
526 0000
527 0000
528 0000
529 -Mode 4-
530 -Final Storage Area 2-
531 0
532 -CR10X ID-
533 0
534 -CR10X Power Up-
535 3
536 -CR10X Compile Setting-
537 3
538 -CR10X RS-232 Setting-
539 -1
540 -DLD File Labels-
541 0
542 -Final Storage Labels-
543 0,60,6084
544 1,Year_RTM,17297
545 1,Day_RTM
546 1,Hour_Minute_RTM
547 2,Wind_Spd_S_WVT^1,25081
548 2,Wind_Dir_D1_WVT^2
549 3,Wind_Spd_MAX^1,30846
550 4,Shortwave_AVG^7,2969
551 5,Rel_Humid^4,2494
552 6,Battery_MIN^5,29813
553 7,240,32715
554 8,Year_RTM,24613
555 8,Day_RTM
556 8,Hour_Minute_RTM
557 9,Wind_Spd_S_WVT^1,7005
558 9,Wind_Dir_D1_WVT^2
559 10,Wind_Spd_MAX^1,15417
560 10,Wind_Spd_Hr_Min_MAX^1
561 11,Temp_F_MIN^3,2028
562 11,Temp_F_Hr_Min_MIN^3
563 12,Temp_F_MAX^3,24663
564 12,Temp_F_Hr_Min_MAX^3
565 13,Temp_F_AVG^3,3412
566 14,Rel_Humid_AVG^4,24183
567 15,Battery_MIN^5,15889
568 16,Shortwave_MIN^7,16675
569 16,Shortwave_Hr_Min_MIN^7
570 17,Shortwave_MAX^7,8487
571 17,Shortwave_Hr_Min_MAX^7
572 18,Longwave_AVG^8,18739
573 19,Longwave_AVG^8,24559

```



APPENDIX B

YCWEATHER USER MANUAL

## B.1 Installation

### B.1.1 System Requirements

YCweather is a Windows based program that was compiled using MATLAB 2008b (The Mathworks, Inc.) and requires MATLAB Component Runtime 7.9. YCweather was designed to automatically update the software as well as the weather data files. Thus, it is recommended that when using YCweather that the computer be connected to the Internet. However, the Internet is not a requirement to run YCweather and for this case the automatic data download option should be turned off, see the Section B.7 for details.

### B.1.2 Installing YCweather

YCweather is available for download from the website of the Subzero Science and Engineering Research Facility<sup>1</sup> at Montana State University. To install the software the following steps must be followed.

1. Download the MATLAB Common Runtime (MCRinstaller.exe) software, this is the background program necessary to run YCweather: [www.coe.montana.edu/ce/subzero/snow/MCRInstaller.exe](http://www.coe.montana.edu/ce/subzero/snow/MCRInstaller.exe).
2. Download the YCweather installer software package, YCinstaller.exe: [www.coe.montana.edu/ce/subzero/snow/YCinstaller.exe](http://www.coe.montana.edu/ce/subzero/snow/YCinstaller.exe).
3. Execute the MCRinstaller.exe file, using the default settings for this program is recommended.

---

<sup>1</sup>[www.coe.montana.edu/ce/subzero/snow](http://www.coe.montana.edu/ce/subzero/snow)

4. Execute the YCinstaller.exe and follow the instructions, it installs similar to most Windows programs.
5. When the installation process is complete, YCweather may be run by using the YCweather.exe file located in the created program directory.

### B.1.3 Updates

YCweather is a software package that is under development, as such updates will be available periodically. When an update is available YCweather will provide the user with a prompt, giving the user the option to update YCweather. It is strongly recommend that if a new version is available that it be installed. The installation of the update will occur automatically. Note, if the computer running YCweather does not have Internet access the automatic update warnings will not be received. In this case, the user should periodically check the download page for a newer version of the software.

In order to install an updated version, simply download the file and install it as explained in the installation instructions above. When installing allow the new version to overwrite the old files, no data will be lost during this process. MCRinstaller.exe only needs to be installed with the initial installation.

## B.2 Program Control Window

Upon executing YCweather.exe, the window that appears is the Program Control window, see Figure B.1. This window acts as the central controls for all operations performed by YCweather. This section focuses on the main purpose of YCweather: creating graphs of weather data. The Program Control window contains four basic parts:

1. the menus, which are drop-down items at the top of the window (e.g., File menu and Plot menu);
2. the toolbar, which contains the buttons just below the menus that act as shortcuts to common menu items;
3. the Date/Time panel, which contains the options for selecting the date range of interest; and
4. the Station panel, which lists the weather stations in the database.

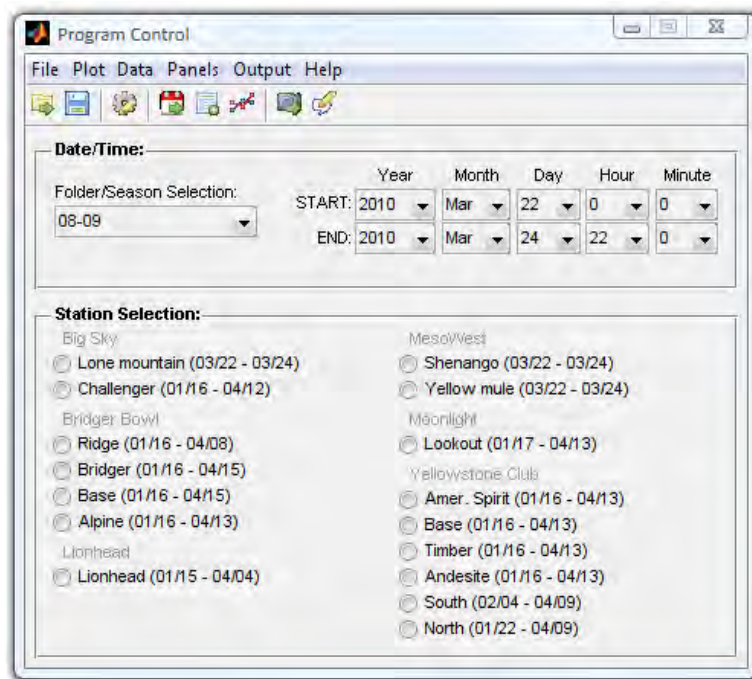


Figure B.1: YCweather Program Control window.

### B.3 Tutorial: Plotting Weather Data

To quickly create a simple plot of weather data:

1. Select a folder from the Folder/Season drop-down option on the Date/Time panel.
2. Select a weather station from the buttons in the Station panel, for example Ridge and Bridger from Bridger Bowl.
3. Choose a start and end date from the drop-down menus, be sure to select a range that lies within the available data, which is given in the parenthesis adjacent to the station radio buttons.
4. Select the Open Data List option. This is available by selecting Open Data List option from the Data menu, pressing the Open Data List button on the toolbar, or by pressing CTRL + V. This will open an additional window, as shown in Figure B.2. Note, this window may take several seconds to open especially if multiple stations are selected and/or if the stations contain a lot of data. The reason being that when this window is open the program is recalling all of the data for each station and storing it in a temporary location. This allows the plots to be generated quickly.
5. In this new window (named Data List) select a weather parameter, such as Air Temperature. Notice, that when you press a button that all variables without the panel labeled Temperature disappear. This will prevent plotting of variables with different units on the same axis.
6. Finally, plot the data. This can be done by pressing the Plot Weather Data toolbar button on either Program Control or Data List window, by selecting Weather Data from the Plot menu on either window, and by CTRL + W.

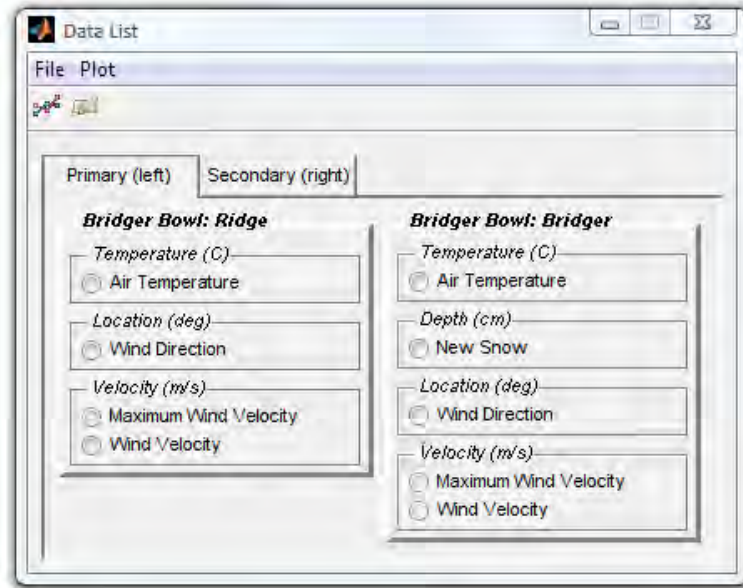


Figure B.2: Example of the Data List window.

## B.4 Creating Graphs

One of the main purposes of YCweather is to produce graphs, these graphs are meant to be customizable and easily exportable. This section details the creation and manipulation available in YCweather created graphs. Graphs are generated using the Data List window as demonstrated in the previous section.

### B.4.1 Dual-axis

When creating a graph, the Data List window (Figure B.2) displays two tabs. Data selected via the Primary and Secondary tabs graph along the left-side and right-side vertical axis, respectively. For example, Figure B.3 was created by selecting Air Temperature under the Primary tab and Incoming Short-wave under the Secondary Tab. The tick marks along the axes are setup to coincide, this sometimes results in

illogical tick mark labels. This problem may be corrected by editing the limits and step size, which is detailed in the following section.

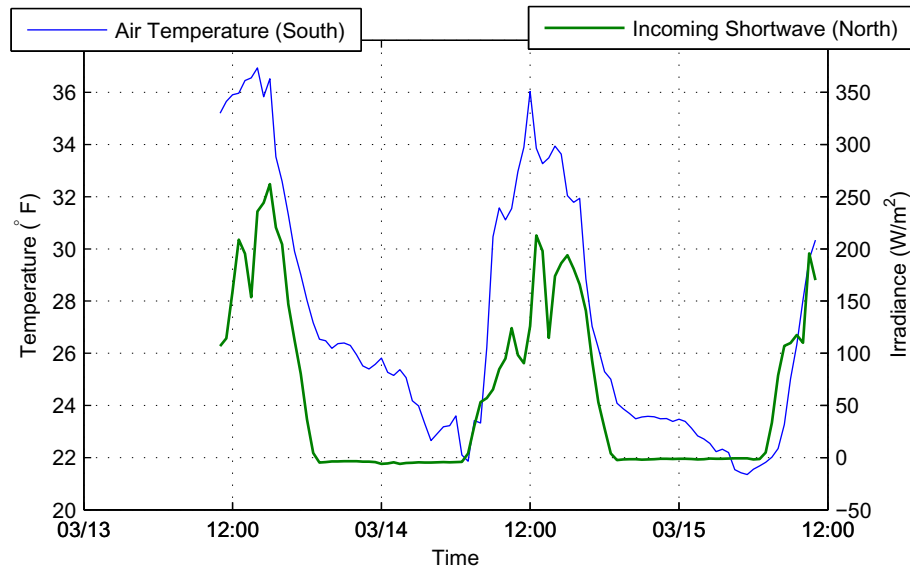


Figure B.3: Example graph showing dual-axis capabilities.

#### B.4.2 Editing Axis Limits and Step-size

In many cases, especially when creating graphs for dissemination, it is desirable to change the tick marks and limits on the graph. YCweather provides this capability via two options: Limit Boxes and Step-size Boxes. These options are available on the figure toolbar by the pairs of green arrows or by selecting the options from the corresponding axis menu (e.g., the X-axis menu).

- **Limit Boxes:** This option creates two text box items near the extremes of the corresponding axis. Simply change the limits to the desired value and press Enter. If the box is empty the axis limits are automatically determined based on the data.

- **Step-size Boxes:** This toggle places a text box item near the lower axis limit. This value dictates the step size between tick marks; leaving the value empty results in automatic tick placement.

### B.4.3 Exploring Data

The YCweather graphs allow the user to explore the data in various ways.

1. **Limit/Step-size Boxes** allow for custom control of axis limits and tick marks, see Section B.4.2 for more details.
2. **Zooming:** This option is toggled by selecting the magnifying glass icon on the figure toolbar.
3. **Data Cursor** allows the user to view the actual numbers associated with the graph by selecting a portion of the plotted line. This option is available on the figure toolbar.
4. **Zoom Slider** operates similar to the zooming feature but restricts the zoom to the associated axis and has a slider bar that controls the zooming from 100% to 0.1% of the data range. The slider feature is available in the menus associated with each axis (e.g., X-Axis menu).
5. **Line highlighting** is activated by left-clicking the mouse button on the desired line, this will make the line large and display the actual data points that make up the line. The highlighting is removed by left-clicking the line a second time.



#### B.4.4 Context Menus

The lines, labels, and legends on YCweather graphs each have menus associated that allow the user to manipulate the data. The menus for these items are accessed by right-clicking on the object.

- **Line Context Menu:** By right clicking on any line the user has control over the appearance of the line for items such as the line thickness, style, color, or markers. Additionally, a line may be deleted.
- **Label Context Menu:** Each text item, such as the axis labels or annotations (see Section B.4.5), allows for the user to edit the text, font, and location or delete the item.
- **Legend Context Menu:** The legend is also editable in its appearance including options for editing the color of the box or the width of the bounding box. Also, when two legends are present. as in Figure B.3. they may be combined into a single legend by selecting the refresh option in this menu. Then simply delete the unwanted legend box.

#### B.4.5 Figure Menus

The axes menus available from graphs created with YCweather include the Options menu as well as a menu for each axis. The Options menu provides generic functionality that applies to the entire figure whereas the axis specific menus only apply to that axis.

File menu (default MATLAB menu):

- **New:** This option creates an empty figure, which is inaccessible with YCweather.

- **Open:** Allows the user to open figure files that were saved with the \*.fig extension.
- **Close:** Closes the current figure.
- **Save:** Saves the figure by overwriting the current file if the figure has previously been saved, otherwise it invokes the Save as option.
- **Save as:** Allows the user to save the figure in a variety of formats, including MATLAB \*.fig format.
- **Export Setup:** Opens MATLAB's export user interface (see Section B.4.6).
- **Print Preview:** Opens MATLAB's print setup user interface (see Section B.4.6).
- **Print:** Sends the figure to the printer.

Options menu:

- **Add/Edit Labels:** Allows user to add and/or edit the axes labels, figure name, and figure title.
- **Interpreter:** Allows user to change the typesetting format,  $\text{T}_{\text{E}}\text{X}$  and  $\text{L}^{\text{A}}\text{T}_{\text{E}}\text{X}$  are usefull when equations and units are being displayed.
- **Edit Font:** Allows the user to change the font, style, and size for all text objects in the figure.
- **Axes Color:** Controls the background color of the figure.
- **Add Annotation:** Enables user to insert items such as text boxes and arrows.

- **Resize Figure:** Allows for editing the size of the figure, which is useful for exporting.
- **Tight Fit:** Moves the axis labels to the outer extent to minimize whitespace around the edges, this option is irreversible.
- **Export figure:** Allows the user to export the figure as an image file (see Section B.4.6).

X-, Y-, and Y2-Axis Menus:

- **Ticks/Labels:** Allows for strict definition of the tick marks and labels used on the associated axis.
- **Step Size Box:** Toggle for the step size controls (see Section B.4.2).
- **Limit Boxes:** Toggle for the axis limit controls (see Section B.4.2).
- **Zoom Slider:** Toggles the presence of the zoom slider (see Section B.4.3).
- **Grid:** Toggles the major grid lines.
- **Minor Grid:** Toggles the minor grid lines.
- **Minor Ticks:** Toggles the axis tick marks.
- **Reversed:** Toggles the orientation of the tick marks and labels along the axis.
- **Add/Edit Legend:** Allows the user to add or edit the legend entries.

### B.4.6 Exporting Figures

YCweather allows the user to output the graphs in a variety of formats. For those familiar with MATLAB, it is possible save the figure as a \*.fig file. The exporting/saving is accomplished in two ways. First, to simply create an image exactly as the figure appears, select Export Figure from the Options Menu or press the associated Toolbar button (see Section B.4.5). This option will output the figure exactly as it appears, so it is imperative to setup the figure precisely as needed. The size of the exported figure can be specified by editing the dimensions via the Resize Figure option in the Options Menu.

The second option for saving/exporting figures is accomplished using the File Menu (Section B.4.5), this menu is the default MATLAB figure menu; thus, for users unfamiliar with MATLAB these options may be difficult to use. This menu provides two options: one for printing the image that uses the Print Preview and Print menu items and an Export Setup option for saving the figure as an image. Both, the Print Preview and Export Setup open user interfaces with a variety of options, details for using these items may be found in the online MATLAB help file: <http://www.mathworks.com/access/helpdesk/help/techdoc/index.html> (in the contents select “Graphics”; “Printing and Exporting”; “How to Print or Export”).

### B.5 Workspaces

YCweather has the ability to save and load workspaces. A workspace is simply a conglomeration windows including the Program Control, Data List, and any graphs. For example, Figure B.4 is a workspace that includes graphs for air temperature and short-wave irradiance.

To create a workspace consider the following example:

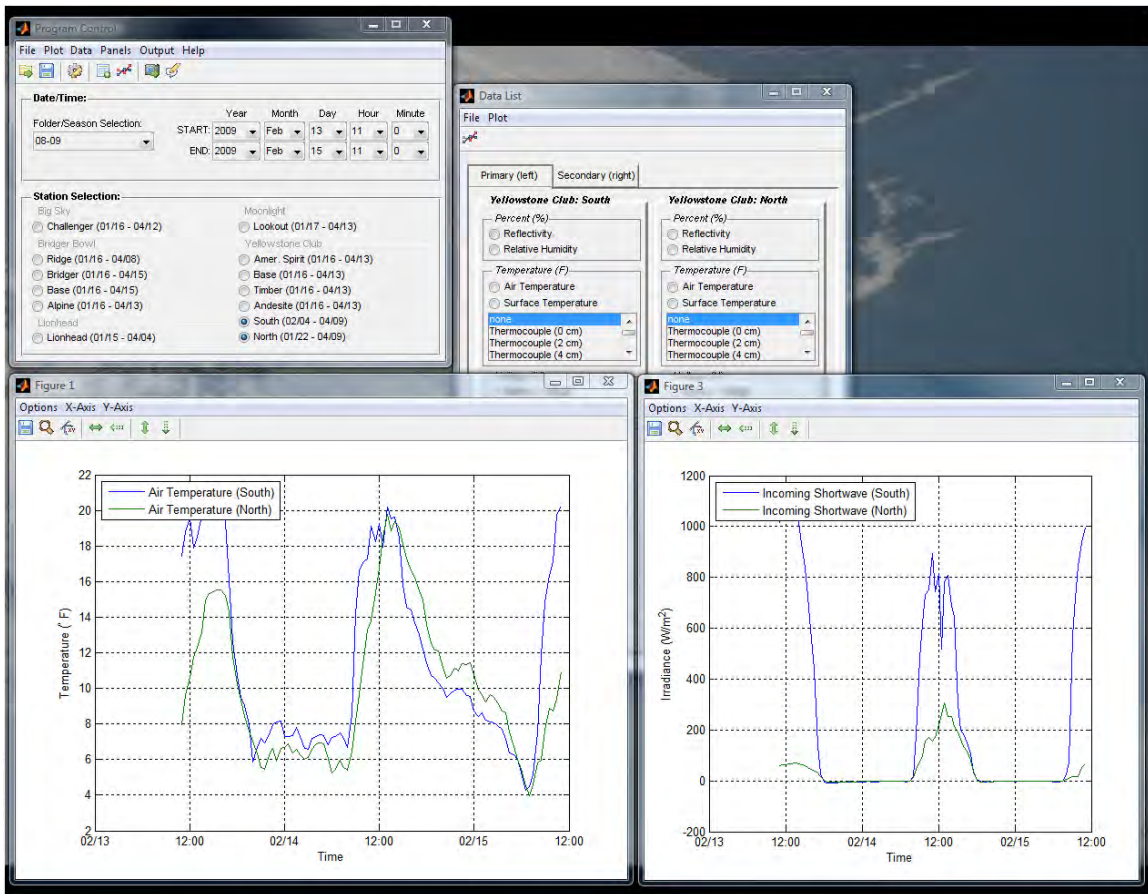


Figure B.4: Example of a YCweather workspace.

1. Begin by creating a graph of some kind, see Section B.3 for instruction on creating a graph.
2. To create a second plot the Clear Figures preference must be turned off, see Section B.7 for details.
3. Arrange the windows as desired.
4. Save the workspace by selecting Save Workspace from the File menu in the Program Control window. The default location is the \saved directory where YCweather was installed. However, the workspace files (\*.mat extension) may be saved in any location.

5. The workspace is now saved.

To load a workspace, simply select the Load Workspace option from the File menu and locate the desired workspace file in the dialog box that appears. Once the workspace has been selected YCweather will provide a prompt, as in Figure B.5, that asks to use the current or stored time.

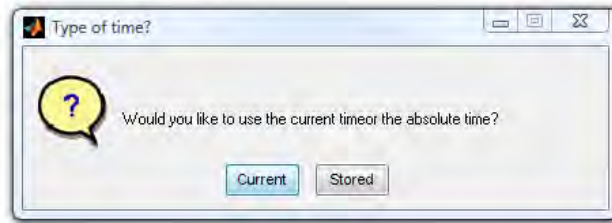


Figure B.5: Prompt that appears by default when opening a workspace.

The “current” option, by default, recalls the workspace using the most recent 48 hrs of data that exists. The stored time option uses the exact times set when the workspace was created. These options exist so that the user can specify historical (“stored”) workspaces of specific events or create workspaces (“current”) of commonly used plots. The YCweather preferences (Section B.7) allow the number of hours to be changed as well as the prompt appearance to be changed. For example, if a workspace is created that is solely intended for a specific event, then the prompting preference should be changed to “Stored” so that when this workspace is recalled it simply opens.

## B.6 MesoWest Data

YCweather is capable of interfacing with weather data archived with MesoWest ([mesowest.utah.edu/index.html](http://mesowest.utah.edu/index.html)). First, a text file named `mesowest.txt` must be present in the season folder within the YCweather database, see Section B.11.2

for details regarding the folder structure. This file contains two columns of comma separated data: the first column contains a list of station identifiers as shown on MesoWest. For example, YLWM8 is the identifier for the Yellow Mule station in Southwest Montana. The second column contains a corresponding group name associated with the station identifier in the same row. For example, the Yellow Mule station mentioned is a part of the RAWS network, thus an appropriate name may be “RAWS Stations” and perhaps another group would include the National Weather Service stations (e.g., “NWS Stations”).

The data available for download from MesoWest is limited to 30 days, as such if changes to range on the Program Control is altered the MesoWest data may require updating. When YCweather opens and MesoWest data is desired, it downloads the data in the date range, by default this is the last 48 hours of the data. The MesoWest data does not update automatically, but can easily be updated via the Toolbar button or using the Data menu (see Section B.8).

## B.7 Preferences

YCweather offers a variety of customizable options for controlling how the program operates. These options are available in the Preferences, which may be opened via the Program Control File menu or with the Toolbar button. Figure B.6 shows the Preferences window. This window is divided into three parts, each of which has a number of options as discussed below.

In order for the changes in preferences to take place, the Apply button must be pressed. The changed setting will only apply to the current YCweather workspace and will return to the default settings when YCweather is reopened. The selected preferences may be defined as the default by selecting the Set Default option in

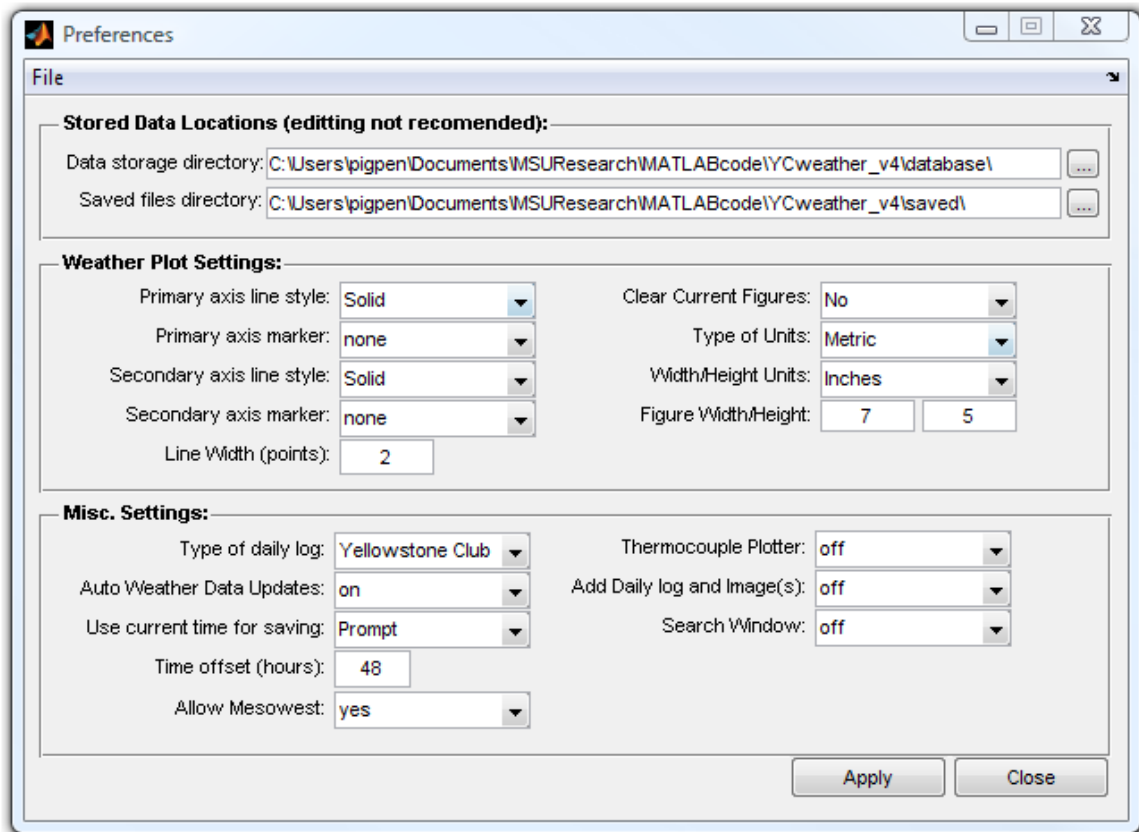


Figure B.6: YCweather preferences window.

the Preferences window File menu. Additionally, if the workspace is saved (Section B.5) the current settings are applied to that workspace file and will remain when this workspace is opened in subsequent executions of this workspace file.

### B.7.1 Stored Data Locations

As indicated in the Preferences window (Figure B.6) editing the “database” and “saved” directory is not recommended unless a thorough understanding of file structure of YCweather is possessed. These details are included in Section B.11, which discuss how YCweather operates. The “database” directory is where all the weather data, images, and log files are stored. And the “saved” directory is the default location for all YCweather related files created by the user.



### B.7.2 Weather Plotting Settings

The left-hand column in this section controls how the lines of weather graphs will appear upon creation, allowing for the adjustment of the line style, line markers, and line width for both the primary (left-side) and secondary (right-side) axes. The right-hand column includes various options, which are summarized in the following list.

- **Clear Current Figures:** If this value is set to “Yes” then each time a graph is created all others are deleted.
- **Type of Units:** Specifies the units to display when graphs are created. Note, if this is changed a new Data List window must be created because the unit conversion occurs during the creation of this window.
- **Width/Height Units:** Sets the units of the graph size upon creation, the numeric value for this setting is provided in the following item.
- **Figure Width/Height:** The width and height of a graph created based on the units specified above.

### B.7.3 Misc. Settings

The settings in Misc. Settings panel, as the name suggests, control various aspects of YCweather. The first three items in the right-hand column toggle the appearance of the corresponding side panels when YCweather opens. These panels are detailed in Section B.9.

The left-hand column allows the user to determine the type of daily log that YCweather should utilize, see Section B.8.2 for details. The Auto Weather Data Update options toggles the automatic download of the latest available weather data, as

detailed in Section B.8. The next two options in this column control the graphing start and end times when graphs are created via workspaces, which is discussed in Section B.5. Finally, the “Allow Mesowest” setting toggles the capability for YCweather to communicate with the MesoWest database, which requires Internet access. Additional details regarding the MesoWest feature may be found in Section B.6.

## B.8 Data Menu

The Data menu in the Program Control window serves two functions: to update the weather data and to access images and daily logs. This section briefly explains data updating.

YCweather is designed to automatically collect the most recent weather data files; however, this is only available from the Montana State University network. If off-campus access is required please contact the MSU Department of Civil Engineering. This automatic update may be disabled in the program Preferences (Section B.7) and accessed manually via the “Check for new weather data” option in the Data menu. This process includes updating the weather files as well as any daily log files that exist. It is also possible to download images from a specific day and time via the daily log viewer (see Section B.8.2).

### B.8.1 Image Viewer

YCweather contains a basic image viewer for accessing images stored in the YCweather database. Adding images to the database is explained in Section B.9.2 and the database file structure is explained in Section B.11. To access images, follow these steps:

1. Select the station(s) of interest,

2. Select the start date desired (the end date is not utilized), and
3. Select Open Images from the Data menu or Toolbar button on the Program Control window.

If images for the selected station(s) exist a window will open displaying the images. One window will appear for each station selected. Figure B.7 provides an example of the image window. In the case where no images exist for selected date, but exist for other dates at this station, an image window will open with the Select Date pop-up menu (see Figure B.7) set to the first date available.

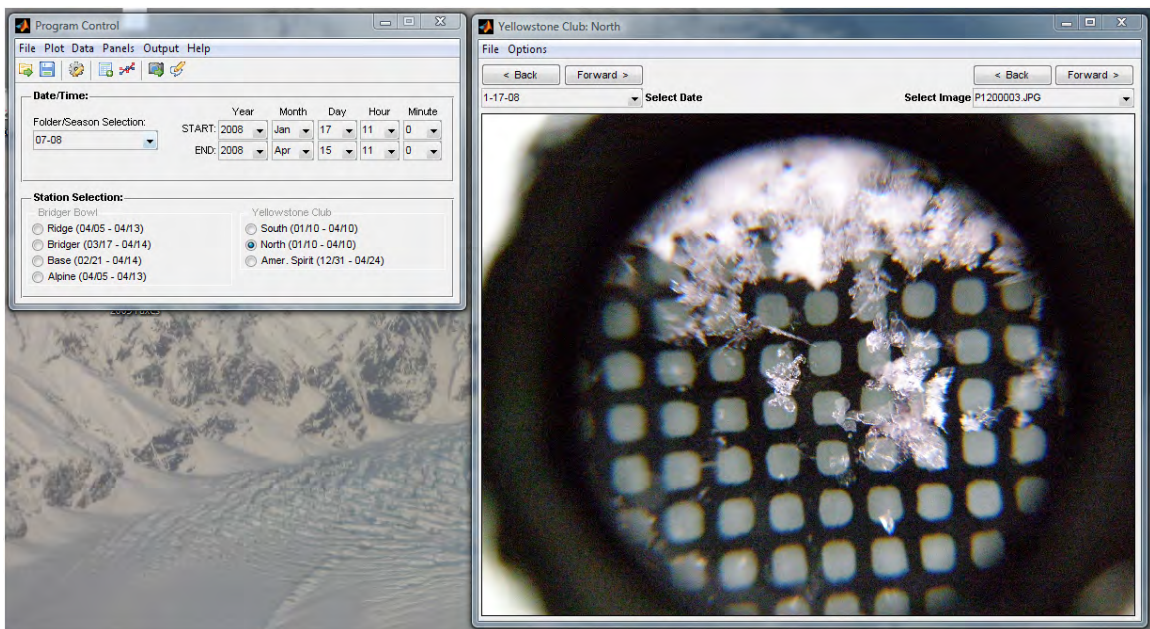


Figure B.7: Example of the image viewer for YCweather.

The YCweather image viewer offers the user the following functionality:

- Toggles for cycling through images on the current date (right-hand buttons and pop-up menu).
- Toggles for changing the date being viewed (left-hand buttons and pop-up menu).

- Zooming via the mouse cursor.
- The ability to export the figure to another location via the Save image as... option in the File menu of the image viewer (this copies the image and does not affect the original).
- Capability of renaming an image in the database (Rename in the Options menu).
- The ability of using the default Windows-based program for viewing images, which is available as the Open with Windows item in the Options menu.

### B.8.2 Daily Logs

One of YCweather's main features is the daily logs, which are text notes associated with each station and date. These logs are stored in the YCweather database (see Section B.11) and added via the panel discussed in Section B.9.2. Two types of daily logs are available, as shown in Figure B.8. The type of log displayed is controlled in the preferences (Section B.7).

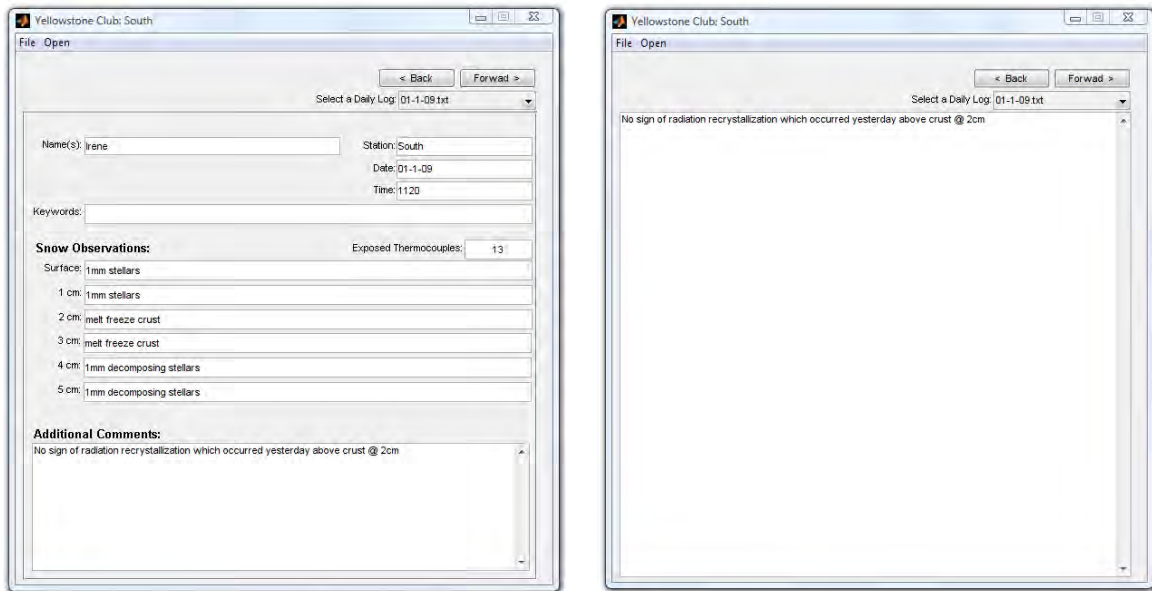
1. **Yellowstone Club:** A form specifically designed for usage with a research project at the Yellowstone Club.
2. **General:** A simple form for typing notes.

To open the daily logs: (1) select the station(s) of interest, (2) select the start date desired (the end date is not utilized), and (3) chose Open Daily Log(s) from the Data menu or Toolbar on the Program Control window.

If daily logs exist then a window, similar to Figure B.8, will appear. The toggles and pop-up menu on the right allow the user to cycle through all the logs for the station. The daily log may be edited and the changes saved using the Save daily log

option in the File menu. Additionally, the log may be opened in a traditional text editor (Open log with Windows in the Open menu); however, this is not recommended for the casual user. Editing the the log in this fashion may render the file unreadable by YCweather.

It is possible to download images associated with the current station and date of the daily log, this is accessible by selecting Download images from the Open menu. Finally, the image viewer for the current station may be opened using the daily log window by selecting Open images from the Open menu.



(a) Yellowstone Club

(b) General

Figure B.8: Examples of the daily log options available in YCweather.

## B.9 Panels Menu

Three additional panels for manipulating data within YCweather are available: Thermocouple Plotter, Add Logs and Images, and Search. These features are available via the Panels menu on the Program Control window. These panels may be

triggered automatically when YCweather opens via the program Preferences (Section B.7). Figure B.9 shows the Program Control window with all the panels. Each of these panels serves a specific function, as defined below, that a typical user will likely not require.

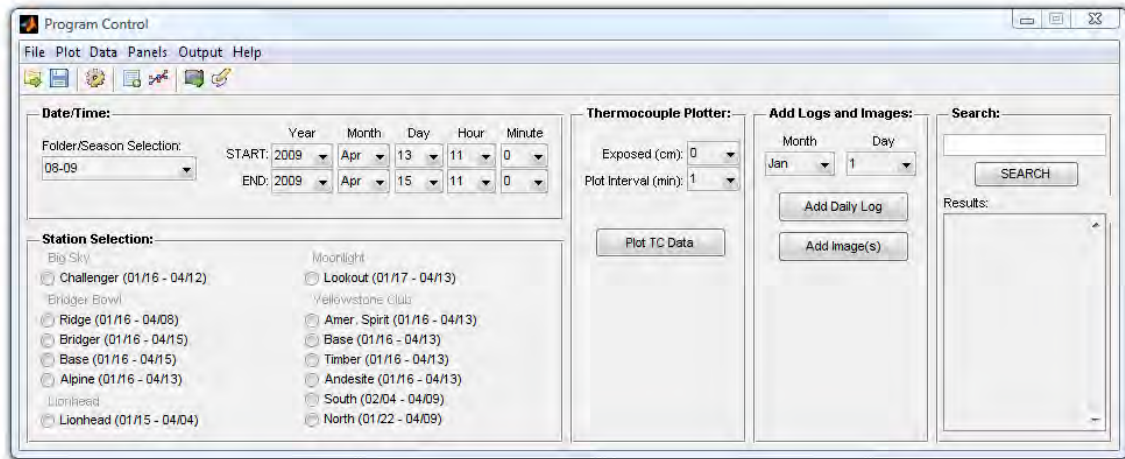


Figure B.9: Program Control with all side panels showing.

### B.9.1 Thermocouple Plotter

A weather station may contain thermocouple data that extends into the snowpack, such as the North and South stations at the Yellowstone Club. In this case it is desirable to graph temperature profiles of the snow pack at various intervals; the Thermocouple Plotter panel serves this purpose. To understand this feature consider the following tutorial, referring to Figure B.10.

1. Open the Yellowstone Club South weather station Data List, as in Figure B.10. In the Data List window a list of thermocouple will be present in the Temperature panel, this indicates that this station has thermocouple data.
2. Open the Thermocouple Plotter panel using the Panels menu on the Program Control window.



3. Select a start and end time on the Program Control for just a few hours as in Figure B.10.
4. Change the Plot Interval pop-up menu to 30 minutes on the Thermocouple Plotter panel.
5. Change the Exposed pop-up menu to a value of four.
6. Press the Plot TC Data button.

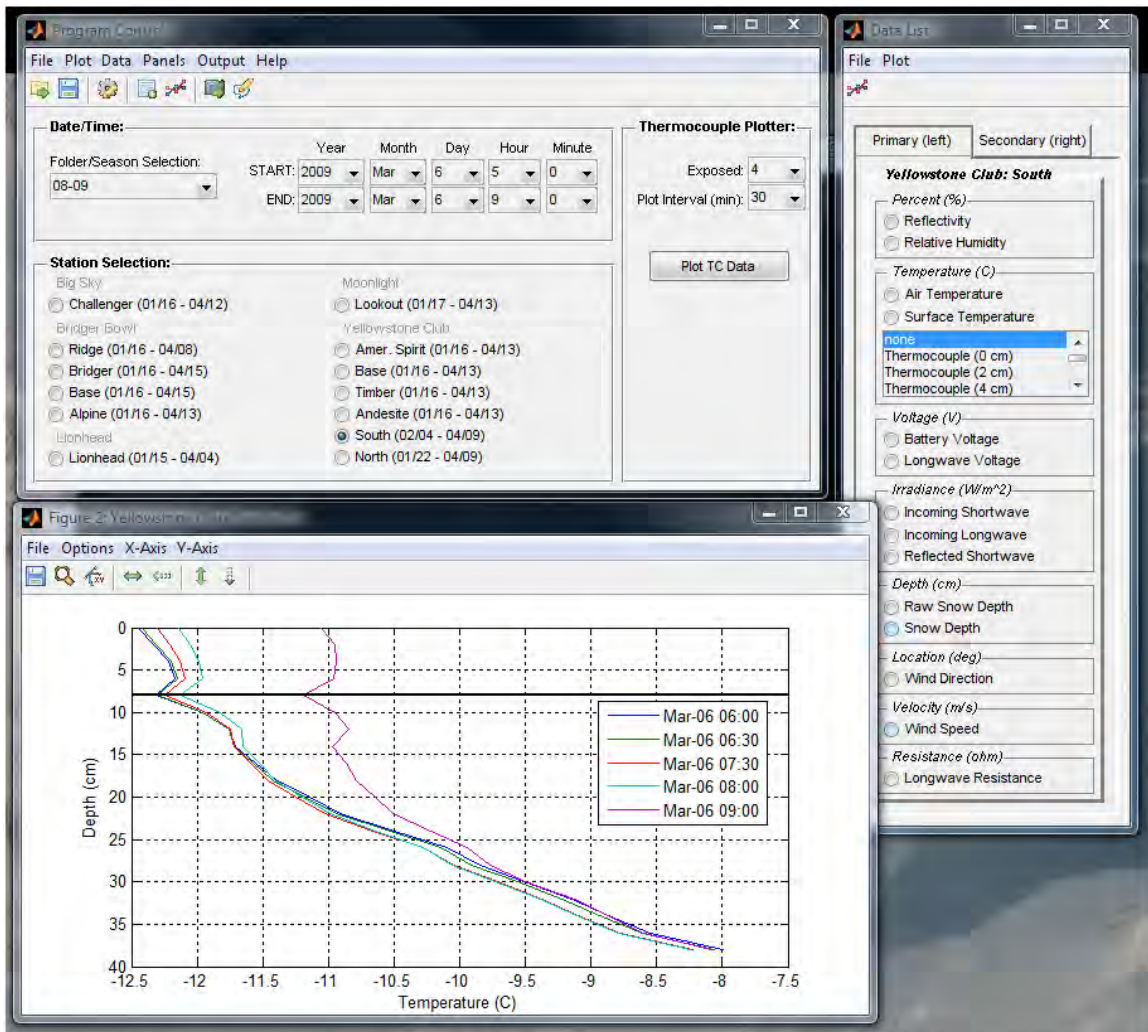


Figure B.10: Example workspace showing a graph of thermocouple data.

Following the above steps should produce a graph similar to that displayed in Figure B.10. This graph displays the thermocouple profiles at 30 minute intervals over the specified time. The horizontal black line is meant to represent the snow surface. For the North and South Yellowstone Club weather stations the number of thermocouples exposed is recorded in the daily logs.

### B.9.2 Add Logs and Images

This panel allows the user to add image files and daily logs to a specific station for a specific date. Each weather station (e.g. South at the Yellowstone Club or Ridge at Bridger Bowl) may have images and a daily log associated with the station for each day. The Add Logs and Images panel allows this data to be assigned. For example, to add a daily log for February 13 at the South Yellowstone Club station:

1. select the South station from the Yellowstone Club panel in the Program Control window,
2. select the appropriate day from the Add Logs and Images panel, and
3. press the “Add Daily Log” button.

Performing these steps opens a window for adding and editing the daily log. Enter the desired information and then select the Save daily log option from the File menu. If a log already exists for the selected station and date, a warning will appear. If it is desired to overwrite the log then continue, otherwise the log should be edited. Editing daily logs is discussed in B.8.2.

Similarly, images can be added to the YCweather database. In this case the program will prompt the user to select the desired images to include, these images will be added to the database and accessible via the image viewer. No changes to the



images occur, YCweather simply builds a reference to the image file(s). For specifics on the YCweather file organization within the database see Section B.11.

### B.9.3 Search

The Search panel provides the user a tool for searching all the daily log (Section B.8.2) files for a specific folder/season. Type the desired keyword(s) in the window with multiple words separated by a comma. If any matches for any of the keywords exist the station and date will appear in the Results list. Selecting the desired result opens the associated daily log.

## B.10 Output Menu

### B.10.1 Output data to file(s)

The weather data from YCweather may be exported as a comma separated text (\*.txt), Microsoft Excel 97-2003 (\*.xls), or Microsoft Excel 2007 (\*.xlsx) file via the Output menu on the Program Control window. Selecting this option causes two options to appear:

- **All data:** This option exports all the available weather variables, as listed in the Data list (Figure B.2), from the selected stations.
- **Selected data:** This option only exports the data selected in the Data list (Figure B.2).

After selecting one of these options YCweather will open a prompt asking: “Would you like to crop the data between the selected date/times or write the entire data set?” By selecting Crop only the data between the times selected on the Program Control window are exported. Selecting Entire exports all available data.

Next, YCweather will prompt for selecting the location and name of the output file, this is where the file type may be specified. If either Excel file formats are selected YCweather will create a single file with each selected station as Worksheets within this file. Outputting as a text file (\*.txt) results in a file for each selected station being created, which will be named as <name>\_station.txt. The <name> is the filename entered by the user and the station is the YCweather designation for the station.

### B.10.2 Output to RadTherm

YCweather is capable of producing a text file for the use with RadTherm/RT (ThermoAnalytics, Inc.), an example file is shown in Figure B.11b. This feature is accessed from the Output menu on the Program Control window. This opens the RadTherm Export window, as shown in Figure B.11a.

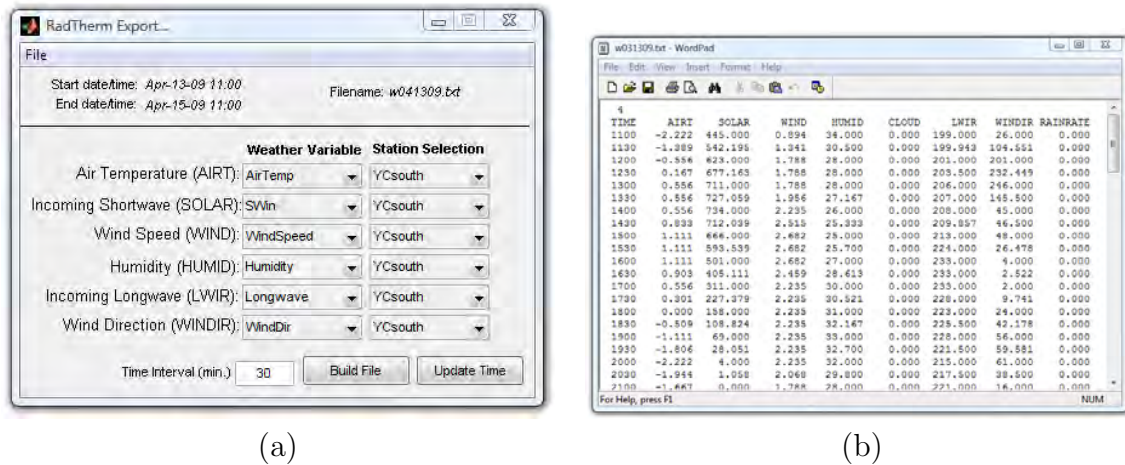


Figure B.11: (a) RadTherm/RT file exporter and (b) an example output file.

When using the exporter, begin by selecting the desired station from the right-column of pop-up menus. When a station is selected the corresponding Weather Variable pop-up menu is changed to include weather variables with the necessary units. The names that appear in both menus correspond to the tags assigned to the

\*.yc file for the stations, as discussed in Section B.11. The start and end date/time values may be changed using the Program Control window and then by pressing the Update Time button. Finally, the file is created by pressing Build File, a prompt will open for selecting the location to save the file. The filename is dictated by the date.

The RadTherm/RT exporter also allows for the configuration of the pop-up menus to be saved. This is available from the File menu on the exporter via the Save and Open Settings options. These settings files utilize a \*.rdt extension.

## B.11 Application Details

The following section details of the operation of YCweather. This section is meant to aid researchers at the Subzero Science and Engineering Research Facility maintain and update the software. YCweather was written with MATLAB version 7.7.0.471 (R2008b). If you are using a newer version of MATLAB for editing YCweather the MATLAB run time component must be updated on all machines attempting to execute YCweather (see Section B.11.5 for additional details).

### B.11.1 Basic YCweather Operations

The executable version of YCweather relies on four primary files that must be located in the same location: `YCweather.exe`, `YCmain.exe`, `default.mat`, and `version.txt`. `YCweather.exe` is a wrapper program that keeps the main program `YCmain.exe` current based on the installed version (`version.txt`) and the available version on the YCweather website (Section B.11.5). `YCmain.exe` may be executed without `YCweather.exe`, but will never update in this case. The source code for `YCweather.exe` and `YCmain.exe` are MATLAB m-files `YCweather.m` and `MAIN.m`,

respectively. `YCweather.m` will not operate correctly via the m-file; `MAIN.m` may be run via MATLAB if desired.

When `YCmain.exe` begins it opens the `default.mat` workspace file, which must be located in the same directory. If this file does not exist or it is the first execution of `YCweather` this file is created. The workspace file includes the location of the database directory that contains all the weather data, daily logs, and image files. This directory may be located anywhere on the machine as long as the workspace file points to the correct location (see Sections B.7). However, when the `default.mat` workspace file is created the location is initially set as the “database” folder in the same directory as the `YCweather` executables.

When `YCmain.exe` (`MAIN.m`) begins operation, after opening the workspace file (`default.mat`), it attempts to download the latest weather data. As mentioned in Section B.8 this option may be turned off. The installation package, Section B.11.5, includes the latest data from the current season. Thus, an Internet connection is not required to run `YCweather` initially, but only to keep the program and data current. Lastly, `YCmain.m` initializes by applying the `default.mat` workspace file (`callback_readWS.m`), prior to this the only two parameters in the workspace file where utilized: the database location and the auto update trigger.

At this point, the `YCweather` is ready for manipulation by the user and the program has opened all available data into the internal data structures.

### B.11.2 Database Directory

The database directory must be organized in a specific fashion for `YCweather` to operate correctly, most of this organization is handled automatically. The directory tree for the `YCweather` database is shown in Figure B.12. The first level of folders in the database directory are for each season of data, these exact folder names show up

in the Program Control window in the Season/Folder pop-up menu. The initialization of the pop-up menu occurs when a workspace file is opened, the source code being `callback_readWS.m`.

When the user selects the season via the pop-up menu YCweather accesses this folder, inside of which the \*.yc format files (see Section B.11.3) for all weather stations are stored. These format files contain, among other things, an abbreviated station name. This name is used in the internal data structure of YCweather as well as for creating the next level of folders.

As described in Section B.8, YCweather acts as an archiving application for daily logs and images. The daily logs, images, or image reference files are contained in folders that exist within the station folders. The folders are named according the aforementioned abbreviated station name. Within each of these folders two additional folders exist: DailyLogs and Images. These folders, as the names suggest, store the archived daily logs and image files. The station folders and sub-folders are created automatically by YCweather when the user adds a daily log or image (see Section B.9.2).

The DailyLog folder contains text files that store the daily log information, each log must be named as `mm-dd-yy.txt`. The Images folder contains folders named as `mm-dd-yy`. Within each folder the images are stored, the names are irrelevant, but the files should be stored only in recognized formats, see MATLAB's help on "imread". This directory may also contain a `images.txt` file which contains a list of image files elsewhere on the computer that have been associated with the station and data by the user, see Section B.9.2.

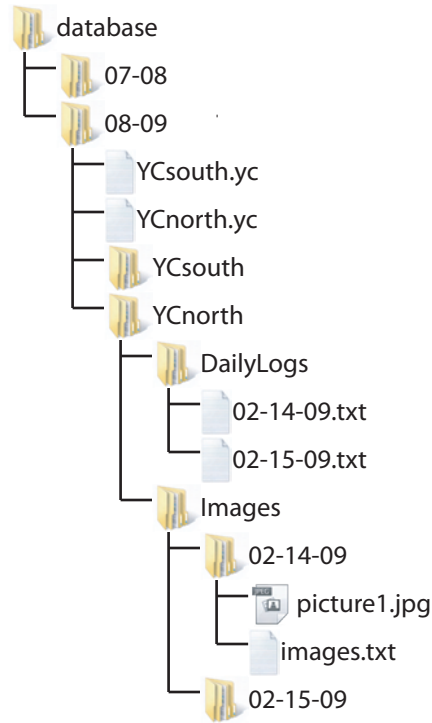


Figure B.12: Example of file structure of the database directory used by YCweather.

### B.11.3 Weather Station Format Files (\*.yc)

YCweather basis its entire operation on format files, which are simply text files with a \*.yc extension. An example, format file is include in Figure B.13. These files communicate to YCweather the necessary information regarding the weather data files. The weather data files may be any comma delimited text file completely composed of columnar numeric entries.

Format files are composed of three parts, with the parts being separated by # sign. The first portion consists of six lines that detail various parts of the data file. Part two details each column of data present in the data file. Finally, part three contains custom functions utilized for making calculations.

Part One: Data File Details: The following list is a line-by-line description of the six components required in the first portion of the \*.yc format files.

```

BBalpine
Alpine
Bridger Bowl
alpine.dat
none
0
#
year,0,0,0
month,0,0,0
day,0,0,0
hrmin,0,0,0
AirTemp,1,F,Air Temperature
Humidity,1,%,Humidity
AirPress,1,inHg,Air Pressure
TotalSnow,1,in,Total Snow Depth
DaySnow,1,in, 24 Hour Snowfall
H2OContent,1,in,Water Content
WindSpeed,1,mph,Wind Velocity
WindMax,1,mph,Maximum Wind Velocity
#
Time,calcwx_time,year,month,day,hrmin,GNFAC

```

Figure B.13: Example format file utilized by YCweather.

1. **Station ID:** The station id must be a single text string that uniquely identifies the weather station associated with this data file. This ID must conform to MATLAB's variable naming convention, see MATLAB's help file on "Naming Variables".
2. **Station name:** This string identifies the weather station and will appear next to the toggle button within the Station Panel in the Program Control window.
3. **Station location:** This value is a text string that identifies the location of the weather station, this name will appear in the Station Panel in the Program Control Window.
4. **Path to data file:** The path to the data file must be any valid complete or relative path and filename that references the data file associated with this

format file. In the example file, Figure B.13, the file `alpine.dat` must then exist in the same directory as the `*.yc` format file.

5. **Array ID:** This value is useful for weather files that are composed of multiple data arrays such as created via Campbell Scientific dataloggers. In many cases data files of this type contain a identifier at the beginning of a row identify the type of data. For example, a row beginning with 60 may represent hourly data and those starting with 24 may indicate daily data. Thus, if the Array ID is 60 in the `*.yc` format file then only the data marked with this ID would be included for this station in YCweather. Another `*.yc` file would need to be established to gather the data from the other array. Figure B.14 includes the Array ID feature. In Array ID is present in the file, **none** should be entered in this location.
6. **Thermocouple ID:** This identifier indicates if a thermocouple array within the snowpack exists. If this data does not exist then 0 (zero) should be entered. For stations with snowpack temperature arrays this ID should correspond the the variable ID's defined in part two of the `*.yc` file, as discussed below and shown in Figure B.14. The variable ID also must contain a numeric portion that indicates the location of each thermocouple in the snowpack. For example, the thermocouples shown in Figure B.14 are space at 2 cm intervals.

Part Two: Weather Variables: Part two details the weather variables, there should be one row for each column that exists in the corresponding data file. Each row in this section has four comma separated values, as detailed below.

1. **Variable Name:** The first value is a single string of text that uniquely defines the variable from others in the format file. This name must conform to



```

YCsouth
South
Yellowstone Club
SOUTHYC.dat
100
TC
#
ArrayID,0,0,0
year,0,0,0
day,0,0,0
hrmin,0,0,0
Battery,1,V,Battery Voltage
WindSpeed,1,m/s,Wind Speed
WindDir,1,deg,Wind Direction
Surface,1,C,Surface Temperature
SWin,1,W/m^2,Incoming Shortwave
SWref,1,W/m^2,Reflected Shortwave
Longwave,1,W/m^2,Incoming Longwave
Depth,1,cm,Snow Depth
TempDepth,1,C,Air Temperature (Depth Sensor)
AirTemp,1,C,Air Temperature
Humidity,1,%,Relative Humidity
PIR_mV,1,V,Longwave Voltage
CaseRes,1,ohm,Longwave Resistance
TC00,1,C,Thermocouple (0 cm)
TC02,1,C,Thermocouple (2 cm)
TC04,1,C,Thermocouple (4 cm)
TC06,1,C,Thermocouple (6 cm)
TC08,1,C,Thermocouple (8 cm)
TC10,1,C,Thermocouple (10 cm)
TC12,1,C,Thermocouple (12 cm)

```

Figure B.14: Example format file utilized by YCweather that includes the thermocouple ID for plotting temperature profile data (this is not a complete file).

MATLAB's variable naming convention, see MATLAB's help file on "Naming Variables".

2. **Inclusion Trigger:** This value indicates to YCweather if the corresponding column of data should be listed as a selectable option in the program. Entries may be 0 or 1, where 0 excludes the data.
3. **Units:** The third entry communicates the units of the data; this value must conform to the units specified in the `units.txt` file as detailed in Section B.11.4.

The units can be in either English or metric units, but must be included in the aforementioned file.

4. **Legend Label:** The last value is a string describing the weather data that is inserted into the legends of YCweather graphs.

Part Three: Custom Functions: This section allows for calculation to be done on the weather variables listed above in Part Two. One function that is a critical component of YCweather will be used here as an example, the `calcwx_time.m` function. **YCweather requires that a variable named Time be present and contain the time stamps for the weather data in MATLAB's serial format.** The `calcwx_time.m` function performs this operation. For information on this format see MATLAB's help on "Types of Date Formats".

Taking a step back, the function `read_dat.m` is responsible for reading the format `*.yc` files, this function outputs the weather data into a structure that is used by YCweather; `read_dat.m` also implements the custom functions listed in the `*.yc` format files.

When the custom function are called from `read_dat.m` they are implemented as follows within MATLAB, using `calcwx_time.m` as an example.

```

MATLAB
>> Time = calcwx_time(d,'year','month','day','hrmin','GNFAC');
```

Comparing this functional operation to the row of inputs in the format file in Figure B.13 shows that the first entry in the format `*.yc` file is the output variable (Time), the next value is the function name (`calcwx_time`), and the remaining items are string input into the custom function. The input variable `d` is the data structure used for storing the weather data and is automatically inputted into the custom

function in `read_dat.m`. This data structure contains all the data present in the weather data file, as listed in Part Two. Hence, the function `calcwx_time.m` uses the input strings (`'year'`, `'month'`, etc.) to compute the new Time variable with the appropriate time format required by YCweather. So, each custom function essentially creates another weather variable for use by YCweather.

The custom functions were setup to allow YCweather to be expandable by the user to perform calculations on the weather data. To best understand the custom functions, it is best to examine the source code, specifically section five of `read_dat.m` and any of the existing custom functions: `calcwx_time.m`, `calcwx_flux.m`, and `calcwx_labLW.m`.

#### B.11.4 Variable Units

As mentioned in Section B.11.3, the format files require that the units for each weather variable be defined. The units prescribed in the format file must be present in the `units.txt` file, which is read by the `getunit.m` function. The `units.txt` defines the units via text abbreviations (e.g., `'kPa'` for pressure) both in Metric and English, the conversion factor between the units, and the appropriate axis labels for use in YCweather generated graphs. The function `getunit.m` is utilized for extracting the various unit related information in various portions of YCweather. Both the function `getunit.m` and text file `units.txt` were designed to allow for additional units to be added, which should only require adding a row to the text file.

The `units.txt` file should be composed of rows containing the following comma separated information: 1) the Metric abbreviation, 2) the English abbreviation, 3) text describing the unit, 4) the Metric abbreviation written in  $\text{\LaTeX}$  math format, 5) the English abbreviation written in  $\text{\LaTeX}$  math format, 6) the Metric unit written as  $\text{\TeX}$ , 7) the English unit written as  $\text{\TeX}$ , 7), and finally 8) the conversion multiplier

from English to Metric. Figure B.15 contains a portion of the `units.txt` file, refer to the file itself for additional examples as well as additional information regarding the format. Note, the `#` is the comment character within the file.

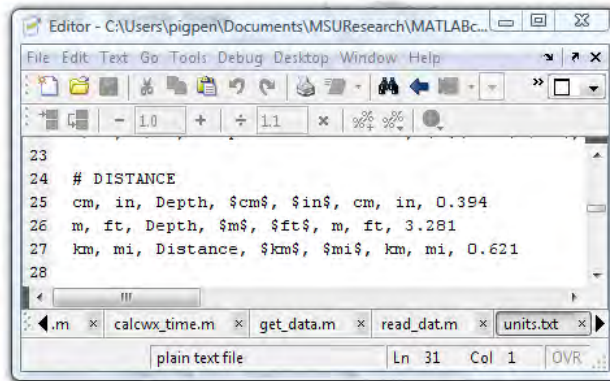


Figure B.15: Example entries for prescribing units within the `units.txt` file, which is utilized by the `getunit.m` function.

### B.11.5 Compiling and Implementing YCweather

The information in this section details the process for building a YCweather executable file from the source code via MATLAB's compiler. If any changes are made to the source code of YCweather the following information will make the updates available to all users running YCweather.

The function `YCbuild.m` acts to automate the process of compiling YCweather into executable form as well as post the updated to the web folder. The function requires two outside programs, WinSCP<sup>2</sup> and InstallJammer<sup>3</sup>.

After changing the source code, implement the the following code from the MATLAB command-line: `>>YCbuild('build',0.5)`, where the second input is the new version number. When this command executes the version is updated, YCweather.exe

<sup>2</sup>WinSCP: [winscp.net](http://winscp.net)

<sup>3</sup>InstallJammer: [www.installjammer.com](http://www.installjammer.com)

and YCmean.exe are compiled, YCmain.zip is packaged, the latest weather data from the current season is prepared, and the installer is compiled (YCinstaller.exe). All of these files are placed in the `release` directory, which are exactly the files need on the YCweather website. Before compiling a new version, the version number in the `MAIN.m` functions should be updated.

This process relies on three files. First, the two project files: `YCweather.prj` and `YCmain.prj`. These files were created with MATLAB's `deploytool` and dictate how `YCweather.exe` and `YCmain.exe` are compiled. If any additional m-files are added to `YCweather` then these files will needed to be added to the list of files in the `YCmain.prj` file. The third file, is the InstallJammer installation file, `YCinstaller.mpi`, which is stored in the `YCinstallerFiles` directory.

Once `YCweather` is compiled it must also be uploaded to the website so that the changes will be made available to all users of the program. This is done by executing the following: `>>YCbuild('web')`. This removes the old files from the web and adds the new via WinSCP; access to the appropriate account on the MSU Department of Civil Engineering server is required.

#### B.11.6 Website and Online Weather Database

The `YCweather` website, [www.coe.montana.edu/ce/subzero/snow](http://www.coe.montana.edu/ce/subzero/snow), is hosted by the MSU College of Engineering and contains the necessary files for initially downloading `YCweather` and the files needed for automatically updating `YCweather`. These files are automatically generated and created during the compilation and posting process described in Section B.11.5.

`YCweather` also relies on an ftp accessible database also hosted by the College of Engineering. This directory contains the weather files database directories that are automatically accessed by `YCweather` for keeping the weather data up to date.

The MATLAB program `GNAFC.m` located on the server is executed hourly to keep the weather data current via CRONTAB.

APPENDIX C

THERMAL MODEL SOFTWARE USER MANUAL

## C.1 Introduction

A heat-equation based thermal model was presented in Chapter 5, which was used as the basis of the sensitivity analysis and Monte Carlo simulations presented in Chapters 7–10. This appendix details the implementation of the thermal model software developed that works in conjunction with the sensitivity analysis software detailed in Appendix D. Additionally, details are provided on other software developed for implementing this model, including a complete stand-alone graphical user interface.

This appendix is divided into three main sections. Section C.2 explains the basic operation of the thermal software. Section C.3 presents an interface that links the thermal model with Microsoft Excel, allowing inputs to be easily modified. Figure C.1 contains a flow chart demonstrating how the various functions detailed in the first two sections (C.2 and C.3) interact. Finally, in Section C.4, a complete graphical user interface is briefly presented that operates as a stand-alone Windows application.

A few notational conventions are utilized throughout this user manual:

- Monospaced typeface indicates a MATLAB m-file, function, or variable (e.g., `sobol.m`).
- MATLAB code is provided in figure windows (e.g., Figure D.2 when referenced many times).
- MATLAB code is also presented in-line with the text as:

---

```
>> 2+2  
ans = 4  
>>
```

---



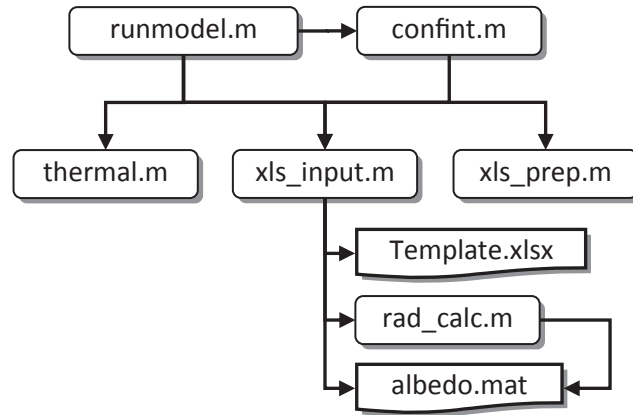


Figure C.1: Flow chart demonstrating how the various functions discussed in Section C.2 and C.3 interact.

## C.2 Basic Application

The basic operation of the thermal model is performed via the MATLAB command-line using two functions: `xls_prep.m` and `thermal.m` (the source code is included in Section C.5). These two functions were utilized by `saMODEL2.m` as detailed in Appendix D. First, `xls_prep.m` is implemented, which requires three input arrays that contain the snow properties, atmospheric conditions, and model constants. The syntax for `xls_prep.m` is as follows:

---

```

function [s,a] = xls_prep(snow,atm,constants)
% XLS_PREP builds arrays for inputting into thermal model
%-----
% SYNTAX:
%   [snow,atm] = prep_input(snow,atm,constants);
  
```

---

The `snow` variable may be arranged in two ways: as a uniform or a varying snowpack. If the snowpack is assumed uniform then `snow` is a 1-D array with six values (in order): depth (cm), density ( $\text{kg/m}^3$ ), thermal conductivity ( $\text{W}/(\text{m}\cdot\text{K})$ ), specific heat capacity ( $\text{J}/(\text{gm}\cdot\text{K})$ ), snow temperature ( $^{\circ}\text{C}$ ), and extinction coefficient ( $1/\text{m}$ ). If the snowpack varies then the array may be composed of any number of rows of the same

parameters that dictates the different layers. The following MATLAB code provides example definitions of the `snow` variable:

---

```
>> snow = [50, 130, 0.06, 2030, -10, 70]
snow =
      50  130  0.06  2030  -10  70
>> snow = [0, 130, 0.06, 2030, -10, 70; 50, 180, 0.1, 2030, -5, 90;...
100, 180, 0.1, 2030, -5, 90]
snow =
      0  130  0.06  2030  -10  70
      50  180  0.1  2030  -5  90
     100  180  0.1  2030  -5  90
>>
```

---

The first example defines a 50 cm thick snow pack with constant properties. The second example defines a 100 cm deep snowpack that increases in density, thermal conductivity, temperature, and extinction coefficient from 0 to 50 cm. Then from 50 to 100 cm the conditions remain constant. The `xls_prep.m` function performs linear interpolation between the rows according to the layer thickness. An additional seventh column is optional that specifies the extinction coefficient for the near-infrared wavebands, in this case the extinction coefficient previously mentioned is used for the visible waveband.

In similar fashion, the atmospheric conditions are defined in the `atm` variable, which includes nine parameters (in order): time (hours), incoming long-wave radiation ( $\text{W}/\text{m}^2$ ), incoming short-wave radiation ( $\text{W}/\text{m}^2$ ), albedo, wind speed (m/s), air temperature ( $^{\circ}\text{C}$ ), relative humidity (%), the lower boundary condition ( $^{\circ}\text{C}$ ), and air pressure (kPa). Two additional columns may also be defined that specify the incoming short-wave radiation and albedo for the near-infrared wavebands. Again, the short-wave radiation and albedo previously defined are then used as the values for the visible spectrum.

The model constants are defined in the `constants` variable, which must include the following (in order): latent heat of sublimation (kJ/kg), the latent heat transfer coefficient, the sensible heat transfer coefficient, the ratio of molecular weights

of dry-air and water-vapor, the gas constant for water-vapor (kJ/(kg·K)), reference temperature (°C), reference vapor-pressure (kPa), the emissivity of snow, the layer thickness (cm), and time step (s).

Once the three input variable arrays are defined the thermal model may be executed, for example:

---

```
>> snow = [50, 130, 0.06, 2030, -10, 70];
>> atm = [0,240,0,0.82,1.7,-10,.2,-10,101; 10,240,500,0.82,1.7,-10,.2,-10,101];
>> constants = [2833,0.0023,0.0023,0.622,0.462,-5,0.402,0.95,1,60,1];
>> [S,A] = xls_prep(snow, atm, constants);
>> [T,Q] = thermal(S, A, constants);
```

---

The `thermal.m` function implements the finite-difference solution presented in Chapter 5. This function outputs an array containing snow temperatures (`T`) as a function of model evaluation time (columns) and depth (rows). The various heat-fluxes—long-wave, sensible, latent, short-wave—are output in the `Q` variable in similar fashion.

## C.3 Spreadsheet Application

### C.3.1 General Application

To make the thermal model more powerful, two additional functions were developed—`xls_input.m` and `runmodel.m`—that provide an interface between MATLAB and Microsoft Excel. This allows the various input matrices previously explained to be easily developed. First, the required structure of the Excel file must be established. The Excel spreadsheet must be composed of three worksheets named “SnowProperties”, “AtmosphericSettings”, and “Constants”. Each worksheet must be formatted in a specific fashion, as shown in Figures C.2 and Figures C.3.<sup>1</sup> Section

---

<sup>1</sup>A template may be downloaded at: [www.coe.montana.edu/ce/subzero/snow/thermalmodel/template.xlsx](http://www.coe.montana.edu/ce/subzero/snow/thermalmodel/template.xlsx).

C.3.2 details some additional features available when using `xls_input.m`, particularly for the “Constants” worksheet.

Snow Property Settings:						
Depth	Density ( $\rho$ )	Thermal Conductivity (k)	Specific Heat (Cp)	Snow Temperature (Tinitial)	Extinction Coefficient (kappa)	NIR Extinction Coefficient (kappa)
(cm)	( $\text{kg}/\text{m}^3$ )	( $\text{W}/\text{m}^{\circ}\text{K}$ )	( $\text{J}/\text{g}^{\circ}\text{K}$ )	( $^{\circ}\text{C}$ )	( $1/\text{m}$ )	( $1/\text{m}$ )
0	130	0.06325	2036	-10	class2	
20	130	0.06325	2036	-10	class2	
40	150	0.05	2036	-9	class2	

(a) Snow Properties

Atmospheric Settings:										
Time	Incoming Longwave (LWin)	Incoming Shortwave (SWin)	Albedo (alpha)	Wind Speed (Vw)	Air Temperature (Ta)	Relative Humidity (RH)	Lower Boundary (bottom)	Air Pressure (Patm)	NIR Incoming Shortwave (SWin)	NIR Albedo (alpha)
(hours)	( $\text{W}/\text{m}^2$ )	( $\text{W}/\text{m}^2$ )		(cm)	( $^{\circ}\text{C}$ )	(%)	( $^{\circ}\text{C}$ )	(kPa)	( $\text{W}/\text{m}^2$ )	
10	185	500	d0.5	1.3	-10	20	-10	100		

(b) Atmospheric Settings

Figure C.2: Example of the (a) “SnowProperties” and (b) “AtmosphericSettings” worksheets for Excel file read by `xls_input.m`.

Once the Excel file is setup as desired, the function `xls_input.m` is used to process the data contained in the spreadsheet. As was the case for the basic operation, the

near-infrared columns are optional. For example, for the template.xlsx file available for download, the following code implements the thermal model:

```
>> filename = 'template.xlsx';
>> [s,a,c] = xls_input(filename);
>> [S,A] = xls_prep(s, a, c);
>> [T,Q] = thermal(S, A, c);
```

The `runmodel.m` function performs the above actions, groups the results into a data structure, and adds the ability to compute confidence level intervals for the snow temperatures. The confidence intervals are explained further in the following section. The code shown in Figure C.4 implements the thermal model via `runmodel.m` and displays the data structure produced. The data structure and details regarding various optional inputs are explained in the help associated with the `runmodel.m`.

Thermal Model Constants:			
MATLAB Code	Description	Value	Error (%)
Ls	Latent heat of sublimation phase change (kJ/kg)	2833	0
Ke	Dimensionless turbulent transfer coefficient for water vapor	0.0023	0
Kh	Dimensionless turbulent transfer coefficient	0.0023	0
MvMa	Ratio of dry-air and water-vapor molecular weights	0.622	0
Rv	Gas constant for water vapor (kJ/kg*K)	0.462	0
T0	Reference temperature for vapor pressure (°C)	-5	0
e0	Reference vapor pressure (kPa)	0.402	0
emis	Emissivity of snow	0.9875	0
dz	Layer thickness (cm)	0.5	
dt	Iteration time step (sec)	60	
Atmospheric Property Multipliers & Error	Incoming Longwave (LWin)	1	5
	Incoming Shortwave (SWin)	1	5
	Albedo (alpha)	1	5
	Wind Speed (Vw)	1	5
	Air Temperature (Ta)	1	5
	Relative Humidity (RH)	1	5
	Lower Boundary (bottom)	1	5
	Air Pressure (Patm)	1	5
Snow Property Multipliers & Error	NIR Incoming Shortwave (SWin)	1	5
	NIR Albedo (alpha)	1	5
	Density (p)	1	5
	Thermal Conductivity (k)	1	5
	Specific Heat (Cp)	1	5
	Snow Temperature (Tinitial)	1	5
	Extinction Coefficient (kappa)	1	5
	NIR Extinction Coefficient (kappa)	1	5

Figure C.3: Example of the “Constants” worksheets for Excel file read by `xls_input.m`.

The data structure was designed to be implemented via the graphical user interface (Section C.4), as such the data structure may contain many model runs, as shown in Figure C.4.

```

1 >> filename = 'template.xlsx';
2 >> data = runmodel(filename)
3 data =
4         xls: 'template.xlsx'
5     bootsettings: []
6         name: ''
7         desc: ''
8         time: '22-Mar-2010 09:58:06'
9         T: [82x601 double]
10        Q: [81x601x5 double]
11        snw: [81x7 double]
12        atm: [601x11 double]
13        const: [1x10 double]
14        Tboot: []
15        Qboot: []
16        Sboot: []
17        Aboot: []
18        Cboot: []
19 >> data(2) = runmodel(filename); % multiple runs may be stored
20 >>

```

Figure C.4: MATLAB implementation of `runmodel.m` and the resulting data structure.

### C.3.2 Additional Features

The usage of the function `xls_input.m` offers additional functionality for inputs, including the usage of tabulated snow micro-structure data, input multipliers, and confidence interval calculations.

Snow Micro-Structure: The snow albedo and extinction coefficient may be input into the Excel document using keys: *dXX*, *classX*, or *type*.<sup>2</sup> The *dXX* key allows the snow grain diameter to be used to compute albedo and extinction coefficient according to Armstrong and Brun (2008, Eq. 2.25, p. 56), where the *XX* is a number

<sup>2</sup>The *italicized* keys are used to reference the inputs, the actual text as would be entered in the Excel worksheets is provide in quotes.



representing the size of the grain in millimeters (e.g., “d5”). Figure C.2b includes the implementation of this option. The *classX* key uses the tabulated values from Armstrong and Brun (2008, Tab. 2.6), where *X* is a value one to six (e.g., “class2”). The type may be one of three strings: “fine”, “medium”, or “coarse”, this option is only available for the computation of albedo. The usage of these keys results in the computation of the albedo from the information provided in Baldrige *et al.* (2009). The albedo and extinction coefficient calculations are preformed in the `albedo` and `extinction` sub-functions of `xls_input.m`.

In all cases, when the optional near-infrared columns are not utilized it is assumed that albedo and extinction coefficients are defined for the “all-wave” spectrum that includes both the visible and near-infrared spectrum. Using ASTM G-173 (2003) the appropriated values are computed based on this spectrum via `rad_calc.m` (see Section C.5.5).

Both `xls_input.m` and `rad_calc.m` require the `albedo.mat` file that contains the data structure shown in Figure C.5. Each component of this structure contains a two-column numeric array, the the first column of which provides the wavelength in nanometers. The second column of `x.atm` contains solar irradiance as defined by ASTM G-173 (2003). For the other items (e.g., `x.fine`), the second column contains albedo values as defined in Baldrige *et al.* (2009).<sup>3</sup>

Finally, the snow density or the thermal conductivity may be automatically computed by using “auto” in either column, but not both. The desired density or thermal

---

<sup>3</sup>This file may downloaded at [www.coe.montana.edu/ce/subzero/snow/thermalmodel/albedo.mat](http://www.coe.montana.edu/ce/subzero/snow/thermalmodel/albedo.mat).

```

1 >> x = load('albedo.mat')
2 x =
3     astm: [2002x2 double]
4     fine: [179x2 double]
5     medium: [179x2 double]
6     coarse: [179x2 double]
7 >>

```

Figure C.5: Required data structure of `albedo.mat`.

conductivity calculations are performed using the relationships presented by Sturm *et al.* (1997).

Input Multipliers: To enable simple modification of entire columns of data, multipliers are provided on the “Constants” worksheet, as shown in Figure C.3. The corresponding column from the other worksheets are simply multiplied by the values listed, allowing the user to quickly modify the various inputs.

Confidence Intervals: The `runmodel.m` function includes the ability to compute confidence intervals via `confint.m`, which uses the percentile bootstrap method presented by Efron and Tibshirani (1993). First, the percent error is prescribed by the values listed in the “Error” column on the “Constants” worksheet, as shown in Figure C.3. These values allow the parameter to vary plus or minus this amount according to a normal distribution, such that the  $n\sigma$  tails of this distribution are at these limits, where  $n\sigma$  is the number of standard deviations. The graphical user interface described in the following sections provides the means for utilizing this feature.

#### C.4 Graphical User Interface

A graphical user interface (GUI), as shown in Figure C.6, was developed to act as front-end to the software explained in the previous sections. This interface was deployed via MATLAB’s `deploytool` tool and wrapped into an installable Windows-



based program. The complete installer, `TMsetup.exe`, may be downloaded at: [www.coe.montana.edu/ce/subzero/snow/thermalmodel/TMsetup.exe](http://www.coe.montana.edu/ce/subzero/snow/thermalmodel/TMsetup.exe).

The stand-alone application may prompt the user to download a newer version, which is recommended. By agreeing to this prompt the website listing the associated files will automatically open in a browser. The only file that needs to be downloaded is `model.exe`, this file should replace the original that is located in the installation directory.

The GUI serves two functions, first it controls the operation of the `runmodel.m` function and manages the data structure produced by this function (see Section C.3). This is done through the use of projects, which are nothing more than MATLAB mat-files that store the data structure produced by `runmodel.m`. However, the extension was changed to `*.prj`. The GUI also provides tools for the visualization of the input and output variables.

#### C.4.1 Performing Model Runs

The following briefly describes the basic steps of performing thermal model evaluations:

1. Select New Project from the file menu.
2. A prompt will appear that gives options regarding the Excel spreadsheet file to utilize. Selecting New copies the `template.xlsx` file previously discussed to a file selected by the user. Selecting Existing allows the user to select a previously created file. In both cases the Excel file will open when the necessary actions are complete.
3. Modify and saved the Excel file created for the desired conditions, as detailed in Section C.3.

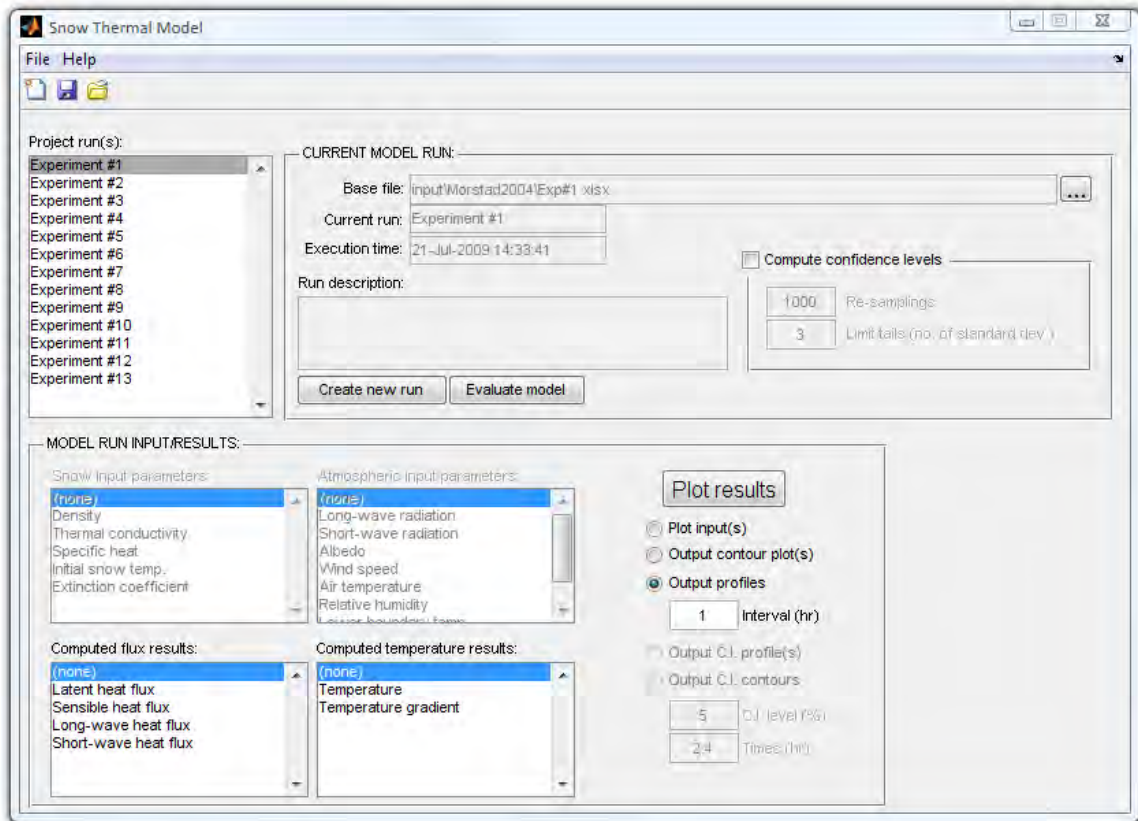


Figure C.6: Graphical user interface for implementing the snow thermal model.

4. Return to the GUI application and type a name for the current run as well as a description. Also, if confidence levels are desired (see Section C.3.2.3) the Compute Confidence Levels option should be checked at this time. The computation of the confidence levels can be extremely time consuming, so begin with a small number of re-samplings.
5. Press the Evaluate Model button on the GUI, this starts the model evaluations which may take several minutes depending on the computer and model inputs. If confidence levels are being computed a window will appear showing the progress of the calculations.

6. When the run is complete it appears in the Project Run(s) menu on the left-side of the GUI.
7. Additional runs may be computed by selecting the Create New Run button and the Excel file may be changed by selecting the “...” button at the right-end of the Base File text. This same button will also open the associated Excel file when a model run is activated. It is not necessary to create a new Excel file, but any changes made to the Excel file for additional model evaluations must be saved, these changes will not be stored and cannot not be recalled (this functionality may be available in future versions). Run names may be edited or runs may be deleted by right-clicking on the run in the Project Run(s) list.
8. After all the desired runs are completed the project should be saved by selecting Save Project from the File menu.

#### C.4.2 Graphing Results

It is possible to create graphs of both the model inputs and outputs, this is done using the lower pane of the GUI shown in Figure C.6. First, a model run must be selected in the Project Run(s) panel. The graphs created share all of the functionality of the graphs presented in Appendix B (Section B.4).

Model Inputs: The model inputs are graphed by selecting the Plot Input(s) radio button, this will cause the Snow and Atmospheric parameter lists to become activated. To create a graph simply select the desired item and press the Plot Results button. A graph will appear for each item selected.

Model Outputs: Two different graph styles of model outputs are available: profiles and contours. Figure C.7 provides examples of the snowpack temperature

graphed with each of the different methods. When plotting profiles the interval, in hours, must also be set (e.g., 2 results in profiles being plotted every 2 hours). It is possible to graph a single profile directly from a contour plot, this is done by right-clicking on the contour where the profile is desired and then selecting either a vertical or horizontal profile.

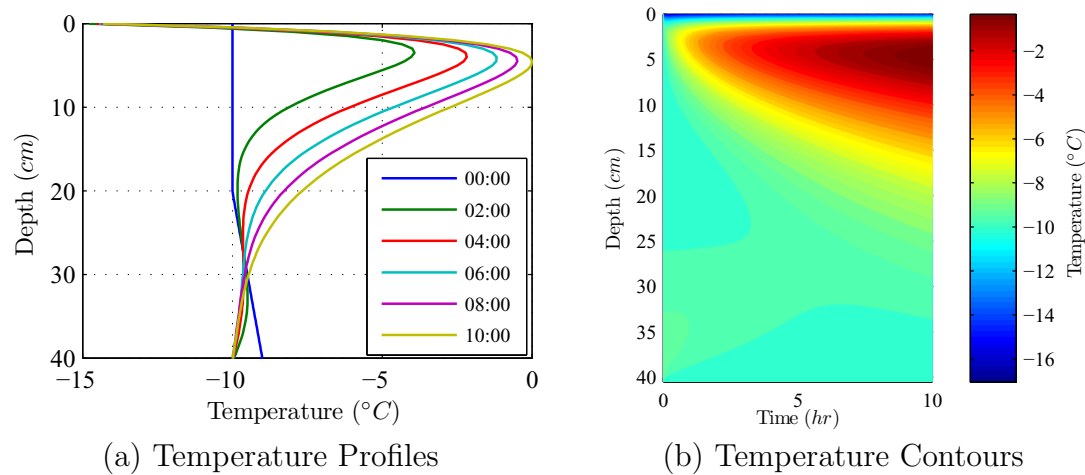


Figure C.7: Example graphs of snowpack temperatures demonstrated the two graphing options available: (a) profiles and (b) contours.

In similar fashion, if confidence intervals were computed it is possible to graph these intervals using the Output C.I. Profiles or Contours radio buttons. Figure C.8 provides examples of temperature data plots with confidence level intervals. Both the profiles and the contours require the confidence level to be specified by a scalar value (in percent) entered into the C.I. Level location. When profiles are plotted the time(s) at which the profiles are desired must be specified in the Times (hr) location (e.g., 2 or 2, 4). The confidence level contour graphs show the absolute value of the largest deviation from the mean value.

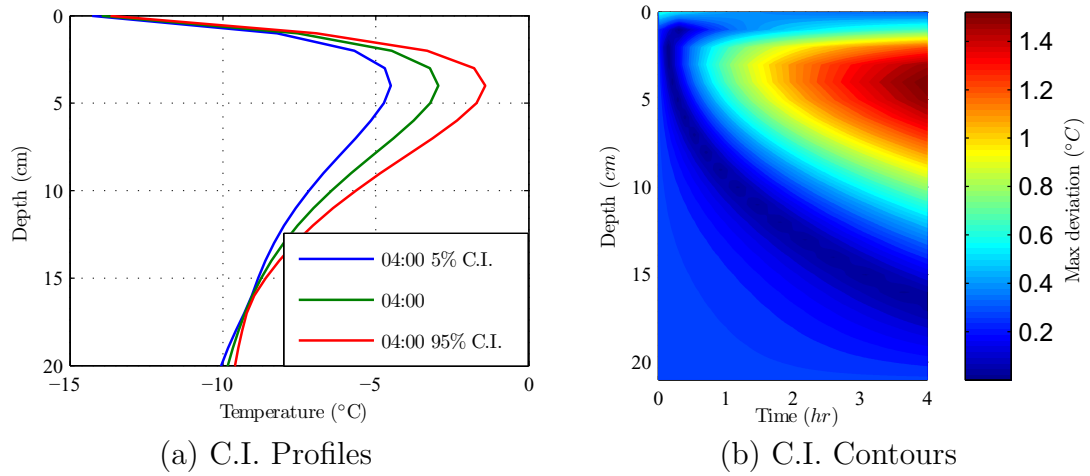


Figure C.8: Example graphs of snowpack temperature demonstrated the two graphing options available for displaying confidence level intervals: (a) C.I. profiles and (b) C.I. contours.

#### C.4.3 Closing Remarks

The information presented in this appendix explains the basic and advanced functionality of the thermal model developed for the work presented throughout this dissertation. The details presented as well as the entire software package was developed to make the model easily accessible, thus please contact the author if more information is required.

## C.5 Source Code

C.5.1 `runmodel.m`

```

1 function data = runmodel(varargin)
2 % RUNMODEL program to execute thermal model using Excel input file.
3 %-----
4 % SYNTAX:
5 %   data = runmodel;
6 %   data = runmodel(filename);
7 %   data = runmodel(filename,name);
8 %   data = runmodel(filename,name,desc);
9 %   data = runmodel(...,[B,N]);
10 %
11 % DESCRIPTION:
12 %   data = runmodel executes the thermal model via Excel input, prompting
13 %   the user for a filename.
14 %   data = runmodel(filename) executes the thermal model for supplied name.
15 %   data = runmodel(filename,name) same as above, but allows the user to
16 %   name the run (e.g. name = 'Model Run #3');
17 %   data = runmodel(filename,name,desc) same as above, but allows user to
18 %   also add a description to the run (e.g. desc = 'This run mimics
19 %   Feb-14-2008 at the South station of the YC');
20 %   data = runmodel(filename,name,desc,[B,N]) runs the model and
21 %   computes the bootstrap confidence intervals, where B = number
22 %   of resamplings, N = number of standard deviations to assume for
23 %   the tails
24 %
25 % OUTPUT:
26 % The data structure has the following fieldnames
27 %   xls: Input Excel filename
28 % bootsettings: Bootstrap settings
29 %   name: Name of current run
30 %   desc: Description of the current run
31 %   time: Start time of model execution
32 %   T: Array of snowpack temperatures
33 %   Q: Array of snowpack heat fluxes
34 %   snw: Input array of snow properties
35 %   atm: Input array of atmospheric conditions
36 %   const: Array of model constants
37 %   Tboot: Bootstrap replicates of temperature
38 %   Qboot: Bootstrap replicates of heat fluxes
39 %   Sboot: Bootstrap replicates of snw inputs
40 %   Aboot: Bootstrap replicates of atm inputs
41 %   Cboot: Bootstrap replicates of const inputs
42 %-----
43
44 % 1 - GATHER OPTIONS
45   data = getoptions(varargin{:});
46
47 % 2 - EXECUTE MODEL
48   [S,A,data.const] = xls_input(data.xls);
49   [data.snw,data.atm] = xls_prep(S,A,data.const);
50   [data.T,data.Q] = thermal(data.snw,data.atm,data.const);
51
52 % 3 - RUN THE BOOTSTRAP
53   if ~isempty(data.bootsettings);
54     B = data.bootsettings;
55     bootdata = confint(data.xls,B(1),B(2));
56     fn = fieldnames(bootdata);
57     for i = 1:length(fn);
58       data.(fn{i}) = bootdata.(fn{i});
59     end
60   end
61
62 %-----
63 function [data,B] = getoptions(varargin)
64 % GETOPTIONS determines/sets the input options
65
66 % 1 - SET THE DEFAULTS
67   filename = '';
68   name = '';
69   desc = '';
70   B = [];
71
72 % 2 - GATHER BOOTSTRAPPING DATA
73   idx = [];
74   for i = 1:nargin; idx(i) = isnumeric(varargin{i}); end
75   ix = find(idx,1,'first');
76   if ~isempty(ix); B = varargin{ix}; end
77
78 % 3 - GATHER FILENAME, NAME, AND DESCRIPTION..
79   if isempty(B); rem = varargin; else rem = varargin(1:nargin-1); end

```

```

80     if length(rem) >= 1; filename = varargin{1}; end
81     if length(rem) >= 2; name = varargin{2}; end
82     if length(rem) == 3; desc = varargin{3}; end
83
84 % 4 - PROMPT FOR FILENAME
85 % 4.1 - Gather/define the "lastdir" preference
86     if ispref('ThermalModel_v5','lastdir');
87         defdir = getpref('ThermalModel_v5','lastdir');
88     else
89         addpref('ThermalModel_v5','lastdir',cd);
90         defdir = cd;
91     end
92
93 % 4.2 - Prompt the user for a filename
94     if isempty(filename);
95         FilterSpec = {'*.xlsx','Excel_Workbook_(*.xlsx)';...
96                     '*.xls','Excel_97-2003_Workbook_(*.xls)';...
97                     '**','All_files_(*.*)'};
98         [fn,pth] = uigetfile(FilterSpec,'Select_file...',defdir);
99         if isnumeric(fn); return; end
100        filename = [pth,fn];
101        setpref('ThermalModel_v5','lastdir',fileparts(filename));
102    end
103
104 % 5 - BUILD DATA STRUCTURE
105 % 5.1 - File information
106     data.xls = filename;
107     data.bootsettings = B;
108     data.name = name;
109     data.desc = desc;
110     data.time = datestr(now);
111
112 % 5.2 - Model evaluation
113     data.T = []; data.Q = [];
114     data.snw = []; data.atm = []; data.const = [];
115
116 % 5.3 - Bootstrap results
117     data.Tboot = []; data.Qboot = [];
118     data.Sboot = []; data.Aboot = []; data.Cboot = [];

```

## C.5.2 xls\_input.m

```

1 function [S,A,C,E] = xls_input(filename)
2 % XLSINPUT builds input matrices for usage with the thermal model (v5).
3 %-----
4 % SYNTAX:
5 %   [S,A,C,E] = xls_input(filename)
6 %-----
7
8 % 1 - CHECK FILE
9     if nargin == 0; filename = 'input/WetSnow/base.xlsx'; end
10    if ~exist(filename,'file');
11        errordlg('File_does_not_exist!'); return;
12    end;
13
14 % 2 - EXTRACT DATA FROM FILE
15 % 2.1 - Read files
16     [S,snwTXT] = xlsread(filename,'SnowProperties');
17     [A,atmTXT] = xlsread(filename,'AtmosphericSettings');
18     [const] = xlsread(filename,'Constants');
19
20 % 2.2 - Separate constants and multipliers
21     C = const(1:10);
22     M = const(11:length(const),1); M(isnan(M)) = 0;
23     aM = M(1:10); % atmospheric multipliers
24     sM = M(11:length(M)); % snow multipliers
25
26 % 2.3 - Separate percent error values
27     Nc = size(const,2);
28     if Nc == 1;
29         E.atm = zeros(length(aM),1); E.atm(:,1) = 0.05;
30         E.snw = zeros(length(sM),1); E.snw(:,1) = 0.05;
31         E.const = zeros(10,1);
32     else
33         E.atm = const(11:length(aM)+10,2)/100;
34         E.snw = const(length(aM)+11:length(const),2)/100;
35         E.const = const(1:10,2)/100;
36     end
37

```

```

38 % 3 - APPLY SPECIAL VALUES TO ALBEDO AND EXTINCTION COLUMNS
39   A = albedo(A,atmTXT,S);
40   S = extinction(S,snwTXT);
41   S = density(S,snwTXT);
42
43 % 4 - APPLY MULTIPLIERS
44 % 4.1 - Re-size multipliers arrays to necessary size
45   aM = [1;aM(1:size(A,2)-1)]; % 1 adds a column for time
46   sM = [1;sM(1:size(S,2)-1)]; % 1 adds a column for the depth
47
48 % 4.2 - Apply multipliers
49   for i = 1:length(sM); S(:,i) = S(:,i) * sM(i); end
50   for i = 1:length(aM); A(:,i) = A(:,i) * aM(i); end
51
52 %-----
53 function A = albedo(A,atmTXT,S)
54 % ALBEDO applies special input into albedo column: dXX, classX, <type>
55 % Special values given in the albedo column (#4) assume that the shortwave
56 % column (3) is an all-wave value, so it is divided into a VIS/NIR
57 % components as is the albedo for all "special" cases
58
59 % 1 - Determine "special" locations
60   idx = find(isnan(A(:,4)));
61
62 % 2 - Cycle through each special value and compute desired albedos
63 for i = 1:length(idx);
64   val = atmTXT{idx(i)+3,4}; % Current special case
65
66   % Optical depth case: dXX
67   if strcmpi('d',val(1)); % Optical depth caer
68     dopt = str2double(val(2:length(val)));
69     if isnan(dopt);
70       error('xls_input:albedo','optical_depth_ill_define.');

```



```

125 % Record an error
126 else
127     error('xls_input:albedo','error with albedo input , column 4!');
128 end
129 end
130
131 %-----
132 function S = density(S,snwTXT)
133 % DENSITY applies special input for density and/or thermal conductivity
134 % columns, either can be 'auto', just not both. The auto values are
135 % replaced it the appropriate value from Sturm, 1997. The quadratic is used
136 % for solving for k and the exponential when solving for density
137
138 for i = 1:size(S,1);
139     rho = S(i,2)/1000; k = S(i,3);
140     if isnumeric(rho) && isnumeric(k); % Both specified
141         S(i,2) = rho*1000; S(i,3) = k;
142     elseif isnan(rho) && isnumeric(k); % Compute density
143         S(i,2) = (log10(k) + 1.652) / 2.65 * 1000;
144     elseif isnumeric(rho) && isnan(k); % Compute k
145         if rho < 0.156;
146             S(i,3) = 0.023 + 0.234 * rho;
147         else
148             S(i,3) = 0.138 - 1.01*rho + 3.233 * rho^2;
149         end
150     else
151         error('xls_input:density',...
152             'error with density/conductivity input , column 2 and/or 3!');
153     end
154 end

```

### C.5.3 xls\_prep.m

```

1 function [s,a] = xls_prep(snow,atm,constants)
2 % XLSPREP builds arrays for inputing into thermal model
3 %-----
4 % SYNTAX:
5 % [snow,atm] = prep_input(snow,atm,constants);
6 %
7 % INPUT:
8 % snow = matrix containing snow data
9 % atm = matrix containing atmospheric data
10 % constants = matrix containing model constants
11 %
12 % EXAMPLE INPUT:
13 % snow = [50,130,0.06,2030,-10,70];
14 % atm = [6,240,500,0.82,1.7,-10,.2,-10,101];
15 % constants = [2833,0.0023,0.0023,0.622,0.462,-5,0.402,0.95,1,60,1];
16 %-----
17
18 % 1 - Fill in atmospheric data
19 atm(:,1) = atm(:,1) .* 3600; % Convert time to seconds
20 dt = constants(10); % Time step in seconds
21 a = fill_array(atm,dt);
22
23 % 2 - Fill and snow properties data
24 dz = constants(9);
25 s = fill_array(snow,dz);
26
27 %-----
28 % SUBFUCTION: fill_array
29 function out = fill_array(in,int)
30 % FILL_ARRAY builds an array from "in" using the interval in "int" based on
31 % the first column of data
32
33 % 1 - Build array for case when data is only a single row (constant data)
34 len = size(in,1);
35 if len == 1;
36     in(2,:) = in(1,:);
37     in(1,1) = 0;
38 end
39
40 % 2 - Build new array with spacing based on "int"
41 % 2.1 - Build the first column of the new array (e.g. time steps)
42 n = size(in,1);
43 xi = (in(1,1):int:in(n,1))';
44
45 % 2.2 - Interpolate the remaining data based on the first column
46 x = in(:,1);

```

```

47 Y = in(:,2:size(in,2));
48 yi = interp1(x,Y,xi,'linear');
49 out = [xi,yi];

```

### C.5.4 thermal.m

```

1 function [T,Q] = thermal(snow,atm,C)
2 % THERMAL executes 1-D heat equation based thermal model
3 %-----
4 % SYNTAX:
5 [T,Q] = thermal(snow,atm,C)
6 %
7 % DESCRIPTION:
8 [T,Q] = thermal(snow,atm,C) based on the information provided in the
9 numeric arrays containing snow properties (snow), atmospheric
10 conditions (atm), and model constants (C) a 1-D thermal analysis is
11 performed resulting in the snowpack temperatures (T) and associated
12 heat fluxes (Q)
13 %-----
14
15 % 1 - PREPARE VARIABLES FOR CALCULATION
16 % 1.1 - Pre-define arrays
17 if size(atm,2) == 11 && size(snow,2) == 7;
18     ndim = 2;
19 else
20     ndim = 1;
21 end
22
23 nt = size(atm,1);           % Number of time steps
24 ns = size(snow,1);         % Number of snow elements
25
26 T = zeros(ns,nt);         % Temperature array
27 q = zeros(ns,nt,ndim);    % Short-wave flux absorbed array
28 qs = zeros(nt,3);         % Surface flux array
29
30 A = zeros(ns+1,ns+1);     % A-matrix for temperature solution
31 b = zeros(ns+1,1);        % b-vector for temperature solution
32
33 % 1.2 - Establish user specified constants
34 Ls = C(1);
35 Ke = C(2);
36 Kh = C(3);
37 MvMa = C(4);
38 Rv = C(5);
39 T0 = C(6) + 273.15;
40 e0 = C(7);
41 emis = C(8);
42 dz = C(9)/100;
43 dt = C(10);
44
45 % 1.3 - Define additional constants needed
46 sb = 5.6696*10^(-8);      % Stefan Boltzmann constant (W/m^2/K^4)
47 R = 0.287;                % Gas constant for air (kJ/kg/K)
48
49 % 1.4 - Compute the properties of air
50 Cp_air = 1003;            % Specific heat @-5C (J/kg/K)
51 rho_air = atm(:,9)./(R*(atm(:,6) + 273.15)); % Density (kg/m^2)
52
53 % 2 - INITILIZE ARRAYS FOR COMPUTATION
54 % 2.1 - Initilize temperature array
55 T(:,1) = snow(:,5);      % Initial snow temperature
56 T(ns+1,:) = atm(:,8);    % Base
57
58 % 2.2 - General Matrix coefficients
59 Ca = snow(:,3) ./ dz^2;   % a
60 Cb = (snow(:,2) .* snow(:,4))./dt; % b
61 Cc = Cb + Ca;            % c
62 Cd = Cb - Ca;            % d
63
64 % 3 - BEGIN COMPUTING FOR EACH TIME STEP (time step = index "j")
65 for j = 2:nt
66 % 3.1 - Establish air/snow surface temperatures
67 Ta = atm(j,6) + 273.15;
68 Ts = T(1,j-1) + 273.15;
69
70 % 3.2 - Compute longwave heat flux
71 qs(j,1) = atm(j,2) - emis*sb*Ts^4;
72
73 % 3.3 - Compute the latent heat flux

```

```

74     ea = e0*exp(Ls/Rv *(1/T0 - 1/Ta))*atm(j,7)/100;
75     es = e0*exp(Ls/Rv *(1/T0 - 1/Ts));
76     qs(j,2) = 1000*MvMa*rho_air(j)*Ls*Ke*atm(j,5)*(ea-es)/atm(j,9);
77
78 % 3.4 - Compute the sensible heat flux
79     qs(j,3) = Kh*rho_air(j)*Cp-air*atm(j,5)*(Ta - Ts);
80
81 % 3.5 - Compute the absorbed shortwave and build solution matrix
82 %     for each layer of snow
83 % 3.5.1 - Compute shortwave absorbed in the top layer
84     q(1,j,1) = atm(j,3)*(1-atm(j,4))*(1-exp(-snow(1,6)*dz));
85
86 % 3.5.2 - Compute shortwave in NIR if present
87     if ndim == 2;
88         q(1,j,2) = atm(j,10)*(1-atm(j,11))*(1-exp(-snow(1,7)*dz));
89     end
90
91 % 3.5.2 - Compute shortwave absorbed for lower layers and build
92 %     solution matrices
93     for i = 2:ns
94         % Short-wave radiation absorbed
95         q(i,j,1) = q(i-1,j,1)*exp(-snow(i,6)*dz); % all-wave or VIS
96         if ndim == 2;
97             q(i,j,2) = q(i-1,j,2)*exp(-snow(i,7)*dz); % NIR
98         end
99
100        % Solution matrices
101        A(i,i-1) = -Ca(i)/2;
102        A(i,i) = Cc(i);
103        A(i,i+1) = -Ca(i)/2;
104        b(i,1) = Ca(i)/2*T(i-1,j-1) + Cd(i)*T(i,j-1) + ...
105                Ca(i)/2*T(i+1,j-1) + sum(q(i,j,:))/dz;
106    end
107
108 % 3.6 - Compute the surface flux
109     sur_flux = sum(qs(j,1:3));
110
111 % 3.7 - Insert matrix values for surface node (i = 1)
112     A(1,1) = Cc(1);
113     A(1,2) = -Ca(1);
114     b(1) = Cd(1)*T(1,j-1) + Ca(1)*T(2,j-1) + 2*sur_flux/dz + ...
115           sum(q(1,j,:))/dz;
116
117 % 3.8 - Insert matrix values for bottom boundary condition
118     A(ns+1,ns+1) = 1;
119     b(ns+1) = atm(j,8);
120
121 % 3.9 - Calculate the new temperature profile
122     Tnew = A\b;
123     Tnew(Tnew>0) = 0;
124     T(:,j) = Tnew;
125 end;
126
127 Q = zeros(ns,nt,ndim+3);
128 Q(1,:,1:3) = qs;
129 Q(:, :, 4:end) = q;

```

## C.5.5 rad\_calc.m

```

1 function varargout = rad_calc(varargin)
2 % RAD_CALC spectral calculations of radiation, albedo, and extinction.
3 %-----
4 % SYNTAX:
5 %     [SWvis,SWnir,SWswir] = rad_calc(SWall);
6 %     [Avis,Anir,Aswir] = rad_calc(curve);
7 %     [Avis,Bvis,Anir,Bvis,Aswir,Bswir] = rad_calc(dopt,rho);
8 %     [Avis,Bvis,Anir,Bvis,Aswir,Bswir] = rad_calc('class',num);
9 %
10 % DESCRIPTION:
11 %     [SWvis,SWnir,SWswir] = rad_calc(SWall) computes spectral components of
12 %     all-wave shortwave radiation based on ASTM standard.
13 %     [Avis,Anir,Aswir] = rad_calc(curve) computes spectral albedo components
14 %     based on curves: 'fine', 'medium', 'coarse'
15 %     [Avis,Bvis,Anir,Bvis,Aswir,Bswir] = rad_calc(dopt,rho) computes
16 %     spectral components of albedo and extinction based on Snow & Climate
17 %     equations given on p.56.
18 %     [Avis,Bvis,Anir,Bvis,Aswir,Bswir] = rad_calc('class',num) computes
19 %     spectral components of albedo and extinction based on Snow & Climate
20 %     table given on p.57, where num must be an integer between 1 and 6.

```

```

21 %-----
22
23 % 1 - Compute desired values, execute as order in SYNTAX/DESCRIPTION above
24 if nargin == 1 && isnumeric(varargin{1});
25     output = shortwave(varargin{1});
26 elseif nargin == 1 && ischar(varargin{1});
27     output = albedo_curve(varargin{1});
28 elseif nargin == 2 && isnumeric(varargin{1});
29     output = albedo_eqn(varargin{:});
30 elseif nargin == 2 && ischar(varargin{1});
31     output = albedo_table(varargin{2});
32 end
33
34 % 2 - Produce output
35 varargout = num2cell(output);
36
37 %-----
38 function out = albedo_table(N)
39 % ALBEDO.TABLE computes albedo and exciction base on Snow&Climate(p.57)
40
41 % Error handling
42 if N < 1 || N > 6;
43     error('Class must be an integer 1 through 6!'); out = NaN; return;
44 end
45
46 % Build Table 2.6 from Snow & Climate (2008), p.57
47 C(:,1) = [94,94,93,93,92,91]/100;
48 C(1:6,2) = 40;
49 C(:,3) = [80,73,68,64,57,42]/100;
50 C(:,4) = [110,136,190,110,112,127];
51 C(:,5) = [59,49,42,37,30,18]/100;
52 C(1:6,6) = inf;
53
54 % Produce output
55 out = C(N,:);
56
57 %-----
58 function out = albedo_eqn(dopt,rho)
59 % ALBEDO.EQN computes albedo and exciction base on Snow&Climate(p.56)
60
61 % Convert units (dopt mm->m; rho kg/m^3->gm/cm^3)
62 dopt = dopt/1000; rho = rho/1000;
63
64 % VIS
65 out(1) = min(0.94,0.96 - 1.58*sqrt(dopt));
66 out(2) = max(0.04, 0.0192*rho/sqrt(dopt))*100;
67
68 % NIR
69 out(3) = 0.95 - 15.4 * sqrt(dopt);
70 out(4) = max(1, 0.1098*rho/sqrt(dopt))*100;
71
72 % SWIR
73 out(5) = 0.88 + 346.6*dopt - 32.31*sqrt(dopt);
74 out(6) = inf;
75
76 %-----
77 function Aout = albedo_curve(curve)
78 % ALBEDO.CURVE computes VIS,NIR,& SWIR albedos based on input curve
79
80 % 1 - Load the desired curve
81 X = load('albedo.mat');
82 A = X.(curve);
83
84 % 2 - Parse out the albedo for each wavelength group
85 L = [285,800; 800,1500; 1500,3500];
86 for i = 1:size(L,1);
87     idx(1) = find(A(:,1)>=L(i,1),1,'first');
88     idx(2) = find(A(:,1)<=L(i,2),1,'last');
89     Aout(i) = mean(A(idx(1):idx(2),2))/100;
90 end
91
92 %-----
93 function SWout = shortwave(SWall)
94 % SHORTWAVE computes spectral components of all-wave based on ASTM standard
95
96 % 1 - Load the solar spectrum desired
97 X = load('albedo.mat');
98 S = X.astm;
99
100 % 2 - Normalize solar spectrum to inputed SW data
101 I = insolation(S,[285,3500]);
102 S(:,2) = (S(:,2)/I)*SWall;
103
104 % 3 - Parse out wavelength groups
105 L = [285,800; 800,1500; 1500,3500];
106 for i = 1:size(L,1); SWout(i) = insolation(S,L(i,:)); end
107

```

```

108 %-----
109 function I = insolation(S,L)
110 % POWER computers the insolation between the a and b wavelenghts
111
112 % 1 - Locate indicies of wavelenghts
113 x = S(:,1); y = S(:,2);
114 i(1) = find(x>L(1),1,'first');
115 i(2) = find(x<L(2),1,'last');
116 idx = i(1):i(2);
117
118 % 2 - Compute the insolation
119 I = sum((y(i(1):i(2)-1)+diff(y(idx))).*diff(x(idx)));

```

### C.5.6 confint.m

```

1 function data = confint(filename,B,n)
2 % CONFINT computes the confidence intervals for temp profiles
3
4 % Read file input
5 [S,A,C,E] = xls_input(filename);
6
7 % Compute the actual temperature profile
8 [Sa,Aa] = xls_prep(S,A,C);
9 T = thermal(Sa,Aa,C);
10
11 % Compute the standard deviation values
12 s = getstd(S,E.snow,n,1); % standard deviation for snow properties
13 a = getstd(A,E.atm,n,1); % standard deviation for atmospheric terms
14 c = getstd(C,E.const,n,0); % standard deviation for constants
15
16 % Compute the Monte Carlo replicates
17 data.Tboot = zeros([size(T),B]); % Initilize storage array
18 h = waitbar(0,'Please wait...');
19 for i = 1:B;
20 r = rand(1);
21 S.b = norminv(r,S,abs(s)); % Re-sample snow
22 S.b(:,1) = S(:,1); % Snow depth does not change
23 S.b(isnan(S.b)) = S(isnan(S.b));
24 A.b = norminv(r,A,abs(a)); % Re-sample atmosphere
25 A.b(:,1) = A(:,1); % Duration does not change
26 A.b(isnan(S.b)) = A(isnan(A.b));
27 C.b = norminv(r,C,abs(c)); % Constant resampling
28 C.b(9) = C(9); % dz constant
29 C.b(10) = C(10); % dt constant
30 C.b(isnan(C.b)) = C(isnan(C.b));
31
32 [SS,AA] = xls_prep(S.b,A.b,C.b); % Build input for evaluation
33 [data.Tboot(:,:,i), data.Qboot(:,:,i)] = thermal(SS,AA,C.b);
34 data.Sboot(:,:,i) = SS;
35 data.Aboot(:,:,i) = AA;
36 data.Cboot(:,:,i) = C.b;
37 waitbar(i/B,h);
38 end
39 close(h);
40
41 %-----
42 function s = getstd(S,E,n,offset)
43 % GETSTD returns the standard deviation of the input items
44 if offset == 1;
45 s(:,1) = S(:,1);
46 for i = 2:size(S,2);
47 s(:,i) = S(:,i).*E(i-offset)/n;
48 end
49 elseif offset == 0;
50 for i = 1:size(S,2);
51 s(:,i) = S(:,i).*E(i)/n;
52 end
53 end

```

APPENDIX D

SENSITIVITY ANALYSIS SOFTWARE USER MANUAL

## D.1 Introduction

The information presented here details the usage of sensitivity analysis software developed to perform the analysis presented in Chapter 8 and 9. The software was developed in MATLAB (The Mathworks, Inc.) based on the theory presented in Chapter 6. The information presented here assumes the user is familiar with the basic operation of the MATLAB language. As detailed in Chapter 6 the SOBOL method is applicable to any function that utilizes discrete input and output. Therefore, the general application of the software is presented followed by the specific application to the thermal model used throughout this dissertation. Finally, the source code is provided. This appendix follows the notational conventions outlined in Appendix C.

The information presented here only details the computation of the sensitivity indices. However, in some respect the storage and visualization of this data is the most difficult task. A variety of visualization tools were developed that yield the various graphs and charts presented in Chapter 8 and 9. Including the instructions for usage of these tools and/or providing the source code for these files was assumed to be unnecessary. However, if this information is desired please contact the author.

## D.2 General Application

### D.2.1 Sensitivity Analysis Program

Inputs: The main function that executes the sensitivity analysis is the `sobol.m` function (Section D.5.1). This function only has a single mandatory input, `func`, which is a string or cell array such that it may be evaluated as defined in Section D.2.2. The `func` variable may also be a data structure that contains the  $\vec{a}$  output vectors (see 6.4.2, Equation (6.32)). These vectors are computed with the `sobolvec.mat`

function. Section D.2.1.2 provides additional information on the function and Section D.2.3 explains the and data structure. This feature allows the model evaluations to be separated from the computation of sensitivity indices.

An additional five optional inputs may be specified, the syntax for which may be retrieved by executing the help from the MATLAB command-line as:

---

```
>> help sobol
SOBOL performs complete SOBOL sensitivity analysis.
-----
SYNTAX:
  r = sobol(func);
  r = sobol(func, outfile);
  r = sobol(...,K);
  r = sobol(...,K,B);
  r = sobol(...,K,B,'off');
  [r, outfile] = sobol(...);
-----
```

---

A string may be specified in the variable `outfile` that contains the name of a `*.mat` file where the output structure will be saved. The `outfile` is optional in all cases and if an empty string is supplied the user will be prompted to select a file and location to store the results. For this scenario, the `outfile` is the second output from the `sobol.m` function. The default value for `outfile` is `NaN`, which does not produce any output file, only the output structure `r` is returned to the command window.

The variable `K` specifies the number of Monte Carlo simulations to perform, i.e., the size for the input sample and re-sample matrices from which the desired function evaluations will be computed (see Section 6.4.2). The default for `K` is 1,024. Similarly, `B` specifies the number of bootstrap replicates to be performed when computing the confidence level intervals (see Section 6.5). Specifying an empty numeric array skips the computation of the confidence levels. The default value for `B` is 10,000. The final optional input is a toggle that allows the user to turn 'off' the progress bar.

Program Flow: The primary sensitivity analysis function, `sobol.m`, relies on several sub functions. A flow chart demonstrating the connection between the various



functions is provided in Figure D.1. A brief description of each function follows and the complete source code is provided in Section D.5.

- `sobol.m`: The main program of the sensitivity analysis software, which handles the inputs; executes the model evaluations, sensitivity index computation, and confidence interval calculations; and outputs the data structure and output file.
- `sobolvec.m`: Performs the model evaluations according to the improved SOBOL method detailed in Section 6.4.2.
- `sobolidx.m`: Computes the total-effect as well as the first-, second-, and higher order sensitivity indices via the methodology described in Section 6.4.2.
- `sobolci2.m`: Calculates the confidence level intervals using the BCa bootstrap methods detailed in Section 6.5.
- `sobol_firstorder.m`: Implements Equation (6.38) that computes the first-order sensitivity index.
- `sobol_secondorder.m`: Implements Equation (6.39) that computes the second-order sensitivity index.
- `sobol_totaleffect.m`: Implements Equation (6.40) that computes the total-effect sensitivity index.

### D.2.2 Input Function

To perform a sensitivity analysis a function that executes the desired calculation must be written that is compatible with the SOBOL software package. This function is passed to the `sobol.m` function via the `func` variable. This function should be executable via the MATLAB command-line as either a string or cell array as:

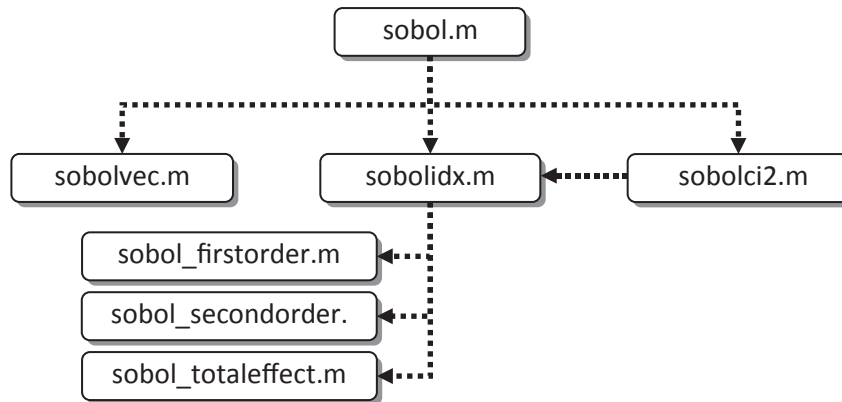


Figure D.1: Flow chart of the main sensitivity analysis function `sobol.m` and associated sub functions.

---

```

>> [Y,x] = feval(func,sk); % Evaluation if func is of class 'char'
>> [Y,x] = feval(func{:},sk); % Evaluation if func is of class 'cell'
  
```

---

The variable `sk` is defined and implemented during the execution of `func` in `sobolvec.m`. When `sk` is an empty numeric, the evaluation of `func` must return either a scalar that is equivalent to the number of input parameters ( $n$ ; Section 6.2) or a cell array of strings containing the variable names such that the `length` of this cell array is equal to the number of input parameters. In the later case, the cell array of strings is added to the output structure. The scalar or cell array should be exported via the `Y` variable.

Using the number of input parameters determined by evaluating `func` with an empty array for `sk`, in subsequent evaluations of `func` the variable `sk` is a numeric array containing the Monte Carlo samplings of the inputs parameters such that the size of `sk` is  $K \times n$  (i.e., the  $W$ ,  $W'$ ,  $N_i$ , and  $N_{-i}$  matrices defined in Section 6.4.2). However, `sobolvec.m` develops these matrices as uniformly distributed values from 0 to 1. From this data `func` should convert these values to the desired distributions (e.g., using MATLAB `norminv` function).

Figure D.2 is a simple example of an appropriate function for usage with `sobol.m`. This function evaluates the simple equation presented in Fang *et al.* (2003). The `g`-function utilized in Section 6.6 is also presented in Figure D.2 as another example of the usage of sensitivity analysis software. Notice, the `saG.m` function contains a second output not discussed in Chapter 6, but included here as an example.

```

1 function [Y,x] = saFANG(sk)
2 % saFANG is the function used by Fang et al. (2003).
3
4 if isempty(sk) Y = 5; x = []; return; end
5
6 % Input variables
7 x(:,1) = expinv(sk(:,1),0.5);
8 x(:,2) = wblinv(sk(:,2),1.5,3);
9 x(:,3) = norminv(sk(:,3),0,sqrt(0.25));
10 x(:,4) = betainv(sk(:,4),1.5,2.5);
11 x(:,5) = gaminv(sk(:,5),3.5,0.5);
12
13 % Analyze function
14 Y(:,1) = sum(x,2);

```

Figure D.2: MATLAB code for `saFANG.m` function.

```

1 function [y,a] = saG(sk)
2 % saG executes the g-function from Chapter 6
3
4 % Return the number variables or continue operation
5 if isempty(sk); y = 6; a = []; return;end
6
7 % Perform the calculations
8 a = [0,0.5,3,9,99,99];
9 g = zeros(size(sk));
10 for i = 1:size(sk,2);
11     g(:,i) = (abs(4*sk(:,i) - 2) + a(i))/(1 + a(i));
12 end
13
14 % Export the desired output(s)
15 y(:,1) = prod(g,2);
16 y(:,2) = sum(g,2);

```

Figure D.3: MATLAB code for `saG.m` function.

When evaluated with the numeric arrays for `sk`, `func` should also provide two outputs: `Y` and `x`. The `Y` variable should be a  $K \times m$  array of the function output, which are the  $\vec{a}$  output vectors used by `sobolidx.m` (see Equation (6.32)). The `x`

variable is a  $K \times n$  numeric array (i.e., the  $W$ ,  $W'$ ,  $N_i$ , and  $N_{-i}$  matrices defined in Section 6.4.2). The following section summarizes the storage of this data in the output data structure.

### D.2.3 Output Structure

The output data structure is composed of the all sensitivity analysis results for a single execution of a function via `sobol.m`, this function contains  $n$  inputs factors,  $m$  outputs factors, and is composed of  $K$  Monte Carlo replicates (see Chapter 6). The following MATLAB code is an example of a data structure produced by `sobol.m` for the `saG.m` function shown in Figure D.3, where  $n = 6$ ,  $m = 2$ , and  $K = 500$ .

---

```
>> r = sobol('saG',1000,500)
r =
    a_0: [1000x2 double]
    a_K: [1000x2 double]
    a_i: [1000x6x2 double]
    a_ni: [1000x6x2 double]
    S: [6x6x2 double]
    ST: [6x2 double]
    STci1: [6x2 double]
    STci2: [6x2 double]
    Sci1: [6x6x2 double]
    Sci2: [6x6x2 double]
    Sbias: [6x6x2 double]
    STbias: [6x2 double]
    bootstrap: 500
```

---

The first four entries contain the  $\vec{a}$  output vectors defined in Equation (6.32) on page 150. The `r.S` and `r.ST` contain the sensitivity indices for each input. The structure components that included a “ci” are the confidence level intervals, where the “1” is the lower or 5% confidence intervals and the “2” is the upper or 95% interval. For example, `r.Sci1` includes the 5% confidence level for `r.S`. The `r.Sbias` and `r.STbias` are the bootstrap computed bias estimates (see Section 6.5), thus the bias adjusted sensitivity indices are computed by `r.S + r.Sbias` and `r.ST + r.STbias`. Finally, `r.bootstrap` contains the number of bootstrap replicates performed.

### D.3 Thermal Model Application

This section briefly details the execution of sensitivity analysis software with the thermal model presented in Chapter 5. The information presented only details a single execution of the thermal model sensitivity analysis, which can be computationally expensive. As such, additional tools to automate the sensitivity analysis were developed. However, these programs are excluded from this discussion. If such an application is desired please contact the author.

The main function is `saMODEL2.m`, which calls a sub-function, `saMODEL2_output.m`. Thus, for implementing with `sobol.m`, the `func` input, in its simplest form is defined

as: `func = 'saMODEL2'`. In addition to the information presented in this section, help regarding the usage of `saMODEL2.m` may be obtained via the MATLAB command-line by typing `help saMODEL2.m`. A portion of this help is displayed in Figure D.4, which displays the various syntax options for `saMODEL2.m`. It is possible to execute the function without any inputs, which uses the default values for the optional inputs as shall be detailed next. For the `saMODEL2.m` function to operate correctly, the thermal model software presented in Appendix C must be in a separate directory on the same level as the directory containing the `saMODEL2.m` functions; the directory containing the thermal model must be named "ThermalModel\_v5".

```

1 function [Y,x,user , varargout] = saMODEL2(varargin)
2 % SAMODEL2 performs analysis for SOBOL and FAST sensitiivty analysis
3 % -----
4 % SYNTAX:
5 %   [Y,x] = saMODEL2(sk)
6 %   [Y,x] = saMODEL2(input , sk)
7 %   [Y,x] = saMODEL2(input , 'PropertyName' , PropertyValue , ... , sk)
8 %   [Y,x,user] = saMODEL2(...)
9 %   L = saMODEL2(... , []) , where sk = []

```

Figure D.4: Syntax for implementation of `saMODEL2.m`.

### D.3.1 Input Files

The first optional input of `saMODEL2.m` (Figure D.4) is the `input` variable, which is the name of a `*.mat` file containing a data structure of the various model inputs. The file must be defined as a complete path or the path must be added to MATLAB via the `addpath` function. The default file is `control2.mat`. A complete example of the required elements of this structure are provided in help of `saMODEL2.m`. The code in Figure D.5 is one portion of the complete file that is presented here to illustrate the usage of these input files.

The input structure is composed of four sub structures: `snow`, `atm`, `constant`, and `dirt`. Within these structures a list of variables is defined, as shown in Figure

```

1 >> w = load('control2.mat')
2 w =
3     snow: [1x1 struct]
4     atm: [1x1 struct]
5     constant: [1x1 struct]
6     dirt: [1x1 struct]
7
8 >> w.snow
9 ans =
10     depth: 50
11     density: {'unif' [50] [500]}
12     conductivity: {'unif' [0.01] [0.7]}
13     specific: {'unif' [1795] [2115]}
14     snowtemp: {'unif' [-40] [0]}
15     kappa: {'unif' [40] [200]}
16     kappaNIR: 0

```

Figure D.5: MATLAB code demonstrating the definition of the input `*.mat` files for the `saMODEL2.m` function.

D.5. Each variable is either a scalar or cell array. Scalar values are evaluated as constants and not considered for the sensitivity analysis. The cell arrays items determine the variables to consider for the sensitivity analysis, which include the name of the statistical distribution to be executed using MATLAB's available inverse distributions functions, e.g., `unifinv` and `norminv`. The “inv” portion of the function should not be included.

After the distribution is defined the distribution parameters are defined, in the case of `unifinv` this is simply the upper and lower limits. If the function is a normal distribution the inputs should be the mean and standard deviation, see `help norminv`. It is also possible to add two additional inputs that limit the distribution to these values. For example, `w.snow.density = {'norm', 150, 50, 50, 300}` would sample from a normal distribution with a mean of 150 and standard deviation of 50, but the resulting sample would be limited to values between 50 and 300. Each of the inputs in the data structure correspond—including the required units—with the inputs defined in Appendix C, which details the usage of the thermal model itself.

For the data presented in Chapters 8 and 9, six input files were used that were defined based on the distributions presented in Table 7.3.

The input labels may also be defined in a separate file: `label.lbl`. This file has the same exact structure as shown in Figure D.5, but contains strings that provide the name of the variable as shown in the following code.

---

```
>> L = load('label.lbl','-mat')
L =
    snow: [1x1 struct]
    atm: [1x1 struct]
    constant: [1x1 struct]
    dirt: [1x1 struct]
    profile: [1x1 struct]

>> L.snow
ans =
    depth: 'Snow depth, $z$ [$cm$]'
    density: 'Snow density, $\rho$ [$kg/m^3$]'
    conductivity: 'Thermal conductivity, $k$ [$W/(mK)$]'
    specific: 'Specific heat, $C_p$ [$kJ/(kgK)$]'
    snowtemp: 'Initial snow temp, $T_s^{\text{int}}$ [$^{\circ}\text{C}$]'
    kappa: 'Extinction coefficient, $\kappa$ [$m^{-1}$]'
    kappaNIR: 'NIR extinction coefficient, $\kappa^{\text{NIR}}$ [$m^{-1}$]'
```

---

These labels are used when producing the various graphs and plots. When executing `saMODEL2.m`, the function `sobolvec.m` includes two additional outputs—`legend` and `input`—in the output data structure defined in Section D.2.3. These additional outputs contain a cell array of legend entries gathered from the `label.lbl` file and the input structure used for the analysis, respectively.

### D.3.2 Evaluation Options

The `saMODEL2.m` is configurable such that the thermal model may be explored beyond what is presented in Chapters 8 and 9. The options must be entered in pairs, as shown in the following example execution:

---

```
>> L = saMODEL2('control2.mat','prog','on','dirt','on',[]);
>> sk = rand(100,length(L));
>> [Y,x] = saMODEL2('control2.mat','prog','on','type','TG','subtype','mean',sk);
```

---

The following list details the various options—including the default values—available in `saMODEL2.m`. The help for the function (i.e., `>> help saMODEL2.m`) also includes a brief description of these options.



- **‘type’**: Specifies the type of output to use for the sensitivity analysis, the available types include the snow temperature (**‘T’**), temperature gradient (**‘TG’**; default), the snow temperature at the “knee” location (**‘Tknee’**, see Section 9.2), “knee” temperature gradient (**‘KTG’**), the “knee” depth (**‘Kdepth’**), the “knee” duration (**‘Kduration’**), and mass-flux at the snow surface (**‘MF’**).
- **‘subtype’**: Specifies the calculation to perform on the output type, options include the mean, minimum, and maximum of the data (**‘mean’** (default), **‘min’**, and **‘max’**, respectively) in addition to the time at which the minimum and maximum occur (**‘min\_time’** and **‘max\_time’**, respectively). Also, the output type may be summed (**‘total’**) or the output may be provided as a function of time using **‘all’**.
- **‘depth’**: Defines the depth (in cm) at which the temperatures or temperature gradients are considered when **‘T’** or **‘TG’** are specified. The default is 5 cm and this property is input as a numeric scalar.
- **‘inc’**: defines the storage increment, in minutes, when the **‘all’** subtype is specified. The default is 20 minutes and this property is input as a numeric scalar.
- **‘day’**: A toggle that may be either **‘on’** (default) or **‘off’** that when set to on modifies the short-wave to act as sine wave, with the mean of the sine-wave to be equal to the inputed value.
- **‘dirt’**: A toggle that may be either **‘on’** or **‘off’** (default) that adds a layer of dirt to the snowpack using the settings specified in the **dirt** structure of the input file (see Figure D.5).

- ‘profile’: Allows the user to turn on a snow profile feature by specifying either ‘on’ or ‘off’ (default). Referring to Figure D.5, the top is assigned temperature given by `w.snow.snowtemp` and the bottom by `w.atm.bottom`. A linear profile between the top and bottom is constructed based on a temperature within the snowpack defined by `w.profile.temp` at a depth of `w.profile.depth`.
- ‘prog’: A toggle that is either ‘on’ or ‘off’ (default) that controls the presence of a progress message.

#### D.4 Closing Remarks

The information presented in this appendix presents information for individuals interested in implementing the SOBOL method of sensitivity analysis. The software written to perform the work presented throughout this dissertation was designed to be flexible, as it is the desire of the author that others would perform further analysis on other functions as well as the thermal model presented in Chapter 5 and Appendix C. The sensitivity analysis software is capable of evaluating any function with discrete input and output, as explained in Section D.2. Additionally, a powerful function was developed for exploration of the aforementioned thermal model, as detailed in Section D.3. However, as mentioned, performing the analysis is only the first step, management and visualization of the data is also required. Additional MATLAB functions were develop for this purpose, but for reasons of brevity excluded, please contact the author for further information.

## D.5 Source Code

D.5.1 `sobol.m`

```

1 function varargout = sobol(func,varargin)
2 % SOBOL performs complete SOBOL sensitivity analysis.
3 %-----
4 % SYNTAX:
5 %   r = sobol(func);
6 %   r = sobol(func,outfile);
7 %   r = sobol(...,K);
8 %   r = sobol(...,K,B);
9 %   r = sobol(...,K,B,'off');
10 %   [r,outfile] = sobol(...);
11 %
12 % DESCRIPTION:
13 %   r = sobol(func) executes the function defined in the string func
14 %   r = sobol(func,outfile) executes the function and saves the results in
15 %   the *.mat file specified in outfile, an empty string will prompt
16 %   the user for a file and NaN (default) will not produce an output
17 %   file
18 %   r = sobol(...,K) allows the user to specify the number of Monte Carlo
19 %   replicates to utilized, the default is 1,024
20 %   r = sobol(...,K,B) allows the user to also specify the number of
21 %   bootstrap samples to use when computing the confidence levels, the
22 %   default is 10,000
23 %   r = sobol(...,K,B,'off') toggles off the progress bar
24 %   [r,outfile] = sobol(...) outputs the outfile name to the command window
25 %-----
26
27 % 1 - GATHER INPUT
28 % 1.1 - Determine m-file/mat-file source
29 spec = {'*.mat','MAT-file\*.mat'}; % Also used in Sec. 3.2
30 if isempty(func);
31     loc = [cd,filesep,'vec'];
32     [fname,pth] = uigetfile(spec,'Select\MAT-file...',loc);
33     if isnumeric(fname); varargout{1} = []; return; end
34     func = [pth,fname];
35 end
36
37 % 1.2 - Gather additional input
38 [K,B,wtbar,outfile] = inputoptions(varargin{:});
39
40 % 2 - PERFORM SOBOL CALCULATIONS
41 % 2.1 - Account for direct structure input
42 if isstruct(func);
43     r = func;
44 elseif ischar(func) || ~iscell(func);
45     [p,f,e] = fileparts(func);
46     if strcmpi(e,'.m'); r = load(func); end
47 end
48 if ~exist('r','var'); r = sobolvec(func,K,wtbar); end
49
50 % 2.2 - Compute SOBOL indices
51 r = sobolidx(r);
52
53 % 2.3 - Compute confidence bounds
54 if ~isempty(B); r = sobolci2(r,B,wtbar); end
55
56 % 3 - OUTPUT DATA
57 % 3.1 - Output data structure
58 r.bootstrap = B;
59 varargout{1} = r;
60
61 % 3.2 - Output to file, if desired
62 if isempty(outfile);
63     [fname,pth] = uiputfile(spec,'Save\as...',...
64         [cd,filesep,'results',filesep]);
65     if isnumeric(fname); return; end
66     outfile = [pth,fname];
67 else
68     if isnan(outfile); varargout{2} = ''; return; end
69 end
70
71 pth = fileparts(outfile);
72 if ~exist(pth,'dir'); mkdir(pth); end
73 save(outfile,'-mat','-struct','r');
74 varargout{2} = outfile;
75
76 %-----
77 function [K,B,wtbar,outfile] = inputoptions(varargin)
78 % INPUTOPTIONS gathers user input from command-line
79

```

```

80 % 1 - SET THE DEFAULT VALUES, RETURN IF NO OPTIONS SPECIFIED
81 outfile = NaN; K = 1024; B = 10000; wtbar = 'on';
82 if nargin == 0; return; end
83
84 % 2 - GATHER USER SUPPLIED OPTIONS
85 % 2.1 - Output filename
86 if ischar(varargin{1});
87     outfile = varargin{1}; N = 1;
88 else N = 0;
89 end
90
91 % 2.2 - Additional input options
92 if nargin >= N+1; K = varargin{N+1}; end
93 if nargin >= N+2; B = varargin{N+2}; end
94 if nargin == N+3; wtbar = varargin{N+3}; end

```

## D.5.2 sobolvec.m

```

1 function output = sobolvec(func,varargin)
2 %SOBOLVEC creates the vectors needed for computing SOBOL indices
3 %-----
4 % SYNTAX:
5 %   output = sobolvec(func);
6 %   output = sobolvec(func,K);
7 %   output = sobolvec(func,K,'off');
8 %-----
9
10 % 1 - ASSIGN DEFAULTS AND/OR USER DEFINED OPTIONS
11 K = 1000; wtbar = 'on';
12 N = length(varargin);
13 if N >= 1 && isnumeric(varargin{1}); K = varargin{1}; end
14 if N == 2 && ischar(varargin{2}); wtbar = varargin{2}; end
15
16 % 2 - BUILD/READ THE SOBOL VECTORS
17 % 2.1 - Case when "func" is a file containing the vectors
18 if ischar(func) && exist(func,'file');
19     [pth,name,ext] = fileparts(func);
20     if strcmpi(ext,'.mat'); output = load(func); return; end
21 end
22
23 % 2.2 - Case when "func" must be evaluated
24 output = analyze_func(func,K,wtbar);
25
26 %-----
27 function r = analyze_func(func,K,wtbar)
28 % ANALYZE_FUNC performs the function evaluations
29
30 % 1 - DETERMINE NUMBER OF VARIABLES
31 addpath([cd,filesep,'func']);
32 addpath([cd,filesep,'input']);
33 if ischar(func); func = {func}; end
34 n_func = nargin(func{1});
35 if n_func == -1 || n_func == 3;
36     [n,x,input] = feval(func{:},[]); r.input = input;
37 else
38     n = feval(func{:},[]);
39 end
40 if iscell(n); r.legend = n; n = length(n); end
41
42 % 2 - INITIALIZE WAITBAR FOR FUNCTION EVALUATIONS
43 C = (n*2 + 2); c = 1;
44 hbar = updatebar(wtbar,0,'Performing function evaluations...');
45
46 % 3 - PERFORM MONTE CARLO SAMPLING AND RE-SAMPLING
47 M1 = rand(K,n); M2 = rand(K,n);
48
49 % 4 - NON-SUBSTITUTED FUNCTION EVALUATIONS
50 r.a_0 = feval(func{:},M2);
51 updatebar(wtbar,c/C,hbar); c = c + 1;
52 r.a_K = feval(func{:},M1);
53 updatebar(wtbar,c/C,hbar); c = c + 1;
54
55 % 5 - PERFORM SOBOL FOR EACH i-th INPUT PARAMETER
56 r.a_i = zeros(K,n,size(r.a_0,2)); r.a_ni = r.a_i;
57
58 for i = 1:n
59     % 5.1 - Solve for M1-matrix, i-th solutions
60     Ni = M2; Ni(:,i) = M1(:,i);
61     r.a_i(:,i,:) = feval(func{:},Ni);

```

```

62     updatebar(wtbar,c/C,hbar); c = c + 1;
63
64     % 5.2 - Solve for M2-matrix, -i-th solutions (only in 'improved')
65     Nni = M1; Nni(:,i) = M2(:,i);
66     r.a_ni(:,i,:) = feval(func{:},Nni);
67     updatebar(wtbar,c/C,hbar); c = c + 1;
68 end
69
70 close(hbar); drawnow; % Closes waitbar
71
72 %-----
73 function varargout = updatebar(trig,progress,varargin)
74 % UPDATEBAR operates the waitbar allowing the user to turn if off
75 varargout{1} = [];
76 if strcmpi(trig,'off'); return; end;
77
78 if ~isunix && ~strcmpi(trig,'screen') % Windows systems, show a graphical waitbar
79 if progress == 0;
80     varargout{1} = waitbar(0,varargin{1});
81 else
82     waitbar(progress,varargin{1});
83 end
84
85 elseif isunix || strcmpi(trig,'screen') % Linux, print progress to the screen
86 if progress == 0;
87     tic;
88     disp('Performing model evaluations, please wait...');
89 else
90     elp = toc;
91     disp(['\n',num2str(progress*100),'% complete;\n',...
92         num2str(elp/3600),'hours elapsed.']);
93 end
94 end

```

### D.5.3 sobolidx.m

```

1 function r = sobolidx(r)
2 % SOBOLIDX computes the sobol indices for the input vectors.
3 %-----
4 % SYNTAX: r = sobolidx(r);
5 %-----
6
7 % 1 - DEFINE THE VECTORS SIZES
8 [K,n,m] = size(r.a_i); % m = number of inputs; n = number of indices
9
10 % 2 - COMPUTE INDICES FOR EACH INPUT (m)
11 for j = 1:m; % loop number of inputs
12     S = zeros(n,n); ST = zeros(n,1); % clear variables from pervious loop
13
14     % 2.1 - Seperate current vectors
15     a_0 = r.a_0(:,j); a_K = r.a_K(:,j);
16     a_i = r.a_i(:,j); a_ni = r.a_ni(:,j);
17
18     % 2.2 - Compute first and total-effect indices
19     for i = 1:n;
20         S(i,i) = sobol_firstorder(a_0,a_K,a_i(:,i),a_ni(:,i));
21         ST(i) = sobol_totaleffect(a_0,a_K,a_i(:,i),a_ni(:,i));
22     end
23
24     % 2.3 - Compute the second-order indices
25     for i = 1:n;
26         for l = i+1:n
27             S(i,l) = sobol_secondorder(a_i(:,i),a_ni(:,i),a_i(:,l)...
28                 ,a_ni(:,l),S(i,i),S(l,l));
29             S(l,i) = S(i,l);
30         end
31     end
32
33     % 2.4 - Store data from current loop for output
34     r.S(:,j) = S;
35     r.ST(:,j) = ST;
36 end

```

## D.5.4 sobolci2.m

```

1 function r = sobolci2(r,varargin)
2 % SOBOLCI2 computes the bootstrap confidence level intervals.
3 %-----
4 % SYNTAX:
5 %   r = sobolci2(r);
6 %   r = sobolci2(r,B);
7 %   r = sobolci2(r,B,'off');
8 %-----
9
10 % 1 - PREPARE FOR ANALYSIS
11 % 1.1 - Gather the user input
12     B = 10000; wtbar = 'on';
13     N = length(varargin);
14     if N >= 1 && isnumeric(varargin{1}); B = varargin{1}; end
15     if N == 2 && ischar(varargin{2}); wtbar = varargin{2}; end
16
17 % 1.2 - Determine size of input arrays
18     [K,n,m] = size(r.a-i);
19
20 % 2 - COMPUTE BOOTSTRAP REPLICATES
21 % 2.1 - Initialize resample storage arrays and rename original values
22     S = zeros(n,n,m,B); ST = zeros(n,m,B);
23     zS = S; zST = ST;
24     s = r.S; st = r.ST; % original values
25
26 % 2.2 - Loop through number of desired resamplings
27     hbar = updatebar(wtbar,0,'Computing bootstrap SOBOL indices...');
28     for i = 1:B;
29         idx = randsample(K,K,true);
30         [S(:,:,:,i),ST(:,:,:,i)] = sobolrep(r,idx);
31         zST(:,:,:,i) = ST(:,:,:,i) < st;
32         zS(:,:,:,i) = S(:,:,:,i) < s;
33         %updatebar(wtbar,i/B,hbar);
34     end
35     %close(hbar);
36
37 % 3 - COMPUTE BOOTSTRAP CONFIDENCE LEVEL INTERVALS
38     hbar = updatebar(wtbar,0,'Computing confidence level intervals...');
39     for j = 1:m % Loop through each output variable
40
41         % 3.1 - Initialize the variables in use
42         Sj = sort(squeeze(S(:,:,:,j)),3); % bootstrap replicates of S
43         STj = sort(squeeze(ST(:,:,:,j)),2); % bootstrap replicates of St
44         zSj = squeeze(zS(:,:,:,j)); % count of values less than original S
45         zSTj = squeeze(zST(:,:,:,j)); % count of values less than original ST
46
47         % 3.2 - Compute the bias adjustment
48         S_z0 = norminv(sum(zSj,3)/B,0,1);
49         ST_z0 = norminv(sum(zSTj,2)/B,0,1);
50
51         % 3.3 - Compute the acceleration (see Efron et al.)
52         % 3.3.1 - Compute jackknife statistics
53         [S_jk,ST_jk] = jackcalc(r,j);
54
55         % 3.3.2 - Compute the inner portion acceleration equation
56         for k = 1:K
57             scr_S(:,:,:,k) = (mean(S_jk,3) - S_jk(:,:,:,k));
58             scr_ST(:,:,:,k) = (mean(ST_jk,2) - ST_jk(:,:,:,k));
59         end
60
61         % 3.3.3 - Compute acceleration
62         aS = 1/6*sum(scr_S.^3,3)/(sum(scr_S.^2,3).^1.5);
63         aST = 1/6*sum(scr_ST.^3,2)/(sum(scr_ST.^2,2).^1.5);
64
65         % 3.4 - Compute the 95% upper and lower percentiles
66         alpha1 = norminv(0.05); alpha2 = -alpha1;
67         fcn_pct = @(z0,alpha,acc)...
68             100*normcdf(z0+(z0+alpha)./(1-acc.*(z0+alpha)));
69         S_pct1 = fcn_pct(S_z0,alpha1,aS);
70         S_pct2 = fcn_pct(S_z0,alpha2,aS);
71         ST_pct1 = fcn_pct(ST_z0,alpha1,aST);
72         ST_pct2 = fcn_pct(ST_z0,alpha2,aST);
73
74         % 3.5 - Gather the correct value for the calculated percentiles
75         for i = 1:n;
76             r.STci1(i,j) = prctile(STj(i,:),ST_pct1(i));
77             r.STci2(i,j) = prctile(STj(i,:),ST_pct2(i));
78             for ii = 1:n;
79                 r.Sci1(i,ii,j) = prctile(Sj(i,ii,:),S_pct1(i,ii));
80                 r.Sci2(i,ii,j) = prctile(Sj(i,ii,:),S_pct2(i,ii));
81             end
82         end
83
84         % 3.6 - Compute bias from original values

```

```

85         r.Sbias(:,:,j) = (r.Sci1(:,:,j) + r.Sci2(:,:,j))/2 - s(:,:,j);
86         r.STbias(:,j) = (r.STci1(:,j) + r.STci2(:,j))/2 - st(:,j);
87
88     updatebar(wtbar, j/m, hbar);
89 end
90 close(hbar);
91
92 %-----
93 function [S_jk,ST_jk] = jackcalc(r,j)
94 % JACKCALC computes the jackknife statistic
95
96 % 1 - Initialize
97 [K,n,m] = size(r.a_i);
98 S_jk = zeros(n,n,K); ST_jk = zeros(n,K);
99
100 % 2 - Loop through each parameter and recalculate SOBOL indices
101 for k = 1:length(K);
102     idx = true(K,1); idx(k) = false;
103     rr.a_0 = r.a_0(idx,j); rr.a_K = r.a_K(idx,j);
104     rr.a_i = r.a_i(idx,:,j); rr.a_ni = r.a_ni(idx,:,j);
105     rr = sobolidx(rr);
106     S_jk(:,:,k) = rr.S;
107     ST_jk(:,k) = rr.ST;
108 end
109
110 %-----
111 function [S,ST] = sobolrep(r,idx)
112 % SOBOLREP executes sobolidx function
113 rr.a_0 = r.a_0(idx,:); rr.a_K = r.a_K(idx,:);
114 rr.a_i = r.a_i(idx,:,:); rr.a_ni = r.a_ni(idx,:,:);
115 rr = sobolidx(rr);
116 S = rr.S;
117 ST = rr.ST;
118
119 %-----
120 function varargout = updatebar(trig,progress,varargin)
121 % UPDATEBAR operates the waitbar allowing the user to turn if off
122 varargout{1} = [];
123 if strcmpi(trig,'off'); return; end;
124
125 if ~isunix && ~strcmpi(trig,'screen') % Windows systems, show a graphical waitbar
126     if progress == 0;
127         varargout{1} = waitbar(0,varargin{1});
128     else
129         waitbar(progress,varargin{1});
130     end
131
132 elseif isunix || strcmpi(trig,'screen') % Linux, print progress to the screen
133     if progress == 0;
134         tic;
135         disp(varargin{1});
136     else
137         elp = toc;
138         disp(['\u25b6',num2str(progress*100),'%\u25b6complete;\u25c4',...
139             num2str(elp/3600),' \u25b6hours\u25c4elapsed.']);
140     end
141 end

```

### D.5.5 sobol\_firstorder.m

```

1 function S = sobol_firstorder(a0,aK,ai,ani)
2 % SOBOL_FIRSTORDER computes the first order SOBOL sensitivity index.
3     K = length(a0); % Number of replicates
4     E2 = 1/K * dot(a0,aK); % Square of expected
5     V = 1/K * dot(aK,aK) - E2; % Total variance
6     U(1) = 1/K * dot(aK,ai); % First estimate of U
7     U(2) = 1/K * dot(a0,ani); % Second estimate of U
8     S = (mean(U) - E2)/V; % First-order index

```

### D.5.6 `sobol_secondorder.m`

```

1 function S2 = sobol_secondorder(ai, ani, aiL, aniL, Si, S1)
2 % SOBOLSECONDORDER computes the second-order SOBOL index.
3   K = length(ai);           % Number of replicates
4   E2 = 1/K * dot(ai, ani);  % Square of expected value
5   V = 1/K * dot(aniL, aniL) - E2; % Total variance
6   U1 = 1/K * dot(ai, aniL); % First estimate of Vi1
7   U2 = 1/K * dot(aiL, ani); % Second estimate of Vi1
8   Sc = (mean([U1, U2]) - E2)/V; % Closed second-order index
9   S2 = Sc - Si - S1;        % Second-order index

```

### D.5.7 `sobol_totaleffect.m`

```

1 function ST = sobol_totaleffect(a0, aK, ai, ani)
2 % SOBOLTOTALEFFECT computes the SOBOL total effect index.
3   K = length(a0);           % Number of replicates
4   E2 = 1/K * dot(a0, aK);   % Square of expected
5   V = 1/K * dot(a0, a0) - E2; % Total variance
6   U(1) = 1/K * dot(a0, ai); % First estimate of U
7   U(2) = 1/K * dot(aK, ani); % Second estimate of U
8   ST = 1 - (mean(U) - E2)/V; % Total-effect index

```

### D.5.8 `saMODEL2.m`

```

1 function [Y,x,user,varargout] = saMODEL2(varargin)
2 % SAMODEL2 performs analysis for SOBOL and FAST sensitivity analysis
3 %-----
4 % SYNTAX:
5 %   [Y,x] = saMODEL2(sk)
6 %   [Y,x] = saMODEL2(input,sk)
7 %   [Y,x] = saMODEL2(input, 'PropertyName', PropertyValue, ..., sk)
8 %   [Y,x,user] = saMODEL2(...)
9 %   L = saMODEL2(...,[]), where sk = []
10 %
11 % DESCRIPTION:
12 %   [Y,x] = saMODEL2(sk) runs thermal model using the 'default.mat' input
13 %   file; all input files should be located in \input directory.
14 %   [Y,x] = saMODEL2(input,sk) allows user to specify an input file or
15 %   structure, using input = '' will prompt for a file.
16 %   [Y,x] = saMODEL2(input, 'PropertyName', PropertyValue, ..., sk) allows user
17 %   to adjust the settings of the model run, the available properties
18 %   are listed below.
19 %   [Y,x,user] = saMODEL2(...) provides an additional output that is a data
20 %   structure that includes the program options structure and the input
21 %   data structure.
22 %   L = saMODEL(...,sk), where sk = [] returns the variables labels
23 %   being explored given the desired input and settings. This value
24 %   should be used to create sk, n = length(L).
25 %
26 % FIXED INPUTS:
27 %   sk = a numeric array containing rand numbers from 0 to 1 that is
28 %   [K x n] in size, where K is the number of model evaluations and n
29 %   is the number of variables being explored. n is given by evaluating
30 %   this function as shown above.
31 %   input = a *.mat file containing an input structure or the structure
32 %   variable itself, the structure must include all snow, atm, and
33 %   constant values shown below, the dirt is only need if the 'dirt'
34 %   property is 'on'.
35 %
36 %   X must be one of two things. If it is a scalar value this variable
37 %   is held constant at the specified. Otherwise, X may be a cell
38 %   array structure as X = {'FuncName', Input1, Input2, ..., Min, Max}.
39 %   'FuncName' should be a string defining the distribution function to
40 %   analyze that matches an available MATLAB inverse function. For
41 %   example, supply 'norm' would invoke the function 'norminv'. The
42 %   inputs: Input1, etc. should be the exact number of inputs required
43 %   by the inverse function, i.e. the distribution parameters. The
44 %   Min and Max values are optional, if the are included the data is

```



```

45 |% restricted to values between these two values.
46 |%
47 |% The following is an example input file , the units of each variable
48 |% are consistent with the thermal model input.
49 |%
50 |% >> input.snow
51 |% ans =
52 |%     depth: 50
53 |%     density: {'unif' [50] [500]}
54 |%     conductivity: {'unif' [0.01] [0.7]}
55 |%     specific: 2030
56 |%     snowtemp: {'gev' [-0.39219] [5.7951] [-16.339] [-20] [-5]}
57 |%     kappa: {'unif' [40] [200]}
58 |%     kappaNIR: 0
59 |%
60 |% >> input.atm
61 |% ans =
62 |%     time: 10
63 |%     longwave: {'gev' [-0.09476] [63.62] [287.97]}
64 |%     shortwave: {'gp' [-0.88865] [575.79] [39.094]}
65 |%     alpha: {'unif' [0.4] [0.95]}
66 |%     wind: {'logn' [0.52448] [0.33004]}
67 |%     airtemp: {'gev' [-0.24391] [4.4744] [-8.1885]}
68 |%     humidity: {'gev' [-0.65934] [15.918] [60.433]}
69 |%     bottom: 0
70 |%     pressure: 85
71 |%     shortwaveNIR: 0
72 |%     alphaNIR: 0
73 |%
74 |% >> input.constant
75 |% ans =
76 |%     Ls: 2833
77 |%     Ke: 0.0023
78 |%     Kh: 0.0023
79 |%     MvMa: 0.622
80 |%     Rv: 0.462
81 |%     T0: -5
82 |%     e0: 0.402
83 |%     emis: 0.9875
84 |%     dz: 0.5
85 |%     dt: 60
86 |%
87 |% >> input.dirt
88 |% ans =
89 |%     depth: {'unif' [1] [5]}
90 |%     kappa: {'unif' [100] [1000]}
91 |%     kappaNIR: 0
92 |%
93 |% >> input.profile
94 |% ans =
95 |%     diurnal: {'unif' [-20] [0]}
96 |%
97 |% OUTPUTS:
98 |% Y = [K x p] vector containing desired output for each model evaluation ,
99 |% with each output occupying a row of length p, where p is the number
100 |% output per evaluation. In the case of output ('type'), for 'TG'
101 |% this p is the number of gradient values stored based on the model
102 |% run duration and the storage increment ('inc').
103 |% x = the sk input with associated variable distributions applied.
104 |% user = a data structure that includes the program options structure and
105 |% the input data structure.
106 |%
107 |% AVAILABLE PROPERTIES (Property and value pairs, see EXAMPLE for help)
108 |% 'type' specifies the type of output to use for analysis 'TG' is the
109 |% default value, the available types includ: 'T', 'TG', 'Tknee',
110 |% 'KTG', 'Kdepth', 'Kduration', 'MF'
111 |% 'subtype' specifies the calculation to perform on the desired output,
112 |% options include: 'mean', 'min', 'min-time', 'max', 'max-time',
113 |% 'total', or 'all'
114 |% 'depth' defines the depth in cm for compute gradients, this values
115 |% should be a scalar, the default is 5 cm.
116 |% 'inc' defines the storage increment for 'TG' and 'MF' options in
117 |% minutes, the value should be scalar and the default is 20 min.
118 |% 'day' modifies the short-wave (including NIR) to act as sine wave, with
119 |% the mean of the sine wave to be equal to the inputted short-wave
120 |% value(s). 'day' is an 'on'/'off' toggle, the default is 'on'.
121 |% 'dirt' is either 'on' or 'off' (default) that adds a layer of dirt
122 |% based on input.dirt settings
123 |% 'profile' allows the user to turn on a snow profile feature, which
124 |% is an 'on'/'off' toggle, the default is 'off'. The top is
125 |% assigned the value given by input.snow.snowtemp, the bottom by
126 |% input.atm.bottom, and at a depth of input.profile.depth and
127 |% temperature of input.profile.temp and a linear fit in between.
128 |% 'prog' is an 'on' or 'off'(default) toggle for the progress message
129 |%
130 |% EXAMPLE:
131 |% >> L = saMODEL2('control2.mat', 'prog', 'on', 'dirt', 'on', []);

```

```

132 % >> sk = rand(100,length(L));
133 % >> [Y,x] = saMODEL2('control2.mat','prog','on','type','TG','subtype',
134 % 'mean',sk);
135 %
136 % NOTES FOR USER:
137 % (1) The \func and \func\input directories that contain this file and
138 % the input files must be added to MATLAB's path (see help addpath),
139 % this is automatically done by sobol.m.
140 % (2) This function utilized two m-files associated with version 5 of the
141 % thermal model, the path to the files thermal.m and xls_prep.m must
142 % also be added (see help addpath), the default location for these
143 % files is a directory that is parallel to the sensitivity directory
144 % which contains sobol.m named ThermalModel_v5, see Section 1.
145 % (3) If input.snow.snowtemp = NaN, the snow temperature is set to the
146 % air temperature.
147 % (4) If input.atm.bottom = NaN, the bottom boundary conditions is set to
148 % the snow temperature.
149 % (5) If input.dirt.kappaNIR = NAN, this value is set to input.dirt.kappa
150 %
151 % PROGRAM OUTLINE:
152 % 1 - ADD DEFAULT PATHS TO THE THERMAL MODEL (v5)
153 % 2 - PREPARE INPUT FROM COMMAND LINE
154 % 3 - BUILD VARIABLE LIST AND RETURN LABELS (sk = [] case)
155 % 4 - CONSTRUCT MODEL INPUT MATRICES
156 % 5 - PERFORM MODEL EVALUATIONS
157 % 6 - BUILD REMAINING OUTPUT
158 %
159 % SUBFUNCTIONS:
160 % GETUSEROPTIONS gather user input
161 % GETLABELS constructs list of variables with distributions
162 % BUILDINPUT constructs input matrices, one row per evaluation
163 % BUILDMATRIX evaluates the distribution functions for sk values
164 % GETLIMITS extracts min/max limits supplied with dist. function input
165 % SPECIALINPUT applies special conditions for input data
166 %-----
167
168 % 1 - ADD DEFAULT PATHS TO THE THERMAL MODEL (v5)
169 loc = cd('..');
170 addpath([cd, filesep, 'ThermalModel_v5']);
171 cd(loc);
172
173 % 2 - PREPARE INPUT FROM COMMAND LINE
174 [in,sk,opt] = getuseroptions(varargin{:});
175 user.input = in;
176 user.options = opt;
177
178 % 3 - OPEN DATA STRUCTURE AND RETURN LABELS
179 % 3.1 - Load distribution structures
180 addpath([cd, filesep, 'input']);
181 if ~isstruct(in) && exist(in,'file'); in = load(in); end
182
183 % 3.2 - Build labels (stop operation in sk = [] case)
184 if isempty(sk);
185 L = getlabels(in,opt);
186 Y = L; x = []; return;
187 end
188
189 % 4 - CONSTRUCT MODEL INPUT MATRICES
190 [S,A,C,D,P,x] = buildinput(in,opt,sk);
191
192 % 5 - PERFORM MODEL EVALUATIONS
193 % 5.1 - Setup loop parameters and initialize arrays
194 K = size(sk,1);
195 e = tic; k = K*0.01;
196
197 % 5.2 - Initialize arrays
198 nn = in.atm.time/(opt.inc/60) + 1;
199 mm = 10/in.constant.dz;
200 ysz = 1;
201 if strcmpi(opt.subtype,'all'); ysz = nn; end
202 Y = zeros(K,ysz);
203 Tout = zeros(K,mm,nn);
204 Qout = zeros(K,nn);
205 %Qout = zeros(K,mm,nn,5);
206
207 % 5.3 - Loop through each model evaluation
208 for i = 1:K;
209 % 5.3.1 - Build full matrices of current input parameters
210 c = C(i,:); s = S(i,:); a = A(i,:);
211 if ~isempty(P); p = P(i,:); else p = []; end
212 [s,a] = specialinput(s,a,p,opt);
213 [s,a] = xls_prep(s,a,c);
214
215 % 5.3.2 - Applies dirt-layer, if desired
216 if strcmpi(opt.dirt,'on') && ~isempty(D);
217 d = D(i,:);
218 idx = find(s(:,1)>d(1),1,'first');

```

```

219         S(idx,6) = d(2); S(idx,7) = d(3);
220     end
221
222     % 5.3.3 - Perform model calculations and build desired output
223     [T,Q] = thermal(s,a,c);
224     Qs = squeeze(Q(1,:,2)); % Qs = latent at surface
225     if nargin == 5;
226         inc = (opt.inc*60)/c(10); % Storage increment
227         idx = 1:inc:size(T,2); % Indices of storage increment
228         Tout(i, :, :) = T(1:10/c(9),idx); % Temps for montecarlo2
229         Qout(i, :) = squeeze(Qs(:,idx)); % Flux usage, only latent
230     else
231         Y(i, :) = saMODEL2_output(T,Qs,c,opt);
232     end
233
234     % 5.3.4 - Print the progress, if desired
235     if strcmpi(opt.prog,'on') && round(i/k) == i/k;
236         disp([num2str(i/K*100), '% Complete, ', ...
237             num2str(toc(e)/3600), ' hrs elapsed.']);
238     end
239 end
240
241 % 6 - BUILD REMAINING OUTPUT
242 x = single(x);
243 if nargin == 5;
244     Y = [];
245     varargout{1} = single(Tout);
246     varargout{2} = single(Qout);
247 end
248
249 %-----
250 function [in,sk,opt] = getuseroptions(varargin)
251 % GETUSEROPTIONS gather user input
252
253 % 1 - Extract mandatory "sk" input and default filename
254 n = nargin; % Number of input variables
255 sk = varargin{n};
256 in = 'control2.mat';
257 q = {};
258
259 % 2 - Gather user specified values
260 if nargin >= 2; in = varargin{1}; end
261 if nargin >= 3; q = varargin(2:nargin-1); end
262
263 % 3 - Set defaults
264 opt.type = 'TG'; opt.subtype = 'mean';
265 opt.depth = 5;
266 opt.inc = 20;
267 opt.day = 'on';
268 opt.profile = 'off';
269 opt.dirt = 'off';
270 opt.prog = 'off';
271 opt.output = '';
272
273 % 4 - apply settings
274 n = length(q); k = 1;
275 list = fieldnames(opt);
276 while k < n
277     itm = q{k}; value = q{k+1}; k = k + 2;
278     if strcmp(lower(itm),list,'exact');
279         opt.(itm) = value;
280     else
281         mes = ['The option, ',itm,', was not recognized.'];
282         disp(mes);
283     end
284 end
285
286 %-----
287 function L = getlabels(A,opt)
288 % GETLABELS constructs list of variables with distributions
289
290 % Pre-define output and load labels files
291 L = {}; LB = load('label.lbl','-mat');
292 TF(1) = ~strcmpi(opt.dirt,'on') || ~isfield(A,'dirt');
293 TF(2) = ~strcmpi(opt.profile,'on') || ~isfield(A,'profile');
294
295 % Correct fieldnames for exclusion of dirt
296 fnA = fieldnames(A);
297 if TF(1); fnA(strcmp('dirt',fnA)) = []; end
298 if TF(2); fnA(strcmp('profile',fnA)) = []; end
299
300 % Search input for cells, bulding
301 for i = 1:length(fnA);
302     fnA2 = fieldnames(A.(fnA{i}));
303     for j = 1:length(fnA2);
304         itm = A.(fnA{i}).(fnA2{j});
305         if iscell(itm); L = [L,LB.(fnA{i}).(fnA2{j])]; end

```

```

306     end
307 end
308
309 %-----
310 function [S,A,C,D,P,x] = buildinput(IN,opt,sk)
311 % BUILDINPUT constructs input matrices, one row per evaluation
312
313 % 1 - Build data structure containing vectors values for each evaluation
314 x = zeros(size(sk)); % matrix of input values
315 cnt = 1; % variable counter
316
317 [X.snow,x,cnt] = buildmatrix(IN.snow,sk,x,cnt);
318 [X.atm,x,cnt] = buildmatrix(IN.atm,sk,x,cnt);
319 [X.constant,x,cnt] = buildmatrix(IN.constant,sk,x,cnt);
320 if isfield(IN,'dirt');
321     [X.dirt,x,cnt] = buildmatrix(IN.dirt,sk,x,cnt);
322 end
323 if isfield(IN,'profile');
324     [X.profile,x] = buildmatrix(IN.profile,sk,x,cnt);
325 end
326
327 % 2 - Build matrices (actual fieldnames used to ensure proper order)
328 s = X.snow;
329 S = [s.depth,s.density,s.conductivity,s.specific,s.snowtemp,...
330     s.kappa,s.kappaNIR];
331
332 a = X.atm;
333 A = [a.time,a.longwave,a.shortwave,a.alpha,a.wind,a.airtemp,...
334     a.humidity,a.bottom,a.pressure,a.shortwaveNIR,a.alphaNIR];
335
336 c = X.constant;
337 C = [c.Ls,c.Ke,c.Kh,c.MvMa,c.Rv,c.T0,c.e0,c.emis,c.dz,c.dt];
338
339 if strcmpi(opt.dirt,'on') && isfield(X,'dirt');
340     d = X.dirt;
341     if isnan(d.kappaNIR); d.kappaNIR = d.kappa; end
342     D = [d.depth,d.kappa,d.kappaNIR];
343 else
344     D = [];
345 end
346 if strcmpi(opt.profile,'on') && isfield(X,'profile');
347     p = X.profile;
348     P = [p.temp,p.temp];
349 else
350     P = [];
351 end
352
353 %-----
354 function [IN,X,cnt] = buildmatrix(IN,sk,X,cnt)
355 % BUILDMATRIX evaluates the distribution functions for sk values
356
357 % 1 - Loop through each structure item
358 K = size(sk,1); % No. of model evaluations
359 fn = fieldnames(IN); % Fieldnames
360 for i = 1:length(fn);
361     if isnumeric(IN.(fn{i})) % Case when variable is constant
362         val = IN.(fn{i});
363         IN.(fn{i}) = zeros(K,1);
364         IN.(fn{i})(:) = val;
365
366     elseif iscell(IN.(fn{i})) % Case when variable is a distribution
367         evl = IN.(fn{i}); % Gathers distribution info
368         func = [evl{1},'inv']; % Extracts distribution function
369         input = evl(2:length(evl)); % Collects dist. function input
370         [lim,n_func] = getlimits(func,input); % Gets limits, if exist
371
372         x = feval(func,sk(:,cnt),input{1:n_func-1}); % evaluates fund
373         X(:,cnt) = x; % builds x-matrix for output
374         cnt = cnt + 1; % increments variable counter
375
376         if ~isempty(lim); % apply limits if the exist
377             x(x<lim{1}) = lim{1};
378             x(x>lim{2}) = lim{2};
379         end
380         IN.(fn{i}) = x;
381     end
382 end
383
384 %-----
385 function [lim,n_func] = getlimits(func,input)
386 % GETLIMITS extracts min/max limits supplied with dist. function input
387
388 % Accounts for inverse function with optional "pcov" and "alpha" inputs
389 switch func
390     case {'evinv','expinv','gaminv','logninv','norminv','wblinv'};
391         n_func = nargin(func) - 2;
392     otherwise

```

```

393     n_func = nargin(func);
394     end
395
396 % Extracts limits
397 n_input = length(input);
398 dn = n_input - (n_func - 1);
399 if dn == 2;
400     lim = input(n_input-1:n_input);
401 else
402     lim = [];
403 end
404
405 %-----
406 function [s,a] = specialinput(S,A,P,opt)
407 % SPECIALINPUT applies special conditions for input data
408
409 % 1 - Apply the NaN conditions for bottom temperature and snow temp.
410 if isnan(S(:,5)); S(:,5) = A(1,6); end % Tsnow = Tair
411 if isnan(A(:,8)); A(:,8) = S(:,5); end % Tbottom = Tsnow
412 s = S; a = A;
413
414 % 2 - Apply sine-wave to shortwave input(s)
415 if strcmpi(opt.day,'on');
416     dur = A(1); %Day-light duration (hr)
417     t = (0:1/60:dur)'; %1-min. intervals in hrs
418     a = zeros(length(t),length(A));
419     SW = A(3)*sin(2*pi/dur*t - pi/2) + A(3);
420     NIR = A(10)*sin(2*pi/dur*t - pi/2) + A(10);
421
422     a(:,1) = t; a(:,3) = SW; a(:,10) = NIR;
423     idx = [2,4:9,11];
424     for i = 1:length(idx); a(:,idx(i)) = A(idx(i)); end
425 end
426
427 % 3 - Insert a temperature profile
428 if strcmpi(opt.profile,'on') && ~isempty(P);
429     s = []; % remove unmodified input
430     bot = A(1,8); % Bottom temp
431     diu = P(1); % Diurnal temp
432     s(1,:) = S; s(1,1) = 0;
433     s(2,:) = S; s(2,1) = P(2); s(2,5) = diu;
434     s(3,:) = S; s(3,1) = S(1); s(3,5) = bot;
435 end

```

## D.5.9 saMODEL2\_output.m

```

1 function y = saMODEL2_output(T,Q,c,opt,varargin)
2 % SAMODEL2_OUTPUT produces the desired output
3 %-----
4 % SYNTAX:
5 % y = saMODEL2_output(T,Q,c,opt)           %saMODEL2.m
6 % y = saMODEL2_output(T,Q,c,opt,'raw')    %saMODEL2sobol.m
7 %
8 % INPUTS:
9 % T,Q,c = Outputs from thermal model evaluation
10 % opt = data structure containing options defined in saMODEL2.m
11 %-----
12
13 [nk,nz,nt] = size(T);
14 if nt > 1;
15     T = permute(T,[2,3,1]); % Re-order so that the replicates occupy the last index
16 end
17 % 1 - GATHER DATA FOR EXPORT AND STORAGE (WHEN CALLED FROM SAMODEL2)
18 % Case when using stored raw files, the data is already incremented
19 if nargin == 5 && strcmpi('raw',varargin{1});
20     idx = 1:size(T,2); % Does not increment the output
21     tstep = opt.inc*60; % Time step is equal to the increment (s)
22
23 % Case when running directly from SOBOL
24 else
25     tstep = c(10); % Time step (s)
26     inc = (opt.inc*60)/c(10); % Storage increment
27     idx = 1:inc:size(T,2); % Indices of storage increment
28 end
29
30 % 2 - DEFINE THE DEPTH INDEX AND MEASURED DEPTH FOR GRAD. CALCULATIONS
31 zi = round(opt.depth/c(9)+1); % Desired depth index
32 dz = opt.depth/100; % Depth in meters
33

```

```

34 % 3 - COMPUTE THE DESIRED DATA TYPE
35 switch lower(opt.type)
36   case 't' % snow temp.
37     y = squeeze(T(zi, :, :));
38   case 'tg' % temp. grad
39     y = squeeze((diff(T([1, zi], :, :))/dz));
40   case 'tknee' % temp. at knee
41     Tk = getknee(T); y = squeeze(Tk(2, :, :));
42   case 'ktg' % knee gradient
43     [Tk,d] = getknee(T);
44     dz = (d-1)*c(9)/100;
45     y = squeeze(diff(Tk,1,1)') ./ dz;
46     %y(isnan(y)) = 0;
47   case 'kdepth' % depth to knee
48     [Tk,d] = getknee(T);
49     y = (d-1)*c(9);
50   case 'kduration';
51     [Tk,d] = getknee(T); d = d-1; d(d>0) = 1;
52     y = d*tstep/3600;
53   case 'mf' % mass flux at surface
54     y = (Q/c(1));
55 end
56
57 % 4 - CORRECT FOR NaN VALUES FROM 'KNEE' OUTPUTS
58 y(isnan(y)) = 0;
59
60 % 5 - APPLY POS/NEG
61 if iscell(opt.subtype);
62   switch lower(opt.subtype{2});
63     case 'pos'; y(y<0) = 0;
64     case 'neg'; y(y>0) = 0;
65   end
66   test = lower(opt.subtype{1});
67 else
68   test = lower(opt.subtype);
69 end
70
71 % 6 - COMPUTE THE SUBTYPE
72 % 6.1 - Re-orient single column data
73 [ry,cy] = size(y);
74 if cy == nk; y = y'; end
75
76 switch test
77   case 'mean'; y = mean(y,2);
78   case 'min'; y = min(y,[1,2]);
79   case 'min_time'; [tmp,y] = min(y,[1,2]); y = y*c(10)/3600;
80   case 'max'; y = max(y,[1,2]);
81   case 'max_time'; [tmp,y] = max(y,[1,2]); y = y*c(10)/3600;
82   case 'total'; y = sum(y,2);
83   otherwise % ALL
84     y = y(:,idx,:);
85 end
86
87 %-----
88 function [Tout,dpth_idx,dur_cnt] = getknee(T)
89 % GETKNEE computes knee difference
90
91 dT = diff(T,1,1);
92
93 % Correct for the cases when the dT < 0 for the entire snowpack
94 A = sum(dT <= 0,1) == 0;
95 B = repmat(A, size(dT,1),1);
96 C = dT <= 0 + B;
97
98 [rr,c] = find(C);
99 % [rr,c] = find(dT <= 0);
100 [c,m,n] = unique(c,'first');
101 r(1:length(m)) = rr(m);
102
103 T = T(1:end-1, :, :);
104 [n1,n2,n3] = size(T);
105
106 T2 = reshape(T,[n1,n2*n3]);
107 ind = sub2ind(size(T2),r,c');
108
109 Tout(1, :, :) = T(1, :, :);
110 Tout(2, :, :) = reshape(T2(ind),1,n2,n3);
111
112 dpth_idx = reshape(r,n2,n3)';
113 dur_cnt = squeeze(sum((diff(Tout,1,1) > 0),2));

```

APPENDIX E

SENSITIVITY ANALYSIS RESULTS FOR SURFACE HOAR

### E.1 Introduction

The tables presented in this appendix provide the complete sensitivity analysis results for Chapter 8 that explored surface hoar formation. The following tables include the first-order, second-order, higher-order, and total-effect indices. The indices are listed using the 90% confidence level intervals. The indices listed in Table 7.1 are used in the tables presented here. The higher-order indices listed were computed from the bias corrected first- and second-order and total-effect indices. The confidence levels for this parameter were not computed, but would be of similar magnitude to the confidence levels for the total-effect.

In this appendix only the night scenario results are listed, since the research focus of Chapter 9 was on surface hoar. The three input “locations” were considered: Control, North, and South. Chapter 7 includes the details on the development of the input scenarios and locations. For each location four “classes” were considered: the mass-flux, positive-only mass-flux, negative-only mass-flux, and snow temperature, all at the snow surface. Note, the snow surface temperature results were not discussed in Chapter 8, but included here since the Monte Carlo results presented in Chapter 8 utilized this parameter.

First, the sensitivity analysis was performed temporally at 20 minute intervals for each of the classes mentioned, resulting in 30 sets of indices for each class. For these temporal results, a table including only the total-effect indices as a function of time in hours and the complete sensitivity results at mid-day are reported. Next, the mean, maximum, and minimum were computed for each class. The caption for each table is organized as location/class/type.



## E.2 Mass Flux at Snow Surface

Table E.1: Control / Mass Flux with Time (Total-effect)

t \ i	1	2	3	4	5	6	7	8
0.33	15.9-21.8	-1.5-4.8	-3.9-2.5	9.7-15.8	33.3-38.3	30.3-35.5	28.8-34.3	23.5-28.9
0.67	15.5-21.4	-2.5-4.0	-3.3-3.1	9.0-15.1	35.0-40.0	31.4-36.5	29.1-34.7	23.1-28.6
1.00	15.3-21.2	-2.6-3.9	-2.9-3.5	8.5-14.7	36.3-41.2	32.0-37.1	29.5-35.1	23.1-28.5
1.33	15.3-21.2	-2.5-3.9	-2.6-3.8	8.7-14.8	37.1-42.0	32.5-37.6	29.9-35.4	23.2-28.6
1.67	15.3-21.2	-2.5-3.9	-2.2-4.2	8.8-14.9	37.5-42.4	32.9-38.0	30.0-35.5	23.2-28.6
2.00	15.2-21.1	-2.5-3.8	-2.2-4.1	8.7-14.9	37.7-42.5	33.1-38.2	30.1-35.6	23.1-28.5
2.33	15.0-20.9	-2.6-3.7	-2.2-4.1	8.6-14.8	37.7-42.6	33.2-38.3	30.2-35.6	23.0-28.4
2.67	14.8-20.7	-2.8-3.6	-2.2-4.1	8.6-14.7	37.8-42.7	33.3-38.3	30.2-35.7	23.0-28.4
3.00	14.8-20.7	-2.7-3.6	-2.1-4.2	8.7-14.9	37.9-42.8	33.4-38.5	30.3-35.8	23.0-28.4
3.33	14.8-20.6	-2.7-3.6	-2.1-4.3	8.7-14.9	38.0-42.9	33.6-38.6	30.4-35.8	23.1-28.5
3.67	14.8-20.6	-2.7-3.6	-1.9-4.4	8.8-15.0	38.1-43.0	33.7-38.7	30.5-35.9	23.1-28.5
4.00	14.7-20.6	-2.7-3.6	-1.9-4.4	8.8-15.0	38.2-43.0	33.8-38.8	30.5-36.0	23.1-28.5
4.33	14.7-20.6	-2.7-3.6	-1.9-4.4	8.8-15.0	38.3-43.1	33.9-38.9	30.6-36.0	23.2-28.6
4.67	14.7-20.6	-2.7-3.7	-1.9-4.5	8.8-15.0	38.3-43.1	34.0-39.0	30.7-36.1	23.2-28.6
5.00	14.7-20.6	-2.6-3.7	-1.8-4.5	8.9-15.1	38.4-43.2	34.1-39.1	30.8-36.2	23.2-28.6
5.33	14.7-20.6	-2.6-3.7	-1.8-4.5	8.9-15.1	38.5-43.3	34.1-39.1	30.8-36.2	23.2-28.6
5.67	14.7-20.6	-2.6-3.7	-1.7-4.5	8.9-15.1	38.5-43.3	34.2-39.2	30.8-36.2	23.2-28.6
6.00	14.6-20.6	-2.5-3.8	-1.7-4.6	8.9-15.1	38.5-43.3	34.3-39.2	30.9-36.3	23.2-28.6
6.33	14.7-20.6	-2.4-3.9	-1.6-4.7	9.0-15.1	38.6-43.4	34.4-39.4	31.0-36.4	23.3-28.7
6.67	14.7-20.6	-2.4-3.9	-1.6-4.7	9.0-15.1	38.6-43.4	34.4-39.4	31.1-36.4	23.3-28.7
7.00	14.6-20.6	-2.4-3.8	-1.6-4.6	9.0-15.1	38.6-43.4	34.4-39.4	31.1-36.4	23.3-28.7
7.33	14.6-20.5	-2.4-3.8	-1.6-4.6	9.0-15.1	38.6-43.4	34.5-39.4	31.1-36.4	23.3-28.7
7.67	14.6-20.5	-2.5-3.9	-1.6-4.6	9.0-15.1	38.6-43.4	34.5-39.5	31.1-36.5	23.3-28.7
8.00	14.6-20.6	-2.5-3.9	-1.6-4.6	9.0-15.2	38.6-43.4	34.5-39.5	31.1-36.5	23.3-28.7
8.33	14.6-20.5	-2.5-3.9	-1.6-4.6	9.0-15.2	38.6-43.4	34.5-39.5	31.1-36.5	23.3-28.7
8.67	14.6-20.5	-2.5-3.9	-1.6-4.6	9.0-15.2	38.6-43.4	34.5-39.5	31.1-36.5	23.3-28.7
9.00	14.6-20.5	-2.5-3.8	-1.6-4.6	9.0-15.2	38.6-43.4	34.5-39.5	31.1-36.5	23.3-28.7
9.33	14.6-20.5	-2.5-3.8	-1.6-4.7	9.1-15.2	38.6-43.4	34.5-39.5	31.1-36.5	23.3-28.7
9.67	14.6-20.5	-2.4-3.9	-1.6-4.7	9.1-15.2	38.6-43.4	34.5-39.5	31.2-36.6	23.3-28.7
10.00	14.6-20.5	-2.5-3.9	-1.6-4.7	9.1-15.2	38.7-43.4	34.5-39.6	31.2-36.6	23.3-28.7

Table E.2: Control / Mass Flux / Mid-day

i \ j	1	2	3	4	6	9	10	11
1	0.7-2.3	-0.7-2.1	-0.7-2.1	0.7-3.7	-1.5-2.3	0.1-3.1	-1.3-2.0	-0.6-2.5
2	-0.7-2.1	-0.0-0.2	-0.4-0.1	-0.4-0.1	-1.2-0.8	-1.2-0.1	-0.7-0.1	-0.4-0.4
3	-0.7-2.1	-0.4-0.1	-0.1-0.2	-0.4-0.3	-1.2-0.9	-1.1-0.2	-0.8-0.2	-0.5-0.4
4	0.7-3.7	-0.4-0.1	-0.4-0.3	-1.0-0.5	-1.4-2.0	-1.1-1.5	-1.1-1.9	-1.1-1.9
6	-1.5-2.3	-1.2-0.8	-1.2-0.9	-1.4-2.0	23.1-26.1	0.8-5.4	0.3-4.5	-2.0-1.9
9	0.1-3.1	-1.2-0.1	-1.1-0.2	-1.1-1.5	0.8-5.4	10.5-12.8	0.1-2.9	2.8-5.4
10	-1.3-2.0	-0.7-0.1	-0.8-0.2	-1.1-1.9	0.3-4.5	0.1-2.9	7.6-10.2	5.5-10.1
11	-0.6-2.5	-0.4-0.4	-0.5-0.4	-1.1-1.9	-2.0-1.9	2.8-5.4	5.5-10.1	9.6-11.7
Total	14.7-20.6	-2.6-3.7	-1.8-4.5	8.9-15.1	38.4-43.2	34.1-39.1	30.8-36.2	23.2-28.6
Higher	9.2	1.1	1.8	8.9	10.4	15.3	12.6	2.1

Table E.3: South / Mass Flux with Time (Total-effect)

t \ i	1	2	3	4	5	6	7	8
0.33	38.2-45.9	1.7-11.2	-3.2-6.7	32.0-41.4	41.3-48.6	32.2-40.9	17.3-26.3	4.7-13.9
0.67	40.0-47.3	-1.7-8.1	-4.2-5.9	33.4-42.9	45.1-52.4	32.8-41.5	15.7-25.0	2.8-12.4
1.00	40.1-47.3	-3.2-6.6	-4.5-5.5	33.2-42.7	47.4-54.7	32.6-41.2	15.4-24.5	2.4-11.8
1.33	39.9-47.0	-4.2-5.7	-4.8-5.2	33.2-42.6	48.8-55.9	32.4-40.9	15.0-24.2	2.2-11.6
1.67	39.9-47.1	-3.8-6.0	-3.9-5.9	33.9-43.2	49.8-56.8	32.7-41.2	15.5-24.7	2.9-12.2
2.00	39.5-46.6	-3.9-5.8	-3.6-6.2	33.8-43.1	50.5-57.5	32.6-41.1	15.4-24.5	2.9-12.1
2.33	39.3-46.4	-4.1-5.6	-3.5-6.2	33.7-43.1	50.9-57.8	32.5-40.9	15.1-24.3	2.8-12.0
2.67	39.2-46.2	-4.1-5.5	-3.5-6.2	33.6-43.0	51.2-58.1	32.4-40.7	15.1-24.2	2.8-12.0
3.00	39.1-46.0	-4.1-5.4	-3.5-6.1	33.5-42.8	51.4-58.3	32.2-40.6	15.1-24.2	2.8-11.9
3.33	39.0-45.9	-4.2-5.3	-3.5-6.1	33.3-42.6	51.7-58.5	32.1-40.5	15.2-24.3	2.9-11.9
3.67	38.9-45.8	-4.3-5.2	-3.5-6.1	33.2-42.5	51.8-58.7	32.1-40.4	15.2-24.3	2.9-11.9
4.00	38.8-45.7	-4.4-5.1	-3.4-6.1	33.2-42.4	52.0-58.8	32.0-40.3	15.2-24.2	2.8-11.8
4.33	38.6-45.5	-4.6-5.0	-3.5-6.0	32.9-42.2	52.2-59.0	31.9-40.2	15.1-24.2	2.6-11.6
4.67	38.5-45.4	-4.6-5.0	-3.4-6.1	32.8-42.1	52.4-59.2	31.9-40.2	15.1-24.2	2.6-11.6
5.00	38.4-45.3	-4.5-5.0	-3.3-6.1	32.8-42.1	52.7-59.4	31.9-40.2	15.1-24.2	2.7-11.6
5.33	38.4-45.3	-4.5-5.0	-3.2-6.2	32.8-42.0	52.8-59.6	31.9-40.2	15.1-24.2	2.7-11.7
5.67	38.3-45.2	-4.5-5.0	-3.2-6.2	32.8-42.0	53.0-59.7	31.9-40.2	15.2-24.2	2.8-11.7
6.00	38.3-45.2	-4.4-5.1	-3.0-6.3	32.8-42.0	53.1-59.8	32.1-40.3	15.2-24.2	2.9-11.8
6.33	38.2-45.1	-4.5-5.0	-3.0-6.3	32.8-41.9	53.1-59.8	32.0-40.3	15.1-24.2	2.9-11.8
6.67	38.2-45.1	-4.5-5.0	-3.0-6.4	32.7-41.9	53.1-59.8	32.0-40.2	15.2-24.2	2.9-11.8
7.00	38.2-45.1	-4.4-5.1	-2.9-6.5	32.7-41.9	53.2-59.9	32.1-40.3	15.3-24.3	3.0-11.9
7.33	38.1-45.0	-4.4-5.1	-2.9-6.5	32.7-41.9	53.3-60.0	32.1-40.3	15.3-24.3	2.9-11.9
7.67	38.1-44.9	-4.4-5.1	-2.8-6.6	32.7-41.9	53.4-60.1	32.2-40.4	15.3-24.3	3.0-11.9
8.00	38.0-44.9	-4.4-5.1	-2.8-6.6	32.7-41.9	53.5-60.1	32.2-40.4	15.3-24.3	3.0-11.9
8.33	38.0-44.8	-4.4-5.1	-2.8-6.6	32.7-41.9	53.5-60.2	32.2-40.4	15.3-24.3	3.0-11.9
8.67	38.0-44.8	-4.3-5.2	-2.7-6.6	32.7-41.8	53.6-60.3	32.2-40.4	15.3-24.3	3.1-12.0
9.00	37.9-44.8	-4.3-5.2	-2.6-6.7	32.7-41.8	53.7-60.3	32.3-40.4	15.4-24.3	3.1-12.0
9.33	37.9-44.8	-4.3-5.2	-2.6-6.7	32.6-41.7	53.7-60.4	32.3-40.4	15.3-24.2	3.1-12.0
9.67	37.8-44.7	-4.3-5.1	-2.6-6.7	32.5-41.7	53.8-60.4	32.3-40.4	15.3-24.2	3.1-12.0
10.00	37.8-44.7	-4.3-5.1	-2.6-6.7	32.5-41.7	53.8-60.4	32.2-40.3	15.2-24.1	3.1-12.0

Table E.4: South / Mass Flux / Mid-day

i \ j	1	2	3	4	6	9	10	11
1	0.4-3.6	-2.4-1.8	-2.3-1.9	4.0-9.4	-1.3-4.8	-1.0-4.5	-2.2-2.4	-2.1-2.2
2	-2.4-1.8	-0.2-0.1	-0.3-0.3	-0.3-0.4	-1.6-2.3	-0.5-0.6	-0.3-0.4	-0.3-0.4
3	-2.3-1.9	-0.3-0.3	-0.2-0.4	-0.9-0.2	-2.1-1.9	-1.1-0.3	-0.9-0.3	-0.8-0.4
4	4.0-9.4	-0.3-0.4	-0.9-0.2	-1.1-2.2	-4.7-1.9	-0.2-4.7	-2.6-2.4	-2.7-2.2
6	-1.3-4.8	-1.6-2.3	-2.1-1.9	-4.7-1.9	33.7-38.7	-2.2-5.2	-2.4-2.7	-1.7-1.8
9	-1.0-4.5	-0.5-0.6	-1.1-0.3	-0.2-4.7	-2.2-5.2	4.4-7.4	-2.3-1.6	-1.6-1.8
10	-2.2-2.4	-0.3-0.4	-0.9-0.3	-2.6-2.4	-2.4-2.7	-2.3-1.6	0.8-3.0	-1.8-1.9
11	-2.1-2.2	-0.3-0.4	-0.8-0.4	-2.7-2.2	-1.7-1.8	-1.6-1.8	-1.8-1.9	2.9-4.2
Total	38.4-45.3	-4.5-5.0	-3.3-6.1	32.8-42.1	52.7-59.4	31.9-40.2	15.1-24.2	2.7-11.6
Higher	30.0	0.1	2.9	30.0	17.5	25.2	18.1	3.7

Table E.5: North / Mass Flux with Time (Total-effect)

t \ i	1	2	3	4	5	6	7	8
0.33	16.1-23.0	1.5-8.6	-4.1-3.1	16.2-23.1	57.2-62.2	10.0-17.2	15.0-21.7	2.0-8.9
0.67	20.4-27.0	0.1-7.1	-3.6-3.6	17.2-24.2	63.6-68.4	12.5-19.6	13.5-20.2	1.9-8.7
1.00	21.6-28.1	-0.9-6.0	-3.3-3.8	17.1-24.2	66.3-70.9	13.0-20.0	13.0-19.7	1.5-8.3
1.33	21.8-28.2	-1.9-5.1	-3.3-3.8	17.1-24.2	67.8-72.4	13.1-20.2	12.6-19.1	1.1-7.9
1.67	21.7-28.0	-2.9-4.2	-3.5-3.7	17.2-24.2	68.7-73.2	12.9-20.0	11.8-18.4	0.9-7.7
2.00	21.9-28.2	-3.1-3.9	-3.5-3.6	17.3-24.2	69.4-73.8	13.0-20.0	11.5-18.1	0.8-7.5
2.33	22.1-28.3	-3.5-3.6	-3.4-3.6	17.2-24.1	70.0-74.4	13.0-20.0	11.4-18.0	0.6-7.4
2.67	22.2-28.4	-3.4-3.6	-3.2-3.9	17.3-24.2	70.6-74.9	13.2-20.1	11.3-18.0	0.7-7.5
3.00	22.1-28.3	-3.5-3.5	-3.1-3.9	17.2-24.1	71.0-75.3	13.3-20.2	11.1-17.8	0.6-7.4
3.33	22.1-28.2	-3.7-3.3	-3.1-3.9	17.3-24.2	71.3-75.6	13.4-20.2	11.0-17.7	0.5-7.3
3.67	21.9-28.1	-3.8-3.2	-3.2-3.8	17.1-24.0	71.6-75.9	13.3-20.2	10.9-17.5	0.4-7.2
4.00	21.9-28.0	-3.8-3.1	-3.2-3.8	17.2-24.0	71.9-76.2	13.5-20.2	10.9-17.6	0.4-7.2
4.33	21.8-28.0	-3.9-3.0	-3.2-3.8	17.2-24.1	72.3-76.5	13.4-20.2	10.8-17.5	0.4-7.1
4.67	21.7-27.9	-4.1-2.9	-3.2-3.8	17.3-24.1	72.5-76.7	13.4-20.2	10.8-17.4	0.3-7.0
5.00	21.7-27.8	-4.1-2.8	-3.2-3.8	17.3-24.1	72.7-76.9	13.4-20.2	10.7-17.3	0.2-6.9
5.33	21.7-27.8	-4.1-2.9	-3.1-3.8	17.3-24.1	72.9-77.1	13.4-20.2	10.7-17.3	0.2-6.9
5.67	21.6-27.8	-4.1-2.8	-3.2-3.8	17.2-24.0	73.0-77.2	13.4-20.2	10.6-17.3	0.2-6.9
6.00	21.6-27.7	-4.2-2.7	-3.2-3.7	17.1-24.0	73.1-77.3	13.3-20.1	10.6-17.2	0.1-6.8
6.33	21.5-27.7	-4.2-2.7	-3.2-3.7	17.1-23.9	73.1-77.3	13.3-20.1	10.5-17.1	0.0-6.8
6.67	21.5-27.6	-4.3-2.7	-3.2-3.7	17.1-23.9	73.1-77.4	13.3-20.1	10.5-17.1	0.1-6.8
7.00	21.4-27.5	-4.3-2.7	-3.2-3.7	17.0-23.8	73.2-77.4	13.3-20.0	10.4-17.0	0.0-6.7
7.33	21.4-27.5	-4.2-2.7	-3.2-3.6	17.0-23.8	73.2-77.5	13.3-20.0	10.3-17.0	-0.0-6.7
7.67	21.3-27.5	-4.3-2.6	-3.3-3.6	16.9-23.7	73.3-77.5	13.2-20.0	10.3-16.9	-0.1-6.7
8.00	21.3-27.4	-4.3-2.6	-3.3-3.6	16.8-23.7	73.3-77.6	13.2-19.9	10.2-16.9	-0.1-6.6
8.33	21.3-27.4	-4.3-2.6	-3.3-3.5	16.8-23.6	73.4-77.6	13.1-19.9	10.2-16.8	-0.1-6.6
8.67	21.2-27.3	-4.4-2.6	-3.3-3.5	16.8-23.6	73.5-77.7	13.1-19.9	10.2-16.8	-0.1-6.6
9.00	21.2-27.3	-4.4-2.5	-3.4-3.5	16.8-23.6	73.5-77.7	13.1-19.8	10.1-16.8	-0.1-6.6
9.33	21.1-27.2	-4.4-2.5	-3.4-3.5	16.7-23.5	73.6-77.8	13.0-19.8	10.1-16.7	-0.1-6.6
9.67	21.1-27.2	-4.4-2.5	-3.4-3.4	16.7-23.5	73.6-77.8	13.0-19.8	10.1-16.7	-0.1-6.6
10.00	21.0-27.1	-4.4-2.5	-3.4-3.4	16.7-23.5	73.7-77.9	13.0-19.8	10.0-16.7	-0.1-6.5

Table E.6: North / Mass Flux / Mid-day

i \ j	1	2	3	4	6	9	10	11
1	-0.8-1.8	-1.3-2.1	-0.9-2.5	4.6-8.8	-0.8-6.5	-0.8-3.2	-0.6-3.0	-0.7-2.7
2	-1.3-2.1	-0.2-0.2	-0.4-0.4	-0.5-0.3	-3.9-2.4	-0.4-0.4	-0.5-0.3	-0.4-0.4
3	-0.9-2.5	-0.4-0.4	-0.5-0.0	0.1-1.1	-3.5-2.8	0.0-0.9	-0.2-0.8	0.0-0.9
4	4.6-8.8	-0.5-0.3	0.1-1.1	-0.8-0.8	-3.5-3.3	-1.5-1.6	-2.3-1.1	-2.6-0.7
6	-0.8-6.5	-3.9-2.4	-3.5-2.8	-3.5-3.3	54.4-59.6	-1.4-4.1	-2.0-2.0	-0.9-1.3
9	-0.8-3.2	-0.4-0.4	0.0-0.9	-1.5-1.6	-1.4-4.1	0.8-2.3	-0.9-1.6	-0.9-1.3
10	-0.6-3.0	-0.5-0.3	-0.2-0.8	-2.3-1.1	-2.0-2.0	-0.9-1.6	4.5-6.1	-0.6-2.2
11	-0.7-2.7	-0.4-0.4	0.0-0.9	-2.6-0.7	-0.9-1.3	-0.9-1.3	-0.6-2.2	3.1-3.9
Total	21.7-27.8	-4.1-2.8	-3.2-3.8	17.3-24.1	72.7-76.9	13.4-20.2	10.7-17.3	0.2-6.9
Higher	10.0	-0.2	-1.9	14.9	14.5	11.6	6.7	-1.7

Table E.7: Control / Mass Flux / Mean

i \ j	1	2	3	4	6	9	10	11
1	0.8-2.5	-0.8-2.1	-0.8-2.1	0.8-3.7	-1.7-2.2	0.1-3.0	-1.3-1.9	-0.6-2.5
2	-0.8-2.1	0.0-0.2	-0.4-0.0	-0.3-0.1	-1.2-0.8	-1.1-0.1	-0.7-0.1	-0.4-0.4
3	-0.8-2.1	-0.4-0.0	-0.1-0.2	-0.4-0.3	-1.2-0.8	-1.0-0.2	-0.7-0.2	-0.5-0.4
4	0.8-3.7	-0.3-0.1	-0.4-0.3	-1.0-0.5	-1.6-1.9	-1.1-1.5	-1.1-1.9	-1.0-1.9
6	-1.7-2.2	-1.2-0.8	-1.2-0.8	-1.6-1.9	23.2-26.0	0.7-5.3	0.1-4.3	-2.0-1.8
9	0.1-3.0	-1.1-0.1	-1.0-0.2	-1.1-1.5	0.7-5.3	10.3-12.6	0.2-2.9	2.9-5.5
10	-1.3-1.9	-0.7-0.1	-0.7-0.2	-1.1-1.9	0.1-4.3	0.2-2.9	7.7-10.3	5.6-10.3
11	-0.6-2.5	-0.4-0.4	-0.5-0.4	-1.0-1.9	-2.0-1.8	2.9-5.5	5.6-10.3	9.7-11.8
Total	14.6-20.3	-2.8-3.5	-2.3-4.0	8.6-14.7	37.7-42.6	33.5-38.6	30.4-35.8	23.4-28.7
Higher	9.2	1.0	1.4	8.7	10.5	14.9	12.3	1.9

Table E.8: South / Mass Flux / Mean

i \ j	1	2	3	4	6	9	10	11
1	0.4-3.7	-2.5-1.7	-2.4-1.8	4.1-9.4	-0.9-4.9	-1.2-4.5	-2.1-2.5	-2.1-2.2
2	-2.5-1.7	-0.1-0.2	-0.2-0.2	-0.4-0.2	-1.6-2.2	-0.7-0.4	-0.3-0.3	-0.3-0.2
3	-2.4-1.8	-0.2-0.2	-0.1-0.4	-0.9-0.2	-2.0-1.8	-1.1-0.3	-0.8-0.2	-0.8-0.3
4	4.1-9.4	-0.4-0.2	-0.9-0.2	-1.1-2.0	-4.5-1.7	-0.5-4.4	-2.7-2.3	-2.7-2.1
6	-0.9-4.9	-1.6-2.2	-2.0-1.8	-4.5-1.7	33.4-38.4	-2.3-5.2	-2.3-2.5	-1.6-1.8
9	-1.2-4.5	-0.7-0.4	-1.1-0.3	-0.5-4.4	-2.3-5.2	4.5-7.5	-2.2-1.5	-1.4-1.9
10	-2.1-2.5	-0.3-0.3	-0.8-0.2	-2.7-2.3	-2.3-2.5	-2.2-1.5	1.1-3.3	-1.6-2.1
11	-2.1-2.2	-0.3-0.2	-0.8-0.3	-2.7-2.1	-1.6-1.8	-1.4-1.9	-1.6-2.1	3.1-4.4
Total	37.9-45.1	-5.1-5.0	-4.1-5.8	32.3-41.8	51.6-58.4	31.7-40.1	14.5-23.8	2.4-11.9
Higher	29.5	0.2	2.4	30.2	16.7	25.4	17.3	3.4

Table E.9: North / Mass Flux / Mean

i \ j	1	2	3	4	6	9	10	11
1	-0.7-1.9	-1.4-1.9	-1.1-2.2	4.5-8.6	-1.1-6.1	-0.9-2.9	-0.8-2.7	-0.9-2.4
2	-1.4-1.9	-0.1-0.2	-0.3-0.4	-0.3-0.3	-2.4-4.0	-0.4-0.2	-0.5-0.2	-0.3-0.3
3	-1.1-2.2	-0.3-0.4	-0.4-0.0	0.1-0.9	-3.9-2.4	-0.0-0.7	-0.3-0.6	-0.0-0.7
4	4.5-8.6	-0.3-0.3	0.1-0.9	-0.7-0.9	-3.8-2.9	-1.7-1.5	-2.4-0.9	-2.7-0.5
6	-1.1-6.1	-2.4-4.0	-3.9-2.4	-3.8-2.9	54.6-59.8	-1.5-3.9	-2.4-1.3	-0.9-1.3
9	-0.9-2.9	-0.4-0.2	-0.0-0.7	-1.7-1.5	-1.5-3.9	0.9-2.3	-1.0-1.2	-0.9-1.2
10	-0.8-2.7	-0.5-0.2	-0.3-0.6	-2.4-0.9	-2.4-1.3	-1.0-1.2	5.1-6.7	-0.5-2.2
11	-0.9-2.4	-0.3-0.3	-0.0-0.7	-2.7-0.5	-0.9-1.3	-0.9-1.2	-0.5-2.2	3.2-4.1
Total	20.7-27.1	-4.1-3.1	-3.7-3.5	16.3-23.3	71.7-75.8	12.6-19.4	10.4-17.3	0.3-7.3
Higher	10.7	-1.3	-1.1	15.1	13.5	11.8	7.4	-1.1

Table E.10: Control / Positive Mass Flux with Time (Total-effect)

t \ i	1	2	3	4	5	6	7	8
0.33	-4.6-10.7	-10.5-5.5	-8.1-6.9	-4.6-11.2	10.1-23.7	11.6-26.1	63.8-71.2	47.7-56.9
0.67	-6.1-9.8	-6.6-8.3	-8.0-7.0	-6.3-9.7	11.5-25.2	11.9-26.4	64.1-71.7	49.7-58.8
1.00	-6.7-9.4	-6.9-8.1	-7.8-7.3	-6.9-9.3	11.9-25.6	11.9-26.6	64.4-72.0	50.6-59.7
1.33	-7.1-9.1	-7.2-8.0	-7.8-7.4	-7.3-9.0	11.8-25.6	11.9-26.7	64.7-72.3	51.2-60.3
1.67	-7.6-8.7	-7.5-7.8	-8.0-7.3	-7.6-8.7	11.6-25.5	11.7-26.7	64.8-72.4	51.5-60.6
2.00	-8.0-8.4	-7.7-7.6	-8.1-7.3	-7.9-8.5	11.5-25.5	11.5-26.6	64.9-72.5	51.7-60.9
2.33	-8.3-8.2	-7.9-7.5	-8.2-7.3	-8.2-8.3	11.4-25.4	11.4-26.7	65.0-72.6	51.9-61.0
2.67	-8.5-8.1	-8.0-7.4	-8.3-7.3	-8.3-8.2	11.3-25.4	11.4-26.7	65.1-72.6	51.9-61.1
3.00	-8.7-8.0	-8.1-7.4	-8.4-7.2	-8.4-8.2	11.2-25.3	11.4-26.7	65.1-72.7	52.1-61.2
3.33	-8.8-7.9	-8.2-7.3	-8.4-7.2	-8.6-8.1	11.2-25.3	11.4-26.7	65.1-72.7	52.1-61.3
3.67	-8.9-7.8	-8.2-7.3	-8.4-7.2	-8.6-8.1	11.1-25.3	11.4-26.7	65.1-72.7	52.2-61.4
4.00	-9.0-7.8	-8.3-7.3	-8.4-7.2	-8.7-8.0	11.0-25.2	11.4-26.7	65.1-72.7	52.2-61.4
4.33	-9.1-7.7	-8.3-7.3	-8.4-7.2	-8.8-8.0	11.0-25.2	11.4-26.7	65.1-72.7	52.3-61.5
4.67	-9.2-7.7	-8.4-7.3	-8.4-7.1	-8.8-8.0	10.9-25.2	11.3-26.7	65.2-72.8	52.3-61.5
5.00	-9.2-7.7	-8.4-7.3	-8.4-7.2	-8.9-8.0	10.9-25.1	11.3-26.8	65.2-72.8	52.4-61.6
5.33	-9.3-7.7	-8.5-7.2	-8.5-7.1	-8.9-8.0	10.9-25.1	11.3-26.8	65.2-72.8	52.4-61.6
5.67	-9.3-7.6	-8.5-7.2	-8.5-7.1	-8.9-8.0	10.8-25.0	11.3-26.7	65.2-72.8	52.5-61.6
6.00	-9.3-7.6	-8.5-7.2	-8.5-7.1	-8.9-8.0	10.8-25.0	11.3-26.8	65.2-72.8	52.5-61.7
6.33	-9.3-7.6	-8.5-7.1	-8.5-7.1	-8.9-8.0	10.7-25.0	11.3-26.7	65.2-72.8	52.5-61.7
6.67	-9.3-7.6	-8.5-7.1	-8.5-7.1	-8.9-8.0	10.7-25.0	11.3-26.8	65.2-72.8	52.5-61.7
7.00	-9.4-7.6	-8.5-7.2	-8.5-7.1	-8.9-8.0	10.7-24.9	11.3-26.8	65.2-72.8	52.5-61.7
7.33	-9.4-7.6	-8.5-7.1	-8.5-7.1	-8.9-7.9	10.6-24.9	11.2-26.8	65.2-72.9	52.6-61.7
7.67	-9.4-7.5	-8.6-7.1	-8.5-7.1	-9.0-7.9	10.6-24.9	11.3-26.8	65.2-72.9	52.6-61.7
8.00	-9.4-7.5	-8.6-7.1	-8.5-7.1	-9.0-7.9	10.5-24.8	11.3-26.8	65.2-72.9	52.6-61.8
8.33	-9.4-7.5	-8.6-7.1	-8.5-7.1	-9.0-7.9	10.5-24.8	11.3-26.8	65.2-72.9	52.6-61.8
8.67	-9.4-7.5	-8.6-7.1	-8.5-7.1	-9.0-7.9	10.4-24.8	11.3-26.8	65.2-72.9	52.6-61.8
9.00	-9.4-7.5	-8.6-7.1	-8.6-7.1	-9.0-7.9	10.4-24.8	11.3-26.8	65.2-72.9	52.6-61.8
9.33	-9.4-7.5	-8.6-7.1	-8.6-7.1	-9.0-7.9	10.4-24.8	11.3-26.8	65.2-72.9	52.7-61.8
9.67	-9.4-7.5	-8.6-7.1	-8.6-7.1	-9.0-7.9	10.4-24.7	11.3-26.8	65.2-72.9	52.6-61.8
10.00	-9.5-7.5	-8.6-7.1	-8.5-7.1	-9.1-7.9	10.3-24.7	11.3-26.8	65.3-72.9	52.7-61.8

Table E.11: Control / Mass Flux / Positive Mid-day

i \ j	1	2	3	4	6	9	10	11
1	-0.4-0.3	-0.4-0.9	-0.5-0.8	-0.2-1.2	-0.7-0.8	-0.5-1.0	-3.2-2.9	-0.7-2.6
2	-0.4-0.9	-0.1-0.1	-0.1-0.1	-0.1-0.2	-0.5-0.1	-0.2-0.2	-3.3-2.3	-0.9-1.9
3	-0.5-0.8	-0.1-0.1	-0.1-0.1	-0.3-0.1	-0.6-0.1	-0.5-0.1	-3.4-2.1	-0.9-2.0
4	-0.2-1.2	-0.1-0.2	-0.3-0.1	-0.7-0.0	-0.5-1.2	-0.2-1.2	-2.5-3.2	-0.6-2.4
6	-0.7-0.8	-0.5-0.1	-0.6-0.1	-0.5-1.2	4.2-6.3	-1.5-2.0	1.2-10.1	2.2-8.3
9	-0.5-1.0	-0.2-0.2	-0.5-0.1	-0.2-1.2	-1.5-2.0	1.0-2.7	0.5-8.0	1.2-5.4
10	-3.2-2.9	-3.3-2.3	-3.4-2.1	-2.5-3.2	1.2-10.1	0.5-8.0	16.8-22.3	24.0-34.9
11	-0.7-2.6	-0.9-1.9	-0.9-2.0	-0.6-2.4	2.2-8.3	1.2-5.4	24.0-34.9	8.5-12.0
Total	-9.2-7.7	-8.4-7.3	-8.4-7.2	-8.9-8.0	10.9-25.1	11.3-26.8	65.2-72.8	52.4-61.6
Higher	-2.7	-0.6	-0.3	-2.6	1.7	8.8	11.1	5.9

Table E.12: South / Positive Mass Flux with Time (Total-effect)

t \ i	1	2	3	4	5	6	7	8
0.33	35.6-46.7	1.4-15.1	-5.5-9.2	32.6-44.1	36.6-47.7	24.3-36.2	42.8-53.4	11.0-23.3
0.67	41.6-52.0	-0.7-13.0	-3.5-10.4	30.9-42.6	43.9-54.2	28.2-39.6	38.5-49.3	10.4-22.7
1.00	43.4-53.3	-1.2-12.7	-2.7-11.4	30.5-42.3	47.0-57.0	29.8-41.3	36.4-47.6	10.4-22.9
1.33	44.2-53.8	-1.6-12.3	-2.5-11.7	30.4-42.2	48.8-58.5	30.5-41.9	35.3-46.6	10.4-22.7
1.67	44.5-54.2	-2.2-11.9	-2.3-11.9	29.9-41.8	49.8-59.5	30.7-42.0	34.6-45.9	10.4-22.7
2.00	44.8-54.4	-2.6-11.5	-2.1-12.0	29.8-41.7	50.4-60.0	30.7-42.0	33.6-45.2	10.3-22.6
2.33	45.1-54.6	-2.4-11.6	-1.6-12.3	29.9-41.9	50.9-60.5	31.0-42.3	33.3-44.9	10.4-22.8
2.67	45.4-54.8	-2.4-11.6	-1.4-12.5	30.1-42.0	51.4-61.0	31.3-42.5	32.9-44.6	10.3-22.6
3.00	45.4-54.9	-2.3-11.7	-1.3-12.5	30.2-42.2	51.8-61.4	31.4-42.6	32.8-44.4	10.3-22.6
3.33	45.5-55.0	-2.2-11.7	-1.2-12.5	30.4-42.4	52.2-61.7	31.5-42.8	32.7-44.3	10.2-22.6
3.67	45.4-55.1	-2.2-11.7	-1.1-12.6	30.5-42.5	52.4-61.9	31.7-42.9	32.5-44.1	10.3-22.5
4.00	45.5-55.1	-2.2-11.7	-1.2-12.5	30.5-42.5	52.6-62.1	31.7-42.9	32.3-43.9	10.3-22.5
4.33	45.6-55.1	-2.1-11.7	-1.1-12.5	30.5-42.5	52.9-62.3	31.8-43.0	32.2-43.7	10.4-22.6
4.67	45.5-55.1	-2.1-11.6	-1.2-12.5	30.4-42.4	53.0-62.4	31.8-43.0	32.0-43.5	10.4-22.5
5.00	45.5-55.0	-2.2-11.6	-1.3-12.4	30.3-42.3	53.1-62.5	31.8-43.0	31.8-43.4	10.3-22.5
5.33	45.4-55.0	-2.2-11.5	-1.3-12.4	30.3-42.3	53.2-62.6	31.8-43.0	31.6-43.2	10.2-22.4
5.67	45.4-55.0	-2.2-11.5	-1.2-12.4	30.3-42.3	53.4-62.7	31.8-43.0	31.5-43.2	10.3-22.4
6.00	45.4-55.0	-2.2-11.5	-1.2-12.4	30.3-42.3	53.5-62.8	31.9-43.1	31.5-43.1	10.3-22.4
6.33	45.4-54.9	-2.2-11.5	-1.2-12.3	30.3-42.3	53.6-62.9	31.9-43.1	31.4-43.0	10.2-22.4
6.67	45.4-54.9	-2.3-11.4	-1.3-12.3	30.2-42.2	53.6-62.9	31.9-43.1	31.3-42.9	10.1-22.4
7.00	45.3-54.9	-2.3-11.4	-1.2-12.3	30.2-42.2	53.7-63.0	31.9-43.1	31.2-42.8	10.1-22.4
7.33	45.3-54.9	-2.3-11.3	-1.2-12.4	30.2-42.1	53.8-63.1	31.9-43.1	31.1-42.8	10.0-22.3
7.67	45.3-54.9	-2.4-11.3	-1.2-12.4	30.2-42.1	53.8-63.1	31.9-43.1	31.0-42.7	10.0-22.3
8.00	45.3-54.8	-2.4-11.3	-1.1-12.4	30.1-42.0	53.9-63.2	31.9-43.2	30.9-42.6	10.0-22.3
8.33	45.3-54.8	-2.4-11.3	-1.1-12.4	30.1-42.0	53.9-63.2	32.0-43.2	30.9-42.6	10.0-22.3
8.67	45.3-54.8	-2.4-11.3	-1.1-12.4	30.1-42.0	54.0-63.3	32.0-43.2	30.8-42.6	10.0-22.3
9.00	45.3-54.8	-2.4-11.3	-1.1-12.5	30.0-42.0	54.0-63.3	32.0-43.2	30.8-42.5	10.0-22.3
9.33	45.3-54.8	-2.4-11.3	-1.1-12.5	30.0-42.0	54.1-63.4	32.0-43.2	30.7-42.5	10.0-22.3
9.67	45.3-54.8	-2.4-11.3	-1.0-12.5	30.0-42.0	54.1-63.4	32.0-43.2	30.7-42.4	10.0-22.3
10.00	45.2-54.8	-2.4-11.3	-1.0-12.5	30.0-42.0	54.1-63.4	32.0-43.2	30.6-42.4	9.9-22.3

Table E.13: South / Mass Flux / Positive Mid-day

i \ j	1	2	3	4	6	9	10	11
1	2.0-6.0	-0.3-3.4	-0.7-3.1	4.7-10.5	-0.4-6.9	5.3-11.3	-1.2-4.4	0.0-4.0
2	-0.3-3.4	-0.1-0.1	-0.3-0.2	-0.2-0.4	-3.4-1.2	-0.3-0.3	-1.2-0.1	-0.4-0.2
3	-0.7-3.1	-0.3-0.2	-0.3-0.3	-0.5-0.6	-3.4-1.2	-0.6-0.4	-1.6-0.1	-0.7-0.5
4	4.7-10.5	-0.2-0.4	-0.5-0.6	-1.0-1.6	-4.2-2.4	0.3-5.4	-2.3-2.5	-1.6-2.6
6	-0.4-6.9	-3.4-1.2	-3.4-1.2	-4.2-2.4	19.4-24.5	-3.3-3.5	1.6-8.2	-0.1-4.3
9	5.3-11.3	-0.3-0.3	-0.6-0.4	0.3-5.4	-3.3-3.5	0.1-2.5	-2.0-1.7	-1.1-2.1
10	-1.2-4.4	-1.2-0.1	-1.6-0.1	-2.3-2.5	1.6-8.2	-2.0-1.7	3.8-7.2	-0.7-3.2
11	0.0-4.0	-0.4-0.2	-0.7-0.5	-1.6-2.6	-0.1-4.3	-1.1-2.1	-0.7-3.2	1.0-2.4
Total	45.5-55.0	-2.2-11.6	-1.3-12.4	30.3-42.3	53.1-62.5	31.8-43.0	31.8-43.4	10.3-22.5
Higher	20.8	4.8	6.4	25.8	28.5	24.7	25.6	8.5

Table E.14: North / Positive Mass Flux with Time (Total-effect)

t \ i	1	2	3	4	5	6	7	8
0.33	9.9-19.8	-2.8-8.1	-5.4-5.3	20.2-29.3	34.2-42.0	2.9-13.3	44.5-51.7	7.2-16.6
0.67	15.7-25.4	-4.7-6.3	-5.1-5.7	18.0-27.6	41.6-49.1	4.9-15.5	40.1-47.8	6.6-16.2
1.00	18.9-28.5	-5.0-5.9	-4.1-6.6	17.2-26.9	45.0-52.5	6.4-16.9	38.5-46.3	6.8-16.4
1.33	20.2-29.6	-5.7-5.3	-7.3-3.8	16.5-26.3	47.0-54.3	6.8-17.4	37.0-44.9	6.3-16.0
1.67	20.8-30.2	-6.1-4.9	-7.2-3.9	16.0-25.7	48.4-55.5	7.1-17.7	35.8-43.8	6.0-15.7
2.00	21.3-30.7	-6.4-4.7	-6.8-4.3	15.7-25.4	49.5-56.5	7.6-18.1	35.1-43.2	6.0-15.7
2.33	21.8-31.1	-6.4-4.7	-6.4-4.6	15.6-25.3	50.4-57.4	7.9-18.4	34.7-42.8	6.1-15.7
2.67	21.9-31.3	-6.4-4.6	-6.2-4.7	15.4-25.1	51.1-58.0	8.1-18.6	34.4-42.5	6.2-15.8
3.00	22.0-31.3	-6.5-4.5	-6.2-4.8	15.2-24.9	51.7-58.4	8.2-18.7	34.1-42.2	6.2-15.8
3.33	22.0-31.3	-6.7-4.3	-6.3-4.7	15.0-24.7	52.1-58.8	8.1-18.7	33.8-41.9	6.1-15.7
3.67	22.0-31.3	-6.8-4.2	-6.4-4.6	14.8-24.5	52.4-59.1	8.1-18.6	33.5-41.6	6.1-15.7
4.00	22.0-31.4	-6.9-4.1	-6.5-4.5	14.6-24.4	52.7-59.4	8.1-18.6	33.3-41.4	6.1-15.7
4.33	22.0-31.4	-7.0-4.1	-6.5-4.6	14.5-24.3	53.0-59.7	8.1-18.6	33.0-41.2	6.1-15.7
4.67	22.0-31.4	-7.0-4.0	-6.4-4.6	14.4-24.3	53.2-59.9	8.2-18.7	32.9-41.0	6.1-15.7
5.00	22.1-31.4	-7.0-4.0	-6.4-4.7	14.4-24.3	53.5-60.1	8.2-18.7	32.7-40.9	6.0-15.6
5.33	22.1-31.4	-7.0-4.0	-6.4-4.7	14.4-24.3	53.6-60.3	8.2-18.7	32.6-40.7	6.0-15.6
5.67	22.1-31.4	-7.1-3.9	-6.5-4.7	14.3-24.2	53.8-60.4	8.1-18.6	32.4-40.5	5.9-15.6
6.00	22.0-31.4	-7.2-3.8	-6.5-4.6	14.2-24.1	53.9-60.5	8.0-18.5	32.2-40.4	5.8-15.5
6.33	22.0-31.3	-7.3-3.8	-6.6-4.5	14.1-24.1	54.0-60.6	7.9-18.5	32.0-40.2	5.7-15.4
6.67	21.9-31.3	-4.1-6.5	-6.6-4.5	14.0-24.0	54.2-60.7	7.9-18.4	31.8-40.1	5.6-15.3
7.00	21.9-31.3	-4.1-6.4	-6.6-4.5	13.9-23.9	54.3-60.8	7.8-18.4	31.7-39.9	5.6-15.2
7.33	21.9-31.2	-4.2-6.3	-6.6-4.5	13.9-23.8	54.4-60.9	7.8-18.3	31.6-39.8	5.5-15.2
7.67	21.9-31.2	-4.3-6.3	-6.6-4.4	13.8-23.7	54.5-61.0	7.7-18.3	31.5-39.7	5.5-15.2
8.00	21.8-31.2	-4.3-6.2	-6.7-4.4	13.7-23.7	54.6-61.1	7.7-18.2	31.4-39.7	5.4-15.1
8.33	21.8-31.1	-4.4-6.2	-6.7-4.4	13.6-23.6	54.7-61.2	7.6-18.2	31.3-39.6	5.4-15.1
8.67	21.7-31.1	-4.4-6.1	-6.7-4.4	13.5-23.5	54.8-61.3	7.6-18.1	31.2-39.5	5.3-15.1
9.00	21.7-31.1	-4.5-6.1	-6.8-4.4	13.5-23.5	54.9-61.4	7.5-18.1	31.1-39.4	5.3-15.0
9.33	21.7-31.0	-4.5-6.1	-6.7-4.3	13.4-23.4	54.9-61.4	7.5-18.1	31.1-39.4	5.3-15.0
9.67	21.7-31.0	-4.5-6.1	-6.7-4.3	13.4-23.4	55.0-61.5	7.5-18.0	31.0-39.3	5.3-15.0
10.00	21.6-31.0	-4.5-6.0	-6.8-4.3	13.4-23.3	55.1-61.6	7.5-18.0	30.9-39.2	5.3-15.0

Table E.15: North / Mass Flux / Positive Mid-day

i \ j	1	2	3	4	6	9	10	11
1	2.1-5.0	-1.7-1.8	-1.6-1.9	1.8-6.0	-0.9-5.6	0.8-4.7	-1.7-2.7	-1.8-1.9
2	-1.7-1.8	-0.1-0.2	-0.4-0.1	-0.4-0.2	-2.9-1.8	-0.4-0.2	-1.8-0.6	-0.4-0.2
3	-1.6-1.9	-0.4-0.1	-0.0-0.4	-0.8-0.1	-3.0-1.8	-0.7-0.1	-2.2-0.3	-0.7-0.2
4	1.8-6.0	-0.4-0.2	-0.8-0.1	-1.1-0.7	-3.3-2.1	-2.0-1.2	-2.0-1.8	-1.3-2.0
6	-0.9-5.6	-2.9-1.8	-3.0-1.8	-3.3-2.1	27.9-32.3	-1.7-2.4	4.3-11.6	2.0-5.3
9	0.8-4.7	-0.4-0.2	-0.7-0.1	-2.0-1.2	-1.7-2.4	0.2-1.6	-2.4-1.1	-1.6-1.0
10	-1.7-2.7	-1.8-0.6	-2.2-0.3	-2.0-1.8	4.3-11.6	-2.4-1.1	15.2-18.3	0.7-3.5
11	-1.8-1.9	-0.4-0.2	-0.7-0.2	-1.3-2.0	2.0-5.3	-1.6-1.0	0.7-3.5	3.8-4.7
Total	22.1-31.4	-7.0-4.0	-6.4-4.7	14.4-24.3	53.5-60.1	8.2-18.7	32.7-40.9	6.0-15.6
Higher	13.5	-0.1	1.4	16.8	14.2	11.1	11.7	1.1

Table E.16: Control / Mass Flux / Positive Mean

i \ j	1	2	3	4	6	9	10	11
1	-0.4-0.4	-0.5-0.9	-0.5-0.8	-0.3-1.2	-0.7-0.8	-0.5-1.0	-3.0-2.8	-0.7-2.6
2	-0.5-0.9	-0.0-0.1	-0.2-0.1	-0.1-0.1	-0.6-0.1	-0.3-0.2	-3.3-2.3	-1.0-1.9
3	-0.5-0.8	-0.2-0.1	-0.1-0.1	-0.3-0.1	-0.6-0.1	-0.5-0.1	-3.4-2.2	-1.0-2.0
4	-0.3-1.2	-0.1-0.1	-0.3-0.1	-0.7-0.1	-0.5-1.2	-0.3-1.2	-2.5-3.2	-0.7-2.5
6	-0.7-0.8	-0.6-0.1	-0.6-0.1	-0.5-1.2	4.2-6.2	-1.5-2.0	1.6-10.1	2.2-8.3
9	-0.5-1.0	-0.3-0.2	-0.5-0.1	-0.3-1.2	-1.5-2.0	1.1-2.7	0.7-7.9	1.2-5.4
10	-3.0-2.8	-3.3-2.3	-3.4-2.2	-2.5-3.2	1.6-10.1	0.7-7.9	17.0-22.5	23.6-34.6
11	-0.7-2.6	-1.0-1.9	-1.0-2.0	-0.7-2.5	2.2-8.3	1.2-5.4	23.6-34.6	8.8-12.2
Total	-8.6-7.7	-7.8-7.1	-8.0-6.9	-8.5-7.9	10.7-24.7	11.5-26.5	65.1-72.7	52.1-61.2
Higher	-2.3	-0.1	-0.0	-2.4	1.2	8.7	10.8	5.8

Table E.17: South / Mass Flux / Positive Mean

i \ j	1	2	3	4	6	9	10	11
1	1.6-5.7	-0.4-3.4	-0.7-3.1	4.6-10.6	-0.2-7.0	5.6-11.3	-1.3-4.5	-0.1-3.9
2	-0.4-3.4	-0.2-0.1	-0.3-0.4	-0.4-0.3	-3.3-1.3	-0.5-0.3	-1.3-0.3	-0.4-0.4
3	-0.7-3.1	-0.3-0.4	-0.3-0.3	-0.5-0.6	-3.3-1.3	-0.5-0.5	-1.6-0.1	-0.6-0.5
4	4.6-10.6	-0.4-0.3	-0.5-0.6	-1.2-1.4	-3.9-2.8	0.5-5.6	-2.3-2.6	-1.5-2.8
6	-0.2-7.0	-3.3-1.3	-3.3-1.3	-3.9-2.8	18.8-24.0	-2.9-3.5	2.0-8.5	0.2-4.6
9	5.6-11.3	-0.5-0.3	-0.5-0.5	0.5-5.6	-2.9-3.5	-0.0-2.3	-2.1-1.8	-1.1-2.1
10	-1.3-4.5	-1.3-0.3	-1.6-0.1	-2.3-2.6	2.0-8.5	-2.1-1.8	4.4-8.0	-0.4-3.6
11	-0.1-3.9	-0.4-0.4	-0.6-0.5	-1.5-2.8	0.2-4.6	-1.1-2.1	-0.4-3.6	1.1-2.4
Total	44.6-54.3	-3.0-11.3	-2.4-11.9	29.6-41.9	51.7-61.5	31.0-42.3	31.8-43.8	9.7-22.5
Higher	20.1	4.2	5.3	24.6	26.4	23.5	24.3	7.3

Table E.18: North / Mass Flux / Positive Mean

i \ j	1	2	3	4	6	9	10	11
1	1.8-4.7	-1.7-1.8	-1.5-2.0	1.9-6.0	-0.8-5.5	0.6-4.5	-1.6-2.9	-1.7-1.9
2	-1.7-1.8	-0.0-0.2	-0.5-0.1	-0.4-0.2	-2.9-1.8	-0.4-0.2	-1.8-0.8	-0.5-0.2
3	-1.5-2.0	-0.5-0.1	-0.1-0.3	-0.7-0.2	-3.0-1.8	-0.6-0.1	-2.1-0.5	-0.6-0.3
4	1.9-6.0	-0.4-0.2	-0.7-0.2	-1.0-0.8	-3.3-2.2	-1.2-2.1	-1.9-2.1	-1.2-2.0
6	-0.8-5.5	-2.9-1.8	-3.0-1.8	-3.3-2.2	27.1-31.5	-1.7-2.4	4.7-11.9	1.9-5.2
9	0.6-4.5	-0.4-0.2	-0.6-0.1	-1.2-2.1	-1.7-2.4	0.3-1.7	-2.4-1.3	-1.5-1.0
10	-1.6-2.9	-1.8-0.8	-2.1-0.5	-1.9-2.1	4.7-11.9	-2.4-1.3	16.1-19.3	0.9-3.8
11	-1.7-1.9	-0.5-0.2	-0.6-0.3	-1.2-2.0	1.9-5.2	-1.5-1.0	0.9-3.8	3.9-4.9
Total	20.7-30.1	-7.1-3.7	-7.0-3.9	13.9-23.8	52.1-58.8	7.3-17.5	33.5-41.5	6.0-15.5
Higher	12.3	-0.3	0.3	14.9	13.2	9.2	10.3	0.6



Table E.19: Control / Negative Mass Flux with Time (Total-effect)

t \ i	1	2	3	4	5	6	7	8
0.33	20.9-28.8	-2.0-6.8	-4.9-4.1	11.3-19.7	39.8-46.2	40.3-46.6	17.8-25.7	13.0-21.0
0.67	20.1-27.7	-3.1-5.6	-4.2-4.6	10.0-18.2	40.5-46.8	40.6-46.8	19.2-26.9	13.3-21.0
1.00	19.7-27.3	-3.1-5.5	-3.6-5.0	9.3-17.4	41.5-47.6	40.9-47.0	20.1-27.6	13.5-21.2
1.33	19.6-27.1	-3.0-5.5	-3.1-5.5	9.5-17.5	42.3-48.3	41.4-47.4	20.7-28.1	14.0-21.5
1.67	19.6-27.0	-2.9-5.5	-2.5-5.9	9.7-17.7	42.6-48.6	41.7-47.7	20.9-28.3	14.1-21.5
2.00	19.4-26.8	-3.0-5.4	-2.4-5.9	9.7-17.6	42.7-48.7	41.8-47.8	21.2-28.5	14.1-21.5
2.33	19.1-26.5	-3.1-5.2	-2.5-5.8	9.6-17.4	42.7-48.6	41.9-47.8	21.4-28.6	14.2-21.5
2.67	18.8-26.3	-3.3-5.1	-2.5-5.8	9.5-17.3	42.8-48.6	41.8-47.8	21.4-28.6	14.2-21.5
3.00	18.7-26.3	-3.2-5.1	-2.3-6.0	9.6-17.4	42.9-48.7	42.0-47.9	21.6-28.8	14.4-21.6
3.33	18.7-26.2	-3.2-5.1	-2.2-6.0	9.6-17.4	43.0-48.8	42.2-48.0	21.7-28.9	14.4-21.7
3.67	18.7-26.2	-3.1-5.2	-2.0-6.2	9.6-17.5	43.1-48.9	42.3-48.1	21.9-29.1	14.6-21.8
4.00	18.7-26.1	-3.1-5.1	-2.0-6.2	9.6-17.5	43.1-48.9	42.4-48.2	22.0-29.1	14.6-21.8
4.33	18.7-26.1	-3.1-5.2	-2.0-6.2	9.6-17.5	43.2-49.0	42.4-48.3	22.1-29.3	14.7-21.9
4.67	18.6-26.1	-3.0-5.2	-2.0-6.2	9.6-17.5	43.2-49.0	42.5-48.3	22.2-29.3	14.7-21.9
5.00	18.6-26.1	-3.0-5.3	-1.9-6.3	9.7-17.6	43.3-49.1	42.6-48.4	22.3-29.5	14.7-21.9
5.33	18.6-26.0	-3.0-5.3	-1.9-6.3	9.8-17.6	43.3-49.1	42.6-48.4	22.4-29.5	14.7-21.9
5.67	18.5-26.0	-3.0-5.3	-1.9-6.3	9.8-17.6	43.4-49.2	42.6-48.4	22.4-29.6	14.8-21.9
6.00	18.5-26.0	-2.9-5.3	-1.8-6.4	9.7-17.5	43.4-49.2	42.7-48.5	22.5-29.6	14.8-22.0
6.33	18.5-26.0	-2.8-5.5	-1.7-6.5	9.8-17.6	43.5-49.3	42.8-48.6	22.7-29.8	14.9-22.1
6.67	18.5-26.0	-2.8-5.5	-1.7-6.5	9.8-17.6	43.5-49.3	42.9-48.7	22.7-29.8	15.0-22.1
7.00	18.5-25.9	-2.8-5.5	-1.8-6.4	9.8-17.5	43.5-49.3	42.9-48.7	22.7-29.8	14.9-22.1
7.33	18.4-25.9	-2.8-5.4	-1.8-6.4	9.7-17.5	43.5-49.2	42.9-48.7	22.8-29.9	15.0-22.1
7.67	18.4-25.9	-2.7-5.5	-1.8-6.4	9.7-17.5	43.5-49.2	42.9-48.7	22.8-29.9	15.0-22.1
8.00	18.4-25.9	-2.7-5.5	-1.8-6.4	9.8-17.6	43.5-49.2	42.9-48.7	22.9-29.9	15.0-22.2
8.33	18.4-25.8	-2.7-5.5	-1.8-6.4	9.8-17.6	43.5-49.2	43.0-48.7	22.9-30.0	15.0-22.2
8.67	18.4-25.8	-2.7-5.5	-1.8-6.4	9.8-17.6	43.5-49.2	43.0-48.7	22.9-30.0	15.0-22.2
9.00	18.4-25.8	-2.7-5.4	-1.8-6.4	9.8-17.6	43.5-49.2	43.0-48.7	22.9-30.0	15.0-22.2
9.33	18.4-25.8	-2.7-5.4	-1.7-6.4	9.8-17.6	43.5-49.2	43.0-48.7	22.9-30.0	15.0-22.2
9.67	18.4-25.8	-2.7-5.5	-1.7-6.5	9.8-17.6	43.5-49.2	43.0-48.7	23.0-30.0	15.0-22.2
10.00	18.4-25.8	-2.7-5.5	-1.7-6.5	9.8-17.6	43.5-49.2	43.0-48.7	23.0-30.0	15.0-22.2

Table E.20: Control / Mass Flux / Negative Mid-Day

i \ j	1	2	3	4	6	9	10	11
1	1.0-3.0	-0.5-2.8	-0.5-2.8	1.0-4.4	-1.7-3.1	-0.3-3.7	-0.5-3.0	-0.5-3.0
2	-0.5-2.8	-0.1-0.2	-0.4-0.2	-0.4-0.2	-1.4-1.3	-2.2-0.4	-0.6-0.2	-0.5-0.3
3	-0.5-2.8	-0.4-0.2	-0.2-0.2	-0.4-0.5	-1.4-1.4	-2.1-0.5	-0.7-0.3	-0.6-0.4
4	1.0-4.4	-0.4-0.2	-0.4-0.5	-0.9-0.7	-2.3-2.0	-1.6-1.9	-1.8-1.6	-1.8-1.5
6	-1.7-3.1	-1.4-1.3	-1.4-1.4	-2.3-2.0	23.4-26.9	-1.0-5.7	0.6-5.1	-2.0-1.9
9	-0.3-3.7	-2.2-0.4	-2.1-0.5	-1.6-1.9	-1.0-5.7	18.8-21.9	-1.5-1.7	1.2-4.1
10	-0.5-3.0	-0.6-0.2	-0.7-0.3	-1.8-1.6	0.6-5.1	-1.5-1.7	2.4-4.7	0.2-4.5
11	-0.5-3.0	-0.5-0.3	-0.6-0.4	-1.8-1.5	-2.0-1.9	1.2-4.1	0.2-4.5	6.2-8.1
Total	18.6-26.1	-3.0-5.3	-1.9-6.3	9.7-17.6	43.3-49.1	42.6-48.4	22.3-29.5	14.7-21.9
Higher	10.4	1.4	2.3	11.3	15.4	19.9	16.2	5.3

Table E.21: South / Negative Mass Flux with Time (Total-effect)

t \ i	1	2	3	4	5	6	7	8
0.33	39.0-48.8	-0.0-12.9	-5.4-8.1	24.4-36.3	37.4-46.6	36.6-47.8	9.9-22.8	1.9-14.6
0.67	40.2-49.7	-3.9-9.3	-6.8-6.9	24.5-36.5	38.9-48.0	36.5-47.3	8.9-21.6	-0.3-12.8
1.00	40.4-49.6	-5.8-7.6	-7.3-6.3	23.7-35.7	40.2-49.1	35.8-46.4	8.6-21.1	-1.1-11.9
1.33	40.2-49.3	-6.9-6.4	-7.4-5.8	23.3-35.3	41.1-49.8	35.3-45.8	8.5-20.8	-1.2-11.7
1.67	40.5-49.4	-6.3-6.8	-6.5-6.7	24.1-35.9	42.1-50.7	35.7-46.2	9.2-21.5	-0.1-12.5
2.00	40.0-48.9	-6.4-6.7	-6.1-7.1	24.1-35.7	42.7-51.2	35.6-46.0	9.1-21.4	-0.1-12.4
2.33	39.7-48.6	-6.7-6.4	-6.2-7.0	23.9-35.5	42.8-51.4	35.3-45.6	8.9-21.3	-0.1-12.3
2.67	39.5-48.4	-6.6-6.4	-6.1-7.0	23.7-35.3	43.1-51.6	35.1-45.4	8.9-21.2	-0.1-12.2
3.00	39.5-48.3	-6.7-6.2	-6.0-6.9	23.6-35.2	43.2-51.7	34.9-45.2	9.0-21.2	-0.1-12.2
3.33	39.3-48.2	-6.8-6.1	-5.9-7.0	23.3-34.9	43.3-51.8	34.9-45.1	9.1-21.3	0.0-12.2
3.67	39.2-48.0	-7.0-6.0	-5.9-6.9	23.1-34.8	43.5-51.9	34.8-45.0	9.1-21.2	0.1-12.2
4.00	39.1-47.9	-7.1-5.9	-5.8-6.9	23.0-34.6	43.5-51.9	34.7-44.8	9.1-21.3	-0.0-12.1
4.33	39.0-47.7	-7.3-5.7	-6.0-6.8	22.7-34.4	43.7-52.1	34.6-44.7	9.1-21.2	-0.3-11.8
4.67	38.9-47.7	-7.2-5.7	-5.9-6.8	22.7-34.3	43.9-52.3	34.5-44.7	9.2-21.2	-0.3-11.8
5.00	38.8-47.6	-7.2-5.8	-5.8-6.8	22.6-34.2	44.2-52.6	34.5-44.7	9.2-21.3	-0.2-11.9
5.33	38.8-47.5	-7.2-5.7	-5.7-6.9	22.6-34.2	44.4-52.7	34.5-44.7	9.3-21.3	-0.2-11.9
5.67	38.7-47.5	-7.2-5.7	-5.6-6.9	22.6-34.2	44.6-52.8	34.5-44.7	9.4-21.3	-0.1-12.0
6.00	38.8-47.5	-7.0-5.8	-5.5-7.0	22.7-34.2	44.8-53.0	34.7-44.7	9.5-21.4	0.1-12.1
6.33	38.7-47.4	-7.1-5.7	-5.5-7.0	22.6-34.1	44.8-53.0	34.7-44.7	9.5-21.4	0.0-12.1
6.67	38.7-47.4	-7.1-5.7	-5.3-7.1	22.6-34.1	44.8-52.9	34.7-44.7	9.6-21.4	0.0-12.1
7.00	38.7-47.4	-6.9-5.8	-5.3-7.2	22.6-34.1	44.8-53.0	34.7-44.8	9.7-21.5	0.2-12.3
7.33	38.6-47.3	-6.9-5.9	-5.2-7.2	22.6-34.1	44.9-53.1	34.8-44.8	9.8-21.5	0.2-12.3
7.67	38.6-47.3	-6.9-5.9	-5.1-7.3	22.7-34.1	45.0-53.1	34.9-44.8	10.0-21.6	0.2-12.3
8.00	38.5-47.2	-6.9-5.9	-5.0-7.3	22.7-34.1	45.1-53.2	34.9-44.8	10.0-21.6	0.2-12.3
8.33	38.4-47.2	-6.9-5.9	-5.0-7.4	22.6-34.0	45.2-53.3	34.9-44.8	10.0-21.6	0.2-12.3
8.67	38.4-47.1	-6.8-6.0	-4.9-7.4	22.6-34.0	45.3-53.3	35.0-44.9	10.1-21.7	0.3-12.4
9.00	38.5-47.2	-6.8-6.0	-4.8-7.5	22.6-33.9	45.4-53.4	35.0-44.9	10.1-21.7	0.3-12.4
9.33	38.4-47.1	-6.8-6.0	-4.8-7.5	22.5-33.9	45.4-53.4	35.0-44.9	10.0-21.6	0.3-12.4
9.67	38.4-47.0	-6.8-6.0	-4.8-7.5	22.5-33.9	45.4-53.5	35.0-44.8	9.9-21.5	0.3-12.4
10.00	38.3-47.0	-6.8-5.9	-4.8-7.5	22.4-33.8	45.5-53.5	34.9-44.8	9.9-21.5	0.3-12.4

Table E.22: South / Mass Flux / Negative Mid-Day

i \ j	1	2	3	4	6	9	10	11
1	4.5-8.0	-2.6-1.7	-2.5-2.0	1.6-6.6	-2.8-4.1	1.9-8.3	-2.4-2.3	-2.4-2.1
2	-2.6-1.7	-0.1-0.2	-0.3-0.4	-0.3-0.4	-2.9-1.7	-1.6-0.8	-0.4-0.3	-0.4-0.3
3	-2.5-2.0	-0.3-0.4	-0.3-0.4	-1.0-0.4	-2.1-2.5	-1.5-1.1	-0.8-0.5	-0.9-0.6
4	1.6-6.6	-0.3-0.4	-1.0-0.4	-1.0-1.8	-4.0-2.5	-1.3-3.7	-2.6-2.2	-2.6-2.1
6	-2.8-4.1	-2.9-1.7	-2.1-2.5	-4.0-2.5	29.8-35.3	-4.0-5.2	-2.3-3.0	-1.9-1.9
9	1.9-8.3	-1.6-0.8	-1.5-1.1	-1.3-3.7	-4.0-5.2	9.4-12.8	-2.9-1.0	-2.1-1.4
10	-2.4-2.3	-0.4-0.3	-0.8-0.5	-2.6-2.2	-2.3-3.0	-2.9-1.0	-0.7-1.4	-1.9-1.7
11	-2.4-2.1	-0.4-0.3	-0.9-0.6	-2.6-2.1	-1.9-1.9	-2.1-1.4	-1.9-1.7	2.3-3.5
Total	38.8-47.6	-7.2-5.8	-5.8-6.8	22.6-34.2	44.2-52.6	34.5-44.7	9.2-21.3	-0.2-11.9
Higher	28.0	0.7	1.3	24.2	15.4	23.4	16.0	4.0

Table E.23: North / Negative Mass Flux with Time (Total-effect)

t \ i	1	2	3	4	5	6	7	8
0.33	16.9-27.8	0.4-12.1	-6.9-5.2	11.5-22.3	64.6-71.0	12.4-23.6	4.5-16.2	-2.2-9.4
0.67	21.5-31.5	-1.0-9.9	-5.8-5.5	11.2-21.8	67.9-73.8	15.2-25.7	4.4-15.6	-1.6-9.2
1.00	22.4-32.2	-2.6-8.5	-5.7-5.6	10.6-21.2	68.7-74.4	15.4-25.8	4.7-15.6	-2.1-8.7
1.33	22.5-32.2	-3.8-7.3	-5.6-5.6	10.2-20.8	69.2-74.8	15.5-25.8	4.5-15.4	-2.5-8.4
1.67	22.2-31.8	-5.1-6.0	-5.8-5.4	10.1-20.6	69.4-75.1	15.0-25.2	3.8-14.6	-2.8-8.1
2.00	22.4-31.9	-5.5-5.6	-6.0-5.2	10.0-20.4	69.6-75.2	14.8-25.0	3.6-14.5	-2.8-7.9
2.33	22.5-31.9	-5.8-5.1	-6.0-5.1	9.7-20.1	70.0-75.5	14.6-24.8	3.6-14.4	-3.0-7.7
2.67	22.7-32.0	-5.7-5.2	-5.5-5.4	9.8-20.1	70.4-75.9	14.8-25.0	3.8-14.6	-2.8-7.8
3.00	22.5-31.9	-5.9-4.9	-5.4-5.5	9.7-19.9	70.6-76.1	14.8-24.9	3.7-14.4	-3.0-7.7
3.33	22.5-31.8	-6.1-4.7	-5.4-5.4	9.7-19.9	70.8-76.3	14.9-25.0	3.7-14.3	-3.0-7.6
3.67	22.3-31.6	-6.3-4.5	-5.6-5.3	9.4-19.7	71.0-76.5	14.7-24.8	3.6-14.2	-3.2-7.3
4.00	22.4-31.7	-6.3-4.5	-5.5-5.3	9.5-19.7	71.3-76.8	14.9-25.0	3.7-14.3	-3.2-7.3
4.33	22.3-31.6	-6.4-4.3	-5.5-5.3	9.5-19.7	71.6-77.0	14.8-24.9	3.7-14.3	-3.4-7.2
4.67	22.2-31.5	-6.7-4.1	-5.5-5.2	9.4-19.6	71.7-77.2	14.8-24.9	3.5-14.2	-3.5-7.0
5.00	22.2-31.4	-6.7-4.1	-5.5-5.2	9.4-19.6	71.9-77.3	14.8-24.8	3.5-14.1	-3.6-6.9
5.33	22.2-31.4	-6.7-4.1	-5.4-5.2	9.5-19.6	72.1-77.5	14.9-24.9	3.6-14.2	-3.6-6.9
5.67	22.1-31.3	-6.8-4.1	-5.5-5.2	9.4-19.6	72.2-77.5	14.8-24.8	3.6-14.1	-3.6-6.9
6.00	22.0-31.3	-6.9-4.0	-5.6-5.1	9.3-19.5	72.2-77.5	14.7-24.7	3.5-14.0	-3.7-6.8
6.33	22.0-31.2	-6.9-3.9	-5.6-5.1	9.3-19.4	72.2-77.6	14.6-24.7	3.5-14.0	-3.7-6.8
6.67	21.9-31.2	-6.9-3.9	-5.5-5.1	9.2-19.4	72.2-77.5	14.7-24.7	3.5-14.0	-3.7-6.8
7.00	21.9-31.1	-6.9-3.9	-5.5-5.1	9.2-19.3	72.2-77.6	14.7-24.7	3.5-14.0	-3.7-6.7
7.33	21.9-31.1	-6.9-3.9	-5.6-5.0	9.1-19.3	72.1-77.5	14.6-24.7	3.5-13.9	-3.7-6.7
7.67	21.8-31.0	-6.9-3.9	-5.7-4.9	9.1-19.2	72.1-77.5	14.6-24.6	3.4-13.9	-3.8-6.6
8.00	21.8-30.9	-6.9-3.9	-5.8-4.9	9.0-19.1	72.2-77.6	14.6-24.6	3.4-13.8	-3.8-6.6
8.33	21.7-30.9	-6.9-3.8	-5.8-4.9	9.0-19.1	72.2-77.6	14.5-24.5	3.4-13.8	-3.8-6.6
8.67	21.7-30.9	-7.0-3.8	-5.8-4.8	8.9-19.1	72.3-77.6	14.5-24.5	3.3-13.8	-3.8-6.6
9.00	21.6-30.8	-7.0-3.8	-5.8-4.8	8.9-19.0	72.3-77.7	14.5-24.4	3.3-13.8	-3.8-6.6
9.33	21.6-30.8	-7.0-3.7	-5.9-4.7	8.8-19.0	72.3-77.7	14.4-24.4	3.3-13.7	-3.8-6.5
9.67	21.5-30.7	-7.0-3.7	-5.9-4.7	8.8-18.9	72.4-77.8	14.4-24.4	3.3-13.7	-3.8-6.5
10.00	21.5-30.7	-7.0-3.7	-5.9-4.7	8.8-18.9	72.4-77.8	14.4-24.4	3.3-13.7	-3.8-6.5

Table E.24: North / Mass Flux / Negative Mid-Day

i \ j	1	2	3	4	6	9	10	11
1	3.4-6.3	-1.6-2.1	-1.2-2.6	2.4-6.7	-3.9-6.9	0.5-4.8	-0.8-3.2	-1.1-2.6
2	-1.6-2.1	-0.3-0.2	-0.6-0.4	-0.5-0.5	-5.9-3.7	-0.6-0.6	-0.6-0.4	-0.6-0.4
3	-1.2-2.6	-0.6-0.4	-0.6-0.1	0.3-1.4	-5.5-4.0	-0.1-1.1	0.1-1.4	0.2-1.2
4	2.4-6.7	-0.5-0.5	0.3-1.4	-0.9-0.8	-4.3-5.7	-1.4-1.8	-2.0-1.5	-2.5-0.8
6	-3.9-6.9	-5.9-3.7	-5.5-4.0	-4.3-5.7	52.0-59.3	-3.5-4.5	-2.9-2.2	-1.7-1.3
9	0.5-4.8	-0.6-0.6	-0.1-1.1	-1.4-1.8	-3.5-4.5	2.9-4.7	-1.0-1.7	-0.6-1.9
10	-0.8-3.2	-0.6-0.4	0.1-1.4	-2.0-1.5	-2.9-2.2	-1.0-1.7	-0.2-1.4	-0.9-1.8
11	-1.1-2.6	-0.6-0.4	0.2-1.2	-2.5-0.8	-1.7-1.3	-0.6-1.9	-0.9-1.8	1.6-2.3
Total	22.2-31.4	-6.7-4.1	-5.5-5.2	9.4-19.6	71.9-77.3	14.8-24.8	3.5-14.1	-3.6-6.9
Higher	10.3	-0.1	-2.5	9.4	18.6	11.1	6.2	-1.7

Table E.25: Control / Mass Flux / Negative Mean

i \ j	1	2	3	4	6	9	10	11
1	1.2-3.2	-0.6-2.7	-0.6-2.8	1.1-4.4	-1.8-3.0	-0.3-3.8	-0.4-3.1	-0.4-3.0
2	-0.6-2.7	-0.0-0.2	-0.4-0.1	-0.3-0.2	-1.4-1.3	-2.2-0.5	-0.5-0.1	-0.4-0.3
3	-0.6-2.8	-0.4-0.1	-0.2-0.2	-0.4-0.4	-1.4-1.3	-2.1-0.6	-0.6-0.2	-0.5-0.3
4	1.1-4.4	-0.3-0.2	-0.4-0.4	-0.9-0.7	-2.2-2.0	-1.6-2.0	-1.7-1.6	-1.7-1.5
6	-1.8-3.0	-1.4-1.3	-1.4-1.3	-2.2-2.0	23.5-26.9	-0.8-5.7	0.5-4.8	-2.0-1.9
9	-0.3-3.8	-2.2-0.5	-2.1-0.6	-1.6-2.0	-0.8-5.7	18.8-21.9	-1.4-1.7	1.3-4.1
10	-0.4-3.1	-0.5-0.1	-0.6-0.2	-1.7-1.6	0.5-4.8	-1.4-1.7	2.3-4.7	0.1-4.4
11	-0.4-3.0	-0.4-0.3	-0.5-0.3	-1.7-1.5	-2.0-1.9	1.3-4.1	0.1-4.4	6.2-8.1
Total	18.4-25.7	-3.4-4.9	-2.6-5.6	9.3-17.2	42.6-48.5	42.1-47.9	21.7-28.8	14.5-21.8
Higher	10.0	1.0	1.6	10.7	14.9	19.0	15.7	5.0

Table E.26: South / Mass Flux / Negative Mean

i \ j	1	2	3	4	6	9	10	11
1	4.8-8.1	-2.7-1.7	-2.5-1.9	1.6-6.6	-2.7-4.2	1.7-8.1	-2.3-2.3	-2.3-2.1
2	-2.7-1.7	-0.1-0.2	-0.2-0.3	-0.4-0.3	-2.9-1.7	-1.1-1.3	-0.2-0.4	-0.3-0.3
3	-2.5-1.9	-0.2-0.3	-0.2-0.4	-0.8-0.3	-2.0-2.7	-1.5-1.0	-0.7-0.4	-0.7-0.4
4	1.6-6.6	-0.4-0.3	-0.8-0.3	-1.1-1.7	-3.9-2.5	-1.5-3.5	-2.6-2.3	-2.7-2.0
6	-2.7-4.2	-2.9-1.7	-2.0-2.7	-3.9-2.5	29.7-35.0	-4.2-5.1	-2.4-2.8	-2.0-1.7
9	1.7-8.1	-1.1-1.3	-1.5-1.0	-1.5-3.5	-4.2-5.1	9.6-13.1	-2.8-1.0	-1.9-1.5
10	-2.3-2.3	-0.2-0.4	-0.7-0.4	-2.6-2.3	-2.4-2.8	-2.8-1.0	-0.7-1.5	-1.7-1.8
11	-2.3-2.1	-0.3-0.3	-0.7-0.4	-2.7-2.0	-2.0-1.7	-1.9-1.5	-1.7-1.8	2.5-3.7
Total	38.7-47.4	-6.9-5.8	-6.0-6.5	22.9-34.2	43.4-51.9	34.7-44.7	8.8-20.7	0.1-12.2
Higher	27.7	0.2	0.9	24.7	15.0	23.2	15.2	3.9

Table E.27: North / Mass Flux / Negative Mean

i \ j	1	2	3	4	6	9	10	11
1	3.5-6.3	-1.8-1.8	-1.4-2.3	2.1-6.3	-4.4-6.5	0.2-4.3	-1.0-2.8	-1.3-2.4
2	-1.8-1.8	-0.2-0.1	-0.4-0.4	-0.3-0.5	-3.6-6.1	-0.5-0.4	-0.5-0.3	-0.4-0.3
3	-1.4-2.3	-0.4-0.4	-0.5-0.0	0.2-1.1	-6.2-3.5	-0.2-0.8	0.0-1.0	0.1-1.0
4	2.1-6.3	-0.3-0.5	0.2-1.1	-0.8-0.9	-4.8-5.3	-1.6-1.6	-2.2-1.1	-2.7-0.6
6	-4.4-6.5	-3.6-6.1	-6.2-3.5	-4.8-5.3	52.6-60.0	-3.7-4.2	-2.0-2.8	-1.5-1.3
9	0.2-4.3	-0.5-0.4	-0.2-0.8	-1.6-1.6	-3.7-4.2	3.2-4.9	-1.1-1.3	-0.5-1.7
10	-1.0-2.8	-0.5-0.3	0.0-1.0	-2.2-1.1	-2.0-2.8	-1.1-1.3	0.2-1.6	-0.8-1.7
11	-1.3-2.4	-0.4-0.3	0.1-1.0	-2.7-0.6	-1.5-1.3	-0.5-1.7	-0.8-1.7	1.7-2.3
Total	21.5-30.6	-6.3-4.5	-6.0-4.9	9.3-19.2	71.4-76.8	14.5-24.3	3.2-13.8	-3.2-7.4
Higher	11.7	-2.0	-1.4	10.6	16.1	11.8	5.9	-0.7

Table E.28: Control / Mass Flux / Maximum

i \ j	1	2	3	4	6	9	10	11
1	-0.6-0.5	-0.9-0.9	-0.9-0.8	-0.5-1.5	-1.0-0.9	-0.6-1.2	-3.2-2.8	-0.2-3.2
2	-0.9-0.9	-0.0-0.4	-0.5-0.3	-0.3-0.4	-1.0-0.2	-0.5-0.4	-3.3-2.3	-0.9-1.8
3	-0.9-0.8	-0.5-0.3	-0.1-0.0	-0.1-0.3	-0.5-0.2	-0.3-0.2	-3.4-2.1	-0.5-2.0
4	-0.5-1.5	-0.3-0.4	-0.1-0.3	-0.6-0.4	-0.4-1.4	-0.4-1.3	-2.5-3.3	0.0-3.3
6	-1.0-0.9	-1.0-0.2	-0.5-0.2	-0.4-1.4	4.5-6.2	-0.9-2.0	1.6-10.0	2.8-8.4
9	-0.6-1.2	-0.5-0.4	-0.3-0.2	-0.4-1.3	-0.9-2.0	1.5-3.0	0.3-7.3	1.7-5.3
10	-3.2-2.8	-3.3-2.3	-3.4-2.1	-2.5-3.3	1.6-10.0	0.3-7.3	17.9-23.0	21.2-30.9
11	-0.2-3.2	-0.9-1.8	-0.5-2.0	0.0-3.3	2.8-8.4	1.7-5.3	21.2-30.9	8.7-11.8
Total	-4.5-10.6	-10.4-5.2	-7.8-6.9	-4.2-11.0	11.6-24.8	11.9-26.0	62.7-70.0	47.4-56.6
Higher	1.1	-2.3	-0.3	-0.3	0.9	8.1	11.2	2.1

Table E.29: South / Mass Flux / Maximum

i \ j	1	2	3	4	6	9	10	11
1	0.3-4.1	-0.7-3.3	-0.9-3.0	4.8-10.7	0.5-6.4	3.4-8.8	-1.3-5.1	-0.3-3.6
2	-0.7-3.3	-0.2-0.3	-0.6-0.4	-0.7-0.6	-2.7-0.8	-0.8-0.5	-2.0-0.5	-0.7-0.3
3	-0.9-3.0	-0.6-0.4	-0.3-0.3	-0.5-0.7	-2.4-1.2	-0.7-0.4	-2.4-0.1	-0.7-0.5
4	4.8-10.7	-0.7-0.6	-0.5-0.7	-1.5-1.5	-3.4-2.7	-1.0-4.2	-2.6-3.3	-1.8-2.7
6	0.5-6.4	-2.7-0.8	-2.4-1.2	-3.4-2.7	16.8-21.0	-2.2-3.4	-0.2-6.9	0.4-4.4
9	3.4-8.8	-0.8-0.5	-0.7-0.4	-1.0-4.2	-2.2-3.4	0.8-3.1	-1.9-2.7	-1.8-1.5
10	-1.3-5.1	-2.0-0.5	-2.4-0.1	-2.6-3.3	-0.2-6.9	-1.9-2.7	9.4-13.7	1.0-5.1
11	-0.3-3.6	-0.7-0.3	-0.7-0.5	-1.8-2.7	0.4-4.4	-1.8-1.5	1.0-5.1	1.8-3.1
Total	39.9-49.2	-0.3-12.1	-1.3-11.2	31.5-41.9	44.4-53.7	27.1-37.8	38.1-48.0	11.7-22.7
Higher	19.1	6.8	5.7	26.9	22.3	22.2	24.4	7.6

Table E.30: North / Mass Flux / Maximum

i \ j	1	2	3	4	6	9	10	11
1	1.4-4.0	-2.0-1.5	-1.6-1.9	1.9-5.9	0.3-5.7	0.4-4.1	-2.8-1.9	-1.8-1.8
2	-2.0-1.5	-0.1-0.4	-0.7-0.2	-0.6-0.4	-2.2-1.5	-0.7-0.3	-2.0-1.3	-0.6-0.4
3	-1.6-1.9	-0.7-0.2	-0.1-0.3	-0.6-0.4	-2.0-1.6	-0.5-0.3	-2.3-0.8	-0.5-0.4
4	1.9-5.9	-0.6-0.4	-0.6-0.4	0.6-2.6	-3.1-2.0	-1.9-1.5	-2.7-1.9	-1.5-1.9
6	0.3-5.7	-2.2-1.5	-2.0-1.6	-3.1-2.0	23.4-27.0	-1.1-2.5	2.4-9.7	1.5-4.6
9	0.4-4.1	-0.7-0.3	-0.5-0.3	-1.9-1.5	-1.1-2.5	1.2-2.5	-2.7-1.2	-1.6-0.9
10	-2.8-1.9	-2.0-1.3	-2.3-0.8	-2.7-1.9	2.4-9.7	-2.7-1.2	20.2-23.7	1.8-4.8
11	-1.8-1.8	-0.6-0.4	-0.5-0.4	-1.5-1.9	1.5-4.6	-1.6-0.9	1.8-4.8	4.7-5.8
Total	18.5-27.4	-5.3-4.9	-6.1-4.2	16.0-25.1	43.2-50.1	6.9-16.8	37.1-44.3	6.8-16.0
Higher	11.6	1.2	0.2	16.2	9.7	8.7	12.1	0.1

Table E.31: Control / Mass Flux / Minimum

i \ j	1	2	3	4	6	9	10	11
1	0.6-2.6	-0.2-3.2	-0.3-3.2	1.4-4.9	-1.6-3.3	-0.3-3.8	-0.3-3.3	-0.2-3.2
2	-0.2-3.2	-0.0-0.2	-0.4-0.1	-0.4-0.1	-1.4-1.2	-2.2-0.5	-0.6-0.0	-0.5-0.2
3	-0.3-3.2	-0.4-0.1	-0.2-0.3	-0.5-0.3	-1.3-1.5	-1.9-0.9	-0.5-0.4	-0.5-0.4
4	1.4-4.9	-0.4-0.1	-0.5-0.3	-1.1-0.6	-2.3-2.1	-1.4-2.3	-1.5-1.9	-1.6-1.7
6	-1.6-3.3	-1.4-1.2	-1.3-1.5	-2.3-2.1	22.6-26.0	-0.7-5.8	0.6-5.0	-2.3-1.6
9	-0.3-3.8	-2.2-0.5	-1.9-0.9	-1.4-2.3	-0.7-5.8	19.7-22.9	-1.3-1.9	1.4-4.2
10	-0.3-3.3	-0.6-0.0	-0.5-0.4	-1.5-1.9	0.6-5.0	-1.3-1.9	2.7-5.0	0.3-4.6
11	-0.2-3.2	-0.5-0.2	-0.5-0.4	-1.6-1.7	-2.3-1.6	1.4-4.2	0.3-4.6	6.5-8.4
Total	18.8-26.1	-2.7-5.5	-1.9-6.3	9.6-17.5	41.9-47.8	43.5-49.3	22.7-29.9	15.0-22.3
Higher	9.1	1.5	1.5	10.3	14.8	18.6	15.6	4.9

Table E.32: South / Mass Flux / Minimum

i \ j	1	2	3	4	6	9	10	11
1	4.0-7.5	-2.5-2.0	-2.5-2.2	1.8-7.0	-2.5-4.3	2.2-8.5	-2.2-2.7	-2.3-2.4
2	-2.5-2.0	-0.1-0.2	-0.4-0.3	-0.5-0.3	-1.8-2.7	-1.1-1.4	-0.3-0.4	-0.4-0.4
3	-2.5-2.2	-0.4-0.3	-0.3-0.4	-1.0-0.4	-2.3-2.4	-1.5-1.2	-0.9-0.5	-0.9-0.6
4	1.8-7.0	-0.5-0.3	-1.0-0.4	-1.1-1.7	-4.3-2.2	-1.4-3.6	-2.5-2.3	-2.6-2.2
6	-2.5-4.3	-1.8-2.7	-2.3-2.4	-4.3-2.2	28.9-34.3	-3.8-5.4	-2.1-3.3	-1.7-2.1
9	2.2-8.5	-1.1-1.4	-1.5-1.2	-1.4-3.6	-3.8-5.4	10.3-13.9	-2.7-1.3	-1.8-1.8
10	-2.2-2.7	-0.3-0.4	-0.9-0.5	-2.5-2.3	-2.1-3.3	-2.7-1.3	-0.2-1.8	-1.7-1.8
11	-2.3-2.4	-0.4-0.4	-0.9-0.6	-2.6-2.2	-1.7-2.1	-1.8-1.8	-1.7-1.8	2.7-3.9
Total	38.8-47.6	-6.7-6.0	-5.4-7.2	21.8-33.3	42.2-50.4	35.8-45.9	9.0-20.9	0.0-12.2
Higher	26.9	-0.7	1.7	23.6	12.8	22.1	14.1	2.9

Table E.33: North / Mass Flux / Minimum

i \ j	1	2	3	4	6	9	10	11
1	2.8-5.8	-1.5-2.5	-1.0-3.0	2.9-7.3	-3.8-6.4	0.7-5.0	-0.6-3.5	-1.0-2.9
2	-1.5-2.5	-0.3-0.1	-0.1-0.7	0.1-0.9	-5.7-3.3	-0.5-0.5	-0.1-0.7	-0.1-0.7
3	-1.0-3.0	-0.1-0.7	-0.6-0.0	0.1-1.3	-5.6-3.3	-0.3-1.0	-0.0-1.3	0.0-1.1
4	2.9-7.3	0.1-0.9	0.1-1.3	-0.8-1.1	-4.8-4.5	-1.4-1.9	-1.7-1.9	-2.5-1.1
6	-3.8-6.4	-5.7-3.3	-5.6-3.3	-4.8-4.5	50.2-57.1	-3.3-4.5	-3.2-2.0	-1.7-1.2
9	0.7-5.0	-0.5-0.5	-0.3-1.0	-1.4-1.9	-3.3-4.5	3.7-5.5	-1.2-1.5	-0.6-1.8
10	-0.6-3.5	-0.1-0.7	-0.0-1.3	-1.7-1.9	-3.2-2.0	-1.2-1.5	0.7-2.4	-0.8-2.0
11	-1.0-2.9	-0.1-0.7	0.0-1.1	-2.5-1.1	-1.7-1.2	-0.6-1.8	-0.8-2.0	1.9-2.6
Total	22.0-31.0	-6.8-3.9	-6.2-4.5	9.6-19.6	68.6-74.1	14.9-24.6	4.0-14.5	-3.7-6.7
Higher	9.1	-2.0	-3.0	8.6	19.1	10.3	5.1	-2.8

### E.3 Snow Surface Temperature

Table E.34: Control / Temp. at 0cm with Time (Total-effect)

t \ i	1	2	3	4	5	6	7	8
0.33	9.3-18.4	-4.7-4.8	-4.8-4.7	22.4-30.7	59.0-64.0	9.3-18.9	19.5-28.0	-4.0-5.4
0.67	10.1-19.0	-4.0-5.3	-5.5-4.0	17.4-25.9	63.9-68.7	9.9-19.2	21.0-29.3	-4.7-4.7
1.00	10.5-19.3	-4.6-4.7	-5.3-4.0	15.1-23.7	66.4-71.1	10.5-19.7	22.1-30.2	-4.6-4.6
1.33	11.1-19.7	-4.4-4.8	-4.8-4.4	14.6-23.3	67.9-72.5	11.3-20.5	23.0-31.0	-4.0-5.1
1.67	11.4-19.9	-4.4-4.8	-4.5-4.6	14.1-22.9	68.7-73.3	11.7-20.9	23.3-31.2	-3.9-5.2
2.00	11.4-19.8	-4.6-4.6	-4.7-4.5	13.7-22.4	69.2-73.7	11.9-21.1	23.4-31.3	-4.1-5.0
2.33	11.3-19.8	-4.7-4.5	-4.7-4.5	13.2-22.0	69.5-74.0	12.0-21.1	23.5-31.4	-4.2-4.9
2.67	11.4-19.8	-4.8-4.4	-4.7-4.4	13.0-21.7	69.9-74.4	12.2-21.3	23.6-31.4	-4.2-4.9
3.00	11.5-19.9	-4.8-4.4	-4.6-4.5	12.9-21.6	70.2-74.7	12.3-21.4	23.7-31.5	-4.1-5.0
3.33	11.5-20.0	-4.8-4.3	-4.6-4.5	12.7-21.4	70.4-74.9	12.5-21.6	23.7-31.5	-4.1-5.0
3.67	11.6-20.0	-4.8-4.3	-4.5-4.6	12.5-21.3	70.7-75.1	12.7-21.7	23.7-31.5	-4.1-5.0
4.00	11.6-20.0	-4.8-4.2	-4.5-4.6	12.4-21.2	70.8-75.2	12.8-21.8	23.7-31.5	-4.1-5.0
4.33	11.6-20.0	-4.8-4.3	-4.4-4.7	12.3-21.0	71.0-75.4	12.9-21.9	23.7-31.5	-4.0-5.0
4.67	11.7-20.1	-4.8-4.3	-4.3-4.8	12.2-21.0	71.1-75.5	13.1-22.0	23.8-31.6	-4.0-5.0
5.00	11.9-20.3	-4.6-4.5	-4.1-4.9	12.3-21.0	71.3-75.7	13.3-22.2	24.0-31.7	-3.8-5.2
5.33	11.8-20.3	-4.6-4.5	-4.1-5.0	12.2-21.0	71.5-75.8	13.4-22.3	24.0-31.8	-3.8-5.2
5.67	11.9-20.3	-4.6-4.4	-4.1-5.0	12.1-20.9	71.5-75.9	13.4-22.3	24.0-31.8	-3.8-5.2
6.00	11.9-20.3	-4.6-4.4	-4.0-5.0	12.0-20.8	71.6-76.0	13.6-22.4	24.1-31.8	-3.8-5.2
6.33	11.9-20.3	-4.6-4.4	-4.0-5.0	12.0-20.7	71.8-76.1	13.7-22.5	24.1-31.8	-3.7-5.2
6.67	11.9-20.3	-4.6-4.4	-4.0-5.0	11.9-20.6	71.9-76.1	13.8-22.6	24.1-31.8	-3.8-5.2
7.00	11.9-20.3	-4.6-4.4	-4.1-5.0	11.8-20.6	71.9-76.2	13.8-22.6	24.1-31.8	-3.8-5.2
7.33	11.9-20.3	-4.7-4.3	-4.1-4.9	11.8-20.5	71.9-76.2	13.8-22.6	24.1-31.8	-3.8-5.2
7.67	11.9-20.3	-4.7-4.3	-4.1-4.9	11.7-20.4	72.0-76.3	13.8-22.6	24.0-31.8	-3.8-5.1
8.00	11.9-20.3	-4.7-4.3	-4.1-4.9	11.6-20.4	72.1-76.3	13.8-22.6	24.0-31.8	-3.8-5.1
8.33	11.9-20.3	-4.7-4.3	-4.1-4.9	11.6-20.4	72.1-76.4	13.9-22.6	24.0-31.8	-3.8-5.1
8.67	11.9-20.3	-4.7-4.3	-4.1-4.9	11.6-20.3	72.1-76.4	13.9-22.6	24.0-31.7	-3.8-5.1
9.00	11.9-20.3	-4.7-4.2	-4.0-4.9	11.6-20.3	72.2-76.4	13.9-22.6	24.0-31.7	-3.7-5.2
9.33	12.0-20.3	-4.8-4.2	-4.0-5.0	11.6-20.3	72.2-76.5	13.9-22.6	24.0-31.7	-3.7-5.2
9.67	12.0-20.3	-4.7-4.3	-4.0-5.0	11.6-20.3	72.3-76.5	14.0-22.7	24.0-31.8	-3.7-5.2
10.00	12.0-20.3	-4.7-4.3	-4.0-5.0	11.6-20.3	72.3-76.6	14.0-22.7	24.0-31.7	-3.7-5.2

Table E.35: Control / Temp. at 0cm / Mid-day

i \ j	1	2	3	4	6	9	10	11
1	-1.1-1.2	-1.0-2.9	-1.0-2.9	0.6-4.9	-3.8-3.8	-0.7-3.7	-0.5-3.6	-1.0-2.8
2	-1.0-2.9	-0.1-0.3	-0.5-0.3	-0.4-0.4	-4.2-3.1	-0.5-0.4	-0.9-0.6	-0.5-0.3
3	-1.0-2.9	-0.5-0.3	-0.1-0.3	-0.6-0.3	-4.1-3.3	-0.6-0.3	-0.8-0.8	-0.6-0.3
4	0.6-4.9	-0.4-0.4	-0.6-0.3	0.5-2.4	-3.0-4.9	-1.5-2.4	-1.1-2.4	-1.5-1.9
6	-3.8-3.8	-4.2-3.1	-4.1-3.3	-3.0-4.9	47.1-52.6	1.5-7.1	-1.1-5.9	-0.3-1.7
9	-0.7-3.7	-0.5-0.4	-0.6-0.3	-1.5-2.4	1.5-7.1	-1.7-0.8	1.5-5.8	-1.3-2.8
10	-0.5-3.6	-0.9-0.6	-0.8-0.8	-1.1-2.4	-1.1-5.9	1.5-5.8	10.1-12.6	-0.3-2.9
11	-1.0-2.8	-0.5-0.3	-0.6-0.3	-1.5-1.9	-0.3-1.7	-1.3-2.8	-0.3-2.9	-0.1-0.4
Total	11.9-20.3	-4.6-4.5	-4.1-4.9	12.3-21.0	71.3-75.7	13.3-22.2	24.0-31.7	-3.8-5.2
Higher	7.5	-0.3	0.3	10.3	16.2	7.7	7.0	-3.0

Table E.36: South / Temp. at 0cm with Time (Total-effect)

t \ i	1	2	3	4	5	6	7	8
0.33	23.1-34.9	-2.3-11.6	-8.6-5.8	38.2-48.5	44.3-53.4	10.0-23.2	12.7-25.3	-8.1-6.4
0.67	25.7-36.9	-7.2-6.9	-6.4-7.2	32.7-43.5	50.6-59.1	10.0-22.8	14.4-26.7	-5.6-8.0
1.00	26.9-37.7	-5.2-7.9	-7.5-5.8	29.9-40.8	54.2-62.2	9.6-22.1	15.7-27.4	-6.6-6.7
1.33	27.4-38.1	-6.6-6.5	-8.0-5.1	28.2-39.2	56.2-64.0	9.5-21.9	16.3-27.8	-7.0-6.1
1.67	27.9-38.3	-6.6-6.3	-7.5-5.4	27.5-38.4	57.5-65.1	9.6-22.0	17.3-28.5	-6.8-6.2
2.00	27.8-38.1	-7.1-5.7	-7.6-5.2	26.4-37.3	58.1-65.6	9.3-21.6	17.1-28.3	-7.1-5.7
2.33	27.9-38.0	-7.6-5.2	-7.8-4.9	25.7-36.6	58.5-65.9	9.2-21.4	17.1-28.2	-7.1-5.6
2.67	27.8-37.9	-7.7-5.0	-7.9-4.7	25.1-36.0	59.0-66.3	9.2-21.3	17.2-28.2	-7.1-5.6
3.00	27.7-37.8	-7.8-4.9	-8.2-4.4	24.7-35.6	59.3-66.6	9.2-21.3	17.4-28.4	-7.1-5.5
3.33	27.8-37.8	-7.9-4.7	-8.2-4.4	24.3-35.3	59.7-66.9	9.4-21.3	17.7-28.5	-7.0-5.5
3.67	28.0-38.0	-7.7-4.8	-8.0-4.5	24.4-35.3	60.2-67.4	9.7-21.6	18.1-28.9	-6.7-5.8
4.00	28.2-38.1	-7.6-4.9	-7.6-4.8	24.4-35.3	60.6-67.8	10.1-21.8	18.5-29.2	-6.4-6.1
4.33	28.3-38.1	-7.7-4.7	-7.6-4.7	24.1-35.0	60.9-68.0	10.0-21.8	18.7-29.3	-6.4-5.9
4.67	28.4-38.1	-7.6-4.7	-7.5-4.8	24.0-34.9	61.2-68.2	10.1-21.9	18.9-29.4	-6.4-5.9
5.00	28.4-38.2	-7.6-4.7	-7.4-4.9	23.9-34.8	61.4-68.4	10.2-22.0	19.0-29.4	-6.3-6.0
5.33	28.5-38.1	-7.6-4.6	-7.3-4.9	23.8-34.6	61.6-68.5	10.3-22.0	19.0-29.5	-6.2-6.0
5.67	28.5-38.1	-7.7-4.5	-7.3-4.9	23.6-34.5	61.7-68.6	10.3-22.0	19.1-29.5	-6.2-6.0
6.00	28.5-38.1	-7.7-4.4	-7.2-4.9	23.6-34.4	61.7-68.7	10.3-22.0	19.2-29.6	-6.1-6.0
6.33	28.5-38.0	-7.7-4.4	-7.2-4.9	23.4-34.3	61.8-68.7	10.3-21.9	19.2-29.5	-6.1-6.0
6.67	28.4-38.0	-7.8-4.4	-7.2-4.9	23.3-34.1	61.8-68.8	10.3-21.9	19.3-29.6	-6.1-6.0
7.00	28.4-37.9	-7.7-4.4	-7.1-4.9	23.3-34.1	61.9-68.8	10.4-21.9	19.4-29.6	-6.0-6.0
7.33	28.4-37.9	-7.7-4.4	-7.0-4.9	23.3-34.0	62.0-68.9	10.4-21.9	19.5-29.7	-6.0-6.0
7.67	28.3-37.9	-7.7-4.4	-7.0-5.0	23.3-34.0	62.1-69.0	10.4-21.9	19.6-29.7	-6.0-6.0
8.00	28.3-37.8	-7.7-4.4	-6.9-5.0	23.2-33.9	62.2-69.0	10.4-21.9	19.6-29.7	-5.9-6.1
8.33	28.3-37.8	-7.6-4.4	-6.9-5.0	23.1-33.9	62.2-69.1	10.4-21.9	19.6-29.7	-5.9-6.1
8.67	28.3-37.8	-7.6-4.4	-6.8-5.1	23.1-33.8	62.2-69.1	10.5-22.0	19.6-29.8	-5.8-6.1
9.00	28.3-37.8	-7.5-4.5	-6.7-5.2	23.1-33.7	62.3-69.1	10.6-22.0	19.6-29.8	-5.8-6.1
9.33	28.3-37.8	-7.5-4.4	-6.7-5.2	23.0-33.6	62.3-69.1	10.5-22.0	19.6-29.7	-5.8-6.1
9.67	28.3-37.7	-7.6-4.4	-6.7-5.1	22.9-33.6	62.3-69.1	10.5-21.9	19.6-29.7	-5.8-6.1
10.00	28.2-37.7	-7.6-4.4	-6.7-5.1	22.9-33.5	62.3-69.1	10.5-21.9	19.6-29.6	-5.8-6.0

Table E.37: South / Temp. at 0cm / Mid-day

i \ j	1	2	3	4	6	9	10	11
1	-3.0-1.8	-3.5-4.7	-3.2-4.9	3.2-11.6	0.4-10.2	-3.8-4.5	-2.5-5.3	-3.2-5.0
2	-3.5-4.7	-0.3-0.4	-0.7-0.7	-1.0-0.6	-3.7-3.9	-0.7-0.6	-0.9-1.0	-0.7-0.7
3	-3.2-4.9	-0.7-0.7	-0.4-0.6	-1.3-0.8	-3.9-3.7	-1.3-0.6	-1.4-1.0	-1.2-0.8
4	3.2-11.6	-1.0-0.6	-1.3-0.8	1.9-6.1	-5.4-4.8	-3.8-3.7	-2.8-4.4	-2.9-4.7
6	0.4-10.2	-3.7-3.9	-3.9-3.7	-5.4-4.8	35.9-42.1	-4.0-3.5	-5.4-2.6	-2.7-2.2
9	-3.8-4.5	-0.7-0.6	-1.3-0.6	-3.8-3.7	-4.0-3.5	-1.9-1.7	-2.9-3.4	-3.2-3.5
10	-2.5-5.3	-0.9-1.0	-1.4-1.0	-2.8-4.4	-5.4-2.6	-2.9-3.4	8.9-12.4	-3.4-1.9
11	-3.2-5.0	-0.7-0.7	-1.2-0.8	-2.9-4.7	-2.7-2.2	-3.2-3.5	-3.4-1.9	-0.6-0.4
Total	28.4-38.2	-7.6-4.7	-7.4-4.9	23.9-34.8	61.4-68.4	10.2-22.0	19.0-29.4	-6.3-6.0
Higher	17.0	-2.1	-1.1	17.0	22.8	16.2	13.3	-0.8



Table E.38: North / Temp. at 0cm with Time (Total-effect)

t \ i	1	2	3	4	5	6	7	8
0.33	11.3-23.5	-0.0-12.9	-6.7-6.8	28.3-38.5	56.2-63.2	1.9-14.8	6.9-19.3	-7.5-6.2
0.67	17.8-29.0	-1.6-10.8	-6.7-6.2	24.6-35.3	63.2-69.5	4.8-17.0	10.0-21.7	-7.0-6.0
1.00	19.3-30.1	-3.8-8.6	-7.0-5.6	22.3-33.1	65.6-71.7	4.9-16.9	11.3-22.6	-7.8-4.9
1.33	19.8-30.5	-5.0-7.2	-7.0-5.4	21.0-31.8	67.1-73.1	4.9-16.8	11.7-22.9	-8.0-4.5
1.67	20.1-30.6	-6.1-5.9	-7.1-5.1	20.2-30.9	67.9-73.8	4.7-16.6	11.6-22.6	-4.7-6.8
2.00	20.5-30.9	-6.8-5.1	-7.3-4.7	19.4-30.1	68.3-74.2	4.5-16.3	11.7-22.6	-5.0-6.4
2.33	20.9-31.2	-7.3-4.6	-7.4-4.6	18.8-29.5	69.0-74.9	4.7-16.3	12.0-22.8	-5.2-6.2
2.67	21.3-31.6	-7.5-4.5	-7.1-4.8	18.7-29.3	69.7-75.5	5.0-16.6	12.3-23.1	-5.0-6.3
3.00	21.5-31.7	-7.8-4.2	-7.1-4.8	18.4-29.0	70.1-75.9	5.1-16.7	12.4-23.1	-5.1-6.2
3.33	21.6-31.8	-4.5-6.8	-7.2-4.7	18.2-28.8	70.4-76.2	5.0-16.6	12.4-23.1	-5.2-6.2
3.67	21.5-31.8	-4.8-6.6	-7.3-4.6	17.7-28.3	70.6-76.4	4.8-16.4	12.3-23.0	-5.4-6.0
4.00	21.6-31.8	-5.0-6.3	-7.5-4.5	17.4-28.1	70.9-76.7	4.8-16.3	12.4-23.1	-5.5-5.8
4.33	21.5-31.8	-5.1-6.2	-7.5-4.4	17.2-27.9	71.1-76.9	4.8-16.3	12.5-23.2	-5.6-5.7
4.67	21.5-31.8	-5.3-6.0	-7.5-4.4	16.9-27.7	71.4-77.1	4.8-16.2	12.5-23.1	-5.7-5.6
5.00	21.5-31.7	-5.3-5.9	-7.5-4.4	16.7-27.5	71.6-77.3	4.8-16.2	12.6-23.1	-5.7-5.5
5.33	21.6-31.8	-5.3-5.9	-7.4-4.4	16.7-27.4	71.8-77.5	4.8-16.2	12.6-23.2	-5.7-5.5
5.67	21.6-31.7	-5.4-5.9	-7.4-4.4	16.6-27.2	71.9-77.6	4.7-16.2	12.6-23.1	-5.7-5.5
6.00	21.6-31.7	-5.4-5.8	-7.5-4.3	16.4-27.1	72.0-77.7	4.7-16.1	12.6-23.1	-5.8-5.4
6.33	21.5-31.6	-5.5-5.7	-7.5-4.3	16.2-26.9	72.1-77.7	4.7-16.0	12.6-23.1	-5.8-5.4
6.67	21.6-31.6	-5.5-5.6	-7.5-4.3	16.1-26.8	72.1-77.7	4.7-16.0	12.7-23.1	-5.8-5.3
7.00	21.6-31.6	-5.5-5.6	-7.5-4.2	16.1-26.7	72.2-77.8	4.7-16.0	12.6-23.0	-5.8-5.3
7.33	21.6-31.6	-5.6-5.6	-7.6-4.2	16.0-26.6	72.2-77.8	4.7-16.0	12.6-23.0	-5.9-5.2
7.67	21.6-31.6	-5.6-5.5	-7.6-4.1	16.0-26.5	72.3-77.9	4.7-16.0	12.6-23.0	-6.0-5.1
8.00	21.6-31.6	-5.7-5.4	-4.2-6.8	15.9-26.4	72.4-77.9	4.7-15.9	12.6-23.0	-6.0-5.1
8.33	21.6-31.6	-5.8-5.4	-4.3-6.7	15.8-26.4	72.4-78.0	4.6-15.9	12.5-22.9	-6.1-5.0
8.67	21.6-31.5	-5.9-5.3	-4.3-6.7	15.7-26.3	72.5-78.0	4.6-15.9	12.5-22.9	-6.2-4.9
9.00	21.5-31.5	-5.9-5.2	-4.4-6.6	15.6-26.2	72.5-78.1	4.6-15.8	12.5-22.9	-6.2-4.9
9.33	21.5-31.5	-6.0-5.2	-4.4-6.6	15.5-26.1	72.6-78.1	4.6-15.8	12.4-22.8	-6.3-4.9
9.67	21.5-31.5	-6.0-5.1	-4.5-6.5	15.4-26.0	72.6-78.1	4.5-15.8	12.4-22.8	-6.3-4.8
10.00	21.5-31.5	-6.0-5.0	-4.5-6.5	15.4-26.0	72.6-78.2	4.6-15.8	12.4-22.8	-6.3-4.8

Table E.39: North / Temp. at 0cm / Mid-day

i \ j	1	2	3	4	6	9	10	11
1	-2.3-2.6	-5.0-3.6	-4.5-4.1	1.2-9.7	-1.5-10.2	-5.1-3.7	-3.3-5.1	-4.6-3.9
2	-5.0-3.6	-0.4-0.3	-0.6-0.8	-0.9-0.8	-5.0-5.0	-0.5-1.0	-0.9-0.8	-0.6-0.8
3	-4.5-4.1	-0.6-0.8	-0.6-0.6	-1.5-0.9	-5.0-4.9	-1.2-1.1	-0.9-1.6	-1.3-1.0
4	1.2-9.7	-0.9-0.8	-1.5-0.9	1.7-5.8	-4.7-6.9	-3.9-3.8	-4.1-3.3	-4.5-3.2
6	-1.5-10.2	-5.0-5.0	-5.0-4.9	-4.7-6.9	48.3-55.8	-3.6-2.9	-4.0-3.8	-1.4-1.7
9	-5.1-3.7	-0.5-1.0	-1.2-1.1	-3.9-3.8	-3.6-2.9	-1.5-1.4	-2.7-2.8	-2.7-3.0
10	-3.3-5.1	-0.9-0.8	-0.9-1.6	-4.1-3.3	-4.0-3.8	-2.7-2.8	6.5-9.8	-2.4-2.7
11	-4.6-3.9	-0.6-0.8	-1.3-1.0	-4.5-3.2	-1.4-1.7	-2.7-3.0	-2.4-2.7	-0.2-0.3
Total	21.5-31.7	-5.3-5.9	-7.5-4.4	16.7-27.5	71.6-77.3	4.8-16.2	12.6-23.1	-5.7-5.5
Higher	17.7	0.7	-1.3	13.2	17.2	11.2	8.8	0.4

Table E.40: Control / Temp. at 0cm / Mean

i \ j	1	2	3	4	6	9	10	11
1	-1.2-1.2	-0.8-3.2	-1.0-3.0	0.7-4.9	-3.6-4.1	-0.6-3.9	-0.5-3.8	-1.0-3.0
2	-0.8-3.2	-0.2-0.3	-0.5-0.4	-0.6-0.4	-3.9-3.3	-0.5-0.5	-0.9-0.7	-0.5-0.3
3	-1.0-3.0	-0.5-0.4	-0.1-0.3	-0.5-0.4	-3.8-3.5	-0.5-0.4	-0.7-0.8	-0.5-0.3
4	0.7-4.9	-0.6-0.4	-0.5-0.4	2.2-4.2	-2.7-5.4	-1.4-2.4	-1.1-2.6	-1.5-2.0
6	-3.6-4.1	-3.9-3.3	-3.8-3.5	-2.7-5.4	46.3-51.9	1.2-6.9	-0.9-6.0	-0.2-1.8
9	-0.6-3.9	-0.5-0.5	-0.5-0.4	-1.4-2.4	1.2-6.9	-1.8-0.8	1.5-6.0	-1.4-3.0
10	-0.5-3.8	-0.9-0.7	-0.7-0.8	-1.1-2.6	-0.9-6.0	1.5-6.0	9.9-12.5	-0.2-3.1
11	-1.0-3.0	-0.5-0.3	-0.5-0.3	-1.5-2.0	-0.2-1.8	-1.4-3.0	-0.2-3.1	-0.1-0.4
Total	10.6-19.5	-5.0-4.3	-4.7-4.5	13.1-22.1	69.5-74.0	11.9-21.1	22.9-30.9	-4.2-4.9
Higher	5.5	-0.9	-0.8	8.9	14.1	6.2	5.6	-3.8

Table E.41: South / Temp. at 0cm / Mean

i \ j	1	2	3	4	6	9	10	11
1	-2.8-2.1	-4.1-4.6	-3.8-4.8	2.2-11.2	0.0-10.1	-4.4-4.4	-3.0-5.1	-3.8-4.9
2	-4.1-4.6	-0.4-0.3	-0.9-0.5	-1.0-0.9	-3.6-3.9	-0.8-0.5	-1.0-0.9	-0.9-0.5
3	-3.8-4.8	-0.9-0.5	-0.3-0.6	-1.6-0.6	-3.9-3.8	-1.2-0.5	-1.5-0.8	-1.1-0.6
4	2.2-11.2	-1.0-0.9	-1.6-0.6	4.3-8.8	-5.8-4.9	-4.4-3.5	-3.3-4.1	-3.3-4.3
6	0.0-10.1	-3.6-3.9	-3.9-3.8	-5.8-4.9	35.4-42.0	-4.4-3.1	-6.0-2.0	-3.0-2.0
9	-4.4-4.4	-0.8-0.5	-1.2-0.5	-4.4-3.5	-4.4-3.1	-1.9-1.7	-3.0-3.4	-3.2-3.5
10	-3.0-5.1	-1.0-0.9	-1.5-0.8	-3.3-4.1	-6.0-2.0	-3.0-3.4	8.9-12.4	-2.1-3.3
11	-3.8-4.9	-0.9-0.5	-1.1-0.6	-3.3-4.3	-3.0-2.0	-3.2-3.5	-2.1-3.3	-0.5-0.5
Total	26.5-36.8	-7.9-4.8	-7.9-4.8	25.2-36.0	58.9-66.2	8.7-20.9	17.1-28.2	-6.6-5.9
Higher	17.9	-1.3	-0.5	17.8	22.3	16.2	12.2	-1.2

Table E.42: North / Temp. at 0cm / Mean

i \ j	1	2	3	4	6	9	10	11
1	-2.4-2.5	-4.9-3.7	-4.5-4.1	0.7-9.4	-2.1-9.9	-5.2-3.5	-3.3-4.9	-4.7-3.9
2	-4.9-3.7	-0.4-0.3	-0.6-0.9	-1.1-0.7	-5.4-5.0	-0.5-1.0	-1.0-0.7	-0.6-0.9
3	-4.5-4.1	-0.6-0.9	-0.4-0.6	-1.1-1.2	-5.4-4.8	-1.2-0.9	-1.0-1.3	-1.2-0.8
4	0.7-9.4	-1.1-0.7	-1.1-1.2	3.8-8.1	-5.9-6.7	-3.9-3.7	-4.3-3.1	-4.4-3.1
6	-2.1-9.9	-5.4-5.0	-5.4-4.8	-5.9-6.7	48.5-56.1	-3.8-2.6	-4.8-3.2	-1.6-1.6
9	-5.2-3.5	-0.5-1.0	-1.2-0.9	-3.9-3.7	-3.8-2.6	-1.6-1.4	-2.7-2.8	-2.6-3.2
10	-3.3-4.9	-1.0-0.7	-1.0-1.3	-4.3-3.1	-4.8-3.2	-2.7-2.8	6.7-9.9	-2.5-2.6
11	-4.7-3.9	-0.6-0.9	-1.2-0.8	-4.4-3.1	-1.6-1.6	-2.6-3.2	-2.5-2.6	-0.2-0.2
Total	19.8-30.3	-5.1-6.4	-8.3-4.3	17.9-28.6	69.5-75.4	3.6-15.5	11.3-22.3	-5.5-5.9
Higher	17.4	1.4	-1.5	13.4	17.8	10.8	9.0	1.0

Table E.43: Control / Temp. at 0cm / Maximum

i \ j	1	2	3	4	6	9	10	11
1	-1.1-0.3	-0.2-2.4	-0.2-2.4	0.3-3.3	-1.4-3.9	-0.1-2.6	0.0-2.7	-0.3-2.3
2	-0.2-2.4	-0.1-0.1	-0.2-0.3	-0.8-1.0	-2.4-2.5	-0.3-0.2	-0.6-0.3	-0.2-0.3
3	-0.2-2.4	-0.2-0.3	-0.1-0.2	-0.9-0.9	-2.3-2.6	-0.5-0.3	-0.5-0.5	-0.5-0.2
4	0.3-3.3	-0.8-1.0	-0.9-0.9	12.7-15.2	7.8-14.9	-1.3-1.1	1.0-3.7	-0.6-1.3
6	-1.4-3.9	-2.4-2.5	-2.3-2.6	7.8-14.9	36.1-40.3	1.7-5.8	-0.2-4.5	-0.4-1.9
9	-0.1-2.6	-0.3-0.2	-0.5-0.3	-1.3-1.1	1.7-5.8	-1.1-0.8	1.6-4.9	-1.0-2.4
10	0.0-2.7	-0.6-0.3	-0.5-0.5	1.0-3.7	-0.2-4.5	1.6-4.9	8.0-10.2	-0.8-2.2
11	-0.3-2.3	-0.2-0.3	-0.5-0.2	-0.6-1.3	-0.4-1.9	-1.0-2.4	-0.8-2.2	-0.0-0.4
Total	3.5-11.1	-3.5-4.3	-3.3-4.4	32.6-38.7	64.7-68.9	8.2-15.8	20.7-27.4	-5.1-2.9
Higher	-1.2	-0.8	-0.7	5.8	9.2	3.4	5.2	-4.8

Table E.44: South / Temp. at 0cm / Maximum

i \ j	1	2	3	4	6	9	10	11
1	-1.7-2.0	-2.9-3.6	-3.0-3.5	-4.3-4.1	-1.3-5.5	-3.1-3.6	-3.8-2.3	-2.9-3.7
2	-2.9-3.6	-0.2-0.3	-0.5-0.4	-3.7-2.0	-1.7-2.2	-0.5-0.5	-0.8-0.3	-0.5-0.5
3	-3.0-3.5	-0.5-0.4	-0.3-0.5	-3.9-1.8	-1.8-2.2	-1.0-0.6	-1.1-0.5	-1.0-0.5
4	-4.3-4.1	-3.7-2.0	-3.9-1.8	30.6-35.8	0.6-9.5	-2.1-2.8	-3.0-2.1	-1.9-2.2
6	-1.3-5.5	-1.7-2.2	-1.8-2.2	0.6-9.5	24.0-28.6	-2.4-3.3	-4.6-1.4	-4.2-0.6
9	-3.1-3.6	-0.5-0.5	-1.0-0.6	-2.1-2.8	-2.4-3.3	-1.2-1.5	-2.3-2.7	-2.5-2.7
10	-3.8-2.3	-0.8-0.3	-1.1-0.5	-3.0-2.1	-4.6-1.4	-2.3-2.7	5.7-8.4	-2.9-1.8
11	-2.9-3.7	-0.5-0.5	-1.0-0.5	-1.9-2.2	-4.2-0.6	-2.5-2.7	-2.9-1.8	-0.3-0.3
Total	12.7-21.8	-6.0-4.6	-5.6-4.9	50.2-56.8	45.0-51.7	5.9-15.6	13.1-22.1	-5.3-5.2
Higher	14.6	-0.2	0.9	17.2	17.3	9.5	14.3	1.9

Table E.45: North / Temp. at 0cm / Maximum

i \ j	1	2	3	4	6	9	10	11
1	-0.4-2.6	-3.0-2.4	-2.8-2.6	-5.1-3.0	-1.7-5.0	-2.8-2.7	-3.4-2.0	-2.9-2.4
2	-3.0-2.4	-0.1-0.3	-0.6-0.2	-3.5-2.6	-2.2-2.6	-0.6-0.3	-0.6-0.2	-0.6-0.2
3	-2.8-2.6	-0.6-0.2	-0.4-0.3	-3.6-2.6	-2.2-2.6	-0.7-0.9	-0.7-0.8	-0.7-0.9
4	-5.1-3.0	-3.5-2.6	-3.6-2.6	34.3-39.5	0.8-10.9	-2.3-1.5	-1.8-2.4	-1.8-1.5
6	-1.7-5.0	-2.2-2.6	-2.2-2.6	0.8-10.9	31.6-36.6	-2.7-1.4	-2.9-1.8	-2.8-0.8
9	-2.8-2.7	-0.6-0.3	-0.7-0.9	-2.3-1.5	-2.7-1.4	-0.8-1.1	-2.1-1.6	-2.2-1.6
10	-3.4-2.0	-0.6-0.2	-0.7-0.8	-1.8-2.4	-2.9-1.8	-2.1-1.6	1.6-3.8	-1.9-2.0
11	-2.9-2.4	-0.6-0.2	-0.7-0.9	-1.8-1.5	-2.8-0.8	-2.2-1.6	-1.9-2.0	-0.2-0.2
Total	8.5-17.5	-5.0-4.9	-4.2-5.6	49.6-55.7	49.3-55.3	1.4-10.8	6.5-15.7	-4.9-5.0
Higher	12.8	1.1	1.1	12.1	12.5	7.6	9.8	1.8

Table E.46: Control / Temp. at 0cm / Minimum

i \ j	1	2	3	4	6	9	10	11
1	-1.5-0.9	-1.2-3.2	-1.4-3.1	-6.0-8.8	-1.4-2.9	-1.1-3.5	-1.2-3.3	-1.4-3.1
2	-1.2-3.2	-0.2-0.3	-0.5-0.4	-7.2-7.7	-0.6-0.6	-0.5-0.5	-0.5-0.5	-0.5-0.4
3	-1.4-3.1	-0.5-0.4	-0.2-0.3	-7.4-7.6	-0.5-0.6	-0.5-0.5	-0.5-0.5	-0.5-0.4
4	-6.0-8.8	-7.2-7.7	-7.4-7.6	68.9-77.9	-1.3-8.6	-3.3-3.8	-2.1-5.2	-0.5-1.5
6	-1.4-2.9	-0.6-0.6	-0.5-0.6	-1.3-8.6	4.3-7.6	-0.3-5.5	-1.2-4.7	-2.3-3.5
9	-1.1-3.5	-0.5-0.5	-0.5-0.5	-3.3-3.8	-0.3-5.5	-1.7-0.7	-1.2-3.5	-1.4-3.2
10	-1.2-3.3	-0.5-0.5	-0.5-0.5	-2.1-5.2	-1.2-4.7	-1.2-3.5	-0.6-1.7	-1.1-3.2
11	-1.4-3.1	-0.5-0.4	-0.5-0.4	-0.5-1.5	-2.3-3.5	-1.4-3.2	-1.1-3.2	-0.3-0.2
Total	2.3-13.2	-6.9-4.6	-6.6-4.9	85.0-89.0	13.8-23.6	1.3-12.6	2.8-13.7	-6.4-4.9
Higher	1.0	-2.4	-1.8	6.0	3.3	1.4	1.2	-4.5

Table E.47: South / Temp. at 0cm / Minimum

i \ j	1	2	3	4	6	9	10	11
1	-2.5-2.0	-2.1-6.3	-1.6-6.6	-9.4-7.2	-0.9-7.4	-1.1-7.1	-1.4-6.7	-1.7-6.7
2	-2.1-6.3	-0.6-0.2	-0.3-1.2	-13.5-1.9	-1.2-1.9	-0.2-1.3	-0.3-1.2	-0.3-1.2
3	-1.6-6.6	-0.3-1.2	-0.4-0.6	-14.1-1.5	-1.3-1.8	-1.2-0.8	-1.1-0.9	-1.2-0.8
4	-9.4-7.2	-13.5-1.9	-14.1-1.5	51.3-62.5	-4.8-11.2	-4.4-5.4	-5.8-4.8	-2.8-2.9
6	-0.9-7.4	-1.2-1.9	-1.3-1.8	-4.8-11.2	9.6-15.0	-5.6-3.2	-3.4-5.4	-3.8-4.8
9	-1.1-7.1	-0.2-1.3	-1.2-0.8	-4.4-5.4	-5.6-3.2	-1.5-2.1	-4.2-2.7	-4.5-2.7
10	-1.4-6.7	-0.3-1.2	-1.1-0.9	-5.8-4.8	-3.4-5.4	-4.2-2.7	1.0-4.7	-4.2-2.7
11	-1.7-6.7	-0.3-1.2	-1.2-0.8	-2.8-2.9	-3.8-4.8	-4.5-2.7	-4.2-2.7	-0.7-0.4
Total	10.9-25.8	-9.8-7.3	-10.2-7.0	73.3-80.2	20.6-34.2	-0.3-16.2	4.1-19.8	-9.4-7.7
Higher	3.6	0.3	1.9	29.8	7.7	6.7	7.1	-2.3

Table E.48: North / Temp. at 0cm / Minimum

i \ j	1	2	3	4	6	9	10	11
1	-2.6-2.6	-3.4-6.3	-3.0-6.6	-10.3-6.1	-2.1-7.6	-2.9-6.7	-2.7-6.5	-3.0-6.5
2	-3.4-6.3	-0.5-0.3	-0.5-1.1	-14.7-0.4	-1.6-2.8	-0.5-1.2	-0.8-1.0	-0.6-1.1
3	-3.0-6.6	-0.5-1.1	-0.7-0.4	-15.0-0.6	-2.4-2.2	-0.9-1.4	-1.0-1.4	-0.9-1.3
4	-10.3-6.1	-14.7-0.4	-15.0-0.6	44.9-56.5	-1.9-16.6	-4.6-5.4	-7.4-4.3	-2.4-3.9
6	-2.1-7.6	-1.6-2.8	-2.4-2.2	-1.9-16.6	12.7-19.2	-2.1-7.3	-2.8-6.8	-2.6-6.3
9	-2.9-6.7	-0.5-1.2	-0.9-1.4	-4.6-5.4	-2.1-7.3	-1.9-1.7	-3.3-3.5	-3.4-3.7
10	-2.7-6.5	-0.8-1.0	-1.0-1.4	-7.4-4.3	-2.8-6.8	-3.3-3.5	2.5-6.6	-4.7-2.8
11	-3.0-6.5	-0.6-1.1	-0.9-1.3	-2.4-3.9	-2.6-6.3	-3.4-3.7	-4.7-2.8	-0.1-0.5
Total	8.2-25.1	-9.9-8.8	-9.8-8.6	65.4-74.1	30.2-43.3	-2.1-16.3	3.8-20.8	-11.1-7.8
Higher	7.2	4.0	4.7	29.6	3.8	1.4	5.9	-5.8

APPENDIX F

SENSITIVITY ANALYSIS RESULTS FOR NEAR-SURFACE FACETS

### F.1 Introduction

The tables presented in this appendix provide the complete sensitivity analysis results for Chapter 9 that explored near-surface facet formation. The following tables include the first-order, second-order, higher-order, and total-effect indices. The indices are listed using the 90% confidence level intervals. Each table uses the indices listed in Table 7.1 that correspond to the specific parameters.

In this appendix only the day-light scenario results are listed, since the research focus of Chapter 9 is on radiation-recrystallization. Refer to Section 9.2 for details regarding the nomenclature used for labeling the tables.

## F.2 Snow Surface Temperature

Table F.1: Control / Temp. at 0cm with Time (Total-effect)

t \ i	1	2	3	4	5	6	7	8	9	10	11
0.33	9.1-17.9	-5.0-4.6	-5.9-3.6	22.0-29.8	-6.3-3.2	60.3-65.4	-6.3-3.2	-6.3-3.2	7.4-16.1	17.2-25.1	-5.2-4.3
0.67	9.6-18.3	-4.2-5.0	-6.5-2.9	17.0-25.3	-6.8-2.7	65.9-70.7	-6.8-2.7	-6.8-2.7	9.3-17.9	18.5-26.2	-5.6-3.8
1.00	10.0-18.6	-4.7-4.5	-6.3-3.2	14.8-23.2	-6.5-2.9	68.4-73.1	-6.4-3.0	-6.5-2.9	10.7-19.1	19.7-27.3	-5.4-4.0
1.33	9.3-17.9	-5.8-3.6	-6.9-2.6	12.5-21.0	-7.4-2.2	68.9-73.5	-6.7-2.8	-7.0-2.5	10.1-18.7	19.8-27.5	-6.4-3.1
1.67	8.8-17.5	-6.4-3.1	-7.3-2.3	11.1-19.8	-7.7-1.9	68.6-73.2	-6.1-3.4	-6.5-3.1	9.9-18.6	20.3-28.0	-6.8-2.7
2.00	8.0-16.9	-7.3-2.4	-8.0-1.8	9.6-18.6	-8.3-1.6	67.4-72.2	-5.1-4.5	-5.9-3.9	9.2-18.1	20.4-28.2	-7.6-2.2
2.33	7.2-16.4	-7.9-2.0	-8.6-1.5	8.4-17.5	-8.8-1.3	65.8-70.9	-6.0-4.0	-4.4-5.4	8.7-17.7	20.5-28.4	-8.3-1.7
2.67	6.5-16.0	-8.4-1.7	-9.2-1.2	7.3-16.7	-9.3-1.1	63.9-69.3	-3.6-6.5	-5.6-4.8	8.4-17.5	20.5-28.4	-9.0-1.3
3.00	5.8-15.5	-9.0-1.3	-9.9-0.8	6.3-15.9	-9.7-1.1	62.1-67.8	-1.4-8.8	-4.1-6.5	7.8-17.1	20.2-28.4	-9.7-1.0
3.33	5.0-15.1	-9.8-1.0	-10.6-0.4	5.3-15.2	-10.3-0.8	60.5-66.5	0.6-10.9	-2.7-8.0	7.0-16.7	19.9-28.4	-10.4-0.6
3.67	4.5-14.8	-10.3-0.7	-11.1-0.2	4.5-14.6	-10.7-0.8	59.3-65.5	2.5-12.9	-1.6-9.3	6.6-16.6	19.8-28.5	-11.0-0.4
4.00	4.1-14.7	-10.5-0.8	-11.4-0.3	3.9-14.2	-11.0-0.9	58.2-64.7	4.0-14.4	-0.6-10.4	6.3-16.6	19.6-28.5	-11.4-0.2
4.33	3.8-14.6	-10.8-0.7	-11.7-0.2	3.4-14.0	-11.3-0.8	57.4-64.1	5.0-15.5	0.1-11.3	6.1-16.6	19.5-28.6	-11.9-0.1
4.67	3.8-14.6	-10.9-0.8	-11.9-0.2	3.1-13.8	-11.4-0.9	56.9-63.8	5.6-16.2	0.5-11.9	6.2-16.7	19.6-28.8	-12.0-0.1
5.00	3.6-14.5	-11.2-0.7	-12.2-0.1	2.7-13.6	-11.7-0.8	56.6-63.5	5.7-16.5	0.4-12.0	6.1-16.8	19.5-28.8	-12.2-0.1
5.33	3.6-14.6	-11.4-0.6	-12.4-0.0	2.6-13.6	-11.9-0.7	56.5-63.4	5.5-16.3	0.2-11.9	6.1-16.9	19.5-28.9	-12.4-0.0
5.67	3.7-14.7	-11.3-0.7	-12.4-0.1	2.8-13.8	-11.9-0.7	56.5-63.5	5.0-16.0	-0.1-11.6	6.3-17.0	19.7-29.1	-12.3-0.0
6.00	4.0-15.0	-11.2-0.7	-12.4-0.1	3.1-14.0	-11.9-0.6	56.7-63.7	4.2-15.2	-0.7-11.1	6.5-17.2	20.0-29.3	-12.3-0.1
6.33	4.4-15.4	-11.1-0.8	-12.2-0.0	3.6-14.3	-11.9-0.6	57.2-64.0	3.2-14.2	-1.4-10.3	6.8-17.4	20.3-29.6	-12.1-0.1
6.67	4.9-15.8	-10.8-0.8	-12.0-0.1	4.3-14.8	-11.7-0.5	57.9-64.6	1.8-12.9	-2.3-9.4	7.2-17.7	20.8-29.9	-11.7-0.3
7.00	5.6-16.3	-10.5-1.0	-11.7-0.1	5.0-15.4	-11.5-0.4	58.8-65.4	0.3-11.3	-3.3-8.3	7.8-18.0	21.3-30.2	-11.3-0.5
7.33	6.4-16.8	-10.0-1.2	-11.2-0.4	5.9-16.1	-11.2-0.5	60.0-66.3	-1.3-9.6	-4.4-7.1	8.4-18.4	21.9-30.6	-10.8-0.8
7.67	7.3-17.5	-9.6-1.4	-10.5-0.7	7.0-16.9	-10.8-0.6	61.5-67.5	-3.0-7.8	-5.5-5.8	9.1-18.8	22.5-31.0	-10.1-1.2
8.00	8.3-18.2	-9.1-1.6	-9.8-1.1	8.1-17.7	-10.3-0.9	63.2-68.9	-4.8-5.9	-6.6-4.5	9.8-19.3	23.1-31.5	-9.4-1.6
8.33	9.3-19.0	-8.5-1.9	-9.0-1.7	9.3-18.6	-9.5-1.2	65.0-70.5	-6.3-4.3	-4.3-6.2	10.4-19.8	23.7-31.9	-8.5-2.2
8.67	10.4-19.7	-7.8-2.3	-8.0-2.4	10.1-19.3	-8.7-1.8	67.0-72.2	-4.4-5.6	-4.9-5.4	11.2-20.2	24.3-32.2	-7.7-2.7
9.00	11.3-20.4	-7.1-2.9	-7.1-3.1	10.6-19.7	-7.9-2.4	68.7-73.7	-5.1-4.9	-5.2-4.9	11.9-20.8	24.7-32.4	-6.8-3.4
9.33	11.9-20.8	-6.4-3.4	-6.4-3.7	11.0-20.0	-7.1-2.9	70.1-75.0	-5.3-4.6	-5.2-4.7	12.4-21.2	24.9-32.5	-6.1-3.9
9.67	12.2-21.0	-5.8-3.9	-5.8-4.2	11.1-20.0	-6.6-3.4	71.2-75.9	-5.3-4.5	-5.1-4.7	12.8-21.5	24.8-32.4	-5.6-4.3
10.00	12.3-20.9	-5.6-4.1	-5.4-4.5	10.9-19.8	-6.3-3.5	71.8-76.5	-5.3-4.5	-5.1-4.7	13.0-21.7	24.6-32.2	-5.3-4.5

Table F.2: Control / Temp. at 0cm / Mid-day

i \ j	1	2	3	4	5	6	7	8	9	10	11
1	-1.0-0.6	-1.5-1.5	-1.5-1.5	-0.4-2.4	-1.6-1.4	-1.8-3.7	-1.7-1.4	-1.7-1.3	-1.4-1.9	-1.9-1.4	-1.6-1.4
2	-1.5-1.5	-0.1-0.3	-0.5-0.4	-0.4-0.6	-0.4-0.4	-1.4-3.7	-0.5-0.7	-0.6-0.5	-0.4-0.6	-0.3-1.3	-0.5-0.4
3	-1.5-1.5	-0.5-0.4	-0.1-0.2	-0.3-0.4	-0.4-0.3	-1.6-3.5	-0.2-0.7	-0.5-0.3	-0.3-0.4	-0.5-0.9	-0.4-0.3
4	-0.4-2.4	-0.4-0.6	-0.3-0.4	0.5-1.9	-1.7-1.0	-2.2-3.5	-1.5-1.2	-1.6-1.2	-1.9-1.0	-1.7-1.2	-1.7-1.0
5	-1.6-1.4	-0.4-0.4	-0.4-0.3	-1.7-1.0	-0.1-0.2	-1.5-3.5	-0.1-0.9	-0.1-0.7	-0.1-0.7	-0.2-1.3	-0.1-0.6
6	-1.8-3.7	-1.4-3.7	-1.6-3.5	-2.2-3.5	-1.5-3.5	24.8-29.2	3.7-7.8	2.3-6.2	-0.9-3.9	2.7-8.6	-0.9-1.3
7	-1.7-1.4	-0.5-0.7	-0.2-0.7	-1.5-1.2	-0.1-0.9	3.7-7.8	4.5-6.0	-0.8-2.1	-1.0-1.8	0.5-3.6	-0.6-1.6
8	-1.7-1.3	-0.6-0.5	-0.5-0.3	-1.6-1.2	-0.1-0.7	2.3-6.2	-0.8-2.1	3.7-5.1	-0.1-2.5	0.4-3.8	-0.3-1.8
9	-1.4-1.9	-0.4-0.6	-0.3-0.4	-1.9-1.0	-0.1-0.7	-0.9-3.9	-1.0-1.8	-0.1-2.5	0.3-2.1	1.9-5.2	-1.5-1.4
10	-1.9-1.4	-0.3-1.3	-0.5-0.9	-1.7-1.2	-0.2-1.3	2.7-8.6	0.5-3.6	0.4-3.8	1.9-5.2	7.2-9.3	-0.9-1.5
11	-1.6-1.4	-0.5-0.4	-0.4-0.3	-1.7-1.0	-0.1-0.6	-0.9-1.3	-0.6-1.6	-0.3-1.8	-1.5-1.4	-0.9-1.5	-0.1-0.2
Total	3.6-14.5	-11.2-0.7	-12.2-0.1	2.7-13.6	-11.7-0.8	56.6-63.5	5.7-16.5	0.4-12.0	6.1-16.8	19.5-28.8	-12.2-0.1
Higher	7.9	-7.2	-7.3	6.9	-7.7	10.9	-3.9	-6.9	3.2	1.4	-7.6

Table F.3: South / Temp. at 0cm with Time (Total-effect)

t \ i	1	2	3	4	5	6	7	8	9	10	11
0.33	16.4-25.7	-0.7-9.8	-5.8-5.0	19.0-28.2	-6.1-4.8	59.8-65.1	-6.0-4.8	-6.1-4.8	2.5-12.9	11.3-20.7	-5.2-5.6
0.67	17.8-26.8	-3.1-7.1	-5.7-4.6	15.3-24.8	-6.3-4.1	65.3-70.2	-6.2-4.1	-6.4-4.0	3.8-13.5	13.5-22.4	-5.5-4.9
1.00	16.2-25.0	-5.8-4.5	-4.5-5.6	12.4-21.9	-4.9-5.0	66.7-71.4	-4.3-5.7	-4.7-5.3	2.2-11.9	14.0-22.6	-3.9-6.1
1.33	13.8-22.7	-4.6-5.4	-5.7-4.2	10.0-19.6	-6.3-3.7	66.2-71.0	-4.0-5.9	-4.8-5.0	1.5-10.9	14.1-22.5	-5.3-4.8
1.67	11.4-20.2	-5.8-4.0	-6.8-3.1	7.5-17.2	-7.2-2.8	64.0-69.0	-4.8-5.1	-6.3-3.8	0.2-9.7	13.6-22.0	-6.6-3.6
2.00	9.3-18.1	-6.8-3.0	-7.6-2.2	5.2-15.0	-7.6-2.3	60.6-65.9	-0.9-8.6	-3.4-6.5	-0.5-8.9	12.7-21.1	-7.3-2.7
2.33	7.3-16.5	-7.5-2.4	-8.4-1.6	3.4-13.4	-8.1-1.9	56.9-62.6	3.5-12.7	0.0-9.7	-1.2-8.3	11.8-20.3	-8.0-2.1
2.67	5.9-15.3	-8.2-2.1	-9.0-1.2	1.7-12.0	-8.5-1.7	53.6-59.7	7.6-16.6	3.1-12.7	-1.8-7.9	10.9-19.7	-8.7-1.6
3.00	4.8-14.4	-8.8-1.7	-9.7-1.0	0.3-11.0	-9.0-1.5	51.0-57.5	11.1-20.1	5.5-15.0	-2.5-7.6	10.1-19.1	-9.4-1.3
3.33	3.7-13.7	-9.4-1.5	-10.3-0.6	-0.8-10.2	-9.5-1.4	49.0-55.9	13.9-22.9	7.1-16.8	-3.0-7.4	9.4-18.7	-10.0-0.8
3.67	2.9-13.3	-9.8-1.3	-10.8-0.6	-1.5-9.7	-9.7-1.5	47.7-54.8	16.1-25.1	8.6-18.4	-3.3-7.3	8.9-18.5	-10.5-0.7
4.00	2.4-13.0	-10.1-1.3	-11.2-0.4	-2.2-9.3	-10.0-1.4	46.8-54.1	17.6-26.8	9.5-19.5	-3.7-7.2	8.3-18.2	-10.9-0.5
4.33	2.1-12.9	-10.4-1.3	-11.7-0.2	-2.8-9.1	-10.2-1.5	46.2-53.7	18.6-27.9	10.1-20.3	-4.1-7.1	7.9-18.1	-11.1-0.5
4.67	1.8-12.8	-10.7-1.2	-12.2-0.1	-3.3-8.8	-10.6-1.3	45.7-53.4	19.1-28.4	10.2-20.6	-4.6-7.0	7.7-18.1	-11.5-0.4
5.00	1.7-12.9	-10.9-1.1	-12.5-0.3	-3.5-8.7	-10.8-1.2	45.6-53.3	19.2-28.7	10.1-20.7	-4.9-6.9	7.6-18.1	-11.7-0.4
5.33	1.8-13.0	-10.9-1.1	-12.6-0.2	-3.6-8.7	-10.9-1.2	45.6-53.3	19.1-28.6	9.9-20.5	-4.8-7.0	7.7-18.2	-11.8-0.4
5.67	2.1-13.3	-10.8-1.2	-12.5-0.2	-3.4-8.8	-10.8-1.2	45.7-53.5	18.6-28.1	9.5-20.2	-4.7-7.2	7.8-18.3	-11.8-0.4
6.00	2.5-13.6	-10.7-1.2	-12.5-0.2	-3.2-9.0	-10.8-1.3	46.2-53.9	17.6-27.2	8.8-19.5	-4.5-7.3	8.0-18.5	-11.7-0.4
6.33	3.2-14.1	-10.4-1.4	-12.2-0.1	-2.7-9.3	-10.6-1.3	46.8-54.5	16.3-25.9	8.0-18.5	-4.1-7.5	8.4-18.7	-11.4-0.6
6.67	4.0-14.8	-10.1-1.6	-11.8-0.2	-2.2-9.8	-10.4-1.4	47.8-55.3	14.7-24.3	6.9-17.4	-3.6-7.7	9.0-19.1	-11.0-0.8
7.00	5.1-15.6	-9.7-1.9	-11.2-0.5	-1.4-10.3	-10.0-1.6	49.2-56.4	12.8-22.4	5.8-16.2	-2.9-8.1	9.7-19.6	-10.4-1.1
7.33	6.4-16.6	-9.2-2.2	-10.5-1.0	-0.4-11.0	-9.6-1.8	50.9-57.9	10.6-20.1	4.4-14.7	-2.3-8.5	10.7-20.2	-9.8-1.6
7.67	8.0-17.9	-8.6-2.5	-9.6-1.6	0.7-11.9	-9.1-2.0	53.1-59.9	8.0-17.5	2.8-13.1	-1.5-8.9	11.8-21.0	-9.1-2.0
8.00	9.7-19.3	-8.0-2.8	-8.6-2.3	1.9-12.8	-8.5-2.4	55.9-62.3	5.2-14.8	0.9-11.3	-0.8-9.4	12.9-22.0	-8.3-2.6
8.33	11.6-21.0	-7.3-3.3	-7.5-3.1	3.1-13.9	-7.6-3.0	59.1-65.1	2.3-12.1	-0.9-9.5	-0.3-9.9	14.3-23.1	-7.4-3.3
8.67	13.8-22.9	-6.2-4.2	-6.1-4.4	4.3-14.8	-6.5-3.9	62.6-68.2	-0.2-9.8	-2.4-8.0	0.7-10.8	15.7-24.4	-6.2-4.3
9.00	15.8-24.7	-4.8-5.4	-4.5-5.9	5.3-15.7	-5.1-5.2	65.8-71.1	-1.7-8.3	-3.1-7.3	1.9-11.9	17.3-25.9	-4.8-5.6
9.33	17.3-26.2	-6.4-4.2	-6.1-4.6	6.0-16.4	-6.7-3.9	68.3-73.5	-2.5-7.7	-3.3-7.1	3.0-13.0	18.5-27.2	-6.6-4.3
9.67	18.3-27.3	-5.2-5.3	-4.8-5.8	6.4-16.9	-5.6-4.9	69.9-75.0	-2.5-7.8	-3.1-7.4	3.8-13.8	19.4-28.1	-5.5-5.4
10.00	18.7-27.6	-4.6-5.9	-4.1-6.4	6.5-17.0	-5.0-5.5	70.9-75.9	-2.4-7.9	-2.9-7.6	4.2-14.2	19.9-28.6	-4.9-5.9

Table F.4: South / Temp. at 0cm / Mid-day

i \ j	1	2	3	4	5	6	7	8	9	10	11
1	0.2-1.7	-1.7-0.8	-2.0-0.5	-0.9-1.5	-1.9-0.6	-2.9-1.7	-1.6-1.6	-1.6-1.3	-1.4-1.1	-1.6-1.0	-1.9-0.6
2	-1.7-0.8	-0.1-0.5	-0.5-0.6	-0.5-0.7	-0.4-0.7	-1.8-2.4	-0.5-1.5	-0.9-0.7	-0.8-0.5	-0.5-0.9	-0.5-0.6
3	-2.0-0.5	-0.5-0.6	-0.2-0.1	-0.2-0.3	-0.2-0.3	-1.8-2.3	-0.1-1.4	-0.4-0.6	-0.1-0.4	-0.0-0.8	-0.1-0.3
4	-0.9-1.5	-0.5-0.7	-0.2-0.3	0.1-1.4	-1.4-1.0	-2.1-2.7	-1.8-1.2	-1.1-1.4	-1.4-1.1	-1.3-1.1	-1.5-1.0
5	-1.9-0.6	-0.4-0.7	-0.2-0.3	-1.4-1.0	0.1-0.5	-1.6-2.6	-0.2-1.8	-0.4-1.0	-0.2-0.8	-0.2-1.0	-0.3-0.6
6	-2.9-1.7	-1.8-2.4	-1.8-2.3	-2.1-2.7	-1.6-2.6	21.2-25.1	6.0-10.8	4.1-8.5	-0.5-2.8	1.9-6.1	-1.0-1.2
7	-1.6-1.6	-0.5-1.5	-0.1-1.4	-1.8-1.2	-0.2-1.8	6.0-10.8	10.4-12.5	-0.8-3.0	-1.0-1.6	1.2-4.3	-0.9-1.3
8	-1.6-1.3	-0.9-0.7	-0.4-0.6	-1.1-1.4	-0.4-1.0	4.1-8.5	-0.8-3.0	7.9-9.8	-0.1-2.5	0.9-4.0	-0.4-1.9
9	-1.4-1.1	-0.8-0.5	-0.1-0.4	-1.4-1.1	-0.2-0.8	-0.5-2.8	-1.0-1.6	-0.1-2.5	0.5-1.6	0.4-2.6	-0.6-1.4
10	-1.6-1.0	-0.5-0.9	-0.0-0.8	-1.3-1.1	-0.2-1.0	1.9-6.1	1.2-4.3	0.9-4.0	0.4-2.6	4.7-6.1	-0.6-1.3
11	-1.9-0.6	-0.5-0.6	-0.1-0.3	-1.5-1.0	-0.3-0.6	-1.0-1.2	-0.9-1.3	-0.4-1.9	-0.6-1.4	-0.6-1.3	-0.0-0.3
Total	1.7-12.9	-10.9-1.1	-12.5-0.3	-3.5-8.7	-10.8-1.2	45.6-53.3	19.2-28.7	10.1-20.7	-4.9-6.9	7.6-18.1	-11.7-0.4
Higher	9.6	-5.6	-7.3	2.0	-6.8	5.5	-1.9	-5.5	-4.6	-4.2	-7.1



Table F.5: North / Temp. at 0cm with Time (Total-effect)

t \ i	1	2	3	4	5	6	7	8	9	10	11
0.33	17.9-30.0	4.8-17.9	-4.4-9.8	39.4-48.7	-4.8-9.2	45.6-54.1	-4.8-9.2	-4.8-9.2	4.0-17.3	9.3-21.7	-3.6-10.2
0.67	21.6-32.9	-0.4-12.7	-6.2-7.6	31.0-41.6	-6.7-7.1	53.2-60.7	-6.7-7.1	-6.7-7.1	3.4-16.5	10.7-22.6	-5.3-8.4
1.00	22.9-34.0	-2.8-10.2	-6.0-7.6	28.7-39.4	-7.6-6.1	56.6-63.8	-7.4-6.2	-7.5-6.2	2.8-15.9	11.7-23.4	-5.5-8.0
1.33	22.1-32.9	-4.9-8.0	-7.1-6.3	25.9-36.8	-8.3-5.0	57.7-64.8	-8.0-5.4	-7.8-5.5	1.8-14.7	11.9-23.1	-6.4-6.8
1.67	21.0-31.6	-6.2-6.5	-7.5-5.5	23.5-34.4	-4.9-7.2	58.4-65.3	-7.9-5.0	-7.7-5.2	1.1-13.6	11.9-22.9	-7.1-5.8
2.00	18.9-29.3	-7.3-5.1	-8.2-4.4	20.8-31.7	-5.9-6.2	58.3-65.0	-7.8-4.7	-7.6-4.9	0.2-12.3	11.3-22.2	-8.1-4.5
2.33	17.2-27.4	-7.6-4.4	-4.7-6.8	18.8-29.5	-5.9-5.7	57.7-64.2	-6.3-5.7	-5.9-6.0	-0.0-11.6	11.5-22.0	-4.7-7.0
2.67	15.5-25.5	-4.6-6.5	-5.2-5.9	16.8-27.1	-6.2-5.0	56.6-62.9	-4.6-6.8	-3.8-7.4	-0.8-10.5	11.2-21.5	-5.2-6.2
3.00	14.0-23.7	-4.9-5.8	-5.5-5.2	14.8-24.9	-6.2-4.6	55.0-61.1	-2.7-8.2	-1.4-9.3	-1.4-9.5	11.1-20.9	-5.3-5.6
3.33	12.8-22.3	-5.1-5.4	-5.5-4.9	13.1-23.0	-6.0-4.4	53.2-59.4	-0.5-9.8	1.3-11.5	-1.7-8.8	10.9-20.4	-5.3-5.2
3.67	11.7-21.1	-5.3-4.8	-5.5-4.7	11.5-21.4	-5.8-4.3	51.3-57.5	1.3-11.1	3.9-13.6	-2.0-8.3	10.8-20.1	-5.4-4.8
4.00	10.9-20.2	-5.5-4.5	-5.6-4.4	10.3-20.1	-5.8-4.1	49.7-55.9	2.6-12.2	6.0-15.4	-2.3-7.8	10.7-19.8	-5.5-4.5
4.33	10.2-19.4	-5.8-4.1	-5.8-4.1	9.3-19.1	-6.0-3.8	48.3-54.5	3.6-13.0	7.5-16.7	-2.6-7.4	10.4-19.4	-5.8-4.0
4.67	9.7-18.9	-6.0-3.9	-6.0-3.8	8.8-18.5	-6.4-3.5	47.2-53.5	4.2-13.5	8.6-17.6	-2.9-7.0	10.1-19.1	-6.2-3.7
5.00	9.4-18.5	-6.2-3.7	-6.2-3.6	8.4-18.1	-6.6-3.3	46.6-52.9	4.5-13.7	9.3-18.2	-3.2-6.7	10.0-19.0	-6.6-3.3
5.33	9.4-18.5	-6.2-3.7	-6.2-3.5	8.3-18.1	-6.7-3.3	46.4-52.8	4.6-13.8	9.6-18.5	-3.1-6.8	10.0-19.0	-6.6-3.3
5.67	9.7-18.8	-6.2-3.7	-6.2-3.7	8.6-18.3	-6.7-3.3	46.7-53.0	4.5-13.7	9.5-18.4	-2.9-7.0	10.2-19.2	-6.5-3.5
6.00	10.2-19.3	-6.3-3.7	-6.2-3.8	9.0-18.8	-6.7-3.3	47.2-53.6	3.9-13.3	8.8-17.8	-2.8-7.1	10.5-19.6	-6.5-3.6
6.33	10.8-20.0	-6.3-3.7	-6.2-3.8	9.6-19.4	-6.8-3.3	48.2-54.6	3.0-12.6	7.6-16.7	-2.8-7.3	10.9-20.0	-6.5-3.7
6.67	11.8-21.0	-6.4-3.8	-6.1-4.0	10.4-20.3	-6.9-3.4	49.6-55.9	1.9-11.6	5.9-15.4	-2.6-7.7	11.3-20.5	-6.4-4.0
7.00	13.0-22.4	-6.4-3.9	-6.1-4.2	11.6-21.6	-7.0-3.5	51.3-57.7	0.5-10.5	3.9-13.7	-2.3-8.1	11.8-21.1	-6.2-4.2
7.33	14.7-24.1	-6.5-4.1	-6.0-4.6	13.1-23.1	-7.0-3.7	53.3-59.6	-1.1-9.3	1.6-11.8	-2.0-8.6	12.4-21.8	-6.1-4.6
7.67	16.6-26.0	-6.5-4.4	-5.8-5.0	14.7-24.9	-7.1-3.9	55.4-61.8	-2.9-7.9	-0.8-9.9	-1.7-9.1	13.0-22.6	-5.9-5.0
8.00	18.7-28.2	-6.5-4.7	-5.6-5.5	16.6-26.8	-7.0-4.2	57.6-63.9	-4.7-6.6	-2.9-8.2	-1.3-9.8	13.7-23.4	-5.6-5.5
8.33	20.8-30.4	-6.5-5.0	-5.4-6.0	18.4-28.7	-6.9-4.6	59.5-65.9	-6.2-5.5	-4.9-6.7	-0.8-10.4	14.2-24.2	-5.3-6.2
8.67	22.8-32.5	-6.4-5.3	-5.2-6.5	20.0-30.5	-6.8-4.9	60.9-67.5	-7.5-4.6	-6.4-5.6	-0.4-11.1	14.7-24.9	-5.1-6.7
9.00	24.5-34.2	-6.4-5.6	-4.9-7.1	21.2-31.9	-6.7-5.3	62.0-68.6	-4.7-7.1	-7.6-4.7	-0.0-11.7	15.1-25.4	-4.8-7.1
9.33	25.7-35.5	-6.4-5.9	-8.1-4.3	22.1-32.9	-6.6-5.6	62.7-69.4	-5.3-6.8	-4.7-7.4	0.3-12.2	15.3-25.7	-4.7-7.4
9.67	26.5-36.4	-6.3-6.1	-7.8-4.6	22.6-33.5	-6.5-5.9	63.2-69.9	-5.7-6.6	-5.0-7.2	0.7-12.7	15.4-26.0	-8.3-4.5
10.00	26.9-36.9	-6.2-6.3	-7.7-4.9	22.8-33.8	-6.4-6.0	63.5-70.3	-5.8-6.6	-5.1-7.2	1.1-13.0	15.4-26.1	-8.1-4.6

Table F.6: North / Temp. at 0cm / Mid-day

i \ j	1	2	3	4	5	6	7	8	9	10	11
1	-0.2-2.3	-2.5-1.7	-2.5-1.8	-0.8-3.5	-2.6-1.7	-0.8-5.2	-2.6-1.5	-2.5-1.5	-2.6-1.7	-2.1-2.1	-2.9-1.4
2	-2.5-1.7	-0.3-0.3	-0.4-0.8	-0.2-1.1	-0.3-0.9	0.1-5.1	-0.3-1.1	-0.4-1.1	-0.4-0.9	-0.4-1.2	-0.4-0.9
3	-2.5-1.8	-0.4-0.8	-0.3-0.4	-0.5-0.8	-0.6-0.6	-0.4-4.6	-0.6-0.6	-0.8-0.8	-0.6-0.7	-0.8-0.7	-0.7-0.6
4	-0.8-3.5	-0.2-1.1	-0.5-0.8	1.4-3.4	-1.8-1.9	-0.6-5.3	-1.5-2.0	-1.8-1.6	-2.0-1.8	-1.1-2.6	-1.6-2.1
5	-2.6-1.7	-0.3-0.9	-0.6-0.6	-1.8-1.9	0.1-0.5	-0.2-4.8	-0.4-0.6	-0.6-0.8	-0.3-0.5	-0.5-0.9	-0.4-0.4
6	-0.8-5.2	0.1-5.1	-0.4-4.6	-0.6-5.3	-0.2-4.8	32.5-36.9	-0.4-3.1	-0.4-3.9	-0.8-2.9	-0.9-4.2	-0.7-1.8
7	-2.6-1.5	-0.3-1.1	-0.6-0.6	-1.5-2.0	-0.4-0.6	-0.4-3.1	8.1-9.8	-2.1-1.3	-1.4-1.1	-1.6-1.4	-1.4-0.9
8	-2.5-1.5	-0.4-1.1	-0.8-0.8	-1.8-1.6	-0.6-0.8	-0.4-3.9	-2.1-1.3	11.5-13.4	-1.3-1.4	-2.0-1.3	-1.3-1.2
9	-2.6-1.7	-0.4-0.9	-0.6-0.7	-2.0-1.8	-0.3-0.5	-0.8-2.9	-1.4-1.1	-1.3-1.4	-0.7-0.8	-1.1-1.8	-1.1-1.8
10	-2.1-2.1	-0.4-1.2	-0.8-0.7	-1.1-2.6	-0.5-0.9	-0.9-4.2	-1.6-1.4	-2.0-1.3	-1.1-1.8	9.5-11.5	-1.6-1.2
11	-2.9-1.4	-0.4-0.9	-0.7-0.6	-1.6-2.1	-0.4-0.4	-0.7-1.8	-1.4-0.9	-1.3-1.2	-1.1-1.8	-1.6-1.2	-0.3-0.3
Total	9.4-18.5	-6.2-3.7	-6.2-3.6	8.4-18.1	-6.6-3.3	46.6-52.9	4.5-13.7	9.3-18.2	-3.2-6.7	10.0-19.0	-6.6-3.3
Higher	12.9	-6.0	-3.4	5.6	-4.6	-2.8	-0.5	0.4	0.2	1.3	-1.8

Table F.7: Control / Temp. at 0cm / Mean

i \ j	1	2	3	4	5	6	7	8	9	10	11
1	-0.8-1.1	-2.2-1.3	-2.2-1.2	0.1-3.4	-2.3-1.2	-1.6-5.6	-1.4-1.9	-1.4-1.9	-2.3-1.5	-1.7-1.9	-2.3-1.2
2	-2.2-1.3	-0.1-0.3	-0.4-0.4	-0.2-0.7	-0.3-0.4	-1.6-5.5	-0.4-0.4	-0.3-0.4	-0.3-0.5	-0.2-1.5	-0.3-0.4
3	-2.2-1.2	-0.4-0.4	-0.2-0.2	-0.3-0.5	-0.4-0.3	-1.7-5.4	-0.3-0.4	-0.4-0.3	-0.3-0.4	-0.4-1.2	-0.4-0.3
4	0.1-3.4	-0.2-0.7	-0.3-0.5	2.9-4.6	-1.7-1.2	-2.0-5.8	-1.7-1.3	-1.7-1.3	-1.9-1.4	-1.4-2.0	-1.7-1.2
5	-2.3-1.2	-0.3-0.4	-0.4-0.3	-1.7-1.2	-0.1-0.1	-1.8-5.2	-0.1-0.4	-0.1-0.4	-0.1-0.4	-0.3-1.3	-0.1-0.3
6	-1.6-5.6	-1.6-5.5	-1.7-5.4	-2.0-5.8	-1.8-5.2	36.9-42.3	0.5-3.6	-0.2-2.7	0.4-5.9	2.4-9.5	-1.1-1.0
7	-1.4-1.9	-0.4-0.4	-0.3-0.4	-1.7-1.3	-0.1-0.4	0.5-3.6	1.5-2.3	-0.5-0.9	-0.7-0.8	-0.2-2.1	-0.5-0.8
8	-1.4-1.9	-0.3-0.4	-0.4-0.3	-1.7-1.3	-0.1-0.4	-0.2-2.7	-0.5-0.9	1.1-1.8	0.0-1.5	0.1-2.5	-0.1-1.1
9	-2.3-1.5	-0.3-0.5	-0.3-0.4	-1.9-1.4	-0.1-0.4	0.4-5.9	-0.7-0.8	0.0-1.5	-0.4-1.5	2.1-5.9	-1.7-1.7
10	-1.7-1.9	-0.2-1.5	-0.4-1.2	-1.4-2.0	-0.3-1.3	2.4-9.5	-0.2-2.1	0.1-2.5	2.1-5.9	9.6-11.9	-0.8-1.8
11	-2.3-1.2	-0.3-0.4	-0.4-0.3	-1.7-1.2	-0.1-0.3	-1.1-1.0	-0.5-0.8	-0.1-1.1	-1.7-1.7	-0.8-1.8	-0.1-0.3
Total	5.9-16.4	-9.9-1.4	-10.6-0.8	8.6-18.6	-10.7-0.9	62.2-68.1	-7.7-4.0	-6.0-5.3	6.3-16.7	19.6-28.7	-10.1-1.3
Higher	8.9	-7.1	-6.7	6.7	-6.8	3.7	-7.4	-6.0	3.3	-1.2	-5.0

Table F.8: South / Temp. at 0cm / Mean

i \ j	1	2	3	4	5	6	7	8	9	10	11
1	0.7-2.8	-1.8-1.4	-2.0-1.3	-1.4-1.8	-2.0-1.3	-4.2-3.2	-2.1-1.3	-1.8-1.5	-2.1-1.4	-1.6-1.9	-2.1-1.2
2	-1.8-1.4	-0.1-0.5	-0.8-0.3	-0.9-0.3	-0.7-0.4	-4.1-3.1	-0.7-0.6	-0.8-0.4	-0.7-0.5	-1.0-0.6	-0.8-0.4
3	-2.0-1.3	-0.8-0.3	-0.2-0.2	-0.4-0.5	-0.4-0.4	-3.9-3.2	-0.4-0.5	-0.5-0.4	-0.3-0.5	-0.4-0.9	-0.3-0.4
4	-1.4-1.8	-0.9-0.3	-0.4-0.5	2.3-3.9	-1.8-1.1	-3.9-4.0	-1.7-1.4	-1.7-1.3	-1.6-1.4	-1.5-1.7	-1.9-1.1
5	-2.0-1.3	-0.7-0.4	-0.4-0.4	-1.8-1.1	-0.0-0.4	-4.0-3.1	-0.6-0.4	-0.4-0.5	-0.5-0.3	-0.7-0.7	-0.4-0.4
6	-4.2-3.2	-4.1-3.1	-3.9-3.2	-3.9-4.0	-4.0-3.1	37.9-43.5	0.3-4.7	-0.3-3.6	-0.9-3.6	0.8-6.8	-1.2-1.0
7	-2.1-1.3	-0.7-0.6	-0.4-0.5	-1.7-1.4	-0.6-0.4	0.3-4.7	4.6-5.8	-1.0-1.1	-1.0-0.9	-0.2-2.2	-0.8-0.9
8	-1.8-1.5	-0.8-0.4	-0.5-0.4	-1.7-1.3	-0.4-0.5	-0.3-3.6	-1.0-1.1	3.6-4.7	-0.5-1.4	-0.2-2.1	-0.5-1.2
9	-2.1-1.4	-0.7-0.5	-0.3-0.5	-1.6-1.4	-0.5-0.3	-0.9-3.6	-1.0-0.9	-0.5-1.4	0.5-1.9	-0.4-2.4	-1.7-0.9
10	-1.6-1.9	-1.0-0.6	-0.4-0.9	-1.5-1.7	-0.7-0.7	0.8-6.8	-0.2-2.2	-0.2-2.1	-0.4-2.4	8.3-10.2	-1.1-1.4
11	-2.1-1.2	-0.8-0.4	-0.3-0.4	-1.9-1.1	-0.4-0.4	-1.2-1.0	-0.8-0.9	-0.5-1.2	-1.7-0.9	-1.1-1.4	0.1-0.6
Total	6.7-17.7	-9.7-2.4	-10.3-1.9	2.5-14.6	-9.9-2.2	56.0-62.7	-0.6-11.0	-4.5-7.5	-4.0-7.9	9.7-20.4	-9.7-2.5
Higher	12.9	-1.7	-3.7	6.6	-2.5	11.3	-2.8	-5.5	-1.1	-1.4	-2.9

Table F.9: North / Temp. at 0cm / Mean

i \ j	1	2	3	4	5	6	7	8	9	10	11
1	-0.4-3.3	-2.4-3.6	-2.4-3.6	0.3-6.5	-2.5-3.5	-1.3-7.6	-2.7-3.2	-2.6-3.1	-2.5-3.6	-3.3-2.2	-3.0-3.1
2	-2.4-3.6	-0.4-0.3	-0.8-0.6	-0.7-1.0	-0.8-0.6	-1.5-6.1	-0.8-0.6	-0.8-0.6	-0.7-0.7	-1.0-0.9	-0.8-0.6
3	-2.4-3.6	-0.8-0.6	-0.2-0.5	-0.8-0.9	-0.9-0.5	-1.8-5.8	-0.9-0.5	-0.9-0.5	-0.9-0.6	-0.9-1.0	-0.9-0.5
4	0.3-6.5	-0.7-1.0	-0.8-0.9	4.4-7.4	-1.4-3.5	-1.5-7.6	-1.2-3.4	-1.5-3.1	-1.7-3.3	-0.9-4.0	-1.2-3.7
5	-2.5-3.5	-0.8-0.6	-0.9-0.5	-1.4-3.5	-0.1-0.2	-1.6-5.9	-0.4-0.2	-0.4-0.2	-0.2-0.3	-0.9-0.6	-0.2-0.3
6	-1.3-7.6	-1.5-6.1	-1.8-5.8	-1.5-7.6	-1.6-5.9	39.4-45.5	-1.3-2.2	-1.3-2.6	-1.9-3.0	-2.9-3.8	-1.0-1.9
7	-2.7-3.2	-0.8-0.6	-0.9-0.5	-1.2-3.4	-0.4-0.2	-1.3-2.2	3.1-4.0	-1.1-0.9	-1.2-0.6	-1.2-1.2	-1.2-0.5
8	-2.6-3.1	-0.8-0.6	-0.9-0.5	-1.5-3.1	-0.4-0.2	-1.3-2.6	-1.1-0.9	4.0-5.1	-1.1-0.8	-1.3-1.3	-1.0-0.8
9	-2.5-3.6	-0.7-0.7	-0.9-0.6	-1.7-3.3	-0.2-0.3	-1.9-3.0	-1.2-0.6	-1.1-0.8	-0.9-1.1	-2.4-1.5	-1.8-2.1
10	-3.3-2.2	-1.0-0.9	-0.9-1.0	-0.9-4.0	-0.9-0.6	-2.9-3.8	-1.2-1.2	-1.3-1.3	-2.4-1.5	10.7-13.4	-1.5-2.1
11	-3.0-3.1	-0.8-0.6	-0.9-0.5	-1.2-3.7	-0.2-0.3	-1.0-1.9	-1.2-0.5	-1.0-0.8	-1.8-2.1	-1.5-2.1	-0.3-0.4
Total	14.6-25.5	-5.9-6.1	-5.9-6.1	17.3-28.2	-6.6-5.5	54.7-61.7	-5.4-7.0	-3.6-8.4	-2.7-9.5	11.1-21.9	-5.5-6.4
Higher	9.8	-2.4	-1.6	3.7	-3.8	0.6	-3.4	-3.1	2.2	3.3	-1.0

Table F.10: Control / Temp. at 0cm / Maximum

i \ j	1	2	3	4	5	6	7	8	9	10	11
1	-0.7-0.7	-1.5-1.1	-1.6-1.0	-0.5-2.0	-1.7-1.0	-0.6-3.9	-1.1-1.6	-1.1-1.7	-1.3-1.6	-1.5-1.2	-1.7-0.9
2	-1.5-1.1	-0.2-0.3	-0.3-0.7	-0.3-0.9	-0.2-0.8	-0.1-3.8	-0.3-0.9	-0.3-0.8	-0.2-0.8	-0.2-1.2	-0.3-0.7
3	-1.6-1.0	-0.3-0.7	-0.1-0.1	-0.3-0.4	-0.3-0.2	-0.4-3.3	-0.3-0.3	-0.3-0.3	-0.2-0.2	-0.5-0.5	-0.2-0.3
4	-0.5-2.0	-0.3-0.9	-0.3-0.4	4.2-5.9	-1.2-0.8	3.2-8.4	-0.8-1.5	-1.4-1.0	-1.1-1.3	0.0-2.6	-1.3-0.7
5	-1.7-1.0	-0.2-0.8	-0.3-0.2	-1.2-0.8	-0.2-0.2	-0.4-3.4	-0.1-0.9	-0.1-0.8	-0.2-0.6	-0.3-0.9	-0.2-0.6
6	-0.6-3.9	-0.1-3.8	-0.4-3.3	3.2-8.4	-0.4-3.4	22.3-25.8	2.6-6.2	2.1-5.6	-1.0-2.8	2.1-6.7	-1.5-0.9
7	-1.1-1.6	-0.3-0.9	-0.3-0.3	-0.8-1.5	-0.1-0.9	2.6-6.2	3.7-5.2	-0.1-2.8	-0.7-2.0	0.3-3.2	-0.3-2.0
8	-1.1-1.7	-0.3-0.8	-0.3-0.3	-1.4-1.0	-0.1-0.8	2.1-5.6	-0.1-2.8	3.1-4.6	-0.1-2.6	0.2-3.1	0.0-2.3
9	-1.3-1.6	-0.2-0.8	-0.2-0.2	-1.1-1.3	-0.2-0.6	-1.0-2.8	-0.7-2.0	-0.1-2.6	0.1-1.9	1.9-5.1	-1.1-1.9
10	-1.5-1.2	-0.2-1.2	-0.5-0.5	0.0-2.6	-0.3-0.9	2.1-6.7	0.3-3.2	0.2-3.1	1.9-5.1	6.5-8.4	-1.2-1.5
11	-1.7-0.9	-0.3-0.7	-0.2-0.3	-1.3-0.7	-0.2-0.6	-1.5-0.9	-0.3-2.0	0.0-2.3	-1.1-1.9	-1.2-1.5	-0.1-0.2
Total	2.2-11.8	-6.4-3.5	-7.4-2.6	20.5-29.2	-6.4-3.4	55.9-61.9	9.8-18.7	6.1-15.4	8.9-18.1	21.2-29.3	-6.8-3.1
Higher	5.4	-5.5	-3.8	11.8	-4.2	9.3	-0.5	-3.1	5.0	4.4	-4.0

Table F.11: South / Temp. at 0cm / Maximum

i \ j	1	2	3	4	5	6	7	8	9	10	11
1	0.0-1.3	-1.9-0.6	-1.9-0.5	-1.1-1.2	-1.9-0.5	-2.6-1.6	-2.1-0.8	-1.7-1.0	-1.6-0.8	-1.8-0.6	-1.9-0.5
2	-1.9-0.6	-0.2-0.4	-0.6-0.6	-0.7-0.6	-0.5-0.7	-1.4-2.2	-0.6-1.2	-0.7-0.9	-0.6-0.7	-0.5-0.9	-0.6-0.6
3	-1.9-0.5	-0.6-0.6	-0.1-0.1	-0.2-0.2	-0.2-0.3	-1.7-1.8	-0.6-0.7	-0.6-0.4	-0.3-0.2	-0.4-0.3	-0.1-0.3
4	-1.1-1.2	-0.7-0.6	-0.2-0.2	0.9-2.1	-1.5-0.5	-1.8-2.4	-1.2-1.2	-1.2-1.0	-1.4-0.6	-1.0-1.0	-1.6-0.4
5	-1.9-0.5	-0.5-0.7	-0.2-0.3	-1.5-0.5	0.1-0.6	-1.4-2.2	-0.6-1.2	-0.5-0.9	-0.2-0.7	-0.4-0.7	-0.4-0.5
6	-2.6-1.6	-1.4-2.2	-1.7-1.8	-1.8-2.4	-1.4-2.2	22.8-26.3	4.5-9.0	3.7-7.8	-0.7-2.2	0.4-4.2	-1.1-1.1
7	-2.1-0.8	-0.6-1.2	-0.6-0.7	-1.2-1.2	-0.6-1.2	4.5-9.0	10.9-13.0	-0.6-3.1	-1.0-1.7	0.4-3.3	-0.9-1.4
8	-1.7-1.0	-0.7-0.9	-0.6-0.4	-1.2-1.0	-0.5-0.9	3.7-7.8	-0.6-3.1	8.6-10.5	-0.5-2.2	0.0-3.0	-0.7-1.8
9	-1.6-0.8	-0.6-0.7	-0.3-0.2	-1.4-0.6	-0.2-0.7	-0.7-2.2	-1.0-1.7	-0.5-2.2	0.8-2.0	-0.3-1.9	-1.1-1.1
10	-1.8-0.6	-0.5-0.9	-0.4-0.3	-1.0-1.0	-0.4-0.7	0.4-4.2	0.4-3.3	0.0-3.0	-0.3-1.9	4.9-6.4	-0.6-1.4
11	-1.9-0.5	-0.6-0.6	-0.1-0.3	-1.6-0.4	-0.4-0.5	-1.1-1.1	-0.9-1.4	-0.7-1.8	-1.1-1.1	-0.6-1.4	-0.0-0.3
Total	0.9-10.6	-7.0-2.6	-8.7-1.2	0.6-10.7	-6.5-3.3	47.9-54.4	21.6-29.6	14.4-22.9	-2.5-7.1	8.7-17.8	-8.1-1.7
Higher	10.4	-2.6	-3.0	5.4	-2.2	10.4	3.2	-0.6	-1.3	1.1	-3.3

Table F.12: North / Temp. at 0cm / Maximum

i \ j	1	2	3	4	5	6	7	8	9	10	11
1	-1.0-1.1	-2.2-1.5	-2.2-1.4	-0.4-3.4	-2.3-1.4	0.3-5.4	-1.4-2.1	-1.4-2.1	-2.4-1.4	-1.9-1.6	-1.4-2.3
2	-2.2-1.5	-0.4-0.2	-0.1-1.0	-0.1-1.2	-0.1-1.1	0.2-4.4	-0.1-1.2	-0.1-1.4	-0.2-1.0	-0.2-1.1	-0.1-1.0
3	-2.2-1.4	-0.1-1.0	-0.3-0.3	-0.6-0.8	-0.6-0.6	-0.4-3.9	-0.6-0.6	-0.8-0.6	-0.6-0.6	-0.6-0.7	-0.6-0.6
4	-0.4-3.4	-0.1-1.2	-0.6-0.8	6.2-8.3	-0.1-2.9	2.5-7.9	0.4-3.4	0.3-3.4	-0.2-2.8	0.9-3.8	0.0-3.0
5	-2.3-1.4	-0.1-1.1	-0.6-0.6	-0.1-2.9	0.1-0.5	-0.2-3.9	-0.5-0.5	-0.5-0.8	-0.5-0.4	-0.7-0.5	-0.5-0.3
6	0.3-5.4	0.2-4.4	-0.4-3.9	2.5-7.9	-0.2-3.9	31.4-35.2	-0.6-2.8	-0.2-3.8	-0.6-2.5	-1.2-3.1	-0.6-1.8
7	-1.4-2.1	-0.1-1.2	-0.6-0.6	0.4-3.4	-0.5-0.5	-0.6-2.8	7.5-9.3	-0.9-2.7	-1.0-1.8	-1.8-1.2	-1.0-1.8
8	-1.4-2.1	-0.1-1.4	-0.8-0.6	0.3-3.4	-0.5-0.8	-0.2-3.8	-0.9-2.7	10.8-12.8	-1.4-1.6	-1.8-1.5	-1.3-1.6
9	-2.4-1.4	-0.2-1.0	-0.6-0.6	-0.2-2.8	-0.5-0.4	-0.6-2.5	-1.0-1.8	-1.4-1.6	-0.5-0.8	-0.8-1.7	-1.1-1.4
10	-1.9-1.6	-0.2-1.1	-0.6-0.7	0.9-3.8	-0.7-0.5	-1.2-3.1	-1.8-1.2	-1.8-1.5	-0.8-1.7	8.7-10.5	-1.1-1.6
11	-1.4-2.3	-0.1-1.0	-0.6-0.6	0.0-3.0	-0.5-0.3	-0.6-1.8	-1.0-1.8	-1.3-1.6	-1.1-1.4	-1.1-1.6	-0.3-0.2
Total	5.7-14.0	-5.7-3.1	-3.9-4.6	18.0-25.6	-3.8-4.6	46.2-51.6	7.8-15.7	12.2-19.7	-2.0-6.7	10.1-18.0	-4.0-4.5
Higher	6.1	-7.3	-1.4	-3.0	-3.0	-3.8	-2.0	-1.4	-1.0	0.7	-3.4

Table F.13: Control / Temp. at 0cm / Minimum

i \ j	1	2	3	4	5	6	7	8	9	10	11
1	-1.0-1.2	-1.7-2.5	-1.8-2.5	-8.2-7.9	-1.8-2.5	-1.3-2.9	-1.7-2.6	-1.8-2.5	-1.9-2.5	-1.5-2.7	-1.6-2.6
2	-1.7-2.5	-0.4-0.3	-0.5-0.8	-9.0-7.1	-0.5-0.8	-0.8-0.6	-0.5-0.8	-0.5-0.8	-0.5-0.8	-0.8-0.5	-0.5-0.8
3	-1.8-2.5	-0.5-0.8	-0.4-0.2	-8.8-7.3	-0.4-0.7	-0.3-0.9	-0.4-0.7	-0.4-0.7	-0.4-0.8	-0.4-0.8	-0.4-0.7
4	-8.2-7.9	-9.0-7.1	-8.8-7.3	73.0-82.8	-1.3-0.5	-2.4-8.1	-1.2-0.8	-0.9-1.3	-3.9-3.5	-1.1-7.1	-1.3-0.8
5	-1.8-2.5	-0.5-0.8	-0.4-0.7	-1.3-0.5	-0.3-0.3	-0.7-0.5	-0.5-0.5	-0.5-0.5	-0.5-0.7	-0.5-0.6	-0.5-0.5
6	-1.3-2.9	-0.8-0.6	-0.3-0.9	-2.4-8.1	-0.7-0.5	3.9-7.1	-3.2-2.6	-3.3-2.5	-2.4-3.5	-3.6-2.2	-3.3-2.5
7	-1.7-2.6	-0.5-0.8	-0.4-0.7	-1.2-0.8	-0.5-0.5	-3.2-2.6	-0.2-0.4	-0.8-0.5	-0.7-0.5	-0.7-0.6	-0.8-0.5
8	-1.8-2.5	-0.5-0.8	-0.4-0.7	-0.9-1.3	-0.5-0.5	-3.3-2.5	-0.8-0.5	-0.4-0.2	-0.4-0.7	-0.4-0.8	-0.5-0.7
9	-1.9-2.5	-0.5-0.8	-0.4-0.8	-3.9-3.5	-0.5-0.7	-2.4-3.5	-0.7-0.5	-0.4-0.7	-1.0-1.1	-1.6-2.5	-2.0-2.2
10	-1.5-2.7	-0.8-0.5	-0.4-0.8	-1.1-7.1	-0.5-0.6	-3.6-2.2	-0.7-0.6	-0.4-0.8	-1.6-2.5	-0.5-1.6	-1.8-2.3
11	-1.6-2.6	-0.5-0.8	-0.4-0.7	-1.3-0.8	-0.5-0.5	-3.3-2.5	-0.8-0.5	-0.5-0.7	-2.0-2.2	-1.8-2.3	-0.4-0.2
Total	3.1-13.6	-5.8-5.4	-6.0-5.3	87.1-90.5	-6.4-4.9	11.1-21.0	-6.3-5.1	-6.1-5.2	0.3-10.9	1.6-12.1	-6.1-5.3
Higher	4.2	-0.2	-1.4	7.7	-1.1	7.9	-0.5	-1.1	3.7	2.4	-0.7

Table F.14: South / Temp. at 0cm / Minimum

i \ j	1	2	3	4	5	6	7	8	9	10	11
1	0.2-3.7	-2.8-3.8	-2.7-3.9	-24.1-0.4	-2.7-3.8	-3.0-3.4	-2.7-3.9	-2.6-3.9	-4.1-2.6	-2.5-4.0	-2.7-3.8
2	-2.8-3.8	-0.7-0.4	-1.2-0.8	-23.3-0.4	-1.3-0.8	-0.8-1.4	-1.3-0.8	-1.2-0.8	-1.2-0.8	-1.2-0.9	-1.2-0.8
3	-2.7-3.9	-1.2-0.8	-0.5-0.7	-23.5-0.4	-1.3-1.0	-1.2-1.1	-1.3-1.0	-1.3-1.0	-1.3-1.1	-1.3-1.0	-1.3-1.0
4	-24.1-0.4	-23.3-0.4	-23.5-0.4	79.7-94.7	-1.6-2.0	-4.9-7.8	-1.5-2.7	-2.1-2.6	-3.0-4.7	-3.0-6.5	-2.1-0.9
5	-2.7-3.8	-1.3-0.8	-1.3-1.0	-1.6-2.0	-0.6-0.5	-0.9-1.3	-0.9-1.3	-1.0-1.2	-0.9-1.3	-1.0-1.2	-1.0-1.2
6	-3.0-3.4	-0.8-1.4	-1.2-1.1	-4.9-7.8	-0.9-1.3	1.3-4.8	-5.9-1.2	-5.7-1.3	-5.7-1.3	-5.3-1.7	-5.8-1.2
7	-2.7-3.9	-1.3-0.8	-1.3-1.0	-1.5-2.7	-0.9-1.3	-5.9-1.2	-0.6-0.5	-1.1-1.2	-1.0-1.2	-1.1-1.1	-1.1-1.1
8	-2.6-3.9	-1.2-0.8	-1.3-1.0	-2.1-2.6	-1.0-1.2	-5.7-1.3	-1.1-1.2	-0.6-0.6	-1.1-1.2	-1.1-1.1	-1.1-1.1
9	-4.1-2.6	-1.2-0.8	-1.3-1.1	-3.0-4.7	-0.9-1.3	-5.7-1.3	-1.0-1.2	-1.1-1.2	-0.3-1.9	-3.6-0.8	-3.6-0.8
10	-2.5-4.0	-1.2-0.9	-1.3-1.0	-3.0-6.5	-1.0-1.2	-5.3-1.7	-1.1-1.1	-1.1-1.1	-3.6-0.8	-1.0-1.4	-3.2-1.7
11	-2.7-3.8	-1.2-0.8	-1.3-1.0	-2.1-0.9	-1.0-1.2	-5.8-1.2	-1.1-1.1	-1.1-1.1	-3.6-0.8	-3.2-1.7	-0.6-0.4
Total	5.0-19.2	-5.4-9.8	-5.7-9.6	88.5-92.1	-5.7-9.7	3.3-17.6	-5.8-9.6	-5.9-9.5	-3.5-11.6	-0.8-13.8	-5.7-9.7
Higher	18.3	14.4	13.9	33.4	0.8	16.1	3.0	3.3	8.2	8.0	6.8

Table F.15: North / Temp. at 0cm / Minimum

i \ j	1	2	3	4	5	6	7	8	9	10	11
1	0.6-4.1	-2.4-4.0	-2.5-3.9	-17.2-7.9	-2.5-3.9	-3.4-2.9	-2.5-3.9	-2.5-3.9	-4.0-2.4	-3.8-2.6	-2.7-3.8
2	-2.4-4.0	-0.3-0.3	-0.7-0.6	-17.3-7.0	-0.7-0.7	-0.5-0.9	-0.7-0.7	-0.7-0.7	-0.6-0.7	-0.6-0.7	-0.7-0.7
3	-2.5-3.9	-0.7-0.6	-0.3-0.6	-17.5-7.0	-1.2-0.7	-1.1-0.9	-1.2-0.7	-1.2-0.7	-1.1-0.8	-1.2-0.7	-1.2-0.7
4	-17.2-7.9	-17.3-7.0	-17.5-7.0	74.4-88.8	-1.0-0.6	-2.6-9.0	-0.8-1.0	-1.3-0.9	-4.2-3.3	-3.6-5.3	-0.8-1.8
5	-2.5-3.9	-0.7-0.7	-1.2-0.7	-1.0-0.6	-0.0-0.3	-0.5-0.3	-0.7-0.0	-0.7-0.0	-0.7-0.1	-0.7-0.1	-0.7-0.0
6	-3.4-2.9	-0.5-0.9	-1.1-0.9	-2.6-9.0	-0.5-0.3	0.9-4.8	-3.6-3.6	-3.7-3.5	-3.7-3.6	-3.2-4.1	-3.7-3.6
7	-2.5-3.9	-0.7-0.7	-1.2-0.7	-0.8-1.0	-0.7-0.0	-3.6-3.6	-0.0-0.4	-0.8-0.1	-0.8-0.1	-0.8-0.1	-0.8-0.1
8	-2.5-3.9	-0.7-0.7	-1.2-0.7	-1.3-0.9	-0.7-0.0	-3.7-3.5	-0.8-0.1	-0.2-0.3	-0.6-0.4	-0.6-0.4	-0.7-0.4
9	-4.0-2.4	-0.6-0.7	-1.1-0.8	-4.2-3.3	-0.7-0.1	-3.7-3.6	-0.8-0.1	-0.6-0.4	-0.9-1.2	-2.2-2.0	-2.4-1.8
10	-3.8-2.6	-0.6-0.7	-1.2-0.7	-3.6-5.3	-0.7-0.1	-3.2-4.1	-0.8-0.1	-0.6-0.4	-2.2-2.0	-0.8-2.0	-3.2-2.1
11	-2.7-3.8	-0.7-0.7	-1.2-0.7	-0.8-1.8	-0.7-0.0	-3.7-3.6	-0.8-0.1	-0.7-0.4	-2.4-1.8	-3.2-2.1	-0.6-0.2
Total	7.7-21.7	-5.2-10.1	-5.1-10.2	89.7-93.7	-5.7-9.7	7.5-21.6	-5.6-9.7	-5.4-9.9	-2.3-12.7	1.0-15.6	-4.8-10.5
Higher	14.5	6.6	8.5	21.5	3.3	8.6	3.1	3.0	7.6	8.5	4.0

## F.3 Snow Temperature at 2 cm

Table F.16: Control / Temp. at 2cm with Time (Total-effect)

t \ i	1	2	3	4	5	6	7	8	9	10	11
0.33	4.0-12.7	0.5-9.5	-3.6-5.6	61.8-65.8	-3.6-5.6	22.2-29.4	-3.6-5.6	-3.6-5.6	-0.2-8.8	4.0-12.5	-3.4-5.7
0.67	1.5-10.2	-0.4-8.5	-5.0-4.1	39.0-44.7	-5.0-4.1	39.6-45.4	-5.0-4.1	-5.0-4.1	0.8-9.6	8.0-16.1	-4.8-4.3
1.00	-0.2-8.5	-1.5-7.2	-5.8-3.2	26.7-33.4	-5.8-3.2	49.1-54.1	-5.6-3.4	-5.7-3.3	1.3-10.0	10.3-18.1	-5.5-3.5
1.33	-1.1-7.4	-2.6-6.0	-3.6-4.7	19.3-26.4	-3.6-4.7	54.2-58.7	-5.3-3.4	-5.6-3.3	1.6-10.0	11.7-19.3	-3.3-5.0
1.67	-1.6-6.8	-3.5-5.0	-4.1-4.0	14.4-21.7	-4.0-4.1	56.5-60.8	-4.2-4.3	-4.5-4.1	1.5-9.7	12.7-20.0	-3.8-4.3
2.00	-2.2-6.1	-4.2-4.2	-4.6-3.4	10.6-18.3	-4.5-3.5	56.9-61.2	-2.1-6.2	-2.5-5.8	0.9-9.2	13.1-20.3	-4.3-3.7
2.33	-2.9-5.6	-5.1-3.6	-5.2-3.0	7.7-15.6	-4.9-3.2	56.1-60.5	1.1-9.1	0.3-8.4	0.3-8.6	13.2-20.5	-4.8-3.2
2.67	-3.5-5.1	-5.5-3.2	-5.6-2.5	5.3-13.4	-5.3-2.9	54.7-59.3	4.9-12.9	3.7-11.7	-0.2-8.3	13.2-20.5	-5.3-2.8
3.00	-4.3-4.5	-6.0-2.9	-6.2-2.3	3.3-11.7	-5.7-2.7	53.3-58.1	8.9-16.7	6.9-14.9	-0.8-7.9	13.0-20.6	-5.9-2.5
3.33	-5.1-4.0	-3.6-4.9	-6.7-2.1	1.6-10.3	-6.2-2.5	52.2-57.2	12.6-20.4	9.8-17.7	-1.3-7.6	12.9-20.7	-6.4-2.4
3.67	-5.9-3.4	-3.9-4.9	-7.1-1.9	0.2-9.2	-6.6-2.4	51.4-56.6	15.7-23.5	12.1-20.0	-1.6-7.5	12.9-20.9	-6.8-2.1
4.00	-3.8-5.2	-4.2-4.9	-7.5-1.8	-1.2-8.2	-7.0-2.3	50.7-56.2	18.2-26.1	14.0-21.9	-2.0-7.4	12.9-21.0	-7.2-2.0
4.33	-4.5-4.8	-4.4-4.9	-7.9-1.7	-2.3-7.4	-7.4-2.1	50.4-56.1	20.1-28.1	15.3-23.4	-2.3-7.4	12.9-21.2	-7.6-1.9
4.67	-5.1-4.3	-4.4-5.0	-8.1-1.6	-3.2-6.7	-7.7-2.0	50.3-56.1	21.6-29.7	16.4-24.5	-2.6-7.4	12.9-21.5	-7.9-1.8
5.00	-5.7-4.0	-4.4-5.1	-8.4-1.5	-4.0-6.1	-7.9-2.0	50.4-56.3	22.6-30.7	17.1-25.3	-2.6-7.5	13.0-21.7	-8.2-1.7
5.33	-6.2-3.6	-4.4-5.3	-8.6-1.4	-4.7-5.6	-8.1-1.8	50.5-56.5	23.1-31.3	17.5-25.8	-2.7-7.5	13.1-22.0	-8.3-1.6
5.67	-6.6-3.3	-4.3-5.4	-8.7-1.4	-5.3-5.1	-8.3-1.7	50.8-56.8	23.2-31.5	17.6-25.9	-2.7-7.6	13.3-22.2	-8.4-1.6
6.00	-6.9-3.0	-4.1-5.6	-8.8-1.3	-5.8-4.7	-8.3-1.7	51.2-57.1	22.8-31.2	17.4-25.7	-2.6-7.7	13.6-22.4	-8.5-1.5
6.33	-7.2-2.7	-4.0-5.7	-8.8-1.2	-6.2-4.2	-8.4-1.6	51.6-57.5	22.1-30.4	16.7-25.1	-2.6-7.7	13.8-22.7	-8.5-1.5
6.67	-7.4-2.4	-3.8-5.8	-8.8-1.1	-6.6-3.8	-8.4-1.6	52.2-58.0	20.8-29.1	15.7-24.1	-2.4-7.8	14.2-22.9	-8.5-1.4
7.00	-7.5-2.2	-6.8-3.4	-8.8-1.1	-6.8-3.4	-8.4-1.4	53.0-58.6	18.9-27.3	14.2-22.7	-2.2-7.8	14.5-23.1	-8.5-1.3
7.33	-7.6-2.1	-6.6-3.4	-8.7-1.0	-4.0-5.5	-8.3-1.3	54.0-59.5	16.4-24.8	12.2-20.7	-2.0-7.9	14.8-23.2	-8.4-1.2
7.67	-7.5-2.0	-6.4-3.5	-8.6-0.9	-4.2-5.2	-8.2-1.2	55.4-60.6	13.3-21.7	9.6-18.1	-1.6-8.0	15.3-23.5	-8.3-1.2
8.00	-7.3-2.0	-6.1-3.5	-8.3-1.0	-4.2-4.9	-8.0-1.3	57.3-62.2	9.5-18.1	6.4-15.0	-1.2-8.1	15.8-23.8	-8.0-1.3
8.33	-6.9-2.2	-5.7-3.6	-8.0-1.1	-4.1-4.9	-7.7-1.4	59.6-64.3	5.5-14.2	3.0-11.6	-0.8-8.3	16.4-24.2	-7.6-1.5
8.67	-6.3-2.5	-5.5-3.7	-7.5-1.4	-3.8-5.0	-7.3-1.6	62.5-66.8	1.7-10.4	-0.4-8.4	-0.3-8.6	17.0-24.6	-7.1-1.8
9.00	-5.7-3.0	-5.4-3.6	-6.9-1.8	-3.5-5.1	-6.8-1.9	65.5-69.4	-1.6-7.2	-3.1-5.7	0.3-9.0	17.5-25.0	-6.5-2.1
9.33	-5.1-3.4	-5.5-3.4	-6.4-2.1	-6.0-3.0	-6.3-2.2	68.2-71.9	-3.9-4.9	-5.0-3.7	0.9-9.5	17.8-25.2	-6.0-2.5
9.67	-4.6-3.7	-5.7-3.0	-6.0-2.3	-5.7-3.1	-6.0-2.4	70.5-73.9	-5.5-3.3	-3.6-4.7	1.5-10.0	18.0-25.2	-5.6-2.8
10.00	-4.4-3.9	-3.5-4.7	-5.8-2.5	-5.6-3.2	-5.7-2.5	72.0-75.3	-3.6-4.6	-4.3-3.9	2.1-10.4	18.0-25.2	-5.3-2.9

Table F.17: Control / Temp. at 2cm / Mid-day

i \ j	1	2	3	4	5	6	7	8	9	10	11
1	-0.1-0.5	-0.4-0.8	-0.3-0.8	0.0-1.1	-0.3-0.8	-1.3-2.7	-0.0-1.6	0.0-1.6	-0.2-1.0	0.0-1.4	-0.3-0.8
2	-0.4-0.8	0.0-0.7	-0.5-0.7	-0.6-0.6	-0.5-0.7	0.1-4.2	-0.2-1.6	-0.3-1.3	-0.4-0.9	0.1-1.4	-0.5-0.7
3	-0.3-0.8	-0.5-0.7	-0.0-0.0	-0.1-0.1	-0.0-0.1	-1.2-2.6	-0.1-0.9	-0.2-0.7	-0.0-0.1	-0.1-0.5	-0.0-0.1
4	0.0-1.1	-0.6-0.6	-0.1-0.1	2.1-2.8	-0.6-0.5	-1.7-2.8	-0.2-1.7	-0.5-1.2	-0.6-0.6	-0.5-1.2	-0.6-0.5
5	-0.3-0.8	-0.5-0.7	-0.0-0.1	-0.6-0.5	-0.0-0.2	-1.4-2.4	-0.3-0.9	-0.4-0.6	-0.3-0.3	-0.2-0.6	-0.2-0.3
6	-1.3-2.7	0.1-4.2	-1.2-2.6	-1.7-2.8	-1.4-2.4	22.7-26.1	7.9-12.3	6.1-10.0	-1.0-1.4	2.0-5.6	-1.3-0.3
7	-0.0-1.6	-0.2-1.6	-0.1-0.9	-0.2-1.7	-0.3-0.9	7.9-12.3	9.0-11.1	0.3-4.2	-0.6-2.2	2.0-5.2	-0.4-2.2
8	0.0-1.6	-0.3-1.3	-0.2-0.7	-0.5-1.2	-0.4-0.6	6.1-10.0	0.3-4.2	7.8-9.7	-0.4-2.3	1.1-4.1	-0.6-1.9
9	-0.2-1.0	-0.4-0.9	-0.0-0.1	-0.6-0.6	-0.3-0.3	-1.0-1.4	-0.6-2.2	-0.4-2.3	-0.5-0.5	0.9-3.0	-1.1-0.9
10	0.0-1.4	0.1-1.4	-0.1-0.5	-0.5-1.2	-0.2-0.6	2.0-5.6	2.0-5.2	1.1-4.1	0.9-3.0	5.7-7.1	-0.2-1.5
11	-0.3-0.8	-0.5-0.7	-0.0-0.1	-0.6-0.5	-0.2-0.3	-1.3-0.3	-0.4-2.2	-0.6-1.9	-1.1-0.9	-0.2-1.5	-0.0-0.2
Total	-5.7-4.0	-4.4-5.1	-8.4-1.5	-4.0-6.1	-7.9-2.0	50.4-56.3	22.6-30.7	17.1-25.3	-2.6-7.5	13.0-21.7	-8.2-1.7
Higher	-5.9	-4.9	-5.5	-3.9	-4.6	2.5	-3.9	-4.1	-2.1	-4.0	-5.2

Table F.18: South / Temp. at 2cm with Time (Total-effect)

t \ i	1	2	3	4	5	6	7	8	9	10	11
0.33	6.5-18.1	1.8-13.9	-3.5-9.1	58.3-63.9	-3.5-9.1	22.8-32.4	-3.5-9.1	-3.5-9.1	-2.7-9.8	1.5-13.5	-3.4-9.2
0.67	4.6-15.3	1.2-12.2	-4.6-7.0	36.6-44.1	-4.6-6.9	39.4-46.5	-4.6-7.0	-4.6-7.0	-3.3-8.2	4.3-14.9	-4.4-7.1
1.00	3.4-13.5	-0.2-10.2	-5.3-5.5	25.2-33.3	-5.3-5.5	47.7-53.7	-4.6-6.2	-4.8-6.0	-3.7-7.0	5.9-15.6	-5.1-5.7
1.33	3.3-12.7	-1.4-8.4	-5.8-4.4	18.0-26.2	-5.7-4.5	50.9-56.1	-2.8-7.0	-3.4-6.6	-4.1-6.0	6.7-15.7	-5.6-4.6
1.67	3.2-12.0	-2.3-6.9	-6.2-3.3	12.8-21.0	-5.9-3.5	50.1-55.1	1.1-9.9	0.1-9.1	-4.4-5.0	6.7-15.2	-6.0-3.5
2.00	2.4-10.8	-3.2-5.6	-3.9-4.6	8.9-16.9	-3.5-5.0	47.0-52.1	6.5-14.4	4.8-12.9	-4.9-4.0	6.3-14.3	-3.6-4.8
2.33	1.2-9.3	-3.8-4.6	-4.5-3.7	5.8-13.8	-3.9-4.2	43.6-48.9	12.7-19.8	10.1-17.5	-5.4-3.2	5.7-13.4	-4.2-3.9
2.67	0.0-8.1	-4.3-4.0	-4.9-3.2	3.5-11.5	-4.3-3.8	40.8-46.2	18.3-25.0	14.6-21.5	-3.3-4.8	5.0-12.8	-4.7-3.4
3.00	-1.1-7.2	-4.5-3.8	-5.3-2.9	1.8-10.0	-4.6-3.6	38.9-44.5	23.2-29.7	18.2-24.9	-3.6-4.5	4.8-12.6	-5.1-3.1
3.33	-2.1-6.3	-5.0-3.6	-5.7-2.7	0.5-8.9	-5.0-3.3	37.6-43.6	27.1-33.4	20.7-27.4	-3.9-4.4	4.6-12.6	-5.5-2.9
3.67	-3.2-5.5	-5.3-3.6	-6.0-2.5	-0.7-7.9	-5.3-3.2	37.0-43.2	30.0-36.4	22.6-29.4	-4.1-4.4	4.4-12.7	-5.8-2.7
4.00	-4.1-4.9	-5.4-3.6	-6.3-2.5	-1.8-7.2	-5.6-3.1	36.8-43.2	32.2-38.6	24.0-30.9	-4.2-4.5	4.2-12.8	-6.1-2.7
4.33	-5.0-4.4	-5.6-3.8	-6.6-2.5	-2.6-6.6	-5.9-3.1	36.9-43.5	33.7-40.3	25.0-32.1	-4.4-4.5	4.2-13.0	-6.4-2.7
4.67	-5.7-3.9	-5.5-4.0	-6.8-2.5	-3.4-6.1	-6.1-3.1	37.2-44.0	34.9-41.6	25.7-32.9	-4.5-4.6	4.2-13.3	-6.6-2.6
5.00	-6.4-3.5	-5.5-4.3	-7.0-2.5	-4.1-5.7	-6.3-3.0	37.6-44.4	35.7-42.4	26.3-33.5	-4.6-4.7	4.2-13.5	-6.8-2.7
5.33	-3.9-5.4	-5.4-4.5	-7.1-2.5	-4.6-5.4	-6.5-3.0	38.0-44.9	36.1-42.9	26.6-33.9	-4.6-4.9	4.3-13.7	-6.9-2.7
5.67	-4.4-5.1	-5.2-4.8	-7.2-2.4	-5.1-5.1	-6.6-3.0	38.5-45.5	36.2-43.0	26.6-34.0	-4.6-4.9	4.4-13.9	-7.0-2.7
6.00	-4.8-4.7	-5.0-5.1	-7.3-2.4	-5.5-4.7	-6.7-2.9	39.1-46.0	35.9-42.8	26.4-33.9	-4.6-4.9	4.6-14.1	-7.0-2.7
6.33	-5.2-4.3	-4.7-5.2	-7.4-2.3	-5.8-4.4	-6.7-2.9	39.7-46.6	35.2-42.2	26.0-33.4	-4.6-4.9	4.8-14.3	-7.0-2.6
6.67	-5.5-3.9	-4.4-5.4	-7.4-2.3	-6.1-4.0	-6.7-2.9	40.4-47.2	34.2-41.1	25.2-32.7	-4.6-4.9	5.0-14.4	-7.0-2.6
7.00	-5.8-3.5	-4.2-5.6	-7.3-2.1	-6.3-3.7	-6.7-2.7	41.3-47.8	32.6-39.5	24.0-31.5	-4.5-4.8	5.3-14.5	-7.0-2.4
7.33	-6.0-3.2	-3.8-5.7	-7.3-2.0	-6.5-3.4	-6.7-2.6	42.4-48.7	30.3-37.3	22.3-29.8	-4.4-4.7	5.6-14.6	-7.0-2.3
7.67	-6.2-2.9	-3.6-5.8	-7.3-1.9	-3.6-5.4	-6.7-2.4	43.8-49.8	27.1-34.2	19.9-27.4	-4.4-4.5	5.9-14.6	-6.9-2.2
8.00	-6.2-2.7	-3.3-5.8	-7.2-1.7	-3.8-5.1	-6.6-2.3	45.8-51.6	22.9-30.1	16.5-24.2	-4.4-4.4	6.3-14.8	-6.9-2.0
8.33	-6.2-2.6	-3.1-5.9	-7.2-1.6	-3.8-4.9	-6.6-2.2	48.9-54.2	17.4-24.9	12.1-20.1	-4.4-4.3	6.9-15.2	-6.8-2.0
8.67	-5.9-2.9	-2.8-6.2	-7.0-1.8	-3.7-5.0	-6.5-2.3	53.2-58.1	11.3-19.2	7.1-15.4	-4.2-4.5	7.6-15.9	-6.6-2.2
9.00	-5.3-3.4	-2.6-6.4	-6.7-2.3	-3.5-5.2	-6.1-2.7	58.6-63.0	5.2-13.6	2.2-10.8	-3.8-4.9	8.6-16.9	-6.2-2.6
9.33	-4.7-4.2	-2.9-6.3	-6.2-2.7	-6.2-3.3	-5.8-3.2	64.0-67.9	0.2-9.1	-1.8-7.3	-3.4-5.3	9.8-18.0	-5.8-3.2
9.67	-4.1-4.7	-3.6-5.7	-5.8-3.1	-5.8-3.6	-5.5-3.5	68.7-72.2	-3.2-6.1	-4.6-4.9	-6.1-3.4	10.7-18.9	-5.4-3.6
10.00	-3.9-5.0	-4.5-5.0	-5.6-3.5	-5.7-3.9	-5.3-3.7	71.8-75.0	-5.0-4.4	-5.8-3.7	-5.8-3.8	11.3-19.5	-5.1-3.9

Table F.19: South / Temp. at 2cm / Mid-day

i \ j	1	2	3	4	5	6	7	8	9	10	11
1	0.4-1.0	-0.3-0.9	-0.3-0.9	0.1-1.2	-0.2-1.0	-0.8-2.1	0.2-2.8	0.2-2.3	-0.2-1.0	-0.0-1.3	-0.3-0.9
2	-0.3-0.9	0.2-0.9	-0.6-0.7	-0.7-0.6	-0.6-0.7	0.1-3.0	-0.1-2.6	-0.2-1.9	-0.6-0.7	-0.2-1.1	-0.6-0.6
3	-0.3-0.9	-0.6-0.7	-0.0-0.0	-0.1-0.1	-0.0-0.1	-0.9-1.5	-0.3-1.8	-0.2-1.3	-0.0-0.1	-0.0-0.3	-0.0-0.1
4	0.1-1.2	-0.7-0.6	-0.1-0.1	1.7-2.3	-0.4-0.6	-1.8-1.3	0.1-2.9	-0.1-2.0	-0.4-0.6	-0.4-0.9	-0.5-0.5
5	-0.2-1.0	-0.6-0.7	-0.0-0.1	-0.4-0.6	-0.0-0.3	-1.1-1.4	-0.3-1.9	-0.4-1.3	-0.4-0.3	-0.2-0.5	-0.4-0.2
6	-0.8-2.1	0.1-3.0	-0.9-1.5	-1.8-1.3	-1.1-1.4	16.3-19.0	9.0-13.9	6.3-10.5	-0.7-0.9	0.0-2.6	-0.9-0.6
7	0.2-2.8	-0.1-2.6	-0.3-1.8	0.1-2.9	-0.3-1.9	9.0-13.9	16.8-19.6	2.3-7.3	-0.5-2.2	2.7-5.8	-0.2-2.3
8	0.2-2.3	-0.2-1.9	-0.2-1.3	-0.1-2.0	-0.4-1.3	6.3-10.5	2.3-7.3	13.1-15.5	-0.2-2.5	1.2-4.3	-0.3-2.2
9	-0.2-1.0	-0.6-0.7	-0.0-0.1	-0.4-0.6	-0.4-0.3	-0.7-0.9	-0.5-2.2	-0.2-2.5	-0.2-0.3	-0.1-1.0	-0.4-0.7
10	-0.0-1.3	-0.2-1.1	-0.0-0.3	-0.4-0.9	-0.2-0.5	0.0-2.6	2.7-5.8	1.2-4.3	-0.1-1.0	3.2-4.1	-0.1-1.1
11	-0.3-0.9	-0.6-0.6	-0.0-0.1	-0.5-0.5	-0.4-0.2	-0.9-0.6	-0.2-2.3	-0.3-2.2	-0.4-0.7	-0.1-1.1	0.0-0.2
Total	-6.4-3.5	-5.5-4.3	-7.0-2.5	-4.1-5.7	-6.3-3.0	37.6-44.4	35.7-42.4	26.3-33.5	-4.6-4.7	4.2-13.5	-6.8-2.7
Higher	-8.8	-5.6	-4.4	-4.5	-3.7	-0.1	-7.4	-6.4	-3.2	-5.8	-5.0

Table F.20: North / Temp. at 2cm with Time (Total-effect)

t \ i	1	2	3	4	5	6	7	8	9	10	11
0.33	2.2-15.6	-0.8-13.0	-2.6-11.3	80.3-83.6	-2.6-11.3	10.7-22.9	-2.5-11.3	-2.6-11.3	-2.1-11.7	0.3-13.9	-2.5-11.3
0.67	1.1-14.9	-1.6-12.5	-4.2-10.2	61.0-67.0	-4.1-10.3	24.0-34.6	-4.1-10.3	-4.1-10.2	-3.1-11.1	2.6-16.1	-4.0-10.3
1.00	0.3-13.9	-2.5-11.5	-4.8-9.3	47.3-55.0	-4.8-9.3	33.8-43.0	-4.8-9.3	-4.8-9.4	-3.5-10.4	4.7-17.6	-4.7-9.4
1.33	-0.5-12.9	-3.3-10.4	-5.5-8.4	37.3-46.1	-5.5-8.4	40.4-48.6	-5.1-8.7	-5.0-8.7	-4.2-9.6	6.2-18.6	-5.3-8.6
1.67	-0.6-12.2	-3.6-9.5	-5.7-7.6	29.9-39.1	-5.7-7.6	44.6-51.9	-4.6-8.6	-4.6-8.6	-4.4-8.8	7.3-19.1	-5.6-7.8
2.00	-0.5-11.7	-3.9-8.6	-5.9-6.7	23.9-33.4	-5.9-6.8	46.5-53.3	-3.4-8.9	-3.2-9.2	-4.6-8.0	7.9-19.0	-5.7-6.9
2.33	-0.2-11.2	-3.6-8.0	-6.0-5.9	19.2-28.6	-5.9-6.0	46.6-52.9	-1.5-10.0	-0.7-10.6	-4.7-7.1	8.2-18.6	-5.8-6.1
2.67	-0.0-10.6	-3.2-7.7	-6.0-5.1	15.3-24.5	-5.7-5.4	45.2-51.3	1.1-11.5	2.6-12.8	-4.8-6.3	8.2-17.9	-5.8-5.3
3.00	-0.1-9.9	-2.6-7.5	-5.9-4.4	12.2-21.1	-5.6-4.7	43.0-49.1	3.9-13.4	6.2-15.5	-4.8-5.5	8.0-17.1	-5.8-4.6
3.33	-0.3-9.1	-2.2-7.3	-6.0-3.8	9.6-18.2	-5.6-4.1	40.7-46.7	6.5-15.2	9.8-18.2	-5.1-4.8	7.7-16.3	-5.8-4.0
3.67	-0.8-8.3	-1.8-7.2	-6.2-3.2	7.4-15.8	-5.8-3.5	38.6-44.4	8.7-16.9	13.0-20.8	-5.2-4.1	7.2-15.5	-6.0-3.4
4.00	-1.3-7.4	-1.6-7.0	-3.6-4.8	5.6-13.8	-3.2-5.2	36.6-42.5	10.5-18.2	15.9-23.2	-5.5-3.5	6.8-14.8	-3.4-5.0
4.33	-1.9-6.6	-1.5-6.9	-3.9-4.3	4.1-12.2	-3.5-4.7	35.1-40.9	11.9-19.3	18.2-25.2	-5.7-3.0	6.4-14.3	-3.7-4.5
4.67	-2.5-5.9	-1.4-6.9	-4.2-3.9	2.9-11.0	-3.8-4.3	34.0-39.8	13.0-20.1	20.1-26.8	-3.3-4.8	6.2-13.9	-4.0-4.1
5.00	-3.0-5.2	-1.1-7.0	-4.3-3.7	1.9-9.9	-3.9-4.0	33.3-39.1	13.6-20.7	21.5-28.0	-3.5-4.5	6.0-13.6	-4.2-3.8
5.33	-3.6-4.6	-0.9-7.2	-4.5-3.4	1.1-9.2	-4.1-3.8	33.0-38.8	14.0-21.0	22.4-28.8	-3.6-4.3	5.9-13.5	-4.3-3.6
5.67	-4.1-4.1	-0.6-7.4	-4.6-3.3	0.5-8.5	-4.2-3.7	33.1-38.9	14.1-21.1	22.6-29.0	-3.7-4.2	5.9-13.5	-4.4-3.5
6.00	-4.5-3.7	-0.3-7.7	-4.6-3.3	-0.0-8.1	-4.2-3.6	33.5-39.3	13.9-20.9	22.4-28.8	-3.7-4.1	6.1-13.6	-4.4-3.4
6.33	-5.0-3.4	-0.0-8.0	-4.7-3.3	-0.4-7.7	-4.3-3.6	34.3-40.1	13.5-20.5	21.6-28.1	-3.7-4.2	6.3-13.8	-4.5-3.5
6.67	-5.3-3.1	0.3-8.4	-4.7-3.3	-0.8-7.5	-4.3-3.7	35.6-41.3	12.7-19.9	20.3-27.0	-3.7-4.3	6.6-14.2	-4.5-3.6
7.00	-5.7-2.9	0.7-8.9	-4.7-3.5	-1.0-7.4	-4.3-3.9	37.3-42.9	11.6-18.9	18.4-25.3	-3.7-4.4	7.0-14.7	-4.5-3.7
7.33	-3.2-5.0	1.0-9.4	-4.6-3.7	-1.2-7.4	-4.2-4.0	39.5-45.0	10.0-17.6	16.1-23.3	-3.6-4.7	7.5-15.3	-4.4-3.9
7.67	-3.4-5.1	1.3-9.8	-4.6-3.9	-1.3-7.5	-4.2-4.3	42.2-47.7	7.9-16.0	13.2-20.9	-3.5-5.1	8.1-16.1	-4.4-4.2
8.00	-3.4-5.4	1.3-10.2	-4.5-4.4	-1.4-7.8	-4.1-4.8	45.5-50.9	5.6-14.2	10.1-18.2	-3.4-5.4	8.8-17.0	-4.3-4.6
8.33	-6.4-3.5	1.1-10.4	-4.4-4.9	-1.5-8.1	-4.1-5.2	49.1-54.4	3.2-12.2	6.6-15.5	-6.3-3.6	9.5-18.0	-4.2-5.1
8.67	-6.4-3.9	0.6-10.3	-4.4-5.3	-1.5-8.5	-4.0-5.6	53.0-58.0	0.8-10.4	3.5-13.0	-6.3-4.1	10.3-19.1	-4.1-5.6
9.00	-6.3-4.4	-0.2-10.0	-4.3-5.7	-1.5-8.8	-4.0-6.1	56.7-61.6	-1.5-8.8	0.7-10.8	-6.3-4.6	11.1-20.2	-4.0-6.1
9.33	-6.3-4.9	-1.3-9.5	-4.3-6.2	-1.6-9.2	-7.5-3.8	60.1-64.7	-3.4-7.5	-1.6-9.1	-6.1-5.0	11.7-21.1	-7.4-3.9
9.67	-6.2-5.3	-2.3-8.9	-4.2-6.6	-1.7-9.4	-7.5-4.1	62.9-67.4	-4.9-6.6	-3.4-7.9	-6.1-5.4	12.2-21.9	-7.4-4.2
10.00	-6.2-5.6	-3.3-8.2	-7.8-4.1	-1.8-9.5	-7.6-4.2	65.0-69.3	-5.7-6.0	-4.6-7.1	-5.9-5.8	12.7-22.4	-7.5-4.4

Table F.21: North / Temp. at 2cm / Mid-day

i \ j	1	2	3	4	5	6	7	8	9	10	11
1	1.5-2.4	-0.8-1.0	-0.9-0.8	-0.9-0.7	-1.0-0.8	-1.2-2.7	-1.2-0.8	-1.4-1.2	-0.9-0.8	-0.9-1.0	-0.9-0.8
2	-0.8-1.0	1.8-2.8	-0.9-1.1	-1.2-0.8	-0.7-1.3	-0.0-3.8	-0.9-1.3	-0.5-2.3	-0.8-1.1	-0.5-1.5	-0.8-1.1
3	-0.9-0.8	-0.9-1.1	-0.0-0.1	-0.4-0.0	-0.1-0.1	-0.7-2.6	-0.4-0.5	-0.5-1.2	-0.1-0.1	-0.2-0.4	-0.1-0.1
4	-0.9-0.7	-1.2-0.8	-0.4-0.0	6.2-7.2	-0.9-0.6	-1.6-2.8	-1.1-0.9	-1.2-1.5	-0.8-0.7	-0.9-1.0	-0.8-0.6
5	-1.0-0.8	-0.7-1.3	-0.1-0.1	-0.9-0.6	-0.2-0.2	-0.5-2.8	-0.4-0.8	-0.5-1.4	-0.4-0.4	-0.3-0.7	-0.4-0.4
6	-1.2-2.7	-0.0-3.8	-0.7-2.6	-1.6-2.8	-0.5-2.8	29.2-32.2	-0.1-3.0	0.2-4.6	-1.1-0.6	-0.6-2.5	-0.8-0.8
7	-1.2-0.8	-0.9-1.3	-0.4-0.5	-1.1-0.9	-0.4-0.8	-0.1-3.0	12.8-14.8	-1.6-2.9	-1.7-1.1	-1.9-1.1	-1.8-1.0
8	-1.4-1.2	-0.5-2.3	-0.5-1.2	-1.2-1.5	-0.5-1.4	0.2-4.6	-1.6-2.9	19.2-21.6	-1.6-1.2	-1.5-1.7	-1.6-1.2
9	-0.9-0.8	-0.8-1.1	-0.1-0.1	-0.8-0.7	-0.4-0.4	-1.1-0.6	-1.7-1.1	-1.6-1.2	-0.2-0.3	-0.2-1.0	-0.6-0.4
10	-0.9-1.0	-0.5-1.5	-0.2-0.4	-0.9-1.0	-0.3-0.7	-0.6-2.5	-1.9-1.1	-1.5-1.7	-0.2-1.0	8.6-9.8	-0.9-0.6
11	-0.9-0.8	-0.8-1.1	-0.1-0.1	-0.8-0.6	-0.4-0.4	-0.8-0.8	-1.8-1.0	-1.6-1.2	-0.6-0.4	-0.9-0.6	0.1-0.2
Total	-3.0-5.2	-1.1-7.0	-4.3-3.7	1.9-9.9	-3.9-4.0	33.3-39.1	13.6-20.7	21.5-28.0	-3.5-4.5	6.0-13.6	-4.2-3.8
Higher	-1.1	-3.5	-1.8	-0.6	-2.2	-4.4	2.2	-0.2	0.8	-1.2	0.4

Table F.22: Control / Temp. at 2cm / Mean

i \ j	1	2	3	4	5	6	7	8	9	10	11
1	0.2-0.9	-0.5-0.8	-0.5-0.7	-0.7-0.7	-0.6-0.7	-1.8-5.0	-0.6-0.7	-0.7-0.6	-0.5-0.9	-0.6-1.0	-0.5-0.7
2	-0.5-0.8	-0.2-0.4	-0.5-0.8	-0.8-0.6	-0.5-0.8	-0.4-6.4	-0.7-0.7	-0.8-0.6	-0.8-0.5	-0.3-1.3	-0.5-0.8
3	-0.5-0.7	-0.5-0.8	-0.0-0.0	-0.7-0.1	-0.1-0.1	-1.5-5.0	-0.1-0.3	-0.1-0.2	-0.1-0.1	-0.3-0.7	-0.1-0.1
4	-0.7-0.7	-0.8-0.6	-0.7-0.1	9.7-11.1	-0.9-0.7	-2.4-6.1	-1.0-1.1	-1.1-0.9	-0.8-1.1	-0.8-1.9	-0.9-0.7
5	-0.6-0.7	-0.5-0.8	-0.1-0.1	-0.9-0.7	-0.0-0.2	-1.6-5.0	-0.2-0.3	-0.3-0.2	-0.2-0.3	-0.3-0.8	-0.2-0.2
6	-1.8-5.0	-0.4-6.4	-1.5-5.0	-2.4-6.1	-1.6-5.0	38.5-43.1	2.2-5.9	1.4-4.8	-0.5-2.5	1.8-6.6	-1.4-0.1
7	-0.6-0.7	-0.7-0.7	-0.1-0.3	-1.0-1.1	-0.2-0.3	2.2-5.9	4.1-5.2	-0.3-1.8	-0.6-1.2	0.3-2.6	-0.4-1.2
8	-0.7-0.6	-0.8-0.6	-0.1-0.2	-1.1-0.9	-0.3-0.2	1.4-4.8	-0.3-1.8	3.6-4.7	-0.5-1.2	-0.1-2.1	-0.6-1.0
9	-0.5-0.9	-0.8-0.5	-0.1-0.1	-0.8-1.1	-0.2-0.3	-0.5-2.5	-0.6-1.2	-0.5-1.2	-0.8-0.5	1.7-4.3	-1.4-1.2
10	-0.6-1.0	-0.3-1.3	-0.3-0.7	-0.8-1.9	-0.3-0.8	1.8-6.6	0.3-2.6	-0.1-2.1	1.7-4.3	9.5-11.2	-0.4-1.6
11	-0.5-0.7	-0.5-0.8	-0.1-0.1	-0.9-0.7	-0.2-0.2	-1.4-0.1	-0.4-1.2	-0.6-1.0	-1.4-1.2	-0.4-1.6	0.0-0.3
Total	-5.1-4.6	-4.9-4.8	-7.3-2.6	4.5-13.9	-7.2-2.7	54.5-59.7	2.7-12.2	0.2-9.9	-2.3-7.7	13.0-21.7	-7.0-2.8
Higher	-3.0	-3.9	-4.5	-3.1	-4.5	-5.3	-4.3	-4.4	-1.9	-4.9	-2.8

Table F.23: South / Temp. at 2cm / Mean

i \ j	1	2	3	4	5	6	7	8	9	10	11
1	1.1-1.8	-0.9-0.6	-0.9-0.5	-0.8-0.7	-0.9-0.5	-2.0-4.5	-0.5-1.4	-0.6-1.1	-0.9-0.6	-0.7-1.0	-0.9-0.6
2	-0.9-0.6	-0.2-0.6	-0.9-0.6	-0.9-0.8	-0.8-0.7	-0.4-5.8	-0.6-1.4	-0.7-1.1	-0.9-0.6	-0.3-1.3	-0.9-0.6
3	-0.9-0.5	-0.9-0.6	-0.0-0.0	-0.7-0.1	-0.1-0.1	-1.7-4.3	-0.2-0.9	-0.1-0.7	-0.1-0.1	-0.1-0.6	-0.1-0.1
4	-0.8-0.7	-0.9-0.8	-0.7-0.1	9.5-11.0	-1.0-0.5	-3.4-4.5	-0.9-1.9	-1.0-1.4	-0.9-0.7	-0.8-1.5	-0.9-0.6
5	-0.9-0.5	-0.8-0.7	-0.1-0.1	-1.0-0.5	-0.0-0.3	-1.7-4.3	-0.3-1.0	-0.3-0.7	-0.4-0.2	-0.2-0.7	-0.4-0.2
6	-2.0-4.5	-0.4-5.8	-1.7-4.3	-3.4-4.5	-1.7-4.3	34.8-39.4	3.3-8.3	2.5-6.8	-1.0-0.9	0.3-4.3	-1.1-0.5
7	-0.5-1.4	-0.6-1.4	-0.2-0.9	-0.9-1.9	-0.3-1.0	3.3-8.3	9.7-11.5	0.2-3.5	-0.3-1.7	1.0-3.5	-0.2-1.7
8	-0.6-1.1	-0.7-1.1	-0.1-0.7	-1.0-1.4	-0.3-0.7	2.5-6.8	0.2-3.5	7.8-9.4	-0.5-1.6	0.1-2.5	-0.5-1.4
9	-0.9-0.6	-0.9-0.6	-0.1-0.1	-0.9-0.7	-0.4-0.2	-1.0-0.9	-0.3-1.7	-0.5-1.6	-0.4-0.3	0.3-1.7	-0.5-0.9
10	-0.7-1.0	-0.3-1.3	-0.1-0.6	-0.8-1.5	-0.2-0.7	0.3-4.3	1.0-3.5	0.1-2.5	0.3-1.7	7.2-8.5	-0.3-1.1
11	-0.9-0.6	-0.9-0.6	-0.1-0.1	-0.9-0.6	-0.4-0.2	-1.1-0.5	-0.2-1.7	-0.5-1.4	-0.5-0.9	-0.3-1.1	0.1-0.3
Total	-7.1-4.1	-4.2-6.3	-7.0-3.8	3.5-13.8	-6.7-4.1	45.8-52.4	11.1-20.8	6.9-16.8	-4.9-5.8	4.8-14.9	-6.7-4.1
Higher	-4.4	-2.3	-3.1	-2.3	-2.9	-7.6	-8.1	-6.8	-1.5	-6.7	-2.4

Table F.24: North / Temp. at 2cm / Mean

i \ j	1	2	3	4	5	6	7	8	9	10	11
1	0.7-1.8	-1.4-0.7	-1.5-0.6	-2.0-0.6	-1.5-0.6	-2.5-4.9	-1.3-0.8	-1.4-0.8	-1.5-0.6	-1.4-0.9	-1.5-0.6
2	-1.4-0.7	0.8-1.9	-1.0-1.1	-2.0-0.8	-0.9-1.2	-1.3-6.0	-1.0-1.1	-0.8-1.6	-1.0-1.1	-0.8-1.4	-1.0-1.1
3	-1.5-0.6	-1.0-1.1	-0.1-0.1	-1.9-0.1	-0.1-0.1	-2.0-5.0	-0.2-0.3	-0.4-0.4	-0.1-0.1	-0.6-0.5	-0.1-0.1
4	-2.0-0.6	-2.0-0.8	-1.9-0.1	16.0-18.4	-1.2-1.0	-3.6-6.3	-1.1-1.6	-2.0-1.2	-1.1-1.2	-1.8-1.7	-1.1-1.1
5	-1.5-0.6	-0.9-1.2	-0.1-0.1	-1.2-1.0	-0.2-0.2	-1.9-5.1	-0.5-0.5	-0.5-0.6	-0.4-0.4	-0.6-0.7	-0.4-0.4
6	-2.5-4.9	-1.3-6.0	-2.0-5.0	-3.6-6.3	-1.9-5.1	40.3-45.5	-1.8-1.9	-1.5-2.9	-0.8-1.3	-2.4-2.8	-0.9-0.8
7	-1.3-0.8	-1.0-1.1	-0.2-0.3	-1.1-1.6	-0.5-0.5	-1.8-1.9	6.2-7.8	-1.8-1.3	-1.6-0.8	-1.5-1.4	-1.6-0.7
8	-1.4-0.8	-0.8-1.6	-0.4-0.4	-2.0-1.2	-0.5-0.6	-1.5-2.9	-1.8-1.3	8.7-10.6	-1.4-1.2	-1.6-1.5	-1.4-1.1
9	-1.5-0.6	-1.0-1.1	-0.1-0.1	-1.1-1.2	-0.4-0.4	-0.8-1.3	-1.6-0.8	-1.4-1.2	-0.3-0.5	-0.6-1.2	-0.9-0.6
10	-1.4-0.9	-0.8-1.4	-0.6-0.5	-1.8-1.7	-0.6-0.7	-2.4-2.8	-1.5-1.4	-1.6-1.5	-0.6-1.2	11.1-12.9	-1.0-0.9
11	-1.5-0.6	-1.0-1.1	-0.1-0.1	-1.1-1.1	-0.4-0.4	-0.9-0.8	-1.6-0.7	-1.4-1.1	-0.9-0.6	-1.0-0.9	0.1-0.3
Total	-4.6-6.8	-3.3-8.0	-7.3-4.4	12.4-22.0	-7.0-4.6	43.0-49.6	2.4-13.0	5.7-16.1	-6.2-5.3	7.5-17.7	-7.0-4.6
Higher	2.2	-1.5	-1.5	1.3	-2.5	-5.7	1.7	1.3	-0.1	0.2	-0.2



Table F.25: Control / Temp. at 2cm / Maximum

i \ j	1	2	3	4	5	6	7	8	9	10	11
1	0.1-0.5	-0.3-0.6	-0.3-0.5	-0.5-0.6	-0.3-0.6	-0.6-2.8	0.0-1.4	-0.0-1.3	-0.3-0.6	0.0-1.1	-0.3-0.5
2	-0.3-0.6	0.1-0.9	-0.6-0.7	-0.9-0.6	-0.6-0.7	0.8-4.4	-0.3-1.6	-0.6-1.3	-0.5-0.9	-0.2-1.2	-0.6-0.7
3	-0.3-0.5	-0.6-0.7	-0.0-0.0	-0.5-0.1	-0.1-0.0	-0.4-2.8	-0.0-0.9	-0.2-0.6	-0.0-0.1	-0.1-0.4	-0.0-0.0
4	-0.5-0.6	-0.9-0.6	-0.5-0.1	4.8-6.2	-0.5-0.4	2.9-7.5	1.3-3.5	0.5-2.5	-0.7-0.5	0.8-2.5	-0.5-0.4
5	-0.3-0.6	-0.6-0.7	-0.1-0.0	-0.5-0.4	-0.1-0.2	-0.5-2.7	-0.2-1.0	-0.4-0.6	-0.4-0.2	-0.2-0.6	-0.3-0.2
6	-0.6-2.8	0.8-4.4	-0.4-2.8	2.9-7.5	-0.5-2.7	18.0-21.1	6.5-10.6	4.8-8.5	-1.4-1.0	1.2-4.5	-1.2-0.5
7	0.0-1.4	-0.3-1.6	-0.0-0.9	1.3-3.5	-0.2-1.0	6.5-10.6	7.6-9.7	0.0-4.1	-0.8-2.1	1.4-4.6	-0.5-2.1
8	-0.0-1.3	-0.6-1.3	-0.2-0.6	0.5-2.5	-0.4-0.6	4.8-8.5	0.0-4.1	6.9-8.9	-0.8-2.1	0.3-3.5	-0.8-1.8
9	-0.3-0.6	-0.5-0.9	-0.0-0.1	-0.7-0.5	-0.4-0.2	-1.4-1.0	-0.8-2.1	-0.8-2.1	-0.2-0.8	0.6-2.7	-0.8-1.2
10	0.0-1.1	-0.2-1.2	-0.1-0.4	0.8-2.5	-0.2-0.6	1.2-4.5	1.4-4.6	0.3-3.5	0.6-2.7	4.4-5.8	-0.4-1.3
11	-0.3-0.5	-0.6-0.7	-0.0-0.0	-0.5-0.4	-0.3-0.2	-1.2-0.5	-0.5-2.1	-0.8-1.8	-0.8-1.2	-0.4-1.3	-0.1-0.1
Total	-5.6-4.3	-5.9-4.3	-7.6-2.5	13.6-22.9	-7.1-2.9	47.7-54.2	23.6-32.0	17.7-26.3	-1.4-8.6	13.2-22.0	-7.3-2.7
Higher	-4.7	-5.6	-4.6	2.6	-4.0	2.7	-0.6	-0.5	0.1	-0.5	-4.0

Table F.26: South / Temp. at 2cm / Maximum

i \ j	1	2	3	4	5	6	7	8	9	10	11
1	0.2-0.7	-0.1-0.8	-0.1-0.8	0.1-1.0	-0.1-0.9	-0.5-2.2	0.4-2.8	0.2-2.2	-0.1-0.9	0.1-1.2	-0.1-0.8
2	-0.1-0.8	0.4-1.1	-0.6-0.7	-0.5-0.8	-0.5-0.8	0.4-3.3	0.1-2.8	-0.1-2.1	-0.5-0.8	-0.2-1.2	-0.6-0.7
3	-0.1-0.8	-0.6-0.7	-0.0-0.0	-0.1-0.1	-0.0-0.1	-0.7-1.6	-0.2-1.9	-0.3-1.2	-0.0-0.1	0.0-0.3	-0.0-0.1
4	0.1-1.0	-0.5-0.8	-0.1-0.1	1.8-2.4	-0.5-0.4	-1.2-1.7	0.3-2.9	-0.2-1.9	-0.5-0.4	-0.4-0.8	-0.5-0.3
5	-0.1-0.9	-0.5-0.8	-0.0-0.1	-0.5-0.4	0.0-0.3	-0.9-1.5	-0.2-2.0	-0.4-1.3	-0.4-0.2	-0.2-0.5	-0.2-0.3
6	-0.5-2.2	0.4-3.3	-0.7-1.6	-1.2-1.7	-0.9-1.5	15.6-18.3	9.1-14.1	6.0-10.0	-0.8-0.9	-0.2-2.3	-0.9-0.5
7	0.4-2.8	0.1-2.8	-0.2-1.9	0.3-2.9	-0.2-2.0	9.1-14.1	16.0-18.8	2.3-7.4	-0.5-2.2	2.7-5.9	-0.2-2.3
8	0.2-2.2	-0.1-2.1	-0.3-1.2	-0.2-1.9	-0.4-1.3	6.0-10.0	2.3-7.4	12.6-15.0	-0.3-2.4	0.9-4.1	-0.4-2.2
9	-0.1-0.9	-0.5-0.8	-0.0-0.1	-0.5-0.4	-0.4-0.2	-0.8-0.9	-0.5-2.2	-0.3-2.4	-0.2-0.4	-0.1-0.9	-0.4-0.6
10	0.1-1.2	-0.2-1.2	0.0-0.3	-0.4-0.8	-0.2-0.5	-0.2-2.3	2.7-5.9	0.9-4.1	-0.1-0.9	3.1-4.1	-0.3-1.0
11	-0.1-0.8	-0.6-0.7	-0.0-0.1	-0.5-0.3	-0.2-0.3	-0.9-0.5	-0.2-2.3	-0.4-2.2	-0.4-0.6	-0.3-1.0	-0.0-0.1
Total	-5.0-4.3	-4.6-4.9	-7.5-2.1	-2.8-7.1	-6.8-2.6	38.0-44.7	36.5-43.3	26.9-34.2	-4.8-4.5	4.9-13.8	-7.2-2.3
Higher	-7.5	-6.3	-5.2	-3.4	-4.4	0.3	-6.4	-4.3	-3.2	-4.4	-5.1

Table F.27: North / Temp. at 2cm / Maximum

i \ j	1	2	3	4	5	6	7	8	9	10	11
1	1.1-1.8	-0.8-0.7	-0.8-0.6	-0.9-0.6	-0.8-0.6	-0.9-2.4	-0.9-0.8	-1.4-0.8	-0.8-0.6	-0.8-0.7	-0.8-0.6
2	-0.8-0.7	2.6-3.7	-1.2-0.9	-1.2-0.9	-1.0-1.1	0.0-3.6	-1.0-1.3	-0.7-2.2	-1.2-0.9	-0.9-1.1	-1.1-0.9
3	-0.8-0.6	-1.2-0.9	-0.0-0.1	-0.8-0.1	-0.1-0.1	-0.4-2.4	-0.3-0.5	-0.6-1.0	-0.1-0.1	-0.3-0.3	-0.1-0.1
4	-0.9-0.6	-1.2-0.9	-0.8-0.1	9.0-10.4	-0.6-0.6	0.5-4.5	0.1-2.1	-0.0-2.6	-0.6-0.7	-0.0-1.7	-0.5-0.7
5	-0.8-0.6	-1.0-1.1	-0.1-0.1	-0.6-0.6	-0.1-0.3	-0.3-2.6	-0.4-0.8	-0.7-1.2	-0.5-0.3	-0.4-0.5	-0.5-0.3
6	-0.9-2.4	0.0-3.6	-0.4-2.4	0.5-4.5	-0.3-2.6	25.7-28.5	0.3-3.4	-0.0-4.0	-0.9-0.9	-0.7-2.2	-0.9-0.8
7	-0.9-0.8	-1.0-1.3	-0.3-0.5	0.1-2.1	-0.4-0.8	0.3-3.4	12.0-14.1	-1.2-3.2	-1.4-1.5	-1.8-1.2	-1.4-1.6
8	-1.4-0.8	-0.7-2.2	-0.6-1.0	-0.0-2.6	-0.7-1.2	-0.0-4.0	-1.2-3.2	18.3-20.7	-1.8-1.3	-2.0-1.3	-1.7-1.3
9	-0.8-0.6	-1.2-0.9	-0.1-0.1	-0.6-0.7	-0.5-0.3	-0.9-0.9	-1.4-1.5	-1.8-1.3	-0.3-0.2	-0.3-0.8	-0.4-0.7
10	-0.8-0.7	-0.9-1.1	-0.3-0.3	-0.0-1.7	-0.4-0.5	-0.7-2.2	-1.8-1.2	-2.0-1.3	-0.3-0.8	7.5-8.7	-1.0-0.8
11	-0.8-0.6	-1.1-0.9	-0.1-0.1	-0.5-0.7	-0.5-0.3	-0.9-0.8	-1.4-1.6	-1.7-1.3	-0.4-0.7	-1.0-0.8	0.0-0.2
Total	-2.9-4.9	1.3-8.8	-3.4-4.2	10.5-17.9	-3.0-4.6	32.6-38.3	15.5-22.1	22.7-28.9	-4.7-3.3	6.3-13.4	-3.3-4.4
Higher	-0.2	-0.3	-0.1	-0.7	-0.7	-3.3	1.6	1.9	-0.5	0.5	0.8

Table F.28: Control / Temp. at 2cm / Minimum

i \ j	1	2	3	4	5	6	7	8	9	10	11
1	-0.0-0.5	-0.9-0.2	-0.9-0.2	-14.5-3.0	-0.9-0.2	-0.8-0.3	-0.9-0.2	-0.9-0.2	-0.8-0.2	-0.8-0.2	-0.9-0.2
2	-0.9-0.2	-0.2-0.2	-0.4-0.5	-14.1-3.4	-0.4-0.5	-0.2-0.6	-0.4-0.5	-0.4-0.5	-0.4-0.5	-0.3-0.5	-0.4-0.5
3	-0.9-0.2	-0.4-0.5	-0.0-0.0	-14.3-3.2	-0.1-0.1	-0.2-0.1	-0.1-0.1	-0.1-0.1	-0.1-0.1	-0.1-0.1	-0.1-0.1
4	-14.5-3.0	-14.1-3.4	-14.3-3.2	86.5-96.2	-0.3-0.2	-1.6-4.6	-0.7-0.7	-0.5-0.7	-1.5-1.1	-1.3-2.5	-0.3-0.2
5	-0.9-0.2	-0.4-0.5	-0.1-0.1	-0.3-0.2	-0.0-0.0	-0.1-0.1	-0.1-0.0	-0.1-0.0	-0.1-0.0	-0.1-0.0	-0.1-0.0
6	-0.8-0.3	-0.2-0.6	-0.2-0.1	-1.6-4.6	-0.1-0.1	2.8-5.3	-3.6-1.1	-3.7-1.0	-3.2-1.4	-3.0-1.7	-3.7-1.0
7	-0.9-0.2	-0.4-0.5	-0.1-0.1	-0.7-0.7	-0.1-0.0	-3.6-1.1	-0.2-0.2	-0.4-0.4	-0.4-0.4	-0.4-0.4	-0.4-0.4
8	-0.9-0.2	-0.4-0.5	-0.1-0.1	-0.5-0.7	-0.1-0.0	-3.7-1.0	-0.4-0.4	-0.2-0.2	-0.4-0.4	-0.4-0.4	-0.4-0.4
9	-0.8-0.2	-0.4-0.5	-0.1-0.1	-1.5-1.1	-0.1-0.0	-3.2-1.4	-0.4-0.4	-0.4-0.4	-0.5-0.4	-0.7-1.2	-0.9-1.1
10	-0.8-0.2	-0.3-0.5	-0.1-0.1	-1.3-2.5	-0.1-0.0	-3.0-1.7	-0.4-0.4	-0.4-0.4	-0.7-1.2	-0.5-0.9	-0.9-1.9
11	-0.9-0.2	-0.4-0.5	-0.1-0.1	-0.3-0.2	-0.1-0.0	-3.7-1.0	-0.4-0.4	-0.4-0.4	-0.9-1.1	-0.9-1.9	-0.1-0.0
Total	-2.4-7.4	-2.5-7.3	-2.8-7.0	92.1-94.6	-2.8-7.0	5.9-15.2	-2.6-7.2	-2.6-7.2	-1.4-8.4	1.0-10.5	-2.8-7.1
Higher	10.9	7.4	8.1	16.8	2.5	10.6	3.8	3.8	4.5	5.0	3.4

Table F.29: South / Temp. at 2cm / Minimum

i \ j	1	2	3	4	5	6	7	8	9	10	11
1	-0.2-0.3	-0.6-0.4	-0.6-0.4	-27.9-2.6	-0.6-0.4	-0.5-0.4	-0.6-0.4	-0.6-0.4	-0.6-0.4	-0.5-0.4	-0.6-0.4
2	-0.6-0.4	-0.2-0.2	-0.3-0.4	-27.8-2.6	-0.3-0.4	-0.3-0.4	-0.3-0.4	-0.3-0.4	-0.3-0.4	-0.3-0.4	-0.3-0.4
3	-0.6-0.4	-0.3-0.4	-0.0-0.0	-27.9-2.7	-0.1-0.1	-0.0-0.1	-0.1-0.1	-0.1-0.1	-0.1-0.1	-0.1-0.1	-0.1-0.1
4	-27.9-2.6	-27.8-2.6	-27.9-2.7	95.6-112.9	-0.1-0.2	-1.3-3.4	-0.7-0.4	-0.5-0.4	-0.5-0.6	-1.1-2.0	-0.3-0.2
5	-0.6-0.4	-0.3-0.4	-0.1-0.1	-0.1-0.2	-0.0-0.0	-0.0-0.1	-0.1-0.1	-0.1-0.1	-0.1-0.1	-0.1-0.1	-0.1-0.1
6	-0.5-0.4	-0.3-0.4	-0.0-0.1	-1.3-3.4	-0.0-0.1	-0.3-1.5	-1.6-1.9	-1.6-1.9	-1.6-1.9	-1.4-2.1	-1.6-1.9
7	-0.6-0.4	-0.3-0.4	-0.1-0.1	-0.7-0.4	-0.1-0.1	-1.6-1.9	-0.1-0.2	-0.4-0.3	-0.4-0.3	-0.4-0.3	-0.4-0.3
8	-0.6-0.4	-0.3-0.4	-0.1-0.1	-0.5-0.4	-0.1-0.1	-1.6-1.9	-0.4-0.3	-0.1-0.2	-0.3-0.3	-0.3-0.3	-0.3-0.3
9	-0.6-0.4	-0.3-0.4	-0.1-0.1	-0.5-0.6	-0.1-0.1	-1.6-1.9	-0.4-0.3	-0.3-0.3	-0.2-0.2	-0.4-0.3	-0.4-0.3
10	-0.5-0.4	-0.3-0.4	-0.1-0.1	-1.1-2.0	-0.1-0.1	-1.4-2.1	-0.4-0.3	-0.3-0.3	-0.4-0.3	-0.8-0.2	-0.2-1.9
11	-0.6-0.4	-0.3-0.4	-0.1-0.1	-0.3-0.2	-0.1-0.1	-1.6-1.9	-0.4-0.3	-0.3-0.3	-0.4-0.3	-0.2-1.9	-0.1-0.1
Total	-1.2-12.6	-1.3-12.5	-1.4-12.4	97.7-99.3	-1.4-12.4	1.2-14.7	-1.3-12.5	-1.3-12.5	-1.2-12.5	-0.1-13.5	-1.4-12.4
Higher	18.9	18.2	18.2	30.7	5.5	5.2	5.8	5.6	5.6	5.5	4.7

Table F.30: North / Temp. at 2cm / Minimum

i \ j	1	2	3	4	5	6	7	8	9	10	11
1	-0.2-0.5	-0.9-0.5	-0.9-0.5	-26.9-2.4	-0.9-0.5	-0.9-0.5	-0.9-0.5	-0.9-0.5	-0.9-0.5	-0.9-0.5	-0.9-0.5
2	-0.9-0.5	-0.3-0.2	-0.4-0.7	-26.4-2.7	-0.4-0.7	-0.3-0.8	-0.4-0.7	-0.4-0.7	-0.4-0.7	-0.4-0.7	-0.4-0.7
3	-0.9-0.5	-0.4-0.7	-0.1-0.1	-26.7-2.4	-0.1-0.2	-0.2-0.1	-0.1-0.2	-0.2-0.1	-0.1-0.2	-0.2-0.1	-0.1-0.2
4	-26.9-2.4	-26.4-2.7	-26.7-2.4	90.6-107.4	-0.2-0.2	-1.4-5.5	-0.6-0.5	-0.7-0.7	-0.6-0.8	-1.9-3.0	-0.4-0.3
5	-0.9-0.5	-0.4-0.7	-0.1-0.2	-0.2-0.2	-0.0-0.1	-0.1-0.1	-0.1-0.1	-0.1-0.1	-0.1-0.1	-0.1-0.1	-0.1-0.0
6	-0.9-0.5	-0.3-0.8	-0.2-0.1	-1.4-5.5	-0.1-0.1	1.3-4.0	-3.7-1.5	-3.7-1.5	-3.7-1.5	-3.3-1.9	-3.8-1.5
7	-0.9-0.5	-0.4-0.7	-0.1-0.2	-0.6-0.5	-0.1-0.1	-3.7-1.5	-0.2-0.2	-0.4-0.5	-0.4-0.5	-0.4-0.5	-0.4-0.5
8	-0.9-0.5	-0.4-0.7	-0.2-0.1	-0.7-0.7	-0.1-0.1	-3.7-1.5	-0.4-0.5	-0.2-0.2	-0.4-0.5	-0.4-0.5	-0.4-0.5
9	-0.9-0.5	-0.4-0.7	-0.1-0.2	-0.6-0.8	-0.1-0.1	-3.7-1.5	-0.4-0.5	-0.4-0.5	-0.3-0.3	-0.4-0.6	-0.5-0.6
10	-0.9-0.5	-0.4-0.7	-0.2-0.1	-1.9-3.0	-0.1-0.1	-3.3-1.9	-0.4-0.5	-0.4-0.5	-0.4-0.6	-0.8-0.8	-0.8-2.4
11	-0.9-0.5	-0.4-0.7	-0.1-0.2	-0.4-0.3	-0.1-0.0	-3.8-1.5	-0.4-0.5	-0.4-0.5	-0.5-0.6	-0.8-2.4	-0.1-0.1
Total	-1.5-12.6	-1.7-12.6	-1.9-12.3	94.7-97.3	-1.9-12.3	3.2-16.9	-1.8-12.4	-1.8-12.4	-1.5-12.5	0.8-14.8	-1.8-12.4
Higher	19.6	16.3	17.4	30.7	5.5	10.5	6.4	6.4	6.4	7.1	5.7

## F.4 Snow Temperature at 5 cm

Table F.31: Control / Temp. at 5cm with Time (Total-effect)

t \ i	1	2	3	4	5	6	7	8	9	10	11
0.33	3.6-11.9	1.2-9.7	-0.9-7.6	91.5-92.7	-1.0-7.6	3.5-11.7	-1.0-7.6	-1.0-7.6	-0.5-8.1	0.1-8.7	-1.0-7.6
0.67	5.3-13.6	3.2-11.7	-1.6-7.2	79.7-82.1	-1.6-7.2	10.5-18.4	-1.6-7.2	-1.7-7.2	-0.1-8.6	1.6-10.2	-1.6-7.2
1.00	5.3-13.7	4.3-12.9	-2.3-6.6	69.2-72.6	-2.3-6.6	16.9-24.4	-2.3-6.6	-2.3-6.6	0.1-8.9	3.0-11.5	-2.2-6.7
1.33	4.9-13.4	4.8-13.4	-3.1-6.0	60.6-64.7	-3.1-5.9	21.9-29.0	-2.9-6.1	-3.0-6.0	0.1-9.0	4.0-12.6	-3.0-6.1
1.67	4.8-13.2	5.0-13.6	-3.6-5.4	53.6-58.2	-3.7-5.4	25.4-32.3	-3.1-5.9	-3.3-5.7	0.1-8.9	4.9-13.3	-3.6-5.4
2.00	4.8-13.1	5.1-13.6	-4.3-4.7	47.7-52.9	-4.1-4.9	27.5-34.3	-2.8-6.1	-3.2-5.9	-0.1-8.5	5.4-13.7	-4.2-4.8
2.33	4.9-13.2	4.9-13.3	-4.9-4.1	42.8-48.4	-4.4-4.6	28.5-35.2	-1.9-6.9	-2.4-6.4	-0.5-8.1	5.6-13.9	-4.8-4.2
2.67	5.0-13.2	4.7-13.0	-5.4-3.5	38.7-44.6	-4.5-4.4	28.7-35.3	-0.5-8.2	-1.3-7.5	-1.0-7.6	5.7-13.9	-5.3-3.6
3.00	4.9-13.0	4.4-12.8	-3.4-5.2	35.2-41.3	-4.5-4.4	28.4-35.1	1.4-9.9	0.2-8.8	-1.4-7.1	5.6-13.7	-3.2-5.4
3.33	4.6-12.7	4.0-12.4	-3.9-4.7	32.1-38.5	-4.4-4.5	27.9-34.7	3.5-11.8	1.9-10.3	-2.0-6.7	5.4-13.6	-3.8-4.9
3.67	4.2-12.4	3.6-12.1	-4.4-4.4	29.5-36.1	-4.2-4.7	27.6-34.4	5.5-13.7	3.4-11.8	-2.4-6.4	5.3-13.6	-4.2-4.6
4.00	3.6-11.9	3.3-11.8	-4.8-4.1	27.2-34.1	-4.1-4.9	27.4-34.3	7.4-15.6	4.8-13.2	-2.7-6.1	5.3-13.6	-4.7-4.2
4.33	3.0-11.4	2.8-11.5	-5.2-3.9	25.2-32.3	-3.9-5.1	27.3-34.3	9.0-17.2	6.2-14.4	-3.1-5.9	5.3-13.6	-5.1-4.0
4.67	2.3-10.9	2.3-11.0	-5.6-3.6	23.4-30.7	-3.8-5.2	27.3-34.4	10.5-18.7	7.3-15.6	-3.3-5.8	5.3-13.7	-5.5-3.7
5.00	1.5-10.3	1.7-10.6	-5.9-3.3	21.7-29.3	-3.8-5.3	27.6-34.8	11.7-19.9	8.2-16.5	-3.5-5.7	5.4-13.9	-5.8-3.4
5.33	0.7-9.6	1.1-10.2	-6.2-3.1	20.2-28.0	-3.9-5.3	28.1-35.4	12.8-21.0	9.0-17.4	-3.7-5.6	5.6-14.2	-6.1-3.3
5.67	-0.1-8.9	0.6-9.7	-6.5-2.9	18.8-26.7	-4.1-5.2	28.8-36.1	13.5-21.8	9.7-18.0	-3.7-5.7	5.8-14.5	-6.4-3.0
6.00	-1.0-8.2	-0.0-9.2	-6.8-2.8	17.4-25.5	-4.4-5.0	29.7-37.0	14.1-22.4	10.1-18.5	-3.8-5.8	6.2-14.9	-6.6-2.9
6.33	-1.9-7.5	-0.6-8.8	-7.0-2.6	16.1-24.3	-4.7-4.8	30.8-38.1	14.5-22.7	10.4-18.9	-3.8-5.8	6.6-15.3	-6.8-2.7
6.67	-2.8-6.7	-1.1-8.3	-7.2-2.5	14.8-23.2	-5.1-4.5	32.2-39.4	14.5-22.8	10.5-19.0	-3.7-5.9	7.0-15.8	-7.0-2.7
7.00	-3.6-6.0	-1.6-7.9	-7.3-2.4	13.6-22.0	-5.5-4.2	33.7-40.8	14.2-22.5	10.2-18.7	-3.6-6.0	7.5-16.3	-7.2-2.6
7.33	-4.4-5.2	-2.1-7.4	-7.5-2.3	12.4-20.9	-6.0-3.8	35.5-42.5	13.4-21.8	9.7-18.2	-3.6-6.2	8.1-16.9	-7.4-2.4
7.67	-5.2-4.6	-2.6-7.1	-7.6-2.2	11.2-19.9	-3.6-5.9	37.6-44.3	12.1-20.5	8.5-17.2	-3.4-6.3	8.7-17.5	-7.5-2.4
8.00	-5.8-4.0	-2.8-6.8	-7.7-2.2	10.3-18.9	-4.0-5.5	39.9-46.5	10.1-18.7	6.8-15.6	-3.1-6.5	9.4-18.2	-7.5-2.4
8.33	-6.1-3.7	-3.1-6.6	-7.6-2.2	9.3-18.0	-4.4-5.1	42.8-49.1	7.6-16.4	4.7-13.6	-2.9-6.8	10.2-18.9	-7.4-2.4
8.67	-6.4-3.5	-3.0-6.6	-7.5-2.4	8.5-17.3	-4.7-4.8	46.0-52.0	4.7-13.8	2.2-11.4	-2.5-7.2	11.0-19.7	-7.2-2.6
9.00	-6.3-3.5	-2.9-6.7	-7.2-2.6	7.7-16.6	-4.9-4.7	49.5-55.1	1.8-11.2	-0.3-9.1	-2.1-7.6	11.9-20.5	-7.0-2.9
9.33	-6.2-3.6	-2.9-6.6	-7.0-2.8	7.0-15.9	-5.1-4.5	53.0-58.3	-0.6-8.8	-2.3-7.2	-1.6-8.0	12.7-21.1	-6.6-3.1
9.67	-6.1-3.8	-3.0-6.5	-6.7-3.1	6.4-15.3	-5.2-4.4	56.1-61.1	-2.7-6.9	-4.1-5.6	-1.0-8.5	13.3-21.7	-6.3-3.4
10.00	-5.8-3.9	-3.2-6.4	-6.4-3.3	5.9-14.8	-5.2-4.4	58.7-63.4	-4.0-5.5	-5.3-4.5	-0.4-9.0	13.8-22.1	-6.0-3.6

Table F.32: Control / Temp. at 5cm / Mid-day

i \ j	1	2	3	4	5	6	7	8	9	10	11
1	4.0-5.2	-0.8-1.3	-1.2-0.7	-0.4-2.3	-0.8-1.1	-1.6-1.9	-0.8-1.5	-0.9-1.4	-1.1-0.9	-1.0-1.2	-1.1-0.8
2	-0.8-1.3	2.7-4.1	-1.4-0.8	-1.1-1.8	-0.8-1.4	-1.1-2.5	-1.4-1.1	-1.4-1.1	-1.5-0.9	-1.0-1.5	-1.5-0.8
3	-1.2-0.7	-1.4-0.8	-0.0-0.1	-1.4-0.4	-0.1-0.1	-0.5-1.7	-0.0-0.6	-0.1-0.5	-0.1-0.1	-0.1-0.3	-0.1-0.1
4	-0.4-2.3	-1.1-1.8	-1.4-0.4	18.0-20.3	-0.8-1.0	-2.3-2.7	-0.8-2.2	-0.7-2.1	-0.9-1.1	-1.0-1.7	-1.0-0.6
5	-0.8-1.1	-0.8-1.4	-0.1-0.1	-0.8-1.0	1.6-2.4	-1.2-1.6	-1.0-0.8	-0.7-1.1	-0.9-0.6	-0.6-0.9	-0.9-0.5
6	-1.6-1.9	-1.1-2.5	-0.5-1.7	-2.3-2.7	-1.2-1.6	16.7-19.4	1.8-5.0	1.1-4.1	-2.1-0.6	-0.9-2.0	-2.8-0.3
7	-0.8-1.5	-1.4-1.1	-0.0-0.6	-0.8-2.2	-1.0-0.8	1.8-5.0	6.8-8.5	-0.1-3.1	-0.6-1.9	0.7-3.3	-0.6-1.9
8	-0.9-1.4	-1.4-1.1	-0.1-0.5	-0.7-2.1	-0.7-1.1	1.1-4.1	-0.1-3.1	6.1-7.7	-1.0-1.5	-0.3-2.2	-1.1-1.2
9	-1.1-0.9	-1.5-0.9	-0.1-0.1	-0.9-1.1	-0.9-0.6	-2.1-0.6	-0.6-1.9	-1.0-1.5	-0.5-0.5	0.1-2.0	-0.7-1.2
10	-1.0-1.2	-1.0-1.5	-0.1-0.3	-1.0-1.7	-0.6-0.9	-0.9-2.0	0.7-3.3	-0.3-2.2	0.1-2.0	3.6-4.9	-0.4-1.6
11	-1.1-0.8	-1.5-0.8	-0.1-0.1	-1.0-0.6	-0.9-0.5	-2.8-0.3	-0.6-1.9	-1.1-1.2	-0.7-1.2	-0.4-1.6	-0.0-0.2
Total	1.5-10.3	1.7-10.6	-5.9-3.3	21.7-29.3	-3.8-5.3	27.6-34.8	11.7-19.9	8.2-16.5	-3.5-5.7	5.4-13.9	-5.8-3.4
Higher	-0.5	2.2	-1.6	3.5	-1.9	6.9	-1.1	-1.1	0.1	-0.8	-0.3

Table F.33: South / Temp. at 5cm with Time (Total-effect)

t \ i	1	2	3	4	5	6	7	8	9	10	11
0.33	5.9-17.8	2.9-15.2	-0.5-12.2	88.8-90.7	-0.5-12.2	4.4-16.5	-0.5-12.2	-0.5-12.2	-0.4-12.2	0.3-12.9	-0.5-12.2
0.67	8.2-19.8	5.5-17.4	-1.3-11.2	75.0-78.6	-1.4-11.2	11.0-22.2	-1.3-11.2	-1.4-11.1	-1.1-11.5	0.9-13.1	-1.3-11.2
1.00	8.8-19.9	7.0-18.4	-2.4-10.0	63.5-68.4	-2.4-10.0	16.8-27.0	-2.3-10.1	-2.4-10.0	-1.7-10.5	1.4-13.3	-2.3-10.0
1.33	9.5-20.1	7.8-18.8	-3.1-8.9	54.0-59.9	-3.1-8.9	20.7-30.1	-2.4-9.4	-2.7-9.2	-2.2-9.5	1.8-13.2	-3.0-8.9
1.67	10.5-20.5	8.2-18.7	-3.6-7.8	46.0-52.5	-3.4-8.0	22.7-31.5	-1.6-9.6	-2.3-9.1	-2.8-8.6	2.0-12.9	-3.6-7.9
2.00	11.4-20.8	8.5-18.4	-4.1-6.8	39.2-46.1	-3.5-7.4	22.8-31.3	0.1-10.6	-1.0-9.8	-3.3-7.6	1.9-12.3	-4.1-6.8
2.33	11.8-20.8	8.5-17.9	-4.7-5.7	33.6-40.7	-3.4-6.9	21.9-30.1	2.5-12.4	1.1-11.1	-3.9-6.5	1.5-11.5	-4.6-5.8
2.67	11.6-20.3	8.2-17.4	-5.3-4.7	29.0-36.3	-3.1-6.8	20.5-28.5	5.4-14.6	3.4-12.7	-4.4-5.6	1.0-10.6	-5.3-4.8
3.00	11.2-19.6	8.0-16.9	-5.8-4.0	25.3-32.8	-2.6-7.1	19.1-27.1	8.2-16.9	5.6-14.5	-4.9-4.8	0.5-9.9	-5.8-4.1
3.33	10.6-18.9	7.9-16.5	-6.3-3.4	22.6-30.1	-1.9-7.4	18.0-25.9	10.8-19.0	7.6-16.1	-5.3-4.3	0.2-9.4	-6.3-3.5
3.67	9.8-18.1	7.5-16.2	-3.8-5.5	20.3-28.0	-1.2-7.9	17.1-25.0	12.8-20.9	9.2-17.6	-5.6-3.9	-0.1-9.0	-3.7-5.5
4.00	8.9-17.3	7.1-15.8	-4.1-5.1	18.5-26.4	-0.7-8.4	16.5-24.6	14.6-22.6	10.6-18.8	-5.8-3.6	-0.3-8.8	-4.0-5.2
4.33	8.1-16.5	6.7-15.4	-4.5-4.9	17.0-25.0	-0.3-8.8	16.2-24.3	16.1-24.1	11.7-19.9	-3.4-5.9	-0.5-8.7	-4.4-4.9
4.67	7.3-15.7	6.1-15.0	-4.8-4.6	15.7-23.8	0.0-9.1	16.2-24.4	17.4-25.3	12.7-20.9	-3.6-5.7	-0.7-8.5	-4.7-4.7
5.00	6.4-15.0	5.6-14.5	-5.0-4.5	14.5-22.8	0.2-9.4	16.4-24.6	18.6-26.4	13.5-21.7	-3.8-5.6	-0.7-8.5	-4.9-4.5
5.33	5.5-14.2	5.1-14.0	-5.3-4.3	13.5-21.9	0.3-9.5	16.8-25.0	19.5-27.4	14.3-22.4	-4.0-5.5	-0.7-8.6	-5.2-4.4
5.67	4.5-13.4	4.4-13.5	-5.5-4.1	12.6-21.1	0.3-9.4	17.4-25.7	20.4-28.3	15.0-23.1	-4.2-5.3	-0.7-8.7	-5.4-4.3
6.00	3.6-12.5	3.8-12.9	-5.7-4.0	11.7-20.3	0.1-9.3	18.3-26.5	21.2-29.1	15.6-23.7	-4.3-5.3	-0.6-8.9	-5.6-4.2
6.33	2.6-11.6	3.2-12.3	-5.8-3.9	10.9-19.6	-0.2-9.1	19.3-27.6	21.9-29.7	16.1-24.2	-4.3-5.3	-0.3-9.2	-5.7-4.0
6.67	1.5-10.6	2.5-11.7	-6.0-3.7	10.1-18.8	-0.5-8.7	20.6-28.8	22.4-30.2	16.5-24.6	-4.3-5.4	-0.0-9.5	-5.9-3.8
7.00	0.4-9.6	1.9-11.1	-6.1-3.7	9.3-18.1	-1.0-8.3	22.1-30.1	22.6-30.4	16.7-24.8	-4.4-5.3	0.4-9.8	-6.0-3.8
7.33	-0.7-8.6	1.2-10.5	-6.3-3.6	8.6-17.5	-1.6-7.8	23.9-31.8	22.5-30.2	16.7-24.7	-4.5-5.3	0.8-10.2	-6.1-3.7
7.67	-1.8-7.6	0.5-9.9	-6.5-3.4	7.9-16.8	-2.3-7.2	25.9-33.6	21.8-29.6	16.2-24.2	-4.5-5.3	1.2-10.6	-6.3-3.6
8.00	-2.9-6.7	-0.1-9.4	-6.7-3.2	7.2-16.2	-3.1-6.5	28.4-35.9	20.4-28.3	15.0-23.1	-4.6-5.2	1.7-11.0	-6.4-3.4
8.33	-3.8-5.9	-0.7-8.9	-6.8-3.1	6.6-15.7	-3.9-5.9	31.5-38.8	18.0-26.1	12.9-21.3	-4.7-5.2	2.3-11.6	-6.5-3.3
8.67	-4.6-5.4	-1.0-8.8	-6.8-3.2	6.1-15.3	-4.5-5.4	35.4-42.5	14.6-23.0	9.9-18.8	-4.6-5.3	2.9-12.4	-6.6-3.4
9.00	-5.0-5.1	-1.1-8.9	-6.8-3.5	5.7-15.1	-5.2-5.0	40.2-47.0	10.4-19.3	6.5-15.8	-4.6-5.5	3.8-13.3	-6.5-3.7
9.33	-5.3-5.2	-1.1-9.1	-6.7-3.7	5.4-15.1	-6.0-4.5	45.5-51.9	6.1-15.6	3.0-12.8	-4.5-5.8	4.7-14.5	-6.4-4.0
9.67	-5.5-5.3	-1.3-9.1	-6.6-4.0	5.1-15.0	-6.5-4.3	50.6-56.6	2.3-12.3	-0.2-10.1	-4.2-6.3	5.7-15.5	-6.3-4.3
10.00	-5.5-5.4	-1.6-9.0	-6.4-4.3	4.7-14.9	-7.0-4.0	55.0-60.5	-0.7-9.8	-2.5-8.2	-4.0-6.5	6.5-16.4	-6.0-4.6

Table F.34: South / Temp. at 5cm / Mid-day

i \ j	1	2	3	4	5	6	7	8	9	10	11
1	7.8-9.2	-0.3-2.1	-1.0-1.0	-0.6-2.2	-1.2-0.9	-1.3-1.8	-0.6-2.5	-0.5-2.3	-0.9-1.1	-0.9-1.3	-1.0-1.0
2	-0.3-2.1	5.3-7.0	-1.2-1.2	-1.2-1.6	-0.6-1.8	-1.2-2.0	-1.0-2.2	-1.7-1.2	-1.2-1.2	-1.5-1.1	-1.2-1.2
3	-1.0-1.0	-1.2-1.2	-0.0-0.1	-1.0-0.4	-0.2-0.1	-0.4-0.9	-0.2-1.1	-0.0-1.0	-0.1-0.1	-0.1-0.2	-0.1-0.1
4	-0.6-2.2	-1.2-1.6	-1.0-0.4	13.5-15.3	-0.7-1.0	-1.3-2.1	-0.5-2.6	-0.2-2.6	-0.7-0.8	-0.8-1.1	-0.8-0.7
5	-1.2-0.9	-0.6-1.8	-0.2-0.1	-0.7-1.0	3.1-4.3	-1.3-1.2	-0.9-1.9	-0.9-1.7	-0.9-1.2	-1.2-0.9	-0.9-1.1
6	-1.3-1.8	-1.2-2.0	-0.4-0.9	-1.3-2.1	-1.3-1.2	10.7-12.9	2.4-5.5	1.8-4.6	-1.9-0.6	-1.0-1.5	-2.0-0.4
7	-0.6-2.5	-1.0-2.2	-0.2-1.1	-0.5-2.6	-0.9-1.9	2.4-5.5	12.5-14.7	0.9-4.7	-0.4-2.3	1.0-3.8	-0.3-2.4
8	-0.5-2.3	-1.7-1.2	-0.0-1.0	-0.2-2.6	-0.9-1.7	1.8-4.6	0.9-4.7	10.0-12.0	-0.8-1.8	-0.2-2.5	-0.9-1.7
9	-0.9-1.1	-1.2-1.2	-0.1-0.1	-0.7-0.8	-0.9-1.2	-1.9-0.6	-0.4-2.3	-0.8-1.8	-0.3-0.2	-0.2-0.7	-0.4-0.6
10	-0.9-1.3	-1.5-1.1	-0.1-0.2	-0.8-1.1	-1.2-0.9	-1.0-1.5	1.0-3.8	-0.2-2.5	-0.2-0.7	1.7-2.5	-0.1-1.3
11	-1.0-1.0	-1.2-1.2	-0.1-0.1	-0.8-0.7	-0.9-1.1	-2.0-0.4	-0.3-2.4	-0.9-1.7	-0.4-0.6	-0.1-1.3	-0.0-0.1
Total	6.4-15.0	5.6-14.5	-5.0-4.5	14.5-22.8	0.2-9.4	16.4-24.6	18.6-26.4	13.5-21.7	-3.8-5.6	-0.7-8.5	-4.9-4.5
Higher	-1.8	1.6	-1.2	0.6	-0.5	1.5	-5.8	-4.1	-0.5	-2.8	-1.6

Table F.35: North / Temp. at 5cm with Time (Total-effect)

t \ i	1	2	3	4	5	6	7	8	9	10	11
0.33	1.7-13.8	0.6-12.7	-0.8-11.6	96.0-97.0	-0.8-11.7	1.5-13.6	-0.8-11.7	-0.8-11.7	-0.7-11.7	-0.4-11.9	-0.7-11.7
0.67	3.1-15.5	1.4-14.1	-1.2-11.7	89.4-91.5	-1.2-11.7	5.3-17.5	-1.2-11.7	-1.2-11.7	-1.1-11.8	-0.0-12.8	-1.2-11.7
1.00	3.4-16.2	1.8-14.8	-1.9-11.4	82.4-85.4	-2.0-11.4	9.5-21.5	-1.9-11.4	-2.0-11.4	-1.6-11.7	0.6-13.6	-1.9-11.4
1.33	3.5-16.3	2.0-15.2	-2.5-11.0	75.4-79.4	-2.5-10.9	13.6-25.1	-2.5-11.0	-2.5-11.0	-2.0-11.3	1.2-14.2	-2.5-11.0
1.67	3.7-16.4	2.2-15.3	-2.9-10.5	68.7-73.5	-3.0-10.5	17.1-28.2	-2.7-10.7	-2.8-10.6	-2.5-10.9	1.8-14.7	-3.0-10.5
2.00	4.0-16.5	2.3-15.2	-3.4-9.9	62.3-67.9	-3.4-9.9	20.3-30.8	-2.7-10.5	-3.0-10.4	-2.9-10.4	2.4-15.0	-3.4-10.0
2.33	4.6-16.7	2.4-15.0	-3.7-9.4	56.3-62.4	-3.6-9.5	22.5-32.5	-2.4-10.6	-2.6-10.6	-3.1-9.9	3.0-15.3	-3.6-9.4
2.67	5.2-16.9	2.4-14.5	-3.9-8.7	50.5-57.1	-3.6-9.0	24.0-33.5	-1.4-11.0	-1.4-11.1	-3.3-9.3	3.3-15.2	-3.9-8.8
3.00	5.9-17.0	2.3-14.0	-4.2-8.0	45.2-52.2	-3.7-8.5	24.6-33.8	-0.2-11.7	0.2-12.0	-3.5-8.7	3.5-14.9	-4.1-8.1
3.33	6.4-17.1	2.3-13.5	-4.4-7.4	40.5-47.7	-3.6-8.1	24.7-33.6	1.3-12.5	2.1-13.3	-3.8-8.0	3.7-14.6	-4.3-7.5
3.67	6.6-16.9	2.0-12.9	-4.6-6.7	36.3-43.6	-3.5-7.8	24.5-33.1	2.9-13.5	4.1-14.7	-4.0-7.3	3.8-14.2	-4.5-6.8
4.00	6.7-16.5	1.8-12.2	-4.9-6.1	32.6-40.1	-3.5-7.4	24.2-32.5	4.4-14.4	6.3-16.2	-4.3-6.6	3.7-13.8	-4.8-6.2
4.33	6.4-15.9	1.4-11.6	-5.2-5.5	29.3-37.0	-3.5-7.1	23.8-31.9	5.7-15.3	8.3-17.7	-4.5-6.0	3.5-13.4	-5.1-5.5
4.67	5.8-15.2	1.1-11.0	-5.4-4.9	26.5-34.3	-3.4-6.8	23.5-31.4	6.8-16.1	10.1-19.2	-4.8-5.5	3.4-13.0	-5.4-5.0
5.00	5.2-14.3	0.7-10.4	-5.7-4.5	24.2-32.0	-3.4-6.6	23.3-31.0	7.8-16.9	11.8-20.5	-5.1-5.0	3.3-12.7	-5.7-4.5
5.33	4.3-13.4	0.3-9.9	-6.0-4.1	22.2-30.0	-3.5-6.4	23.3-30.9	8.6-17.4	13.1-21.6	-5.3-4.6	3.2-12.5	-5.9-4.1
5.67	3.5-12.6	0.0-9.5	-6.2-3.8	20.5-28.4	-3.5-6.2	23.6-31.1	9.2-17.9	14.3-22.5	-5.5-4.4	3.2-12.4	-6.1-3.8
6.00	2.7-11.7	-0.2-9.2	-6.4-3.5	19.1-27.1	-3.6-6.1	24.1-31.5	9.6-18.2	15.0-23.1	-5.7-4.2	3.3-12.5	-6.3-3.6
6.33	1.8-10.9	-0.5-9.0	-3.6-5.8	17.9-25.9	-3.7-5.9	24.9-32.2	9.7-18.3	15.4-23.4	-5.8-4.0	3.5-12.6	-6.5-3.5
6.67	0.8-10.0	-0.7-8.9	-3.7-5.7	16.9-25.0	-3.9-5.8	26.0-33.3	9.7-18.3	15.4-23.4	-6.0-3.9	3.8-12.8	-3.6-5.9
7.00	-0.1-9.2	-0.8-8.9	-3.8-5.7	16.2-24.4	-4.1-5.7	27.4-34.6	9.3-18.1	14.9-23.1	-6.1-3.9	4.1-13.1	-3.7-5.8
7.33	-1.0-8.6	-0.8-9.0	-3.9-5.7	15.5-23.9	-4.3-5.6	29.2-36.3	8.7-17.6	14.0-22.3	-6.2-4.0	4.4-13.6	-3.8-5.9
7.67	-1.9-8.0	-0.7-9.3	-3.9-5.8	15.0-23.5	-4.6-5.6	31.2-38.3	7.7-16.9	12.5-21.2	-6.3-4.1	4.9-14.2	-3.8-6.0
8.00	-2.7-7.5	-0.6-9.6	-4.0-6.0	14.6-23.4	-4.9-5.6	33.6-40.6	6.3-15.8	10.7-19.7	-6.4-4.2	5.3-14.8	-3.8-6.2
8.33	-3.4-7.2	-0.5-10.0	-4.0-6.2	14.2-23.4	-5.3-5.6	36.2-43.2	4.5-14.5	8.4-18.0	-6.5-4.5	5.8-15.6	-7.2-3.8
8.67	-3.9-7.1	-0.5-10.4	-7.6-3.8	14.0-23.4	-5.6-5.6	39.1-46.0	2.7-13.2	6.1-16.3	-6.6-4.7	6.4-16.3	-7.3-4.0
9.00	-4.3-7.1	-0.4-10.7	-7.7-4.1	13.9-23.5	-6.0-5.7	42.0-48.8	0.9-11.9	3.9-14.5	-6.6-5.0	6.9-17.2	-7.4-4.3
9.33	-4.6-7.3	-0.5-11.0	-7.8-4.3	13.7-23.6	-6.3-5.7	44.9-51.6	-0.8-10.7	1.9-13.0	-6.6-5.4	7.4-18.0	-7.6-4.6
9.67	-4.7-7.4	-0.6-11.1	-7.8-4.6	13.4-23.7	-6.5-5.8	47.5-54.0	-2.2-9.7	0.1-11.7	-6.6-5.7	8.0-18.7	-7.5-4.9
10.00	-4.7-7.6	-0.9-11.1	-7.8-4.8	13.1-23.6	-6.7-5.9	49.8-56.2	-3.3-8.9	-1.3-10.7	-6.6-6.1	8.5-19.4	-7.5-5.1

Table F.36: North / Temp. at 5cm / Mid-day

i \ j	1	2	3	4	5	6	7	8	9	10	11
1	6.1-8.0	-1.6-1.7	-2.2-0.9	-2.9-1.6	-2.4-0.8	-2.5-1.9	-1.7-1.6	-1.9-1.7	-2.2-0.9	-2.2-1.1	-2.2-0.9
2	-1.6-1.7	0.2-1.9	-1.8-1.2	-1.8-2.1	-1.2-1.7	-0.5-3.4	-1.5-1.4	-1.7-1.3	-1.8-1.2	-1.5-1.5	-1.8-1.2
3	-2.2-0.9	-1.8-1.2	-0.1-0.1	-2.9-0.1	-0.2-0.2	-0.8-1.9	-0.3-0.4	-0.5-0.7	-0.1-0.2	-0.2-0.4	-0.1-0.2
4	-2.9-1.6	-1.8-2.1	-2.9-0.1	23.3-26.5	-1.2-1.0	-2.6-3.2	-1.9-1.3	-2.2-1.7	-1.0-1.2	-1.5-1.7	-1.0-1.1
5	-2.4-0.8	-1.2-1.7	-0.2-0.2	-1.2-1.0	0.5-1.4	-1.2-1.9	-1.2-0.8	-1.2-1.0	-0.8-1.0	-1.1-0.7	-0.8-1.0
6	-2.5-1.9	-0.5-3.4	-0.8-1.9	-2.6-3.2	-1.2-1.9	22.1-25.2	-1.4-1.6	-1.3-2.4	-1.3-1.2	-1.6-1.4	-1.4-1.1
7	-1.7-1.6	-1.5-1.4	-0.3-0.4	-1.9-1.3	-1.2-0.8	-1.4-1.6	8.3-10.3	-1.8-2.2	-1.5-1.6	-1.2-1.8	-1.5-1.5
8	-1.9-1.7	-1.7-1.3	-0.5-0.7	-2.2-1.7	-1.2-1.0	-1.3-2.4	-1.8-2.2	12.4-14.7	-2.6-0.6	-2.5-0.8	-2.6-0.6
9	-2.2-0.9	-1.8-1.2	-0.1-0.2	-1.0-1.2	-0.8-1.0	-1.3-1.2	-1.5-1.6	-2.6-0.6	-0.3-0.2	-0.5-0.7	-0.5-0.7
10	-2.2-1.1	-1.5-1.5	-0.2-0.4	-1.5-1.7	-1.1-0.7	-1.6-1.4	-1.2-1.8	-2.5-0.8	-0.5-0.7	6.1-7.4	-1.2-0.7
11	-2.2-0.9	-1.8-1.2	-0.1-0.2	-1.0-1.1	-0.8-1.0	-1.4-1.1	-1.5-1.5	-2.6-0.6	-0.5-0.7	-1.2-0.7	0.0-0.2
Total	5.2-14.3	0.7-10.4	-5.7-4.5	24.2-32.0	-3.4-6.6	23.3-31.0	7.8-16.9	11.8-20.5	-5.1-5.0	3.3-12.7	-5.7-4.5
Higher	7.1	3.6	0.8	5.1	1.3	0.8	2.9	5.1	1.5	2.5	1.5

Table F.37: Control / Temp. at 5cm / Mean

i \ j	1	2	3	4	5	6	7	8	9	10	11
1	2.5-3.7	-1.0-1.1	-1.1-0.9	-2.5-2.2	-1.3-0.8	-1.5-2.6	-0.9-1.3	-1.0-1.1	-1.1-1.0	-0.8-1.5	-1.1-0.9
2	-1.0-1.1	1.2-2.7	-1.5-1.2	-2.7-2.1	-1.2-1.4	-0.4-3.9	-1.2-1.5	-1.5-1.2	-1.6-1.1	-1.6-1.1	-1.5-1.1
3	-1.1-0.9	-1.5-1.2	-0.1-0.0	-3.8-0.4	-0.1-0.1	-0.7-2.3	-0.0-0.3	-0.1-0.2	-0.1-0.1	-0.1-0.4	-0.1-0.1
4	-2.5-2.2	-2.7-2.1	-3.8-0.4	33.7-37.7	-1.1-0.8	-2.8-5.0	-0.9-2.2	-1.2-1.8	-1.4-1.0	-1.0-2.7	-1.0-0.7
5	-1.3-0.8	-1.2-1.4	-0.1-0.1	-1.1-0.8	0.5-1.1	-1.0-2.3	-0.8-0.4	-0.5-0.7	-0.6-0.5	-0.6-0.5	-0.6-0.5
6	-1.5-2.6	-0.4-3.9	-0.7-2.3	-2.8-5.0	-1.0-2.3	21.7-24.9	-0.7-2.4	-1.1-1.9	-1.8-1.3	-1.0-2.4	-2.8-0.0
7	-0.9-1.3	-1.2-1.5	-0.0-0.3	-0.9-2.2	-0.8-0.4	-0.7-2.4	3.0-4.1	-0.3-1.8	-0.5-1.3	0.1-2.0	-0.5-1.3
8	-1.0-1.1	-1.5-1.2	-0.1-0.2	-1.2-1.8	-0.5-0.7	-1.1-1.9	-0.3-1.8	2.9-3.9	-0.9-0.9	-0.6-1.3	-1.0-0.7
9	-1.1-1.0	-1.6-1.1	-0.1-0.1	-1.4-1.0	-0.6-0.5	-1.8-1.3	-0.5-1.3	-0.9-0.9	-0.6-0.5	0.3-2.5	-0.9-1.5
10	-0.8-1.5	-1.6-1.1	-0.1-0.4	-1.0-2.7	-0.6-0.5	-1.0-2.4	0.1-2.0	-0.6-1.3	0.3-2.5	4.9-6.4	-0.8-1.5
11	-1.1-0.9	-1.5-1.1	-0.1-0.1	-1.0-0.7	-0.6-0.5	-2.8-0.0	-0.5-1.3	-1.0-0.7	-0.9-1.5	-0.8-1.5	-0.0-0.2
Total	-1.2-8.6	-0.6-9.3	-4.6-4.9	37.4-43.9	-6.0-4.2	28.1-35.7	1.4-10.9	-0.4-9.2	-3.1-6.8	5.3-14.5	-4.5-5.0
Higher	0.1	1.6	1.0	4.6	-1.9	3.4	-1.7	-0.6	0.6	-0.5	1.0

Table F.38: South / Temp. at 5cm / Mean

i \ j	1	2	3	4	5	6	7	8	9	10	11
1	6.1-7.6	-1.4-1.1	-1.1-1.2	-3.4-2.1	-1.3-1.0	-1.7-2.5	-1.4-1.4	-1.4-1.2	-1.0-1.3	-1.6-0.9	-1.1-1.2
2	-1.4-1.1	3.0-4.8	-1.2-1.9	-3.3-2.0	-1.4-1.6	-0.5-3.9	-1.4-1.8	-2.0-1.2	-1.2-1.9	-1.6-1.6	-1.2-1.8
3	-1.1-1.2	-1.2-1.9	-0.0-0.1	-4.0-0.3	-0.1-0.2	-0.8-1.8	-0.2-0.6	-0.1-0.5	-0.1-0.1	-0.1-0.3	-0.1-0.1
4	-3.4-2.1	-3.3-2.0	-4.0-0.3	29.0-33.3	-1.4-0.7	-3.4-3.4	-1.3-2.8	-1.1-2.6	-0.8-1.0	-1.0-2.0	-1.0-0.6
5	-1.3-1.0	-1.4-1.6	-0.1-0.2	-1.4-0.7	1.3-2.2	-1.1-2.0	-0.9-1.2	-1.0-1.0	-0.7-1.1	-1.0-0.8	-0.7-1.1
6	-1.7-2.5	-0.5-3.9	-0.8-1.8	-3.4-3.4	-1.1-2.0	17.8-21.0	0.2-3.7	-0.2-3.3	-1.9-1.2	-1.8-1.5	-2.2-0.9
7	-1.4-1.4	-1.4-1.8	-0.2-0.6	-1.3-2.8	-0.9-1.2	0.2-3.7	6.9-8.6	0.1-3.1	-0.3-2.1	0.4-2.9	-0.2-2.1
8	-1.4-1.2	-2.0-1.2	-0.1-0.5	-1.1-2.6	-1.0-1.0	-0.2-3.3	0.1-3.1	5.9-7.4	-1.1-1.2	-0.7-1.6	-1.1-1.2
9	-1.0-1.3	-1.2-1.9	-0.1-0.1	-0.8-1.0	-0.7-1.1	-1.9-1.2	-0.3-2.1	-1.1-1.2	-0.4-0.3	-0.2-1.0	-0.6-0.7
10	-1.6-0.9	-1.6-1.6	-0.1-0.3	-1.0-2.0	-1.0-0.8	-1.8-1.5	0.4-2.9	-0.7-1.6	-0.2-1.0	3.2-4.4	-0.7-1.3
11	-1.1-1.2	-1.2-1.8	-0.1-0.1	-1.0-0.6	-0.7-1.1	-2.2-0.9	-0.2-2.1	-1.1-1.2	-0.6-0.7	-0.7-1.3	0.0-0.2
Total	2.6-13.6	2.0-13.2	-7.8-4.3	30.6-38.9	-3.9-7.7	20.9-30.4	6.9-17.4	4.0-14.9	-6.6-5.4	0.1-11.3	-7.7-4.4
Higher	2.1	1.9	-1.3	5.1	-0.4	0.8	-4.0	-1.5	-2.3	-1.0	-2.7

Table F.39: North / Temp. at 5cm / Mean

i \ j	1	2	3	4	5	6	7	8	9	10	11
1	2.7-4.4	-2.1-1.1	-2.4-0.7	-7.4-1.0	-2.5-0.6	-2.6-2.7	-2.2-1.0	-2.4-0.8	-2.5-0.7	-2.3-1.0	-2.4-0.7
2	-2.1-1.1	-0.9-1.0	-2.0-1.6	-6.1-1.8	-1.6-2.0	-0.6-4.4	-1.9-1.7	-1.9-1.6	-2.0-1.6	-1.5-2.0	-2.0-1.6
3	-2.4-0.7	-2.0-1.6	-0.1-0.1	-7.6-0.1	-0.2-0.2	-1.2-2.5	-0.2-0.3	-0.3-0.3	-0.1-0.2	-0.4-0.3	-0.1-0.2
4	-7.4-1.0	-6.1-1.8	-7.6-0.1	40.0-46.3	-1.6-0.8	-4.1-5.9	-2.4-1.4	-2.6-1.9	-1.0-1.3	-2.3-2.4	-1.0-1.2
5	-2.5-0.6	-1.6-2.0	-0.2-0.2	-1.6-0.8	0.0-0.8	-1.4-2.6	-1.0-0.6	-1.0-0.7	-0.6-1.0	-1.0-0.6	-0.6-0.9
6	-2.6-2.7	-0.6-4.4	-1.2-2.5	-4.1-5.9	-1.4-2.6	23.9-28.0	-2.1-1.3	-1.9-1.8	-1.3-1.7	-2.3-1.5	-1.4-1.5
7	-2.2-1.0	-1.9-1.7	-0.2-0.3	-2.4-1.4	-1.0-0.6	-2.1-1.3	4.2-5.6	-1.7-1.2	-1.3-1.2	-1.2-1.2	-1.3-1.1
8	-2.4-0.8	-1.9-1.6	-0.3-0.3	-2.6-1.9	-1.0-0.7	-1.9-1.8	-1.7-1.2	6.2-7.9	-2.0-0.6	-2.0-0.8	-2.0-0.6
9	-2.5-0.7	-2.0-1.6	-0.1-0.2	-1.0-1.3	-0.6-1.0	-1.3-1.7	-1.3-1.2	-2.0-0.6	-0.4-0.3	-0.7-0.8	-0.6-0.9
10	-2.3-1.0	-1.5-2.0	-0.4-0.3	-2.3-2.4	-1.0-0.6	-2.3-1.5	-1.2-1.2	-2.0-0.8	-0.7-0.8	6.4-7.9	-1.3-1.0
11	-2.4-0.7	-2.0-1.6	-0.1-0.2	-1.0-1.2	-0.6-0.9	-1.4-1.5	-1.3-1.1	-2.0-0.6	-0.6-0.9	-1.3-1.0	0.0-0.2
Total	0.5-12.7	-0.8-11.6	-5.5-7.3	41.9-49.5	-4.3-8.3	24.9-34.3	1.1-13.2	3.1-14.9	-4.9-7.8	3.3-15.1	-5.5-7.4
Higher	12.2	6.6	5.1	11.8	2.3	0.2	4.4	5.7	2.6	3.8	2.4

Table F.40: Control / Temp. at 5cm / Maximum

i \ j	1	2	3	4	5	6	7	8	9	10	11
1	2.7-3.6	-0.6-1.0	-0.9-0.7	-1.7-1.4	-1.0-0.6	-0.9-2.3	-0.5-1.6	-0.6-1.4	-0.9-0.7	-0.6-1.2	-0.9-0.7
2	-0.6-1.0	0.9-2.0	-1.3-0.8	-1.9-1.2	-1.2-0.8	-0.5-2.8	-1.2-1.1	-1.2-1.0	-1.3-0.8	-0.8-1.3	-1.3-0.7
3	-0.9-0.7	-1.3-0.8	-0.0-0.1	-2.0-0.5	-0.1-0.1	-0.2-2.0	-0.0-0.7	-0.2-0.5	-0.1-0.1	-0.1-0.3	-0.1-0.1
4	-1.7-1.4	-1.9-1.2	-2.0-0.5	19.7-22.4	-0.5-0.7	1.5-6.8	1.1-4.2	0.5-3.3	-1.0-0.6	0.4-2.9	-0.4-0.6
5	-1.0-0.6	-1.2-0.8	-0.1-0.1	-0.5-0.7	1.5-2.3	-0.9-1.9	-1.0-1.0	-0.7-1.1	-1.0-0.6	-0.6-1.0	-0.9-0.6
6	-0.9-2.3	-0.5-2.8	-0.2-2.0	1.5-6.8	-0.9-1.9	13.9-16.5	2.5-5.8	1.5-4.6	-1.8-0.7	-0.8-2.1	-2.2-0.0
7	-0.5-1.6	-1.2-1.1	-0.0-0.7	1.1-4.2	-1.0-1.0	2.5-5.8	6.3-8.1	0.1-3.6	-0.5-2.2	0.9-3.6	-0.3-2.2
8	-0.6-1.4	-1.2-1.0	-0.2-0.5	0.5-3.3	-0.7-1.1	1.5-4.6	0.1-3.6	6.0-7.7	-1.2-1.4	-0.6-2.1	-1.2-1.2
9	-0.9-0.7	-1.3-0.8	-0.1-0.1	-1.0-0.6	-1.0-0.6	-1.8-0.7	-0.5-2.2	-1.2-1.4	-0.2-0.8	-0.1-1.8	-1.0-0.9
10	-0.6-1.2	-0.8-1.3	-0.1-0.3	0.4-2.9	-0.6-1.0	-0.8-2.1	0.9-3.6	-0.6-2.1	-0.1-1.8	3.0-4.2	-0.3-1.6
11	-0.9-0.7	-1.3-0.7	-0.1-0.1	-0.4-0.6	-0.9-0.6	-2.2-0.0	-0.3-2.2	-1.2-1.2	-1.0-0.9	-0.3-1.6	-0.0-0.2
Total	-2.6-7.1	-2.8-7.0	-6.5-3.4	30.3-37.9	-4.9-5.1	29.3-36.8	14.2-22.8	9.9-18.7	-3.5-6.5	5.7-15.0	-6.3-3.5
Higher	-2.5	0.6	-1.9	3.9	-2.0	4.3	-2.2	-0.9	0.6	-0.9	-1.3

Table F.41: South / Temp. at 5cm / Maximum

i \ j	1	2	3	4	5	6	7	8	9	10	11
1	4.9-6.0	-0.4-1.4	-0.8-0.9	-0.5-1.7	-0.9-0.9	-1.0-2.1	-0.3-2.8	-0.3-2.4	-0.8-1.0	-0.6-1.4	-0.8-0.9
2	-0.4-1.4	1.5-2.8	-1.1-1.2	-1.5-0.9	-0.5-1.7	-0.7-2.3	-0.8-2.3	-1.4-1.4	-1.1-1.1	-1.4-1.0	-1.1-1.1
3	-0.8-0.9	-1.1-1.2	-0.0-0.1	-0.8-0.3	-0.1-0.1	-0.4-1.2	-0.2-1.5	-0.1-1.2	-0.1-0.1	-0.0-0.2	-0.1-0.1
4	-0.5-1.7	-1.5-0.9	-0.8-0.3	11.5-13.2	-0.7-0.8	-1.8-1.7	-0.0-3.5	-0.1-2.9	-0.7-0.7	-0.6-1.3	-0.7-0.6
5	-0.9-0.9	-0.5-1.7	-0.1-0.1	-0.7-0.8	3.1-4.2	-1.3-1.4	-0.8-2.2	-1.0-1.7	-1.0-0.9	-1.2-0.8	-1.0-0.9
6	-1.0-2.1	-0.7-2.3	-0.4-1.2	-1.8-1.7	-1.3-1.4	11.6-14.0	4.3-8.1	2.8-6.1	-1.8-0.6	-1.6-1.0	-1.9-0.4
7	-0.3-2.8	-0.8-2.3	-0.2-1.5	-0.0-3.5	-0.8-2.2	4.3-8.1	13.9-16.4	1.5-6.0	-0.0-2.7	1.8-4.8	0.0-2.7
8	-0.3-2.4	-1.4-1.4	-0.1-1.2	-0.1-2.9	-1.0-1.7	2.8-6.1	1.5-6.0	11.2-13.4	-0.7-2.1	0.1-3.0	-0.8-1.9
9	-0.8-1.0	-1.1-1.1	-0.1-0.1	-0.7-0.7	-1.0-0.9	-1.8-0.6	-0.0-2.7	-0.7-2.1	-0.2-0.3	-0.3-0.8	-0.5-0.6
10	-1.0-2.1	-1.4-1.0	-0.0-0.2	-0.6-1.3	-1.2-0.8	-1.6-1.0	1.8-4.8	0.1-3.0	-0.3-0.8	1.9-2.8	-0.0-1.5
11	-0.8-0.9	-1.1-1.1	-0.1-0.1	-0.7-0.6	-1.0-0.9	-1.9-0.4	0.0-2.7	-0.8-1.9	-0.5-0.6	-0.0-1.5	-0.0-0.1
Total	-0.1-9.5	-1.4-8.3	-6.5-3.4	11.2-20.2	-2.2-7.5	21.5-29.5	24.0-31.7	17.3-25.4	-4.8-4.9	-0.1-9.5	-6.3-3.5
Higher	-5.3	-1.0	-3.1	-0.2	-2.3	1.9	-8.4	-5.4	-1.9	-3.5	-3.4

Table F.42: North / Temp. at 5cm / Maximum

i \ j	1	2	3	4	5	6	7	8	9	10	11
1	3.9-5.2	-1.3-1.1	-1.6-0.7	-3.0-0.8	-1.8-0.6	-1.8-2.1	-1.2-1.5	-1.6-1.4	-1.7-0.6	-1.7-0.7	-1.6-0.7
2	-1.3-1.1	-0.7-0.7	-1.0-1.7	-2.8-0.7	-1.0-1.6	-0.4-3.0	-1.4-1.2	-1.5-1.2	-0.9-1.7	-1.4-1.1	-1.0-1.7
3	-1.6-0.7	-1.0-1.7	-0.0-0.1	-3.0-0.2	-0.1-0.1	-0.6-2.0	-0.3-0.5	-0.6-0.8	-0.2-0.1	-0.2-0.3	-0.2-0.1
4	-3.0-0.8	-2.8-0.7	-3.0-0.2	23.4-26.5	-1.0-0.7	-0.5-5.0	-0.6-2.5	-0.9-3.0	-0.8-0.8	-0.4-2.2	-0.7-0.9
5	-1.8-0.6	-1.0-1.6	-0.1-0.1	-1.0-0.7	0.6-1.5	-0.8-2.2	-1.1-1.0	-1.2-1.2	-0.8-1.0	-1.1-0.7	-0.8-1.0
6	-1.8-2.1	-0.4-3.0	-0.6-2.0	-0.5-5.0	-0.8-2.2	21.0-23.8	-0.5-2.6	-0.8-3.2	-1.3-1.0	-1.1-1.8	-1.3-0.9
7	-1.2-1.5	-1.4-1.2	-0.3-0.5	-0.6-2.5	-1.1-1.0	-0.5-2.6	9.2-11.3	-1.2-3.1	-1.2-1.9	-1.9-1.3	-1.2-1.9
8	-1.6-1.4	-1.5-1.2	-0.6-0.8	-0.9-3.0	-1.2-1.2	-0.8-3.2	-1.2-3.1	14.1-16.5	-2.4-0.8	-2.5-0.8	-2.4-0.8
9	-1.7-0.6	-0.9-1.7	-0.2-0.1	-0.8-0.8	-0.8-1.0	-1.3-1.0	-1.2-1.9	-2.4-0.8	-0.3-0.2	-0.5-0.7	-0.5-0.7
10	-1.7-0.7	-1.4-1.1	-0.2-0.3	-0.4-2.2	-1.1-0.7	-1.1-1.8	-1.9-1.3	-2.5-0.8	-0.5-0.7	5.9-7.1	-0.9-0.9
11	-1.6-0.7	-1.0-1.7	-0.2-0.1	-0.7-0.9	-0.8-1.0	-1.3-0.9	-1.2-1.9	-2.4-0.8	-0.5-0.7	-0.9-0.9	-0.0-0.2
Total	1.3-10.4	-1.2-8.0	-5.3-4.3	26.8-34.0	-2.9-6.5	25.3-32.5	11.2-19.4	16.0-23.7	-4.6-5.0	3.7-12.7	-5.2-4.4
Higher	4.9	2.3	0.3	4.0	0.5	-0.8	1.6	4.0	0.7	2.3	-0.0

Table F.43: Control / Temp. at 5cm / Minimum

i \ j	1	2	3	4	5	6	7	8	9	10	11
1	-0.2-0.4	-0.7-0.4	-0.7-0.4	-15.1-3.1	-0.7-0.4	-0.6-0.5	-0.7-0.4	-0.7-0.4	-0.7-0.4	-0.6-0.5	-0.7-0.4
2	-0.7-0.4	-0.4-0.2	-0.6-0.5	-14.8-3.3	-0.6-0.5	-0.5-0.7	-0.6-0.5	-0.6-0.5	-0.6-0.5	-0.6-0.6	-0.6-0.5
3	-0.7-0.4	-0.6-0.5	-0.0-0.0	-15.0-3.1	-0.1-0.1	-0.1-0.1	-0.1-0.1	-0.1-0.1	-0.1-0.1	-0.1-0.1	-0.1-0.1
4	-15.1-3.1	-14.8-3.3	-15.0-3.1	91.1-101.0	-0.1-0.1	-1.9-2.7	-0.8-0.5	-0.5-0.7	-0.8-1.0	-0.9-1.9	-0.2-0.1
5	-0.7-0.4	-0.6-0.5	-0.1-0.1	-0.1-0.1	-0.0-0.1	-0.1-0.1	-0.1-0.1	-0.1-0.1	-0.1-0.1	-0.1-0.1	-0.1-0.1
6	-0.6-0.5	-0.5-0.7	-0.1-0.1	-1.9-2.7	-0.1-0.1	1.3-3.1	-2.7-0.9	-2.8-0.8	-2.6-1.0	-2.4-1.1	-2.8-0.8
7	-0.7-0.4	-0.6-0.5	-0.1-0.1	-0.8-0.5	-0.1-0.1	-2.7-0.9	-0.3-0.2	-0.4-0.6	-0.4-0.6	-0.4-0.6	-0.4-0.6
8	-0.7-0.4	-0.6-0.5	-0.1-0.1	-0.5-0.7	-0.1-0.1	-2.8-0.8	-0.4-0.6	-0.3-0.2	-0.5-0.4	-0.5-0.4	-0.5-0.3
9	-0.7-0.4	-0.6-0.5	-0.1-0.1	-0.8-1.0	-0.1-0.1	-2.6-1.0	-0.4-0.6	-0.5-0.4	-0.4-0.3	-0.5-0.9	-0.6-0.8
10	-0.6-0.5	-0.6-0.6	-0.1-0.1	-0.9-1.9	-0.1-0.1	-2.4-1.1	-0.4-0.6	-0.5-0.4	-0.5-0.9	-0.6-0.5	-0.7-1.5
11	-0.7-0.4	-0.6-0.5	-0.1-0.1	-0.2-0.1	-0.1-0.1	-2.8-0.8	-0.4-0.6	-0.5-0.3	-0.6-0.8	-0.7-1.5	-0.1-0.0
Total	-2.0-7.5	-2.1-7.5	-2.5-7.1	95.1-97.0	-2.5-7.1	2.5-11.7	-2.2-7.4	-2.2-7.4	-1.6-7.9	-0.3-9.1	-2.5-7.1
Higher	9.6	8.8	8.4	16.9	2.5	8.8	3.5	3.8	3.7	4.1	3.0

Table F.44: South / Temp. at 5cm / Minimum

i \ j	1	2	3	4	5	6	7	8	9	10	11
1	-0.2-0.2	-0.4-0.5	-0.4-0.5	-27.8-2.7	-0.4-0.5	-0.4-0.5	-0.4-0.5	-0.4-0.5	-0.4-0.5	-0.4-0.5	-0.4-0.5
2	-0.4-0.5	-0.2-0.2	-0.5-0.4	-27.8-2.8	-0.5-0.4	-0.5-0.4	-0.5-0.4	-0.5-0.4	-0.5-0.4	-0.5-0.4	-0.5-0.4
3	-0.4-0.5	-0.5-0.4	-0.0-0.0	-27.9-2.7	-0.0-0.1	-0.0-0.1	-0.0-0.1	-0.0-0.1	-0.0-0.1	-0.0-0.1	-0.0-0.1
4	-27.8-2.7	-27.8-2.8	-27.9-2.7	96.9-114.2	-0.1-0.2	-1.0-2.4	-0.7-0.5	-0.5-0.5	-0.3-0.5	-0.8-1.3	-0.3-0.2
5	-0.4-0.5	-0.5-0.4	-0.0-0.1	-0.1-0.2	-0.0-0.0	-0.1-0.1	-0.1-0.1	-0.1-0.1	-0.1-0.1	-0.1-0.1	-0.1-0.1
6	-0.4-0.5	-0.5-0.4	-0.0-0.1	-1.0-2.4	-0.1-0.1	-0.5-0.8	-1.0-1.6	-1.0-1.6	-1.0-1.6	-1.6-1.0	-1.0-1.6
7	-0.4-0.5	-0.5-0.4	-0.0-0.1	-0.7-0.5	-0.1-0.1	-1.0-1.6	-0.2-0.1	-0.3-0.5	-0.3-0.5	-0.3-0.5	-0.3-0.5
8	-0.4-0.5	-0.5-0.4	-0.0-0.1	-0.5-0.5	-0.1-0.1	-1.0-1.6	-0.3-0.5	-0.1-0.2	-0.4-0.3	-0.4-0.3	-0.4-0.3
9	-0.4-0.5	-0.5-0.4	-0.0-0.1	-0.3-0.5	-0.1-0.1	-1.0-1.6	-0.3-0.5	-0.4-0.3	-0.2-0.1	-0.2-0.3	-0.2-0.3
10	-0.4-0.5	-0.5-0.4	-0.0-0.1	-0.8-1.3	-0.1-0.1	-1.6-1.0	-0.3-0.5	-0.4-0.3	-0.2-0.3	-0.6-0.2	-0.2-1.3
11	-0.4-0.5	-0.5-0.4	-0.0-0.1	-0.3-0.2	-0.1-0.1	-1.0-1.6	-0.3-0.5	-0.4-0.3	-0.2-0.3	-0.2-1.3	-0.0-0.1
Total	-1.1-12.5	-1.2-12.4	-1.4-12.2	98.6-99.7	-1.4-12.2	0.1-13.6	-1.4-12.3	-1.3-12.4	-1.2-12.4	-0.7-12.9	-1.4-12.2
Higher	18.0	18.3	18.0	30.3	5.3	5.0	4.9	5.2	5.0	5.7	4.5

Table F.45: North / Temp. at 5cm / Minimum

i \ j	1	2	3	4	5	6	7	8	9	10	11
1	-0.3-0.4	-0.7-0.8	-0.7-0.7	-26.4-3.0	-0.7-0.7	-0.6-0.8	-0.7-0.8	-0.7-0.8	-0.7-0.8	-0.7-0.8	-0.7-0.8
2	-0.7-0.8	-0.5-0.3	-0.5-1.0	-26.0-3.2	-0.5-1.0	-0.4-1.1	-0.5-1.0	-0.5-1.1	-0.5-1.0	-0.5-1.1	-0.5-1.0
3	-0.7-0.7	-0.5-1.0	-0.1-0.0	-26.4-2.9	-0.1-0.1	-0.1-0.1	-0.1-0.1	-0.1-0.1	-0.1-0.1	-0.1-0.1	-0.1-0.1
4	-26.4-3.0	-26.0-3.2	-26.4-2.9	93.4-109.9	-0.2-0.2	-1.1-3.9	-0.5-0.6	-0.8-0.6	-0.5-0.6	-1.2-2.3	-0.3-0.2
5	-0.7-0.7	-0.5-1.0	-0.1-0.1	-0.2-0.2	-0.1-0.1	-0.1-0.2	-0.1-0.1	-0.1-0.1	-0.1-0.1	-0.1-0.1	-0.1-0.1
6	-0.6-0.8	-0.4-1.1	-0.1-0.1	-1.1-3.9	-0.1-0.2	0.5-2.5	-2.8-1.2	-2.8-1.2	-2.8-1.2	-2.6-1.4	-2.8-1.2
7	-0.7-0.8	-0.5-1.0	-0.1-0.1	-0.5-0.6	-0.1-0.1	-2.8-1.2	-0.3-0.2	-0.5-0.3	-0.5-0.3	-0.5-0.3	-0.5-0.3
8	-0.7-0.8	-0.5-1.1	-0.1-0.1	-0.8-0.6	-0.1-0.1	-2.8-1.2	-0.5-0.3	-0.3-0.2	-0.4-0.6	-0.4-0.6	-0.4-0.6
9	-0.7-0.8	-0.5-1.0	-0.1-0.1	-0.5-0.6	-0.1-0.1	-2.8-1.2	-0.5-0.3	-0.4-0.6	-0.2-0.2	-0.4-0.3	-0.4-0.3
10	-0.7-0.8	-0.5-1.1	-0.1-0.1	-1.2-2.3	-0.1-0.1	-2.6-1.4	-0.5-0.3	-0.4-0.6	-0.4-0.3	-0.5-0.7	-0.6-2.0
11	-0.7-0.8	-0.5-1.0	-0.1-0.1	-0.3-0.2	-0.1-0.1	-2.8-1.2	-0.5-0.3	-0.4-0.6	-0.4-0.3	-0.6-2.0	-0.1-0.1
Total	-1.3-12.2	-1.3-12.2	-1.9-11.8	96.5-98.5	-1.9-11.8	1.2-14.5	-1.7-11.9	-1.6-12.0	-1.7-11.9	-0.1-13.3	-1.8-11.8
Higher	16.7	14.6	16.3	28.8	4.6	8.2	6.0	5.5	5.5	5.4	4.9



## F.5 Snow Temperature at 8 cm

Table F.46: Control / Temp. at 8cm with Time (Total-effect)

t \ i	1	2	3	4	5	6	7	8	9	10	11
0.33	0.9-9.4	-0.2-8.3	-1.0-7.7	97.6-98.1	-1.0-7.6	0.2-8.6	-1.0-7.6	-1.0-7.6	-0.9-7.7	-0.7-7.8	-0.9-7.6
0.67	3.4-11.9	1.4-10.0	-1.0-7.9	92.6-93.7	-1.0-7.8	2.8-11.4	-1.0-7.8	-1.0-7.8	-0.7-8.2	-0.2-8.6	-1.0-7.8
1.00	4.8-13.3	2.8-11.5	-1.1-7.8	87.1-88.7	-1.2-7.8	5.8-14.3	-1.2-7.8	-1.2-7.7	-0.4-8.6	0.5-9.4	-1.2-7.8
1.33	5.5-14.0	4.0-12.7	-1.4-7.6	81.6-83.8	-1.5-7.5	8.6-16.9	-1.4-7.6	-1.4-7.5	-0.1-8.8	1.1-10.0	-1.4-7.6
1.67	6.0-14.5	5.0-13.7	-1.7-7.3	76.5-79.2	-1.8-7.3	11.0-19.1	-1.6-7.4	-1.7-7.3	-0.1-8.8	1.7-10.5	-1.7-7.3
2.00	6.3-14.8	6.0-14.5	-2.1-7.0	71.8-74.9	-2.1-7.0	12.8-20.7	-1.7-7.4	-1.8-7.2	-0.2-8.7	2.2-10.9	-2.1-7.0
2.33	6.7-15.2	6.8-15.3	-2.4-6.7	67.5-71.0	-2.4-6.7	14.0-21.8	-1.5-7.5	-1.8-7.2	-0.4-8.6	2.5-11.2	-2.4-6.7
2.67	7.2-15.5	7.5-16.0	-2.7-6.3	63.6-67.4	-2.6-6.5	14.6-22.4	-1.2-7.8	-1.5-7.5	-0.6-8.3	2.6-11.3	-2.7-6.3
3.00	7.5-15.9	8.2-16.6	-3.1-5.9	60.0-64.2	-2.8-6.3	14.9-22.7	-0.5-8.3	-1.0-7.8	-0.9-8.0	2.6-11.2	-3.1-5.9
3.33	7.7-16.0	8.9-17.1	-3.5-5.5	56.9-61.4	-2.9-6.1	15.0-22.7	0.2-9.0	-0.5-8.3	-1.2-7.7	2.5-11.1	-3.4-5.6
3.67	7.9-16.1	9.4-17.6	-3.8-5.2	54.2-58.9	-2.9-6.0	14.8-22.6	1.0-9.7	0.0-8.8	-1.5-7.4	2.5-11.0	-3.8-5.2
4.00	7.9-16.0	9.9-18.0	-4.3-4.8	51.8-56.6	-3.0-6.0	14.6-22.5	1.7-10.4	0.6-9.3	-1.9-7.1	2.3-10.9	-4.2-4.8
4.33	7.7-15.9	10.2-18.4	-4.6-4.5	49.6-54.7	-3.0-6.0	14.5-22.4	2.6-11.2	1.1-9.8	-2.2-6.8	2.3-10.8	-4.6-4.5
4.67	7.4-15.7	10.4-18.7	-5.0-4.2	47.6-52.9	-2.9-6.1	14.5-22.3	3.3-11.9	1.6-10.2	-2.4-6.6	2.2-10.7	-4.9-4.2
5.00	7.0-15.4	10.5-18.8	-5.3-3.9	45.9-51.4	-2.9-6.1	14.4-22.4	4.0-12.6	2.1-10.7	-2.7-6.4	2.1-10.7	-5.3-3.9
5.33	6.6-15.0	10.6-18.8	-5.7-3.6	44.3-50.0	-3.0-6.1	14.5-22.5	4.6-13.2	2.4-11.1	-2.9-6.2	2.0-10.7	-5.7-3.6
5.67	6.1-14.6	10.4-18.8	-3.4-5.7	42.8-48.7	-3.0-6.1	14.8-22.8	5.1-13.7	2.7-11.5	-3.1-6.1	2.0-10.7	-3.4-5.8
6.00	5.5-14.1	10.2-18.6	-3.8-5.5	41.4-47.4	-3.1-6.1	15.3-23.3	5.6-14.2	3.1-11.8	-3.3-6.0	2.0-10.8	-3.7-5.5
6.33	4.8-13.5	9.9-18.4	-4.1-5.2	40.1-46.3	-3.3-6.0	15.8-23.9	5.9-14.6	3.4-12.2	-3.5-5.8	2.1-11.0	-4.0-5.3
6.67	3.9-12.8	9.5-18.1	-4.4-5.0	38.9-45.1	-3.5-5.9	16.6-24.6	6.2-14.8	3.6-12.4	-3.7-5.8	2.3-11.2	-4.4-5.0
7.00	3.1-12.1	9.0-17.6	-4.7-4.7	37.6-44.0	-3.8-5.7	17.5-25.6	6.3-15.0	3.7-12.6	-3.8-5.7	2.5-11.5	-4.6-4.8
7.33	2.2-11.3	8.4-17.1	-5.0-4.6	36.4-42.9	-4.2-5.4	18.7-26.8	6.3-15.0	3.7-12.6	-3.9-5.7	2.9-11.8	-4.9-4.7
7.67	1.4-10.5	7.6-16.5	-5.2-4.4	35.2-41.9	-4.6-5.1	20.3-28.2	5.9-14.8	3.4-12.4	-3.9-5.8	3.3-12.3	-5.1-4.5
8.00	0.4-9.8	6.8-15.8	-5.5-4.2	34.0-40.8	-5.1-4.7	22.1-29.9	5.4-14.2	2.8-12.0	-4.0-5.8	3.8-12.8	-5.4-4.3
8.33	-0.4-9.0	6.1-15.1	-5.6-4.1	32.9-39.8	-5.5-4.4	24.3-32.0	4.4-13.4	2.0-11.3	-3.9-6.0	4.4-13.4	-5.5-4.2
8.67	-1.1-8.4	5.3-14.4	-5.8-4.0	31.7-38.8	-5.9-4.1	26.9-34.4	3.1-12.3	0.9-10.3	-3.7-6.1	5.0-14.1	-5.6-4.1
9.00	-1.7-7.9	4.5-13.7	-5.9-4.0	30.6-37.7	-6.2-3.8	29.8-37.1	1.6-11.0	-0.4-9.1	-3.5-6.4	5.8-14.8	-5.7-4.1
9.33	-2.1-7.6	3.8-13.2	-5.9-3.9	29.4-36.7	-3.6-6.1	32.9-40.0	0.1-9.6	-1.8-7.9	-3.2-6.7	6.6-15.6	-5.7-4.1
9.67	-2.4-7.4	3.3-12.6	-5.9-4.0	28.1-35.5	-3.9-5.8	36.0-42.9	-1.3-8.3	-3.0-6.8	-2.9-7.0	7.3-16.3	-5.7-4.2
10.00	-2.6-7.1	2.7-12.1	-5.8-4.1	26.9-34.4	-4.1-5.6	38.9-45.6	-2.5-7.2	-4.0-5.9	-2.4-7.4	8.0-16.9	-5.6-4.3

Table F.47: Control / Temp. at 8cm / Mid-day

i \ j	1	2	3	4	5	6	7	8	9	10	11
1	6.7-8.2	-1.1-1.6	-1.1-1.0	-2.3-3.8	-1.4-0.8	-1.1-1.8	-1.4-1.0	-1.0-1.4	-1.0-1.2	-0.9-1.5	-1.1-1.0
2	-1.1-1.6	7.7-9.6	-1.8-0.8	-3.7-2.7	-1.7-0.9	-1.5-2.0	-1.3-1.6	-1.7-1.1	-1.9-0.8	-1.4-1.4	-1.8-0.8
3	-1.1-1.0	-1.8-0.8	-0.1-0.1	-4.3-0.8	-0.1-0.1	-0.3-0.8	-0.0-0.3	-0.0-0.2	-0.1-0.2	-0.0-0.2	-0.1-0.2
4	-2.3-3.8	-3.7-2.7	-4.3-0.8	37.9-42.2	-1.1-0.5	-2.3-2.6	-0.8-2.1	-1.0-1.7	-1.1-0.8	-0.7-2.0	-0.8-0.5
5	-1.4-0.8	-1.7-0.9	-0.1-0.1	-1.1-0.5	1.2-1.9	-0.8-1.0	-0.9-0.5	-1.0-0.4	-1.1-0.2	-1.0-0.4	-1.1-0.2
6	-1.1-1.8	-1.5-2.0	-0.3-0.8	-2.3-2.6	-0.8-1.0	10.6-12.7	-1.6-1.4	-1.8-1.0	-2.5-0.4	-1.5-1.3	-3.0-0.1
7	-1.4-1.0	-1.3-1.6	-0.0-0.3	-0.8-2.1	-0.9-0.5	-1.6-1.4	2.7-4.0	-0.4-2.0	-0.7-1.6	-0.1-2.2	-0.6-1.6
8	-1.0-1.4	-1.7-1.1	-0.0-0.2	-1.0-1.7	-1.0-0.4	-1.8-1.0	-0.4-2.0	2.7-4.0	-0.9-1.3	-1.2-1.0	-1.0-1.2
9	-1.0-1.2	-1.9-0.8	-0.1-0.2	-1.1-0.8	-1.1-0.2	-2.5-0.4	-0.7-1.6	-0.9-1.3	-0.4-0.5	-0.4-1.3	-0.8-0.9
10	-0.9-1.5	-1.4-1.4	-0.0-0.2	-0.7-2.0	-1.0-0.4	-1.5-1.3	-0.1-2.2	-1.2-1.0	-0.4-1.3	2.0-3.1	-0.8-1.3
11	-1.1-1.0	-1.8-0.8	-0.1-0.2	-0.8-0.5	-1.1-0.2	-3.0-0.1	-0.6-1.6	-1.0-1.2	-0.8-0.9	-0.8-1.3	-0.1-0.1
Total	7.0-15.4	10.5-18.8	-5.3-3.9	45.9-51.4	-2.9-6.1	14.4-22.4	4.0-12.6	2.1-10.7	-2.7-6.4	2.1-10.7	-5.3-3.9
Higher	2.3	8.1	0.8	8.7	2.6	8.9	1.6	2.2	2.7	1.5	1.0

Table F.48: South / Temp. at 8cm with Time (Total-effect)

t \ i	1	2	3	4	5	6	7	8	9	10	11
0.33	2.0-14.9	0.8-13.6	-0.5-12.6	96.6-97.3	-0.5-12.6	0.8-13.7	-0.5-12.6	-0.5-12.6	-0.4-12.6	-0.4-12.7	-0.5-12.6
0.67	5.7-18.0	3.0-15.7	-0.5-12.5	89.7-91.4	-0.5-12.5	3.7-16.2	-0.5-12.5	-0.5-12.5	-0.4-12.6	0.1-13.0	-0.5-12.5
1.00	7.9-19.8	5.0-17.3	-0.8-12.2	82.5-85.2	-0.8-12.1	6.5-18.6	-0.7-12.2	-0.8-12.1	-0.6-12.3	0.5-13.2	-0.7-12.2
1.33	9.5-20.9	7.0-18.8	-1.2-11.6	75.5-79.0	-1.3-11.5	9.0-20.6	-1.1-11.7	-1.1-11.6	-0.9-11.8	0.5-13.1	-1.2-11.5
1.67	10.8-21.9	8.6-20.0	-1.6-10.9	68.7-73.0	-1.6-10.9	10.6-21.8	-1.1-11.3	-1.3-11.1	-1.3-11.2	0.9-13.0	-1.6-10.9
2.00	12.3-22.8	10.1-21.0	-1.9-10.2	62.3-67.2	-1.9-10.2	11.5-22.3	-0.6-11.3	-1.1-10.9	-1.6-10.5	0.9-12.7	-2.0-10.2
2.33	13.4-23.5	11.5-21.9	-2.4-9.4	56.3-61.8	-2.1-9.7	11.8-22.1	0.1-11.6	-0.6-11.0	-2.0-9.8	0.8-12.2	-2.4-9.4
2.67	14.0-23.9	12.7-22.7	-2.9-8.6	51.1-57.0	-2.3-9.2	11.3-21.5	1.0-12.1	0.1-11.3	-2.4-9.0	0.4-11.5	-2.9-8.6
3.00	14.4-24.0	13.6-23.3	-3.3-7.9	46.5-52.9	-2.3-8.8	10.7-20.7	2.1-12.7	0.9-11.7	-2.9-8.3	0.0-10.9	-3.3-7.8
3.33	14.6-23.9	14.6-24.0	-3.7-7.3	42.8-49.5	-2.2-8.7	10.0-19.8	3.2-13.6	1.6-12.2	-3.2-7.7	-0.3-10.3	-3.7-7.2
3.67	14.6-23.7	15.4-24.6	-4.1-6.7	39.8-46.6	-2.0-8.7	9.3-19.0	4.3-14.3	2.4-12.7	-3.5-7.2	-0.6-9.9	-4.1-6.7
4.00	14.3-23.3	16.2-25.1	-4.4-6.3	37.2-44.2	-1.7-8.8	8.7-18.4	5.2-15.1	3.1-13.1	-3.8-6.8	-0.8-9.5	-4.4-6.3
4.33	14.0-22.9	16.8-25.5	-4.7-5.9	35.1-42.3	-1.3-9.1	8.3-17.9	6.1-15.7	3.6-13.5	-4.2-6.4	-1.1-9.1	-4.8-5.9
4.67	13.5-22.5	17.1-25.8	-5.1-5.5	33.3-40.6	-1.0-9.3	7.9-17.5	6.8-16.3	4.0-13.9	-4.5-6.0	-1.3-8.8	-5.1-5.5
5.00	12.9-21.9	17.3-26.0	-5.5-5.1	31.6-39.1	-0.8-9.4	7.7-17.2	7.4-16.8	4.4-14.2	-4.8-5.7	-1.6-8.5	-5.5-5.1
5.33	12.3-21.3	17.4-26.1	-5.8-4.8	30.2-37.9	-0.5-9.6	7.5-17.1	7.9-17.2	4.8-14.5	-5.1-5.4	-1.9-8.4	-5.8-4.8
5.67	11.6-20.6	17.3-26.0	-6.1-4.5	29.0-36.8	-0.4-9.7	7.5-17.2	8.3-17.7	5.2-14.8	-5.4-5.2	-2.0-8.2	-6.2-4.6
6.00	10.7-19.9	17.1-25.9	-6.5-4.3	28.0-35.9	-0.4-9.8	7.7-17.4	8.7-18.2	5.4-15.2	-5.6-5.0	-2.1-8.1	-6.4-4.3
6.33	9.8-19.2	16.8-25.6	-6.7-4.0	27.1-35.1	-0.4-9.8	8.1-17.8	9.2-18.6	5.8-15.5	-5.9-4.8	-2.2-8.1	-6.7-4.1
6.67	9.0-18.4	16.4-25.3	-3.9-6.4	26.3-34.4	-0.5-9.7	8.6-18.3	9.6-19.1	6.1-15.9	-6.1-4.6	-2.2-8.2	-3.8-6.5
7.00	8.0-17.5	15.8-24.8	-4.2-6.2	25.6-33.8	-0.8-9.6	9.4-19.1	10.0-19.5	6.4-16.2	-6.3-4.5	-2.2-8.2	-4.1-6.3
7.33	6.8-16.6	15.0-24.1	-4.4-6.0	24.9-33.2	-1.0-9.3	10.4-20.0	10.3-19.8	6.7-16.5	-6.5-4.3	-2.2-8.4	-4.3-6.1
7.67	5.6-15.6	14.1-23.4	-4.7-5.9	24.3-32.7	-1.5-9.0	11.6-21.2	10.5-20.0	6.9-16.7	-6.8-4.2	-2.1-8.6	-4.6-6.0
8.00	4.4-14.5	13.0-22.5	-5.0-5.7	23.8-32.2	-1.9-8.7	13.1-22.7	10.3-19.8	6.8-16.7	-7.0-4.1	-1.9-8.8	-4.9-5.8
8.33	3.2-13.5	11.9-21.5	-5.3-5.6	23.3-31.9	-2.5-8.2	15.1-24.6	9.8-19.4	6.3-16.3	-4.1-6.7	-1.6-9.1	-5.1-5.8
8.67	1.9-12.5	10.6-20.6	-5.6-5.5	23.0-31.8	-3.2-7.8	17.8-27.1	8.7-18.5	5.4-15.6	-4.2-6.7	-1.2-9.6	-5.4-5.7
9.00	0.8-11.7	9.4-19.6	-5.8-5.5	22.9-31.7	-3.9-7.4	21.0-30.2	7.0-17.2	3.9-14.4	-4.4-6.8	-0.8-10.2	-5.6-5.7
9.33	-0.3-11.0	8.3-18.8	-5.9-5.5	22.7-31.8	-4.6-6.9	24.9-33.8	4.9-15.5	2.1-13.0	-4.5-6.9	-0.1-11.0	-5.8-5.7
9.67	-1.0-10.6	7.3-18.0	-6.1-5.6	22.5-31.8	-5.1-6.6	29.0-37.6	2.6-13.6	0.3-11.6	-4.4-7.1	0.6-11.8	-5.8-5.9
10.00	-1.5-10.2	6.2-17.2	-6.0-5.8	22.2-31.6	-5.6-6.4	33.0-41.3	0.7-12.0	-1.3-10.2	-7.8-4.4	1.4-12.7	-5.8-6.0

Table F.49: South / Temp. at 8cm / Mid-day

i \ j	1	2	3	4	5	6	7	8	9	10	11
1	12.8-15.0	-2.4-1.9	-1.0-1.1	-2.9-3.2	-1.6-0.8	-1.9-1.1	-1.3-1.6	-1.5-1.2	-1.0-1.3	-1.5-0.9	-1.0-1.1
2	-2.4-1.9	14.4-17.0	-1.4-1.3	-2.8-3.6	-1.2-1.5	-1.5-2.1	-1.3-2.0	-2.0-1.2	-1.4-1.3	-1.8-1.1	-1.4-1.3
3	-1.0-1.1	-1.4-1.3	-0.0-0.1	-3.4-0.7	-0.2-0.1	-0.2-0.5	-0.1-0.4	-0.1-0.4	-0.1-0.1	-0.1-0.2	-0.1-0.1
4	-2.9-3.2	-2.8-3.6	-3.4-0.7	27.6-31.4	-1.2-0.6	-1.4-2.0	-0.9-2.1	-0.8-1.8	-0.6-0.7	-0.7-1.2	-0.7-0.5
5	-1.6-0.8	-1.2-1.5	-0.2-0.1	-1.2-0.6	2.5-3.6	-1.3-0.7	-1.0-1.3	-1.2-1.0	-1.5-0.5	-1.4-0.6	-1.5-0.4
6	-1.9-1.1	-1.5-2.1	-0.2-0.5	-1.4-2.0	-1.3-0.7	6.7-8.6	-0.6-2.1	-0.9-1.8	-2.0-0.8	-1.6-1.2	-2.1-0.7
7	-1.3-1.6	-1.3-2.0	-0.1-0.4	-0.9-2.1	-1.0-1.3	-0.6-2.1	5.4-7.2	-0.2-2.9	-0.6-2.3	-0.0-2.8	-0.5-2.3
8	-1.5-1.2	-2.0-1.2	-0.1-0.4	-0.8-1.8	-1.2-1.0	-0.9-1.8	-0.2-2.9	4.8-6.4	-1.0-1.6	-1.5-1.1	-1.1-1.6
9	-1.0-1.3	-1.4-1.3	-0.1-0.1	-0.6-0.7	-1.5-0.5	-2.0-0.8	-0.6-2.3	-1.0-1.6	-0.3-0.2	-0.4-0.5	-0.5-0.4
10	-1.5-0.9	-1.8-1.1	-0.1-0.2	-0.7-1.2	-1.4-0.6	-1.6-1.2	-0.0-2.8	-1.5-1.1	-0.4-0.5	0.8-1.6	-0.4-1.2
11	-1.0-1.1	-1.4-1.3	-0.1-0.1	-0.7-0.5	-1.5-0.4	-2.1-0.7	-0.5-2.3	-1.1-1.6	-0.5-0.4	-0.4-1.2	-0.0-0.1
Total	12.9-21.9	17.3-26.0	-5.5-5.1	31.6-39.1	-0.8-9.4	7.7-17.2	7.4-16.8	4.4-14.2	-4.8-5.7	-1.6-8.5	-5.5-5.1
Higher	4.5	6.0	0.7	5.5	3.5	5.1	-0.8	1.6	0.3	1.4	-0.3

Table F.50: North / Temp. at 8cm with Time (Total-effect)

t \ i	1	2	3	4	5	6	7	8	9	10	11
0.33	0.2-12.4	-0.4-11.8	-0.8-11.5	98.8-99.2	-0.7-11.5	-0.1-12.0	-0.7-11.5	-0.7-11.5	-0.8-11.5	-0.7-11.5	-0.7-11.5
0.67	1.6-14.0	0.5-13.0	-0.8-11.8	96.2-97.2	-0.7-11.8	1.3-13.6	-0.8-11.8	-0.7-11.8	-0.7-11.8	-0.5-12.1	-0.8-11.8
1.00	2.7-15.3	1.4-14.0	-1.0-11.9	93.0-94.5	-1.0-11.9	3.1-15.5	-1.0-11.9	-1.0-11.9	-0.9-12.0	-0.4-12.5	-1.0-11.9
1.33	3.4-16.1	2.0-14.8	-1.1-11.9	89.4-91.5	-1.2-11.9	4.9-17.4	-1.1-12.0	-1.2-11.9	-1.1-12.0	-0.0-12.9	-1.2-11.9
1.67	4.0-16.6	2.5-15.4	-1.5-11.7	85.6-88.2	-1.5-11.7	6.8-19.2	-1.4-11.8	-1.5-11.8	-1.3-11.9	0.1-13.3	-1.5-11.8
2.00	4.6-17.1	3.1-16.0	-1.8-11.5	81.6-84.7	-1.9-11.5	8.6-20.8	-1.7-11.7	-1.8-11.6	-1.6-11.7	0.5-13.6	-1.8-11.5
2.33	5.2-17.6	3.7-16.4	-2.2-11.2	77.3-81.0	-2.2-11.2	10.2-22.2	-1.7-11.6	-1.8-11.5	-1.9-11.4	0.8-13.8	-2.1-11.2
2.67	5.8-18.1	4.2-16.8	-2.3-10.9	73.0-77.1	-2.3-10.9	11.6-23.2	-1.6-11.6	-1.6-11.5	-2.0-11.1	1.0-13.8	-2.3-10.9
3.00	6.6-18.6	4.8-17.1	-2.6-10.5	68.6-73.2	-2.5-10.5	12.6-24.0	-1.2-11.7	-1.2-11.7	-2.3-10.7	1.3-13.8	-2.5-10.5
3.33	7.4-19.1	5.2-17.2	-2.8-10.0	64.3-69.3	-2.6-10.2	13.3-24.4	-0.7-11.9	-0.5-12.0	-2.5-10.3	1.4-13.7	-2.8-10.0
3.67	8.1-19.4	5.7-17.4	-3.0-9.6	60.2-65.6	-2.7-9.8	13.8-24.6	0.1-12.3	0.4-12.6	-2.7-9.8	1.5-13.6	-2.9-9.6
4.00	8.5-19.6	6.1-17.5	-3.1-9.1	56.3-62.1	-2.6-9.5	14.2-24.7	0.9-12.7	1.5-13.2	-2.8-9.4	1.6-13.4	-3.1-9.1
4.33	8.9-19.6	6.3-17.5	-3.3-8.7	52.8-58.8	-2.7-9.2	14.4-24.6	1.6-13.1	2.6-13.9	-3.0-9.0	1.7-13.2	-3.3-8.7
4.67	9.0-19.5	6.4-17.4	-3.5-8.2	49.6-55.9	-2.8-8.9	14.5-24.5	2.3-13.5	3.6-14.6	-3.2-8.5	1.7-12.9	-3.5-8.2
5.00	8.9-19.2	6.5-17.2	-3.9-7.8	46.8-53.3	-2.9-8.6	14.7-24.4	3.0-13.9	4.6-15.3	-3.5-8.1	1.6-12.6	-3.9-7.8
5.33	8.4-18.7	6.4-17.0	-4.1-7.4	44.3-51.0	-3.0-8.4	14.8-24.4	3.6-14.3	5.5-15.9	-3.7-7.7	1.6-12.4	-4.1-7.4
5.67	7.9-18.2	6.3-16.7	-4.4-7.0	42.2-49.0	-3.0-8.2	15.0-24.5	4.1-14.6	6.3-16.5	-4.0-7.3	1.6-12.3	-4.3-7.0
6.00	7.3-17.5	6.0-16.4	-4.7-6.6	40.3-47.4	-3.1-7.9	15.4-24.7	4.5-14.9	7.0-17.0	-4.3-7.0	1.6-12.2	-4.6-6.7
6.33	6.6-16.8	5.8-16.1	-4.8-6.4	38.8-45.9	-3.3-7.8	15.9-25.2	4.8-15.1	7.4-17.5	-4.5-6.7	1.6-12.2	-4.8-6.4
6.67	5.7-16.0	5.4-15.8	-5.1-6.1	37.5-44.8	-3.4-7.6	16.6-25.8	5.0-15.2	7.8-17.7	-4.7-6.5	1.7-12.3	-5.1-6.2
7.00	4.8-15.2	5.1-15.5	-5.4-5.9	36.4-43.8	-3.6-7.5	17.6-26.7	4.9-15.3	7.9-17.9	-4.8-6.4	1.8-12.4	-5.3-6.0
7.33	3.9-14.4	4.7-15.2	-5.5-5.8	35.7-43.1	-3.8-7.3	18.8-27.8	4.8-15.2	7.6-17.8	-5.0-6.3	2.0-12.6	-5.5-5.9
7.67	2.9-13.6	4.3-14.9	-5.8-5.7	35.0-42.6	-4.0-7.3	20.2-29.2	4.4-15.0	7.2-17.5	-5.2-6.2	2.2-12.9	-5.7-5.8
8.00	1.9-12.9	3.9-14.6	-5.9-5.7	34.6-42.3	-4.2-7.2	21.8-30.8	3.8-14.5	6.5-16.9	-5.4-6.2	2.5-13.3	-5.9-5.7
8.33	1.0-12.2	3.5-14.5	-6.1-5.7	34.3-42.1	-4.5-7.2	23.7-32.6	3.1-14.0	5.5-16.2	-5.5-6.2	2.9-13.8	-6.0-5.8
8.67	0.2-11.7	3.0-14.3	-6.3-5.7	34.1-42.1	-4.8-7.1	25.6-34.6	2.2-13.3	4.3-15.3	-5.6-6.3	3.2-14.3	-6.1-5.8
9.00	-0.5-11.3	2.7-14.2	-6.5-5.8	33.8-42.0	-5.0-7.1	27.8-36.7	1.1-12.5	3.0-14.4	-5.7-6.5	3.7-14.9	-6.3-5.9
9.33	-1.0-11.1	2.2-14.1	-6.5-5.9	33.7-42.0	-5.3-7.2	30.0-38.8	0.0-11.8	1.7-13.4	-5.8-6.6	4.1-15.4	-6.3-6.1
9.67	-1.5-10.9	1.9-14.1	-6.7-6.1	33.4-41.9	-5.6-7.2	32.1-40.8	-1.1-11.1	0.4-12.6	-5.9-6.8	4.5-16.0	-6.5-6.2
10.00	-1.8-10.7	1.5-14.0	-6.7-6.2	33.0-41.7	-5.7-7.2	34.1-42.7	-2.1-10.4	-0.7-11.8	-5.9-7.0	4.9-16.5	-6.6-6.3

Table F.51: North / Temp. at 8cm / Mid-day

i \ j	1	2	3	4	5	6	7	8	9	10	11
1	8.0-10.3	-2.5-1.1	-2.7-0.8	-7.8-2.0	-3.0-0.6	-1.9-2.4	-2.3-1.4	-2.4-1.3	-2.8-0.7	-2.6-1.0	-2.7-0.7
2	-2.5-1.1	3.8-5.9	-2.2-1.5	-6.2-3.1	-2.1-1.5	-0.7-3.5	-1.9-1.8	-2.2-1.5	-2.3-1.4	-1.9-1.8	-2.2-1.5
3	-2.7-0.8	-2.2-1.5	-0.1-0.1	-7.7-0.4	-0.1-0.2	-0.6-1.0	-0.2-0.3	-0.2-0.4	-0.1-0.3	-0.1-0.3	-0.1-0.2
4	-7.8-2.0	-6.2-3.1	-7.7-0.4	42.4-48.7	-1.4-0.6	-3.2-3.2	-1.9-1.4	-1.5-2.4	-0.7-1.2	-1.5-1.9	-0.7-1.0
5	-3.0-0.6	-2.1-1.5	-0.1-0.2	-1.4-0.6	0.4-1.1	-0.8-1.3	-0.9-0.7	-0.9-0.7	-1.0-0.5	-0.9-0.6	-1.0-0.5
6	-1.9-2.4	-0.7-3.5	-0.6-1.0	-3.2-3.2	-0.8-1.3	14.0-16.7	-2.0-1.3	-2.0-1.3	-1.4-1.8	-2.2-1.2	-1.5-1.7
7	-2.3-1.4	-1.9-1.8	-0.2-0.3	-1.9-1.4	-0.9-0.7	-2.0-1.3	3.6-5.2	-1.6-1.6	-1.8-1.1	-1.7-1.1	-1.8-1.1
8	-2.4-1.3	-2.2-1.5	-0.2-0.4	-1.5-2.4	-0.9-0.7	-2.0-1.3	-1.6-1.6	6.1-8.0	-2.9-0.3	-2.8-0.4	-2.9-0.3
9	-2.8-0.7	-2.3-1.4	-0.1-0.3	-0.7-1.2	-1.0-0.5	-1.4-1.8	-1.8-1.1	-2.9-0.3	-0.3-0.3	-0.7-0.4	-0.6-0.5
10	-2.6-1.0	-1.9-1.8	-0.1-0.3	-1.5-1.9	-0.9-0.6	-2.2-1.2	-1.7-1.1	-2.8-0.4	-0.7-0.4	3.6-4.9	-0.8-1.4
11	-2.7-0.7	-2.2-1.5	-0.1-0.2	-0.7-1.0	-1.0-0.5	-1.5-1.7	-1.8-1.1	-2.9-0.3	-0.6-0.5	-0.8-1.4	-0.0-0.2
Total	8.9-19.2	6.5-17.2	-3.9-7.8	46.8-53.3	-2.9-8.6	14.7-24.4	3.0-13.9	4.6-15.3	-3.5-8.1	1.6-12.6	-3.9-7.8
Higher	14.2	9.7	6.3	12.2	4.6	2.8	6.3	7.6	5.4	5.5	4.6

Table F.52: Control / Temp. at 8cm / Mean

i \ j	1	2	3	4	5	6	7	8	9	10	11
1	3.8-5.0	-1.3-1.0	-1.2-0.9	-6.1-3.1	-1.4-0.7	-1.4-1.4	-1.1-1.2	-1.2-1.0	-1.2-1.0	-1.0-1.3	-1.2-0.9
2	-1.3-1.0	4.0-5.6	-1.5-1.1	-5.7-3.5	-1.5-1.2	-0.8-2.4	-1.3-1.4	-1.6-1.1	-1.7-1.0	-1.2-1.6	-1.6-1.1
3	-1.2-0.9	-1.5-1.1	-0.1-0.0	-7.5-0.9	-0.1-0.1	-0.3-0.9	-0.0-0.2	-0.1-0.2	-0.1-0.1	-0.1-0.2	-0.1-0.1
4	-6.1-3.1	-5.7-3.5	-7.5-0.9	54.2-60.3	-1.3-0.3	-2.7-3.8	-0.8-2.3	-1.2-1.7	-1.1-1.1	-0.8-2.7	-0.6-0.4
5	-1.4-0.7	-1.5-1.2	-0.1-0.1	-1.3-0.3	0.5-0.9	-0.8-0.7	-0.6-0.5	-0.6-0.4	-0.6-0.3	-0.5-0.4	-0.6-0.3
6	-1.4-1.4	-0.8-2.4	-0.3-0.9	-2.7-3.8	-0.8-0.7	11.0-13.3	-1.4-1.7	-1.7-1.4	-2.4-0.9	-1.5-1.6	-2.8-0.4
7	-1.1-1.2	-1.3-1.4	-0.0-0.2	-0.8-2.3	-0.6-0.5	-1.4-1.7	1.2-2.1	-0.4-1.4	-0.5-1.2	-0.2-1.5	-0.5-1.3
8	-1.2-1.0	-1.6-1.1	-0.1-0.2	-1.2-1.7	-0.6-0.4	-1.7-1.4	-0.4-1.4	1.4-2.3	-0.7-1.0	-1.0-0.6	-0.7-0.9
9	-1.2-1.0	-1.7-1.0	-0.1-0.1	-1.1-1.1	-0.6-0.3	-2.4-0.9	-0.5-1.2	-0.7-1.0	-0.5-0.5	-0.4-1.4	-0.8-1.1
10	-1.0-1.3	-1.2-1.6	-0.1-0.2	-0.8-2.7	-0.5-0.4	-1.5-1.6	-0.2-1.5	-1.0-0.6	-0.4-1.4	2.2-3.4	-1.1-1.2
11	-1.2-0.9	-1.6-1.1	-0.1-0.1	-0.6-0.4	-0.6-0.3	-2.8-0.4	-0.5-1.3	-0.7-0.9	-0.8-1.1	-1.1-1.2	-0.1-0.1
Total	2.9-12.1	5.2-14.2	-4.9-4.8	60.8-65.1	-3.9-5.8	13.4-21.8	-0.2-9.2	-1.2-8.2	-2.5-7.0	1.6-10.9	-4.9-4.9
Higher	5.5	6.2	3.2	9.7	1.8	5.8	-0.2	1.3	2.5	1.0	1.2

Table F.53: South / Temp. at 8cm / Mean

i \ j	1	2	3	4	5	6	7	8	9	10	11
1	8.7-10.6	-1.5-1.8	-1.3-1.0	-8.0-2.8	-1.7-0.7	-1.7-1.6	-1.6-1.1	-1.1-1.5	-1.3-1.1	-1.1-1.4	-1.3-1.0
2	-1.5-1.8	8.7-11.0	-1.2-1.8	-7.7-3.1	-1.9-1.1	-0.8-3.1	-1.5-1.8	-2.0-1.2	-1.2-1.8	-1.6-1.5	-1.2-1.8
3	-1.3-1.0	-1.2-1.8	-0.0-0.1	-8.1-0.9	-0.1-0.1	-0.3-0.7	-0.1-0.3	-0.1-0.3	-0.1-0.1	-0.1-0.2	-0.1-0.1
4	-8.0-2.8	-7.7-3.1	-8.1-0.9	45.1-52.0	-1.8-0.3	-2.9-2.9	-1.2-2.7	-1.1-2.3	-0.5-0.9	-0.7-2.0	-0.7-0.4
5	-1.7-0.7	-1.9-1.1	-0.1-0.1	-1.8-0.3	1.1-2.0	-0.7-1.1	-0.7-1.1	-0.8-0.9	-1.0-0.6	-0.9-0.8	-1.0-0.6
6	-1.7-1.6	-0.8-3.1	-0.3-0.7	-2.9-2.9	-0.7-1.1	8.6-11.1	-1.5-1.9	-1.8-1.6	-2.1-1.4	-1.6-1.8	-2.2-1.3
7	-1.6-1.1	-1.5-1.8	-0.1-0.3	-1.2-2.7	-0.7-1.1	-1.5-1.9	3.1-4.5	-0.3-2.4	-0.4-2.0	-0.1-2.3	-0.4-2.0
8	-1.1-1.5	-2.0-1.2	-0.1-0.3	-1.1-2.3	-0.8-0.9	-1.8-1.6	-0.3-2.4	2.9-4.2	-0.9-1.3	-1.4-0.9	-0.9-1.3
9	-1.3-1.1	-1.2-1.8	-0.1-0.1	-0.5-0.9	-1.0-0.6	-2.1-1.4	-0.4-2.0	-0.9-1.3	-0.3-0.2	-0.4-0.6	-0.6-0.4
10	-1.1-1.4	-1.6-1.5	-0.1-0.2	-0.7-2.0	-0.9-0.8	-1.6-1.8	-0.1-2.3	-1.4-0.9	-0.4-0.6	1.3-2.3	-0.9-1.1
11	-1.3-1.0	-1.2-1.8	-0.1-0.1	-0.7-0.4	-1.0-0.6	-2.2-1.3	-0.4-2.0	-0.9-1.3	-0.6-0.4	-0.9-1.1	-0.0-0.1
Total	7.2-18.3	10.0-20.9	-5.4-7.1	49.5-56.0	-3.0-9.2	9.2-20.2	2.5-14.0	0.6-12.5	-4.8-7.6	-1.5-10.6	-5.4-7.1
Higher	6.5	6.3	3.8	11.4	3.2	4.0	-0.4	1.3	0.5	0.8	0.4

Table F.54: North / Temp. at 8cm / Mean

i \ j	1	2	3	4	5	6	7	8	9	10	11
1	3.5-5.4	-2.4-0.9	-2.6-0.7	-13.3-2.1	-2.7-0.6	-1.4-2.6	-2.4-1.0	-2.5-0.8	-2.6-0.7	-2.4-0.9	-2.6-0.7
2	-2.4-0.9	0.9-2.9	-1.9-1.8	-11.9-3.0	-1.8-1.9	-0.3-3.8	-1.8-1.9	-1.9-1.7	-1.9-1.8	-1.5-2.1	-1.9-1.8
3	-2.6-0.7	-1.9-1.8	-0.1-0.1	-13.5-0.8	-0.2-0.1	-0.6-1.1	-0.2-0.2	-0.2-0.2	-0.2-0.1	-0.2-0.2	-0.2-0.1
4	-13.3-2.1	-11.9-3.0	-13.5-0.8	58.8-68.6	-1.6-0.2	-3.7-5.1	-2.2-1.5	-1.6-2.6	-0.7-1.0	-2.2-2.3	-0.6-0.8
5	-2.7-0.6	-1.8-1.9	-0.2-0.1	-1.6-0.2	0.1-0.7	-1.0-0.9	-0.7-0.6	-0.7-0.6	-0.7-0.5	-0.6-0.6	-0.7-0.5
6	-1.4-2.6	-0.3-3.8	-0.6-1.1	-3.7-5.1	-1.0-0.9	12.6-15.6	-2.0-1.4	-2.0-1.5	-1.3-2.3	-2.1-1.4	-1.3-2.2
7	-2.4-1.0	-1.8-1.9	-0.2-0.2	-2.2-1.5	-0.7-0.6	-2.0-1.4	1.9-3.1	-1.3-1.1	-0.8-1.4	-0.8-1.4	-0.8-1.4
8	-2.5-0.8	-1.9-1.7	-0.2-0.2	-1.6-2.6	-0.7-0.6	-2.0-1.5	-1.3-1.1	3.4-4.8	-2.1-0.2	-2.1-0.2	-2.1-0.2
9	-2.6-0.7	-1.9-1.8	-0.2-0.1	-0.7-1.0	-0.7-0.5	-1.3-2.3	-0.8-1.4	-2.1-0.2	-0.3-0.3	-0.7-0.5	-0.5-0.6
10	-2.4-0.9	-1.5-2.1	-0.2-0.2	-2.2-2.3	-0.6-0.6	-2.1-1.4	-0.8-1.4	-2.1-0.2	-0.7-0.5	3.2-4.5	-1.4-0.9
11	-2.6-0.7	-1.9-1.8	-0.2-0.1	-0.6-0.8	-0.7-0.5	-1.3-2.2	-0.8-1.4	-2.1-0.2	-0.5-0.6	-1.4-0.9	-0.0-0.2
Total	3.2-15.4	2.7-15.1	-3.8-9.3	63.3-68.4	-3.4-9.7	13.5-24.5	-0.1-12.5	0.5-13.1	-3.5-9.5	1.1-13.5	-3.8-9.3
Higher	16.8	10.3	9.9	18.0	4.8	1.7	4.3	6.3	4.2	5.3	4.1

Table F.55: Control / Temp. at 8cm / Maximum

i \ j	1	2	3	4	5	6	7	8	9	10	11
1	4.8-5.9	-0.8-1.1	-0.6-0.9	-2.6-3.3	-0.8-0.8	-1.1-1.5	-0.8-1.2	-1.0-1.0	-0.6-1.0	-0.9-1.0	-0.6-1.0
2	-0.8-1.1	5.6-7.3	-1.6-0.9	-2.7-3.4	-1.2-1.2	-1.2-2.2	-1.0-1.7	-1.5-1.2	-1.6-0.9	-1.2-1.4	-1.6-0.9
3	-0.6-0.9	-1.6-0.9	-0.0-0.1	-4.1-0.9	-0.1-0.1	-0.1-1.0	-0.0-0.3	-0.1-0.2	-0.1-0.1	-0.1-0.2	-0.1-0.1
4	-2.6-3.3	-2.7-3.4	-4.1-0.9	36.2-40.5	-0.6-0.8	0.3-5.7	0.6-3.8	-0.1-2.8	-1.0-0.8	0.2-3.0	-0.4-0.4
5	-0.8-0.8	-1.2-1.2	-0.1-0.1	-0.6-0.8	1.3-2.0	-0.9-0.9	-0.6-0.9	-0.8-0.7	-0.9-0.4	-0.7-0.6	-0.9-0.4
6	-1.1-1.5	-1.2-2.2	-0.1-1.0	0.3-5.7	-0.9-0.9	9.6-11.7	-0.2-2.5	-0.7-2.0	-2.2-0.6	-1.1-1.6	-2.5-0.1
7	-0.8-1.2	-1.0-1.7	-0.0-0.3	0.6-3.8	-0.6-0.9	-0.2-2.5	3.1-4.5	0.0-2.7	-0.3-2.1	0.4-2.8	-0.2-2.1
8	-1.0-1.0	-1.5-1.2	-0.1-0.2	-0.1-2.8	-0.8-0.7	-0.7-2.0	0.0-2.7	3.3-4.6	-1.4-0.9	-1.1-1.1	-0.8-1.4
9	-0.6-1.0	-1.6-0.9	-0.1-0.1	-1.0-0.8	-0.9-0.4	-2.2-0.6	-0.3-2.1	-1.4-0.9	-0.2-0.7	-0.6-1.2	-1.1-0.8
10	-0.9-1.0	-1.2-1.4	-0.1-0.2	0.2-3.0	-0.7-0.6	-1.1-1.6	0.4-2.8	-1.1-1.1	-0.6-1.2	1.8-2.9	-0.6-1.4
11	-0.6-1.0	-1.6-0.9	-0.1-0.1	-0.4-0.4	-0.9-0.4	-2.5-0.1	-0.2-2.1	-0.8-1.4	-1.1-0.8	-0.6-1.4	-0.1-0.1
Total	1.9-11.0	5.6-14.8	-4.5-4.8	47.5-53.2	-4.1-5.6	16.4-24.8	5.7-14.8	2.9-12.2	-3.8-6.0	1.9-11.1	-4.3-4.9
Higher	-0.4	3.5	1.2	4.9	-0.6	5.7	-2.5	0.3	1.4	-0.1	0.4

Table F.56: South / Temp. at 8cm / Maximum

i \ j	1	2	3	4	5	6	7	8	9	10	11
1	8.8-10.3	-0.7-2.1	-1.1-0.8	-1.7-2.9	-0.9-1.1	-1.2-1.7	-0.7-2.2	-0.7-1.9	-1.0-1.0	-0.9-1.3	-1.1-0.8
2	-0.7-2.1	9.6-11.8	-1.2-1.5	-1.8-3.1	-1.2-1.4	-1.1-2.5	-0.9-2.5	-1.6-1.6	-1.2-1.6	-1.5-1.4	-1.2-1.5
3	-1.1-0.8	-1.2-1.5	-0.0-0.1	-2.6-0.7	-0.2-0.1	-0.2-0.7	-0.1-0.8	-0.0-0.6	-0.1-0.1	-0.1-0.2	-0.1-0.1
4	-1.7-2.9	-1.8-3.1	-2.6-0.7	23.4-26.7	-1.1-0.7	-2.0-1.8	-0.5-3.0	-0.5-2.7	-0.7-0.7	-0.5-1.5	-0.8-0.4
5	-0.9-1.1	-1.2-1.4	-0.2-0.1	-1.1-0.7	2.8-3.9	-0.8-1.4	-1.1-1.3	-1.3-1.0	-1.2-0.7	-1.0-0.9	-1.2-0.7
6	-1.2-1.7	-1.1-2.5	-0.2-0.7	-2.0-1.8	-0.8-1.4	8.2-10.3	1.1-4.2	0.3-3.3	-2.1-0.9	-1.5-1.4	-2.2-0.7
7	-0.7-2.2	-0.9-2.5	-0.1-0.8	-0.5-3.0	-1.1-1.3	1.1-4.2	7.8-9.8	0.9-4.3	-0.0-2.9	1.0-3.9	0.0-2.9
8	-0.7-1.9	-1.6-1.6	-0.0-0.6	-0.5-2.7	-1.3-1.0	0.3-3.3	0.9-4.3	6.6-8.4	-1.2-1.6	-0.7-2.0	-1.2-1.5
9	-1.0-1.0	-1.2-1.6	-0.1-0.1	-0.7-0.7	-1.2-0.7	-2.1-0.9	-0.0-2.9	-1.2-1.6	-0.3-0.3	-0.3-0.7	-0.5-0.5
10	-0.9-1.3	-1.5-1.4	-0.1-0.2	-0.5-1.5	-1.0-0.9	-1.5-1.4	1.0-3.9	-0.7-2.0	-0.3-0.7	1.0-1.9	-0.2-1.5
11	-1.1-0.8	-1.2-1.5	-0.1-0.1	-0.8-0.4	-1.2-0.7	-2.2-0.7	0.0-2.9	-1.2-1.5	-0.5-0.5	-0.2-1.5	-0.1-0.1
Total	5.6-15.6	10.1-19.9	-4.8-5.5	26.1-34.3	-2.3-8.4	11.2-20.8	11.5-21.0	7.2-17.1	-7.1-4.0	-2.2-8.3	-4.7-5.6
Higher	-1.9	0.8	0.3	2.5	0.0	2.3	-6.4	-2.6	-2.7	-3.0	-0.8

Table F.57: North / Temp. at 8cm / Maximum

i \ j	1	2	3	4	5	6	7	8	9	10	11
1	5.6-7.3	-1.7-1.1	-2.0-0.6	-6.4-1.2	-2.2-0.5	-2.4-1.4	-1.6-1.3	-2.0-1.1	-2.1-0.5	-2.1-0.7	-2.1-0.6
2	-1.7-1.1	1.6-3.3	-1.2-1.9	-5.5-1.6	-1.7-1.4	-0.7-3.1	-1.7-1.4	-1.3-1.9	-1.2-1.9	-1.9-1.3	-1.2-1.9
3	-2.0-0.6	-1.2-1.9	-0.1-0.1	-6.3-0.2	-0.2-0.1	-0.5-1.3	-0.2-0.3	-0.4-0.4	-0.1-0.1	-0.2-0.2	-0.1-0.1
4	-6.4-1.2	-5.5-1.6	-6.3-0.2	38.6-43.8	-0.9-0.9	-1.5-4.9	-1.0-2.4	-1.8-2.3	-0.9-0.7	-0.8-2.3	-0.7-0.7
5	-2.2-0.5	-1.7-1.4	-0.2-0.1	-0.9-0.9	0.5-1.3	-1.1-1.3	-0.7-1.1	-0.8-1.1	-0.9-0.7	-0.7-0.8	-0.9-0.8
6	-2.4-1.4	-0.7-3.1	-0.5-1.3	-1.5-4.9	-1.1-1.3	15.5-18.1	-0.9-2.0	-1.2-2.1	-1.5-1.2	-1.3-1.6	-1.5-1.1
7	-1.6-1.3	-1.7-1.4	-0.2-0.3	-1.0-2.4	-0.7-1.1	-0.9-2.0	5.4-7.2	-1.2-2.3	-1.7-1.3	-1.6-1.3	-1.7-1.3
8	-2.0-1.1	-1.3-1.9	-0.4-0.4	-1.8-2.3	-0.8-1.1	-1.2-2.1	-1.2-2.3	8.8-10.9	-2.9-0.3	-2.9-0.3	-2.8-0.3
9	-2.1-0.5	-1.2-1.9	-0.1-0.1	-0.9-0.7	-0.9-0.7	-1.5-1.2	-1.7-1.3	-2.9-0.3	-0.3-0.3	-0.7-0.5	-0.5-0.6
10	-2.1-0.7	-1.9-1.3	-0.2-0.2	-0.8-2.3	-0.7-0.8	-1.3-1.6	-1.6-1.3	-2.9-0.3	-0.7-0.5	4.2-5.4	-1.0-0.9
11	-2.1-0.6	-1.2-1.9	-0.1-0.1	-0.7-0.7	-0.9-0.8	-1.5-1.1	-1.7-1.3	-2.8-0.3	-0.5-0.6	-1.0-0.9	-0.0-0.2
Total	4.1-14.2	2.3-12.6	-4.6-6.3	43.3-49.8	-3.0-7.7	18.1-26.9	5.8-15.7	8.1-17.9	-4.1-6.7	2.0-12.2	-4.6-6.3
Higher	10.6	5.3	3.8	9.8	2.1	2.0	3.3	5.8	3.7	4.0	2.9

Table F.58: Control / Temp. at 8cm / Minimum

i \ j	1	2	3	4	5	6	7	8	9	10	11
1	-0.2-0.3	-0.6-0.5	-0.6-0.5	-15.4-2.8	-0.6-0.5	-0.5-0.5	-0.6-0.5	-0.5-0.5	-0.6-0.5	-0.5-0.5	-0.6-0.5
2	-0.6-0.5	-0.3-0.2	-0.6-0.4	-15.3-2.9	-0.6-0.4	-0.5-0.5	-0.6-0.4	-0.6-0.4	-0.6-0.4	-0.6-0.5	-0.6-0.4
3	-0.6-0.5	-0.6-0.4	-0.0-0.0	-15.3-2.9	-0.1-0.1	-0.1-0.1	-0.1-0.1	-0.1-0.1	-0.1-0.1	-0.1-0.1	-0.1-0.1
4	-15.4-2.8	-15.3-2.9	-15.3-2.9	93.8-103.7	-0.1-0.1	-1.7-1.8	-0.7-0.5	-0.3-0.7	-0.5-0.9	-0.7-1.4	-0.1-0.1
5	-0.6-0.5	-0.6-0.4	-0.1-0.1	-0.1-0.1	-0.0-0.0	-0.1-0.1	-0.1-0.1	-0.1-0.1	-0.1-0.1	-0.1-0.1	-0.1-0.1
6	-0.5-0.5	-0.5-0.5	-0.1-0.1	-1.7-1.8	-0.1-0.1	0.6-2.0	-2.1-0.7	-2.2-0.6	-2.1-0.7	-2.0-0.8	-2.2-0.6
7	-0.6-0.5	-0.6-0.4	-0.1-0.1	-0.7-0.5	-0.1-0.1	-2.1-0.7	-0.2-0.2	-0.4-0.5	-0.4-0.5	-0.3-0.5	-0.4-0.5
8	-0.5-0.5	-0.6-0.4	-0.1-0.1	-0.3-0.7	-0.1-0.1	-2.2-0.6	-0.4-0.5	-0.2-0.2	-0.4-0.4	-0.4-0.4	-0.4-0.4
9	-0.6-0.5	-0.6-0.4	-0.1-0.1	-0.5-0.9	-0.1-0.1	-2.1-0.7	-0.4-0.5	-0.4-0.4	-0.4-0.2	-0.3-0.8	-0.3-0.7
10	-0.5-0.5	-0.6-0.5	-0.1-0.1	-0.7-1.4	-0.1-0.1	-2.0-0.8	-0.3-0.5	-0.4-0.4	-0.3-0.8	-0.3-0.6	-0.6-1.2
11	-0.6-0.5	-0.6-0.4	-0.1-0.1	-0.1-0.1	-0.1-0.1	-2.2-0.6	-0.4-0.5	-0.4-0.4	-0.3-0.7	-0.6-1.2	-0.1-0.0
Total	-1.6-7.6	-1.7-7.5	-2.0-7.1	96.6-98.1	-2.1-7.1	1.0-10.0	-1.8-7.4	-1.8-7.4	-1.5-7.7	-0.6-8.5	-2.1-7.1
Higher	9.5	9.9	9.0	16.6	2.7	7.7	3.4	3.4	3.3	3.5	3.0

Table F.59: South / Temp. at 8cm / Minimum

i \ j	1	2	3	4	5	6	7	8	9	10	11
1	-0.2-0.2	-0.4-0.5	-0.4-0.5	-27.9-2.3	-0.4-0.5	-0.4-0.5	-0.4-0.5	-0.4-0.5	-0.4-0.5	-0.4-0.5	-0.4-0.5
2	-0.4-0.5	-0.2-0.2	-0.5-0.3	-27.9-2.4	-0.5-0.3	-0.4-0.3	-0.5-0.3	-0.5-0.3	-0.5-0.3	-0.5-0.3	-0.5-0.3
3	-0.4-0.5	-0.5-0.3	-0.0-0.0	-28.0-2.4	-0.0-0.0	-0.0-0.0	-0.0-0.0	-0.0-0.0	-0.0-0.0	-0.0-0.0	-0.0-0.0
4	-27.9-2.3	-27.9-2.4	-28.0-2.4	97.8-115.0	-0.2-0.1	-0.9-1.7	-0.6-0.4	-0.5-0.4	-0.2-0.4	-0.7-0.9	-0.2-0.1
5	-0.4-0.5	-0.5-0.3	-0.0-0.0	-0.2-0.1	-0.0-0.0	-0.0-0.1	-0.0-0.1	-0.0-0.1	-0.0-0.1	-0.0-0.1	-0.0-0.1
6	-0.4-0.5	-0.4-0.3	-0.0-0.0	-0.9-1.7	-0.0-0.1	-0.5-0.5	-1.3-0.8	-1.3-0.8	-1.3-0.7	-1.2-0.8	-1.3-0.8
7	-0.4-0.5	-0.5-0.3	-0.0-0.0	-0.6-0.4	-0.0-0.1	-1.3-0.8	-0.2-0.1	-0.3-0.4	-0.3-0.4	-0.3-0.4	-0.3-0.4
8	-0.4-0.5	-0.5-0.3	-0.0-0.0	-0.5-0.4	-0.0-0.1	-1.3-0.8	-0.3-0.4	-0.1-0.2	-0.3-0.2	-0.3-0.2	-0.3-0.2
9	-0.4-0.5	-0.5-0.3	-0.0-0.0	-0.2-0.4	-0.0-0.1	-1.3-0.8	-0.3-0.4	-0.3-0.2	-0.2-0.1	-0.1-0.2	-0.1-0.3
10	-0.4-0.5	-0.5-0.3	-0.0-0.0	-0.7-0.9	-0.0-0.1	-1.2-0.8	-0.3-0.4	-0.3-0.2	-0.1-0.3	-0.4-0.2	-0.3-0.9
11	-0.4-0.5	-0.5-0.3	-0.0-0.0	-0.2-0.1	-0.0-0.1	-1.3-0.8	-0.3-0.4	-0.3-0.2	-0.1-0.3	-0.3-0.9	-0.0-0.1
Total	-0.9-12.4	-1.0-12.3	-1.1-12.2	99.0-99.9	-1.1-12.2	-0.2-13.1	-1.0-12.3	-1.0-12.3	-1.0-12.3	-0.6-12.6	-1.1-12.2
Higher	18.2	18.9	18.4	31.0	5.5	7.3	5.7	6.0	5.7	5.8	5.4

Table F.60: North / Temp. at 8cm / Minimum

i \ j	1	2	3	4	5	6	7	8	9	10	11
1	-0.3-0.4	-0.6-0.8	-0.6-0.8	-26.3-2.3	-0.6-0.8	-0.5-0.8	-0.6-0.8	-0.6-0.8	-0.6-0.8	-0.6-0.8	-0.6-0.8
2	-0.6-0.8	-0.4-0.3	-0.5-0.9	-26.1-2.4	-0.5-0.9	-0.4-1.0	-0.5-0.9	-0.5-0.9	-0.5-0.9	-0.5-1.0	-0.5-0.9
3	-0.6-0.8	-0.5-0.9	-0.1-0.0	-26.4-2.0	-0.1-0.1	-0.1-0.1	-0.1-0.1	-0.1-0.1	-0.1-0.1	-0.1-0.1	-0.1-0.1
4	-26.3-2.3	-26.1-2.4	-26.4-2.0	95.4-111.6	-0.1-0.2	-1.1-2.8	-0.4-0.6	-0.6-0.7	-0.3-0.5	-0.9-1.8	-0.1-0.3
5	-0.6-0.8	-0.5-0.9	-0.1-0.1	-0.1-0.2	-0.1-0.1	-0.1-0.1	-0.1-0.1	-0.1-0.1	-0.1-0.1	-0.1-0.1	-0.1-0.1
6	-0.5-0.8	-0.4-1.0	-0.1-0.1	-1.1-2.8	-0.1-0.1	0.1-1.7	-2.1-1.0	-2.1-1.0	-2.1-1.0	-2.0-1.1	-2.1-1.0
7	-0.6-0.8	-0.5-0.9	-0.1-0.1	-0.4-0.6	-0.1-0.1	-2.1-1.0	-0.2-0.2	-0.5-0.3	-0.5-0.3	-0.5-0.3	-0.5-0.3
8	-0.6-0.8	-0.5-0.9	-0.1-0.1	-0.6-0.7	-0.1-0.1	-2.1-1.0	-0.5-0.3	-0.3-0.2	-0.6-0.3	-0.6-0.4	-0.4-0.6
9	-0.6-0.8	-0.5-0.9	-0.1-0.1	-0.3-0.5	-0.1-0.1	-2.1-1.0	-0.5-0.3	-0.6-0.3	-0.1-0.2	-0.3-0.2	-0.4-0.2
10	-0.6-0.8	-0.5-1.0	-0.1-0.1	-0.9-1.8	-0.1-0.1	-2.0-1.1	-0.5-0.3	-0.6-0.4	-0.3-0.2	-0.5-0.5	-0.5-1.5
11	-0.6-0.8	-0.5-0.9	-0.1-0.1	-0.1-0.3	-0.1-0.1	-2.1-1.0	-0.5-0.3	-0.4-0.6	-0.4-0.2	-0.5-1.5	-0.1-0.1
Total	-1.1-12.0	-1.0-12.1	-1.5-11.6	97.5-99.1	-1.5-11.6	0.5-13.4	-1.4-11.8	-1.3-11.8	-1.5-11.7	-0.3-12.7	-1.5-11.7
Higher	16.6	15.6	16.9	29.2	4.6	7.5	5.8	5.7	5.6	5.6	4.8

### F.6 Temperature at “Knee”

Table F.61: Control / “Knee” Temp. with Time (Total-effect)

t \ i	1	2	3	4	5	6	7	8	9	10	11
0.33	0.6-8.2	-0.7-6.9	-4.5-3.4	27.2-33.3	-4.6-3.2	59.4-63.3	-4.6-3.2	-4.7-3.2	6.3-13.7	13.8-20.5	-4.0-3.7
0.67	0.8-8.2	-2.5-5.1	-3.0-4.6	17.1-23.8	-3.1-4.5	67.4-70.8	-3.1-4.5	-3.1-4.5	7.8-15.0	15.3-21.8	-4.7-3.1
1.00	1.1-8.4	-3.3-4.4	-3.3-4.2	11.7-18.8	-3.4-4.0	70.6-73.8	-3.2-4.2	-3.4-4.1	8.2-15.4	16.0-22.5	-2.8-4.6
1.33	1.2-8.5	-3.8-3.8	-3.6-3.9	8.3-15.5	-3.8-3.6	71.5-74.7	-2.9-4.6	-3.1-4.4	8.0-15.1	16.4-22.9	-3.2-4.2
1.67	0.9-8.4	-4.3-3.4	-4.1-3.5	5.8-13.1	-4.3-3.2	70.9-74.2	-4.0-3.7	-4.5-3.2	7.1-14.4	16.6-23.0	-3.8-3.7
2.00	0.7-8.3	-4.6-3.2	-4.7-3.0	4.0-11.5	-4.9-2.8	69.4-72.7	-1.7-5.9	-2.6-5.1	6.1-13.4	16.5-23.1	-4.5-3.2
2.33	0.3-8.0	-5.0-3.0	-5.5-2.5	2.3-10.1	-5.5-2.4	67.1-70.7	1.5-9.1	0.1-7.8	4.9-12.5	16.3-23.0	-5.3-2.6
2.67	-0.2-7.8	-3.0-5.0	-6.0-2.2	0.9-9.1	-6.1-2.1	64.7-68.6	5.5-13.2	3.4-11.2	4.0-11.9	15.9-22.9	-5.9-2.4
3.00	-0.9-7.5	-3.4-5.0	-6.7-1.9	-0.3-8.2	-6.7-1.8	62.5-66.8	9.3-17.1	6.4-14.3	2.9-11.2	15.4-22.7	-6.6-2.0
3.33	-1.7-7.1	-4.0-4.8	-7.6-1.4	-1.6-7.4	-7.5-1.4	60.6-65.2	12.5-20.4	8.8-16.9	1.8-10.6	14.9-22.5	-7.4-1.6
3.67	-2.5-6.7	-4.3-4.9	-8.2-1.2	-2.7-6.8	-8.2-1.3	59.2-64.1	15.3-23.4	10.9-19.2	1.0-10.2	14.6-22.5	-8.1-1.3
4.00	-3.0-6.6	-4.5-5.0	-8.5-1.2	-3.4-6.4	-8.5-1.2	58.1-63.3	17.8-26.0	12.8-21.3	0.6-10.2	14.3-22.5	-8.4-1.3
4.33	-3.5-6.4	-4.6-5.2	-8.8-1.2	-4.1-6.1	-8.8-1.2	57.3-62.7	19.6-27.9	14.3-22.9	0.3-10.1	14.1-22.6	-8.7-1.3
4.67	-3.9-6.2	-4.7-5.3	-9.1-1.2	-4.6-5.9	-9.0-1.2	56.8-62.4	20.9-29.3	15.4-24.0	0.1-10.1	14.0-22.6	-8.9-1.3
5.00	-4.3-6.1	-4.8-5.4	-9.4-1.0	-5.1-5.6	-9.4-1.0	56.3-62.1	21.7-30.3	15.9-24.7	-0.0-10.2	13.9-22.7	-9.2-1.1
5.33	-4.5-5.9	-4.7-5.5	-9.5-1.0	-5.4-5.4	-9.5-1.0	56.1-62.0	22.3-30.9	16.3-25.1	-0.1-10.2	13.8-22.7	-9.4-1.1
5.67	-4.7-5.8	-4.6-5.6	-9.6-0.9	-5.6-5.2	-9.6-0.9	56.0-61.9	22.4-31.0	16.4-25.2	-0.2-10.2	13.8-22.7	-9.5-1.0
6.00	-5.0-5.6	-4.6-5.7	-9.7-0.8	-5.8-5.0	-9.7-0.9	56.0-61.9	22.1-30.7	16.1-25.0	-0.2-10.2	13.9-22.7	-9.6-0.9
6.33	-5.1-5.4	-4.5-5.8	-9.8-0.6	-5.9-4.8	-9.7-0.8	56.1-61.9	21.3-29.9	15.5-24.4	-0.1-10.2	13.9-22.7	-9.7-0.8
6.67	-5.0-5.4	-4.1-5.9	-9.7-0.7	-5.6-4.9	-9.4-0.9	56.3-62.1	20.2-28.8	14.8-23.6	0.3-10.4	14.1-22.8	-9.5-0.8
7.00	-4.8-5.4	-3.9-6.0	-9.5-0.7	-5.3-5.0	-9.3-0.9	56.8-62.3	18.7-27.3	13.7-22.4	0.6-10.6	14.3-22.8	-9.4-0.7
7.33	-4.4-5.5	-6.5-3.6	-9.2-0.8	-4.7-5.2	-8.9-1.0	57.4-62.8	16.7-25.2	12.0-20.7	1.3-10.9	14.5-22.9	-9.1-0.8
7.67	-3.7-5.9	-5.7-4.1	-8.6-1.1	-3.9-5.7	-8.3-1.3	58.2-63.5	14.5-22.9	10.1-18.7	1.9-11.3	15.0-23.1	-8.5-1.2
8.00	-3.1-6.2	-5.0-4.4	-8.3-1.1	-3.4-5.9	-8.0-1.4	59.5-64.5	11.2-19.6	7.5-16.1	2.6-11.6	15.4-23.3	-8.1-1.2
8.33	-2.1-6.9	-4.1-5.0	-7.5-1.5	-2.4-6.6	-7.4-1.6	61.6-66.3	7.9-16.2	4.5-13.1	3.3-12.2	16.3-23.8	-7.5-1.6
8.67	-0.7-7.8	-2.8-5.9	-6.6-2.1	-1.0-7.6	-6.7-2.0	64.0-68.3	4.6-12.9	1.9-10.3	4.5-13.0	17.1-24.4	-6.6-2.0
9.00	0.1-8.4	-2.0-6.5	-6.2-2.2	-0.3-8.1	-6.4-2.0	66.4-70.3	1.4-9.7	-0.8-7.6	5.6-13.8	17.6-24.6	-6.2-2.2
9.33	1.2-9.3	-1.6-6.7	-5.6-2.5	0.2-8.4	-5.8-2.4	68.6-72.3	-1.3-7.0	-2.9-5.5	6.7-14.6	18.1-25.1	-5.5-2.7
9.67	1.9-9.9	-1.0-7.0	-5.0-3.0	0.5-8.6	-5.3-2.7	70.5-74.0	-2.7-5.5	-3.8-4.3	7.4-15.2	18.6-25.3	-4.9-3.1
10.00	2.3-10.0	-0.9-7.0	-4.7-3.2	0.6-8.5	-5.2-2.7	72.0-75.5	-3.5-4.6	-4.6-3.5	8.2-15.8	18.7-25.3	-4.6-3.3

Table F.62: Control / “Knee” Temp. / Mid-day

i \ j	1	2	3	4	5	6	7	8	9	10	11
1	0.4-1.3	-1.2-0.6	-1.1-0.6	-0.7-1.1	-1.1-0.6	-0.9-3.5	-1.1-1.0	-0.9-1.1	-1.2-0.7	-0.5-1.4	-1.1-0.6
2	-1.2-0.6	0.5-1.1	-0.3-0.7	-0.3-0.8	-0.3-0.7	-0.6-3.7	-0.2-1.6	-0.2-1.4	-0.3-0.9	-0.0-1.3	-0.3-0.7
3	-1.1-0.6	-0.3-0.7	-0.1-0.1	-0.3-0.2	-0.2-0.2	-1.7-2.3	-0.4-0.7	-0.3-0.5	-0.2-0.2	-0.4-0.3	-0.2-0.2
4	-0.7-1.1	-0.3-0.8	-0.3-0.2	0.9-1.7	-1.1-0.5	-2.0-2.4	-1.0-1.0	-1.2-0.7	-1.3-0.4	-1.1-0.7	-1.1-0.4
5	-1.1-0.6	-0.3-0.7	-0.2-0.2	-1.1-0.5	-0.1-0.1	-1.9-2.0	-0.2-0.7	-0.2-0.6	-0.2-0.2	-0.3-0.4	-0.2-0.1
6	-0.9-3.5	-0.6-3.7	-1.7-2.3	-2.0-2.4	-1.9-2.0	21.5-25.1	8.5-12.9	6.3-10.3	-0.7-2.3	1.7-5.3	-1.2-0.5
7	-1.1-1.0	-0.2-1.6	-0.4-0.7	-1.0-1.0	-0.2-0.7	8.5-12.9	6.9-9.0	-0.4-3.5	-1.3-1.7	0.8-4.1	-0.9-1.7
8	-0.9-1.1	-0.2-1.4	-0.3-0.5	-1.2-0.7	-0.2-0.6	6.3-10.3	-0.4-3.5	6.0-7.8	-1.1-1.7	0.4-3.5	-1.0-1.4
9	-1.2-0.7	-0.3-0.9	-0.2-0.2	-1.3-0.4	-0.2-0.2	-0.7-2.3	-1.3-1.7	-1.1-1.7	-0.7-0.5	0.2-2.6	-1.1-1.1
10	-0.5-1.4	-0.0-1.3	-0.4-0.3	-1.1-0.7	-0.3-0.4	1.7-5.3	0.8-4.1	0.4-3.5	0.2-2.6	5.2-6.7	-1.0-1.0
11	-1.1-0.6	-0.3-0.7	-0.2-0.2	-1.1-0.4	-0.2-0.1	-1.2-0.5	-0.9-1.7	-1.0-1.4	-1.1-1.1	-1.0-1.0	-0.0-0.2
Total	-4.3-6.1	-4.8-5.4	-9.4-1.0	-5.1-5.6	-9.4-1.0	56.3-62.1	21.7-30.3	15.9-24.7	-0.0-10.2	13.9-22.7	-9.2-1.1
Higher	-0.7	-4.9	-4.5	-0.3	-4.3	9.6	1.8	0.4	2.9	2.1	-4.0

Table F.63: South / “Knee” Temp. with Time (Total-effect)

t \ i	1	2	3	4	5	6	7	8	9	10	11
0.33	1.1-9.8	1.6-10.2	-4.0-5.0	15.9-23.7	-4.1-4.9	64.8-68.5	-4.1-4.9	-4.1-4.9	-0.8-8.0	10.3-18.2	-3.7-5.3
0.67	2.0-10.1	-1.0-7.4	-4.5-4.1	9.1-17.0	-4.6-3.9	71.3-74.3	-4.5-4.0	-4.6-3.9	-0.5-7.8	12.1-19.6	-4.2-4.3
1.00	2.1-10.0	-2.4-5.8	-4.8-3.5	6.1-13.9	-4.9-3.5	72.5-75.4	-4.2-4.1	-4.5-3.9	-0.9-7.2	12.9-20.0	-4.5-3.8
1.33	1.9-9.6	-2.9-5.1	-5.2-2.9	4.0-11.7	-5.4-2.8	70.7-73.7	-2.4-5.6	-2.9-5.1	-1.3-6.5	12.9-19.9	-5.0-3.1
1.67	1.2-8.8	-3.1-4.7	-3.8-3.9	2.0-9.6	-3.6-4.0	66.3-69.6	1.1-8.7	-0.0-7.6	-2.5-5.2	12.0-18.9	-3.5-4.2
2.00	0.3-7.9	-3.3-4.4	-4.7-3.0	0.3-8.0	-4.4-3.2	61.0-64.8	6.5-13.7	4.3-11.6	-3.5-4.3	10.8-17.7	-4.3-3.4
2.33	-0.5-7.2	-3.6-4.2	-5.4-2.4	-1.0-6.9	-5.1-2.7	56.2-60.4	12.7-19.4	9.1-16.2	-4.2-3.6	9.8-16.8	-5.0-2.9
2.67	-1.6-6.5	-4.1-4.0	-6.0-2.1	-2.2-6.0	-5.8-2.3	52.2-56.9	18.2-24.8	13.0-20.2	-5.1-3.1	8.7-16.1	-5.7-2.4
3.00	-2.5-6.1	-4.6-3.9	-6.6-1.9	-3.2-5.4	-6.5-2.0	49.4-54.5	22.7-29.3	16.3-23.5	-3.2-5.1	8.1-15.8	-6.2-2.2
3.33	-3.4-5.6	-5.1-3.8	-7.2-1.7	-4.2-4.8	-7.0-1.8	47.5-53.0	26.1-32.9	18.8-26.0	-3.7-4.9	7.5-15.6	-6.9-1.9
3.67	-4.3-5.0	-5.6-3.7	-7.8-1.5	-5.0-4.3	-7.7-1.4	46.2-52.0	28.8-35.6	20.5-27.9	-4.1-4.8	6.8-15.2	-7.5-1.6
4.00	-5.1-4.6	-5.7-3.8	-8.2-1.4	-5.7-4.1	-8.2-1.3	45.4-51.5	30.8-37.9	21.9-29.5	-4.5-4.8	6.4-15.2	-7.9-1.5
4.33	-5.7-4.4	-6.1-3.8	-8.6-1.3	-6.3-3.8	-8.6-1.2	44.8-51.2	32.2-39.3	22.9-30.7	-4.9-4.7	6.1-15.2	-8.3-1.5
4.67	-6.3-4.2	-6.2-3.9	-8.9-1.3	-6.8-3.6	-8.9-1.1	44.5-51.0	33.1-40.5	23.6-31.6	-5.1-4.7	5.9-15.3	-8.6-1.5
5.00	-6.7-4.0	-6.2-4.2	-9.1-1.3	-4.0-6.1	-9.2-1.1	44.3-51.0	33.8-41.3	24.2-32.2	-5.2-4.8	5.8-15.4	-8.9-1.4
5.33	-7.0-3.9	-6.2-4.3	-9.3-1.3	-4.2-6.0	-9.3-1.1	44.2-51.0	34.2-41.7	24.4-32.6	-5.3-4.8	5.7-15.4	-9.0-1.4
5.67	-4.0-6.3	-6.1-4.4	-9.4-1.2	-4.3-5.9	-9.4-1.0	44.1-51.0	34.3-41.8	24.5-32.7	-5.4-4.8	5.7-15.4	-9.2-1.3
6.00	-4.4-5.9	-6.1-4.4	-9.6-1.0	-4.6-5.7	-9.6-0.9	44.1-50.9	34.0-41.5	24.1-32.4	-5.5-4.7	5.5-15.3	-9.3-1.2
6.33	-4.6-5.7	-6.0-4.5	-9.6-0.8	-4.5-5.7	-9.6-0.8	44.3-51.1	33.3-40.8	23.7-31.9	-5.5-4.6	5.6-15.3	-9.3-1.1
6.67	-4.7-5.4	-5.6-4.6	-9.5-0.8	-4.3-5.7	-9.4-0.9	44.6-51.3	32.3-39.7	23.1-31.1	-5.4-4.6	5.8-15.3	-9.3-0.9
7.00	-4.4-5.4	-5.0-5.0	-9.1-0.8	-3.7-6.0	-9.0-1.0	45.1-51.6	30.9-38.2	22.1-30.1	-5.0-4.8	6.2-15.4	-8.9-1.0
7.33	-4.2-5.3	-4.4-5.3	-8.8-0.9	-6.3-3.7	-8.6-1.1	45.8-52.0	29.0-36.3	20.7-28.6	-4.5-4.9	6.5-15.5	-8.6-1.1
7.67	-4.0-5.3	-4.0-5.5	-8.6-0.9	-5.8-3.9	-8.3-1.2	46.8-52.7	26.3-33.6	18.6-26.4	-4.4-4.8	6.8-15.5	-8.4-1.1
8.00	-6.3-3.3	-3.0-6.0	-8.1-1.0	-5.2-4.2	-7.7-1.4	48.3-54.0	22.7-30.0	16.0-23.8	-3.9-5.0	7.3-15.7	-7.9-1.3
8.33	-5.5-3.7	-2.7-6.2	-7.7-1.2	-4.4-4.7	-7.3-1.6	50.7-56.1	18.2-25.7	12.4-20.3	-3.4-5.3	7.8-16.0	-7.5-1.4
8.67	-3.8-5.2	-1.2-7.4	-6.6-2.1	-2.9-5.9	-6.3-2.3	54.4-59.3	13.2-20.9	8.9-16.9	-5.2-3.8	9.7-17.6	-6.6-2.1
9.00	-1.8-6.9	0.2-8.7	-6.2-2.4	-2.0-6.8	-5.7-2.8	59.2-63.6	8.4-16.3	4.4-12.7	-4.3-4.5	10.9-18.6	-6.0-2.6
9.33	-0.3-8.2	1.0-9.4	-5.6-2.9	-1.2-7.5	-5.3-3.2	63.8-67.8	3.4-11.6	0.7-9.2	-3.7-5.0	12.2-19.7	-5.6-2.9
9.67	1.9-10.2	2.4-10.6	-3.9-4.3	0.3-8.8	-3.8-4.5	68.4-72.0	1.0-9.3	-1.0-7.5	-1.8-6.8	14.1-21.4	-4.0-4.3
10.00	2.6-10.9	1.8-10.0	-3.1-5.0	0.4-9.0	-3.2-5.0	71.1-74.6	-0.8-7.5	-2.1-6.5	-1.1-7.4	15.1-22.3	-3.3-5.0

Table F.64: South / “Knee” Temp. / Mid-day

i \ j	1	2	3	4	5	6	7	8	9	10	11
1	0.6-1.4	-1.0-0.4	-0.9-0.4	-1.2-0.4	-0.9-0.5	-1.0-2.2	-0.7-1.7	-0.8-1.3	-0.9-0.4	-0.8-0.6	-0.9-0.4
2	-1.0-0.4	0.7-1.4	-0.5-0.7	-0.4-0.7	-0.5-0.7	-0.4-2.8	0.1-2.7	-0.1-2.0	-0.6-0.7	-0.2-1.2	-0.5-0.7
3	-0.9-0.4	-0.5-0.7	-0.0-0.0	-0.1-0.0	-0.1-0.0	-1.2-1.5	-0.3-1.5	-0.2-1.1	-0.1-0.1	-0.0-0.4	-0.1-0.0
4	-1.2-0.4	-0.4-0.7	-0.1-0.0	0.6-1.3	-0.7-0.6	-1.6-1.7	-0.7-1.8	-0.5-1.4	-0.8-0.7	-0.7-0.8	-0.8-0.6
5	-0.9-0.5	-0.5-0.7	-0.1-0.0	-0.7-0.6	-0.1-0.0	-1.3-1.5	-0.1-1.7	-0.1-1.3	-0.0-0.3	0.0-0.5	-0.0-0.3
6	-1.0-2.2	-0.4-2.8	-1.2-1.5	-1.6-1.7	-1.3-1.5	16.4-19.4	9.8-14.9	7.5-11.6	-0.7-1.1	0.5-3.4	-1.0-0.5
7	-0.7-1.7	0.1-2.7	-0.3-1.5	-0.7-1.8	-0.1-1.7	9.8-14.9	13.3-15.9	1.7-6.5	-0.8-2.1	2.4-5.7	-0.7-1.9
8	-0.8-1.3	-0.1-2.0	-0.2-1.1	-0.5-1.4	-0.1-1.3	7.5-11.6	1.7-6.5	10.3-12.5	-0.7-2.1	1.2-4.3	-0.7-1.8
9	-0.9-0.4	-0.6-0.7	-0.1-0.1	-0.8-0.7	-0.0-0.3	-0.7-1.1	-0.8-2.1	-0.7-2.1	-0.3-0.4	0.1-1.4	-0.2-1.1
10	-0.8-0.6	-0.2-1.2	-0.0-0.4	-0.7-0.8	0.0-0.5	0.5-3.4	2.4-5.7	1.2-4.3	0.1-1.4	3.4-4.5	-0.9-0.6
11	-0.9-0.4	-0.5-0.7	-0.1-0.0	-0.8-0.6	-0.0-0.3	-1.0-0.5	-0.7-1.9	-0.7-1.8	-0.2-1.1	-0.9-0.6	0.0-0.3
Total	-6.7-4.0	-6.2-4.2	-9.1-1.3	-4.0-6.1	-9.2-1.1	44.3-51.0	33.8-41.3	24.2-32.2	-5.2-4.8	5.8-15.4	-8.9-1.4
Higher	-1.8	-6.3	-5.1	-0.6	-5.8	3.8	-2.6	-3.4	-2.9	-3.6	-4.9



Table F.65: North / “Knee” Temp. with Time (Total-effect)

t \ i	1	2	3	4	5	6	7	8	9	10	11
0.33	1.6-13.7	1.8-13.7	-4.4-8.3	37.2-45.3	-4.4-8.2	44.1-51.3	-4.5-8.2	-4.4-8.2	-1.0-11.2	7.5-18.7	-4.1-8.5
0.67	2.8-14.1	-0.9-10.8	-5.8-6.3	23.0-32.4	-5.8-6.3	54.7-60.5	-6.0-6.1	-6.0-6.2	-1.3-10.4	9.5-20.1	-5.5-6.7
1.00	3.6-14.5	-2.3-9.1	-6.1-5.6	16.8-26.5	-6.5-5.3	59.3-64.5	-6.4-5.4	-6.5-5.3	-1.5-9.9	10.7-20.8	-5.9-5.8
1.33	4.0-14.4	-3.4-7.8	-6.3-5.1	13.0-22.7	-6.8-4.6	61.3-66.2	-6.6-4.8	-6.5-4.9	-1.6-9.3	11.2-20.9	-6.3-5.1
1.67	4.0-14.1	-3.8-6.9	-6.2-4.7	10.4-20.0	-6.8-4.1	61.6-66.2	-5.9-5.0	-5.6-5.2	-2.1-8.5	11.3-20.6	-6.5-4.5
2.00	3.6-13.3	-3.9-6.4	-6.3-4.1	8.3-17.7	-3.9-6.1	60.2-64.8	-4.6-5.7	-4.2-6.1	-2.6-7.6	11.3-20.3	-6.6-3.8
2.33	3.3-12.4	-3.2-6.4	-6.2-3.6	6.5-15.6	-3.8-5.7	57.6-62.3	-2.1-7.4	-1.4-8.1	-2.8-6.8	11.1-19.6	-6.4-3.4
2.67	2.9-11.5	-2.5-6.6	-3.6-5.5	5.1-13.8	-4.0-5.1	54.1-58.9	0.4-9.3	1.7-10.6	-3.3-5.9	10.6-18.7	-3.8-5.3
3.00	2.5-10.8	-1.9-6.8	-3.8-4.9	3.9-12.2	-4.2-4.5	50.7-55.5	3.1-11.4	5.2-13.3	-3.7-5.1	10.0-17.7	-3.9-4.8
3.33	1.9-9.9	-1.3-7.0	-4.0-4.4	2.8-11.0	-4.3-4.1	47.4-52.4	5.7-13.4	8.6-16.2	-4.0-4.4	9.3-16.8	-4.1-4.3
3.67	1.5-9.3	-0.8-7.2	-4.1-4.0	2.0-9.9	-4.3-3.8	44.5-49.5	8.0-15.3	11.7-18.9	-4.1-4.0	8.8-16.1	-4.2-3.9
4.00	1.1-8.7	-0.4-7.3	-4.2-3.7	1.2-9.0	-4.5-3.5	42.1-47.2	9.9-16.8	14.6-21.4	-4.3-3.7	8.4-15.5	-4.4-3.5
4.33	0.5-8.0	-0.3-7.3	-4.4-3.4	0.5-8.3	-4.8-3.1	40.2-45.3	11.2-18.0	16.8-23.4	-4.6-3.3	7.8-15.0	-4.6-3.2
4.67	0.0-7.6	-0.2-7.3	-4.6-3.1	0.1-7.8	-4.9-2.8	38.8-44.0	12.2-18.8	18.5-25.0	-4.7-3.1	7.5-14.6	-4.8-2.9
5.00	-0.3-7.2	-0.1-7.3	-4.7-2.9	-0.3-7.3	-5.1-2.6	37.9-43.1	12.8-19.4	19.8-26.1	-4.9-2.9	7.3-14.4	-4.9-2.7
5.33	-0.6-6.9	0.1-7.5	-4.8-2.8	-0.5-7.1	-5.1-2.5	37.4-42.7	13.2-19.8	20.6-26.8	-4.9-2.8	7.3-14.3	-5.0-2.6
5.67	-0.8-6.7	0.3-7.7	-4.8-2.8	-0.7-7.0	-5.2-2.4	37.3-42.5	13.4-19.9	20.9-27.0	-4.9-2.8	7.3-14.3	-5.0-2.6
6.00	-1.0-6.6	0.5-7.9	-4.7-2.8	-0.7-7.0	-5.1-2.5	37.6-42.8	13.3-19.8	20.6-26.8	-4.9-2.9	7.5-14.5	-5.0-2.6
6.33	-1.0-6.5	0.7-8.1	-4.8-2.9	-0.7-7.0	-5.1-2.5	38.2-43.4	12.8-19.4	19.8-26.1	-4.9-2.9	7.6-14.7	-5.0-2.6
6.67	-1.0-6.7	1.0-8.5	-4.7-3.0	-0.4-7.3	-5.1-2.6	39.2-44.4	12.1-18.8	18.5-25.0	-4.7-3.1	8.0-15.1	-5.0-2.7
7.00	-0.8-6.8	1.2-8.7	-4.7-3.1	-0.2-7.6	-5.0-2.8	40.7-45.8	11.0-17.8	16.7-23.4	-4.7-3.3	8.2-15.4	-5.0-2.8
7.33	-0.6-7.2	1.5-9.2	-4.5-3.5	0.5-8.3	-4.8-3.2	42.5-47.6	9.6-16.7	14.7-21.6	-4.5-3.6	8.8-16.1	-4.8-3.2
7.67	0.0-8.0	2.0-9.9	-4.1-4.0	1.3-9.3	-4.6-3.5	44.8-49.9	8.1-15.5	12.4-19.6	-4.0-4.2	9.6-17.0	-4.5-3.6
8.00	0.8-8.9	2.5-10.5	-3.8-4.5	2.4-10.5	-4.3-4.0	47.5-52.5	6.2-13.9	9.7-17.2	-3.7-4.8	10.4-17.8	-4.2-4.1
8.33	1.2-9.7	2.4-10.7	-4.0-4.6	3.2-11.6	-4.4-4.3	50.5-55.4	3.6-11.8	6.5-14.6	-3.7-5.1	10.7-18.5	-4.4-4.2
8.67	2.4-11.1	2.7-11.3	-3.7-5.1	4.4-12.9	-4.1-4.8	53.9-58.7	1.5-10.2	3.9-12.5	-3.2-5.8	11.8-19.7	-4.2-4.7
9.00	3.9-12.7	2.8-11.6	-6.1-3.4	5.7-14.4	-3.8-5.3	56.9-61.6	-0.2-8.9	1.8-10.7	-2.7-6.6	13.0-21.0	-3.8-5.2
9.33	5.0-14.0	2.5-11.6	-5.7-4.0	6.7-15.6	-3.6-5.7	59.7-64.3	-1.5-7.9	-0.0-9.2	-2.1-7.4	14.0-22.1	-6.1-3.5
9.67	5.9-15.0	1.9-11.3	-5.7-4.2	6.8-15.8	-6.4-3.5	62.2-66.7	-3.0-6.7	-1.8-7.9	-1.9-7.8	14.2-22.5	-6.2-3.8
10.00	6.5-15.6	1.3-10.8	-5.3-4.7	6.9-16.1	-6.2-3.9	63.9-68.4	-3.6-6.2	-2.7-7.1	-1.6-8.1	14.7-23.1	-5.8-4.1

Table F.66: North / “Knee” Temp. / Mid-day

i \ j	1	2	3	4	5	6	7	8	9	10	11
1	2.0-3.2	-1.8-0.4	-1.8-0.3	-1.6-0.8	-1.8-0.3	-1.1-3.0	-1.7-0.6	-1.5-1.1	-2.0-0.3	-1.4-0.7	-1.8-0.3
2	-1.8-0.4	3.1-4.2	-0.8-0.9	-0.9-0.9	-0.8-0.9	-0.5-3.5	-0.9-1.3	-0.6-2.0	-0.8-0.9	-0.7-1.2	-0.8-0.9
3	-1.8-0.3	-0.8-0.9	-0.2-0.2	-0.4-0.5	-0.3-0.5	-1.0-2.3	-0.6-0.5	-0.8-0.8	-0.3-0.5	-0.5-0.4	-0.3-0.5
4	-1.6-0.8	-0.9-0.9	-0.4-0.5	2.9-3.9	-1.1-0.8	-1.7-2.4	-0.9-1.2	-1.1-1.3	-1.2-0.7	-1.2-0.8	-1.1-0.8
5	-1.8-0.3	-0.8-0.9	-0.3-0.5	-1.1-0.8	-0.1-0.1	-0.8-2.5	-0.3-0.6	-0.6-0.9	-0.2-0.3	-0.3-0.5	-0.2-0.3
6	-1.1-3.0	-0.5-3.5	-1.0-2.3	-1.7-2.4	-0.8-2.5	29.5-32.5	0.4-3.3	0.6-4.5	-0.7-1.1	-0.6-2.6	-0.9-0.8
7	-1.7-0.6	-0.9-1.3	-0.6-0.5	-0.9-1.2	-0.3-0.6	0.4-3.3	11.6-13.5	-2.2-1.9	-1.8-0.9	-1.1-1.8	-1.8-0.8
8	-1.5-1.1	-0.6-2.0	-0.8-0.8	-1.1-1.3	-0.6-0.9	0.6-4.5	-2.2-1.9	17.2-19.4	-1.6-1.1	-1.5-1.7	-1.6-1.1
9	-2.0-0.3	-0.8-0.9	-0.3-0.5	-1.2-0.7	-0.2-0.3	-0.7-1.1	-1.8-0.9	-1.6-1.1	-0.3-0.5	-0.6-1.0	-1.0-0.6
10	-1.4-0.7	-0.7-1.2	-0.5-0.4	-1.2-0.8	-0.3-0.5	-0.6-2.6	-1.1-1.8	-1.5-1.7	-0.6-1.0	8.9-10.2	-0.8-0.9
11	-1.8-0.3	-0.8-0.9	-0.3-0.5	-1.1-0.8	-0.2-0.3	-0.9-0.8	-1.8-0.8	-1.6-1.1	-1.0-0.6	-0.8-0.9	-0.1-0.2
Total	-0.3-7.2	-0.1-7.3	-4.7-2.9	-0.3-7.3	-5.1-2.6	37.9-43.1	12.8-19.4	19.8-26.1	-4.9-2.9	7.3-14.4	-4.9-2.7
Higher	5.1	-2.2	-1.1	0.7	-1.8	-0.4	2.6	1.9	0.3	-0.1	0.6

Table F.67: Control / “Knee” Temp. / Mean

i \ j	1	2	3	4	5	6	7	8	9	10	11
1	0.1-1.2	-1.2-0.8	-1.3-0.8	-1.3-0.9	-1.2-0.8	-1.4-5.3	-0.7-1.3	-1.2-0.8	-1.2-1.1	-0.6-1.5	-1.2-0.8
2	-1.2-0.8	1.0-1.5	-0.3-0.5	-0.6-0.5	-0.4-0.5	-1.1-5.6	-0.2-0.9	-0.3-0.8	-0.3-0.6	-0.2-1.2	-0.3-0.5
3	-1.3-0.8	-0.3-0.5	-0.1-0.1	-0.4-0.2	-0.2-0.2	-2.1-4.4	-0.4-0.3	-0.4-0.2	-0.3-0.2	-0.5-0.5	-0.2-0.2
4	-1.3-0.9	-0.6-0.5	-0.4-0.2	4.5-5.7	-1.1-0.8	-1.8-5.7	-0.8-1.3	-0.9-1.2	-1.3-0.9	-1.0-1.3	-1.1-0.8
5	-1.2-0.8	-0.4-0.5	-0.2-0.2	-1.1-0.8	-0.1-0.1	-2.3-4.1	-0.2-0.2	-0.3-0.1	-0.1-0.2	-0.5-0.5	-0.2-0.2
6	-1.4-5.3	-1.1-5.6	-2.1-4.4	-1.8-5.7	-2.3-4.1	38.5-43.2	2.9-6.5	1.9-5.2	0.7-4.2	1.8-6.5	-0.8-0.7
7	-0.7-1.3	-0.2-0.9	-0.4-0.3	-0.8-1.3	-0.2-0.2	2.9-6.5	3.1-4.2	-0.6-1.5	-0.9-0.9	-0.1-2.0	-0.6-1.0
8	-1.2-0.8	-0.3-0.8	-0.4-0.2	-0.9-1.2	-0.3-0.1	1.9-5.2	-0.6-1.5	2.8-3.8	-0.7-1.0	-0.4-1.7	-0.8-0.8
9	-1.2-1.1	-0.3-0.6	-0.3-0.2	-1.3-0.9	-0.1-0.2	0.7-4.2	-0.9-0.9	-0.7-1.0	-0.8-0.7	1.1-3.9	-1.2-1.6
10	-0.6-1.5	-0.2-1.2	-0.5-0.5	-1.0-1.3	-0.5-0.5	1.8-6.5	-0.1-2.0	-0.4-1.7	1.1-3.9	8.9-10.7	-0.9-1.2
11	-1.2-0.8	-0.3-0.5	-0.2-0.2	-1.1-0.8	-0.2-0.2	-0.8-0.7	-0.6-1.0	-0.8-0.8	1.2-1.6	-0.9-1.2	0.0-0.3
Total	-3.3-6.4	-4.6-4.8	-7.7-1.9	1.3-10.9	-7.9-1.7	61.8-66.5	2.3-11.7	-0.4-9.1	1.2-10.9	14.0-22.4	-7.5-2.1
Higher	-0.4	-4.5	-3.6	-0.7	-3.8	0.3	-3.8	-3.8	0.8	-1.0	-3.2

Table F.68: South / “Knee” Temp. / Mean

i \ j	1	2	3	4	5	6	7	8	9	10	11
1	0.7-1.8	-1.5-0.4	-1.5-0.5	-1.7-0.6	-1.6-0.5	-2.6-4.3	-1.2-1.0	-1.2-0.9	-1.6-0.5	-0.9-1.1	-1.5-0.5
2	-1.5-0.4	1.7-2.3	-0.4-0.6	-0.6-0.4	-0.4-0.6	-1.9-4.9	-0.3-1.4	-0.3-1.1	-0.4-0.6	-0.2-1.2	-0.4-0.6
3	-1.5-0.5	-0.4-0.6	-0.1-0.1	-0.4-0.1	-0.2-0.2	-2.8-3.6	-0.3-0.7	-0.3-0.4	-0.2-0.2	-0.3-0.6	-0.2-0.2
4	-1.7-0.6	-0.6-0.4	-0.4-0.1	4.0-5.1	-1.2-0.6	-3.0-4.3	-1.4-0.9	-1.3-0.8	-1.2-0.7	-0.9-1.2	-1.2-0.7
5	-1.6-0.5	-0.4-0.6	-0.2-0.2	-1.2-0.6	-0.1-0.1	-2.9-3.6	-0.3-0.6	-0.3-0.4	-0.2-0.2	-0.3-0.6	-0.2-0.1
6	-2.6-4.3	-1.9-4.9	-2.8-3.6	-3.0-4.3	-2.9-3.6	38.0-42.6	4.0-8.7	3.0-7.1	-0.6-1.6	1.1-5.4	-1.0-0.5
7	-1.2-1.0	-0.3-1.4	-0.3-0.7	-1.4-0.9	-0.3-0.6	4.0-8.7	7.6-9.2	-0.2-2.7	-0.6-1.5	0.8-3.3	-0.4-1.5
8	-1.2-0.9	-0.3-1.1	-0.3-0.4	-1.3-0.8	-0.3-0.4	3.0-7.1	-0.2-2.7	6.1-7.5	-0.7-1.2	0.1-2.4	-0.6-1.2
9	-1.6-0.5	-0.4-0.6	-0.2-0.2	-1.2-0.7	-0.2-0.2	-0.6-1.6	-0.6-1.5	-0.7-1.2	-0.3-0.5	0.1-1.9	-0.6-1.1
10	-0.9-1.1	-0.2-1.2	-0.3-0.6	-0.9-1.2	-0.3-0.6	1.1-5.4	0.8-3.3	0.1-2.4	0.1-1.9	8.0-9.4	-0.8-0.8
11	-1.5-0.5	-0.4-0.6	-0.2-0.2	-1.2-0.7	-0.2-0.1	-1.0-0.5	-0.4-1.5	-0.6-1.2	-0.6-1.1	-0.8-0.8	0.2-0.5
Total	-6.2-4.6	-4.0-6.0	-8.3-2.1	-2.6-8.0	-8.4-1.9	54.3-59.8	9.3-18.6	4.5-14.3	-4.9-5.2	6.8-16.5	-7.9-2.3
Higher	0.6	-3.7	-3.4	-0.5	-3.1	-1.9	-5.6	-5.7	-1.7	-5.7	-3.2

Table F.69: North / “Knee” Temp. / Mean

i \ j	1	2	3	4	5	6	7	8	9	10	11
1	1.4-3.1	-2.1-1.0	-2.1-1.1	-1.6-2.0	-2.2-1.0	-1.9-5.6	-2.1-0.9	-2.1-1.0	-2.3-0.9	-1.5-1.5	-2.2-1.0
2	-2.1-1.0	3.1-4.1	-1.0-0.8	-1.0-1.0	-1.0-0.8	-2.1-5.4	-1.1-0.9	-0.9-1.3	-1.0-0.8	-1.0-1.1	-1.0-0.8
3	-2.1-1.1	-1.0-0.8	-0.3-0.2	-0.7-0.5	-0.4-0.7	-2.2-4.6	-0.7-0.4	-0.5-0.7	-0.4-0.7	-0.8-0.6	-0.4-0.6
4	-1.6-2.0	-1.0-1.0	-0.7-0.5	7.1-8.8	-1.4-1.4	-2.8-5.5	-1.4-1.5	-1.7-1.3	-1.6-1.3	-1.2-2.1	-1.3-1.5
5	-2.2-1.0	-1.0-0.8	-0.4-0.7	-1.4-1.4	-0.1-0.1	-2.1-4.7	-0.3-0.4	-0.4-0.4	-0.3-0.3	-0.7-0.5	-0.3-0.3
6	-1.9-5.6	-2.1-5.4	-2.2-4.6	-2.8-5.5	-2.1-4.7	42.2-47.2	-1.2-2.1	-1.4-2.5	-1.2-1.2	-2.1-3.0	-1.0-0.7
7	-2.1-0.9	-1.1-0.9	-0.7-0.4	-1.4-1.5	-0.3-0.4	-1.2-2.1	5.5-6.9	-1.2-1.6	-1.5-0.7	-1.4-1.3	-1.5-0.7
8	-2.1-1.0	-0.9-1.3	-0.5-0.7	-1.7-1.3	-0.4-0.4	-1.4-2.5	-1.2-1.6	7.5-9.1	-1.2-1.2	-1.4-1.5	-1.2-1.2
9	-2.3-0.9	-1.0-0.8	-0.4-0.7	-1.6-1.3	-0.3-0.3	-1.2-1.2	-1.5-0.7	-1.2-1.2	-0.6-0.6	-1.4-1.1	-1.0-1.4
10	-1.5-1.5	-1.0-1.1	-0.8-0.6	-1.2-2.1	-0.7-0.5	-2.1-3.0	-1.4-1.3	-1.4-1.5	-1.4-1.1	11.6-13.5	-0.8-1.4
11	-2.2-1.0	-1.0-0.8	-0.4-0.6	-1.3-1.5	-0.3-0.3	-1.0-0.7	-1.5-0.7	-1.2-1.2	-1.0-1.4	-0.8-1.4	-0.2-0.3
Total	-0.1-9.7	-2.0-8.1	-4.2-5.7	5.8-15.2	-4.7-5.2	49.7-55.2	1.4-11.0	4.2-13.6	-4.8-5.5	9.3-18.4	-4.3-5.6
Higher	4.6	-1.4	0.2	0.9	-0.5	-1.0	1.0	0.1	1.6	0.4	1.1

Table F.70: Control / “Knee” Temp. / Maximum

i \ j	1	2	3	4	5	6	7	8	9	10	11
1	0.1-0.9	-0.7-1.1	-0.6-1.1	-0.9-0.9	-0.6-1.1	-0.3-3.4	-0.9-1.0	-0.8-1.1	-1.0-0.9	-0.7-1.1	-0.6-1.0
2	-0.7-1.1	0.4-1.1	-0.5-0.7	-0.6-0.8	-0.5-0.7	0.4-4.2	-0.3-1.5	-0.5-1.3	-0.4-0.9	-0.3-1.2	-0.5-0.7
3	-0.6-1.1	-0.5-0.7	-0.1-0.1	-0.5-0.1	-0.2-0.1	-0.8-2.5	-0.3-0.6	-0.4-0.4	-0.2-0.1	-0.3-0.3	-0.2-0.1
4	-0.9-0.9	-0.6-0.8	-0.5-0.1	3.4-4.9	-0.7-0.7	2.9-7.5	0.4-2.7	-0.3-1.8	-1.0-0.7	0.2-2.2	-0.8-0.6
5	-0.6-1.1	-0.5-0.7	-0.2-0.1	-0.7-0.7	-0.1-0.1	-0.8-2.4	-0.2-0.8	-0.3-0.6	-0.2-0.2	-0.1-0.5	-0.2-0.2
6	-0.3-3.4	0.4-4.2	-0.8-2.5	2.9-7.5	-0.8-2.4	17.1-20.5	6.6-10.8	4.8-8.7	-1.5-1.3	1.4-4.9	-1.2-0.7
7	-0.9-1.0	-0.3-1.5	-0.3-0.6	0.4-2.7	-0.2-0.8	6.6-10.8	5.9-7.9	-0.2-3.7	-1.1-2.0	1.0-4.2	-0.6-2.2
8	-0.8-1.1	-0.5-1.3	-0.4-0.4	-0.3-1.8	-0.3-0.6	4.8-8.7	-0.2-3.7	5.5-7.5	-1.2-1.7	-0.0-3.3	-1.1-1.6
9	-1.0-0.9	-0.4-0.9	-0.2-0.1	-1.0-0.7	-0.2-0.2	-1.5-1.3	-1.1-2.0	-1.2-1.7	-0.6-0.6	0.2-2.5	-1.3-1.0
10	-0.7-1.1	-0.3-1.2	-0.3-0.3	0.2-2.2	-0.1-0.5	1.4-4.9	1.0-4.2	-0.0-3.3	0.2-2.5	4.1-5.6	-1.0-1.1
11	-0.6-1.0	-0.5-0.7	-0.2-0.1	-0.8-0.6	-0.2-0.2	-1.2-0.7	-0.6-2.2	-1.1-1.6	-1.3-1.0	-1.0-1.1	-0.0-0.2
Total	-4.5-6.0	-5.4-5.1	-7.4-3.2	14.3-24.1	-7.5-3.2	53.7-59.9	23.2-31.9	17.4-26.2	1.1-11.2	15.4-24.4	-7.2-3.4
Higher	-2.6	-5.6	-3.2	6.7	-3.8	8.9	3.6	3.2	4.2	4.2	-2.9

Table F.71: South / “Knee” Temp. / Maximum

i \ j	1	2	3	4	5	6	7	8	9	10	11
1	0.5-1.3	-1.1-0.3	-1.1-0.2	-1.3-0.2	-1.1-0.3	-1.1-1.9	-0.9-1.5	-1.0-1.0	-1.1-0.3	-0.6-0.8	-1.1-0.3
2	-1.1-0.3	0.8-1.5	-0.5-0.7	-0.4-0.9	-0.5-0.7	-0.1-3.0	0.2-2.8	-0.1-2.1	-0.5-0.7	-0.4-1.0	-0.5-0.7
3	-1.1-0.2	-0.5-0.7	-0.0-0.1	-0.2-0.0	-0.1-0.0	-1.1-1.5	-0.4-1.4	-0.3-1.0	-0.2-0.0	-0.2-0.2	-0.1-0.0
4	-1.3-0.2	-0.4-0.9	-0.2-0.0	1.0-1.8	-1.0-0.4	-1.0-2.1	-0.7-1.9	-0.6-1.4	-1.0-0.4	-0.9-0.6	-1.0-0.4
5	-1.1-0.3	-0.5-0.7	-0.1-0.0	-1.0-0.4	-0.1-0.1	-1.0-1.5	-0.3-1.6	-0.2-1.1	-0.2-0.2	-0.1-0.4	-0.2-0.2
6	-1.1-1.9	-0.1-3.0	-1.1-1.5	-1.0-2.1	-1.0-1.5	15.6-18.6	9.0-14.0	6.5-10.7	-1.1-0.9	-0.2-2.7	-1.2-0.5
7	-0.9-1.5	0.2-2.8	-0.4-1.4	-0.7-1.9	-0.3-1.6	9.0-14.0	13.3-16.0	1.6-6.5	-1.0-1.9	2.1-5.4	-0.8-1.9
8	-1.0-1.0	-0.1-2.1	-0.3-1.0	-0.6-1.4	-0.2-1.1	6.5-10.7	1.6-6.5	10.4-12.7	-1.0-1.9	0.6-3.9	-1.0-1.7
9	-1.1-0.3	-0.5-0.7	-0.2-0.0	-1.0-0.4	-0.2-0.2	-1.1-0.9	-1.0-1.9	-1.0-1.9	-0.3-0.4	-0.2-1.2	-0.4-0.9
10	-0.6-0.8	-0.4-1.0	-0.2-0.2	-0.9-0.6	-0.1-0.4	-0.2-2.7	2.1-5.4	0.6-3.9	-0.2-1.2	3.2-4.4	-0.6-1.0
11	-1.1-0.3	-0.5-0.7	-0.1-0.0	-1.0-0.4	-0.2-0.2	-1.2-0.5	-0.8-1.9	-1.0-1.7	-0.4-0.9	-0.6-1.0	-0.0-0.3
Total	-6.4-3.8	-4.8-5.2	-8.5-1.6	-3.7-6.8	-8.5-1.5	43.6-50.2	35.1-42.4	25.9-33.5	-4.8-5.0	6.5-15.7	-8.1-1.9
Higher	-0.4	-5.4	-3.9	0.1	-4.4	6.1	0.1	0.2	-0.8	-1.0	-3.5

Table F.72: North / “Knee” Temp. / Maximum

i \ j	1	2	3	4	5	6	7	8	9	10	11
1	1.5-2.6	-1.4-0.6	-1.4-0.6	-1.3-1.0	-1.4-0.6	-0.4-3.1	-1.1-1.0	-1.2-1.3	-1.5-0.6	-1.1-0.9	-1.4-0.6
2	-1.4-0.6	3.5-4.6	-1.2-0.7	-0.8-1.2	-1.2-0.7	-0.0-3.7	-1.0-1.2	-0.8-1.9	-1.2-0.7	-1.0-1.0	-1.2-0.7
3	-1.4-0.6	-1.2-0.7	-0.2-0.2	-0.6-0.3	-0.3-0.4	-0.4-2.5	-0.5-0.5	-0.7-0.8	-0.3-0.4	-0.5-0.3	-0.3-0.4
4	-1.3-1.0	-0.8-1.2	-0.6-0.3	6.2-7.6	-0.5-1.3	1.4-5.2	0.2-2.3	-0.1-2.5	-0.5-1.3	0.4-2.4	-0.4-1.4
5	-1.4-0.6	-1.2-0.7	-0.3-0.4	-0.5-1.3	-0.1-0.1	-0.3-2.6	-0.4-0.5	-0.7-0.8	-0.3-0.3	-0.4-0.3	-0.3-0.2
6	-0.4-3.1	-0.0-3.7	-0.4-2.5	1.4-5.2	-0.3-2.6	25.4-28.4	0.8-3.7	0.4-4.2	-0.6-1.5	-0.5-2.7	-0.6-1.3
7	-1.1-1.0	-1.0-1.2	-0.5-0.5	0.2-2.3	-0.4-0.5	0.8-3.7	11.0-12.9	-1.5-2.6	-1.4-1.4	-1.9-1.1	-1.4-1.3
8	-1.2-1.3	-0.8-1.9	-0.7-0.8	-0.1-2.5	-0.7-0.8	0.4-4.2	-1.5-2.6	16.6-18.8	-1.7-1.2	-1.9-1.3	-1.6-1.2
9	-1.5-0.6	-1.2-0.7	-0.3-0.4	-0.5-1.3	-0.3-0.3	-0.6-1.5	-1.4-1.4	-1.7-1.2	-0.4-0.4	-0.5-1.0	-0.9-0.7
10	-1.1-0.9	-1.0-1.0	-0.5-0.3	0.4-2.4	-0.4-0.3	-0.5-2.7	-1.9-1.1	-1.9-1.3	-0.5-1.0	7.3-8.7	-1.0-1.0
11	-1.4-0.6	-1.2-0.7	-0.3-0.4	-0.4-1.4	-0.3-0.2	-0.6-1.3	-1.4-1.3	-1.6-1.2	-0.9-0.7	-1.0-1.0	-0.1-0.2
Total	-0.2-7.4	1.5-9.0	-3.6-4.1	10.3-17.3	-3.9-3.8	36.4-41.8	14.2-21.0	20.9-27.3	-4.0-3.8	7.4-14.5	-3.6-4.0
Higher	2.5	-0.1	-0.0	-1.4	-1.0	-2.9	1.9	2.6	-0.2	1.2	0.2

Table F.73: Control / “Knee” Temp. / Minimum

i \ j	1	2	3	4	5	6	7	8	9	10	11
1	-0.6-0.5	-0.8-1.3	-0.8-1.3	-13.3-4.2	-0.8-1.3	-1.2-0.9	-0.9-1.3	-0.8-1.3	-1.3-0.8	-1.3-0.8	-0.8-1.3
2	-0.8-1.3	-0.3-0.4	-0.7-0.8	-13.2-4.2	-0.7-0.8	-0.6-0.9	-0.7-0.8	-0.7-0.8	-0.7-0.8	-0.7-0.8	-0.7-0.8
3	-0.8-1.3	-0.7-0.8	-0.1-0.1	-13.4-4.0	-0.2-0.3	-0.2-0.3	-0.2-0.3	-0.2-0.3	-0.2-0.3	-0.2-0.3	-0.2-0.3
4	-13.3-4.2	-13.2-4.2	-13.4-4.0	85.6-95.2	-0.5-0.1	-2.8-3.6	-0.8-0.9	-0.8-0.5	-2.0-1.4	-1.4-2.2	-0.4-0.2
5	-0.8-1.3	-0.7-0.8	-0.2-0.3	-0.5-0.1	-0.1-0.2	-0.4-0.2	-0.3-0.2	-0.3-0.2	-0.3-0.3	-0.3-0.2	-0.3-0.2
6	-1.2-0.9	-0.6-0.9	-0.2-0.3	-2.8-3.6	-0.4-0.2	2.7-5.2	-3.8-0.9	-3.9-0.8	-3.1-1.6	-3.2-1.4	-3.9-0.8
7	-0.9-1.3	-0.7-0.8	-0.2-0.3	-0.8-0.9	-0.3-0.2	-3.8-0.9	-0.2-0.3	-0.5-0.5	-0.5-0.6	-0.5-0.5	-0.5-0.5
8	-0.8-1.3	-0.7-0.8	-0.2-0.3	-0.8-0.5	-0.3-0.2	-3.9-0.8	-0.5-0.5	-0.2-0.2	-0.4-0.5	-0.4-0.5	-0.4-0.5
9	-1.3-0.8	-0.7-0.8	-0.2-0.3	-2.0-1.4	-0.3-0.3	-3.1-1.6	-0.5-0.6	-0.4-0.5	-0.7-0.6	-0.9-1.6	-1.0-1.5
10	-1.3-0.8	-0.7-0.8	-0.2-0.3	-1.4-2.2	-0.3-0.2	-3.2-1.4	-0.5-0.5	-0.4-0.5	-0.9-1.6	-0.5-0.9	-1.3-1.4
11	-0.8-1.3	-0.7-0.8	-0.2-0.3	-0.4-0.2	-0.3-0.2	-3.9-0.8	-0.5-0.5	-0.4-0.5	-1.0-1.5	-1.3-1.4	-0.2-0.1
Total	-1.8-8.0	-2.4-7.5	-3.2-6.7	92.1-94.6	-3.2-6.6	5.6-14.8	-2.9-6.9	-3.0-6.9	-0.6-9.0	-0.0-9.6	-3.2-6.7
Higher	7.0	6.4	5.9	16.5	2.0	12.0	3.1	3.3	4.8	4.8	2.9

Table F.74: South / “Knee” Temp. / Minimum

i \ j	1	2	3	4	5	6	7	8	9	10	11
1	-0.2-0.6	-1.1-0.4	-1.1-0.4	-27.9-2.6	-1.1-0.4	-1.0-0.5	-1.1-0.4	-1.1-0.4	-1.1-0.4	-1.1-0.4	-1.1-0.4
2	-1.1-0.4	-0.2-0.3	-0.6-0.5	-27.8-2.7	-0.6-0.5	-0.6-0.5	-0.6-0.5	-0.6-0.5	-0.6-0.5	-0.6-0.5	-0.6-0.5
3	-1.1-0.4	-0.6-0.5	-0.1-0.1	-27.8-2.5	-0.3-0.2	-0.3-0.2	-0.3-0.2	-0.3-0.2	-0.3-0.2	-0.3-0.2	-0.3-0.2
4	-27.9-2.6	-27.8-2.7	-27.8-2.5	94.6-111.9	-0.4-0.4	-3.3-2.1	-0.8-0.3	-0.6-0.5	-1.0-0.9	-1.7-1.7	-0.5-0.2
5	-1.1-0.4	-0.6-0.5	-0.3-0.2	-0.4-0.4	-0.2-0.1	-0.3-0.3	-0.3-0.3	-0.3-0.3	-0.3-0.3	-0.3-0.3	-0.3-0.3
6	-1.0-0.5	-0.6-0.5	-0.3-0.2	-3.3-2.1	-0.3-0.3	0.3-2.4	-2.9-1.2	-2.9-1.2	-2.9-1.2	-2.6-1.4	-2.9-1.2
7	-1.1-0.4	-0.6-0.5	-0.3-0.2	-0.8-0.3	-0.3-0.3	-2.9-1.2	-0.1-0.3	-0.6-0.1	-0.6-0.1	-0.6-0.1	-0.6-0.1
8	-1.1-0.4	-0.6-0.5	-0.3-0.2	-0.6-0.5	-0.3-0.3	-2.9-1.2	-0.6-0.1	-0.2-0.2	-0.4-0.3	-0.4-0.3	-0.4-0.3
9	-1.1-0.4	-0.6-0.5	-0.3-0.2	-1.0-0.9	-0.3-0.3	-2.9-1.2	-0.6-0.1	-0.4-0.3	-0.2-0.5	-1.0-0.3	-1.0-0.3
10	-1.1-0.4	-0.6-0.5	-0.3-0.2	-1.7-1.7	-0.3-0.3	-2.6-1.4	-0.6-0.1	-0.4-0.3	-1.0-0.3	-0.6-0.6	-0.8-1.6
11	-1.1-0.4	-0.6-0.5	-0.3-0.2	-0.5-0.2	-0.3-0.3	-2.9-1.2	-0.6-0.1	-0.4-0.3	-1.0-0.3	-0.8-1.6	-0.0-0.2
Total	-1.9-12.3	-1.7-12.3	-1.9-12.2	97.2-99.0	-1.9-12.2	1.0-14.6	-2.0-12.1	-1.9-12.2	-1.8-12.3	-0.5-13.3	-2.0-12.1
Higher	20.8	18.8	18.3	33.9	5.5	11.3	7.4	6.8	7.3	7.6	6.6

Table F.75: North / “Knee” Temp. / Minimum

i \ j	1	2	3	4	5	6	7	8	9	10	11
1	-0.3-0.8	-1.3-0.9	-1.3-0.9	-25.8-3.1	-1.3-0.9	-1.2-1.0	-1.3-0.9	-1.3-0.9	-1.3-0.9	-1.2-1.0	-1.4-0.9
2	-1.3-0.9	-0.3-0.5	-0.9-0.7	-25.5-3.2	-0.9-0.7	-0.8-0.7	-0.9-0.7	-0.9-0.7	-0.9-0.7	-0.9-0.7	-0.9-0.7
3	-1.3-0.9	-0.9-0.7	-0.1-0.1	-25.6-3.2	-0.3-0.3	-0.3-0.3	-0.3-0.3	-0.3-0.3	-0.3-0.3	-0.2-0.3	-0.3-0.3
4	-25.8-3.1	-25.5-3.2	-25.6-3.2	87.6-104.2	-0.4-0.3	-2.7-5.2	-0.8-0.4	-1.0-0.3	-1.2-1.2	-2.6-2.8	-0.5-0.3
5	-1.3-0.9	-0.9-0.7	-0.3-0.3	-0.4-0.3	-0.2-0.1	-0.3-0.5	-0.3-0.5	-0.3-0.5	-0.3-0.5	-0.3-0.5	-0.3-0.5
6	-1.2-1.0	-0.8-0.7	-0.3-0.3	-2.7-5.2	-0.3-0.5	2.0-5.0	-4.5-1.4	-4.5-1.3	-4.4-1.5	-4.0-1.9	-4.5-1.4
7	-1.3-0.9	-0.9-0.7	-0.3-0.3	-0.8-0.4	-0.3-0.5	-4.5-1.4	-0.2-0.2	-0.4-0.4	-0.4-0.4	-0.4-0.4	-0.4-0.4
8	-1.3-0.9	-0.9-0.7	-0.3-0.3	-1.0-0.3	-0.3-0.5	-4.5-1.3	-0.4-0.4	-0.3-0.2	-0.3-0.6	-0.6-0.3	-0.3-0.6
9	-1.3-0.9	-0.9-0.7	-0.3-0.3	-1.2-1.2	-0.3-0.5	-4.4-1.5	-0.4-0.4	-0.3-0.6	-0.4-0.5	-0.9-0.9	-0.9-0.9
10	-1.2-1.0	-0.9-0.7	-0.2-0.3	-2.6-2.8	-0.3-0.5	-4.0-1.9	-0.4-0.4	-0.6-0.3	-0.9-0.9	-0.7-1.2	-1.4-2.3
11	-1.4-0.9	-0.9-0.7	-0.3-0.3	-0.5-0.3	-0.3-0.5	-4.5-1.4	-0.4-0.4	-0.3-0.6	-0.9-0.9	-1.4-2.3	-0.2-0.1
Total	-2.1-12.4	-2.3-12.3	-2.7-11.9	93.6-96.6	-2.8-11.8	4.0-17.8	-2.7-11.9	-2.6-12.0	-2.2-12.3	0.6-14.8	-2.7-11.9
Higher	18.1	17.1	16.1	32.2	4.4	13.6	6.5	6.8	6.6	8.1	5.9

F.7 Temperature Gradient at 2 cm

Table F.76: Control / Temp. Gradient at 2cm with Time (Total-effect)

t \ i	1	2	3	4	5	6	7	8	9	10	11
0.33	38.4-44.0	11.6-17.9	-3.7-3.3	46.7-52.5	-4.4-2.5	38.9-44.6	-4.4-2.5	-4.4-2.4	14.6-20.7	17.2-23.3	-3.3-3.6
0.67	50.3-56.3	8.5-15.9	-4.9-3.1	50.6-57.7	-6.0-2.1	40.5-47.3	-6.0-2.1	-6.0-2.1	19.2-26.1	20.0-27.2	-4.6-3.3
1.00	57.6-63.7	6.3-14.7	-5.3-4.1	52.3-60.3	-6.7-2.7	42.4-49.9	-6.8-2.6	-6.7-2.6	22.4-30.1	22.9-30.7	-5.4-3.8
1.33	62.6-69.0	3.6-13.3	-6.3-4.6	52.5-61.3	-7.9-3.2	42.8-51.1	-8.0-2.9	-7.9-2.9	23.6-32.1	24.6-33.2	-6.8-3.8
1.67	65.6-72.3	1.5-12.3	-7.0-5.3	52.1-61.8	-8.2-4.3	43.3-52.4	-8.4-3.6	-8.0-4.0	24.8-34.1	26.0-35.4	-7.8-4.1
2.00	67.1-74.1	-0.7-11.4	-8.2-5.3	51.1-61.4	-8.8-5.0	43.5-53.3	-8.5-4.7	-8.3-4.8	25.3-35.3	26.9-37.0	-9.1-4.1
2.33	67.2-74.5	-1.8-11.2	-8.8-5.7	49.6-60.6	-8.3-6.4	43.9-54.3	-7.6-6.4	-7.6-6.4	25.8-36.4	27.9-38.6	-9.7-4.4
2.67	66.0-73.5	-1.8-11.7	-8.9-6.2	47.9-59.3	-7.4-7.9	44.8-55.6	-5.8-8.7	-6.2-8.4	26.5-37.3	29.3-40.2	-10.1-4.7
3.00	64.2-72.0	-2.0-12.2	-9.2-6.5	45.7-57.4	-6.9-9.1	45.6-56.9	-9.3-6.8	-10.4-6.2	26.8-37.9	29.9-41.4	-10.5-4.9
3.33	62.1-70.4	-2.4-12.4	-9.5-6.7	43.4-55.6	-6.9-9.7	46.4-58.0	-8.4-8.2	-10.2-6.9	26.6-38.2	30.5-42.4	-11.0-4.8
3.67	60.4-68.9	-2.6-12.9	-9.6-7.1	41.7-54.3	-6.5-10.6	47.2-59.1	-7.6-9.3	-10.1-7.6	27.1-38.9	31.2-43.4	-11.2-5.0
4.00	58.5-67.4	-2.2-13.5	-9.7-7.3	39.5-52.6	-11.5-6.7	47.8-59.9	-6.9-10.3	-9.7-8.1	27.2-39.2	31.3-43.9	-11.3-5.3
4.33	56.8-66.0	-1.7-14.2	-9.9-7.4	37.8-51.2	-11.7-6.9	48.4-60.6	-6.4-10.9	-9.4-8.6	27.0-39.3	31.6-44.4	-11.5-5.4
4.67	55.1-64.6	-0.8-15.0	-9.9-7.5	36.2-49.8	-11.7-7.1	48.9-61.3	-5.7-11.6	-9.0-9.0	26.9-39.4	31.9-45.0	-11.4-5.8
5.00	53.4-63.3	-0.6-15.3	-10.3-7.2	34.6-48.4	-12.0-6.9	49.3-61.7	-5.6-11.8	-9.1-9.0	26.4-39.1	32.0-45.1	-11.4-5.8
5.33	52.1-62.2	-0.2-15.6	-10.6-7.0	33.8-47.6	-7.0-11.2	49.7-62.0	-5.7-11.7	-9.1-9.0	26.0-38.8	32.1-45.2	-11.4-5.8
5.67	51.1-61.2	0.3-16.1	-10.5-6.9	33.3-47.1	-7.0-11.0	50.3-62.5	-5.8-11.5	-8.9-9.0	25.9-38.6	32.5-45.3	-11.2-5.9
6.00	50.4-60.5	0.8-16.3	-10.3-6.9	33.2-46.8	-7.2-10.5	50.8-62.8	-6.2-11.1	-8.9-8.8	25.8-38.3	32.6-45.3	-10.9-5.9
6.33	49.9-60.0	1.0-16.3	-10.1-6.8	33.4-46.7	-7.6-9.8	51.4-63.1	-6.7-10.4	-9.0-8.6	25.6-38.0	32.7-45.2	-10.7-5.9
6.67	49.6-59.6	1.3-16.3	-10.0-6.8	33.8-46.8	-8.1-9.0	52.0-63.4	-7.4-9.5	-9.0-8.3	25.5-37.7	32.9-45.1	-10.6-5.8
7.00	49.6-59.5	1.6-16.3	-9.6-6.7	34.5-47.2	-8.3-8.4	52.8-63.8	-8.0-8.8	-9.0-8.0	25.3-37.4	33.2-45.1	-10.2-5.8
7.33	50.0-59.8	2.0-16.3	-9.3-6.6	35.6-47.9	-8.5-7.8	53.6-64.3	-8.3-8.2	-8.9-7.7	25.2-37.2	33.6-45.1	-9.8-5.8
7.67	50.8-60.4	2.3-16.3	-8.9-6.6	37.1-49.0	-8.8-7.1	54.2-64.7	-8.7-7.5	-8.7-7.3	25.5-37.2	33.8-45.1	-9.3-5.9
8.00	52.1-61.4	2.5-16.1	-8.7-6.5	38.8-50.4	-9.0-6.4	54.9-65.1	-8.9-7.0	-8.8-6.9	26.0-37.5	34.2-45.2	-9.0-6.0
8.33	54.0-63.1	2.7-16.1	-8.0-6.9	41.0-52.4	-8.7-6.3	55.9-65.8	-8.9-6.7	-8.6-6.9	26.9-38.1	34.8-45.6	-8.3-6.3
8.67	56.6-65.3	3.3-16.2	-7.0-7.5	43.4-54.7	-7.9-6.7	57.1-66.7	-8.5-6.9	-8.0-7.3	28.3-39.3	35.7-46.3	-7.4-7.0
9.00	59.5-68.0	3.7-16.4	-5.8-8.5	46.1-57.4	-6.8-7.6	58.4-67.8	-7.6-7.6	-6.9-8.1	30.3-41.2	37.2-47.7	-6.0-8.1
9.33	62.8-71.0	3.8-16.5	-9.0-6.2	49.0-60.3	-10.1-5.1	59.7-69.1	-6.5-8.4	-6.0-8.8	32.8-43.5	39.0-49.5	-9.0-5.9
9.67	66.2-74.0	3.5-16.2	-7.5-7.4	51.8-63.3	-8.8-6.2	61.0-70.3	-5.7-9.1	-5.1-9.5	35.3-45.8	40.8-51.3	-7.5-7.1
10.00	69.3-76.8	2.8-15.6	-6.6-8.2	54.2-65.8	-7.7-6.9	61.9-71.3	-5.2-9.6	-4.6-9.9	37.4-47.8	42.2-52.8	-6.6-8.0

Table F.77: Control / Temp. Gradient at 2cm / Mid-day

i \ j	1	2	3	4	5	6	7	8	9	10	11
1	-2.0-2.0	-3.0-1.5	-1.5-2.0	4.3-9.8	-2.1-1.9	-3.4-3.2	-1.5-2.4	-2.6-1.6	-3.0-2.5	-3.4-2.7	-1.9-1.6
2	-3.0-1.5	2.4-3.8	-1.1-0.7	-1.1-1.4	-1.3-0.7	2.4-6.3	-0.9-1.1	-1.0-0.9	-1.1-2.0	0.6-3.6	-1.1-0.7
3	-1.5-2.0	-1.1-0.7	-0.2-0.1	-0.4-0.4	-0.3-0.3	-0.6-1.1	-0.2-0.3	-0.3-0.3	-0.3-0.5	-0.5-0.5	-0.3-0.3
4	4.3-9.8	-1.1-1.4	-0.4-0.4	-1.1-0.7	-1.8-1.4	-2.0-2.2	-1.8-1.4	-2.1-1.2	-2.2-1.4	-2.5-1.6	-1.8-1.2
5	-2.1-1.9	-1.3-0.7	-0.3-0.3	-1.8-1.4	1.5-2.4	-1.4-1.4	-1.2-0.4	-1.2-0.3	-0.8-1.3	-1.2-1.0	-1.1-0.4
6	-3.4-3.2	2.4-6.3	-0.6-1.1	-2.0-2.2	-1.4-1.4	4.0-6.8	-2.0-1.1	-1.5-1.5	-1.9-2.7	-2.1-2.8	-1.7-1.1
7	-1.5-2.4	-0.9-1.1	-0.2-0.3	-1.8-1.4	-1.2-0.4	-2.0-1.1	-0.3-0.7	-0.9-1.0	-1.1-1.2	-1.2-1.0	-0.7-1.1
8	-2.6-1.6	-1.0-0.9	-0.3-0.3	-2.1-1.2	-1.2-0.3	-1.5-1.5	-0.9-1.0	-0.5-0.6	-1.2-1.1	-0.7-1.6	-0.8-1.1
9	-3.0-2.5	-1.1-2.0	-0.3-0.5	-2.2-1.4	-0.8-1.3	-1.9-2.7	-1.1-1.2	-1.2-1.1	1.1-3.1	-1.2-3.4	-1.8-1.1
10	-3.4-2.7	0.6-3.6	-0.5-0.5	-2.5-1.6	-1.2-1.0	-2.1-2.8	-1.2-1.0	-0.7-1.6	-1.2-3.4	1.5-3.5	-1.2-1.4
11	-1.9-1.6	-1.1-0.7	-0.3-0.3	-1.8-1.2	-1.1-0.4	-1.7-1.1	-0.7-1.1	-0.8-1.1	-1.8-1.1	-1.2-1.4	-0.0-0.2
Total	53.4-63.3	-0.6-15.3	-10.3-7.2	34.6-48.4	-12.0-6.9	49.3-61.7	-5.6-11.8	-9.1-9.0	26.4-39.1	32.0-45.1	-11.4-5.8
Higher	52.8	-1.4	-2.0	36.4	-3.0	45.5	3.2	0.8	29.3	32.9	-1.8

Table F.78: South / Temp. Gradient at 2cm with Time (Total-effect)

t \ i	1	2	3	4	5	6	7	8	9	10	11
0.33	46.5-51.5	17.2-23.1	-3.9-2.9	31.7-38.1	-2.6-4.0	34.1-39.8	-2.6-4.0	-2.6-4.0	8.4-14.8	10.8-17.2	-3.6-3.3
0.67	57.3-62.2	13.2-19.7	-4.2-3.0	34.5-41.8	-3.3-3.7	34.5-41.0	-3.3-3.6	-3.4-3.6	10.8-17.5	12.9-19.8	-4.3-3.0
1.00	63.4-68.3	9.6-16.7	-3.3-4.3	36.1-44.2	-4.4-3.3	35.0-42.0	-4.5-3.2	-4.6-3.0	11.0-18.1	13.8-21.3	-3.2-4.7
1.33	67.7-72.5	6.5-14.6	-4.3-4.0	37.3-46.1	-5.1-3.6	34.8-42.6	-5.0-3.5	-5.4-3.0	11.1-18.9	14.3-22.5	-4.3-4.5
1.67	69.8-74.8	4.7-13.6	-5.0-4.2	38.0-47.6	-4.6-4.9	34.7-43.3	-4.2-5.0	-4.7-4.4	11.2-19.5	14.9-23.6	-5.0-4.7
2.00	70.2-75.4	3.6-13.2	-5.0-4.9	37.8-48.1	-5.9-4.6	35.0-44.3	-5.0-5.4	-5.5-4.7	11.5-20.5	15.5-24.8	-4.9-5.5
2.33	68.9-74.4	3.0-13.5	-5.4-5.2	36.9-47.8	-4.7-6.5	35.5-45.5	-2.4-8.6	-3.3-7.6	11.6-21.3	16.0-26.0	-5.1-6.0
2.67	66.9-72.7	3.0-14.2	-5.6-5.9	35.6-47.1	-3.7-8.3	36.5-47.1	0.6-12.1	-1.4-10.2	11.6-22.2	16.1-26.9	-5.3-6.7
3.00	64.7-71.2	3.1-15.1	-5.5-6.6	34.4-46.5	-2.9-9.8	37.8-48.8	3.2-15.2	0.1-12.4	11.8-23.0	16.6-28.1	-5.2-7.6
3.33	62.5-69.5	2.9-15.7	-6.1-6.8	32.6-45.5	-2.6-10.9	38.6-50.1	4.8-17.5	0.6-13.6	11.6-23.6	16.8-28.9	-5.6-7.8
3.67	60.4-67.9	3.2-16.5	-6.7-7.0	31.1-44.6	-2.4-11.7	39.6-51.3	6.4-19.6	1.2-14.9	11.5-24.2	17.1-29.9	-6.0-8.3
4.00	58.4-66.3	3.9-17.4	-7.1-7.1	29.6-43.5	-2.6-12.2	40.4-52.4	7.7-21.3	1.7-15.9	11.1-24.6	17.4-30.6	-6.3-8.5
4.33	56.4-64.8	4.6-18.5	-7.5-7.2	28.2-42.5	-2.6-12.6	41.3-53.5	9.0-22.8	2.3-16.9	10.7-24.7	17.6-31.2	-6.3-8.9
4.67	54.5-63.2	4.7-19.0	-8.1-7.0	26.7-41.4	-3.2-12.4	41.9-54.3	9.4-23.6	2.3-17.3	10.2-24.6	17.9-31.7	-6.7-8.9
5.00	52.8-61.8	5.2-19.6	-8.4-7.0	25.5-40.4	-3.6-12.3	42.5-55.0	9.7-24.0	2.5-17.7	9.6-24.5	18.1-32.1	-6.7-9.2
5.33	51.2-60.4	5.6-19.9	-8.4-7.0	24.7-39.6	-3.9-12.1	43.1-55.6	9.6-23.9	2.3-17.7	9.5-24.4	18.3-32.3	-6.7-9.2
5.67	50.1-59.4	6.1-20.3	-8.2-7.1	24.2-39.1	-4.1-11.8	43.9-56.1	9.2-23.6	2.1-17.5	9.5-24.3	18.5-32.3	-6.6-9.2
6.00	49.2-58.5	6.3-20.4	-8.0-7.1	23.8-38.6	-4.4-11.4	44.7-56.7	8.5-22.8	1.8-17.0	9.5-24.0	18.5-32.3	-6.4-9.1
6.33	48.6-57.9	6.7-20.4	-7.6-7.1	23.9-38.3	-4.6-10.8	45.7-57.4	7.7-21.6	1.5-16.3	9.6-23.9	18.9-32.2	-6.1-9.1
6.67	48.6-57.5	7.1-20.4	-7.0-7.3	24.1-38.1	-4.9-10.2	46.7-58.1	6.6-20.3	1.3-15.7	10.0-23.7	19.2-32.2	-10.3-5.4
7.00	48.8-57.6	7.6-20.4	-6.1-7.7	24.8-38.3	-4.8-9.7	48.0-59.0	5.7-19.0	1.2-15.3	10.6-23.6	19.8-32.4	-9.4-5.6
7.33	49.5-57.9	8.0-20.4	-9.5-4.9	25.6-38.6	-4.7-9.2	49.3-59.8	4.7-17.7	1.4-14.8	11.1-23.5	20.6-32.6	-8.5-5.8
7.67	50.4-58.6	8.4-20.5	-8.3-5.5	26.6-39.2	-4.4-8.9	50.6-60.6	3.9-16.5	1.6-14.5	11.6-23.5	21.3-32.9	-7.7-6.1
8.00	52.0-59.8	9.1-20.7	-7.0-6.3	27.9-40.1	-4.0-8.8	52.0-61.5	3.5-15.8	2.1-14.5	12.4-23.7	22.2-33.3	-6.6-6.6
8.33	54.3-61.6	10.4-21.5	-5.0-7.7	29.3-41.3	-3.1-9.2	53.0-62.4	3.7-15.7	3.0-15.1	13.6-24.3	23.4-34.1	-5.1-7.5
8.67	57.5-64.4	12.2-22.9	-2.2-9.9	31.1-42.8	-1.1-10.7	54.2-63.4	5.1-16.8	5.2-16.7	15.7-26.2	25.5-35.6	-2.8-9.1
9.00	61.3-67.8	14.3-24.7	1.0-12.8	33.0-44.4	1.6-13.1	55.8-64.8	7.6-18.9	7.6-19.0	19.0-29.2	27.9-37.9	-0.1-11.5
9.33	65.5-71.7	16.2-26.4	4.6-16.0	34.8-46.4	4.6-16.0	58.0-66.7	10.7-21.7	10.6-21.7	22.8-32.7	31.1-40.9	2.8-14.1
9.67	69.9-75.7	17.0-27.2	8.0-19.1	37.0-48.6	7.7-18.9	60.3-68.9	13.5-24.4	13.2-24.2	26.4-36.2	34.2-43.9	5.6-16.7
10.00	73.8-79.2	16.8-27.2	10.1-21.2	39.1-50.7	9.8-20.9	62.3-70.8	15.4-26.2	14.9-25.8	29.2-39.0	36.4-46.2	7.5-18.6

Table F.79: South / Temp. Gradient at 2cm / Mid-day

i \ j	1	2	3	4	5	6	7	8	9	10	11
1	1.9-6.1	-0.2-4.3	-0.8-2.4	3.3-8.4	-1.2-2.9	-3.0-3.5	1.1-5.3	0.8-4.9	-0.1-4.5	-2.0-3.3	-0.8-2.6
2	-0.2-4.3	3.0-4.6	-1.0-0.9	-1.4-1.2	-0.5-1.7	2.2-5.9	-0.7-1.6	-0.9-1.2	-0.3-2.2	0.3-2.8	-1.1-0.7
3	-0.8-2.4	-1.0-0.9	-0.2-0.1	-0.0-0.7	-0.2-0.5	-0.6-1.0	-0.1-0.5	-0.2-0.5	-0.2-0.6	-0.1-0.6	-0.1-0.5
4	3.3-8.4	-1.4-1.2	-0.0-0.7	-1.2-0.3	-0.7-2.0	-1.8-2.2	-0.6-2.1	-1.0-1.7	-0.6-2.0	-0.6-2.7	-0.8-1.7
5	-1.2-2.9	-0.5-1.7	-0.2-0.5	-0.7-2.0	2.9-4.2	-1.9-1.3	-1.3-0.9	-1.6-0.5	-1.4-0.8	-1.2-1.2	-1.3-0.5
6	-3.0-3.5	2.2-5.9	-0.6-1.0	-1.8-2.2	-1.9-1.3	4.4-7.8	-2.1-1.7	-1.5-2.1	-0.3-3.9	0.3-5.0	-0.9-2.3
7	1.1-5.3	-0.7-1.6	-0.1-0.5	-0.6-2.1	-1.3-0.9	-2.1-1.7	-0.8-0.7	-0.2-2.3	-1.4-1.4	-0.9-1.8	-0.9-1.4
8	0.8-4.9	-0.9-1.2	-0.2-0.5	-1.0-1.7	-1.6-0.5	-1.5-2.1	-0.2-2.3	-0.7-0.6	-1.4-1.1	-1.3-1.2	-1.0-1.2
9	-0.1-4.5	-0.3-2.2	-0.2-0.6	-0.6-2.0	-1.4-0.8	-0.3-3.9	-1.4-1.4	-1.4-1.1	0.5-2.0	0.8-3.5	0.1-2.4
10	-2.0-3.3	0.3-2.8	-0.1-0.6	-0.6-2.7	-1.2-1.2	0.3-5.0	-0.9-1.8	-1.3-1.2	0.8-3.5	0.3-2.0	-0.3-2.0
11	-0.8-2.6	-1.1-0.7	-0.1-0.5	-0.8-1.7	-1.3-0.5	-0.9-2.3	-0.9-1.4	-1.0-1.2	0.1-2.4	-0.3-2.0	-0.2-0.2
Total	52.8-61.8	5.2-19.6	-8.4-7.0	25.5-40.4	-3.6-12.3	42.5-55.0	9.7-24.0	2.5-17.7	9.6-24.5	18.1-32.1	-6.7-9.2
Higher	33.6	-0.9	-3.0	23.2	0.2	33.1	10.9	5.9	7.0	14.4	-2.9

Table F.80: North / Temp. Gradient at 2cm with Time (Total-effect)

t \ i	1	2	3	4	5	6	7	8	9	10	11
0.33	44.6-50.9	22.2-28.6	-2.5-5.1	48.3-55.1	-3.7-3.7	31.5-37.9	-3.8-3.7	-3.8-3.7	9.6-16.8	9.4-16.7	-2.7-4.9
0.67	60.0-65.5	16.5-23.6	-3.3-4.8	50.2-58.0	-5.3-2.9	33.0-40.2	-5.2-2.9	-5.3-2.8	11.7-19.3	11.0-19.1	-3.7-4.4
1.00	68.3-73.4	12.1-19.7	-2.2-6.3	52.7-61.4	-5.5-3.2	34.8-42.6	-5.5-3.2	-5.5-3.1	13.7-22.0	12.8-21.4	-3.2-5.6
1.33	73.0-77.9	8.7-16.9	-2.8-6.4	54.4-63.6	-5.8-3.3	35.7-44.0	-5.8-3.3	-5.8-3.3	14.6-23.2	13.7-22.6	-3.5-5.7
1.67	76.4-81.1	6.9-15.4	-2.5-7.1	55.5-65.3	-5.5-4.1	36.6-45.2	-5.5-3.9	-5.4-4.1	15.5-24.3	14.9-24.0	-3.6-6.0
2.00	78.6-83.1	5.5-14.4	-2.7-7.3	56.0-66.0	-5.7-4.5	36.8-45.7	-5.8-4.2	-5.4-4.5	15.8-24.8	15.2-24.8	-4.1-6.0
2.33	79.7-84.1	5.1-14.4	-2.4-7.8	55.7-66.0	-4.7-5.8	36.9-46.2	-4.8-5.4	-4.3-5.8	16.5-25.6	16.0-25.9	-3.7-6.6
2.67	79.7-84.2	4.9-14.6	-3.0-7.5	55.0-65.3	-4.4-6.3	36.9-46.2	-4.3-6.0	-3.7-6.5	16.0-25.4	16.1-26.2	-4.3-6.4
3.00	78.8-83.5	5.2-15.1	-3.6-7.3	53.7-64.3	-4.0-7.0	36.7-46.1	-3.8-6.8	-3.3-7.4	15.3-24.9	15.9-26.2	-4.8-6.3
3.33	77.4-82.2	6.0-16.0	-3.8-7.3	52.1-62.9	-3.2-7.8	36.6-46.1	-3.2-7.7	-2.0-8.9	14.8-24.5	15.8-26.3	-5.0-6.3
3.67	75.4-80.5	6.3-16.7	-4.1-7.2	50.3-61.1	-3.0-8.3	36.0-45.7	-3.2-8.0	-1.0-10.1	14.2-24.0	15.4-26.0	-5.6-5.9
4.00	73.2-78.5	7.4-17.8	-4.4-7.0	48.1-59.0	-2.6-8.7	35.8-45.4	-3.1-8.3	-0.0-11.1	13.4-23.5	15.2-25.9	-5.9-5.7
4.33	71.1-76.6	8.3-18.8	-4.8-6.9	46.1-57.3	-2.5-8.9	35.5-45.3	-2.9-8.6	0.7-11.9	12.9-23.1	15.1-25.9	-6.3-5.5
4.67	69.1-74.9	9.2-19.8	-5.3-6.5	44.7-56.0	-2.9-8.7	35.2-45.1	-2.9-8.7	1.0-12.4	12.3-22.6	14.9-25.7	-7.0-5.1
5.00	67.5-73.4	10.2-20.7	-5.7-6.3	43.5-54.8	-3.3-8.5	35.2-45.1	-3.0-8.8	1.0-12.6	11.6-22.1	14.7-25.6	-7.5-4.7
5.33	66.3-72.3	11.0-21.5	-5.8-6.2	42.8-54.1	-3.4-8.4	35.4-45.4	-3.0-8.9	1.2-12.8	11.5-22.0	14.7-25.7	-7.5-4.7
5.67	65.4-71.5	11.7-22.1	-5.6-6.3	42.5-53.8	-3.6-8.2	35.8-45.8	-2.9-8.9	1.4-12.9	11.5-22.0	14.7-25.8	-7.4-4.8
6.00	64.8-70.9	12.2-22.5	-5.8-6.1	42.5-53.6	-4.0-7.8	36.0-46.0	-3.0-8.7	1.2-12.8	11.3-21.8	14.9-25.9	-7.4-4.8
6.33	64.6-70.7	12.5-22.7	-6.0-5.9	42.5-53.7	-4.6-7.1	36.3-46.2	-3.2-8.4	0.8-12.3	11.1-21.6	15.0-26.0	-7.4-4.7
6.67	64.9-70.9	12.6-22.7	-5.9-5.7	43.1-54.2	-5.2-6.5	36.6-46.4	-3.4-8.1	0.4-11.8	11.2-21.5	15.1-26.1	-7.3-4.7
7.00	65.6-71.5	12.6-22.6	-5.8-5.6	44.0-54.9	-5.7-5.9	37.0-46.8	-3.6-7.8	-0.1-11.2	11.4-21.6	15.5-26.3	-7.1-4.9
7.33	66.7-72.5	12.3-22.2	-5.6-5.7	45.2-56.1	-6.1-5.4	37.5-47.3	-3.8-7.6	-0.6-10.6	11.7-21.9	15.9-26.6	-6.8-5.0
7.67	68.3-73.8	11.7-21.7	-5.2-6.0	47.0-57.7	-6.5-4.9	38.2-47.9	-3.8-7.5	-0.9-10.2	12.3-22.3	16.5-27.1	-6.5-5.2
8.00	70.2-75.6	11.0-20.9	-4.9-6.3	49.2-59.7	-6.8-4.6	39.0-48.7	-3.7-7.5	-1.1-9.8	12.9-22.9	17.3-27.7	-6.1-5.5
8.33	72.5-77.7	10.0-19.9	-4.4-6.8	51.6-62.0	-6.9-4.5	40.1-49.8	-3.6-7.5	-1.2-9.6	13.7-23.6	18.3-28.6	-5.6-5.9
8.67	75.0-80.0	8.7-18.6	-3.7-7.3	54.0-64.4	-6.9-4.5	41.3-51.0	-3.5-7.5	-1.4-9.3	14.6-24.4	19.3-29.6	-5.1-6.4
9.00	77.8-82.6	7.0-17.1	-2.9-8.0	56.6-67.1	-6.7-4.5	42.6-52.4	-3.6-7.4	-1.7-9.0	15.7-25.4	20.4-30.7	-4.5-6.8
9.33	80.6-85.2	5.3-15.5	-2.2-8.7	59.0-69.7	-6.6-4.7	44.0-53.8	-3.7-7.3	-1.9-8.7	16.9-26.6	21.5-31.8	-3.9-7.3
9.67	83.3-87.7	3.7-14.1	-1.5-9.4	61.1-71.9	-6.2-5.0	45.2-55.2	-3.8-7.2	-2.1-8.6	18.1-27.8	22.6-32.9	-3.4-7.8
10.00	85.4-89.7	2.4-12.9	-0.9-10.0	62.9-73.7	-5.8-5.3	46.2-56.2	-3.9-7.1	-2.2-8.5	19.0-28.8	23.4-33.8	-2.9-8.3

Table F.81: North / Temp. Gradient at 2cm / Mid-day

i \ j	1	2	3	4	5	6	7	8	9	10	11
1	4.5-10.6	-2.8-1.8	-1.7-2.3	10.1-17.7	-2.7-1.6	0.1-7.8	-2.6-1.7	-2.8-1.9	-3.2-2.4	-3.1-3.3	-2.6-1.6
2	-2.8-1.8	6.9-8.9	-1.5-0.7	-2.0-1.4	-0.4-1.8	1.0-4.4	-1.0-1.4	-1.0-1.5	-1.2-1.8	-0.9-1.7	-1.3-0.9
3	-1.7-2.3	-1.5-0.7	-0.4-0.5	-0.0-1.5	-0.2-1.1	-0.1-1.7	-0.3-0.9	-0.3-1.1	-0.1-1.3	-0.4-1.1	-0.4-0.9
4	10.1-17.7	-2.0-1.4	-0.0-1.5	-0.7-2.1	-0.4-3.0	-0.5-4.1	-0.2-3.4	-0.3-3.3	-0.3-3.6	-0.3-3.5	-0.1-3.4
5	-2.7-1.6	-0.4-1.8	-0.2-1.1	-0.4-3.0	2.5-3.6	-1.2-1.2	-0.7-1.1	-1.1-0.9	-1.3-0.8	-1.3-0.8	-1.0-0.8
6	0.1-7.8	1.0-4.4	-0.1-1.7	-0.5-4.1	-1.2-1.2	0.9-3.2	-0.5-2.7	-0.6-2.9	-1.2-2.5	-0.4-3.4	-0.4-2.6
7	-2.6-1.7	-1.0-1.4	-0.3-0.9	-0.2-3.4	-0.7-1.1	-0.5-2.7	-0.2-0.6	-0.4-1.4	-0.2-1.7	-0.3-1.6	-0.4-1.3
8	-2.8-1.9	-1.0-1.5	-0.3-1.1	-0.3-3.3	-1.1-0.9	-0.6-2.9	-0.4-1.4	0.3-1.3	-1.1-1.0	-1.3-0.8	-0.8-1.1
9	-3.2-2.4	-1.2-1.8	-0.1-1.3	-0.3-3.6	-1.3-0.8	-1.2-2.5	-0.2-1.7	-1.1-1.0	-0.2-1.2	-1.3-1.4	-1.4-1.1
10	-3.1-3.3	-0.9-1.7	-0.4-1.1	-0.3-3.5	-1.3-0.8	-0.4-3.4	-0.3-1.6	-1.3-0.8	-1.3-1.4	-0.4-1.2	-1.0-1.7
11	-2.6-1.6	-1.3-0.9	-0.4-0.9	-0.1-3.4	-1.0-0.8	-0.4-2.6	-0.4-1.3	-0.8-1.1	-1.4-1.1	-1.0-1.7	-0.4-0.3
Total	67.5-73.4	10.2-20.7	-5.7-6.3	43.5-54.8	-3.3-8.5	35.2-45.1	-3.0-8.8	1.0-12.6	11.6-22.1	14.7-25.6	-7.4-4.7
Higher	47.5	4.5	-3.6	23.2	-1.8	23.4	-2.6	2.9	13.3	15.2	-4.4

Table F.82: Control / Temp. Gradient at 2cm / Mean

i \ j	1	2	3	4	5	6	7	8	9	10	11
1	-1.3-3.0	-2.1-2.1	-2.1-1.4	7.6-13.4	-1.5-2.1	-1.4-5.4	-2.3-1.5	-2.3-1.3	-3.3-2.8	-3.6-2.6	-2.2-1.3
2	-2.1-2.1	0.2-1.3	-1.0-0.5	-0.5-1.8	-0.8-0.8	3.4-6.5	-0.9-0.7	-0.8-0.8	-0.8-1.7	1.0-3.4	-1.0-0.6
3	-2.1-1.4	-1.0-0.5	-0.2-0.2	-0.5-0.5	-0.4-0.3	-0.2-1.5	-0.3-0.3	-0.5-0.3	-0.1-0.6	-0.4-0.7	-0.3-0.4
4	7.6-13.4	-0.5-1.8	-0.5-0.5	-1.2-1.2	-1.5-1.7	-2.6-2.2	-1.4-1.7	-1.9-1.4	-1.5-2.4	-1.8-2.2	-1.5-1.6
5	-1.5-2.1	-0.8-0.8	-0.4-0.3	-1.5-1.7	0.6-1.1	-1.1-1.1	-0.8-0.3	-0.7-0.3	-0.6-0.7	-0.9-0.6	-0.8-0.3
6	-1.4-5.4	3.4-6.5	-0.2-1.5	-2.6-2.2	-1.1-1.1	5.1-8.0	-1.9-1.4	-2.1-1.2	-1.8-2.8	-2.3-2.7	-2.0-1.3
7	-2.3-1.5	-0.9-0.7	-0.3-0.3	-1.4-1.7	-0.8-0.3	-1.9-1.4	-0.1-0.5	-0.6-0.6	-0.6-0.9	-0.5-0.9	-0.6-0.6
8	-2.3-1.3	-0.8-0.8	-0.5-0.3	-1.9-1.4	-0.7-0.3	-2.1-1.2	-0.6-0.6	-0.4-0.3	-0.7-0.9	-0.2-1.4	-0.4-0.8
9	-3.3-2.8	-0.8-1.7	-0.1-0.6	-1.5-2.4	-0.6-0.7	-1.8-2.8	-0.6-0.9	-0.7-0.9	-0.0-1.8	-1.1-3.3	-1.0-1.8
10	-3.6-2.6	1.0-3.4	-0.4-0.7	-1.8-2.2	-0.9-0.6	-2.3-2.7	-0.5-0.9	-0.2-1.4	-1.1-3.3	1.2-3.2	-1.1-1.8
11	-2.2-1.3	-1.0-0.6	-0.3-0.4	-1.5-1.6	-0.8-0.3	-2.0-1.3	-0.6-0.6	-0.4-0.8	-1.0-1.8	-1.1-1.8	-0.1-0.2
Total	61.1-69.2	-3.5-10.8	-9.9-5.7	44.2-56.0	-9.6-6.5	51.4-61.9	-7.9-7.1	-8.4-7.0	26.3-37.6	31.7-42.7	-10.1-5.2
Higher	53.9	-4.7	-2.4	38.5	-1.9	43.1	-0.1	-0.2	27.8	30.6	-2.2

Table F.83: South / Temp. Gradient at 2cm / Mean

i \ j	1	2	3	4	5	6	7	8	9	10	11
1	7.6-12.4	-0.9-3.2	-1.3-1.9	4.9-10.6	-1.5-2.2	-3.5-3.9	-1.0-2.7	-0.8-2.8	0.6-5.3	-2.9-2.9	-1.6-1.8
2	-0.9-3.2	0.6-1.6	-1.1-0.3	-0.8-1.4	-0.6-0.9	2.2-5.1	-0.9-0.7	-1.1-0.5	-1.0-0.9	-0.2-1.7	-1.0-0.5
3	-1.3-1.9	-1.1-0.3	-0.2-0.2	-0.4-0.5	-0.5-0.3	-0.7-1.0	-0.5-0.3	-0.5-0.3	-0.5-0.4	-0.5-0.4	-0.4-0.4
4	4.9-10.6	-0.8-1.4	-0.4-0.5	-1.0-1.1	-0.3-2.7	-1.2-3.5	-0.0-2.9	-0.5-2.4	0.2-3.5	-0.1-4.1	-0.3-2.6
5	-1.5-2.2	-0.6-0.9	-0.5-0.3	-0.3-2.7	1.6-2.4	-1.7-0.8	-1.4-0.2	-1.5-0.1	-1.2-0.6	-1.5-0.3	-1.4-0.1
6	-3.5-3.9	2.2-5.1	-0.7-1.0	-1.2-3.5	-1.7-0.8	6.5-9.8	-1.7-2.0	-1.3-2.3	-0.8-3.4	-0.3-4.9	-1.3-2.2
7	-1.0-2.7	-0.9-0.7	-0.5-0.3	-0.0-2.9	-1.4-0.2	-1.7-2.0	-0.2-0.6	-0.8-0.9	-1.1-0.7	-1.1-0.8	-1.0-0.6
8	-0.8-2.8	-1.1-0.5	-0.5-0.3	-0.5-2.4	-1.5-0.1	-1.3-2.3	-0.8-0.9	-0.4-0.5	-1.1-0.7	-1.0-0.7	-0.8-0.7
9	0.6-5.3	-1.0-0.9	-0.5-0.4	0.2-3.5	-1.2-0.6	-0.8-3.4	-1.1-0.7	-1.1-0.7	0.3-1.8	0.0-2.9	-0.3-2.0
10	-2.9-2.9	-0.2-1.7	-0.5-0.4	-0.1-4.1	-1.5-0.3	-0.3-4.9	-1.1-0.8	-1.0-0.7	0.0-2.9	0.7-2.5	-0.4-2.1
11	-1.6-1.8	-1.0-0.5	-0.4-0.4	-0.3-2.6	-1.4-0.1	-1.3-2.2	-1.0-0.6	-0.8-0.7	-0.3-2.0	-0.4-2.1	-0.1-0.4
Total	63.7-70.1	1.0-13.2	-5.6-6.9	33.9-46.0	-6.2-7.0	46.3-56.5	-2.6-10.2	-4.5-8.5	12.1-23.4	20.0-30.9	-8.4-5.1
Higher	42.2	1.1	1.0	22.0	0.0	33.8	2.5	0.9	9.1	17.5	-4.0

Table F.84: North / Temp. Gradient at 2cm / Mean

i \ j	1	2	3	4	5	6	7	8	9	10	11
1	4.9-11.7	-2.5-1.9	-1.9-1.9	15.2-23.7	-1.4-2.2	1.6-10.2	-2.2-1.4	-2.4-1.4	-3.2-2.7	-2.5-4.0	-2.7-1.3
2	-2.5-1.9	2.6-3.8	-1.2-0.5	-0.7-1.9	-1.0-0.7	0.9-3.4	-0.9-0.8	-1.0-0.8	-1.1-1.2	-1.0-0.9	-1.2-0.5
3	-1.9-1.9	-1.2-0.5	-0.4-0.3	-0.1-1.4	-0.3-0.9	-0.1-1.7	-0.3-0.9	-0.2-1.0	-0.1-1.2	-0.4-0.8	-0.3-0.9
4	15.2-23.7	-0.7-1.9	-0.1-1.4	0.2-3.1	-0.8-2.3	-0.6-4.1	-0.5-2.7	-0.5-2.6	-1.0-2.6	-0.8-2.9	-0.5-2.6
5	-1.4-2.2	-1.0-0.7	-0.3-0.9	-0.8-2.3	0.8-1.4	-1.0-0.5	-0.7-0.5	-0.7-0.5	-0.8-0.5	-1.1-0.2	-0.8-0.3
6	1.6-10.2	0.9-3.4	-0.1-1.7	-0.6-4.1	-1.0-0.5	1.4-3.8	-0.3-3.0	-0.2-3.2	-1.3-2.8	-0.3-3.7	-0.2-3.0
7	-2.2-1.4	-0.9-0.8	-0.3-0.9	-0.5-2.7	-0.7-0.5	-0.3-3.0	-0.2-0.4	-0.2-0.9	-0.1-1.1	-0.1-1.1	-0.2-0.8
8	-2.4-1.4	-1.0-0.8	-0.2-1.0	-0.5-2.6	-0.7-0.5	-0.2-3.2	-0.2-0.9	0.2-0.9	-0.7-0.7	-0.6-0.8	-0.6-0.7
9	-3.2-2.7	-1.1-1.2	-0.1-1.2	-1.0-2.6	-0.8-0.5	-1.3-2.8	-0.1-1.1	-0.7-0.7	-0.2-1.2	-1.2-1.3	-1.3-1.0
10	-2.5-4.0	-1.0-0.9	-0.4-0.8	-0.8-2.9	-1.1-0.2	-0.3-3.7	-0.1-1.1	-0.6-0.8	-1.2-1.3	-0.2-1.3	-1.3-1.2
11	-2.7-1.3	-1.2-0.5	-0.3-0.9	-0.5-2.6	-0.8-0.3	-0.2-3.0	-0.2-0.8	-0.6-0.7	-1.3-1.0	-1.3-1.2	-0.3-0.3
Total	77.1-81.8	4.3-14.7	-5.2-6.2	52.7-63.4	-5.8-5.6	39.2-48.6	-5.5-5.8	-3.7-7.5	13.4-23.2	16.3-26.7	-5.5-6.0
Higher	46.8	4.9	-2.7	28.2	-1.3	24.2	-3.9	-1.4	15.8	17.2	-1.4



Table F.85: Control / Temp. Gradient at 2cm / Maximum

i \ j	1	2	3	4	5	6	7	8	9	10	11
1	2.6-6.1	-1.6-2.8	-1.7-1.8	4.1-8.9	-1.7-2.0	0.2-6.4	-1.5-2.2	-1.9-1.8	0.8-5.7	-1.1-3.9	-1.7-2.0
2	-1.6-2.8	4.3-6.0	-1.0-0.7	-0.6-2.0	-0.8-0.9	3.8-9.2	-0.9-0.8	-0.6-1.1	-0.8-2.0	1.5-4.7	-0.9-0.8
3	-1.7-1.8	-1.0-0.7	-0.3-0.2	-0.4-0.8	-0.4-0.5	-0.8-2.8	-0.3-0.5	-0.4-0.5	-0.1-1.1	-0.2-1.2	-0.3-0.5
4	4.1-8.9	-0.6-2.0	-0.4-0.8	-1.0-1.1	-1.2-2.2	-2.8-2.3	-2.0-1.4	-1.4-2.1	-1.9-1.8	-1.6-2.2	-1.2-2.2
5	-1.7-2.0	-0.8-0.9	-0.4-0.5	-1.2-2.2	0.0-0.6	-1.1-2.6	-0.6-0.5	-0.5-0.6	-0.6-0.7	-0.9-0.9	-0.6-0.5
6	0.2-6.4	3.8-9.2	-0.8-2.8	-2.8-2.3	-1.1-2.6	11.8-15.7	-1.3-1.5	-1.6-1.2	-1.1-3.6	-0.7-4.6	-1.7-1.1
7	-1.5-2.2	-0.9-0.8	-0.3-0.5	-2.0-1.4	-0.6-0.5	-1.3-1.5	0.1-0.9	-0.8-0.6	-0.8-0.9	-0.8-1.2	-0.7-0.6
8	-1.9-1.8	-0.6-1.1	-0.4-0.5	-1.4-2.1	-0.5-0.6	-1.6-1.2	-0.8-0.6	-0.1-0.5	-0.9-0.8	-0.2-1.7	-0.6-0.7
9	0.8-5.7	-0.8-2.0	-0.1-1.1	-1.9-1.8	-0.6-0.7	-1.1-3.6	-0.8-0.9	-0.9-0.8	1.4-3.4	0.7-4.5	-1.7-1.2
10	-1.1-3.9	1.5-4.7	-0.2-1.2	-1.6-2.2	-0.9-0.9	-0.7-4.6	-0.8-1.2	-0.2-1.7	0.7-4.5	3.5-5.6	-1.4-1.4
11	-1.7-2.0	-0.9-0.8	-0.3-0.5	-1.2-2.2	-0.6-0.5	-1.7-1.1	-0.7-0.6	-0.6-0.7	-1.7-1.2	-1.4-1.4	-0.2-0.3
Total	40.4-52.5	3.1-18.3	-11.5-6.3	21.6-33.9	-11.3-6.4	46.9-58.0	-9.2-8.3	-9.0-8.3	18.3-32.2	20.8-34.4	-11.1-6.5
Higher	26.4	-5.9	-5.0	19.3	-4.2	24.5	-1.3	-1.7	14.9	12.3	-2.5

Table F.86: South / Temp. Gradient at 2cm / Maximum

i \ j	1	2	3	4	5	6	7	8	9	10	11
1	15.9-20.6	-1.9-2.9	-0.8-2.4	0.9-5.5	-0.8-2.5	0.6-7.3	-1.3-2.1	-1.1-2.1	2.4-6.6	-0.6-4.4	-1.0-2.1
2	-1.9-2.9	6.2-7.9	-1.1-0.8	-1.2-1.1	-0.9-1.1	0.1-4.5	-0.9-1.1	-1.3-0.7	-0.9-1.5	-0.1-2.4	-1.0-0.9
3	-0.8-2.4	-1.1-0.8	-0.4-0.3	-0.7-0.5	-0.6-0.7	-1.5-1.2	-0.5-0.8	-0.5-0.8	-0.4-0.8	-0.5-0.7	-0.5-0.7
4	0.9-5.5	-1.2-1.1	-0.7-0.5	-0.8-0.7	-1.7-0.9	-2.0-1.7	-1.5-1.1	-1.2-1.5	-1.6-1.2	-1.8-1.4	-1.2-1.6
5	-0.8-2.5	-0.9-1.1	-0.6-0.7	-1.7-0.9	0.4-1.2	-1.9-1.1	-0.9-0.6	-1.0-0.4	-0.8-0.7	-1.1-0.4	-1.0-0.4
6	0.6-7.3	0.1-4.5	-1.5-1.2	-2.0-1.7	-1.9-1.1	12.2-15.4	-1.0-1.8	-1.3-1.6	-1.2-2.4	-0.4-3.4	-1.3-1.4
7	-1.3-2.1	-0.9-1.1	-0.5-0.8	-1.5-1.1	-0.9-0.6	-1.0-1.8	0.5-1.4	-0.9-0.8	-0.7-1.0	-1.1-0.9	-1.1-0.6
8	-1.1-2.1	-1.3-0.7	-0.5-0.8	-1.2-1.5	-1.0-0.4	-1.3-1.6	-0.9-0.8	0.3-1.2	-0.9-0.7	-1.1-0.6	-1.0-0.6
9	2.4-6.6	-0.9-1.5	-0.4-0.8	-1.6-1.2	-0.8-0.7	-1.2-2.4	-0.7-1.0	-0.9-0.7	1.2-2.7	-0.7-1.8	-1.3-1.0
10	-0.6-4.4	-0.1-2.4	-0.5-0.7	-1.8-1.4	-1.1-0.4	-0.4-3.4	-1.1-0.9	-1.1-0.6	-0.7-1.8	2.4-4.0	-1.0-1.3
11	-1.0-2.1	-1.0-0.9	-0.5-0.7	-1.2-1.6	-1.0-0.4	-1.3-1.4	-1.1-0.6	-1.0-0.6	-1.3-1.0	-1.0-1.3	-0.1-0.3
Total	51.2-59.3	6.2-18.7	-5.7-7.7	8.4-21.8	-8.5-5.6	39.2-49.6	-8.1-6.1	-7.7-6.3	5.5-18.2	8.7-20.9	-6.5-7.1
Higher	19.8	1.6	-0.0	12.9	-1.4	22.4	-2.4	-1.2	4.2	7.2	0.1

Table F.87: North / Temp. Gradient at 2cm / Maximum

i \ j	1	2	3	4	5	6	7	8	9	10	11
1	21.4-27.6	-2.2-3.0	-1.7-1.9	8.6-15.1	-1.8-1.7	0.7-6.8	-1.3-2.3	-2.0-1.6	2.1-7.3	-0.8-4.1	-1.7-2.0
2	-2.2-3.0	11.5-14.1	-1.8-0.7	-2.0-1.8	-1.5-0.9	0.1-3.8	-1.2-1.3	-1.0-1.5	-2.0-1.3	-1.8-1.2	-1.7-0.7
3	-1.7-1.9	-1.8-0.7	-0.1-0.6	-0.6-0.7	-0.5-0.5	-0.8-0.5	-0.5-0.7	-0.6-0.6	-0.5-0.7	-0.7-0.6	-0.6-0.6
4	8.6-15.1	-2.0-1.8	-0.6-0.7	-0.8-1.4	-0.4-2.8	-0.3-3.3	-0.2-3.1	-0.0-3.1	-0.4-3.0	-0.2-3.1	-0.2-3.0
5	-1.8-1.7	-1.5-0.9	-0.5-0.5	-0.4-2.8	0.6-1.3	-1.1-0.4	-0.9-0.5	-0.9-0.4	-1.2-0.4	-1.2-0.3	-1.0-0.3
6	0.7-6.8	0.1-3.8	-0.8-0.5	-0.3-3.3	-1.1-0.4	1.4-3.5	-0.2-2.7	-0.2-2.6	-0.7-2.5	-0.1-3.1	-0.4-2.4
7	-1.3-2.3	-1.2-1.3	-0.5-0.7	-0.2-3.1	-0.9-0.5	-0.2-2.7	0.5-1.3	-0.5-0.9	-0.6-0.9	-0.6-1.0	-0.7-0.7
8	-2.0-1.6	-1.0-1.5	-0.6-0.6	-0.0-3.1	-0.9-0.4	-0.2-2.6	-0.5-0.9	1.3-2.3	-1.5-0.4	-1.4-0.6	-1.4-0.4
9	2.1-7.3	-2.0-1.3	-0.5-0.7	-0.4-3.0	-1.2-0.4	-0.7-2.5	-0.6-0.9	-1.5-0.4	-0.0-1.6	-1.4-1.7	-1.8-1.1
10	-0.8-4.1	-1.8-1.2	-0.7-0.6	-0.2-3.1	-1.2-0.3	-0.1-3.1	-0.6-1.0	-1.4-0.6	-1.4-1.7	-0.2-1.3	-1.2-1.5
11	-1.7-2.0	-1.7-0.7	-0.6-0.6	-0.2-3.0	-1.0-0.3	-0.4-2.4	-0.7-0.7	-1.4-0.4	-1.8-1.1	-1.2-1.5	-0.3-0.2
Total	64.3-70.9	12.2-23.9	-8.7-5.2	26.3-37.1	-9.0-5.1	21.7-33.2	-7.7-6.3	-5.5-8.2	5.9-18.3	3.3-16.2	-5.4-7.8
Higher	20.4	4.8	-1.5	9.8	-1.8	12.4	-5.3	-1.8	5.8	5.3	0.2

Table F.88: Control / Temp. Gradient at 2cm / Minimum

i \ j	1	2	3	4	5	6	7	8	9	10	11
1	0.2-3.4	-3.4-1.5	-3.8-0.8	-1.3-5.0	-3.9-0.7	1.8-7.9	-3.9-0.8	-3.7-0.9	-2.8-2.6	-3.0-2.3	-3.6-1.0
2	-3.4-1.5	9.7-11.8	-1.6-0.5	0.3-5.3	-1.4-0.7	-0.5-3.3	-1.3-0.8	-1.4-0.8	-1.6-1.3	-1.0-1.9	-1.5-0.7
3	-3.8-0.8	-1.6-0.5	-0.2-0.4	-2.8-0.2	-0.8-0.4	-1.1-0.7	-0.8-0.4	-0.8-0.4	-0.8-0.5	-1.0-0.3	-0.8-0.4
4	-1.3-5.0	0.3-5.3	-2.8-0.2	19.4-23.3	-1.8-1.3	0.6-6.7	-1.6-1.5	-1.7-1.4	-1.9-2.2	-2.5-2.1	-1.7-1.4
5	-3.9-0.7	-1.4-0.7	-0.8-0.4	-1.8-1.3	-0.1-0.4	-1.1-0.3	-0.7-0.2	-0.7-0.2	-0.6-0.3	-0.7-0.3	-0.7-0.2
6	1.8-7.9	-0.5-3.3	-1.1-0.7	0.6-6.7	-1.1-0.3	6.2-9.3	-2.3-2.0	-2.1-2.1	-1.7-3.1	-3.2-2.0	-2.3-1.9
7	-3.9-0.8	-1.3-0.8	-0.8-0.4	-1.6-1.5	-0.7-0.2	-2.3-2.0	-0.3-0.2	-0.4-0.7	-0.4-0.7	-0.4-0.7	-0.4-0.7
8	-3.7-0.9	-1.4-0.8	-0.8-0.4	-1.7-1.4	-0.7-0.2	-2.1-2.1	-0.4-0.7	-0.3-0.3	-0.5-0.7	-0.5-0.7	-0.5-0.6
9	-2.8-2.6	-1.6-1.3	-0.8-0.5	-1.9-2.2	-0.6-0.3	-1.7-3.1	-0.4-0.7	-0.5-0.7	-0.7-1.1	-1.5-2.2	-1.4-2.0
10	-3.0-2.3	-1.0-1.9	-1.0-0.3	-2.5-2.1	-0.7-0.3	-3.2-2.0	-0.4-0.7	-0.5-0.7	-1.5-2.2	0.3-2.4	-1.9-1.9
11	-3.6-1.0	-1.5-0.7	-0.8-0.4	-1.7-1.4	-0.7-0.2	-2.3-1.9	-0.4-0.7	-0.5-0.6	-1.4-2.0	-1.9-1.9	-0.2-0.2
Total	31.6-39.4	16.6-25.0	-4.3-5.5	46.2-52.7	-5.3-4.6	35.5-43.1	-4.7-5.1	-4.8-5.1	10.0-19.1	14.8-23.3	-4.7-5.1
Higher	35.7	8.4	5.4	21.8	3.4	22.3	2.1	2.1	13.3	18.4	2.3

Table F.89: South / Temp. Gradient at 2cm / Minimum

i \ j	1	2	3	4	5	6	7	8	9	10	11
1	1.8-4.8	-3.0-2.2	-4.2-0.4	-0.8-5.1	-4.1-0.6	1.9-8.3	-4.1-0.6	-3.9-0.7	-3.4-1.6	-2.7-2.3	-4.2-0.4
2	-3.0-2.2	15.5-18.4	-2.3-0.1	-0.3-4.9	-1.9-0.5	0.5-5.5	-2.0-0.5	-1.9-0.6	-2.0-0.8	-1.7-1.4	-2.1-0.3
3	-4.2-0.4	-2.3-0.1	-0.0-0.8	-2.3-0.7	-1.6-0.1	-1.4-1.1	-1.6-0.1	-1.6-0.1	-1.7-0.1	-1.9-0.0	-1.6-0.2
4	-0.8-5.1	-0.3-4.9	-2.3-0.7	15.7-19.0	-2.0-1.2	-0.1-6.2	-1.9-1.3	-1.8-1.4	-2.0-1.7	-1.9-2.1	-1.9-1.3
5	-4.1-0.6	-1.9-0.5	-1.6-0.1	-2.0-1.2	-0.5-0.3	-1.2-1.4	-1.0-0.6	-1.0-0.7	-1.0-0.7	-0.7-1.0	-1.0-0.7
6	1.9-8.3	0.5-5.5	-1.4-1.1	-0.1-6.2	-1.2-1.4	10.8-14.1	-2.1-2.0	-2.1-2.1	-1.8-2.8	-1.6-3.3	-2.2-1.9
7	-4.1-0.6	-2.0-0.5	-1.6-0.1	-1.9-1.3	-1.0-0.6	-2.1-2.0	-0.4-0.6	-1.2-0.9	-1.2-1.0	-1.5-0.8	-1.2-0.9
8	-3.9-0.7	-1.9-0.6	-1.6-0.1	-1.8-1.4	-1.0-0.7	-2.1-2.1	-1.2-0.9	-0.5-0.4	-0.7-1.1	-0.8-1.0	-0.7-1.1
9	-3.4-1.6	-2.0-0.8	-1.7-0.1	-2.0-1.7	-1.0-0.7	-1.8-2.8	-1.2-1.0	-0.7-1.1	-0.9-0.6	-1.3-1.7	-1.3-1.5
10	-2.7-2.3	-1.7-1.4	-1.9-0.0	-1.9-2.1	-0.7-1.0	-1.6-3.3	-1.5-0.8	-0.8-1.0	-1.3-1.7	1.4-3.2	-1.5-1.9
11	-4.2-0.4	-2.1-0.3	-1.6-0.2	-1.9-1.3	-1.0-0.7	-2.2-1.9	-1.2-0.9	-0.7-1.1	-1.3-1.5	-1.5-1.9	-0.2-0.7
Total	29.3-37.7	25.5-33.6	-3.8-6.5	34.8-42.3	-3.7-6.6	37.1-44.8	-2.8-7.5	-3.5-6.9	3.2-13.3	8.8-18.4	-3.8-6.6
Higher	33.4	12.5	9.6	15.8	5.5	16.3	6.7	4.7	10.1	11.5	4.9

Table F.90: North / Temp. Gradient at 2cm / Minimum

i \ j	1	2	3	4	5	6	7	8	9	10	11
1	0.1-4.6	-2.0-3.2	-2.2-2.8	5.7-13.0	-2.5-2.4	5.1-12.4	-2.8-2.1	-2.3-2.7	-2.8-2.9	-1.8-4.0	-2.8-2.1
2	-2.0-3.2	8.6-10.9	-1.0-1.1	0.7-5.8	-0.7-1.1	0.6-4.9	-1.0-1.0	-0.7-1.3	-1.2-1.3	-1.1-1.5	-0.8-1.1
3	-2.2-2.8	-1.0-1.1	-0.3-0.5	-2.1-1.0	-1.2-0.6	-1.2-1.2	-0.6-0.9	-1.2-0.6	-1.1-0.6	-0.7-0.9	-1.2-0.6
4	5.7-13.0	0.7-5.8	-2.1-1.0	14.0-18.0	-2.2-1.9	-1.3-6.1	-2.2-2.0	-2.1-2.1	-2.0-3.1	-2.0-3.4	-2.4-1.8
5	-2.5-2.4	-0.7-1.1	-1.2-0.6	-2.2-1.9	-0.1-0.2	-1.0-0.6	-0.3-0.2	-0.3-0.3	-0.3-0.3	-0.4-0.2	-0.3-0.3
6	5.1-12.4	0.6-4.9	-1.2-1.2	-1.3-6.1	-1.0-0.6	7.3-10.5	-1.8-2.1	-1.6-2.4	-1.3-3.4	-2.0-2.9	-1.8-2.1
7	-2.8-2.1	-1.0-1.0	-0.6-0.9	-2.2-2.0	-0.3-0.2	-1.8-2.1	-0.3-0.3	-0.5-0.6	-0.8-0.5	-0.5-0.6	-0.5-0.6
8	-2.3-2.7	-0.7-1.3	-1.2-0.6	-2.1-2.1	-0.3-0.3	-1.6-2.4	-0.5-0.6	-0.3-0.2	-0.5-0.7	-0.6-0.6	-0.6-0.6
9	-2.8-2.9	-1.2-1.3	-1.1-0.6	-2.0-3.1	-0.3-0.3	-1.3-3.4	-0.8-0.5	-0.5-0.7	-0.7-0.9	-0.4-2.2	-0.2-2.2
10	-1.8-4.0	-1.1-1.5	-0.7-0.9	-2.0-3.4	-0.4-0.2	-2.0-2.9	-0.5-0.6	-0.6-0.6	-0.4-2.2	0.7-2.4	-1.6-1.3
11	-2.8-2.1	-0.8-1.1	-1.2-0.6	-2.4-1.8	-0.3-0.3	-1.8-2.1	-0.5-0.6	-0.6-0.6	-0.2-2.2	-1.6-1.3	-0.1-0.2
Total	42.9-51.8	16.1-26.0	-3.5-7.9	45.3-53.2	-6.3-5.3	35.1-43.8	-5.5-6.1	-5.1-6.4	5.4-16.2	10.8-21.2	-5.4-6.1
Higher	25.4	3.8	3.2	18.1	0.1	14.6	0.4	0.0	7.4	11.2	0.0

### F.8 Temperature Gradient at 5 cm

Table F.91: Control / Temp. Gradient at 5cm with Time (Total-effect)

t \ i	1	2	3	4	5	6	7	8	9	10	11
0.33	18.9-23.5	4.5-9.5	-2.9-2.5	46.7-50.5	-3.3-2.1	41.4-45.4	-3.3-2.1	-3.3-2.1	10.4-15.3	15.9-20.6	-2.4-2.9
0.67	25.4-30.2	5.4-10.6	-3.2-2.2	48.9-53.0	-2.2-3.2	40.5-44.7	-2.2-3.2	-2.2-3.2	11.9-16.8	16.3-21.1	-2.8-2.6
1.00	29.8-34.6	6.9-12.3	-3.3-2.4	50.1-54.5	-2.3-3.3	39.6-44.2	-2.3-3.4	-2.3-3.3	13.2-18.3	17.0-22.0	-3.1-2.6
1.33	32.9-37.9	8.0-13.7	-3.6-2.5	50.9-55.7	-2.5-3.5	37.8-42.7	-2.4-3.5	-2.5-3.4	13.8-19.2	17.4-22.6	-3.6-2.4
1.67	35.4-40.6	9.1-15.0	-3.5-3.0	51.7-56.8	-3.9-2.5	36.0-41.2	-3.6-2.7	-3.9-2.6	14.5-20.2	17.9-23.4	-3.7-2.6
2.00	37.3-42.8	10.0-16.3	-3.7-3.2	52.3-57.6	-3.5-3.4	33.8-39.5	-3.0-3.7	-3.4-3.4	14.8-20.8	17.9-23.8	-4.0-2.9
2.33	38.9-44.5	10.8-17.4	-3.9-3.4	52.4-58.1	-2.8-4.7	31.8-37.9	-2.4-4.8	-2.9-4.3	14.9-21.1	17.7-23.9	-4.3-2.9
2.67	40.1-45.9	11.6-18.3	-4.0-3.6	52.3-58.2	-1.8-6.0	30.3-36.6	-1.5-5.9	-2.3-5.2	14.9-21.3	17.6-24.1	-4.6-2.9
3.00	41.0-46.9	12.0-18.9	-4.3-3.6	51.7-57.8	-0.5-7.6	29.1-35.7	-1.0-6.7	-2.0-5.8	14.7-21.4	17.4-24.2	-4.9-3.0
3.33	41.6-47.6	12.1-19.1	-4.8-3.5	50.8-57.2	0.6-8.9	28.3-35.2	-0.7-7.3	-1.9-6.1	14.4-21.4	17.3-24.3	-3.1-5.0
3.67	42.0-48.1	11.9-19.2	-5.2-3.4	49.8-56.5	1.9-10.5	27.9-35.1	-0.3-7.9	-1.8-6.5	14.4-21.6	17.4-24.6	-3.4-4.9
4.00	42.3-48.5	11.7-19.2	-5.7-3.3	48.6-55.5	2.9-11.7	27.8-35.3	-0.1-8.4	-1.8-6.7	14.5-21.8	17.4-24.8	-3.8-4.8
4.33	42.6-48.9	11.3-19.0	-3.4-5.5	47.7-54.8	3.6-12.7	28.1-35.7	-0.4-8.6	-2.1-6.8	14.7-22.2	17.8-25.3	-4.2-4.6
4.67	42.8-49.3	10.8-18.7	-3.8-5.5	46.5-53.9	4.2-13.5	28.7-36.5	-0.4-8.7	-2.4-6.8	14.9-22.6	18.4-26.1	-4.6-4.6
5.00	43.0-49.5	9.9-18.1	-4.3-5.3	45.3-52.9	4.2-13.9	29.4-37.5	-0.8-8.6	-2.9-6.6	15.2-23.1	19.0-26.9	-5.0-4.4
5.33	43.2-49.9	8.9-17.4	-4.9-5.1	44.2-52.1	4.0-13.9	30.5-38.7	-1.4-8.3	-3.6-6.3	15.6-23.6	19.7-27.8	-5.5-4.3
5.67	43.4-50.3	8.1-16.8	-5.3-5.0	43.3-51.3	3.5-13.8	32.0-40.3	-2.0-8.1	-4.1-6.0	16.1-24.3	20.6-28.8	-5.8-4.3
6.00	43.7-50.6	7.1-16.0	-5.6-4.9	42.3-50.5	2.8-13.3	33.8-42.1	-2.6-7.6	-4.7-5.7	16.7-25.0	21.6-29.9	-6.1-4.2
6.33	44.0-51.0	6.0-15.2	-6.0-4.8	41.4-49.7	1.7-12.4	35.8-44.2	-3.4-7.1	-5.3-5.4	17.2-25.6	22.7-31.0	-6.5-4.1
6.67	44.3-51.3	5.0-14.3	-6.3-4.6	40.5-49.0	0.5-11.4	38.2-46.5	-4.2-6.5	-5.8-5.1	17.8-26.3	23.8-32.2	-6.7-4.1
7.00	44.5-51.6	4.1-13.6	-6.5-4.6	39.9-48.3	-1.0-10.1	40.8-48.9	-4.9-6.0	-6.1-4.9	18.5-27.0	25.0-33.4	-6.8-4.1
7.33	44.6-51.8	3.4-12.9	-6.5-4.6	39.3-47.8	-2.3-8.8	43.5-51.4	-5.5-5.5	-6.2-4.8	19.2-27.6	26.1-34.5	-6.8-4.2
7.67	44.8-52.0	2.8-12.4	-6.4-4.7	38.9-47.3	-3.6-7.5	46.3-53.9	-5.9-5.2	-6.2-4.8	19.9-28.3	27.3-35.6	-6.6-4.3
8.00	45.1-52.2	2.4-12.0	-6.3-4.8	38.8-47.1	-4.7-6.3	49.0-56.3	-6.1-4.9	-6.1-4.8	20.5-28.9	28.3-36.5	-6.4-4.4
8.33	45.6-52.6	2.4-11.9	-5.8-5.0	38.8-47.1	-5.4-5.5	51.7-58.8	-5.9-5.0	-5.5-5.2	21.3-29.6	29.2-37.3	-5.9-4.8
8.67	46.2-53.2	2.9-12.1	-5.1-5.5	39.1-47.3	-5.7-5.0	54.1-61.0	-5.3-5.4	-4.8-5.8	22.1-30.4	30.0-38.1	-5.2-5.3
9.00	47.1-54.0	3.4-12.6	-4.4-6.2	39.5-47.8	-5.7-4.9	56.2-63.0	-4.7-6.0	-3.8-6.5	23.3-31.6	30.8-38.8	-4.4-6.0
9.33	48.0-55.1	4.1-13.3	-6.6-4.2	40.2-48.7	-5.5-5.0	57.9-64.6	-4.0-6.6	-3.2-7.1	24.6-32.9	31.8-39.7	-6.7-3.9
9.67	49.3-56.3	4.7-13.9	-5.9-4.9	41.2-49.8	-5.4-5.3	59.2-65.9	-3.5-7.1	-2.9-7.5	25.9-34.2	32.6-40.6	-6.1-4.6
10.00	50.9-57.8	5.0-14.3	-5.6-5.3	42.5-51.2	-5.2-5.4	60.0-66.8	-3.3-7.3	-2.9-7.6	27.0-35.4	33.3-41.3	-5.7-5.0

Table F.92: Control / Temp. Gradient at 5cm / Mid-day

i \ j	1	2	3	4	5	6	7	8	9	10	11
1	5.6-9.1	-2.7-1.8	-2.6-1.3	4.6-10.5	-3.3-1.2	-2.6-3.2	-2.9-1.1	-2.9-1.1	-2.5-2.7	-2.6-3.0	-2.8-0.9
2	-2.7-1.8	1.9-3.6	-1.3-0.2	0.2-4.1	-0.3-1.5	0.7-3.2	-1.3-0.4	-1.8-0.1	-1.2-1.1	-0.8-1.5	-1.2-0.3
3	-2.6-1.3	-1.3-0.2	-0.2-0.2	-0.8-1.2	-0.4-0.5	-0.6-0.6	-0.3-0.5	-0.3-0.5	-0.4-0.3	-0.5-0.4	-0.3-0.4
4	4.6-10.5	0.2-4.1	-0.8-1.2	12.0-15.1	-0.5-2.6	-2.2-2.4	-1.1-1.8	-1.4-1.4	-1.5-2.3	-2.2-1.8	-1.0-1.6
5	-3.3-1.2	-0.3-1.5	-0.4-0.5	-0.5-2.6	4.7-6.4	-1.9-1.7	-1.3-1.5	-1.5-1.2	-1.5-1.6	-1.9-1.4	-1.7-1.0
6	-2.6-3.2	0.7-3.2	-0.6-0.6	-2.2-2.4	-1.9-1.7	2.9-5.4	-2.6-2.0	-2.8-1.8	-2.8-2.1	-2.5-2.7	-1.8-2.7
7	-2.9-1.1	-1.3-0.4	-0.3-0.5	-1.1-1.8	-1.3-1.5	-2.6-2.0	-0.5-0.5	-0.5-1.3	-0.6-1.4	-0.7-1.3	-0.5-1.3
8	-2.9-1.1	-1.8-0.1	-0.3-0.5	-1.4-1.4	-1.5-1.2	-2.8-1.8	-0.5-1.3	-0.4-0.5	-1.1-0.8	-0.6-1.4	-0.7-1.0
9	-2.5-2.7	-1.2-1.1	-0.4-0.3	-1.5-2.3	-1.5-1.6	-2.8-2.1	-0.6-1.4	-1.1-0.8	0.2-1.9	-0.4-3.2	-1.0-1.9
10	-2.6-3.0	-0.8-1.5	-0.5-0.4	-2.2-1.8	-1.9-1.4	-2.5-2.7	-0.7-1.3	-0.6-1.4	-0.4-3.2	1.4-3.1	-2.2-1.0
11	-2.8-0.9	-1.2-0.3	-0.3-0.4	-1.0-1.6	-1.7-1.0	-1.8-2.7	-0.5-1.3	-0.7-1.0	-1.0-1.9	-2.2-1.0	0.0-0.3
Total	43.0-49.5	9.9-18.1	-4.3-5.3	45.3-52.9	4.2-13.9	29.4-37.5	-0.8-8.6	-2.9-6.6	15.2-23.1	19.0-26.9	-5.0-4.4
Higher	35.6	9.1	1.3	23.7	3.4	27.7	3.5	3.3	15.9	19.1	0.2

Table F.93: South / Temp. Gradient at 5cm with Time (Total-effect)

t \ i	1	2	3	4	5	6	7	8	9	10	11
0.33	26.3-31.5	8.2-14.1	-2.5-3.8	36.2-41.1	-2.9-3.4	41.9-46.4	-2.9-3.4	-2.9-3.4	5.9-11.8	11.1-16.9	-2.1-4.2
0.67	33.3-38.2	9.5-15.2	-2.4-3.7	37.5-42.6	-3.0-3.1	38.7-43.4	-3.0-3.1	-3.0-3.1	6.6-12.4	11.6-17.3	-2.2-3.9
1.00	36.7-41.7	10.4-16.3	-3.1-3.3	38.0-43.4	-3.7-2.7	36.0-41.0	-3.5-2.9	-3.7-2.7	6.3-12.3	11.4-17.4	-2.8-3.6
1.33	38.7-43.7	11.4-17.6	-3.5-3.2	38.7-44.3	-3.8-2.9	32.8-38.3	-3.2-3.5	-3.8-2.9	6.4-12.6	11.1-17.4	-3.3-3.4
1.67	40.1-45.3	13.1-19.4	-3.4-3.6	39.0-44.8	-2.8-4.2	29.7-35.6	-2.0-5.0	-2.9-4.1	6.4-12.9	10.8-17.4	-3.2-3.8
2.00	41.4-46.7	14.6-21.1	-2.9-4.2	39.1-45.1	-1.0-6.2	26.9-33.1	-0.0-7.0	-1.2-5.9	6.7-13.4	10.6-17.3	-2.8-4.5
2.33	42.6-48.0	15.8-22.3	-2.8-4.6	38.8-44.9	1.1-8.4	24.4-30.9	1.6-8.8	0.1-7.3	6.7-13.6	10.1-17.1	-2.5-4.9
2.67	43.3-48.7	16.7-23.3	-2.8-4.7	38.1-44.4	3.2-10.6	22.5-29.2	2.8-10.1	0.8-8.1	6.3-13.5	9.5-16.8	-2.6-5.0
3.00	43.3-48.9	17.0-23.8	-3.1-4.7	37.0-43.5	5.2-12.6	20.8-27.9	3.4-10.9	1.1-8.6	5.8-13.1	8.9-16.2	-2.9-4.9
3.33	43.0-48.8	17.2-24.1	-3.4-4.5	35.8-42.5	7.3-14.7	19.7-27.0	3.9-11.6	1.5-9.1	5.3-12.8	8.4-15.9	-3.2-4.8
3.67	42.7-48.6	17.1-24.2	-3.7-4.3	34.8-41.8	9.3-16.7	19.2-26.6	4.3-12.1	1.8-9.5	5.1-12.8	8.2-15.9	-3.5-4.7
4.00	42.5-48.5	17.0-24.2	-4.0-4.2	34.0-41.1	11.0-18.6	18.9-26.5	4.6-12.6	2.0-9.8	5.0-12.8	8.2-16.0	-3.7-4.6
4.33	42.4-48.5	16.8-24.0	-4.3-4.0	33.3-40.6	12.5-20.1	19.0-26.7	5.0-13.0	2.2-10.1	4.9-12.9	8.4-16.3	-3.9-4.6
4.67	42.3-48.6	16.2-23.5	-4.7-3.7	32.5-40.0	13.5-21.1	19.3-27.2	5.1-13.2	2.1-10.1	4.8-13.0	8.7-16.7	-4.2-4.4
5.00	42.4-48.7	15.5-23.0	-5.0-3.5	31.8-39.4	14.3-21.9	20.1-28.1	5.1-13.3	2.0-10.2	5.0-13.2	9.2-17.2	-4.4-4.3
5.33	42.4-48.9	14.7-22.2	-5.4-3.3	31.1-38.9	14.7-22.4	21.2-29.2	5.1-13.4	1.8-10.1	5.2-13.5	9.7-17.8	-4.7-4.1
5.67	42.6-49.2	13.8-21.4	-3.3-5.3	30.5-38.5	14.8-22.6	22.7-30.8	5.0-13.4	1.6-10.0	5.4-13.8	10.3-18.5	-5.0-4.0
6.00	42.9-49.4	12.6-20.3	-3.6-5.1	29.8-37.9	14.3-22.2	24.5-32.7	4.8-13.2	1.3-9.8	5.6-14.1	11.0-19.2	-5.3-3.8
6.33	43.3-49.8	11.3-19.1	-3.8-5.1	29.2-37.5	13.3-21.4	26.8-34.9	4.3-12.8	0.8-9.5	6.0-14.5	11.8-20.1	-5.6-3.6
6.67	43.6-50.1	10.0-17.9	-3.9-4.9	28.6-37.0	12.0-20.2	29.5-37.5	3.8-12.4	0.6-9.3	6.4-14.9	12.8-21.0	-5.8-3.5
7.00	44.0-50.5	8.7-16.7	-3.8-5.1	28.1-36.6	10.4-18.7	32.6-40.5	3.4-12.0	0.4-9.2	7.0-15.5	13.9-22.0	-5.8-3.5
7.33	44.5-50.9	7.5-15.6	-3.6-5.3	27.9-36.4	8.7-17.0	36.0-43.7	2.9-11.6	0.3-9.2	7.6-16.0	15.2-23.2	-5.7-3.6
7.67	45.0-51.3	6.6-14.8	-5.7-3.5	27.7-36.2	6.8-15.2	39.6-47.1	2.6-11.3	0.6-9.4	8.3-16.5	16.5-24.5	-5.4-3.9
8.00	45.6-51.8	6.0-14.2	-4.9-4.2	27.7-36.2	5.1-13.6	43.3-50.6	2.4-11.1	1.1-9.8	8.8-17.0	17.9-25.7	-4.9-4.3
8.33	46.5-52.6	5.9-14.3	-3.8-5.2	27.8-36.4	3.9-12.5	46.9-54.0	2.6-11.4	1.8-10.6	9.6-17.8	19.3-27.2	-4.2-5.0
8.67	47.7-53.8	6.7-15.1	-2.1-6.8	28.2-36.9	3.6-12.2	50.3-57.2	3.6-12.4	3.1-12.0	11.0-19.3	21.1-29.0	-2.8-6.3
9.00	49.4-55.4	8.6-16.9	0.1-9.1	28.8-37.6	4.1-12.8	53.3-60.0	5.5-14.3	5.2-14.1	13.1-21.4	23.3-31.1	-1.0-8.1
9.33	51.4-57.3	10.7-18.9	2.4-11.4	29.4-38.4	5.2-14.0	55.7-62.3	7.8-16.6	7.5-16.4	15.5-23.9	25.5-33.3	1.0-10.1
9.67	53.6-59.4	12.5-20.7	4.7-13.6	30.4-39.5	6.4-15.4	57.6-64.3	9.9-18.7	9.6-18.5	17.8-26.3	27.6-35.4	2.9-11.9
10.00	55.8-61.6	13.7-21.8	6.2-15.2	31.6-40.9	7.4-16.5	59.0-65.8	11.3-20.1	10.8-19.8	19.7-28.2	29.2-37.0	4.2-13.2

Table F.94: South / Temp. Gradient at 5cm / Mid-day

i \ j	1	2	3	4	5	6	7	8	9	10	11
1	14.5-17.9	-0.4-4.3	-1.7-2.0	0.9-6.2	-2.2-2.3	-2.2-3.2	-2.1-2.2	-2.2-2.0	-2.4-2.0	-2.9-1.8	-1.6-2.1
2	-0.4-4.3	4.6-6.6	-1.1-0.2	-1.2-2.2	1.5-3.4	-0.1-2.1	-1.1-0.7	-1.7-0.0	-1.0-0.9	-0.9-1.1	-1.3-0.3
3	-1.7-2.0	-1.1-0.2	-0.1-0.3	-1.1-0.4	-0.5-0.6	-0.5-0.4	-0.3-0.4	-0.3-0.4	-0.3-0.4	-0.3-0.5	-0.3-0.4
4	0.9-6.2	-1.2-2.2	-1.1-0.4	10.3-12.7	-0.4-2.6	-1.4-2.2	-0.2-2.4	-0.7-1.9	-0.3-2.4	-0.4-2.4	-0.4-2.0
5	-2.2-2.3	1.5-3.4	-0.5-0.6	-0.4-2.6	9.4-11.6	-2.2-1.5	-1.4-1.9	-2.0-1.2	-1.7-1.5	-1.9-1.4	-2.1-0.8
6	-2.2-3.2	-0.1-2.1	-0.5-0.4	-1.4-2.2	-2.2-1.5	1.5-3.9	-1.3-3.1	-1.0-3.3	-1.1-3.3	-0.7-4.1	-1.6-2.7
7	-2.1-2.2	-1.1-0.7	-0.3-0.4	-0.2-2.4	-1.4-1.9	-1.3-3.1	-0.6-0.7	-0.6-1.8	-0.9-1.6	-0.5-1.9	-0.7-1.7
8	-2.2-2.0	-1.7-0.0	-0.3-0.4	-0.7-1.9	-2.0-1.2	-1.0-3.3	-0.6-1.8	-0.7-0.4	-1.0-1.1	-0.8-1.4	-0.8-1.2
9	-2.4-2.0	-1.0-0.9	-0.3-0.4	-0.3-2.4	-1.7-1.5	-1.1-3.3	-0.9-1.6	-1.0-1.1	-0.1-1.3	-0.5-2.3	-0.8-1.8
10	-2.9-1.8	-0.9-1.1	-0.3-0.5	-0.4-2.4	-1.9-1.4	-0.7-4.1	-0.5-1.9	-0.8-1.4	-0.5-2.3	0.0-1.5	-1.8-1.1
11	-1.6-2.1	-1.3-0.3	-0.3-0.4	-0.4-2.0	-2.1-0.8	-1.6-2.7	-0.7-1.7	-0.8-1.2	-0.8-1.8	-1.8-1.1	-0.3-0.3
Total	42.4-48.7	15.5-23.0	-5.0-3.5	31.8-39.4	14.3-21.9	20.1-28.1	5.1-13.3	2.0-10.2	5.0-13.2	9.2-17.2	4.4-4.3
Higher	23.7	9.5	-0.5	14.3	5.3	14.3	4.8	4.5	4.8	8.7	-1.5

Table F.95: North / Temp. Gradient at 5cm with Time (Total-effect)

t \ i	1	2	3	4	5	6	7	8	9	10	11
0.33	23.4-28.7	10.8-16.0	-1.4-4.2	51.2-55.4	-2.2-3.4	34.1-38.6	-2.2-3.4	-2.1-3.4	6.1-11.5	9.6-14.9	-1.4-4.2
0.67	32.7-37.9	10.3-15.5	-1.8-3.8	51.2-55.9	-2.9-2.7	34.0-38.7	-2.9-2.7	-2.9-2.6	6.8-12.2	10.3-15.6	-2.0-3.6
1.00	38.7-43.9	9.9-15.3	-1.3-4.4	52.1-57.2	-3.1-2.7	34.3-39.2	-3.0-2.7	-3.1-2.6	7.8-13.4	11.1-16.6	-1.7-4.1
1.33	42.1-47.3	9.6-15.1	-1.6-4.3	52.6-58.2	-3.3-2.6	34.0-39.1	-3.3-2.7	-3.3-2.7	8.1-14.0	11.2-17.1	-2.1-4.0
1.67	44.4-49.7	9.7-15.4	-1.5-4.7	53.0-58.8	-3.2-3.0	33.5-39.0	-3.0-3.1	-3.0-3.2	8.5-14.5	11.7-17.7	-2.0-4.2
2.00	46.0-51.3	9.9-15.7	-1.5-4.9	52.8-58.9	-3.1-3.3	32.7-38.2	-2.9-3.4	-2.9-3.5	8.7-14.8	11.7-17.9	-2.3-4.1
2.33	47.0-52.3	10.3-16.3	-1.4-5.2	52.5-58.6	-2.2-4.3	31.8-37.5	-2.2-4.3	-2.1-4.4	8.9-15.2	11.9-18.3	-2.1-4.4
2.67	47.8-53.1	10.6-16.7	-1.5-5.2	51.9-58.2	-1.5-5.1	30.7-36.5	-1.5-5.0	-1.5-5.1	8.8-15.1	11.8-18.3	-2.2-4.5
3.00	48.6-53.9	10.8-17.0	-1.8-5.1	51.3-57.7	-0.7-6.0	29.5-35.4	-1.1-5.6	-1.1-5.7	8.5-14.9	11.5-18.2	-2.3-4.6
3.33	49.3-54.6	10.9-17.3	-1.7-5.2	50.6-57.1	0.5-7.2	28.5-34.6	-0.5-6.3	-0.3-6.4	8.4-14.9	11.3-18.1	-2.3-4.6
3.67	50.1-55.4	10.8-17.2	-1.8-5.3	49.9-56.5	1.6-8.4	27.5-33.7	-0.4-6.6	0.2-7.0	8.1-14.7	11.1-17.9	-2.5-4.5
4.00	50.9-56.2	10.6-17.1	-2.0-5.2	49.1-55.9	2.7-9.5	26.9-33.2	-0.3-6.7	0.5-7.4	8.0-14.6	10.9-17.8	-2.7-4.4
4.33	51.7-57.0	10.3-16.9	-2.2-5.1	48.5-55.4	3.6-10.5	26.5-32.8	-0.4-6.8	0.6-7.6	7.9-14.6	10.8-17.9	-3.0-4.3
4.67	52.6-57.9	9.9-16.7	-2.5-4.9	47.9-55.0	4.1-11.2	26.4-32.8	-0.5-6.7	0.5-7.6	7.8-14.6	10.8-17.9	-3.4-4.0
5.00	53.5-58.8	9.5-16.4	-2.7-4.7	47.5-54.7	4.6-11.7	26.5-33.1	-0.9-6.5	0.3-7.6	7.7-14.6	11.0-18.2	-3.7-3.8
5.33	54.5-59.8	8.9-15.9	-3.0-4.6	47.1-54.6	4.9-12.1	27.2-33.8	-1.2-6.3	0.0-7.4	7.6-14.7	11.1-18.4	-3.9-3.7
5.67	55.6-60.9	8.3-15.5	-3.2-4.6	47.0-54.7	4.8-12.2	28.1-34.8	-1.6-6.1	-0.2-7.4	7.8-15.0	11.4-18.9	-4.1-3.7
6.00	56.7-62.0	7.6-15.0	-3.5-4.4	47.1-54.8	4.4-11.9	29.2-36.0	-2.1-5.7	-0.7-7.1	7.9-15.2	11.8-19.4	-4.5-3.6
6.33	57.9-63.2	6.9-14.4	-3.9-4.2	47.2-55.1	3.6-11.4	30.5-37.4	-2.6-5.3	-1.2-6.8	7.9-15.4	12.3-20.0	-4.8-3.4
6.67	59.1-64.5	6.2-13.9	-4.2-4.1	47.5-55.6	2.5-10.6	31.9-39.0	-3.2-5.0	-1.7-6.6	8.2-15.8	12.8-20.6	-5.1-3.4
7.00	60.5-65.9	5.7-13.5	-4.5-4.0	47.9-56.1	1.3-9.6	33.5-40.7	-3.6-4.9	-2.1-6.3	8.5-16.3	13.4-21.4	-5.3-3.4
7.33	62.0-67.3	5.2-13.2	-4.6-4.1	48.4-56.9	-0.1-8.4	35.1-42.4	-3.9-4.8	-2.2-6.3	8.8-16.8	14.0-22.1	-5.4-3.5
7.67	63.4-68.7	4.8-13.0	-4.5-4.3	49.3-57.8	-1.4-7.4	36.8-44.2	-4.0-5.0	-2.2-6.5	9.3-17.4	14.7-23.0	-5.4-3.8
8.00	64.8-70.1	4.6-12.9	-4.4-4.6	50.3-58.8	-2.6-6.5	38.4-45.8	-3.9-5.2	-2.0-6.8	9.9-18.0	15.5-23.8	-5.2-4.1
8.33	66.1-71.3	4.5-12.9	-4.1-5.0	51.3-60.0	-3.5-5.7	39.7-47.2	-3.7-5.6	-1.6-7.3	10.5-18.7	16.2-24.7	-5.0-4.4
8.67	67.3-72.6	4.4-12.9	-3.7-5.4	52.3-61.1	-4.2-5.1	40.8-48.4	-3.4-5.9	-1.3-7.6	11.1-19.4	16.9-25.5	-4.7-4.8
9.00	68.6-73.8	4.3-13.0	-3.3-5.9	53.5-62.4	-4.8-4.7	41.7-49.5	-3.2-6.2	-1.1-7.9	11.8-20.2	17.6-26.3	-4.5-5.1
9.33	69.9-75.0	4.1-12.9	-2.9-6.5	54.6-63.7	-5.1-4.5	42.6-50.4	-3.1-6.4	-1.0-8.1	12.6-21.1	18.3-27.0	-4.2-5.5
9.67	71.2-76.3	4.0-12.8	-2.4-7.0	55.9-65.1	-5.1-4.5	43.4-51.4	-3.0-6.5	-0.9-8.2	13.6-22.0	19.1-27.8	-3.8-5.9
10.00	72.6-77.6	3.9-12.7	-1.8-7.5	57.1-66.4	-5.0-4.6	44.2-52.3	-2.9-6.5	-1.0-8.2	14.4-22.9	19.7-28.6	-3.4-6.3

Table F.96: North / Temp. Gradient at 5cm / Mid-day

i \ j	1	2	3	4	5	6	7	8	9	10	11
1	11.1-15.7	-1.9-2.4	-2.4-1.6	6.3-12.5	-3.0-1.2	-2.2-4.0	-3.0-1.0	-2.8-1.5	-2.8-2.2	-2.5-2.7	-3.6-0.3
2	-1.9-2.4	1.0-2.4	-0.6-0.9	2.2-5.0	0.5-2.0	1.5-3.7	-0.6-0.9	-0.9-0.7	-0.8-1.0	-0.2-1.4	-0.6-0.8
3	-2.4-1.6	-0.6-0.9	-0.3-0.4	-0.7-1.1	-0.3-1.0	-0.2-1.3	-0.4-0.8	-0.4-0.8	-0.3-1.0	-0.4-0.9	-0.4-0.8
4	6.3-12.5	2.2-5.0	-0.7-1.1	13.4-16.5	-1.8-1.4	-1.7-2.6	-1.9-1.3	-1.2-1.9	-1.7-1.8	-1.9-1.7	-1.1-2.0
5	-3.0-1.2	0.5-2.0	-0.3-1.0	-1.8-1.4	4.2-5.5	-1.6-1.1	-1.5-0.8	-1.3-1.1	-1.2-1.2	-1.6-0.8	-1.3-0.8
6	-2.2-4.0	1.5-3.7	-0.2-1.3	-1.7-2.6	-1.6-1.1	5.0-7.2	-1.8-2.0	-1.8-2.2	-1.9-2.3	-1.7-2.6	-1.7-2.1
7	-3.0-1.0	-0.6-0.9	-0.4-0.8	-1.9-1.3	-1.5-0.8	-1.8-2.0	-0.4-0.4	-0.7-0.8	-0.6-0.9	-0.6-1.0	-0.5-0.9
8	-2.8-1.5	-0.9-0.7	-0.4-0.8	-1.2-1.9	-1.3-1.1	-1.8-2.2	-0.7-0.8	-0.2-0.7	-1.1-0.7	-0.9-1.0	-0.9-0.8
9	-2.8-2.2	-0.8-1.0	-0.3-1.0	-1.7-1.8	-1.2-1.2	-1.9-2.3	-0.6-0.9	-1.1-0.7	-0.6-0.6	-0.4-2.1	-0.5-1.8
10	-2.5-2.7	-0.2-1.4	-0.4-0.9	-1.9-1.7	-1.6-0.8	-1.7-2.6	-0.6-1.0	-0.9-1.0	-0.4-2.1	1.4-2.9	-2.1-0.7
11	-3.6-0.3	-0.6-0.8	-0.4-0.8	-1.1-2.0	-1.3-0.8	-1.7-2.1	-0.5-0.9	-0.9-0.8	-0.5-1.8	-2.1-0.7	-0.3-0.3
Total	53.5-58.8	9.5-16.4	-2.7-4.7	47.5-54.7	4.6-11.7	26.5-33.1	-0.9-6.5	0.3-7.6	7.7-14.6	11.0-18.2	-3.7-3.8
Higher	37.0	2.6	-1.0	22.3	4.2	18.4	3.4	4.0	9.2	11.2	0.9

Table F.97: Control / Temp. Gradient at 5cm / Mean

i \ j	1	2	3	4	5	6	7	8	9	10	11
1	3.3-6.7	-1.8-2.3	-2.4-1.4	5.2-10.8	-2.9-1.2	-3.1-2.9	-2.7-1.2	-2.6-1.2	-2.6-2.7	-2.6-2.8	-2.5-1.2
2	-1.8-2.3	1.0-2.1	-0.8-0.5	0.9-4.3	-0.6-0.7	1.7-4.3	-0.8-0.5	-0.9-0.4	-1.3-0.7	0.1-2.0	-0.7-0.6
3	-2.4-1.4	-0.8-0.5	-0.1-0.2	-1.1-0.9	-0.4-0.3	-0.7-1.0	-0.4-0.3	-0.4-0.3	-0.3-0.5	-0.4-0.6	-0.4-0.3
4	5.2-10.8	0.9-4.3	-1.1-0.9	13.0-16.3	-1.1-1.9	-2.5-2.8	-1.5-1.5	-1.7-1.2	-1.4-2.4	-2.2-2.0	-1.3-1.5
5	-2.9-1.2	-0.6-0.7	-0.4-0.3	-1.1-1.9	1.5-2.4	-1.4-1.2	-1.1-0.7	-1.1-0.6	-1.1-0.7	-1.3-0.7	-1.2-0.5
6	-3.1-2.9	1.7-4.3	-0.7-1.0	-2.5-2.8	-1.4-1.2	10.4-13.3	-2.5-1.6	-2.5-1.6	-1.7-3.1	-1.6-3.6	-2.5-1.5
7	-2.7-1.2	-0.8-0.5	-0.4-0.3	-1.5-1.5	-1.1-0.7	-2.5-1.6	-0.3-0.3	-0.3-0.7	-0.3-0.8	-0.2-1.0	-0.3-0.7
8	-2.6-1.2	-0.9-0.4	-0.4-0.3	-1.7-1.2	-1.1-0.6	-2.5-1.6	-0.3-0.7	-0.2-0.3	-0.6-0.5	-0.3-1.0	-0.4-0.6
9	-2.6-2.7	-1.3-0.7	-0.3-0.5	-1.4-2.4	-1.1-0.7	-1.7-3.1	-0.3-0.8	-0.6-0.5	-0.4-1.3	-0.1-3.5	-1.0-2.0
10	-2.6-2.8	0.1-2.0	-0.4-0.6	-2.2-2.0	-1.3-0.7	-1.6-3.6	-0.2-1.0	-0.3-1.0	-0.1-3.5	2.7-4.6	-1.6-1.6
11	-2.5-1.2	-0.7-0.6	-0.4-0.3	-1.3-1.5	-1.2-0.5	-2.5-1.5	-0.3-0.7	-0.4-0.6	-1.0-2.0	-1.6-1.6	-0.0-0.3
Total	41.6-47.8	5.1-12.7	-4.7-3.8	47.2-53.9	-3.6-5.2	38.9-45.4	-3.4-4.9	-3.8-4.5	16.3-23.1	21.9-28.6	-4.7-3.6
Higher	34.9	1.4	0.1	24.6	0.7	26.8	1.2	1.7	16.0	17.3	0.1

Table F.98: South / Temp. Gradient at 5cm / Mean

i \ j	1	2	3	4	5	6	7	8	9	10	11
1	13.6-17.1	-1.8-2.4	-1.9-1.8	1.8-7.0	-2.1-1.9	-2.5-3.5	-1.8-2.1	-1.6-2.3	-1.8-2.7	-2.1-2.9	-2.1-1.7
2	-1.8-2.4	3.2-4.5	-1.2-0.1	-1.1-1.8	-0.2-1.1	0.3-2.7	-1.2-0.1	-1.2-0.1	-0.9-0.7	-0.7-1.1	-1.2-0.1
3	-1.9-1.8	-1.2-0.1	-0.1-0.3	-1.2-0.3	-0.4-0.5	-0.9-0.6	-0.4-0.4	-0.4-0.4	-0.4-0.5	-0.4-0.5	-0.4-0.5
4	1.8-7.0	-1.1-1.8	-1.2-0.3	11.2-13.9	-0.5-2.4	-1.9-2.7	-0.6-2.3	-0.9-1.9	-0.2-3.0	-0.6-3.0	-0.6-2.1
5	-2.1-1.9	-0.2-1.1	-0.4-0.5	-0.5-2.4	3.7-5.0	-2.4-0.6	-1.6-0.7	-1.7-0.5	-1.6-0.7	-1.9-0.5	-1.9-0.3
6	-2.5-3.5	0.3-2.7	-0.9-0.6	-1.9-2.7	-2.4-0.6	10.3-13.0	-1.8-2.4	-1.5-2.6	-1.4-3.0	-0.6-4.3	-1.9-2.3
7	-1.8-2.1	-1.2-0.1	-0.4-0.4	-0.6-2.3	-1.6-0.7	-1.8-2.4	-0.5-0.3	-0.8-0.7	-1.0-0.6	-0.8-0.8	-0.8-0.7
8	-1.6-2.3	-1.2-0.1	-0.4-0.4	-0.9-1.9	-1.7-0.5	-1.5-2.6	-0.8-0.7	-0.3-0.4	-0.8-0.7	-0.7-0.8	-0.6-0.8
9	-1.8-2.7	-0.9-0.7	-0.4-0.5	-0.2-3.0	-1.6-0.7	-1.4-3.0	-1.0-0.6	-0.8-0.7	-0.3-1.2	-0.1-2.7	-0.6-2.1
10	-2.1-2.9	-0.7-1.1	-0.4-0.5	-0.6-3.0	-1.9-0.5	-0.6-4.3	-0.8-0.8	-0.7-0.8	-0.1-2.7	1.9-3.5	-1.5-1.5
11	-2.1-1.7	-1.2-0.1	-0.4-0.5	-0.6-2.1	-1.9-0.3	-1.9-2.3	-0.8-0.7	-0.6-0.8	-0.6-2.1	-1.5-1.5	-0.1-0.5
Total	44.7-50.1	9.3-16.3	-4.5-3.1	35.7-42.6	3.0-10.3	32.5-39.1	-0.9-6.7	-1.9-5.4	6.8-13.9	12.9-20.0	-3.9-3.9
Higher	25.9	8.5	0.2	16.2	5.0	19.0	3.0	1.5	5.9	9.4	-0.5

Table F.99: North / Temp. Gradient at 5cm / Mean

i \ j	1	2	3	4	5	6	7	8	9	10	11
1	7.4-12.4	-2.0-2.0	-1.7-2.0	10.3-16.8	-2.1-1.6	-0.1-6.6	-2.1-1.5	-2.0-1.7	-2.1-2.9	-3.1-2.4	-2.9-0.9
2	-2.0-2.0	0.3-1.3	-0.5-0.7	2.4-4.8	-0.1-1.0	1.9-3.9	-0.5-0.7	-0.4-0.7	-0.7-0.8	-0.1-1.3	-0.6-0.6
3	-1.7-2.0	-0.5-0.7	-0.3-0.2	-0.5-1.1	-0.3-0.7	-0.2-1.3	-0.3-0.7	-0.3-0.7	-0.2-0.9	-0.4-0.7	-0.3-0.7
4	10.3-16.8	2.4-4.8	-0.5-1.1	13.7-16.9	-1.9-1.2	-1.6-3.1	-1.8-1.2	-1.8-1.3	-2.0-1.5	-2.2-1.5	-2.0-1.1
5	-2.1-1.6	-0.1-1.0	-0.3-0.7	-1.9-1.2	1.3-2.1	-1.0-0.8	-0.7-0.7	-0.7-0.8	-0.9-0.6	-1.2-0.4	-0.9-0.5
6	-0.1-6.6	1.9-3.9	-0.2-1.3	-1.6-3.1	-1.0-0.8	8.8-11.2	-1.8-1.9	-1.6-2.1	-2.0-2.2	-1.9-2.3	-1.7-2.0
7	-2.1-1.5	-0.5-0.7	-0.3-0.7	-1.8-1.2	-0.7-0.7	-1.8-1.9	-0.2-0.2	-0.3-0.5	-0.2-0.6	-0.2-0.6	-0.3-0.5
8	-2.0-1.7	-0.4-0.7	-0.3-0.7	-1.8-1.3	-0.7-0.8	-1.6-2.1	-0.3-0.5	-0.2-0.3	-0.5-0.4	-0.4-0.6	-0.4-0.5
9	-2.1-2.9	-0.7-0.8	-0.2-0.9	-2.0-1.5	-0.9-0.6	-2.0-2.2	-0.2-0.6	-0.5-0.4	-0.7-0.5	-0.7-1.7	-0.7-1.5
10	-3.1-2.4	-0.1-1.3	-0.4-0.7	-2.2-1.5	-1.2-0.4	-1.9-2.3	-0.2-0.6	-0.4-0.6	-0.7-1.7	2.1-3.6	-1.8-0.8
11	-2.9-0.9	-0.6-0.6	-0.3-0.7	-2.0-1.1	-0.9-0.5	-1.7-2.0	-0.3-0.5	-0.4-0.5	-0.7-1.5	-1.8-0.8	-0.1-0.4
Total	55.6-60.7	6.5-13.0	-2.9-4.1	52.7-59.6	-1.2-5.8	34.0-40.2	-3.4-3.6	-2.9-4.1	8.7-15.2	13.0-19.8	-3.0-4.0
Higher	33.0	1.0	-1.8	24.6	1.4	19.1	-0.2	0.2	10.5	13.5	1.4

Table F.100: Control / Temp. Gradient at 5cm / Maximum

i \ j	1	2	3	4	5	6	7	8	9	10	11
1	1.0-4.4	-1.6-2.7	-2.3-1.7	3.4-8.5	-2.2-1.7	-0.6-6.2	-2.0-2.0	-2.4-1.6	-0.9-4.2	-1.6-3.5	-2.0-1.9
2	-1.6-2.7	1.8-2.7	-0.6-0.7	-0.1-1.9	-0.5-0.9	1.7-7.1	-0.4-0.8	-0.3-0.9	-0.5-1.3	0.9-3.4	-0.4-0.9
3	-2.3-1.7	-0.6-0.7	-0.3-0.2	-0.5-0.8	-0.5-0.5	-1.0-3.7	-0.4-0.6	-0.4-0.6	-0.2-1.0	-0.1-1.4	-0.3-0.6
4	3.4-8.5	-0.1-1.9	-0.5-0.8	-1.3-1.2	-2.2-1.7	-2.1-4.1	-2.2-1.6	-2.3-1.5	-2.5-1.8	-1.7-2.5	-2.2-1.6
5	-2.2-1.7	-0.5-0.9	-0.5-0.5	-2.2-1.7	-0.3-0.3	-0.7-4.0	-0.4-0.7	-0.4-0.7	-0.1-1.1	-0.3-1.5	-0.4-0.7
6	-0.6-6.2	1.7-7.1	-1.0-3.7	-2.1-4.1	-0.7-4.0	16.7-21.3	-1.4-1.5	-1.4-1.5	-0.7-4.4	0.3-6.5	-1.8-1.1
7	-2.0-2.0	-0.4-0.8	-0.4-0.6	-2.2-1.6	-0.4-0.7	-1.4-1.5	-0.0-0.6	-0.7-0.5	-0.9-0.6	-0.3-1.6	-0.8-0.5
8	-2.4-1.6	-0.3-0.9	-0.4-0.6	-2.3-1.5	-0.4-0.7	-1.4-1.5	-0.7-0.5	-0.2-0.4	-0.8-0.7	0.1-1.9	-0.4-0.8
9	-0.9-4.2	-0.5-1.3	-0.2-1.0	-2.5-1.8	-0.1-1.1	-0.7-4.4	-0.9-0.6	-0.8-0.7	-0.1-2.0	0.7-4.6	-1.7-1.6
10	-1.6-3.5	0.9-3.4	-0.1-1.4	-1.7-2.5	-0.3-1.5	0.3-6.5	-0.3-1.6	0.1-1.9	0.7-4.6	4.1-6.2	-1.3-1.5
11	-2.0-1.9	-0.4-0.9	-0.3-0.6	-2.2-1.6	-0.4-0.7	-1.8-1.1	-0.8-0.5	-0.4-0.8	-1.7-1.6	-1.3-1.5	-0.2-0.3
Total	38.5-50.4	-3.9-11.3	-11.2-5.7	26.0-37.3	-11.0-5.9	55.4-64.5	-9.5-7.1	-8.8-7.5	17.3-30.2	23.3-35.4	-10.9-5.6
Higher	30.9	-8.0	-5.4	24.8	-5.6	24.8	-1.9	-1.6	15.9	11.7	-2.7

Table F.101: South / Temp. Gradient at 5cm / Maximum

i \ j	1	2	3	4	5	6	7	8	9	10	11
1	13.3-18.0	-1.8-2.4	-0.9-2.5	0.4-5.2	-0.9-2.5	-0.2-7.1	-1.5-2.0	-1.3-2.1	1.5-5.9	-0.9-4.2	-1.3-2.0
2	-1.8-2.4	2.5-3.5	-1.7-0.1	-1.5-0.3	-1.3-0.3	-2.3-1.9	-1.3-0.3	-1.7-0.1	-1.4-0.5	-1.3-0.8	-1.4-0.1
3	-0.9-2.5	-1.7-0.1	-0.4-0.4	-0.8-0.7	-1.0-0.6	-2.2-1.3	-0.8-0.6	-0.9-0.6	-0.9-0.7	-0.8-0.7	-0.9-0.6
4	0.4-5.2	-1.5-0.3	-0.8-0.7	-0.8-1.0	-1.2-1.7	-3.0-1.4	-2.0-1.0	-1.5-1.5	-1.2-1.9	-1.5-2.0	-1.5-1.6
5	-0.9-2.5	-1.3-0.3	-1.0-0.6	-1.2-1.7	0.3-1.2	-2.2-1.6	-0.8-0.9	-1.1-0.5	-0.7-1.1	-1.2-0.6	-1.0-0.6
6	-0.2-7.1	-2.3-1.9	-2.2-1.3	-3.0-1.4	-2.2-1.6	14.7-18.2	-1.4-1.8	-2.0-1.1	-2.4-1.5	-1.1-3.4	-1.2-1.9
7	-1.5-2.0	-1.3-0.3	-0.8-0.6	-2.0-1.0	-0.8-0.9	-1.4-1.8	0.6-1.5	-1.0-0.7	-0.8-1.0	-1.0-1.0	-1.2-0.5
8	-1.3-2.1	-1.7-0.1	-0.9-0.6	-1.5-1.5	-1.1-0.5	-2.0-1.1	-1.0-0.7	0.5-1.4	-1.4-0.5	-1.3-0.6	-1.4-0.4
9	1.5-5.9	-1.4-0.5	-0.9-0.7	-1.2-1.9	-0.7-1.1	-2.4-1.5	-0.8-1.0	-1.4-0.5	0.4-1.9	-1.3-1.6	-1.1-1.5
10	-0.9-4.2	-1.3-0.8	-0.8-0.7	-1.5-2.0	-1.2-0.6	-1.1-3.4	-1.0-1.0	-1.3-0.6	-1.3-1.6	3.2-4.9	-1.5-0.9
11	-1.3-2.0	-1.4-0.1	-0.9-0.6	-1.5-1.6	-1.0-0.6	-1.2-1.9	-1.2-0.5	-1.4-0.4	-1.1-1.5	-1.5-0.9	-0.1-0.5
Total	53.3-61.7	-0.8-12.8	-9.3-5.5	12.0-25.5	-7.4-7.2	46.1-55.9	-7.1-7.5	-6.4-8.1	5.8-19.0	12.8-24.9	-6.0-8.0
Higher	27.4	7.7	-0.5	16.9	-0.4	32.1	0.1	2.6	7.8	12.9	1.9

Table F.102: North / Temp. Gradient at 5cm / Maximum

i \ j	1	2	3	4	5	6	7	8	9	10	11
1	18.5-24.7	-2.1-2.4	-1.6-2.3	9.2-16.7	-1.5-2.2	1.3-7.8	-1.0-2.8	-1.5-2.4	1.8-7.2	-0.6-4.6	-2.6-1.5
2	-2.1-2.4	4.1-5.4	-1.3-0.5	-0.8-1.9	-1.0-0.7	0.3-2.9	-0.9-0.7	-0.7-1.1	-1.3-0.9	-1.0-1.0	-1.2-0.5
3	-1.6-2.3	-1.3-0.5	-0.2-0.6	-0.8-0.8	-0.7-0.5	-0.9-0.7	-0.7-0.6	-0.7-0.6	-0.7-0.7	-0.8-0.7	-0.7-0.5
4	9.2-16.7	-0.8-1.9	-0.8-0.8	1.4-4.3	-0.5-3.3	0.5-5.0	-0.5-3.3	-0.2-3.5	-0.7-3.5	-0.2-3.9	-0.4-3.4
5	-1.5-2.2	-1.0-0.7	-0.7-0.5	-0.5-3.3	0.2-0.9	-0.8-0.9	-0.6-0.6	-0.7-0.6	-0.9-0.6	-1.0-0.4	-0.8-0.5
6	1.3-7.8	0.3-2.9	-0.9-0.7	0.5-5.0	-0.8-0.9	3.8-6.2	-0.4-2.6	-0.2-2.8	-0.8-2.6	-0.1-3.5	-0.4-2.5
7	-1.0-2.8	-0.9-0.7	-0.7-0.6	-0.5-3.3	-0.6-0.6	-0.4-2.6	0.2-0.9	-0.1-1.2	-0.4-1.1	-0.2-1.2	-0.4-0.9
8	-1.5-2.4	-0.7-1.1	-0.7-0.6	-0.2-3.5	-0.7-0.6	-0.2-2.8	-0.1-1.2	0.8-1.7	-1.3-0.5	-1.4-0.6	-1.3-0.5
9	1.8-7.2	-1.3-0.9	-0.7-0.7	-0.7-3.5	-0.9-0.6	-0.8-2.6	-0.4-1.1	-1.3-0.5	-0.4-1.2	-1.4-2.0	-1.9-1.1
10	-0.6-4.6	-1.0-1.0	-0.8-0.7	-0.2-3.9	-1.0-0.4	-0.1-3.5	-0.2-1.2	-1.4-0.6	-1.4-2.0	0.8-2.4	-1.2-1.6
11	-2.6-1.5	-1.2-0.5	-0.7-0.5	-0.4-3.4	-0.8-0.5	-0.4-2.5	-0.4-0.9	-1.3-0.5	-1.9-1.1	-1.2-1.6	-0.3-0.3
Total	66.3-73.0	0.3-13.7	-5.5-8.0	35.6-45.9	-5.8-7.8	28.4-39.6	-8.9-5.5	-7.6-6.7	5.4-18.2	6.4-19.1	-6.0-7.7
Higher	22.4	0.9	1.5	12.5	-0.5	14.1	-7.3	-4.6	5.1	5.3	-0.3

Table F.103: Control / Temp. Gradient at 5cm / Minimum

i \ j	1	2	3	4	5	6	7	8	9	10	11
1	0.4-2.7	-2.7-1.2	-2.4-1.5	-2.9-3.8	-2.4-1.4	-1.6-3.2	-2.6-1.3	-2.4-1.5	-2.1-2.2	-2.6-1.7	-2.4-1.5
2	-2.7-1.2	5.1-6.3	-1.2-0.6	-3.9-2.2	-1.2-0.7	-1.4-1.6	-1.1-0.7	-1.2-0.7	-1.1-1.0	-1.1-1.1	-1.1-0.7
3	-2.4-1.5	-1.2-0.6	-0.2-0.3	-4.8-0.4	-0.5-0.3	-1.3-0.5	-0.5-0.3	-0.5-0.3	-0.5-0.3	-0.6-0.3	-0.5-0.3
4	-2.9-3.8	-3.9-2.2	-4.8-0.4	37.1-41.8	-1.5-0.6	0.3-6.7	-1.2-1.0	-1.4-0.8	-1.7-1.5	-1.8-2.3	-1.2-0.9
5	-2.4-1.4	-1.2-0.7	-0.5-0.3	-1.5-0.6	0.1-0.7	-1.8-0.3	-0.9-0.2	-0.9-0.3	-0.9-0.3	-1.0-0.2	-0.9-0.2
6	-1.6-3.2	-1.4-1.6	-1.3-0.5	0.3-6.7	-1.8-0.3	13.7-16.6	-1.4-2.3	-1.4-2.3	-1.5-2.6	-1.7-2.8	-1.5-2.1
7	-2.6-1.3	-1.1-0.7	-0.5-0.3	-1.2-1.0	-0.9-0.2	-1.4-2.3	-0.2-0.5	-0.5-0.8	-0.6-0.8	-0.6-0.8	-0.5-0.8
8	-2.4-1.5	-1.2-0.7	-0.5-0.3	-1.4-0.8	-0.9-0.3	-1.4-2.3	-0.5-0.8	-0.2-0.5	-0.8-0.5	-0.6-0.8	-0.6-0.8
9	-2.1-2.2	-1.1-1.0	-0.5-0.3	-1.7-1.5	-0.9-0.3	-1.5-2.6	-0.6-0.8	-0.8-0.5	-0.7-1.0	-0.9-2.7	-1.6-1.7
10	-2.6-1.7	-1.1-1.1	-0.6-0.3	-1.8-2.3	-1.0-0.2	-1.7-2.8	-0.6-0.8	-0.6-0.8	-0.9-2.7	2.8-4.8	-2.2-1.4
11	-2.4-1.5	-1.1-0.7	-0.5-0.3	-1.2-0.9	-0.9-0.2	-1.5-2.1	-0.5-0.8	-0.6-0.8	-1.6-1.7	-2.2-1.4	-0.1-0.3
Total	16.7-23.9	8.8-16.4	-1.4-6.8	56.7-61.2	-1.0-7.1	32.7-38.8	-0.5-7.5	-0.7-7.3	8.3-15.9	14.2-21.5	-1.2-6.9
Higher	21.2	9.6	6.6	19.3	6.4	14.9	3.7	3.9	10.9	13.7	3.7

Table F.104: South / Temp. Gradient at 5cm / Minimum

i \ j	1	2	3	4	5	6	7	8	9	10	11
1	2.9-5.5	-2.4-1.8	-2.6-1.6	-3.5-2.9	-2.5-1.7	-1.1-4.8	-2.5-1.8	-2.4-1.8	-2.0-2.5	-1.9-2.6	-2.6-1.6
2	-2.4-1.8	9.8-11.6	-1.3-0.7	-3.5-2.4	-1.3-0.7	-1.7-2.8	-1.3-0.7	-1.2-0.9	-1.0-1.1	-1.2-1.1	-1.2-0.8
3	-2.6-1.6	-1.3-0.7	-0.1-0.6	-3.8-0.6	-1.1-0.2	-1.3-1.7	-1.1-0.2	-1.1-0.2	-1.1-0.2	-1.2-0.1	-1.1-0.2
4	-3.5-2.9	-3.5-2.4	-3.8-0.6	28.1-32.2	-1.6-1.0	-0.8-6.5	-1.2-1.5	-1.5-1.1	-1.5-1.6	-1.5-2.2	-1.2-1.3
5	-2.5-1.7	-1.3-0.7	-1.1-0.2	-1.6-1.0	0.3-1.2	-1.3-2.1	-1.1-0.7	-1.1-0.8	-1.2-0.6	-1.3-0.6	-1.2-0.6
6	-1.1-4.8	-1.7-2.8	-1.3-1.7	-0.8-6.5	-1.3-2.1	19.7-23.3	-1.6-2.3	-1.7-2.1	-1.5-2.6	-1.1-3.4	-1.6-2.1
7	-2.5-1.8	-1.3-0.7	-1.1-0.2	-1.2-1.5	-1.1-0.7	-1.6-2.3	0.2-1.2	-1.0-1.1	-1.1-1.0	-1.2-1.0	-1.0-1.1
8	-2.4-1.8	-1.2-0.9	-1.1-0.2	-1.5-1.1	-1.1-0.8	-1.7-2.1	-1.0-1.1	0.1-1.1	-0.9-1.0	-1.1-0.9	-0.9-1.0
9	-2.0-2.5	-1.0-1.1	-1.1-0.2	-1.5-1.6	-1.2-0.6	-1.5-2.6	-1.1-1.0	-0.9-1.0	-0.8-0.8	-0.6-2.4	-0.7-2.2
10	-1.9-2.6	-1.2-1.1	-1.2-0.1	-1.5-2.2	-1.3-0.6	-1.1-3.4	-1.2-1.0	-1.1-0.9	-0.6-2.4	3.3-5.0	-1.4-1.7
11	-2.6-1.6	-1.2-0.8	-1.1-0.2	-1.2-1.3	-1.2-0.6	-1.6-2.1	-1.0-1.1	-0.9-1.0	-0.7-2.2	-1.4-1.7	-0.1-0.5
Total	17.8-25.9	14.7-23.0	-2.0-7.5	41.6-47.7	-0.1-9.1	36.1-42.7	0.6-9.7	-0.4-8.9	3.4-12.4	8.6-17.2	-1.6-7.8
Higher	17.8	9.8	7.5	14.0	6.0	9.7	5.3	4.7	6.1	7.0	3.0

Table F.105: North / Temp. Gradient at 5cm / Minimum

i \ j	1	2	3	4	5	6	7	8	9	10	11
1	-0.9-2.3	-1.9-2.6	-1.9-2.7	0.8-7.8	-1.9-2.5	1.8-7.8	-2.1-2.4	-1.9-2.6	-2.4-2.6	-1.8-3.2	-2.2-2.3
2	-1.9-2.6	7.0-8.4	-0.8-0.8	-2.5-3.2	-0.8-0.7	-1.3-2.6	-1.0-0.6	-0.7-0.9	-1.2-0.7	-1.0-0.9	-0.8-0.7
3	-1.9-2.7	-0.8-0.8	-0.3-0.4	-3.6-0.8	-0.8-0.5	-1.0-1.6	-0.8-0.5	-0.8-0.5	-0.8-0.5	-0.5-0.8	-0.8-0.5
4	0.8-7.8	-2.5-3.2	-3.6-0.8	28.0-32.7	-1.7-1.5	-1.9-5.7	-1.7-1.6	-1.9-1.4	-1.5-2.6	-2.7-1.9	-1.9-1.4
5	-1.9-2.5	-0.8-0.7	-0.8-0.5	-1.7-1.5	-0.0-0.5	-1.1-1.4	-0.5-0.6	-0.5-0.6	-0.6-0.5	-0.7-0.4	-0.6-0.5
6	1.8-7.8	-1.3-2.6	-1.0-1.6	-1.9-5.7	-1.1-1.4	15.6-19.0	-1.6-2.1	-1.6-2.1	-1.9-2.3	-2.6-1.8	-1.4-2.1
7	-2.1-2.4	-1.0-0.6	-0.8-0.5	-1.7-1.6	-0.5-0.6	-1.6-2.1	-0.0-0.6	-0.5-0.9	-0.6-0.8	-0.8-0.7	-0.6-0.7
8	-1.9-2.6	-0.7-0.9	-0.8-0.5	-1.9-1.4	-0.5-0.6	-1.6-2.1	-0.5-0.9	0.1-0.9	-0.7-0.8	-0.9-0.6	-0.7-0.7
9	-2.4-2.6	-1.2-0.7	-0.8-0.5	-1.5-2.6	-0.6-0.5	-1.9-2.3	-0.6-0.8	-0.7-0.8	-0.9-0.4	-0.5-2.1	-0.4-2.1
10	-1.8-3.2	-1.0-0.9	-0.5-0.8	-2.7-1.9	-0.7-0.4	-2.6-1.8	-0.8-0.7	-0.9-0.6	-0.5-2.1	2.5-4.2	-1.7-1.1
11	-2.2-2.3	-0.8-0.7	-0.8-0.5	-1.9-1.4	-0.6-0.5	-1.4-2.1	-0.6-0.7	-0.7-0.7	-0.4-2.1	-1.7-1.1	-0.0-0.3
Total	25.2-33.1	11.8-20.1	-1.8-7.4	49.8-55.7	-1.9-7.2	33.9-40.8	-1.5-7.7	-1.6-7.5	4.0-12.8	9.4-18.0	-2.7-6.5
Higher	17.0	7.5	4.1	17.8	2.4	11.5	2.4	2.0	6.4	10.2	1.3



F.9 Temperature Gradient at 8 cm

Table F.106: Control / Temp. Gradient at 8cm with Time (Total-effect)

t \ i	1	2	3	4	5	6	7	8	9	10	11
0.33	13.0-17.7	1.2-6.2	-2.6-2.5	46.8-50.4	-2.9-2.2	42.4-46.2	-2.9-2.2	-2.9-2.2	9.5-14.2	15.8-20.3	-2.1-2.9
0.67	17.4-21.8	1.7-6.6	-2.5-2.5	49.2-52.8	-2.9-2.1	41.3-45.1	-2.9-2.1	-2.9-2.1	10.3-14.8	15.8-20.2	-2.1-2.9
1.00	20.4-24.9	3.0-7.9	-2.3-2.7	50.6-54.3	-2.8-2.3	40.2-44.1	-2.7-2.4	-2.8-2.3	10.9-15.6	16.0-20.5	-2.1-3.0
1.33	22.4-27.1	4.2-9.3	-2.3-3.0	51.9-55.7	-2.9-2.4	38.2-42.3	-2.5-2.7	-2.6-2.6	11.1-16.0	15.9-20.7	-2.2-3.1
1.67	24.2-29.0	5.6-10.8	-2.0-3.5	53.3-57.3	-2.6-3.0	35.9-40.3	-1.8-3.7	-2.0-3.6	11.5-16.6	16.1-21.0	-2.1-3.4
2.00	25.6-30.5	7.0-12.5	-1.8-3.9	54.8-58.9	-2.2-3.6	33.3-38.0	-0.7-5.0	-1.0-4.7	11.8-17.1	16.0-21.1	-1.9-3.8
2.33	26.7-31.8	8.4-14.1	-1.6-4.4	55.9-60.1	-1.6-4.4	30.7-35.7	0.4-6.4	0.0-6.0	11.9-17.3	15.7-21.0	-1.8-4.2
2.67	27.6-33.0	9.8-15.7	-1.4-4.9	56.8-61.1	-1.0-5.2	28.3-33.7	1.6-7.7	1.0-7.1	11.9-17.5	15.4-21.0	-1.7-4.5
3.00	28.6-34.0	11.2-17.2	-1.3-5.2	57.1-61.6	-0.3-6.2	26.4-32.0	2.5-8.7	1.7-7.9	11.8-17.7	15.1-20.8	-1.6-4.8
3.33	29.3-34.9	12.3-18.4	-1.2-5.4	57.2-61.7	0.3-7.0	24.9-30.8	3.0-9.4	1.9-8.4	11.6-17.6	14.7-20.6	-1.6-5.0
3.67	29.9-35.6	13.1-19.3	-1.3-5.5	56.9-61.5	0.9-7.8	23.8-29.8	3.2-9.8	2.1-8.7	11.5-17.6	14.3-20.5	-1.8-5.0
4.00	30.5-36.2	13.8-20.1	-1.5-5.5	56.3-61.1	1.5-8.5	23.1-29.2	3.3-10.0	2.1-8.8	11.3-17.5	14.1-20.3	-1.9-5.0
4.33	31.1-36.9	14.4-20.7	-1.6-5.4	55.7-60.6	2.0-9.1	22.6-28.8	3.2-10.0	1.9-8.8	11.2-17.6	13.9-20.3	-2.2-4.9
4.67	31.6-37.5	14.8-21.2	-1.9-5.3	54.9-59.9	2.4-9.6	22.4-28.7	3.0-9.9	1.6-8.6	11.3-17.6	14.0-20.4	-2.4-4.8
5.00	32.1-38.0	14.8-21.3	-2.2-5.0	54.0-59.2	2.7-9.9	22.4-28.8	2.6-9.6	1.2-8.2	11.3-17.7	14.1-20.6	-2.6-4.6
5.33	32.6-38.5	14.7-21.2	-2.6-4.7	53.1-58.4	2.8-10.1	22.7-29.2	2.1-9.3	0.6-7.8	11.4-17.9	14.4-20.9	-3.1-4.3
5.67	33.1-39.1	14.3-20.9	-3.0-4.4	52.1-57.6	2.7-10.2	23.4-30.0	1.6-8.8	0.1-7.3	11.7-18.1	14.8-21.4	-3.5-4.0
6.00	33.7-39.7	13.8-20.4	-3.4-4.1	51.1-56.7	2.6-10.1	24.5-31.1	1.0-8.2	-0.5-6.8	12.0-18.5	15.5-22.1	-3.8-3.7
6.33	34.4-40.4	13.1-19.8	-3.8-3.8	50.1-55.7	2.2-9.8	26.0-32.6	0.3-7.6	-1.1-6.2	12.5-18.9	16.4-22.9	-4.2-3.3
6.67	35.0-41.1	12.2-18.9	-4.2-3.4	48.8-54.6	1.7-9.3	28.0-34.5	-0.5-6.9	-1.8-5.6	13.0-19.5	17.4-23.8	-4.6-3.0
7.00	35.6-41.7	11.2-17.9	-4.6-3.1	47.6-53.4	1.0-8.6	30.5-36.8	-1.3-6.2	-2.4-5.1	13.8-20.1	18.5-24.9	-2.7-4.7
7.33	36.2-42.3	10.1-16.8	-2.7-4.7	46.3-52.2	0.1-7.7	33.3-39.5	-2.0-5.5	-2.7-4.7	14.5-20.9	19.9-26.1	-2.9-4.4
7.67	36.7-42.8	9.0-15.6	-2.9-4.5	45.0-50.9	-0.9-6.8	36.4-42.5	-2.7-4.8	-3.1-4.4	15.3-21.6	21.2-27.4	-3.1-4.3
8.00	37.2-43.2	7.9-14.5	-3.2-4.3	43.7-49.6	-1.9-5.8	39.9-45.7	-3.3-4.3	-3.4-4.1	16.0-22.3	22.5-28.6	-3.2-4.1
8.33	37.6-43.6	7.0-13.7	-3.1-4.3	42.6-48.6	-2.6-5.1	43.4-49.0	-3.4-4.1	-3.4-4.1	16.8-23.0	23.7-29.8	-3.1-4.2
8.67	38.0-43.9	6.4-13.1	-2.8-4.5	41.6-47.6	-3.0-4.7	46.7-52.1	-3.3-4.2	-3.2-4.4	17.5-23.8	24.8-30.9	-2.8-4.5
9.00	38.4-44.3	6.1-12.9	-4.7-3.0	40.8-46.9	-3.1-4.5	49.6-54.9	-3.0-4.6	-2.7-4.9	18.5-24.8	25.7-31.8	-4.5-3.0
9.33	38.9-44.8	6.1-12.9	-4.3-3.5	40.3-46.5	-3.1-4.5	51.9-57.2	-2.5-5.1	-2.2-5.4	19.5-25.9	26.4-32.6	-4.1-3.5
9.67	39.3-45.3	6.1-13.1	-3.9-3.9	40.3-46.6	-3.2-4.5	53.7-58.9	-2.2-5.6	-1.8-5.8	20.4-26.8	27.0-33.3	-3.8-3.8
10.00	40.0-46.0	6.4-13.3	-3.8-4.1	40.7-47.1	-3.3-4.5	54.8-60.1	-2.1-5.7	-1.8-5.9	21.1-27.6	27.4-33.7	-3.7-4.0

Table F.107: Control / Temp. Gradient at 8cm / Mid-day

i \ j	1	2	3	4	5	6	7	8	9	10	11
1	8.0-10.8	-2.5-1.5	-3.1-0.5	1.4-7.4	-3.6-0.2	-3.1-1.8	-3.4-0.3	-3.4-0.3	-3.1-1.3	-3.0-1.5	-3.3-0.3
2	-2.5-1.5	6.3-8.0	-1.1-0.3	-0.6-4.6	-0.7-0.8	-0.1-2.0	-1.2-0.4	-1.4-0.2	-1.1-0.8	-1.0-0.9	-1.1-0.4
3	-3.1-0.5	-1.1-0.3	-0.2-0.2	-2.5-1.1	-0.4-0.3	-0.6-0.4	-0.3-0.5	-0.3-0.5	-0.4-0.3	-0.3-0.5	-0.3-0.4
4	1.4-7.4	-0.6-4.6	-2.5-1.1	28.7-32.6	-1.2-1.4	-2.4-1.9	-1.1-1.5	-1.0-1.7	-1.2-2.2	-1.9-1.6	-0.8-1.4
5	-3.6-0.2	-0.7-0.8	-0.4-0.3	-1.2-1.4	2.7-3.9	-1.9-0.6	-1.3-0.9	-1.4-0.8	-1.6-0.7	-1.6-0.6	-1.6-0.5
6	-3.1-1.8	-0.1-2.0	-0.6-0.4	-2.4-1.9	-1.9-0.6	2.6-5.0	-1.8-2.9	-2.0-2.7	-2.5-2.2	-2.0-2.8	-2.7-1.8
7	-3.4-0.3	-1.2-0.4	-0.3-0.5	-1.1-1.5	-1.3-0.9	-1.8-2.9	-0.7-0.5	-0.9-1.2	-1.1-1.1	-1.0-1.2	-1.0-1.1
8	-3.4-0.3	-1.4-0.2	-0.3-0.5	-1.0-1.7	-1.4-0.8	-2.0-2.7	-0.9-1.2	-0.4-0.6	-1.0-1.1	-0.6-1.5	-0.8-1.2
9	-3.1-1.3	-1.1-0.8	-0.4-0.3	-1.2-2.2	-1.6-0.7	-2.5-2.2	-1.1-1.1	-1.0-1.1	-0.3-1.3	-0.5-2.9	-1.0-2.0
10	-3.0-1.5	-1.0-0.9	-0.3-0.5	-1.9-1.6	-1.6-0.6	-2.0-2.8	-1.0-1.2	-0.6-1.5	-0.5-2.9	1.0-2.8	-2.2-1.3
11	-3.3-0.3	-1.1-0.4	-0.3-0.4	-0.8-1.4	-1.6-0.5	-2.7-1.8	-1.0-1.1	-0.8-1.2	-1.0-2.0	-2.2-1.3	0.0-0.3
Total	32.1-38.0	14.8-21.3	-2.2-5.0	54.0-59.2	2.7-9.9	22.4-28.8	2.6-9.6	1.2-8.2	11.3-17.7	14.1-20.6	-2.6-4.6
Higher	31.7	10.3	3.6	19.2	7.2	21.9	7.2	5.4	13.5	15.1	3.0

Table F.108: South / Temp. Gradient at 8cm with Time (Total-effect)

t \ i	1	2	3	4	5	6	7	8	9	10	11
0.33	19.6-24.9	3.9-9.9	-2.2-3.9	38.2-42.8	-2.6-3.6	45.3-49.6	-2.6-3.6	-2.6-3.6	5.4-11.3	11.7-17.3	-1.8-4.3
0.67	24.6-29.7	4.5-10.3	-1.9-4.1	40.1-44.6	-2.4-3.6	42.2-46.6	-2.4-3.7	-2.4-3.6	5.8-11.5	11.9-17.5	-1.7-4.3
1.00	27.1-32.2	5.7-11.6	-2.2-4.0	41.1-45.8	-2.8-3.5	39.4-44.0	-2.4-3.8	-2.6-3.6	5.5-11.4	11.8-17.5	-2.0-4.3
1.33	28.3-33.5	7.1-13.2	-2.4-4.2	42.1-46.9	-2.9-3.7	35.9-40.9	-1.8-4.8	-2.2-4.4	5.4-11.6	11.4-17.3	-2.2-4.4
1.67	29.0-34.4	9.0-15.4	-2.2-4.7	42.9-48.0	-2.2-4.6	32.1-37.5	-0.0-6.7	-0.8-6.0	5.4-11.9	10.9-17.2	-1.9-5.0
2.00	29.8-35.4	11.0-17.7	-1.5-5.6	43.6-48.8	-1.0-6.1	28.6-34.4	2.4-9.3	1.2-8.2	5.9-12.6	10.5-17.1	-1.3-5.8
2.33	31.0-36.6	13.2-19.9	-0.9-6.3	44.1-49.4	0.2-7.5	25.5-31.6	4.6-11.5	3.0-10.1	6.3-13.1	10.2-17.0	-0.7-6.6
2.67	32.1-37.9	15.0-21.9	-0.6-6.9	44.2-49.6	1.4-8.8	22.9-29.3	5.8-13.0	3.9-11.2	6.2-13.3	9.8-16.8	-0.3-7.2
3.00	32.8-38.7	16.6-23.4	-0.6-7.1	43.7-49.3	2.3-9.8	20.6-27.3	6.4-13.6	4.0-11.5	5.8-13.1	9.0-16.2	-0.4-7.3
3.33	33.3-39.2	17.9-24.8	-0.7-7.1	42.9-48.6	3.2-10.8	18.8-25.8	6.4-13.8	4.0-11.5	5.3-12.8	8.3-15.7	-0.6-7.3
3.67	33.6-39.6	19.0-26.0	-1.0-7.0	42.1-47.9	4.1-11.8	17.6-24.7	6.2-13.8	3.8-11.5	4.9-12.6	7.8-15.4	-0.8-7.2
4.00	33.8-39.9	20.0-27.0	-1.2-6.9	41.2-47.1	5.0-12.7	16.6-23.7	6.0-13.7	3.6-11.4	4.6-12.4	7.4-15.1	-1.0-7.2
4.33	34.1-40.2	20.9-27.8	-1.4-6.7	40.4-46.3	6.0-13.6	15.8-23.1	5.8-13.5	3.4-11.2	4.4-12.2	7.2-14.9	-1.1-7.1
4.67	34.3-40.4	21.3-28.3	-1.6-6.5	39.4-45.5	6.7-14.3	15.4-22.7	5.5-13.3	3.1-10.9	4.2-12.0	7.0-14.8	-1.4-6.9
5.00	34.5-40.6	21.6-28.5	-2.0-6.2	38.5-44.6	7.3-15.0	15.2-22.6	5.2-13.0	2.7-10.5	3.9-11.9	6.9-14.7	-1.6-6.7
5.33	34.7-40.8	21.5-28.4	-2.3-5.9	37.6-43.8	7.8-15.5	15.4-22.7	4.8-12.6	2.3-10.2	3.8-11.7	7.0-14.7	-1.9-6.4
5.67	35.0-41.1	21.1-28.0	-2.7-5.5	36.7-43.0	8.2-15.8	15.9-23.2	4.4-12.2	1.9-9.7	3.7-11.6	7.2-14.8	-2.2-6.0
6.00	35.4-41.5	20.5-27.4	-2.9-5.1	35.9-42.2	8.4-15.9	16.9-24.1	4.0-11.7	1.6-9.3	3.9-11.6	7.5-15.0	-2.5-5.6
6.33	35.9-41.9	19.6-26.4	-3.2-4.7	35.0-41.4	8.4-15.7	18.3-25.3	3.6-11.2	1.2-8.8	4.0-11.6	7.9-15.3	-2.7-5.2
6.67	36.5-42.3	18.4-25.1	-3.4-4.3	34.0-40.5	8.0-15.3	20.1-27.0	3.1-10.6	0.8-8.3	4.3-11.7	8.5-15.7	-2.9-4.8
7.00	37.2-42.9	17.1-23.7	-3.6-4.0	33.2-39.6	7.5-14.6	22.6-29.2	2.8-10.0	0.6-7.8	4.8-12.0	9.4-16.4	-3.1-4.5
7.33	37.9-43.5	15.7-22.1	-3.5-3.7	32.4-38.8	6.8-13.7	25.7-32.0	2.4-9.5	0.4-7.5	5.3-12.2	10.6-17.3	-3.1-4.2
7.67	38.7-44.1	14.2-20.5	-3.4-3.7	31.7-38.0	5.9-12.6	29.4-35.4	2.1-9.0	0.5-7.3	5.9-12.6	11.9-18.5	-3.2-4.0
8.00	39.3-44.7	12.9-19.0	-3.1-3.8	30.8-37.1	4.8-11.4	33.4-39.2	1.8-8.6	0.6-7.3	6.5-13.0	13.5-19.7	-3.0-4.0
8.33	40.0-45.2	11.8-17.8	-2.6-4.1	30.1-36.4	3.8-10.4	37.6-43.2	1.7-8.3	1.0-7.5	7.0-13.4	14.9-21.1	-2.7-4.2
8.67	40.8-46.0	11.3-17.2	-1.5-5.1	29.6-36.0	3.4-9.9	41.8-47.3	2.2-8.7	1.8-8.3	8.1-14.3	16.6-22.7	-1.9-4.8
9.00	41.8-47.0	11.5-17.5	-0.1-6.6	29.2-35.8	3.7-10.2	45.7-51.0	3.4-10.0	3.2-9.7	9.6-15.9	18.7-24.7	-0.6-6.1
9.33	43.0-48.2	12.2-18.2	1.5-8.3	29.2-35.9	4.4-11.0	48.8-54.1	5.2-11.8	5.0-11.6	11.3-17.7	20.6-26.7	0.7-7.5
9.67	44.3-49.4	13.0-19.1	3.0-9.9	29.5-36.4	5.2-12.0	51.2-56.6	6.9-13.6	6.7-13.3	13.0-19.5	22.3-28.4	2.0-8.9
10.00	45.5-50.7	13.5-19.8	4.1-11.1	30.3-37.3	5.9-12.8	52.9-58.3	8.0-14.8	7.8-14.5	14.4-21.0	23.6-29.8	2.8-9.8

Table F.109: South / Temp. Gradient at 8cm / Mid-day

i \ j	1	2	3	4	5	6	7	8	9	10	11
1	17.8-20.9	-2.8-2.6	-2.2-1.3	-2.5-3.7	-3.1-0.9	-2.5-2.2	-1.9-2.1	-2.0-1.9	-1.9-2.0	-2.2-1.9	-2.0-1.5
2	-2.8-2.6	12.9-15.2	-1.1-0.4	-2.9-2.1	-0.9-0.9	-1.0-1.2	-1.0-0.9	-1.3-0.5	-1.0-0.8	-1.1-0.9	-1.1-0.4
3	-2.2-1.3	-1.1-0.4	-0.0-0.3	-2.8-0.2	-0.6-0.2	-0.5-0.4	-0.4-0.3	-0.4-0.3	-0.4-0.3	-0.4-0.4	-0.4-0.3
4	-2.5-3.7	-2.9-2.1	-2.8-0.2	22.2-25.6	-1.1-1.6	-1.3-2.1	-0.0-2.6	-0.8-1.7	-0.2-2.3	-0.5-2.2	-0.3-2.0
5	-3.1-0.9	-0.9-0.9	-0.6-0.2	-1.1-1.6	5.6-7.1	-2.2-0.7	-1.6-1.1	-2.0-0.7	-2.0-0.7	-2.2-0.6	-2.2-0.3
6	-2.5-2.2	-1.0-1.2	-0.5-0.4	-1.3-2.1	-2.2-0.7	0.8-3.1	-0.5-4.1	-0.6-3.9	-1.2-3.2	-0.9-3.8	-1.5-2.8
7	-1.9-2.1	-1.0-0.9	-0.4-0.3	-0.0-2.6	-1.6-1.1	-0.5-4.1	-0.7-0.8	-1.4-1.4	-1.0-1.8	-1.4-1.5	-1.6-1.2
8	-2.0-1.9	-1.3-0.5	-0.4-0.3	-0.8-1.7	-2.0-0.7	-0.6-3.9	-1.4-1.4	-0.7-0.5	-1.3-1.2	-1.0-1.5	-1.2-1.2
9	-1.9-2.0	-1.0-0.8	-0.4-0.3	-0.2-2.3	-2.0-0.7	-1.2-3.2	-1.0-1.8	-1.3-1.2	-0.3-1.1	-1.0-1.8	-1.2-1.5
10	-2.2-1.9	-1.1-0.9	-0.4-0.4	-0.5-2.2	-2.2-0.6	-0.9-3.8	-1.4-1.5	-1.0-1.5	-1.0-1.8	-0.2-1.4	-1.2-2.0
11	-2.0-1.5	-1.1-0.4	-0.4-0.3	-0.3-2.0	-2.2-0.3	-1.5-2.8	-1.6-1.2	-1.2-1.2	-1.2-1.5	-1.2-2.0	-0.4-0.2
Total	34.5-40.6	21.6-28.5	-2.0-6.2	38.5-44.6	7.3-15.0	15.2-22.6	5.2-13.0	2.7-10.5	3.9-11.9	6.9-14.7	-1.6-6.7
Higher	19.7	12.9	4.5	13.7	10.0	10.8	6.0	5.5	5.4	7.9	2.4

Table F.110: North / Temp. Gradient at 8cm with Time (Total-effect)

i \ t	1	2	3	4	5	6	7	8	9	10	11
0.33	17.7-22.7	6.6-11.7	-1.2-4.1	52.3-56.0	-1.9-3.4	35.0-39.1	-1.9-3.4	-1.9-3.4	5.3-10.5	9.6-14.6	-1.2-4.1
0.67	24.0-28.9	5.7-10.6	-1.5-3.6	52.5-56.4	-2.4-2.7	34.8-38.9	-2.4-2.8	-2.4-2.7	5.5-10.5	10.2-15.0	-1.6-3.6
1.00	28.4-33.1	5.7-10.6	-1.1-4.1	53.2-57.3	-2.4-2.8	34.7-39.1	-2.4-2.8	-2.4-2.8	6.2-11.3	10.8-15.7	-1.3-3.9
1.33	30.6-35.5	5.8-10.9	-1.2-4.1	53.6-57.9	-2.6-2.8	34.3-38.8	-2.4-2.9	-2.4-3.0	6.2-11.5	10.9-15.9	-1.5-3.9
1.67	32.1-37.0	6.3-11.5	-1.2-4.4	53.7-58.3	-2.5-3.1	33.6-38.3	-2.1-3.4	-2.0-3.5	6.4-11.8	11.0-16.3	-1.5-4.0
2.00	32.9-37.8	6.8-12.2	-1.3-4.5	53.5-58.2	-2.6-3.2	32.5-37.3	-1.9-3.9	-1.7-4.1	6.3-11.9	10.9-16.4	-1.7-4.0
2.33	33.2-38.3	7.6-13.2	-1.2-4.8	53.1-57.8	-2.2-3.8	31.4-36.3	-1.1-4.9	-0.8-5.1	6.4-12.0	10.9-16.5	-1.7-4.3
2.67	33.3-38.5	8.3-14.0	-1.2-4.9	52.4-57.4	-1.9-4.2	29.9-35.0	-0.2-5.8	0.1-6.1	6.2-12.0	10.6-16.4	-1.7-4.5
3.00	33.4-38.6	8.8-14.8	-1.3-5.0	51.8-56.9	-1.5-4.7	28.3-33.6	0.5-6.7	0.9-7.0	5.8-11.8	10.2-16.2	-1.8-4.6
3.33	33.6-39.0	9.4-15.5	-1.3-5.2	51.2-56.4	-1.0-5.4	26.9-32.3	1.2-7.5	1.8-8.0	5.7-11.8	9.9-16.0	-1.8-4.7
3.67	34.1-39.5	9.9-16.0	-1.3-5.2	50.7-55.9	-0.5-6.0	25.5-31.0	1.6-8.0	2.4-8.8	5.4-11.7	9.6-15.8	-1.8-4.8
4.00	34.8-40.2	10.3-16.5	-1.4-5.3	50.2-55.5	0.1-6.6	24.4-30.0	1.8-8.3	2.9-9.3	5.3-11.7	9.3-15.6	-1.9-4.8
4.33	35.8-41.2	10.6-16.9	-1.4-5.4	49.9-55.2	0.5-7.1	23.7-29.4	1.8-8.4	3.0-9.5	5.3-11.8	9.1-15.5	-1.9-4.9
4.67	36.8-42.2	11.0-17.3	-1.4-5.4	49.7-55.0	1.0-7.6	23.2-29.0	1.8-8.4	3.0-9.5	5.4-11.9	9.1-15.5	-1.9-4.8
5.00	38.0-43.4	11.2-17.5	-1.4-5.3	49.4-54.9	1.3-7.9	23.1-28.9	1.6-8.2	2.7-9.3	5.4-11.9	9.2-15.6	-2.0-4.7
5.33	39.4-44.7	11.3-17.6	-1.5-5.2	49.2-54.8	1.6-8.2	23.3-29.1	1.2-7.8	2.3-8.8	5.5-12.0	9.3-15.7	-2.1-4.7
5.67	40.9-46.2	11.2-17.4	-1.5-5.1	49.2-54.8	1.7-8.2	23.9-29.6	0.8-7.3	1.8-8.3	5.7-12.1	9.6-16.0	-2.1-4.6
6.00	42.5-47.7	10.9-17.1	-1.7-4.9	49.1-54.8	1.6-8.1	24.6-30.4	0.2-6.7	1.1-7.5	5.8-12.1	9.9-16.3	-2.3-4.3
6.33	44.2-49.3	10.5-16.6	-2.0-4.6	49.2-55.0	1.3-7.8	25.7-31.4	-0.6-6.0	0.2-6.7	5.9-12.2	10.2-16.6	-2.6-4.1
6.67	46.1-51.2	9.9-16.0	-2.3-4.3	49.4-55.2	0.8-7.2	27.0-32.7	-1.3-5.2	-0.7-5.8	6.1-12.3	10.7-17.0	-2.8-3.8
7.00	48.0-53.1	9.2-15.3	-2.6-4.0	49.6-55.6	0.2-6.6	28.7-34.4	-1.9-4.5	-1.5-5.0	6.4-12.6	11.2-17.6	-3.1-3.6
7.33	50.1-55.2	8.5-14.5	-2.7-3.8	49.9-56.0	-0.6-5.9	30.6-36.2	-2.5-4.0	-2.1-4.4	6.8-12.9	11.9-18.2	-3.2-3.4
7.67	52.2-57.2	7.8-13.9	-2.8-3.8	50.3-56.6	-1.3-5.3	32.6-38.2	-2.9-3.7	-2.5-4.1	7.2-13.4	12.6-19.0	-3.3-3.4
8.00	54.1-59.1	7.1-13.2	-2.7-3.9	50.9-57.4	-2.0-4.6	34.5-40.2	-3.0-3.6	-2.5-4.1	7.7-14.0	13.4-19.8	-3.2-3.5
8.33	55.8-60.9	6.4-12.7	-2.6-4.1	51.5-58.1	-2.6-4.2	36.2-42.0	-3.0-3.7	-2.3-4.4	8.3-14.6	14.1-20.7	-3.1-3.7
8.67	57.4-62.4	5.9-12.4	-2.5-4.4	52.1-58.9	-3.1-3.8	37.6-43.6	-2.9-4.0	-1.9-4.9	8.8-15.3	14.8-21.5	-3.0-3.9
9.00	58.7-63.7	5.5-12.1	-2.3-4.8	52.6-59.7	-3.5-3.6	38.7-44.9	-2.7-4.3	-1.5-5.4	9.4-16.0	15.4-22.2	-2.9-4.2
9.33	59.7-64.7	5.2-11.9	-2.0-5.1	53.3-60.5	-3.8-3.5	39.7-46.0	-2.6-4.6	-1.2-5.8	9.9-16.7	16.0-22.9	-2.8-4.4
9.67	60.7-65.7	5.0-11.9	-1.7-5.5	54.1-61.4	-3.8-3.6	40.6-47.0	-2.5-4.9	-1.0-6.2	10.6-17.5	16.5-23.5	-2.6-4.7
10.00	61.6-66.5	5.0-11.9	-1.4-5.9	54.9-62.4	-3.8-3.6	41.3-47.8	-2.4-5.0	-0.9-6.4	11.2-18.2	16.9-24.1	-2.4-5.0

Table F.111: North / Temp. Gradient at 8cm / Mid-day

i \ j	1	2	3	4	5	6	7	8	9	10	11
1	10.3-13.8	-2.2-1.9	-2.7-1.1	2.5-8.5	-3.3-0.6	-2.9-2.4	-3.2-0.7	-2.9-1.1	-3.1-1.4	-2.7-1.9	-3.5-0.3
2	-2.2-1.9	4.9-6.2	-0.8-0.6	0.6-4.3	-0.5-0.8	0.1-2.2	-1.1-0.4	-0.7-0.8	-1.0-0.6	-0.7-0.9	-0.8-0.5
3	-2.7-1.1	-0.8-0.6	-0.3-0.4	-1.6-1.2	-0.5-0.7	-0.5-0.9	-0.6-0.6	-0.6-0.6	-0.4-0.8	-0.5-0.7	-0.5-0.7
4	2.5-8.5	0.6-4.3	-1.6-1.2	24.2-27.7	-1.5-1.4	-2.1-1.9	-1.4-1.7	-1.9-1.2	-1.9-1.3	-1.4-2.1	-1.4-1.4
5	-3.3-0.6	-0.5-0.8	-0.5-0.7	-1.5-1.4	2.1-3.0	-1.3-0.7	-0.7-0.9	-0.6-1.0	-1.0-0.8	-1.2-0.6	-1.0-0.6
6	-2.9-2.4	0.1-2.2	-0.5-0.9	-2.1-1.9	-1.3-0.7	7.7-10.0	-2.4-1.6	-2.3-1.8	-2.5-1.8	-2.3-1.9	-2.4-1.6
7	-3.2-0.7	-1.1-0.4	-0.6-0.6	-1.4-1.7	-0.7-0.9	-2.4-1.6	1.1-2.0	-0.8-1.0	-0.8-1.1	-0.7-1.2	-0.8-1.1
8	-2.9-1.1	-0.7-0.8	-0.6-0.6	-1.9-1.2	-0.6-1.0	-2.3-1.8	-0.8-1.0	1.8-2.9	-1.2-0.9	-1.2-1.0	-1.1-0.9
9	-3.1-1.4	-1.0-0.6	-0.4-0.8	-1.9-1.3	-1.0-0.8	-2.5-1.8	-0.8-1.1	-1.2-0.9	-0.5-0.7	-0.3-2.1	-0.4-1.9
10	-2.7-1.9	-0.7-0.9	-0.5-0.7	-1.4-2.1	-1.2-0.6	-2.3-1.9	-0.7-1.2	-1.2-1.0	-0.3-2.1	2.4-3.9	-2.3-0.5
11	-3.5-0.3	-0.8-0.5	-0.5-0.7	-1.4-1.4	-1.0-0.6	-2.4-1.6	-0.8-1.1	-1.1-0.9	-0.4-1.9	-2.3-0.5	-0.1-0.3
Total	38.0-43.4	11.2-17.5	-1.4-5.3	49.4-54.9	1.3-7.9	23.1-28.9	1.6-8.2	2.7-9.3	5.4-11.9	9.2-15.6	-2.0-4.7
Higher	30.7	5.8	2.3	18.8	3.8	18.1	4.4	5.2	8.5	9.5	3.7

Table F.112: Control / Temp. Gradient at 8cm / Mean

i \ j	1	2	3	4	5	6	7	8	9	10	11
1	4.3-7.1	-2.5-1.4	-2.6-1.1	2.7-7.9	-3.0-0.9	-2.0-3.0	-2.9-0.8	-2.9-0.8	-2.8-1.9	-2.7-2.0	-2.7-1.0
2	-2.5-1.4	3.2-4.3	-0.7-0.3	0.3-4.3	-0.5-0.6	0.3-2.4	-0.8-0.3	-0.8-0.3	-0.7-0.8	-0.3-1.3	-0.6-0.4
3	-2.6-1.1	-0.7-0.3	-0.2-0.1	-1.4-1.5	-0.4-0.2	-0.5-0.9	-0.4-0.3	-0.4-0.3	-0.3-0.4	-0.4-0.4	-0.4-0.3
4	2.7-7.9	0.3-4.3	-1.4-1.5	26.1-29.7	-1.2-1.4	-2.9-2.0	-1.5-1.2	-1.1-1.5	-1.5-2.1	-2.1-1.7	-1.2-1.3
5	-3.0-0.9	-0.5-0.6	-0.4-0.2	-1.2-1.4	1.0-1.6	-1.4-0.5	-0.8-0.5	-0.9-0.5	-1.0-0.5	-1.0-0.5	-1.0-0.3
6	-2.0-3.0	0.3-2.4	-0.5-0.9	-2.9-2.0	-1.4-0.5	12.5-15.1	-2.1-1.9	-2.2-1.8	-1.4-3.1	-1.0-3.6	-2.3-1.6
7	-2.9-0.8	-0.8-0.3	-0.4-0.3	-1.5-1.2	-0.8-0.5	-2.1-1.9	-0.3-0.3	-0.5-0.7	-0.5-0.7	-0.4-0.8	-0.5-0.6
8	-2.9-0.8	-0.8-0.3	-0.4-0.3	-1.1-1.5	-0.9-0.5	-2.2-1.8	-0.5-0.7	-0.2-0.3	-0.6-0.6	-0.4-0.8	-0.5-0.6
9	-2.8-1.9	-0.7-0.8	-0.3-0.4	-1.5-2.1	-1.0-0.5	-1.4-3.1	-0.5-0.7	-0.6-0.6	-0.6-1.0	0.0-3.4	-1.1-2.0
10	-2.7-2.0	-0.3-1.3	-0.4-0.4	-2.1-1.7	-1.0-0.5	-1.0-3.6	-0.4-0.8	-0.4-0.8	0.0-3.4	3.1-5.0	-1.6-1.9
11	-2.7-1.0	-0.6-0.4	-0.4-0.3	-1.2-1.3	-1.0-0.3	-2.3-1.6	-0.5-0.6	-0.5-0.6	-1.1-2.0	-1.6-1.9	0.0-0.3
Total	30.3-35.8	7.7-13.8	-3.7-2.9	52.2-57.1	-1.9-4.8	32.7-38.1	-2.7-3.9	-3.1-3.5	12.2-17.9	17.5-23.0	-3.7-2.9
Higher	27.7	3.9	0.6	19.2	2.8	19.0	1.8	1.3	12.0	12.9	0.4

Table F.113: South / Temp. Gradient at 8cm / Mean

i \ j	1	2	3	4	5	6	7	8	9	10	11
1	14.0-17.0	-1.8-2.5	-2.3-1.5	-1.0-4.5	-2.6-1.4	-2.7-2.8	-2.4-1.6	-2.2-1.7	-2.8-1.7	-2.4-2.3	-2.4-1.4
2	-1.8-2.5	7.8-9.2	-1.1-0.0	-2.3-1.4	-0.6-0.6	-1.0-1.3	-1.2-0.1	-1.1-0.1	-0.9-0.6	-0.9-0.8	-1.1-0.1
3	-2.3-1.5	-1.1-0.0	-0.1-0.3	-2.4-0.1	-0.5-0.4	-0.9-0.4	-0.5-0.4	-0.5-0.4	-0.5-0.5	-0.5-0.4	-0.5-0.4
4	-1.0-4.5	-2.3-1.4	-2.4-0.1	21.3-24.5	-0.8-1.9	-2.1-2.4	-0.6-2.1	-1.1-1.7	-0.3-2.7	-0.8-2.5	-0.7-1.9
5	-2.6-1.4	-0.6-0.6	-0.5-0.4	-0.8-1.9	2.4-3.4	-1.9-0.4	-1.3-0.7	-1.4-0.5	-1.4-0.6	-1.6-0.4	-1.6-0.3
6	-2.7-2.8	-1.0-1.3	-0.9-0.4	-2.1-2.4	-1.9-0.4	11.6-14.1	-1.5-2.8	-1.4-2.9	-1.4-3.0	-0.7-4.0	-1.8-2.4
7	-2.4-1.6	-1.2-0.1	-0.5-0.4	-0.6-2.1	-1.3-0.7	-1.5-2.8	-0.3-0.6	-0.8-1.0	-0.9-0.9	-1.2-0.7	-0.8-1.0
8	-2.2-1.7	-1.1-0.1	-0.5-0.4	-1.1-1.7	-1.4-0.5	-1.4-2.9	-0.8-1.0	-0.5-0.4	-0.9-0.8	-0.8-0.9	-0.8-0.9
9	-2.8-1.7	-0.9-0.6	-0.5-0.5	-0.3-2.7	-1.4-0.6	-1.4-3.0	-0.9-0.9	-0.9-0.8	-0.5-1.0	-0.3-2.6	-0.7-2.0
10	-2.4-2.3	-0.9-0.8	-0.5-0.4	-0.8-2.5	-1.6-0.4	-0.7-4.0	-1.2-0.7	-0.8-0.9	-0.3-2.6	2.2-3.9	-1.8-1.4
11	-2.4-1.4	-1.1-0.1	-0.5-0.4	-0.7-1.9	-1.6-0.3	-1.8-2.4	-0.8-1.0	-0.8-0.9	-0.7-2.0	-1.8-1.4	-0.1-0.5
Total	34.5-40.0	12.9-19.4	-2.8-4.4	40.1-45.8	1.6-8.7	27.4-33.4	0.1-7.2	-1.1-6.0	5.0-11.8	10.4-17.0	-2.2-5.0
Higher	22.3	9.8	3.3	15.5	5.5	14.1	3.4	2.4	5.6	8.0	1.2

Table F.114: North / Temp. Gradient at 8cm / Mean

i \ j	1	2	3	4	5	6	7	8	9	10	11
1	7.1-11.0	-1.4-2.4	-1.8-1.8	6.0-11.9	-2.2-1.4	-0.9-4.8	-2.2-1.4	-2.1-1.5	-2.1-2.4	-3.0-1.8	-2.7-1.0
2	-1.4-2.4	2.4-3.3	-0.4-0.5	1.4-4.3	-0.5-0.4	1.0-2.8	-0.6-0.4	-0.4-0.6	-0.6-0.7	-0.2-1.0	-0.5-0.5
3	-1.8-1.8	-0.4-0.5	-0.3-0.2	-1.0-1.3	-0.3-0.6	-0.4-1.0	-0.3-0.6	-0.3-0.6	-0.2-0.7	-0.4-0.6	-0.3-0.6
4	6.0-11.9	1.4-4.3	-1.0-1.3	23.8-27.3	-1.3-1.6	-1.9-2.6	-1.2-1.6	-1.4-1.5	-1.3-2.1	-1.5-2.0	-1.3-1.5
5	-2.2-1.4	-0.5-0.4	-0.3-0.6	-1.3-1.6	0.7-1.2	-0.8-0.7	-0.5-0.5	-0.5-0.6	-0.7-0.5	-0.8-0.3	-0.6-0.4
6	-0.9-4.8	1.0-2.8	-0.4-1.0	-1.9-2.6	-0.8-0.7	12.9-15.2	-2.2-1.4	-2.2-1.5	-2.1-1.8	-2.2-1.7	-2.1-1.5
7	-2.2-1.4	-0.6-0.4	-0.3-0.6	-1.2-1.6	-0.5-0.5	-2.2-1.4	-0.1-0.4	-0.5-0.3	-0.5-0.4	-0.5-0.4	-0.5-0.4
8	-2.1-1.5	-0.4-0.6	-0.3-0.6	-1.4-1.5	-0.5-0.6	-2.2-1.5	-0.5-0.3	-0.0-0.5	-0.5-0.5	-0.5-0.5	-0.4-0.5
9	-2.1-2.4	-0.6-0.7	-0.2-0.7	-1.3-2.1	-0.7-0.5	-2.1-1.8	-0.5-0.4	-0.5-0.5	-0.6-0.6	-0.5-1.8	-0.6-1.6
10	-3.0-1.8	-0.2-1.0	-0.4-0.6	-1.5-2.0	-0.8-0.3	-2.2-1.7	-0.5-0.4	-0.5-0.5	-0.5-1.8	3.4-4.8	-1.9-0.8
11	-2.7-1.0	-0.5-0.5	-0.3-0.6	-1.3-1.5	-0.6-0.4	-2.1-1.5	-0.5-0.4	-0.4-0.5	-0.6-1.6	-1.9-0.8	-0.0-0.4
Total	40.8-45.8	7.4-13.1	-2.2-4.0	53.1-58.4	-1.7-4.5	31.1-36.2	-2.3-3.8	-2.2-3.9	6.0-11.8	11.2-16.9	-2.1-3.9
Higher	25.2	1.7	-0.5	16.8	0.9	16.7	1.4	1.0	7.2	10.2	1.7

Table F.115: Control / Temp. Gradient at 8cm / Maximum

i \ j	1	2	3	4	5	6	7	8	9	10	11
1	0.9-4.3	-1.7-2.4	-2.6-1.5	2.8-8.1	-2.4-1.6	-0.9-6.1	-2.2-1.8	-2.6-1.5	-1.8-3.6	-1.9-3.3	-2.2-1.8
2	-1.7-2.4	0.5-1.1	-0.5-0.6	-0.1-1.5	-0.5-0.6	0.2-5.4	-0.4-0.7	-0.3-0.7	-0.5-0.9	0.4-2.5	-0.4-0.7
3	-2.6-1.5	-0.5-0.6	-0.3-0.2	-0.4-1.0	-0.4-0.6	-1.2-3.8	-0.3-0.6	-0.3-0.7	-0.2-1.0	-0.0-1.5	-0.3-0.7
4	2.8-8.1	-0.1-1.5	-0.4-1.0	-0.4-2.2	-2.2-1.6	-1.1-5.6	-2.4-1.4	-2.5-1.4	-2.8-1.7	-2.7-1.7	-2.3-1.5
5	-2.4-1.6	-0.5-0.6	-0.4-0.6	-2.2-1.6	-0.4-0.2	-0.7-4.2	-0.1-0.9	-0.1-0.9	0.1-1.3	-0.0-1.7	-0.1-0.9
6	-0.9-6.1	0.2-5.4	-1.2-3.8	-1.1-5.6	-0.7-4.2	18.8-23.4	-1.6-1.4	-1.5-1.5	-0.4-4.9	1.0-7.3	-1.2-1.8
7	-2.2-1.8	-0.4-0.7	-0.3-0.6	-2.4-1.4	-0.1-0.9	-1.6-1.4	-0.1-0.5	-0.4-0.8	-0.9-0.6	-0.4-1.5	-0.7-0.5
8	-2.6-1.5	-0.3-0.7	-0.3-0.7	-2.5-1.4	-0.1-0.9	-1.5-1.5	-0.4-0.8	-0.4-0.3	-0.5-0.9	0.2-2.1	-0.3-0.9
9	-1.8-3.6	-0.5-0.9	-0.2-1.0	-2.8-1.7	0.1-1.3	-0.4-4.9	-0.9-0.6	-0.5-0.9	-0.7-1.4	0.5-4.5	-1.7-1.7
10	-1.9-3.3	0.4-2.5	-0.0-1.5	-2.7-1.7	-0.0-1.7	1.0-7.3	-0.4-1.5	0.2-2.1	0.5-4.5	4.2-6.3	-1.3-1.5
11	-2.2-1.8	-0.4-0.7	-0.3-0.7	-2.3-1.5	-0.1-0.9	-1.2-1.8	-0.7-0.5	-0.3-0.9	-1.7-1.7	-1.3-1.5	-0.3-0.3
Total	39.5-50.8	-8.2-6.7	-9.7-5.9	30.9-41.0	-10.3-5.4	59.4-67.8	-8.8-6.7	-8.0-7.2	18.2-30.3	24.9-36.1	-9.7-5.6
Higher	34.4	-7.8	-4.7	29.2	-6.3	25.3	-1.7	-2.0	17.4	13.7	-2.8

Table F.116: South / Temp. Gradient at 8cm / Maximum

i \ j	1	2	3	4	5	6	7	8	9	10	11
1	13.6-18.4	-1.7-2.1	-1.2-2.2	-0.5-4.5	-1.4-2.1	0.0-7.8	-1.8-1.8	-1.6-1.8	1.0-5.5	-1.2-4.0	-1.8-1.6
2	-1.7-2.1	0.6-1.5	-1.7-0.2	-1.6-0.1	-1.5-0.1	-2.4-1.5	-1.2-0.3	-1.7-0.1	-1.4-0.3	-1.2-0.6	-1.4-0.1
3	-1.2-2.2	-1.7-0.2	-0.4-0.5	-1.0-0.6	-1.0-0.7	-2.3-1.4	-0.9-0.6	-1.0-0.5	-1.0-0.7	-0.9-0.8	-0.9-0.7
4	-0.5-4.5	-1.6-0.1	-1.0-0.6	-0.2-1.7	-1.4-1.7	-3.1-1.7	-1.2-1.8	-1.6-1.5	-1.5-1.8	-1.9-1.9	-1.6-1.5
5	-1.4-2.1	-1.5-0.1	-1.0-0.7	-1.4-1.7	-0.1-0.8	-2.1-1.7	-0.6-1.1	-0.9-0.7	-1.0-0.7	-1.1-0.7	-0.8-0.9
6	0.0-7.8	-2.4-1.5	-2.3-1.4	-3.1-1.7	-2.1-1.7	14.8-18.4	-1.8-1.5	-1.5-1.7	-1.9-2.1	-1.2-3.4	-1.7-1.5
7	-1.8-1.8	-1.2-0.3	-0.9-0.6	-1.2-1.8	-0.6-1.1	-1.8-1.5	0.3-1.2	-0.9-0.9	-1.1-0.7	-0.9-1.1	-1.1-0.6
8	-1.6-1.8	-1.7-0.1	-1.0-0.5	-1.6-1.5	-0.9-0.7	-1.5-1.7	-0.9-0.9	0.2-1.2	-1.2-0.8	-1.1-0.8	-1.2-0.6
9	1.0-5.5	-1.4-0.3	-1.0-0.7	-1.5-1.8	-1.0-0.7	-1.9-2.1	-1.1-0.7	-1.2-0.8	0.1-1.7	-1.6-1.3	-1.2-1.4
10	-1.2-4.0	-1.2-0.6	-0.9-0.8	-1.9-1.9	-1.1-0.7	-1.2-3.4	-0.9-1.1	-1.1-0.8	-1.6-1.3	3.3-5.0	-0.9-1.5
11	-1.8-1.6	-1.4-0.1	-0.9-0.7	-1.6-1.5	-0.8-0.9	-1.7-1.5	-1.1-0.6	-1.2-0.6	-1.2-1.4	-0.9-1.5	-0.1-0.5
Total	58.7-66.4	-5.4-8.9	-8.6-6.0	15.7-28.8	-7.6-7.1	48.8-58.4	-6.5-7.8	-6.2-8.3	6.9-20.0	15.5-27.4	-9.9-5.1
Higher	34.9	6.2	0.6	20.6	0.1	33.7	0.3	1.9	10.4	15.2	-1.6

Table F.117: North / Temp. Gradient at 8cm / Maximum

i \ j	1	2	3	4	5	6	7	8	9	10	11
1	17.9-23.9	-1.6-2.6	-1.6-2.3	8.8-16.7	-1.7-2.1	1.3-8.0	-1.1-2.6	-1.3-2.7	1.5-6.8	-0.5-4.7	-2.7-1.5
2	-1.6-2.6	1.3-2.1	-1.0-0.4	-0.3-1.9	-0.7-0.6	-0.2-1.9	-0.7-0.5	-0.7-0.6	-0.9-0.8	-0.9-0.6	-0.8-0.5
3	-1.6-2.3	-1.0-0.4	-0.1-0.7	-0.9-1.0	-0.8-0.5	-1.1-0.7	-0.8-0.5	-0.9-0.5	-0.8-0.6	-0.8-0.7	-0.8-0.5
4	8.8-16.7	-0.3-1.9	-0.9-1.0	3.8-6.9	-0.6-3.3	1.4-6.5	-0.7-3.4	-0.5-3.5	-0.9-3.6	-0.1-4.3	-0.6-3.4
5	-1.7-2.1	-0.7-0.6	-0.8-0.5	-0.6-3.3	-0.1-0.5	-0.9-0.7	-0.5-0.5	-0.5-0.5	-0.8-0.5	-0.7-0.5	-0.5-0.5
6	1.3-8.0	-0.2-1.9	-1.1-0.7	1.4-6.5	-0.9-0.7	5.0-7.5	-0.7-2.4	-0.5-2.6	-1.1-2.4	-0.1-3.6	-0.8-2.3
7	-1.1-2.6	-0.7-0.5	-0.8-0.5	-0.7-3.4	-0.5-0.5	-0.7-2.4	0.0-0.6	-0.1-1.1	-0.3-1.0	-0.2-1.1	-0.3-0.9
8	-1.3-2.7	-0.7-0.6	-0.9-0.5	-0.5-3.5	-0.5-0.5	-0.5-2.6	-0.1-1.1	0.5-1.3	-1.2-0.5	-1.3-0.6	-1.2-0.5
9	1.5-6.8	-0.9-0.8	-0.8-0.6	-0.9-3.6	-0.8-0.5	-1.1-2.4	-0.3-1.0	-1.2-0.5	-0.7-1.0	-1.3-2.2	-1.7-1.3
10	-0.5-4.7	-0.9-0.6	-0.8-0.7	-0.1-4.3	-0.7-0.5	-0.1-3.6	-0.2-1.1	-1.3-0.6	-1.3-2.2	1.3-3.0	-1.1-1.8
11	-2.7-1.5	-0.8-0.5	-0.8-0.5	-0.6-3.4	-0.5-0.5	-0.8-2.3	-0.3-0.9	-1.2-0.5	-1.7-1.3	-1.1-1.8	-0.2-0.3
Total	67.3-74.1	-5.8-8.0	-9.3-4.8	41.6-51.1	-6.8-6.3	31.8-42.5	-5.2-7.7	-8.1-5.7	6.0-18.4	8.8-21.0	-5.7-7.3
Higher	24.2	-1.9	-1.6	14.2	-1.5	16.8	-3.4	-4.6	5.9	6.3	-0.5

Table F.118: Control / Temp. Gradient at 8cm / Minimum

i \ j	1	2	3	4	5	6	7	8	9	10	11
1	0.3-2.2	-2.3-1.3	-2.1-1.5	-4.5-3.3	-2.1-1.4	-2.8-1.6	-2.3-1.3	-2.1-1.5	-2.1-1.8	-1.7-2.2	-2.1-1.5
2	-2.3-1.3	3.2-4.2	-1.4-0.3	-4.4-3.2	-1.5-0.2	-2.1-0.5	-1.5-0.2	-1.5-0.3	-1.3-0.6	-1.4-0.5	-1.4-0.3
3	-2.1-1.5	-1.4-0.3	-0.2-0.2	-5.8-1.2	-0.4-0.3	-1.2-0.4	-0.4-0.3	-0.4-0.3	-0.4-0.3	-0.5-0.3	-0.4-0.3
4	-4.5-3.3	-4.4-3.2	-5.8-1.2	47.3-52.7	-1.5-0.2	-0.9-5.4	-1.1-0.7	-1.3-0.6	-1.4-1.8	-2.0-2.1	-0.7-0.9
5	-2.1-1.4	-1.5-0.2	-0.4-0.3	-1.5-0.2	0.1-0.7	-1.6-0.3	-0.8-0.4	-0.8-0.4	-0.9-0.3	-0.9-0.3	-0.9-0.3
6	-2.8-1.6	-2.1-0.5	-1.2-0.4	-0.9-5.4	-1.6-0.3	13.1-15.8	-2.4-1.6	-2.2-1.7	-1.8-2.2	-1.8-2.6	-2.4-1.3
7	-2.3-1.3	-1.5-0.2	-0.4-0.3	-1.1-0.7	-0.8-0.4	-2.4-1.6	0.2-1.1	-0.8-1.0	-1.0-0.9	-1.1-0.8	-0.9-0.9
8	-2.1-1.5	-1.5-0.3	-0.4-0.3	-1.3-0.6	-0.8-0.4	-2.2-1.7	-0.8-1.0	0.0-0.9	-1.0-0.7	-0.7-1.1	-0.7-1.1
9	-2.1-1.8	-1.3-0.6	-0.4-0.3	-1.4-1.8	-0.9-0.3	-1.8-2.2	-1.0-0.9	-1.0-0.7	-0.8-0.9	-0.3-3.2	-1.2-2.1
10	-1.7-2.2	-1.4-0.5	-0.5-0.3	-2.0-2.1	-0.9-0.3	-1.8-2.6	-1.1-0.8	-0.7-1.1	-0.3-3.2	2.9-4.9	-1.8-1.7
11	-2.1-1.5	-1.4-0.3	-0.4-0.3	-0.7-0.9	-0.9-0.3	-2.4-1.3	-0.9-0.9	-0.7-1.1	-1.2-2.1	-1.8-1.7	-0.1-0.3
Total	12.1-19.3	5.8-13.3	-0.3-7.6	63.3-67.1	0.1-8.0	28.3-34.5	1.7-9.5	1.5-9.3	8.4-15.7	13.4-20.5	-0.1-7.8
Higher	17.7	11.6	7.5	17.3	7.3	17.7	7.1	6.5	10.7	11.8	4.7

Table F.119: South / Temp. Gradient at 8cm / Minimum

i \ j	1	2	3	4	5	6	7	8	9	10	11
1	3.5-6.0	-2.4-1.8	-2.5-1.8	-3.9-4.0	-2.4-1.8	-2.5-3.0	-2.3-2.1	-2.2-2.0	-2.1-2.6	-2.0-2.5	-2.5-1.9
2	-2.4-1.8	7.4-9.0	-1.3-0.8	-4.1-3.4	-1.4-0.7	-2.4-1.5	-1.5-0.7	-1.2-0.9	-1.1-1.0	-1.4-0.9	-1.3-0.8
3	-2.5-1.8	-1.3-0.8	0.0-0.5	-5.2-1.1	-1.1-0.0	-1.4-1.1	-1.0-0.0	-1.1-0.0	-1.1-0.0	-1.1-0.0	-1.0-0.1
4	-3.9-4.0	-4.1-3.4	-5.2-1.1	36.3-41.4	-1.4-1.0	-1.7-5.4	-1.4-1.4	-1.3-1.3	-1.2-1.7	-1.6-2.0	-1.0-1.2
5	-2.4-1.8	-1.4-0.7	-1.1-0.0	-1.4-1.0	0.9-1.9	-1.7-1.5	-1.5-0.4	-1.6-0.3	-1.7-0.3	-1.7-0.3	-1.7-0.2
6	-2.5-3.0	-2.4-1.5	-1.4-1.1	-1.7-5.4	-1.7-1.5	17.5-21.0	-1.5-3.0	-1.7-2.7	-1.6-2.8	-1.3-3.3	-1.8-2.4
7	-2.3-2.1	-1.5-0.7	-1.0-0.0	-1.4-1.4	-1.5-0.4	-1.5-3.0	1.6-3.1	-1.3-1.4	-1.6-1.2	-1.5-1.3	-1.5-1.3
8	-2.2-2.0	-1.2-0.9	-1.1-0.0	-1.3-1.3	-1.6-0.3	-1.7-2.7	-1.3-1.4	1.3-2.6	-1.2-1.3	-1.2-1.3	-1.2-1.3
9	-2.1-2.6	-1.1-1.0	-1.1-0.0	-1.2-1.7	-1.7-0.3	-1.6-2.8	-1.6-1.2	-1.2-1.3	-0.9-0.7	-0.1-2.8	-0.3-2.6
10	-2.0-2.5	-1.4-0.9	-1.1-0.0	-1.6-2.0	-1.7-0.3	-1.3-3.3	-1.5-1.3	-1.2-1.3	-0.1-2.8	2.8-4.6	-2.1-1.2
11	-2.5-1.9	-1.3-0.8	-1.0-0.1	-1.0-1.2	-1.7-0.2	-1.8-2.4	-1.5-1.3	-1.2-1.3	-0.3-2.6	-2.1-1.2	-0.1-0.5
Total	15.0-23.4	11.2-19.9	-0.6-8.9	47.4-53.2	1.3-10.6	30.8-38.0	4.5-13.4	3.1-12.3	4.2-13.3	8.3-17.1	-0.3-9.2
Higher	15.0	10.2	9.8	11.6	9.5	10.6	7.8	6.5	6.7	8.2	5.0

Table F.120: North / Temp. Gradient at 8cm / Minimum

i \ j	1	2	3	4	5	6	7	8	9	10	11
1	-0.2-2.5	-1.9-2.2	-2.3-2.0	-2.0-5.2	-2.3-2.0	-0.2-5.1	-2.3-1.9	-2.1-2.1	-2.6-2.1	-2.4-2.2	-2.5-1.8
2	-1.9-2.2	6.3-7.6	-0.9-0.6	-2.6-3.7	-1.0-0.5	-1.2-2.2	-1.1-0.5	-0.8-0.7	-0.8-0.9	-0.7-1.1	-1.0-0.5
3	-2.3-2.0	-0.9-0.6	-0.2-0.3	-4.5-0.8	-0.7-0.4	-1.2-1.2	-0.4-0.6	-0.4-0.6	-0.7-0.4	-0.4-0.7	-0.7-0.4
4	-2.0-5.2	-2.6-3.7	-4.5-0.8	34.6-39.3	-1.8-1.1	-3.3-3.8	-1.8-1.3	-2.2-0.9	-1.5-2.1	-1.6-2.6	-1.7-1.1
5	-2.3-2.0	-1.0-0.5	-0.7-0.4	-1.8-1.1	0.3-0.8	-1.4-1.0	-0.6-0.5	-0.6-0.5	-0.7-0.4	-0.6-0.6	-0.5-0.6
6	-0.2-5.1	-1.2-2.2	-1.2-1.2	-3.3-3.8	-1.4-1.0	16.8-19.9	-1.9-1.8	-2.0-1.8	-2.1-1.8	-1.7-2.5	-1.6-1.9
7	-2.3-1.9	-1.1-0.5	-0.4-0.6	-1.8-1.3	-0.6-0.5	-1.9-1.8	1.2-2.2	-0.8-0.9	-1.1-0.7	-0.9-0.9	-0.7-1.0
8	-2.1-2.1	-0.8-0.7	-0.4-0.6	-2.2-0.9	-0.6-0.5	-2.0-1.8	-0.8-0.9	1.7-2.7	-1.2-0.8	-1.5-0.6	-1.3-0.7
9	-2.6-2.1	-0.8-0.9	-0.7-0.4	-1.5-2.1	-0.7-0.4	-2.1-1.8	-1.1-0.7	-1.2-0.8	-1.0-0.2	-0.3-2.1	-0.3-2.1
10	-2.4-2.2	-0.7-1.1	-0.4-0.7	-1.6-2.6	-0.6-0.6	-1.7-2.5	-0.9-0.9	-1.5-0.6	-0.3-2.1	3.1-4.7	-1.7-1.1
11	-2.5-1.8	-1.0-0.5	-0.7-0.4	-1.7-1.1	-0.5-0.6	-1.6-1.9	-0.7-1.0	-1.3-0.7	-0.3-2.1	-1.7-1.1	0.0-0.3
Total	19.0-26.7	9.9-18.0	-1.1-7.7	51.2-56.5	-0.7-8.1	29.9-36.5	1.5-10.0	1.7-10.2	3.4-11.8	8.5-16.6	-1.6-7.1
Higher	18.6	6.6	5.6	17.2	4.4	11.7	4.8	5.5	6.9	7.5	2.9

## F.10 “Knee” Temperature Gradient

Table F.121: Control / “Knee” Temp. Gradient with Time (Total-effect)

t \ i	1	2	3	4	5	6	7	8	9	10	11
0.33	78.6-88.4	1.4-24.4	-18.0-10.9	17.6-40.8	-21.0-7.0	27.8-49.3	-21.0-6.9	-21.1-6.9	30.4-49.0	14.2-36.6	-17.6-10.1
0.67	79.0-88.6	-3.8-19.0	-16.3-11.0	19.5-40.9	-20.1-6.6	29.5-49.3	-19.6-7.1	-19.0-7.3	34.3-50.8	16.8-37.2	-16.5-9.9
1.00	78.6-88.6	-5.0-18.5	-12.8-12.3	29.6-44.3	-16.4-8.5	32.3-51.0	-16.5-8.2	-16.2-8.3	34.0-50.9	18.5-37.8	-12.6-11.6
1.33	75.0-85.7	-4.7-18.2	-12.4-12.0	30.3-45.2	-16.3-7.4	31.5-49.4	-14.3-8.9	-13.8-9.4	33.7-51.1	19.8-38.4	-13.0-10.4
1.67	68.3-80.3	-1.9-21.6	-14.5-9.6	28.2-43.8	-16.6-7.4	34.8-51.8	-13.4-10.8	-13.6-12.1	30.2-48.4	18.3-37.9	-14.1-10.1
2.00	59.1-72.1	5.3-26.8	-13.6-11.4	26.0-41.9	-14.9-10.8	37.0-55.7	-18.1-8.5	-11.6-12.5	27.5-45.2	16.7-37.3	-14.8-9.9
2.33	42.8-62.5	9.0-29.6	-21.0-7.4	18.6-37.0	-20.1-8.6	35.7-54.9	-10.3-13.7	-14.2-11.3	18.1-40.1	17.4-36.7	-21.7-5.9
2.67	25.9-55.5	12.4-30.6	-30.3-4.4	16.1-34.5	-21.0-9.0	37.2-55.8	-16.3-11.9	-15.9-11.3	7.5-36.7	18.3-37.8	-29.4-4.9
3.00	24.2-51.5	17.5-36.0	-26.3-6.2	13.1-31.5	-26.6-5.5	40.7-56.8	-11.7-14.8	-22.1-9.4	8.0-36.4	20.5-38.7	-26.5-5.9
3.33	23.0-47.9	22.5-39.9	-21.4-7.4	11.3-29.2	-20.6-8.5	43.9-59.0	-25.8-12.2	-16.7-11.9	13.6-37.5	23.6-40.8	-20.7-7.9
3.67	22.2-45.1	24.9-41.2	-16.6-9.5	9.7-27.6	-15.3-11.5	45.6-59.9	-19.3-14.5	-12.2-13.8	15.6-37.2	25.1-41.0	-15.9-10.2
4.00	23.5-44.9	26.1-43.0	-13.7-10.5	10.5-29.3	-21.6-9.7	44.4-59.3	-14.3-17.4	-8.0-17.0	17.9-36.5	25.5-41.5	-12.8-11.7
4.33	20.1-41.6	27.1-43.6	-16.3-8.4	7.0-26.6	-14.2-13.2	43.2-58.4	-15.1-16.0	-11.7-15.4	15.9-34.2	24.3-40.8	-15.1-9.8
4.67	18.9-40.2	27.7-44.5	-16.5-8.1	5.5-25.5	-14.0-13.1	43.0-58.4	-14.9-16.0	-10.6-15.9	15.4-33.6	24.3-40.7	-15.6-9.2
5.00	14.5-37.7	27.4-44.5	-21.7-3.2	-10.1-21.0	-19.9-11.7	43.3-58.4	-21.2-13.8	-15.1-14.1	13.5-32.2	23.0-39.9	-23.3-7.1
5.33	14.1-37.0	27.6-44.7	-19.0-6.7	1.0-22.5	-16.1-12.1	42.9-58.2	-18.5-13.7	-13.4-14.4	13.1-32.0	23.2-40.1	-17.6-8.3
5.67	13.5-36.9	30.1-46.2	-17.7-7.9	1.5-22.9	-15.3-12.7	43.9-58.8	-17.1-15.1	-12.3-15.5	12.6-31.8	24.3-40.7	-15.5-9.9
6.00	15.1-38.5	32.5-48.4	-15.7-9.8	4.0-24.9	-22.6-9.7	45.4-60.1	-16.2-16.6	-8.0-18.1	13.7-33.3	25.4-41.5	-13.4-12.1
6.33	11.2-36.9	34.3-49.0	-18.1-9.3	2.1-22.3	-15.3-12.8	46.9-61.3	-20.9-15.0	-9.2-17.0	11.2-34.3	24.2-41.0	-15.6-11.3
6.67	8.0-36.8	34.8-49.7	-21.7-8.3	0.4-21.9	-21.5-9.9	45.2-60.4	-26.8-13.5	-13.7-15.7	5.7-32.7	23.2-41.2	-21.2-9.0
7.00	2.3-37.0	33.4-48.9	-30.2-6.2	-4.2-20.5	-32.1-5.0	40.9-58.0	-22.9-11.2	-20.2-13.6	-3.7-29.5	17.5-38.3	-29.2-7.0
7.33	-4.3-35.7	33.4-47.7	-36.4-4.7	-1.3-22.5	-23.0-11.1	39.8-58.9	-14.3-15.9	-13.4-16.8	-9.5-27.2	16.7-39.4	-34.1-6.6
7.67	11.0-40.9	36.9-52.6	-20.3-11.8	1.7-25.8	-19.3-13.8	41.8-61.7	-11.3-17.7	-14.6-16.1	5.3-33.9	20.9-42.2	-20.0-11.7
8.00	26.8-50.0	39.0-55.0	-17.6-12.5	12.4-33.3	-21.3-11.6	43.6-64.2	-5.3-22.9	-7.3-20.4	19.4-41.6	24.3-46.3	-18.4-11.8
8.33	29.5-51.8	26.5-46.6	-20.0-8.2	14.8-37.1	-19.0-10.8	40.6-60.8	-13.8-18.4	-8.6-18.1	18.6-42.8	25.6-46.3	-15.1-14.8
8.67	50.5-67.0	18.8-40.2	-15.4-12.3	32.7-49.1	-17.5-11.1	48.7-65.2	-8.3-19.0	-3.1-21.4	24.5-48.2	34.2-52.2	-13.9-14.1
9.00	64.3-75.5	6.5-29.4	-14.6-10.3	37.9-54.0	-14.1-10.8	53.3-67.4	-2.6-19.9	-2.9-20.6	34.0-51.8	39.1-55.9	-17.8-9.2
9.33	72.1-80.9	2.0-23.6	-8.8-13.6	41.6-55.9	-13.1-9.6	56.0-68.6	-2.1-19.2	3.4-24.7	42.9-57.2	41.0-55.3	-9.7-13.5
9.67	76.8-84.4	-0.7-20.8	-5.4-16.7	40.7-55.9	-12.9-11.0	52.1-65.5	-2.7-18.1	3.8-23.3	44.3-59.5	40.7-55.3	-6.9-16.4
10.00	78.4-86.0	-3.6-18.0	-8.2-14.2	38.5-53.8	-8.8-12.8	49.5-62.8	-6.3-15.7	-1.0-19.3	44.1-59.4	38.8-52.7	-10.9-12.2

Table F.122: Control / “Knee” Temp. Gradient / Mid-day

i \ j	1	2	3	4	5	6	7	8	9	10	11
1	-0.1-2.1	-2.8-3.7	-1.8-1.2	0.7-4.0	-1.2-1.8	-2.6-2.6	-1.7-1.4	-1.3-2.0	-1.0-3.1	-2.2-2.1	-1.2-1.7
2	-2.8-3.7	8.3-12.4	-0.2-2.4	-1.7-3.1	-1.4-1.8	6.3-14.6	-1.5-1.9	-1.1-2.5	0.1-5.9	4.5-12.3	-0.7-1.5
3	-1.8-1.2	-0.2-2.4	-0.3-0.2	-0.4-0.5	-0.4-0.3	-0.7-2.6	-0.5-0.4	-0.5-0.5	-0.4-0.9	-0.1-1.7	-0.4-0.4
4	0.7-4.0	-1.7-3.1	-0.4-0.5	-0.3-1.1	-1.5-1.2	-2.6-2.1	-1.6-1.2	-1.7-1.1	-1.1-1.8	-1.8-1.8	-1.3-1.0
5	-1.2-1.8	-1.4-1.8	-0.4-0.3	-1.5-1.2	-0.6-0.5	-1.0-2.9	-0.7-1.4	-0.8-1.3	-0.5-2.0	-0.5-2.3	-0.5-1.4
6	-2.6-2.6	6.3-14.6	-0.7-2.6	-2.6-2.1	-1.0-2.9	5.1-8.9	-1.6-2.2	-1.6-2.4	-0.9-4.9	-0.6-5.4	-1.0-1.8
7	-1.7-1.4	-1.5-1.9	-0.5-0.4	-1.6-1.2	-0.7-1.4	-1.6-2.2	-1.0-0.6	-1.4-1.4	-1.3-2.1	-0.9-2.6	-1.5-1.3
8	-1.3-2.0	-1.1-2.5	-0.5-0.5	-1.7-1.1	-0.8-1.3	-1.6-2.4	-1.4-1.4	-0.9-0.4	-0.2-2.8	0.6-4.1	-0.1-2.4
9	-1.0-3.1	0.1-5.9	-0.4-0.9	-1.1-1.8	-0.5-2.0	-0.9-4.9	-1.3-2.1	-0.2-2.8	1.4-3.2	2.0-6.2	-0.7-1.3
10	-2.2-2.1	4.5-12.3	-0.1-1.7	-1.8-1.8	-0.5-2.3	-0.6-5.4	-0.9-2.6	0.6-4.1	2.0-6.2	1.8-3.9	-1.3-1.2
11	-1.2-1.7	-0.7-1.5	-0.4-0.4	-1.3-1.0	-0.9-1.4	-1.0-1.8	-1.5-1.3	-0.1-2.4	-0.7-1.3	-1.3-1.2	-0.2-0.2
Total	14.5-37.7	27.4-44.5	-21.7-3.2	-10.1-21.0	-19.9-11.7	43.3-58.4	-21.2-13.8	-15.1-14.1	13.5-32.2	23.0-39.9	-23.3-7.1
Higher	20.9	-0.0	-12.0	2.5	-8.1	26.1	-5.2	-6.4	7.1	8.9	-10.8

Table F.123: South / “Knee” Temp. Gradient with Time (Total-effect)

t \ i	1	2	3	4	5	6	7	8	9	10	11
0.33	88.0-94.1	14.7-30.3	-7.6-13.1	17.5-32.6	-11.7-8.2	25.0-40.6	-12.0-7.9	-11.9-8.0	23.1-39.6	7.0-24.1	-9.4-10.1
0.67	87.6-93.9	3.3-18.8	-12.2-8.3	12.2-27.5	-9.6-8.5	23.6-38.9	-9.7-8.1	-9.6-8.2	19.6-35.5	2.8-19.5	-8.3-9.3
1.00	86.6-93.3	0.4-17.4	-9.0-8.9	14.5-28.5	-9.5-8.4	26.5-41.3	-10.6-6.5	-8.2-9.5	18.8-35.2	4.5-21.5	-7.8-9.7
1.33	85.4-90.8	2.7-20.6	-8.1-9.7	15.0-29.1	-8.1-9.5	28.2-43.3	-8.5-9.2	-10.5-6.9	20.9-35.1	7.6-23.2	-11.5-6.6
1.67	70.1-81.2	6.8-25.1	-7.7-11.5	9.3-26.3	-10.3-8.9	29.1-44.5	-7.1-10.9	-8.5-9.6	14.5-31.5	6.2-23.6	-11.8-8.3
2.00	59.1-70.3	13.0-28.7	-13.4-7.4	3.7-22.8	-13.7-6.2	30.0-46.3	-9.6-9.6	-11.0-8.4	7.1-26.3	4.3-21.4	-15.3-5.2
2.33	53.5-64.2	18.0-34.0	-10.3-8.9	5.8-23.7	-9.3-9.3	33.9-48.4	-7.3-13.0	-6.1-12.5	10.3-28.1	8.9-24.9	-11.2-7.1
2.67	46.8-58.2	22.8-37.9	-10.0-8.1	6.7-24.1	-10.7-8.0	37.4-51.4	-2.9-16.8	-2.9-16.3	10.3-26.7	10.6-26.1	-8.8-8.7
3.00	42.0-56.8	29.9-46.6	-14.5-10.1	3.4-25.4	-7.5-19.1	40.4-58.5	5.7-28.5	1.7-22.2	13.5-30.6	14.3-31.8	-16.2-7.9
3.33	36.5-52.1	28.4-43.1	-9.4-13.4	0.5-22.6	-8.6-18.9	40.1-58.0	4.4-24.6	1.2-21.8	10.4-27.2	10.7-28.8	-10.2-11.7
3.67	32.8-48.8	30.9-44.0	-15.9-8.1	0.1-21.7	-5.2-21.3	33.8-56.9	7.8-26.5	4.9-23.8	11.5-27.3	12.3-29.2	-9.1-11.8
4.00	28.6-45.2	30.3-43.9	-9.6-12.4	-1.8-20.1	-5.8-21.4	31.8-55.5	4.6-25.1	4.3-23.1	9.2-25.7	11.5-28.4	-11.2-10.1
4.33	25.0-42.4	32.1-45.2	-11.6-10.8	-2.6-19.2	-4.2-21.8	32.6-55.6	5.2-25.5	5.3-23.7	7.8-24.8	11.3-28.1	-11.9-9.6
4.67	22.1-39.8	31.6-45.0	-13.0-9.4	-4.1-17.9	-6.5-20.0	31.4-54.8	4.8-25.2	3.9-22.8	4.3-22.1	9.3-26.8	-13.3-8.4
5.00	19.7-38.2	32.4-45.5	-13.9-8.6	-4.8-17.3	-6.2-20.2	31.3-54.8	4.1-24.9	3.9-22.9	3.0-21.0	7.7-25.4	-13.8-8.0
5.33	17.0-36.1	32.5-45.4	-14.3-8.5	-6.3-16.2	-7.0-20.0	30.4-54.6	3.8-24.6	3.0-22.0	2.6-20.3	8.4-26.2	-14.5-7.7
5.67	17.2-36.4	34.7-47.1	-13.0-9.7	-5.6-17.0	-4.4-22.1	32.0-55.7	5.3-25.4	4.6-23.3	4.7-22.2	9.6-27.1	-12.7-9.3
6.00	18.8-38.1	35.1-47.6	-11.1-11.5	-4.7-18.3	-4.2-23.1	32.0-56.4	6.1-26.1	5.6-24.5	6.3-23.5	9.9-27.5	-10.8-10.9
6.33	21.8-41.1	38.1-50.1	-16.1-8.3	-2.7-20.2	-3.1-24.1	33.5-58.1	7.8-27.2	5.7-25.1	8.2-25.0	12.7-30.0	-15.5-8.2
6.67	23.2-43.1	40.7-52.5	-15.4-9.9	-1.7-21.6	-2.7-24.5	43.2-61.3	7.4-27.5	5.9-26.4	8.8-26.2	13.4-31.1	-14.2-9.8
7.00	24.5-45.2	44.3-58.3	-13.0-12.7	-1.7-23.1	-3.3-24.5	44.3-63.0	9.3-32.6	7.5-28.6	10.1-28.9	15.9-33.8	-13.3-11.6
7.33	24.0-40.6	43.6-55.9	-11.0-8.5	-0.8-19.1	-4.5-14.2	44.6-58.9	6.0-25.6	6.1-26.6	6.3-24.1	13.3-29.3	-9.5-9.7
7.67	21.1-40.1	40.9-55.0	-14.6-8.3	-8.2-14.8	-13.9-9.0	40.6-56.6	-1.6-21.2	3.3-25.1	1.4-23.7	9.8-27.7	-13.8-7.7
8.00	25.0-43.2	41.8-55.6	-15.4-9.3	-10.5-16.1	-17.9-8.9	38.9-56.7	2.2-23.5	1.4-24.3	-0.1-24.3	11.3-28.6	-14.1-10.1
8.33	28.8-50.6	35.0-52.9	-10.3-12.2	-12.5-18.6	-10.8-14.1	42.0-58.5	4.3-25.6	0.3-25.4	1.4-26.3	13.4-31.7	-17.1-9.4
8.67	50.3-64.3	22.9-43.9	-14.4-11.3	2.7-25.9	-15.3-9.5	43.1-60.1	0.9-23.8	1.9-24.5	7.0-29.2	13.8-33.2	-12.7-12.3
9.00	66.6-77.2	10.0-30.2	-17.2-7.7	12.7-35.6	-14.5-9.0	47.6-61.4	1.7-22.6	-0.0-23.1	8.0-29.2	19.5-37.1	-13.8-9.0
9.33	74.9-84.6	-4.8-18.3	-13.2-10.1	8.8-32.0	-14.6-8.9	47.7-61.8	-3.0-19.6	-8.8-15.2	11.6-31.9	17.6-35.5	-18.1-5.6
9.67	80.1-88.5	-4.7-16.5	-14.5-9.2	11.3-33.2	-10.0-11.7	47.8-61.2	-6.8-16.2	-5.6-16.5	18.0-36.8	17.2-35.5	-12.7-9.9
10.00	83.6-90.7	-1.8-18.6	-9.7-12.0	15.4-35.7	-14.6-8.4	48.7-61.6	-5.6-16.0	-4.1-16.3	22.5-40.4	19.1-36.5	-14.6-8.6

Table F.124: South / “Knee” Temp. Gradient / Mid-day

i \ j	1	2	3	4	5	6	7	8	9	10	11
1	0.1-3.5	-0.7-7.4	-0.5-2.8	1.2-5.0	-0.3-3.8	-2.6-2.9	0.2-4.8	0.5-4.7	1.3-5.6	-0.6-4.4	-0.3-3.1
2	-0.7-7.4	10.9-15.4	0.0-2.4	0.1-4.4	0.1-3.5	1.4-9.4	-3.6-2.1	-1.9-2.8	1.2-6.1	1.4-7.4	-0.1-2.2
3	-0.5-2.8	0.0-2.4	-0.4-0.1	-0.1-1.0	-0.3-0.8	-1.6-1.2	-0.3-0.9	-0.1-1.1	-0.0-1.0	-0.2-1.1	-0.1-0.8
4	1.2-5.0	0.1-4.4	-0.1-1.0	-0.7-0.2	-0.7-1.4	-2.4-0.9	-0.5-1.4	-0.4-1.5	-0.2-1.7	-0.6-1.4	-0.6-1.2
5	-0.3-3.8	0.1-3.5	-0.3-0.8	-0.7-1.4	-0.7-0.9	-2.4-1.6	-1.5-1.6	-1.2-1.9	-1.0-2.1	-1.8-1.7	-1.1-1.7
6	-2.6-2.9	1.4-9.4	-1.6-1.2	-2.4-0.9	-2.4-1.6	7.4-11.1	-2.7-2.5	-2.0-2.7	-1.0-3.9	-2.1-3.3	-2.2-1.6
7	0.2-4.8	-3.6-2.1	-0.3-0.9	-0.5-1.4	-1.5-1.6	-2.7-2.5	-1.8-0.9	-1.4-2.9	-1.9-2.6	-2.1-2.6	-2.0-2.0
8	0.5-4.7	-1.9-2.8	-0.1-1.1	-0.4-1.5	-1.2-1.9	-2.0-2.7	-1.4-2.9	-1.1-1.0	-0.8-2.8	-1.2-2.7	-0.7-2.5
9	1.3-5.6	1.2-6.1	-0.0-1.0	-0.2-1.7	-1.0-2.1	-1.0-3.9	-1.9-2.6	-0.8-2.8	0.8-2.3	0.0-2.8	-0.5-1.6
10	-0.6-4.4	1.4-7.4	-0.2-1.1	-0.6-1.4	-1.8-1.7	-2.1-3.3	-2.1-2.6	-1.2-2.7	0.0-2.8	0.7-3.3	-2.1-1.7
11	-0.3-3.1	-0.1-2.2	-0.1-0.8	-0.6-1.2	-1.1-1.7	-2.2-1.6	-2.0-2.0	-0.7-2.5	-0.5-1.6	-2.1-1.7	-0.2-0.2
Total	19.7-38.2	32.4-45.5	-13.9-8.6	-4.8-17.3	-6.2-20.2	31.3-54.8	4.1-24.9	3.9-22.9	3.0-21.0	7.7-25.4	-13.8-8.0
Higher	5.7	2.9	-7.5	-1.5	2.0	27.5	11.1	5.3	-3.1	4.6	-7.3



Table F.125: North / “Knee” Temp. Gradient with Time (Total-effect)

t \ i	1	2	3	4	5	6	7	8	9	10	11
0.33	93.8-98.0	23.2-40.3	-8.5-14.9	27.6-42.6	-14.1-9.9	15.5-34.8	-14.1-9.8	-14.1-9.8	23.0-40.7	-0.4-21.0	-12.0-11.2
0.67	94.3-97.8	15.1-31.5	-6.2-14.6	27.2-41.6	-12.1-8.5	16.8-34.6	-12.0-8.6	-11.5-9.5	22.2-39.4	2.4-22.0	-10.3-10.0
1.00	94.1-97.5	9.3-25.6	-6.6-12.4	25.7-39.4	-7.5-10.7	17.8-34.2	-12.9-6.8	-12.5-7.0	20.9-37.3	0.2-18.5	-10.4-9.0
1.33	93.2-96.9	6.3-23.3	-6.5-12.6	27.5-40.9	-11.9-7.3	18.3-34.5	-11.4-7.8	-10.7-8.7	18.5-35.3	1.4-19.2	-10.6-8.7
1.67	91.6-95.6	4.9-21.9	-3.7-13.6	28.1-41.7	-12.4-7.3	18.4-34.1	-9.0-8.9	-8.4-10.7	16.6-33.6	1.6-19.1	-11.1-8.0
2.00	87.7-92.4	5.8-22.1	-4.0-12.5	26.2-39.9	-10.8-6.9	17.9-33.1	-7.3-9.4	-8.0-9.5	16.6-31.5	1.2-17.9	-10.0-7.5
2.33	81.9-87.6	9.0-24.7	-7.1-9.6	25.2-38.7	-7.4-9.6	16.7-31.8	-6.2-10.8	-6.3-10.4	12.5-28.3	-0.0-16.6	-10.1-7.2
2.67	74.6-81.8	14.9-31.3	-8.0-10.1	23.4-38.3	-7.5-10.4	18.6-34.0	-3.2-14.7	-4.5-12.9	11.7-27.9	0.1-17.4	-11.0-7.2
3.00	66.8-75.2	20.7-35.6	-10.3-7.7	20.7-35.8	-12.4-7.3	18.9-33.9	-1.7-15.7	-2.2-14.2	6.9-23.3	-0.6-16.9	-10.7-7.4
3.33	57.5-67.9	26.6-40.1	-8.6-10.2	15.4-31.6	-9.8-9.3	17.4-33.3	-1.3-16.0	-2.5-14.7	-0.2-19.5	-4.7-14.3	-11.5-8.4
3.67	49.6-61.4	32.9-45.8	-14.0-6.6	15.0-31.0	-15.0-7.2	19.4-35.6	1.1-18.8	1.4-18.4	1.4-21.2	-0.7-17.7	-9.8-9.5
4.00	46.0-58.0	37.2-49.5	-12.8-7.4	14.2-30.0	-14.1-7.3	20.5-36.4	1.7-19.2	3.5-20.3	2.0-21.4	0.8-18.7	-8.2-10.8
4.33	42.3-54.5	40.4-52.2	-13.3-6.6	12.5-28.2	-13.8-6.8	21.5-36.8	1.4-18.8	4.8-21.6	1.4-20.3	0.8-18.7	-8.3-10.2
4.67	39.4-51.8	42.4-53.8	-13.2-6.9	11.5-27.5	-12.8-7.5	21.5-36.6	0.4-18.7	5.3-21.9	0.4-19.3	0.4-18.3	-8.8-9.8
5.00	36.9-49.8	42.9-54.2	-8.5-9.7	10.1-26.5	-13.4-7.2	20.6-36.0	-1.3-17.5	3.3-20.4	-1.4-17.9	-0.5-17.5	-10.5-8.4
5.33	35.9-48.8	44.7-55.8	-8.4-10.1	9.6-26.2	-12.8-7.9	19.8-35.6	-0.1-18.4	4.5-21.7	-1.5-18.1	-1.3-17.1	-10.0-9.0
5.67	35.3-48.4	45.9-56.8	-8.4-10.2	9.9-26.5	-14.1-7.2	20.0-36.0	1.3-18.7	4.7-21.9	-1.1-18.8	-0.8-17.7	-9.4-9.8
6.00	36.0-49.3	46.6-57.3	-8.8-10.4	10.6-27.5	-13.3-9.1	19.4-35.9	1.4-19.0	4.0-21.4	-2.1-18.7	-1.2-17.8	-9.1-10.6
6.33	37.2-50.8	46.7-57.9	-9.0-10.9	11.3-28.6	-12.1-11.0	18.2-35.5	2.7-21.0	5.5-23.2	-2.4-19.3	-0.6-18.7	-8.5-11.6
6.67	36.6-50.5	45.2-56.7	-12.0-9.3	8.9-28.4	-13.8-8.9	15.3-32.6	0.2-19.1	3.8-22.0	-6.7-15.7	-5.8-14.5	-12.9-8.6
7.00	42.1-54.8	42.0-54.0	-12.3-7.2	12.0-29.5	-10.1-8.9	16.1-32.3	-0.0-17.4	5.2-20.9	-0.1-17.7	-3.7-14.8	-12.3-6.6
7.33	48.0-59.9	35.8-51.5	-10.4-10.1	14.0-32.5	-13.3-8.9	14.8-32.4	0.7-19.4	7.1-24.0	4.4-22.2	-3.5-16.0	-13.4-7.7
7.67	50.4-61.8	32.3-47.7	-8.5-9.4	18.1-33.4	-11.8-8.4	15.1-31.3	2.0-18.3	7.2-22.2	6.7-22.9	1.6-17.9	-12.6-8.3
8.00	58.6-69.7	28.8-45.0	-5.4-14.4	25.6-41.8	-9.2-11.6	21.6-38.4	6.5-23.8	9.3-27.9	12.2-29.9	9.0-27.5	-9.8-13.1
8.33	70.8-80.5	16.8-35.6	-6.2-16.9	33.2-50.8	-9.5-12.9	29.3-46.5	-7.3-16.2	1.0-22.1	17.0-35.5	14.5-35.8	-10.9-12.7
8.67	81.4-88.6	4.9-26.0	-7.8-15.7	37.5-54.3	-10.4-11.8	34.3-51.2	-6.1-16.8	-0.9-21.6	20.4-39.3	16.6-37.8	-13.6-11.8
9.00	87.2-93.6	-7.0-16.7	-12.9-11.9	36.5-53.8	-17.8-6.7	33.5-51.5	-17.3-8.7	-7.6-16.3	17.3-36.8	14.0-35.8	-14.3-10.4
9.33	90.2-96.0	-7.4-15.2	-7.5-15.4	40.4-56.0	-14.7-9.0	36.6-53.4	-12.5-10.9	-5.5-16.8	21.4-39.2	19.4-39.2	-12.0-10.7
9.67	91.7-97.1	-8.3-14.2	-8.8-14.0	39.2-54.0	-14.1-8.3	33.2-50.4	-12.0-10.7	-6.4-15.5	21.2-38.5	15.9-34.9	-10.3-10.9
10.00	93.0-97.8	-6.7-13.9	-3.9-16.7	37.6-51.9	-9.6-10.8	35.1-51.1	-7.7-12.9	-3.4-15.8	23.5-39.3	16.7-34.6	-14.1-7.9

Table F.126: North / “Knee” Temp. Gradient / Mid-day

i \ j	1	2	3	4	5	6	7	8	9	10	11
1	7.6-11.9	-7.6-5.0	-1.5-1.8	4.5-9.3	-1.3-2.0	-0.5-4.7	-1.1-3.2	-0.2-3.8	0.6-5.0	-1.5-2.6	-1.4-1.7
2	-7.6-5.0	23.2-30.2	-1.8-1.2	-0.5-5.7	-2.3-1.4	-0.4-7.2	-2.6-3.9	1.1-6.4	-2.3-2.7	-2.3-3.1	-1.4-1.0
3	-1.5-1.8	-1.8-1.2	-0.3-0.4	-0.5-0.9	-0.5-0.7	-0.3-1.3	-0.4-0.9	-0.3-1.0	-0.3-1.1	-0.4-1.0	-0.5-0.7
4	4.5-9.3	-0.5-5.7	-0.5-0.9	-0.6-0.8	-0.1-2.1	-0.0-2.6	-0.1-2.6	0.1-2.7	-0.1-2.5	-0.1-2.5	-0.1-2.3
5	-1.3-2.0	-2.3-1.4	-0.5-0.7	-0.1-2.1	-0.1-0.6	-0.8-0.7	-1.1-0.6	-1.2-0.6	-1.1-0.6	-1.1-0.4	-1.2-0.3
6	-0.5-4.7	-0.4-7.2	-0.3-1.3	-0.0-2.6	-0.8-0.7	0.2-2.4	-0.3-3.0	0.0-3.4	-1.0-2.5	-0.5-3.1	-0.9-2.2
7	-1.1-3.2	-2.6-3.9	-0.4-0.9	-0.1-2.6	-1.1-0.6	-0.3-3.0	-0.2-1.0	-0.4-1.8	-0.8-1.5	-0.5-1.8	-0.6-1.5
8	-0.2-3.8	1.1-6.4	-0.3-1.0	0.1-2.7	-1.2-0.6	0.0-3.4	-0.4-1.8	1.1-2.3	-1.9-0.7	-1.4-1.2	-1.7-0.6
9	0.6-5.0	-2.3-2.7	-0.3-1.1	-0.1-2.5	-1.1-0.6	-1.0-2.5	-0.8-1.5	-1.9-0.7	0.2-1.4	-1.2-0.9	-0.9-1.1
10	-1.5-2.6	-2.3-3.1	-0.4-1.0	-0.1-2.5	-1.1-0.4	-0.5-3.1	-0.5-1.8	-1.4-1.2	-1.2-0.9	-0.9-0.5	-0.8-1.3
11	-1.4-1.7	-1.4-1.0	-0.5-0.7	-0.1-2.3	-1.2-0.3	-0.9-2.2	-0.6-1.5	-1.7-0.6	-0.9-1.1	-0.8-1.3	-0.2-0.2
Total	36.9-49.8	42.9-54.2	-8.5-9.7	10.1-26.5	-13.4-7.2	20.6-36.0	-1.3-17.5	3.3-20.4	-1.4-17.9	-0.5-17.5	-10.5-8.4
Higher	19.0	13.1	-1.6	-0.0	-2.8	14.0	1.2	2.0	2.6	4.6	-2.6

Table F.127: Control / “Knee” Temp. Gradient / Mean

i \ j	1	2	3	4	5	6	7	8	9	10	11
1	2.6-6.1	-1.9-4.0	-1.2-1.6	3.9-8.8	-1.7-1.2	-0.4-5.4	-1.7-1.7	-1.1-2.0	2.4-7.3	-1.2-4.3	-1.6-1.6
2	-1.9-4.0	5.9-9.1	-0.3-1.6	-0.2-3.8	-0.4-1.6	4.6-10.6	-0.5-1.9	0.1-2.4	-0.1-4.1	3.2-9.1	-0.3-1.7
3	-1.2-1.6	-0.3-1.6	-0.3-0.2	-0.6-0.6	-0.5-0.4	-0.8-1.7	-0.5-0.4	-0.6-0.4	-0.4-0.9	-0.3-1.4	-0.5-0.5
4	3.9-8.8	-0.2-3.8	-0.6-0.6	-0.8-0.7	-1.7-1.0	-2.6-1.8	-1.6-1.3	-1.1-1.8	-1.2-2.0	-2.3-1.4	-1.7-1.0
5	-1.7-1.2	-0.4-1.6	-0.5-0.4	-1.7-1.0	-0.2-0.3	-0.6-1.8	-0.4-0.5	-0.4-0.5	-0.4-0.9	-0.3-1.3	-0.4-0.5
6	-0.4-5.4	4.6-10.6	-0.8-1.7	-2.6-1.8	-0.6-1.8	4.4-7.4	-1.3-1.5	-1.2-1.6	-0.7-3.5	-1.1-3.7	-1.1-1.4
7	-1.7-1.7	-0.5-1.9	-0.5-0.4	-1.6-1.3	-0.4-0.5	-1.3-1.5	-0.4-0.4	-0.7-1.1	-1.3-1.0	-1.0-1.4	-0.8-1.0
8	-1.1-2.0	0.1-2.4	-0.6-0.4	-1.1-1.8	-0.4-0.5	-1.2-1.6	-0.7-1.1	-0.7-0.2	-0.3-1.8	0.6-2.9	-0.1-1.7
9	2.4-7.3	-0.1-4.1	-0.4-0.9	-1.2-2.0	-0.4-0.9	-0.7-3.5	-1.3-1.0	-0.3-1.8	1.9-3.8	1.6-5.5	-0.8-1.2
10	-1.2-4.3	3.2-9.1	-0.3-1.4	-2.3-1.4	-0.3-1.3	-1.1-3.7	-1.0-1.4	0.6-2.9	1.6-5.5	1.7-3.9	-1.4-1.0
11	-1.6-1.6	-0.3-1.7	-0.5-0.5	-1.7-1.0	-0.4-0.5	-1.1-1.4	-0.8-1.0	-0.1-1.7	-0.8-1.2	-1.4-1.0	-0.1-0.2
Total	36.1-57.0	10.3-29.7	-20.0-7.2	14.5-32.8	-21.8-6.3	36.0-53.4	-16.5-10.7	-13.7-11.6	16.5-37.6	18.5-36.5	-18.9-8.4
Higher	25.5	-9.9	-8.3	16.6	-9.4	24.9	-3.9	-6.5	10.7	9.9	-6.8

Table F.128: South / “Knee” Temp. Gradient / Mean

i \ j	1	2	3	4	5	6	7	8	9	10	11
1	9.8-14.2	-2.8-4.6	-0.5-2.4	1.4-5.9	-1.0-2.3	-0.2-5.8	-1.1-2.7	-0.5-3.1	4.4-9.5	-0.8-4.3	-0.6-2.3
2	-2.8-4.6	9.7-13.0	-0.9-1.2	-1.6-1.4	-0.9-1.4	2.5-7.8	-1.5-1.2	-1.4-1.1	-0.0-3.6	1.4-5.2	-0.7-1.3
3	-0.5-2.4	-0.9-1.2	-0.2-0.2	-0.4-0.5	-0.6-0.4	-0.9-1.1	-0.5-0.5	-0.5-0.5	-0.4-0.7	-0.4-0.6	-0.4-0.5
4	1.4-5.9	-1.6-1.4	-0.4-0.5	-0.6-0.4	-1.3-1.1	-1.2-2.1	-1.0-1.3	-1.1-1.2	-0.6-2.1	-1.4-1.5	-1.5-1.1
5	-1.0-2.3	-0.9-1.4	-0.6-0.4	-1.3-1.1	-0.1-0.6	-1.7-0.3	-0.6-0.6	-0.7-0.5	-0.5-0.9	-0.8-0.7	-0.6-0.5
6	-0.2-5.8	2.5-7.8	-0.9-1.1	-1.2-2.1	-1.7-0.3	5.8-8.7	-1.2-1.7	-1.1-1.9	0.1-3.7	-0.2-3.6	-0.5-2.1
7	-1.1-2.7	-1.5-1.2	-0.5-0.5	-1.0-1.3	-0.6-0.6	-1.2-1.7	-0.5-0.7	-0.9-1.3	-0.7-1.7	-1.0-1.5	-1.0-1.1
8	-0.5-3.1	-1.4-1.1	-0.5-0.5	-1.1-1.2	-0.7-0.5	-1.1-1.9	-0.9-1.3	-0.5-0.6	-0.9-1.3	-1.0-1.3	-0.8-1.3
9	4.4-9.5	-0.0-3.6	-0.4-0.7	-0.6-2.1	-0.5-0.9	0.1-3.7	-0.7-1.7	-0.9-1.3	1.5-3.0	-0.1-2.5	-0.8-1.3
10	-0.8-4.3	1.4-5.2	-0.4-0.6	-1.4-1.5	-0.8-0.7	-0.2-3.6	-1.0-1.5	-1.0-1.3	-0.1-2.5	0.9-2.4	-0.6-1.6
11	-0.6-2.3	-0.7-1.3	-0.4-0.5	-1.5-1.1	-0.6-0.5	-0.5-2.1	-1.0-1.1	-0.8-1.3	-0.8-1.3	-0.6-1.6	-0.1-0.2
Total	48.2-60.5	15.0-31.2	-10.7-9.1	1.5-21.0	-9.3-12.8	29.2-48.0	-11.0-10.9	-10.2-10.6	8.2-24.6	4.5-21.8	-11.5-8.0
Higher	21.7	0.2	-2.3	6.5	1.5	18.5	-2.2	-2.1	0.3	2.7	-4.6

Table F.129: North / “Knee” Temp. Gradient / Mean

i \ j	1	2	3	4	5	6	7	8	9	10	11
1	22.1-28.8	-4.2-3.8	-1.7-2.1	7.5-14.5	-1.3-1.6	0.6-6.9	-0.6-3.1	0.2-4.1	4.2-10.1	-2.0-2.5	-1.7-1.2
2	-4.2-3.8	12.3-15.7	-1.4-1.2	-1.7-2.5	-1.8-0.5	-1.5-2.8	-1.2-1.6	0.2-3.0	-1.5-2.1	-1.7-1.5	-1.4-1.0
3	-1.7-2.1	-1.4-1.2	-0.4-0.5	-0.9-0.9	-1.0-0.6	-0.9-0.9	-0.9-0.7	-1.2-0.7	-0.8-0.9	-1.1-0.7	-1.1-0.6
4	7.5-14.5	-1.7-2.5	-0.9-0.9	-0.8-0.8	-0.0-2.0	0.0-2.7	0.3-2.5	0.3-2.5	0.1-2.6	0.2-2.5	0.1-2.2
5	-1.3-1.6	-1.8-0.5	-1.0-0.6	-0.0-2.0	0.0-0.4	-0.7-0.1	-0.7-0.1	-0.7-0.1	-0.7-0.2	-0.6-0.1	-0.7-0.0
6	0.6-6.9	-1.5-2.8	-0.9-0.9	0.0-2.7	-0.7-0.1	-0.9-0.8	0.1-2.8	0.1-2.9	-0.7-2.4	0.6-3.4	-0.2-2.3
7	-0.6-3.1	-1.2-1.6	-0.9-0.7	0.3-2.5	-0.7-0.1	0.1-2.8	-0.3-0.6	-0.6-1.1	-0.6-1.1	-0.5-1.1	-0.6-1.0
8	0.2-4.1	0.2-3.0	-1.2-0.7	0.3-2.5	-0.7-0.1	0.1-2.9	-0.6-1.1	0.3-1.2	-1.4-0.5	-1.2-0.7	-1.3-0.5
9	4.2-10.1	-1.5-2.1	-0.8-0.9	0.1-2.6	-0.7-0.2	-0.7-2.4	-0.6-1.1	-1.4-0.5	0.6-2.1	-1.3-1.2	-1.7-0.6
10	-2.0-2.5	-1.7-1.5	-1.1-0.7	0.2-2.5	-0.6-0.1	0.6-3.4	-0.5-1.1	-1.2-0.7	-1.3-1.2	-0.5-0.7	-1.3-1.2
11	-1.7-1.2	-1.4-1.0	-1.1-0.6	0.1-2.2	-0.7-0.0	-0.2-2.3	-0.6-1.0	-1.3-0.5	-1.7-0.6	-1.3-1.2	-0.3-0.2
Total	68.4-75.6	16.3-29.2	-10.1-6.4	20.9-34.2	-8.5-7.6	16.1-30.0	-6.0-9.8	-3.4-11.7	7.9-22.5	-1.4-14.1	-6.7-9.0
Higher	21.1	6.8	-1.1	7.2	0.9	10.6	-3.2	-1.9	5.2	3.3	0.9

Table F.130: Control / “Knee” Temp. Gradient / Maximum

i \ j	1	2	3	4	5	6	7	8	9	10	11
1	3.6-7.0	-1.5-3.9	-1.5-1.9	3.5-8.5	-1.3-1.9	0.8-6.4	-1.2-2.3	-1.6-2.1	2.5-7.4	0.2-5.2	-1.4-2.0
2	-1.5-3.9	6.2-9.0	-1.0-1.2	-0.9-2.8	-0.9-1.1	3.8-8.9	-0.5-1.7	-0.3-2.2	-1.0-2.7	2.6-6.6	-1.0-1.2
3	-1.5-1.9	-1.0-1.2	-0.3-0.4	-0.7-1.1	-0.9-0.7	-1.0-1.7	-1.0-0.7	-1.1-0.6	-0.8-1.0	-0.6-1.3	-0.8-0.7
4	3.5-8.5	-0.9-2.8	-0.7-1.1	-0.1-2.3	-2.1-1.2	-2.5-2.4	-2.1-1.4	-2.4-1.2	-2.7-1.5	-2.2-2.0	-2.3-1.1
5	-1.3-1.9	-0.9-1.1	-0.9-0.7	-2.1-1.2	-0.2-0.2	-0.3-2.0	-0.3-0.5	-0.4-0.4	-0.4-0.8	-0.0-1.2	-0.4-0.4
6	0.8-6.4	3.8-8.9	-1.0-1.7	-2.5-2.4	-0.3-2.0	5.2-8.2	-0.5-2.4	-1.1-1.9	-1.1-3.4	-0.1-4.5	-1.4-1.6
7	-1.2-2.3	-0.5-1.7	-1.0-0.7	-2.1-1.4	-0.3-0.5	-0.5-2.4	0.2-0.9	-0.9-0.7	-0.8-1.2	-0.6-1.3	-0.7-0.7
8	-1.6-2.1	-0.3-2.2	-1.1-0.6	-2.4-1.2	-0.4-0.4	-1.1-1.9	-0.9-0.7	-0.2-0.7	-0.5-1.3	0.3-2.3	-0.3-1.2
9	2.5-7.4	-1.0-2.7	-0.8-1.0	-2.7-1.5	-0.4-0.8	-1.1-3.4	-0.8-1.2	-0.5-1.3	2.2-4.2	0.9-4.9	-1.6-1.3
10	0.2-5.2	2.6-6.6	-0.6-1.3	-2.2-2.0	-0.0-1.2	-0.1-4.5	-0.6-1.3	0.3-2.3	0.9-4.9	1.6-3.7	-1.3-1.4
11	-1.4-2.0	-1.0-1.2	-0.8-0.7	-2.3-1.1	-0.4-0.4	-1.4-1.6	-0.7-0.7	-0.3-1.2	-1.6-1.3	-1.3-1.4	-0.4-0.2
Total	38.7-53.8	12.2-27.0	-13.6-6.0	15.4-31.7	-18.4-2.4	35.8-49.1	-10.6-9.0	-8.9-9.4	20.7-36.8	17.3-31.8	-14.2-6.2
Higher	20.9	-3.7	-4.6	18.1	-9.6	19.8	-3.5	-2.8	15.7	7.0	-4.1

Table F.131: South / “Knee” Temp. Gradient / Maximum

i \ j	1	2	3	4	5	6	7	8	9	10	11
1	16.3-21.4	-2.8-4.1	-1.0-2.7	0.4-5.4	-1.3-2.1	-1.2-5.7	-1.9-1.7	-1.4-2.2	4.6-10.1	-1.5-3.8	-1.4-2.0
2	-2.8-4.1	8.9-11.7	-1.2-1.4	-1.2-1.9	-1.1-1.5	1.0-5.8	-1.6-1.1	-1.0-1.7	-1.8-1.6	0.2-3.5	-1.0-1.5
3	-1.0-2.7	-1.2-1.4	-0.6-0.5	-1.1-1.2	-1.1-1.0	-1.4-1.3	-1.1-1.1	-1.0-1.1	-1.0-1.3	-0.9-1.3	-1.0-1.1
4	0.4-5.4	-1.2-1.9	-1.1-1.2	-1.0-0.7	-1.4-1.8	-1.7-2.1	-2.2-1.2	-1.3-1.7	-2.6-1.7	-2.8-1.4	-1.8-1.7
5	-1.3-2.1	-1.1-1.5	-1.1-1.0	-1.4-1.8	-0.3-0.4	-0.9-1.1	-0.7-0.7	-0.7-0.6	-0.4-1.0	-0.7-0.8	-0.7-0.7
6	-1.2-5.7	1.0-5.8	-1.4-1.3	-1.7-2.1	-0.9-1.1	6.7-9.5	-0.7-2.3	-0.8-2.3	-0.8-3.0	-0.1-3.6	-1.0-2.0
7	-1.9-1.7	-1.6-1.1	-1.1-1.1	-2.2-1.2	-0.7-0.7	-0.7-2.3	0.3-1.1	-0.9-0.9	-1.0-1.0	-0.9-1.1	-0.9-0.8
8	-1.4-2.2	-1.0-1.7	-1.0-1.1	-1.3-1.7	-0.7-0.6	-0.8-2.3	-0.9-0.9	-0.1-0.9	-1.1-0.9	-1.2-0.8	-0.7-1.2
9	4.6-10.1	-1.8-1.6	-1.0-1.3	-2.6-1.7	-0.4-1.0	-0.8-3.0	-1.0-1.0	-1.1-0.9	0.9-2.7	-0.6-2.5	-1.0-1.9
10	-1.5-3.8	0.2-3.5	-0.9-1.3	-2.8-1.4	-0.7-0.8	-0.1-3.6	-0.9-1.1	-1.2-0.8	-0.6-2.5	1.1-2.7	-1.3-1.2
11	-1.4-2.0	-1.0-1.5	-1.0-1.1	-1.8-1.7	-0.7-0.7	-1.0-2.0	-0.9-0.8	-0.7-1.2	-1.0-1.9	-1.3-1.2	-0.3-0.2
Total	54.0-63.0	15.9-28.1	-9.0-7.3	8.0-22.2	-7.1-8.0	31.5-44.2	-8.9-7.2	-8.4-7.4	12.3-25.9	6.6-20.0	-7.2-7.9
Higher	23.5	4.9	-2.2	13.0	-0.6	19.0	-1.7	-2.5	7.7	6.3	-1.2

Table F.132: North / “Knee” Temp. Gradient / Maximum

i \ j	1	2	3	4	5	6	7	8	9	10	11
1	22.2-29.0	-3.3-3.3	-2.2-2.3	5.8-13.7	-1.4-2.1	-1.2-6.0	-1.4-3.1	-1.9-2.6	4.2-11.5	-1.3-4.7	-1.5-2.2
2	-3.3-3.3	12.1-15.6	-1.9-1.2	-2.8-2.0	-2.1-0.4	-2.3-2.2	-1.9-1.3	-0.8-2.3	-2.0-2.3	-1.6-2.3	-1.5-1.3
3	-2.2-2.3	-1.9-1.2	-0.1-0.9	-1.0-0.9	-1.3-0.3	-1.3-0.4	-1.3-0.4	-1.4-0.5	-1.4-0.4	-1.5-0.3	-1.2-0.3
4	5.8-13.7	-2.8-2.0	-1.0-0.9	-1.2-1.0	-0.9-2.5	-0.7-3.5	-0.9-2.7	-0.8-2.7	-0.9-3.4	-1.0-2.8	-1.0-2.5
5	-1.4-2.1	-2.1-0.4	-1.3-0.3	-0.9-2.5	0.0-0.5	-1.0-0.1	-1.0-0.1	-0.8-0.3	-1.4-0.0	-1.0-0.1	-1.1-0.0
6	-1.2-6.0	-2.3-2.2	-1.3-0.4	-0.7-3.5	-1.0-0.1	-1.0-1.1	-0.4-3.2	0.0-3.5	-0.7-3.4	-0.1-4.2	-0.7-3.0
7	-1.4-3.1	-1.9-1.3	-1.3-0.4	-0.9-2.7	-1.0-0.1	-0.4-3.2	0.4-1.1	-0.4-1.0	-0.8-0.9	-0.6-0.8	-0.7-0.8
8	-1.9-2.6	-0.8-2.3	-1.4-0.5	-0.8-2.7	-0.8-0.3	0.0-3.5	-0.4-1.0	1.4-2.6	-3.0-0.1	-3.1-0.1	-2.5-0.0
9	4.2-11.5	-2.0-2.3	-1.4-0.4	-0.9-3.4	-1.4-0.0	-0.7-3.4	-0.8-0.9	-3.0-0.1	-0.8-1.7	-1.8-3.2	-2.1-1.7
10	-1.3-4.7	-1.6-2.3	-1.5-0.3	-1.0-2.8	-1.0-0.1	-0.1-4.2	-0.6-0.8	-3.1-0.1	-1.8-3.2	-1.3-0.7	-1.6-2.1
11	-1.5-2.2	-1.5-1.3	-1.2-0.3	-1.0-2.5	-1.1-0.0	-0.7-3.0	-0.7-0.8	-2.5-0.0	-2.1-1.7	-1.6-2.1	-0.3-0.2
Total	68.7-75.5	14.2-27.8	-6.5-9.6	26.1-37.9	-8.4-6.9	20.3-33.8	-6.8-9.0	-4.3-10.9	12.7-26.9	5.7-20.3	-6.3-8.8
Higher	22.9	8.0	4.9	15.9	2.2	16.3	-2.0	2.3	10.9	9.9	1.2

APPENDIX G

YELLOWSTONE CLUB DAILY LOGS

The following sections contain verbatim copies of the daily logs recorded by the Yellowstone Club Ski Patrol for the 2006/2007 through 2008/2009 seasons. The logs from the 2006/2007 season were received as handwritten notes, these notes were transcribed into a digital format consistent with the other seasons using the YCweather software package (see Appendix B). The fields are typeset in *italic* and the notes in typewriter text.

### G.1 2008/2009 Season

January 01, 2009 \_\_\_\_\_

—— North ——

*NO DAILY LOG RECORDED*

—— South ——

*Names: Irene Station: South Date: 01-1-09 Time: 1120 Exposed thermocouples: 13 Keywords:*

*Surface: 1mm stellars*

*Layer 1: 1mm stellars*

*Layer 2: melt freeze crust*

*Layer 3: melt freeze crust*

*Layer 4: 1mm decomposing stellars*

*Layer 5: 1mm decomposing stellars*

January 18, 2009 \_\_\_\_\_

—— North ——

*Names: Doug M Station: North Date: 01-18-09  
Time: 1300 Exposed thermocouples: 1 Keywords:  
Surface: 1mm decomposing  
Layer 1: 2mm grauple  
Layer 2: 0.5mm rounds  
Layer 3: 0.5mm rounds  
Layer 4: 0.5mm rounds  
Layer 5: 0.5mm rounds*

—— South ——

*NO DAILY LOG RECORDED*

January 19, 2009

— North —

— South —

*Names:* Doug C, Virginia *Station:* North *Date:*01-19-09 *Time:* 1100 *Exposed thermocouples:* 2*Keywords:**Surface:*

soft surface crust (0.5-1mm thick)melt-freeze?

*Layer 1:* 0.5mm mixed forms*Layer 2:* 0.5mm mixed forms*Layer 3:* 0.5mm mixed forms*Layer 4:* 0.5mm mixed forms*Layer 5:* 0.5mm mixed forms

NO DAILY LOG RECORDED

January 20, 2009

— North —

— South —

*Names:* Doug C, Danielle *Station:* North *Date:*01-20-09 *Time:* 1120 *Exposed thermocouples:* 2*Keywords:**Surface:* 0.5 mm thick melt-freeze crust*Layer 1:* 0.5mm mixed forms*Layer 2:* 0.5mm mixed forms*Layer 3:* 0.5mm mixed forms*Layer 4:* 0.5mm mixed forms*Layer 5:* 0.5mm mixed forms

NO DAILY LOG RECORDED

January 21, 2009

— North —

— South —

*Names:* Tom, Coop, Katy *Station:* north *Date:*01-21-09 *Time:* 1130 *Exposed thermocouples:* 2*Keywords:* facets*Surface:* 0.5mm mixed facets*Layer 1:* 0.5mm mixed facets*Layer 2:* 0.5mm rounds*Layer 3:* 0.5mm rounds*Layer 4:* 0.5mm rounds*Layer 5:* 0.5mm rounds

NO DAILY LOG RECORDED

January 22, 2009

— North —

— South —

Names: Irene, Doug C, Ed, Pat, Rich (MSU), Dan  
 Station: north Date: 01-22-09 Time: 1410 Exposed  
 thermocouples: 2 Keywords:  
 Surface: 2-3mm stellars  
 Layer 1: 0.5mm mixed forms  
 Layer 2: 0.5mm mixed forms  
 Layer 3: 0.5mm rounds  
 Layer 4: 0.5mm rounds  
 Layer 5: 0.5mm rounds

NO DAILY LOG RECORDED

January 23, 2009

— North —

— South —

Names: Doug M Station: north Date: 01-23-09  
 Time: 1315 Exposed thermocouples: 2 Keywords:  
 surface hoar  
 Surface: 0.5mm surface hoar  
 Layer 1: 0.5mm decomposing  
 Layer 2: 0.5mm decomposing  
 Layer 3: 0.5mm rounds  
 Layer 4: 0.5mm rounds  
 Layer 5: 0.5mm rounds

NO DAILY LOG RECORDED

January 24, 2009

— North —

— South —

Names: 1/24/09 @ 1245 hours Station: ovc Skys  
 Date: calm Time: Doug M and tom Exposed  
 thermocouples: Keywords: 0cm-New snow 1.0mm +  
 surface hoar 0.5mm (old from yesterday)  
 Surface: 1cm-decomposing 0.5mm  
 Layer 1: 2cm-rounds 0.5mm  
 Layer 2: 3cm-rounds 0.5mm  
 Layer 3: 4cm-rounds 0.5mm  
 Layer 4: 5cm-rounds 0.5mm  
 Layer 5:

NO DAILY LOG RECORDED

January 25, 2009

— North —

— South —

*Names: Tom, Coop Station: north Date: 01-25-09**Time: 0900 Exposed thermocouples: 0 Keywords:**Surface: 1-2mm stellars**Layer 1: 1-2mm stellars**Layer 2: 1-2mm stellars**Layer 3: 1-2mm stellars**Layer 4: 1-2mm stellars**Layer 5: 1-2mm stellars**NO DAILY LOG RECORDED*

January 26, 2009

— North —

— South —

*Names: Doug C, Danielle Station: north Date:**01-26-09 Time: 1220 Exposed thermocouples: 12**Keywords:**Surface: 0.5mm new snow**Layer 1: 0.5mm new snow**Layer 2: 0.5mm new snow**Layer 3: 1mm decomposing**Layer 4: 1mm decomposing**Layer 5: 1mm decomposing**NO DAILY LOG RECORDED*

January 27, 2009

— North —

— South —

*Names: Doug C, Warren Station: north Date:**01-27-09 Time: 1330 Exposed thermocouples: 12**Keywords:**Surface: 0.5-1mm decomposing**Layer 1: 0.5-1mm decomposing**Layer 2: 0.5-1mm decomposing**Layer 3: 0.5-1mm decomposing**Layer 4: 0.5-1mm decomposing**Layer 5: 0.5-1mm decomposing**NO DAILY LOG RECORDED*



January 28, 2009

— North —

— South —

*Names: Irene Station: 1/27/09 @ 1145 Date:**Names: NO observations**OVC with light snow falling, light gusts,  
moderate winds from West Time:**10" of new snow overnight Exposed thermocouples:**Keywords: 0cm 1mm heavily rimed new snow**Surface: 1cm 1mm heavily rimed new snow**Layer 1: 2cm 1mm heavily rimed new snow**Layer 2: 3cm 1mm heavily rimed new snow**Layer 3: 4cm 1mm heavily rimed new snow**Layer 4: 5cm 1mm heavily rimed new snow**Layer 5:*

January 29, 2009

— North —

— South —

*Names: Doug C, Irene, Ed, Pat, Dan Station: north**NO DAILY LOG RECORDED**Date: 01-29-09 Time: 1330 Exposed thermocouples:**7 Keywords:**Surface: 0.5-1mm decomposing new snow**Layer 1: 0.5-1mm decomposing new snow**Layer 2: 0.5-1mm decomposing new snow**Layer 3: 0.5-1mm decomposing new snow**Layer 4: 0.5-1mm decomposing new snow**Layer 5: 0.5-1mm decomposing new snow*

January 30, 2009

— North —

— South —

*Names: Irene, Kristin Station: north Date:**NO DAILY LOG RECORDED**01-30-09 Time: 1215 Exposed thermocouples: 8**Keywords: surface hoar**Surface: 0.5mm surface hoar**Layer 1: 0.5-1mm decomposing**Layer 2: 0.5-1mm decomposing**Layer 3: 0.5-1mm decomposing**Layer 4: 0.5-1mm decomposing**Layer 5: 0.5-1mm decomposing*

January 31, 2009

— North —

Names: Doug M Station: north Date: 01-31-09  
 Time: 1030 Exposed thermocouples: 9 Keywords:  
 surface hoar  
 Surface: 1mm surface hoar  
 Layer 1: 0.25mm decomposing  
 Layer 2: 0.25mm decomposing  
 Layer 3: 0.25mm decomposing  
 Layer 4: 0.25mm decomposing  
 Layer 5: 0.25mm decomposing

— South —

NO DAILY LOG RECORDED

February 01, 2009

— North —

Names: Doug M, Tom Station: north Date: 02-1-09  
 Time: 1400 Exposed thermocouples: 10 Keywords:  
 Surface: wind crust  
 Layer 1: 0.25mm decomposing  
 Layer 2: 0.25mm decomposing  
 Layer 3: 0.25mm decomposing  
 Layer 4: 0.25mm decomposing  
 Layer 5: 0.25mm decomposing

— South —

Names: Doug M, Tom Station: 2/1/09 @ 1430 Date:  
 Ovc Time: Light West winds w/ moderate gusts  
 Exposed thermocouples: Keywords:  
 0cm melt-freeze crust  
 Surface: 1cm melt-freeze crust  
 Layer 1: 2cm 0.25mm rounds  
 Layer 2: 3cm 0.25mm rounds  
 Layer 3: 4cm 0.25mm rounds  
 Layer 4: 5cm 0.5mm decomposing  
 Layer 5:

February 02, 2009

— North —

Names: 2/2/09 Doug C and Jeff L Station:  
 North 1100 hours Date:  
 ovc, Light wind from the south Time:  
 0cm rimed new snow 1mm Exposed thermocouples:  
 1cm decomposing snow to rounds .5mm Keywords:  
 2cm decomposing snow to rounds .5mm  
 Surface: 3cm decomposing snow to rounds .5mm  
 Layer 1: 4cm decomposing snow to rounds .5mm  
 Layer 2: 5cm decomposing snow to rounds .5mm  
 Layer 3:  
 Layer 4: 10 Thermocouples exposed  
 Layer 5: S-1 snow

— South —

Names: 2/2/09 Station: South, 0945 hours Date:  
 OVC, Light wind from the south with Mod gusts  
 Time: 0cm grouple 1-2mm Exposed thermocouples:  
 0-1cm meltfreeze crust Keywords: 2cm rounds .5mm  
 Surface: 3cm rounds .5mm  
 Layer 1: 4cm decomposing snow .5-1mm  
 Layer 2: 5cm decomposing snow .5-1mm  
 Layer 3:  
 Layer 4: 8 Thermocouples exposed  
 Layer 5: S-1 precip

February 04, 2009

— North —

*Names:* Irene, Pat, Jared *Station:*  
*North Study Plot Date:* 02-4-09 *Time:* 1245  
*Exposed thermocouples:* 11 *Keywords:* Surface hoar  
*Surface:* 5mm surface hoar  
*Layer 1:* 1mm rounds  
*Layer 2:* 1mm rounds  
*Layer 3:* 1mm rounds  
*Layer 4:* 1mm rounds  
*Layer 5:* 1mm rounds; 1mm decomposing stellars

— South —

*Names:* Irene, Pat, Jared *Station:*  
*South Weather Station Date:* 02-4-09 *Time:* 1130  
*Exposed thermocouples:* 10 *Keywords:* surface hoar  
*Surface:* .5mm facets- surface hoar  
*Layer 1:* melt freeze crust  
*Layer 2:* melt freeze crust  
*Layer 3:* 1mm decomposing stellars  
*Layer 4:* 1mm decomposing stellars  
*Layer 5:* 1mm decomposing stellars

February 05, 2009

— North —

*Names:* Doug C *Station:* North *Date:* 02-05-09  
*Time:* 945 *Exposed thermocouples:* 11 *Keywords:*  
 Surface Hoar  
*Surface:* Surface Hoar, 2-3mm  
*Layer 1:* small facets beginning to round, .5mm  
*Layer 2:* mixed forms, .5mm  
*Layer 3:* mixed forms, .5mm  
*Layer 4:* mixed forms, .5mm  
*Layer 5:* mixed forms, .5mm

— South —

*Names:* Doug C *Station:* South *Date:* 02-05-09  
*Time:* 1015 *Exposed thermocouples:* 18 *Keywords:*  
 surface hoar  
*Surface:*  
 decomposing surface hoar (or facets?), .5mm  
*Layer 1:* melt freeze crust  
*Layer 2:* melt freeze crust  
*Layer 3:* melt freeze crust  
*Layer 4:* decomposing snow to rounds, .5-1mm  
*Layer 5:* decomposing snow to rounds, .5-1mm

February 06, 2009

— North —

*Names:* Doug M, JJ *Station:* North *Date:* 02-6-09  
*Time:* 1200 *Exposed thermocouples:* 10 *Keywords:*  
*Surface:* 1mm new snow  
*Layer 1:* 1mm new snow  
*Layer 2:* 1mm new snow  
*Layer 3:* 1mm new snow  
*Layer 4:* 1mm new snow  
*Layer 5:* 1mm new snow

— South —

*Names:* Doug M *Station:* South *Date:* 02-6-09 *Time:*  
 1030 *Exposed thermocouples:* 16 *Keywords:*  
*Surface:* 1mm new snow  
*Layer 1:* 1mm new snow  
*Layer 2:* melt-freeze crust  
*Layer 3:* melt-freeze crust  
*Layer 4:* melt-freeze crust  
*Layer 5:* rounds

February 07, 2009

— North —

*Names: Doug M Station: north Date: 02-7-09 Time:**1115 Exposed thermocouples: 9 Keywords:***surface hoar***Surface: 2mm new snow, 1mm surface hoar**Layer 1: 2mm new snow, 0.25 decomposing**Layer 2: 2mm new snow, 0.25 decomposing**Layer 3: 2mm new snow, 0.25 decomposing**Layer 4: 2mm new snow, 0.25 decomposing**Layer 5: 2mm new snow, 0.25 decomposing*

— South —

*Names: Doug M Station: South Date: 02-7-09 Time:**1000 Exposed thermocouples: 12 Keywords:**Surface: 1.5mm new snow**Layer 1: 1.5mm new snow**Layer 2: 1.5mm new snow**Layer 3: 1.5mm new snow**Layer 4: 1.5mm new snow**Layer 5: 1.5mm new snow*

February 08, 2009

— North —

*Names: Doug M Station: north Date: 02-8-09 Time:**0945 Exposed thermocouples: 9 Keywords:***surface hoar***Surface: 5mm surface hoar**Layer 1: 0.25mm highly decomposed**Layer 2: 0.25mm highly decomposed**Layer 3: 0.25mm highly decomposed**Layer 4: 0.25mm highly decomposed**Layer 5: 0.25mm highly decomposed*

— South —

*Names: Doug M, Tom, Coop Station: south Date:**02-8-09 Time: 1045 Exposed thermocouples: 15**Keywords: surface hoar, facets**Surface: 1mm surface hoar, 1mm facets**Layer 1: melt-freeze (moist)**Layer 2: melt-freeze (moist)**Layer 3: melt-freeze (moist)**Layer 4: 0.5mm rounds**Layer 5: 0.5mm rounds*

February 09, 2009

— North —

*Names: Tom, Warren Station: North Date: 02-9-09**Time: 1:15 Exposed thermocouples: 9 Keywords:***none***Surface: 1mm rimed stellars**Layer 1: 1mm rimed stellars w/some surface hoar from yesterday**Layer 2: 1mm broken stellars going rounds**Layer 3: .5 - 1mm rounds**Layer 4: .5 rounds**Layer 5: .5 rounds*

— South —

*Names: Tom Station: South Date: 02-9-09 Time:**11:30 Exposed thermocouples: 11 Keywords:**Surface: 1mm rimed stellars**Layer 1: 1mm rimed stellars**Layer 2: 1mm rimed stellars**Layer 3: 1mm rimed stellars**Layer 4: 1mm rimed stellars w/ a few facets from yesterday**Layer 5: MF Crust*

February 10, 2009

— North —

Names: Doug C, Linda Station: North Date: 02-10-09 Time: 1230 Exposed thermocouples: 0  
 Keywords: New Snow  
 Surface: New Snow, 1-2mm  
 Layer 1: New Snow, 1-2mm  
 Layer 2: New Snow, 1-2mm  
 Layer 3: New Snow, 1-2mm  
 Layer 4: New Snow, 1-2mm  
 Layer 5: New Snow, 1-2mm

— South —

Names: Doug C, Lance Station: South Date: 02-10-09 Time: 1115 Exposed thermocouples: 7  
 Keywords: New Snow  
 Surface: new snow, 1-2mm  
 Layer 1: new snow, 1-2mm  
 Layer 2: new snow, 1-2mm  
 Layer 3: new snow, 1-2mm  
 Layer 4: new snow, 1-2mm  
 Layer 5: new snow, 1-2mm

February 11, 2009

— North —

Names: Doug C Station: North Date: 02-11-09 Time: 1300 Exposed thermocouples: 5 Keywords: New Snow  
 Surface: New Snow, .5-1mm  
 Layer 1: New Snow, .5-1mm  
 Layer 2: New Snow, .5-1mm  
 Layer 3: Decomposing Snow, 1-2mm  
 Layer 4: Decomposing Snow, 1-2mm  
 Layer 5: Decomposing Snow, 1-2mm

— South —

Names: Doug C, Brittany Station: South Date: 02-11-09 Time: 1115 Exposed thermocouples: 8  
 Keywords: New Snow  
 Surface: New Snow, .5-1mm  
 Layer 1: New Snow, .5-1mm  
 Layer 2: New Snow, .5-1mm  
 Layer 3: decomposing snow, 1-2mm  
 Layer 4: decomposing snow, 1-2mm  
 Layer 5: decomposing snow, 1-2mm

February 12, 2009

— North —

Names: Doug C, Katy Station: North Date: 02-12-09 Time: 1345 Exposed thermocouples: 5 Keywords: New Snow  
 Surface: Rimed new snow, 1-2mm  
 Layer 1: Rimed new snow, 1-2mm  
 Layer 2: Rimed new snow, 1-2mm  
 Layer 3: decomposing new snow to rounds, 1mm  
 Layer 4: decomposing new snow to rounds, 1mm  
 Layer 5: decomposing new snow to rounds, 1mm

— South —

Names: Doug C, Doug M, Tom, Katy Station: South Date: 02-12-09 Time: 1015 Exposed thermocouples: 6 Keywords: New Snow, Radiation Recrystallization  
 Surface: New Snow, 1-2mm  
 Layer 1: New Snow, 1-2mm  
 Layer 2: New Snow, 1-2mm  
 Layer 3: rhimed New Snow, 1-2mm  
 Layer 4: Decomposing snow, 1mm  
 Layer 5: Decomposing snow, 1mm

February 13, 2009

— North —

*Names:* Tom, Wes *Station:* North *Date:* 02-13-09  
*Time:* 14:03 *Exposed thermocouples:* 5 *Keywords:*  
*Surface:* 1/2 surface hoar and 1/2 decomposing  
 stellars. 1mm  
*Layer 1:* 1/2 surface hoar and 1/2 decomposing  
 stellars. 1mm  
*Layer 2:* Decomposing stellars. .5 - 1 mm  
*Layer 3:* Rounds. .5mm  
*Layer 4:* Rounds .5mm  
*Layer 5:* Rounds. 5mm

— South —

*Names:* Tom *Station:* South *Date:* 02-13-09 *Time:*  
 13:13 *Exposed thermocouples:* 8 *Keywords:*  
 Near Surface Facets  
*Surface:* NSF, 1mm  
*Layer 1:* NSF, 1mm  
*Layer 2:* MF Crust  
*Layer 3:* MF Crust  
*Layer 4:* Rounds, .5mm  
*Layer 5:* Rounds, .5mm

February 14, 2009

— North —

*Names:* Doug M, Warren *Station:* North *Date:*  
 02-14-09 *Time:* 1230 *Exposed thermocouples:* 6  
*Keywords:*  
*Surface:* 1.5mm decomposing surface hoar  
*Layer 1:* 0.5mm decomposing and rounds  
*Layer 2:* 0.5mm decomposing and rounds  
*Layer 3:* 0.5mm decomposing and rounds  
*Layer 4:* 0.5mm decomposing and rounds  
*Layer 5:* 0.5mm decomposing and rounds

— South —

*Names:* Doug M, Tom *Station:* South *Date:* 02-14-09  
*Time:* 0945 *Exposed thermocouples:* 9 *Keywords:*  
 near-surface facets  
*Surface:* 0.5-1mm facets  
*Layer 1:* melt-freeze crust  
*Layer 2:* melt-freeze crust  
*Layer 3:* melt-freeze crust  
*Layer 4:* melt-freeze crust  
*Layer 5:* melt-freeze crust

February 15, 2009

— North —

*Names:* Doug M, Robin *Station:* North *Date:*  
 02-15-09 *Time:* 1030 *Exposed thermocouples:* 3  
*Keywords:*  
*Surface:* 0.25 decomposing & broken new snow  
*Layer 1:* 0.25 decomposing & broken new snow  
*Layer 2:* 0.25 decomposing & broken new snow  
*Layer 3:* 0.25 decomposing & broken new snow  
*Layer 4:* 0.5mm stellars and decomposing  
*Layer 5:* 0.5mm stellars and decomposing

— South —

*Names:* Doug M, Tom (PM), Coop (PM) *Station:* South  
*Date:* 02-15-09 *Time:* 0845 *Exposed thermocouples:*  
 6 *Keywords:* facets  
*Surface:* 0.5 decomposing & broken new snow  
*Layer 1:* 0.5 decomposing & broken new snow  
*Layer 2:* 0.5 decomposing & broken new snow  
*Layer 3:* 0.5 decomposing & broken new snow  
*Layer 4:* 1mm stellars  
*Layer 5:* 1mm stellars

February 16, 2009

— North —

*Names:* Doug C, Little B *Station:* North *Date:*  
02-16-09 *Time:* 1245 *Exposed thermocouples:* 4  
*Keywords:*  
*Surface:* Rounds, .5mm  
*Layer 1:* Rounds, .5mm  
*Layer 2:* Rounds, .5mm  
*Layer 3:* Rounds, .5mm  
*Layer 4:* decomposing snow to rounds, .5-1mm  
*Layer 5:* decomposing snow to rounds, .5-1mm

— South —

*Names:* Doug C, Danielle *Station:* South *Date:*  
02-16-09 *Time:* 1045 *Exposed thermocouples:* 10  
*Keywords:*  
*Surface:* rounds, .5mm  
*Layer 1:* rounds, .5mm  
*Layer 2:* decomposing snow, 1-1.5mm  
*Layer 3:* decomposing snow, 1-1.5mm  
*Layer 4:* decomposing snow, 1-1.5mm  
*Layer 5:* decomposing snow, 1-1.5mm

February 17, 2009

— North —

*Names:* Doug C, Anderson *Station:* North *Date:*  
02-17-09 *Time:* 1345 *Exposed thermocouples:* 1  
*Keywords:*  
*Surface:* Rimed new snow, 1-2mm  
*Layer 1:* Rimed new snow, 1-2mm  
*Layer 2:* Rimed new snow, 1-2mm  
*Layer 3:* Rimed new snow, 1-2mm  
*Layer 4:* Rimed new snow, 1-2mm  
*Layer 5:* Rimed new snow, 1-2mm

— South —

*Names:* Doug C *Station:* South *Date:* 02-17-09  
*Time:* 915 *Exposed thermocouples:* 5 *Keywords:*  
*Surface:* Rimed new snow, 1-2mm  
*Layer 1:* Rimed new snow, 1-2mm  
*Layer 2:* Rimed new snow, 1-2mm  
*Layer 3:* Rimed new snow, 1-2mm  
*Layer 4:* Rimed new snow, 1-2mm  
*Layer 5:* Rimed new snow, 1-2mm

February 18, 2009

— North —

*Names:* Irene *Station:* North *Date:* 02-18-09 *Time:*  
1020 *Exposed thermocouples:* 6 *Keywords:*  
*Surface:* 1-2mm rimed stellars  
*Layer 1:* 1-2mm rimed stellars  
*Layer 2:* 1-2mm rimed stellars  
*Layer 3:* 1-2mm rimed stellars  
*Layer 4:* 1-2mm rimed stellars  
*Layer 5:* 1-2mm rimed stellars

— South —

*Names:* Doug C, Irene *Station:* South *Date:*  
02-18-09 *Time:* 1345 *Exposed thermocouples:* 0  
*Keywords:*  
*Surface:* rimed New Snow, 1-2mm  
*Layer 1:* rimed New Snow, 1-2mm  
*Layer 2:* rimed New Snow, 1-2mm  
*Layer 3:* rimed New Snow, 1-2mm  
*Layer 4:* rimed New Snow, 1-2mm  
*Layer 5:* rimed New Snow, 1-2mm

February 19, 2009

— North —

*Names:* Irene, Pat, Rich (MSU) *Station:* North  
*Date:* 02-19-09 *Time:* 1400 *Exposed thermocouples:*  
 8 *Keywords:*  
*Surface:* 1-2mm stellars  
*Layer 1:* 1-2mm stellars  
*Layer 2:* 1-2mm stellars  
*Layer 3:* 1-2mm stellars  
*Layer 4:* 1-2mm stellars  
*Layer 5:* 1-2mm stellars

— South —

*Names:* Doug C, Doug M *Station:* South *Date:*  
 02-19-09 *Time:* 1245 *Exposed thermocouples:* 12  
*Keywords:* Near Surface Facets  
*Surface:* New Snow, 1mm, Rad rec facets, .3mm  
*Layer 1:* Decomposing Snow, 1mm  
*Layer 2:* Decomposing Snow, 1mm  
*Layer 3:* Decomposing Snow, 1mm  
*Layer 4:* Decomposing Snow, 1mm  
*Layer 5:* Decomposing Snow, 1mm

February 20, 2009

— North —

*Names:* Irene, Virginia *Station:* North *Date:*  
 02-20-09 *Time:* 1240 *Exposed thermocouples:* 10  
*Keywords:* none  
*Surface:* 1mm stellars, decomposing stellars  
*Layer 1:* 1mm stellars, decomposing stellars  
*Layer 2:* 1mm stellars, decomposing stellars  
*Layer 3:* 1mm stellars, decomposing stellars  
*Layer 4:* 1mm stellars, decomposing stellars  
*Layer 5:* 1mm stellars, decomposing stellars

— South —

*Names:* Irene *Station:* South *Date:* 02-20-09 *Time:*  
 1120 *Exposed thermocouples:* 13 *Keywords:*  
*Surface:* 1mm stellars  
*Layer 1:* 1mm stellars  
*Layer 2:* melt freeze crust  
*Layer 3:* melt freeze crust  
*Layer 4:* 1mm decomposing stellars  
*Layer 5:* 1mm decomposing stellars

February 21, 2009

— North —

*Names:* Doug M *Station:* North *Date:* 02-21-09 *Time:*  
 0900 *Exposed thermocouples:* 10 *Keywords:* facets  
*Surface:* 0.5mm facets  
*Layer 1:* 0.5mm decomposing and rounds  
*Layer 2:* 0.5mm decomposing and rounds  
*Layer 3:* 0.5mm decomposing and rounds  
*Layer 4:* 0.5mm decomposing and rounds  
*Layer 5:* 0.5mm decomposing and rounds

— South —

*Names:* Doug M *Station:* South *Date:* 02-21-09 *Time:*  
 1045 *Exposed thermocouples:* 14 *Keywords:* facets  
*Surface:* 0.5mm facets  
*Layer 1:* 0.5mm decomposing  
*Layer 2:* melt-freeze (moist)  
*Layer 3:* melt-freeze (moist)  
*Layer 4:* melt-freeze (moist)  
*Layer 5:* 0.5mm rounds



February 22, 2009

— North —

*Names: Tom Station: North Date: 02-22-09 Time: 10:30 Exposed thermocouples: 11 Keywords: none*  
*Surface: 3mm thick soft wind crust*  
*Layer 1: mixed facets. .5mm*  
*Layer 2: mixed facets. .5mm*  
*Layer 3: mixed facets. .5mm*  
*Layer 4: mixed facets going rounds. 1mm*  
*Layer 5: mixed facets going rounds. 1mm*

— South —

*Names: Tom Station: South Date: 02-22-09 Time: 9:30 Exposed thermocouples: 17 Keywords: facets*  
*Surface: facets .5mm*  
*Layer 1: facets .5mm*  
*Layer 2: melt freeze crust*  
*Layer 3: melt freeze crust*  
*Layer 4: decomposing stellars going to rounds. 1mm*  
*Layer 5: decomposing stellars going to rounds. 1mm*

February 23, 2009

— North —

*Names: Doug C Station: North Date: 02-23-09 Time: 1130 Exposed thermocouples: 12 Keywords:*  
*Surface: rimed new snow, 1-2mm*  
*Layer 1: decomposing snow heavily rounded, .5mm*  
*Layer 2: decomposing snow heavily rounded, .5mm*  
*Layer 3: decomposing snow heavily rounded, .5mm*  
*Layer 4: decomposing snow heavily rounded, .5mm*  
*Layer 5: decomposing snow heavily rounded, .5mm*

— South —

*Names: Doug C Station: South Date: 02-23-09 Time: 1030 Exposed thermocouples: 20 Keywords:*  
*Surface: rimed new snow, 1-2mm*  
*Layer 1: Melt Freeze crust*  
*Layer 2: Melt Freeze crust*  
*Layer 3: Melt Freeze crust*  
*Layer 4: rorunds, .5-1mm*  
*Layer 5: rorunds, .5-1mm*

February 24, 2009

— North —

*Names: Doug C Station: North Date: 02-24-09 Time: 1100 Exposed thermocouples: 0 Keywords:*  
*Surface: New Snow (Group), 2mm*  
*Layer 1: Decomposing snow tuirning to rounds, .5-1.5mm*  
*Layer 2: Decomposing snow tuirning to rounds, .5-1.5mm*  
*Layer 3: Decomposing snow tuirning to rounds, .5-1.5mm*  
*Layer 4: Decomposing snow tuirning to rounds, .5-1.5mm*  
*Layer 5: Decomposing snow tuirning to rounds, .5-1.5mm*

— South —

*Names: Irene Station: South Date: 02-24-09 Time: 1130 Exposed thermocouples: 14 Keywords:*  
*Surface: 2mm graupel*  
*Layer 1: 2mm graupel*  
*Layer 2: melt freeze crust*  
*Layer 3: melt freeze crust*  
*Layer 4: melt freeze crust*  
*Layer 5: melt freeze crust*

February 25, 2009

— North —

*Names:* Wes/ Coop *Station:* north *Date:* 02-25-09  
*Time:* 13:40 *Exposed thermocouples:* 13 *Keywords:*  
*Surface:* 2mm graupel  
*Layer 1:* 2mm graupel  
*Layer 2:* 2mm graupel  
*Layer 3:* .5-1mm rounds  
*Layer 4:* .5-1mm rounds  
*Layer 5:* .5-1mm rounds

— South —

*Names:* Wes/Coop *Station:* south *Date:* 02-25-09  
*Time:* 10:10 *Exposed thermocouples:* 16 *Keywords:*  
*Surface:* 1-2 mm melt freeze crust  
*Layer 1:* 1-2 mm melt freeze crust  
*Layer 2:* 1-2 mm melt freeze crust  
*Layer 3:* .5-1 mm rounds  
*Layer 4:* 1-2 mm melt freeze crust  
*Layer 5:* 1-2 mm melt freeze crust

February 26, 2009

— North —

*Names:* Irene, Doug C, Ed, Jared, Dan *Station:*  
*North Date:* 02-26-09 *Time:* 1300 *Exposed*  
*thermocouples:* 14 *Keywords:* none  
*Surface:* 1mm decomposing stellars, graupel  
*Layer 1:* 1mm decomposing stellars, graupel  
*Layer 2:* 1mm decomposing stellars, graupel  
*Layer 3:* 1mm decomposing stellars, graupel  
*Layer 4:* 1mm decomposing stellars, graupel  
*Layer 5:* 1mm decomposing stellars, graupel

— South —

*Names:* Irene, Doug C, Ed, Jared, Dan *Station:*  
*South Date:* 02-26-09 *Time:* 1255 *Exposed*  
*thermocouples:* 11 *Keywords:*  
*Surface:* 1mm decomposing stellars, graupel  
*Layer 1:* 1mm decomposing stellars, graupel  
*Layer 2:* 1mm decomposing stellars, graupel  
*Layer 3:* 1mm decomposing stellars, graupel  
*Layer 4:* 1mm decomposing stellars, graupel  
*Layer 5:* 1mm decomposing stellars, graupel

February 27, 2009

— North —

*Names:* Irene *Station:* North *Date:* 02-27-09 *Time:*  
 1300 *Exposed thermocouples:* 6 *Keywords:* none  
*Surface:* 1mm stellars  
*Layer 1:* 1mm stellars  
*Layer 2:* 1mm stellars, decomposing stellars  
*Layer 3:* 1mm stellars, decomposing stellars  
*Layer 4:* 1mm stellars, decomposing stellars  
*Layer 5:* 1mm stellars, decomposing stellars

— South —

*Names:* Doug McCabe, Irene Henninger (@1400)  
*Station:* South *Date:* 02-27-09 *Time:* 1200/1400  
*Exposed thermocouples:* 2 *Keywords:*  
 radiation recrystallization  
*Surface:* 0.5-3mm new snow, 0.25mm facets  
*Layer 1:* 0.5mm new snow  
*Layer 2:* 0.25mm new snow and decomposing  
*Layer 3:* 0.25mm new snow and decomposing  
*Layer 4:* 0.25-3mm new snow and decomposing  
*Layer 5:* 0.25-3mm new snow and decomposing

February 28, 2009

— North —

Names: Doug M Station: North Date: 02-28-09  
 Time: 1400 Exposed thermocouples: 6 Keywords:  
 surface hoar  
 Surface: 1.5mm surface hoar  
 Layer 1: 0.25mm highly decomposed  
 Layer 2: 0.25mm highly decomposed  
 Layer 3: 0.25mm highly decomposed  
 Layer 4: 0.25mm highly decomposed  
 Layer 5: 0.25mm highly decomposed

— South —

Names: Doug M (AM & PM), Katy (AM) Station: South  
 Date: 02-28-09 Time: 1000 Exposed thermocouples:  
 3 Keywords: facets  
 Surface: 0.5mm facets  
 Layer 1: 0.25mm rounds  
 Layer 2: 0.25mm rounds  
 Layer 3: 0.25mm rounds/ melt-freeze  
 Layer 4: 0.25mm rounds/ melt-freeze  
 Layer 5: 0.25mm rounds/ melt-freeze

March 01, 2009

— North —

Names: Doug M Station: North Date: 03-1-09 Time:  
 1130 Exposed thermocouples: 6 Keywords:  
 surface hoar  
 Surface:  
 1mm surface hoar (decomposing from yesterday)  
 Layer 1: 0.25mm rounds  
 Layer 2: 0.25mm rounds  
 Layer 3: 0.25mm rounds  
 Layer 4: 0.25mm rounds  
 Layer 5: 0.25mm rounds

— South —

Names: Doug M Station: South Date: 03-1-09 Time:  
 1045 Exposed thermocouples: 6 Keywords: facets  
 Surface: 0.5mm facets (decomposing)  
 Layer 1: melt-freeze crust  
 Layer 2: melt-freeze crust  
 Layer 3: melt-freeze crust  
 Layer 4: 0.25mm rounds  
 Layer 5: 0.25mm rounds

March 02, 2009

— North —

Names: Doug C, Tom, Ethan Station: North Date:  
 03-2-09 Time: 1315 Exposed thermocouples: 7  
 Keywords:  
 Surface: Rounds, 1mm  
 Layer 1: Rounds, 1mm  
 Layer 2: Rounds, 1mm  
 Layer 3: Rounds, 1mm  
 Layer 4: Rounds, 1mm  
 Layer 5: Rounds, 1mm

— South —

Names: Doug C Station: South Date: 03-2-09 Time:  
 1015 Exposed thermocouples: 12 Keywords:  
 Surface: Melt Freeze Crust  
 Layer 1: Polyclusters/wet grains, 2-3mm  
 Layer 2: Polyclusters/wet grains, 2-3mm  
 Layer 3: Polyclusters/wet grains, 2-3mm  
 Layer 4: Polyclusters/wet grains, 2-3mm  
 Layer 5: Polyclusters/wet grains, 2-3mm

March 04, 2009

— North —

Names: Irene, Tom Station: North Date: 03-4-09  
 Time: 1215 Exposed thermocouples: 5 Keywords:  
 Surface: 1-3mm stellars, rimed stellars  
 Layer 1: 1-3mm stellars, rimed stellars  
 Layer 2: 1-3mm stellars, rimed stellars, graupel  
 Layer 3: 1mm decomposing stellars  
 Layer 4: 1mm decomposing stellars  
 Layer 5: 1mm decomposing stellars

— South —

Names: Irene, Tom Station: South Date: 03-4-09  
 Time: 1120 Exposed thermocouples: 11 Keywords:  
 none  
 Surface: 1-2 mm stellars, some rimed  
 Layer 1: 1-2 mm stellars, some rimed  
 Layer 2: 1-2 mm stellars, graupel  
 Layer 3: melt freeze crust  
 Layer 4: melt freeze crust  
 Layer 5: .5mm rounds

March 05, 2009

— North —

Names: no one Station: North Date: 03-5-09 Time:  
 Exposed thermocouples: 0 Keywords: snow  
 Surface:  
 Layer 1:  
 Layer 2:  
 Layer 3:  
 Layer 4:  
 Layer 5:

— South —

Names: No one Station: South Date: 03-5-09 Time:  
 Exposed thermocouples: 0 Keywords: snow  
 Surface:  
 Layer 1:  
 Layer 2:  
 Layer 3:  
 Layer 4:  
 Layer 5:

March 06, 2009

— North —

Names: Irene Station: North Date: 03-6-09 Time:  
 1025 Exposed thermocouples: 7 Keywords:  
 Surface: 1-4mm stellars, rimed stellars  
 Layer 1: 1-4mm stellars, rimed stellars  
 Layer 2: 1-4mm stellars, rimed stellars  
 Layer 3: 1-4mm stellars, rimed stellars  
 Layer 4: 1-4mm stellars, rimed stellars  
 Layer 5: 1-4mm stellars, rimed stellars

— South —

Names: Doug McCabe Station: South Date: 03-6-09  
 Time: 1200 Exposed thermocouples: 4 Keywords:  
 Surface: 0.5-2mm new snow  
 Layer 1: 0.5-2mm new snow  
 Layer 2: 0.5-2mm new snow  
 Layer 3: 0.5-2mm new snow  
 Layer 4: 0.5-2mm new snow  
 Layer 5: 0.5-2mm new snow

March 07, 2009

---

— North —

*Names:* Doug McCabe *Station:* North *Date:* 03-7-09  
*Time:* 0900 *Exposed thermocouples:* 6 *Keywords:*  
*Surface:* 1-2mm new snow  
*Layer 1:* 0.5mm decomposing  
*Layer 2:* 0.5mm decomposing  
*Layer 3:* 0.5mm decomposing  
*Layer 4:* 0.5mm decomposing  
*Layer 5:* 0.5mm decomposing

— South —

*Names:* Doug McCabe *Station:* South *Date:* 03-7-09  
*Time:* 0945 *Exposed thermocouples:* 4 *Keywords:*  
 near surface facets  
*Surface:* 1-2mm new snow  
*Layer 1:* 0.5mm decomposing  
*Layer 2:* 0.5mm decomposing  
*Layer 3:* 0.5mm decomposing  
*Layer 4:* 0.5mm decomposing  
*Layer 5:* 0.5mm decomposing

March 08, 2009

---

— North —

*Names:* Doug McCabe *Station:* North *Date:* 03-8-09  
*Time:* 1300 *Exposed thermocouples:* 5 *Keywords:*  
*Surface:* 1-2mm new snow  
*Layer 1:* 1-2mm new snow  
*Layer 2:* 1-2mm new snow  
*Layer 3:* 1-2mm new snow  
*Layer 4:* 1-2mm new snow  
*Layer 5:* 1-2mm new snow

— South —

*Names:* Doug McCabe *Station:* South *Date:* 03-8-09  
*Time:* 1430 *Exposed thermocouples:* 4 *Keywords:*  
*Surface:* 1-2mm new snow  
*Layer 1:* 1-2mm new snow  
*Layer 2:* 1-2mm new snow  
*Layer 3:* 1-2mm new snow  
*Layer 4:* 1-2mm new snow  
*Layer 5:* 1-2mm new snow

March 09, 2009

---

— North —

*Names:* Doug C *Station:* North *Date:* 03-9-09 *Time:*  
 1100 *Exposed thermocouples:* 0 *Keywords:*  
*Surface:* New Snow, 1mm  
*Layer 1:* New Snow, 1mm  
*Layer 2:* New Snow, 1mm  
*Layer 3:* New Snow, 1mm  
*Layer 4:* New Snow, 1mm  
*Layer 5:* New Snow, 1mm

— South —

*Names:* Doug C *Station:* South *Date:* 03-9-09 *Time:*  
 1145 *Exposed thermocouples:* 0 *Keywords:*  
*Surface:* New Snow to Decomposing Snow, 1mm  
*Layer 1:* New Snow to Decomposing Snow, 1mm  
*Layer 2:* New Snow to Decomposing Snow, 1mm  
*Layer 3:* New Snow to Decomposing Snow, 1mm  
*Layer 4:* New Snow to Decomposing Snow, 1mm  
*Layer 5:* New Snow to Decomposing Snow, 1mm

March 10, 2009

---

— North —

*Names:* Doug C *Station:* North *Date:* 03-10-09  
*Time:* 1330 *Exposed thermocouples:* 8 *Keywords:*  
*Surface:* New Snow, .5mm  
*Layer 1:* Decomposing Snow transitioning to rounds  
, .3-5 mm  
*Layer 2:* Decomposing Snow transitioning to rounds  
, .3-5 mm  
*Layer 3:* Decomposing Snow transitioning to rounds  
, .3-5 mm  
*Layer 4:* Decomposing Snow , .5 mm  
*Layer 5:* Decomposing Snow, .5 mm

— South —

*Names:* Doug C *Station:* South *Date:* 03-10-09  
*Time:* 1045 *Exposed thermocouples:* 6 *Keywords:*  
*Surface:* New Snow, .5mm  
*Layer 1:* Decomposing Snow transitioning to rounds  
, .3-5 mm  
*Layer 2:* Decomposing Snow transitioning to rounds  
, .3-5 mm  
*Layer 3:* Decomposing Snow transitioning to rounds  
, .3-5 mm  
*Layer 4:* Decomposing Snow transitioning to rounds  
, .3-5 mm  
*Layer 5:* Decomposing Snow, .5 mm

March 11, 2009

---

— North —

*Names:* Doug C , Virginia *Station:* North *Date:*  
03-11-09 *Time:* 1315 *Exposed thermocouples:* 11  
*Keywords:*  
*Surface:* decomposing snow to rounds .5mm with  
small surface hoar, 1-3mm  
*Layer 1:* decomposing snow to rounds .5mm  
*Layer 2:* decomposing snow to rounds .5mm  
*Layer 3:* decomposing snow to rounds .5mm  
*Layer 4:* decomposing snow to rounds .5mm  
*Layer 5:* decomposing snow to rounds .5mm

— South —

*Names:* Doug C, (Tom, Coop PM) *Station:* South  
*Date:* 03-11-09 *Time:* 930 *Exposed thermocouples:* 7  
*Keywords:* Surface Hoar or Near Surface Facets  
*Surface:*  
Near Surface Facets or Surface Hoar, .1-.3mm  
*Layer 1:* Decomposing Snow, .5-1mm  
*Layer 2:* Decomposing Snow, .5-1mm  
*Layer 3:* Decomposing Snow, .5-1mm  
*Layer 4:* Decomposing Snow, .5-1mm  
*Layer 5:* Melt Freeze Crust

March 12, 2009

---

— North —

*Names:* Irene, Pat, Rich *Station:* North *Date:*  
03-12-09 *Time:* 1245 *Exposed thermocouples:* 3  
*Keywords:* facets  
*Surface:* .5-1mm facets  
*Layer 1:* 1mm highly decomposed particles  
*Layer 2:* 1mm highly decomposed particles  
*Layer 3:* 1mm highly decomposed particles  
*Layer 4:* 1mm highly decomposed particles  
*Layer 5:* 1mm highly decomposed particles

— South —

*Names:* Doug M (am), Doug C (am) *Station:* South  
*Date:* 03-12-09 *Time:* 0945 *Exposed thermocouples:*  
8 *Keywords:* Facets  
*Surface:* 0.5mm facets?, 0.5mm surface hoar?, 0.5  
mm decomposing  
*Layer 1:* 0.5 decomposing  
*Layer 2:* 0.5 decomposing  
*Layer 3:* 0.5 decomposing  
*Layer 4:* melt-freeze  
*Layer 5:* melt-freeze

March 13, 2009

---

— North —

*Names: Irene, Jake Z Station: North Date: 03-13-09 Time: 0930 Exposed thermocouples: 4*  
*Keywords: surface hoar*  
*Surface: .5-1mm surface hoar,*  
*Layer 1: .5mm highly decomposed particles*  
*Layer 2: .5mm highly decomposed particles*  
*Layer 3: .5mm highly decomposed particles*  
*Layer 4: 1mm decomposing particles*  
*Layer 5: 1mm decomposing particles*

— South —

*Names: Irene, Virginia Station: South Date: 03-13-09 Time: 1220 Exposed thermocouples: 8*  
*Keywords: Radiation Recrystallization*  
*Surface: 1-2mm RR facets*  
*Layer 1: melt layer*  
*Layer 2: melt layer*  
*Layer 3: melt layer*  
*Layer 4: 1mm decomposing particles*  
*Layer 5: 1mm decomposing particles*

March 14, 2009

---

— North —

*Names: Irene Station: North Date: 03-14-09 Time: 0945 Exposed thermocouples: 4*  
*Keywords:*  
*Surface: .5mm mixed forms rounding*  
*Layer 1: .5mm rounds*  
*Layer 2: .5mm rounds*  
*Layer 3: .5mm rounds*  
*Layer 4: .5mm highly decomposed particles*  
*Layer 5: .5mm highly decomposed stellars*

— South —

*Names: Doug (am)Irene, Tom (pm) Station: South Date: 03-14-09 Time: 11:20; 3:40 Exposed thermocouples: 10*  
*Keywords: Radiation Recrystallization*  
*Surface: .5-2mm RR facets*  
*Layer 1: melt layer*  
*Layer 2: melt layer*  
*Layer 3: melt layer*  
*Layer 4: melt layer*  
*Layer 5: melt layer*

March 15, 2009

---

— North —

*Names: Doug McCabe Station: North Date: 03-15-09 Time: 1100 Exposed thermocouples: 4*  
*Keywords:*  
*Surface: 0.75mm rounds*  
*Layer 1: 0.75mm rounds*  
*Layer 2: 0.75mm rounds*  
*Layer 3: 0.75mm rounds*  
*Layer 4: 0.75mm rounds*  
*Layer 5: 0.75mm rounds*

— South —

*Names: Doug McCabe Station: South Date: 03-15-09 Time: 1300 Exposed thermocouples: 12*  
*Keywords:*  
*Surface: melt-freeze crust (frozen)*  
*Layer 1: melt-freeze crust (frozen)*  
*Layer 2: melt-freeze crust (frozen)*  
*Layer 3: melt-freeze crust (frozen)*  
*Layer 4: melt-freeze crust (frozen)*  
*Layer 5: 0.5mm rounds*

March 16, 2009

---

— North —

*Names:* Doug C *Station:* Date: 03-16-09 *Time:*

*Exposed thermocouples:* 0 *Keywords:*

*Surface:*

*Layer 1:*

*Layer 2:*

*Layer 3:*

*Layer 4:*

*Layer 5:*

— South —

*Names:* Doug C *Station:* South *Date:* 03-16-09

*Time:* 1130 *Exposed thermocouples:* 14 *Keywords:*

*Surface:* Melt Freeze Crust with observable facets

*Layer 1:* Melt Freeze Crust

*Layer 2:* Melt Freeze Crust

*Layer 3:* Melt Freeze Crust

*Layer 4:* Decomposing Snow to Rounds, .5mm

*Layer 5:* Decomposing Snow to Rounds, .5mm

March 18, 2009

---

— North —

*Names:* Doug C, Pat, Andrew *Station:* North *Date:*

03-18-09 *Time:* 1215 *Exposed thermocouples:* 11

*Keywords:*

*Surface:* Decomposing Snow, 1mm

*Layer 1:* Decomposing Snow, 1mm

*Layer 2:* Decomposing Snow, 1mm

*Layer 3:* Decomposing Snow, 1mm

*Layer 4:* Decomposing Snow, 1mm

*Layer 5:* Decomposing Snow, 1mm

— South —

*Names:* Doug C, Pat Andrew, Irene *Station:* South

*Date:* 03-18-09 *Time:* 1300 *Exposed thermocouples:*

11 *Keywords:*

*Surface:* decomposing snow to rounds, .5-1mm

*Layer 1:* decomposing snow to rounds, .5-1mm

*Layer 2:* decomposing snow to rounds, .5-1mm

*Layer 3:* decomposing Snow, .5-1mm

*Layer 4:* decomposing snow, .5-1mm

*Layer 5:* decomposing snow, .5-1mm

March 19, 2009

---

— North —

*Names:* Doug McCabe, Peter Cooch *Station:* North

*Date:* 03-19-09 *Time:* 1300 *Exposed thermocouples:*

12 *Keywords:*

*Surface:* 0.25-1.0mm decomposing to rounds

*Layer 1:* 0.25-1.0mm decomposing to rounds

*Layer 2:* 0.25-1.0mm decomposing to rounds

*Layer 3:* 0.25-1.0mm decomposing to rounds

*Layer 4:* 0.25-1.0mm decomposing to rounds

*Layer 5:* 0.25-1.0mm decomposing to rounds

— South —

*Names:* Doug McCabe, Jeremy *Station:* South *Date:*

03-19-09 *Time:* 0945 *Exposed thermocouples:* 12

*Keywords:*

*Surface:* 1.5mm new snow, 1.0mm decomposing

*Layer 1:* 0.5mm decomposing

*Layer 2:* melt-freeze

*Layer 3:* melt-freeze

*Layer 4:* 0.25mm decomposing

*Layer 5:* 0.25mm decomposing



March 20, 2009

— North —

*Names: Irene, Doug M Station: North Date: 03-20-09 Time: 0930 Exposed thermocouples: 12*  
*Keywords:*  
*Surface: 1-2mm graupel*  
*Layer 1: 1-2mm decomposing stellars, rounds*  
*Layer 2: 1-2mm decomposing stellars, rounds*  
*Layer 3: 1-2mm decomposing stellars, rounds*  
*Layer 4: 1-2mm decomposing stellars, rounds*  
*Layer 5: 1-2mm decomposing stellars, rounds*

— South —

*Names: Irene, Morgan Station: South Date: 03-20-09 Time: 1120 Exposed thermocouples: 14*  
*Keywords: radiation recrystallization*  
*Surface: 1mm graupel, 1mm rr forms*  
*Layer 1: 1mm wet grains*  
*Layer 2: 1mm wet grains*  
*Layer 3: 1mm wet grains*  
*Layer 4: 1mm wet grains*  
*Layer 5: 1mm wet grains*

March 21, 2009

— North —

*Names: Irene Station: North Date: 03-21-09 Time: 1250 Exposed thermocouples: 14*  
*Keywords:*  
*Surface: 1mm decomposing wet new snow*  
*Layer 1: 2-3mm graupel*  
*Layer 2: 1mm decomposing wet grains*  
*Layer 3: 1mm decomposing wet grains*  
*Layer 4: 1mm decomposing wet grains*  
*Layer 5: 1mm decomposing wet grains*

— South —

*Names: Doug McCabe, Brittany Station: South Date: 03-21-09 Time: 1015 Exposed thermocouples: 4*  
*Keywords:*  
*Surface: 1.0mm new snow*  
*Layer 1: melt-freeze crust*  
*Layer 2: melt-freeze crust*  
*Layer 3: melt-freeze crust*  
*Layer 4: melt-freeze crust*  
*Layer 5: melt-freeze crust*

March 22, 2009

— North —

*Names: Doug M Station: North Date: 03-22-09 Time: 1130 Exposed thermocouples: 9*  
*Keywords:*  
*Surface: 0.5-2mm new and decomposing snow*  
*Layer 1: 0.5-2mm new and decomposing snow*  
*Layer 2: 0.5-2mm new and decomposing snow*  
*Layer 3: 0.5-2mm new and decomposing snow*  
*Layer 4: 0.5-2mm new and decomposing snow*  
*Layer 5: 0.5-2mm new and decomposing snow*

— South —

*Names: Doug M, Tom, Coop Station: South Date: 03-22-09 Time: 0915 Exposed thermocouples: 0*  
*Keywords:*  
*Surface: 1-2mm new rimed snow*  
*Layer 1: 1-2mm new rimed snow*  
*Layer 2: 1-2mm new rimed snow*  
*Layer 3: 1-2mm new rimed snow*  
*Layer 4: 1-2mm new rimed snow*  
*Layer 5: 1-2mm new rimed snow*

March 23, 2009

---

— North —

*Names: Not Observed Station: Date: 03-23-09*

*Time: Exposed thermocouples: 0 Keywords:*

*Surface:*

*Layer 1:*

*Layer 2:*

*Layer 3:*

*Layer 4:*

*Layer 5:*

— South —

*Names: Doug C, Jeremy Station: South Date:*

*03-23-09 Time: 945 Exposed thermocouples: 0*

*Keywords:*

*Surface: New Snow, 1-2mm*

*Layer 1: New Snow, 1-2mm*

*Layer 2: New Snow, 1-2mm*

*Layer 3: New Snow, 1-2mm*

*Layer 4: New Snow, 1-2mm*

*Layer 5: New Snow, 1-2mm*

March 24, 2009

---

— North —

*Names: Doug C Station: North Date: 03-24-09*

*Time: 1115 Exposed thermocouples: 4 Keywords:*

*Surface: New Snow, 1-2mm*

*Layer 1: New Snow, 1-2mm*

*Layer 2: New Snow, 1-2mm*

*Layer 3: New Snow, 1-2mm*

*Layer 4: New Snow, 1-2mm*

*Layer 5: New Snow, 1-2mm*

— South —

*Names: Doug C Station: South Date: 03-24-09*

*Time: 1000 Exposed thermocouples: 7 Keywords:*

*Surface: New snow, 1-2mm*

*Layer 1: New snow, 1-2mm*

*Layer 2: New snow, 1-2mm*

*Layer 3: New snow, 1-2mm*

*Layer 4: New snow, 1-2mm*

*Layer 5: New snow, 1-2mm*

March 26, 2009

---

— North —

*Names: Doug M, Tom Station: North Date: 03-26-09*

*Time: 1145 Exposed thermocouples: 10 Keywords:*

*Surface: 0.5mm new snow (broken up)w/ rime*

*Layer 1: 0.5mm new snow (broken up)w/ rime*

*Layer 2: 0.5mm new snow (broken up)w/ rime*

*Layer 3: 0.5mm new snow (broken up)w/ rime*

*Layer 4: 0.5mm new snow (broken up)w/ rime*

*Layer 5: 0.5mm new snow (broken up)w/ rime*

— South —

*Names: Doug M, Tom Station: South Date: 03-26-09*

*Time: 1015 Exposed thermocouples: 5 Keywords:*

*Surface: 0.5-3mm new snow*

*Layer 1: 0.5-3mm new snow*

*Layer 2: 0.5-3mm new snow*

*Layer 3: 0.5-3mm new snow*

*Layer 4: 0.5-3mm new snow*

*Layer 5: 0.5-3mm new snow*

March 27, 2009

— North —

*Names:* Doug M *Station:* North *Date:* 03-27-09  
*Time:* 1230 *Exposed thermocouples:* 10 *Keywords:*  
 facets, surface hoar  
*Surface:* thin (1mm)wind crust w/ small (0.5mm)  
 facets and plates on top.  
*Layer 1:* 0.25mm highly decomposed and rounds  
*Layer 2:* 0.25mm highly decomposed and rounds  
*Layer 3:* 0.25mm highly decomposed and rounds  
*Layer 4:* 0.25mm highly decomposed and rounds  
*Layer 5:* 0.25mm highly decomposed and rounds

— South —

NO DAILY LOG RECORDED

March 28, 2009

— North —

*Names:* Doug M, Katy *Station:* North *Date:* 03-28-09  
*Time:* 1230 *Exposed thermocouples:* 10 *Keywords:*  
*Surface:* 0.5-2.0mm new snow  
*Layer 1:* 0.5-2.0mm new snow and decomposing  
*Layer 2:* 0.5-2.0mm new snow and decomposing  
*Layer 3:* 0.5-2.0mm new snow and decomposing  
*Layer 4:* 0.5-2.0mm new snow and decomposing  
*Layer 5:* 0.5-2.0mm new snow and decomposing

— South —

*Names:* Doug m, Katy *Station:* South *Date:* 03-28-09  
*Time:* 1130 *Exposed thermocouples:* 8 *Keywords:*  
*Surface:* 1.5mm new snow  
*Layer 1:* melt-freeze crust  
*Layer 2:* melt-freeze crust  
*Layer 3:* 0.5-2mm decomposing to rounds  
*Layer 4:* 0.5-2mm decomposing to rounds  
*Layer 5:* 0.5-2mm decomposing to rounds

March 30, 2009

— North —

*Names:* Tom, Waren *Station:* 1330 *Date:* 03-30-09  
*Time:* *Exposed thermocouples:* 0 *Keywords:*  
*Surface:* New Snow, Decomposing Snow, .5mm  
*Layer 1:* Decomposing Snow, .5mm  
*Layer 2:* Decomposing Snow, .5mm  
*Layer 3:* Decomposing Snow, .5mm  
*Layer 4:* Decomposing Snow, .5mm  
*Layer 5:* Decomposing Snow, .5mm

— South —

*Names:* Doug C, Virg (Doug , Tom PM) *Station:*  
 South *Date:* 03-30-09 *Time:* 1130 (1415 pm)  
*Exposed thermocouples:* 0 *Keywords:*  
*Surface:*  
 New SNOW, 1-2 mm (PM Facets on stellars .3mm)  
*Layer 1:* New SNOW, 1-2 mm (PM Rounds, .5mm)  
*Layer 2:* New SNOW, 1-2 mm (PM Rounds, .5mm)  
*Layer 3:* New SNOW, 1-2 mm (PM Rounds, .5mm)  
*Layer 4:* New SNOW, 1-2 mm (PM Rounds, .5mm)  
*Layer 5:* New SNOW, 1-2 mm (PM Rounds, .5mm)

April 01, 2009

— North —

Names: Doug C Station: North Date: 04-1-09 Time:  
1030 Exposed thermocouples: 0 Keywords:  
Surface: New Snow, 1mm  
Layer 1: New Snow, 1mm  
Layer 2: New Snow, 1mm  
Layer 3: New Snow, 1mm  
Layer 4: New Snow, 1mm  
Layer 5: New Snow, 1mm

— South —

Names: Doug C, Tom , Katy Station: South Date:  
04-1-09 Time: 1400 Exposed thermocouples: 1  
Keywords:  
Surface: rounds, .5mm  
Layer 1: decomposing snow, 1mm  
Layer 2: decomposing snow, 1mm  
Layer 3: decomposing snow, 1mm  
Layer 4: decomposing snow, 1mm  
Layer 5: decomposing snow, 1mm

April 02, 2009

— North —

Names: Irene, Pat, Andrew, Rich Station: North  
Date: 04-2-09 Time: 1320 Exposed thermocouples:  
11 Keywords:  
Surface: 1-3mm stellars  
Layer 1: 1-3mm stellars  
Layer 2: 1-3mm stellars  
Layer 3: 1-3mm stellars  
Layer 4: 1-3mm stellars  
Layer 5: 1-3mm stellars

— South —

Names: Irene, Pat, Andrew, Rich Station: South  
Date: 04-2-09 Time: 1240 Exposed thermocouples:  
10 Keywords: none  
Surface: 1-3mm stellars  
Layer 1: 1-3mm stellars  
Layer 2: 1-3mm stellars  
Layer 3: 1-3mm stellars  
Layer 4: 1-3mm stellars  
Layer 5: 1-3mm stellars

April 05, 2009

— North —

NO DAILY LOG RECORDED

— South —

Names: Doug M, Tom Station: South Date: 04-5-09  
Time: 1100 Exposed thermocouples: 4 Keywords:  
surface hoar, new snow, NSF  
Surface: 0.5-3mm new snow and some surface hoar  
Layer 1: 0.5mm decomposing  
Layer 2: 0.5mm decomposing  
Layer 3: 0.5mm decomposing  
Layer 4: 0.5mm decomposing  
Layer 5: 0.5mm decomposing

April 06, 2009

— North —

*Names: Doug C Station: North Date: 04-6-09 Time:**1245 Exposed thermocouples: 14 Keywords:***Near Surface facets***Surface: Near surface facets, .3-.5**Layer 1: rounds, .3-.5mm**Layer 2: rounds, .3-.5mm**Layer 3: rounds, .3-.5mm**Layer 4: rounds, .3-.5mm**Layer 5: rounds, .3-.5mm*

— South —

*Names: Doug C Station: South Date: 04-6-09 Time:**1200 Exposed thermocouples: 12 Keywords:***near surface facets, .3-.5***Surface: Near surface facets, .3-.5mm**Layer 1: wet grains, 2-3mm**Layer 2: wet grains, 2-3mm**Layer 3: wet grains, 2-3mm**Layer 4: wet grains, 2-3mm**Layer 5: wet grains, 2-3mm*G.2 2007/2008 Season

January 17, 2008

— North —

*NO DAILY LOG RECORDED*

— South —

*Names: Henry Station: YC\_South Date: 01-17-08**Time: 11:00 Exposed thermocouples: 0 Keywords:***none***Surface:**1-4mm stellars, heavily rimed other new snow**Layer 1:**1-4mm stellars, heavily rimed other new snow**Layer 2:**1-4mm stellars, heavily rimed other new snow**Layer 3:**1-4mm stellars, heavily rimed other new snow**Layer 4:**1-4mm stellars, heavily rimed other new snow**Layer 5:**1-4mm stellars, heavily rimed other new snow*

January 18, 2008

— North —

*Names:* Doug *Station:* YC\_North *Date:* 01-18-08  
*Time:* 1:00 *Exposed thermocouples:* 5 *Keywords:*  
 none

*Surface:* 1-2mm rimed stellars  
*Layer 1:* 1-2mm rimed stellars  
*Layer 2:* 1-2mm rimed stellars  
*Layer 3:* 1-2mm rimed stellars  
*Layer 4:* 1-2mm rimed stellars  
*Layer 5:* 1-2mm rimed stellars

— South —

*Names:* Henry, Doug *Station:* YC\_South *Date:*  
 01-18-08 *Time:* 12:00 *Exposed thermocouples:* 0  
*Keywords:* none

*Surface:* 1-2mm heavily rimed new snow  
*Layer 1:* 1-2mm heavily rimed new snow  
*Layer 2:* 1-2mm heavily rimed new snow  
*Layer 3:* 1-2mm heavily rimed new snow  
*Layer 4:* 1-2mm heavily rimed new snow  
*Layer 5:* 1-2mm heavily rimed new snow

January 19, 2008

— North —

*Names:* Doug *Station:* YC\_North *Date:* 01-19-08  
*Time:* 12:00 *Exposed thermocouples:* 0 *Keywords:*  
 none

*Surface:* 2mm lightly rimed stellars  
*Layer 1:* 2mm lightly rimed stellars  
*Layer 2:* 2mm lightly rimed stellars  
*Layer 3:* 2mm lightly rimed stellars  
*Layer 4:* 2mm lightly rimed stellars  
*Layer 5:* 2mm lightly rimed stellars

— South —

*Names:* Doug *Station:* YC\_South *Date:* 01-19-08  
*Time:* 1:30 *Exposed thermocouples:* 0 *Keywords:*  
 none

*Surface:* 1-2mm rimed new snow  
*Layer 1:* 2mm stellars  
*Layer 2:* 2mm stellars  
*Layer 3:* 2mm stellars  
*Layer 4:* 2mm stellars  
*Layer 5:* 2mm stellars

January 20, 2008

— North —

*Names:* Doug C *Station:* NorthYC *Date:* 01-20-08  
*Time:* 10:30 *Exposed thermocouples:* 0 *Keywords:*  
 none

*Surface:* rimed stellars and plates .5-1mm  
*Layer 1:* rimed stellars and plates .5-1mm  
*Layer 2:* rimed stellars and plates .5-1mm  
*Layer 3:* rimed stellars and plates .5-1mm  
*Layer 4:* rimed stellars and plates .5-1mm  
*Layer 5:* rimed stellars and plates .5-1mm

— South —

*Names:* Doug C *Station:* SouthYC *Date:* 01-20-08  
*Time:* 9:00 *Exposed thermocouples:* 0 *Keywords:*  
 none

*Surface:* rimed stellars and plates .2-.5mm  
*Layer 1:* rimed stellars and plates .2-.5mm  
*Layer 2:* rimed stellars and plates .2-.5mm  
*Layer 3:* rimed stellars and plates .5-1mm  
*Layer 4:* rimed stellars and plates .5-1mm  
*Layer 5:* rimed stellars and plates .5-1mm

January 22, 2008

— North —

Names: Doug C Station: NorthYC Date: 01-22-08  
 Time: 1030 Exposed thermocouples: 0 Keywords:  
 near surface facet  
 Surface: rimed stellar 2mm  
 Layer 1: facet <.5mm  
 Layer 2: facet <.5mm  
 Layer 3: facet <.5mm  
 Layer 4: facet <.5mm  
 Layer 5: facet <.5mm

— South —

Names: Doug C, Virginia Station: SouthYC Date:  
 01-22-08 Time: 900 Exposed thermocouples: 0  
 Keywords: surface hoar, surface facet  
 Surface: surface hoar 4-6mm  
 Layer 1: facet w/ broken stellars still sligtly  
 vis. <.5mm  
 Layer 2: facet w/ broken stellars still sligtly  
 vis. <.5mm  
 Layer 3: facet w/ broken stellars still sligtly  
 vis. <.5mm  
 Layer 4: broken stellars with rounding 1mm  
 Layer 5: broken stellars with rounding 1mm

January 23, 2008

— North —

Names: TEST Station: YC\_North Date: 01-23-08  
 Time: none Exposed thermocouples: none Keywords:  
 none  
 Surface: none  
 Layer 1: none  
 Layer 2: none  
 Layer 3: none  
 Layer 4: none  
 Layer 5: none

— South —

NO DAILY LOG RECORDED

January 24, 2008

— North —

Names: Henry Doug Station: YC\_North Date:  
 01-24-08 Time: 1:00 Exposed thermocouples: 0  
 Keywords: none  
 Surface: 2-3mm surface hoar  
 Layer 1: 1-3mm stellars, plates  
 Layer 2: 1-3mm stellars, plates  
 Layer 3: 1-3mm stellars, plates  
 Layer 4: 1-3mm stellars, plates  
 Layer 5: 1-3mm stellars, plates

— South —

Names: Henry Station: YC\_South Date: 01-24-08  
 Time: 10:30 Exposed thermocouples: 0 Keywords:  
 none  
 Surface: decomposing surface hoar 1-2mm  
 Layer 1: 1mm decomposing new snow  
 Layer 2: 1mm decomposing new snow  
 Layer 3: sun crust .5mm  
 Layer 4: sun crust .5mm  
 Layer 5: decomposing new snow 1mm / .5mm rounds

January 25, 2008

— North —

*Names:* Doug *Station:* YC\_North *Date:* 01-25-08  
*Time:* 1:00 *Exposed thermocouples:* 0 *Keywords:*  
 surface hoar  
*Surface:* 1-2mm lightly rimed stellars and plates  
*Layer 1:* 1-2mm lightly rimed stellars and plates  
*Layer 2:* 1-2mm lightly rimed stellars and plates  
*Layer 3:* 1-2mm partially decomposed surface hoar  
*Layer 4:* 1-2mm stellars  
*Layer 5:* 1-2mm stellars

— South —

*Names:* Henry, Doug, Irene *Station:* YC\_South *Date:*  
 01-25-08 *Time:* 11:00 *Exposed thermocouples:* none  
*Keywords:* surface hoar  
*Surface:* 1-3mm stellars, plates  
*Layer 1:* 1-2mm partially decomposed surface hoar  
*Layer 2:* .5mm sun crust  
*Layer 3:* .5mm sun crust  
*Layer 4:* 1mm decomposing new snow, .5mm rounds  
*Layer 5:* 1mm decomposing new snow, .5mm rounds

January 26, 2008

— North —

*Names:* Doug, Irene, Peter *Station:* NorthYC *Date:*  
 01-26-08 *Time:* 2:00pm *Exposed thermocouples:* 0  
*Keywords:* surface hoar  
*Surface:* surface hoar .5mm-1mm  
*Layer 1:* wind crust (.5mm thick).5mm  
*Layer 2:*  
 stellars 1mm, partly decomposed new snow 1mm  
*Layer 3:* partly decomposed surface hoar 2mm  
*Layer 4:*  
 stellars 2mm, partly decomposed new snow 1mm  
*Layer 5:*  
 stellars 2mm, partly decomposed new snow 1mm

— South —

*Names:* Henry, Wes *Station:* YC\_South *Date:*  
 01-26-08 *Time:* 12:30 *Exposed thermocouples:* 0  
*Keywords:* surface hoar  
*Surface:* .5mm surface hoar remnants  
*Layer 1:* .3-.5mm sun crust  
*Layer 2:* .3-.5mm sun crust  
*Layer 3:* .3-.5mm sun crust  
*Layer 4:*  
 mostly decomposed new snow crystals .5mm-1mm  
*Layer 5:*  
 mostly decomposed new snow crystals .5mm-1mm

January 27, 2008

— North —

*Names:* doug C, Danielle *Station:* NorthYC *Date:*  
 01-27-08 *Time:* 1345 *Exposed thermocouples:* 0  
*Keywords:* surface hoar  
*Surface:* decomposing particals.5-1mm, broken  
 surface hoar observable but not prolific ~1mm  
*Layer 1:* decomposing particals. 5-1mm  
*Layer 2:* decomposing particals. 5-1mm  
*Layer 3:* decomposing particals. 5-1mm  
*Layer 4:* decomposing particals. 5-1mm  
*Layer 5:* decomposing particals. 5-1mm

— South —

*Names:* Doug, Tom *Station:* SouthYC *Date:* 01-27-08  
*Time:* 10:00 *Exposed thermocouples:* 0 *Keywords:*  
 surface hoar  
*Surface:* partly decomposed surface hoar 1mm  
*Layer 1:* crust .5 mm  
*Layer 2:* crust .5 mm  
*Layer 3:* crust .5 mm  
*Layer 4:* decomposing new snow 1mm  
*Layer 5:* decomposing new snow 1mm



January 28, 2008

— North —

*Names: Doug C Station: NorthYC Date: 01-28-08**Time: 1130 Exposed thermocouples: 0 Keywords:***none***Surface: rimed stellars, 1mm**Layer 1: rimed stellars, 1mm**Layer 2: rimed stellars, 1mm**Layer 3: rimed stellars and graupel, 2mm**Layer 4: rimed stellars and graupel, 2mm**Layer 5: rimed stellars and graupel, 2mm*

— South —

*Names: Doug C, Shawn R Station: SouthYC Date:**01-28-08 Time: 1230 Exposed thermocouples: 0**Keywords: none**Surface: rhimed stellars, 1mm**Layer 1: rhimed stellars, 1mm**Layer 2: rhimed stellars, 1mm**Layer 3: rhimed stellars, 1mm**Layer 4: rhimed stellars, 1mm**Layer 5: rhimed stellars, 1mm*

January 29, 2008

— North —

*NO DAILY LOG RECORDED*

— South —

*Names: Henry, Jan Station: SouthYC Date: 01-29-08**Time: 11:30 Exposed thermocouples: 0 Keywords:***none***Surface: .5mm sun crust**Layer 1: .5mm sun crust**Layer 2: .5mm sun crust**Layer 3: .5-1mm decomposing new snow**Layer 4: .5-1mm decomposing new snow**Layer 5: .5-1mm decomposing new snow*

January 30, 2008

— North —

*NO DAILY LOG RECORDED*

— South —

*Names: Irene Station: SouthYC Date: 01-30-08**Time: 11:00 Exposed thermocouples: 0 Keywords:***none***Surface: .5-1mm rimed stellars -some columns**Layer 1: .5-1mm rimed stellars-some columns**Layer 2: .5-1mm rimed stellars-some columns**Layer 3: .5-1mm rimed stellars-some columns**Layer 4: .5-1mm rimed stellars-some columns**Layer 5: .5-1mm rimed stellars-some columns*

January 31, 2008

— North —

*Names:* Doug, Irene *Station:* NorthYC *Date:*  
01-31-08 *Time:* 1:00 *Exposed thermocouples:* 9  
*Keywords:* none  
*Surface:* stellars 3 mm, highly broken new snow w/  
rime .5 mm  
*Layer 1:* highly broken new snow w/ rime .5 mm  
*Layer 2:* highly broken new snow w/ rime .5 mm  
*Layer 3:* highly broken new snow w/ rime .5 mm  
*Layer 4:* highly broken new snow w/ rime .5 mm  
*Layer 5:* highly broken new snow w/ rime .5 mm

— South —

*Names:* Doug, Irene *Station:* SouthYC *Date:*  
01-31-08 *Time:* 11:00 *Exposed thermocouples:* 10  
*Keywords:* none  
*Surface:* stellars 3 mm, highly broken new snow .5  
mm light rime, columns 1 mm  
*Layer 1:* highly broken new snow .5 mm light rime,  
columns 1 mm  
*Layer 2:* highly broken new snow .5 mm light rime,  
columns 1 mm  
*Layer 3:* highly broken new snow .5 mm light rime,  
columns 1 mm  
*Layer 4:* highly broken new snow .5 mm light rime,  
columns 1 mm  
*Layer 5:* highly broken new snow .5 mm light rime,  
columns 1 mm

February 01, 2008

— North —

*Names:* Doug *Station:* NorthYC *Date:* 02-01-08 *Time:*  
10:30 *Exposed thermocouples:* 7 *Keywords:* none  
*Surface:* graupel 1 mm - 2 mm, stellars 1 mm rimed  
*Layer 1:* stellars 1 mm rimed, partly decomposed 1  
mm, columns .5 mm  
*Layer 2:* stellars 1 mm rimed, partly decomposed 1  
mm, columns .5 mm  
*Layer 3:* partly decomposed 1 mm  
*Layer 4:* highly broken .5 mm  
*Layer 5:* highly broken .5 mm

— South —

*Names:* Doug *Station:* SouthYC *Date:* 02-01-08 *Time:*  
9:30 *Exposed thermocouples:* 8 *Keywords:* graupel  
*Surface:* graupel 3 mm  
*Layer 1:* graupel 1.5 mm, partly decomposed 1 mm,  
columns .5 mm  
*Layer 2:* graupel 1.5 mm, partly decomposed 1 mm,  
columns .5 mm  
*Layer 3:* highly broken .5 mm  
*Layer 4:* highly broken .5 mm  
*Layer 5:* crust 1 mm (2 cm thick)

February 02, 2008

— North —

*Names:* Doug, Doug C, Coop *Station:* NorthYC *Date:* 02-02-08  
*Time:* 2:15 *Exposed thermocouples:* 6  
*Keywords:* none  
*Surface:* highly broken 1 mm w/ rime  
*Layer 1:* highly broken .5 mm  
*Layer 2:* highly broken .5 mm  
*Layer 3:* highly broken .5 mm  
*Layer 4:* highly broken .25 mm  
*Layer 5:* highly broken .25 mm, stellars 1 mm

— South —

*Names:* Doug C *Station:* SouthYC *Date:* 02-02-08  
*Time:* 1030 *Exposed thermocouples:* 7 *Keywords:* none  
*Surface:* heavily rhimed stellars, 1-1.5 mm  
*Layer 1:* heavily rhimed stellars, 1-1.5 mm  
*Layer 2:* heavily rhimed stellars, 1-1.5 mm  
*Layer 3:* heavily rhimed stellars, 1-1.5 mm  
*Layer 4:* heavily rhimed stellars, 1-1.5 mm  
*Layer 5:* heavily rhimed stellars, 1-1.5 mm

February 03, 2008

— North —

*Names:* Doug, Doug C, Coop *Station:* NorthYC *Date:* 02-03-08  
*Time:* 1:00 *Exposed thermocouples:* 5  
*Keywords:* none  
*Surface:* plates 1 mm, stellars 1 mm  
*Layer 1:* plates 1 mm, stellars 1 mm  
*Layer 2:* plates 1 mm, stellars 1 mm  
*Layer 3:* plates 1 mm, stellars 1 mm  
*Layer 4:* highly broken .25 mm  
*Layer 5:* highly broken .25 mm

— South —

*Names:* Doug, Coop *Station:* SouthYC *Date:* 02-03-08  
*Time:* 10:30 *Exposed thermocouples:* 7 *Keywords:* none  
*Surface:* stellars 1 mm heavy rime, plates .5 mm  
*Layer 1:* plates .5 mm - 1mm  
*Layer 2:* highly broken .25 mm  
*Layer 3:* partly decomposed 1 mm  
*Layer 4:* partly decomposed 1 mm  
*Layer 5:* crust 1 mm

February 04, 2008

— North —

*Names:* Doug C *Station:* NorthYC *Date:* 02-04-08  
*Time:* 1100 *Exposed thermocouples:* 2 *Keywords:*  
*Surface:* rimed new snow, .5-1mm  
*Layer 1:* rimed new snow, .5-1mm  
*Layer 2:* new snow, 1mm  
*Layer 3:* new snow, 1mm  
*Layer 4:* new snow, 1mm  
*Layer 5:* new snow, 1.5mm

— South —

*Names:* Doug C, Linda W *Station:* SouthYC *Date:* 02-04-08  
*Time:* 1130 *Exposed thermocouples:* 0  
*Keywords:* none  
*Surface:* rimed stellars, 1-1.5mm  
*Layer 1:* rimed stellars, 1-1.5mm  
*Layer 2:* new snow (sectors, columns), 1mm  
*Layer 3:* new snow (sectors, columns), 1mm  
*Layer 4:* new snow (sectors, columns), 1mm  
*Layer 5:* new snow (sectors, columns), 1mm

February 05, 2008

— North —

*Names:* Doug C, Brian S *Station:* NorthYC *Date:* 02-05-08  
*Time:* 1400 *Exposed thermocouples:* 2  
*Keywords:*  
*Surface:* rimed broken particles, .5-1mm  
*Layer 1:* new snow, .5-1mm  
*Layer 2:* new snow, .5-1mm  
*Layer 3:* new snow, .5-1mm  
*Layer 4:* new snow, .5-1mm  
*Layer 5:* new snow, .5-1mm

— South —

*Names:* Henry *Station:* SouthYC *Date:* 02-05-08  
*Time:* *Exposed thermocouples:* 5 *Keywords:*  
*Surface:* .5 mm surface hoar sporadic, highly decomposed new snow becoming sun crust  
*Layer 1:* .5-1mm decomposed new snow, signs of sun penetration  
*Layer 2:* 1mm decomposing stellars  
*Layer 3:* .5mm columns  
*Layer 4:* .5mm columns  
*Layer 5:* .5mm columns

February 06, 2008

— North —

*Names:* Irene *Station:* NorthYC *Date:* 02-06-08  
*Time:* 12:00 *Exposed thermocouples:* 0 *Keywords:*  
*Surface:* 1-2mm stellars, 1-2mm rimed stellars  
*Layer 1:* 1-2mm stellars, 1-2mm rimed stellars  
*Layer 2:* 1-2mm stellars, 1-2mm rimed stellars  
*Layer 3:* 1-2mm stellars, 1-2mm rimed stellars  
*Layer 4:* 1-2mm stellars, 1-2mm rimed stellars  
*Layer 5:* 1-2mm stellars, 1-2mm rimed stellars

— South —

*Names:* Irene *Station:* SouthYC *Date:* 02-06-08  
*Time:* 11:00 *Exposed thermocouples:* 0 *Keywords:*  
*Surface:* 1-2mm stellars, 1-2mm rimed stellars  
*Layer 1:* 1-2mm stellars, 1-2mm rimed stellars  
*Layer 2:* 1-2mm stellars, 1-2mm rimed stellars  
*Layer 3:* 1-2mm stellars, 1-2mm rimed stellars  
*Layer 4:* 1-2mm stellars, 1-2mm rimed stellars  
*Layer 5:* 1-2mm stellars, 1-2mm rimed stellars

February 07, 2008

— North —

*Names:* Henry *Station:* NorthYC *Date:* 02-07-08  
*Time:* 1:00 *Exposed thermocouples:* 0 *Keywords:*  
*Surface:* 2-3mm graupel  
*Layer 1:* 1-2mm heavily rimed stellars, plates  
*Layer 2:* 1-2mm heavily rimed stellars, plates  
*Layer 3:* 1-2mm heavily rimed stellars, plates  
*Layer 4:* 1-2mm heavily rimed stellars, plates  
*Layer 5:* 1-2mm heavily rimed stellars, plates

— South —

NO DAILY LOG RECORDED

February 08, 2008

— North —

*Names:* Henry, Wes *Station:* NorthYC *Date:* 02-08-08  
*Time:* 11:00 *Exposed thermocouples:* 0 *Keywords:*  
*Surface:* 2mm graupel  
*Layer 1:* 1-2mm mechanically decomposed new snow  
*Layer 2:* 1-2mm mechanically decomposed new snow  
*Layer 3:* 1-2mm mechanically decomposed new snow  
*Layer 4:* 2-3mm partially decomposed stellars  
*Layer 5:* 2-3mm partially decomposed stellars

— South —

*Names:* Henry, Tom *Station:* SouthYC *Date:* 02-08-08  
*Time:* 12:00 *Exposed thermocouples:* 0 *Keywords:*  
*Surface:* 2mm heavily rimed new snow / graupel  
*Layer 1:* 1mm wind crust  
*Layer 2:* 1mm wind crust  
*Layer 3:* 1-3mm decomposing stellars, plates  
*Layer 4:* 1-3mm decomposing stellars, plates  
*Layer 5:* 1-3mm decomposing stellars, plates

February 09, 2008

— North —

*Names:* Doug *Station:* NorthYC *Date:* 02-09-08  
*Time:* 11:45 *Exposed thermocouples:* 0 *Keywords:*  
*Surface:* heavily rimed stellars 3-5 mm  
*Layer 1:* heavily rimed stellars 3-5 mm  
*Layer 2:* partly decomposed .5 mm  
*Layer 3:* partly decomposed .5 mm  
*Layer 4:* partly decomposed .5 mm  
*Layer 5:* highly broken .25 mm

— South —

*Names:* Doug, Robin *Station:* SouthYC *Date:* 02-09-08  
*Time:* 10:15 *Exposed thermocouples:* 9  
*Keywords:*  
*Surface:* heavily rimed stellars 2 mm  
*Layer 1:* crust (melt freeze)1 mm  
*Layer 2:* partly decomposed and rounds 1 mm  
*Layer 3:* partly decomposed and rounds 1 mm  
*Layer 4:* partly decomposed and rounds .5 mm  
*Layer 5:* partly decomposed and rounds .5 mm

February 10, 2008

— North —

*Names:* Doug *Station:* NorthYC *Date:* 02-10-08  
*Time:* 2:15 *Exposed thermocouples:* 0 *Keywords:*  
*Surface:* wind crust .25 mm  
*Layer 1:* partly decomposed .5 mm  
*Layer 2:* heavily rimed new snow 3 mm  
*Layer 3:* partly decomposed and rounds .5 mm  
*Layer 4:* partly decomposed and rounds .5 mm  
*Layer 5:* partly decomposed and rounds .5 mm

— South —

*Names:* Doug *Station:* SouthYC *Date:* 02-10-08  
*Time:* 1:15 *Exposed thermocouples:* 9 *Keywords:*  
*Surface:* wind crust .25mm  
*Layer 1:* crust (melt freeze)1mm  
*Layer 2:* partly decomposed and rounds 1mm  
*Layer 3:* partly decomposed and rounds 1mm  
*Layer 4:* partly decomposed and rounds 1mm  
*Layer 5:* partly decomposed and rounds 1mm

February 11, 2008

— North —

*Names:* Henry Station: NorthYC *Date:* 02-11-08  
*Time:* 1:00 *Exposed thermocouples:* 3 *Keywords:*  
*Surface:*  
 .5mm highly broken wind affected crystals  
*Layer 1:* 2-3mm stellars, broken stellars  
*Layer 2:* 2-3mm stellars, broken stellars  
*Layer 3:* 2-3mm stellars, broken stellars  
*Layer 4:* decomposing rimed snow  
*Layer 5:* decomposing rimed snow

— South —

*Names:* Henry Station: SouthYC *Date:* 02-11-08  
*Time:* 12:00 *Exposed thermocouples:* 6 *Keywords:*  
*Surface:* 1-2mm stellars, 50% rimed  
*Layer 1:* 2-3mm stellars, no rime  
*Layer 2:* 2-3mm stellars, no rime  
*Layer 3:* 1-2mm rimed stellars, 1mm rimed plates  
*Layer 4:* .5-1mm decomposing new snow  
*Layer 5:* .5-1mm decomposing new snow

February 12, 2008

— North —

*Names:* Henry Station: NorthYC *Date:* 02-12-08  
*Time:* 11:00 *Exposed thermocouples:* 0 *Keywords:*  
 none  
*Surface:* 2-4mm stellars, stellar fragments  
*Layer 1:* 2-4mm stellars, stellar fragments, .25  
 x1mm capped columns  
*Layer 2:* 2-4mm stellars, stellar fragments, .25  
 x1mm capped columns  
*Layer 3:* 2-4mm stellars, stellar fragments  
*Layer 4:* 2-4mm stellars, stellar fragments  
*Layer 5:* 2-4mm stellars, stellar fragments

— South —

*Names:* Doug C, Wes H. Station: SouthYC *Date:*  
 02-12-08 *Time:* 1015 *Exposed thermocouples:* 3  
*Keywords:*  
*Surface:* new snow, 2mm  
*Layer 1:* new snow with riming, 2mm  
*Layer 2:* new snow with riming, 2mm  
*Layer 3:* new snow with riming, 2mm  
*Layer 4:* new snow with heavy riming, 2mm  
*Layer 5:* new snow with heavy riming, 2mm

February 13, 2008

— North —

*Names: Irene Station: NorthYC Date: 02-13-08*  
*Time: 11:50 Exposed thermocouples: 0 Keywords:*  
 none

*Surface: 1-2mm stellars, some lightly rimed*  
*Layer 1: 1-2mm stellars, some lightly rimed*  
*Layer 2: 1-2mm stellars, some lightly rimed*  
*Layer 3: 1-2mm stellars, some lightly rimed*  
*Layer 4: 1-2mm stellars, some lightly rimed*  
*Layer 5: 1-2mm stellars, some lightly rimed*

— South —

*Names: Doug, Brian Station: SouthYC Date:*  
*02-13-08 Time: 1:00 Exposed thermocouples: 0*  
*Keywords:*

*Surface:*  
*New snow, stellars rimed 2 mm, plates 1 mm*  
*Layer 1:*  
*New snow, stellars rimed 2 mm, plates 1 mm*  
*Layer 2:*  
*New snow, stellars rimed 2 mm, plates 1 mm*  
*Layer 3:*  
*New snow, stellars rimed 2 mm, plates 1 mm*  
*Layer 4:*  
*New snow, stellars rimed 2 mm, plates 1 mm*  
*Layer 5:*  
*New snow, stellars rimed 2 mm, plates 1 mm*

February 14, 2008

— North —

*Names: Irene Station: NorthYC Date: 02-14-08*  
*Time: 12:00 Exposed thermocouples: 0 Keywords:*  
 Surface hoar

*Surface: .5 mm surface hoar; 2mm stellars; 1mm*  
*columns; 1mm partially rimed stellars*  
*Layer 1:*  
*2mm stellars; 1mm partially rimed stellars*  
*Layer 2: 2mm stellars; 1mm partially rimed*  
*stellars, partially decomposed stellars*  
*Layer 3: 2mm stellars; 1mm partially rimed*  
*stellars, partially decomposed stellars*  
*Layer 4: 2mm stellars; 1mm partially rimed*  
*stellars, partially decomposed stellars*  
*Layer 5: 2mm stellars; 1mm partially rimed*  
*stellars, partially decomposed stellars*

— South —

*Names: Henry, Irene Station: SouthYC Date:*  
*02-14-08 Time: 11:00 Exposed thermocouples: 10*  
*Keywords:*

*radiation recrystalization, surface hoar*  
*Surface: .5mm surface hoar*  
*Layer 1: .5-1mm decomposing new snow*  
*Layer 2: .5-1mm decomposing new snow*  
*Layer 3: 1mm plates, 2mm stellars*  
*Layer 4: 1mm plates, 2mm stellars*  
*Layer 5: 1mm plates, 2mm stellars*

February 15, 2008

— North —

*Names:* Irene, Tom *Station:* NorthYC *Date:* 02-15-08*Time:* 1:00 *Exposed thermocouples:* 0 *Keywords:*

surface hoar, near surface facets

*Surface:*

stellars 2 mm, surface hoar 1 mm, facets 1mm

*Layer 1:* stellars 2mm, facets .5 mm*Layer 2:* partly decomposed 1 mm, stellars 2mm*Layer 3:* partly decomposed 1 mm, stellars 2mm*Layer 4:* partly decomposed 1 mm, stellars 2mm*Layer 5:* partly decomposed 1 mm, stellars 2mm

— South —

*Names:* Doug, Irene, Tom *Station:* SouthYC *Date:*02-15-08 *Time:* 11:00 *Exposed thermocouples:* 14*Keywords:* surface hoar, near surface facets*Surface:*

facets 2 mm, stellars 4 mm, surface hoar 1 mm

*Layer 1:* stellars 4 mm, partly decomposed 2 mm*Layer 2:* melt freeze crust (wet).5 mm*Layer 3:* melt freeze crust (wet).5 mm*Layer 4:* partly decomposed 1 mm*Layer 5:* partly decomposed 1 mm

February 16, 2008

— North —

*Names:* Doug C, Ben *Station:* NorthYC *Date:*02-16-08 *Time:* 1330 *Exposed thermocouples:* 12*Keywords:**Surface:* broken stellars, .5mm*Layer 1:* broken stellars, .5mm*Layer 2:* broken stellars, .5mm*Layer 3:* broken stellars, .5mm*Layer 4:* broken stellars, .5mm*Layer 5:* broken stellars, .5mm

— South —

*Names:* Doug, Irene *Station:* SouthYC *Date:*02-16-08 *Time:* 11:00 *Exposed thermocouples:* 16*Keywords:* facets*Surface:* stellars with lt rime 2 mm, plates .5 mm  
, highly broken .5 mm*Layer 1:* highly broken .5 mm*Layer 2:* highly broken .5 mm*Layer 3:* highly broken .5 mm*Layer 4:* highly broken .5 mm*Layer 5:* highly broken .5 mm, facets 1 mm



February 17, 2008

— North —

*Names:* Coop and Tom *Station:* NorthYC *Date:*  
 02-17-08 *Time:* 2:00pm *Exposed thermocouples:* 0  
*Keywords:* none  
*Surface:* irregular crystals, 1mm  
*Layer 1:*  
 irregular crystals and broken stellars, 1mm  
*Layer 2:*  
 irregular crystals and broken stellars, 1mm  
*Layer 3:*  
 irregular crystals and broken stellars, 1mm  
*Layer 4:*  
 irregular crystals and broken stellars, 1mm  
*Layer 5:*  
 irregular crystals and broken stellars, 1mm

— South —

*Names:* Coop and Tom *Station:* SouthYC *Date:*  
 02-17-08 *Time:* 1:30pm *Exposed thermocouples:* 14  
*Keywords:*  
*Surface:* Rim Stel  
*Layer 1:* Rim Stel and decomp Stel  
*Layer 2:* Rim Stel and decomp Stel  
*Layer 3:* Rim Stel and decomp Stel  
*Layer 4:* Rim Stel and decomp Stel  
*Layer 5:* Rim Stel and decomp Stel

February 18, 2008

— North —

*Names:* Doug C, Tom L *Station:* NorthYC *Date:*  
 02-18-08 *Time:* 1230 *Exposed thermocouples:* 12  
*Keywords:* facet  
*Surface:* surface facet, 1mm  
*Layer 1:* irregular crystal, 1mm  
*Layer 2:* decomposing stellaras, .75 mm  
*Layer 3:* decomposing stellaras, .75 mm  
*Layer 4:* decomposing stellaras, .75 mm  
*Layer 5:* decomposing stellaras, .75 mm

— South —

*Names:* Doug C, Pete C *Station:* SouthYC *Date:*  
 02-18-08 *Time:* 924 *Exposed thermocouples:* 16  
*Keywords:* surface facet  
*Surface:* surface facet, .5 mm  
*Layer 1:* decomposing stellaras, 1mm  
*Layer 2:* decomposing stellaras, 1mm  
*Layer 3:* decomposing stellaras, .5mm  
*Layer 4:* decomposing stellaras, .5mm  
*Layer 5:* decomposing stellaras, .5mm

February 19, 2008

— North —

*Names:* Henry, Doug C., Coop *Station:* NorthYC  
*Date:* 02-19-08 *Time:* 12:00 *Exposed thermocouples:*  
 0 *Keywords:* surface hoar  
*Surface:* .5mm surface hoar on top of thin 1mm  
 thick rounded wind crust  
*Layer 1:* .5-1mm decomposing stellar crystals  
*Layer 2:* .5-1mm decomposing stellar crystals  
*Layer 3:* .5-1mm decomposing stellar crystals  
*Layer 4:* .5-1mm decomposing stellar crystals  
*Layer 5:* .5-1mm decomposing stellar crystals

— South —

*Names:* Henry, Doug C. *Station:* SouthYC *Date:*  
 02-19-08 *Time:* 11:00 *Exposed thermocouples:* 18  
*Keywords:* surface hoar, diurnally recrystallized  
 near surface facets  
*Surface:* .5mm surface hoar  
*Layer 1:* .25x1mm spaghetti chains  
*Layer 2:* .25-.5mm rounded poly crystals moist  
*Layer 3:* .25-.5mm rounded poly crystals moist  
*Layer 4:* .25-.5mm sun crust rounds  
*Layer 5:* .25-.5mm sun crust rounds

February 20, 2008

— North —

*Names:* Henry, Tom, Wes *Station:* NorthYC *Date:*  
 02-20-08 *Time:* 11:00 *Exposed thermocouples:* 15  
*Keywords:* surface hoar  
*Surface:*  
 .5mm surface hoar, still bonded to thin crust  
*Layer 1:* .5-1mm decomposing stellars  
*Layer 2:* .5-1mm decomposing stellars  
*Layer 3:* .5-1mm decomposing stellars  
*Layer 4:* .5-1mm decomposing stellars  
*Layer 5:* .5-1mm decomposing stellars

— South —

*Names:* Henry *Station:* SouthYC *Date:* 02-20-08  
*Time:* 9:30 *Exposed thermocouples:* 20 *Keywords:*  
 surface hoar  
*Surface:* 1-2mm surface hoar  
*Layer 1:* melt freeze/sun crust  
*Layer 2:* melt freeze/sun crust  
*Layer 3:* melt freeze/sun crust  
*Layer 4:* melt freeze/sun crust  
*Layer 5:* .5-1mm mixed forms

February 21, 2008

— North —

*Names:* Henry, Doug, Tom, Irene *Station:* NorthYC  
*Date:* 02-21-08 *Time:* 11:00 *Exposed thermocouples:*  
 0 *Keywords:*  
*Surface:* .5mm surface hoar goblets  
*Layer 1:* .5-1mm decomposing new snow with  
 evidence of minor faceting  
*Layer 2:* .5-1mm decomposing new snow with  
 evidence of minor faceting  
*Layer 3:* .5-1mm decomposing new snow with  
 evidence of minor faceting  
*Layer 4:* .5-1mm decomposing new snow  
*Layer 5:* .5-1mm decomposing new snow

— South —

*Names:* Henry, Doug, Tom *Station:* SouthYC *Date:*  
 02-21-08 *Time:* 12:30 *Exposed thermocouples:* 12  
*Keywords:* surface hoar  
*Surface:* 1mm surface hoar\*  
*Layer 1:*  
 2mm poly crystals with free water evident  
*Layer 2:*  
 2mm poly crystals with free water evident  
*Layer 3:*  
 2mm poly crystals with free water evident  
*Layer 4:*  
 2mm poly crystals with free water evident  
*Layer 5:*  
 2mm poly crystals with free water evident

February 22, 2008

— North —

*Names:* Henry, Tom *Station:* NorthYC *Date:* 02-22-08  
*Time:* 1:00 *Exposed thermocouples:* 13 *Keywords:*  
 surface hoar  
*Surface:* 1-2mm surface hoar  
*Layer 1:* .5-1mm decomposing snow with evidence of  
 faceting  
*Layer 2:* .5-1mm decomposing snow with evidence of  
 faceting  
*Layer 3:* .5-1mm decomposing snow with evidence of  
 faceting  
*Layer 4:* .5-1mm decomposing snow with evidence of  
 faceting  
*Layer 5:* .5-1mm decomposing snow with evidence of  
 faceting

— South —

*Names:* Henry, Tom *Station:* SouthYC *Date:* 02-22-08  
*Time:* 1:45 *Exposed thermocouples:* 0 *Keywords:*  
*Surface:*  
 .5mm surface hoar attached to melt freeze crust  
*Layer 1:* moist melt freeze crust  
*Layer 2:* moist melt freeze crust  
*Layer 3:* moist melt freeze crust  
*Layer 4:* melt freeze crust  
*Layer 5:* melt freeze crust

February 23, 2008

— North —

*Names:* Doug C, Warren *Station:* NorthYC *Date:* 02-23-08 *Time:* 930 *Exposed thermocouples:* 17  
*Keywords:* surface hoar  
*Surface:* new snow, 1mm  
*Layer 1:* new snow, 1mm  
*Layer 2:* new snow, 1mm  
*Layer 3:* surface hoar (.5)with new snow, 1mm  
*Layer 4:* decomposing snow, .5mm  
*Layer 5:* decomposing snow, .5mm

— South —

*Names:* Doug C, Waren *Station:* SouthYC *Date:* 02-23-08 *Time:* Exposed thermocouples: 13  
*Keywords:*  
*Surface:* new snow, rimed, 1-2mm  
*Layer 1:* new snow, rimed, 1-2mm  
*Layer 2:* new snow, rimed, 1-2mm  
*Layer 3:* new snow, rimed, 1-2mm  
*Layer 4:* surface hoar, possible facets (1-3)mm w/  
 new snow, rimed, 1-2mm  
*Layer 5:* ice crust

February 24, 2008

— North —

*Names:* Doug C *Station:* NorthYC *Date:* 02-24-08  
*Time:* 1015 *Exposed thermocouples:* 12 *Keywords:*  
*Surface:* 2-3 mm, rimed snow  
*Layer 1:* 2-3 mm, rimed snow  
*Layer 2:* 2 mm, heavily rimed snow  
*Layer 3:* 2 mm, heavily rimed snow  
*Layer 4:* 2 mm, heavily rimed snow  
*Layer 5:* 2 mm, heavily rimed snow

— South —

*Names:* Doug C *Station:* SouthYC *Date:* 02-24-08  
*Time:* 1100 *Exposed thermocouples:* 8 *Keywords:*  
*Surface:* rimed new snow, 1-2mm  
*Layer 1:* rimed new snow, 1-2mm  
*Layer 2:* rimed new snow, 1-2mm  
*Layer 3:* rimed new snow, 1-2mm  
*Layer 4:* rimed new snow, 1-2mm  
*Layer 5:* rimed new snow, 1-2mm

February 25, 2008

— North —

*Names:* Henry *Station:* NorthYC *Date:* 02-25-08  
*Time:* 1:00 *Exposed thermocouples:* 10 *Keywords:*  
*Surface:* 2-3mm stellar dendrites, some heavily  
 rimed, some not at all  
*Layer 1:* 2-3mm stellar dendrites, some heavily  
 rimed, some not at all  
*Layer 2:* 2-3mm stellar dendrites, some heavily  
 rimed, some not at all  
*Layer 3:* 2-3mm stellar dendrites, some heavily  
 rimed, some not at all  
*Layer 4:* 2mm stellar fragments  
*Layer 5:* 2mm stellar fragments

— South —

*Names:* henry *Station:* SouthYC *Date:* 02-25-08  
*Time:* 1:30 *Exposed thermocouples:* 0 *Keywords:*  
*Surface:* 2-3mm stellar dendrites, some heavily  
 rimed, some not at all  
*Layer 1:* 2-3mm stellar dendrites, some heavily  
 rimed, some not at all  
*Layer 2:* 2-3mm stellar dendrites, some heavily  
 rimed, some not at all  
*Layer 3:* 2-3mm stellar dendrites, some heavily  
 rimed, some not at all  
*Layer 4:* 2mm stellar fragments  
*Layer 5:* 2mm stellar fragments

February 26, 2008

— North —

*Names:* henry, coup *Station:* NorthYC *Date:*  
02-26-08 *Time:* 11:00 *Exposed thermocouples:* 10  
*Keywords:* surface hoar  
*Surface:* 4-8mm surface hoars  
*Layer 1:* broken stellars 2-3mm  
*Layer 2:* broken stellars 2-3mm  
*Layer 3:* broken stellars 2-3mm  
*Layer 4:* broken stellars 2-3mm  
*Layer 5:* broken stellars 2-3mm

— South —

*Names:* Doug C, Coop *Station:* SouthYC *Date:*  
02-26-08 *Time:* 830 *Exposed thermocouples:* 3  
*Keywords:* Surface Hoar  
*Surface:* surface hoar, 2-4mm  
*Layer 1:* rimed new snow, 2mm  
*Layer 2:* rimed new snow, 2mm  
*Layer 3:* rimed new snow, 2mm  
*Layer 4:* rimed new snow, 2mm  
*Layer 5:* rimed new snow, 2mm

February 27, 2008

— North —

*Names:* Irene, Tom *Station:* NorthYC *Date:* 02-27-08  
*Time:* 11:30 *Exposed thermocouples:* 13 *Keywords:*  
Surface Hoar  
*Surface:* 2-4mm surface hoar, 2mm stellars and  
decomposing stellars  
*Layer 1:* 1-2mm stellars and decomposing stellars  
*Layer 2:* 2mm stellars and decomposing stellars  
*Layer 3:* 2mm stellars and decomposing stellars  
*Layer 4:* 1-2mm stellars and decomposing stellars  
*Layer 5:* 1-2mm decomposing stellars

— South —

*Names:* Irene, Coop, Hayes *Station:* SouthYC *Date:*  
02-27-08 *Time:* 10:00 *Exposed thermocouples:* 10  
*Keywords:* Surface Hoar, Near Surface Facets  
*Surface:* 1mm columns, needles, surface hoar  
*Layer 1:* melt freeze crust with 1mm grains  
*Layer 2:* melt freeze crust with 1mm grains  
*Layer 3:* melt freeze crust with 1mm grains  
*Layer 4:* 2mm decomposing stellars, 1mm mixed  
forms, 1mm facets  
*Layer 5:* 2mm decomposing stellars, .5mm rounds

February 28, 2008

— North —

*Names:* Doug, Henry, Irene, Tom *Station:* NorthYC  
*Date:* 02-28-08 *Time:* 11:30 *Exposed thermocouples:*  
14 *Keywords:*  
*Surface:* stellars w/ rime 2 mm  
*Layer 1:* partly decomposed 1 mm  
*Layer 2:* partly decomposed 1 mm  
*Layer 3:* surface hoar 2 mm  
*Layer 4:* stellars 3 mm, partly decomposed 2 mm  
*Layer 5:* stellars 3 mm, partly decomposed 2 mm

— South —

*Names:* Doug, Henry, Tom *Station:* SouthYC *Date:*  
02-28-08 *Time:* 12:30 *Exposed thermocouples:* 9  
*Keywords:* near surface facets  
*Surface:* wind crust (.25 mm thick), highly broken  
snow below crust .25 mm  
*Layer 1:*  
partly decomposed 1 mm, highly broken .25 mm  
*Layer 2:*  
partly decomposed 1 mm, highly broken .25 mm  
*Layer 3:*  
partly decomposed 1 mm, highly broken .25 mm  
*Layer 4:* facets 1 mm  
*Layer 5:* melt freeze crust

February 29, 2008

— North —

*Names:* Doug M *Station:* NorthYC *Date:* 02-29-08  
*Time:* 1:30 *Exposed thermocouples:* 15 *Keywords:*  
**surface hoar**  
*Surface:* surface hoar .75 mm (partly decomposed)  
*Layer 1:* highly broken .25 mm  
*Layer 2:* highly broken .25 mm  
*Layer 3:* highly broken .25 mm  
*Layer 4:* surface hoar 2 mm  
*Layer 5:* stellars 3 mm, partly decomposed 1 mm

— South —

*Names:* Doug M *Station:* SouthYC *Date:* 02-29-08  
*Time:* 12:30 *Exposed thermocouples:* 9 *Keywords:*  
**surface hoar**  
*Surface:* surface hoar 1 mm (partly decomposed)  
*Layer 1:* highly broken .25 mm  
*Layer 2:* highly broken .25 mm  
*Layer 3:* highly broken .25 mm  
*Layer 4:* highly broken .25 mm  
*Layer 5:* partly decomposed 1 mm

March 01, 2008

— North —

*Names:* Doug M, Neil *Station:* NorthYC *Date:*  
 03-01-08 *Time:* 10:30 *Exposed thermocouples:* 17  
*Keywords:*  
*Surface:* highly broken .25 mm  
*Layer 1:*  
 highly broken .25 mm, partly decomposed 1 mm  
*Layer 2:*  
 highly broken .25 mm, partly decomposed 1 mm  
*Layer 3:*  
 highly broken .25 mm, partly decomposed 1 mm  
*Layer 4:* partly decomposed 1 mm  
*Layer 5:* partly decomposed 1 mm

— South —

*Names:* Doug C *Station:* SouthYC *Date:* 03-01-08  
*Time:* 1345 *Exposed thermocouples:* 9 *Keywords:*  
*Surface:* rimed stellars, 1mm  
*Layer 1:* heavily rimed stellars, 1mm  
*Layer 2:* heavily rimed stellars, 1mm  
*Layer 3:* heavily rimed stellars, 1mm  
*Layer 4:* graupel, 1-2 mm  
*Layer 5:* crust

March 02, 2008

---

— North —

*Names:* Doug M, Doug C *Station:* NorthYC *Date:* 03-02-08 *Time:* 10:45 *Exposed thermocouples:* 10  
*Keywords:*  
*Surface:* stellars rimed 1-2 mm, plates 1 mm  
*Layer 1:* stellars rimed 1-2 mm, plates 1 mm  
*Layer 2:* stellars rimed 1-2 mm, plates 1 mm  
*Layer 3:* stellars rimed 1-2 mm, plates 1 mm, columns .5 mm  
*Layer 4:* stellars rimed 1-2 mm, plates 1 mm, columns .5 mm  
*Layer 5:* stellars rimed 1-2 mm, plates 1 mm, columns .5 mm

— South —

*Names:* Doug M, Doug C *Station:* SouthYC *Date:* 03-02-08 *Time:* 1:00 *Exposed thermocouples:* 0  
*Keywords:*  
*Surface:* stellars rimed 1-2 mm  
*Layer 1:* stellars rimed 1-2 mm  
*Layer 2:* stellars rimed 1-2 mm  
*Layer 3:* stellars rimed 1-2 mm  
*Layer 4:* stellars rimed 1-2 mm  
*Layer 5:* stellars rimed 1-2 mm

March 03, 2008

---

— North —

*Names:* Tom *Station:* NorthYC *Date:* 03-03-08 *Time:* 14:30 *Exposed thermocouples:* 12 *Keywords:*  
*Surface:*  
 Stellars and some broken stekkers up to 3 mm  
*Layer 1:* Broken stellars 1-2 mm  
*Layer 2:* Broken stellars 1 mm  
*Layer 3:*  
 Some broken stellars w/ beginning rounding .5 mm  
*Layer 4:*  
 Broken stellars w/ beginning rounding .5 mm  
*Layer 5:*  
 Broken stellars w/ beginning rounding .5 mm

— South —

*Names:* Coop *Station:* SouthYC *Date:* 03-03-08  
*Time:* Noon *Exposed thermocouples:* 0 *Keywords:*  
*Surface:* Highly broken .25 mm  
*Layer 1:* Highly broken .25 mm  
*Layer 2:* Highly broken .25 mm  
*Layer 3:* Highly broken .25 mm  
*Layer 4:* Partly decomposed .5 - 1 mm  
*Layer 5:* Partly decomposed .5 - 1 mm

March 05, 2008

---

— North —

*Names: Irene Station: NorthYC Date: 03-05-08*  
*Time: 1:20 Exposed thermocouples: 6 Keywords:*  
*Surface:*  
 1mm rimed stellars; 2 mm stellars; 1 mm plates  
*Layer 1:*  
 1mm rimed stellars; 2 mm stellars; 1 mm plates  
*Layer 2:*  
 1mm rimed stellars; 2 mm stellars; 1 mm plates  
*Layer 3:* 1mm rimed stellars; 2 mm stellars; 1 mm plates, 3mm stellars, 1mm decomposing stellars  
*Layer 4:* 1mm rimed stellars; 2 mm stellars; 1 mm plates, 3mm stellars, 1mm decomposing stellars  
*Layer 5:* 1mm rimed stellars; 2 mm stellars; 1 mm plates, 1mm decomposing stellars

— South —

*Names: Irene Station: SouthYC Date: 03-05-08*  
*Time: 12:10 Exposed thermocouples: 0 Keywords:*  
*Surface:* 1mm rimed stellars, 2mm stellars  
*Layer 1:* 1mm rimed stellars, 2mm stellars  
*Layer 2:*  
 1mm rimed stellars, 2mm stellars, 1mm plates  
*Layer 3:*  
 1mm rimed stellars, 2mm stellars, 1mm plates  
*Layer 4:* 1mm rimed stellars, 2mm stellars, decomposing stellars  
*Layer 5:* 1mm rimed stellars, 2mm stellars, decomposing stellars

March 06, 2008

---

— North —

*Names: Henry, Irene Station: NorthYC Date: 03-06-08*  
*Time: 12:30 Exposed thermocouples: 0*  
*Keywords:*  
*Surface:* 2mm wind crust  
*Layer 1:* 2-3mm stellars, stellar fragments  
*Layer 2:* 2-3mm stellars, stellar fragments  
*Layer 3:* 2-3mm stellars, stellar fragments  
*Layer 4:* 2-3mm stellars, stellar fragments  
*Layer 5:* 2-3mm stellars, stellar fragments

— South —

*Names: Henry, Irene Station: SouthYC Date: 03-06-08*  
*Time: 1:30 Exposed thermocouples: 0*  
*Keywords:*  
*Surface:*  
 1-2mm radiation recrystalized cups, needles  
*Layer 1:* 1-2mm radiation recrystalized cups, needles, 1-2mm stellar fragments  
*Layer 2:* moist melting snow  
*Layer 3:* moist melting snow  
*Layer 4:* moist melting snow  
*Layer 5:* very moist (free water evident from a distance)melting snow



March 07, 2008

---

— North —

*Names:* Henry Station: NorthYC *Date:* 03-07-08  
*Time:* 11:30 *Exposed thermocouples:* 9 *Keywords:*  
*Surface:* .5mm surface hoar  
*Layer 1:* 2-3mm stellars, stellar fragments  
*Layer 2:* 2-3mm stellars, stellar fragments  
*Layer 3:* 2-3mm stellars, stellar fragments,  
 increasingly decomposed  
*Layer 4:* 2-3mm stellars, stellar fragments,  
 increasingly decomposed  
*Layer 5:* 2-3mm stellars, stellar fragments,  
 increasingly decomposed

— South —

*Names:* Henry Station: SouthYC *Date:* 03-07-08  
*Time:* 10:30 *Exposed thermocouples:* 10 *Keywords:*  
*Surface:* 1-2mm facets, wind affected surface snow  
 (looks like decomposing new snow)  
*Layer 1:* 1-2mm facets  
*Layer 2:* sun crust  
*Layer 3:* sun crust  
*Layer 4:* sun crust  
*Layer 5:* highly decomposed new snow

March 08, 2008

---

— North —

*Names:* Doug M Station: NorthYC *Date:* 03-08-08  
*Time:* 10:30 *Exposed thermocouples:* 9 *Keywords:*  
 surface hoar  
*Surface:* surface hoar .5 mm, thin wind crust  
 under surface hoar .25 mm thick  
*Layer 1:* partly decomposed 1 mm  
*Layer 2:* partly decomposed 1 mm  
*Layer 3:* partly decomposed .75 mm  
*Layer 4:* partly decomposed .75 mm  
*Layer 5:* partly decomposed 1 mm, stellars 2 mm

— South —

*Names:* Doug M Station: SouthYC *Date:* 03-08-08  
*Time:* 1:30 *Exposed thermocouples:* 11 *Keywords:*  
 surface hoar  
*Surface:* surface hoar 1.5 mm  
*Layer 1:* partly decomposed 1 mm  
*Layer 2:* melting snow 1 mm  
*Layer 3:* melt freeze crust 1.5 mm, melting  
*Layer 4:* melt freeze crust 1.5 mm, melting  
*Layer 5:* highly broken (dry).25 mm

March 09, 2008

---

— North —

*Names:* Doug M Station: NorthYC *Date:* 03-09-08  
*Time:* 1:00 *Exposed thermocouples:* 10 *Keywords:*  
*Surface:*  
 stellars rimed 1 mm, partly decomposed 1 mm  
*Layer 1:* stellars 3 mm, partly decomposed 1 mm  
*Layer 2:* stellars 2 mm, partly decomposed 1 mm  
*Layer 3:* stellars 2 mm, partly decomposed 1 mm  
*Layer 4:* partly decomposed 1 mm  
*Layer 5:* partly decomposed 1 mm

— South —

*Names:* Doug M Station: SouthYC *Date:* 03-09-08  
*Time:* 2:30 *Exposed thermocouples:* 12 *Keywords:*  
*Surface:* highly broken .25 mm (dry)  
*Layer 1:* small rounds .75 mm (dry)  
*Layer 2:* melt freeze crust 1.5 mm - wet  
*Layer 3:* melt freeze crust 1.5 mm - wet  
*Layer 4:* melt freeze crust 1.5 mm - frozen  
*Layer 5:* small rounds .5 mm (dry)

March 10, 2008

---

— North —

*Names:* Doug M *Station:* NorthYC *Date:* 03-10-08

*Time:* 11:15 *Exposed thermocouples:* 11 *Keywords:*

**Surface Hoar**

*Surface:*

surface hoar .75mm, few small facets .5mm

*Layer 1:* partly decomposed 1 mm

*Layer 2:* partly decomposed 1 mm

*Layer 3:* partly decomposed 1 mm, rounds .5mm

*Layer 4:* partly decomposed 1 mm, rounds .5mm

*Layer 5:* partly decomposed 1 mm, rounds .5mm

— South —

*Names:* Doug M *Station:* SouthYC *Date:* 03-10-08

*Time:* 10:15 *Exposed thermocouples:* 13 *Keywords:*

**Near Surface Facets, surface hoar**

*Surface:* surface hoar 1 mm, near surface facets

.5 mm - 1mm

*Layer 1:* melt freeze crust (frozen/dry)1.5 mm

*Layer 2:* melt freeze crust (frozen/dry)1.5 mm

*Layer 3:* melt freeze crust (frozen/dry)1.5 mm

*Layer 4:* rounds .5 mm, partly decomposed 1 mm

*Layer 5:* rounds .5 mm, partly decomposed 1 mm

March 11, 2008

---

— North —

*Names:* Henry, Irene *Station:* NorthYC *Date:*

03-11-08 *Time:* 1:30 *Exposed thermocouples:* 12

*Keywords:*

*Surface:* .5mm decomposing surface hoar

*Layer 1:* .5-1mm highly decomposed stellars

*Layer 2:* .5-1mm highly decomposed stellars

*Layer 3:* .5-1mm highly decomposed stellars

*Layer 4:* 1-2mm decomposing stellars

*Layer 5:* 1-2mm decomposing stellars

— South —

*Names:* Henry, Irene *Station:* SouthYC *Date:*

03-11-08 *Time:* 1:00 *Exposed thermocouples:* 17

*Keywords:*

*Surface:* .5mm melting facets

*Layer 1:* wet melt/freeze polycrystals

*Layer 2:* wet melt/freeze polycrystals

*Layer 3:* wet melt/freeze polycrystals

*Layer 4:* wet melt/freeze polycrystals

*Layer 5:* wet melt/freeze polycrystals

March 12, 2008

---

— North —

*Names:* Henry *Station:* NorthYC *Date:* 03-12-08  
*Time:* 1:00 *Exposed thermocouples:* 10 *Keywords:*  
**none**  
*Surface:* wind affected new snow .5mm  
*Layer 1:*  
 decomposing stellars 1-2mm, small facets .5mm  
*Layer 2:*  
 decomposing stellars 1-2mm, small facets .5mm  
*Layer 3:* highly decomposed new snow 1mm  
*Layer 4:* highly decomposed new snow 1mm  
*Layer 5:* highly decomposed new snow 1mm

— South —

*Names:* Irene *Station:* SouthYC *Date:* 03-12-08  
*Time:* 12:45 *Exposed thermocouples:* 17 *Keywords:*  
**facets**  
*Surface:* 2mm stellars, 1mm decomposing stellars,  
 1mm facets  
*Layer 1:*  
 .5-1mm grains in melt/freeze crust (frozen)  
*Layer 2:*  
 .5-1mm grains in melt/freeze crust (frozen)  
*Layer 3:*  
 .5-1mm grains in melt/freeze crust (frozen)  
*Layer 4:*  
 .5-1mm grains in melt/freeze crust (frozen)  
*Layer 5:*  
 .5-1mm grains in melt/freeze crust (frozen)

March 13, 2008

---

— North —

*Names:* Henry, Irene *Station:* NorthYC *Date:*  
 03-13-08 *Time:* 1:00 *Exposed thermocouples:* 14  
*Keywords:*  
*Surface:* stellar capped columns, stellars  
*Layer 1:* decomposing new snow with evidence of  
 surface faceting .5mm  
*Layer 2:* decomposing new snow with evidence of  
 surface faceting .5mm  
*Layer 3:* decomposing new snow with evidence of  
 surface faceting .5mm  
*Layer 4:* decomposing new snow .5-1mm  
*Layer 5:* decomposing new snow .5-1mm

— South —

*Names:* Henry, Irene *Station:* SouthYC *Date:*  
 03-13-08 *Time:* 12:00 *Exposed thermocouples:* 18  
*Keywords:*  
*Surface:* melt freeze crust  
*Layer 1:* melt freeze crust  
*Layer 2:* melt freeze crust  
*Layer 3:* melt freeze crust  
*Layer 4:* .5mm facets  
*Layer 5:* .5mm facets

March 14, 2008

---

— North —

*Names:* Doug M, Tom *Station:* NorthYC *Date:*  
03-14-08 *Time:* 1:30 *Exposed thermocouples:* 10  
*Keywords:*  
*Surface:* stellars rimed 1-2 mm  
*Layer 1:* stellars partly rimed 1-2 mm  
*Layer 2:* stellars 1-2 mm  
*Layer 3:* stellars 1-2 mm  
*Layer 4:* stellars 2-3 mm  
*Layer 5:* stellars 2-3 mm

— South —

*Names:* Doug M, Irene *Station:* SouthYC *Date:*  
03-14-08 *Time:* 11:30 *Exposed thermocouples:* 12  
*Keywords:*  
*Surface:* stellars rimed 1-2 mm  
*Layer 1:* stellars partly rimed 1-2 mm  
*Layer 2:* stellars 1-2 mm  
*Layer 3:* stellars 1-2 mm  
*Layer 4:* stellars 1-2 mm  
*Layer 5:* stellars 1-2 mm

March 15, 2008

---

— North —

*Names:* Doug C, Tom L *Station:* NorthYC *Date:*  
03-15-08 *Time:* 1200 *Exposed thermocouples:* 11  
*Keywords:*  
*Surface:* new snow, 1-2 mm  
*Layer 1:* decomposing new snow, 1mm  
*Layer 2:* decomposing new snow, 1mm  
*Layer 3:* decomposing new snow, 1mm  
*Layer 4:* decomposing new snow, 1mm  
*Layer 5:* decomposing new snow, 1mm

— South —

*Names:* Doug C, Tom L/ Doug C, Neil D *Station:*  
SouthYC *Date:* 03-15-08 *Time:* 1045/1400 *Exposed*  
*thermocouples:* 15 *Keywords:* near surface facet  
*Surface:* new snow, 1-2mm  
*Layer 1:* small facet, .5mm  
*Layer 2:* crust  
*Layer 3:* crust  
*Layer 4:* decomposing new snow, 1mm  
*Layer 5:* decomposing new snow, 1mm

March 16, 2008

---

— North —

*Names:* Tom L *Station:* NorthYC *Date:* 03-16-08  
*Time:* 13:00 *Exposed thermocouples:* 11 *Keywords:*  
*Surface:* Stellars w/ some rimmed grains 1-2 mm  
*Layer 1:* Stellars 1-1.5mm  
*Layer 2:* Decomposing Stellars .75-1 mm  
*Layer 3:* Decomposing Stellars .75-1 mm  
*Layer 4:*  
Decomposing Stellars w/ some rounding .5-.75mm  
*Layer 5:* Rounding .5mm

— South —

*Names:* Tom L *Station:* SouthYC *Date:* 03-16-08  
*Time:* 14:00 *Exposed thermocouples:* 14 *Keywords:*  
Near Surface Facets  
*Surface:* Stellars w/ some rimed grains 2mm  
*Layer 1:* Stellars 2mm  
*Layer 2:* Stellars 2mm  
*Layer 3:* Stellars w/ some capped stellars 1-2mm  
*Layer 4:* NSF .5-.75  
*Layer 5:* Crust

March 17, 2008

---

— North —

*Names:* Doug C *Station:* NorthYC *Date:* 03-17-08  
*Time:* 1245 *Exposed thermocouples:* 13 *Keywords:*  
*Surface:* rhimed new snow, 1mm  
*Layer 1:* decomposing new snow, 1-1.5mm  
*Layer 2:* decomposing new snow, 1-1.5mm  
*Layer 3:* decomposing new snow, 1-1.5mm  
*Layer 4:* decomposing new snow, 1-1.5mm  
*Layer 5:* decomposing new snow, 1-1.5mm

— South —

*Names:* Doug C, Tom L *Station:* SouthYC *Date:*  
 03-17-08 *Time:* 1100 *Exposed thermocouples:* 15  
*Keywords:* near surface facets  
*Surface:* rhimed new snow, 1-2mm  
*Layer 1:* decomposing new snow, 1mm  
*Layer 2:*  
 decomposing new snow with begining facets, 1mm  
*Layer 3:*  
 decomposing new snow with begining facets, 1mm  
*Layer 4:* facets, .5mm  
*Layer 5:* crust

March 18, 2008

---

— North —

*Names:* Henry *Station:* NorthYC *Date:* 03-18-08  
*Time:* 2:15 *Exposed thermocouples:* 0 *Keywords:*  
*Surface:* 2-3mm stellars and stellar fragments  
*Layer 1:* 2-3mm stellars and stellar fragments  
*Layer 2:* 2-3mm stellars and stellar fragments  
*Layer 3:* 2-3mm stellars and stellar fragments  
*Layer 4:* 2-3mm stellars and stellar fragments  
*Layer 5:* 2-3mm stellars and stellar fragments

— South —

NO DAILY LOG RECORDED

March 19, 2008

---

— North —

*Names:* Henry *Station:* NorthYC *Date:* 03-19-08  
*Time:* 10:30 *Exposed thermocouples:* 6 *Keywords:*  
*Surface:* 2-3mm rimed stellars, 1-2mm graupel on  
 top of 3mm thick wind skin  
*Layer 1:* 2-3mm rimed stellars, 1-2mm graupel  
*Layer 2:* 2-3mm rimed stellars, 1-2mm graupel  
*Layer 3:* 2-3mm rimed stellars, 1-2mm graupel  
*Layer 4:* 2-3mm rimed stellars, 1-2mm graupel  
*Layer 5:* 2-3mm rimed stellars, 1-2mm graupel

— South —

*Names:* Henry, Irene *Station:* SouthYC *Date:*  
 03-19-08 *Time:* 1:30 *Exposed thermocouples:* 6  
*Keywords:*  
*Surface:* .25-.5mm facets  
*Layer 1:* 2-3mm rimed stellars, 1-2mm graupel  
*Layer 2:* 2-3mm rimed stellars, 1-2mm graupel  
*Layer 3:* 2-3mm rimed stellars, 1-2mm graupel  
*Layer 4:* 2-3mm rimed stellars  
*Layer 5:* 2-3mm rimed stellars

March 20, 2008

— North —

*NO DAILY LOG RECORDED*

— South —

*Names: Doug, Tom Station: SouthYC Date: 03-20-08**Time: 13:00 Exposed thermocouples: 8 Keywords:**Surface: stellars rimed 2-3 mm, plates rimed 1 mm**Layer 1: stellars rimed 2-3 mm, plates rimed 1 mm**Layer 2: stellars rimed 2-3 mm, plates rimed 1 mm**Layer 3: stellars rimed 2-3 mm, plates rimed 1 mm**Layer 4: stellars heavily rimed 1-2 mm**Layer 5: stellars heavily rimed 1-2 mm*

March 21, 2008

— North —

*Names: Doug Station: NorthYC Date: 03-21-08**Time: 13:00 Exposed thermocouples: 2 Keywords:**Surface: stellars heavily rimed 3 mm, stellars rimed 1-2 mm**Layer 1: stellars heavily rimed 3 mm, stellars rimed 1-2 mm**Layer 2:**stellars rimed 1-2 mm, partly decomposed 1 mm**Layer 3:**stellars rimed 1-2 mm, partly decomposed 1 mm**Layer 4:**stellars rimed 1-2 mm, partly decomposed 1 mm**Layer 5:**stellars rimed 1-2 mm, partly decomposed 1 mm*

— South —

*Names: Irene, Henry Station: SouthYC Date:**03-21-08 Time: 11:20 Exposed thermocouples: 10**Keywords:**Surface:**1mm plates, columns, capped columns, stellars**Layer 1: 1mm stellars, rimed stellars, graupel**Layer 2: 1mm decomposing stellars, graupel**Layer 3: .5-1mm decomposing stellars**Layer 4: .5-1mm decomposing stellars**Layer 5: .5-1mm decomposing stellars*

March 22, 2008

— North —

*Names: Doug, Tom Station: NorthYC Date: 03-22-08**Time: 11:00 Exposed thermocouples: 2 Keywords:**Surface Hoar, Near Surface Facets**Surface: surface hoar 1 mm, facets 1 mm**Layer 1: highly broken .25 mm**Layer 2: highly broken .25 mm**Layer 3: highly broken .25 mm - 1 mm**Layer 4: highly broken .25 mm - 1 mm**Layer 5: highly broken .25 mm - 1 mm*

— South —

*Names: Doug C, Tom L Station: SouthYC Date:**03-22-08 Time: 1345 Exposed thermocouples: 10**Keywords: near surface faceting**Surface: surface facet, .3-.5mm**Layer 1: melt freeze crust**Layer 2: decomposing stellars, 1-2mm**Layer 3: decomposing stellars, 1-2mm**Layer 4: decomposing stellars, 1-2mm**Layer 5: decomposing stellars, 1-2mm*

March 23, 2008

---

— North —

*Names:* Doug C *Station:* North *YC Date:* 03-23-08  
*Time:* 1030 *Exposed thermocouples:* 4 *Keywords:*  
 near surface facet  
*Surface:* near surface facet, .3-.5  
*Layer 1:* rounds, .3-.5  
*Layer 2:* rounds, .3-.5  
*Layer 3:* decomposing stellars, .5-1  
*Layer 4:* decomposing stellars, .5-1  
*Layer 5:* decomposing stellars, .5-1

— South —

*Names:* Doug C *Station:* South *YC Date:* 03-23-08  
*Time:* 1000 *Exposed thermocouples:* 10 *Keywords:*  
 near surface facet  
*Surface:* near surface facets, .3-.5mm  
*Layer 1:* crust  
*Layer 2:* crust  
*Layer 3:* decomposing stellars, .5-1mm  
*Layer 4:* decomposing stellars, .5-1mm  
*Layer 5:* decomposing stellars, .5-1mm

March 24, 2008

---

— North —

*Names:* Tom L, Coop *Station:* North *YC Date:*  
 03-24-08 *Time:* 13:30 *Exposed thermocouples:* 7  
*Keywords:* Graupel  
*Surface:* Graupel and rimmed grains 1-2 mm  
*Layer 1:* Graupel and rimmed grains 1-2 mm  
*Layer 2:* Graupel and rimmed grains 1 mm  
*Layer 3:* Rounds .5 mm  
*Layer 4:* Rounds .5 mm  
*Layer 5:* Rounds .25-.5 mm

— South —

*Names:* Tom L and Coop *Station:* South *YC Date:*  
 03-24-08 *Time:* 12:30 *Exposed thermocouples:* 12  
*Keywords:*  
*Surface:* Mixed grains. Rounds with some (few)  
 facets. .5 - 1 mm  
*Layer 1:* Crust  
*Layer 2:* Crust  
*Layer 3:* Crust  
*Layer 4:* Crust  
*Layer 5:* Rounds .5 mm

March 25, 2008

---

— North —

*Names:* Henry, Pete *Station:* North *YC Date:*  
 03-25-08 *Time:* 1:00 *Exposed thermocouples:* 5  
*Keywords:*  
*Surface:* 2-4mm stellar dendrites, 1-2mm rounds  
*Layer 1:* 2-4mm stellar dendrites, 1-2mm rounds  
*Layer 2:* 2-4mm stellar dendrites, 1-2mm rounds  
*Layer 3:* 2-4mm stellar dendrites, 1-2mm rounds  
*Layer 4:* 1mm rounds  
*Layer 5:* 1mm rounds

— South —

*Names:* Henry *Station:* South *YC Date:* 03-25-08  
*Time:* 11:00 *Exposed thermocouples:* 13 *Keywords:*  
*Surface:* 2-4mm stellar dendrites, 1-2mm plates  
*Layer 1:* 2-4mm stellar dendrites, 1-2mm plates  
*Layer 2:* 2-4mm stellar dendrites, 1-2mm plates  
*Layer 3:*  
 .5-1mm facets on top of rounded/crust layer  
*Layer 4:* .5mm rounds  
*Layer 5:* .5mm rounds

March 27, 2008

— North —

*Names: Irene Station: NorthYC Date: 03-27-08*  
*Time: 10:45 Exposed thermocouples: 0 Keywords:*  
 none

*Surface: 1mm rimed stellars, 2mm graupel*  
*Layer 1: 1mm rimed stellars, 2mm graupel*  
*Layer 2: 1mm rimed stellars,*  
*Layer 3: 1mm rimed stellars*  
*Layer 4: 1mm rimed stellars*  
*Layer 5: 1mm rimed stellars*

— South —

NO DAILY LOG RECORDED

March 28, 2008

— North —

*Names: Doug, Tom Station: NorthYC Date: 03-28-08*  
*Time: 1:30 Exposed thermocouples: 0 Keywords:*  
*Surface:*

*highly broken .25 mm, partly decomposed .5 mm*  
*Layer 1:*  
*highly broken .25 mm, partly decomposed .5 mm*  
*Layer 2:*  
*highly broken .25 mm, partly decomposed .5 mm*  
*Layer 3:*  
*highly broken .25 mm, partly decomposed .5 mm*  
*Layer 4:*  
*highly broken .25 mm, partly decomposed .5 mm*  
*Layer 5:*  
*highly broken .25 mm, partly decomposed .5 mm*

— South —

*Names: Henry, Tom Station: SouthYC Date: 03-28-08*  
*Time: 11:30 Exposed thermocouples: 10 Keywords:*  
*Surface:*

*.5mm facets on decomposing rimed new snow*  
*Layer 1: decomposing rimed new snow .5-1mm*  
*Layer 2: decomposing rimed new snow .5-1mm*  
*Layer 3: decomposing rimed new snow .5-1mm*  
*Layer 4: decomposing rimed new snow .5-1mm*  
*Layer 5: decomposing rimed new snow .5-1mm*



March 29, 2008

---

— North —

*Names:* Doug *Station:* NorthYC *Date:* 03-29-08  
*Time:* 1:30 *Exposed thermocouples:* 0 *Keywords:*  
*Surface:*  
 highly broken .25 mm, partly decomposed 1 mm  
*Layer 1:*  
 highly broken .25 mm, partly decomposed 1 mm  
*Layer 2:*  
 highly broken .25 mm, partly decomposed 1 mm  
*Layer 3:*  
 highly broken .25 mm, partly decomposed 1 mm  
*Layer 4:*  
 highly broken .25 mm, partly decomposed 1 mm  
*Layer 5:*  
 highly broken .25 mm, partly decomposed 1 mm

— South —

*Names:* Doug C *Station:* SouthYC *Date:* 03-29-08  
*Time:* 1315 *Exposed thermocouples:* 4 *Keywords:*  
*Surface:* highly broken new snow, .5mm  
*Layer 1:* highly broken new snow, .5mm  
*Layer 2:* decomposing new snow, .5-1mm  
*Layer 3:* decomposing new snow, .5-1mm  
*Layer 4:* decomposing new snow, .5-1mm  
*Layer 5:* decomposing new snow, .5-1mm

March 30, 2008

---

— North —

*Names:* Doug *Station:* NorthYC *Date:* 03-30-08  
*Time:* 11:30 *Exposed thermocouples:* 2 *Keywords:*  
 Surface Hoar, Near Surface Facets  
*Surface:*  
 surface hoar 1 mm, near surface facets 1 mm  
*Layer 1:* highly broken .25 mm  
*Layer 2:* highly broken .25 mm  
*Layer 3:* highly broken .25 mm  
*Layer 4:* highly broken .25 mm  
*Layer 5:* highly broken .25 mm

— South —

*Names:* Doug *Station:* SouthYC *Date:* 03-30-08  
*Time:* 9:30 *Exposed thermocouples:* 4 *Keywords:*  
 Near Surface Facets, Surface Hoar  
*Surface:* Facets 1 mm, surface hoar 1 mm  
*Layer 1:*  
 highly broken .25 mm, partly decomposed .5 mm  
*Layer 2:*  
 highly broken .25 mm, partly decomposed .5 mm  
*Layer 3:*  
 highly broken .25 mm, partly decomposed .5 mm  
*Layer 4:*  
 highly broken .25 mm, partly decomposed .5 mm  
*Layer 5:*  
 highly broken .25 mm, partly decomposed .5 mm

March 31, 2008

---

— North —

*Names:* doug C *Station:* NorthYC *Date:* 03-31-08  
*Time:* 1315 *Exposed thermocouples:* 3 *Keywords:*  
 none

*Surface:* highly broken stellars, .5mm  
*Layer 1:* highly broken stellars, .5mm  
*Layer 2:* highly broken stellars, .5mm  
*Layer 3:* highly broken stellars, .5mm  
*Layer 4:* highly broken stellars, .5mm  
*Layer 5:* highly broken stellars, .5mm

— South —

*Names:* Doug C, bear *Station:* SouthYC *Date:*  
 03-31-08 *Time:* 1145 *Exposed thermocouples:* 4  
*Keywords:*

*Surface:* rimed new snow, 1mm  
*Layer 1:* rimed new snow, 1mm  
*Layer 2:* rimed new snow, 1mm, some decintegrating  
 facets observable, .5mm  
*Layer 3:* crust  
*Layer 4:* rounded demposing stellars, .5-1mm  
*Layer 5:* rounded demposing stellars, .5-1mm

April 01, 2008

---

— North —

*Names:* Doug C, Shawn *Station:* NorthYC *Date:*  
 04-01-08 *Time:* 1200 *Exposed thermocouples:* 5  
*Keywords:*

*Surface:* rimed new snow, .5-1mm  
*Layer 1:* rimed new snow, .5-1mm  
*Layer 2:* rimed new snow, .5-1mm  
*Layer 3:* rimed new snow, .5-1mm  
*Layer 4:* decomposing stellars, 1mm  
*Layer 5:* decomposing stellars, 1mm

— South —

*Names:* doug c *Station:* SouthYC *Date:* 04-01-08  
*Time:* 1030 *Exposed thermocouples:* 5 *Keywords:*

*Surface:* rimed stellars, 1mm  
*Layer 1:* rimed stellars, 1mm  
*Layer 2:* rimed stellars, 1mm  
*Layer 3:* rimed stellars, 1mm  
*Layer 4:* highly broken stellars, .5mm  
*Layer 5:* crust

April 02, 2008

---

— North —

*Names:* Irene *Station:* NorthYC *Date:* 04-02-08  
*Time:* 1:40 *Exposed thermocouples:* 4 *Keywords:*

*Facets, Surface hoar*  
*Surface:* .5 mm facets, 1 mm surface hoar  
*Layer 1:* .5-1mm facets  
*Layer 2:* 1mm decomposing stellars  
*Layer 3:* 1mm decomposing stellars  
*Layer 4:* 1mm decomposing stellars  
*Layer 5:* 1mm decomposing stellars

— South —

*Names:* Irene *Station:* SouthYC *Date:* 04-02-08  
*Time:* 12:00 *Exposed thermocouples:* 6 *Keywords:*

*Facets*  
*Surface:* .5mm facets  
*Layer 1:* .5-1mm facets  
*Layer 2:* 1mm decomposing stellars  
*Layer 3:* 1-2mm decomposing stellars  
*Layer 4:* 1-2mm decomposing stellars  
*Layer 5:* 1-2mm decomposing stellars

April 03, 2008

— North —

*NO DAILY LOG RECORDED*

— South —

*Names: Doug, Tom, Henry Station: SouthYC Date: 04-03-08 Time: 11:30 Exposed thermocouples: 6*  
*Keywords: near surface facets*  
*Surface: facets .5 - 1 mm*  
*Layer 1: stellars 1 mm, partly decomposed 1 mm*  
*Layer 2: partly decomposed 1 mm*  
*Layer 3: rounds .5 mm*  
*Layer 4: rounds .5 mm*  
*Layer 5: rounds .5 mm*

April 04, 2008

— North —

*Names: Irene Station: NorthYC Date: 04-04-08*  
*Time: 10:15 Exposed thermocouples: 7 Keywords:*  
**Facets**  
*Surface:*  
 1-2mm stellars and dendrites, 1 mm facets  
*Layer 1: 1 mm decomposing stellars, .5mm facets*  
*Layer 2: 1 mm decomposing stellars*  
*Layer 3: 1 mm decomposing stellars*  
*Layer 4: 1 mm decomposing stellars*  
*Layer 5: 1 mm decomposing stellars*

— South —

*Names: Henry Station: SouthYC Date: 04-04-08*  
*Time: 9:30 Exposed thermocouples: 0 Keywords:*  
**facets**  
*Surface: 1mm facets--well developed needle and sheath, striated cups*  
*Layer 1: melt freeze crust*  
*Layer 2: melt freeze crust*  
*Layer 3: .5mm faceted forms, solid type, some remaining evidence of new snow forms*  
*Layer 4: melt freeze crust*  
*Layer 5: melt freeze crust*

April 05, 2008

— North —

*Names: Tom L, Doug M Station: NorthYC Date: 04-05-08 Time: 14:15 Exposed thermocouples: 5*  
*Keywords:*  
*Surface: New Snow. Irregular grains w/ some riming and a few little columns. .75 - 1 mm*  
*Layer 1: Same*  
*Layer 2: Same*  
*Layer 3: Same*  
*Layer 4: Same*  
*Layer 5: Same*

— South —

*Names: Tom L Station: SouthYC Date: 04-05-08*  
*Time: 13:15 Exposed thermocouples: 8 Keywords:*  
*Surface: New Snow. Rimed Irregular Grains. 1mm*  
*Layer 1: Same*  
*Layer 2: Melt freeze crust*  
*Layer 3: Melt freeze crust*  
*Layer 4: Rounds. .75 - 1mm*  
*Layer 5: Melt freeze crust.*

April 06, 2008

— North —

*Names:* Doug C, John L *Station:* NorthYC *Date:*  
04-06-08 *Time:* 1330 *Exposed thermocouples:* 5  
*Keywords:*

*Surface:* new snow, 1mm

*Layer 1:* new snow, 1mm

*Layer 2:* decomposing stellars, .5-1

*Layer 3:* decomposing stellars, .5-1

*Layer 4:* decomposing stellars, .5-1

*Layer 5:* decomposing stellars, .5-1

— South —

*Names:* Doug *Station:* SouthYC *Date:* 04-06-08  
*Time:* 10:30 *Exposed thermocouples:* 7 *Keywords:*  
Surface Hoar, Radiation Recrystallization

*Surface:* surface hoar 1 mm, stellars 1 - 3 mm,  
facets 1 mm in PM

*Layer 1:*

partly decomposed 1 mm, highly broken .25 mm

*Layer 2:*

partly decomposed 1 mm, highly broken .25 mm

*Layer 3:*

partly decomposed 1 mm, highly broken .25 mm

*Layer 4:*

partly decomposed 1 mm, highly broken .25 mm

*Layer 5:*

partly decomposed 1 mm, highly broken .25 mm

April 07, 2008

— North —

*Names:* Doug C *Station:* NorthYC *Date:* 04-07-08  
*Time:* 1345 *Exposed thermocouples:* 2 *Keywords:*

*Surface:* rimed new snow, 1mm

*Layer 1:* new snow, 1mm

*Layer 2:* new snow, 1mm

*Layer 3:* new snow, 1mm

*Layer 4:* new snow, 1mm

*Layer 5:* new snow, 1mm

— South —

*Names:* Doug C *Station:* SouthYC *Date:* 04-07-08  
*Time:* 830 *Exposed thermocouples:* 5 *Keywords:*

surface hoar

*Surface:* surface hoar, .5mm

*Layer 1:* new snow, 1mm

*Layer 2:* new snow, 1mm

*Layer 3:* new snow, 1mm

*Layer 4:* new snow, 1mm

*Layer 5:* new snow, 1mm

April 08, 2008

— North —

Names: Doug C, Warren Station: NorthYC Date:  
 04-08-08 Time: 1045 Exposed thermocouples: 0  
 Keywords:  
 Surface: new snow, 1mm  
 Layer 1: rimed new snow, 1mm  
 Layer 2: rimed new snow, 1mm  
 Layer 3: rimed new snow, 1mm  
 Layer 4: rimed new snow, 1mm  
 Layer 5: rimed new snow, 1mm

— South —

Names: Doug C, Coop Station: SouthYC Date:  
 04-08-08 Time: 1000 Exposed thermocouples: 3  
 Keywords:  
 Surface: new snow, 1mm  
 Layer 1: rimed new snow, 1mm  
 Layer 2: heavily rimed new snow, 1mm  
 Layer 3: heavily rimed new snow, 1mm  
 Layer 4: heavily rimed new snow, 1mm  
 Layer 5: heavily rimed new snow, 1mm

April 09, 2008

— North —

Names: Irene Station: NorthYC Date: 04-09-08  
 Time: 12:00 Exposed thermocouples: 0 Keywords:  
 Surface: 1-2mm Stellars, 1 mm Plates  
 Layer 1: 2 mm stellars, 1 mm decomposing stellars  
 Layer 2: 1 mm decomposing stellars  
 Layer 3: .5-1mm decomposing stellars  
 Layer 4: .5-1mm decomposing stellars  
 Layer 5: .5-1mm decomposing stellars

— South —

Names: Henry Station: SouthYC Date: 04-09-08  
 Time: 9:30/2:00 Exposed thermocouples: 6  
 Keywords:  
 Surface: .5-1mm facets  
 Layer 1: melt freeze crust  
 Layer 2: melt freeze crust  
 Layer 3: melt freeze crust  
 Layer 4: melt freeze crust  
 Layer 5: melt freeze crust

April 14, 2008

— North —

Names: test Station: NorthYC(07-08) Date:  
 04-14-08 Time: Exposed thermocouples: 0 Keywords:  
 Surface:  
 Layer 1:  
 Layer 2:  
 Layer 3:  
 Layer 4:  
 Layer 5:

— South —

Names: TEst Station: SouthYC(07-08) Date:  
 04-14-08 Time: Exposed thermocouples: 0 Keywords:  
 Surface:  
 Layer 1:  
 Layer 2:  
 Layer 3:  
 Layer 4:  
 Layer 5:

G.3 2006/2007 Season

January 18, 2007

— North —

*Names:* Rich Chandler, Henry Munter *Station:* North*Date:* 01-18-07 *Time:* 12:00 pm *Exposed**thermocouples:* 14 *Keywords:**Surface:*

0.5 mm rimed new snow 2B highly broken particles

*Layer 1:*

0.5 mm rimed new snow highly broken particles

*Layer 2:* 2.0 mm diurnally recrystallized NSFC*Layer 3:* 1.0 mm solid faceted particles small facets highly broken particles*Layer 4:* 1.0 mm solid faceted particles small facets highly broken particles*Layer 5:* 1.0 mm solid faceted particles small facets highly broken particles

— South —

*Names:* Rich Chandler/Henry Munter *Station:* South*Date:* 01-18-07 *Time:* 9:45 am *Exposed**thermocouples:* 0 *Keywords:* none*Surface:* 0.5 mm new rimed stellar*Layer 1:* 0.5 mm new rimed stellar*Layer 2:* 1.0 mm surface hoar?*Layer 3:* melt freeze crust*Layer 4:* melt freeze crust*Layer 5:*

0.5 mm small facets (solid faceted particles)

January 19, 2007

— North —

*Names:* Henry Doug *Station:* North *Date:* 01-19-07*Time:* 11:00 am *Exposed thermocouples:* 14*Keywords:**Surface:* 0.5 mm rimed stellars*Layer 1:* 0.5 mm rimed stellars*Layer 2:* 2.0 mm diurnally recrystallized NSFC*Layer 3:* 1.0 mm facets solid faceted particles*Layer 4:* 1.0 mm facets solid faceted particles*Layer 5:* 1.0 mm facets solid faceted particles

— South —

*Names:* Henry Doug *Station:* South *Date:* 01-19-07*Time:* 10:00 am *Exposed thermocouples:* 15*Keywords:* none*Surface:* 0.5 mm new rimed stellar*Layer 1:* 0.5 mm new rimed stellar*Layer 2:* 1.0 mm surface hoar?*Layer 3:* melt freeze crust*Layer 4:* melt freeze crust*Layer 5:*

0.5 mm small facets (solid faceted particles)

January 20, 2007

— North —

*Names:* Doug Coop Station: North *Date:* 01-20-07*Time:* 11:00 am *Exposed thermocouples:* 13*Keywords:**Surface:*

2.0-3.0 mm stellar dendrite crystals riming

*Layer 1:*

2.0-3.0 mm stellar dendrite crystals riming

*Layer 2:*

2.0-3.0 mm stellar dendrite crystals riming

*Layer 3:*

1.0 mm decomposing precipitation particles

*Layer 4:* 2.0 mm diurnally recrystallized NSFC*Layer 5:* 2.0 mm diurnally recrystallized NSFC

— South —

*Names:* Doug Coop Station: South *Date:* 01-20-07*Time:* 9:30 am *Exposed thermocouples:* 13 *Keywords:*

none

*Surface:* 2.0-3.0 mm stellar dendrite crystal*Layer 1:* 2.0-3.0 mm stellar dendrite crystal*Layer 2:* 2.0-3.0 mm stellar dendrite crystal*Layer 3:* 0.5 mm decomposing stellars*Layer 4:* 0.5 mm faceted crystals*Layer 5:* melt freeze crust

January 21, 2007

— North —

*Names:* Coop Station: North *Date:* 01-21-07 *Time:*12:30 pm *Exposed thermocouples:* 8 *Keywords:**Surface:* precipitation particles 2.0 mm*Layer 1:* precipitation particles 2.0 mm*Layer 2:* precipitation particles 2.0 mm*Layer 3:* precipitation particles 2.0 mm*Layer 4:* precipitation particles 2.0 mm*Layer 5:* precipitation particles 2.0 mm

— South —

*Names:* Doug Coop Station: South *Date:* 01-21-07*Time:* 11:15 am *Exposed thermocouples:* 8 *Keywords:*

none

*Surface:* (precipitation particles)2.0 mm*Layer 1:* (precipitation particles)2.0 mm*Layer 2:* (precipitation particles)2.0 mm*Layer 3:* (precipitation particles)2.0 mm*Layer 4:* (precipitation particles)2.0 mm*Layer 5:* (precipitation particles)2.0 mm

January 22, 2007

— North —

*Names:* Doug Coop Station: North *Date:* 01-22-07  
*Time:* 11:00 am *Exposed thermocouples:* 9 *Keywords:*  
*Surface:* 1.0 mm surface hoar  
*Layer 1:*  
 1.0 mm slightly decomposed precip. particles  
*Layer 2:*  
 1.0 mm slightly decomposed precip. particles  
*Layer 3:*  
 1.0 mm slightly decomposed precip. particles  
*Layer 4:*  
 1.0 mm slightly decomposed precip. particles  
*Layer 5:*  
 1.0 mm slightly decomposed precip. particles

— South —

*Names:* Doug Coop Station: South *Date:* 01-22-07  
*Time:* 1:30 pm *Exposed thermocouples:* 8 *Keywords:*  
 none  
*Surface:* 0.5 mm surface hoar  
*Layer 1:*  
 1.0 mm decomposing stellars (needles)rounds  
*Layer 2:*  
 1.0 mm decomposing stellars (needles)rounds  
*Layer 3:* 1.0 mm (partly decomposed particles)(  
 needles)(large rounded particles)  
*Layer 4:* 1.0 mm (partly decomposed patricles)  
*Layer 5:* 1.0 mm (partly decomposed particles)

January 23, 2007

— North —

*Names:* Coop Henry Station: North *Date:* 01-23-07  
*Time:* 11:00 *Exposed thermocouples:* 10 *Keywords:*  
*Surface:* 1.0 mm surface hoar  
*Layer 1:*  
 1.0 mm partly decomposed precip. particles  
*Layer 2:*  
 1.0 mm partly decomposed precip. particles  
*Layer 3:*  
 1.0 mm partly decomposed precip. particles  
*Layer 4:*  
 1.0 mm partly decomposed precip. particles  
*Layer 5:*  
 1.0 mm partly decomposed precip. particles

— South —

*Names:* Doug Henry Station: South *Date:* 01-23-07  
*Time:* 10:00 am *Exposed thermocouples:* 9 *Keywords:*  
 none  
*Surface:* 1.0 mm surface hoar  
*Layer 1:* 0.5 mm rounds  
*Layer 2:* 0.5 mm rounds  
*Layer 3:* 0.5 mm rounds (partly decomposed  
 particles)1.0 mm decomposing stellars  
*Layer 4:* 1.0 mm decomposing stellars  
*Layer 5:* 1.0 mm decomposing stellars



January 24, 2007

— North —

*Names:* Michelle Copersteiin Doug Henry Station:*North Date:* 01-24-07 *Time:* Exposed thermocouples:*11 Keywords:**Surface:* 1.5 mm surface hoar*Layer 1:*

1.0 mm partly decomposed precip. particles

*Layer 2:*

1.0 mm partly decomposed precip. particles

*Layer 3:*

1.0 mm partly decomposed precip. particles

*Layer 4:*

1.0 mm partly decomposed precip. particles

*Layer 5:*

1.0 mm partly decomposed precip. particles

— South —

*Names:* Coop Doug Henry Station: *South Date:**01-24-07 Time:* 10:00 am *Exposed thermocouples:* 10*Keywords:**Surface:* 1.5 mm surface hoar*Layer 1:* 0.5 mm rounds*Layer 2:* 0.5 mm ice crust*Layer 3:* 1.0 mm decomposing stellars*Layer 4:* 1.0 mm decomposing stellars*Layer 5:* 1.0 mm decomposing stellars

January 25, 2007

— North —

*Names:* Henry Station: *North Date:* 01-25-07 *Time:**2:00 pm Exposed thermocouples:* 12 *Keywords:**Surface:* 2.0-3.0 mm surface hoar*Layer 1:* 1.0 mm stellars decomposing*Layer 2:* 1.0 mm stellars*Layer 3:* 1.0 mm stellars*Layer 4:* 1.0 mm stellars*Layer 5:* 1.0 mm stellars

— South —

*Names:* Henry Station: *South Date:* 01-25-07 *Time:**1:00 pm Exposed thermocouples:* 9 *Keywords:* none*Surface:* globular ice crust: 0.25 mm grain-ish*Layer 1:* 0.5 mm rounds with free water*Layer 2:*

0.5 mm (large rounded particles)with free water

*Layer 3:* 0.5 mm (large rounded particles)/ 1.0 mm decomposing particles with water*Layer 4:* 1.0 mm decomposing particles with water*Layer 5:* 1.0 mm decomposing particles with water

January 26, 2007

— North —

*Names: Henry Station: North Date: 01-26-07 Time:**10:00 am Exposed thermocouples: 12 Keywords:**Surface: 2.0-3.0 mm surface hoar**Layer 1: 1.0 mm decomposing stellars**Layer 2: 1.0 mm decomposing stellars**Layer 3: 1.0 mm decomposing stellars**Layer 4: 1.0 mm partly decomposed precip.**particles, some rounding and bonding**Layer 5:**0.5 mm rounded grains, thing bonded layer*

— South —

*Names: Henry Station: South Date: 01-26-07 Time:**9:00 am Exposed thermocouples: 0 Keywords: none**Surface: (rime)2.0-3.0 mm frozen grains**Layer 1: (rime)2.0-3.0 mm frozen grains**Layer 2: (rime)2.0-3.0 mm frozen grains**Layer 3: (rime)2.0-3.0 mm frozen grains**Layer 4:**(solid faceted particles/ mixed forms)0.5 mm**facets/ 1.0 mm round but not bonded crystals**Layer 5: (rime)1.0-2.0 mm grains*

January 27, 2007

— North —

*Names: Henry Station: North Date: 01-27-07 Time:**1:30 pm Exposed thermocouples: 15 Keywords:**Surface: 3.0 mm stellars, needles, plates**Layer 1: 2.0-3.0 mm surface hoar crystals, 3.0 mm  
thick rime, 1.0 mm small facets under crust**Layer 2: decomposing stellars**Layer 3: decomposing stellars**Layer 4: decomposing stellars**Layer 5: decomposing stellars*

— South —

*Names: Henry Station: South Date: 01-27-07 Time:**1:00 pm Exposed thermocouples: 14 Keywords:**Surface:**2.0 mm stellar dendrites with some needles (new)**Layer 1:**melt freeze crust breaking down with freewater**Layer 2:**melt freeze crust breaking down with freewater**Layer 3:**melt freeze crust breaking down with freewater**Layer 4:**melt freeze crust breaking down with freewater**Layer 5:**melt freeze crust breaking down with freewater*

January 28, 2007

— North —

*Names: Doug Station: North Date: 01-28-07 Time:**12:00 pm Exposed thermocouples: 15 Keywords:**Surface: 2.0 mm decomposing stellar dendrites  
plates needles**Layer 1:**2.0 mm surface hoar crystals, 4.0 mm thick rime**Layer 2: 1.0 mm decomposing stellar dendrites and  
plates 1.0 mm solid faceted particles**Layer 3: 1.0 mm decomposing stellar dendrites and  
plates 1.0 mm solid faceted particles**Layer 4: 1.0 mm decomposing stellar dendrites and  
plates 1.0 mm solid faceted particles**Layer 5: 1.0 mm decomposing stellar dendrites and  
plates 1.0 mm solid faceted particles*

— South —

*Names: Doug Station: South Date: 01-28-07 Time:**10:45 am Exposed thermocouples: 15 Keywords:**Surface:**1.5 mm decomposing dendrites with some needles**Layer 1: melt freeze crust (frozen)**Layer 2: melt freeze crust (frozen)**Layer 3: melt freeze crust (frozen)**Layer 4: melt freeze crust (frozen)**Layer 5: melt freeze crust (frozen)*

January 29, 2007

— North —

*Names: Doug Coop Station: North Date: 01-29-07**Time: 1:00 pm Exposed thermocouples: 16 Keywords:**Surface: 2.0 mm surface hoar crystals**Layer 1: 4.0 mm thick crust**Layer 2: 1.0 mm decomposing stellars 1.0 mm solid  
faceted particles**Layer 3: 1.0 mm decomposing stellars 1.0 mm solid  
faceted particles**Layer 4: 1.0 mm decomposing stellars 1.0 mm solid  
faceted particles**Layer 5: 1.0 mm decomposing stellars 1.0 mm solid  
faceted particles*

— South —

*Names: Doug Coop Station: South Date: 01-29-07**Time: 10:15 am Exposed thermocouples: 16**Keywords: none**Surface: 2.0 mm radiation recrystallized cups**Layer 1: melt freeze crust (rounds)**Layer 2: melt freeze crust (rounds)**Layer 3: 1.0 mm broken stellars**Layer 4: 1.0 mm broken stellars**Layer 5: (rime)*

January 30, 2007

— North —

*Names:* Henry Doug *Station:* North *Date:* 01-30-07  
*Time:* 2:00 *Exposed thermocouples:* 15 *Keywords:*  
*Surface:* new stellars partly decomposed precip.  
 particles rimed stellars 2.0\*4.0 mm  
*Layer 1:* rime with surface hoar frozen to top  
*Layer 2:* 1.0 mm facets (small)  
*Layer 3:* 1.0 mm facets (small)  
*Layer 4:* 1.0 mm facets (small)  
*Layer 5:* 1.0 mm facets (small)

— South —

*Names:* Henry *Station:* South *Date:* 01-30-07 *Time:*  
 9:30 am *Exposed thermocouples:* 16 *Keywords:* none  
*Surface:* 2.0 mm radiation recrystalized cups  
*Layer 1:* melt freeze crust  
*Layer 2:* melt freeze crust  
*Layer 3:* melt freeze crust  
*Layer 4:* decomposing stellars (needles)facets  
*Layer 5:* decomposing stellars (needles)facets

January 31, 2007

— North —

*Names:* Coop Doug *Station:* North *Date:* 01-31-07  
*Time:* 1:30 pm *Exposed thermocouples:* 14 *Keywords:*  
*Surface:* highly broken particles, wind crust  
*Layer 1:* highly broken particles, wind crust  
*Layer 2:* highly broken particles, wind crust  
*Layer 3:* highly broken particles, wind crust  
*Layer 4:* 3.0 mm stellars, partly deomposed precip  
 . particles  
*Layer 5:* 3.0 mm stellars, partly deomposed precip  
 . particles

— South —

*Names:* Henry Doug *Station:* South *Date:* 01-31-07  
*Time:* 11:00 am *Exposed thermocouples:* 14  
*Keywords:*  
*Surface:* 2.0 mm rimed new particles  
*Layer 1:* 2.0 mm rimed new particles  
*Layer 2:* 2.0 rimed new snow/3.0 mm stellars  
*Layer 3:* 2.0 rimed new snow/3.0 mm stellars  
*Layer 4:* melt freeze crust  
*Layer 5:* melt freeze crust

February 01, 2007

— North —

*Names:* Henry *Station:* North *Date:* 02-1-07 *Time:*  
 1:00 pm *Exposed thermocouples:* 13 *Keywords:*  
*Surface:* 0.5 mm columns 1.0 mm rimed particles  
*Layer 1:* 0.5 mm columns 1.0 mm rimed particles  
*Layer 2:* 0.5 mm columns 1.0 mm rimed particles  
*Layer 3:* 0.5 mm columns 1.0 mm rimed particles  
*Layer 4:* 0.5 mm columns partly, 1.0 mm plates,  
 rimed particles  
*Layer 5:* 0.5 mm columns partly, 1.0 mm plates,  
 rimed particles

— South —

*Names:* Henry *Station:* South *Date:* 02-1-07 *Time:*  
 11:00 am *Exposed thermocouples:* 12 *Keywords:*  
*Surface:* 0.5 mm columns/ 1.0 mm rimed particles  
*Layer 1:* 0.5 mm columns/ 1.0 mm rimed particles  
*Layer 2:* 0.5 mm columns/ 1.0 mm rimed particles  
*Layer 3:* 0.5 mm columns/ 1.0 mm rimed particles  
*Layer 4:* 2.0 mm rimed stellars  
*Layer 5:* 2.0 mm rimed stellars

February 02, 2007

— North —

*Names: Henry Station: North Date: 02-2-07 Time:**10:30 Exposed thermocouples: 14 Keywords:**Surface: 2.0 mm rimed stellars**Layer 1:**0.5-1.0 mm rimed needles, columns, plates**Layer 2:**0.5-1.0 mm rimed needles, columns, plates**Layer 3: 0.5 mm rimed columns 1mm rimed particles**Layer 4: 0.5 mm rimed columns 1mm rimed particles**Layer 5: 0.5 mm rimed columns 1mm rimed particles*

— South —

*Names: Henry Ellie Blake Station: South Date:**02-2-07 Time: 10:55 am Exposed thermocouples: 13**Keywords:**Surface: 0.5 mm broken rimed particles**Layer 1: 0.5 mm broken rimed particles**Layer 2: 0.5 mm broken rimed particles**Layer 3:**0.5 mm columns rimed/1.0 mm rimed stellars**Layer 4:**0.5 mm columns rimed/1.0 mm rimed stellars**Layer 5: 2.0 mm rimed stellars*

February 03, 2007

— North —

*Names: Coop Station: North Date: 02-3-07 Time:**2:30 Exposed thermocouples: 13 Keywords:**Surface: BKN particles wind blown**Layer 1: BKN particles wind blown**Layer 2: BKN particles wind blown**Layer 3: BKN particles wind blown**Layer 4: BKN particles wind blown**Layer 5: BKN particles wind blown*

— South —

*Names: Coop Station: South Date: 02-3-07 Time:**3:00 pm Exposed thermocouples: 12 Keywords: none**Surface: broken particles still arms present 2b (highly broken particles)**Layer 1: broken particles mixed stellars (highly broken particles)**Layer 2: broken particles mixed stellars (highly broken particles)**Layer 3: broken particles mixed stellars (highly broken particles)**Layer 4: broken particles mixed stellars (highly broken particles)**Layer 5: broken particles mixed stellars (highly broken particles)*

February 04, 2007

— North —

*Names:* Doug Station: North *Date:* 02-4-07 *Time:*  
10:45 *Exposed thermocouples:* 12 *Keywords:*  
*Surface:* heavily rimed new particles  
precipitation particles 1.0 mm  
*Layer 1:* heavily rimed new particles  
precipitation particles 1.0 mm  
*Layer 2:* heavily rimed new particles  
precipitation particles 1.0 mm  
*Layer 3:* 0.5 mm highly broken particles  
*Layer 4:* 0.5 mm highly broken particles  
*Layer 5:* 0.5 mm highly broken particles

— South —

*Names:* Doug Blake Station: South *Date:* 02-4-07  
*Time:* 9:30 am *Exposed thermocouples:* 11 *Keywords:*  
none  
*Surface:* heavily rimed particles (precipitation  
particles)1.0 mm  
*Layer 1:* heavily rimed particles (precipitation  
particles)1.0 mm  
*Layer 2:* heavily rimed particles (precipitation  
particles)1.0 mm  
*Layer 3:* heavily rimed particles (precipitation  
particles)1.0 mm  
*Layer 4:* heavily rimed particles (precipitation  
particles)1.0 mm  
*Layer 5:* heavily rimed particles (precipitation  
particles)1.0 mm

February 05, 2007

— North —

*Names:* Doug Rich Station: North *Date:* 02-5-07  
*Time:* 11:45 *Exposed thermocouples:* 13 *Keywords:*  
*Surface:* 2.0 m partly decomposed precip.  
particles stellars  
*Layer 1:* 0.5 mm rounds  
*Layer 2:* 0.5 mm rounds  
*Layer 3:* 0.5 mm rounds  
*Layer 4:* 0.5 mm rounds  
*Layer 5:* 0.5 mm rounds

— South —

*Names:* Doug Station: South *Date:* 02-5-07 *Time:*  
8:45 am *Exposed thermocouples:* 12 *Keywords:* none  
*Surface:* (graupell)3.0-6.0 mm and 2.0 mm  
decomposing rimed stellars  
*Layer 1:* 2.0 mm decomposing rimed stellars  
*Layer 2:* 0.5 heavily rimed particles  
*Layer 3:* (rime)4.0 mm thick melt freeze crust  
*Layer 4:* 0.5 mm mixed forms  
*Layer 5:* 0.5 mm mixed forms

February 06, 2007

— North —

*Names:* Doug Henry Station: North *Date:* 02-6-07  
*Time:* 2:00 *Exposed thermocouples:* 13 *Keywords:*  
*Surface:*  
 1.0 mm broken stellars 2.0 mm intact stellars  
*Layer 1:* 0.5 mm rounds  
*Layer 2:* 0.5 mm rounded grains  
*Layer 3:* 0.5 mm rounded grains  
*Layer 4:* 0.5 mm rounded grains  
*Layer 5:* 0.5 mm rounded grains

— South —

*Names:* Doug Henry Station: South *Date:* 02-6-07  
*Time:* 12:00 pm *Exposed thermocouples:* 13  
*Keywords:* none  
*Surface:* (rime)  
*Layer 1:* (rime)  
*Layer 2:* 0.5 mm mixed form (mixed particles)  
*Layer 3:* 0.5 mm mixed form (mixed particles)  
*Layer 4:* (rime)  
*Layer 5:* (rime)

February 07, 2007

— North —

*Names:* Henry Station: North *Date:* 02-7-07 *Time:*  
 2:30 pm *Exposed thermocouples:* 13 *Keywords:*  
*Surface:* 1.0 mm partly decomposed precip.  
 particles 2.0 mm precipitation particles  
*Layer 1:* 0.5 mm rounded grains  
*Layer 2:* 0.5 mm rounded grains  
*Layer 3:* 0.5 mm rounded grains  
*Layer 4:* 0.5 mm rounded grains  
*Layer 5:* 0.5 mm rounded grains

— South —

*Names:* Henry Doug Irene Station: South *Date:*  
 02-7-07 *Time:* 1:30 pm *Exposed thermocouples:* 20  
*Keywords:* none  
*Surface:* 0.5 mm (rounded grains)/ wet grains  
*Layer 1:* 0.5 mm (rounded grains)/ wet grains  
*Layer 2:* (rime)with water  
*Layer 3:* (rime)with water  
*Layer 4:* 0.5 mm (solid faceted particles)/ (mixed  
 forms)with water  
*Layer 5:* 0.5 mm (solid faceted particles)/ (mixed  
 forms)with water

February 08, 2007

— North —

*Names:* 1.0 mm rimed needles parti Station: North  
*Date:* 02-8-07 *Time:* 11:00 *Exposed thermocouples:*  
 11 *Keywords:*  
*Surface:* 1.0 mm rimed needles  
*Layer 1:* 1.0 mm rimed needles  
*Layer 2:* 1.0 mm rimed needles partly decomposed  
 precip. particles 1.5 mm plates  
*Layer 3:* 1.5 rimed needles partly decomposed  
 precip. particles 1.5 mm plates  
*Layer 4:* 2.0 mm stellars  
*Layer 5:* 2.0 mm stellars

— South —

*Names:* Henry Station: South *Date:* 02-8-07 *Time:*  
 10:30 am *Exposed thermocouples:* 13 *Keywords:* none  
*Surface:* 1.0 mm rimed needles  
*Layer 1:*  
 1.0 mm rimed needles/ 1.5 mm rimed plates  
*Layer 2:*  
 1.5 mm rime plates (less rime than above)  
*Layer 3:* 2.0 mm new stellars  
*Layer 4:* (rime)ice crust  
*Layer 5:* (rime)ice crust

February 09, 2007

— North —

*Names:* Ellie Maictin *Station:* North *Date:* 02-9-07  
*Time:* 10:15 am *Exposed thermocouples:* 11  
*Keywords:* none  
*Surface:* Dendrites 20% rimed 1square mm  
*Layer 1:* Dendrites 20% rimed 1.5 square mm  
*Layer 2:* Dendrites 20% rimed 2square mm  
*Layer 3:*  
 Dendrites, thin plates 20% rimed 2 square mm  
*Layer 4:*  
 Dendrites, thin plates 60% rimed 1.5 square mm  
*Layer 5:* Dendrites, 75% rimed 1.5 square mm

— South —

*Names:* Henry *Station:* South *Date:* 02-9-07 *Time:*  
 8:30 *Exposed thermocouples:* 11 *Keywords:*  
*Surface:* 2.0 mm rimed needles, plates, stellars  
*Layer 1:* 2.0mm rimed needles plates  
*Layer 2:* 2.0mm rimed needles plates  
*Layer 3:* 2.0mm heavily rimed particles  
*Layer 4:* 2.0mm heavily rimed particles  
*Layer 5:* 0.5-1.0mm decomposing stellars/ rounds

February 10, 2007

— North —

*Names:* Coop *Station:* North *Date:* 02-10-07 *Time:*  
 9:00 am *Exposed thermocouples:* 7 *Keywords:*  
*Surface:* 2mm surface hoar  
*Layer 1:* Highly broken particles 2-3mm  
*Layer 2:* Precipitation particles 2-3mm  
*Layer 3:* Precipitation particles 2-3mm  
*Layer 4:* Precipitation particles 2-3mm  
*Layer 5:* Precipitation particles 2-3mm

— South —

*Names:* Coop *Station:* South *Date:* 02-10-07 *Time:*  
 10:00 *Exposed thermocouples:* 6 *Keywords:* none  
*Surface:* 0.5-1.0 (surface hoar)  
*Layer 1:* 1.0mm rimed (partly decomposed precip.  
 particles)  
*Layer 2:*  
 2.0-3.0mm rimed (precipitation particles)  
*Layer 3:*  
 2.0-3.0mm rimed (precipitation particles)  
*Layer 4:*  
 2.0-3.0mm rimed (precipitation particles)  
*Layer 5:*  
 2.0-3.0mm rimed (precipitation particles)



February 11, 2007

— North —

*Names:* Doug M, Doug C *Station:* North *Date:*  
02-11-07 *Time:* 11:30 am *Exposed thermocouples:* 3  
*Keywords:*  
*Surface:* Heavily rimed now snow  
*Layer 1:* Heavily rimed stellars 2mm, needles and  
rimed needles 2mm  
*Layer 2:* Lightly rimed stellars 2mm, capped  
columns 2mm, needles 2mm  
*Layer 3:* Lightly rimed stellars 2mm, capped  
columns 2mm, needles 2mm  
*Layer 4:*  
Stellar plates 2mm, needles 2mm, plates 1mm  
*Layer 5:*  
Rimed stellars 2mm, needles 2mm, capped columns

— South —

*Names:* Doug M, Doug C *Station:* South *Date:*  
02-11-07 *Time:* 10:30 *Exposed thermocouples:* 3  
*Keywords:*  
*Surface:* Heavily rimes stellars 2.0mm needles and  
rimed needles 2.0-4.0mm  
*Layer 1:* Heavily rimes stellars 2.0mm needles and  
rimed needles 2.0-4.0mm  
*Layer 2:* Rimed stellars 2.0-3.0mm, capped columns  
2.0mm, needle clusters 2.0-4.0mm  
*Layer 3:* Rimed stellars 2.0-3.0mm, capped columns  
2.0mm, needle clusters 2.0-4.0mm  
*Layer 4:* Sectoried plates 2.0mm, plates 1.0mm,  
needles 2.0mm, heavily rimed stellars 2.0mm  
*Layer 5:* Sectoried plates 2.0mm, plates 1.0mm,  
needles 2.0mm, heavily rimed stellars 2.0mm

February 12, 2007

— North —

*Names:* Doug M *Station:* North *Date:* 02-12-07  
*Time:* 11:15 *Exposed thermocouples:* 0 *Keywords:*  
*Surface:* Plates 0.5-1mm, columns 1mm, sectoried  
plates 1.5mm  
*Layer 1:* Plates 0.5-1mm, columns 1mm, sectoried  
plates 1.5mm  
*Layer 2:* Plates 0.5-1mm, broken stellars 1-2mm  
*Layer 3:* Plates 0.5-1mm, broken stellars 1-2mm  
*Layer 4:* Broken stellars 1-2mm (lightly rimed),  
0.5mm plates  
*Layer 5:* Broken stellars 1-2mm (lightly rimed),  
0.5mm plates

— South —

*Names:* Doug M *Station:* South *Date:* 02-12-07  
*Time:* 12:30 *Exposed thermocouples:* 0 *Keywords:*  
*Surface:*  
Stellars 2.0-3.0mm, plates 1.0mm, sectors 2.0mm  
*Layer 1:*  
Stellars 2.0-3.0mm, plates 1.0mm, sectors 2.0mm  
*Layer 2:* Sectoried plates 2.0mm, plates 1.0mm,  
heavily rimed stellars 2.0mm  
*Layer 3:* Rimed stellars 2.0mm, plates 1.0mm,  
rimed plates 1.0mm  
*Layer 4:* Rimed stellars 2.0mm, plates 1.0mm,  
rimed plates 1.0mm  
*Layer 5:* Rimed stellars 2.0mm, plates 1.0mm,  
rimed plates 1.0mm

February 13, 2007

— North —

*Names:* Henry, Rich *Station:* North *Date:* 02-13-07  
*Time:* 11:00 am *Exposed thermocouples:* 0 *Keywords:*  
*Surface:*  
 0.5mm columns, 2mm plates, 3mm stellars, needles  
*Layer 1:*  
 0.5mm columns, 2mm plates, 3mm stellars, needles  
*Layer 2:* 2mm plates, 3mm stellars  
*Layer 3:* 2mm plates, 3mm stellars  
*Layer 4:* 2mm plates, 0.5mm columns  
*Layer 5:* 2mm plates, 0.5mm columns

— South —

*Names:* Doug Henry *Station:* South *Date:* 02-13-07  
*Time:* 10:00 *Exposed thermocouples:* 0 *Keywords:*  
*Surface:*  
 0.5mm wrapped columns/ 1.0-1.5mm sectored plates  
*Layer 1:* 1.5mm stellars/ sectored plates  
*Layer 2:* 3.0-4.0 stellar dendrites  
*Layer 3:* 2.0mm stellar/ 1.0mm plates  
*Layer 4:* lightly rimed broken stellars 2.0mm  
*Layer 5:* lightly rimed broken stellars 2.0mm

February 14, 2007

— North —

*Names:* Doug M, Blake *Station:* North *Date:*  
 02-14-07 *Time:* 11:30 am *Exposed thermocouples:* 0  
*Keywords:*  
*Surface:* Rimed stellars 1-2mm  
*Layer 1:* Rimed stellars 1-2mm  
*Layer 2:* Rimed stellars 1-2mm  
*Layer 3:* Rimed stellars 1-2mm  
*Layer 4:* Rimed stellars 1-2mm  
*Layer 5:* Rimed stellars 1-2mm

— South —

*Names:* Henry, Rich *Station:* South *Date:* 02-14-07  
*Time:* 11:00 *Exposed thermocouples:* 0 *Keywords:*  
*Surface:* 1.0-2.0mm rimed stellars  
*Layer 1:* 1.0-2.0mm rimed stellars  
*Layer 2:* 1.0-2.0mm rimed stellars  
*Layer 3:* 1.0-2.0mm rimed stellars  
*Layer 4:* 1.0-2.0mm rimed stellars  
*Layer 5:* 1.0-2.0mm rimed stellars

February 15, 2007

— North —

*Names:* Henry, Blake *Station:* North *Date:* 02-15-07  
*Time:* 12:00 pm *Exposed thermocouples:* 14  
*Keywords:*  
*Surface:* 2mm rimed stellars  
*Layer 1:* 2-4mm stellars  
*Layer 2:* 2-4mm stellars  
*Layer 3:* 2-4mm stellars  
*Layer 4:* 2-4mm stellars  
*Layer 5:* 2-4mm stellars

— South —

*Names:* Henry *Station:* South *Date:* 02-15-07 *Time:*  
 11:00 *Exposed thermocouples:* 15 *Keywords:*  
*Surface:* 2.0mm rimed stellars  
*Layer 1:* 2.0-4.0mm stellars  
*Layer 2:* 2.0-4.0mm stellars  
*Layer 3:* 2.0-4.0mm stellars  
*Layer 4:* 2.0-4.0mm stellars  
*Layer 5:* 2.0-4.0mm stellars

February 16, 2007

— North —

*Names: Henry Station: North Date: 02-16-07 Time:**none given Exposed thermocouples: 0 Keywords:**Surface: No observations taken**Layer 1: No observations taken**Layer 2: No observations taken**Layer 3: No observations taken**Layer 4: No observations taken**Layer 5: No observations taken*

— South —

*Names: Henry Station: South Date: 02-16-07 Time:**12:00 Exposed thermocouples: 20 Keywords:**Surface: 1.0mm wind crust**Layer 1: 2.0-3.0mm broken stellars**Layer 2: 2.0-3.0mm broken stellars**Layer 3: 2.0-3.0mm broken stellars**Layer 4: 2.0-3.0mm broken stellars**Layer 5: 2.0-3.0mm broken stellars*

February 17, 2007

— North —

*Names: Coop Station: North Date: 02-17-07 Time:**1:00 pm Exposed thermocouples: 15 Keywords:**Surface: Wind crust**Layer 1: Highly broken particles 0.5-1mm**Layer 2: Highly broken particles 0.5-1mm**Layer 3: Partly decomposed precipitation particles 0.5-1mm**Layer 4: Partly decomposed precipitation particles 0.5-1mm**Layer 5: Partly decomposed precipitation particles 0.5-1mm*

— South —

*Names: Coop Station: South Date: 02-17-07 Time:**12:00 Exposed thermocouples: 20 Keywords: none**Surface: (surface hoar crystals)> 0.5mm**Layer 1: (partly decomposed precip. particles)**2.0-3.0mm moist**Layer 2: (partly decomposed precip. particles)**2.0-3.0mm moist**Layer 3: (partly decomposed precip. particles)**2.0-3.0mm moist**Layer 4: (partly decomposed precip. particles)**2.0-3.0mm dry**Layer 5: (partly decomposed precip. particles)**2.0-3.0mm dry*

February 18, 2007

— North —

*Names:* Doug, JJ *Station:* North *Date:* 02-18-07  
*Time:* 2:30 pm *Exposed thermocouples:* 16 *Keywords:*  
*Surface:* Surface hoar 1mm  
*Layer 1:* Wind crust 5mm thick, highly broken particles 0.5mm  
*Layer 2:* Highly broken particles 0.5mm  
*Layer 3:* Highly broken particles 0.5mm  
*Layer 4:* Highly broken particles 0.5mm  
*Layer 5:* Highly broken particles 0.5mm

— South —

*Names:* Doug, JJ *Station:* South *Date:* 02-18-07  
*Time:* 10:45 *Exposed thermocouples:* 20 *Keywords:*  
 none  
*Surface:* (surface hoar crystals)0.5mm broken  
*Layer 1:* Melt freeze crust 1.0cm thick  
*Layer 2:* 0.5mm rounds  
*Layer 3:* 0.5mm-1.0mm (partly decomposed precip. particles)(needles)(rounded grains)0.5mm  
*Layer 4:* 0.5mm-1.0mm (partly decomposed precip. particles)(needles)(rounded grains)0.5mm  
*Layer 5:* 0.5mm-1.0mm (partly decomposed precip. particles)(needles)(rounded grains)0.5mm

February 19, 2007

— North —

*Names:* Doug, Coop *Station:* North *Date:* 02-19-07  
*Time:* 10:00 am *Exposed thermocouples:* 14  
*Keywords:*  
*Surface:* wind crust 3mm thick, partially decomposed precipitation particles 0.5mm  
*Layer 1:* Precipitation particles 1-3mm  
*Layer 2:* Precipitation particles 1-3mm  
*Layer 3:* Precipitation particles 1-3mm  
*Layer 4:* Precipitation particles 1-3mm  
*Layer 5:* Precipitation particles 1-3mm

— South —

*Names:* Coop, Doug *Station:* South *Date:* 02-19-07  
*Time:* 9:00 *Exposed thermocouples:* 20 *Keywords:*  
 none  
*Surface:*  
 (precipitation particles)light rime 1.0-2.0mm  
*Layer 1:*  
 (precipitation particles)light rime 1.0-2.0mm  
*Layer 2:*  
 (precipitation particles)light rime 1.0-2.0mm  
*Layer 3:*  
 (precipitation particles)light rime 1.0-2.0mm  
*Layer 4:*  
 (precipitation particles)light rime 1.0-2.0mm  
*Layer 5:*  
 (precipitation particles)light rime 1.0-2.0mm

February 20, 2007

— North —

*Names:* Doug *Station:* North *Date:* 02-20-07 *Time:* 12:30 pm *Exposed thermocouples:* 15 *Keywords:*  
*Surface:* Wind crust 2mm thick, highly broken particles 0.25mm  
*Layer 1:* Partially decomposed precipitation particles 0.5-1mm  
*Layer 2:* Partially decomposed precipitation particles 0.5-1mm  
*Layer 3:* Partially decomposed precipitation particles 0.5-1mm  
*Layer 4:* Highly broken particles 0.25mm  
*Layer 5:* Highly broken particles 0.25mm

— South —

*Names:* Doug, Rich *Station:* South *Date:* 02-20-07 *Time:* 10:30 *Exposed thermocouples:* 20 *Keywords:* none  
*Surface:* (highly broken particles)0.5mm  
*Layer 1:* (highly broken particles)0.5mm  
*Layer 2:* Melt freeze crust 4cm thick  
*Layer 3:* Melt freeze crust 4cm thick  
*Layer 4:* Melt freeze crust 4cm thick  
*Layer 5:* Melt freeze crust 4cm thick

February 21, 2007

— North —

*Names:* Doug, Henry *Station:* North *Date:* 02-21-07 *Time:* 10:15 *Exposed thermocouples:* 8 *Keywords:*  
*Surface:*  
 1-4mm rimed stellars, 1mm clustered columns  
*Layer 1:*  
 1-4mm rimed stellars, 1mm clustered columns  
*Layer 2:*  
 1-4mm rimed stellars, 1mm clustered columns  
*Layer 3:* 1-4mm rimed stellars  
*Layer 4:* 1-4mm rimed stellars  
*Layer 5:* 1-4mm rimed stellars

— South —

*Names:* Doug, Hanry *Station:* South *Date:* 02-21-07 *Time:* 9:15 am *Exposed thermocouples:* 20 *Keywords:*  
*Surface:*  
 1-4mm stellars with rime, some 2mm needles  
*Layer 1:* 1-4mm stellars with rime, some clustered and capped columns 1mm  
*Layer 2:* 1-4mm stellars with rime, some clustered and capped columns 1mm  
*Layer 3:* 1-4mm stellars with rime, some clustered and capped columns 1mm  
*Layer 4:* 1-4mm stellars with rime, some clustered and capped columns 1mm  
*Layer 5:* 1-4mm stellars with rime, some clustered and capped columns 1mm

February 22, 2007

— North —

*Names: Henry Station: North Date: 02-22-07 Time:**12:00 pm Exposed thermocouples: 16 Keywords:**Surface: 1-4mm decomposing particles**Layer 1: 1-4mm decomposing particles**Layer 2: 1-4mm decomposing particles**Layer 3: 1-4mm decomposing particles**Layer 4: 1-4mm decomposing particles**Layer 5: 1-4mm decomposing particles*

— South —

*Names: Henry Station: South Date: 02-22-07 Time:**11:00 Exposed thermocouples: 11 Keywords:**Surface: 1mm rounds (from wind)**Layer 1: 1-4mm decomposing particles**Layer 2: 1-4mm decomposing particles**Layer 3: 1-4mm decomposing particles**Layer 4: 1-4mm decomposing particles**Layer 5: 1-4mm decomposing particles*

February 23, 2007

— North —

*Names: Henry Station: North Date: 02-23-07 Time:**10:00 am Exposed thermocouples: 9 Keywords:**Surface:**3-4mm stellars: well formed and intricate**Layer 1: 2-4mm stellars: slightly rimed**Layer 2: 2-4mm stellars: slightly rimed**Layer 3: 2-4mm stellars: slightly rimed**Layer 4: 2-4mm stellars: slightly rimed**Layer 5: 2-4mm stellars: slightly rimed*

— South —

*Names: Henry Station: South Date: 02-23-07 Time:**9:00 am Exposed thermocouples: 6 Keywords:**Surface: 3.4mm stellars, no rime**Layer 1: 2-4mm stellars, slightly rimed**Layer 2: 2-4mm stellars, slightly rimed**Layer 3: Broken particles: 1-2mm stelar fragments  
, 1mm plates**Layer 4: Broken particles: 1-2mm stelar fragments  
, 1mm plates**Layer 5: Broken particles: 1-2mm stelar fragments  
, 1mm plates*

February 24, 2007

— North —

*Names:* Coop, Doug C *Station:* North *Date:* 02-24-07  
*Time:* 11:45 am *Exposed thermocouples:* 3 *Keywords:*  
*Surface:* rimed precipitation particles 1-2mm,  
 partly decomposed precipitation particles  
*Layer 1:* rimed precipitation particles 1-2mm,  
 partly decomposed precipitation particles  
*Layer 2:* rimed precipitation particles 1-2mm,  
 partly decomposed precipitation particles  
*Layer 3:* rimed precipitation particles 1-2mm,  
 partly decomposed precipitation particles  
*Layer 4:* rimed precipitation particles 1-2mm,  
 partly decomposed precipitation particles  
*Layer 5:* rimed precipitation particles 1-2mm,  
 partly decomposed precipitation particles

— South —

*Names:* Coop, Blake *Station:* South *Date:* 02-24-07  
*Time:* 10:45 *Exposed thermocouples:* 3 *Keywords:*  
 none  
*Surface:* (precipitation particles)1-2mm  
*Layer 1:* (precipitation particles)1-2mm  
*Layer 2:* (precipitation particles)1-2mm  
*Layer 3:* (precipitation particles)1-2mm  
*Layer 4:* (precipitation particles)1-2mm  
*Layer 5:* (precipitation particles)1-2mm

February 25, 2007

— North —

*Names:* Coop *Station:* North *Date:* 02-25-07 *Time:*  
 10:00 am *Exposed thermocouples:* 0 *Keywords:*  
*Surface:* Precipitation particles 3-4mm  
*Layer 1:* Precipitation particles 3-4mm  
*Layer 2:* Precipitation particles 3-4mm  
*Layer 3:* Precipitation particles 3-4mm  
*Layer 4:* Precipitation particles 3-4mm  
*Layer 5:* Precipitation particles 3-4mm

— South —

*Names:* Coop *Station:* South *Date:* 02-25-07 *Time:*  
 none given *Exposed thermocouples:* 0 *Keywords:* none  
*Surface:* (precipitation particles)2-3mm  
*Layer 1:* (precipitation particles)2-3mm  
*Layer 2:* (precipitation particles)2-3mm  
*Layer 3:* (precipitation particles)2-3mm  
*Layer 4:* (precipitation particles)2-3mm  
*Layer 5:* (precipitation particles)2-3mm

February 26, 2007

— North —

*Names:* Rich, Doug *Station:* North *Date:* 02-26-07  
*Time:* 11:00 am *Exposed thermocouples:* 0 *Keywords:*  
*Surface:*  
 Stellars 2-3mm, plates 1-2mm, columns 1-2mm  
*Layer 1:*  
 Stellars 2-3mm, plates 1-2mm, columns 1-2mm  
*Layer 2:*  
 Stellars 2-3mm, plates 1-2mm, columns 1-2mm  
*Layer 3:*  
 Stellars 2-3mm, plates 1-2mm, columns 1-2mm  
*Layer 4:* Stellars 3-5mm  
*Layer 5:* Stellars 3-5mm

— South —

*Names:* Rich, Doug *Station:* South *Date:* 02-26-07  
*Time:* 10:00 am *Exposed thermocouples:* 0 *Keywords:*  
*Surface:* It(?)rimed stellars 2-3mm, plates 2mm,  
 stellar plates 2-3mm, capped columns 1-2mm  
*Layer 1:* It(?)rimed stellars 2-3mm, plates 2mm,  
 stellar plates 2-3mm, capped columns 1-2mm  
*Layer 2:* It(?)rimed stellars 2-3mm, plates 2mm,  
 stellar plates 2-3mm, capped columns 1-2mm  
*Layer 3:* It(?)rimed stellars 2-3mm, plates 2mm,  
 stellar plates 2-3mm, capped columns 1-2mm  
*Layer 4:* It(?)rimed stellars 2-3mm, plates 2mm,  
 stellar plates 2-3mm, capped columns 1-2mm  
*Layer 5:* It(?)rimed stellars 2-3mm, plates 2mm,  
 stellar plates 2-3mm, capped columns 1-2mm

February 27, 2007

— North —

*Names:* Doug, Irene *Station:* North *Date:* 02-27-07  
*Time:* 10:30 am *Exposed thermocouples:* 0 *Keywords:*  
*Surface:* Stellars 1-3mm, plates 1mm  
*Layer 1:* Lightly rimed stellars 1-2mm, lightly  
 rimed plates 1mm  
*Layer 2:* rimed stellars 1mm, partly decomposed  
 precipitation particles 1mm  
*Layer 3:* rimes partly decomposed precipitation  
 particles 0.5-1mm  
*Layer 4:* heavily rimed stellars 1mm, partly  
 decomposed precipitation particles 0.5-1mm  
*Layer 5:* Heavily rimed stellars 1-2mm

— South —

*Names:* Henry *Station:* South *Date:* 02-27-07 *Time:*  
 9:40 am *Exposed thermocouples:* 0 *Keywords:*  
*Surface:* 1mm needles, plates, 2mm stellars  
*Layer 1:* 0.5mm highly broken particles  
*Layer 2:* 0.5mm highly broken particles  
*Layer 3:* 1mm broken particles  
*Layer 4:* 1mm broken particles  
*Layer 5:* 2mm broken particles



February 28, 2007

— North —

*Names: Henry, Ellie Station: North Date: 02-28-07**Time: 10:40 Exposed thermocouples: 0 Keywords:**Surface: 1-2mm rimed stellars**Layer 1: 1-2mm rimed stellars**Layer 2: 1-2mm rimed stellars**Layer 3: 1-2mm rimed stellars, needles, plates**Layer 4: 1-2mm rimed stellars, needles, plates**Layer 5: 1-2mm rimed stellars, needles, plates*

— South —

*Names: Doug Wolf Station: South Date: 02-28-07**Time: 10:45 am Exposed thermocouples: 0 Keywords:**none**Surface:**(partly decomposed precip. particles)0.5-2mm rimed, (precipitation particles)1-2mm, H rime**Layer 1: (partly decomposed precip. particles)**0.25-mm heavy rime**Layer 2: (partly decomposed precip particles)**0.5-2mm heavy rime, 2mm (graupel), (precip. particles)1-2mm**Layer 3: (partly decomposed precip particles)**0.5-2mm heavy rime, 2mm (graupel), (precip. particles)1-2mm**Layer 4: (partly decomposed precip particles)**0.5-2mm heavy rime, 2mm (graupel), (precip. particles)1-2mm**Layer 5: (partly decomposed precip particles)**0.5-2mm heavy rime, 2mm (graupel), (precip. particles)1-2mm*

March 01, 2007

— North —

*Names: Henry Station: North Date: 03-1-07 Time:**10:00 am Exposed thermocouples: 0 Keywords:**Surface: 0.5mm heavily rimed columns, needles**Layer 1: 0.5mm heavily rimed columns, needles**Layer 2: 0.5mm heavily rimed columns, needles**Layer 3: 1mm rimed columns, needles, plates**Layer 4: 1mm rimed columns, needles, plates**Layer 5: 1mm rimed columns, needles, plates*

— South —

*Names: Henry Station: South Date: 03-01-07 Time:**11:30 am Exposed thermocouples: 0 Keywords:**Surface: 2mm graupel**Layer 1: 0.5-1mm heavily rimed columns, needles**Layer 2: 0.5-1mm heavily rimed columns, needles**Layer 3: 0.5-1mm heavily rimed columns, needles**Layer 4: 1mm rimed columns needles, plates, 3mm rimed stellars**Layer 5: 1mm rimed columns needles, plates, 3mm rimed stellars*

March 02, 2007

— North —

*Names: Henry Station: North Date: 03-2-07 Time: 2:00 pm Exposed thermocouples: 0 Keywords:*  
*Surface: 4mm wind crust*  
*Layer 1: less that 0.5mm highly broken particles*  
*Layer 2: less that 0.5mm highly broken particles*  
*Layer 3: less that 0.5mm highly broken particles*  
*Layer 4: 0.5-1mm decomposing plates, columns and needles*  
*Layer 5: 0.5-1mm decomposing plates, columns and needles*

— South —

*Names: Henry Station: South Date: 03-02-07 Time: 1:00 pm Exposed thermocouples: 0 Keywords:*  
*Surface: 0.25mm faceted cups, 0.5-1mm broken rimed particles*  
*Layer 1: 0.5-1mm decomposing rimed columns, needles*  
*Layer 2: 0.5-1mm decomposing rimed columns, needles*  
*Layer 3: 0.5-1mm decomposing rimed columns, needles*  
*Layer 4: 0.5-1mm decomposing rimed columns, needles, plates*  
*Layer 5: 0.5-1mm decomposing rimed columns, needles, plates*

March 03, 2007

— North —

*Names: Blake Lowrey Station: North Date: 03-3-07 Time: 1:00 pm Exposed thermocouples: 0 Keywords:*  
*Surface: Highly broken particles, signs of bonding*  
*Layer 1: Highly broken particles, signs of bonding*  
*Layer 2: Highly broken particles*  
*Layer 3: Highly broken particles*  
*Layer 4: Highly broken particles*  
*Layer 5: Highly broken particles*

— South —

*Names: Coop Station: South Date: 03-03-07 Time: 10:00 am Exposed thermocouples: 0 Keywords: none*  
*Surface: (highly broken particles)0.5mm signs of bonding*  
*Layer 1: (highly broken particles)0.5mm signs of bonding*  
*Layer 2: (highly broken particles)0.5mm signs of bonding*  
*Layer 3: (highly broken particles)0.5mm signs of bonding*  
*Layer 4: (highly broken particles)0.5mm signs of bonding*  
*Layer 5: (highly broken particles)0.5mm signs of bonding*

March 04, 2007

— North —

*Names:* Doug Station: North *Date:* 03-4-07 *Time:*  
11:00 am *Exposed thermocouples:* 0 *Keywords:*  
*Surface:* Surface hoar 1-3mm  
*Layer 1:*  
Highly broken particles, signs of bonding  
*Layer 2:*  
Highly broken particles, signs of bonding  
*Layer 3:*  
Highly broken particles, signs of bonding  
*Layer 4:*  
Highly broken particles, signs of bonding  
*Layer 5:*  
Highly broken particles, signs of bonding

— South —

*Names:* D0ug Station: South *Date:* 03-04-07 *Time:*  
10:00 am *Exposed thermocouples:* 0 *Keywords:* none  
*Surface:* 4mm (surface hoar crystals)  
*Layer 1:* 0.25-0.5mm (rounded grains)  
*Layer 2:* 0.25-0.5mm (rounded grains)  
*Layer 3:* 0.25-0.5mm (rounded grains)  
*Layer 4:* (highly broken particles)0.25-0.5mm  
signs of bonding  
*Layer 5:* (highly broken particles)0.25-0.5mm  
signs of bonding

March 05, 2007

— North —

*Names:* Rich Station: North *Date:* 03-5-07 *Time:*  
1:35 *Exposed thermocouples:* 0 *Keywords:*  
*Surface:* 3mm surface hoar  
*Layer 1:* 0.5mm rounded grains  
*Layer 2:* 0.5mm rounded grains  
*Layer 3:* 0.5mm rounded grains  
*Layer 4:* 0.5mm rounded grains  
*Layer 5:* 0.5mm rounded grains

— South —

*Names:* Rich Station: South *Date:* 03-05-07 *Time:*  
12:38 pm *Exposed thermocouples:* 3 *Keywords:* none  
*Surface:* 2mm (surface hoar crystals)  
*Layer 1:* 0.5mm (rounded grains)  
*Layer 2:* 0.5mm (rounded grains)  
*Layer 3:* 0.5mm (rounded grains)  
*Layer 4:* 0.5mm (rounded grains)  
*Layer 5:* 0.5mm (rounded grains)

March 06, 2007

— North —

*Names:* Henry, Doug Station: North *Date:* 03-6-07  
*Time:* 12:00 pm *Exposed thermocouples:* 0 *Keywords:*  
*Surface:* 2mm surface hoar  
*Layer 1:* 0.5mm rounded grains  
*Layer 2:* 0.5mm rounded grains  
*Layer 3:* 0.5mm rounded grains  
*Layer 4:* 0.5mm rounded grains  
*Layer 5:* 0.5mm rounded grains

— South —

*Names:* Henry, Doug Station: South *Date:* 03-06-07  
*Time:* 11:00 am *Exposed thermocouples:* 4 *Keywords:*  
none  
*Surface:* 2mm (surface hoar crystals)wet  
*Layer 1:* 0.5mm (wet grains)  
*Layer 2:* 0.5mm (wet grains)  
*Layer 3:* 0.5mm (wet grains)  
*Layer 4:* 0.5mm (wet grains)  
*Layer 5:* 0.5mm (wet grains)

March 07, 2007

---

— North —

*Names:* Doug Station: North *Date:* 03-7-07 *Time:*  
 9:30 am *Exposed thermocouples:* 5 *Keywords:*  
*Surface:* 3mm surface hoar (new growth)  
*Layer 1:* 0.5mm rounded grains  
*Layer 2:* 0.5mm rounded grains  
*Layer 3:* 0.5mm rounded grains  
*Layer 4:* 0.5mm rounded grains  
*Layer 5:* 0.5mm rounded grains

— South —

*Names:* Coop Station: South *Date:* 03-07-07 *Time:*  
 9:00 am *Exposed thermocouples:* 8 *Keywords:* none  
*Surface:*  
 (solid faceted particles)0.5mm and rounds  
*Layer 1:* sun crust  
*Layer 2:* sun crust  
*Layer 3:* sun crust  
*Layer 4:* sun crust  
*Layer 5:* small rounded grains well bonded

March 08, 2007

---

— North —

*Names:* Rich, Doug C Station: North *Date:* 03-8-07  
*Time:* 11:15 am *Exposed thermocouples:* 4 *Keywords:*  
*Surface:* 1-2mm rimed stellars, needles, columns  
*Layer 1:* 1-2mm rimed stellars, needles, columns  
*Layer 2:* 1-2mm rimed stellars, needles, columns  
*Layer 3:* 1-2mm rimed stellars, needles, columns  
*Layer 4:* 3-4mm rimed stellars, needles, columns  
*Layer 5:* 3-4mm rimed stellars, needles, columns

— South —

*Names:* Rich, Doug C. Station: South *Date:*  
 03-08-07 *Time:* 10:15 *Exposed thermocouples:* 10  
*Keywords:*  
*Surface:*  
 1-2mm rimed stellars, needles and columns  
*Layer 1:*  
 1-2mm rimed stellars, needles and columns  
*Layer 2:*  
 1-2mm rimed stellars, needles and columns  
*Layer 3:*  
 1-2mm rimed stellars, needles and columns  
*Layer 4:*  
 1-2mm rimed stellars, needles and columns  
*Layer 5:*  
 1-2mm rimed stellars, needles and columns

March 09, 2007

---

— North —

*Names:* Marc, Ellie *Station:* North *Date:* 03-9-07  
*Time:* 12:10 pm *Exposed thermocouples:* 6 *Keywords:*  
*Surface:* 0.5-1mm partly decomposed precipitation  
 particles  
*Layer 1:* 0.25mm rounded grains, partly decomposed  
 precipitation  
*Layer 2:* 0.25mm rounded grains, partly decomposed  
 precipitation  
*Layer 3:* 0.25mm rounded grains, partly decomposed  
 precipitation  
*Layer 4:* 0.25mm rounded grains, partly decomposed  
 precipitation  
*Layer 5:* 0.25mm rounded grains

— South —

*Names:* Ellie, Mark *Station:* South *Date:* 03-09-07  
*Time:* 2:00 pm *Exposed thermocouples:* 13 *Keywords:*  
 none  
*Surface:* (melt freeze crust)0.25-0.5 individual  
 grain size, some grains were wet clumping of  
 grains 2mm  
*Layer 1:* (melt freeze crust)0.5 mm (rounded  
 grains)no visible wet grains, 2.0 mm clumps  
*Layer 2:* (melt freeze crust)0.5 mm (rounded  
 grains)no visible wet grains, 2.0 mm clumps  
*Layer 3:* (melt freeze crust)0.5 mm (rounded  
 grains)no visible wet grains, 2.0 mm clumps  
*Layer 4:* (melt freeze crust)0.5 mm (rounded  
 grains)no visible wet grains, 2.0 mm clumps  
*Layer 5:* (melt freeze crust)0.5 mm (rounded  
 grains)no visible wet grains, 2.0 mm clumps

March 10, 2007

---

— North —

*Names:* Coop *Station:* North *Date:* 03-10-07 *Time:*  
 9:35 am *Exposed thermocouples:* 6 *Keywords:*  
*Surface:* Precipitation particles 3mm  
*Layer 1:* partly decomposed precipitation  
 particles, needles, rounded grains 0.5mm  
*Layer 2:* partly decomposed precipitation  
 particles, needles, rounded grains 0.5mm  
*Layer 3:* partly decomposed precipitation  
 particles, needles, rounded grains 0.5mm  
*Layer 4:* partly decomposed precipitation  
 particles, needles, rounded grains 0.5mm  
*Layer 5:* partly decomposed precipitation  
 particles, needles, rounded grains 0.5mm

— South —

*Names:* Coop *Station:* South *Date:* 03-10-07 *Time:*  
 8:30 am *Exposed thermocouples:* 13 *Keywords:* none  
*Surface:* (precipitation particles)3mm  
*Layer 1:* (rounded grains)0.5mm, sun crust  
*Layer 2:* (rounded grains)0.5mm, sun crust  
*Layer 3:* (rounded grains)0.5mm, sun crust  
*Layer 4:* (rounded grains)0.5mm, sun crust  
*Layer 5:* (rounded grains)0.5mm, sun crust

March 11, 2007

---

— North —

*Names: Coop Station: North Date: 03-11-07 Time: 10:45 am Exposed thermocouples: 7 Keywords:*  
*Surface: Precipitation particles 3mm*  
*Layer 1: Precipitation particles 3mm*  
*Layer 2: partly decomposed precipitation particles 0.5-1mm*  
*Layer 3: partly decomposed precipitation particles 0.5-1mm*  
*Layer 4: partly decomposed precipitation particles 0.5-1mm*  
*Layer 5: partly decomposed precipitation particles 0.5-1mm*

— South —

*Names: Coop Station: South Date: 03-11-07 Time: 9:00 am Exposed thermocouples: 13 Keywords: none*  
*Surface: (rounded grains)0.5mm*  
*Layer 1: (rounded grains)0.5mm*  
*Layer 2: (rounded grains)0.5mm*  
*Layer 3: (rounded grains)0.5mm*  
*Layer 4: (rounded grains)0.5mm*  
*Layer 5: (rounded grains)0.5mm*

March 12, 2007

---

— North —

*Names: Doug Station: NOrth Date: 03-12-07 Time: 11:45 am Exposed thermocouples: 12 Keywords:*  
*Surface: Melt freeze crust, rounded grains 2mm*  
*Layer 1: Melt freeze crust, rounded grains 2mm*  
*Layer 2: Rounded grains 0.5mm*  
*Layer 3: Rounded grains 0.5mm*  
*Layer 4: Rounded grains 0.5mm*  
*Layer 5: Melt freeze crust 1cm thick, rounded grains 0.5mm*

— South —

*Names: Doug Station: South Date: 03-12-07 Time: 9:15 am Exposed thermocouples: 15 Keywords: none*  
*Surface: (melt freeze crust)to 5 cm, (rounded grains)1mm-3mm*  
*Layer 1: (melt freeze crust)to 5 cm, (rounded grains)1mm-3mm*  
*Layer 2: (melt freeze crust)to 5 cm, (rounded grains)1mm-3mm*  
*Layer 3: (melt freeze crust)to 5 cm, (rounded grains)1mm-3mm*  
*Layer 4: (melt freeze crust)to 5 cm, (rounded grains)1mm-3mm*  
*Layer 5: (melt freeze crust)to 5 cm, (rounded grains)1mm-3mm*

March 13, 2007

---

— North —

*Names: Coop Station: North Date: 03-13-07 Time: 11:45 am Exposed thermocouples: 13 Keywords: Surface: Graupel 3-4mm Layer 1: Melt freeze crust 1mm Layer 2: Rounded grains 0.5mm Layer 3: Rounded grains 0.5mm Layer 4: Rounded grains 0.5mm Layer 5: Rounded grains 0.5mm*

— South —

*Names: Coop Station: South Date: 03-13-07 Time: 12:47 Exposed thermocouples: 20 Keywords: none Surface: GP (graupel)3-4mm Layer 1: (melt freeze crust)0.5mm Layer 2: (melt freeze crust)0.5mm Layer 3: (melt freeze crust)0.5mm Layer 4: (melt freeze crust)0.5mm Layer 5: (melt freeze crust)0.5mm*

March 14, 2007

---

— North —

*Names: Doug Station: North Date: 03-14-07 Time: 1:00 pm Exposed thermocouples: 15 Keywords: Surface: Melt freeze crust 0.5mm Layer 1: Melt freeze crust 0.5mm Layer 2: Melt freeze crust 0.5mm Layer 3: Rounded grains 0.5mm Layer 4: Rounded grains 0.5mm Layer 5: Melt freeze crust 0.5 cm thick, 0.5mm rounded grains*

— South —

*Names: Doug Station: South Date: 03-14-07 Time: 10:45 Exposed thermocouples: 20 Keywords: none Surface: (melt freeze crust), (rounded grains)2mm Layer 1: (melt freeze crust), (rounded grains)2mm Layer 2: (melt freeze crust), (rounded grains)2mm Layer 3: (melt freeze crust), (rounded grains)2mm Layer 4: (melt freeze crust), (rounded grains)2mm Layer 5: (rounded grains)1mm*

March 15, 2007

---

— North —

*Names: Rich Station: North Date: 03-15-07 Time: 9:35 am Exposed thermocouples: 16 Keywords: Surface: Melt freeze crust 1mm Layer 1: Melt freeze crust 1mm Layer 2: Melt freeze crust 1mm Layer 3: Rounded grains 0.5mm Layer 4: Rounded grains 0.5mm Layer 5: Melt freeze crust 0.5mm*

— South —

*Names: Rich Station: South Date: 03-15-07 Time: 9:00 am Exposed thermocouples: 20 Keywords: none Surface: (melt freeze crust)2-3mm Layer 1: (melt freeze crust)2-3mm Layer 2: (melt freeze crust)2-3mm Layer 3: (melt freeze crust)2-3mm Layer 4: (melt freeze crust)2-3mm Layer 5: (melt freeze crust)2-3mm*

March 16, 2007

---

— North —

*Names:* Henry, Blake *Station:* North *Date:* 03-16-07

*Time:* 11:30 am *Exposed thermocouples:* 20

*Keywords:*

*Surface:* 1mm wet new snow

*Layer 1:* 2mm wet melt freeze snow

*Layer 2:* 2mm wet melt freeze snow

*Layer 3:* 2mm wet melt freeze snow

*Layer 4:* 2mm wet melt freeze snow

*Layer 5:* 2mm wet melt freeze snow

— South —

*Names:* Henry, Blake *Station:* South *Date:* 03-16-07

*Time:* 10:30 am *Exposed thermocouples:* 20

*Keywords:* none

*Surface:* 2mm surface hoar, 2-3mm (melt freeze crust)1mm heavily rimed new snow

*Layer 1:* 2-3mm (melt freeze crust)

*Layer 2:* 2-3mm (melt freeze crust)

*Layer 3:* 2-3mm (melt freeze crust)

*Layer 4:* 2-3mm (melt freeze crust)

*Layer 5:* 2-3mm (melt freeze crust)

March 17, 2007

---

— North —

*Names:* Coop *Station:* North *Date:* 03-17-07 *Time:*

11:25 am *Exposed thermocouples:* 20 *Keywords:*

*Surface:* 2mm wet

*Layer 1:* 2mm wet

*Layer 2:* 2mm wet

*Layer 3:* 2mm wet

*Layer 4:* 2mm wet

*Layer 5:* 2mm wet

— South —

*Names:* Coop *Station:* South *Date:* 03-17-07 *Time:*

12:45 *Exposed thermocouples:* 20 *Keywords:*

*Surface:* 2mm wet

*Layer 1:* 2mm wet

*Layer 2:* 2mm wet

*Layer 3:* 2mm wet

*Layer 4:* 2mm wet

*Layer 5:* 2mm wet

March 18, 2007

---

— North —

*Names:* Doug *Station:* North *Date:* 03-18-07 *Time:*

10:00 am *Exposed thermocouples:* 20 *Keywords:*

*Surface:* Melt freeze crust, 2mm frozen rounded poly crystals

*Layer 1:* Melt freeze crust, 2mm frozen rounded poly crystals

*Layer 2:* Melt freeze crust, 2mm frozen rounded poly crystals

*Layer 3:* 1mm rounded grains

*Layer 4:* 0.5mm rounded grains

*Layer 5:* 0.5mm rounded grains

— South —

*Names:* Doug, Doug *Station:* South *Date:* 03-18-07

*Time:* 11:15 *Exposed thermocouples:* 20 *Keywords:*

none

*Surface:* melt freeze crust

*Layer 1:* melt freeze crust

*Layer 2:* (rounded poly-crystals)1mm

*Layer 3:* (rounded poly-crystals)1mm

*Layer 4:* (rounded grains)1mm

*Layer 5:* (rounded grains)1mm



March 19, 2007

---

— North —

*Names:* Coop Station: North *Date:* 03-19-07 *Time:*  
12:00 pm *Exposed thermocouples:* 20 *Keywords:*  
*Surface:* 2mm wet  
*Layer 1:* Melt freeze crust 1mm  
*Layer 2:* Melt freeze crust 1mm  
*Layer 3:* Melt freeze crust 1mm  
*Layer 4:* Rounded grains 0.5mm  
*Layer 5:* Rounded grains 0.5mm

— South —

*Names:* Coop Station: South *Date:* 03-19-07 *Time:*  
11:15 am *Exposed thermocouples:* 20 *Keywords:* none  
*Surface:* 2-3mm wet grains  
*Layer 1:* 2-3mm wet  
*Layer 2:* 2-3mm wet  
*Layer 3:* melt freeze crust  
*Layer 4:* melt freeze crust  
*Layer 5:* melt freeze crust

March 20, 2007

---

— North —

*Names:* Doug, Henry *Station:* North *Date:* 03-20-07  
*Time:* 9:00 am *Exposed thermocouples:* 20 *Keywords:*  
*Surface:* 2mm melt freeze crust with a few 1mm  
surface hoar crystals evident  
*Layer 1:* 2mm melt freeze crust  
*Layer 2:* 2mm melt freeze crust  
*Layer 3:* 2mm melt freeze crust, melt freeze crust  
3 cm thick  
*Layer 4:* 1mm rounded grains  
*Layer 5:* 0.5mm rounded grains

— South —

*Names:* Henry, Doug *Station:* South *Date:* 03-20-07  
*Time:* 10:00 am *Exposed thermocouples:* 20  
*Keywords:* none  
*Surface:*  
(wet grains)0.5x(rounded poly-crystals)3mm moist  
*Layer 1:*  
(wet grains)0.5x(rounded poly-crystals)3mm moist  
*Layer 2:*  
(wet grains)0.5x(rounded poly-crystals)3mm moist  
*Layer 3:*  
(wet grains)0.5x(rounded poly-crystals)3mm moist  
*Layer 4:*  
(wet grains)0.5x(rounded poly-crystals)3mm moist  
*Layer 5:*  
(wet grains)0.5x(rounded poly-crystals)3mm moist

March 21, 2007

— North —

*Names:* Henry, Doug and Irene *Station:* North *Date:* 03-21-07 *Time:* none given *Exposed thermocouples:* 11 *Keywords:*

*Surface:*

2mm stellar dendrites, 0.25-0.5 mm surface hoar

*Layer 1:* 1mm irregular crystals with rime

*Layer 2:* 1mm irregular crystals with rime

*Layer 3:* 1mm irregular crystals with rime

*Layer 4:* 1mm irregular crystals with rime

*Layer 5:* 1mm irregular crystals with rime

— South —

*Names:* Henry, Doug *Station:* South *Date:* 03-21-07 *Time:* 9:15 *Exposed thermocouples:* 20 *Keywords:* none

*Surface:* stellar dendrites 2mm heavily rimed

*Layer 1:* irregular crystals 0.2x1mm very rimed

*Layer 2:* irregular crystals 0.2x1mm very rimed

*Layer 3:* irregular crystals 0.2x1mm very rimed

*Layer 4:* irregular crystal)0.2x1mm very rimed

*Layer 5:* irregular crystals 0.2x1mm very rimed

March 22, 2007

— North —

*Names:* Rich, Doug C. *Station:* North *Date:* 03-22-07 *Time:* 11:45 am *Exposed thermocouples:* 11 *Keywords:*

*Surface:*

Partly decomposed precipitation particles 1mm

*Layer 1:* rounded grains 1-2mm

*Layer 2:* rounded grains 1-2mm

*Layer 3:* rounded grains 1-2mm

*Layer 4:* rounded grains 1-2mm

*Layer 5:* rounded grains 1-2mm

— South —

*Names:* Rich C *Station:* South *Date:* 03-22-07 *Time:* 10:55 *Exposed thermocouples:* 20 *Keywords:* none

*Surface:* (melt freeze crust)3mm

*Layer 1:* (melt freeze crust)3mm

*Layer 2:* (melt freeze crust)3mm

*Layer 3:* (melt freeze crust)3mm

*Layer 4:* (melt freeze crust)3mm

*Layer 5:* (melt freeze crust)3mm

March 23, 2007

— North —

*Names:* Henry *Station:* North *Date:* 03-23-07 *Time:* 1:15 pm *Exposed thermocouples:* 11 *Keywords:*

*Surface:* 1mm highly broken particles slightly wet

*Layer 1:* 1mm highly broken particles slightly wet

*Layer 2:* Rounded grains (3A)0.5mm slightly wet

*Layer 3:* Rounded grains (3A)0.5mm slightly wet

*Layer 4:* Rounded grains (3A)0.5mm slightly wet

*Layer 5:* Rounded grains (3A)0.5mm slightly wet

— South —

*Names:* Henry *Station:* South *Date:* 03-23-07 *Time:* 12:40 *Exposed thermocouples:* 20 *Keywords:* none

*Surface:* 1mm columns, 2mm needles, 1mm stellar dendrites with beginning melt

*Layer 1:* 1mm columns, 2mm needles, 1mm stellar dendrites with beginning melt

*Layer 2:* 0.5mm slush (BA)

*Layer 3:* 0.5mm slush (BA)

*Layer 4:* 0.5mm slush (BA)

*Layer 5:* melt freeze crust 0.5x5mm

March 24, 2007

---

— North —

*Names:* Coop Station: North *Date:* 03-24-07 *Time:*  
2:30 pm *Exposed thermocouples:* 12 *Keywords:*  
*Surface:* Highly broken particles, needles,  
rounded grains 0.5mm  
*Layer 1:* Highly broken particles, needles,  
rounded grains 0.5mm  
*Layer 2:* Highly broken particles, needles,  
rounded grains 0.5mm  
*Layer 3:* Highly broken particles 0.5mm  
*Layer 4:* Highly broken particles 0.5mm  
*Layer 5:* Highly broken particles 0.5mm

— South —

*Names:* Coop Station: South *Date:* 03-24-07 *Time:*  
9:00 am *Exposed thermocouples:* 20 *Keywords:* none  
*Surface:* small faceted partilces 0.5mm  
*Layer 1:* melt freeze crust, sun crust noticeable  
with more air spaces  
*Layer 2:* melt freeze crust in crust begining to  
*Layer 3:* melt freeze crust  
*Layer 4:* melt freeze crust  
*Layer 5:* melt freeze crust

March 25, 2007

---

— North —

*Names:* Coop Station: North *Date:* 03-25-07 *Time:*  
12:00 pm *Exposed thermocouples:* 12 *Keywords:*  
*Surface:* Highly broken particles, needles,  
rounded grains 0.5mm moist  
*Layer 1:* Highly broken particles, needles,  
rounded grains 0.5mm moist  
*Layer 2:* Highly broken particles, needles,  
rounded grains 0.5mm moist  
*Layer 3:* Highly broken particles, needles,  
rounded grains 0.5mm moist  
*Layer 4:* Highly broken particles, needles,  
rounded grains 0.5mm moist  
*Layer 5:* Highly broken particles, needles,  
rounded grains 0.5mm moist

— South —

*Names:* Coop Station: South *Date:* 03-25-07 *Time:*  
10:00 am *Exposed thermocouples:* 20 *Keywords:*  
*Surface:* Melt freeze crust  
*Layer 1:* Melt freeze crust  
*Layer 2:* Melt freeze crust  
*Layer 3:* Melt freeze crust  
*Layer 4:* Melt freeze crust  
*Layer 5:* Melt freeze crust

March 26, 2007

---

— North —

*Names:* Doug *Station:* North *Date:* 03-26-07 *Time:*  
10:00 am *Exposed thermocouples:* 9 *Keywords:*  
*Surface:* Irregular crystals, 0.5-1mm, graupel 3mm  
*Layer 1:* Irregular crystals, 0.5-1mm, graupel 3mm  
*Layer 2:* Irregular crystals 0.5mm  
*Layer 3:* Irregular crystals 0.5mm  
*Layer 4:* Irregular crystals 0.5mm  
*Layer 5:* melt freeze crust 3cm thick

— South —

*Names:* Doug *Station:* South *Date:* 03-26-07 *Time:*  
10:30 *Exposed thermocouples:* 20 *Keywords:*  
*Surface:* Irregular crystals 0.5-1mm, graupel 2mm  
*Layer 1:* Irregular crystals 0.5-1mm, graupel 2mm  
*Layer 2:* Irregular crystals 0.5-1mm  
*Layer 3:* Irregular crystals 0.5-1mm  
*Layer 4:* Irregular crystals 0.5-1mm  
*Layer 5:* Irregular crystals 0.5-1mm

March 27, 2007

---

— North —

*Names:* Doug, Henry *Station:* North *Date:* 03-27-07  
*Time:* none given *Exposed thermocouples:* 8  
*Keywords:*  
*Surface:* 1-2mm highly broken particles  
*Layer 1:* 1-2mm highly broken particles  
*Layer 2:* 0.5x2mm clustered rounded grains  
*Layer 3:* 0.5x2mm clustered rounded grains  
*Layer 4:* 0.5x2mm clustered rounded grains  
*Layer 5:* 0.5x2mm clustered rounded grains

— South —

*Names:* Doug, Henry *Station:* South *Date:* 03-27-07  
*Time:* Not Given *Exposed thermocouples:* 20  
*Keywords:*  
*Surface:* 1mm highly broken particles (melting)  
*Layer 1:* 1mm highly broken particles (melting)  
*Layer 2:* 0.5x3mm slush  
*Layer 3:* 0.5x3mm slush  
*Layer 4:* 0.5x3mm slush  
*Layer 5:* 0.5x3mm slush

March 28, 2007

---

— North —

*Names:* Doug, Henry *Station:* North *Date:* 03-28-07  
*Time:* 9:45 am *Exposed thermocouples:* 3 *Keywords:*  
*Surface:* 3-5mm stellar dendrites  
*Layer 1:* 3-5mm stellar dendrites  
*Layer 2:* 3-5mm stellar dendrites  
*Layer 3:* 3-5mm stellar dendrites  
*Layer 4:* 3-5mm stellar dendrites  
*Layer 5:* 1mm highly broken particles

— South —

*Names:* Doug, Henry *Station:* South *Date:* 03-28-07  
*Time:* 10:30 am *Exposed thermocouples:* 20  
*Keywords:*  
*Surface:*  
3-5mm stellar dendrites lightly to heavily rimed  
*Layer 1:*  
3-5mm stellar dendrites lightly to heavily rimed  
*Layer 2:*  
3-5mm stellar dendrites lightly to heavily rimed  
*Layer 3:*  
3-5mm stellar dendrites lightly to heavily rimed  
*Layer 4:* 1-2mm highly broken particles  
*Layer 5:* 1-2mm highly broken particles

March 29, 2007

---

— North —

*Names: Henry Station: North Date: 03-29-07 Time: 12:30 pm Exposed thermocouples: 3 Keywords:*  
*Surface: 1mm highly broken particles*  
*Layer 1: 2-4mm stellar dendrites*  
*Layer 2: 2-4mm stellar dendrites*  
*Layer 3: 2-4mm stellar dendrites*  
*Layer 4:*  
*1-2mm partly decomposed precipitation particles*  
*Layer 5:*  
*1-2mm partly decomposed precipitation particles*

— South —

*Names: Henry Station: South Date: 03-29-07 Time: 11:00 am Exposed thermocouples: 7 Keywords:*  
*Surface: 0.5-1mm surface hoar*  
*Layer 1: 2-3mm stellar dendrites*  
*Layer 2: 2-3mm stellar dendrites*  
*Layer 3: 2-3mm stellar dendrites*  
*Layer 4:*  
*1-2mm partly decomposed precipitation particles*  
*Layer 5:*  
*1-2mm partly decomposed precipitation particles*

March 30, 2007

---

— North —

*Names: Ellie Station: North Date: 03-30-07 Time: 11:55 am Exposed thermocouples: 4 Keywords:*  
*Surface: 1mm partly decomposed precipitation particles (broken stellars initial necking)*  
*Layer 1: 1mm partly decomposed precipitation particles, evidence of 1mm surface hoar (minor)*  
*Layer 2: 0.5-1mm partly decomposed precipitation particles, mixed forms (partly decomposed precipitation particles to rounded grains)*  
*Layer 3:*  
*1-2mm surface hoar (80%) partly decomposed precipitation particles to rounded grains (20%)*  
*Layer 4: 0.5-1mm partly decomposed precipitation particles, solid faceted particles, mixed forms*  
*Layer 5: 0.5-1mm partly decomposed precipitation particles, solid faceted particles*

— South —

*Names: Ellie Station: South Date: 03-30-07 Time: 10:35 am Exposed thermocouples: 10 Keywords:*  
*Surface: 1mm partly decomposed precipitation particles, rounded grains, needles becoming wet, surface was elastic*  
*Layer 1:*  
*1mm partly decomposed precipitation particles*  
*Layer 2:*  
*0.5mm partly decomposed precipitation particles*  
*Layer 3:*  
*0.5mm partly decomposed precipitation particles*  
*Layer 4:*  
*0.5mm partly decomposed precipitation particles*  
*Layer 5:*  
*0.5mm partly decomposed precipitation particles*

March 31, 2007

— North —

*Names:* Coop Station: North *Date:* 03-31-07 *Time:*  
 10:45 am *Exposed thermocouples:* 5 *Keywords:*  
*Surface:* Highly broken particles, needles,  
 rounded grains 1mm  
*Layer 1:* Highly broken particles, needles,  
 rounded grains 1mm  
*Layer 2:* Rounded grains 0.5mm  
*Layer 3:* Rounded grains 0.5mm  
*Layer 4:* Rounded grains 0.5mm  
*Layer 5:* Rounded grains 0.5mm

— South —

*Names:* Coop Station: South *Date:* 03-31-07 *Time:*  
 10:00 am *Exposed thermocouples:* 11 *Keywords:*  
*Surface:* Rounded grains 0.5mm  
*Layer 1:* Rounded grains 0.5mm  
*Layer 2:* Rounded grains 0.5mm  
*Layer 3:* Rounded grains 0.5mm  
*Layer 4:* Rounded grains 0.5mm  
*Layer 5:* Rounded grains 0.5mm

April 01, 2007

— North —

*Names:* Doug Station: North *Date:* 04-1-07 *Time:*  
 9:30 am *Exposed thermocouples:* 0 *Keywords:*  
*Surface:* Stellar dendrites, needles, rimed to  
 heavily rimed 1-2mm  
*Layer 1:* Stellar dendrites, needles, rimed to  
 heavily rimed 1-2mm  
*Layer 2:* Stellar dendrites, needles, rimed to  
 heavily rimed 1-2mm  
*Layer 3:* Stellar dendrites, needles, rimed to  
 heavily rimed 1-2mm  
*Layer 4:* Stellar dendrites, needles, rimed to  
 heavily rimed 1-2mm  
*Layer 5:* Stellar dendrites, needles, rimed to  
 heavily rimed 1-2mm

— South —

*Names:* Doug McCabe Station: South *Date:* 04-01-07  
*Time:* 8:30 am *Exposed thermocouples:* 7 *Keywords:*  
 none  
*Surface:* Stellar dendrites, needles rimed to  
 heavily rimed 1-2mm  
*Layer 1:* Stellar dendrites, needles rimed to  
 heavily rimed 1-2mm  
*Layer 2:* Stellar dendrites, needles rimed to  
 heavily rimed 1-2mm  
*Layer 3:* Stellar dendrites, needles rimed to  
 heavily rimed 1-2mm  
*Layer 4:* Stellar dendrites, needles rimed to  
 heavily rimed 1-2mm  
*Layer 5:* Stellar dendrites, needles rimed to  
 heavily rimed 1-2mm

April 02, 2007

— North —

*Names:* Coop Station: North *Date:* 04-2-07 *Time:* 1:45 pm *Exposed thermocouples:* 0 *Keywords:*

*Surface:* Precipitation particles slightly rimed  
1-2mm moist

*Layer 1:* Precipitation particles slightly rimed  
1-2mm moist

*Layer 2:* Precipitation particles slightly rimed  
1-2mm moist

*Layer 3:* Precipitation particles slightly rimed  
1-2mm moist

*Layer 4:* Precipitation particles slightly rimed  
1-2mm moist

*Layer 5:* Precipitation particles slightly rimed  
1-2mm moist

— South —

*Names:* Doug Station: South *Date:* 04-02-07 *Time:* 12:30 pm *Exposed thermocouples:* 0 *Keywords:*

*Surface:* Stellar dendrites 0.5-2mm, plates 0.5-1 mm, capped columns 0.5mm, all particles lightly rimed

*Layer 1:* Stellar dendrites 0.5-2mm, plates 0.5-1 mm, capped columns 0.5mm, all particles lightly rimed

*Layer 2:* Stellar dendrites 0.5-2mm, plates 0.5-1 mm, capped columns 0.5mm, all particles lightly rimed

*Layer 3:* Stellar dendrites 0.5-2mm, plates 0.5-1 mm, capped columns 0.5mm, all particles lightly rimed

*Layer 4:* Stellar dendrites 1-3mm, plates 0.5-1mm rimed, needles heavily rimed

*Layer 5:* Stellar dendrites 1-3mm, plates 0.5-1mm rimed, needles heavily rimed

April 03, 2007

— North —

*Names:* Doug Station: North *Date:* 04-3-07 *Time:* 9:30 am *Exposed thermocouples:* 0 *Keywords:*

*Surface:* Stellar dendrites 1-3mm, needles 1mm, plates 0.5mm, heavy rime on some particles

*Layer 1:* Stellar dendrites 1-3mm, needles 1mm, plates 0.5mm, heavy rime on some particles

*Layer 2:* Stellar dendrites 1-3mm, needles 1mm, plates 0.5mm, heavy rime on some particles

*Layer 3:* Stellar dendrites 1-3mm, needles 1mm, plates 0.5mm, heavy rime on some particles

*Layer 4:*  
Stellar dendrites 1-3mm, rime on some particles

*Layer 5:*  
Stellar dendrites 1-3mm, rime on some particles

— South —

*Names:* Doug Station: South *Date:* 04-03-07 *Time:* 11:00 am *Exposed thermocouples:* 0 *Keywords:* none

*Surface:* Wind crust 1mm thick

*Layer 1:* Stellar dendrites 1-3mm thick, plates 0.5mm, light rime on some particles

*Layer 2:* Stellar dendrites 1-3mm thick, plates 0.5mm, light rime on some particles

*Layer 3:* Stellar dendrites 1-3mm thick, plates 0.5mm, light rime on some particles

*Layer 4:* Stellar dendrites 1-3mm thick, plates 0.5mm, light rime on some particles

*Layer 5:* Stellar dendrites 1-3mm thick, plates 0.5mm, light rime on some particles

April 04, 2007

— North —

*Names: Henry Station: North Date: 04-4-07 Time: 10:30 am Exposed thermocouples: 0 Keywords:*  
*Surface: Stellar dendrites 1-3mm, 1mm needles, 0.5mm plates*  
*Layer 1: Highly broken particles 1mm*  
*Layer 2: Highly broken particles 1mm*  
*Layer 3: Highly broken particles 1mm*  
*Layer 4: Highly broken particles 1mm*  
*Layer 5:*  
 Partly decomposed precipitation particles 1-2mm

— South —

*Names: Henry Station: South Date: 04-04-07 Time: 1:45 pm Exposed thermocouples: 2 Keywords:*  
*Surface: 2-4mm stellar dendrites*  
*Layer 1: 0.25x4mm rounded poly crystals*  
*Layer 2: 0.25x4mm rounded poly crystals*  
*Layer 3: 0.25x4mm rounded poly crystals*  
*Layer 4: 0.25x4mm rounded poly crystals*  
*Layer 5: 0.5-2mm rounded poly crystals*

April 05, 2007

— North —

*Names: Henry Station: North Date: 04-5-07 Time: 1:00 pm Exposed thermocouples: 0 Keywords:*  
*Surface: 1mm graupel becoming wet*  
*Layer 1: 0.25x3mm needles becoming wet*  
*Layer 2:*  
 0.25x1-2mm needles, 1mm columns, 2mm plates  
*Layer 3:*  
 0.25x1-2mm needles, 1mm columns, 2mm plates  
*Layer 4:*  
 0.25x1-2mm needles, 1mm columns, 2mm plates  
*Layer 5:*  
 0.25x1-2mm needles, 1mm columns, 2mm plates

— South —

*Names: Henry Station: South Date: 04-05-07 Time: 11:00 am Exposed thermocouples: 5 Keywords:*  
*Surface: 1mm graupel*  
*Layer 1: 0.25-3mm needles*  
*Layer 2: 0.25-3mm needles*  
*Layer 3: 0.25x1-2mm needles, 1mm columns, 2mm stellar dendrites*  
*Layer 4: 0.25x1-2mm needles, 1mm columns, 2mm stellar dendrites*  
*Layer 5: 0.25x1-2mm needles, 1mm columns, 2mm stellar dendrites*

April 06, 2007

— North —

*Names: Henry Station: North Date: 04-6-07 Time: 2:40 pm Exposed thermocouples: 0 Keywords:*  
*Surface: 0.5mm striated cups*  
*Layer 1: 0.25mm melt freeze crust 2cm thick (dry)*  
*Layer 2: 0.25mm melt freeze crust 2cm thick (dry)*  
*Layer 3: 0.5mm highly broken particles (dry)*  
*Layer 4: 0.5mm highly broken particles*  
*Layer 5: 0.25mm melt freeze crust*

— South —

NO DAILY LOG RECORDED



April 07, 2007

— North —

— South —

*Names: Coop Station: North Date: 04-7-07 Time:**1:25 pm Exposed thermocouples: 0 Keywords:**NO DAILY LOG RECORDED**Surface: rounded grains 0.5-1mm wet**Layer 1: rounded grains 0.5-1mm wet**Layer 2: rounded grains 0.5-1mm wet**Layer 3: rounded grains 0.5-1mm wet**Layer 4: rounded grains 0.5-1mm wet**Layer 5: rounded grains 0.5-1mm wet*

April 08, 2007

— North —

— South —

*Names: Doug Station: North Date: 04-8-07 Time:**9:30 am Exposed thermocouples: 0 Keywords:**NO DAILY LOG RECORDED**Surface: Surface hoar 1-2mm**Layer 1: Mixed forms 0.5-2mm**Layer 2: Mixed forms 0.5-2mm**Layer 3: Melt freeze crust 3cm thick**Layer 4: Melt freeze crust 3cm thick**Layer 5: Melt freeze crust 3cm thick*

April 09, 2007

— North —

— South —

*Names: Doug, Irene Station: North Date: 04-9-07**Time: 12:00 pm Exposed thermocouples: 0 Keywords:**NO DAILY LOG RECORDED**Surface: Graupel 0.5-2mm**Layer 1: Graupel 0.5-2mm**Layer 2: Graupel 0.5-2mm**Layer 3: Graupel 0.5-2mm**Layer 4: Graupel 0.5-2mm**Layer 5: Graupel 0.5-2mm*

April 10, 2007

— North —

— South —

*Names: Doug Station: North Date: 04-10-07 Time:**11:30 am Exposed thermocouples: 0 Keywords:**Surface: Columns 1mm with heavy rime, plates 1mm with heavy rime, precipitation particles 0.5-1mm rimed to heavily rimed**Layer 1: Precipitation particles 0.5-1mm heavily rimed, heavily broken particles 0.5-1mm rimed**Layer 2: Precipitation particles 0.5-1mm heavily rimed, heavily broken particles 0.5-1mm rimed**Layer 3: Precipitation particles 0.5-1mm heavily rimed, heavily broken particles 0.5-1mm rimed**Layer 4: Precipitation particles 0.5-1mm heavily rimed, heavily broken particles 0.5-1mm rimed**Layer 5: Precipitation particles 0.5-1mm heavily rimed, heavily broken particles 0.5-1mm rimed**NO DAILY LOG RECORDED*

April 11, 2007

— North —

— South —

*Names: Doug Station: North Date: 04-11-07 Time:**1:00 pm Exposed thermocouples: 0 Keywords:**Surface: Stellar dendrites 2-5mm**Layer 1: Stellar dendrites 2-5mm**Layer 2: Stellar dendrites 2-5mm**Layer 3: Stellar dendrites 2-5mm**Layer 4: Stellar dendrites 2-5mm**Layer 5: Stellar dendrites 2-5mm**NO DAILY LOG RECORDED*

April 15, 2007

— North —

— South —

*Names: tewrete Station: Date: 04-15-07 Time:**Exposed thermocouples: 0 Keywords:**Surface:**Layer 1:**Layer 2:**Layer 3:**Layer 4:**Layer 5:**NO DAILY LOG RECORDED*